# Conjugate Margins Conference | Halifax 2008

# Extended Abstracts

**August 13-15, 2008**
**Dalhousie University**
**Halifax, Nova Scotia, Canada**

Atlantic Canada Opportunities Agency
Agence de promotion économique du Canada atlantique
Canada

ISBN: 0-9810595-1

Conjugate Margins Conference | Halifax 2008

*"Sharing Ideas – Embracing Opportunities"*

# Program & Extended Abstracts

**13 – 15 August 2008**
**Dalhousie University**
**Halifax, Nova Scotia**
**Canada**

**EDITOR: David E. Brown**

***Conjugatemargins.com***

Program & Abstracts Publication Sponsor:

Atlantic Canada Opportunities Agency
Agence de promotion économique du Canada atlantique
Canada

**Halifax 2008 Steering Committee**

Committee Co-Chairs
David E. Brown – Canada-Nova Scotia Offshore Petroleum Board
Grant D. Wach – Dalhousie University

Committee
Trudy Lewis – Lewis Conference Service International
Paul J. Post – U.S. Minerals Management Service
Sonya A. Dehler – Geological Survey of Canada
Andre MacRae – Saint Mary's University
Mladen Nedimovic – Dalhousie University
Jürgen Adam – Royal Holloway University
Neil Watson – Consultant

**ISBN: 0-9810595-2**

# Sponsors and Supporters

***The Halifax 2008 Steering Committee extends our sincerest thanks and appreciation to all our sponsors and supporters for their generous financial and in-kind support in helping to make this Conference a reality and success.***

**DIAMOND - $20,000 +**

Nova Scotia Offshore Energy Technical Research Association (OETRA)
- *Foundation Funding*

Canada-Nova Scotia Offshore Petroleum Board
- *Foundation Funding, Core Workshop, CNSOPB Reception*

Nova Scotia Department of Energy
- *Foundation Funding*

**PLATINUM - $14,999 - $10,000**

Petrobras
- *Conference CD, Delegate Tote Bag, Short Courses*

BHP Billiton
- *Oral Session "Margin Evolution & Development, Poster Session, Opening Reception*

**GOLD - $9,999 - $6,000**

EnCana
- *Student Registration, Student Breakfast, Delegate Badge Holders, Foundation Funding*

ExxonMobil
- *Foundation Funding*

Husky Energy
- *Oral Session "Petroleum Systems", Foundation Funding*

Atlantic Canada Opportunities Agency (ACOA)
- *Conference Program, Foundation Funding*

**BRONZE - $3,999 - $2,000**

Canadian Superior
- *Foundation Funding*

ION-GEO (GXTechnology)
- *Seismic Data Room*

RPS Energy
- *Harbour Cruise*

**PATRON - $1,999 - $1,000**

Schlumberger – SIS
- *Field Trips*

Petroleum Research–Atlantic Canada (PR-AC)
- *Foundation Funding*

**PARTNER - $999 - $500**

Natural Resources Canada – Geological Survey of Canada
- Foundation Funding

US Minerals management Service
- Foundation Funding

**SUPPORTERS**

Dalhousie University
Atlantic Geoscience Society
Canadian Association of Petroleum Geologists
American Association of Petroleum Geologists
Petroleum Exploration Society of Great Britain
Houston Geological Society
Geological Journal

We sincerely thank all our sponsors, partners and supporters who contributed to the success of the

# Conjugate Margins Conference | Halifax 2008

**Diamond $15,000+**

OETR

CNSOPB — Canada-Nova Scotia Offshore Petroleum Board

Nova Scotia Department of Energy

**Platinum $10,000 – $14,999**

BR Petrobras

bhpbilliton — resourcing the future

**Gold $6,000 – $9,999**

ExxonMobil

Husky Energy

Atlantic Canada Opportunities Agency / Agence de promotion économique du Canada atlantique — Canada

EnCana — energy for people

**Bronze $2,000 – $3,999**

Canadian Superior Energy Inc.

RPS Energy

ion

**Patron $1,000 – $1,999**

Schlumberger

Petroleum Research Atlantic Canada

**Partners $500 – $999**

Natural Resources Canada / Ressources naturelles Canada

Canada

Minerals Management Service

**Supporters**

Canadian Society of Petroleum Geologists

American Association of Petroleum Geologists

ACS

Houston Geological Society

Geological Journal

PESGB

Dalhousie University — Inspiring Minds

# Halifax 2008 Organization

## STEERING COMMITTEE

**David E. Brown – Co-Chair**
*Canada-Nova Scotia Offshore Petroleum Board*
*Halifax, Nova Scotia, CANADA*

**Grant D. Wach – Co-Chair**
*Dalhousie University*
*Halifax, Nova Scotia, CANADA*

**Sonya A. Dehler**
*Geological Survey of Canada – Atlantic*
*Dartmouth, Nova Scotia, CANADA*

**Paul J. Post**
*U.S. Minerals Management Service*
*New Orleans, Louisiana, USA*

**Neil Watson**
*Consultant*
*Halifax, Nova Scotia, CANADA*

**Andrew MacRae,**
*Saint Mary's University*
*Halifax, Nova Scotia, CANADA*

**Jürgen Adam**
*Royal Holloway University of London*
*London, ENGLAND*

**Mladen R. Nedimovic**
*Dalhousie University*
*Halifax, Nova Scotia, CANADA*

**Trudy Lewis – Conference Agent**
*Lewis Conference Services International*
*Halifax, Nova Scotia, CANADA*

## PROGRAM ADVISORY COMMITTEE

**Michal Nemčok**
*Energy & Geoscience Institute-University of Utah*
*Bratislava, SLOVAKIA*

**Mark G. Rowan**
*Rowan Consulting Inc.*
*Boulder, Colorado, USA*

**Tako Koning**
*Consultant / Tullow Oil*
*Luanda, ANGOLA*

**Ian Davison**
*Earthmoves Ltd.*
*Camberley, ENGLAND*

**Webster U. Mohriak**
*Petrobras E&P*
*Rio de Janeiro, BRAZIL*

**Gabor C. Tari**
*OMV (Österreichische Mineralölverwaltung)*
*Vienna, AUSTRIA*

**Paul J. Post**
*U.S. Minerals Management Service*
*New Orleans, Louisiana, USA*

## AUDIO-VISUAL & FACILITIES COMMITTEE

**Peter Wallace**
*Dalhousie University*
*Halifax, Nova Scotia, CANADA*

**Tom Duffett**
*Dalhousie University*
*Halifax, Nova Scotia, CANADA*

**Charlie Walls**
*Dalhousie University*
*Halifax, Nova Scotia, CANADA*

# Table of Contents


Sponsors & Supporters……4

Halifax 2008 Organisation……6

Table of Contents……7

**ORAL SESSIONS**

Margin Evolution & Development – Session 1A……9

Margin Evolution & Development – Session 1B……41

Margin Evolution & Development – Session 1C……63

Petroleum Systems – Session 2A……103

Petroleum Systems – Session 2B……145

Petroleum Systems – Session 2C……221

**POSTER SESSIONS**

Margin Evolution & Development – Poster Session 1……275

Petroleum Systems – Poster Session 2……391

CORE WORKSHOP……485


Central Atlantic
Conjugate Margins Conference
Halifax 2008

# NOTES

# Session 1A:
# MARGIN EVOLUTION & DEVELOPMENT

## KEYNOTE ADDRESS

**DEPTH-DEPENDENT EXTENSION AND MANTLE EXHUMATION: AN EXTREME PASSIVE MARGIN END-MEMBER OR A NEW PARADIGM?**
**Karner, Garry D.**

**CONTINENTAL BREAK-UP MECHANISM; LESSONS FROM SLOW-, INTERMEDIATE- AND FAST-EXTENSION SETTINGS**
Nemčok, Michal; Stuart, C.; Rosendahl, B. R.; Welker, C.; Smith, S.; Sheya, C.; Sinha, S. T.; Choudhuri, M.; Yalamanchili, S.V.; Allen, R.; Reeves, C.; Sharma, S.; Srivastava, D.; Venkatraman, S. and Sinha, N.

**U.S. EAST COAST: CONTINENTAL MARGIN EVALUATION WITH NEW TOOLS, DATA AND TECHNIQUES**
Dickson, William; Odegard, Mark; and Post, Paul J.

**MESOZOIC SEAFLOOR SPREADING HISTORY OF THE CENTRAL ATLANTIC OCEAN**
Bird, Dale E.; Hall, Stuart A.; Burke, Kevin; Casey, John F. and Sawyer, Dale S.

**VARIATIONS IN CRUSTAL THICKNESS AND EXTENSIONAL STYLE ALONG THE SCOTIAN MARGIN, ATLANTIC CANADA: CONSTRAINTS FROM SEISMIC DATA AND 3D GRAVITY INVERSION**
Dehler, Sonya A. and Welford, J. Kim

**NEW PROFILE MODELS OVER THE U.S. EAST COAST CONTINENTAL MARGIN**
Odegard, Mark; Post, Paul J. and Dickson, William

**SYSTEMATIC VARIATIONS IN BASEMENT MORPHOLOGY AND RIFTING GEOMETRY ALONG THE NOVA SCOTIA AND MOROCCO CONJUGATE MARGINS**
Wu, Yue; Louden, Keith and Tari, Gabor

**THE POST-RIFT EVOLUTION OF THE ATLANTIC MARGIN OF NW AFRICA: A NOT-SO-QUIET PERIOD OF EXHUMATION AND EROSION**
Bertotti, Giovanni; Andriessen, Paul; Barrie, Ibrahim; Beunk, Frank; Ghorbal, Badr and Wijbrans, Jan

**BACK**

# Depth-dependent Extension and Mantle Exhumation: An Extreme Passive Margin End-member or a New Paradigm?

**Garry D. Karner**
ExxonMobil Upstream Research Company
P.O. Box 2189
Houston, Texas 77252-2189
USA
e-mail: garry.d.karner@exxonmobil.com

## ABSTRACT

The discovery of exhumed continental mantle rocks and lack of magmas in ocean continent transitions, the existence of top-basement detachments, and the recognition of an "extension discrepancy" across many passive continental margins, as exhibited by preferential thinning of lower crust and the rapid thinning of continental crust in the absence of obvious faulting, have seriously challenged the accepted paradigms for the formation of passive continental margins and the way in which continental lithosphere is deformed in extension. Recent studies have clearly demonstrated that rifting, that is, the offset across high-angle basin bounding normal faults, is only a minor component in the thinning of continental lithosphere. During extension, early fault controlled subsidence tends to be limited to the proximal regions of passive margins while later brittle deformation dominates the distal regions.

Kinematic considerations of passive margin subsidence require preferential bulk thinning of the lower crust and lithospheric mantle relative to the upper crust, an observation supported by seismic refraction results across the West African margin and the Exmouth Plateau, northwest Australia. Age considerations indicate that this depth-dependent extension (DDE) of the lithosphere is the significant process for thinning continental crust from its 30-40 km pre-rift thickness to a thickness of ~10 km, but surprisingly, depositional environments seem to be characterized by shallow water and quiescent conditions, as evidenced by Tithonian carbonates of the Iberian margin now at abyssal depths. Such extension partitioning requires a lateral strain balance, which may take the following form: 1) a counterbalancing of upper crustal extension leading to late-stage brittle deformation in the vicinity of the ocean-continent transition zone (*e.g.* the low angle detachment systems of the distal Iberian margin), and/or 2) the lateral emplacement and exposure of serpentinized and magmatically modified continental mantle and lower crust out from under the adjacent continental lithosphere. While isostatic considerations of DDE allow the distribution and amplitude of syn- and post-extension accommodation to be calculated, a geological understanding of the thinning process and the modes of crustal and mantle deformation cannot be addressed. Thus, the fundamental question remains: what mechanism(s) allow the continental lithosphere to be thinned from ~30 km to ~10 km and thence to the point of rupture?

It has been suggested, using field observations from the exposed Tethyan margin in the Swiss Alps and geodynamic modeling, that the Iberia-Newfoundland system is the result of a complex rifting history that can be described as a sequence of different modes of extension. This sequence initiates with a broadly-distributed brittle deformation (stretching phase) and is followed by strain localization and crustal thinning along upper crustal and mantle ductile shear zones decoupled along a mid-crustal décollement, localized and controlled by a relatively weak middle crustal rheology (thinning phase). If and when coupling of the thinned upper and lower crust occurs (*i.e.* once the crust has reached a thickness of ~10 km), crustal embrittlement and continued extension leads to the formation of crustal-scale detachments along downward-concave faults that are conducive to mantle exhumation (exhumation phase). While this sequencing is a working hypothesis for how continental lithosphere extends, the view is that the final crustal architecture of at least the Iberia-Newfoundland margin is controlled by the stacking of these different modes of extension. Thus, given the field and drilling observations from the Iberia-

Newfoundland and Tethyan margins, the proxy for extensional strain partitioning in the crust is the existence of syn-extensional sags and the exhumation of lower crust and continental mantle.

The width of these exhumed zones may be 100's km wide and contain organized magnetic anomalies. However, these magnetic anomalies are likely a consequence of mantle exhumation and serpentinization rather than mid-ocean ridge basalt production at the spreading center. Many passive continental margins are characterized by such observations, for example, Galicia Bank and the Iberian margin, the Exmouth, Queensland and Marion Plateaus, the Woodlark basin, the West African margin, and the Norwegian margin. While the geological details and sedimentary facies differ between the various margins, the style of deformation is remarkably similar. It would appear that what was once considered an extreme end-member of passive margin formation (*viz.* the Iberian-Newfoundland margin) may instead be a template for the development of many hyperextended margins around the world, that is, continental lithosphere that has undergone 100's of percent of extension to the point of rupture. The modes of extension discussed above have immense implications for the heat flow history, environments of deposition, syn-extensional stratigraphy, and basin architecture of passive margin systems. A goal of this presentation is to show examples of depth-dependent extension and changing modes of crustal deformation. Our future challenge is to understand exactly how to link crustal deformation with lithospheric mantle thinning in a predictive way.

## Introduction

The discovery of exhumed continental mantle rocks and a lack of magmas in ocean continent transitions, the existence of top-basement detachments, and the recognition of an "extension discrepancy" across many passive continental margins, as exhibited by preferential thinning of lower crust in the absence of obvious faulting, have seriously challenged the accepted paradigms for the formation of passive continental margins and the way in which continental lithosphere is thinned in extension. Recent studies have clearly demonstrated that rifting, that is, the brittle deformation of the crust via high-angle basin bounding normal faults, is only a minor component in the thinning of continental lithosphere. In some instances, finding any faults of the appropriate age at all is problematic. For example, Figure 1 shows seismic reflection and refraction profiles across the Cuvier margin (northwest Australia; Tischer 2006), which was formed by extension of the continental lithosphere during the latest Tithonian-Valanginian (Karner et al., 1999). During 2001, R/V Ewing cruise EW0113 collected over 2000 km of multi-channel seismic reflection and more than 800 km of OBS wide-angle refraction data across the continent-ocean transition zones of the Exmouth Plateau and Cuvier passive margins in order to address specifically the question of how extension is balanced vertically and horizontally across the Exmouth Plateau and the Cuvier margin.

## Observations and Examples

In general, the Cuvier margin (and the Bernier Platform) is sediment starved with maximum Cretaceous-Neogene sediment thicknesses only being 0.5-1.0 sec (two-way travel time). The seismic section images folded and faulted Mesozoic and Paleozoic sediments separated from a thin late Early Cretaceous section by a major truncational unconformity of Valanginian age – this is the age of breakup on this margin. There are no obvious faults of Tithonian-Valanginian age and yet the crustal refraction profile indicates a major change in crustal thickness, from 30 km to approx. 15 km. Despite the lack of obvious faulting, the upper crustal velocity structure is clearly truncated between 190-240 km and the lower crustal velocity structure is truncated from between 165-190 km. The conclusion is that this "beheading" of the crustal velocity structure and the progressive removal of the upper crust between 165-240 km is controlled by a low-angle, top-basement detachment. This detachment is not easily recognized in the seismic section but likely is responsible for producing the truncational unconformity prior to the Valanginian and the smooth "roll-over" morphology of the basement. The lower crustal velocity structure seems to be intact from between 190-300 km. Thus, any counterbalancing lower crustal extension would

need to exist on the conjugate margin, perhaps explaining the lack of ductile shear zones on the Cuvier margin lower crust (Fig. 1).

Recognizing top-basement detachments on many margins is often confounded by later high-angle normal faults that result in impressive deformation of the upper crust. This deformation tends to dominate what is seen in seismic sections and dismembers and obscures the geometry and thus the "true" identity and role of the low-angle detachment systems that fundamentally drive upper crustal thinning.

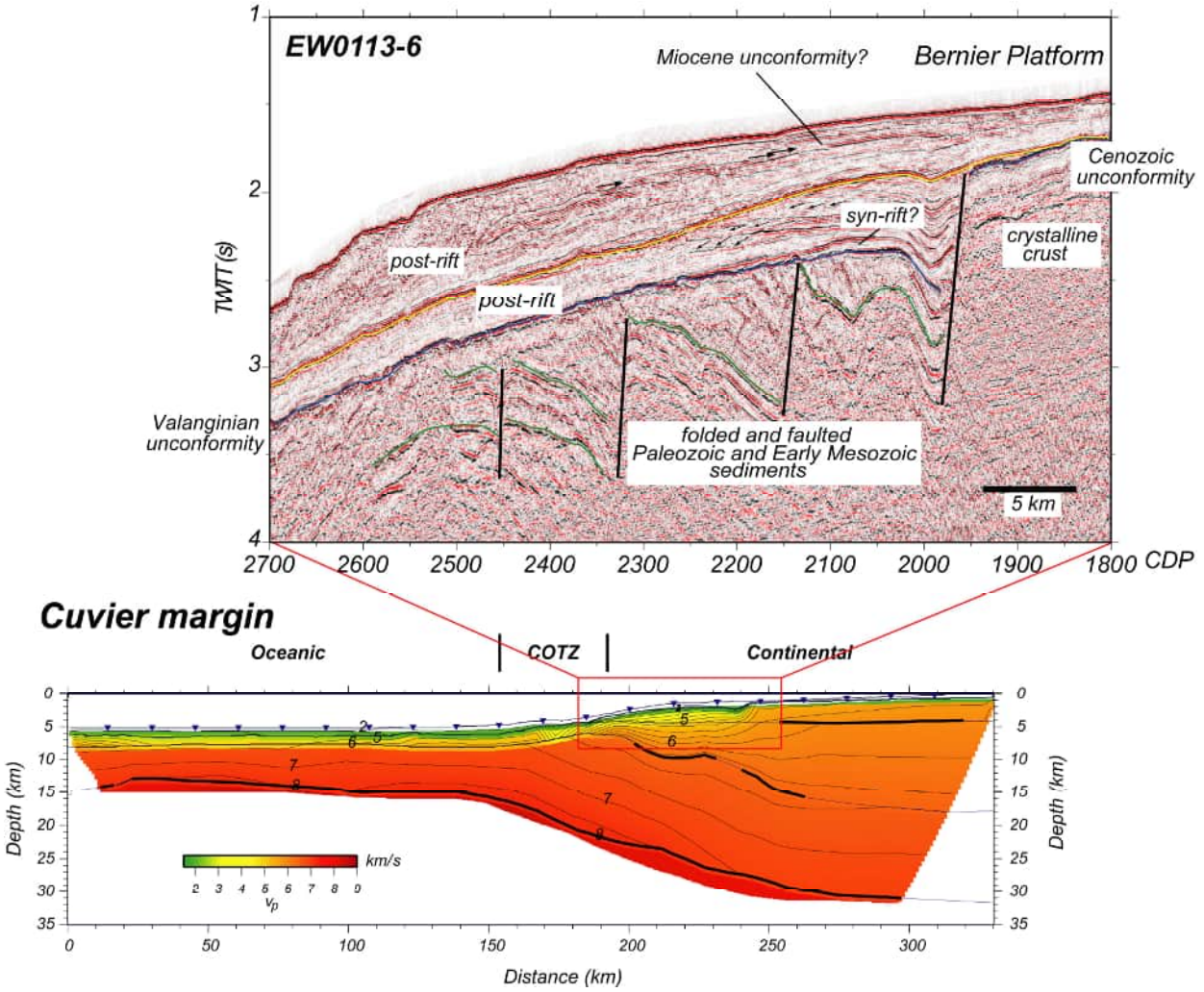


**Figure 1. Contoured P-wave velocity model of the Cuvier margin, Northwest Australia (modified from Tischer, 2006). Thick black lines mark horizons sampled by wide-angle reflections. OBS positions are indicated by blue triangles. Interpreted seismic section EW0113-6 shows a major truncational unconformity (Valanginian age) separating Jurassic, Carboniferous and Silurian sediments from thin late Cretaceous and Tertiary sediment packages. The high-standing crustal block in the east is the Bernier Platform.**

In general, for extensional systems that go to breakup, early but regionally distributed fault controlled subsidence tends to be replaced by syn-extensional sagging with a paucity of high-angle faulting (Karner and Driscoll 1999; Huismans and Beaumont 2008). Kinematic considerations of passive margin subsidence require preferential bulk thinning of the lower crust and lithospheric mantle relative to the upper crust, an observation supported by seismic refraction results across the West African margin and the Exmouth Plateau, Northwest Australia. For example, Figure 2, a seismic refraction profile across the western margin of the Exmouth Plateau (Tischer 2006), clearly shows that the lower crust is

preferentially thinned relative to the upper crust over a broad area. Further, in terms of a lateral strain balance, it would seem that the relatively higher velocities normally associated with the lower crust form a thickened zone of lower crust to the west of the margin proper. That is, we might expect both exhumed lower crust and eventually exhumed continental mantle in the ultra-deep water region to the west of the plateau and over many 100's km. Because the upper crust has extended very differently in both style and magnitude relative to the lower crust, this process is termed depth-dependent extension (DDE; Driscoll and Karner 1998).

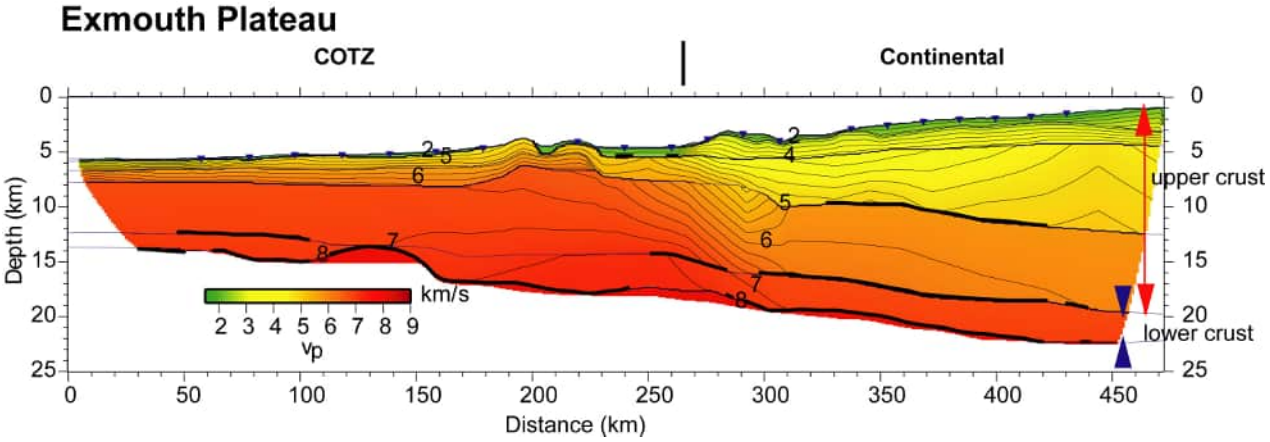


**Figure 2. P-wave velocity model of the Exmouth Plateau (modified from Tischer, 2006) showing the stretched continental crust of the plateau edge and part of the continent-ocean transition zone (COTZ). The velocity distribution (thin black lines, contour interval: 0.2 km/s) indicates a distinct preferential thinning of the upper continental crust relative to the lower crust underlying the plateau. A prominent lateral velocity gradient marks the boundary between continental crust and the COTZ.**

Age considerations indicate that this depth-dependent extension of the lithosphere is the dominant process for thinning continental crust from its 30-40 km pre-rift thickness to a thickness of approximately 10-15 km. For example, Karner and Driscoll (1999) required that the Exmouth Plateau crust was thinned by ~100% during the syn-rift period while for the hyper-extended portion of the Iberian margin, Manatschal *et al.* (2007), using Ocean Drilling Program results and seismic reflection and refraction data, determined that the thickness of the restored pre-Tithonian margin was only 6-10 km. During depth-dependent extension, depositional environments seem to be characterized by shallow water and quiescent conditions. This is evidenced by Tithonian shallow-water carbonates of the Iberian margin now at abyssal depths or the progradation of the Barrow delta across the Exmouth Plateau where clinoform amplitudes suggest a minimum water depth of 400-600 m. The water depth observations are extremely important and may relate to thinning of the lithospheric mantle and thus the input of significant heat, which should offset the subsidence induced by crustal extension.

The Manatschal *et al*. (2007) reconstruction of the hyper-extended Iberian margin is fundamental because it indicates that the region characterized by extreme brittle deformation (*i.e.* the famous "S-reflector" of the Iberian margin; Reston *et al.* 2007) and the zone of eventual continental mantle exhumation is *not* the most important extension event of the margin; rather, this extreme brittle deformation is the terminal extension phase immediately prior to breakup and responsible for thinning the crust from 6-10 km to zero. This exhumation phase of extension was necessarily preceded by a phase of bulk thinning of the crust (and presumably continental lithospheric mantle). This bulk thinning or extension partitioning requires: 1) the need for a lateral strain balance, which leads to upper crustal extension in adjacent regions, most notably in the vicinity of the future ocean-continent transition zone, 2) the lateral emplacement and exposure of serpentinized and magmatically modified continental mantle and lower crust out from under the adjacent continental lithosphere, and 3) that during this bulk thinning phase, environments of deposition appear to be shallow water, quiescent, and associated with minor

sediment accumulations, belying the fact that significant "damage" is being done to the lower crust and lithospheric mantle.

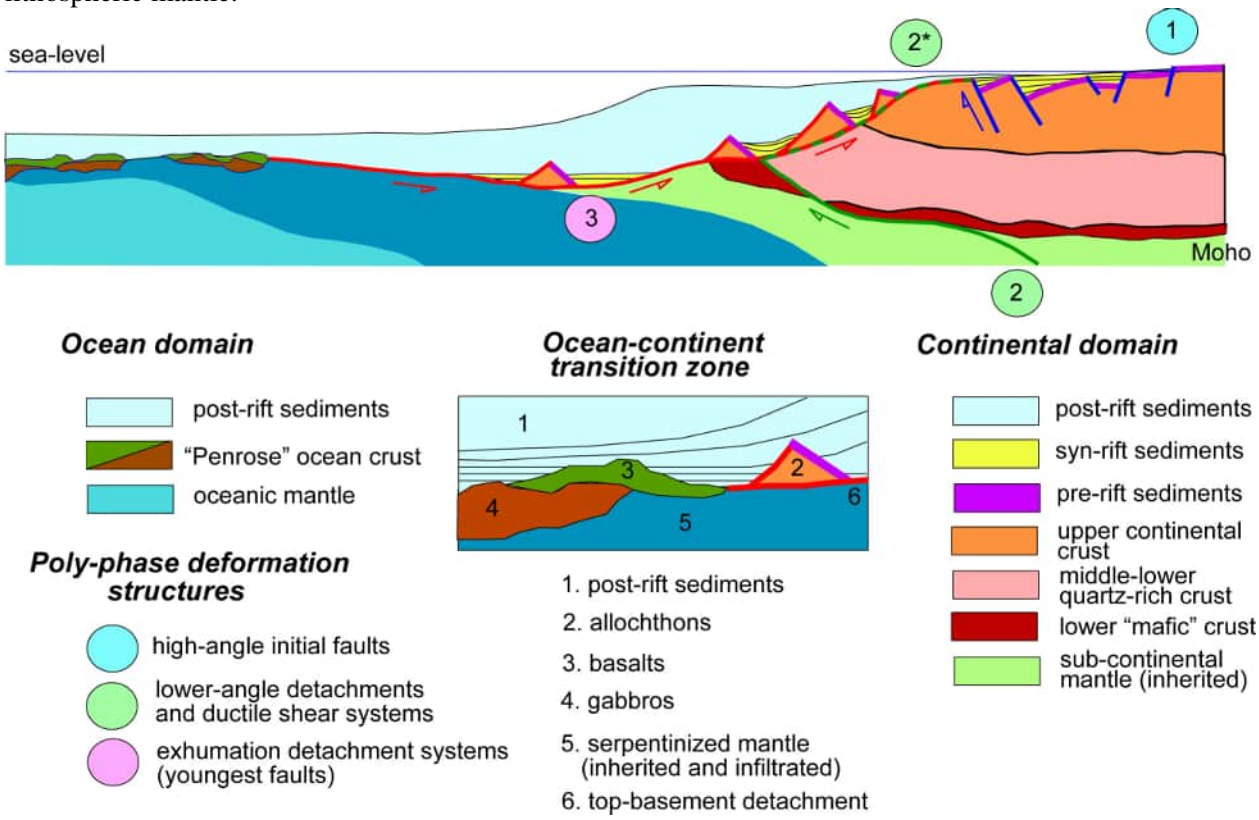


**Figure 3. Architecture of the Ocean-Continent Transition Zone produced by polyphase deformation of a rheologically layered continental lithosphere that resulted in mantle exhumation along top-basement detachment faults (modified from Péron-Pinvidic and Manatschal, 2008). Crustal thinning occurs by both upper crustal detachment systems and lower crustal ductile shear zones. The upper crustal detachment system allows the formation of allochthons. Continental and oceanic crusts are separated by a zone of exhumed continental mantle.**

While isostatic considerations of DDE allow the distribution and amplitude of syn- and post-extension accommodation to be appreciated, a geological understanding of the thinning process and the modes of crustal and mantle deformation cannot be addressed. Thus, the fundamental question still remains: what mechanism(s) allow the continental lithosphere to be thinned from ~30 km to ~10 km and thence to the point of rupture? Lavier and Manatschal (2006), using field observations from the exposed Tethyan margin in the Swiss Alps and supplemented with geodynamic modeling results, have suggested that the Iberia-Newfoundland system is the result of a poly-phase rifting history that can be described as a sequence of different modes of extension. This sequence initiates with a broadly-distributed brittle deformation (stretching phase) and is followed by strain localization and crustal thinning along upper crustal and mantle ductile shear zones decoupled along a mid-crustal decollement, localized and controlled by a relatively weak middle crustal rheology (thinning phase). If and when coupling of the thinned upper and lower crust occurs (*i.e.* once the crust has reached a thickness of ~10 km), crustal embrittlement and continued extension leads to the formation of crustal-scale detachments along downward-concave faults that are conducive to mantle exhumation (exhumation phase).

While this sequencing is a working hypothesis for how continental lithosphere extends, the view is that the final crustal architecture of at least the Iberia-Newfoundland margin is controlled by the stacking and temporal interplay of these different modes of extension (Fig. 3). Given the field and drilling observations from the Iberia-Newfoundland and Tethyan margins, the proxy for extensional strain

partitioning in the crust is the existence of syn-extensional sags and the exhumation of lower crust and continental mantle. The width of these exhumed zones may be 100's km wide and contain organized magnetic anomalies. However, these magnetic anomalies, rather than being produced as part of the seafloor spreading process, are likely a consequence of mantle exhumation and serpentinization rather than mid-ocean ridge basalt production at the spreading center, a review of which was recently published by Sibuet *et al.* (2007).

Figure 3 summarizes the structural complexity and architecture of a hyper-extended margin in terms of the poly-phase deformation of the margin (Péron-Pinvidic *et al.* 2007; Péron-Pinvidic and Manatschal, 2008). Discrete high-angle faulting restricted to the upper crust (Blue faults) produces a series of localized rift basins that are characterized by block rotations and depositional wedges. As extension continues, the upper crust is thinned by a top-basement detachment with ductile shear zones thinning the lithospheric mantle. These mantle shear zones may be responsible for the advection of heat into the extended region thereby offsetting the subsidence induced by thinning of the upper crust.

In Figure 3, the top-basement detachment is responsible for completely necking the upper crust while truncating the lower crust. The color scheme indicates that this same fault system may initiate during the thinning phase (Green faults) but may be reactivated during the exhumation phase (Red faults). Because this scheme was based on the Iberian margin, note that concave-down faults, necessary to exhume the continental mantle in the Lavier and Manatschal (2006) model, do not exist on this figure - these faults should characterize the final stages of extension and exhumation of the conjugate Newfoundland margin implying that the exposed continental mantle (Unit 5, Fig. 3) originated from under the Grand Banks.

## Conclusions

In summary, many passive continental margins are characterized by the above features and observations; for example, Galicia Bank and the Iberian margin, the Exmouth, Queensland and Marion Plateaus, the Woodlark basin, the West African margin, and the Norwegian margin. While the geological details and sedimentary facies differ between the various margins, the style and history of deformation is remarkably similar. It would appear that what was once considered an extreme end-member of passive margin formation (*viz.* the Iberian-Newfoundland margin) may instead be a template for the development of many non-volcanic (and possibly volcanic) hyper-extended margins around the world, that is, continental lithosphere that has undergone 100's of percent of extension to the point of rupture. The modes of extension discussed above have immense implications for the heat flow history, environments of deposition, syn-extensional stratigraphy, and basin architecture of passive margin systems. A goal of this presentation is to show examples of depth-dependent extension and changing modes of crustal deformation. Our future challenge is to understand exactly how to link crustal deformation with lithospheric mantle thinning in a predictive way.

## References


Driscoll, N.W., and G.D. Karner, 1998. Lower crustal extension across the northern Carnarvon basin, Australia: Evidence for an eastward dipping detachment. J. Geophys. Res., v.103, 4975-4992.

Huismans, R., and C. Beaumont, 2008. Complex rifted continental margins explained by dynamical models of depth-dependent lithospheric extension. Geology, v.36, 163–166; doi: 10.1130/G24231A.1

Karner, G.D., and N.W. Driscoll, 1999. Style, timing, and distribution of tectonic deformation across the Exmouth Plateau, northwest Australia, determined from stratal architecture and quantitative basin modelling. In: "Continental Tectonics", Mac Niocaill, C., and P.D. Ryan (eds), Spec. Publ. Geol. Soc. Lond., v.164, p.271-311.

Lavier, L., and G. Manatschal, 2006. A mechanism to thin the continental lithosphere at magma-poor margins, Nature, v.440, 3p.24-328.

Manatschal, G., O. Müntener, L.L. Lavier, T. A. Minshull and G. Péron-Pinvidic, 2007. Observations from the Alpine Tethys and Iberia–Newfoundland margins pertinent to the interpretation of continental breakup. In:

Karner, G. D., Manatschal, G. & Pinheiro, L. M. (eds.) Imaging, Mapping and Modelling Continental Lithosphere Extension and Breakup. Geological Society, London, Special Publications, v.282, p.291–324.

Péron-Pinvidic, G., G. Manatschal, T.A. Minshull, and D. Sawyer, 2007. Tectono-sedimentary evolution of the deep Iberia–Newfoundland margins: Evidence for a complex breakup history. Tectonics, v.26, TC2011, doi:10.1029/2006TC001970.

Péron-Pinvidic, G., and G. Manatschal, 2008. The final rifting evolution at deep magma-poor passive margins from Iberia-Newfoundland: A new point of view. Int. J. Earth Sci. (Geol. Rundsch.) DOI 10.1007/s00531-008-0337-9

Reston, T. J., T. Leythaeuser, G. Booth-Rea, D. Sawyer, D. Klaeschen, and C. Long, 2007. Movement along a low-angle normal fault: The S reflector west of Spain, Geochem. Geophys. Geosyst., v.8, Q06002, doi:10.1029/2006GC001437.

Sibuet, J.C., S. Srivastava, and G. Manatschal, 2007. Exhumed mantle forming transitional crust in the Newfoundland-Iberia rift and associated magnetic anomalies, Journal of Geophysical Research, v.112, B06105, doi:10.1029/ 2005JB003856.

Tischer, M.J., 2006. The structure and development of the continent-ocean transition zone of the Exmouth Plateau and Cuvier margin. Northwest Australia: Implications for extensional strain partitioning, Ph.D. thesis, Columbia University, New York.

**BACK**

# Continental Break-up Mechanism; Lessons from Slow-, Intermediate- and Fast-Extension Settings

**Michal Nemčok**
**C. Stuart**
**Bruce R. Rosendahl**
**C. Welker**
**S. Smith**
**C. Sheya**
**R. Allen**
Energy and Geoscience Institute
University of Utah
423 Wakara Way, Suite 300
Salt Lake City, UT 84108
United States
e-mail: mnemcok@egi.utah.edu

**S.T. Sinha**
**M. Choudhuri**
**S. Sharma**
**D. Srivastava**
**N. Sinha**
Reliance Industries Ltd.
Petroleum Business (E&P)
Reliance Corporate Park, Block 5, A Wing
Navi Mumbai-400701
India

**S.V. Yalamanchili**
Fugro Robertson Inc.
6100 Hillcroft, 5th floor
P.O. Box
740010, Houston, TX 77274
United States

**C. Reeves**
Earthworks bv.
Achterom 41a
2611 PL Delft
Netherlands

**S. Venkatraman**
ION Geophysical
2105 CityWest Boulevard, Suite 900
Houston, TX 77042-3847
United States

## ABSTRACT

Sea-floor spreading mechanisms vary among slow, intermediate and fast-spreading systems. Do continental break-up mechanisms vary for slow-, intermediate- and fast-extension systems? Because the slow-extension break-up mechanism is established by studies of conjugate Iberia and Newfoundland margins of the Central Atlantic and European and Adria margins of the Liguria-Piemonte Ocean, this study focuses on intermediate and fast rates, which are known from Gabon-Cameroon and East India, respectively. The study draws from synthetic interpretation of ultra-deep reflection seismic, well, gravity, magnetic and outcrop-derived paleostress data.

The interpretation indicates that continental break-up is done by a single continental mantle unroofing mechanism in all systems, just progressively more masked by magmatism at faster-extension systems. Breaking-up of the intermediately fast Gabon system is characterized by upper continental crust partially decoupled from the continental mantle, while the fast E India system underwent decoupling and its lower crust underwent up-bulging in zones in immediate footwalls of main normal faults. Regardless of the extension rate, the upper crustal break-up is controlled by pre-existing anisotropies, which form a system of constraining "rails" for extending continental crust and which influence the local stress regime. Such local stress regime regains the regional character once the function of constraining rails vanishes during the unroofing of the upper continental mantle. Different regions reach different amounts of upper crustal stretching prior to break-up initiation. The break-up location is then controlled by the upper crustal energy balance principle of "wound linkage", trying to use the minimum physical work for linking major upper crustal "wounds" and developing the upper crustal break-up.

BACK

# U.S. East Coast: Continental Margin Evaluation with New Tools, Data and Techniques

**William Dickson**
Dickson International Geosciences (DIGs)
10260 Westheimer Rd, Suite 320
Houston, TX 77042-3160
United States
e-mail: billd@hal-pc.org

**Mark Odegard**
Grizzly Geosciences, Inc.
14019 SW Freeway, Suite 301-735
Sugar Land, TX 77478
United States

**Paul J. Post**
Minerals Management Service
1201 Elmwood Park Blvd.
New Orleans, LA 70123
United States

## ABSTRACT

Exploration discussions of the Central Atlantic margins typically omit the U.S. East Coast Continental Margin (ECUS) which has been dormant, without drilling since 1984, despite on-going E&P activities to the north (offshore Nova Scotia), south (offshore northern Cuba), and on the conjugate African margin (Morocco to Mauritania). Shell has documented its exploration success with new ideas and new technology. After a more than twenty year hiatus, we too have new data, technology and ideas along the ECUS, suggesting that timing is favourable for a thorough review.

Our data compilation began with advanced coverage of public domain bathymetry, gravity and magnetic data, all re-leveled, cross-correlated and merged. Our Central Atlantic data set includes five million-odd line-kms each of gravity and magnetic profiles plus a half-million data points. Each data set was carefully merged to regional backgrounds derived from multiple satellites. Stunning imagery of bathymetry, gravity, magnetic and auxiliary data were generated from the final 4 km (super-regional) and 1 km (basin-level) grids. Including multiple data attributes that are somewhat area-dependent, we generated about 40 images, each with specific and general interpretation value.

Evolution of passive margins and adjacent oceanic crust has been studied extensively since the mid-1980's, with continued academic work along the ECUS. The Minerals Management Service is conducting a re-analysis of pre-1985 drilling and seismic data augmenting the older ECUS literature. We make initial comparisons between published interpretations and our new imagery, presenting adjustments, revisions, extrapolations and some speculation. While the dominant structural features are largely unchanged, they are better delineated. This includes evidence of more subtle correlations with published depictions of play-defining features such as areas of salt tectonics and carbonate bank edges. The interaction of these features with plate tectonic elements is also better defined. Each of these observations is illustrated with specific imagery on which feature changes and extensions are highlighted.

BACK

# Mesozoic Seafloor Spreading History of the Central Atlantic Ocean

**Dale E. Bird**
Bird Geophysical
16903 Clan Macintosh
Houston, Texas 77084
Email: dale@birdgeo.com

**Stuart A. Hall**
**Kevin Burke**
**John F. Casey**
Department of Geosciences
University of Houston
Houston, Texas 77204-5503

**Dale S. Sawyer**
Department of Earth Science
Rice University
Keith-Wiess Geological Labs
6100 Main Street,
Houston, Texas 77005

## ABSTRACT

The history of Mesozoic seafloor spreading in the Central Atlantic Ocean includes asymmetric spreading between Chrons M25 and M0 (154.1 Ma to 120.6 Ma), and two ridge jumps at about 170 Ma and 160 Ma. We identify and map twenty-three Mesozoic Chrons, including several in the Jurassic Magnetic Quiet Zone (JQMZ), between the Atlantis and Fifteen-Twenty fracture zones on the North American Plate, and between the Atlantis and Kane fracture zones on the African Plate. Chron M40 (167.5 Ma) is mapped about 65 km outboard of the conjugate Blake Spur and S1 magnetic anomalies, over the respective North American and African flanks of the ocean basin. Inboard of these prominent anomalies, the conjugate East Coast and S3 magnetic anomalies, are respectively located about 180 km and 30 km inboard of the BSMA-S1 pair. Therefore the ridge jump to the east between BSMA and ECMA anomalies at about 170 Ma theorized by Vogt and others in 1971 is supported by this study. The width of the African JMQZ is about 70 km greater (22%) than the North American JMQZ. A second ridge jump is suggested by additional, correlable anomalies over the African flank. Modeling results indicate that this jump occurred between 164 Ma and 159 Ma (Chrons M38 and M32). The ridge jumps can be related to plate interactions as North America separated from Gondwana. It has not escaped our attention that these ridge jumps, especially the latter, could correspond with the opening of the Gulf of Mexico.

## Introduction

Closing ocean basins along geomagnetic isochrons is an objective method for analyzing reconstructed continental margins. If similar geophysical or geological features can then be identified on conjugate margins, then these features can be used to further close ocean basins. We close the Central Atlantic Ocean by focusing on the oldest magnetic anomaly provinces: Mesozoic Chrons M25 to M0; JMQZ Chrons M40 to M28; and a zone of low amplitude anomalies between the ECMA and BSMA over

the North American flank of the ocean basin (Table 1). The conjugates to ECMA and BSMA, S3 and S1, are located over the African flank inboard of Chron M40 (Bird *et al*. 2007).

**Table 1. Finite rotation poles for North America relative to Africa.**

| Chron | Age (Ma) | Latitude | Longitude | Rotation Angle |
|---|---|---|---|---|
| M0 | 120.6 | 66.7ºN | 18.55ºW | 54.23º |
| M25 | 154.1 | 66.10ºN | 16.40ºW | 65.83º |
| M40 | 165.1 | 65.50ºN | 15.30ºW | 71.76º |
| -- | ~185.0 | 67.76ºN | 5.42ºW | 72.97º |

The overall kinematic history of the Central Atlantic Ocean is well understood (Klitgord and Schouten 1986; Muller and Roest 1992; Muller *et al.* 1999; Withjack *et al*. 1998). Following Middle to Late Triassic rifting between North America and Africa, seafloor spreading began at approximately 185 Ma (Withjack *et al*. 1998). We combine flow lines, approximated from fracture zones, and magnetic anomalies to determine the age and relative Mesozoic rotation history between the North American and African Plates. This history includes asymmetric seafloor spreading (120.6 Ma to 154.1 Ma), ridge jumps at 170 Ma (Vogt *et al.* 1971) and between 164 Ma and 159 Ma (Bird *et al*. 2007), and variable extension of the continental crust along-strike. The position of the Bahaman Islands directly along the intersection of the Demarara Rise and Guinea Nose as the basin is closed from Chron M40 (165.1) to final closure (ca. 185 Ma), suggests that the Central Atlantic Magmatic Province (CAMP) plume track lies beneath the Bahaman Islands (Dietz 1973).

## Data and Methods

Open-file geophysical data were used in this study: two magnetic anomaly grids, two gravity anomaly grids, and three magnetic anomaly profile data sets. The magnetic grids partially cover the Central Atlantic Ocean (Hinze *et al*. 1988; Verhoef *et al.* 1996). The gravity grids include one that partially covers the Central Atlantic Ocean and another that covers the world's oceans and seas (Tanner *et al.* 1988; Sandwell and Smith 1997). The magnetic anomaly profile data sources are: NOAA / NGDC GEOphysical DAta System (GEODAS) database, Geological Survey of Canada Kroonvlag project data (Collette *et al.* 1984), and 42 lines digitized from Vogt *et al.* (1971).

The Fifteen-Twenty, Kane, and Atlantis Fracture Zones span most of the Central Atlantic and extend close to the coasts of North America and Africa. We infer flowlines related to these fracture zones on maps of gravity and magnetic anomalies by tracing gravity minima through the transform offsets. Magnetic anomalies produced by sea-floor spreading are identified in a two-step process: 1) by simultaneous interpretation of gridded and profile magnetic anomalies to correlate significant anomaly trends, and 2) by comparison of selected anomaly profiles with synthetic anomaly profiles that are

calculated from 2D magnetic models based on the geomagnetic polarity reversal time scales of Channell *et al*. (1995) and Sager *et al*. (1998).

Total reconstruction poles were calculated for M0 (120.6 Ma), M25 (154.1 Ma) and M40 (165.1 Ma). A method similar to that described by Engebretson *et al.* (1984) was used to find the best fit Euler pole for pairs of control points defined by the intersections between interpreted geomagnetic isochrons and fracture zones. Each pair of control points is assumed to have been originally coincident such that a plate rotation exists that will restore them to a single point and a computer program minimized mismatch between one set of control points and the rotated set of control points by least squares approximation (Bird 2004). The final closure pole is estimated from two pairs of control points located along the 1000 m isobaths along the North American and African coasts, and a third pair of control points that connect the Florida shelf with the intersection of the Guinea Nose and Demarara Rise (Pindell and Dewey 1982). The two pairs of points located on the 1000 m isobaths were interpreted by comparing combinations of gravity and magnetic data and conjugate terranes of North America and Africa (Dallmeyer *et al.* 1987; Mueller *et al.* 1996; Murphy *et al.* 2004; Stillman 1988).

## Reconstructions

Twenty-three geomagnetic Chrons from M40 to M0 have been interpreted and mapped outboard of the North American and African continental slopes: M40, M38, M32, M29, M28, M25, M24, M23, M22, M21, M20, M20n-1, M19, M18, M17, M16, M14, M12A, M10N, M4, M3, M1 and M0. Inboard of the anomalies, the conjugate pairs Blake Spur Magnetic Anomaly (BSMA) – S1 and East Coast Magnetic Anomaly (ECMA) – S3 have also been interpreted and mapped. Bird *et al.* 2007) described the character and correlation of these anomaly sequences in detail.

The spreading rate for the high amplitude M25 through M0 Chrons in the North American plate (14.4 mm/a) is about 10.5% faster than the 12.9 mm/a spreading rate for the African plate, which indicates asymmetric spreading in this interval. The spreading rate for the North American JMQZ of 19 mm/a differs significantly from the African JMQZ rate of 24.6 mm/a, which is about 22% greater. This large difference in spreading rates suggests that a ridge jump may have occurred in this time interval. Therefore the magnetic data over the African side were inspected for repeated anomalies. A sequence of anomalies near M38 appears to repeat on the few profiles we analyzed and could account for an additional ~70 km of oceanic crust that seems to be absent from the North American side. The seafloor spreading models were modified by removing these chrons from the North American model and inserting them into the African model. Comparing JMQZ anomalies with those calculated from our ridge jump models suggests that a sequence of anomalies approximately between M38 and M32 could be produced by a sliver of oceanic lithosphere that was abandoned by a ridge jump. We suggest that the difference in JMQZ widths indicate that a ridge jump occurred between 164 and 159 Ma (Chrons M38 to M32), abandoning about 35 km of North American lithosphere on the African side of the Central Atlantic ocean basin.

Our identification of M40 along North America suggests that the high-amplitude western and eastern basin bounding anomalies, ECMA-S3 and BSMA-S1, are conjugate pairs. The asymmetric spreading required to create oceanic crust from ECMA to BSMA (180 km), and S3 to S1 (50 km), greatly exceeds the maximum asymmetry reported by Muller *et al*. (1998). We conclude that a ridge jump occurred within the IMQZ, substantiating the ridge jump hypothesized Vogt *et al*. (1971).

Gravity and magnetic anomalies suggest tectonic relationships between the North American and African Plates after closing the basin to M40 (Fig. 1). Gravity anomalies over the Guinea Nose of Africa, and Demarara Rise of South America, show the pre-Gondwana breakup position between these two plates (Hall and Bird 2007; Pindell and Dewey 1982). The northern end of the BSMA in the North America magnetic data appear to be continuous with an anomaly in southern end of the Africa magnetic data.

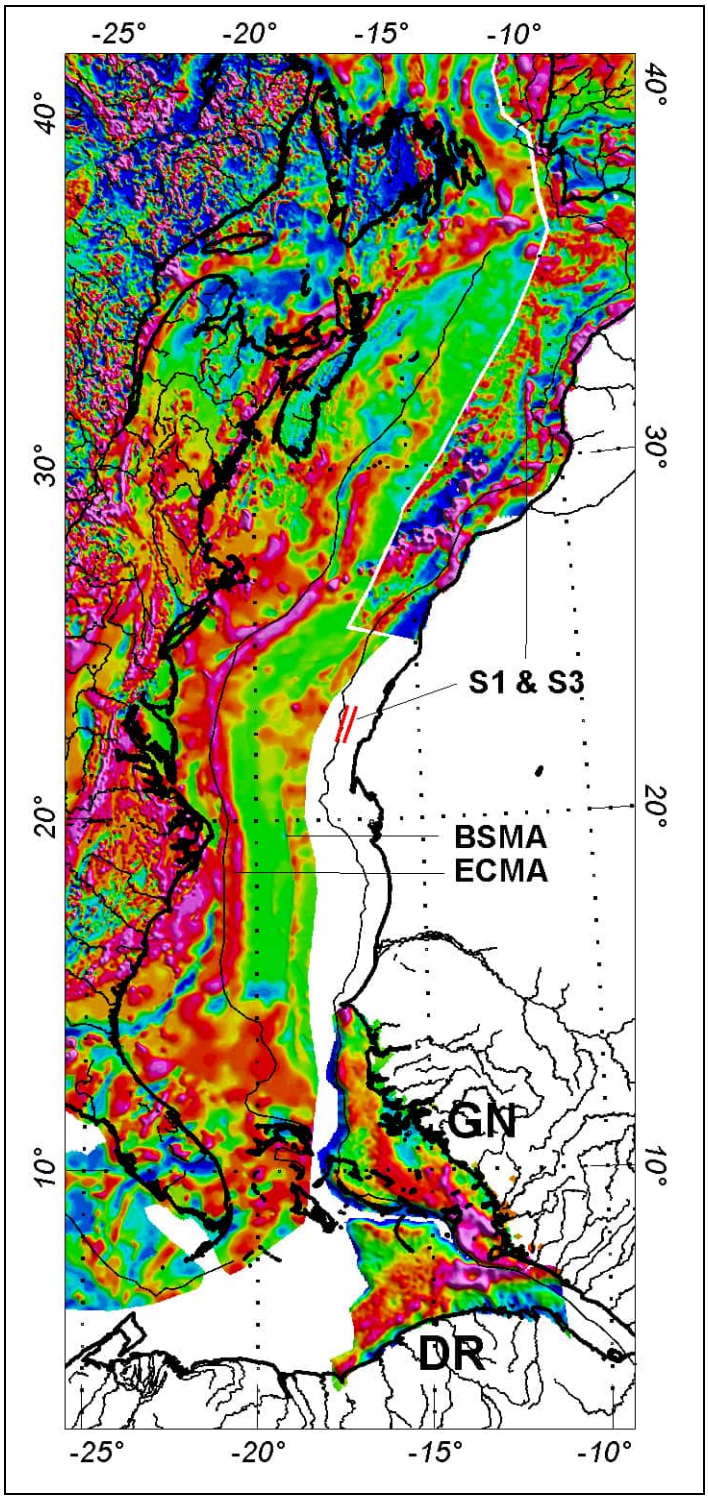


**Figure 1. M40 (165.1 Ma) reconstruction relative to Africa, with 1000 m isobaths for North America and Africa. Magnetic anomaly data: North America = Decade of North American Geology (DNAG) (Hinze *et al.* 1988). Gravity anomaly data = satellite-derived free air anomalies (Sandwell and Smith, 1997). S1 & S3 = magnetic anomalies; identified offshore northwest Africa (Roeser *et al.*, 2002), and identified (red lines) offshore Western Sahara (Bird *et al.* 2007). BSMA = Blake Spur Magnetic Anomaly, ECMA = East Coast Magnetic Anomaly, GN = Guinea Nose, DR = Demarara Rise.**

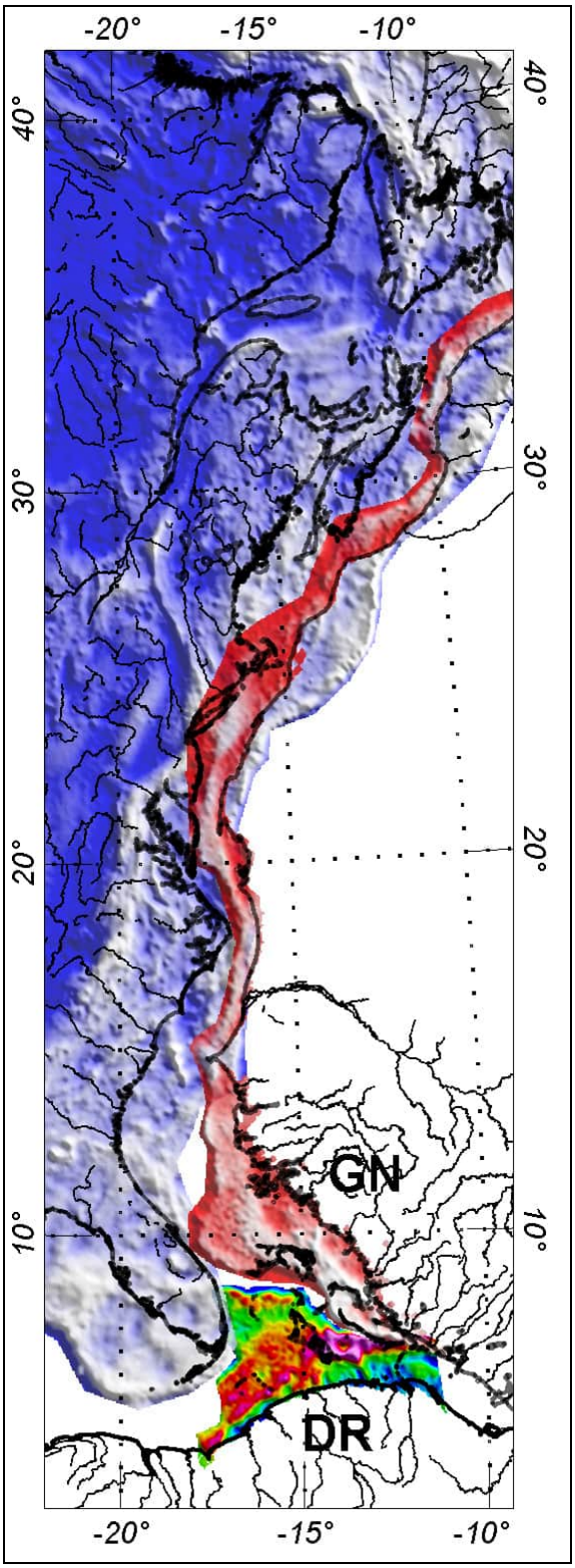


**Figure 2. Final closure reconstruction (ca. 185 Ma) and gravity anomalies. North American gravity (blue) = Decade of North American Geology (DNAG) (Tanner *et al.* 1988). African gravity (red) and Demarara Rise (red-blue color stretch) = Satellite-derived free air anomalies (Sandwell and Smith 1997). GN = Guinea Nose, DR = Demarara Rise.**

We chose to identify rotation control points along the 1000 m isobaths because: 1) the continental crust beneath this depth is interpreted to be partially extended and located near the ocean-continent boundaries, 2) prominent gravity anomalies correlate with the 1000 m isobaths, and 3) ECMA and S1 / S3 magnetic anomalies also correlate with the 1000 m isobaths. Figure 2 shows our final closure of the Central Atlantic Ocean with gravity data masked just outboard of prominent anomalies correlated with 1000 m isobaths. Gravity anomalies are shaded blue over North America, red over Africa, and by a typical red-blue color stretch over the Demarara Rise. The overlap of gravity data north of about 23° N suggests greater continental extension. For this and the M40 reconstructions, the Bahaman Islands map directly over the intersection between Guinea Nose and Demarara Rise suggesting that these structures were formed by the CAMP plume (Dietz 1973).

## Conclusions

We calculate a new Euler total reconstruction pole that closes the Central Atlantic Ocean, completing our kinematic reconstructions of the Central Atlantic Ocean (Bird *et al*. 2007), South Atlantic (Hall and Bird 2007), and the Gulf of Mexico (Bird *et al*. 2005**).**

Recently mapped M-Series Chrons in the Jurassic Magnetic Quiet Zone (JMQZ), and interpretations of geological and geophysical data, support the identification of:

- asymmetric seafloor spreading from M25 (154.1 Ma) to M0 (120.6 Ma) (Bird *et al*. 2007),
- a previously theorized eastward ridge jump at approximately 170 Ma as (Vogt *et al*. 1971),
- westward ridge jump between M32 and M38 (159 Ma and 164 Ma) (Bird *et al*. 2007),
- variable continental extension between North America and Africa north of 23°N, and
- the CAMP hotspot track beneath the Bahaman Islands (previously theorized by Dietz, 1973).

## Acknowledgements

We would like to thank Walter Roest at the Geologic Survey of Canada for sending a copy of the Kroonvlag project, which is a ship-track magnetic dataset (also known as the “Collette Data”).

## References

Bird, D. E., 2004, Jurassic tectonics of the Gulf of Mexico and Central Atlantic Ocean: Univ. of Houston, Ph.D. Dissertation, 161p.

Bird, D. E., K. Burke, S. A. Hall, and J. F. Casey, 2005, Gulf of Mexico tectonic history: Hotspot tracks, crustal boundaries, and early salt distribution: American Association of Petroleum Geologists Bull., v.89, p.311-328.

Bird, D. E., S. A. Hall, K. Burke, J. F. Casey, and D. S. Sawyer, 2007, Early Central Atlantic Ocean seafloor spreading history: Geosphere, v.3, n.5, p.282-298.

Channell, J. E. T., E. Erba, M. Nakanishi, and K. Tamaki, 1995, Late Jurassic – Early Cretaceous time scales and oceanic magnetic anomaly block models: in, Geochronology, Time Scales and Global Stratigraphic Correlation: SEPM Special Publication 54, p.51-63.

Collette, B. J., A. P. Slootweg, J. Verhoef, and W. R. Roest, 1984, Geophysical investigations of the floor of the Atlantic Ocean between 10° and 38°N (Kroonvlag-project): *in*, Amsterdam, Proceedings Koninklijke Nederlandse Akadademie van Wetenschappen, Series B, v.87, p.1-80.

Dallmeyer, R. D., M. Caen-Vachette, and M. Villeneuve, 1987, Emplacement age of post-tectonic granites in southern Guinea (West Africa) and the peninsular Florida subsurface: Implications for origins of southern Appalachian exotic terranes: Geological Society of America Bulle., v.99, p.87-93.

Dietz, R. S., 1973, Morphologic fits of North America / Africa and Gondwana: A review: *in*, Tarling, D. H., and S. K. Runcorn, eds., Implications of Continental Drift to the Earth Sciences, v.2: London, Academic Press, p.865-872.

Engebretson, D. C., A. Cox, and R. G. Gordon, 1984, Relative motions between oceanic plates of the Pacific basin: Jour. of Geophysical Research, v.89, p.10291-10310.

Hall, S. A., and D. E. Bird, 2007, Tristan da Cuhna hotspot tracks and the seafloor spreading history of the South Atlantic: Eos, Transactions, American Geophysical Union, v.88, Fall Meeting Supplement, V31F-04.

Hinze, W. J., P. J. Hood, W. E. Bonini, J. E. Case, M. de la Fuente, R. H. Godson, S. A. Hall, W. F. Hanna, J. R. Heirtzler, R. H. Higgs, M. D. Kleinkopf, H. Meyers, A. R. Palmer, N. W. Peddie, M. S. Reford, D. J. Teskey, L. Thorning, I. and Zietz, 1988, Magnetic anomaly map of North America: The Leading Edge, v.7, n.11, p.19-21.

Klitgord, K. D., and H. Schouten, 1986, Plate kinematics of the central Atlantic: *in*, Vogt, P. R., and B. E. Tucholke, eds., The Geology of North America, The western North Atlantic Region: Boulder, Geological Society of America, Volume M, p.351-378.

Mueller, P. A., M. Kozuch, A. L. Heatherington, J. L. Wooden, T. W. Offield, R. P. Koeppen, T. L. Klein, and A. P. Nutman, 1996, Evidence for Mesoproterozoic basement in the Carolina terrane and speculations on its origin: *in*, Nance, R. D., and M. D. Thompson, eds., Avalonion and related peri-Gondwanan terranes of the circum-North Atlantic: Geological Society of America Special Paper 304, p.207-217.

Muller, R. D., and W. R. Roest, 1992, Fracture zones in the North Atlantic from combined Geosat and Seasat data: Jour. of Geophysical Research, v.97, p.3337-3350.

Muller, R. D., W. R. Roest, and J. –Y. Royer, 1998, Asymmetric sea-floor spreading caused by ridge-plume interactions: Nature, v.396, p.455-459.

Muller, R. D., J. –Y. Royer, S. C. Cande, W. R. Roest, and S. Maschenkov, 1999, New constraints on the Late Cretaceous / Tertiary plate tectonic evolution of the Caribbean: in, Mann, P. (Hsu, K. J., series editor), Caribbean basins. Sedimentary Basins of the World, v.4: Amsterdam, Elsevier Science B.V., p.33-59.

Murphy, J. B., J. Fernandez-Suarez, J. D. Keppie, T. E. and Jeffries, 2004, Contiguous rather than discrete Paleozoic histories for the Avalon and Meguma terranes based on detrital zircon data: Geology, v.32, n. 7, p.585-588.

Pindell, J. L., and J. F. Dewey, 1982, Permo-Triassic reconstruction of western Pangea and the evolution of the Gulf of Mexico / Caribbean region: Tectonics, v.1, p.179-211.

Roeser, H. A., C. Steiner, B. Schreckenberger, and M. Block, 2002, Structural development of the Jurassic Magnetic Quiet Zone off Morocco and identification of Middle Jurassic magnetic lineations: Jour. of Geophysical Research, v.107, p.2207, doi:10.1029/2000JB000094.

Sager, W. W., C. J. Weiss, M. A. Tivey, and H. P. Johnson, 1998, Geomagnetic polarity reversal model of deep-tow profiles from the Pacific Jurassic Quiet Zone: Jour. of Geophysical Research, v.103, p.5269-5286.

Sandwell, D. T., and W. H. F. Smith, 1997, Marine gravity anomaly from Geosat and ERS 1 satellite altimetry: Jour. of Geophysical Research, v.102, p.10039-10054.

Stillman, C. J., 1988, Ordovician to Silurian volcanism in the Appalachian – Caledonian orogen: *in*, Harris, A. L., and D. J. Fettes, eds., Geological Society Special Publication 38, p.275-290.

Tanner, J. G., C. L. V. Aiken, P. Dehlinger, W. T. Dewhurst, M. de la Fuente, V. M. Godley, R. H. Godson, W. F. Hanna, T. G. Hildebrand, M. D. Kleinkopf, G. A. McCalpin, R. K. McConnell, H. D. Meyers, N. W. O'Hara, A. Palmer, D. M. Scheibe, R. E. Sweeney, and L. Thorning, 1988, Gravity anomaly map of North America, The Leading Edge, v.7, n.11, p.15-18.

Verheof, J., W. R. Roest, R. Macnab, and J. Arkani-Hamed, and Members of the Project Team, 1996, Magnetic anomalies of the Arctic and North Atlantic Oceans and adjacent Land areas: Dartmouth, Geological Survey of Canada (Atlantic), scales 1:10,000,000 and 1:6,000,000, 2 sheets.

Vogt, P. R., C. N. Anderson, and D. R. Bracey, 1971, Mesozoic magnetic anomalies, sea-floor spreading, and geomagnetic reversals in the southwestern North Atlantic: Jour. of Geophysical Research, v.76, p.4796-4823.

Withjack, M. O., R. W. Schlische, and P. E. Olsen, 1998, Diachronous rifting, drifting, and inversion on the passive margin of central eastern North America: An analog for other passive margins: American Association of Petroleum Geologists Bull., v.82, p.817-835.

**BACK**

# Variations in Crustal Thickness and Extensional Style along the Scotian Margin, Atlantic Canada: Constraints from Seismic Data and 3D Gravity Inversion

**Sonya A. Dehler**
Geological Survey of Canada
Natural Resources Canada
Dartmouth, NS, B2Y 4A2
Canada
e-mail: sdehler@nrcan.gc.ca

**J. Kim Welford**
Memorial University of Newfoundland
Department of Earth Sciences
St. John's, NL, A1B 3X5
Canada
Email: kwelford@mun.ca

## ABSTRACT

Rifted margins form during lithospheric extension and break up associated with the opening of ocean basins. Extension is accommodated by a combination of ductile stretching and brittle faulting, and is accompanied by synrift sedimentation, enhanced heat flow, and often basaltic magmatism. After break up, the margin enters a post-rift stage of cooling, and post-rift sediments are deposited in broad basins as the margin subsides. The interplay of various controlling factors, namely heat flow, lithospheric strength, and pre-existing structural weaknesses, can produce a variety of margin geometries, faulting styles and basin shapes. Nowhere is this more evident than along the Canadian east coast.

The opening of the North Atlantic Ocean produced a wide range of rifted margin geometries, with broad differences in subsidence patterns, basement faulting styles, margin geometry, and volcanism. The continental margin off Nova Scotia marks the interpreted transition from a volcanic-style margin in the southwest, as observed along the US Atlantic margin, to a non-volcanic style that extends to the east and north as far as Labrador. Other characteristics, such as the depth and width of the overlying sedimentary basin, also vary dramatically along the length of the margin.

The understanding of margin evolution has been aided by the recognition of basic relationships between deep lithospheric structure and sediment fill. By combining observations and models of lithospheric extension with the regional coverage of sediment thickness information and geophysical observations, it has become possible to make quantitative predictions of subsidence rates, paleo-heat flow, and thermal maturity. These regional maps are constrained by measurements in well-studied areas, and can serve as predictive tools in unexplored areas.

## Crustal Thinning

The first step is to establish the present day geometry of the thinned continental crust along the margin. Multichannel seismic data, collected during and prior to the late 1980s, have provided images of the crust and overlying sedimentary basin along several cross-sectional profiles across the Scotian margin. Wide-angle reflection/ refraction data, collected in 2001, provided information on crustal geometry and velocities across the southern, central and northeastern parts of the margin. The velocity models highlight both the different responses of these sections of the margin to extension, as well as the variability in the

transition zone separating thinned continental crust from characteristic oceanic crust (Fig. 1). There are dramatic differences in the width of the extended zone of continental crust, the width and depth of the overlying sedimentary basin, and position of the present day shelf break with respect to the edge of unstretched crust.

Several lines of multichannel seismic data collected by GX Technology in 2003 have also imaged the Moho reflector at the base of the continental crust. We have interpreted these depth-migrated strike line data to obtain constraints on crustal thickness along the length of the margin, joining the other profile lines.

Gravity data, which cover the entire margin and adjacent continental and oceanic regions, provide a means of extending these interpretations across the Scotian margin (Fig. 2). The gravity data respond to density anomalies associated with variable sediment fill and crustal geometry, as well as compositional changes in the various layers. The constraints provided by the seismic data sets and interpretations, together with regional data compilations of water depth and sediment thickness, have supported a 3D inversion approach to examine the regional crustal thickness and links to variations in extensional style along the margin.

## Gravity Inversion

We have used the GRAV3D inversion algorithm developed by Li and Oldenburg (1996; 1998) to invert gravity observations at the Earth's surface and obtain a sub-surface 3D density anomaly distribution, relative to a background density of 2670 kg/m$^3$, below the observation locations. Our model mesh onto which the 3D density anomaly distribution is modelled consists of flattened cubes with lateral dimensions of 15 km by 15 km and which are 500 m deep. The mesh contains 52 cells in the easting direction, 52 cells in the northing direction and 50 cells in depth.

For our inversion, we opted for GRAV3D to generate a 3D density anomaly model that was smooth over length scales of 150 km in the easting and northing directions and smooth over a length scale of 6 km in depth. In terms of fitting the data, given the coarseness of the mesh and the dense data coverage, we opted for a misfit value of five times the number of data points.

## Model Development

Bathymetric data for the margin were obtained from the Geological Survey of Canada (GSC) and were incorporated into the reference density anomaly model by forcing all model prisms above the bathymetric depths to contain density anomalies corresponding to ocean water. These anomalies were kept fixed during the inversion.

Depth-to-basement constraints for the margin were obtained from a GSC compilation based on several decades of interpretation of single and multichannel seismic data. This information was incorporated into the reference density anomaly model by assigning density anomalies consistent with sedimentary rocks to the prisms lying between the seabed and the basement. These anomalies were allowed to vary within a prescribed range during the inversion and this range was chosen to force the prisms to contain reasonable densities for sedimentary rocks whilst allowing the inversion to stratify (as needed) the densities within the sedimentary column and within individual basins.

Once the ocean water and sedimentary portions of the reference density anomaly model were assigned, all remaining mesh prisms were assigned a density anomaly corresponding to the background density. During the inversion, the density anomaly in each of these prisms was allowed to vary within a broader range. Thus, below the base of sediments, the inversion was given great flexibility in assigning density anomalies to reproduce the observed gravity response and no constraints were placed on which prisms should correspond to crustal rocks and which prisms should correspond to upper mantle rocks. In effect, this allowed the inversion to determine the crustal and sub-crustal geometries from the gravity data and initial constraints.

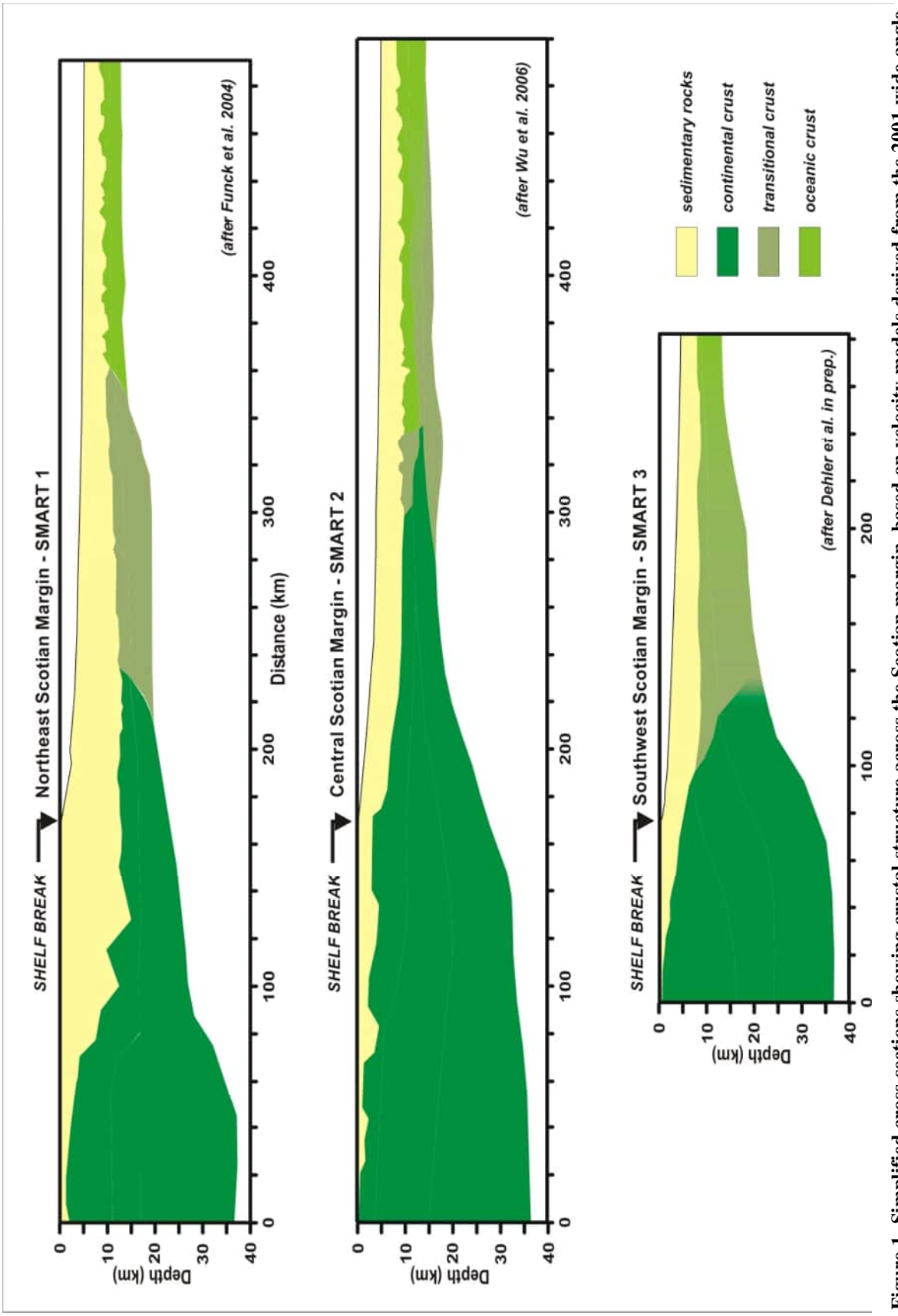


**Figure 1. Simplified cross-sections showing crustal structure across the Scotian margin, based on velocity models derived from the 2001 wide-angle reflection/ refraction survey (SMART). Locations of seismic lines shown in Figure 2.**

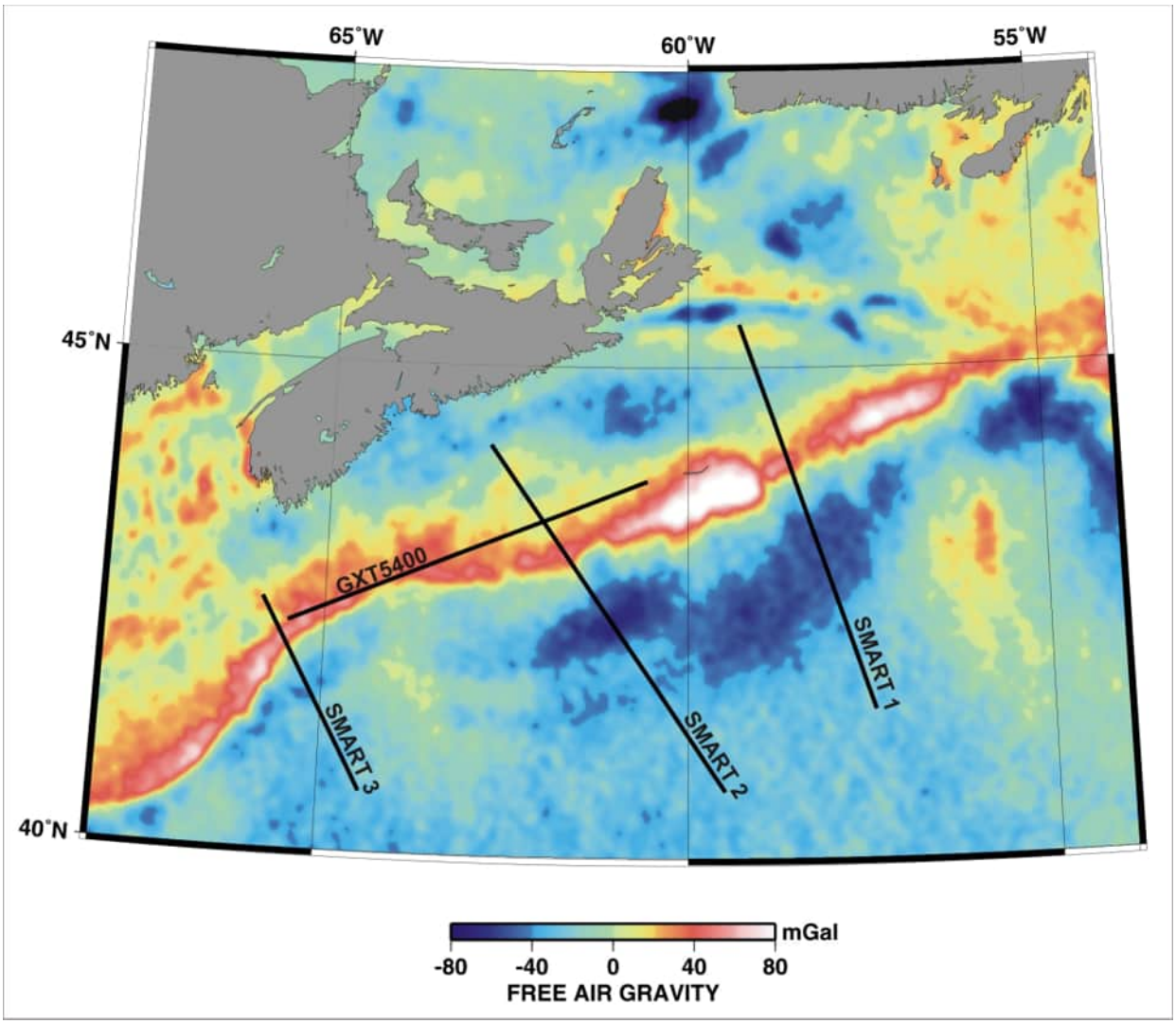


**Figure 2. Map showing free-air gravity anomalies for the study area, based on data from the Geological Survey of Canada. The locations of several key seismic lines are shown.**

## Preliminary Results

Figure 3 shows preliminary inversion results for the main seismic profile lines. While it will take many iterations to satisfy all constraints, the preliminary models already include many of the characteristic features of the margin, such as the variable width of necking, or zone of extensional thinning, of the continental crust. In addition, the variability in thickness of the oceanic crust is also evident, matching the trend toward thinner crust to the northeast as seen in the velocity models.

The final model is one that will satisfy all constraints and produce an acceptable match to the observations of crustal thickness. This 3D model will then provide the basis for additional studies examining the subsidence history and thermal evolution of the margin.

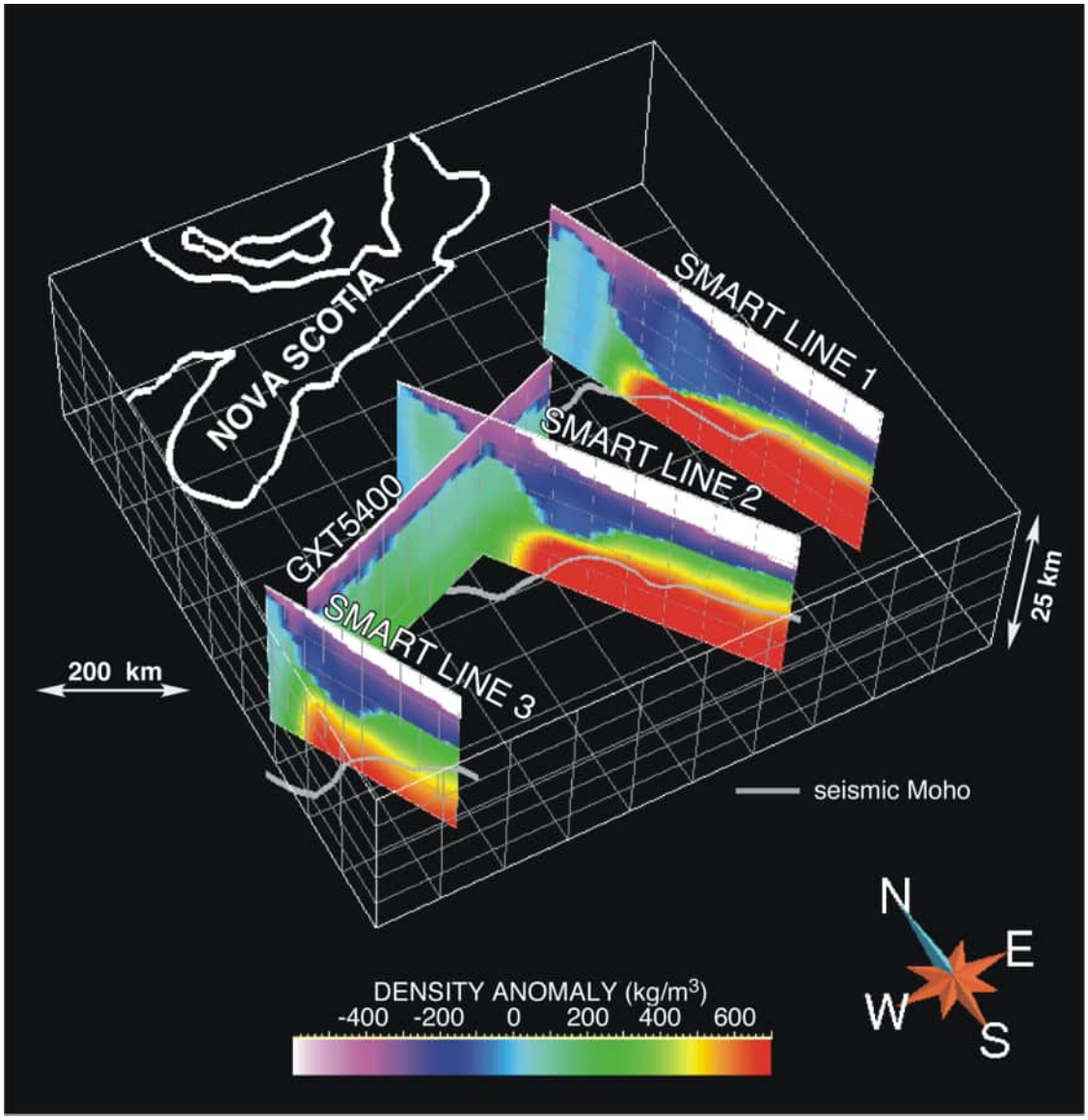


**Figure 3. Preliminary gravity inversion results, shown as density anomalies relative to 2670 kg/m$^3$, along the key seismic lines.**

## References


Funck, T., H.R. Jackson, K. Louden, S.A. Dehler and Y. Wu, 2004, Crustal structure of the northern Nova Scotia rifted continental margin (Eastern Canada): Journal of Geophysical Research, v.109, B09102 (doi:10.1029/2004JB003008).

Li, Y. and D.W. Oldenburg, 1996, 3D inversion of magnetic data: Geophysics, v.61, n.2, p.394–408.

Li, Y. and D.W. Oldenburg, 1998, 3D inversion of gravity data: Geophysics, v.63, p.109–119.

Wu, Y., K.E. Louden, T. Funck, H.R. Jackson and S.A. Dehler, 2006, Crustal structure of the central Nova Scotia margin off Eastern Canada: Geophysical Journal International, v.166, p.878-906 (doi:10.1111/j.1365-246X.2006.02991.x).


**BACK**

# New Profile Models over the U.S. East Coast Continental Margin

**Mark Odegard**
Grizzly Geosciences, Inc.
14019 SW Freeway, Suite 301-735
Sugar Land, TX, 77478
United States
e-mail: meo@grizgeo.com

**Paul J. Post**
U.S. Department of the Interior
1201 Elmwood Park Blvd.
New Orleans, LA, 70123
United States

**William Dickson**
Dickson International Geosciences (DIGs)
10260 Westheimer Rd, Suite 320
Houston, TX, 77042-3160
United States

## ABSTRACT

Profile-based models are excellent for incorporating multiple data sets to illustrate basin architecture. New models across the U.S. East Coast Continental Margin incorporate reprocessed seismic lines, depth-stretched with projected well data, stacking functions and published refraction velocities. Four dip profiles (ranging from 220-480 km each) were tied to a composite (~2,300 km) strike profile; then extended landward and seaward to model long-wavelength crustal variations (from unthinned continental to fully oceanic regimes) defined by our latest gravity and magnetic data.

The seismic interpretation constrains shallower horizons while deep crustal structure derives largely from potential field and published refraction data. Intermediate levels, especially acoustic basement, are revealed as other layers are defined. Models frequently constrain the nature and volume of intrusives such as the lamprophyre dike swarm cored Great Stone Dome (Schlee Dome), and allochthonous salt diapirs, as targeted in the profile model. The feature extents were then interpreted areally, away from seismic coverage, based on gravity and magnetic imagery.

Comparing our profiles with published interpreted and modeled seismic lines; *i.e.*, DNAG volumes, the authors note significant differences. Previously interpreted "salt structures" in the Georges Bank Basin (GBB) do not exist. Salt structures in the Baltimore Canyon Trough (BCT) appear limited to a small, seismically defined diapir and the salt penetrated in the Hudson Canyon 676-1 well on the flank of Schlee Dome. We validated salt structures in the Carolina Trough (CT), although the CT appears to be more complex and separate from the Blake Plateau Basin and BCT. Sediment thickness maxima in the GBB were confirmed on one model and matched to gravity data that improves the definition of previously indicated sub-basins with some exploration potential. Ongoing work is extending the interpretation of the models across the entire margin and will no doubt reveal further interpretation changes.

BACK

# Systematic Variations in Basement Morphology and Rifting Geometry along the Nova Scotia and Morocco Conjugate Margins

**Yue Wu**
Department of Earth Sciences
Dalhousie University
Halifax, Nova Scotia B3H 4J1
Canada
e-mail: wuyue@phys.ocean.dal.ca

**Keith Louden**
Department of Oceanography
Dalhousie University
Halifax, Nova Scotia B3H 4J1
Canada
e-mail: Keith.Louden@Dal.Ca

**Gabor Tari**
OMV Exploration and Production
Gerasdorfer Strasse 151
Vienna 1210
Austria
e-mail: Gabor.Tari@omv.com

## ABSTRACT

The Nova Scotia and Morocco margins formed within a complex transition region between volcanic-style margins to the south and non-volcanic margins to the north. We present new results including recent deep seismic profiles that help document the nature of this transition. Seismic profiles along and across the Nova Scotia margin show two abrupt transitions from south to north. The first transition represents a sharp reduction in syn-rift volcanism at ~64$^{o}$W, coincident with major changes in the East Coast Magnetic Anomaly (ECMA) and with the southern limit of the Slope Diapiric Province. The second transition at ~ 60$^{o}$W represents a further restriction in syn- and post-rift volcanism that leads to exposure of serpentinized mantle basement or creation of highly tectonized ultra-slow spreading oceanic crust. This transition is represented by a major change in basement morphology marked by an oblique zone of highly extended and faulted continental crustal blocks. It is also coincident with a transition in salt deformation from autochthonous diapiric structures to allochthonous canopies.

Revised plate reconstructions of maximum and minimum closure (*i.e.* before rifting and at final separation), constrained by a set of combined seismic profiles, show similar transitions along the Moroccan margin. The southern transition occurs at a major change in the West Africa Coast Magnetic Anomaly (WACMA) and the southern limit of the Morocco Salt Basin. Thus the two margins are basically non-volcanic except at their southern extremes. The second transition occurs at a major oblique basement structural high (Tafelney Plateau), which has been considered as a high relief accommodation zone (HRAZ), and contains highly extended faulted crustal blocks similar to those in conjugate position off central Nova Scotia. This transition marks a major change in rifting asymmetry and separates the margins into two fundamentally distinct segments.

## Introduction

The Nova Scotia margin was formed within the Appalachian Orogen by the separation of Africa from North America during the Mesozoic breakup of Pangaea (Jansa and Wade 1975; Wade and Maclean 1990). Rifting of the Nova Scotia margin began in the Middle Triassic to Early Jurassic (230-175 Ma) (Welsink *et al.* 1989), followed by Jurassic seafloor spreading (Klitgord and Schouten 1986). Across the southern and central Nova Scotia margin (Fig. 1), the Lahave Platform occupies the outer shelf and continental slope area, with the Shelburne Basin located on the continental slope. In contrast, across the northern margin segment, the Sable Basin with a thick wedge of both syn- and post-rift sediments is situated beneath the outer shelf. The oldest syn-rift deposits in the Sable Basin are nonmarine Triassic redbeds, which are generally found between fault blocks (Wade and MacLean 1990). These are overlain by shallow marine sediments of Late Triassic-Early Jurassic age, including the extensive salt diapirs in the Slope Diapiric Province (Fig. 1). The continent-ocean boundary is generally located seaward of the salt front (Funck *et al.* 2004; and Wu *et al.* 2006), except possibly for the northern Nova Scotia margin where the salt front moved seaward to form a series of salt tongues and canopies (Shimeld 2004).

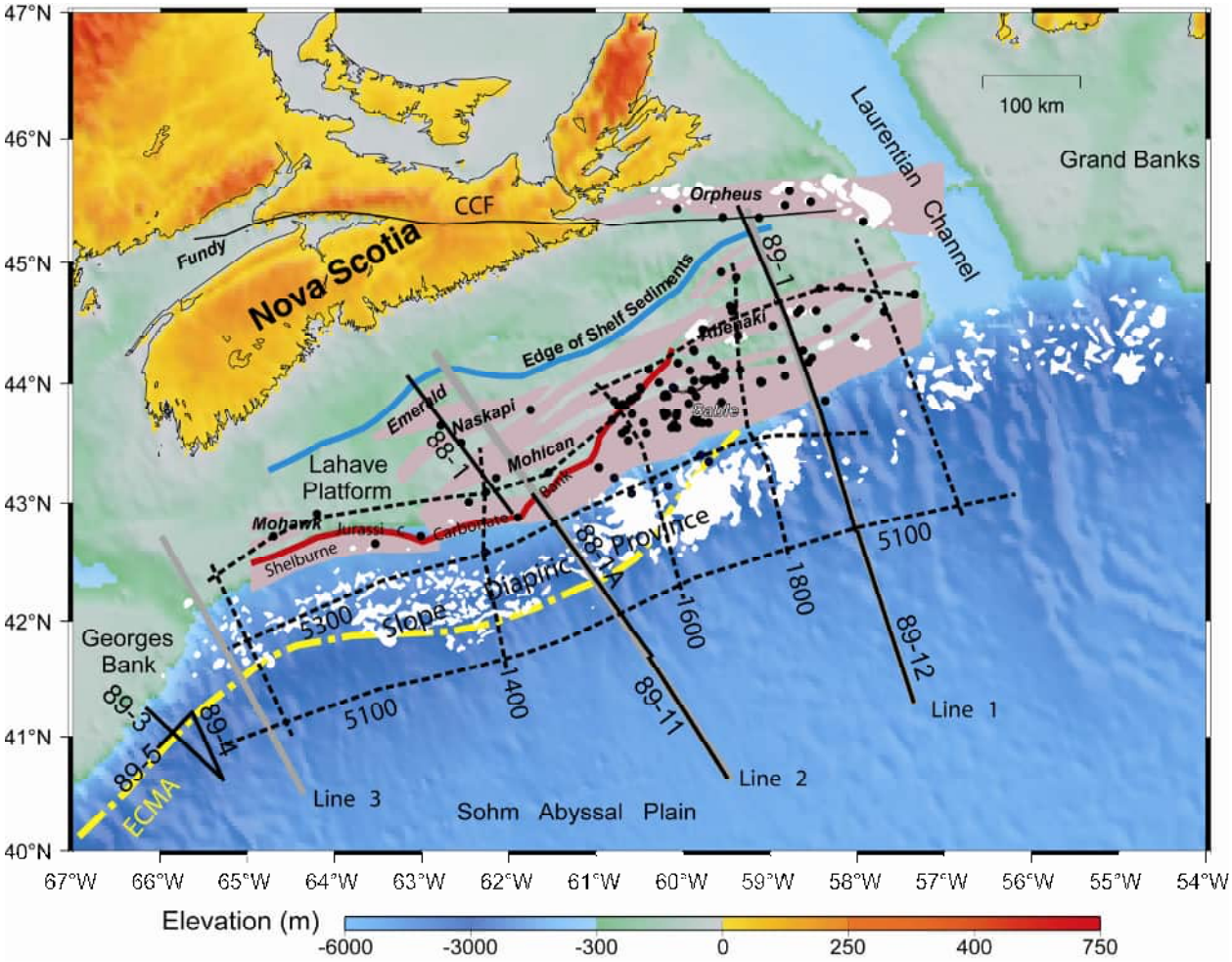


**Figure 1. Location map of seismic profiles and sediment structures across the Nova Scotian margin. Seismic profiles include GXT NovaSPAN MCS profiles (broken lines), Lithoprobe and BGR MCS profiles (solid black) and SMART wide angle profiles (solid gray). Sediment structures include shallow-water basins (solid pink fill) and boundaries of shelf sediment and Jurassic carbonate bank (blue and red lines) from Enachescu and Hogg (2005), and major salt bodies (white fill) from Shimeld (2004). Also shown are locations of the Cobequid Chedabucto fault (CCF, thin black line), East Coast Magnetic Anomaly (ECMA, yellow dashed line), exploration wells (filled circles), and shaded seafloor topography (colour scale).**

The Nova Scotia margin is located at the transition from volcanic margins to the south to non-volcanic margins to the north (Fig. 1). At its southern limit near Georges Bank, a strong, linear magnetic anomaly, referred to as the East Coast Magnetic Anomaly (ECMA), is well developed. The ECMA progressively weakens northward and eventually disappears within the northern margin offshore Sable Island. The northern margin has been classified as a non-volcanic rifted margin without SDR sequences on line 89-1 (Funck *et al.* 2004, Keen and Potter 1995b). However, in the central segment of the Nova Scotia margin, the magnetic anomaly is still pronounced, but there is no evidence for a SDR sequence on line 88-1A (Wu *et al.* 2006; and Keen *et al.* 1991) unless it is obscured by salt. The concurrence of magnetic and seismic signatures leads to an ambiguous character for the central margin segment. The purpose of this work is to further examine crustal-scale variations along the Nova Scotian margin related to the transition between volcanic to non-volcanic rifting, and to compare them with structures offshore Morocco that were formed during rifting and separation of the two margin conjugates.

## Crustal Transitions along the Nova Scotian Margin

The structural variation along the strike of the Scotian margin is shown in Figure 2 (NB: Large size 11x17 inch figure. See end of paper), using recent regional NovaSPAN MCS profiles collected by GX Technology. At the southwestern end of the strike line NovaSPAN 5100 (Fig. 2c), dipping reflections are imaged in the basement. The seismic expression of these reflections is characterized on dip sections 89-3 and 89-4 as seaward dipping reflectors (Keen and Potter 1995a), which are also observed along the dip profile NovaSPAN 1100 (SDR, Fig. 2a). These SDR are thought to be seismic expressions of extrusive rocks of rift volcanism across the SW Scotian margin (Keen and Potter 1995a). Northeast of profile NovaSPAN 1100, SDR sequences are no longer observed (*e.g.* NovaSPAN 1400 (Fig. 2b) and 88-1A (Wu 2007)). A ~100-km-wide zone (VNT, Fig. 2c), featured by rugged basement topography, with greater depths than the basement on either side, occurs at the disappearance of the SDR sequences and ends at a major basement high (BH, Fig. 2c). This zone seems to be highly faulted or compressed, illustrated by the V-shape basement topography, and marks a transition where the SDR sequences occur to the southwest but no longer appear to the northeast. This transition is coincident with a major change in the character of the East Coast Magnetic Anomaly (ECMA) and with the southern limit of the Slope Diapiric Province. We suggest that it represents a sharp reduction in syn-rift volcanism.

Further northeast, faulted basement blocks (FBs) are imaged on NovaSPAN 5100 between shot points (SP) 10000-11500. These FBs are spatially coincident with those which appear on lines 88-1A and NovaSPAN 1600 (Fig. 1), forming a zone of FBs at the continental breakup front between the central and northern segments of the margin. From this FB zone to almost the northeast end of profile 5100, the crust is characterized by an irregular reflector (W), which starts from the base of the FBs and extends ~250 km towards northeast until it reach the top of the basement around SP 16000, where a 30-km-wide band of NE dipping reflections appear in the basement (F). Similar events are also imaged at the seaward end of the dip profile NovaSPAN 1800 and LITHOPROBE 89-1 (Funck *et al.* 2004; Keen and Potter 1995b) and on BGR 89-12 (unpublished). We propose that this second transition represents a further restriction in syn- and post-rift volcanism that leads to exposure of serpentinized mantle basement or creation of highly tectonized ultra-slow spreading oceanic crust. This transition is also coincident with a transition in salt deformation from autochthonous diapiric structures to allochthonous canopies.

## Nova Scotia – Morocco Margin Conjugates

The general structures derived from seismic profiles are summarized in the map of minimum reconstruction of the Nova Scotia and Morocco margin conjugates (Fig. 3; Wu 2007). The VNT transition, which separates the volcanic SW Scotian margin from the non-volcanic northeast margin and marks the SW termination of the Slope Salt Diapiric Province, also marks the SW termination of the Moroccan salt basin. Therefore, the majority of the Scotian/Moroccan conjugate margins, except for the southwestern most part, were rifted by non-volcanic extension. Between the central (Line 2) and northern

conjugate segments (Line 1), the zone of fault blocks (FB) appears near the continental break-up front (CBF). Across the central segment, these FBs are symmetric, with their seaward limits consistent with the CBF on both sides. Northeast of Line 2, FBs still appear on both sides of the conjugate profiles until they disappear north of the Tafelney Plateau or south of the Sable basin in the proposed minimum closure. The elongated FB zone extends obliquely against the general strike of the conjugates such that the continental breakup front also deviates from the CBF toward the Scotian side, leaving an irregular breakup boundary in this region (dotted blue line CBF-2, Fig. 3). We suggest that the irregular breakup boundary in this region is related to different rifting styles along the margin pair.

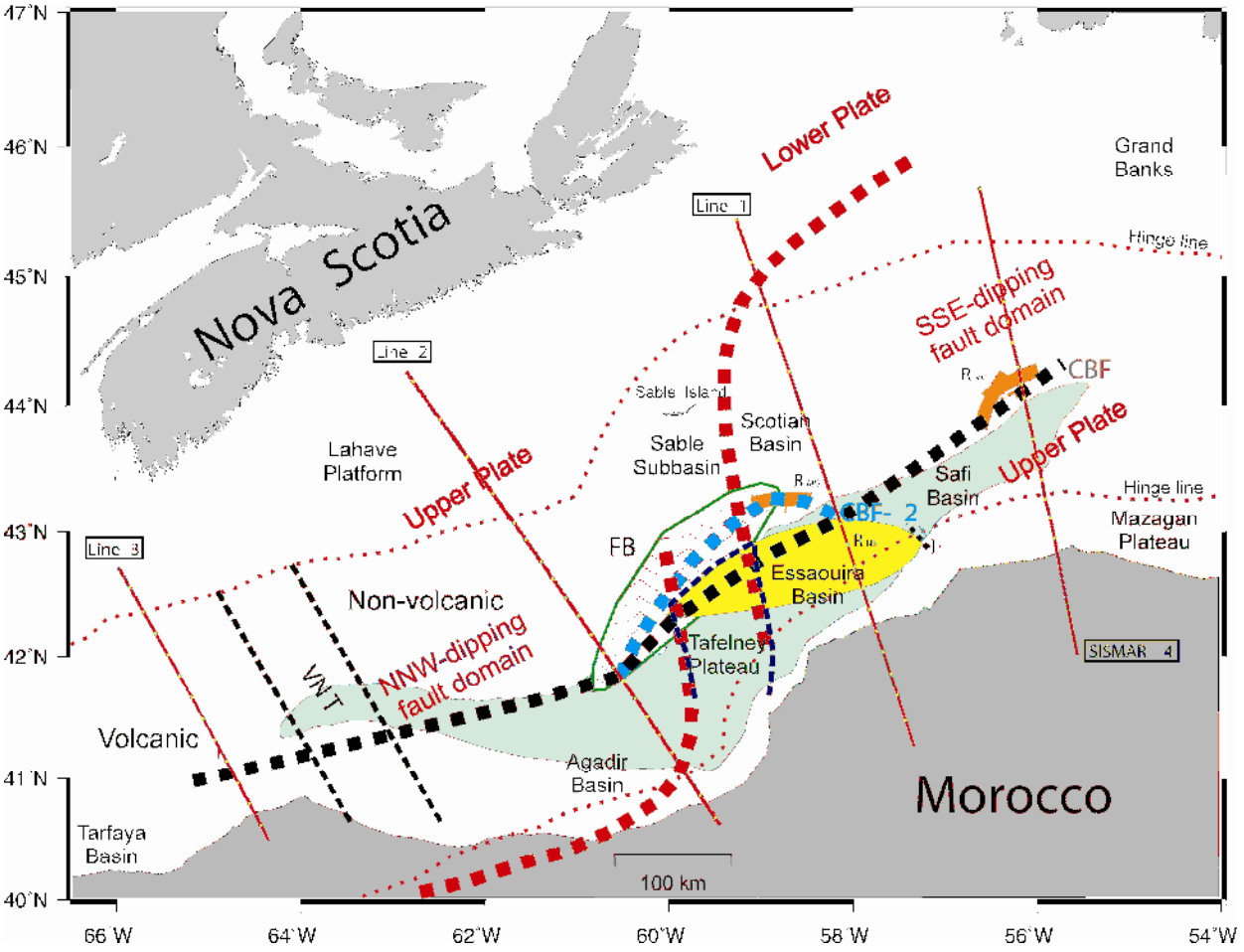


**Figure 3. Major structural features across the Scotian/Moroccan conjugates at the time of breakup. The black and light-blue dotted lines represent the continental breakup front based on plate reconstructions (CBF) and seismic profiles (CBF2), respectively. Light green area delineates the Moroccan salt province and the region of fault blocks (FB) off Nova Scotia are defined by green boundary with wavy fill. The yellow area indicates the distribution of base crustal reflections (W) off Nova Scotia ($R_{NS}$) and the orange bars denote the locations of crustal reflection observed off Morocco ($R_{MO}$), as derived from MCS profiles. The thin red dotted lines indicate the hinge lines and the thick red dashed lines and red labeled features indicate the conceptual plate separation geometries of Tari and Molnar (2005). The two black dashed lines indicate the volcanic to non-volcanic transition (VNT) along the conjugate margins. The boundary of the Tafelney Plateau is marked by a dark-blue dashed line. Bold red dashed lines show conjugate locations of main refraction profiles.**

The northeast margin pair is characterized by intra-basement reflections on both sides. For the Nova Scotia margin, the strong reflections (W) are consistently imaged on the dip profiles of LITHOPROBE 89-1 and NovaSPAN 1800 and the strike profile NovaSPAN 5100 at depths of 11-15 km,

indicating one major crustal reflector (yellow patch, $R_{NS}$). The southwest limit of the reflector is delimited by the FBs and the east boundary delimited by a band of NE dipping events F. However, it is not clear whether these reflections extend further landward or seaward. The landward limit may have been obscured by overlying salt or salt related structures. More seismic data are also required further seaward in order to delineate the seaward limit of this major reflector. On the Morocco side, a crustal reflection ($R_{MO}$) is locally imaged beneath a faulted basement. Toward the NE end of the Moroccan margin, a similar intra-basement reflection is also imaged near SISMAR-4 (Contrucci *et al.* 2004). From existing profiles, however, it is uncertain if these features are continuous or represent separate structures.

Figure 3 also shows the conceptual model for breakup of the Scotian and Moroccan conjugates proposed by Tari and Molnar (2005) and Maillard *et al.* (2006). According to this model, the SW and NE segments of the Scotian/Moroccan conjugates break up in opposite asymmetries, leaving the upper plate on the Morocco side and a lower plate to the Scotian side for the NE segment and the opposite configuration for breakup of the SW segment. This model is characterized by asymmetrical rifting along a low-angle detachment within the Moroccan plate. As rifting began during middle Triassic, the central Nova Scotia margin experienced thermal uplift and erosion. This is constrained by previous depth-dependent geodynamic models across the Lahave Platform, which indicated that lithospheric thinning extended about 100 km further landward of the crustal thinning (Keen and Beaumont 1990; Wu *et al.* 2006). There is no such evidence indicative of uplift and erosion off Morocco at syn-rift age (Broughton and Trepaniér 1993). Therefore, the central segment of the conjugate margins may have started to form by asymmetrical rifting across the conjugate segments, separate by a transfer zone (bold dashed lines, Fig. 3), marked by the Tafelney Plateau on the Moroccan side and the crustal fault blocks (FB) on the Nova Scotian side.

## Summary

Revised plate reconstructions of minimum closure (*i.e.* at final separation), constrained by a set of combined seismic profiles, show similar transitions along both the Nova Scotian and Moroccan margins. The southern transition (VNT) off Nova Scotia occurs at a major change in the West Africa Coast Magnetic Anomaly and the southern limit of the Morocco Salt Basin. Thus the two margins are basically non-volcanic except at their southern extremes. The second transition occurs at a major oblique basement structural high (Tafelney Plateau), which has been considered as a high relief accommodation zone, and contains highly extended faulted crustal blocks similar to those in conjugate position off central Nova Scotia. This transition marks a major change in rifting asymmetry and separates the margins into two fundamentally distinct segments.

## References


Broughton, P., and Trepaniér, A., 1993. Hydrocarbon Generation in the Essaouira Basin of Western Morocco. AAPG Bull.., v.77, n.6, p.999 -1015.

Contrucci I., F. Klingelhofer, J. Perrot, R. Bartolome, M.A. Gutscher, M. Sahabi, J. Malod and Rehault, J. P., 2004. The crustal structure of the NW Moroccan continental margin from wide-angle and reflection seismic data, Geophys. J. Int., 159, n.1, p.117-128.

Enachescu, M.E. and Hogg, J.R.., 2005. Exploring for Atlantic Canada's next giant petroleum discovery. CSEG Recorder, v.30, n.5, p.19-30.

Funck, T., Jackson, H.R., Louden, K.E., Dehler, S.A. and Wu, Y., 2004. Crustal structure of the northern Nova Scotia rifted continental margin (Eastern Canada), J. Geophys. Res., 109, B09102

Jansa, L.F. and Wade, J.A., 1975, Geology of the continental margin off Nova Scotia and Newfoundland: in Offshore Geology of Eastern Canada, Vol. 2, Regional Geology, Van der Linden, W.J.M. and Wade, J.A. (Eds.), Geol. Sur. Can., Paper 74-30, p.51-106.

Keen, C.E. and Beaumont, C., 1990. Geodynamics of rifted continental margins, in Geology of the Continental Margin of Eastern Canada, Edited by Keen, M. J. and Williams, G.L., Geological Survey of Canada, Geology of Canada, No. 2, p.393-472.

Keen, C.E., MacLean, B.C. and Kay, W.A., 1991. A deep seismic reflection profile across the Nova Scotia continental margin, offshore eastern Canada, Can. J. Earth Sci., v.28, p.1112-1120.

Keen, C.E. and Potter, P., 1995a. The transition from a volcanic to non-volcanic rifted margin off eastern Canada, Tectonics, v.14, p.359-371.

Keen, C.E. and Potter, P., 1995b. Formation and evolution of the Nova Scotian rifted margin: Evidence from deep seismic reflection data, Tectonics, v.14, p.918-932.

Klitgord, K. D. and Schouten, H., 1986. Plate kinematics of the central Atlantic, in The Geology of North America, Volume M, The Western North Atlantic Region, edited by Vogt P.R. and Tucholke, B.E., p.351-378, Geological Society of America, Boulder, Colo.

Maillard A., J. Malod, E. Thiébot, F. Klingelhoefer and Réhault, J.-P., 2006. Imaging a lithospheric detachment at the continent–ocean crustal transition off Morocco, Earth Planet. Sci. Lett., 241, p.686-698.

Shimeld, J., 2004. A comparison of salt tectonic subprovinces beneath the Scotian Slope and Laurentian Fan, in: Post, P.J. et al. (Eds.), Salt-sediment interactions and hydrocarbon prospectivity: Concepts, applications and case studies for the 21st century, Proc. 24th Bob Perkins Conf., Gulf Coast Section SEPM, p.291-306, CD-ROM, ISSN 1544-2462.

Tari, G., and Molnar, J., 2005. Correlation of syn-rift structural between Morocco and Nova Scotia, Canada, 25th Annual GCSSEPM Foundation Bob F. Perkins Research Conference, Petroleum Systems of Divergent Continental Margin Basins, Houston, Texas.

Wade, J.A. and McLean, B.C., 1990. The geology of the southeastern margin of Canada: in Keen, M.J. and Williams, G.L. (Eds.), Geology of the Continental Margin of Eastern Canada, The Geology of North America, Vol. I-1, Geol. Sur. Can.,p. 169-238.

Welsink, H.J., Dwyer, J.D., Knight, R.J., 1989. Tectono-stratigraphy of the passive margin off Nova Scotia: Extensional Tectonics and Stratigraphy of the North Atlantic Margin, Tankard, A.J. and Balkwill, H.R. (Eds.), Am. Assoc. Pet. Geol., Mem. 46, p.215-231.

Wu, Y., 2007. Crustal structure of the central Nova Scotia margin and the transition from volcanic to non-volcanic rifting off eastern Canada, Ph.D. thesis, Dalhousie University, 341p.

Wu, Y., Louden, K.E., Funck, T., Jackson, H.R., and Dehler, S.A., 2006. Crustal structure of the central Nova Scotia margin off Eastern Canada, Geophy. J. Int., 166, p.878-906.

**BACK**

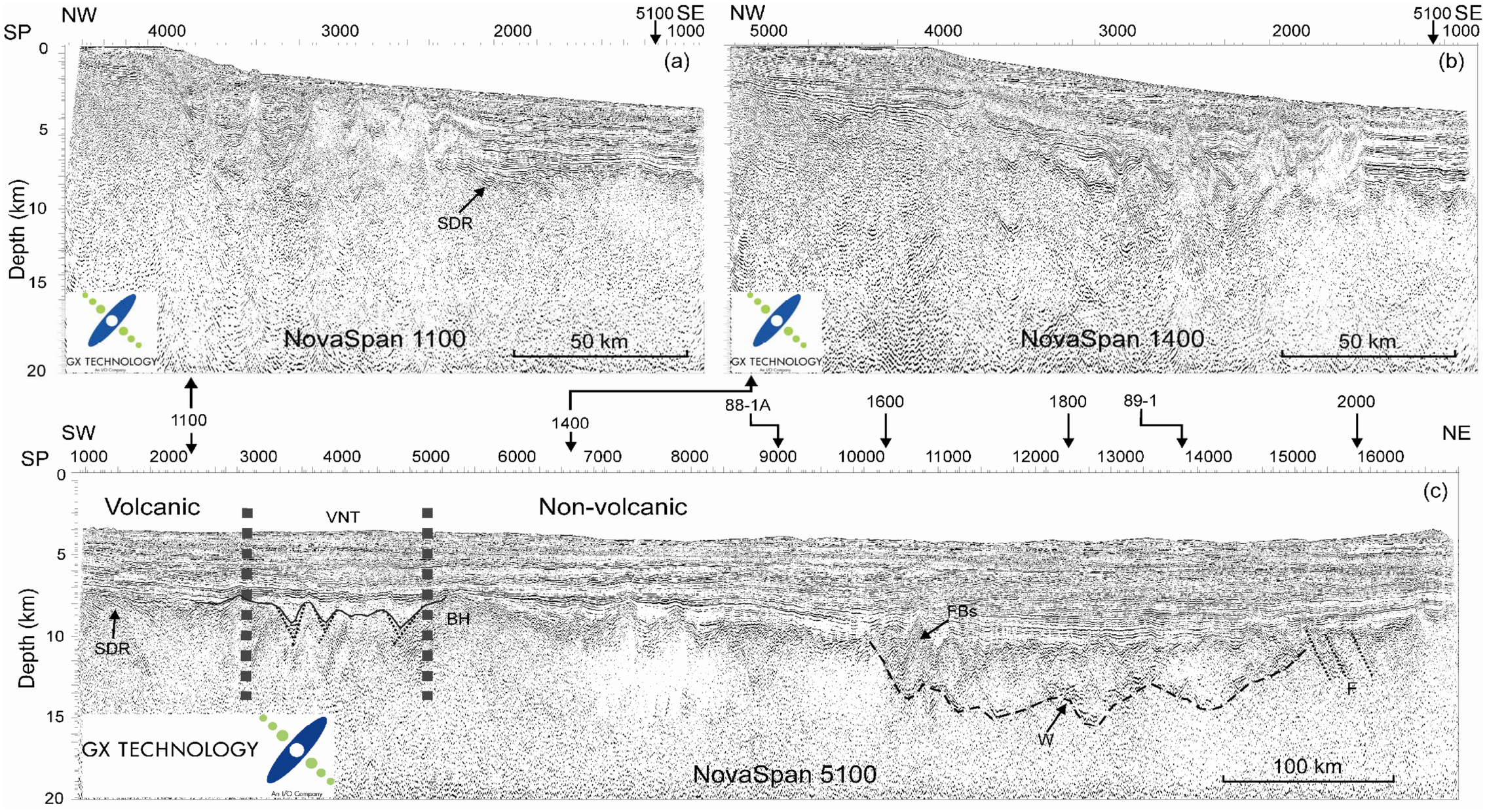


**Figure 2. Depth sections of the strike profile NovaSPAN 5100 and two dip profiles NovaSPAN 1100 and 1400. The crossing points for all dip profiles are marked along the strike line NovaSPAN 5100. The volcanic to non-volcanic transition (VNT) is indicated by a vertical dashed line. BH: basement high; SDR: seaward dipping reflectors; FBs: fault blocks; W: crustal reflector; F: faults**

# The Post-Rift Evolution of the Atlantic Margin of Northwest Africa: a not-so-Quiet Period of Exhumation and Erosion

**Giovanni Bertotti**
**Paul Andriessen**
**Ibrahim Barrie**
**Frank Beunk**
**Badr Ghorbal**
**Jan Wijbrans**
VU University -Amsterdam
De Boelelaan 1085
Amsterdam, 1081HV
Netherlands
e-mail: Giovanni.bertotti@falw.vu.nl

## ABSTRACT

The post-rift stage of passive continental margins is generally characterized by gentle subsidence decreasing through time. Until now, this is also thought for the Atlantic margin of NW Africa and, in particular, the Moroccan and Sierra Leone transects. In the last years, however, absolute ages obtained with a variety of thermochronometers ranging from $^{40}Ar/^{39}Ar$ to Apatite Fission Tracks and (U-Th)/He on apatites have documented fully unexpected vertical movements, incompatible with the simple scheme hitherto accepted. In Morocco, samples from areas considered as stable, such as the Meseta and the Anti Atlas have provided evidence for a stage of Early to Middle Jurassic subsidence followed by exhumation bringing sampled rocks at the Earth's surface before the late Cretaceous. At this time, relief developed during the exhumation must have been eroded away as shown by the flat and fairly regular basis of the Upper Cretaceous shallow water sediments. In Sierra Leone, the Freetown Layered Igneous Complex was emplaced at depths of at least a few kilometers at 210-190Ma and was then exhumed in a poorly constrained time span possibly in the Late Jurassic.

The emerging picture is one where a very large segment of the rifted continental margin elongated parallel to the margin and located several tens of km E of the continent-ocean transition was exhumed during the post-rift evolution. Km-scale exhumation provoked major erosion and production of terrigenous sediments most of which were brought offshore forming the peculiar coarse-grained terrigenous intercalations in the otherwise monotonous succession encountered in the deep offshore.

BACK

# NOTES

# Session 1B:
# MARGIN EVOLUTION & DEVELOPMENT

## KEYNOTE ADDRESS

**THE MESOZOIC ATLANTIC CANADA OFFSHORE MARGIN: HISTORY OF EXPLORATION, PRODUCTION AND FUTURE EXPLORATION POTENTIAL**
**Hogg, John R. and Enachescu, Michael E.**

**LOW-T THERMOCHRONOLOGY PROVIDES NEW INSIGHTS IN THE MESOZOIC TO PRESENT**
Ghorbal, Badr; Bertotti, Giovanni; Foeken, Jurgen; Stuart, Fin and Andriessen, Paul

**GEOTECTONIC SCENARIOS FOR THE EVOLUTION OF THE SOUTH ATLANTIC BRAZILIAN MARGIN: LEFT-LATERAL LOWER CRETACEOUS OBLIQUE RIFTING FOLLOWED BY UPPER CRETACEOUS TO PRESENT ONGOING COMPRESSION**
De Lima, Claudio Coelho; Lopes, Marcos Fetter; Gontijo, Rogerio and Pessoa Neto, Otaviano Da Cruz

**REVISITING CRETACEOUS TECTONISM AND VOLCANISM IN THE LAURENTIAN SUB-BASIN AND ORPHEUS GRABEN, OFFSHORE NOVA SCOTIA**
Bowman, Sarah; Pe-Piper, Georgia and Piper, David J.W.

**$^{40}$AR-$^{39}$AR STUDY OF THE FREETOWN LAYERED IGNEOUS COMPLEX (FLIC), FREETOWN, SIERRA LEONE, WEST AFRICA: IMPLICATIONS FOR THE INITIAL BREAK-UP OF PANGAEA TO FORM THE CENTRAL ATLANTIC OCEAN**
Barrie, Ibrahim Jorgor; Wijbrans, Jan R.; Beunk, Frank F.; Bertotti, Giovanni; Andriessen, Paul A.M.; Strasser-King, Victor E.H. and Fode, Daniel V.A.

**THE INS AND OUTS OF BUTTRESS FOLDS: EXAMPLES FROM THE INVERTED FUNDY RIFT BASIN, NOVA SCOTIA AND NEW BRUNSWICK, CANADA**
Baum, Mark S.; Withjack, Martha Oliver and Schlische, Roy W.

**SECOND-ORDER SEQUENCES AND THEIR APPLICATION FOR EXPLORATION IN THE DEEP-WATER SCOTIAN SLOPE**
Davies, Andrew; Etienne, James L.; Simmons, Mike D.; Davies, Roger B.; Sharland, Peter R.; and Sutcliffe, Owen E.

**BACK**

# NOTES

# The Mesozoic Atlantic Canada Offshore Margin: History of Exploration, Production and Future Exploration Potential

**John R. Hogg**
**Michael E. Enachescu**
MGM Energy Corporation
4100, 350 Seventh Avenue SW
Calgary, Alberta, T2P 3N9
Canada
e-mail: john.hogg@mgmenergy.com

## ABSTRACT

The Mesozoic Basins of the western Atlantic Margin are a result of intermittent rifting and separation of North America from Africa and Europe during the Late Triassic to Early Cretaceous. The extensional tectonics produced elongated, up to 20km deep, basins and subbasins, containing both synrift and syn-drift sedimentary sequences that contain excellent reservoir and source rocks. Numerous structural, stratigraphic and combination traps were formed during the synrift and post-rift stages.

Exploration in Atlantic Canada began in the late 1960's with sporadic successes and considerable exploration failures that have caused several boom and bust cycles. The late 1970's through to the mid-1980's was a time of significant discoveries in 1) Newfoundland's Jeanne d'Arc Basin with giant oilfields Hibernia, Terra Nova, Hebron and White Rose and 2) in the Sable Subbasin, offshore Nova Scotia with gas discoveries at Venture, Thebaud and North Triumph fields. As is typical in most basins, the largest fields were found quite early in the exploration cycle hosted in structural features, easily mapped with seismic data. The following exploration cycle, post 1988, was slowed by a combination of low resources prices and size potential of prospects seen on 2D seismic near the discovered fields.

By the late 1990's, a new round of exploration began in both Newfoundland and Nova Scotia that was focused on unexplored deepwater basins, the Flemish Pass and Orphan Basins off Newfoundland and the Scotian Slope basin. More than 256,105 km of new 2D seismic and 53,318 $km^2$ of 3D seismic surveys combined to give a much better understanding of the basins and detail structure and stratigraphy control. In the deepwater Nova Scotia one discovery was made at Annapolis, with the subsequent delineation well proving unsuccessful. More, recently, the first deep water, deep penetration well in the Orphan Basin was also an economic failure.

Future exploration in the Canadian East Coast Basins will focus around producing fields in Jeanne d'Arc Basin and new field wildcat work in the East Orphan, Laurentian and Hopedale basins, off Newfoundland and Labrador, while Nova Scotia offshore will witness a return to shelf exploration to support the pipelines. In the long-range we believe that the Industry will resume exploration in the Flemish Pass, Carson and Saglek basins of Newfoundland, the Scotian Slope Basin and Jurassic Carbonate Trend and in 2012, if the George's Bank moratorium is lifted, we will see exploration in the Georges Bank Basin adjacent to the US border.

Canada's Atlantic Margin remains an underexplored geological province with high risk and high reward situated in the proximity of world's largest oil and gas market, in a harsh environment that has been conquered in both the Jeanne d'Arc and Scotian basins by on the shelf technologies.

**BACK**

# Low-T Thermochronology Provides New Insights in the Mesozoic to Present

**Badr Ghorbal**
**Giovanni Bertotti**
**Paul Andriessen**
VU University-Isotope Geochemistry
De Boelelaan 1085
Amsterdam, 1081 HV
Netherlands
e-mail: badr.ghorbal@falw.vu.nl

**Jurgen Foeken**
**Fin Stuart**
Scottish Universities Environmental Research Centre
East Kilbride, Scotland, G75 0QF
United Kingdom

## ABSTRACT

To constrain upward and downward vertical movements in Northwest Africa we have sampled for low-T thermochronology a 500km long transect from the Mediterranean coast to the Anti Atlas of Morocco. The analysis of this large data set has provided major surprises requiring a reconsideration of generally accepted ideas.

The data we have produced document an Early to Middle Jurassic stage of subsidence and of Late Jurassic to Early Cretaceous exhumation affecting a large elongated region stretching from the Moroccan Meseta to the Anti Atlas. These domains are typically considered as stable during the same time span. Late Jurassic to Early Cretaceous exhumation caused the erosion of a large amount of terrigenous sediments transported offshore and deposited in the otherwise monotonous and fine-grained succession of the Moroccan Atlantic passive continental margin.

Alpine deformations began in the Late Cretaceous and continue until present. They were initially associated with the development of large scale, WNW-ESE trending folds and then with localization of shortening and exhumation in the Atlas system.

BACK

# Geotectonic Scenarios for the Evolution of the South Atlantic Brazilian Margin: Left-Lateral Lower Cretaceous Oblique Rifting Followed by Upper Cretaceous to Present Ongoing Compression

**Claudio Coelho De Lima**
Petrobras – SA
Ilha do Fundão Q7
Cidade Universitária
Rio de Janeiro, RJ, 21941-915
Brazil
e-mail: claudiolima@petrobras.com.br

**Marcos Fetter Lopes**
**Rogerio Gontijo**
**Pessoa Neto**
**Otaviano Da Cruz**
Petrobras- SA
Rio de Janeiro, RJ, 20031-912
Brazil

## ABSTRACT

We propose that the evolution of South Atlantic Brazilian margin was performed in two successive geotectonic scenarios. The first one was dominated by left-lateral Lower Cretaceous oblique rifting that culminated with South Atlantic seafloor spreading. This scenario produced right stepped NNE-SSW-trending blocks where kitchens are found.

The second scenario has been produced as the South America (SA) plate have been moving westwards with respect to the Africa plate. While moving, this plate is frontally or obliquely "colliding" against other plates (Nazca, Caribbean, Scotia) that are moving eastwards. This geotectonic scenario that began to be delineated in the Upper Cretaceous, was definitely established during the Tertiary and is prevailing in the Present. This scenario is analogous to a huge traffic accident that started in Mid-Upper Cretaceous and is still going on. As a result, the bulk of SA plate has been in horizontal compression since the Upper Cretaceous up until the Present. In such a mechanical environment, we infer that the intraplate deformation across the SA plate will be concentrated along its favorably oriented mechanical discontinuities. On the basis of this rational, the post-rifting evolution of the Brazilian Margin Basins and their petroleum systems should be influenced by compressional/strike-slip reactivation of rift-related and basement structures, modulated by salt tectonics. Results of analyses and modeling of a comprehensive geological and geophysical data set have supported this inference.

Given that intrinsically similar geotectonic scenarios (*i.e*. rifting followed by sea floor spreading; frontal or "collision") should be operating across the Central Atlantic conjugate margins as well, we speculate that using such a frame could help understanding the evolution of their petroleum systems eventually.

BACK

# Revisiting Cretaceous Tectonism and Volcanism in the Laurentian Subbasin and Orpheus Graben, Offshore Nova Scotia

**Sarah Bowman**
**Georgia Pe-Piper**
Department of Geology
Saint Mary's University
Halifax, Nova Scotia, B3H 3C3
Canada
e-mail: sarah_j_bowman@hotmail.com

**David J.W. Piper**
Geological Survey of Canada (Atlantic)
Bedford Institute of Oceanography
P.O. Box 1006
Dartmouth, Nova Scotia, B2Y 4A2
Canada

## ABSTRACT

This study is concerned with the impact of Cretaceous tectonism and volcanism on the maturation and diagenesis of the petroleum system in the Orpheus Graben and the Laurentian sub-basin, components of the Mesozoic-Cenozoic Scotian Basin located offshore of Nova Scotia. The Laurentian subbasin and Orpheus Graben have been strongly affected by early Cretaceous motion on the Cobequid-Chedabucto-Southwest Grand Banks fault system. The region is relatively unexplored although about a dozen wells have been drilled. Hydrocarbon shows are known from the eastern portion of the Laurentian subbasin. Previous work has shown regional unconformities in Orpheus graben corresponding to the base-Missisauga Formation (base Cretaceous), base-Logan Canyon Formation (early Aptian) and top Cree Member (early Albian).

Regional seismic reflection profiles from the shelf off southern Newfoundland and on the SW Grand Banks have been studied and similar unconformities have been mapped throughout the region. This sequence stratigraphic approach to seismic interpretation allows details of the lower Cretaceous stratigraphy determined from wells on the SW Grand Banks to be correlated and refined within many wells within the Orpheus Graben and Laurentian subbasin. The precise stratigraphic position of volcanic products within the wells has been re-evaluated and the volcanic character of the rocks refined by study of cuttings and well logs. Volcanic products within the wells have been compared with detrital volcanic material found distally in the Scotian Basin. The timing of regional unconformities appears to mark the onset of different components of the volcanic system. Deformation on the unconformities and distribution of volcanism are related to the complex opening history of Europe from North America. The widespread volcanic activity indicates a regional and long-lived magma source, which would have manifested itself in an elevated heat flow in the area, which in turn influenced organic maturation and diagenetic processes in the petroleum system.

BACK

# $^{40}$Ar-$^{39}$Ar of the Freetown Layered Igneous Complex (FLIC), Freetown, Sierra Leone, West Africa: Implications for the Initial Break-up of Pangea to form the Central Atlantic Ocean

**Ibrahim Jorgor Barrie**
**Jan R. Wijbrans**
**Frank F. Beunk**
**G. Bertotti,**
VU University Amsterdam,
De Boelelaan 1085, 1081 HV
Amsterdam
The Netherlands
e-mail: jorgor.barrie@falw.vu.nl

**Ibrahim Jorgor Barrie**
**Victor E.H. Strasser-King**
**Daniel V.A. Fode**
Fourah Bay College
University of Sierra Leone
Private Mailbag
Freetown
Sierra Leone

## ABSTRACT

The break-up of the Pangaea super-continent to form the Central Atlantic Ocean and its passive margins began in the Early Jurassic. Geo-tectonically, the break-up was notably accompanied by the outpouring of extensive flood basaltic magma expressed as dykes, sills and lava-flows covering once-contiguous parts of North America, Europe, Africa and South America to form the Central Atlantic Magmatic Province (CAMP). The Freetown Layered Igneous Complex (FLIC) emplaced within the heart of CAMP and measuring on surface 65 x 14 x 7 km, is the largest single layered igneous intrusion yet known on either side of the Central Atlantic Ocean. Geophysical investigations indicate that the intrusion extends beneath the Atlantic Ocean to a depth of at least 20 km and that it is lopolithic in shape with a radius of about 30 km. Geologically, the Complex is a rhythmically layered elongated mafic-ultramafic body divisible into four major zones each comprising repeated sequences of troctolitic, gabbroic and anorthositic rocks.

A first series of $^{40}$Ar-$^{39}$Ar analyses of plagioclases, biotites and amphiboles from the first two zones (Zones 1 and 2) yields plateau ages ranging from 196.3 ± 3 Ma to 228.6 ± 6 Ma. Because $^{40}$Ar-$^{39}$Ar dates of these minerals represent cooling ages, we interpret these dates as representing a minimum intrusion-age of the Complex implying that its true emplacement age might be somewhat older than 230 Ma. Given that most established CAMP ages revolve around 200 Ma or younger, we hypothesize that FLIC represents a hitherto unknown pre-CAMP magmatic event that might have thermally triggered the initial break-up of Pangaea to form the Central Atlantic. This view is consistent with field-observations that the Complex is cross-cut by predominantly coast-parallel mafic dykes we attribute to the well know CAMP dyke-swarms. To ascertain the hypothesis, we are currently carrying out additional $^{40}$Ar-$^{39}$Ar dating of zones 3 and 4 and the cross-cutting dykes to be followed-up by U-Pb zircon dating to establish, precisely, the true emplacement age of the Complex.

## Introduction

The Atlantic Passive Continental Margins form the longest continental borderland systems of the Earth's surface. They show remarkable similarities and are perhaps the best studied rifted-margins in the world. Yet, despite these similarities, various segments of the margins show profound differences as to the occurrences of magmatism and vertical movements. This is particularly true of the Sierra Leone passive margin, a unique transitional margin the magmatic and geo-tectonic study of which, will, in our view, lead to a better understanding of the break-up of Pangaea to form the Central Atlantic Ocean.

The Sierra Leone margin is unique and transitional because it is located at the place where the West African Margin shifts from north-south to east-west (Fig. 1).) With respect to the Atlantic Ocean, this implies a transition from orthogonal (normal) spreading (Central Atlantic Ocean: ~ 180 Ma) to spreading controlled by transform rifting (South Atlantic Ocean: ~ 130 Ma) (*e.g.* Turner *et al.* 2003).

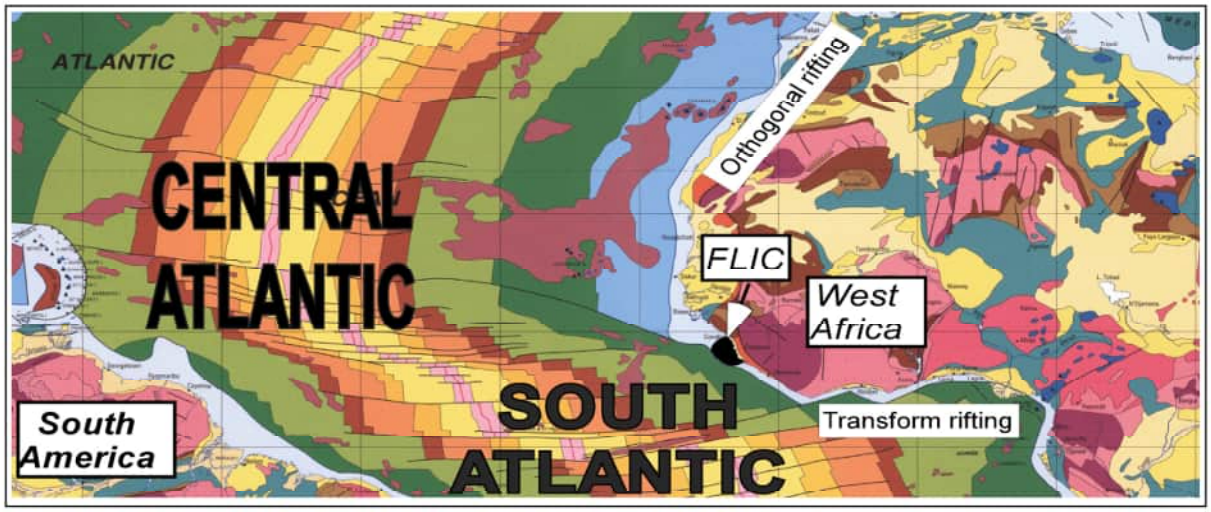


**Fig.1**. Geological map of the Central Atlantic Ocean and adjacent West Africa (taken from the Geological Map of the World; 1:25.000.000, Unesco 2000). Central Atlantic opening started in the Early Jurassic (~180 Ma ago: light blue). Opening of the South Atlantic proceeded from Early Cretaceous onward (~130 Ma ago: dark green). Note the transitional nature of the Sierra Leone margin. Note also that the FLIC is somewhat exaggerated for the purpose of clarity.

On the other hand, the margin is magmatically and geo-tectonically unique because it hosts FLIC, the largest single rift-related layered igneous intrusion yet known on either side of the Central Atlantic Ocean. According to Venkatakrishan and Culver (1989), the spatial relationships between magmatic and tectonic features in Sierra Leone, Liberia and Guinea suggest that the Jurassic continental break-up in central West Africa is not related to plume-magmatism but to a rift-rift-transform junction centred on FLIC (Fig. 2). This observation suggests that the FLIC might have been the thermal engine that initiated and led to the break-up of the Pangaean super-continent in the Jurassic to form the Central Atlantic Ocean, a view convincingly consistent with the $^{40}$Ar-$^{39}$Ar plateau ages we obtain from our mineral dating of zones 1 and 2 of the Complex.

## General Geology of the FLIC

The Freetown Layered Igneous Complex (FLIC) is a very large crescent-shaped rift-related tholeiitic intrusion associated with the Jurassic opening of the Central Atlantic Ocean. On surface, the Complex comprises an eastern area of westward-dipping rhythmically layered elongated mafic-ultramafic

body measuring 65 x 14 x 7 km in volume. Geophysical investigations (Jones et al., 1988; Krause, 1963) indicate that the intrusion extends westwards beneath the Atlantic Ocean to a depth of at least 20 km and that it is lopolithic in shape with a radius of about 30 km.

Wells (1962) laid the foundation for the modern study of the FLIC in a memoir in which he subdivided the Complex into four major zones (Fig. 3) and concluded that the intrusion as a whole crystallised in situ from a single parental magma with little or no crystal settling. Mineralogically, the principal constituents are labradorite, common olivine and augite, and, orthopyroxenes of bronzite-hypersthene composition that show evidence of having inverted from pigeonite.

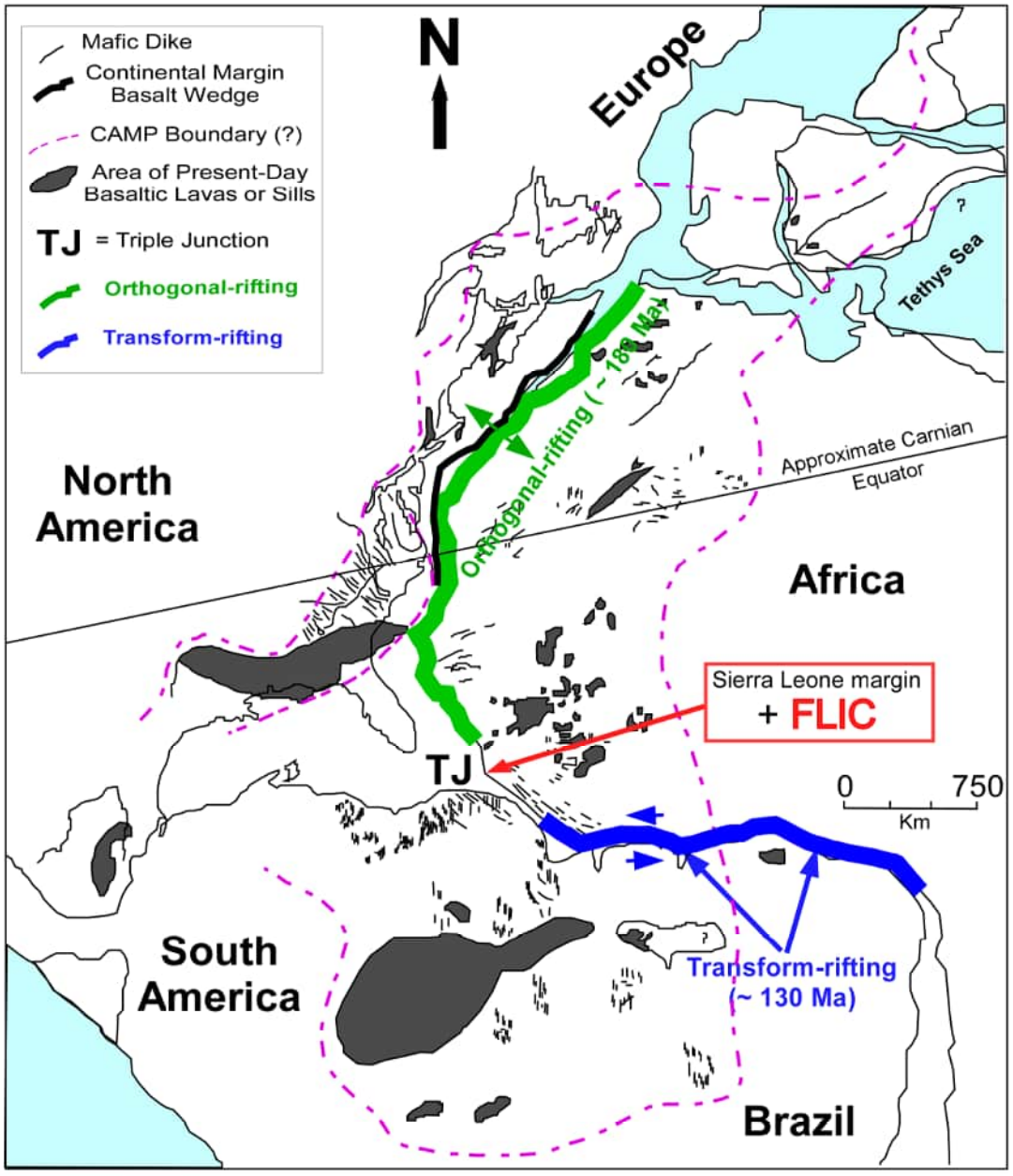


**Fig. 2.** Early Jurassic Basalt Provinces of the Central Atlantic Pangaean rift. Note the location of the Sierra Leone margin and its FLIC: at the triple junction (TJ) between Central Atlantic Orthogonal rifting, South Atlantic Transform rifting and Caribbean opening. Figure modified after McHone 2000

According to Wells (1962), despite the great thickness of the Complex (7 km) and the strong differentiation in terms of mineral proportions, there is no progressive variation in the composition of the minerals. However Chalokwu *et al.* (1995) and Chalokwu (2001) disagree. In both papers, it is argued that the Complex do exhibit both normal and reverse cryptic variation in the composition of the solid solution minerals attributable to the periodic influxes of magmas into the Freetown chamber followed by mixing of new and evolved resident magmas without any discharge.

## Previous Geochronological Studies of the FLIC

Geochronological studies of the FLIC are at best, scarce. So far the only known ages are 180 Ma and 220 Ma years respectively derived from K/Ar whole-rock age determinations and palaeomagnetic studies by Briden *et al.* (1971) and, 193 Ma based on Rb/Sr dating of acid veins contemporaneous with the early stages of the cooling history of the Complex by Beckinsale *et al.* (1977).

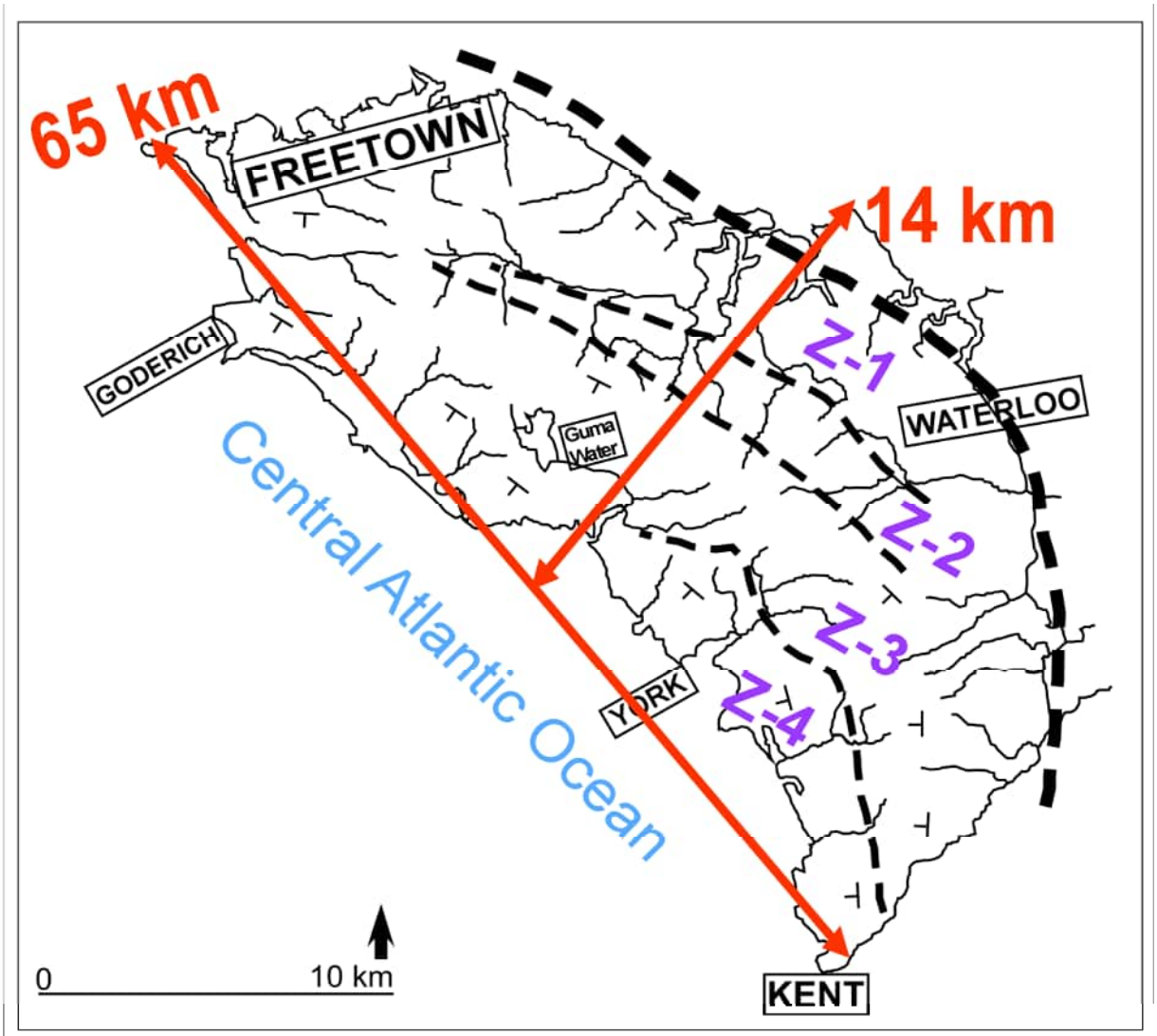


**Fig. 3.** Sketch-map of the exposed part of the Freetown Layered Igneous Complex showing the zone boundries. Note the westward-dipping nature of the Complex. Figure modified after Chalokwu (2001).

## Samples and Methodology

Nine samples (5 plagioclases, 3 amphiboles and 1 biotite) from olivine-gabbros and anorthosites of Zones 1 and 2 of FLIC were analysed. All samples are coarse-grained in texture with sizes greater than 180 µm.

The grains were selected using standard mineral separation techniques and, the fresh and unbroken grains were manually picked under a binocular microscope. About 30 mg of the plagioclase grains and 15 mg of the amphibole (hornblende) and biotite grains were then packed in 9 mm aluminium-foil packages and stacked with packages containing the DRA-1 sanidine standard having a K/Ar age of 25.26 Ma. The grains and standard were then irradiated for 12 hours in the RODEO CD-Line rotating facility at the Petten High-flux reactor in the Netherlands.

After irradiation, laser incremental-heating was carried out using a Synrad 48-5 $CO_2$ laser and then mass-spectrometrically analysed at the Argon-lab of the VU University, Amsterdam. A typical mass-spectrometer run consists of stepping through the argon mass spectrum from m/e: 40 to m/e: 35.5 at steps of a half mass unit, taking a preset number of digital voltmeter readings on each mass step. The beam signal, on all 10 mass steps ,were measured on a Balzers 217 SEM detector.

Aliquots of air and of $^{38}Ar$ spiked air were measured routinely during the measurement runs to monitor the mass-discrimination (for full description, see Kuiper 2003). For off-line data reduction, the ArArCalc2.2c (Koppers 2002) was employed.

## Results and Conclusion

All the grains analysed yield well-defined spectra with plateau ages that range from 196.3 ± 3 Ma to 228.6 ± 6 Ma which, to some extent, seem to agree with the palaeomagnetic age (220 Ma) obtained by Briden et al. (1971) for the Complex. All the ages are quoted at the 2σ uncertainty level. Because $^{40}Ar$-$^{39}Ar$ ages of minerals in general represent cooling ages, we interpret these ages as representing a minimum intrusion-age of the FLIC implying that its true emplacement age might be somewhat older than 230 Ma.

Given that most established CAMP ages revolve around 200 Ma or younger, we therefore conclude that FLIC represents a hitherto unknown pre-CAMP magmatic event that might have thermally triggered the initial break-up of Pangaea to form the Central Atlantic. This view is consistent with field-observations that the Complex is crosscut by predominantly coast-parallel mafic dykes we attribute to the CAMP dyke-swarm observed on the Atlantic passive margins of eastern North America, Western Europe, West Africa and northern South America. To confirm the hypothesis, we are currently carrying out additional $^{40}Ar$-$^{39}Ar$ dating of zones 3 and 4 of the Complex and its cross-cutting dykes to be followed-up by U-Pb zircon dating to establish, precisely, its true emplacement age.

## References


Barrie, I.J., P.A.M. Andriessen, F.F. Beunk, J.R. Wijbrans, V.E.H. Strasser-King, D.V.A. Fode, 2006, Tectonothermal evolution of the Sierra Leone Passive Continental Margin, West Africa: Constraints from thermochronology. Geochemica et Cosmochemica Acta 70 (18): A36-A36 Suppl. S Aug-Sep 2006

Beckinsale, R.D., J.F.W. Bowles, R.J. Pankhurst, M.K. Wells, 1977, Rubidium-strontium age studies and geochemistry of acid veins in the Freetown complex, Sierra Leone. Mineralogical Magazine, v.41, p.501-511.

Briden, J.C., D.I. Henthorn, D.C. Rex, 1971, Palaeomagnetic and Radiometric Evidence for the Age of the Freetown Igneous Complex, Sierra Leone. Earth and Planetary Science Letters 12, p.385-391.

Chalokwu, C.I., P.J. Seney, C.A. Wurie, M. Bersch, 1995, Petrology of the Freetown layered complex of Sierra Leone: Part I. Stratigraphy and mineral-chemical evidence for multiple magma injection. International Geology Review 37, p.230-253.

Chalokwu, C.I., 2001, Petrology of the Freetown Layered Complex, Sierra Leone: Part II. Magma evolution and crystallization conditions. Journal of African Earth Sciences, v.32. n. 3, p.519-540.

Jones, E.J.W., B.R. Clayton, C.C.S. Mgbatogu, C.G. Stevenson, 1988, A Geophysical Survey of the Sierra Leone Continental Margin. Annual Offshore Technology Conference, Dallas, United States, 1988, p.283-292.

Koppers, A.A.P., 2002, ArArCALC-software for $^{40}Ar/^{39}Ar$ age calculations. Computer & geosciences, 28, 605-619.

Krause, D.C., 1963, Seaward Extension and origin of the Freetown Layered Basic Complex of Sierra Leone. Nature, v.200, p.1280-1281.

Kuiper, K.F., 2003, Direct Intercaliberation of Radio-sisotopic and astronomical time in the Mediterranean Neogene. PhD thesis, VU University, Amsterdam, The Netherlands. 223p.

Marzoli, A., P.R. Renne, E.M. Piccirillo, M. Ernesto, G. Bellieni, A. De Min, 1999, Extensive 200-Million-Year-Old Continental Flood Basalts of the Central Atlantic Magmatic Province. Science 284, p.616-618.

McHone, J.G., 2000, Non-plume magmatism and rifting during the opening of the central Atlantic Ocean. Tectonophysics 316, p.287-296.

Turner, J.P., B.R. Rosendahl, P.G. Wilson, 2003, Structure and Evolution of an obliquely sheared continental margin: Rio Muni, West Africa. Tectonophysics 374, p.41-55.

Venkatakrishnan, R., S.J. Culver, 1989, Tectonic fabric of Sierra Leone, West Africa: implications for Mesozoic continental breakup. Journal of the Geological Society, London, v.146, p.991-1002.

Wells, M.K., 1962, Structure and Petrology of the Freetown Layered Basic Complex of Sierra Leone, Overseas Geol. Mineral. Res. Bull. Suppl., 4, 115p.

**BACK**

# The Ins and Outs of Buttress Folds: Examples from the Inverted Fundy Rift Basin, Nova Scotia and New Brunswick, Canada

**Mark S. Baum**
Chevron Energy Technology Company
1500 Louisiana Street
Houston, Texas 77002
USA
e-mail: mark.baum@chevron.com

**Martha Oliver Withjack**
Department of Earth & Planetary Sciences
Rutgers University
610 Taylor Road
Piscataway, New Jersey 08854
USA
e-mail: drmeow3@rci.rutgers.edu

**Roy W. Schlische**
Department of Earth & Planetary Sciences
Rutgers University
610 Taylor Road
Piscataway, New Jersey 08854
USA
e-mail: schlische@rci.rutgers.edu

## ABSTRACT

Buttress folds form in the hanging walls of non-planar normal faults during basin inversion. Slip occurs more easily along the lower, more gently dipping fault segments, whereas the upper, more steeply dipping fault segments act as buttresses, inhibiting slip and causing the hanging-wall strata to shorten and fold. We have examined the geometry of buttress folds in the inverted Fundy rift basin, Canada, using seismic (both offshore and onshore), field, aeromagnetic, and DEM data. Generally, the hinges of the buttress folds in the Fundy rift basin parallel the strikes of the adjacent extensional fault zones. The tightest folds occur adjacent to the more steeply dipping, upper fault segments, whereas broader folds occur adjacent to the more gently dipping, upper fault segments. The folds commonly occur as trains of hanging-wall synclines and anticlines, indicating that a detachment level exists at depth. Therefore, many of the buttress folds in the Fundy basin are combinations of buttress and detachment (buckle) folds. Most natural examples of buttress folds, and those produced in analogue models, consist of a single hanging-wall anticline adjacent to the fault zone. The combination buttress/detachment folds in the Fundy rift basin, however, consist of either a syncline or an anticline adjacent to the fault zone.

Based on kinematically compatible slip vectors on differently oriented segments of the border-fault system, the relative displacement direction of hanging-wall blocks to footwall blocks during inversion of the Fundy rift basin was northeast-southwest. This inversion-related deformation is, at least partially, partitioned into pure-shear and simple-shear components. The fault-parallel buttress/detachment folds accommodate the pure-shear component, whereas fault-parallel, left-lateral strike-slip faults accommodate the simple-shear component. Thus, the buttress/detachment folds in the Fundy basin do not necessarily indicate the relative displacement direction of hanging-wall blocks to footwall blocks. Instead,

their trends reflect the variable local shortening direction associated with the pure-shear component of the deformation.

## Introduction

Buttress folds form in the hanging walls of non-planar normal faults during basin inversion (*e.g.* Dart *et al.* 1995; McClay 1995). Slip occurs more easily along lower, more gently dipping fault segments; however, upper, more steeply dipping fault segments act as a buttress, thereby inhibiting slip and causing the hanging-wall strata to shorten and fold (Fig. 1A). Most geologic examples of buttress folds, as well as those produced in experimental (analogue) models, have a single hanging-wall anticline whose axis parallels the border-fault system (*e.g.* Dart *et al.* 1995; Eisenstadt and Withjack 1995; McClay 1995; Baum, 2006) (Figs. 1Aiii and 1B). How representative are these examples of buttress folds? Do all buttress folds have anticlinal geometries? How do the trends of the axes of buttress folds relate to the regional shortening direction?

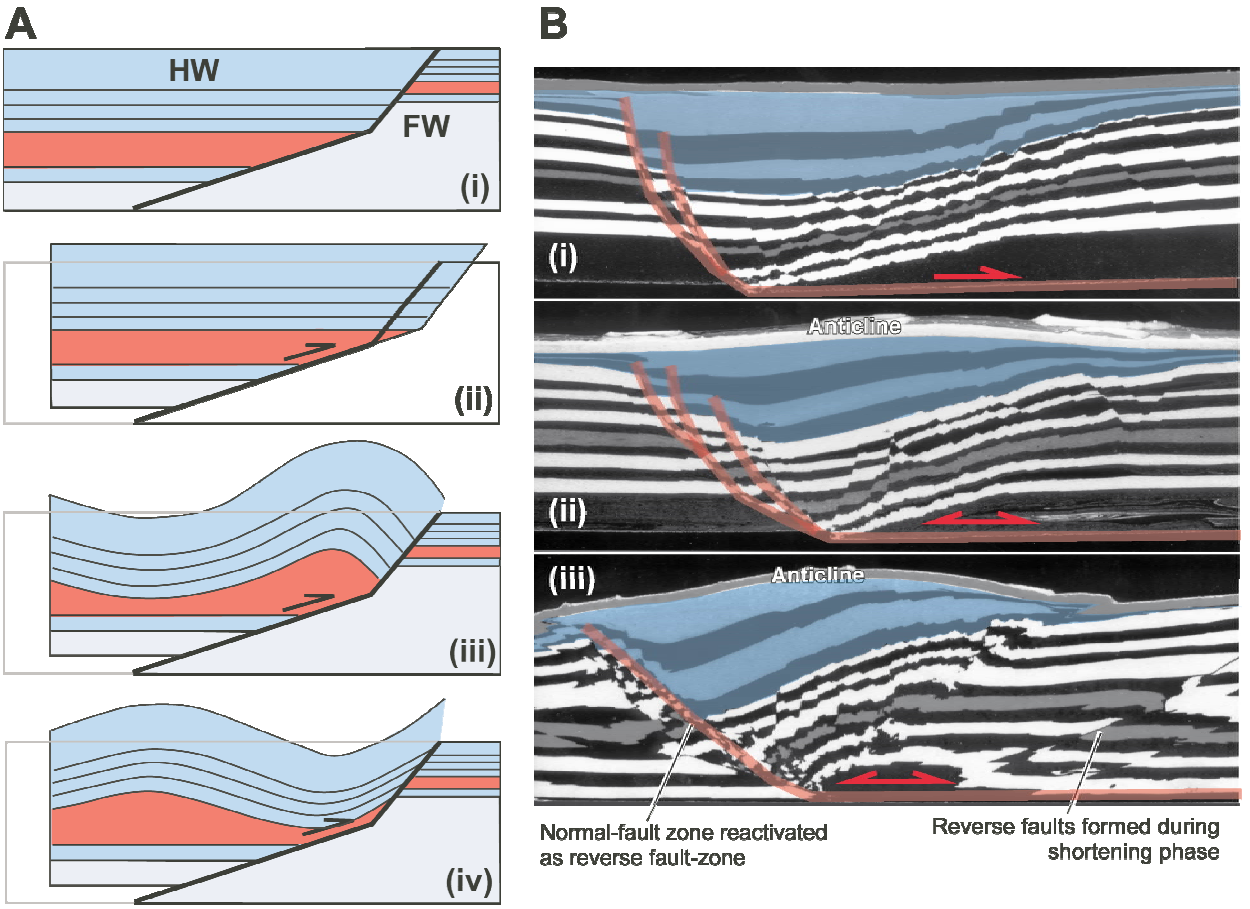


**Figure 1. A. Development of buttress folds. (i) Geometry prior to folding showing pre-existing normal fault whose dip decreases with depth. Generally, footwall is stronger than hanging wall because footwall has thinner sedimentary cover above strong crystalline basement. (ii) Reverse slip would create space problem (overlap) at shallow depths. In response to space problem, folds form in hanging wall. The fold adjacent to the fault may be an anticline (iii) or a syncline (iv). The cross sections are line-length balanced, and the ductile unit (red) is area-balanced. B. Experimental models of inversion-related buttress folds (modified from Eisenstadt and Withjack, 1995). (i) After extension. (ii) After extension and mild inversion. (iii) After extension and severe inversion. The red lines are major faults that formed during extension. The anticline in (ii) and (iii) is a buttress fold.**

We have used geological and geophysical data from the inverted Fundy rift basin, Nova Scotia and New Brunswick, Canada (Fig. 2), to address these questions. Specifically, we have reinterpreted 2D seismic-reflection data from the Bay of Fundy, including several key reprocessed seismic lines. We have also: 1) interpreted new seismic data from onshore Nova Scotia; 2) mapped, in detail, cliff and tidal-flats outcrops from onshore Nova Scotia; 3) incorporated high-resolution, digital elevation model data (Nova Scotia Department of Natural Resources 2004; Canadian Council on Geomatics 2008) and aeromagnetic data (King 2005a, 2005b; Oneschuk and Dumont 2005a 2005b) from the Bay of Fundy region; and 4) compared the structures in the Fundy rift basin to those in scaled experimental models of inversion (orthogonal and oblique) (Baum, 2006).

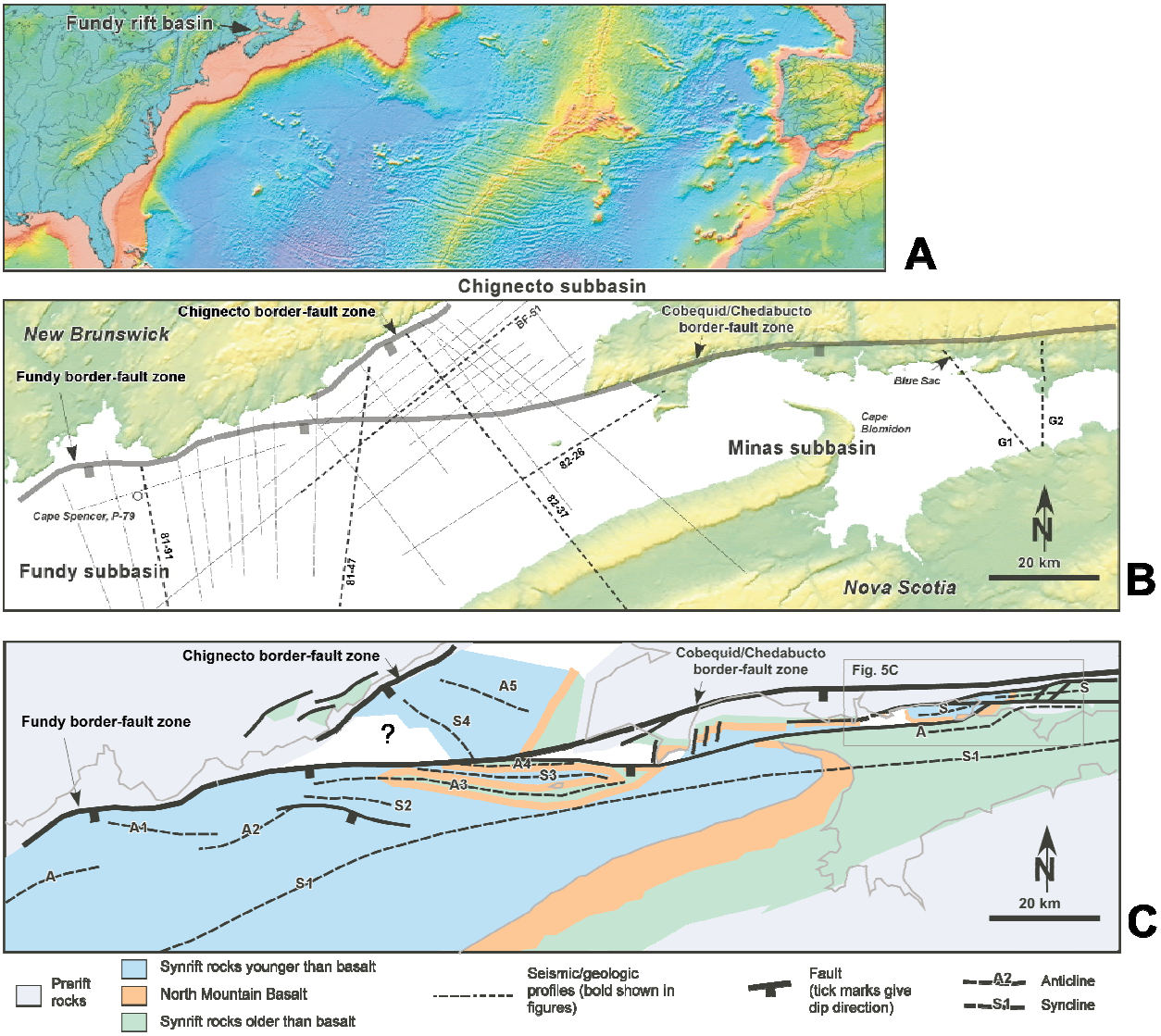


**Figure 2. A. Topographic map of Atlantic Ocean and conjugate continental margins: http://topex.ucsd.edu/marine_topo/gif_topo_track/topo8.gif). B. Map of northern Fundy rift basin showing junction of three structural subbasins (Fundy, Minas, and Chignecto subbasins), geographic features, major faults, seismic coverage, locations of cross sections (G1 and G2), and field sites. Shaded-relief map based on data from Canadian Council on Geomatics (2008). C. Geologic map of northern Fundy rift basin based on seismic data, outcrop and well data (Withjack *et al.*, 1995), seafloor topography and subcrop information (Swift and Lyall, 1968), and aeromagnetic data (King, 2005a, 2005b; Oneschuk and Dumont, 2005a, 2005b).**

## Geometries of Faults and Folds

The Fundy rift basin is the northernmost exposed basin in the eastern North American Mesozoic rift system that formed during the fragmentation of Pangea (Fig. 2A). It has three distinct structural constituents: the Chignecto, Fundy, and Minas subbasins (Olsen and Schlische, 1990; Figs. 2B and 2C). The offshore and onshore seismic data show that the border-fault system of the Fundy rift basin is complex, consisting of linked northeast- and east-striking fault zones (Fig. 2C). The Chignecto and Fundy subbasins are bounded on the northwest by the northeast-striking Chignecto and Fundy border-fault zones, respectively. The Fundy and Minas subbasins are bounded on the north by the east-striking Cobequid/Chedabucto border-fault zone (*e.g,* Olsen and Schlische, 1990; Withjack *et al.* 1995). All fault zones have gentle dips at depth, whereas the east-striking Cobequid/Chedabucto fault zone has steep dips at shallow levels (Fig. 3).

Folds are present in the hanging wall of the entire linked border-fault system of the Fundy rift basin (Fig. 2C). An absence of growth beds indicates that most of this folding occurred after rifting during a subsequent shortening/inversion event. Most of these inversion-related folds are subparallel to the adjacent fault zone (Fig. 2C). Thus, the trends of the fault-parallel folds vary, reflecting the trends of the adjacent fault zones. Generally, broad anticlines develop in the hanging wall of the northeast-striking Fundy fault zone (Fig. 3G), whereas a train of anticlines and synclines develops in the hanging wall of the east-striking Cobequid/Chedabucto fault zone (Fig. 2C). The tightest and narrowest folds occur adjacent to the most steeply dipping, upper segments of the Cobequid/Chedabucto fault zone (Figs. 3C and 3D). Hanging-wall anticlines (*e.g.* Fig. 3D) and synclines (*e.g.,* Fig. 3C) occur directly adjacent to the east-striking Cobequid/Chedabucto fault zone.

Based on these characteristics, we propose that the fault-parallel, hanging-wall folds in the Fundy rift basin are, at least in part, buttress folds. The onshore seismic data show that the train of folds in the hanging wall of the east-striking Cobequid/Chedabucto fault zone does not affect the gently dipping, lower segment of the fault zone, indicating that a detachment exists between the base of the synrift section and the border-fault surface (Fig. 3A). Considering the limited distance between the base of the synrift section and the border-fault surface, the most likely detachment is the border-fault surface itself. Other potential detachment levels include pre-existing, low-angle Paleozoic thrust faults and evaporite units in the pre-rift section (*e.g.* Waldron and Rygel 2005). Thus, many of the fault-parallel folds in the hanging wall of the east-striking Cobequid/Chedabucto fault zone are actually a combination of buttress and detachment (buckle) folds. These combination buttress/detachment folds differ from traditional anticlinal buttress folds in that multiple folds develop and either an anticline or a syncline is present directly adjacent to the fault zone (Figs. 1Aiii and 1Aiv).

To define the small-scale structures associated with the buttress/detachment folding, we have mapped, in detail, several field sites within the east-striking Cobequid/Chedabucto fault zone (Figs. 2C, 4, 5). The small-scale deformation at these field sites consists predominantly of east- to northeast-striking, steeply dipping, left-lateral strike-slip faults (based on slickensided fault surfaces) and minor post-depositional folds. The faults cut and/or bound the minor post-depositional folds (Fig 4). Thus, the small-scale, left-lateral strike-slip faults are also post-depositional structures.

## Displacement Directions and Strain Partitioning

Scaled experimental (analogue) models of oblique rift-basin inversion show that the trends of the axes of buttress folds are parallel to the trends of the adjacent fault zones, regardless of the displacement direction of the hanging wall relative to the footwall (Baum 2006). Thus, the models suggest that the deformation produced by oblique inversion is at least partially partitioned into fault-perpendicular and fault-parallel components.

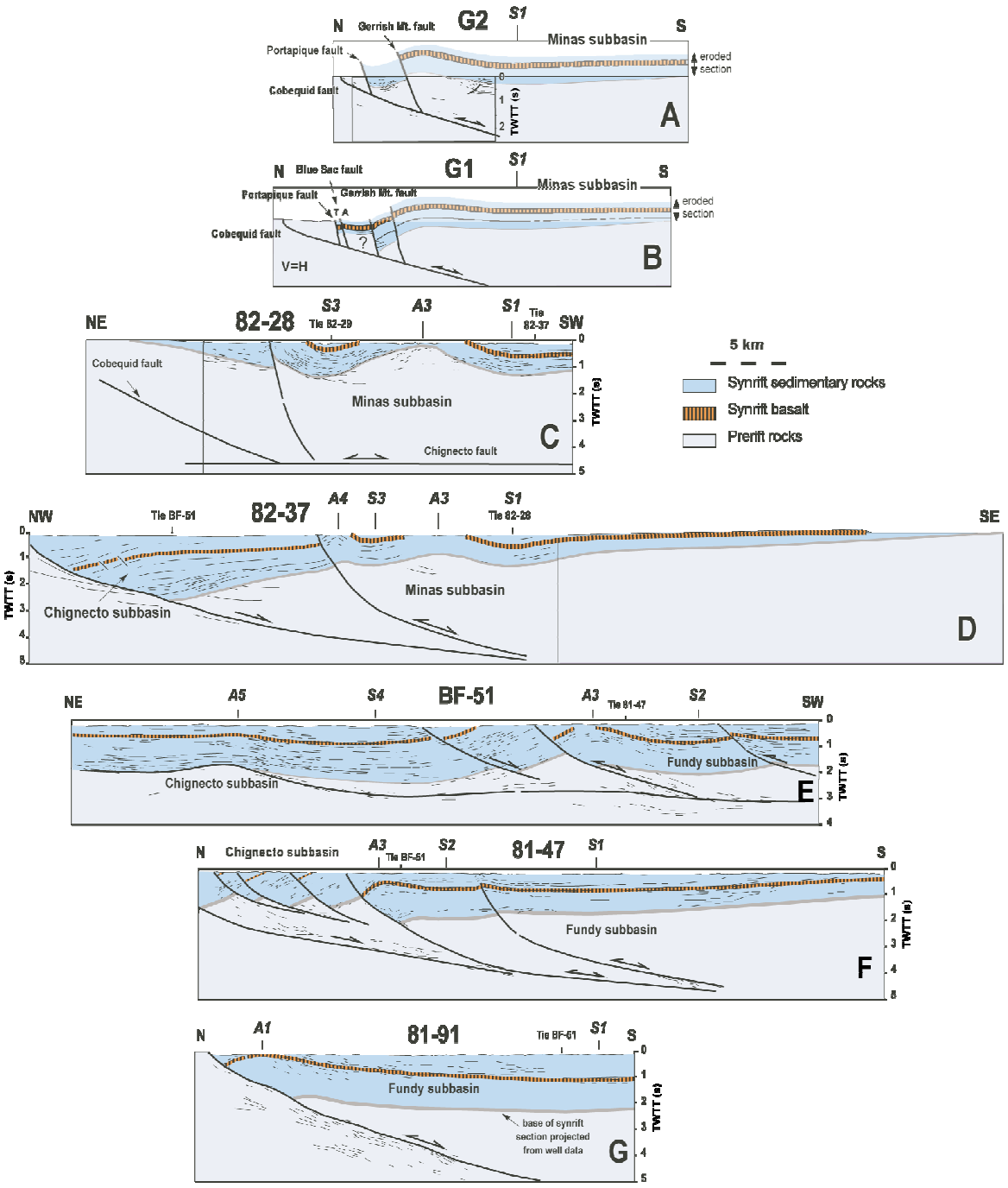


**Figure 3. Sections across Fundy basin based on field, well, and seismic data. See Figure 2 for locations. Boxed portions are interpreted line drawings of seismic profiles, displayed at approximately 1:1 assuming an average velocity of 3.5 km/s. (A) Cross section G2 based in part on onshore seismic data. Contacts in center of basin are projected from Cape Blomidon (see Fig. 2 for location). (B) Cross section G1, based in part on work by Donohoe and Wallace (1982). Contacts in center of basin are projected from Cape Blomidon (see Fig. 2 for location). (C) Northeastern portion of seismic line 82-28 and onshore continuation. (D) Seismic line 82-37 and onshore continuation. (E) Seismic line BF-51. (F) Seismic line 81-47. (G) Seismic line 81-91. Arrows show components of fault slip in plane of cross section. *A* and *S* indicate anticlines and synclines in Figure 2C.**

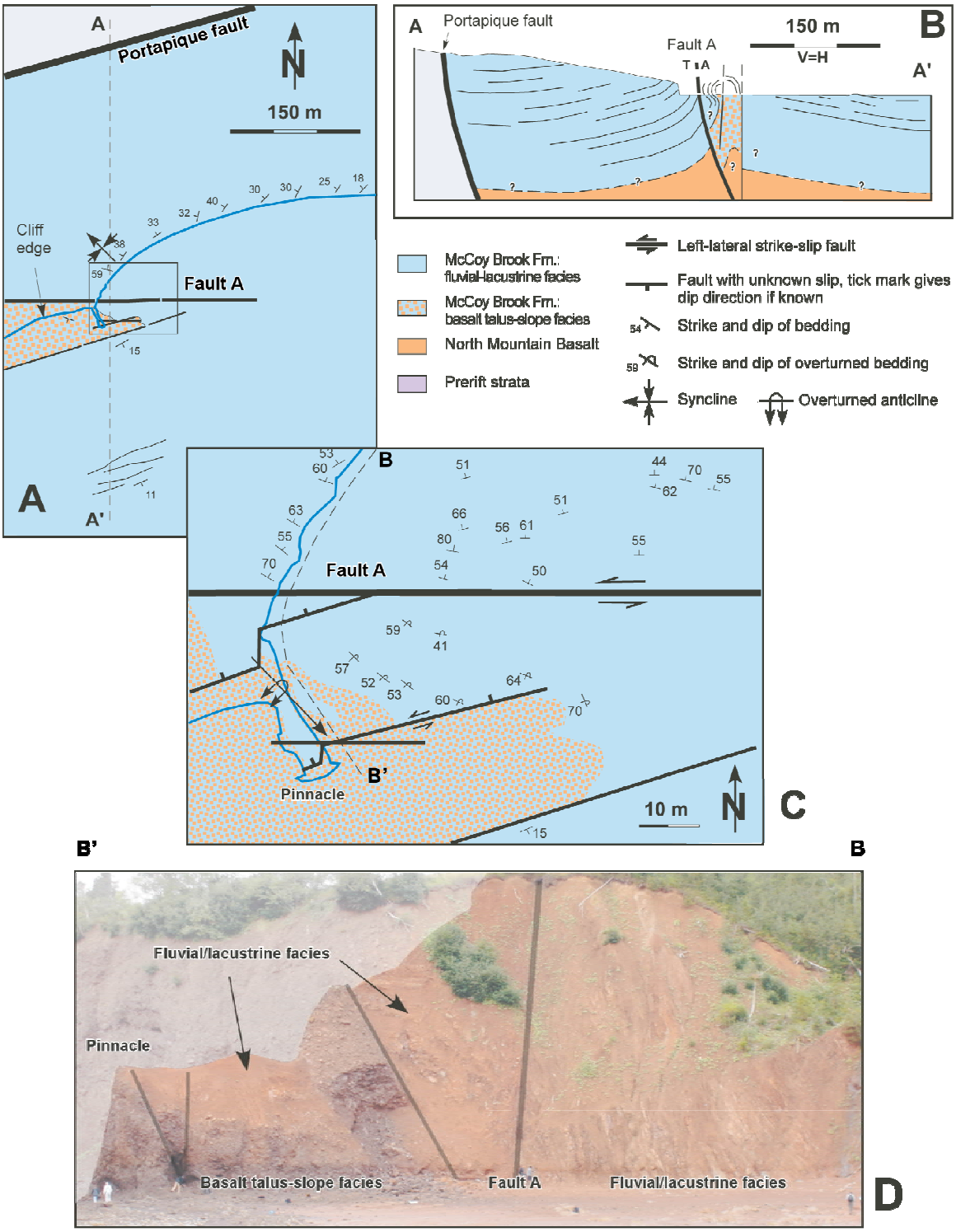


**Figure 4: Geology of the Blue Sac area. A) Simplified geologic map showing faults and distribution of facies in the McCoy Brook Formation. Bedding on north side of Fault A steepens and rotates counterclockwise with increasing proximity to fault. B) Geologic cross section A-A' [location shown in (A)], showing overturned anticline. C) Detailed geologic map of boxed area in (A). Fault A strikes due east, dips steeply to the south, and has shallow southwest-raking slickenlines. Minor faults show left-lateral separation and subhorizontal slickenlines. Anticline has overturned NE limb. D) Photo of north-south trending cliff face from pinnacle to north of Fault A viewed toward the west. Geologists for scale.**

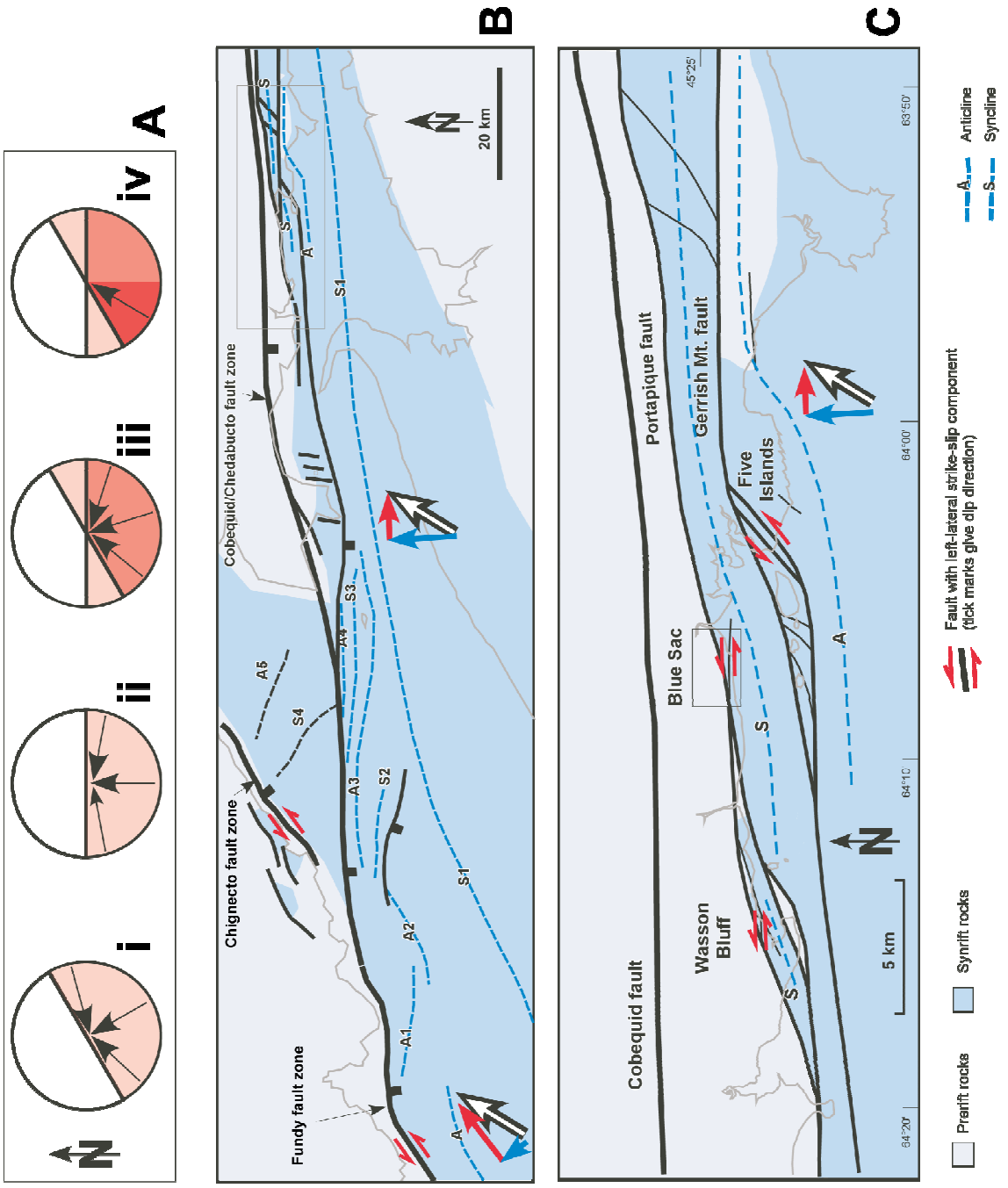


**Figure 5. (A) Displacement direction of hanging wall relative to footwall of linked border-fault system of Fundy rift basin during inversion. (i) Possible range of relative displacement directions based on presence of buttress folds in hanging wall of northeast-striking Fundy fault zone. (ii) Possible range of relative displacement directions based on presence of buttress/detachment folds in hanging wall of east-striking Cobequid/Chedabucto fault zone. (iii) Possible range of relative displacement directions combining information from i and ii. (iv) Possible range of relative displacement directions combining information from i and ii and considering presence of east-striking, left-lateral strike-slip faults observed at field sites. Regional (B) and local (C) maps of northern Fundy rift basin. White arrows with black borders show displacement direction of hanging wall relative to footwall of linked border-fault system during inversion. The northeast-striking fault zones underwent highly oblique inversion, whereas the east-striking fault zones underwent oblique inversion. Blue arrows show pure-shear component and resultant fault-parallel, buttress/detachment folding, and red arrows show simple-shear component and resultant east-striking faults with left-lateral strike-slip components. Many faults have a significant reverse-slip component as well as the left-lateral strike-slip component.**

As mentioned previously, the linked border-fault system of the Fundy rift basin has fault zones with two trends: the northeast-striking Fundy fault zone and the east-striking Cobequid/Chedabucto fault zone (Fig. 2). Therefore, the presence of fault-parallel buttress/detachment folds in the hanging walls of both fault zones indicates a component of fault-perpendicular shortening along both margins and, thus, restricts the displacement direction of the hanging wall relative to the footwall of the linked border-fault system during inversion (Figs. 5i and 5ii). Specifically, the relative displacement direction could range from northeast to west during inversion (Fig. 5Aiii).

The abundance of small-scale, east- to northeast-striking, left-lateral strike-slip faults at the field sites within the east-striking Cobequid/Chedabucto fault zone suggests a fault-parallel component of left-lateral shear and further restricts the displacement direction of the hanging wall relative to the footwall of the linked border-fault system during inversion. Specifically, the relative displacement direction must have had an eastward component during inversion. Together, the fault-parallel buttress/detachment folds and the east- to northeast-striking, left-lateral strike-slip faults indicate that the hanging wall of the linked border-fault system of the Fundy rift basin moved northeast relative to its footwall during inversion (Fig. 5iv).

The seismic and field data show that the postrift deformation in the inverted Fundy rift basin is, at least partially, partitioned into a pure-shear component and a simple-shear component (*e.g.*, Sanderson and Marchini 1984; Jones and Tanner 1995). The fault-parallel, buttress/detachment folds accommodated the pure-shear component, whereas the left-lateral strike-slip faults accommodated the simple-shear component (Figs. 5B and 5C). The strain partitioning in the inverted Fundy rift basin is similar to strain partitioning observed in other transpressional zones (Jones and Tanner 1995).

## Summary and Conclusions

Two distinct deformation styles developed during inversion of the Fundy rift basin: 1) high-angle, left-lateral strike-slip faults that are subparallel to the border-fault zones, and 2) buttress and combination buttress/detachment folds whose axes are subparallel to the border-fault zones. Thus, the inversion-related deformation in the Fundy rift basin is, at least partially, partitioned into simple-shear (*i.e.*, strike-slip faulting) and pure-shear (*i.e.*, buttress/detachment folding) components. The tightest and narrowest buttress/detachment folds occur adjacent to the most steeply dipping, upper segments of the border-fault zones. Most natural examples of buttress folds, and those produced in analogue models, consist of a single hanging-wall anticline. The combination buttress/detachment folds in the inverted Fundy rift basin, however, consist of trains of folds, with either a syncline or an anticline adjacent to the border-fault zone. The geometries of these buttress/detachment folds reflect the local, fault-perpendicular shortening direction associated with the pure-shear component of deformation; therefore, they are biased indicators of the displacement direction of the hanging wall relative to the footwall. However, their occurrence along two border-fault zones with different trends, combined with the presence of left-lateral strike-slip faults subparallel to the border-fault zones, constrains the relative displacement direction of the hanging wall to the footwall to the northeast.

## References


Baum, M.S., 2006, Controls on the deformation produced by oblique inversion of rift basins: Which structures reflect the paleostrain state? Rutgers Univ. Ph.D. thesis.

Dart, C.J., K.R. McClay, and P.N. Hollings, 1995, 3D analysis of inverted extensional fault systems, southern Bristol Channel basin, UK, *in* J.G. Buchanan and P.G. Buchanan, eds., Basin Inversion, Geological Society of London Special Publication 88, p.393-413.

Donahoe, H.V. and P.I. Wallace, 1982, Geologic map of the Cobequid Highlands, Colchester, Cumberland, and Pictou counties, Nova Scotia, scale 1:50,000, Nova Scotia Dept. of Mines and Energy, Halifax, N. S., Canada.

Eisenstadt, G. and M.O. Withjack, 1995, Estimating inversion: results from clay models, *in* J.G. Buchanan and P.G. Buchanan, eds., Basin Inversion, Geological Society of London Special Publication 88, p.119-136.

Jones, R.R. and P.W.G. Tanner, 1995, Strain partitioning in transpression zones: Jour. of Structural Geology, v.17, p.793-802.

King, M.S., 2005a, Airborne magnetic calculated first vertical derivative map for NT 21H/07, Cape Chignecto Area, NS: Nova Scotia Dept. of Natural Resources, Mineral Resources Branch, OpenFile Map ME 2005-36.

King, M.S., 2005b, Airborne magnetic calculated first vertical derivative map for NT 21H/08, Parrsboro Area, NS: Nova Scotia Dept. of Natural Resources, Mineral Resources Branch, OpenFile Map ME 2005-37.

McClay, K.R., 1995, 2D and 3D analogue modelling of extensional fault structures: templates for seismic interpretation: Petroleum Geoscience, v.1, p.163-178.

Nova Scotia Department of Natural Resources (2004), shaded relief images (AZ_000-Alt_45-Z_05), available at: http://gis4.natr.gov.ns.ca/website/nsgeomap/viewer.htm.

Olsen, P.E. and R.W. Schlische, 1990, Transtensional arm of the early Mesozoic Fundy rift basin: penecontemporaneous faulting and sedimentation: Geology, v.18, p.695-698.

Oneschuk, D. and R. Dumont, 2005a, Residual total magnetic field, Parts NTS 21A, B, G, H, Bay of Fundy: Geological Survey of Canada, Open File 5008.

Oneschuk, D. and R. Dumont, 2005b, First vertical derivative of the total magnetic field, Parts NTS 21A, B, G, H, Bay of Fundy: Geological Survey of Canada, Open File 5009.

Sanderson, D.J. and W.R.D. Marchini, 1984, Transpression: Jour, of Structural Geology, v.6, p.449-458.

Swift, D.J.P. and A.K. Lyall, 1968, Reconnaissance of bedrock geology by subbottom profiler, Bay of Fundy: Geological Society of America Bull., v.79, p.639-646.

Waldron, J.W.F., and M.C. Rygel, 2005, Role of evaporite withdrawal in the preservation of a unique coal-bearing succession: Pennsylvanian Joggins Formation, Nova Scotia. Geology, v.33, p.337-340.

Withjack, M.O., P.E. Olsen, and R.W. Schlische, 1995, Tectonic evolution of the Fundy rift basin, Canada: Evidence of extension and shortening during passive margin development. Tectonics, v.14, p.390-405.

Withjack, M.O., R.W. Schlische, and P.E. Olsen, 1998, Diachronous rifting, drifting, and inversion on the passive margin of central eastern North America: an analog for other passive margins: AAPG Bull., v.82, p.817-835.

Withjack, M.O. and R.W. Schlische, 2005, A review of tectonic events on the passive margin of eastern North America, *in* P. Post, ed., Petroleum Systems of Divergent Continental Margin Basins: 25th Bob S. Perkins Research Conference, Gulf Coast Section of SEPM, p.203-235.

**BACK**

# Second-Order Sequences and their Application for Exploration in the Deep Water Scotian Slope

**Andrew Davies**
**James L. Etienne**
**Mike D. Simmons**
**Roger B. Davies**
**Peter R. Sharland**
**Owen E. Sutcliffe**
Neftex Petroleum Consultancy Ltd.
115BD Milton Park
Abingdon, OX14 4SA
United Kingdom
e-mail: andrew.davies@neftex.com

## ABSTRACT

Large-scale changes in lithofacies and stratigraphic architecture resulting from relative sea-level changes have been a prime research focus for the past few decades. Within industry, prediction of hydrocarbon play elements using sequence stratigraphic techniques is well-established. Our previous work demonstrated the veracity of a sequence stratigraphic model for the Arabian Plate identifying 63 major Maximum Flooding Surfaces (MFS) and Sequence Boundaries (SB). Ongoing work, incorporating nearly all of Earths sedimentary basins, now demonstrates the occurrence of 118 biostratigraphically-constrained sequences that are global and observed independent of tectonics or sediment supply. The rapidity and magnitude of sea-level changes inferred from our model implicate eustatic forcing.

In Eastern Canada, recent exploration has shifted focus towards the deepwater of the Scotian Slope driven by successes in other circum-Atlantic deepwater basins. Despite a proven petroleum system, the slope remains underexplored. Sandy lowstand fans comprise the principal reservoir targets, but are risky, borne out by few commercial successes.

Biostratigraphically constrained sections from the Scotian Shelf provide a framework within which sequence stratigraphy can be applied. The recognition of large hiatus relating to second-order SB's allows prediction of viable lowstand reservoirs down systems-tract. For example, the absence of Early Paleocene in many shelf wells, relates to an important late Maastrichtian SB during which significant down-slope transport of sediment is predicted. Major transgressions are often associated with development of organic-rich facies. Such is the case for Naskapi Member source rocks which relate to a second-order intra-Aptian MFS.

Here, major second-order sea-level fluctuations are identified which are postulated to have exerted an important control on reservoir and source rock development on the Scotian Slope.

BACK

# Session 1C:
# MARGIN EVOLUTION & DEVELOPMENT

## KEYNOTE ADDRESS

**SLOPES, BASIN FLOORS, DIAPIRS, AND CANOPIES: REGIONAL-SCALE SALT-SEDIMENT INTERACTION IN THE NORTHERN GULF OF MEXICO AND THE SCOTIAN OFFSHORE**
**Rowan, Mark G.**

**SEISMIC STRATIGRAPHY, SALT STRUCTURES AND THERMAL AND PETROLEUM SYSTEMS MODELS ACROSS THE CENTRAL NOVA SCOTIA SLOPE BASIN**
Louden, Keith; Mukhopadhyay, P.K.; Wu, Yu; Negulic, Eric and Nedimovic, Mladen

**BASIN-SCALE SALT TECTONIC PROCESSES AND SEDIMENT PROGRADATION IN THE SLOPE AND DEEPWATER BASIN OF THE NORTH-CENTRAL SCOTIAN MARGIN**
Adam, Jürgen; Kreszek, Csaba; MacDonald, Cody; Campbell, Clarke; Cribb, Jonathan; Nedimovic, Mladen; Louden, Keith and Grujic, Djordje

**4D PHYSICAL MODELLING OF SALT TECTONICS IN SABLE SUB-BASIN, SCOTIAN MARGIN**
MacDonald, Cody; Campbell, Clarke; Cribb, Jonathan; Adam, Juergen; Nedimovic, Mladen; Louden, Keith and Kreszek, Csaba

**THERMAL EFFECTS OF SALT ON THE PETROLEUM SYSTEM: EVIDENCE FROM FISSION TRACK THERMOCHRONOLOGY, FLUID INCLUSIONS AND BASIN MODELLING**
Zentilli, Marcos; Wielens, Hans; Grist, Sandy M.; Kettanah, Yawooz; Negulic, Eric and Brown, Evan T.

**THE EVOLUTION OF THE PERDIDO FOLD BELT IN THE CONTEXT OF SALT TECTONICS OF THE NORTHWESTERN MARGIN OF THE GULF OF MEXICO – INSIGHTS FROM NUMERICAL MODELING**
Gradmann, Sofie and Beaumont, Christopher

**SEDIMENTARY BASINS IN THE CENTRAL AND SOUTH ATLANTIC CONJUGATE MARGINS: DEEP STRUCTURES AND SALT TECTONICS**
Mohriak, Webster Ueipass; Brown, David E. and Tari, Gabor C.

**BACK**

# NOTES

# Slopes, Basin Floors, Diapirs, and Canopies: Regional-Scale Salt-Sediment Interaction in the Northern Gulf of Mexico and the Scotian Offshore

**Mark G. Rowan**
Rowan Consulting, Inc.
850 8th Street
Boulder, CO, 80302
United States
e-mail: mgrowan@frii.com

## ABSTRACT

Salt diapirs and allochthonous canopies are well known from the northern Gulf of Mexico and the Nova Scotian offshore. Canopies can be divided into two end-member styles: salt-stock canopies, in which the canopy is linked to the autochthonous salt layer by vertical feeder diapirs and intervening minibasins are characterized by turtle structures; and salt-tongue systems, where the canopies are connected to the deep layer by counterregional welds that have basinward-dipping expulsion-rollover structures in their hanging walls.

The fundamental difference between the two styles is the degree of asymmetry. In salt-stock canopies, diapirs grow vertically and spread radially before amalgamating, and sub-canopy withdrawal geometries tend to be symmetrical. In salt-tongue canopies, diapirs grow up and basinward and extrude basinward, and the withdrawal basins are correspondingly asymmetric. Because both diapirs and allochthonous bodies grow passively at the sea floor, the simplest explanation for the difference is the slope of the sea floor. If it is horizontal, there will be no preferred direction of growth and extrusion, resulting in vertical diapirs and salt-stock canopies. If the sea floor slopes, diapirs will lean basinward and extrude salt tongues basinward. Thus, the structural style is largely determined by the evolving bathymetric profile of the passive margin, which in turn is controlled by the history of sediment progradation.

In the northern Gulf of Mexico, a regional boundary between more proximal salt-tongue canopies and more distal salt-stock canopies roughly parallels the margin and probably represents a long-lived base of slope initially established during Paleogene Wilcox deposition. In the Scotian deepwater, a similar boundary is oriented highly oblique to the margin, with vertical diapirs to the southwest (Shelburne Subbasin) and salt-tongue canopies to the northeast (Sable Subbasin). The structural boundary is located along the southwestern edge of the Upper Jurassic to Lower Cretaceous Mic Mac and Missisauga progradational system, and thus represents a lateral boundary to a broad slope to the northeast, with a basin floor along strike to the southwest. One of the key applications of this model is that it can be used to estimate the paleo-toe of slope and thus regional turbidite facies distribution, with channelized slope facies dominant in areas of salt-tongue canopies and ponded basinal facies more likely in areas with vertical diapirs and salt-stock canopies.

BACK

# Seismic Stratigraphy, Salt Structures and Thermal and Petroleum Systems Models across the Central Nova Scotia Slope Basin

**Keith Louden**
Department of Oceanography
Dalhousie University
Halifax, Nova Scotia B3H 4J1
Canada
e-mail: Keith.Louden@Dal.Ca

**P. K. Mukhopadhyay**
Global Geoenergy Research Ltd.
Halifax, Nova Scotia B3J 2A1
Canada
e-mail: muki@global-geoenergy.com

**Yue Wu**
**Eric Negulic**
**Mladen Nedimovic**
Department of Earth Sciences
Dalhousie University
Halifax, Nova Scotia B3H 4J1
Canada

## ABSTRACT

Two regional deep seismic profiles, GXT NovaSPAN 1400 and Lithoprobe 88-1A, are used to better characterize the sediment, salt and basement structures across the Central Nova Scotian Slope Province. Imaging of deeper structures is especially improved, using either pre-stack depth migration with the long offset streamer (NovaSPAN 1400) or a combination of pre-stack time migration and wide-angle velocity models (Lithoprobe 88-1A). Seaward of the salt, basement morphology and crustal velocities suggest that highly-stretched and rotated continental crustal blocks extend further into the ultra-deep basin. Beneath the salt, basement is also well-defined except locally beneath major salt diapirs.

Petroleum systems models are derived along the two profiles for various potential source rocks and reservoirs. Along both profiles, salt flank and salt crest Late Jurassic and Early Cretaceous reservoirs form the primary exploration targets. However, significant differences also exist for the two profiles, primarily associated with variations in salt structures. Along NovaSPAN 1400, the Jurassic Verrill Canyon formation is the main source rock for both the Jurassic and Cretaceous reservoirs. For the Early Cretaceous reservoir, hydrocarbons may contain a major volume of liquids (>75%) with an API of 45-55$^{o}$ and only mild overpressures. Along Lithoprobe 88-1A, Early Jurassic lacustrine and Late Jurassic salt-associated marine reservoirs are potential exploration targets, although these would lie within an over-pressured, dry-to-wet gas regime. Mass balance calculations for both seismic lines indicate that more preserved hydrocarbons are expected within the various reservoirs on NovaSPAN 1400.

Model calculations of present-day sea-floor heat flow predict a gradual landward reduction from 55 mW/m$^2$ in the ultra deep-water basin to 45 mW/m$^2$ on the upper slope. However, large variations are caused by high conductivity associated with salt diapirs, yielding values as high as 85 mW/m$^2$. In July 2008, we plan to take detailed measurements along both profiles in order to verify these predictions.

## Introduction

Rifting on the Scotian margin occurred in the Late Triassic to Early Jurassic (~230-190 Ma), when red beds, evaporites and dolomites formed in fault-controlled half-grabens (*e.g.* Jansa and Wade, 1975). Basement subsidence continued in three main post-rift periods during the Jurassic, Cretaceous and Tertiary. The result of this subsidence was to create a number of major sedimentary subbasins (Fig. 1). Most studies have previously been undertaken in the Sable Subbasin leading to the discovery of significant gas reserves. The sandstone reservoirs are located within shallow marine to deltaic sediments and are probably sourced from the Late Jurassic to Early Cretaceous prodelta to pelagic shales of the Verrill Canyon formation (Welsink *et al.* 1989; Wade and McLean 1990). Maturation of the source rock was accomplished by increased post-rift subsidence during the Late Jurassic to Early Cretaceous. Other, more minor occurrences of both gas and oil are associated with Early Cretaceous clastic sequences (Missisauga and Logan Canyon formations) and are related to the edge of the Late Jurassic Abenaki formation carbonate bank following the present shelf edge (Fig. 1).

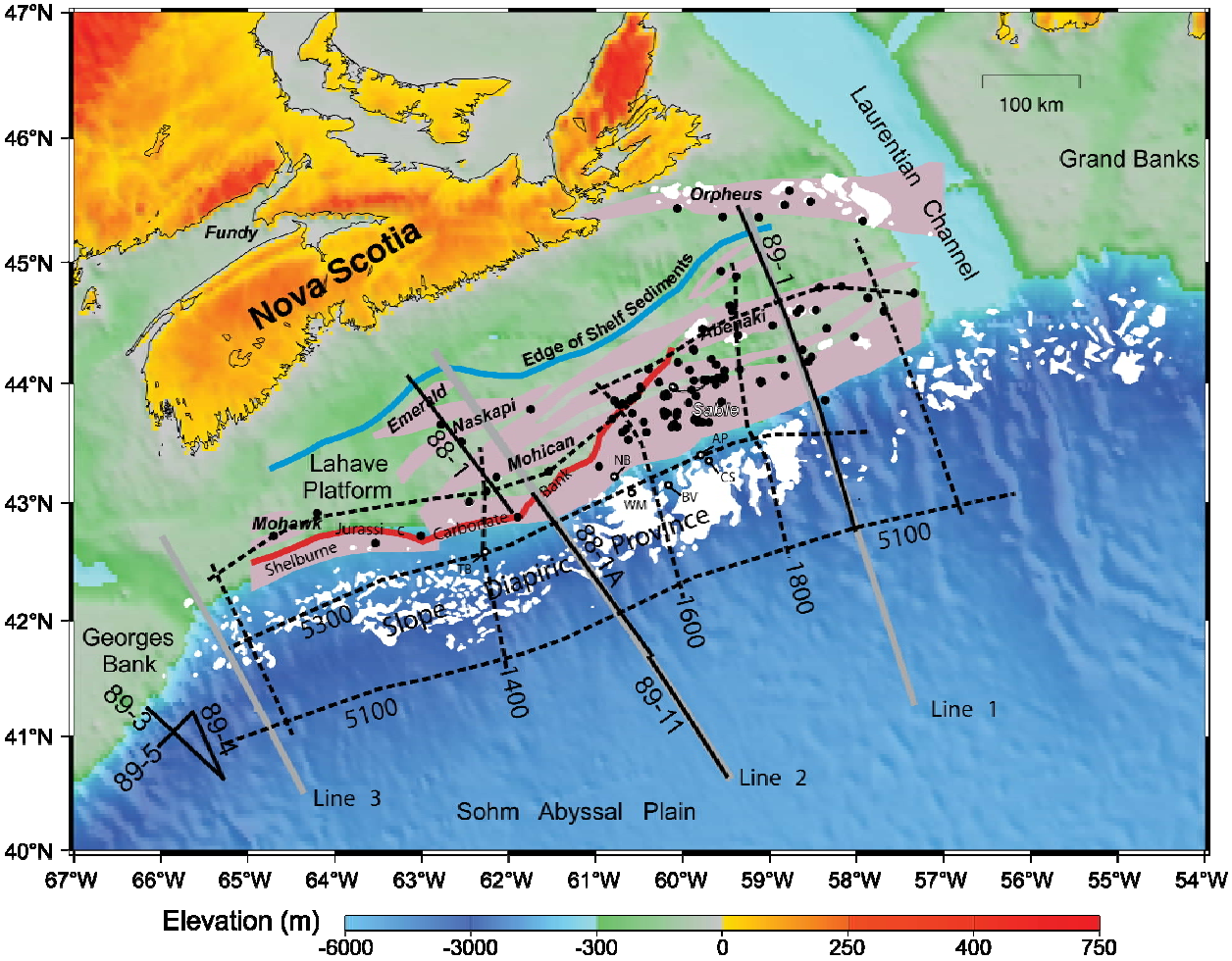


**Figure 1 Location map of seismic profiles and sediment structures across the Nova Scotian margin. Seismic profiles include GXT NovaSPAN MCS profiles (broken lines), Lithoprobe and BGR MCS profiles (solid black) and SMART wide angle profiles (solid gray). Sediment structures include shallow-water basins (solid pink fill) and boundaries of shelf sediment and Jurassic carbonate bank (blue and red lines) from Enachescu and Hogg (2005), and major salt bodies (white fill) from Shimeld (2004). Also shown are exploration wells (filled circles, with selected deep water wells identified as TB=Torbrook, NB=Newburn, WM=Weymouth, BV=Balvenie, AP=Annapolis, CS=Crimson) and shaded seafloor topography (colour scale).**

Further offshore, large thicknesses of sediment also occur beneath the lower continental slope and rise of the Sable and Shelburne subbasins (Fig. 1). It was expected that reservoirs for these deepwater prospects might be associated with Cretaceous and Early Tertiary channels, turbidites and fan deposits, trapped by the steep walls of salt diapirs (Hogg 2000) that extend along the margin within the Salt Diapiric Province southwest of seismic profile 89-1 (Fig. 1). The location of the salt previously had been used to mark the offshore boundary between the rifted continental crust and post-rift formation of oceanic crust. However, recent seismic models now suggest that highly thinned continental crust may in places extend well seaward of the salt (Wu *et al.* 2006) into the ultra-deep water basin (>4000 m). The apparent lack of reservoir indicated by more recent wells on the upper slope, and especially those closest to the Sable gas fields (Fig. 1), suggests the need for wider investigations of the petroleum system in other areas of the margin (Enachescu and Wach 2005). The purpose of this work is to produce petroleum systems models based on new interpretations of these seismic data across the entire region of potential hydrocarbon generation, beginning first with the central slope region.

## Seismic Profiles GXT1400 and Lithoprobe 88-1A

In this paper, we use two profiles, GXT NovaSPAN 1400 and Lithoprobe 88-1A, to better characterize the sediment, salt and basement structures across the Central Slope Province. Imaging of deeper structures in depth section is especially improved, using either pre-stack depth migration with the 9-km-long offset streamer (NovaSPAN 1400) or a combination of pre-stack time migration and wide-angle velocity models (Lithoprobe 88-1A; Wu 2007). Stratigraphic and lithologic interpretation of the profiles is shown in Figure 2, based on neighboring wells and previous interpretations (*e.g.* Kidston *et al.* 2002; Young 2005). Note, however, that there are no hard ties to these interpretations over most of the deep water and it is difficult to tie reflectors which much certainty across the salt. Seaward of the salt, basement morphology and crustal velocities on Lithoprobe 88-1A suggest that highly-stretched and rotated continental crustal blocks extend further into the ultra-deep basin. Beneath the salt, basement is also well-defined except locally beneath major salt diapirs.

## Petroleum System Models

Petroleum systems models, following on previous work by Mukhopadhyay (2006), are derived along the two profiles for various potential source rocks and reservoirs (*e.g.* Figs. 2 and 3). Along both profiles, salt flank and salt crest Late Jurassic and Early Cretaceous reservoirs form the primary exploration targets. However, significant differences also exist for the two profiles, primarily associated with variations in salt structures and stratigraphic thicknesses.

As revealed on line 88-1A, since 35 Ma the Jurassic Verrill Canyon and Cretaceous Verrill Canyon source rocks are situated within the wet gas and dry gas zone. They have expelled 90% of the generated hydrocarbons. The Early Jurassic lacustrine source rocks, which remain within the dry gas zone since 90 Ma, have been fully depleted in generated hydrocarbons (maturity >4% Ro). Distinct prospects of dry gas saturation exist within the syn-rift Early Jurassic reservoirs of the ultra-deep water (beyond 3500 m water depth). These hydrocarbons were solely saturated by the syn-rift Early Jurassic source rocks between 145 and 65 Ma. Although the reservoir contains more than 10% porosity, the reservoirs lie within a temperature $\geq 200^{\circ}$C and pore pressure >125 MPa. The Late Jurassic reservoirs contain a ratio of 90:10 dry to condensate that has not been fully charged with gas and oil until 65 Ma in two distinct expulsion phases. These reservoirs were mainly charged from the Jurassic Verrill Canyon source rock. The Early Cretaceous reservoirs contain a ratio of 60:10 dry gas and condensate. Although both the Late Jurassic and Early Cretaceous reservoirs may have a porosity >10-15%, both reservoirs will be within the overpressure regime.

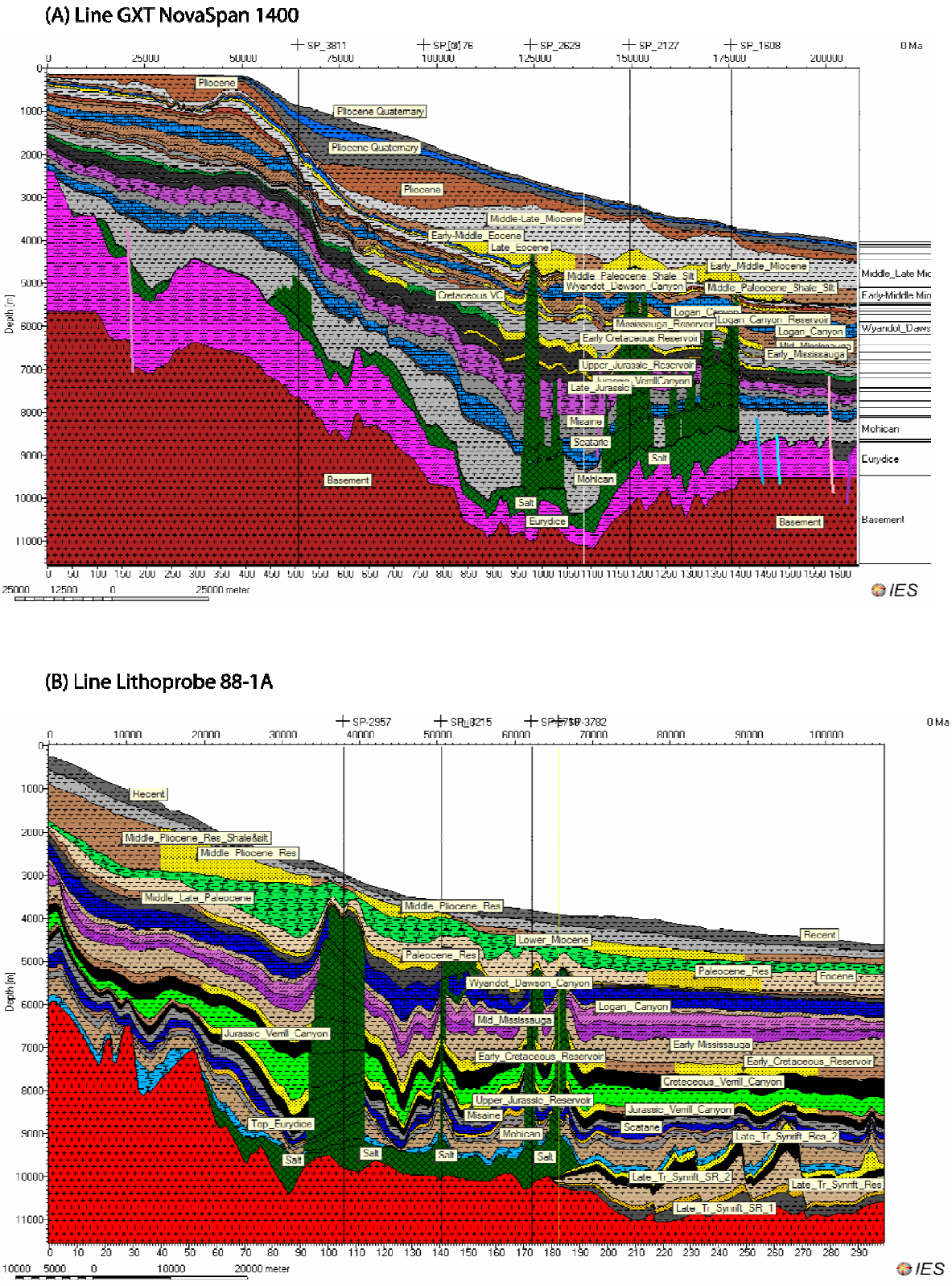


**Figure 2 Lithologic and stratigraphic units interpreted along seismic profiles (A) GXT NovaSPAN 1400 and (B) Lithoprobe 88-1A. Yellow dotted areas are conceptual target sandstone reservoirs and dark and medium gray units are potential source rocks, as identified.**

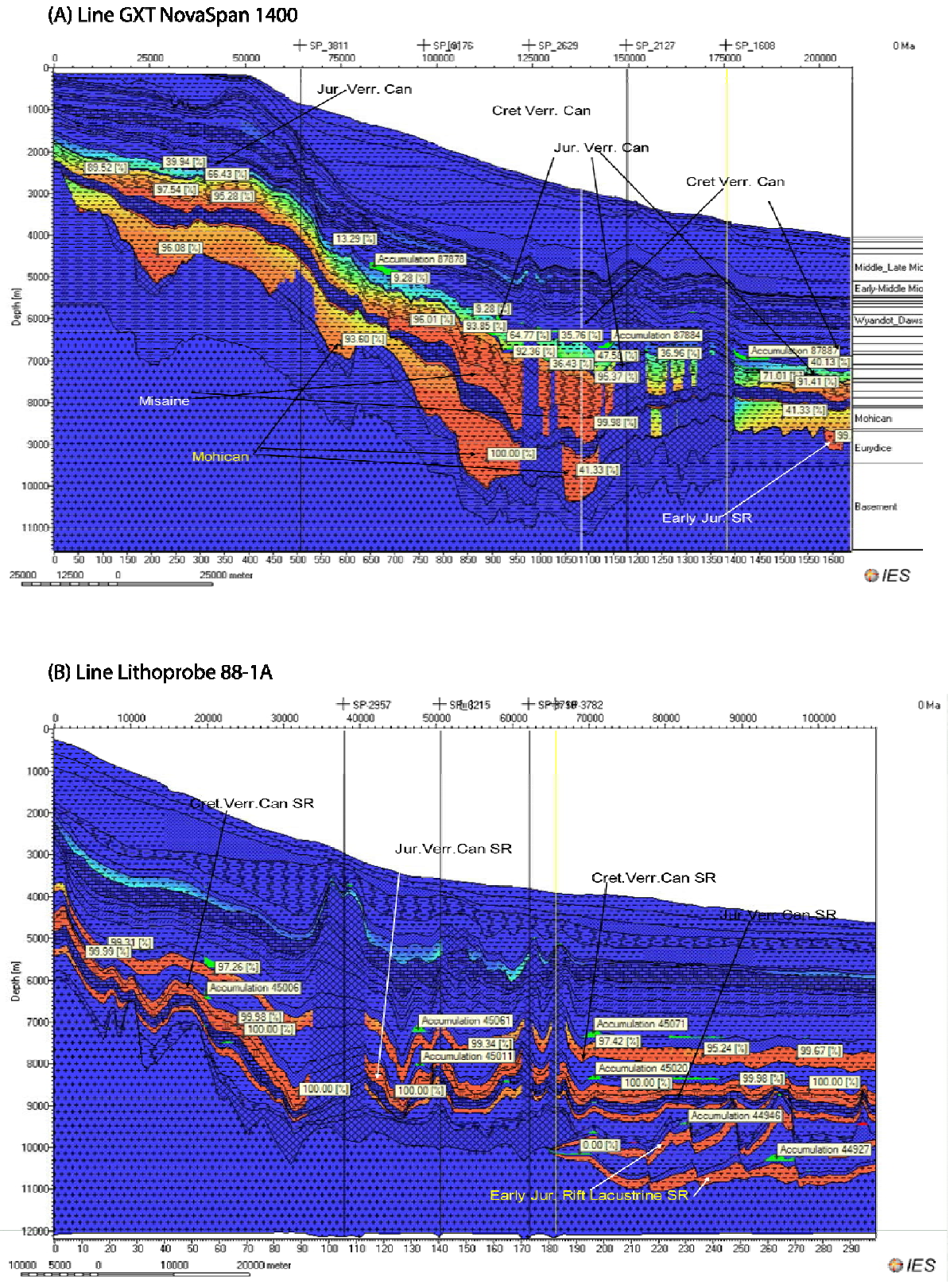


**Figure 3 Simulation output file showing the variations in hydrocarbon transformation ratios in various source rocks and target reservoirs for (A) GXT NovaSPAN 1400 and (B) Lithoprobe 88-1A.**

On line GXT NovaSPAN 1400, the Early Jurassic source rocks occur within the dry gas zone while both the Jurassic and Cretaceous Verrill Canyon source rocks still remain within the oil window (0.5% to 1.35% Ro). Only the source rocks older than the Jurassic Verrill Canyon have expelled more than 50% hydrocarbons. Jurassic Verrill Canyon source rocks have contributed major volumes of hydrocarbons within various reservoirs. The Late Jurassic and Early Cretaceous reservoir hydrocarbons will contain a major component of liquids (>75% for Early Cretaceous with 50% C15+; 40% [low C15+]). The Early Cretaceous reservoirs may lie within moderate pore pressure regime with a temperature <100ºC, while the Late Jurassic reservoirs would remain within the overpressure regime with a temperature >100ºC. These reservoir hydrocarbons were mainly derived from the Jurassic Verrill canyon source rocks. The Late Jurassic reservoir hydrocarbons may contain a liquid to gas mixture of 60:40 with an API of 55º.

**Table 1**

| Seismic Line | Total Mass Generated ($10^9$ kg/m$^3$) | Total Mass Expelled ($10^9$ kg/m$^3$) | Total Mass Accumulated ($10^9$ kg/m$^3$) | Total Hydrocarbons Lost ($10^9$ kg/m$^3$) | Main Hydrocarbon Reservoirs (%) |
|---|---|---|---|---|---|
| Lithoprobe 88-1A | 5253 | 4853 | 247 | 4601 | U. Jurassic (60%)<br>Syn-rift (34%) |
| NovaSPAN 1400 | 6906 | 3165 | 1326 | 1839 | E. Cretaceous (75%)<br>L. Jurassic (25%) |

## Summary

The mass balance reservoir hydrocarbons of both seismic lines (Table 1) indicate that more preserved hydrocarbons could be expected within various reservoirs for line GXT NovaSPAN 1400. For both lines, the salt flank and salt crest Late Jurassic and Early Cretaceous reservoirs could be best for future exploration targets. On line 1400, reservoir hydrocarbons may contain a major volume of liquids (>75% for Early Cretaceous with 50% C15+; 40% [low C15+]) with an API of 45-55º. Jurassic Verrill Canyon is the main source rock for both the Jurassic and Cretaceous reservoirs. On line 88-1A, Early Jurassic lacustrine and Late Jurassic salt-associated marine reservoirs could also become potential exploration targets for future exploration. Both data indicates that stratigraphically older reservoirs (Early Jurassic and Late Jurassic) could be future exploration targets. However, deep drilling is necessary in order to verify these predictions.

Model calculations of present-day sea-floor heat flow predict a gradual landward reduction from 55 mW/m$^2$ in the ultra deep-water basin, to 45 mW/m$^2$ on the upper slope. Within this trend, large variations are caused by high conductivity associated with salt diapirs, yielding values as high as 85 mW/m$^2$. There are presently only a few poorly resolved measurements across the slope (Lewis and Hyndman 1976). In July 2008, detailed measurements along both profiles are planned in order to verify these predictions.

## References

Enachescu, M.E. and Hogg, J.R.., 2005. Exploring for Atlantic Canada's next giant petroleum discovery. CSEG Recorder, 30 (5), p.19-30.

Enachescu, M. and Wach, G., 2005. Exploration offshore Nova Scotia: Quo vadis? Ocean-Resources, 23(3), 5p.

Hogg, J.R., 2000, The Scotian basin, new exploration trends for the nest decade, offshore Nova Scotia, Canada: GeoCanada 2000, Conference CD, Abstract No. 1096, 4p.

Jansa, L.F. and Wade, J.A., 1975, Geology of the continental margin off Nova Scotia and Newfoundland: in Offshore Geology of Eastern Canada, Vol. 2, Regional Geology, Van der Linden, W.J.M. and Wade, J.A. (Eds.), Geol. Sur. Can., Paper 74-30, p51-106.

Kidston, A.G., Brown, D.E., Altheim, B., and Smith, B.M., 2002. Hydrocarbon potential of the deep-water Scotian slope, Canada-Nova Scotia Offshore Petroleum Board, 111p.

Lewis, J.F., and Hyndman, R.D., 1976. Oceanic heat flow measurements over the continental margins of eastern Canada, Can. J. Earth Sci., 13, p.1031.

Mukhopadhyay, P.K., 2006. Evaluation of the petroleum systems by 1D and 2D numerical modeling and geochemical analysis in the area of most recent exploration wells on the deepwater Scotian slope, offshore Nova Scotia, Nova Scotia Department of Energy, unpublished report.

Shimeld, J., 2004. A comparison of salt tectonic subprovinces beneath the Scotian Slope and Laurentian Fan, in: Post, P.J. et al. (Eds.), Salt-sediment interactions and hydrocarbon prospectivity: Concepts, applications and case studies for the 21st century, Proc. 24th Bob Perkins Conf., Gulf Coast Section SEPM, p.291-306, CD-ROM, ISSN 1544-2462.

Wade, J.A. and McLean, B.C., 1990. The geology of the southeastern margin of Canada: in Keen, M.J. and Williams, G.L. (Eds.), Geology of the Continental Margin of Eastern Canada, The Geology of North America, Vol. I-1, Geol. Sur. Can., p.169-238.

Welsink, H.J., Dwyer, J.D., Knight, R.J., 1989. Tectono-stratigraphy of the passive margin off Nova Scotia: Extensional Tectonics and Stratigraphy of the North Atlantic Margin, Tankard, A.J. and Balkwill, H.R. (Eds.), Am. Assoc. Pet. Geol., Mem. 46, p.215-231.

Wu, Y., 2007. Crustal structure of the central Nova Scotia margin and the transition from volcanic to non-volcanic rifting off eastern Canada, Ph.D. thesis, Dalhousie University, 341p.

Wu, Y., Louden, K.E., Funck, T., Jackson, H.R., and Dehler, S.A., 2006. Crustal structure of the central Nova Scotia margin off Eastern Canada, Geophy. Jour. Int., 166, p.878-906.

Young, J.L., 2005. The stratigraphy and structural history of the Mesozoic and Cenozoic of the central Nova Scotian Slope, eastern Canada, M.Sc. thesis, Memorial University of Newfoundland, 229p.

**BACK**

# Basin-Scale Salt Tectonic Processes and Sediment Progradation in the Slope and Deepwater Basin of the North-Central Scotian Margin

**Jürgen Adam**
Department of Geology
Royal Holloway University of London
Egham, Surrey
United Kingdom
e-mail: j.adam@gl.rhul.ac.uk

**Csaba Kreszek**
Chevron Norge AS
Karenslyst Alle 2, P.O. Box 97
Sköyen, 0212 Oslo
Norway

**Louden, Keith**
Department of Oceanography
Dalhousie University
Halifax, Nova Scotia, B3J 3J5
Canada

**Cody MacDonald**
**Clarke Campbell**
**Jonathan Cribb**
**Djordje Grujic**
**Mladen Nedimovic**
Salt Dynamics Group
Department of Earth Sciences
Dalhousie University
Halifax, Nova Scotia, B3J 3J5
Canada

## ABSTRACT

The complex salt deformation styles characterizing the diverse Scotian Basin salt provinces are the result of complex basement topography in the narrow linked rift basins, variable salt thickness, and high clastic sediment input during the Jurassic and Cretaceous. Salt tectonics concepts developed in salt basins around the Atlantic margins cannot be adapted reliably to the Scotian margin. Consequently, the next generation of basin models must investigate the role of the unique basin characteristics including palaeogeography, sediment supply, and rift basin geometry.

Basin-scale seismic sections of the GXT NovaSPAN data allow structural modelling and provide the parameter for scaled physical experiments of regional transects of the Laurentian, Abenaki, and Sable subbasins extending from the shelf to the deepwater basin. The Salt Dynamics Group utilizes physical experiments to analyze salt tectonic processes and their interaction with depositional systems. 4D strain data and experiment sections enable mechanical modelling of salt tectonic processes from early post-rift salt mobilization to late post-rift allochthonous salt complexes. Salt tectonic concepts derived from our experiments relate characteristic salt structures to the palaeo-depositional environment and kinematic stages of the basin evolution.

Our study demonstrates that the Scotian salt provinces differ strongly from the salt basins of the Gulf of Mexico and the younger South Atlantic salt basins. Low mechanical coupling of the sediment overburden due to thick original salt in narrow linked rift basins has favored rapid down-building and sediment aggradation rather than progradation in the early post-rift stage. Salt mobilization and basinward salt inflation started in the Laurentian Basin and propagated in southward direction along the margin due to shelf-parallel sediment transport sourced by the Laurentian Fan from the NE. This depositional pattern has led to diachronous salt extrusion shown by southward younging of allochthonous salt complexes in the North-Central Scotian Basin.

BACK

# 4D Physical Modelling of Salt Tectonics in Sable Subbasin Scotian Margin

**Cody MacDonald**
**Clarke Campbell,**
**Jonathan Cribb**
**Mladen Nedimovic**
Salt Dynamics Group
Department of Earth Sciences
Dalhousie University
Halifax, Nova Scotia, B3J 3J5
Canada
e-mail: macdonc2@dal.ca

**Jürgen Adam**
Department of Earth Sciences
Royal Holloway University of London
Egham, Surrey, TW20 0EX
United Kingdom

**Keith Louden**
Department of Oceanography
Dalhousie University
Halifax, Nova Scotia, B3J 3J5
Canada

**Csaba Kreszek**
Chevron Norge AS
Karenslyst Alle 2, P.O. Box 97
Sköyen, 0212 Oslo
Norway

## ABSTRACT

Salt tectonic structures of the interconnected Sable, Abenaki, and Laurentian sub-basins at the north-central Scotian margin indicate variable rift-basin geometries and tectono-sedimentary environments with high rates of sedimentation and progradation during the Jurassic and Early Cretaceous. The understanding of the deepwater tectono-stratigraphic framework in this area depends on our ability to accurately interpret the variable depositional systems and corresponding salt tectonic structures in these sub-basins.

This study integrates seismic interpretation with analogue experiments to gain insight into the mechanics of thin-skinned deformation and halokinetic sequence stratigraphy in the Sable sub-basin. The experimental setup including salt basin morphology, sedimentation patterns and rates, and initial salt thickness is determined using the GXT NovaSPAN survey and other public domain seismic reflection and well data. The initial salt basin morphology is modeled as two rift half grabens. Variable original salt thickness combined with high, shelf-oblique, sediment input in landward salt-withdrawal basins during the Middle Jurassic to Early Cretaceous has caused major salt inflation in the mid to distal salt basin. This inflated salt complex had a positive, pronounced, and irregular topography that resulted in localized depocentres throughout the Early to Late Cretaceous. These localized depocentres of the deepwater slope and basin have led to the development of a confined mini-basin bounded by a salt wall or diapir and an extensive allochthonous salt tongue. A compressional phase is seen during the Late Cretaceous in features such as thrusted packages of rafted sediments over a salt pillow and squeezed diapirs.

The next phase of the study will focus on the 3D depositional patterns of the entire north-central Scotian margin to analyze the linked structural evolution of the Laurentian, Abenaki, and Sable sub-basins. Improved understanding of the structurally dynamic depositional system of the Scotian Basin will support future exploration activities in the slope and deepwater basin.

BACK

# Thermal Effects of Salt on the Petroleum System: Evidence from Fission track Thermochronology, Fluid Inclusions and Basin Modelling

**Marcos Zentilli**
**Yahwooz Kettanah**
**Eric Negulic**
Department of Earth Sciences
Dalhousie University
Halifax, Nova Scotia B3H 4J1
Canada
e-mail: marcos.zentilli@dal.ca

**Hans Wielens**
Geological Survey of Canada – Atlantic
NRCAN
Dartmouth, Nova Scotia B2Y 4A2
Canada
e-mail: hwielens@nrcan.gc.ca

**Alexander M. Grist**
Department of Earth Sciences
University of Queensland
Brisbane, Queensland 4072
Australia

**Evan T. Brown**
MGM Energy Corporation
4100, 350 Seventh Ave. SW
Calgary, Alberta T2P 3N9
Canada
e-mail: evan.brown@mgmenergy.com

## ABSTRACT

The thermal conductivity of salt is up to four times greater than other sedimentary rocks, thus salt diapirs focus geothermal heat resulting in a high-temperature anomaly in overlying basinal sediments. Depending on the shape of the salt body and its depth, the heat flow over the salt can be 2 to 3 times greater than away from the salt, with consequent drastic effects on diagenesis and hydrocarbon maturation; *i.e.*, over mature above, and under mature below salt. In addition to heat conduction, advection of warm fluids (brines, oil and gas) produces highly localized heat anomalies on top of diapirs, as previously proposed by others for offshore Atlantic Canada.

In the Maritimes basin, Early Carboniferous salt of the Windsor Group has risen to the surface locally from a depth of ca. 8 km. Apatite fission track data indicate that the basin was inverted and rocks now at surface cooled below ca. 100°C during the Triassic-Jurassic Atlantic margin breakup, whereas apatite within siltstone in the salt diapir yields apparent Cretaceous ages; the temperature-sensitive fission-track lengths having been significantly shortened (equivalent to what happens >3 km depth in a well). Time-temperature modelling of the data requires re-burial of the salt structure post-Early

Cretaceous, and heating the diapir to higher temperatures than the regional background, confirming the focused thermal effects of the diapir. We have demonstrated similar thermal effects from evaporite diapirs in the Sverdrup Basin in the Canadian Arctic.

We have studied fluid inclusions in autochthonous and allochthonous salt in Atlantic Canada. Supposedly impermeable salt contains a variety of generations of fluid inclusions, some with brines, some with oil and gas. It is evident that salt has been permeable to various fluids. Entrapment temperatures of the fluids vary from 25°C to more than 100°C. For autochthonous Jurassic salt this implies a sub-salt source rock or an algal source within the salt.

Modelling of Scotian Basin wells; *e.g.*, Wyandot, using Petromod® shows that the presence of salt in the stratigraphic column results in drastic changes in the thermal evolution of the petroleum system.

## Introduction

In this paper we show that salt can have a fundamental thermal effect on the petroleum system of the Atlantic margin. The thermal conductivity of salt is up to four times greater than other sedimentary rocks (*e.g.* Evans 1977), thus salt diapirs focus geothermal heat flow resulting in a high-temperature anomalies in overlying basinal sediments. Depending on the shape of the salt body and its depth, the heat flow in the salt can be 2 times greater than away from the salt, with consequent drastic effects on diagenesis and hydrocarbon maturation; *i.e.,* over mature above, and under mature below salt. In addition to heat conduction, advection of warm fluids (brines, oil and gas) produces highly localised heat anomalies on the sides and top of diapirs. In Atlantic Canada, anomalously high heat flow values were detected in wells in the proximity of salt (*e.g.* Lewis and Hyndman 1976; Rashid and McAlary (1977), Rashid 1978, Issler 1984, Keen and Beaumont 1990), with geothermal gradients varying from about 20 to 34ºC/km, the highest values being due to salt in the subsurface. Keen (1983) proposed that upward circulating warm basinal fluids must be involved to explain the abrupt thermal effect at the diapir/clastic rock boundary.

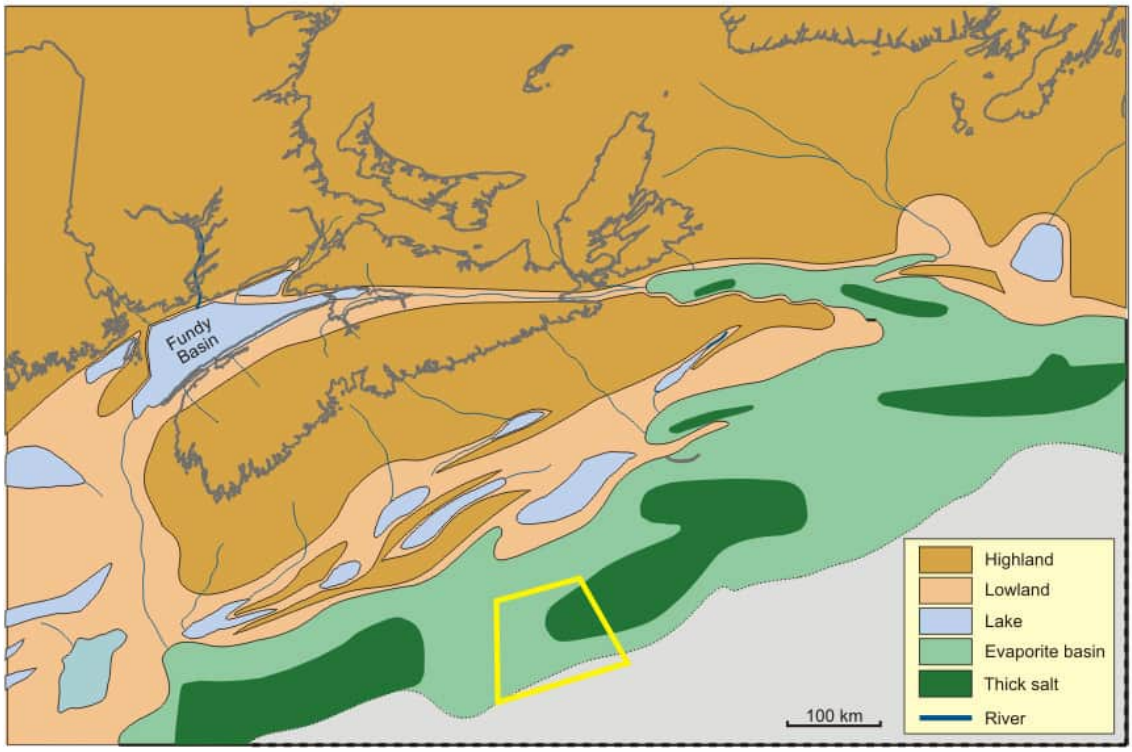

**Figure 1. Paleogeography and distribution of Triassic-Jurassic (Argo) salt (green) in the Scotian Basin. Modified from Wade & MacLean (1990) and "The Last Billion Years" Atlantic Geoscience Society Special Publication #15 (2001). Area for Fig. 5 model is delineated in yellow.**

Salt of Triassic-Jurassic depositional age (Argo Fm.) is ubiquitous in parts of the Scotian Basin (Fig. 1). In the Maritimes Basin to the north of Nova Scotia, Early Carboniferous salt of the Windsor Group has risen to the surface as a large number of diapirs, locally from a depth of 8 km. Apatite fission track data (*e.g.* Ryan and Zentilli 1993; Li *et al.* 1995; Grist *et al.* 1995; Grist and Zentilli 2003) indicate that the basin was inverted and rocks now at surface cooled below ca. 100ºC during the Triassic Atlantic margin breakup. However, apatite within siltstone near surface within a diapir being exploited for road salt in the Magdalen Islands (Mines Seleine) yields the youngest cooling ages; the temperature-sensitive fission-track lengths having been significantly shortened (Fig. 2), evidence for having been heated to the equivalent to what happens >3 km depth in a well; we have demonstrated similar thermal effects from evaporite diapirs in the Sverdrup Basin in the Canadian Arctic (Zentilli *et al.* 2006a, b).

We have studied fluid inclusions in autochthonous and allochthonous salt in Windsor Group (Carboniferous) salt and Argo (Triassic-Jurassic) salt. The salt contains a variety of generations of fluid inclusions, some with brines, some with oil and gas (Fig. 3). Although temperature data from salt must be considered carefully because of the weakness of halite (*e.g.* Roedder 1984), it is evident that salt has been permeable to various fluids during its history; fluids were trapped during deposition as well as later in the basin's evolution. For example, Argo salt in the Osprey G-84 well yields homogenisation temperatures (minimum temperatures of brine entrapment) clustered around 32ºC and 125ºC (secondary inclusions).

Petroleum-rich inclusions observed in autochthonous Argo salt require a within-salt algal source, or a sub-salt petroleum source, demonstrating that the petroleum system of the Scotian Basin may be more complex than previously envisaged.

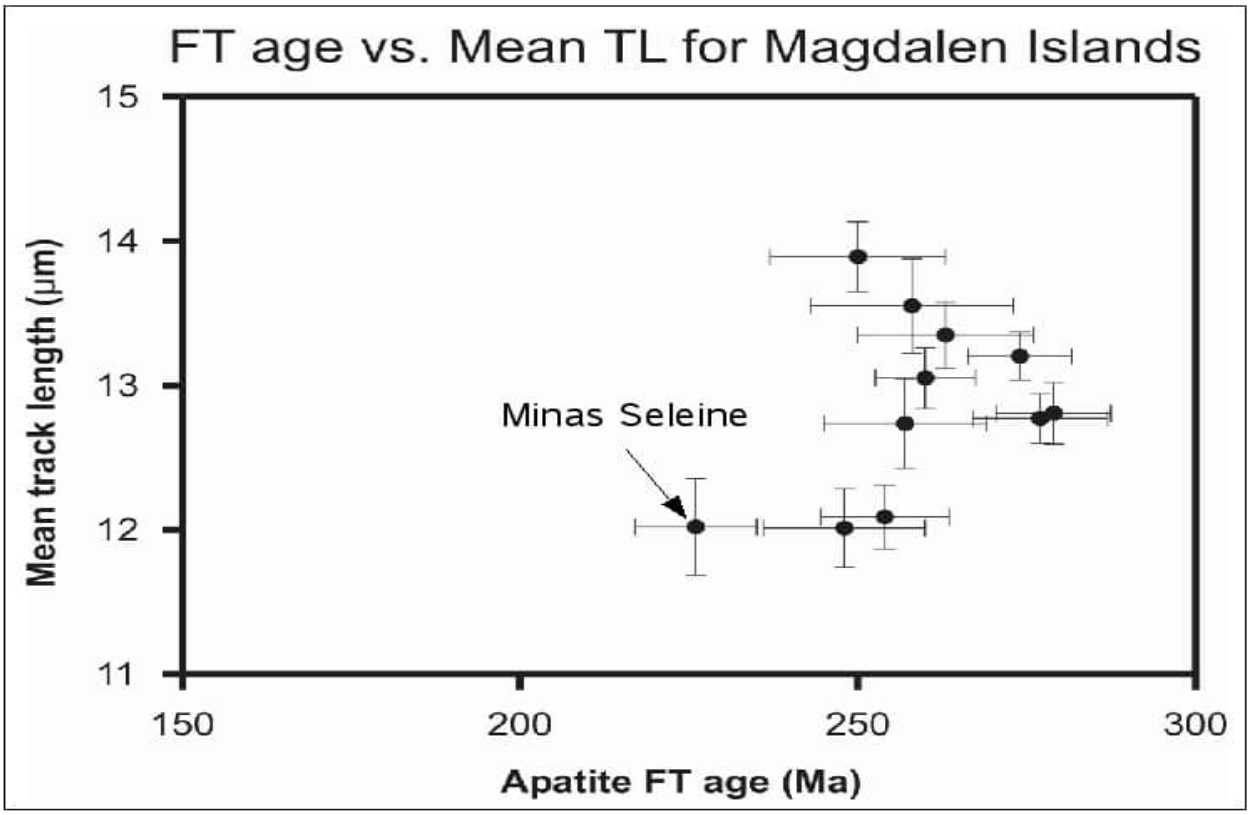


**Figure 2. Plot of apatite fission-track length versus apparent age for a suite of rocks from the Magdalen Islands, Quebec. The apatite from siltstone within the salt mine (Mines Seleine) yields short tracks and the**

**youngest age, indicating it has remained hotter than in the rocks away from the salt diapir. Time-temperature modelling of apatite fission-track length data (*e.g.* Grist and Zentilli 2003) suggests the rocks were the warmest of the suite, and remained so even into post- Cretaceous times (Zentilli *et al.*, 2006a).**

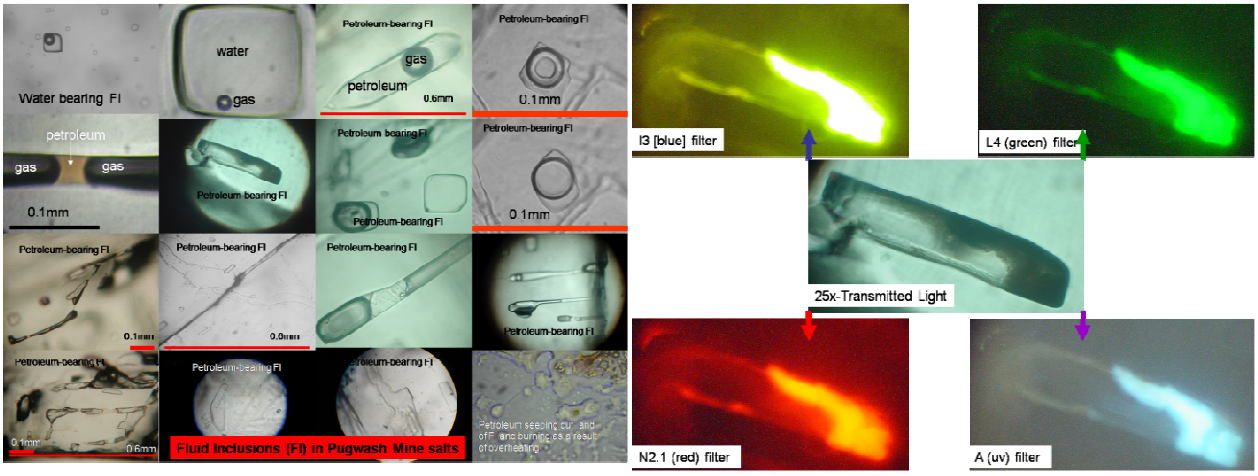


**Figure 3. Brine and petroleum-rich fluid inclusions in salt from the Pugwash Mine, Nova Scotia (left). Fluorescence microscopy (right) indicates the presence of complex hydrocarbons in the inclusions. From Kettanah *et al.* (2004).**

Halite is generally assumed to be extremely impermeable to brines and hydrocarbons, yet our fluid inclusions study demonstrates that brines and hydrocarbons permeated the salt in more than one occasion. This observation is compatible with recent studies of deeply buried salt, which indicate considerable water-halite interaction. For instance, Lewis and Holness (1996) demonstrated experimentally that in sedimentary basins with normal geothermal gradients, halite bodies at depths exceeding 3 km will contain a stable interconnected brine-filled porosity, resulting in permeabilities comparable to those of sandstones. Therefore, salt must be considered having been a conduit for brines and hydrocarbons and advective heat rather than merely a seal as traditionally assumed.

(Continued on next page.)

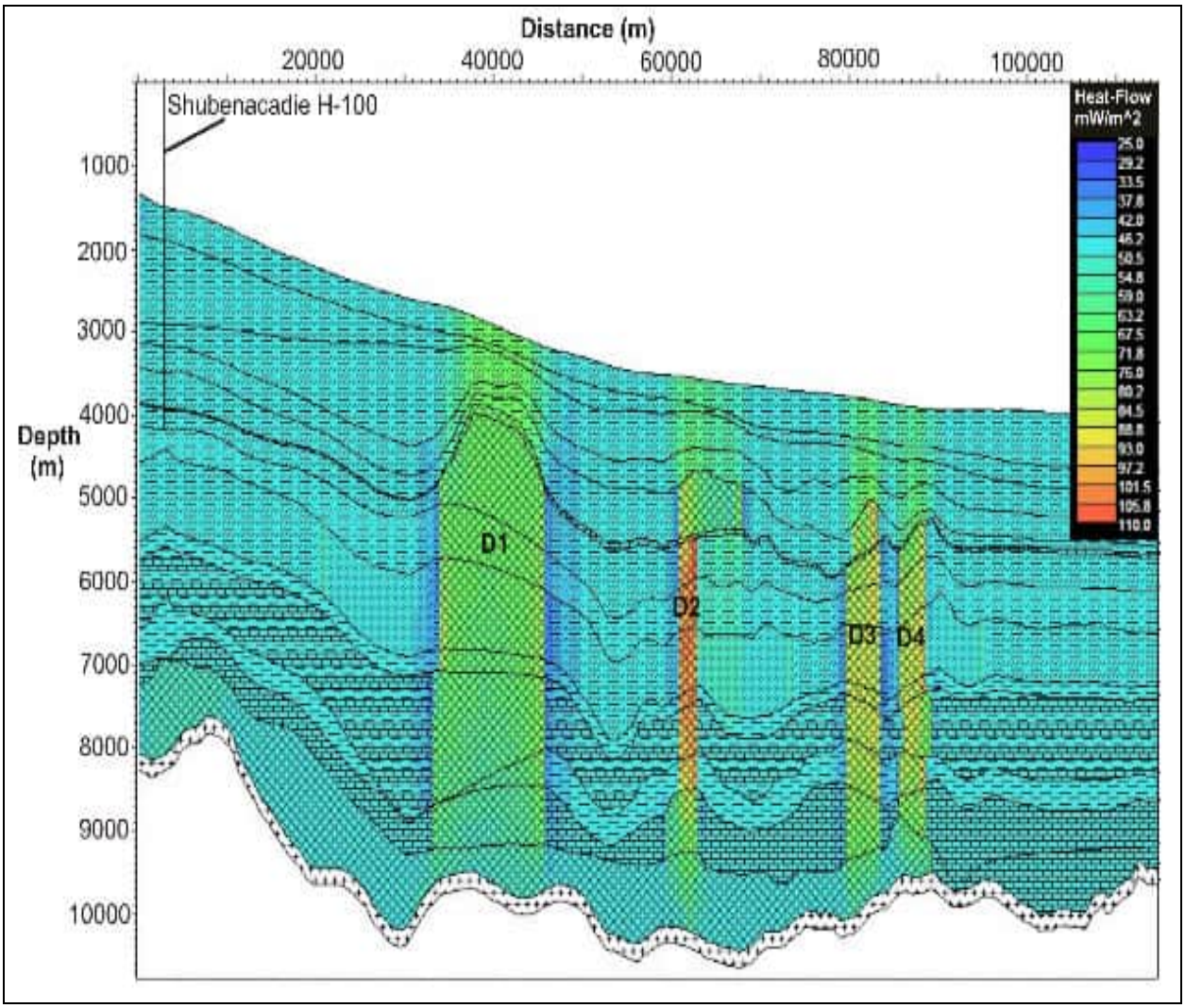


**Figure 4. Cross section through a Petromod® model with salt diapirs, along seismic line 88-1a, showing the effect of salt diapirs (D1-D4) on heat-flow. The lithology is outlined by the black patterns, salt being cross-hatched. The colours indicate the heatflow, red being high, blue is low. Note the cooling effect of most of the diapirs to their sides. The canopy on D2 also increases heatflow above it. From Negulic (2008).**

The petroleum system can now be analyzed best in a comprehensive way using specialised software in a 1D mode (*e.g.* Jones *et al.* 2007) and 3D mode (*e.g.* Wielens *et al.* 2006).

Modelling of Scotian Basin wells using Petromod® (Figs. 4, 5) demonstrates that the presence of salt in the stratigraphic column results in drastic changes in the thermal evolution of the petroleum system. PetroMod10® (Integrated Exploration Systems, Germany) was chosen for model construction and simulation; the software deals effectively with the presence of salt in the system.

(Continued on next page.)

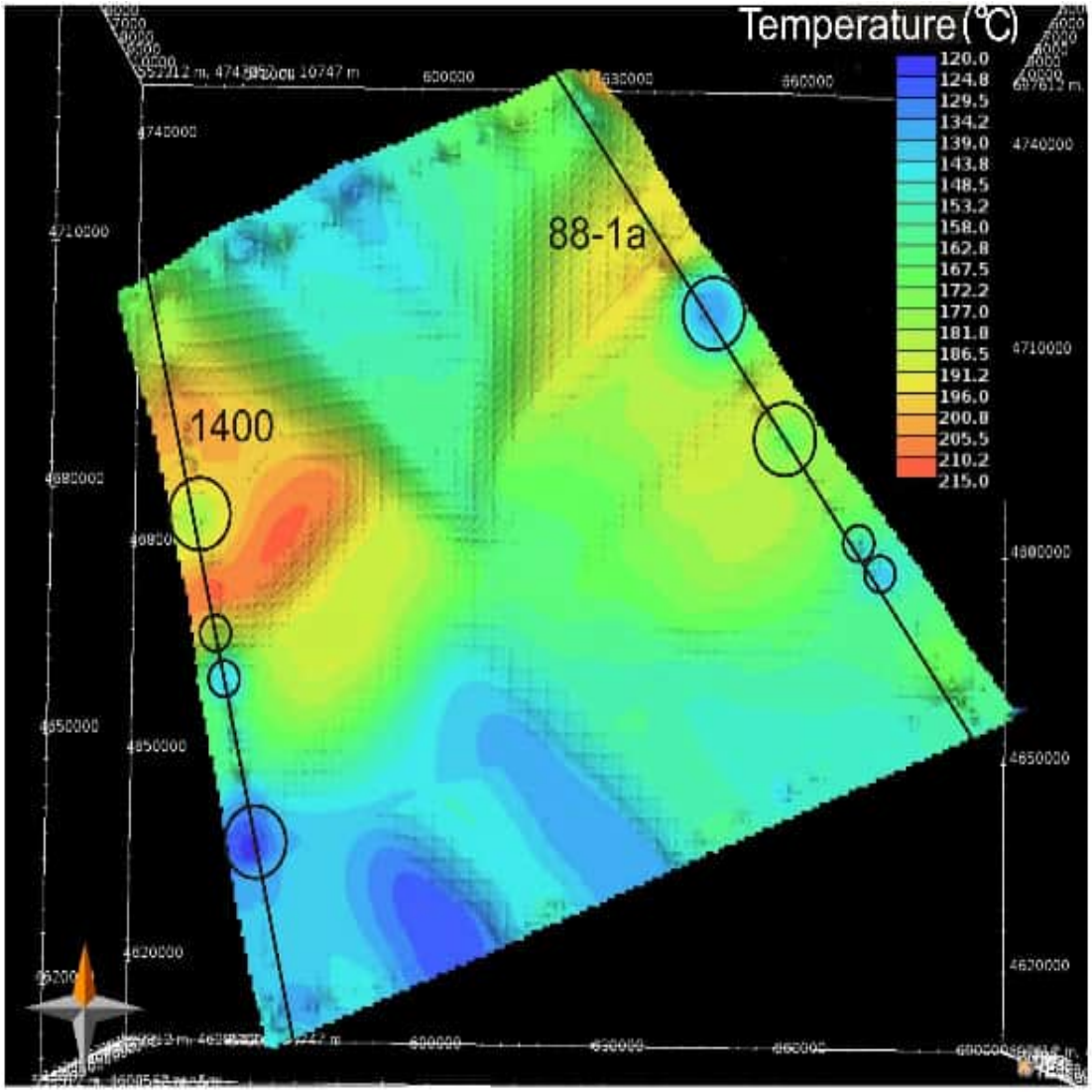


**Figure 5. This 3D basement image from a Petromod® model (area outlined in yellow in Fig. 1) shows the temperature effects of the diapirs. The colours indicate the temperature, red being high, blue is low. The circles show where the diapirs are. Heat flow is anomalously low below some diapirs, potentially leading to relative under-maturity of source rocks. From Negulic (2008).**

## Conclusions

- Heat flow measurements have demonstrated that salt, due to its relatively high thermal conductivity (in comparison with sandstones and shales) is associated with positive thermal anomalies above it.
- These thermal anomalies have been long-lasting, can be detected by apatite fission track thermochronology, and these time-temperature data are important to the petroleum system.
- Brine and petroleum-bearing fluid inclusions in salt provide evidence for past permeability of the salt and lead to recognise the possibility of an in-salt (algal) petroleum source and/or a sub-salt petroleum source in the Scotian Basin.
- Petroleum systems modelling that takes into consideration all available data shows that salt can produce positive thermal anomalies above and negative thermal anomalies below and adjacent to salt in the Scotian Basin.

## Acknowledgments

This research has been funded by Petroleum Research Atlantic Canada (PRAC), the Natural Sciences and Engineering Research Council of Canada (NSERC). The Geological Survey of Canada – Atlantic has supported the research on fluid inclusions and basin modelling.

## References

Atlantic Geoscience Society, 2001. The Last Billion Years. A Geological History of the Maritime Provinces of Canada: Atlantic Geoscience Society Special Publications No.15, 212p.

Evans, T.R., 1977. Thermal properties of North Sea rocks: Log Analyst, v.18, p.3-12.

Grist, A., R.J. Ryan and M. Zentilli, 1995. The thermal evolution and timing of hydrocarbon generation in the Maritimes Basin of eastern Canada, from apatite fission track data: Bulletin Canadian Society of Petroleum Geologists, v.43, no.2, p.145-155.

Grist, A.M., and M. Zentilli, 2003. Post-Paleocene Cooling in the Southern Canadian Atlantic Region: Evidence from Apatite Fission Track Models: Canadian Journal of Earth Sciences, v.40, no.9, p.1279-1297.

Issler, D., R., 1984. Calculation of organic maturation levels for offshore eastern Canada-implications for general application of Lopatin's method: Canadian Journal of Earth Sciences, v.21, p.477 -488.

Jones, S.F., H. Wielens, M-C. Williamson and M. Zentilli, 2007. Impact of magmatism on hydrocarbon systems of the Sverdrup basin, Canadian Arctic Islands, Nunavut; a numerical modelling study: Journal of Petroleum Geology, v.30, no.3, p.237-256.

Keen, C.E., 1983. Salt diapirs and thermal maturity, Scotian Basin: Bulletin Canadian Society of Petroleum Geologists, v.31, p.101-108.

Keen, C.E. and C. Beaumont, 1990. Geodynamics of continental margins. Chapter 9 *in*: M.J. Keen and G.L. Williams (Eds.), Geology of the Continental Margin of Eastern Canada. Geological Survey of Canada, Geology of Canada, no 2, p. 391-472.

Kettanah, Y., M. Zentilli M. and H. Wielens, 2004. Pilot study on fluid inclusions in salt (halite) from the Osprey H-84 well, Carson Sub-basin, Grand Banks, Newfoundland: Atlantic Geology, v.40, no.1, p.144-145.

Lewis, S. and M. Holness, 1996. Equilibrium halite-H2O dihedral angles: High rock-salt permeability in the shallow crust?: Geology, v.24; no.5; p.431-434.

Lewis, J. F., and R.D. Hyndman, 1976. Oceanic heat flow measurements over the continental margins of eastern Canada: Canadian Journal of Earth Sciences, v.13, p.1031-1038.

Li, G., C.E. Ravenhurst, and M. Zentilli, 1995. Implications of apatite fission track analysis for the thermal history of the Scotian basin, offshore Nova Scotia, Canada: Bulletin Canadian Society of Petroleum Geologists, v. 43, no.2, p.127-144.

Negulic, E., 2008. 4D Thermal and Petroleum Systems Modelling of the Central Scotian Slope in and around the Eastern Shelburne Sub-Basin: Unpublished B.Sc. (Honours) Thesis, Dalhousie University, Department of earth Sciences, 88p.

Rashid, M.A. and J.D. McAlary, 1977. Early maturation of organic matter and genesis of hydrocarbons as a result of heat from a shallow piercement salt dome: J. Geochem. Expl., v.8, p.549-569.

Rashid, M.A., 1978. The influence of a salt dome on the diagenesis of organic matter in the Jeanne d'Arc Subbasin of the northeast Grand banks of Newfoundland: Org. Geochem, v.1, p.67-77.

Roedder, E., 1984. The fluids in salt: American Mineralogist, v.69; no.5-6, p.413-439.

Ryan, R. and M. Zentilli, (1993) Allocyclic and thermochronological constraints on the evolution of the Maritimes Basin of Eastern Canada: Atlantic Geology, (ISSN -0843-5561), v.29, p.187-197.

Wade, J.A. & B.C MacLean, 1990. The geology of the southeastern margin of Canada, Chapter 5 *in*: M.J. Keen and G.L. Williams (Eds.), Geology of the Continental Margin of Eastern Canada. Geological Survey of Canada, Geology of Canada, no 2, p.169–238.

Wielens, J.B.W., C.D. Jauer, and G.L. Williams, (2006). Is there a viable petroleum system in the Carson and Salar basins, offshore Newfoundland?: Journal of Petroleum Geology, v.29, no.4, p.303-326.

Zentilli, M., A.M. Grist, M.C Williamson, 2006a. Paleothermal effects of salt diapirs detected by apatite fission track thermochronology and (U-Th)/He dating: Poster #35, European Conference on Thermochronology, 30 July–04 August 2006, Bremen (Germany).

Zentilli, M., A.M. Grist, M.C Williamson, D.T Andersen, & W. Pollard, 2006b. Thermal effects of warm fluid circulation associated with the rise of evaporite diapirs in the east-central Sverdrup Basin, Canadian Arctic Archipelago: Atlantic Geology, v.42, no.1, 125.

**BACK**

# The Evolution of the Perdido Fold Belt in the Context of Salt Tectonics of the Northwestern Gulf of Mexico: Insights from Numerical Modelling

**Sofie Gradmann**
**Christopher Beaumont**
Department of Earth Sciences
Dalhousie University
1355 Oxford Street
Halifax, Nova Scotia, B3H 4J1
Canada
e-mail: s.gradmann@dal.ca

## ABSTRACT

The Perdido Fold Belt is a prominent salt-cored deep-water structure in the northwestern Gulf of Mexico. In the last decade it has become a major target for hydrocarbon exploration. It is characterised by a unique geometry (thick, pre-kinematic, kink-folded sedimentary section, lack of significant syn-kinematic sedimentation, seaward tilt of the fold envelope) and its location above the pinch-out of the autochthonous salt and adjacent to and below the extensive Sigsbee Salt Canopy.

We use 2D finite-element models to study the evolution of the PFB by gravitational spreading during sediment progradation, in which a viscous salt layer is overlain by a frictional-plastic passive margin sedimentary sequence. Model experiments include sediment compaction, flexural isostasy, loading by the overlying water column, and parametric calculations of the effects of pore-fluid pressures in the frictional-plastic sediments.

Limit analysis calculations of the stability of this system reveal that the PFB can have formed by gravity spreading alone if moderately high pore-fluid pressure ratios of approximately 0.8 developed. Under these circumstances, the numerical finite-element model fold belt shows good correlation with the kink-type folds, geometry and dimensions of the PFB. Timing, rate, and extent of folding in the model fold belt are shown to be controlled by the system parameters of overburden strength, continental slope width, salt thickness, and salt viscosity. Variability in the latter two generates two end-member fold belt types: toe-of-slope folding that propagates progressively seaward, and synchronous toe-of-salt folding above the distal section of the salt layer. The numerical model results are interpreted to imply that landward Cretaceous toe-of-slope folding started long before the Oligocene-Miocene folding of the PFB. This allowed proximal allochthonous salt structures to develop through breached anticlines in the propagating fold belt while distal sedimentation continued. Only later did folding propagate and fold the PFB, which represents only the nose of a much older and larger fold belt.

## Introduction

The Perdido Fold Belt (PFB) in the northwestern Gulf of Mexico (GoM) is a prominent deep-water salt-tectonic structure that has recently become a focus of intensive hydrocarbon-related studies, but still remains imperfectly understood. Deep-water fold and thrust belts develop on continental margins as a result of gravity spreading and gliding above a weak substratum (such as salt) which produces paired proximal extensional and distal compressional domains.

The PFB is the best studied salt-cored deep-water fold belt worldwide and several unique features distinguish it from many other deep-water fold belts. These include the large, 4.5 km, thickness of the pre-kinematic section and the absence of earlier folding, the highly symmetric kink folds extending for

60-100 km, the seaward tilt of the entire fold belt, the almost synchronous evolution of its folds within less than 10 Ma during Oligo-Miocene times and its vicinity to the large allochthonous salt structure of the Sigsbee Canopy.

The goal of this work is to explain the first-order structures of the PFB in a dynamical context by comparing its evolution with those of a series of finite element model experiments. The modelling is designed to place quantitative constraints on the conditions under which the PFB may have evolved (overburden strength and geometry, sedimentation rates, salt thickness, salt geometry and salt viscosity), to test whether the system was driven by gravity alone, and to enhance the general understanding of the evolution of gravity-driven deep-water fold belts.

## Limit Analysis for Stability of Continental Margin

Gemmer *et al.* (2005) developed an analytic description for the forces acting on a simplified salt bearing continental margin. By balancing the seaward and landward acting forces, a description of the condition of failure can be obtained. We expand the existing calculations to include the isostatic response to sediment loading and a description of pore-fluid pressure that is related to the mean stress instead of the lithostatic stress and apply it to the Oligocene northwestern Gulf of Mexico. Using estimated values for the geometry of the salt basin and sedimentary overburden as well as respective densities, we obtain values for the maximum sediment strengths that allows gravity spreading to set in of $\varphi_{eff}$=5-6.5°. The effective angle of friction $\varphi_{eff}$ is a combination of internal angle of friction of the dry sediment $\varphi_0$ and pore-fluid pressure ratio $\lambda$ ($\sin \varphi_{eff} = (1- \lambda) \sin \varphi_0$). For fine grained clastic material ($\varphi_0$=25°), the implied pore-fluid pressures correspond to $\lambda$=0.8, representing moderately overpressured sediments, commonly found in large, deep sedimentary basins subject to rapid sedimentation. The outcome of the limit analysis shows that gravity spreading alone can be responsible for the formation of the PFB, provided overpressures of this level developed.

## Numerical Modelling

We use 2D finite-element models in which frictional-plastic sediments overlie a viscous salt layer. The models comprise a passive margin sedimentary sequence from shelf to deep water to account for the dynamical interaction of gravity spreading caused by shelf progradation. Model experiments include sediment compaction, flexural isostasy, loading by the overlying water column as well as parametric calculations of the effects of pore fluid pressures in the frictional-plastic sediments.

A reference model that represents a simplified configuration of the Oligocene northwestern Gulf of Mexico continental margin shows the development of a deep-water fold belt driven by gravity spreading (Fig. 1A, B). The salt basin is 260 km wide and 3 km thick, salt has a viscosity of $10^{18}$ Pas and a density of 2200 kg/m$^3$, sediment strength ($\varphi_{eff}$ = 4.8) is chosen according to the calculations of the limit analysis, and sediment density follows a depth-dependent compaction curve from the Gulf of Mexico. Maximum water depth is 3 km, and sediments prograde with a constant rate of 0.5 cm/a. Several parameters of the reference model are changed in subsequent numerical experiments to investigate their influence on the temporal and spatial development of the deep-water fold belt.

The reference model shows good correlation with the natural example from the Gulf of Mexico (Figs. 1B-1D). Both fold belts show approximately 10 km long kink-type folds of the 4.5 km thick pre-kinematic section. The fold belts extend for 60-80 km and are uplifted and tilted seawards. Variations of the model parameters show that lower sediment strength and smaller continental slope width decrease the stability of the system leading to a faster evolution as well as a longer extent of the fold belt. In particular, a stronger sedimentary overburden inhibits gravity spreading and the system remains largely undeformed (apart from vertical subsidence of the shelf overburden where salt is expelled laterally and corresponding moderate seaward inflation of the salt layer). Although the geometry of the salt layer has some effect on the deformation of the fold belt, it is only when the salt is thin (<1 km) that its effect is profound. Here, folding develops at the toe of the slope before propagating to the distal end of the salt basin. The high

basal traction force at the base of the overburden that leads to toe-of-slope folding can also be achieved with higher salt viscosities. Basement steps or different tapers in the distal section can localise and slow down folding, but do not significantly change the nature of the salt-cored fold belt.

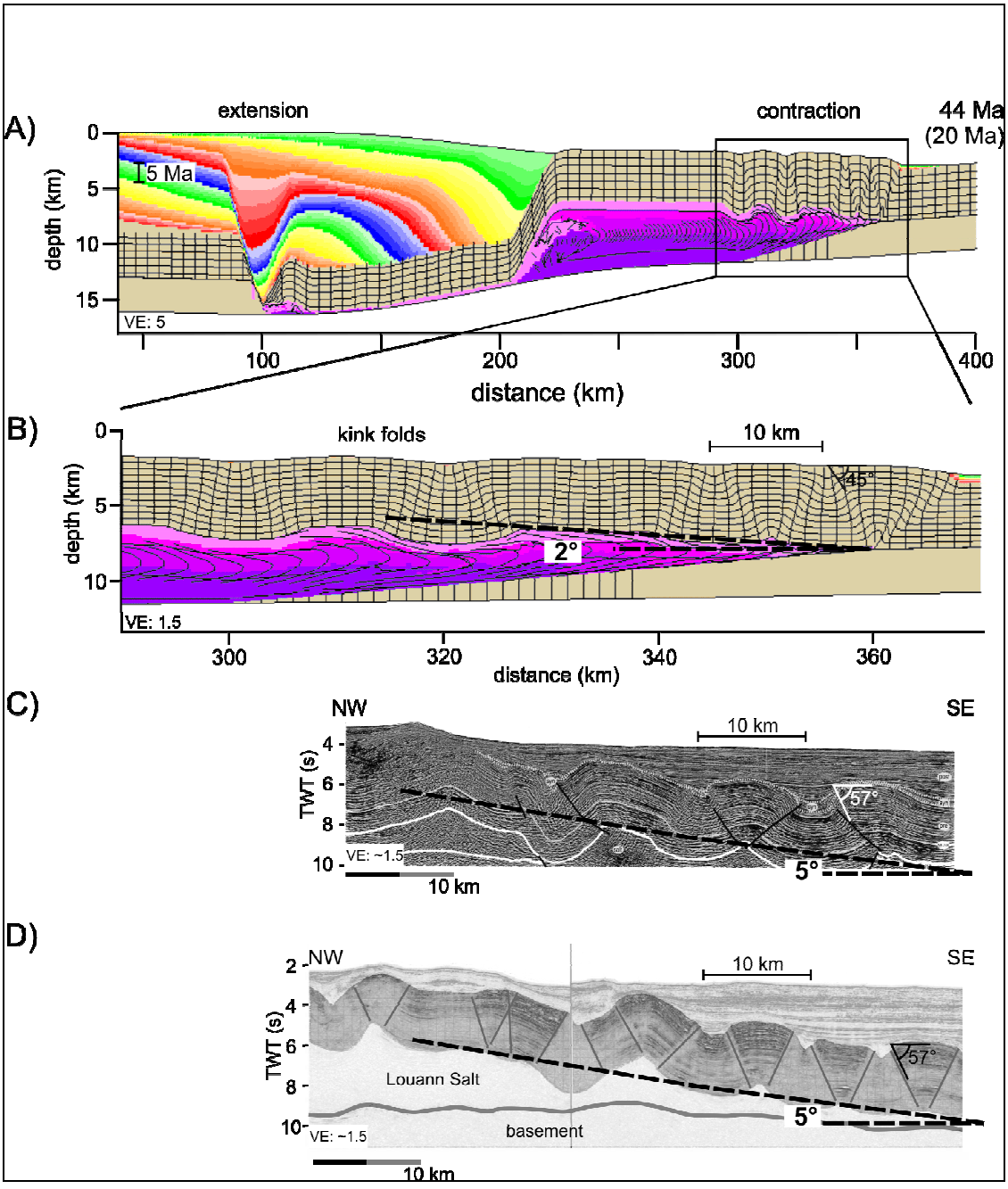


**Figure 1. Comparison of numerical model results with seismic sections from Perdido Fold Belt, northwestern Gulf of Mexico. A) Reference model after 44 Ma model run time (age in brackets denotes time since onset of gravity spreading). The colour scale shows the chronostratigraphy in 5 Ma major bands, each divided into 1 Ma sub-bands. Salt is coloured in magenta. Same coding is used in later figures. B) Close-up of numerical model showing the fold belt with highly symmetric kink folds of ~10 km wavelength. C), D) Seismic sections of PFB (From Rowan *et al.* 2000; Camerlo and Benson, 2006, AAPG©2006, reprinted by permission of the AAPG whose permission is required for further use).**

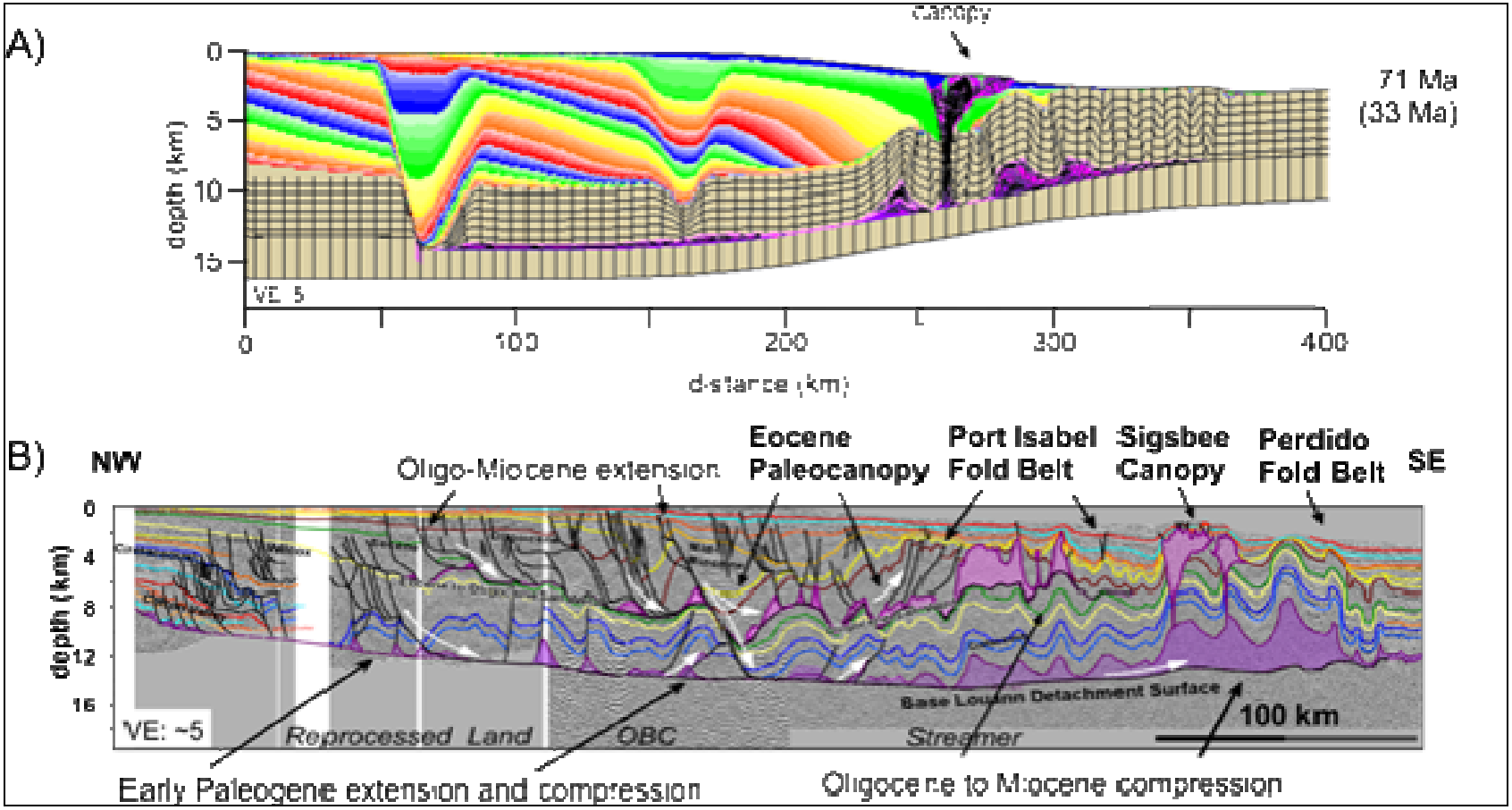


**Figure 2. Comparison of regional numerical model (Fig. 2A, for colour coding and ages see Figure 1) with seismic section from northwestern Gulf of Mexico margin (Fig. 2B) (From Radovich *et al.* 2007). Both sections show landward extension, a distal fold belt and an allochthonous salt canopy located directly adjacent and above the fold belt. Figure 2A shows a simplified model result whereas Figure 2B shows remnants of pre-**

A second set of models was run to investigate the relationship between allochthonous salt structures and deep-water fold belts. Two allochthonous salt structures can be identified from seismic data from the northwestern Gulf of Mexico (Fig. 2B). An early canopy formed during Eocene (Peel *et al.* 1995; Radovich *et al.* 2007), which acted as a shallow detachment surface for the Miocene Port Isabel Fold Belt and is now in most parts deflated. The second structure is the Sigsbee Canopy which formed further seaward in Oligocene times and now partly overlies the PFB. It has recently been inferred from modern seismic data that contraction occurred throughout large parts of the entire Gulf of Mexico deep water (Philippe *et al.* 2005; Guerin *et al.* 2006; Radovich *et al.* 2007). The evolution of allochthonous salt structures in deep water has been associated with compressional deformation, where shortening of salt-cored folds leads to breaching of the anticlines and expulsion of salt onto the seafloor (Vendeville and Gaullier, 2005).

For the numerical experiments we chose values for the model parameters that lead to toe-of-slope folding (thinner salt layer and higher salt viscosity) in order to achieve folding over a wider region and salt expulsion landward of a fold belt located over the distal end of the basin. A comparison of numerical model results and a seismic section is shown in Figure 2. The model presented in Figure 2A develops an allochthonous salt canopy directly adjacent to or above the distal fold belt (similar to the modern Sigsbee Canopy in Figure 2B). By also changing the width of the salt basin we obtain models (not shown here) that develop allochthonous salt canopies >100 km landward of the distal fold belt (similar to the Eocene paleo-canopy).

## Conclusions

Using numerical models and analytic calculations we are able to reconstruct the evolution of a Perdido-like deep-water salt-cored fold belt. Gravity spreading in the Oligocene Gulf of Mexico has been a sufficiently strong mechanism to fold the sediment carapace above the salt provided the overburden developed moderate pore-fluid pressures. Timing and extent of the folding of the model fold belt are shown to be controlled by system parameters such as overburden strength, continental slope width, salt thickness and salt viscosity. The numerical model results are interpreted to imply that landward Cretaceous toe-of-slope folding started long before the Oligocene-Miocene folding of the PFB. This allowed proximal allochthonous salt structures to develop through breached anticlines in the propagating fold belt while distal sedimentation continued. Only later did folding propagate and fold the PFB. By implication, the modern PFB is only the nose of a much older and larger fold belt.

## Acknowledgements

We would like to thank Markus Albertz for many discussions and contributions to the development of this research and Steven Ings for the GoM sediment compaction parameters. Funding for this project was provided by an Atlantic Innovation Fund contract to Dalhousie University, an IBM Shared University Research grant, a Killam Scholarship and a Government of Canada Award to S.G., and the Canada Research Chair in Geodynamics to C.B. We would also like to thank Shell International Exploration and Production, Inc. and Frank Peel for their kind support and advice, and Chris Connors for providing Figure 2B.

## References

Camerlo, R.H. and E.F. Benson, 2006, Geometric and seismic interpretation of the Perdido fold belt; northwestern deep-water Gulf of Mexico: AAPG Bull., v.90, p.363-386.

Gemmer, L. *et al.*, 2005, Dynamic modelling of passive margin salt tectonics: effects of water loading, sediment properties, and sedimentation patterns: Basin Research, v.17, p.383-402.

Guerin, G. *et al.*, 2006, Impact of amount of gravity-driven compression and intermediate decollement levels on the Sigsbee Salt Canopy formation, Gulf of Mexico: AAPG Annual Convention Abstracts.

Peel, F.J. *et al.*, 1995, Genetic structural provinces and salt tectonics of the Cenozoic offshore U.S. Gulf of Mexico: a preliminary analysis, *in* M.P.A. Jackson, D.G. Roberts, and S. Snelson, eds., Salt tectonics, a global perspective: AAPG Memoir, v.65, p.153-175.

Philippe, Y. *et al.*, 2005, Importance of gravity-driven compressional tectonics in northern offshore and deep-offshore Gulf of Mexico: New observations and implications for subsalt interpretation: AAPG Annual Convention Abstracts.

Radovich, B. *et al.*, 2007, Deep imaging of the Paleogene, Miocene structure and stratigraphy of the western Gulf of Mexico using 2D pre-stack depth migration of mega-regional onshore to deep water, long-offset seismic data: GCSSEPM Conference Proceedings, p.307-322.

Rowan, M.G., *et al.,* 2000, Deep-water, salt-cored foldbelts: Lessons from the Mississippi Fan and Perdido Foldbelts, northern Gulf of Mexico, *in* W. Mohriak and M. Talwani, eds., Atlantic rifts and continental margins, Geophys. Monograph, v.115, p.173-191.

Trudgill, B.D. *et al.*, 1999, The Perdido fold belt, northwestern deep Gulf of Mexico; Part 1, Structural geometry, evolution and regional implications: AAPG Bull., v.83, p.88-113.

Vendeville, B. and V. Gaullier, 2005, Salt diapirism generated by shortening and buckle folding: AAPG Annual Convention Abstracts.

**BACK**

# Sedimentary Basins in the Central and South Atlantic Conjugate Margins: Deep Structures and Salt Tectonics

**Webster U. Mohriak**
Petrobras
Av. República do Chile 65
Suite 1302, Centro
CEP 20 031-912
Rio de Janeiro - RJ
Brazil
Email: webmohr@petrobras.com.br

**David E. Brown**
Canada-Nova Scotia Offshore Petroleum Board
1791 Barrington Street
Halifax, Nova Scotia B3J 3K9
Canada
e-mail: dbrown@cnsopb.ns.ca

**Gabor Tari**
OMV Exploration and Production
Gerasdorfer Strasse 151
1210 Vienna
Austria
e-mail: gabor.tari@omv.com

## ABSTRACT

The tectonic evolution of the Central and South Atlantic conjugate margins has recently been constrained by the integration of geological and geophysical data, including deep seismic reflection profiles extending from the coastline towards the oceanic crust. Syn-rift and halokinetic structures imaged in these profiles have a fundamental impact on petroleum exploration of deep-water regions, allowing the identification of sedimentary depocentres with pre-salt and post-salt source rocks. Well and seismic data from conjugate basins along the Canadian (Nova Scotian) and Northwest African (Moroccan) margins indicate an initial phase of subsidence (Middle to Late Triassic rifting) followed by deposition of latest Triassic – earliest evaporites. These were coeval with a major magmatic event that is registered in the conjugate margins. Igneous intrusions within evaporite layers have also been recently recognized as part of the CAMP magmatism in the intracratonic Paleozoic basins in northern Brazil, with important effects on the petroleum systems.

The South Atlantic rifting in the Early Cretaceous formed conjugate basins along the Eastern Brazilian and West African margins. The new vintage of regional deep seismic profiles indicate that several segments of the incipient margin are characterized by the presence of seaward-dipping reflectors in the transition from continental to oceanic crust that appear to be coeval with salt deposition. The pre-salt sedimentary package is characterized by a belt of proximal syn-rift tilted blocks that are overlain by an extremely thick sag basin in more distal areas. Several boreholes have drilled though the salt layer and resulted in important hydrocarbon discoveries in the South Atlantic. We discuss the analogies between structures imaged in the Central (Canada-Morocco) and South Atlantic (Eastern Brazil – West Africa), particularly in the ultra-deep water regions that are exploratory frontiers for petroleum exploration.

## Introduction

Petroleum exploration in the South Atlantic continental margin sedimentary basins has resulted in important oil and gas discoveries since the early 1970's, particularly with several giant oil fields discovered along the Brazilian (Santos, Campos and Espírito Santo Basins) and West African (Angola) continental margins (Fig. 1). The daily oil production offshore Brazil and Angola is currently approaching 2 million barrels for each country, with an excellent prospective for substantial increases in the near future.

In the past three decades, the main focus of petroleum exploration was concentrated on post-salt turbidite reservoirs, which are mainly sourced by underlying syn-rift continental lacustrine rocks. Seismic interpretation of deep-water siliciclastic systems (turbidites) was the main exploratory tool in the geological investigation. More recently, a new approach has been undertaken in the Southeastern Brazilian margin, with significant discoveries in the older pre-salt sequence. These results indicate that pre-salt reservoirs and syn-rift structures in deep-water regions are the new frontiers to be explored in the next decades. The high investments required to drill exploratory boreholes in water depths beyond 2000 m and total penetrating depth exceeding 7000 m require a profound understanding of the basin-forming processes, the reservoir distribution in the context of active rifting, and the identification of continental and oceanic crust structures.

Most of the hydrocarbon fields offshore Eastern Brazil and Angola are related to salt tectonics, which is responsible for controlling reservoir facies in carbonate rocks, and turbidite accumulation in fans, canyons and sedimentary troughs. Salt tectonism also creates efficient pathways for oil migration from source rocks in the pre-salt sequence to reservoirs that range in age from Albian to Upper Tertiary. Oil migration is commonly associated with extensional listric faults detaching on the Aptian salt layer. Salt welds, resulting from salt evacuation, also provide a connection between pre- and post-salt strata. More recently, salt has also been recognized as a very efficient seal for subsalt reservoirs in the ultra-deep-water giant fields discovered in the Santos Basin.

This work discusses the deep crustal structures and the role salt tectonics has played in some of the Brazilian and West African marginal basins, and comparing this to analog structures recognized in the North Atlantic. Based on 2D and 3D seismic data interpretation, we identify possible exploratory plays related to allochthonous salt structures that are classic petroleum plays in the Gulf of Mexico but have yet to be successfully tested in the South and North Atlantic conjugate margins.

We also integrate regional 2D deep seismic profiles and potential field data (gravity and magnetics) to constrain the crustal architecture and rift structures of the South and North Atlantic margin sedimentary basins from platform to oceanic crust, and discuss the magmatic events that are observed at several stratigraphic sequences, including the pre-rift, syn-rift and drift phases of tectonic evolution. We apply some of the recently developed concepts and interpretations (based on high-quality industry and academic seismic data, as well as on IODP drilling results) to analyze the transition from continental to oceanic crust in the North Atlantic region, particularly the Moroccan and Nova Scotian margins, frontier areas which are sparsely tested by exploratory drilling.

## Tectonic Evolution of the Atlantic Margin Sedimentary Basins

The sedimentary basins along the South and North Atlantic (Fig. 1) were formed as a result of extensional processes that diachronously ruptured the continental crust of Pangea. By Late Permian times (around 250 Ma) the amalgamated continental mass straddled the globe including cratons within the North American and Northwest African landmasses in the northern hemisphere. The southern hemisphere was dominated by the Gondwana landmass, incorporating cratonic nuclei within South America, Africa, Australia, Antarctica, and India. Pangea was bordered to the west by the Panthalassic Ocean and to the east by the Tethys Ocean, with active subduction zones at their respective western margins (Scotese 2002).

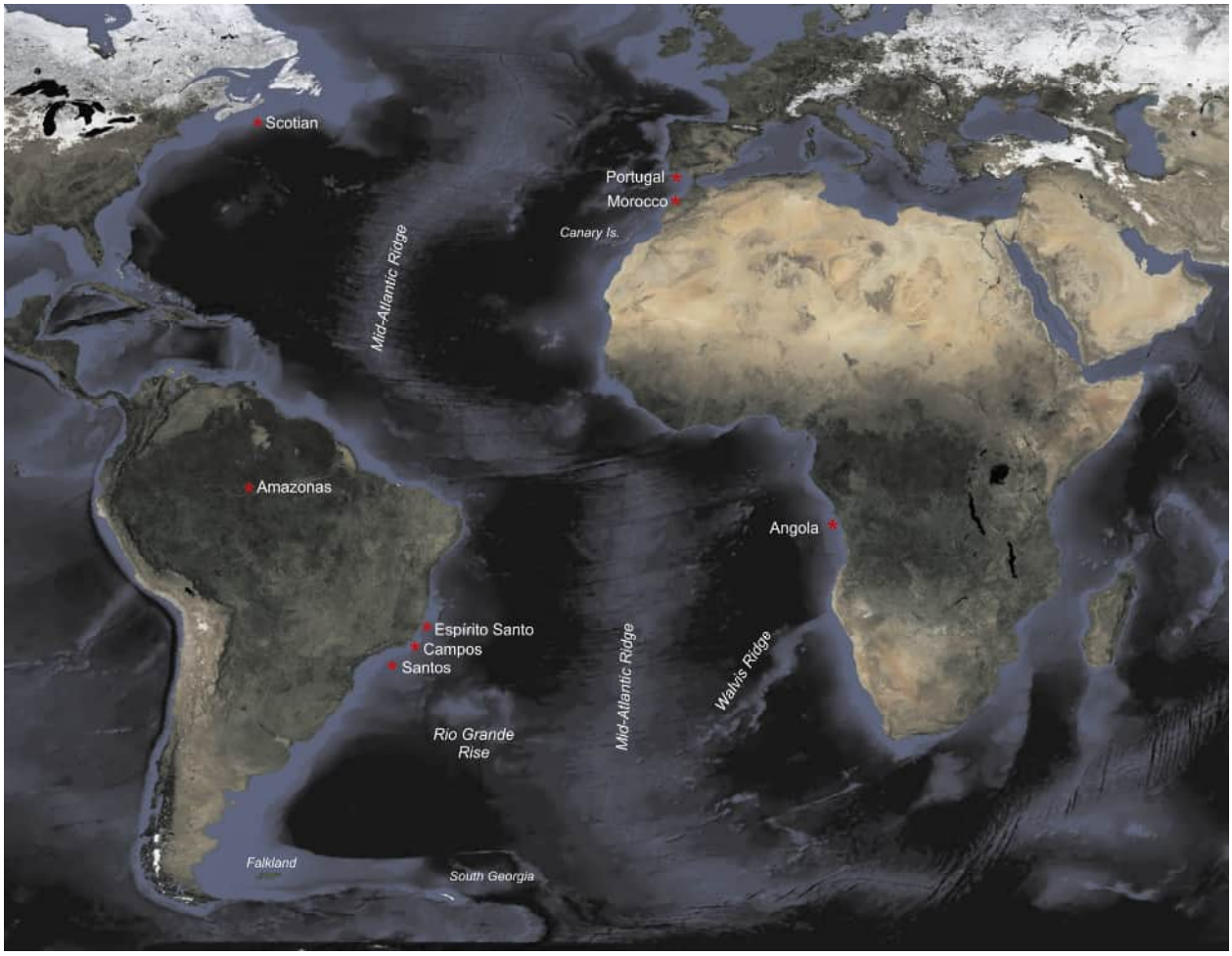


**Figure 1. Satellite image showing the North and South Atlantic margins.**

The syn-rift depocentres along the Moroccan marginal basins are dated as Late Triassic. Underlying pre-rift sequences are composed of Permian to Carboniferous sediments that were deposited in an expansive Paleozoic basin that extended from Northwest Africa to Eastern North America (Uchupi 1989; Uchupi & Emery 1991). A marked unconformity separates the pre-rift and syn-rift sequences, which in the North Atlantic is dated as Lower to Middle Triassic (Fig. 2).

In the incipient North Atlantic margin, basement-involved faults were active up to the Late Triassic and Early Jurassic, when evaporites were deposited in a large area extending from Iberia to south of Morocco in West Africa, and from the Grand Banks towards Nova Scotia and Georges Bank in North America (Davison 2005). A major magmatic event is registered at the Triassic-Jurassic boundary (about 200 Ma), corresponding to the Central Atlantic Magmatic Province (CAMP) volcanic episode (Knight *et al*. 2004).

The Amazon Basin, an intracratonic Paleozoic basin located in northern Brazil (Fig. 1), contains Late Triassic age igneous rocks preferentially intruded into a salt sequence (Costa and Wanderley Filho, 2008). Similarly, within the Moroccan Essaouira Basin, geochronological dating of volcanics indicates a magmatic event around 200 Ma, which indicates that the Amazon Basin may also be included in the Central Atlantic Magmatic Province (CAMP) as suggested by some authors (*e.g.* Marzoli *et al.* 1999). This interpretation promotes the CAMP magmatic episodic to the largest igneous episode in the world.

By Late Triassic time, the wide Tethys Ocean separated the northern Laurasian and southern Gondwanan landmasses. Oceanic propagators started to rupture the continental crust by advancing through the incipient continental margins of North America and Northwest Africa, but could not penetrate

into the Amazon craton. The Amazon and Solimões Basins were uplifted and the previous sedimentary sequences were eroded, resulting in a major stratigraphic gap spanning the Late Permian to Early Cretaceous.

The early development of the North Atlantic passive margin (Fig. 2) is characterized by widespread deposition of shallow to deep-water carbonate rocks dated as Lower to Middle Jurassic (Emery and Uchupi 1991). The oceanic crust propagator advanced towards the north, and by 150 Ma the Iberian margin was ruptured by active spreading centres. Siliciclastic deposition in Tethyan deep-water settings is registered from the Upper Jurassic to Early Cretaceous (Maldonado *et al.* 1999), resulting in a transgressive marine environment.

The Atlantic Ocean was developed in two stages: by breaking apart the North American and Northwest African plates in the Late Triassic, and the South American and West African plates in the Late Jurassic/Early Cretaceous, with oceanic propagators advancing from south (Argentina) to north (Muller *et al.* 2008). The Early Cretaceous syn-rift phase of subsidence in the Santos, Campos and Espírito Santo Basins (Fig. 1) was preceded by widespread magmatic activity dated around 135-130 Ma. Seaward-dipping reflectors mark the inception of oceanic crust and are characterized at several volcanic sectors that segment the margin (Mohriak 2001). The Central Atlantic equatorial margin (around Northeastern Brazil) was the last segment to be ruptured by transform faulting around Aptian-Albian times, permanently connecting the North and South Atlantic oceans (Matos 2000). However, it is not clear from where the first ocean water ingressions advanced from. Marine waters may have advanced from the already formed Argentine Basin in the south, penetrating the Eastern Brazilian/Western African evaporite basins in Late Aptian time. Alternatively, the first marine ingressions may have come from the South Atlantic gulf (extending from northeast Brazil–West Africa towards the Florianópolis High-Rio Grande Fracture Zone/Walvis Ridge in the south) being derived from the Central Atlantic Ocean as indicated by paleontological analysis of the fauna content of the Early Albian carbonate rocks (Azevedo 2004).

The evaporite sequence (Fig. 2) is mainly registered in an elongated gulf extending from the Sergipe-Alagoas Basins in Brazil (with conjugate Rio Muni-Douala Basins in Africa) towards the Santos-Namibe conjugate margins. Salt deposition was associated with a transitional environment, with the first marine ingressions by Late Aptian times (Jackson *et al.,* 2000). However, some recent works have suggested that salt might be deposited diachronously in different sectors of the Atlantic margin (*e.g.* Davison 2005).

## Rift Structures and Crustal Architecture

Recent sub-salt discoveries in the ultra-deep water region of the Brazilian continental margin have highlighted the importance of understanding the syn-rift structures, volcanism and salt tectonics along the South Atlantic divergent margins (Mohriak 2001).

Several similarities in the rift structures along regional basin profiles are observed between the South and North Atlantic margins. For example, an impressive correlation is observed between the geological sections comparing the Campos and Scotian Basins (Fig. 3). These basins have proximal syn-rift depocentres and internal highs that are covered by a thin evaporite layer. The Badejo and Carson highs are analogous structures probably formed by similar geodynamic processes. Basinward of these highs the evaporite layer is thicker, forming extensional salt pillows and diapirs that are locally observed in the Corvina-Parati low (Campos Basin) and Abenaki Subbasin (Scotian Basin). A number of internal highs are present in the platform of both margins (example, Sable High in the Scotian margin), but the most important regional high is located beyond the shelf break. In the Campos Basin, the Outer High is a very important region for focusing hydrocarbons migrated from the syn-rift source rocks (Guardado *et al.* 1989; Cainelli and Mohriak 1998). Beyond the shelf break, the salt basin is more developed and extensional structures predominate; in the slope and deep basin compressional structures are common, and huge salt diapirs and salt walls are observed near the continent-ocean boundary (Fig. 4).

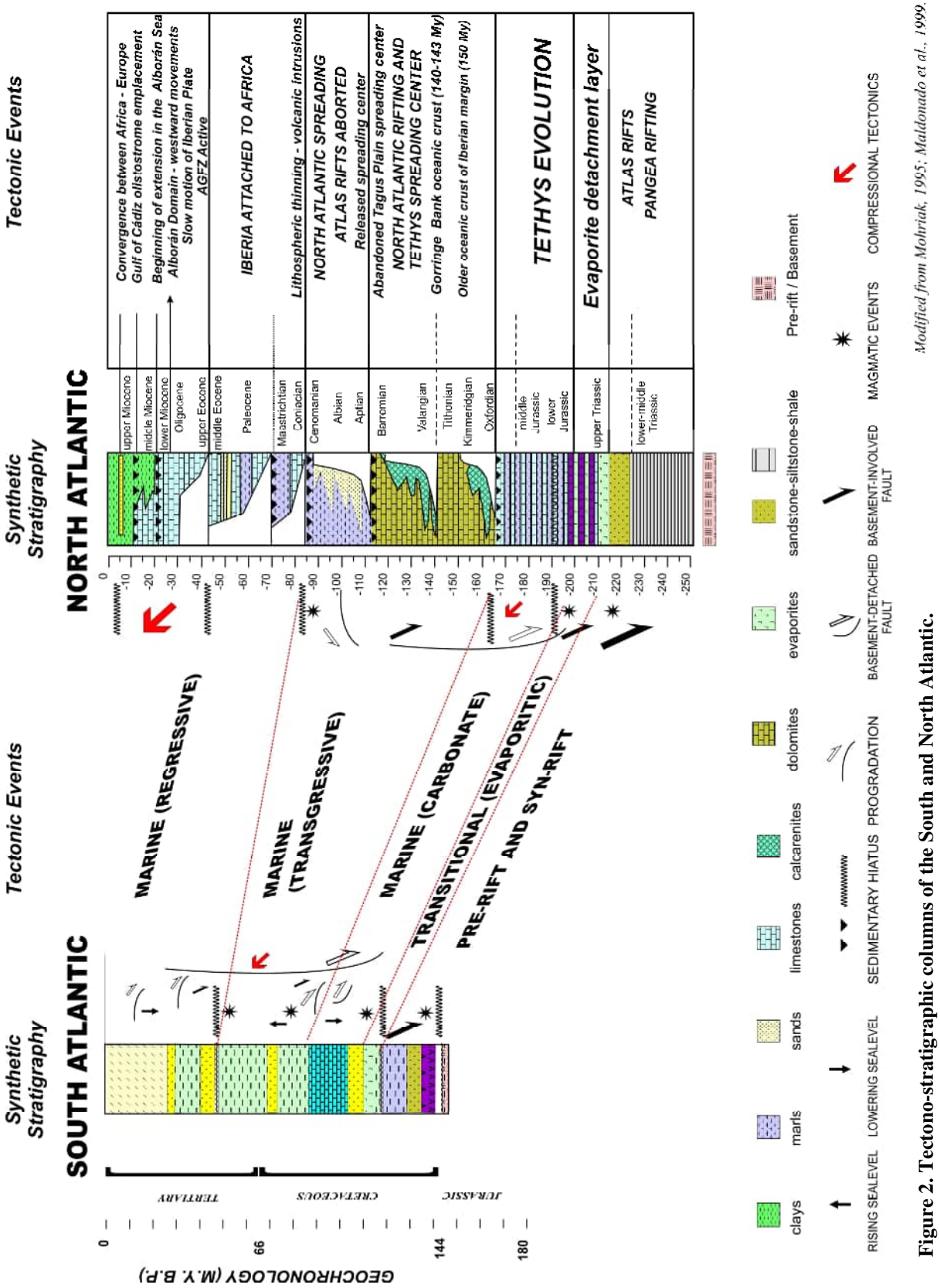


**Figure 2. Tectono-stratigraphic columns of the South and North Atlantic.**

*Modified from Mohriak, 1995; Maldonado et al., 1999.*

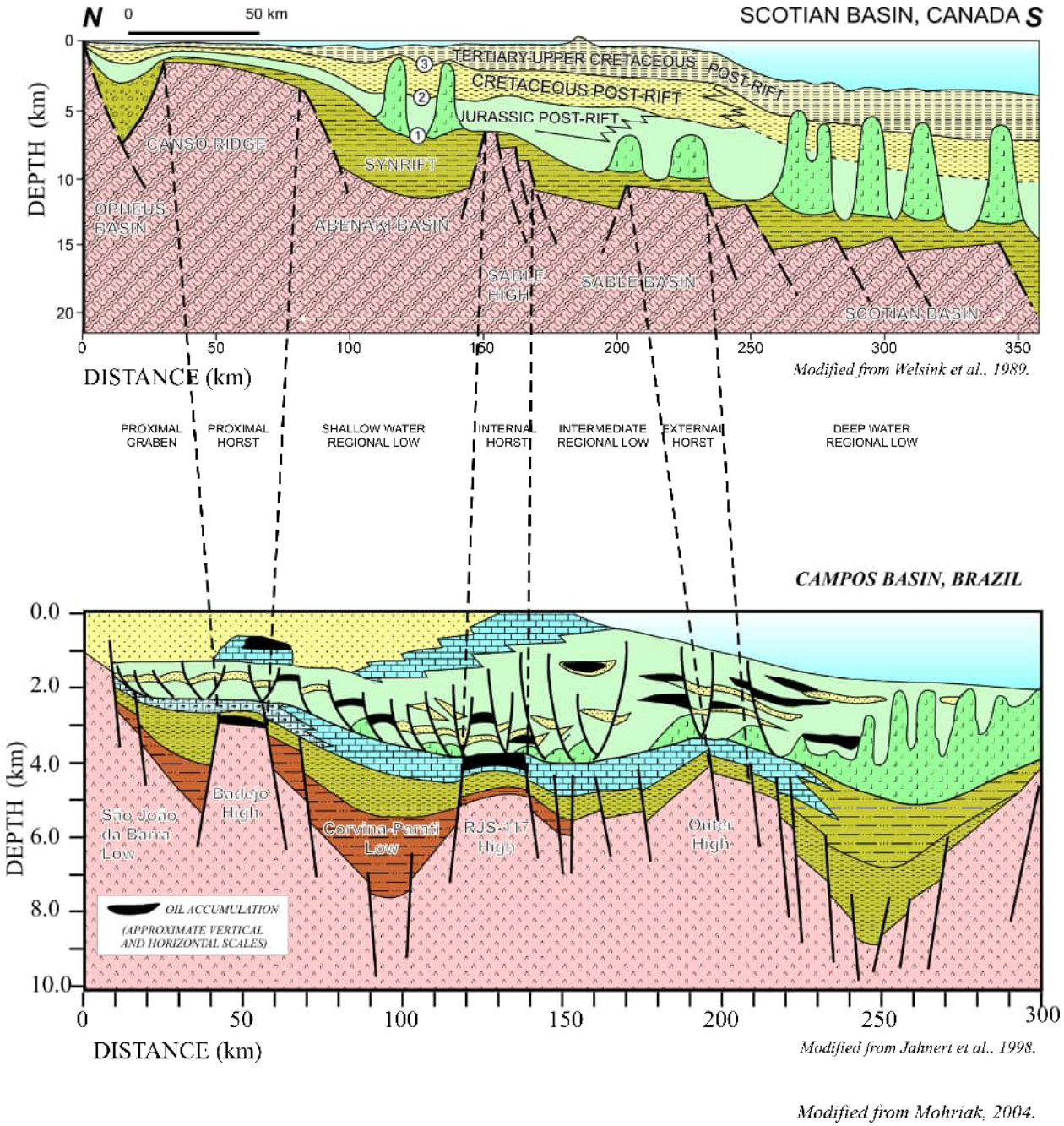


**Figure 3. Comparison between Canada (Scotian) and South Atlantic (Campos) sedimentary basins.**

The sub-salt syn-rift structures are not clearly visible in the slope and deep water basins offshore Nova Scotia and Morocco. Seismic refraction and seismic reflection data in the Scotian Basin indicate that the crustal thickness changes from 37 km to less than 10 km beyond the shelf break (Funck *et al.,* 2004). Wu *et al.* (2006) interpreted an anomalous velocity layer (ranging from 7.2 to 7.6 km/s) corresponding with a lense-shaped body of serpentinized mantle. This body might correspond to the oceanic layer-3, which is interpreted as composed of gabbroic rocks. On oceanic crust, the Moho underlies this layer and is interpreted around 15 km in depth, resulting in a composite column of 5 km of water, 3-4 km of sediments, and 7 km of oceanic crust (basalt, diabase and gabbro).

The deep basin along the Nova Scotian margin is characterized by tilted blocks that are apparently controlled by listric faults. Several alternative interpretations have been proposed for these structures (example, Keen & Potter 1991; Salisbury & Keen 1993): (1) oceanic crustal blocks affected by extensional tectonics with listric faults; (2) continental crust blocks affected by syn-rift extensional faults; and (3) post-rift blocks controlled by listric faults that detach on salt.

The conjugate margin (Talfeney Plateau, offshore Morocco) is characterized by a rather thick Cretaceous to Jurassic sedimentary succession covering syn-rift structures that are not well imaged on existing data sets. Autochthonous and allochthonous salt bodies are present along the margin, extending from the platform towards the oceanic crust region (Tari *et al.* 2000)

The African margin is characterized by a very thick sag basin in northern Angola and by the massive salt in southern Angola, which apparently advances towards oceanic crust volcanic highs (Marton *et al.* 2000). The sag basin is underlain by continental crust in the slope province, and some models (e.g., Henry *et al.,* 2007) suggest that the continental crust extends towards the salt limit and beyond, with drift-phase volcanics overlying remnants of Precambrian age upper and lower crust. Other models (*e.g.,* Contrucci *et al*. 2004; Moulin *et al.* 2005) suggest a marked thinning of continental crust and presence of oceanic crust beyond the salt limit. The platform and slope is marked by a lower crust body interpreted as under-plated material or serpentinized mantle (Karner and Gamboa 2007).

The crustal architecture of the Brazilian margin has been studied since the 1990's using regional deep seismic profiles extending from the platform towards oceanic crust (Mohriak *et al.* 1990; Mohriak *et al.* 2000). A regional crustal transect in the Campos Basin (Fig. 4) shows a marked crustal thinning in the platform and slope, with allochthnous salt tongues advancing towards oceanic crust (Mohriak *et al.* 1998; Mohriak *et al.* 2004).

Recently acquired deep seismic profiles in the Brazilian margin indicate that the Campos Basin model can be applied to other segments of the margin, particularly in the Espírito Santo Basin (Mohriak *et al.,* 2008). Regional seismic profiles extending from the platform towards the deep basin indicate that the sag basin is underlain by remarkably strong reflectors that could correspond to a shear zone or detachment fault, to the top of an underplated body, to lower crust / upper mantle transition (Moho), or to the Conrad discontinuity. Depth-converted of the seismic profile shows the reflector ranges in depth from about 30-35 km in unextended crust, where the pre-salt sedimentary cover is thin and partially eroded. Gravity and seismic data indicate that the Moho rises rapidly to about 20 km in the shelf break where salt tectonics is more developed. It may reach less than 15 km in regions of hypertextended crust below a thick sag basin. The reflectivity of this discontinuity is stronger in the platform and slope, particularly at the proximal limit of the sag basin. Basinwards of the thick sag basin the rift structures are not imaged, and the presalt sequence is probably intruded by igneous rocks. Mohriak *et al*. (2008) have interpreted a massive igneous body below the compressional salt mass that locally advances as an allochthonous tongue. Below the compressional salt tectonics domain the reflectors looses its energy, and the base of the crust is not clearly imaged. The oceanic crust domain is again marked by a very strong reflector which we interpret as the Moho (Mohriak 2005). The oceanic crust is marked by a marked discontinuity that ranges from 13 to 15 km in depth, resulting in a crustal profile similar to the Canadian margin interpretation.

## Rift Structures and Salt Tectonics

The salt tectonics styles in the Moroccan and Brazilian margins have some similarities, particularly expressed by the early development of extensional structures. However, the Northwest African margin was strongly influenced by compressional episodes in the late Tertiary, resulting in marked differences (Fig. 2). The kinematics and geodynamic controls on extensional, compressional and salt tectonics structures can be improved by comparing similar structures observed in the South and North Atlantic salt basins (Mohriak 2005).

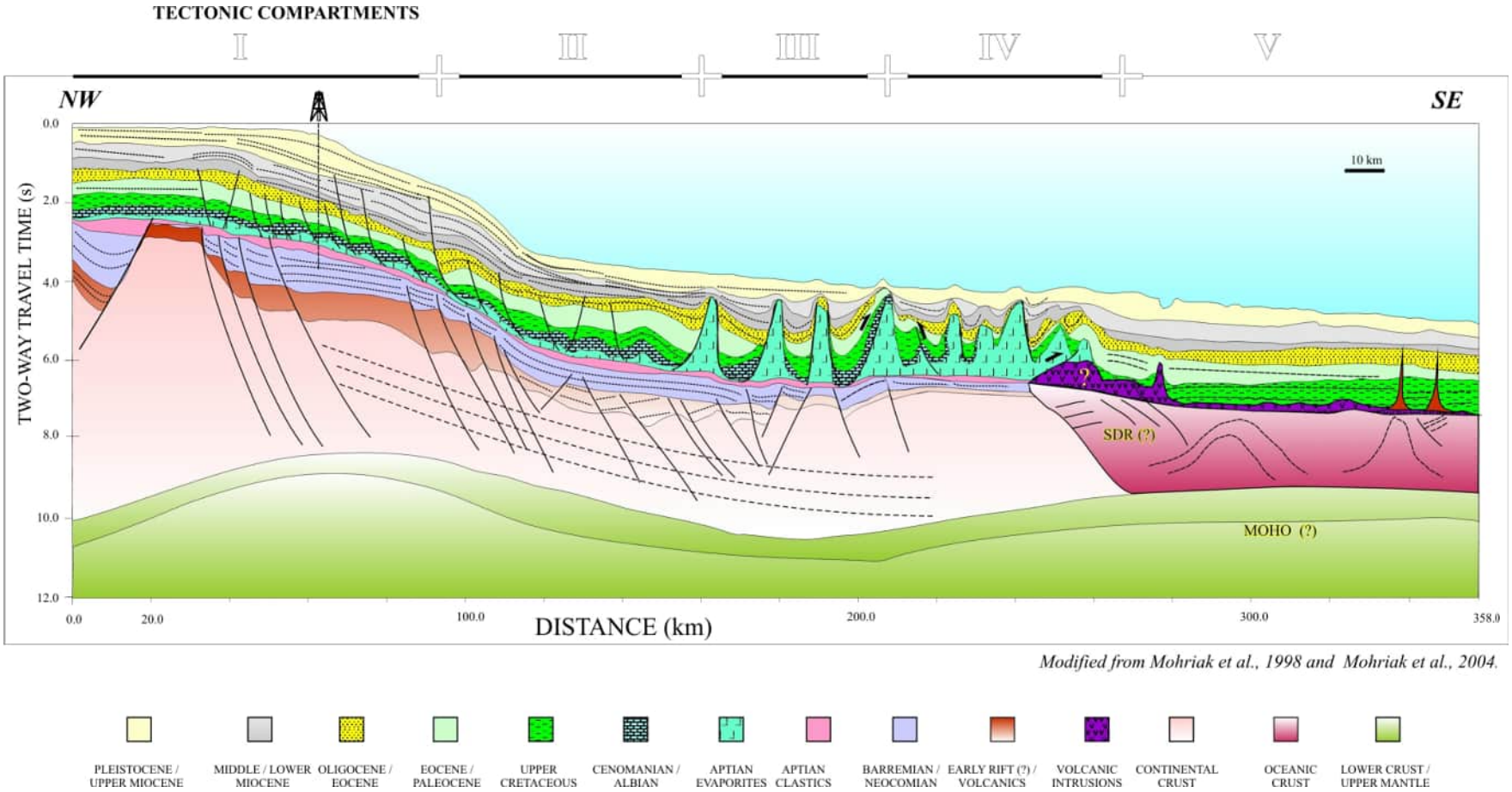


**Figure 4. Regional geological section based on deep seismic profiles from the Campos Basin, offshore Brazil. Structural Domains with salt tectonics compartments (I-IV) are identified from platform to deep basin. Oceanic crust domain (compartment V) is characterized by sub-horizontal reflectors overlying a volcanic basement.**

Important changes in salt tectonics interpretation can be registered along the Brazilian and Angolan margins, where several structures previously interpreted as extensional salt diapirs increasing in height and width towards the deep water region are now re-interpreted as compressional structures and allochthonous salt, similar to many structures observed in the Gulf of Mexico (Mohriak *et al.* 2004; Fiduk *et al.* 2004). Regional seismic profiles and geological sections along the Angolan margin also provide a benchmark for the conceptual interpretation of elusive structures associated with salt tectonics.

In the Campos Basin (Fig. 4) the salt tectonics structural styles can be associated with different compartments along a dip direction, from thin salt with extensional structures (Domain I), salt pillows and extensional diapirs (Domain II), compressional diapirs and salt walls (Domain III) ,and a strongly compressional domain with reverse faults and salt nappes advancing towards oceanic crust (Domain IV).

Extensional tectonics, salt flow and overburden translation from the platform to the deep-water basin has long been recognized in the South Atlantic and Gulf of Mexico as an efficient mechanism to form compressional structures at the distal margin of the basin, with allochthonous salt tongues overriding basement highs near the continent-ocean boundary. The allochthonous salt tongues formed near the boundary between the continental and oceanic crust along the Brazilian and Angolan margins are strongly reminiscent of nappe structures.

The exploratory plays in the Campos Basin, and in the South Atlantic in general, are mostly related with salt tectonics. To date, the successful plays are related to autochthonous salt structures. Subsalt plays are classical targets in the Gulf of Mexico, where several hydrocarbon fields discovered in the 1990's are characterized by siliciclastic reservoirs covered by salt; a perfect seal for hydrocarbon accumulations (Montgomery & Moore 1997). Subsalt plays remain undrilled in the Brazilian and Moroccan margins, but they constitute robust exploratory opportunities in the deep-water region in the North Atlantic continental margins (Haddou & Tari 2007). Allochthonous salt structures (including canopies, salt drops and salt tongues) are present in the Brazilian, Angolan, Iberian and Moroccan margins (Mohriak, 2005). These structures have also been recognized in the Scotian Basin (Fig. 5).and constitute important exploratory plays in the deep-water slope (Kidston *et al.,* 2002).

Some possible exploratory plays in these basins, similar to the Gulf of Mexico structures, can be interpreted with the new 2D and 3D seismic data. The comparison of structures with teardrop geometry in the Canadian and Moroccan margins (*e.g.* Fig. 6) is a clear indication that conceptual plays from one basin might be effectively applied to others, and the risk analysis will mainly depend on particular aspects such as the presence of mature source rocks at the prospect, reservoir presence, and effective migration pathways.

## Discussion-And Conclusions

The tectonic evolution of the North and South Atlantic continental margin sedimentary basins is marked by extensional tectonics, magmatism, salt tectonics and particularly in the Northwest African margin, compressional episodes in the late Tertiary that resulted in inversion of syn-rift troughs. The Iberian margin has suffered the impact of compressional tectonics related to Tertiary plate convergence between Africa and Europe affecting salt structures

In the South Atlantic, the evaporite sequence is thicker than in the North Atlantic margin, and forms massive salt walls towards the continental/oceanic crust boundary, which is marked by allochthonous salt tongues advancing over volcanic highs. The North Atlantic Triassic salt basin offshore Morocco and Iberia shows several isolated and amalgamated canopies in the slope and deep basin, but smaller salt tongues near the continent-ocean boundary.

The Southeastern Brazilian and West African margins are characterized by Late Cretaceous-Tertiary continental uplifts that formed a mountainous region along the rift basins, whose erosion resulted in several episodes of clastic progradation that loaded the salt basin. Compressional structures are uncommon onshore and offshore, and the uplift is probably epeirogenic. The Northwest African margin was strongly affected by Tertiary compressional tectonics that deformed many salt structures and inverted the Atlas rift basin onshore Morocco (Hafid 2000).

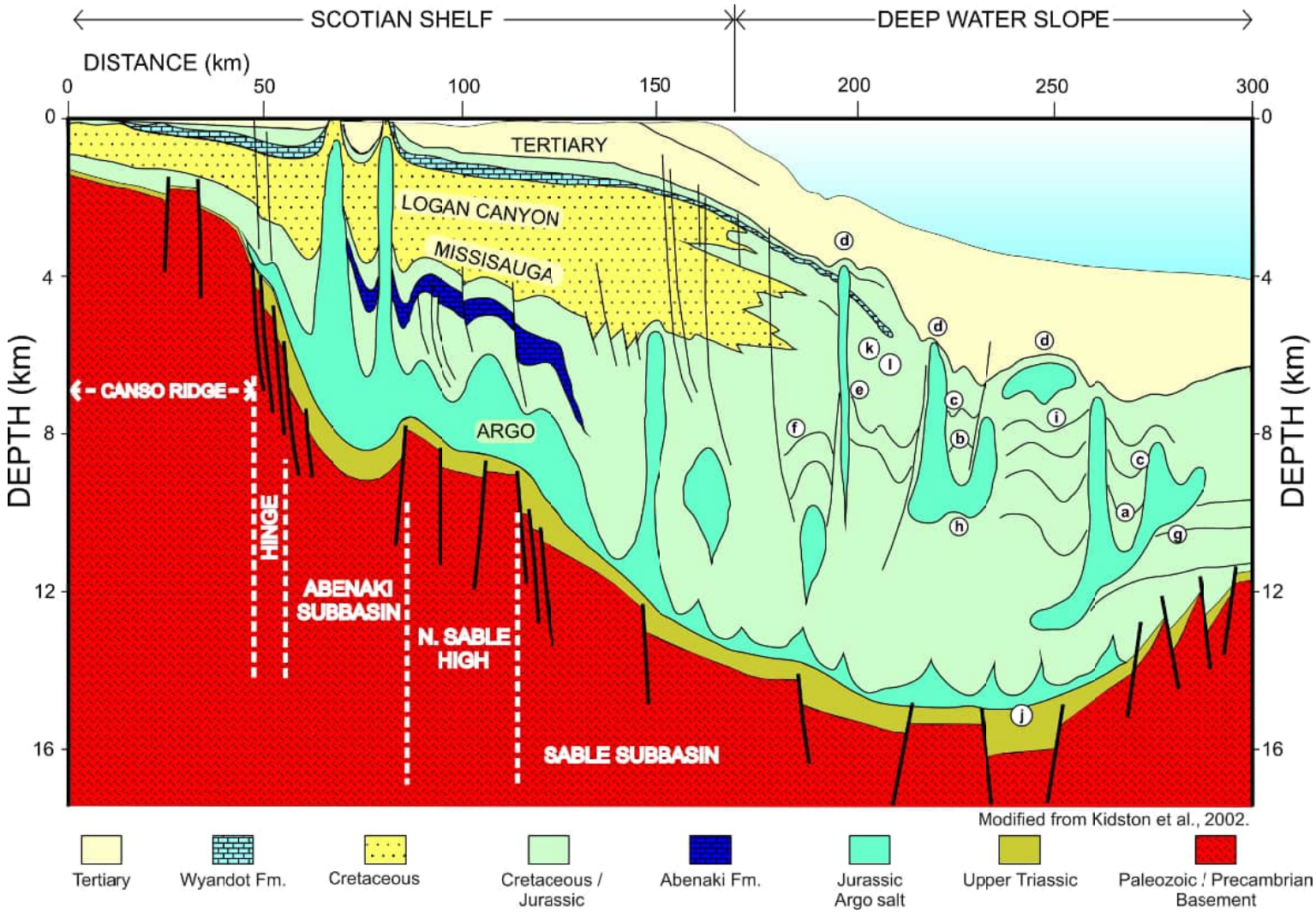


**Figure 5. Schematic geological section with conceptual exploratory play types in the deep-water slope, offshore Nova Scotia. Legend: a - Mini-basin floor, unstructured b - Mini-basin floor, structured c - Mini-basin flanks d - Salt crest e - Salt flank f - Anticline or turtle g - Jurassic subsalt h - Cretaceous subsalt i - Tertiary subsalt j - Triassic subsalt k - Slope fans (stratigraphic / structural) l - Rollover anticlines / tilted fault blocks.**

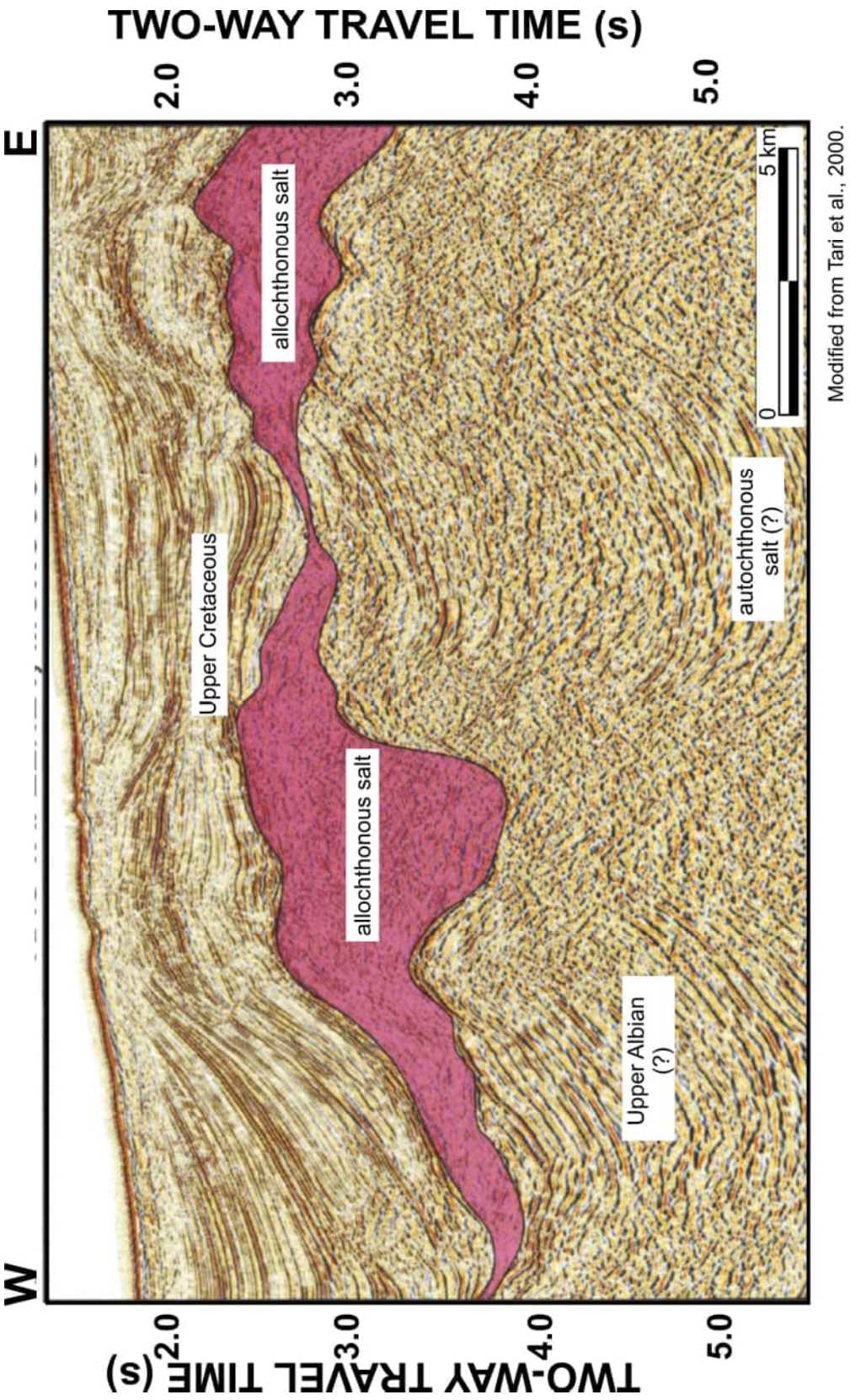


**Figure 6. Seismic profile in the Ras Tafelney region (Essaouira Basin, offshore Morocco).**

Salt tectonics along the Canadian margin is well known, with extensional structures and salt diapirs in deep waters. A number of exploratory boreholes have drilled through allochthonous salt in the North Atlantic basins, but none of these have penetrated the pre-salt stratigraphy in the deep-water Scotian Basin. The conjugate Iberian margin is characterized by few salt diapirs onshore, with later compressional tectonics affecting the diapiric structures.

The Scotian Basin bears similarities with the Campos Basin: extensional divergent margin rift, salt tectonics; whereas the Iberian margin bears similarities with Northeast Brazilian margin: non-volcanic pre-salt sequence, narrow rift, reduced salt tectonics, salt layers affected by basement-involved faults, etc.

Salt tectonics plays a fundamental role in the deep-water petroleum prospectivity along the South Atlantic basins, particularly along the Brazilian and Angolan margins. Structural and stratigraphic plays related to autochthonous and allochthonous salt is present both along the South Atlantic and North Atlantic margins. The comparison of the hydrocarbon accumulations in more explored basins may contribute important lessons to the discovery of oil accumulations in less explored areas.

## Acknowledgements

We thank Petrobras E&P management for the incentive to prepare this work, and several explorationists from Petrobras-E&P and Petrobras-ANI (International Business Unit) for many enlightening discussions. We also acknowledge the contributions from several CNSOPB and ONHYM explorationists for this work.

# References

Azevedo, R.L.M., 2004. Paleoceanografia e a evolução do Atlântico Sul no Albiano. Boletim de Geociências da Petrobras, v.12, n.2, p.231-249.

Cainelli, C., and W.U. Mohriak, 1998. Geology of Atlantic Eastern Brazilian basins. 1998 AAPG International Conference & Exhibition Short Course–Brazilian Geology Part II, November 8–11, 1998, Rio de Janeiro, Brazil, 67p. + figures.

Contrucci, I., L. Matias, M. Moulin, L. Géli, F. Klingelhofer, H. Nouzé, D. Aslanian, J.L. Olivet, J. P. Réhault, and J.C. Sibuet, 2004. Deep structure of the West African continental margin (Congo, Zaïre, Angola), between 5°S and 8°S, from reflection/refraction seismics and gravity data. Geophysical Journal International, v.158, p.529-553.

Costa, A.R.A. & Wanderley Filho, J.R., 2008. Os evaporitos e halocinese na Amazônia. In: Mohriak, W., Szatmari, P. & Anjos, S.M.C., Sal: Geologia e Tectônica. Capítulo 8, p.208-219.

Davison, I., 2005. Central Atlantic margin basins of North West Africa: Geology and hydrocarbon potential (Morocco to Guinea). Journal of African Earth Sciences, 43, p.254-274.

Guardado, L.R., L.A.P. Gamboa, and C.F. Luchesi, 1989. Petroleum geology of the Campos Basin, a model for a producing Atlantic-type basin. In: J. D. Edwards and P.A. Santogrossi (eds.), Divergent/Passive Margin Basins. AAPG Memoir 48: p 3-79.

Hafid, M., 2000. Triassic-early Liassic extensional systems and their Tertiary inversion, Essaouira Basin (Morocco). Marine and Petroleum Geology, v.17, p.409-429.

Henry, S.G., A. Danforth, G. Tari, and S. Venkatraman, 2007. Pre-Salt and Salt Geometry as Controlling Factors in Post-Salt Tectonics. First MAPG International Conference & Exhibition, October 28-31, 2007, Marrakech, Morocco. Poster Session. Abstract: http://www.searchanddiscovery.com/documents/2008/08006morocco_abs

Jabour, H. and G. Tari, 2007. Subsalt exploration potential of the Moroccan salt basin. The Leading Edge, v. 26, p. 1454-1460.

Jackson, M.P.A., C. Cramez and J.M.Fonck, 2000. Role of subaerial volcanic rocks and mantle plumes in creation of South Atlantic margins: implications for salt tectonics and source rocks. Marine and Petroleum Geology, v.17, p.477–498.

Karner, G.D. and L.A.P. Gambôa, 2007. Timing and origin of the South Atlantic pre-salt sag basins and their capping evaporites. In: Schreiber, B.C., Lugli, S., and Babel, M. (eds.), Evaporites through space and time. Geological Society of London, Special Publication 285, p.15-35.

Keen, C.E. and D.P. Potter, 1995. Formation and evolution of the Nova Scotian rifted margin: evidence from deep seismic reflection data. Tectonics, v. 14, n. 4, p. 918-932.

Kidston, A.G., D.E. Brown, B. Altheim, and B. M. Smith, 2002: Hydrocarbon potential of the deep-water Scotian slope. Canada-Nova Scotia Offshore Petroleum Board, Halifax, Nova Scotia, 111p.

Knight, K.B., S.,Nomade, P.R. Renne,. A. Marzoli, H. Bertrand, and N. Youbi, 2004. The Central Atlantic Magmatic Province at the Triassic - Jurassic boundary: paleomagnetic and $^{40}$ Ar / $^{39}$ Ar evidence from Morocco for brief, episodic volcanism. Earth and Planetary Science Letters, v 228, p.143-160.

Maldonado, A., L. Somoza, and L. Pallarés, L., 1999. The Betic Orogen and the Iberian – African boundary in the Gulf of Cadiz: geological evolution (central North Atlantic). Marine Geology, 155, p.9-43.

Marton, L.G., G.C Tari. and C.T. Lehmann, 2000. Evolution of the Angolan passive margin, West Africa, with emphasis on post-salt structural styles. In: W. U. Mohriak and M. Talwani (eds.), Atlantic rifts and continental margins, AGU Geophysical Monograph 115, p.129-149.

Marzoli, A., P.R. Renne, E.M. Piccirillo, M. Ernesto, G. Bellieni and A. De Min, 1999. Extensive 200 Ma-year-old continental flood basalts of the Central Atlantic Magmatic Province. Science, v.284, p.616-618.

Matos, R.M.D., 2000. Tectonic evolution of the equatorial South Atlantic. In: W.U. Mohriak and M. Talwani (eds.), Atlantic rifts and continental margins, AGU Geophysical Monograph 115, p.331–354.

Mohriak, W.U., 2001. Salt tectonics, volcanic centers, fracture zones and their relationship with the origin and evolution of the South Atlantic Ocean: geophysical evidence in the Brazilian and West African margins. 7th International Congress of the Brazilian Geophysical Society, Salvador, Bahia, Brazil, October 28-31, 2001, Expanded Abstract, p.1594.

Mohriak, W.U., 2005. Salt tectonics in Atlantic-type sedimentary basins: Brazilian and West African perspectives applied to the North Atlantic Margin. In: GCSSEPM 25th Annual Bob F. Perkins Research Conference, Petroleum Systems of Divergent Continental Margin Basins, p.75-413.

Mohriak, W.U., R. Hobbs and J.F Dewey, 1990. Basin-forming processes and the deep structure of the Campos Basin, offshore Brazil. Marine and Petroleum Geology, v.7, n.2, p.94-122.

Mohriak, W.U., M.R. Mello, M. Bassetto, I.S. Vieira, and E.A.M. Koutsoukos, 2000. Crustal architecture, sedimentation, and petroleum systems in the Sergipe-Alagoas Basin, Northeastern Brazil. In: M.R. Mello and B.J. Katz, eds., Petroleum systems of South Atlantic margins: AAPG Memoir 73, p.273-300.

Mohriak, W.U., B. Fernandez and A.S. Biassussi, 2004. Salt tectonics domains and structural provinces: analogies between the South Atlantic and the Gulf of Mexico. In: P. J. Post, D. L. Olson, K.T. Lyons, S.L. Palmes, P.F. Harrison and N.C. Rosen (eds.), Salt–sediment interactions and hydrocarbon prospectivity: concepts, applications, and case studies for the 21st century. 24th Annual GCSSEPM Foundation, Bob F. Perkins Research Conference, December 5-8, 2004, Houston, Texas, USA, CD ROM p.551–587.

Mohriak, W.U., M. Nemcok and G. Enciso, 2008. South Atlantic divergent margin evolution: rift-border uplift and salt tectonics in the basins of SE Brazil. In: Pankhurst, R.J., Trouw, R.A.J., Brito Neves, B.B. & de Wit, M.J. (eds.), West Gondwana pre-Cenozoic correlations across the South Atlantic region. Geological Society of London, Special Publication 294, p.365-398.

Montgomery, S. L. and D.W. Moore, 1997. Subsalt play, Gulf of Mexico: a review. AAPG Bulletin, v.81, n.6, p.871-896.

Moulin, M., D. Aslanian, J.L Olivet, I. Contrucci, L. Matias, L. Géli, F. Klingelhoefer, H. Nouzé, J.P. Réhault and P. Unternehr, 2005. Geological constraints on the evolution of the Angolan margin based on reflection and refraction seismic data (ZaiAngo project). Geophysical Journal International, v.162, p.793-810.

Muller, R.D., M. Sdrolias, C. Gaina, and W.R. Roest, 2008. Age, spreading rates and spreading symmetry of the world's ocean crust, Geochem. Geophys. Geosyst., 9, Q04006, doi:10.1029/2007GC001743.

Salisbury, M.H. and C.E., Keen, 1993. Listric faults imaged in oceanic crust. Geology, v.21, p.117-120.

Scotese, C.R., 2002. Paleomap Project. http://www.scotese.com

Tari, G., J. Molnar, P. Ashton, and R. Hedley, 2000. Salt tectonics in the Atlantic margin of Morocco. The Leading Edge, v.19, n.10, p.1074-1078.

Uchupi, E., 1989. The tectonic style of the Atlantic Mesozoic rift system. Journal of African Earth Sciences, v.8, p.143-164.

Uchupi, E. and K.O. Emery, 1991. Pangaean divergent margins: historical perspective. Marine Geology, v.102, p.1-28.

Wu, Y., K.E Louden,. T. Funck, H.R. Jackson and S.A. Dehler, 2006. Crustal structure of the central Nova Scotia margin off Eastern Canada. Geophysical Journal International, v.166, p.878-906.

**BACK**

# Session 2A:
# PETROLEUM SYSTEMS

Husky Energy

## KEYNOTE ADDRESS

**PETROLEUM SYSTEMS OF THE U.S. CENTRAL ATLANTIC MARGIN**
**Post, Paul J. and Sassen, Roger**

**UNUSUAL JURASSIC CONDENSATE OF THE HUDSON CANYON AREA, U.S. ATLANTIC**
Sassen, Roger; and Post, Paul J.

**BALTIMORE CANYON UNTESTED GAS POTENTIAL**
Epstein, Samuel Abraham; and Clark, Donald

**PALEOCEANOGRAPHIC AND PALEOENVIRONMENTAL IMPLICATIONS FOR HYDROCARBON EXPLORATION OF THE CONTINENTAL SLOPE OFF NOVA SCOTIA**
Jansa, Lubomir F.

**THE PENICHE BASIN: TECNO-SEDIMENTATION AND EXPLORATORY ASPECTS**
França, Almério Barros; Gontijo, Rogério Cardoso and Bueno, Gilmar Vital

**GEOLOGICAL EVOLUTION AND HYDROCARBON POTENTIAL OF THE HATTON BASIN (UK SECTOR), NE ATLANTIC OCEAN**
McInroy, David and Hitchen, Kenneth

**REVISITING THE EAST GEORGES BANK BASIN, OFFSHORE NOVA SCOTIA - WHAT THE EXPLORATIONISTS SAW TWO DECADES AGO**
Koning, Tako

BACK

# NOTES

# Petroleum Systems of the U.S. Central Atlantic Margin

**Paul J. Post**
U.S. Minerals Management Service
1201 Elmwood Park Blvd.
New Orleans, LA, 70123
United States
e-mail: paul.post@mms.gov

**Roger Sassen**
Dept. of Geology & Geophysics
Geochemical & Environmental Research Group
Texas A&M University
College Station, TX, 7784
United States
e-mail: sassen@gerg.tamu.edu

## ABSTRACT

From 1975–1988, a single stage of expensive, disappointing hydrocarbon exploration took place on the U.S. Atlantic margin (USAM). Fifty-one wells (5 COST – 46 industry) were drilled in the Georges Bank basin, Baltimore Canyon Trough (BCT), and Southeast Georgia Embayment: none were drilled in the Carolina Trough.

Tested play types included drape/compaction structures, amplitude anomalies, listric fault traps, a dyke-swarm cored uplift, various carbonate margin plays, and slope-apron siliciclastics. The only positive results in the USAM were the gas encountered and/or tested in the eight wells drilled in the four-block Hudson Canyon (HC) 598 area, a listric fault trap in the BCT.

Analogs previously applied to USAM basins are inappropriate. While the same geologic age, they differ in regional and local setting. Carbonate and clean/mature siliciclastic reservoir analogs in the Gulf of Mexico Mesozoic basins are located on salt rollers, or related to salt-cored or salt-withdrawal structures. Other than in the Carolina Trough, similar structures are not widely recognized in USAM basins. The productive Sable sub-basin siliciclastic depocentre is located basinward from the carbonate margin and reservoirs are often overpressured, preserving porosity and permeability. In USAM basins, siliciclastic depocentres are generally landward from the margin and reservoirs encountered to date are not overpressured.

Throughout the USAM, issues regarding petroleum system elements include: generally degrading siliciclastic reservoir quality with depth, poorly developed carbonate reservoir facies, identification and areal distribution of source rocks, and timing of seal deposition/lithification in carbonate margin tests drilled to date. Petroleum system processes; i.e., timing of hydrocarbon generation–migration–accumulation are also poorly understood and appreciated.

Assessment of these basins using a forensic petroleum system approach may provide guidance for future exploration strategies.

BACK

# Unusual Jurassic Condensate of the Hudson Canyon Area U.S. Atlantic

**Roger Sassen**
Dept. of Geology & Geophysics
Geochemical & Environmental Research Group
Texas A&M University
College Station, TX, 7784
United States
e-mail: sassen@gerg.tamu.edu

**Paul J. Post**
U.S. Minerals Management Service
1201 Elmwood Park Blvd.
New Orleans, LA, 70123
United States
e-mail: paul.post@mms.gov

## ABSTRACT

Gas and minor condensate was discovered in Late Jurassic and Early Cretaceous reservoirs in the Hudson Canyon (HC) 598 area of the Baltimore Canyon Trough (BCT). The oldest sedimentary rocks in the BCT are interpreted to be Triassic syn-rift deposits. Predominantly carbonate Early to Middle Jurassic units overlie the Triassic and underlie the Late Jurassic-Early Cretaceous siliciclastic reservoirs.

Condensates from the Kimmeridgian (HC 598-1) and Albian (HC 642-2) reservoirs originate from the same source rock. While biomarkers are absent or in low relative abundance in the condensate, diamondoids, consisting primarily of adamantane and diamantane, along with their methyl and ethyl derivatives, are relatively abundant. The diamondoids have been concentrated during intense thermal cracking of an original oil. The carbon isotopic properties of the condensate are extremely enriched in 13C (-23.7‰ to -24.6‰ PDB), consistent with a Jurassic marine kerogen source. Triassic source rocks appear unlikely to have sourced these condensates because Triassic-sourced oils in the Newark and Culpepper basins are strongly depleted in 13C. The unusual geochemistry of the condensate is interpreted to be the result of extreme thermal cracking of oil sourced from the underlying Early to Middle Jurassic carbonate-rich source rocks. Diamondoid maturity indices suggest that the maturity of the condensate ranges from ~1.3% to ~1.6% vitrinite reflectance (Ro), significantly higher than the estimated ~0.9% Ro of the deepest Kimmeridgian reservoir. Vertical migration of deeper, more mature hydrocarbons into shallower reservoirs was facilitated by faults connecting the source and the reservoir.

The enrichment of diamondoids and 13C are similar to condensates sourced by the Late Jurassic Smackover Formation of the U.S. Gulf Coast. The role of Jurassic oil-prone source rocks in the Central Atlantic is underappreciated.

BACK

# Baltimore Canyon Untested Gas Potential

**Samuel Abraham Epstein**
Geoval Consultants
3701 173 Beach 134th Street
Belle Harbor, New York, 11694
USA
e-mail: samuelepstein@geovalconsulting.com

**Donald Clark**
Geoval Consultants / Northeastern Science Foundation
Staten Island, New York, 10304
USA

## ABSTRACT

Hydrocarbon exploration in the Baltimore Canyon during the 1970's and 1980's targeted Upper Jurassic and younger clastics and carbonates in structural traps. Five wells encountered hydrocarbons with cumulative flow rates testing 90 mm cfg/d. The apparent discontinuity in reservoir extent resulted in project abandonment. Highly mature, organic source rocks in this area were not identified. A recent organic reinterpretation of gas condensates from the Hudson Canyon suggests a deeper Lower Jurassic source, analogous to that of the U.S. Gulf Coast's Smackover formation, Late Jurassic in age.

Reprocessed seismic data (AVO Analysis) indicates reflectors typical of widespread salt layers deposited during the Early Jurassic (60 m thick and 25 km wide) suggesting arid and restricted (anoxic) depositional climatic conditions in the Early Jurassic. Impermeable evaporites and shales, between the Lower and Upper Jurassic, may provide excellent seals explaining the lack of significant migration of hydrocarbons into porous rocks of the Upper Jurassic and Cretaceous. The Gulf Coast Smackover may be an excellent analog for this area.

A Baltimore Canyon Isopach map of the Triassic-Jurassic suggests that a significant area of Lower Jurassic age rocks is buried to depths of mature hydrocarbon generation (gas). Reservoirs should be in carbonates and shelf clastics. A new exploration strategy should focus on deeper sections of the Lower and Middle Jurassic, nearer to the Baltimore Canyon Jurassic depocentre, at much greater depths than previously drilled. Drilling should also be significant distances from igneous emplacements, which may have breached upper reservoir seals.

## Introduction

Emerging markets demand-pull for energy resources have altered the historical petroleum pricing cycle to the upside. Energy demands in countries such as China and India and the Latin American countries have gone from less than 50 quadrillion BTU in 1970 to over 150 quadrillion BTU in 2000 and is projected to reach over 250 quadrillion BTU in 2020 (Energy Information Administration 2008). Within the industrialized countries, energy consumption has increased from 150 quadrillion BTU in 1970 to over 200 quadrillion BTU in 2000 and is projected to reach over 275 quadrillion in 2020. In the past, political instability in the Middle-East was the major factor in spikes in oil and gas prices.

Starting in the late 1970's, hydrocarbon exploration in the Baltimore Canyon Trough (32 wells) targeted Upper Jurassic and younger clastics and carbonates in structural traps. Five wells encountered hydrocarbons with cumulative flow rates testing 90 mm cfg/d (Ball 1982). Apparent discontinuity in reservoir extent resulted in project abandonment.

Deeper gas bearing pay zones have recently been found at depths greater than 4000 meters on the shallow shelf waters of the Gulf of Mexico by McMoran Exploration. The company is currently drilling

the Blackbeard prospect with the target zones between depths of 9000 and 10000 meters. This paper presents another possible deep play, the Baltimore Canyon Trough, which may contain gas in the offshore eastern United States, an area very close to high demand urban areas.

Thermally mature hydrocarbon source rocks within the Late Jurassic and Early Cretaceous have not been identified in the Baltimore Canyon Trough (Prather 1991; Scholle 1977; Sassen and Post 2008; Claypool 1977). An organic reinterpretation of gas condensate from the Hudson Canyon suggests a deeper, Lower Jurassic source, analogous to that of the U.S. Gulf Coast's Smackover formation, Late Jurassic in age (Sassen and Post 2007). Laminated lime mudstones within the Lower Smackover are the hydrocarbon source rock (Sassen 1987; Sassen 1988; Sassen 1990; Sassen and Moore, 1998; Sassen *et al.* 2005). Reservoirs are bounded above and below by evaporites that act as impermeable boundaries to hydrocarbon migration. The Smackover carbonates are extremely productive at depth (6100 meters).

Reprocessed seismic data (AVO Analysis) from the Baltimore Canyon Trough reveal reflectors typical of widespread salt layers in the Early Jurassic deposits (60 m thick and 25 km wide) suggesting arid climatic conditions and possibly restricted depositional conditions in the Early Jurassic (Figs. 1 and 2) (McKinney, *et al.* 2004). Periods of eustatic sea level rise, suggested by Vail, during the Early and Middle Jurassic could have set the stage for anoxic conditions and the deposition of rich organic limestone source rocks in restricted basins similar to that found in the U.S Gulf Coast Smackover formation (Schlee 1980). Modern rift zone carbonates currently possess excellent reservoir characteristics (Epstein and Friedman 1983).

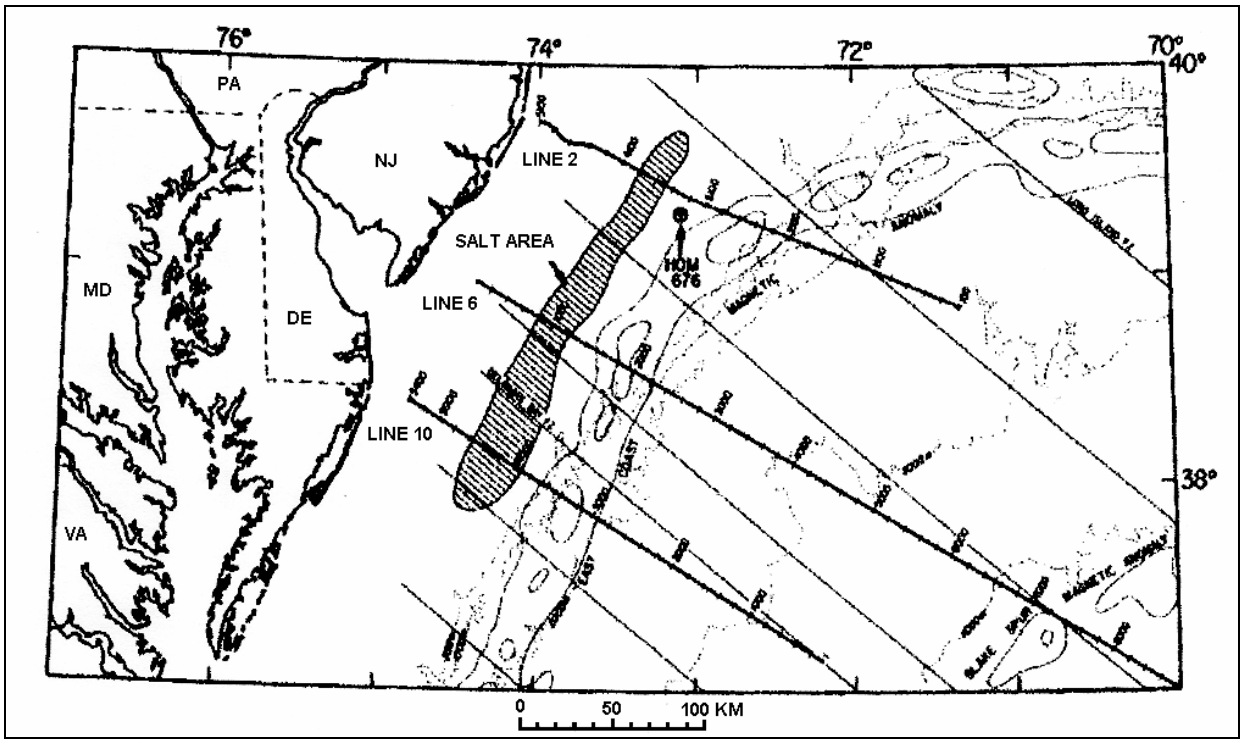


**Figure 1. Map view of the area believed to be a major salt lens in the Baltimore Canyon Trough. The salt lens is Toarcian to Aalenian in age (McKinney *et al.* 2004.**

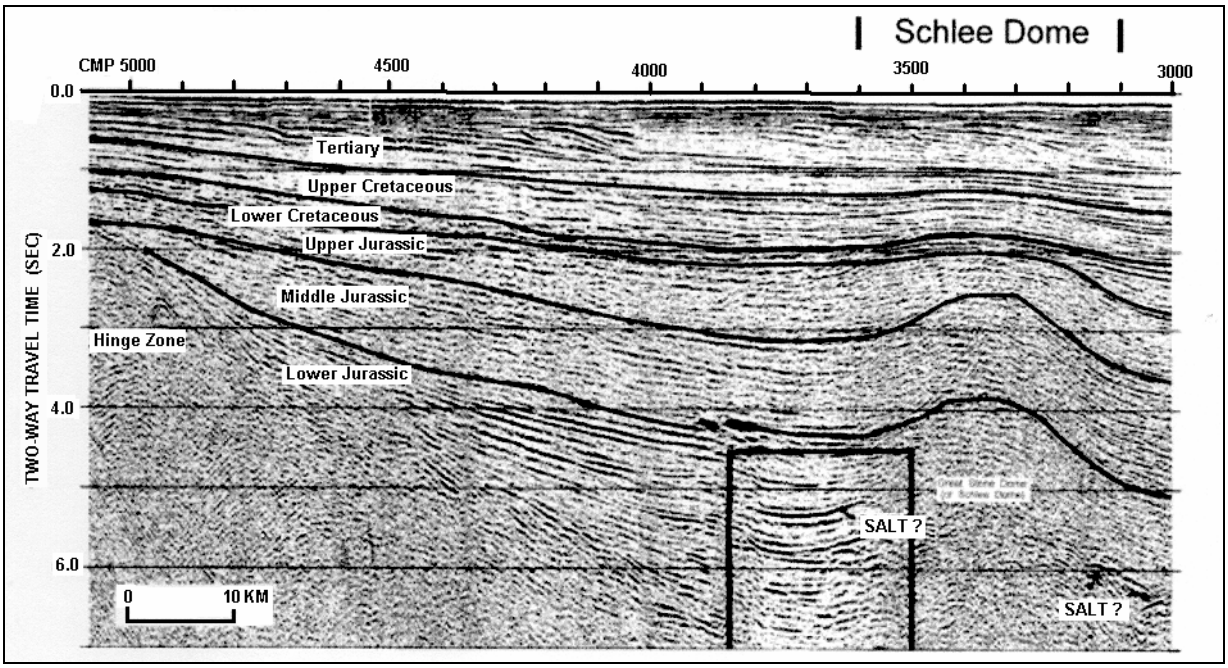


**Figure 2. Cross section of the Baltimore Canyon Trough showing the location (in the highlighted box) of the layers believed to be a major salt lens. The salt lens is Toarcian to Aalenian in age (McKinney *et al.* 2004).**

## Purpose of the Study

The purpose of this study was to further explore the possibility that significant quantities of hydrocarbons are locked in the Early to Middle Jurassic sediments within the Baltimore Canyon Trough. This was done by modeling the thermal maturity of the area and comparing these results to the results of a recently published organic geochemical analysis of condensates taken from Late Jurassic (Kimmeridgian) and Early Cretaceous (Albian) sandstones in the late 1970's (Sassen and Post 2007). The depositional environment of the Baltimore Canyon Trough was also compared to both modern and Mesozoic aged rift zone analogs in order to help determine a future exploration strategy for finding commercial quantities of hydrocarbons.

## Geologic Setting of the Baltimore Canyon Trough

The Baltimore Canyon Trough is a southwestward trending, seaward thickening basin that lies beneath the coastal plain, continental shelf and slope between Cape Hatteras, North Carolina and Long Island, New York (Fig. 3) (Poag 1979; Schlee 1980; Jan Libby-French 1981; Prather 1991; and Withjack, *et al.* 1998). The Baltimore Canyon Trough is one of several basins that formed during the rifting between North America and Africa that began in the Middle to Late Triassic. The trough is asymmetrical with the thickest sediments beneath the outer part of the shelf. More than 15 km of Triassic and younger sediments have been deposited in the trough (Fig. 4). The oldest sediments are Late Triassic in age and are thought to be made up of both non-marine and restricted marine sediments that were deposited during the early stages of rifting. The thickest units are Jurassic in age. These sediments are composed of mixed carbonate and evaporite deposits that were deposited in a rapidly subsiding basin that formed as sea floor spreading widened the newly forming Atlantic Ocean. These Jurassic age deposits record the transition from a restricted marine environment to a more open marine environment. A prograding carbonate shelf complex, made up of coral and grain supported carbonate sediments, marks the maximum seaward extent of these deposits. Overlying the open marine deposits are both marginal marine deposits composed of carbonates, sandstones and shales and coastal plain deposits composed of sandstones, shales and coal that are Late Jurassic to Cretaceous in age.

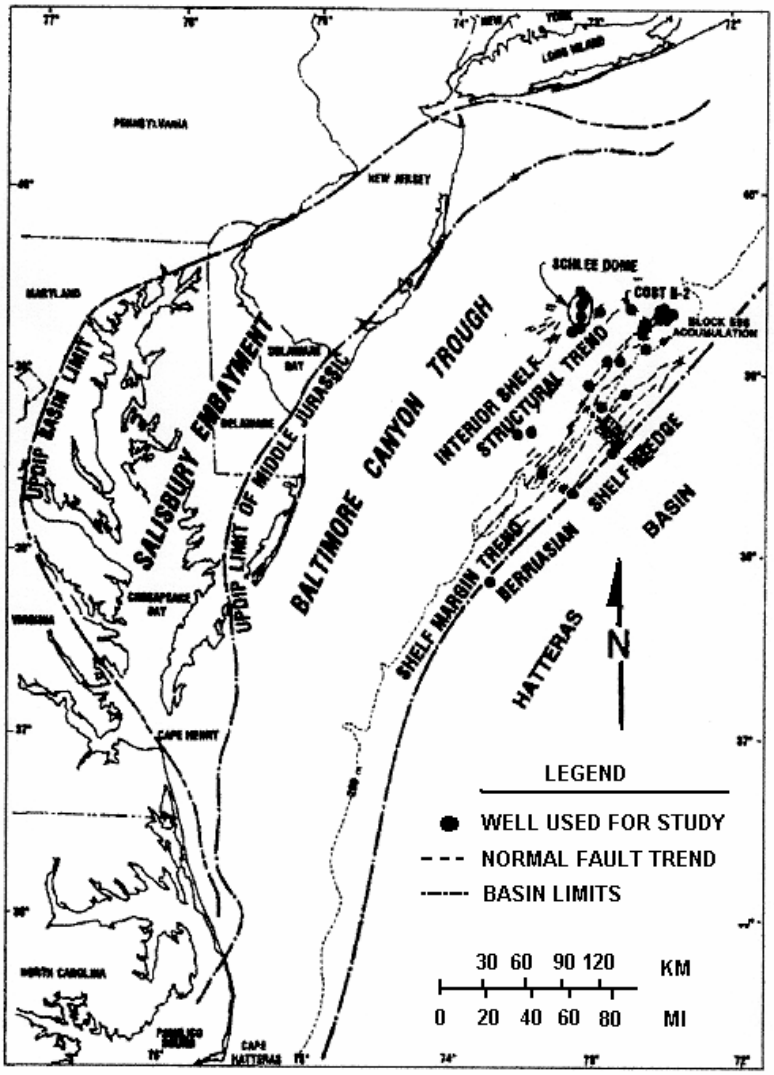


**Figure 3. Map view of the Baltimore Canyon Trough (Prather 1991).**

## History of Petroleum Exploration in the Baltimore Canyon Trough

Exploration for petroleum in the Baltimore Canyon Trough began in 1975 with the drilling of the Continental Offshore Stratigraphic Test (COST) B-2 test well (Fig. 3) (Prather 1991). Of the 32 exploratory wells that were drilled, only a few had hydrocarbon shows or noncommercial quantities of gas and gas condensates. The most significant finds were within some of the sandstone units in the prograding coastal plain and transitional marine deposits. Wells drilled into structural/stratigraphic closures along the downdip termination of the Late Jurassic to Early Cretaceous carbonate shelf edge encountered no hydrocarbons. There was also a failure to find hydrocarbons around the Schlee Dome. Cores and rock samples taken from exploratory wells showed both good and poor reservoir rock. The Upper Jurassic prograded carbonates generally lacked good porosity with less than 200 net meters of reservoir quality limestone (greater than 8% porosity) found in 1830 net meters of these rocks. The transitional marine sandstones contained significant quantities of authigenic clay and calcite cement, reducing their porosity and limiting their value as a reservoir rock. On a positive note, grain supported rocks were encountered (ooids and coral/reef debris), indicating the presence of high energy

environments, reducing the possibility of fine grained sediments filling in valuable pore space. In addition, Berriasian reefal limestones showed evidence of leaching due to subaerial exposure and freshwater diagenesis. This resulted in good reservoir quality rock (porosity greater than 8%).

Failure to find hydrocarbons was thought to be due to an absence of mature source rocks, an absence of migratory pathways from source rock to reservoir rock, an absence of a top seal at the time of hydrocarbon migration, or a combination of all three (Prather 1991). Emplacement of igneous rocks (beneath the Schlee Dome) from the Middle Jurassic to Cretaceous may have breached the trapped hydrocarbon. Impermeable evaporites and shales, between the Early and Late Jurassic, may provide excellent seals explaining the lack of significant migrated hydrocarbons into porous rocks of the Late Jurassic and Early Cretaceous.

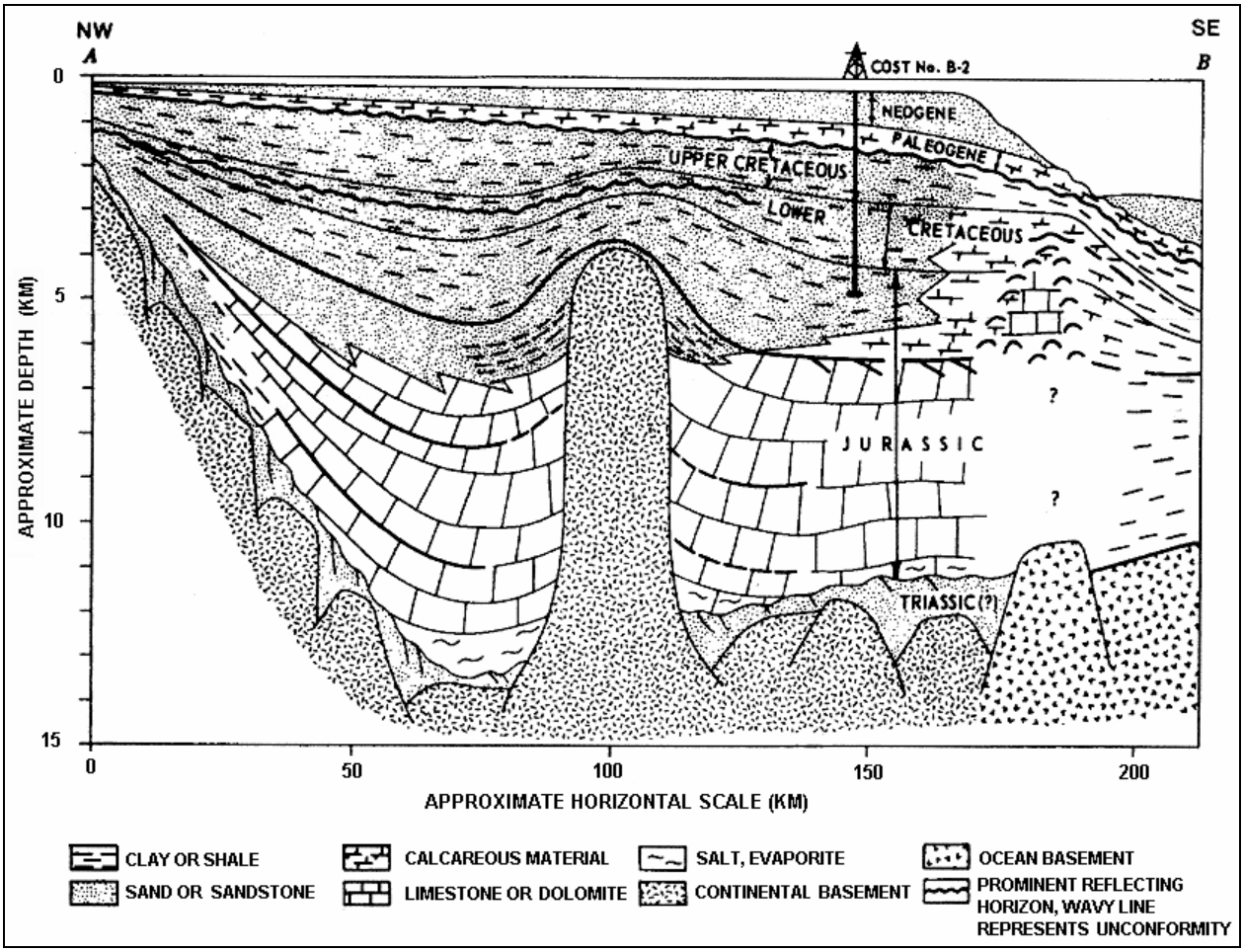


**Figure 4. Schematic geologic cross section of the Baltimore Canyon Trough. Thick black lines indicate major seismic reflectors. Vertical exaggeration approximately 8:1. Cenozoic strata not to scale (Poag 1979).**

## The East African-Red Sea-Dead Sea Rift Zone as a Modern Analog for the Mesozoic Margin of the East Coast of North America

Many similarities exist between the modern East African-Red Sea-Dead Sea rift zone and the Mesozoic margin of the United States East Coast, such as climatic conditions, tectonics, and sedimentary environments (Fig. 5) (Epstein and Friedman 1983). A rift zone formed in the Gulf of Elat (Aqaba) by left lateral shearing between the Arabian plate and the Sinai sub-plate. A normal fault system parallels the

axis of the Gulf of Elat (Aqaba). Consequently, the strata underlying the shelf and adjacent areas overlie a series of uplifted blocks forming a step-like series of raised terraces. The Gulf of Elat (Aqaba) is located in an extremely arid climate. Alluvial fans, algal mats, carbonate deposits and reef complexes are present along the shelf, shelf break, and slope terraces to the limits of the photic zone (approximately 300 ft., 100m) (Fig. 6). Clastics are being deposited penecontemporaneously in alluvial-fan complexes which spill out onto a narrow shelf. Rocks of the adjacent uplifted blocks are composed of Quaternary age coarse, sandy gravel sequences and reefs with associated carbonates sequences.

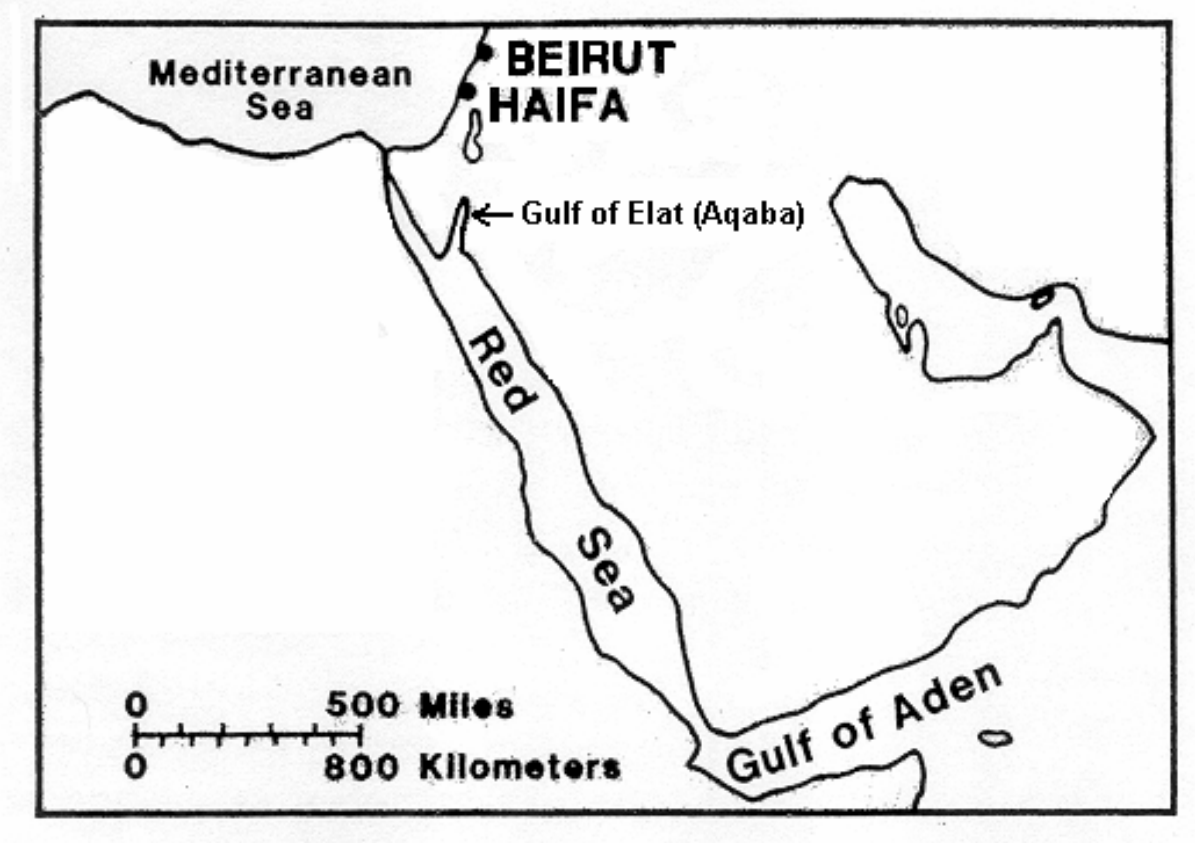


**Figure 5. Location of the Gulf of Elat (Aqaba) in the Middle East (Epstein and Friedman 1983).**

In the Gulf of Elat (Aqaba) a series of uplifted fault blocks, related to active rifting, are found subaerially exposed adjacent to the shelf (Fig. 7) (Epstein and Friedman 1983). Although preferential dissolution and subsurface carbon dioxide degassing may result in localized areas of low porosity and permeability, subaerial exposure of carbonates is more likely to enhance porosity than destroy it. The importance of subaerial exposure to the creation and enhancement of secondary porosity and permeability is clearly demonstrated in the emergent reefs of the Gulf of Elat (Aqaba) where a sequence of diagenetic changes occurred that can be traced from living reefs, through modern dead, but still submerged reefs, to emerged reefs in adjacent uplifted blocks (Fig. 8) (Friedman *et al.* 1976; Gvirtzman and Friedman, 1977; Epstein and Friedman 1981a; 1981b; Epstein and Friedman 1983).

Four stages have been recognized sequentially; (1) stage I, the primary limestone fabric in living corals having 30% to 40% porosity and up to 100 md permeability, (2) stage II, marine cementation as a result of high pH fluid in the dead, but still submerged reefs, reducing porosity to 28% to 30% and permeability to 0.01 md, (3) stage III, leaching under subaerial exposure, increasing porosity to up to 60% and permeability to10,000 md, and (4) stage IV, the limited precipitation of low-magnesium calcite through saturated meteoric waters coating only the micritic envelopes. Porosity and permeability is the same range as in stage III.

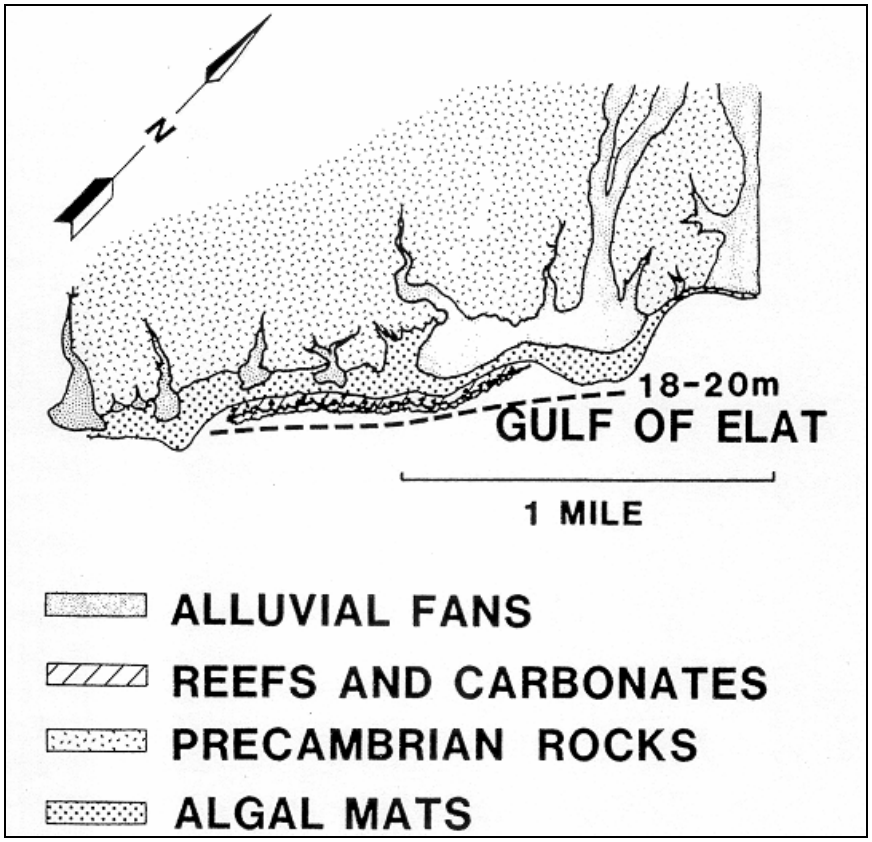


**Figure 6. Distribution of depositional environments along the shoreline of the Gulf of Elat (Epstein and Friedman 1983).**

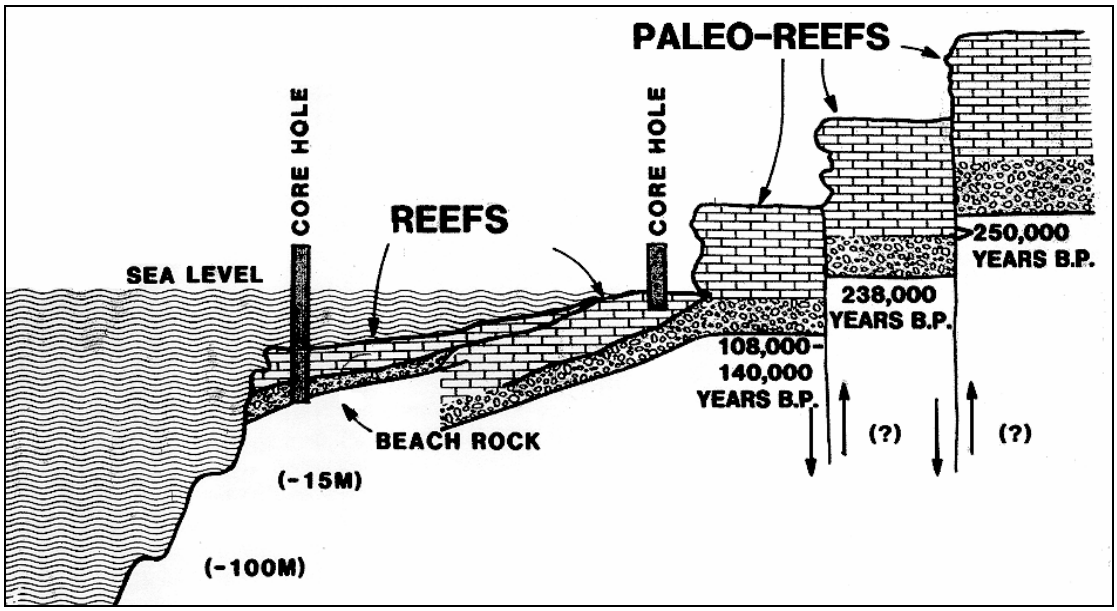


**Figure 7. Diagrammatic representation of raised Pleistocene reef terraces and modern fringing reefs in the Gulf of Elat (Aqaba) (Epstein and Friedman 1983).**

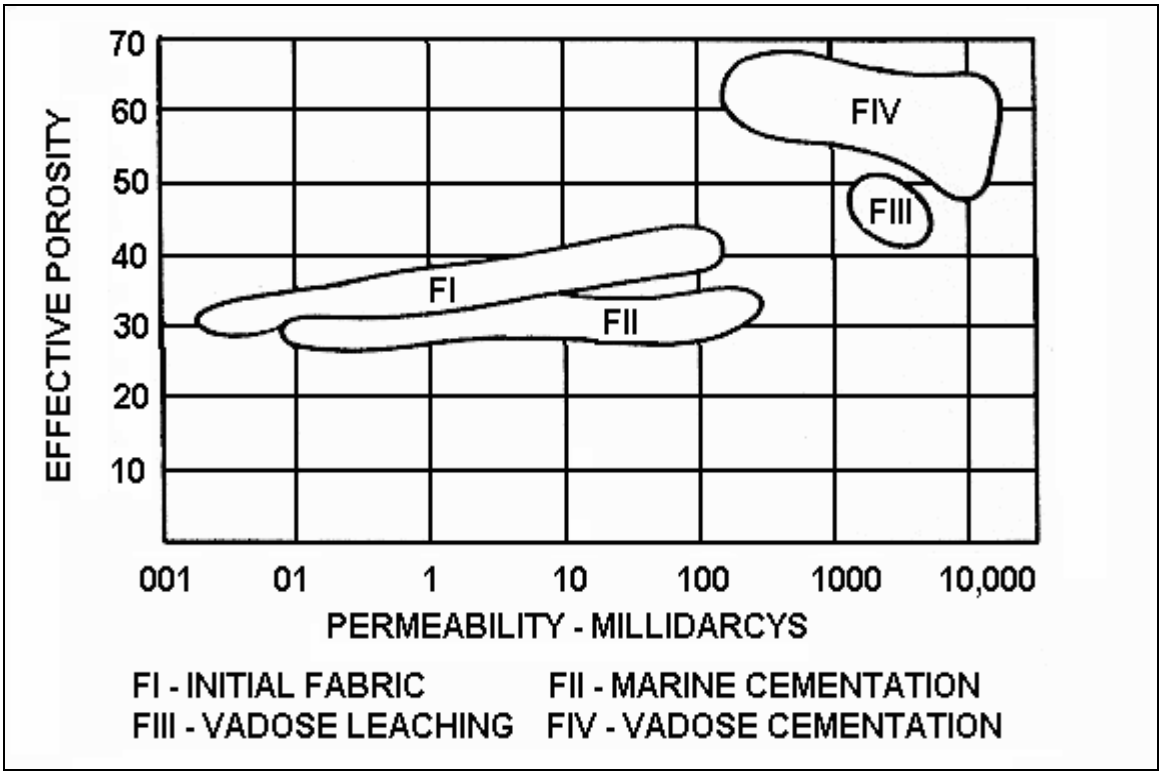


**Figure 8. Plot of effective porosity (%) versus permeability (md) for Pleistocene emergent reefs and modern submerged reefs in the Gulf of Elat (Aqaba) (Epstein and Friedman 1983.**

The Dead Sea is currently undergoing transform motion as an extension of the East-African Rift Zone and is the lowest place on earth (Shamir 2006). Currently, the hypersaline waters of the Dead Sea are evaporating at a rate of 1 meter per year. Beneath the Dead Sea, 5 km of subsidence has occurred since the Pliocene, exceeding the subsidence rates of Early Jurassic Baltimore Canyon Trough (Gvirtzman 2006; Lawrence *et. al.*1990; Friedman, Sanders and Kopaska-Merkel 1992).

## The Jurassic Smackover Formation as an Analog for the Identifying Deeper Target Locations within the Baltimore Canyon Trough Sediments

The Jurassic Smackover formation, beneath the Gulf Coast States (Texas to Florida) has produced tremendous amounts of oil and natural gas (Fig. 9) (Sassen and Moore 1988). Depositional basins formed within the Smackover during the Upper Jurassic as rifting opened up the Gulf of Mexico. Although the timing of rifting in the Gulf Coast States region differs from the timing of rifting along the western Atlantic margin, physical similarities between the two areas may have produced the same depositional environments. If this is the case, then an understanding of the mechanisms for the preservation of organic material and the subsequent generation of hydrocarbons in the Smackover formation may hold the key to a successful exploration strategy in the Baltimore Canyon Trough.

Rifting during the Upper Jurassic formed a series of basins beneath the Gulf Coast States (Fig. 9) (Sassen and Moore 1988). These basins were rimmed on the Gulf side by marginal positive features. The first major marine transgression during the Middle Jurassic deposited thick evaporite sequences, the Louann/Werner formation, in these basins. This salt sequence is more than 1800 m thick in some of the basins. The overlying Lower Smackover is made up of laminated lime muds that were deposited during a rapid sea level rise beginning in the Late Jurassic. A rapid sea level rise under highly evaporative

conditions within a restricted basin environment is thought to have lead to a strong density-stratified water column. A strong density stratification would have cut off bottom water from upper oxygen rich surface water leading to anoxic bottom conditions.

The absence of fossils in the Lower Smackover is a strong indication of a hypersaline and anoxic environment. These environmental conditions also lead to the preservation of the algae that later became the kerogen from which the hydrocarbons were generated. These conditions existed in all four of the Gulf interior salt basins. As the sea level stabilized, the rate of sedimentation equilibrated with the rate of basin subsidence (Fig. 10). As a result, shallow, high energy and well oxygenated waters dominated allowing for the development of normal marine fauna and extensive precipitation of ooids. This was the depositional environment of the Upper Smackover. Many of these oolitic grainstones are dolomitized and are associated with evaporite deposits. The highest TOC concentrations are found in the anoxic laminated lime mudstones of the Lower Smackover formation, particularly along pressure seams and stylolites where insoluble material is concentrated. The laminated lime mud of the Lower Smackover is the source rock whereas the ooid grainstones of the Upper Smackover is the reservoir rock.

Hydrocarbon generation and migration within the Smackover started to occur when the level of thermal maturity reached approximately 0.55% vitrinite reflectance (Fig. 11) (Sassen and Moore 1988). Liquid hydrocarbon generation continued until a thermal maturity of approximately 1.0% vitrinite reflectance. Above this level of vitrinite reflectance, liquid hydrocarbons start converting to gas. The depths that these transformations occur are between approximately 3700 meters and 5100 meters for oil generation, 5600 meters for gas condensate generation and 6000 meters for methane generation (Fig. 12).

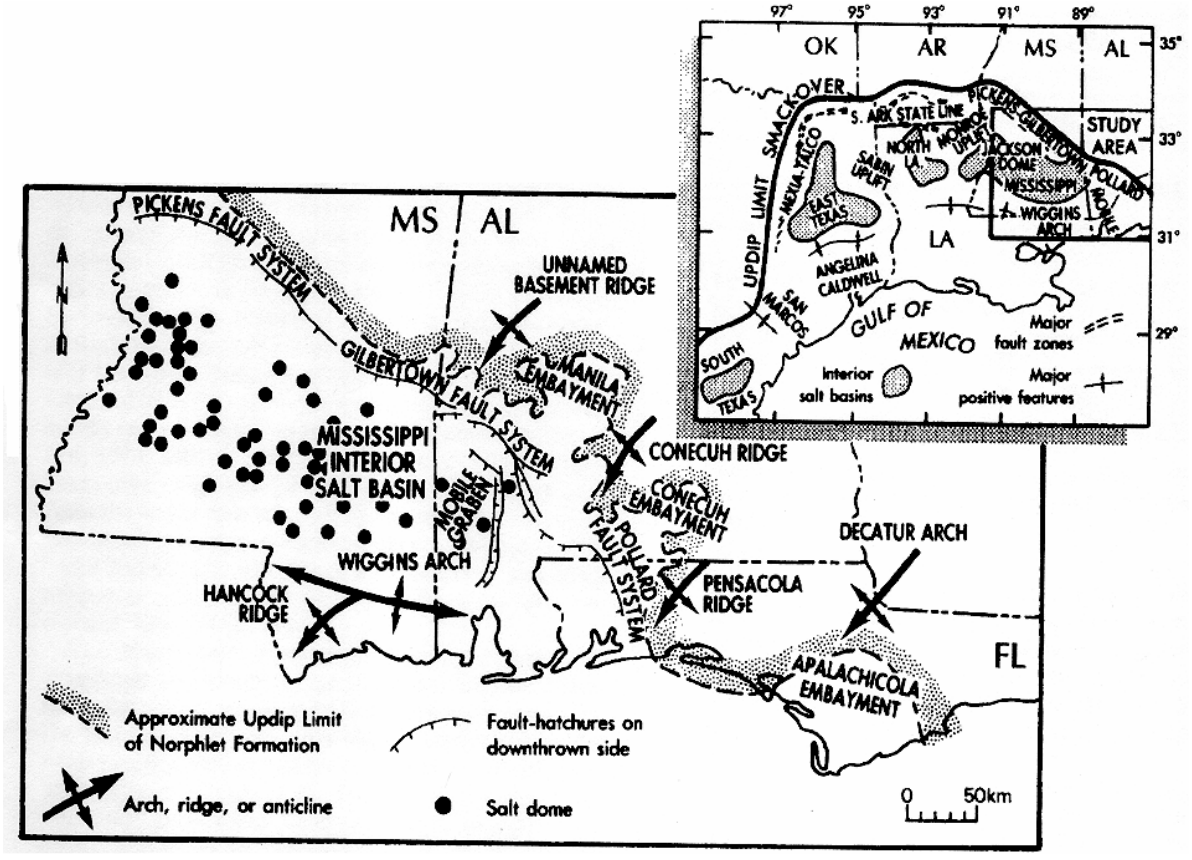


**Figure 9. Geologic setting of the Upper Jurassic across the Gulf of Mexico and the locations of resultant interior salt basins (Sassen and Moore 1988).**

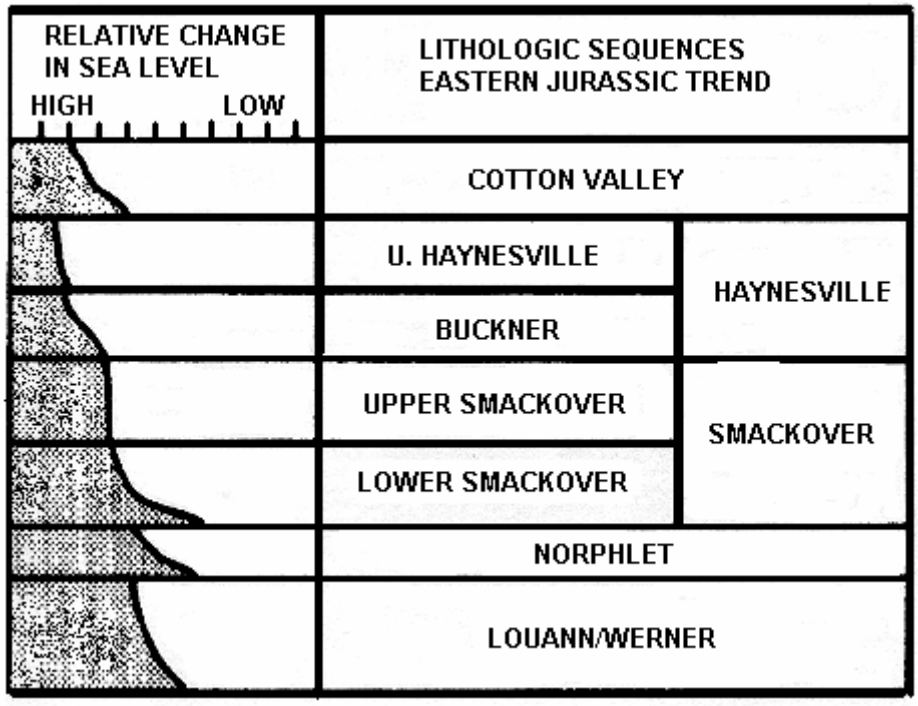


**Figure 10. The relative change in sea level and the lithologic units deposited during the Jurassic in the Gulf Coast, USA. The sea level increased sharply during the time when the Lower Smackover was deposited. The sea level was relatively stabile during the deposition of the Upper Smackover (Sassen and Moore 1988.)**

## Organic Geochemical Assessment of Baltimore Canyon Condensates

Sassen and Post (2007) discussed the significance of relatively high concentrations of diamondoids found in condensate samples taken from an Upper Jurassic (Kimmeridgian) sandstone and a Lower Cretaceous (Albian) sandstone in the Baltimore Canyon Trough in the late 1970's. Diamondoids are the most thermally stable of the complex saturated hydrocarbons and, as a result, are not found in high concentrations unless a significant fraction of the oil has been thermal cracked. Methyladamantane (MAI) and methyldiamantane (MDI) maturity indices were calculated for the condensate samples taken from the Kimmeridgian (MAI = 0.71; MDI = 0.48) and the Albian (MAI = 0.75; MDI = 0.54). These values are roughly equivalent to 1.3 to 1.6% Ro. High temperatures also destroy the biomarkers at thermal maturity levels equivalent to 1.3 to 1.4% Ro. There were low concentrations of biomarkers in the condensates.

Sassen and Post (2007) reported that the thermal maturity of the Kimmeridgian ranges from ~0.7 % to ~0.9%, indicating that condensates could not have originated from sediments of this age. The discrepancy for the Albian sample is even greater, since the thermal maturity for the Albion is ~0.5% Ro. Sassen and Post (2007) concluded that the condensates originated from the Early to Middle Jurassic and migrated up into the Late Jurassic and Early Cretaceous formations. Supporting the assertion that the source rock is from the Early to Middle Jurassic is the fact that the condensates are highly enriched in $^{13}C$. Oils derived from marine kerogen from the Triassic and older age sediments tend to be depleted in $^{13}C$. Further comparisons between the condensates from the Baltimore Canyon Trough and the Smackover and underlying Norphlet reservoirs from the Mobile Bay area of the Gulf Coast indicate that the condensates from the Baltimore Canyon Trough may have originated at depths as great as 6 km (Figs.11 and 12).

Sassen and Post (2007) also discussed the fact that clays act as catalysts for diamondoid formation whereas calcium carbonate may inhibit diamondoid formation. The richest source rock from the Smackover is the laminated lime mud where oil prone kerogen, quartz and clay are closely associated. The interbedding of clastics containing clay within the carbonate bedrock appears to be necessary for the formation of diamondoids.

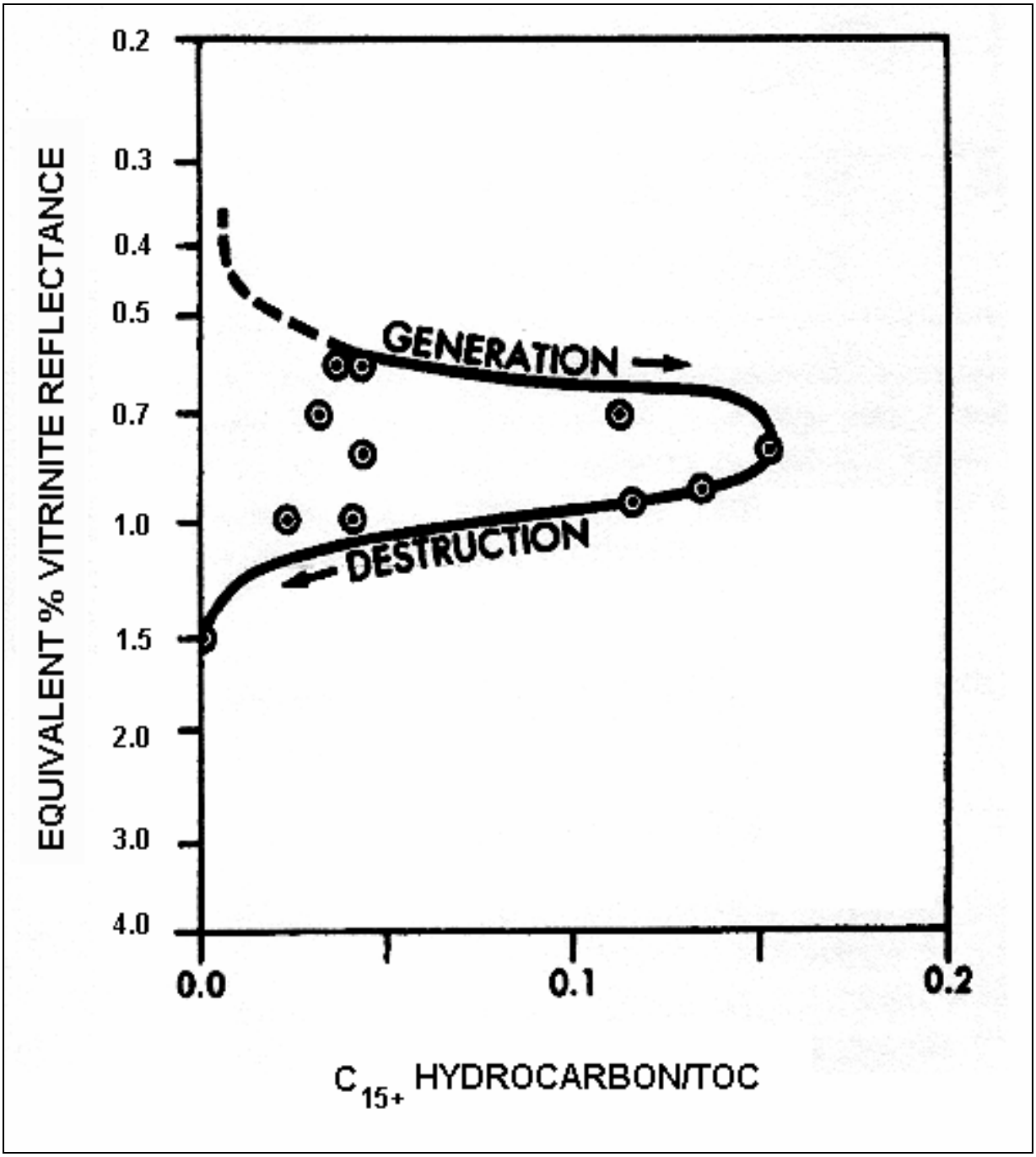


**Figure 11. The generation and destruction of residual hydrocarbons in the organic rich Lower Smackover Formation (Sassen and Moore 1988).**

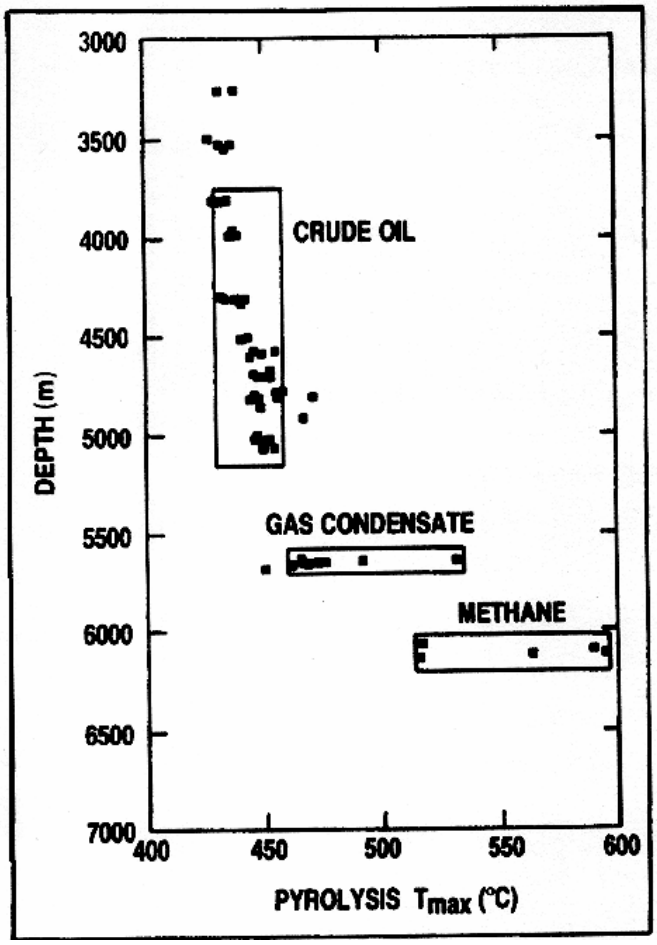


**Figure 12. Thermal maturation depths for crude oil, gas condensates and methane for the Smackover Formation. Data taken from various fields from Mississippi, Alabama and Florida (Sassen and Moore 1988.)**

## Carbonate-Evaporite Complex within the Lower through Upper Jurassic of the Baltimore Canyon Trench

The Early and Middle Jurassic within the Baltimore Canyon Trough have not been penetrated by exploration wells. Despite the lack of physical samples, the case for a carbonate-evaporite complex in the Lower and Middle Jurassic has been made. Poag (1979) has indicated that seismic velocities in the strata below a depth of 6 km exceeded 5 km/sec, suggesting a thick section of carbonate rock (Fig. 4). Indirect evidence for deeply buried evaporites comes in the form of multiple diapers (salt) on seismic profiles off the coast of Cape Hatteras and the coast of New Jersey. Lawrence *et al.* (1990) indicated that the Lower Jurassic is either an aggradational clastic sequence, or an aggradational carbonate/evaporite sequence that interfinger with clastics along the landward margin. As sea floor spreading progressed, carbonates platform formed and was fully established by the Middle Jurassic. This carbonate platform interfingered with clastic rocks along the landward margin. As discussed above, a modern analog for the Mesozoic coast of eastern North America is the Gulf of Elat (Aqaba) in the Middle East. Here, carbonate deposits and reef complexes are present along the shelf, shelf break and slope terraces (Figs. 5 and 6) (Epstein and Friedman 1983).

Reprocessed seismic data analyzed using amplitude versus offset methods indicates reflectors typical of a single widespread salt layer in the Baltimore Canyon Trough (Figs. 1 and 2) (McKinney *et al.* 2004). One dimensional modeling suggests that this layer is as thick as 60 meters near the center of the

layer and thins to approximately 20 meters at the edges. This salt layer extends over an area up to 25 km wide and 230 km long and may ultimately cover an area up to 7,500 km$^2$. The presence of this layer strongly suggests an arid, restrictive and potentially anoxic depositional environment, which may have resulted in the preservation of significant amounts of organic matter. The presence of this salt layer, above Early Jurassic potential source rocks, may partially explain the lack of significant migration of hydrocarbons into the overlying Late Jurassic and Early Cretaceous reservoir rocks. McKinney *et al.* (2004) indicated that the salt layer was deposited during the Late Toarcian or Early Aalenian (Fig. 13). There was a rapid rise in sea level during the Aalenian, which may have flooded the area where the salt is deposited. As discussed above, a rapid rise in sea level under evaporative conditions is thought to have resulted in the deposition of the evaporite beds, laminated carbonate muds and clay rich clastics of the Gulf Coast Smackover formation (Fig. 10) (Sassen and Moore 1988).

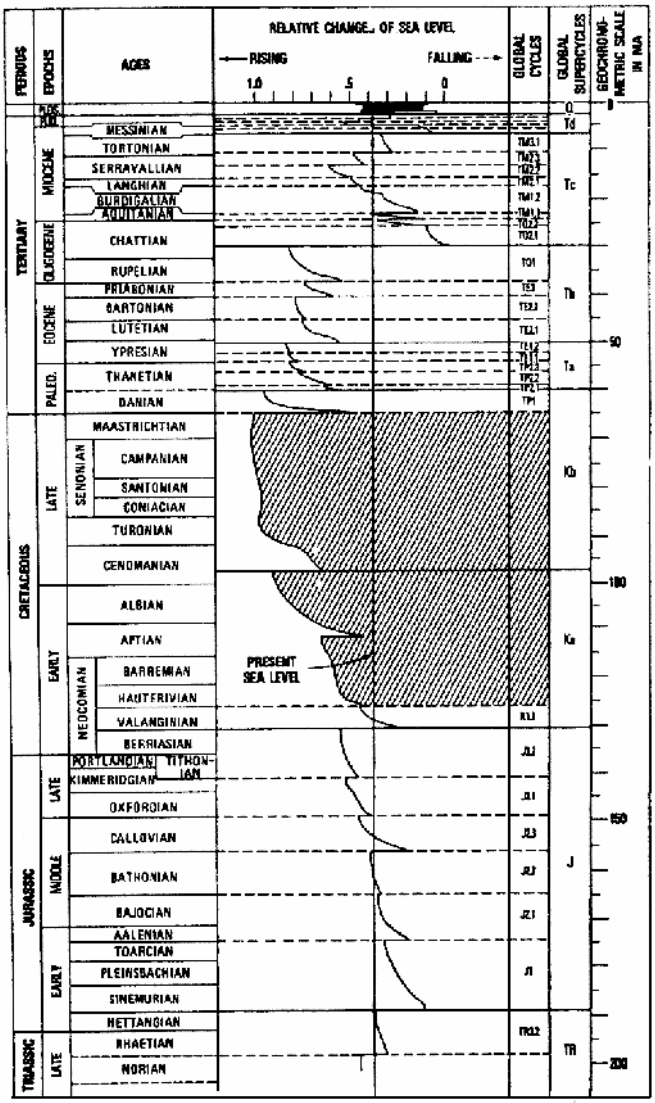


**Figure 13. Global changes in sea level indicate periods of sea level rise in the Early Jurassic (Sinemurian through Toarcian and Aalenian) and a stabilizing of the sea level during the Middle Jurassic (Bathonian). The sea level dropped at the beginning of the Callovian. McKinney *et al.* (2004) indicated that the salt lens in the Baltimore Canyon Trough was deposited during the Late Toarcian or Early Aalenian (Schlee 1980).**

Stable sea level conditions in the Middle Jurassic (Bathonian) may have allowed carbonate deposition to come into equilibrium with, or exceed the rate of basin subsidence in the Baltimore Canyon Trough (Fig. 13). Such conditions may have resulted in the creation of shallow, high energy waters and the precipitation of oolite beds, extensive sabkhas, additional evaporite beds and possibly subaerial exposure. A stable sea level is credited with creating the oolite beds with the Gulf Coast Smackover formation (Sassen and Moore, 1988) (Fig. 10). Sabhkas are commonly found in the supratidal environment when arid conditions dominate the area (Friedman 1980). The sabkha environment is a site of active dolomitization. Subtidal carbonates, associated with evaporites in lagoon settings are also subject to extensive dolomitization (Mazzullo *et al*. 1978; Friedman 1980; Conway and Friedman 1984; Montanez and Read 1992; Sun 1995). Therefore, a significant amount of dolomite may be present in the Middle Jurassic carbonates within the Baltimore Canyon Trough.

An increase in sea level during the Late Jurassic and Early Cretaceous appears to have been responsible for the formation and progradation of a 600 m thick carbonate shelf edge-reef complex (Fig. 14) (Prather 1991). Progradation of carbonate shelf margin extended as much as 60 km in the northern portion of the trough. The extent of progradation of this complex decreases from north to south. The limestone is composed of highly abraded, bioclastic grainstone and coral-hydrozoan boundstone indicative of a high energy environment.

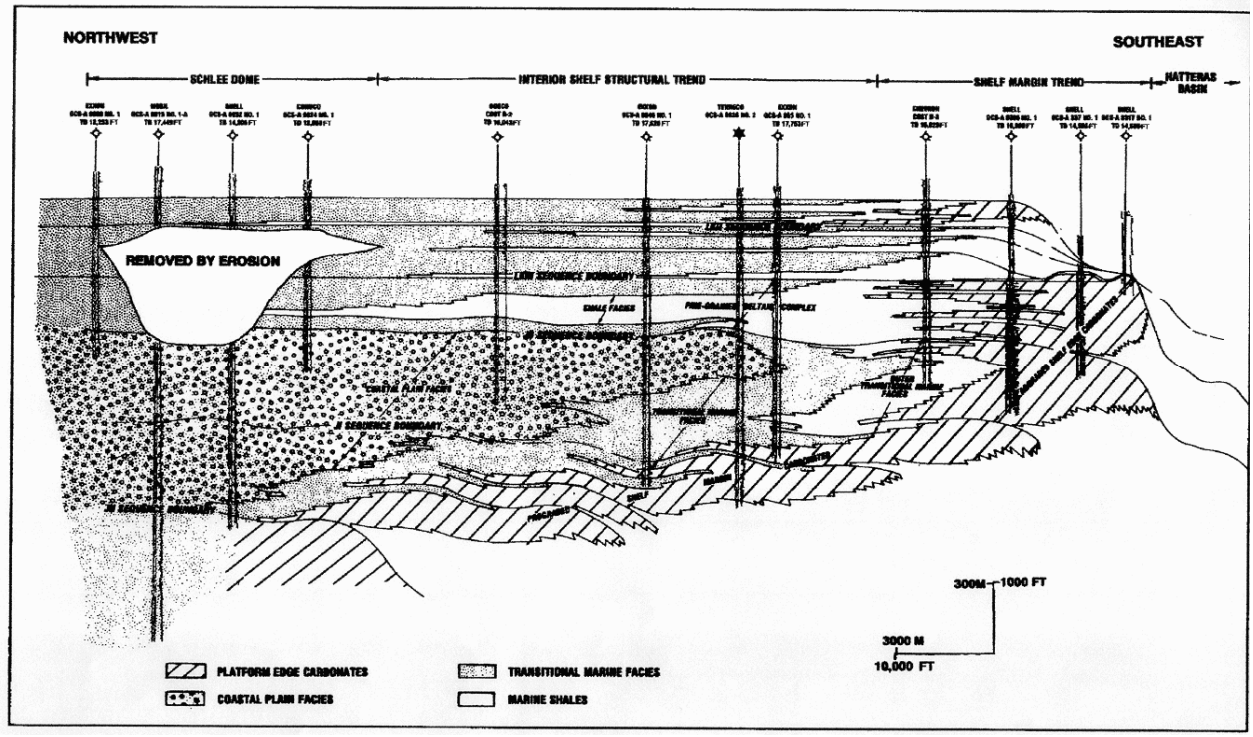


**Figure 14. The prograding platform edge carbonates and younger transitional marine and coastal plain deposits within the Baltimore Canyon Trough (Prather, 1991).**

## Thermal Maturity Model for the Baltimore Canyon Trough

Thermal maturation for the strata in the Baltimore Canyon Trough was modeled using Platte River Associates BasinMod® 1D software. The information used by this software includes formation ages, tops, thicknesses, geothermal gradient of the area and the thermal conductivities of the rock units. Formation tops and thicknesses were based on the Shell 273-1 well (Table 1) (Jan-Libby French 1981).

The base of the Lower Jurassic was placed at ~10,000 m (Lawrence, 1990; Prather, 1991). A geothermal gradient of 1.43$^{OF}$/100 ft. was used.

| Formation | Basal Age | Top Depth (m) | Present Thickness (m) | Lithology |
|---|---|---|---|---|
| Overburden | 5.3 | 0 | 500 | Mudstone |
| Miocene | 25.2 | 500 | 500 | Dolomitic Mudstone |
| Oligocene | 38.1 | 1000 | 400 | Dolomitic Mudstone |
| Eocene | 55.2 | 1400 | 50 | Mudstone |
| Paleocene | 66.8 | 1450 | 50 | Mudstone |
| Upper Cretaceous | 99.6 | 1500 | 600 | Sandy Mudstone |
| Albion | 108.0 | 2100 | 100 | Sandstone |
| Albion to Late Aptian | 116.0 | 2200 | 100 | Shale |
| Early Aptian to Hauterivian | 130.0 | 2300 | 900 | 60% Sandstone 40% Shale |
| Valaginian | 136.0 | 3200 | 150 | 45% Shale 40% Sandstone 15% Coal |
| Berriasian | 141.0 | 3350 | 150 | 45% Shale 40% Sandstone 15% Coal |
| Tithonian | 146.0 | 3500 | 200 | 45% Shale 40% Sandstone 15% Coal |
| Kimmeridgian | 155.0 | 3700 | 1600 | Brown Shaly Sand |
| Middle to Late Jurassic | 200.0 | 5300 | 4700 | Limestone Evaporite Sandstone Siltstone |

**Table 1. The input variables for the BasinMod® 1D software program modeling the thermal Maturity of the Baltimore Canyon Trough.**

Sediments from the Early to Middle Jurassic entered the early mature oil window at a depth of burial of approximately 2500 m to 3000 m and passed into the main gas generation window at a depth of approximately 6500 m to 5000 m (Figs. 15 and 16). These sediments entered the main gas generation window during the Late Jurassic. Gas generation continued throughout the Tertiary. Sediments from the Late Jurassic passed into the early mature window at a depth of approximately 2200 m to 2500 m and stayed in the mid mature window throughout the Middle to Late Cretaceous and into the Tertiary. The only Cretaceous sediments that entered into the early mature window were the ones that were deposited at the very beginning of the Cretaceous. Sediments younger than the Middle Cretaceous never reached the early mature window.

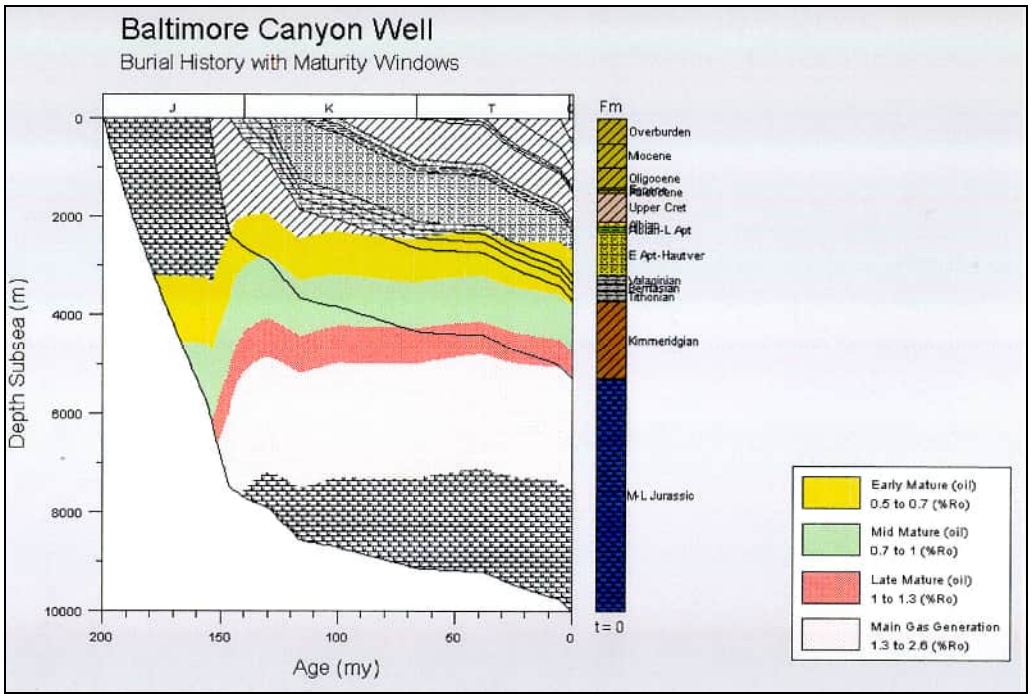


**Figure 15. The thermal maturation profile for the Shell 273-1 well in the Baltimore Canyon Trough. Early to Mid Jurassic sediments entered the early mature (oil) phase at a depth of approximately 2500 m and entered into the main gas generation window at a depth of approximately 5000 m. Gas was generated though the Tertiary. Sediments younger than the late Early Cretaceous never became thermally mature.**

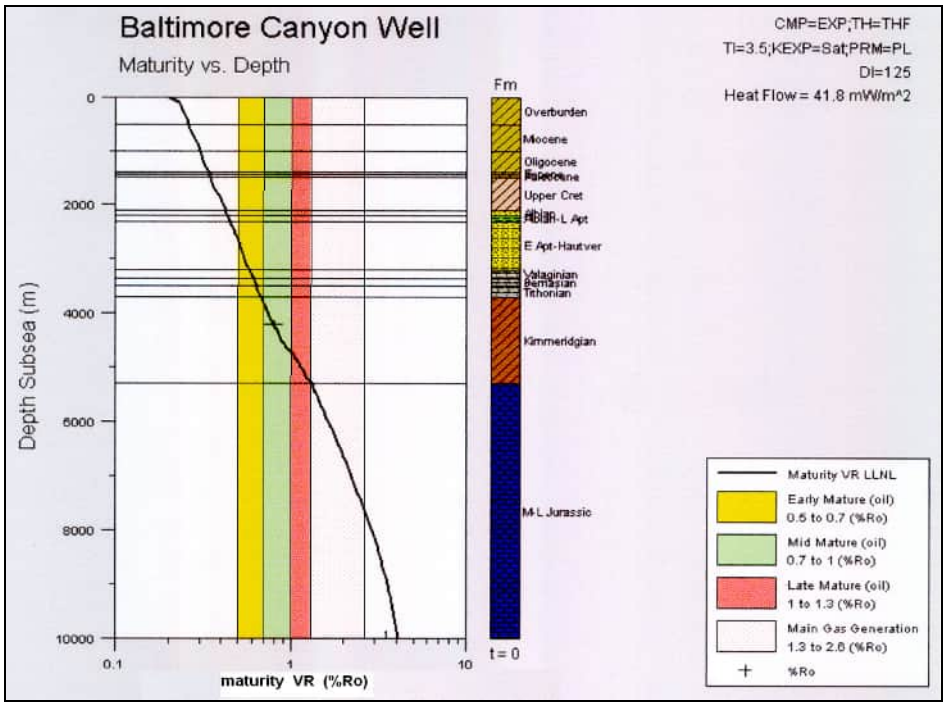


**Figure 16. The black sloping line represents the change in thermal maturity versus depth for rocks in the Baltimore Canyon Trough. Kimmeridgian aged rocks are in the oil window whereas all rocks below the Kimmeridgian are in the main gas generating window.**

## Discussion

The results of the thermal maturation model in this study are consistent with the observations of Sassen and Post (2007). Sassen and Post (2007) reported that the thermal maturity of the Kimmeridgian ranges from ~0.7% to ~0.9% Ro, whereas the thermal maturity of the Albian is ~0.5% Ro. The thermal maturity values, calculated in this study, for most of the Kimmeridgian ranges from 0.7% to 1.0% Ro and less than 0.5% Ro for Albian age sediments (Figs. 15 and 16). Sassen and Post (2007) determined thermal maturity values for the condensates taken from the Kimmeridgian and Albion sandstones to be roughly equivalent to 1.3 to 1.6% Ro and had concluded that the condensates originated from Early to Middle Jurassic sediments . These values are consistent with the values from the main gas generation window (1.3 to 2.6% Ro), calculated in this study, for the Early to Middle Jurassic.

Hydrocarbon generation in the Smackover started to occur when thermal maturity reached approximately 0.55% Ro (Fig. 12) (Sassen and Moore, 1988). Oil generation continued until a thermal maturity of approximately 1.0% Ro was reached. Above this level, liquid hydrocarbons were progressively converted to gas. This corresponds to depths of between 3700 and 5100 meters for oil generation and over 6000 meters for gas generation (Fig. 13). For Early Jurassic rocks, oil generation in the Baltimore Canyon Trough began at a thermal maturity level of 0.5% Ro at a depth of burial of approximately 3000 m (Fig. 15). The main gas generation window started at a thermal maturity level of 1.3% Ro at a depth of approximately 6000 to 5000 meters.

Similarities between the thermal maturity histories of the Gulf Coast Smackover formation and the Early to Middle Jurassic sediments in the Baltimore Canyon Trough strengthen the opinion of Sassen and Post (2007) that the Smackover formation may be a useful analog for the study of the Baltimore Canyon Trough.

As mentioned above, a rapid rise in sea level under evaporative conditions set the stage for a strong density stratification in restricted marine basins and the subsequent deposition of the Lower Smackover evaporites, laminated carbonate muds and clay rich clastics (Sassen and Moore 1988). This environment was ideally suited for the preservation of organic matter. Both the Gulf Coast Smackover formation and the Lower to Middle Jurassic sediments of the Baltimore Canyon Trough appear to have been affected by similar fluctuations in sea level (Figs. 10 and 13). A relatively stabile sea level, after this initial rapid sea level rise, may have allowed for the rate of carbonate production to come into equilibrium with, or exceed basin subsidence. This would have lead to a shoaling of the water in the basins and the production of oolite deposits. Sassen and Moore (1988) indicated that ooid grainstones are present in the Upper Smackover formation and that they are productive reservoirs. A similar occurrence may have occurred during the Bathonian in the Baltimore Canyon Trough (Fig. 13).

In addition to oolite production, shoaling waters due to excessive carbonate production may have lead to the development of extensive sabkhas, the precipitation of evaporite beds and subaerial exposure in the Baltimore Canyon Trough during the Middle Jurassic (Bathonian). Such conditions would have favored the formation of significant dolomite deposits (Mazzullo *et al.* 1978; Friedman, 1980; Conway and Friedman 1984; Montanez and Read 1992; Sun 1995). Sassen and Moore (1988) indicated that ooid grainstones in the Upper Smackover formation are commonly dolomitized and associated with thick evaporative units.

Any drops in sea level, such as the one at the beginning of the Callovian, could have subaerial exposed these dolomite, or mixed dolomite and limestone, deposits and may have lead to karst diagenesis and enhanced secondary porosity (Fig. 13). Early Cretaceous (Berriasian) reefal limestones showed evidence of leaching due to subaerial exposure and freshwater diagenesis (Prather 1991). Karst diagenesis has enhanced the porosity of many carbonate reservoirs in North America (Clark and Friedman 2008). An examination of a modern rift zone analog, the Gulf of Elat (Aqaba) in the Middle East, has demonstrated that subaerially exposed reefs are subject to enhanced secondary porosity due to subaerial exposure (Epstein and Friedman 1983). The possible subaerial exposure of carbonate deposits in the Baltimore Canyon Trough during the Middle Jurassic (Bathonian or Early Callovian) could also have lead to enhanced secondary porosity. The presence of extensive dolomite deposits would certainly make

excellent reservoir rock. Dolomites usually are a better reservoir rock than limestones due to fracturing, karstification and burial corrosion due to organic or sulfuric acids. Dolomite reservoirs account for approximately 80% of the recoverable oil and gas that comes from carbonate rocks in North America (Sun 1995). The distribution of porosity and permeability in dolomite reservoirs is complex and is dependent upon the original fabric of the rock, the volume of dolomitizing fluids that passes through the rock and post dolomitization diagenesis. A review of this topic is beyond the scope of this paper, interested readers are referred to Sun (1995) for a more complete treatment of this topic.

In addition to changes in eustatic sea level, tectonic forces may have had an effect on the relative sea level of the Baltimore Canyon Trough during the Middle Jurassic (Prather 1991 and Withjack *et al.* 1998). Transverse fracture zones separated the western Atlantic margin into basins and platforms, igneous intrusions uplifted overlying sedimentary beds (one notable example is the Schlee dome) and differences in the rates of lithospheric displacement, close to and distant from asthenospheric upwelling, lead to inversion and uplifting. The degree that each of these processes affected relative sea level in the Early to Middle Jurassic may vary depending upon the exact location within the Baltimore Canyon Trough.

Prather (1991) indicated that a highly pressurized gas-bearing zone in a predominantly limestone Oxfordian sequence was encountered at a depth of 5200 meters by the Texaco-Tenneco OCS-A 0038 No. 1 well. The presence of a highly pressurized gas zone at this depth is consistent with the thermal maturity model produced for this study, which indicates that the main gas generation window for Oxfordian age rocks starts at a depth of approximately 5000 m (Fig. 15). Although it is not know whether the gas found in this zone originated in place, or if it migrated from deeper source rocks, it is encouraging that it is located at a depth predicted by the thermal maturation model.

Overall, the Oxfordian limestone has poor porosity due to sparry calcite filling interparticle pore spaces (Prather 1991). This tight limestone, although a poor reservoir rock, may be an excellent caprock for the rock beneath it (Bathonian to Callovian), which may be composed of dolomite with good reservoir qualities. The presence of tight limestones may help to explain why wells drilled into Cretaceous (Berriasian and Aptian) aged rocks had no significant hydrocarbon shows despite the presence of large structural closures. Prather (1991) indicated that much of the prograded carbonate shelf margin complex that was tested lacks good reservoir quality rock.

The timing of hydrocarbon generation and expulsion is critical when considering reservoir and trap formation. The Early and Middle Jurassic beds passed into the main gas generation window during the Late Jurassic and/or Early Cretaceous (Figs. 15). Gas production continued throughout the Cretaceous and into the Tertiary. This would suggest that traps and top seals formed in the Late Jurassic and the Cretaceous would have formed in time to stop the vertical migration of hydrocarbons. Therefore, the tight Oxfordian limestones and other sparry calcite cemented shelf margin rocks could very well have acted as a top seal preventing vertical migration of hydrocarbons into the overlying strata. This may partially explain why wells drilled into Berriasian and Aptian aged rocks had no significant shows of hydrocarbons. Early to Middle Jurassic evaporite beds, formed as surface features, would clearly have been in place to act as seals before the depth of burial was sufficient enough for the generation of hydrocarbons.

Dolomitization of limestone is a very complex process, which often occurs in various stages close to the surface, during progressive burial and as a result of deep burial (Mazzullo *et al.* 1978; Friedman 1980; Conway and Friedman 1984; Montanez and Read 1992; Sun 1995; Phillips and Friedman,2001a). If dolomite deposits formed at the surface and during progressive burial in the Baltimore Canyon Trench during the Middle Jurassic, they would have been in place before the thermal maturation of the Early Jurassic source rocks.

The vertical migration of gas generated from deeply buried source rocks may have encountered several different types of seals. These seals include either single, or, multiple beds of evaporites, tight limestones and shales. Because these different types of seals were deposited in different environmental settings, there may be multiple layers of seals throughout the Baltimore Canyon Trough.

## Conclusions

Prather (1991) listed several possible reasons why exploration wells drilled into the Baltimore Canyon Trench failed to find commercial quantities of hydrocarbons, these are (1) absence of mature source rocks, (2) absence of migration pathways (3) absence of top seals at the time of hydrocarbon migration. Each of these three concerns will be addressed below.

The results of this study, combined with the results of Sassen and Post (2007) indicate that mature source rocks are present in the Baltimore Canyon Trough, but at depths exceeding the depths penetrated by early exploratory wells. The thermally mature rocks of the Baltimore Canyon Trough are Early to Middle Jurassic in age, and not Cretaceous.

Fault and fracture zones associated with the rifting phase and early drifting phase of this area should supply ample migration pathways for the vertical migration of hydrocarbons in the Early and Middle Jurassic. The vertical extent of these zones may be limited due to reduced tectonic activity as drifting progressed. Hydrocarbons may also have migrated directly through overlying rocks, depending upon the degree of permeability of those rocks.

Early through Middle Jurassic evaporite deposits, Late Jurassic tight limestones and possibly shale beds should have been in place before the Early Jurassic source rocks reached a depth of burial sufficiently deep for the production of hydrocarbons. Such top seals, in sufficient number and/or areal extent, may have stopped significant quantities of hydrocarbons before they reached the overlying Cretaceous rocks.

It is very possible that the only reason that the early exploration wells did not encounter significant quantities of hydrocarbons is that the wells were not drilled deep enough. A new exploration strategy for the Baltimore Canyon Trough would be to target deeper potential reservoir rocks. The first target would be the Bathonian to Callovian aged carbonates beneath the tight Oxfordian limestones described by Prather (1991). These rocks may be extensively dolomitized and may have been subject to subaerial exposure and karst diagenesis, which would make this an excellent reservoir rock. In addition, these rocks are above the potentially anoxic and hypersaline Toarcian to Bajocian carbonate/evaporite complex a potentially rich source rock.

A deeper target would be the area below the Toarcian to Aalenian salt lens described by McKinney *et al.* (2004). The areal extent of this salt lens makes it a significant seal for any hydrocarbons that were generated below it. In addition to marine source rocks below this salt lens, non marine lacustrine rocks may also prove to be an organic rich source rock. Up to 5 km of alluvial and lacustrine sediments were deposited in half-grabens in the Baltimore Canyon Trough during the Late Triassic and Early Jurassic (Schlee 1980; Lawrence *et al.* 1990). Lacustrine synrift source rocks are found inter-fingering with the major evaporitic sequences (salt) in Gabon, West Africa and serve as source rocks for productive hydrocarbon reservoirs there (Little and Wilkes 1995; Harris *et. al.* 2004; Henry 1998).

An isopach map of probable Jurassic rocks in the Baltimore Canyon Trough indicates that thicknesses of up to 10 to 12 km were deposited (Fig. 17) (Schlee 1980). The result of this and other recent studies indicates that this area should be further explored for untapped hydrocarbons, mainly in the form of natural gas at depths of 5000 to 7000 meters.

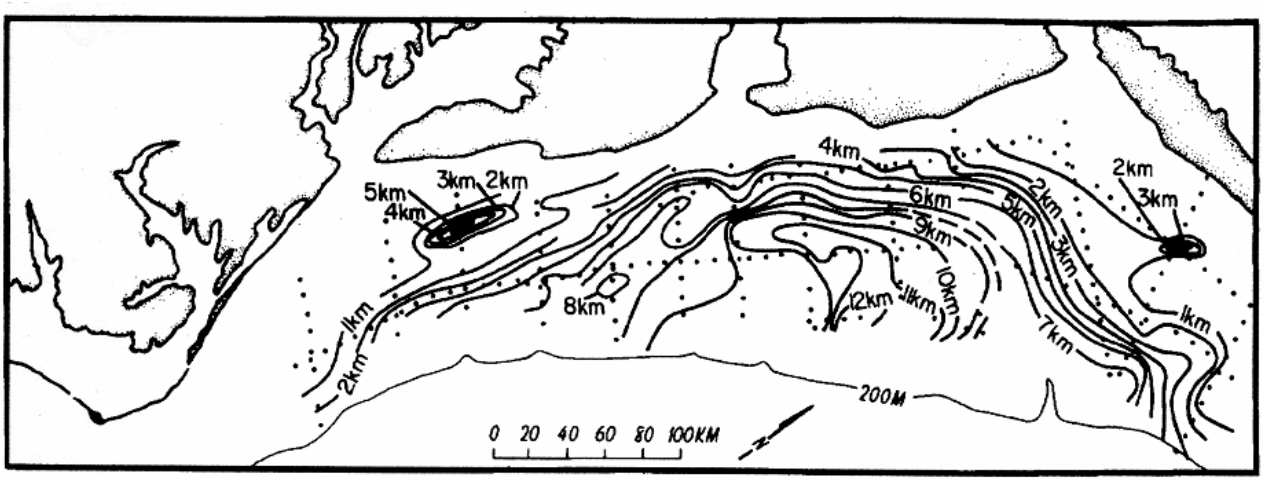


**Figure 17. Isopach map of probable Jurassic and possibly Triassic rocks in the Baltimore Canyon Trough (Schlee 1980).**

## Acknowledgments

We would like to thank Platte River Associates for determining the thermal maturation profile of the Baltimore Canyon Trough using their BasinMod® 1D software, Roger Sassen for valuable input into this research project, John Smythe of Fairfield Industries for seismic interpretation and input, Richard Wilkerson for early input, direction and encouragement and William Ruocco for helping to prepare the manuscript.

## References

Adinolfi, F., 1991, Hydrocarbon Potential of the Baltimore Canyon Trough (abstract): AAPG Bulletin, v.75, p.1514.

Amato, R.V. and Giordano, A.C., 1985 Great Stone Dome- great disappointment (abstract): AAPG Bulletin, v.69, p.1443.

Ball, M.M. Schlee, J.S., Swift, B.A., Sawyer, D.S., and Hinz, K., 1982, Exploration History, North U.S. Atlantic Margin (abstract): AAPG Bulletin, v.66, p.545.

Clark, D. and G. M. Friedman., 2005, Fracture Development and Properties Within the Beekmantown Group Carbonates of Eastern New York State, USA: Northeastern Geology and Environmental Sciences, v.27, n.3, p.197-228.

Clark, D. and G. M. Friedman., 2008, Searching for Natural Gas in the Beekmantown Group Carbonates of Eastern New York State, USA: Northeastern Geology and Environmental Sciences, v.30, n.1, p. 21-45.

Claypool, G.E. et al, 1977, Organic geochemistry in geological studies on the COST No. B-2 well, U.S. Mid-Atlantic outer continental shelf area: U.S. Geol. Survey Circ. 750, p.46-59.

Conway, S. W. and G. M. Friedman, 1984, Depositional environments and diagenesis of the Lower Ordovician Gailor Formation, Schenectady, New York: Northeastern Geology, v.6, n.3, p.135–150.

Durham, L.S. 2008, Shallow water, Deep Miocene Play, American Association of Petroleum Geologist, Explorer p.12-13.

Eliuk, L.S., and Prather, B.E., 2005, Baltimore Canyon Trough Mesozoic Carbonate Margin Cones, Offshore U.S.A. Atlantic (abstract): AAPG Bulletin, v.89 p.676.

Energy Information Administration: www.iea.org

Epstein, S.A., 1995, Revisiting our Predictions of Petroleum Reservoir Properties, U.S. East Coast Mesozoic Offshore: AAPG Bulletin, v.79, p.1412.

Epstein, S.A., 1995, The Geological Thought Process: A Help in Developing Business Instincts: AAPG Bulletin, v.79, p.1412.

Epstein, S.A. and Brink A., 1982, The petroleum Geology of the Bahamas and Thermal Maturation Models, Unpublished manuscript, 48 p.

Epstein, S.A. and Friedman, G.M. 1981, Field and Experimental Studies of Biogeochemical Processes Governing Diagenesis in and Near Reefs, Gulf of Elat, Red Sea (abstract): AAPG Bulletin, v.65, p.923.

Epstein, S.A. and Friedman, G.M., 1981, Gulf of Elat (Aqaba): A Modern Analogue to the Mesozoic U.S. East Coast Shelf and Slope (abstract): AAPG Bulletin, v.65, p.1661.

Epstein, S.A. and Friedman G.M., 1982, Processes controlling precipitation of Carbonate Cement and Dissolution of Silica in reef and Near-Reef Settings: Sedimentary Geology, v.33, p.157-172.

Epstein, S.A. and Friedman, G.M. 1983, Depositional and Diagenetic Relationships Between the Gulf of Elat (Aqaba) and the Mesozoic U.S. East Coast Offshore: AAPG Bulletin, v.67, p.953-962.

Epstein, S.A. and R.F Epstein, 2005, Potential Future petroleum geological pressures created by demand-pulls from emerging markets: Friedman Geoscience Conference, northeastern science foundation conference notes, Troy, New York.

Epstein, S.A. 2008, An Attempt to Quantify Eustatic Sea Level Fluctuations – A geological perspective: Carbonates and Evaporites v. 22, no.2, p. 149-177.

Friedman, G.M., 1968, Geology and geochemistry of reefs, carbonate sediments and water, Gulf of Elat (Aqaba), Read Sea: Journal of Sedimentary Petrology v.46, p.895-919.

Friedman, G.M. Ali, S.A. and Krinsley, D.H. 1976. Solution of quartz accompanying carbonate precipitation in reefs: Example from the Red Sea. J. Sediment, Petrol, v.46, p.970-973.

Friedman, G. M., 1980, Dolomite is and evaporative mineral: Evidence from the rock record and from sea-marginal ponds of the Red Sea: in Concepts and Models of Dolomitization: SEPM Special publication n.28 p.69–80.

Friedman, G.M., Sanders, J.E., and Kopaska-Merkel, D.C., 1992 Principles of Sedimentary Deposits: Stratigraphy and Sedimentology, McMillan Publishing Co., New York, 717p.

Gamboa, L.S., Tauchan, M. and Stoffa, P.L., 1985, Middle and Upper Jurassic Depositional Environments at Outer Shelf and Slope of Baltimore Canyon Trough: AAPG Bulletin, v.69, p.610-621.

Gvirtzman, G. and G.M. Friedman, 1977, Sequence of progressive diagenesis in Quaternary reefs, Red Sea. AAPG Studies in Geology 4, p.357-380.

Gvirtzman, M. 2006, Groundwater hydrology and paleohydrology of the dead sea rift valley in Enzel, Y., Agnon, A., and Stein , M,. eds. New frontiers in Dead Sea Paleoenvironmental Research: GSA special paper 401, p. 95-111.

Harris, N. B., K.H. Freeman, R.D. Pancost, T. White, and G.D. Mitchell, 2004, The character and origin of the lacustrine source rocks in the lower cretaceous synrift section, Congo Basin, west Africa: AAPG Bulletin. v.88. n.8. p1163 -1184

Henry, S.G. and V. Abreu, 1998, Marine transgressions in pre-salt of the South Atlantic. New models for rifting and continental breakup. Extended Abstract, 1998 AAPG annual convention, Salt lake city, Utah

Jana, L.F. and G. Pe-Piper, 1988, Middle Jurassic to Early Cretaceous igneous rocks along eastern North American continental margin: AAPG Bulletin, v.72, n.3, p.347-366.

Lawrence, D.T. Doyle, Mark and Aigner, Thomas, 1990, Stratigraphic simulation of sedimentary basins; Concepts and calculation: AAPG Bulletin, v.74, n.3, p 273-295.

Libby-French, J., 1981, Lithostratigraphy of Shell 272-1 and 273-1 Wells. Implications as to Depositional History of Baltimore Canyon Trough, Mid-Atlantic OCA: AAPG Bulletin, v.65, n.8, p.1476–1484.

Little, R and M. Wilkes, 1995, Organic Matter Accumulation in a thick lacustrine lower Cretaceous sedimentary sequence in Gabon: Facies and maturity Variations: AAPG Bulletin v.79, n.8, p.1231

Mazzullo et al., 1978, Stratigraphy and depositional environments of the Upper Cambrian-Lower Ordovician Sequence, Saratoga Springs, New York: Journal of Sedimentary Petrology, v.48, n.1, p.99–116.

Mancini, E.A., M. Badali, T.M. Puckett, J.C. Llians and W.C. Parcell, 2001a, Mesozoic carbonate petroleum systems in the northeastern Gulf of Mexico area, in R.H. Fillion, N.C. Rosen, and P. Weimer, (Eds.),

Petroleum systems of deep-water basins: Global and Gulf of Mexico experience: Proceedings of the 21st Annual Gulf Coast Section SEPM Foundation, Bob F. Perkins Research Conference, p.423-451.

Mancini, E.A., P. Li, D.A. Goddard, and R.K. Zimmerman, 2005 Petroleum source rocks on the onshore interior salt basins, north central and northeastern Gulf of Mexico; Gulf Coast Association of Geological Societies Transactions, v.55, p.486-504.

Mancini, E.A., D.A. Goddard, P. Li, and O. Ramirez, 2007, Gas potential of deeply buried Mesozoic facies and reservoirs in the onshore interior salt basins, north central and north eastern Gulf of Mexico; Gulf Coast Association of Geological Societies Transactions, v.57, p.543-555.

Mancini, E.A., P. Li, D. Goddard, V. Ramirezm and S.C. Talukdar, 2008, Meszoic (Upper Jurassic-Lower Cretaceous) deep gas reservoir play, central and eastern Gulf Coastal plain: AAPG, Bulletin, v.92, n.3, p.283-308.

Mattick, R.E. et al, 1975, Sediments, structural framework, petroleum potential, environmental conditions, and operational considerations of the Mid-Atlantic area; U.S. Geol. Survey Open-File Rept. 75-61, 143p.

Mattick, et al, 1978, Petroleum potential of U.S. Atlantic slope, rise and abyssal plain: AAPG Bulletin, v.62, p.592-608.

McKinney, B.A., Myung, W.L., Agens, W.F. and Poag, C.W. 2004. Early to Middle Jurassic Salt in Baltimore Canyon Trough: U.S. Geological Survey Open-File Report 2004-1435.

Montanez, I. P. and J. F. Read, 1992, Eustatic control of early dolomitization of cyclic peritidal carbonates: Evidence from the Early Ordovician Upper Know Group, Appalachians: GSA Bull. v.104, p.872–886.

Phillips, S. S. and G. M. Friedman, 2001(a), Carbonate Diagenesis and Dolomitization of Cambro-Ordovician (Sauk Sequence) Platform Strata in Central New York: Depositional Environments, Parasequences and Facies: Northeastern Geology and Environmental Science, v.23, n.2, p.127-169.

Phillips, S. S. and G. M. Friedman, 2001(b), Carbonate Diagenesis and Dolomitization of Cambro-Ordovician (Sauk Sequence) Platform Strata in Central New York: Part 2: Northeastern Geology and Environmental Science, v.23, n.2, p.205-252.

Pindell, J. and Dewey, J. 1982, Permo-Triassic, Reconstruction of Western Pangea and the Evolution of the Gulf of Mexico/Caribbean Region: Tectonics, v.1, p.179-211.

Poag, C.W. 1979, Stratigraphy and depositional environments of Baltimore Canyon Trough: AAPG Bulletin v.63, p.1452-1467.

Poag, C.W., 1980, Foraminiferal stratigraphy, paleoenvironments, and depositional cycles in the outer Baltimore Canyon Trough, in Geological studies of the COST No.B-3 well, United States Mid-Atlantic continental slope area: U.S. Geol. Survey Circ. 833, p.44-63.

Poag, C.W. and J.S. Schlee, 1981, Chronostratigraphic sequences beneath northeastern United States Continental margin (abs): AAPG Bulletin, v.65, p.973.

Prather, B.E., 1991, Petroleum Geology of the Upper Jurassic and Lower Cretaceous, Baltimore Canyon Trough, Western North Atlantic Ocean: AAPG Bulletin, v.73, p.258-277.

Sassen, R., C.H. Moore, and F.C. Meendsen, 1987, Distribution of hydrocarbon source potential in the Jurassic Smackover Formation: Organic Geochemistry, v.11, p.379-383.

Sassen, R. and Moore, C.H., 1988, Frameworks of Hydrocarbon Generation and Destruction in Eastern Smackover Trend: AAPG Bulletin, v.72, p.649-663.

Sassen, R., 1988, Geochemical and carbon isotopic studies of crude oil destruction, bitumen precipitation and sulfate reduction in the deep Smackover Formation. Organic Geochemistry v.12, p.351-361.

Sassen, R., 1990, Lower Tertiary and Upper Cretaceous source rocks in Louisiana and Mississippi: Implications to Gulf of Mexico crude oil: AAPG Bulletin, v.74, p.857-878.

Sassen, R., Post, P., Jung, W. DeFreitas, D.A., McDade, E.C., 2005, Laminated lime mudstone of the Early Oxfordian Smackover Formation of the Northern Gulf Rim: Significance to environments of deposition of carbonate source rocks in rifted basins. In Post, P.J. et al, (Eds.) Petroleum Systems of Divergent Continental Margin Basins, 25th Annual Meeting Gulf Coast Section Society of Economic, Paleontologists and Mineralogists Foundation Bob F. Perkins Research Conference, p.832-861.

Sassen, R. and Post, P, 2007, Enrichment of diamondoids and $^{13}C$ in Condensate from Hudson Canyon, Y.S. Atlantic: Organic Geochemistry

Schlee, J. S., J. C. Behrendt, J. A. Grow, J. M. Rovv, R.E. Mattick, P. T. Taylor and J.J. Lawson, 1976, Regional geologic framework off northeastern United States: AAPG Bulletin v.60, p.926-951.

Schlee, J.S., and J.A. Grow, 1980, Seismic stratigraphy in the vicinity of the COST B-3 well, In: P.S. Schlee, ed., Geological studies of the COST B-3 well, United States mid-Atlantic Continental Slope area: USGS Circular 833, p.111-116.

Schmidt, S., B. Cramer, P. Gerling, Rend R. Little, 1002, The Hydrocarbon Potential of the Southern Atlantic Continental Margins of Argentina and Nambia/South Africa (Extended abstract), American Association of Petroleum Geologists Hedberg Conference Section on Hydrocarbon Habitat of Volcanic Rifted Passive Margins, Stavanger, Norway.

Scholle, P.A. ed., 1977, Geological studies on the COST B-2 well, U.S. Mid-Atlantic outer continental shelf area: U.S. Geol. Survey Circ. 750, 71p.

Sun, S, Q., 1995, Dolomite reservoirs: Porosity evolution and reservoir characteristics: AAPG Bull., v.79, n.2, p.186–204.

Vail, P.R., Mitchum, RM, Jr., Tood, R.G. Widmeir, J.M. Thompson, III, Sangree, J.B. Bubb, J.N. and Hatelid, W.G., 1977, Seismic Stratigraphy and Global Sea Level Changes of Sea Level in Seismic Stratigraphy-Application to Hydrocarbon Exploration: American Association of Petroleum Geologists Memoir, n.26, p.49-207.

Withjack M. O., R. Schlishe, and P.E. Olsen 1998, Diachronous rifting, drifting, and inversion of the passive margin of Central Eastern North America: An analog for other passive margins: AAPG Bulletin, v.82, n.5a, p.817-835.

Zimmerman, R.K. and R. Sassen, 1993, Hydrocarbon transfer pathways from Smackover source rocks to younger reservoir traps in the Monroe gas field, northeast Louisiana: Gulf Coast Association of Geological Societies Transactions, v.43, p.473-480.

**BACK**

# Paleoceanographic and Paleoenvironmental Implications for Hydrocarbon Exploration of the Continental Slope off Nova Scotia

**Lubomir F. Jansa**
Emeritus Scientist
Geological Survey of Canada-Atlantic
P.O. Box 1006
Dartmouth, Nova Scotia B2Y4A2
Canada
e-mail: lujansa@nrcan.gc.ca

## ABSTRACT

The continental slope off Nova Scotia has recently become of interest for oil exploration as a potentially new gas province, under the assumption that past success in exploration on the shelf can be extended onto the continental slope. Is such an assumption supported by the sediment depositional history on the shelf and by the general paleoceanography of the Central Atlantic Ocean during the late Mesozoic?

Of all elements of the Petroleum System, only the source rock and presence of reservoir rocks will be discussed. Source rock occurrences depend on marine organic matter generation and preservation. The former are controlled by the availability of nutrients supplied either by continental runoff (therefore controlled by climate), or as a result of coastal upwelling, surface water mixing, and open ocean divergence. Could such conditions have developed during the Mesozoic on the Scotian Slope? An additional constraint to be considered is ocean bottom water oxygenation, as such conditions changed dramatically during Mesozoic-Cenozoic time in the Central Atlantic. During the Late Jurassic, Late Cretaceous and early Cenozoic, oceanic bottom waters in this region were highly oxygenated, resulting in the destruction of organic matter deposited in ocean bottom sediments. In contrast, the middle Cretaceous was a period of organic matter preservation in deep sea and marginal basin sediments, either due to changes in deep water circulation, climate and/or increases in depositional rates.

Occurrence of reservoir rocks is another important parameter to be considered. The existence of both sandstone and carbonate reservoirs was proven by drilling on the shelf. For continental slope exploration, the petroleum industry applied known models of turbidite fans, apparently without giving sufficient consideration to the sediment supply and sea level changes affecting development of the shelf area during the Cretaceous. This may prove to be the major factor in a lack of commercial hydrocarbon discoveries in exploration wells drilled on the Scotian Slope. Deeper understanding of the geologic evolution of the continental margin and paleoceanographic conditions affecting it, together with a modification of exploration strategy are needed to improve the success of hydrocarbon exploration in the Scotian upper slope domain.

BACK

# The Peniche Basin: Tectono-Sedimentation and Exploratory Aspects

**Almério Barros França**
**Rogério Cardoso Gontijo**
**Gilmar Vital Bueno**
Petrobras
Avenida Chile
65 sala 1401
Rio de Janeiro, RJ, 20031-912
Brazil
e-mail: almeriobfranca@petrobras.com.br

## ABSTRACT

Petrobras in partnership with Galp and Partex, has acquired a total of 12,000 km$^2$ in the Peniche basin, offshore Portugal - a counterpart to some northeast North American basins. The main subject of the present work is to show some geological aspects of the Peniche basin, based mostly on seismic data and a few wells drilled nearby. No wells have been drilled in the whole concession area.

The Jurassic Peniche basin is bounded by SW-NE lineaments, which subdivide the basin into horst and grabens, and by NW-SE lineaments, which are most likely transfer faults. From the end of the Jurassic to the present-day, compressional stress seems to have predominated in the basin, reactivating old lineaments, and creating thrust faults and a series of flower structures. Normal faulting associated with sediment deposition related to middle to late Jurassic salt movement is also a common features on seismic lines. Uplifting in the shallow portion of the Peniche basin brought about slumping and rotation of huge blocks in the deep water realm.

Three major unconformities are easily mapped on seismic, and corroborated by well data: 1) base of lower Cretaceous; 2) pre upper Jurassic sequence (strongly erosive), and 3) Cretaceous-Tertiary boundary. The erosive phases associated with these unconformities have great potential to provide sediment that can be transported deep into the basin, suggesting the possibility of sandstones reservoirs, either as channelized or unconfined lobe deposits. Channelized, coarse-grained Cretaceous sandstones are well exposed along the coast in Santa Cruz, Portugal. The wells drilled in the shallow part of the basin have shown porosity ranging from 15% to 30% (Cretaceous) and 15% in deeper sandstones (Jurassic).

Carbonates are another possibility as reservoir rocks, with porosity ranging from 15% to 20% based on bioconstruction, probably rudist reefs such as the ones exposed in several onshore locations and along the coast, such as Praia do Guincho, near Estoril.

The potential source rocks (Pliensbachian and Kimmeridgian), present in outcrops and wells in the Lusitanian basin, have been traced to deep horizons in the Peniche basin, where the sedimentary section is thicker, suggesting greater potential source rock thickness than in the shallow-water areas.

BACK

# Geological Evolution and Hydrocarbon Potential of the Hatton Basin (UK Sector), Northeast Atlantic Ocean

**David McInroy**
**Ken Hitchen**
British Geological Survey
Murchison House
West Mains Road
Edinburgh, EH9 3LA
United Kingdom
e-mail: dbm@bgs.ac.uk

## ABSTRACT

The deep-water Hatton Basin (flanked by the Hatton and Rockall Highs) is located 600km west of Scotland (NE Atlantic Ocean) on the western margin of the Eurasian continental plate. Prior to Atlantic opening, the area was adjacent to SE Greenland. The basin straddles the UK/Irish median line. Water depths increase southwards from 1000 m to over 1300 m.

The basin has never been licensed for hydrocarbon exploration and is currently the subject of ownership negotiations related to the UN Convention on Law of the Sea. Consequently it is under-explored. The deepest borehole penetration is by DSDP borehole 116 which terminated at 854m below sea bed in the Upper Eocene.

The Pre-Cambrian metamorphic basement only crops out on Rockall Bank where high-grade gneiss and granulite have been sampled and dated at c. 1900 to 1700 Ma. This is a different terrane from that which underlies most of Scotland. Palaeozoic rocks have not been proved in the area but may provide some of the pre-rift basin infill. The Hatton Basin probably opened during the Cretaceous. Recent (2007) seismic data suggest the presence of tilted fault blocks on the basin margins. Mid Cretaceous (Albian) sandstones and mudstones have been proved at shallow depth on the Hatton High. The area was affected by massive Late Paleocene to earliest Eocene volcanism which emplaced several large central igneous complexes and caused widespread lavas which degrade the seismic data from the deeper geology. Atlantic rifting commenced west of the Hatton High at about 56 Ma. During the Cenozoic the Hatton Basin was affected by differential subsidence and several unconformity-forming compressional events.

Numerous potential hydrocarbon trap styles have been identified including syn-rift tilted fault blocks, folds, truncations, prograding fans, pinch-outs, scarp fans and traps related to sill intrusions. Reservoir intervals are likely to be present in the Cretaceous, Paleocene and Eocene. The overlying Oligocene to Recent sediments are mudstones and oozes and may provide a seal. The main risks for an accumulation are the presence of a source rock and the shallow occurrence of some of the potential traps.

## Introduction

During the Mesozoic and Early Cenozoic, and before sea floor spreading occurred in the North Atlantic Ocean, the North American and Eurasian continents were closely juxtaposed (Fig. 1). In mid-Cretaceous times, the southwestern limit of the Hatton Basin, currently in Irish waters, was close to the rift basins now situated in the Labrador Sea and on Canada's eastern continental margin. Also, the northwestern margin of Hatton Basin was adjacent to southeast Greenland. At present, the Hatton Basin is located on the extreme western margin of the European continent approximately 600 km due west of Scotland (Fig. 2). The extent of the Hatton Basin is defined by the Hatton High (to the west) and the Rockall High (to the east) (Fig. 3). Water depths increase southwards from 1000 m to over 1300 m. The continent/ocean crustal boundary underlies the western flank of Hatton Bank (Kimbell *et al* 2005).

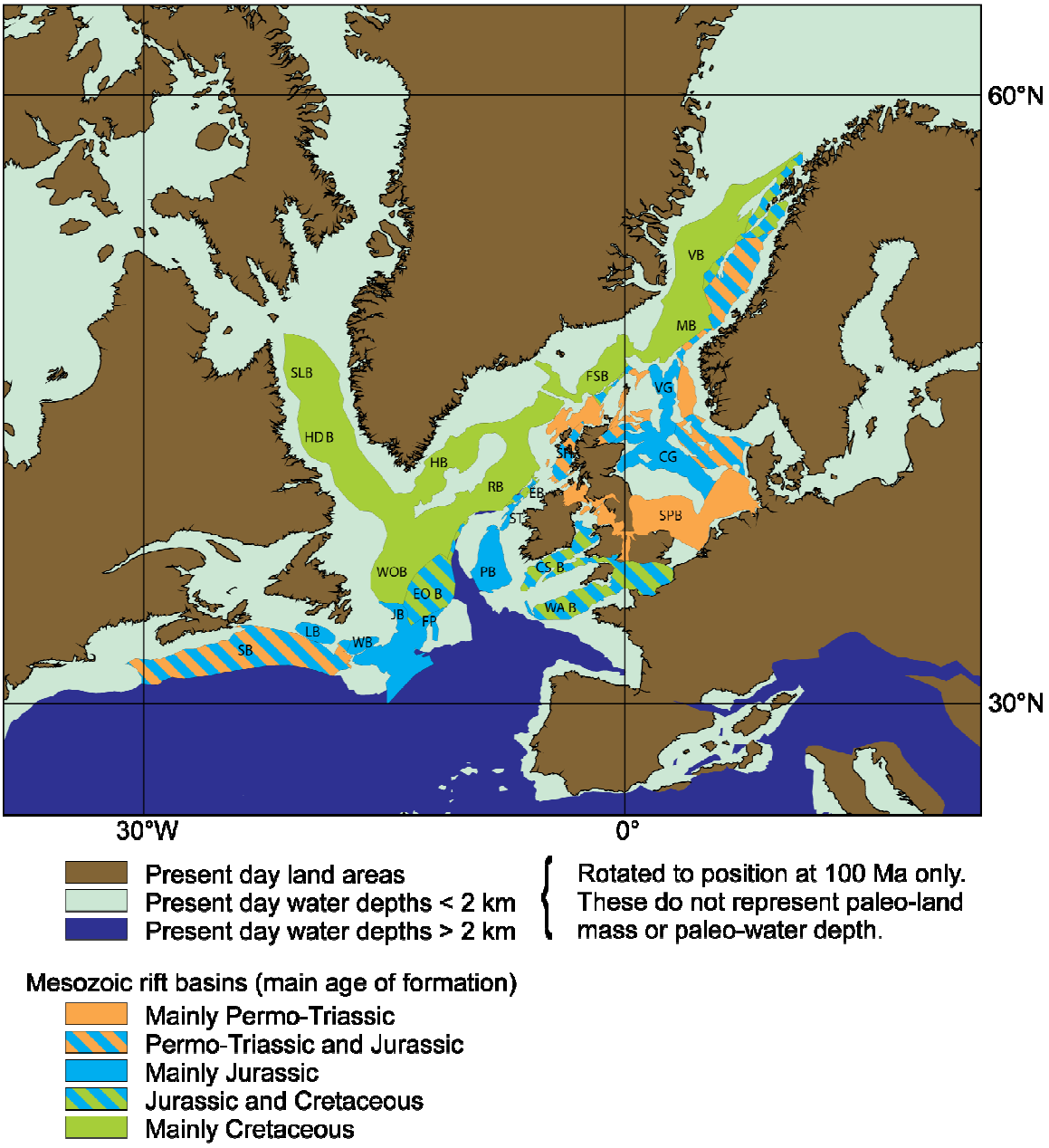


**Figure 1. Reconstruction of the North Atlantic region at approximately 100 Ma (mid-Cretaceous) showing the palaeo-location of the Hatton Basin. Reconstruction based on output from ATLAS plate reconstruction software, Cambridge Paleomap Services Ltd. CG: Central Graben, CSB: Celtic Sea Basin, EB: Erris Basin, EOB: East Orphan Basin, FP: Flemish Pass Basin, FSB: Faroe-Shetland Basin, HB: Hatton Basin, HDB: Hopedale Basin, JB: Jeanne d'Arc Basin, LB: Laurentian Basin, MB: Møre Basin, PB: Porcupine Basin, RB: Rockall Basin, SB: Scotian Basin, SH: Sea of Hebrides Basin, SLB: Saglek Basin, SPB: Southern Permian Basin, ST: Slyne Trough, VB: Vøring basin, VG: Viking Graben, WAB: Western Approaches Basin, WB: Whale Basin, WOB: West Orphan Basin.**

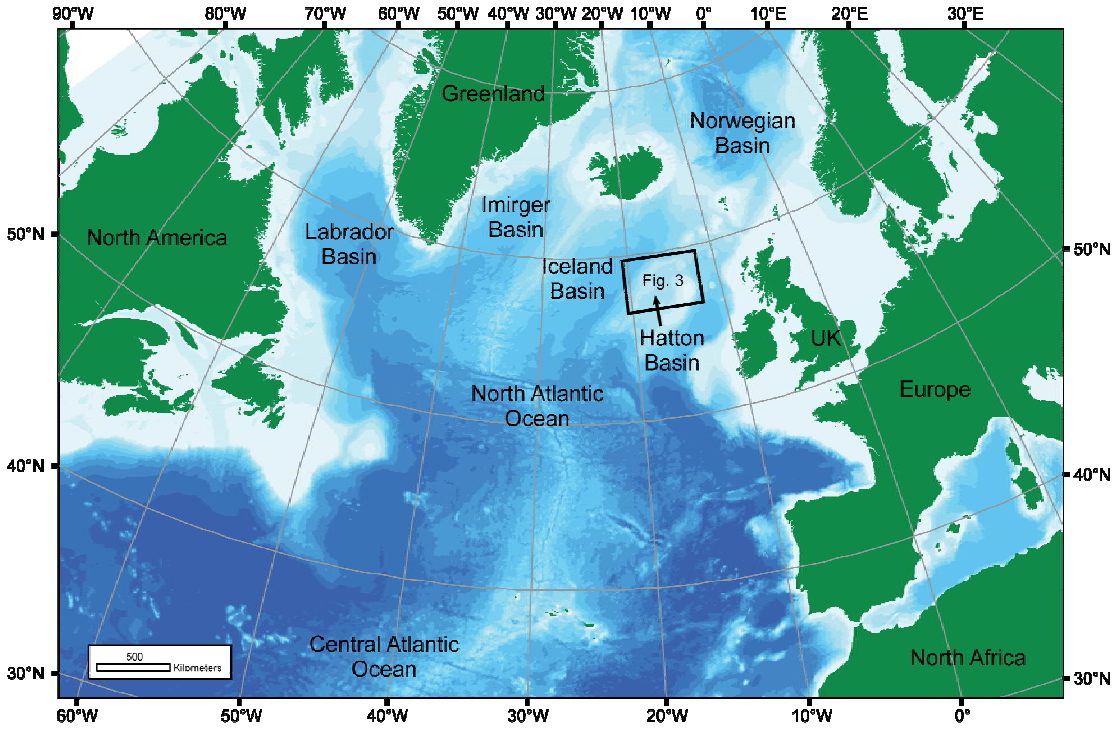


**Figure 2. Present day location of the Hatton Basin in the North Atlantic Ocean.**

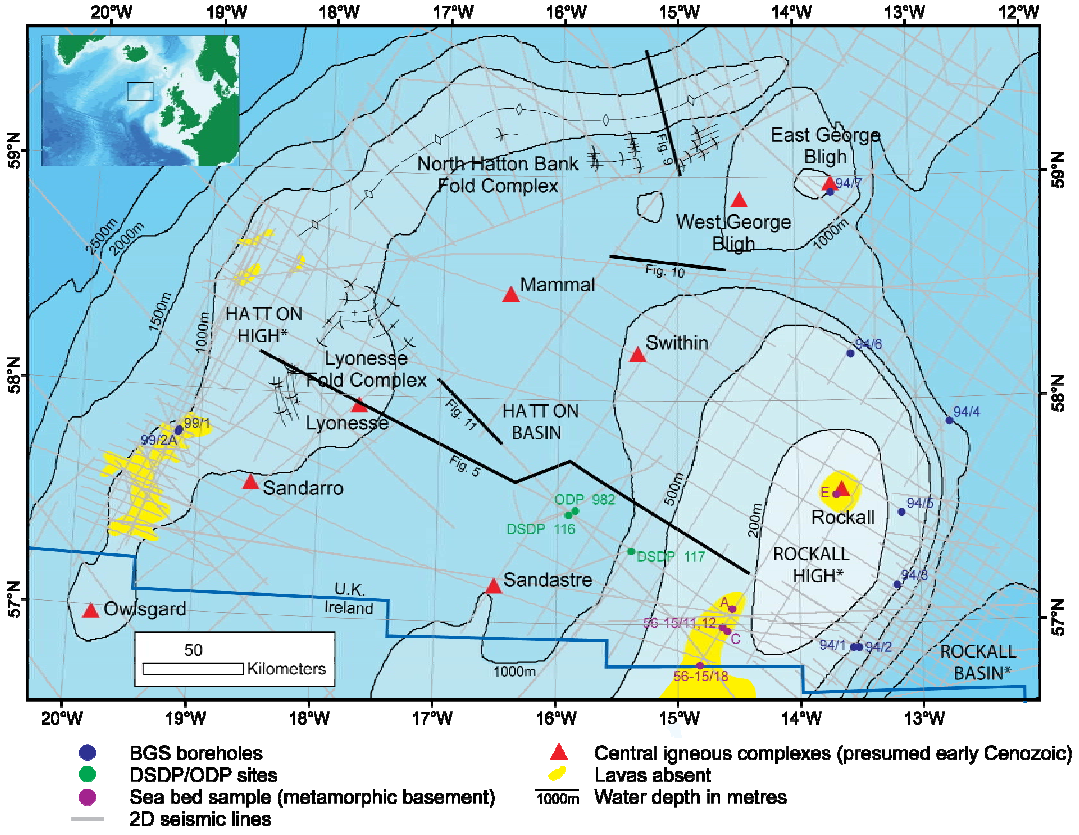


**Figure 3. Principal features of the Hatton Basin and adjacent structural highs. *Denotes geological feature name (bathymetric feature names are, from west to east, Hatton Bank, Hatton Basin, Rockall Bank and Rockall Trough). Precise locations of the TGS profiles illustrated in this abstract (Figs. 6, 7 & 8) have been omitted for commercial reasons.**

Commercially, the Hatton Basin is very remote, under-explored and has never been licensed for hydrocarbon exploration. It is currently the subject of ownership negotiations related to the UN Convention on Law of the Sea. It straddles the bilaterally-agreed median line between the UK and Ireland. Owing to data availability, this paper deals only with the northern part of the basin (the UK sector).

## Data

This paper is based on 20,000 km of post-1992 mainly high-resolution and conventional industry 2D seismic data, most of which have coincident gravity and magnetic data. The deepest borehole penetration in the basin is currently at Deep Sea Drilling Project (DSDP) Site 116 which terminated at 854 m below sea bed in the uppermost Eocene. Other borehole data include DSDP Site 117 and Ocean Drilling Program (ODP) Site 982 (drilled in the eastern part of the basin) and British Geological Survey (BGS) shallow boreholes 99/1 and 99/2A (maximum penetration 46.5 m) drilled on the top of the Hatton High. The BGS also has a small number of short sea-bed cores taken on the top of Rockall High.

## Regional Considerations

As might be expected, the gravity map across the Hatton Basin (Fig. 4) shows it to be broadly coincident with a gravity 'low' albeit containing two large near-circular positive anomalies which correspond to the Mammal and Sandastre igneous centres. Several short sea-bed cores comprising gneiss and granulite (including BGS rockdrill cores 56-15/11 and /12 dated at 1900–1700 Ma) and mainly basic igneous rocks (dated at 57–56 Ma) have been obtained from the Rockall High. Combined with interpretation of the seismic and gravity data, this suggests that Rockall High comprises a massive early Proterozoic metamorphic basement block overlain by Late Paleocene lavas and younger sediments. Consequently the coincident gravity signature is a broad gravity 'high'. In contrast, the gravity signature across the Hatton High (Fig. 4) is much more variable and suggests a more complex structure and geological history. This is corroborated by seismic data which reveal inverted ?Mesozoic basins within the high and a large anticline which constitutes the sinuous high at its northern end. Folds and faults, which are absent on seismic data across the Rockall High, are imaged on the seismic data across the Hatton High.

## Hatton Basin Evolution

The crust beneath the basin comprises high-grade early Proterozoic metamorphic basement. This crops out on Rockall High, where it has been sampled, but not on Hatton High where seismic data suggest it does not occur at sea bed. This basement probably constitutes a separate terrane which is younger and significantly different to the Archaean Lewisian Gneiss Complex of the northern Rockall Basin and western Scotland. The boundary between these terranes may coincide with the north-west to south-east oriented feature termed a suture by Dickin and Bowes (2002), the Anton Dohrn transfer (Doré *et al*. 1997) or the Anton Dohrn lineament (Kimbell *et al*. 2005).

Although Atlantic rifting adjacent to the western flank of Hatton High probably started during anomaly 24 time (Early Eocene) (Kimbell *et al*. 2005), the main phase of Hatton Basin rifting (*i.e.* when the basin 'opened') was probably Early to mid Cretaceous although plate tectonic modelling suggests there may have been an earlier minor precursor phase (Cole and Peachey 1999). Consequently the fill of the Hatton Basin probably constitutes:

1. pre-opening Palaeozoic and Mesozoic sedimentary rocks,
2. syn-rift Cretaceous sediments,
3. post-rift Late Cretaceous to Paleocene sediments,
4. extensive Late Paleocene flood lavas,
5. post-lava Eocene to Recent sediments.

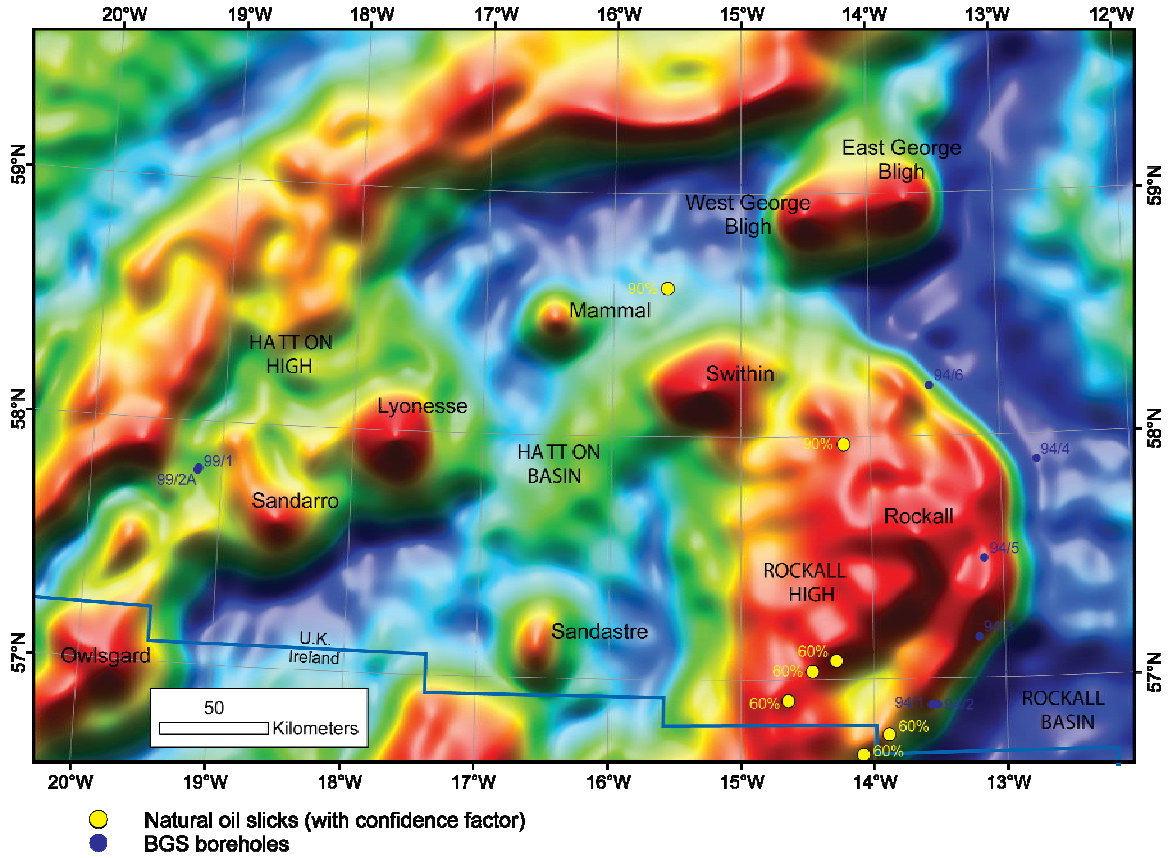


**Figure 4. Bouguer gravity anomaly map of the Hatton Basin and adjacent structural highs. Most central igneous complexes (see also Fig. 3) correspond with near-circular positive anomalies. See text for comment about natural oil slicks. Confidence ratings of individual oil slicks taken from Hitchen (2004).**

A regional cross-section across the basin illustrates much of the post-rift infill and the nature of the Cenozoic basin margins (Fig. 5). From gravity modelling, the combined pre-lava sedimentary thickness of intervals (1), (2) and (3) above has been estimated at up to 4 km thick (Kimbell *et al*. 2007), whereas interpretation of wide-angle seismic data has yielded a figure of up to 5 km for the same interval (Smith 2006). Pre-lava interval velocities have been estimated in the range 4.5–6.1 km/s, although this figure may be somewhat inflated due to igneous intrusions. However, a similar figure of 5.1–5.3 km/s has also been suggested by Keser Neish (1993) for pre-Cenozoic sedimentary rocks within the Hatton High. Although not drilled in the centre of the basin, BGS boreholes 99/1 and 99/2A proved Albian (mid-Cretaceous) mudstones and sandstones on the Hatton High (Hitchen 2004).

Smith (2006) suggested the presence of sub-lava syn-rift tilted fault blocks on the western side of the Hatton Basin based on traveltime inversion of wide-angle data. Wedge-shaped syn-rift seismic packages have also been imaged by new (2007) TGS data from the eastern and western margins of the Hatton Basin (Figs. 6 and 7). Such geometries are probably Cretaceous in age and include potential hydrocarbon traps.

Differential subsidence and uplift has been a feature of the Hatton Basin area through time. During the Albian to Paleocene interval, the ?Mesozoic basin on Hatton High was inverted, folded, faulted and eroded (Fig. 8) whereas the Hatton Basin appears to have escaped similar tectonics. This may in part be due to igneous underplating of the Hatton High associated with the Iceland Plume (White *et al*. 1987).

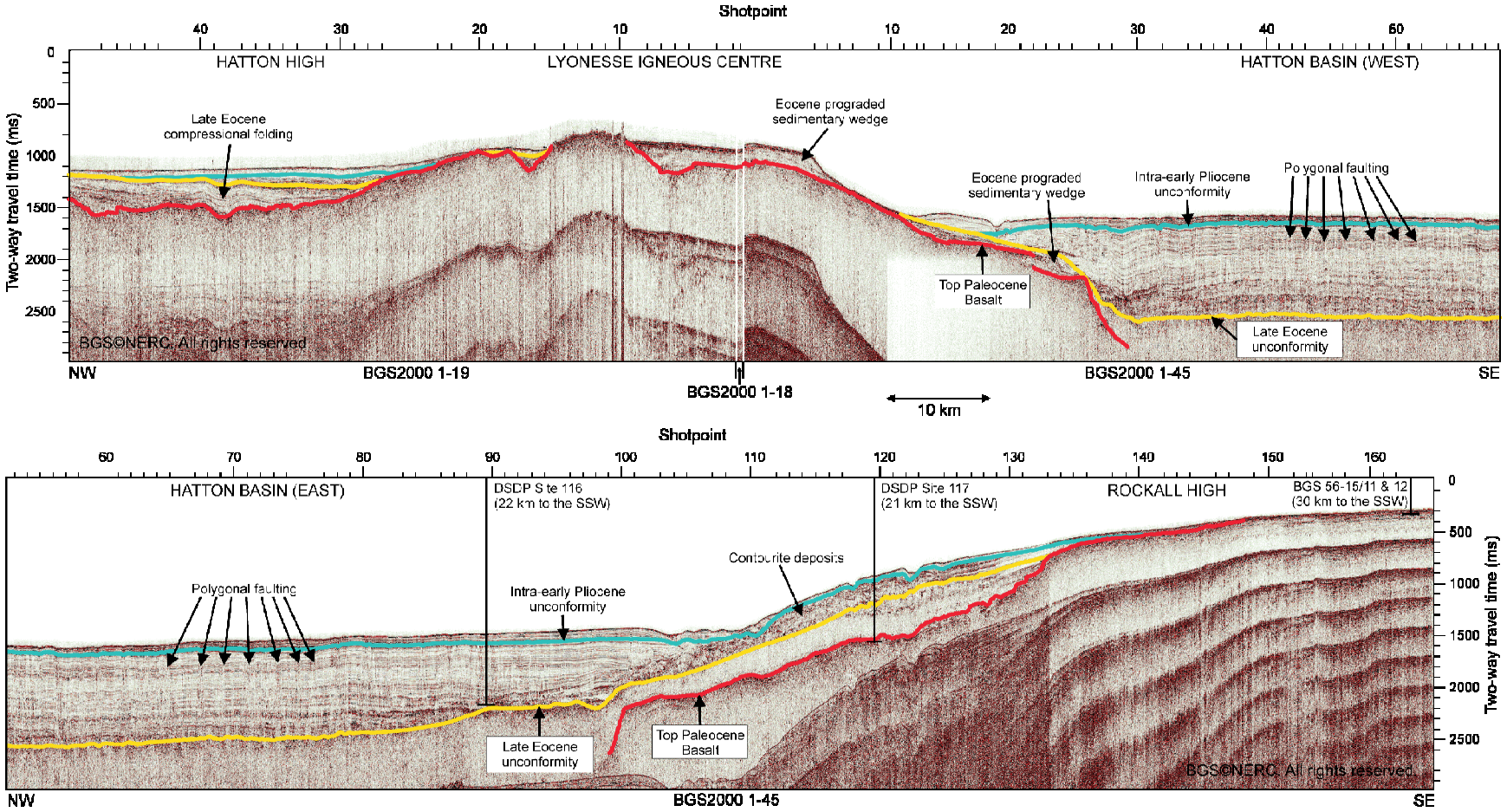


**Figure 5. BGS high-resolution seismic profile (00/01-19, 18 & 45) across the Hatton Basin (located in Fig. 3) illustrating the simple post-rift Cenozoic geometry of the basin.**

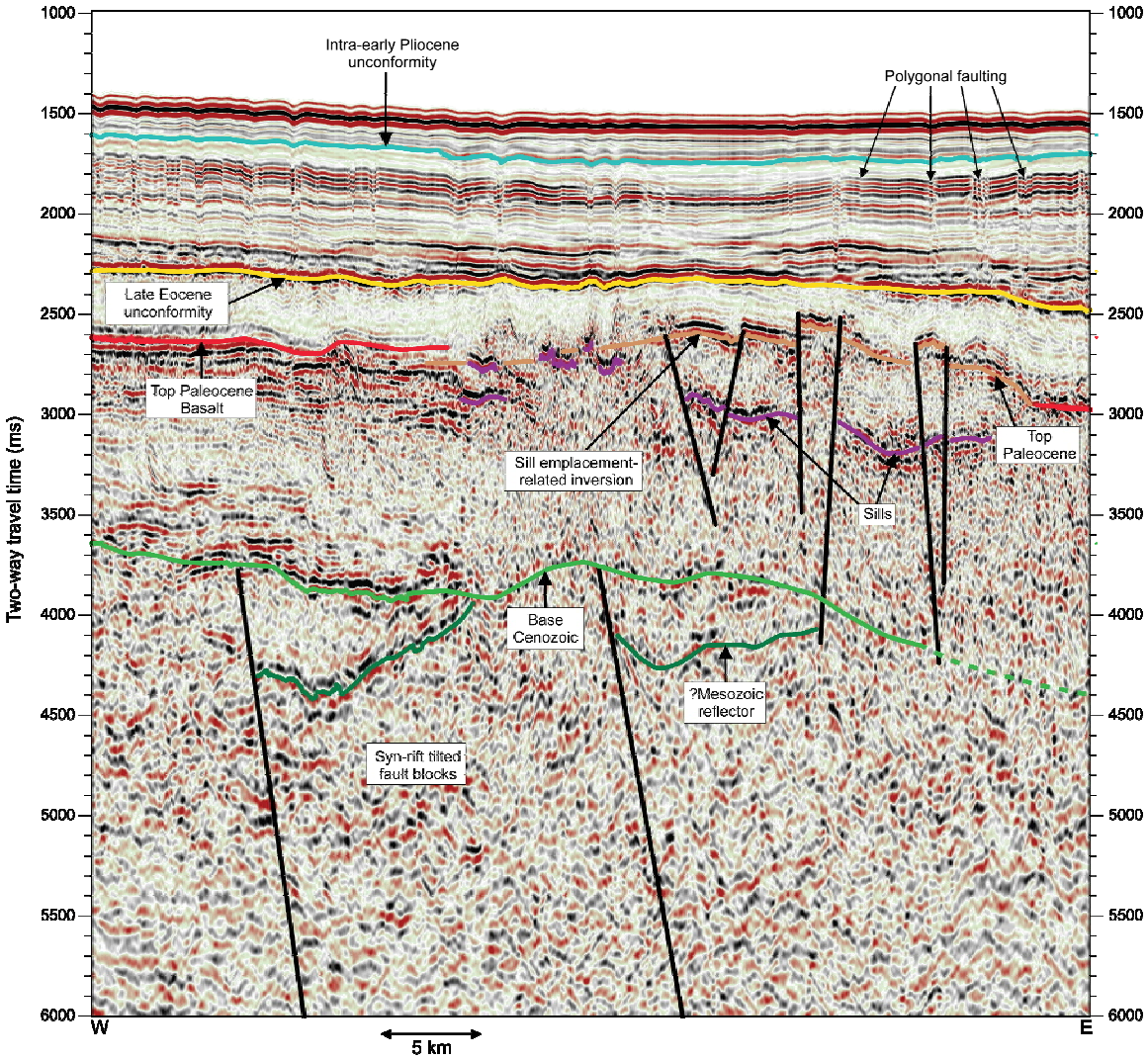


**Figure 6. Seismic profile from the northern Hatton Basin illustrating possible syn-rift tilted fault blocks in the pre-Cenozoic succession and a small inversion structure possibly related to Early Cenozoic sill intrusion. Data shown courtesy of TGS (UK).**

Several large igneous centres were emplaced during the ?Late Paleocene, and extensive lavas were extruded across most of the area (see Fig. 3 for locations, Fig. 4 for gravity signatures, and Fig. 5 for seismic example across Lyonesse igneous centre). The lavas are estimated to be 1200 m thick in the basin (Smith 2006) but thinner across the adjacent highs. The lavas degrade the seismic response from deeper levels and hence hinder the identification of Mesozoic hydrocarbon exploration plays in the basin.

Following this volcanic episode, the Hatton and Rockall highs were probably emergent and acted as source areas for shallow-water nearshore sandstones deposited as prograding wedges (McInroy *et al.* 2006). At the end of the Eocene a major compressional event created the North Hatton High anticline (with associated minor thrusts on its southern limb) and 'pop-up' structures in the northern Hatton Basin (Fig. 9) (Johnson *et al.* 2005). However the Hatton Basin underwent subsidence and, with a new oceanic current regime in place, began to collect a thick sequence of fine-grained mudstones and oozes as proven in DSDP borehole 116.

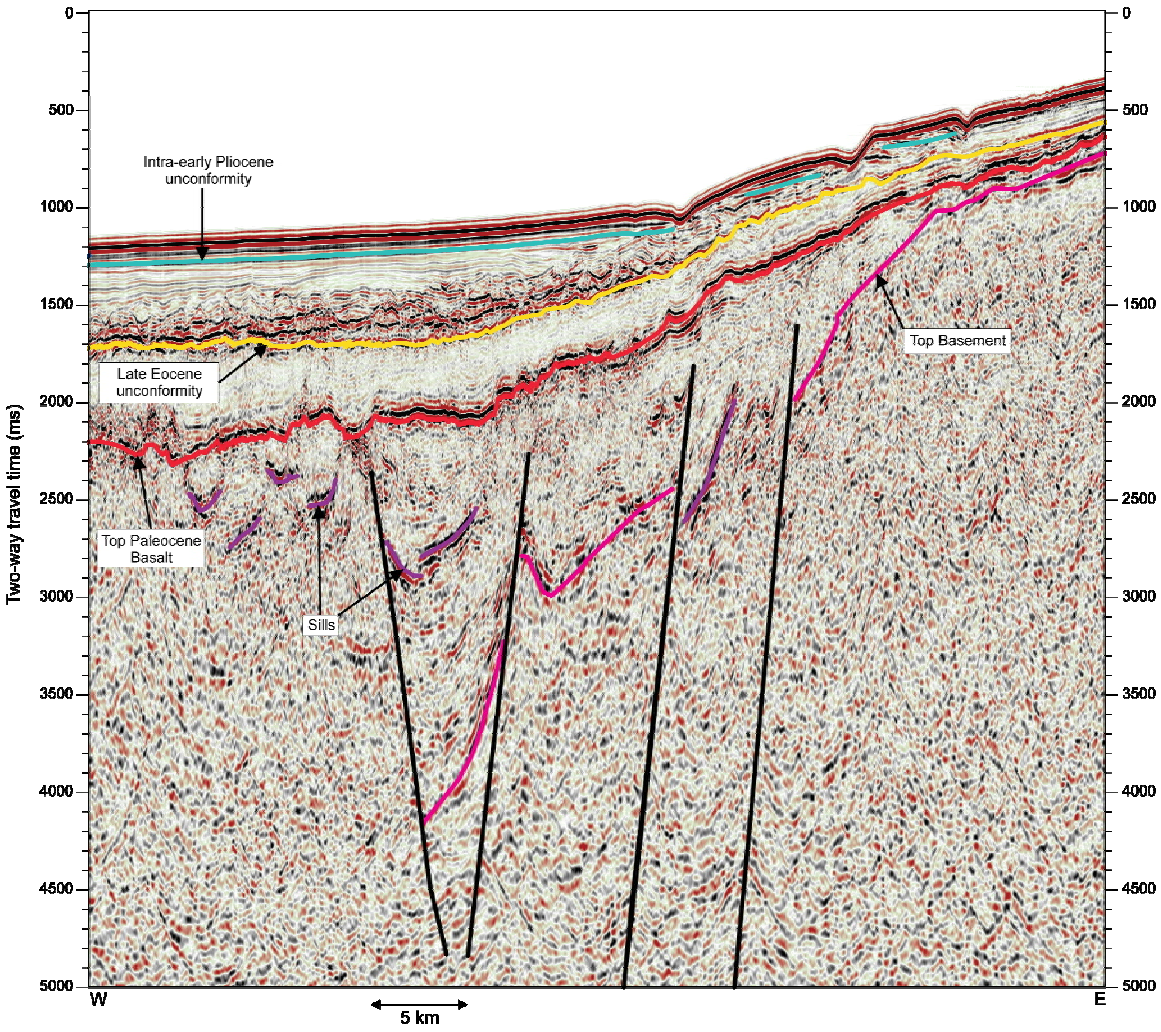


**Figure 7. Seismic profile from the eastern flank of the Hatton Basin illustrating pre-Cenozoic sub-basalt syn-rift wedge-shaped seismic packages. Data shown courtesy of TGS (UK).**

## Hydrocarbon Prospectivity

The presence of a source rock is the biggest single risk for a working petroleum system in the Hatton Basin. However, on a regional pre-Atlantic opening scale, the southern end of the Hatton Basin may have been adjacent to the Labrador margin, which includes the Hopedale Basin which has proven gas fields (DeSilva 1999) with possible source intervals in the Cretaceous through to the Eocene. Numerous examples of Lower, Middle and Upper Jurassic and Lower Cretaceous potential source rocks have been proved by drilling along the Atlantic seaboard of the British Isles (Hitchen and Stoker 1993; Butterworth *et al*. 1999) and in the Rockall Basin gas and condensate have been recovered from UK and Irish wells 154/1-1 and 12/2-1 respectively. Based on an assumed present depth of burial of 5.5 km below sea bed, Jurassic source rocks (if present) in the Hatton Basin would have been mature for oil throughout the Cenozoic. Several natural oil slicks have been documented in the area (Hitchen 2004) including one in the northern Hatton Basin (Fig. 4). Potential reservoir intervals in the Hatton Basin include Cretaceous syn-rift packages, Paleocene sandstones related to thermal uplift and Eocene fans and prograding wedges. There are numerous potential trap styles in and around the Hatton Basin. These include Cretaceous syn-rift tilted fault blocks, truncation of dipping ?Mesozoic sediments beneath the base Cenozoic unconformity, Eocene prograding wedges, updip Eocene pinchouts at the basin margin (Fig. 10), fans at

the base of lava escarpments (Fig. 11) and compressional and inversion structures created during the Late Eocene.

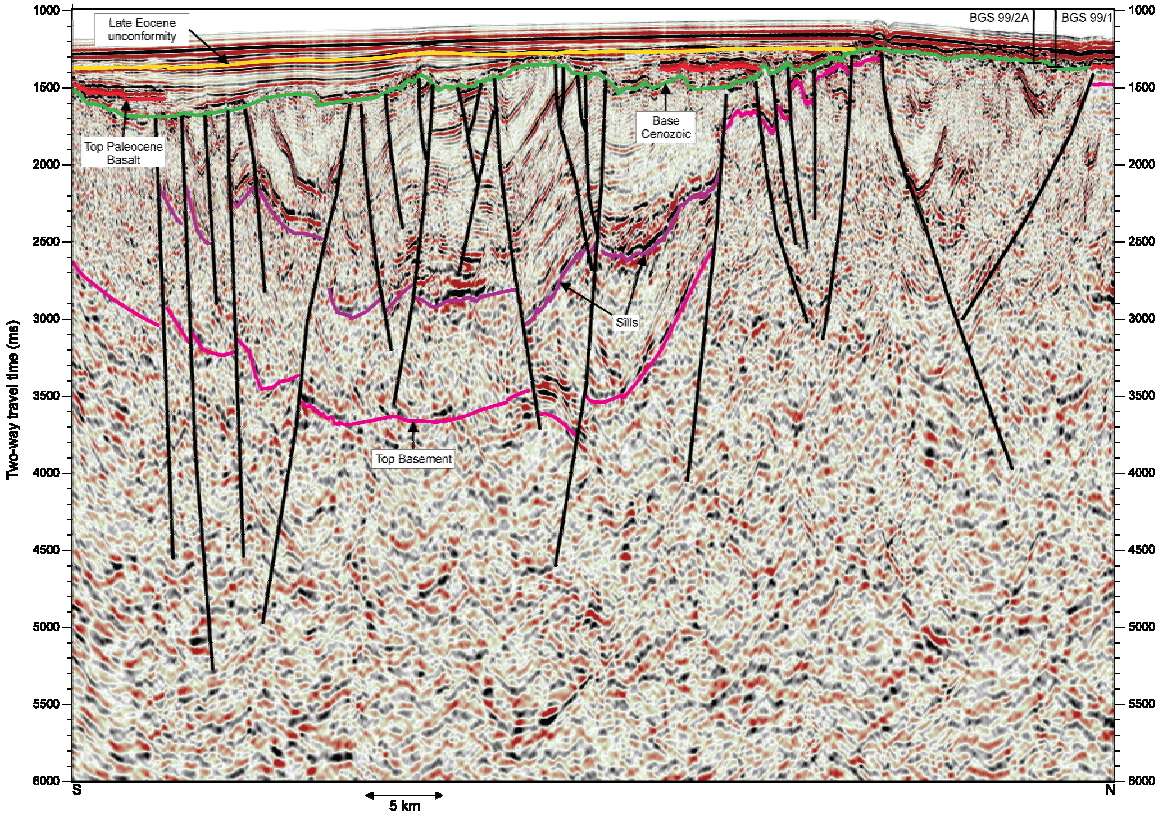


**Figure 8. Seismic profile across part of Hatton High illustrating an inverted basin containing a faulted, folded and eroded ?Mesozoic succession. BGS boreholes 99/1 and 99/2A, projected onto this profile, proved Albian rocks just below sea bed. Data shown courtesy of TGS (UK).**

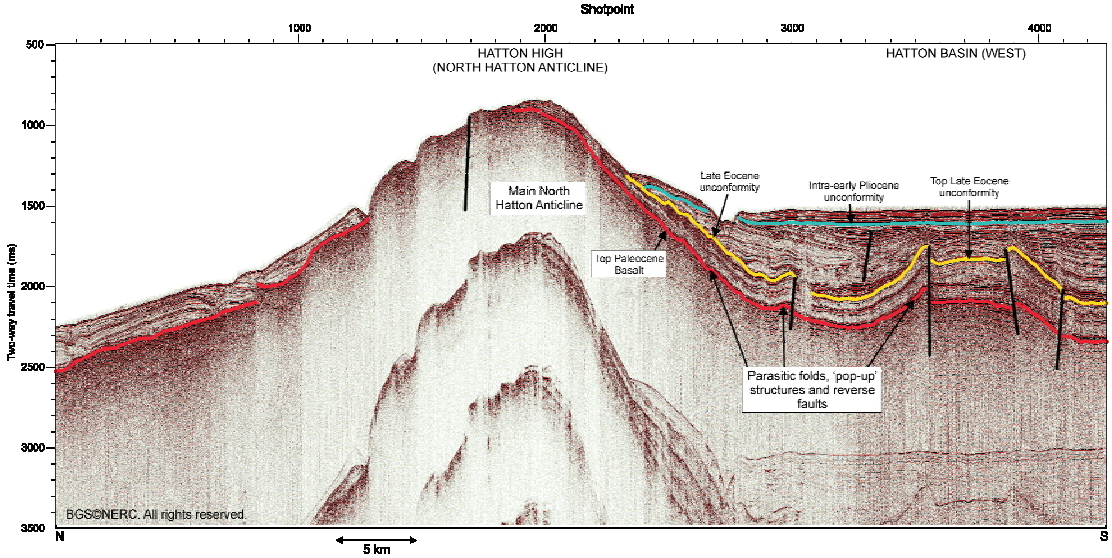


**Figure 9. BGS high-resolution seismic profile (02/02-15) across the northern part of Hatton Bank (located in Fig. 3) illustrating ?Late Eocene compressional features which both affect the sea bed (the North Hatton Bank anticline) or are completely buried by thick younger Cenozoic sediments.**

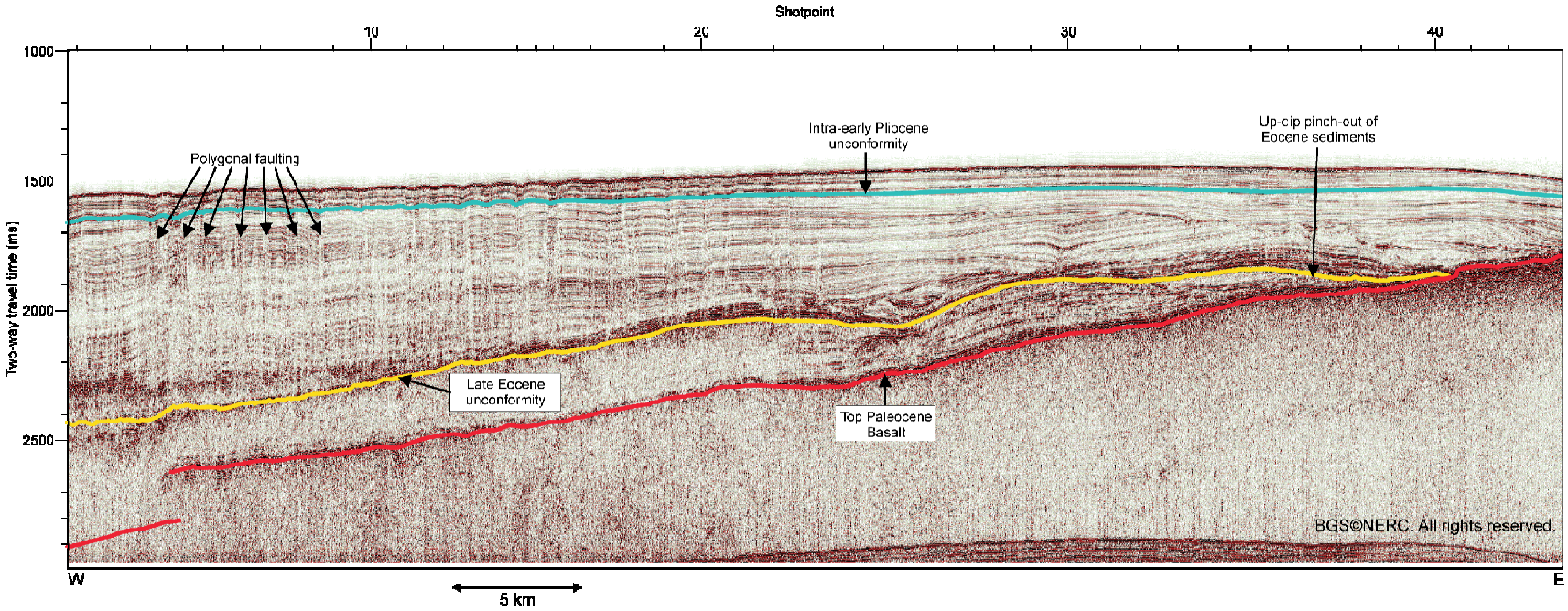


**Figure 10. BGS high-resolution seismic profile (00/01-56) from the north-east Hatton Basin (located in Fig. 3) illustrating the updip pinch-out of the sand-prone Eocene interval beneath younger mud-prone sediments.**

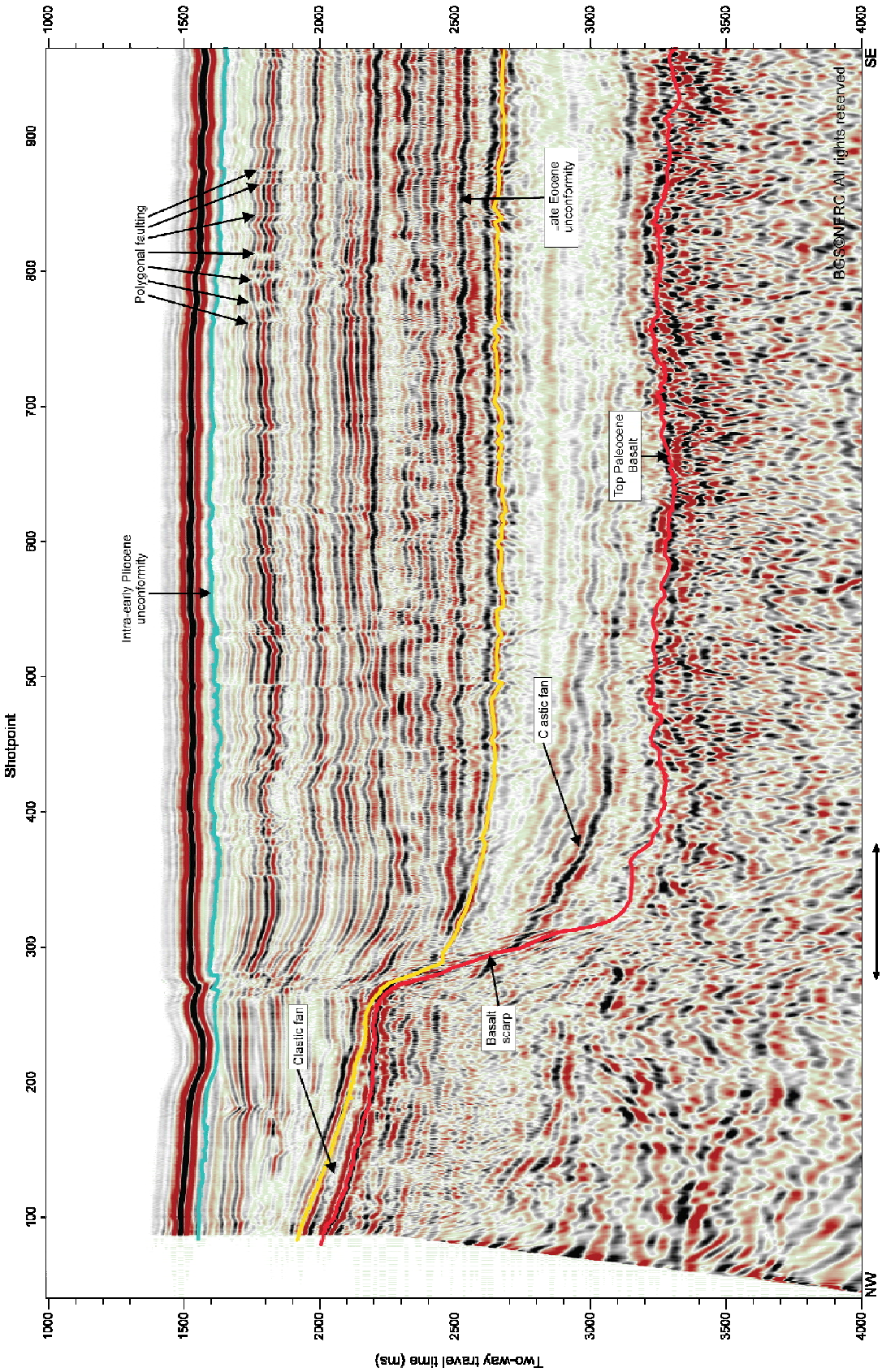


**Figure 11. BGS seismic profile (93/02-C) from the central Hatton Basin (located in Fig. 3) illustrating the presence of a clastic fan at the base of a large basalt scarp.**

## Acknowledgements

The seismic data shown in Figures 6-8 is taken from the TGS HR07 (2007) survey and is shown with the permission of TGS (www.tgsnopec.com). This paper is published with permission of the Executive Director of the British Geological Survey (NERC).

## References

Butterworth, P., A. Holba, S. Hertig, W. Hughes, and C. Atkinson, 1999, Jurassic non-marine source rocks and oils of the Porcupine Basin and other North Atlantic margin basins, *in* A.J. Fleet, and S.A.R. Boldy (eds.), Petroleum Geology of Northwest Europe: Proceedings of the 5th Conference: The Geological Society, London, p.471-486.

Cole, J.E., and J. Peachey, 1999, Evidence for pre-Cretaceous rifting in the Rockall Trough: an analysis using quantitative plate tectonic modelling, *in* A.J. Fleet, and S.A.R. Boldy (eds.), Petroleum Geology of Northwest Europe: Proceedings of the 5th Conference: The Geological Society, London, p.359-370.

DeSilva, N.R., 1999, Sedimentary basins and petroleum systems offshore Newfoundland and Labrador, *in* A.J. Fleet, and S.A.R. Boldy (eds.), Petroleum Geology of Northwest Europe: Proceedings of the 5th Conference: The Geological Society, London, p.501-515.

Dickin, A.P., and G.P. Bowes, 2002, The Blackstones Bank igneous complex: geochemistry and crustal context of a submerged Tertiary igneous centre in the Scottish Hebrides: Geological Magazine, v.139, p. 199-207.

Doré, A.G., E.R. Lundin, Ø. Birkeland, P.E. Eliasson, and L.N. Jensen, 1997, The NE Atlantic Margin: implications of late Mesozoic and Cenozoic events for hydrocarbon prospectivity: Petroleum Geoscience, v.3, p.117-131.

Hitchen, K., 2004, The geology of the UK Hatton-Rockall margin: Marine and Petroleum Geology, v.21, p.993-1012.

Hitchen, K., and M.S. Stoker, 1993, Mesozoic rocks from the Hebrides Shelf and the implications for hydrocarbon prospectivity in the northern Rockall Trough: Marine & Petroleum Geology, v.10, p.246-254.

Johnson, H., J.D. Ritchie, K. Hitchen, D.B. McInroy, and G.S. Kimbell, 2005, Aspects of the Cenozoic deformational history of the northeast Faroe-Shetland Basin and the Wyville-Thomson Ridge and Hatton Bank areas, *in* A.G. Doré, and B.A. Vining (eds.), Petroleum Geology: North-West Europe and Global Perspectives – Proceedings of the 6th Conference: The Geological Society, London, p.993-1007.

Keser Neish, J., 1993, Seismic structure of the Hatton-Rockall area: an integrated seismic/modelling study from composite datasets, *in* J.R., Parker (ed.), Petroleum Geology of Northwest Europe: Proceedings of the 4th Conference: The Geological Society, London, p.1047-1056.

Kimbell, G.S., J.D. Ritchie, H. Johnson, and R.W. Gatliff, 2005, Controls on the structure and evolution of the NE Atlantic margin revealed by regional potential field imaging and 3D modelling, *in* A.G. Doré, and B.A. Vining (eds.), Petroleum Geology: North-West Europe and Global Perspectives – Proceedings of the 6th Conference: The Geological Society, London, p.933-945.

Kimbell, G. S., J.D. Ritchie, and A.F. Henderson, 2007, Three-dimensional gravity and magnetic modelling of the Irish Continental Shelf: Poster presented at the Geological Society Bicentenary Conference: Earth Sciences in the Services of Society, 10-11th Sept. 2007, QEII Conference Centre, London.

McInroy, D.B., K. Hitchen, and M.S. Stoker, 2006, Potential Eocene and Oligocene stratigraphic traps of the Rockall Plateau, NE Atlantic Margin, *in* M.R. Allen, G.P. Goffey, R.K. Morgan, and I.M. Walker (eds.), The Deliberate Search for the Stratigraphic Trap: The Geological Society, London, Special Publications, v.254, p.247-266.

Smith, L.K., 2006, Crustal structure of Hatton Bank volcanic continental margin from traveltime inversion of wide-angle data. Unpublished PhD thesis, Cambridge University (UK), 227 p.

White, R.S., G.D. Spence, S.R. Fowler, D.P. McKenzie, G.K. Westbrook and A.N. Bowen, 1987, Magmatism at rifted continental margins: Nature, v.330, p.439-444.

**BACK**

# Revisiting the East Georges Bank Basin, Offshore Nova Scotia - What the Explorationists saw Two Decades Ago

**Tako Koning**
Advisor, Tullow Oil Angola
No 43, Largo Ingombotas
Luanda
Angola
e-mail: ta_koni@tullowoil.com

## ABSTRACT

The East Georges Bank basin is located offshore Nova Scotia on the southeastern Canadian continental shelf. The basin covers 10,000 km2 (~2.5 million acres) and is one of the last undrilled basins in North America.

The geological understanding of this basin is based on 16,000 km of seismic data which was studied and interpreted in the 1980's by Texaco Canada's geoscientists. The first public presentation of the interpreted data was at a CSPG-GAC-MAC conference in 1988 in St. John's, Newfoundland. Subsequently, the geological and geophysical interpretations were presented at a number of oil industry conferences worldwide (San Diego, Calgary, Lagos, Rio de Janeiro). This presentation is a re-presentation of the 1988 and subsequent papers.

In 1988, the Canadian government placed an oil activity moratorium on Georges Bank. Consequently, no activity such as modern seismic surveying has taken place since that time. Therefore, although this presentation is based on vintage seismic data, it must be viewed as up-to-date since no new data has been acquired on the bank for over twenty years.

The Georges Bank basin formed during the Triassic when the landmass of Pangea began separating along rift zones. A prominent Paleozoic basement high, the Yarmouth Arch, separated the East Georges Bank Basin from the West Georges Bank Basin, and had a dominant influence on sedimentation until Middle Jurassic. During the Middle Jurassic, major growth faulting and halokinesis commenced in the basin.

The structural and stratigraphic evolution of the East Georges Bank basin has resulted in the development of a number of economically attractive seismically-defined prospects. The Geological Survey of Canada (GSC) in 1983 estimated that the average hydrocarbon expectation of the basin was 168 x 106m3 barrels oil (1.0 billion barrels) and 150 x 109m3 natural gas (5.3 TCFG). The GSC's speculative (higher) estimate for the basin was 350 x 106m3 barrels of oil (2.1 billion barrels) and 307 x 109m3 gas (10.8 TCFG).

BACK

# Session 2B:
# PETROLEUM SYSTEMS

## KEYNOTE ADDRESS

**GEOLOGY AND HYDROCARBON POTENTIAL OF THE NW AFRICAN ATLANTIC MARGIN**
**Davison, Ian**

**MID TO LATE CRETACEOUS STRUCTURAL AND SEDIMENTARY ARCHITECTURE AT THE TERRA NOVA OILFIELD, OFFSHORE NEWFOUNDLAND - IMPLICATIONS FOR TECTONIC HISTORY OF THE NORTH ATLANTIC**
Sinclair, Iain K.; and Withjack, Martha O.

**RESERVOIR CONNECTIVITY ANALYSIS, HYDROCARBON DISTRIBUTION, RESOURCE POTENTIAL & PRODUCTION PERFORMANCE IN THE CLASTIC PLAYS OF THE SABLE SUBBASIN, SCOTIAN SHELF**
Richards, Bill; Fairchild, Lee H.; Vrolijk, Peter J.; and Hippler, Susan J.

**REGIONAL SETTING OF THE LATE JURASSIC DEEP PANUKE FIELD, OFFSHORE NOVA SCOTIA, CANADA - CUTTINGS-BASED SEQUENCE STRATIGRAPHY AND DEPOSITIONAL FACIES ASSOCIATIONS ABENAKI FORMATION CARBONATE MARGIN**
Eliuk, Leslie

**LITHOLOGY-BASED, HIGH-RESOLUTION SEQUENCE STRATIGRAPHIC FRAMEWORK OF LOWER CRETACEOUS, MIXED CARBONATE-SILICICLASTIC SEDIMENTS, ATLANTIC COASTAL PLAIN, EASTERN UNITED STATES**
Sunde, Richard A.; and Coffey, Brian P.

**DISTRIBUTION OF DIAGENETIC MINERALS IN LOWER CRETACEOUS SANDSTONES WITHIN A DEPOSITIONAL FACIES AND SEQUENCE STRATIGRAPHIC FRAMEWORK: GLENELG, THEBAUD, AND CHEBUCTO FIELDS, OFFSHORE SCOTIAN BASIN**
Karim, Atika; Pe-Piper, Georgia; and Piper, David J.W.

**HYPERPYCNAL RIVER FLOODS AND THE DEPOSITION OF LOWER CRETACEOUS SANDS, SCOTIAN BASIN**
Piper, David J.W.; Karim, Atika; Pratt, Heidi; Noftall, Ryan; Gould, Kathleen; Foley, James and Pe-Piper, Georgia

**RIVER SOURCE AND DISPERSION OF LOWER CRETACEOUS SANDS, SCOTIAN BASIN**
Pe-Piper, Georgia; Triantafyllidis, Stavros and Piper, David J.W.

**BACK**

# Geology and Hydrocarbon Potential of the NW African Atlantic Margin

**Ian Davison**
Earthmoves Ltd.
Chartley, 38-42 Upper Park Road
Camberley, Surrey, GU15 2EF
United Kingdom
e-mail: i.davison@earthmoves.co.uk

## ABSTRACT

The NW African Atlantic Rift System began to open in Carnian times (ca. 235 Ma) and produced a series of half graben with red-bed clastic fill in Morocco. Near the end of rifting, a 1-2 km thick salt was deposited, and is interpreted to be the same age as the CAMP volcanic rocks (200±1 Ma). Farther south, the deep Triassic rifts have not been drilled, but they could contain good oil prone source rocks similar to the southern USA basins. New evidence is presented that salt is present along the Cap Boujdour area of Aaiun Basin 450 km farther to the south of present mapped salt limit. The salt on the North American margin may also extend farther south, linking the South Georges Basin with the Baltimore Canyon Stone Dome occurrence. The northern limit of the Moroccan salt basin is currently mapped to terminate at the overthrusted southern edge of the Rif Thrust Belt, but the salt must continue northward below the Rif. A sub-thrust play exists in Northern Morocco, which has never been tested due to the lack of good imaging below the thrust belt. The Cenomanian-Turonian source rock may be mature in this area, due to the tectonic loading in the Oligo-Miocene. The overlying Jurassic sequence is mainly a carbonate slope facies, but occasionally a rimmed platform edge developed (Senegal, Gambia and Mauritania). The carbonate play has still to be fully tested, because the wells drilled on the USA margin appear to miss the rimmed carbonate edge, and very few wells have drilled the carbonates in NW Africa. The carbonate platform eventually became drowned in the Early Cretaceous, when clastic deltas were deposited. The increased clastic sediment input may be due to the internal rifting and flank uplift occurring throughout North Africa. Cretaceous -Cenozoic clastic sediments constitute the main deepwater target reservoirs. Recent wells in Morocco appear to have failed due to lack of reservoir.

BACK

# Mid to Late Cretaceous Structural and Sedimentary Architecture at the Terra Nova Oilfield, offshore Newfoundland – Implications for the Tectonic History of the North Atlantic

**Iain K. Sinclair**
Husky Energy
Suite 901, Scotia Centre
235 Water Street
St. John's, Newfoundland A1C 1B6
Canada
e-mail: iain.sinclair@huskyenergy.com

**Martha O. Withjack**
Rutgers University
Department of Earth and Planetary Sciences
610 Taylor Road
Piscataway, NJ, 08854-8066
USA
e-mail: drmeow3@rci.rutgers.edu

## ABSTRACT

Multiple exploration, delineation, and development wells, in association with a high-quality 3D seismic survey over the Terra Nova oilfield, provide a detailed data set for the analysis of the mid to Late Cretaceous structural and stratigraphic development of the Jeanne d'Arc basin on the Grand Banks of Newfoundland. These data provide evidence for falling relative sea level during the Hautervian to Barremian. This falling relative sea-level was coeval with, and followed by, uplift originating in the south of the basin. Facies stacking patterns indicate rising relative sea level during the mid-Aptian to Middle to Late Albian contemporaneous with development of west- to northwest-striking detached normal faults. We believe that these normal faults are associated with basement-involved extension beneath the Jeanne d'Arc basin. Crustal extension produced both basement-involved, west- to northwest-striking subsalt normal faults and detached, west- to northwest-striking suprasalt normal faults. The basement-involved and detached normal faults occur exclusively above and to the east of the border fault of the Jeanne d'Arc basin (*i.e.* the Murre fault). Thus, the Murre fault would have had both normal and strike-slip components of displacement during the mid-Cretaceous extension.

## Introduction and Geological Setting

The oil-rich Jeanne d'Arc basin has important economic value to Canada, in general, and to the province of Newfoundland and Labrador, in particular (PRAC 2005; Locke 2006). Additionally, it provides an increasingly rich, well-sampled data base, derived through petroleum exploration and production, which documents the tectonic development of the extended continental crust bordering the spreading North Atlantic Ocean. Widely spaced exploration wells and 2D seismic data, in combination with dense development drilling of the prolific oilfields at Hibernia, Terra Nova, and White Rose (Fig. 1) and several 3D seismic surveys, define a complex tectonostratigraphic history.

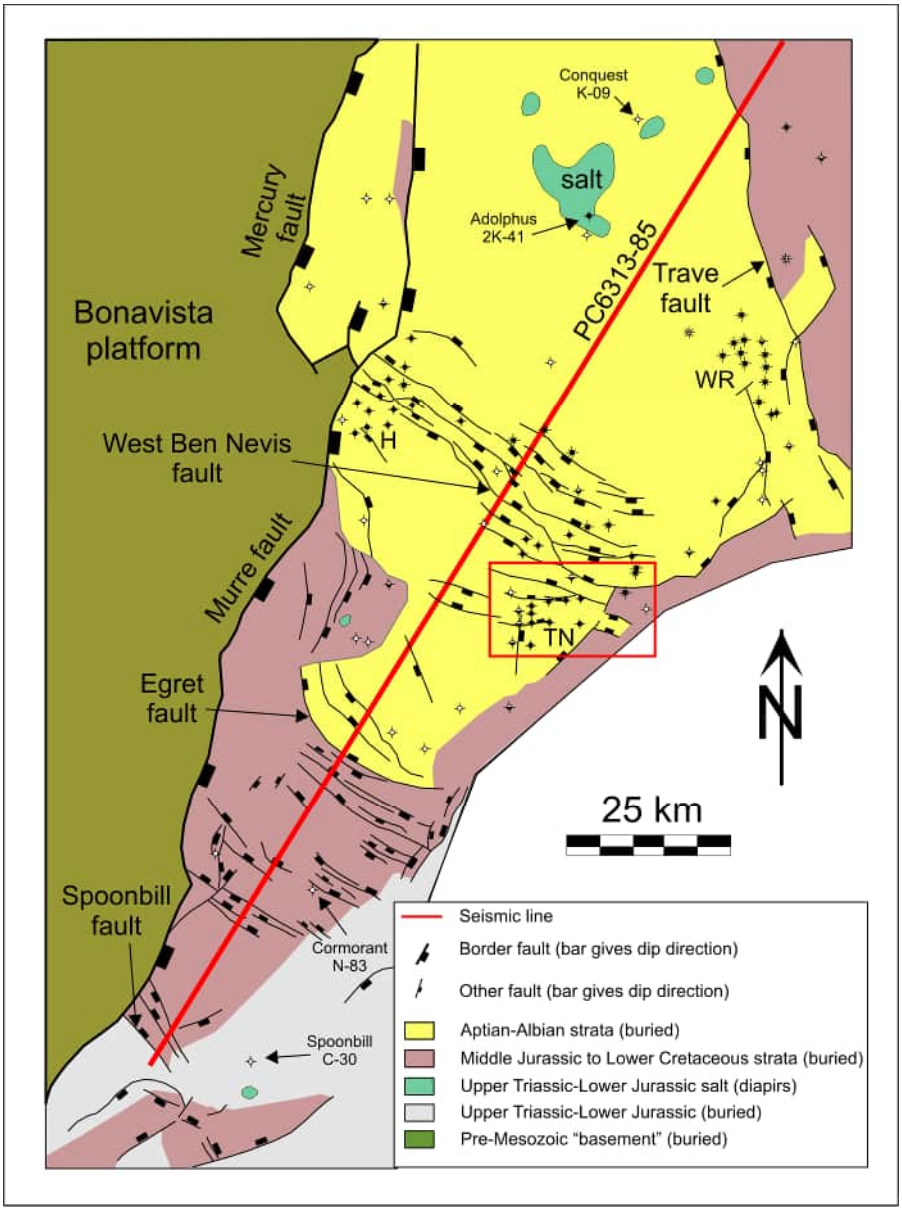


**Figure 1: Location map of the Jeanne d'Arc basin (compiled from Sinclair 1994; Withjack, and Schlische 2005; and McIntyre *et al.* 2004). The stratigraphic packages illustrated are buried beneath relatively unstructured Upper Cretaceous and Tertiary strata. The red line shows the location of a seismic profile in Figure 11. Diapiric salt structures have been drilled at the north end of the basin (Adolphus 2K-41), whereas bedded Upper Triassic to Lower Jurassic salt have been drilled at the south end of the basin at Cormorant N-83 and Spoonbill C-30. Producing oilfields in the basin are: H-Hibernia, WR-White Rose, TN-Terra Nova.**

The Jeanne d'Arc basin is one of many fault-bound rift basins that transect the Grand Banks crustal promontory. The faults that bound and cut across the basin (Fig. 1) resulted from episodic crustal extension leading to the breakup of the Pangean supercontinent and active seafloor spreading from the Central Atlantic to the Labrador Sea (Hubbard *et al.* 1985). Industry, government, and academic researchers broadly conclude that at least two distinct rifting episodes occurred during Late Triassic to Early Jurassic and Late Jurassic to Early Cretaceous (*e.g.* Enachescu 1987; Tankard and Welsink 1987; Grant *et al.* 1988, Tankard *et al.* 1989; Hiscott *et al.* 1990; Sinclair 1988, 1993; Driscoll *et al.* 1995; Withjack and Schlische 2005). A wider range of interpretations, however, exists regarding the age and nature of the youngest extensional episode affecting the Jeanne d'Arc basin. In the following sections, we

describe the lithostratigraphic framework of the mid-Cretaceous strata using well data from the Terra Nova Oilfield and discuss the tectonic implications of these observations for the cause of the mid-Cretaceous extension.

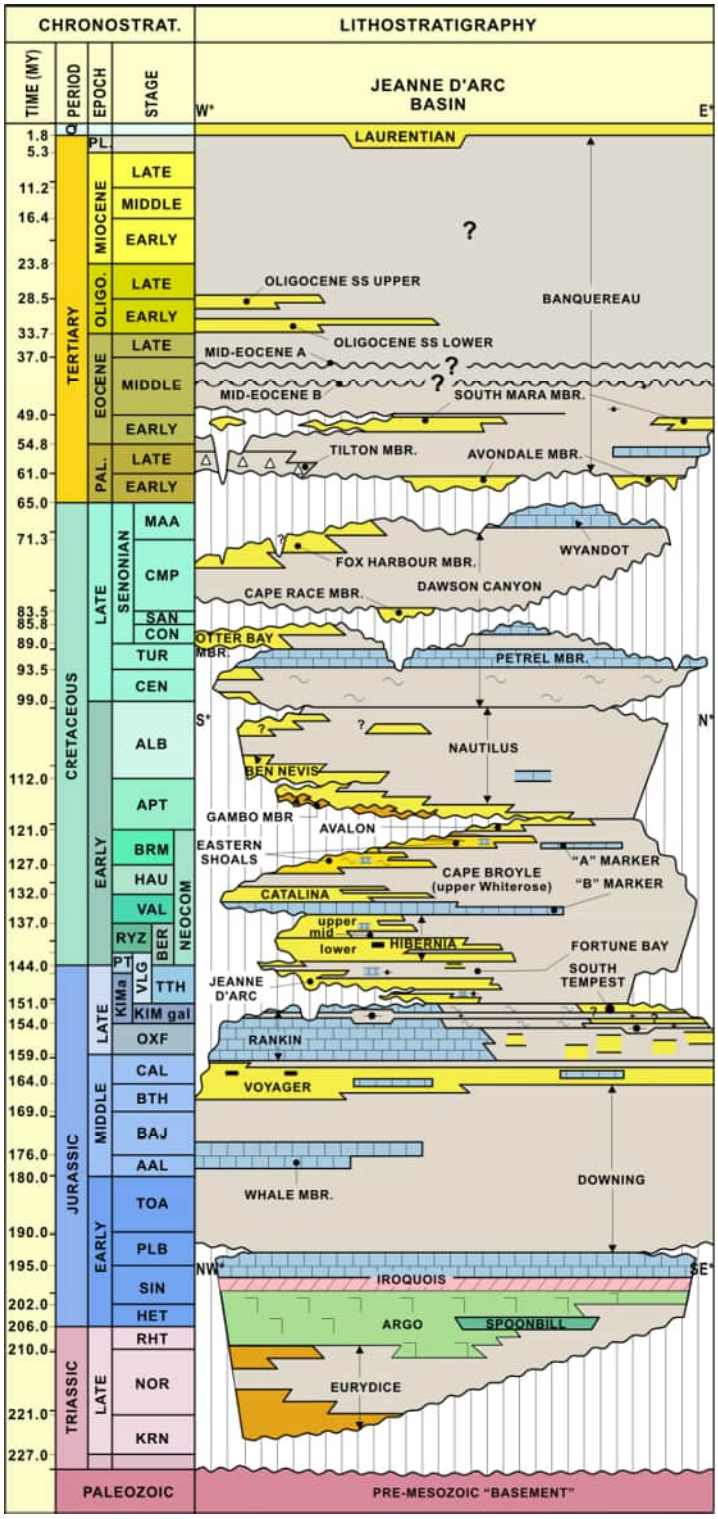


**Figure 2: Stratigraphic column of the Jeanne d'Arc basin, modified after Sinclair (1993) and incorporating McAlpine (1990) and Deptuck *et al.* (2003).**

## Lithostratigraphic Framework

The Terra Nova field produces from Upper Jurassic sandstones of the Jeanne d'Arc formation (Wilcox *et al*. 1991, Skaug *et al*. 2001, Haugen *et al.* 2007) (Fig. 2). The Tertiary and Cretaceous strata in this area are mainly considered as overburden, providing the burial required for source-rock maturation, but otherwise of limited economic interest. Nonetheless, the field operator, Petro-Canada on behalf of the partnership, has collected abundant, publicly available, wireline log and lithological data while drilling producer and injector wells through these strata.

### Eastern Shoals Formation

The Eastern Shoals formation is dated as mainly Barremian, possibly extending into the Hauterivian, as reported by McAlpine (1990). These ages are supported by more recent industry-derived ages in the Terra Nova area (*e.g.* Ainsworth and Riley 2003; Ainsworth *et al*. 2004). Closely spaced wells allow for correlation of progradational parasequences of the Eastern Shoals formation, documenting gradational variations (lateral and vertical) from proximal to distal facies in the Terra Nova area (Figs. 3 and 4). The Eastern Shoals formation is composed of a thick stack of clean sandstones, rich in calcite cements and bioclastic debris, at the south end of the field (*e.g*. Terra Nova I-97). Correlation of gamma-ray and sonic curves, in combination with lithology and grain-size data, indicate that the lowermost bioclastic sandstones of the Eastern Shoals formation are increasingly fine-grained to the north and become gradational with underlying silty shales. This pattern is repeated in overlying sandstones within the Eastern Shoals Formation, corresponding to stacked parasequences of northward-migrating shoreface to shallow marine paleodepositional settings. These stacked parasequences of shoreface to shelf silciclastic sedimentary rocks reflect falling relative sea level from Hauterivian through Barremian time. The northward translation of the coastline with progressive truncation of the parasequences to the south demonstrates that regional uplift of the southern margin of the Jeanne d'Arc basin occurred during and immediately following deposition of these progradational parasequences.

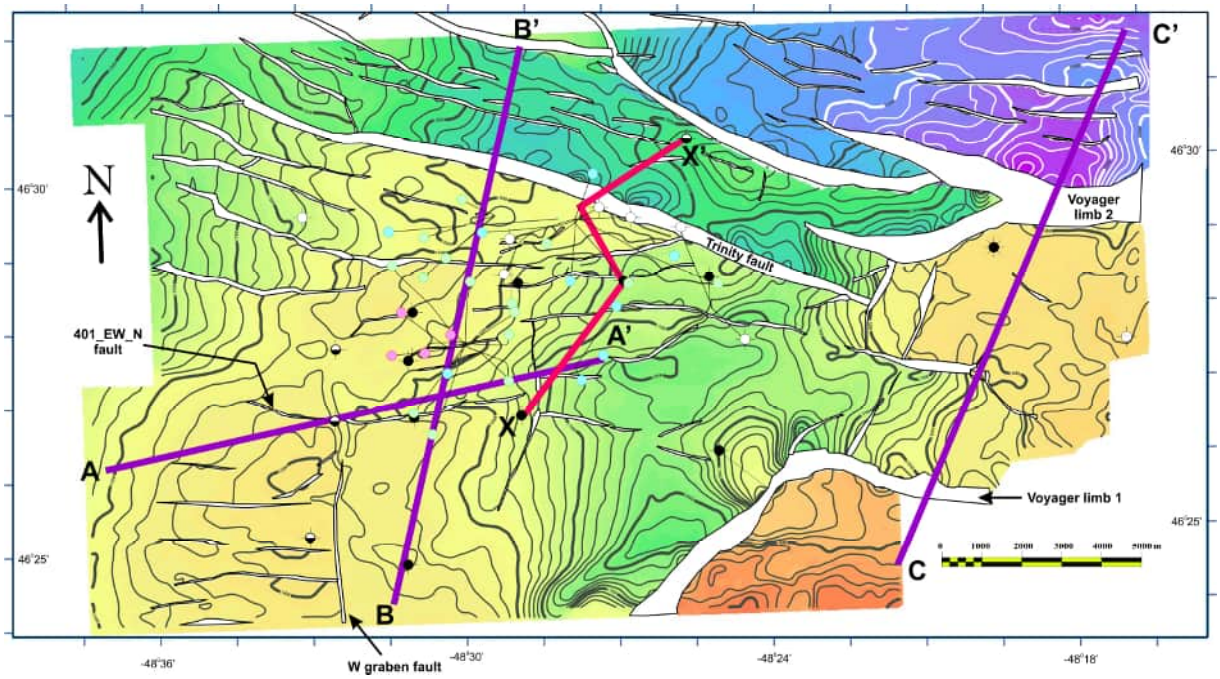


**Figure 3: Time structure map of the mid-Aptian unconformity in the Terra Nova oilfield area mapped with the assistance of Judith McIntyre of Husky Energy. The map shows the location of wells used in Figure 4 and the location of seismic profiles included in Figures 5, 8 and 9. Faults identified in the cross-sections are also labeled on this map.**

Correlations of wellbore thicknesses indicate that most faults in the Terra Nova area were not active during deposition of the Eastern Shoals formation. Post-depositional uplift and differential erosion are indicated, however, by the stratal thickness patterns on opposing sides of major west- to northwest-striking normal faults such as the Trinity fault. Specifically, a significant part of the Eastern Shoals formation is missing from the footwall of the Trinity fault (Terra Nova G-90 4) but is preserved in the hanging wall (North Trinity H-71) (Fig. 4 NB: Large 11x17 inch figure; see end of paper). Additionally, minor increases in the preservation of Eastern Shoals Formation are observed on the downthrown sides of older, north-striking faults (Fig. 5). This latter pattern of differential preservation indicates minor local re-activation of the north-striking faults during the subsequent Aptian-Albian episode of deformation (addressed in the following sections).

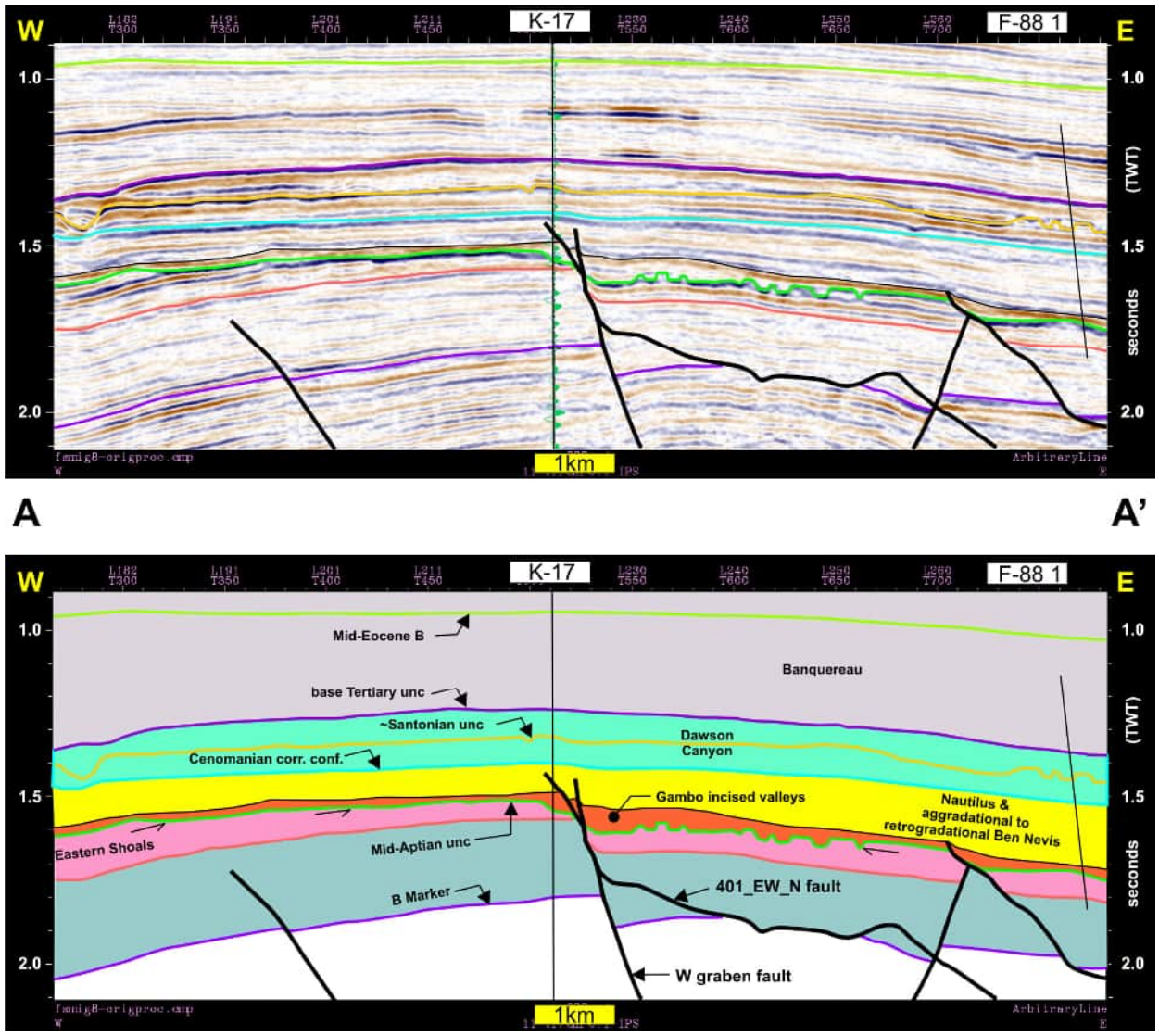


**Figure 5: Seismic profile A-A' across incised valleys at the mid-Aptian unconformity and showing increased preservation of Eastern Shoals strata in the hanging wall of the north-trending west graben fault. The amplitude of the mid-Aptian reflection varies with depth of incision and thickness of weakly cemented sandstones in the overlying Gambo member. Note also the angular truncation of Eastern Shoals strata on the west side of the seismic profile. Location is shown on Figure 3.**

### Sequence Bounding Unconformity

The sequence boundary limiting the preservation of the Eastern Shoals formation previously has been interpreted as a major angular unconformity on 2D seismic data in the southern portion of the Jeanne d'Arc basin (Meneley 1986; Tankard and Welsink 1987; Tankard *et al*. 1989). The lithostratigraphic chart of Tankard and Welsink (1987) places this unconformity within the early Aptian. This is consistent with the recent biostratigraphic analysis of Ainsworth *et al*. (2004). The 3D seismic survey of the Terra Nova oilfield allows for increased resolution of the geophysical characteristics of this unconformity across a significant portion of the southern Jeanne d'Arc basin (Fig. 3). The 3D seismic data show clear indications of valley incision within the oilfield area (Fig. 5) and marked lateral variations in the reflectivity of the unconformity. These variations are attributed to systematic changes in the character of strata on either side of the unconformity (*i.e*. depth of incision of underlying marine strata and thickness of overlying weakly cemented non-marine sandstones). The mid-Aptian unconformity is recognized basin-wide and has been correlated on well and seismic data from Terra Nova to an angular unconformity seen at the base of fluvial sandstones cored in the basin centre at South Mara C-13 (Sinclair 1993). This is a critical surface to the petroleum industry as it provides the basal boundary to a major oil-producing reservoir (*i.e*. Ben Nevis formation) in the areas such as the southern portion of the White Rose oilfield where it also provides a crucial surface for seismic mapping (Kaderali *et al.* 2007) and reservoir modeling.

## Ben Nevis and Nautilus Formations

The Ben Nevis and Nautilus formations overlie the mid-Aptian unconformity. McAlpine (1990) reports their age as ranging from at least Late Aptian to Late Albian. Ainsworth and Riley (2003) and Ainsworth *et al*. (2004) provide a comparable age range for the combined section but with the basal strata of the Ben Nevis possibly extending into the Early Aptian. The lower, variably developed subunit of the Ben Nevis formation, as described by McAlpine (1990), displays a distinctive low-velocity signature on the sonic logs and consists of interbedded shale, sandstone and local coal beds. Such a low-velocity unit can be correlated around much of the Terra Nova oilfield (Fig. 3). Fine to coarse-grained graded sandstones, sandstones with abundant woody carbonaceous debris and partially consolidated intra-clasts are observed in a thin core recovered from this unit at North Trinity H-71, core 5 (Figs. 4, 6A and 6B). These are interpreted to be fluvial sandstones of the Gambo member, laterally equivalent to the fluvial conglomerates and trough cross-bedded, coarse-grained sandstones that were more completely cored at the South Mara C-13 well (Sinclair 1993). Highly carbonaceous shales with sparsely bioturbated silt and very fine sand interbeds, interpreted to represent lower floodplain to coastal plain fines, are also observed in core 5.

The aggradational middle portion of Ben Nevis formation immediately overlying the Gambo member was also cored at North Trinity H-71 (core 4, Fig. 4). The presence of swaley cross beds in clean sandstones and layers with abundant thick-walled shell debris indicate deposition above a high-energy wave base (Figs. 7A and 7B). These shallow marine strata can be correlated over a wide area on the basis of cuttings and wireline log character, (*i.e*., low gamma in clean, winnowed sandstones with highly variable travel-time readings on the sonic log corresponding to porous sandstones alternating with pervasively calcite-cemented sandstones).

Clean sandstones interbedded with pervasively bioturbated argillaceous and silty sandstones were cored in the retrogradational upper portion of the Ben Nevis formation at North Trinity H-71 (Sinclair 1993, his Figure 14). These are interpreted to represent stacked storm and fair-weather deposits (*ibid*.), a common feature documented by others studying Lower Cretaceous strata in the Jeanne d'Arc basin (Harding 1988, Hiscott *et al.* 1990; Pemberton *et al*. 2001). These transitional facies of the upper Ben Nevis are observed to grade laterally and vertically into offshore shales of the Nautilus formation with progressively fewer storm-generated sandstone interbeds. Vertical stacking of back-stepping coastal plain, shoreface, and marine shelf strata document a long-term increase in relative sea level during the

deposition of the Ben Nevis and Nautilus formations. This relative sea level trend, combined with highly variable sediment thicknesses, is interpreted to correspond to high rates of fault-controlled subsidence in the Jeanne d'Arc basin gradually out-pacing high rates of sediment supply during mid-Aptian to Middle or Late Albian times.

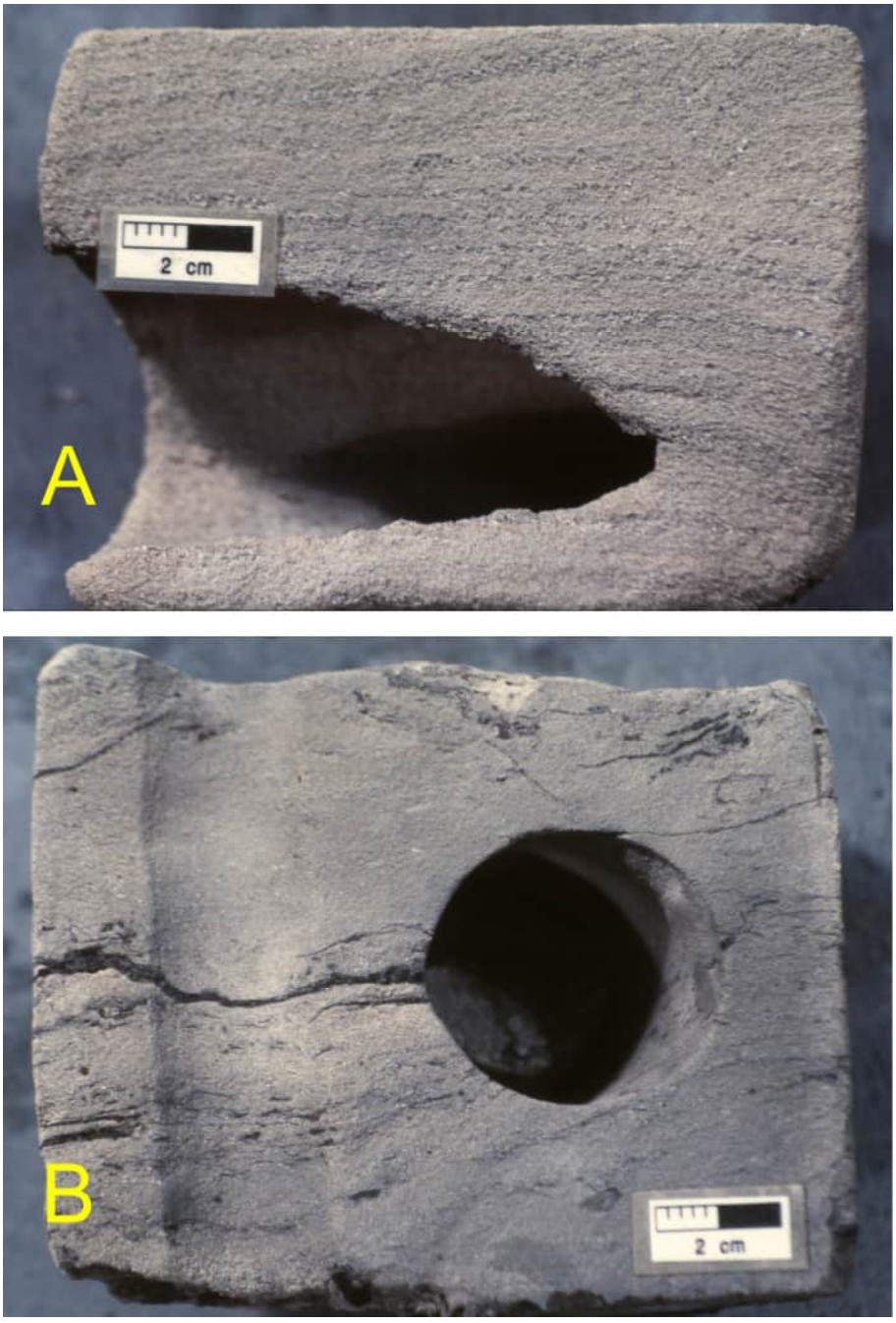


**Figure 6: Photographs of the basal Ben Nevis Formation at North Trinity H-71, core location shown on Fig. 4. Depths are core depths, unadjusted for wireline logs (add about 2m to match wireline)., A; Clean, fine to coarse-grained, friable, graded quartz in fluvial sandstone, core 5, 2164.8 mMD, small plug 293 with 25.8% porosity and 1260 millidarcy air permeability , B, fine to medium grained sandstone with abundant floating woody plant debris, core 5, 2165.75 mMD, small plug 297 with 23.6% porosity and 225 millidarcy air permeability (Core Laboratories, 1985).**

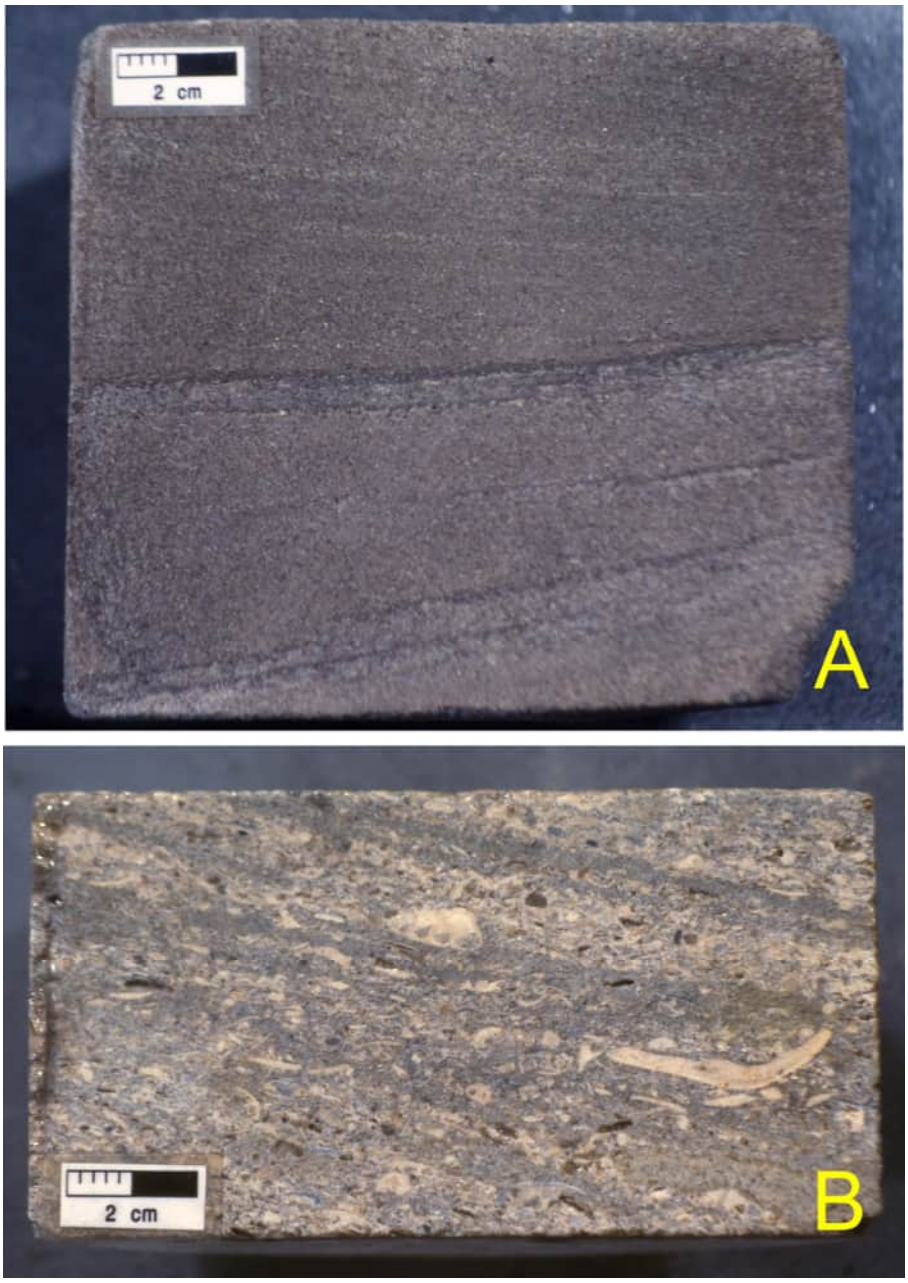


**Figure 7: Photographs of the middle (aggradational) Ben Nevis formation at North Trinity H-71, core location shown on Fig. 4. Depths are core depths, unadjusted for wireline logs (add about 2.8 m to match wireline). A; Weakly divergent (swaley) bedding in fine to medium-grained marine sandstone, core 4,2088.35 mMD, , 2165.75 mMD, small plug 257 with 25.4% porosity and 886 millidarcy air permeability , B; Pervasively calcite cement sandstone with abundant thick-walled bioclastic debris., core 4, 2093.82 mMD, small plug 280 with 5.2% porosity and 0.19 millidarcy air permeability (Core Laboratories, 1985).**

The Ben Nevis and Nautilus formations increase in thickness from 123 to 444 metres moving from Terra Nova G-90 4 to North Trinity H-71, respectively located on the footwall and hanging wall of the west- to northwest-striking Trinity fault (Fig. 4). This change in wellbore penetrations of compacted sandstones and shales is interpreted to represent fault growth during deposition of the Ben Nevis and Nautilus formations in contrast to the post-depositional variations in depth of erosion interpreted for the Eastern Shoals Formation. The 3D seismic data over the Terra Nova oilfield also provide clear evidence

of fault growth during mid-Aptian through Middle or Late Albian deposition on west- to northwest-striking normal faults (Figs. 8 and 9).

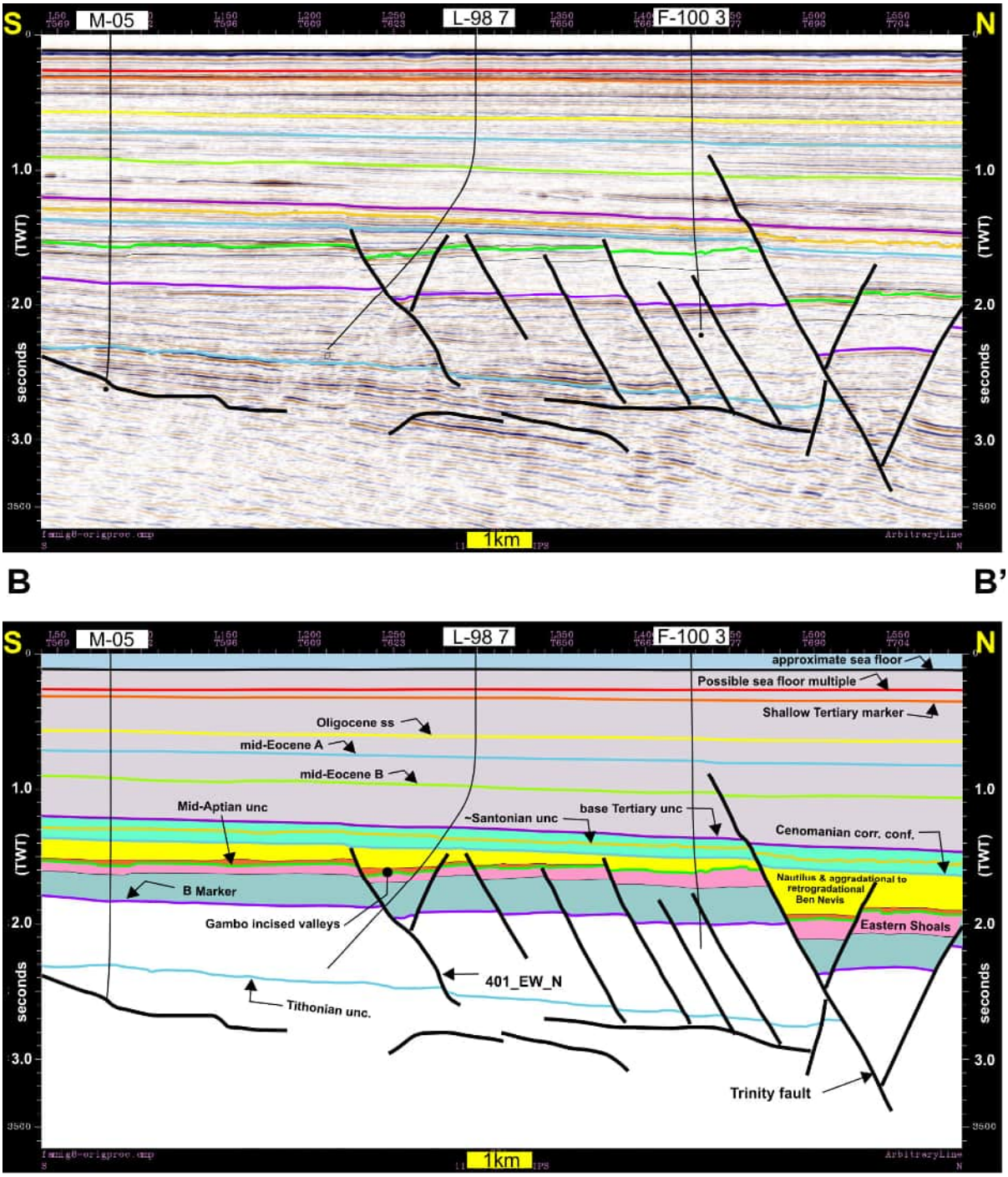


**Figure 8: Seismic profile B-B'across Trinity Fault which bounds the Terra Nova oilfield to the North. Location is shown on Figure 3. This shows that most west- to northwest-trending faults terminate upward within the Aptian-Albian strata highlighted in yellow. The ~Santonian and base Tertiary unconformities are seen to be slightly folded above the moderate-sized 401_EW_N fault. In contrast, the larger-throw Trinity fault does not tip out until well into the Tertiary Banquereau Formation (*i.e.* above the mid-Eocene B marker bed) with a minor forced fold observed at the overlying mid-Eocene A marker.**

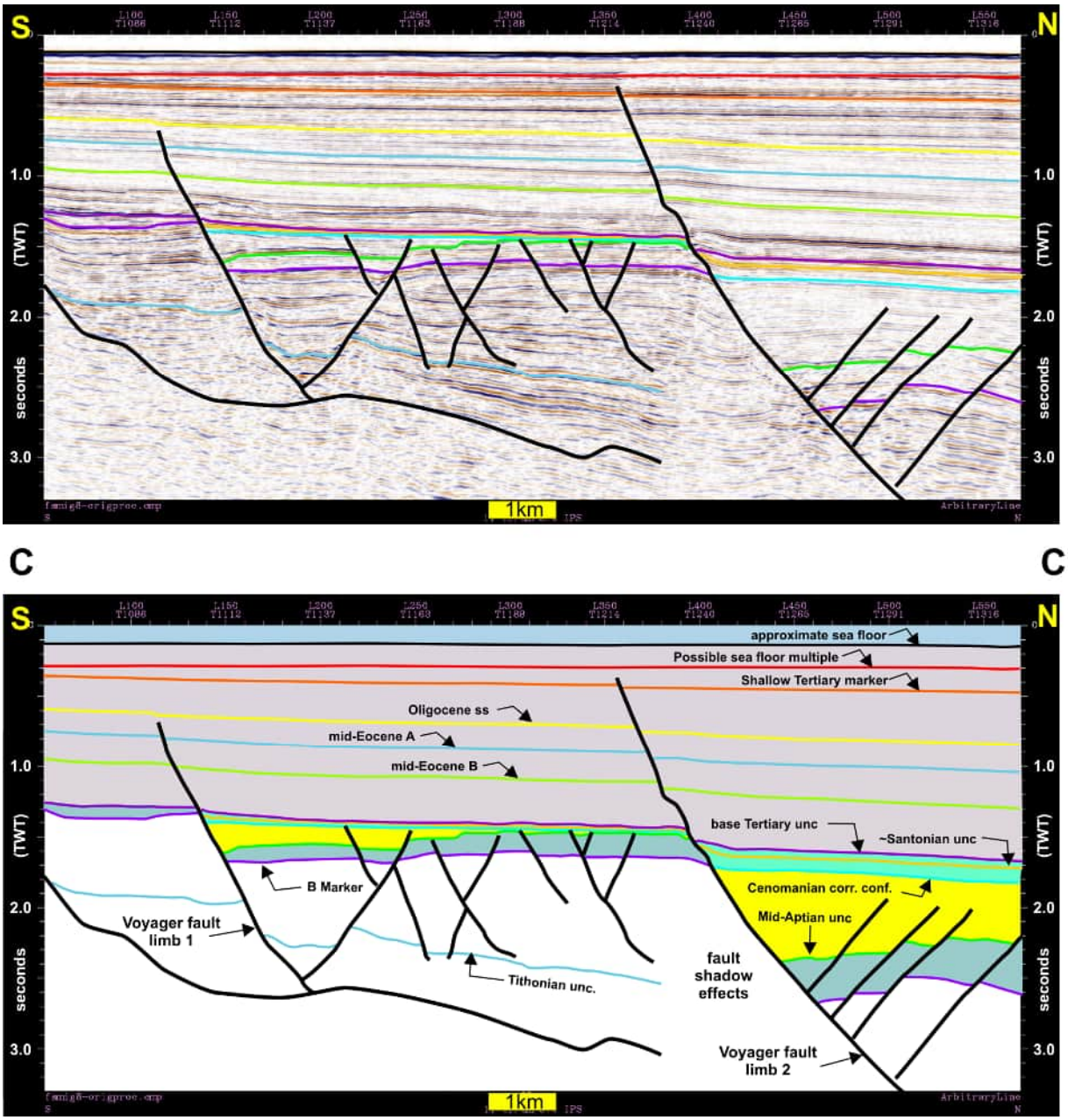


**Figure 9: Seismic profile across basin-bounding Voyager Fault Zone. Location is shown on Figure 3. Patterns of syn-depositional fault growth are again documented by Aptian-Albian thickness variations highlighted yellow. Minor offset and folding is observed on the upper reaches of Voyager fault limb 1 up to mid-way through Tertiary strata. The tip line for the major Voyager Fault limb 2, however, is seen to reach up to uppermost Tertiary beds as shallow as 400 milliseconds Two Way Time (less than 350 m burial depth).**

Seismic profiles also show that the largest throw faults tip out upward at various levels within Upper Cretaceous and Tertiary strata. Figure 9, which crosses two major slip planes of the basin-bounding Voyager fault zone, shows the more northerly fault plane as reaching to within 400 milliseconds two-way time of the sea floor, within Oligocene or younger strata. However the amounts of throw and thickness differences in Upper Cretaceous and Tertiary strata from footwall to hanging wall are minor especially compared to those of Aptian-Albian strata across the lower reaches of the same fault plane. Using relationships derived by Sclater and Christie (1980) for porosity loss/compaction in normally

pressured sediments of the North Sea, we created a subsidence/compaction model to approximate the stratigraphic section observed at Terra Nova G-90 4 and North Trinity H-71 (Fig. 4). This model indicates that stacked intervals of sands, sand and shale, and shale deposited during 692m of subsidence on an active hanging wall block would compact to 458 m thickness during 1500 m of post-extensional burial. Similar ratios of sediments deposited during 208 m of subsidence on an active footwall block would compact to 129 m of strata during equivalent post-extensional burial. These calculations estimate about 155 m of post-extensional differential compaction on either side of such a fault. This 155 m difference in compaction subsidence would require deformation above the previously active fault plane, first by development of minor forced folds and eventually by propagation of discrete fault plane slip. These results compare favourable with patterns of observed deformation across and above the Trinity fault on Figure 8.

## Discussion

What do these patterns of uplift, subsidence, and faulting reveal about the tectonics of the Jeanne d'Arc basin during the mid-Cretaceous? The widespread development of west- to northwest-striking, syn-depositional normal faults in Aptian-Albian strata are variously attributed to two end-member models: 1) purely gravity-driven processes facilitated by mobilization of thick Upper Triassic to Lower Jurassic salt, or 2) deep-seated, rift-related crustal extension with salt and shale units decoupling the deep-seated faults from coeval faults in the overlying Jurassic and Cretaceous strata.

Early exploration wells drilled at the south end of the Jeanne d'Arc basin and in other basins of the southern Grand Banks region have penetrated thick occurrences of Triassic/Jurassic bedded salt (Jansa *et al*. 1977, 1980; Grant *et al.* 1986; Balkwill and Legall 1989). Additionally, salt diapirs have been drilled at the north end of the Jeanne d'Arc basin (*i.e*. Adolphus 2K-41, Fig. 1), attesting to the widespread occurrence of salt beneath the Jurassic and Cretaceous strata in the Jeanne d'Arc basin (Enachescu 1987). Tilting of a salt-floored basin could induce gravity-driven processes including salt mobilization (*e.g*. Hudec and Jackson, 2006, 2007) (Fig. 10a, top row). The Jeanne d'Arc basin experienced multiple times of northward tilting as defined by well and regional seismic data. Specifically, Tithonian to early Valanginian, Hauterivian to Barremian (described above), and most obviously Late Cretaceous through Tertiary (Fig. 11) were times of northward tilting and the development of the Avalon uplift. However, erosion in the south and deposition in the north of the basin as occurred during the Tithonian to early Valanginian and Hauterivian to Barremian times would have inhibited the northward flow of salt (*e.g*. Hudec and Jackson 2006, 2007) (Fig. 10a, bottom row). Furthermore, these two tilt episodes preceded the Aptian-Albian episode of west- to northwest-striking faulting, whereas the Late Cretaceous to Tertiary tilt post-dated most faulting. Additionally, gravity-driven processes produce systems of detached extensional faults that link with synchronous detached fold and thrust belts (*e.g*., the Rhone Fan, offshore southern Mediterranean, Fig. 10b). Evidence of such coeval detached shortening is lacking in the northern Jeanne d'Arc basin (Fig. 11). Instead, the observed patterns of faulting and folding in the Jeanne d'Arc basin resemble those in analog models of basement-involved extension with silicone polymer (Withjack and Callaway 2000) (Fig. 12A) and those in rift basins with basement-involved normal faulting and salt (*e.g*. the Haltenbanken area of offshore Norway, Fig.12B). In both the seismic examples and models, large fault-propagation folds form above basement-involved normal faults and numerous detached normal faults form in the sedimentary cover above the salt or salt analog (Fig. 12). The models suggest that the basement-involved normal faults would produce subparallel detached normal faults (Withjack and Callaway 2000). The intra-sedimentary deformation patterns mapped on seismic data and inferred at depth (Fig. 11) closely resemble the analog models. The deformational patterns around the Egret fault are consistent with a through-going fault eventually linking deformation in the basement and sedimentary cover (Fig. 12A, bottom), whereas the deformation patterns around the West Ben Nevis fault are consistent with the development of a forced fold and an offset, detached normal fault in the sedimentary column (Fig. 12A, top.). Considerable variations in the thickness of bedded salt were encountered during an early phase of exploration drilling across the Grand Banks basins (Hosler *et al.*

1988). This, along with the presence of multiple prominent salt diapirs in the area of the Adolphus and Conquest wells in the north-central Jeanne d'Arc basin (Fig. 1), allows for the possibility that the distinct patterns of detachment and offset at the West Ben Nevis fault are a consequence of crustal extension affecting an area with thicker salt deposits, consistent with analog modeling results of Withjack and Callaway (2000).

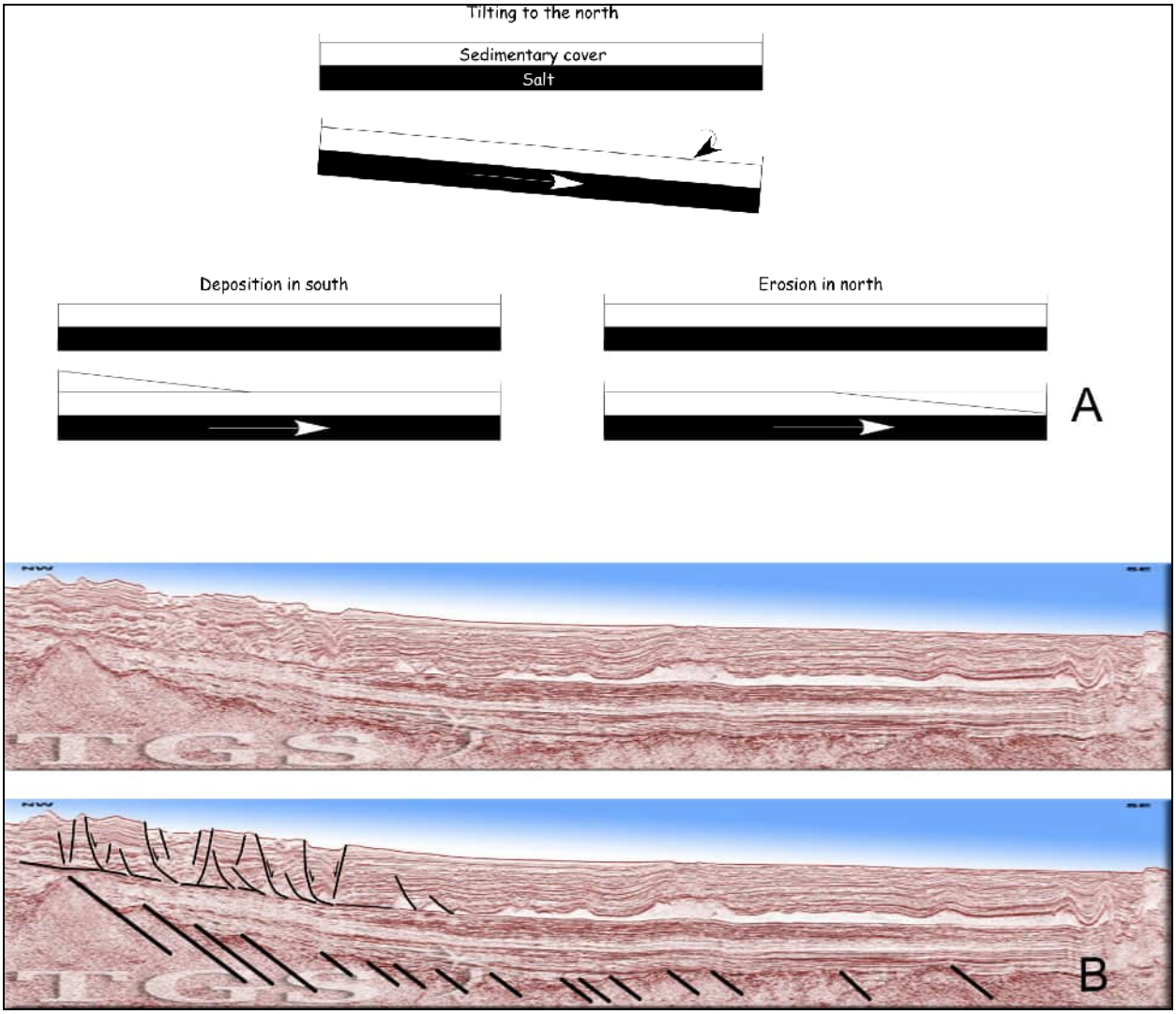


**Figure 10: A. Processes that would promote the flow of salt to the north in the Jeanne d'Arc basin: (top) tilting to the north; (bottom, left) deposition (i.e., progradation) in the south; (bottom, right) erosion in the north. Alternatively, processes that would inhibit the flow of salt to the north include tilting to the south, erosion in the south, and deposition in the north. Although the Jeanne d'Arc basin underwent northward tilting during the Early Cretaceous (Aptian), erosion in the south and deposition in the north associated with this tilting would, at least partially, negate the effect of the tilting. B. Uninterpreted (top) and interpreted (bottom) versions of seismic profile RM01 from the Rhone fan, northern Mediterranean, showing linked extensional and shortening related detached structures (uninterpreted version courtesy of TGS-NOPEC, Virtual Seismic Atlas, www.seismicatlas.org). Black lines show interpreted suprasalt and older subsalt normal faults. The suprasalt normal faults on the northwest end of the line detach within the Messinian salt section. Coeval detachment folds, cored by salt, affect the southeast end of the line.**

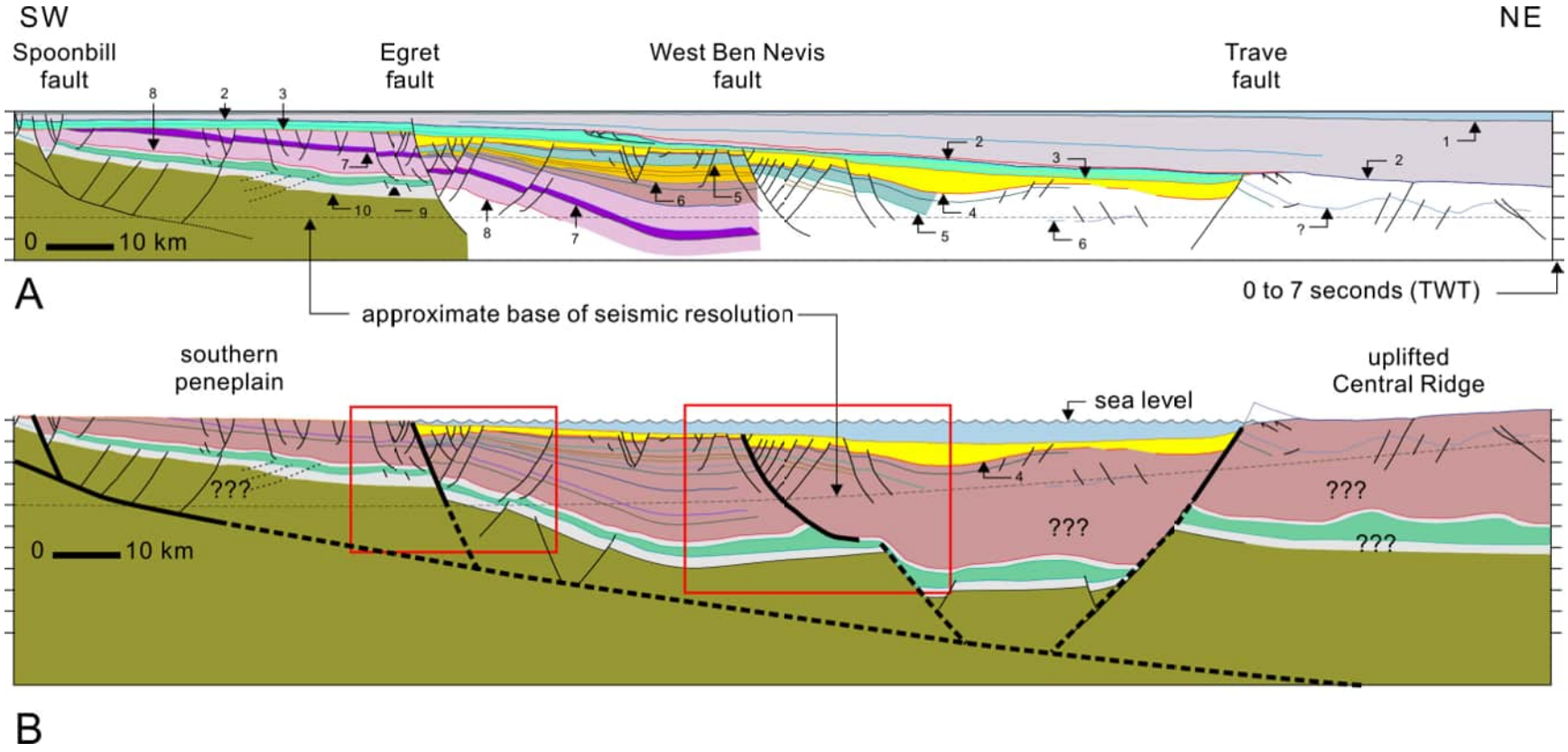


**Figure 11: (A) Line drawing of a portion of Petro-Canada seismic profile 6313-85 with detailed lithostratigraphic subdivisions within the interval of seismic resolution, and (B) restoration to end of mid-Aptian to late Albian extension with inferred structural interpretation below level of seismic resolution (modified from Sinclair, 1994) and the coarse lithostratigraphic subdivision used on Fig. 1. The seismic profile is along the axis of the Jeanne d'Arc basin, highly oblique to the basin-bounding Murre fault (location on Fig. 1). Vertical exaggeration is about 1:1 assuming a velocity of 4 km/s. Seismic reflections in A are: 1, sea floor; 2, base Tertiary unconformity; 3, Cenomanian unconformity and correlative conformity; 4, mid-Aptian unconformity; 5, mid-Valanginian unconformity and correlative conformity; 6, Tithonian unconformity; 7, near top of Whale member; 8, top Iroquois formation; 9, top basal Jurassic basalt; 10, near top of basement. Colour-code for detailed intervals are: mauve – Tertiary, light blue – Upper Cretaceous, yellow – Aptian-Albian, orange – Tithonian to lower Valanginian. Purple –Middle and Upper Jurassic, green –Lower Jurassic to Upper Triassic salt, olive – pre-Mesozoic "basement". Compare structural features in red boxes to those observed in analog models and basins illustrated in**

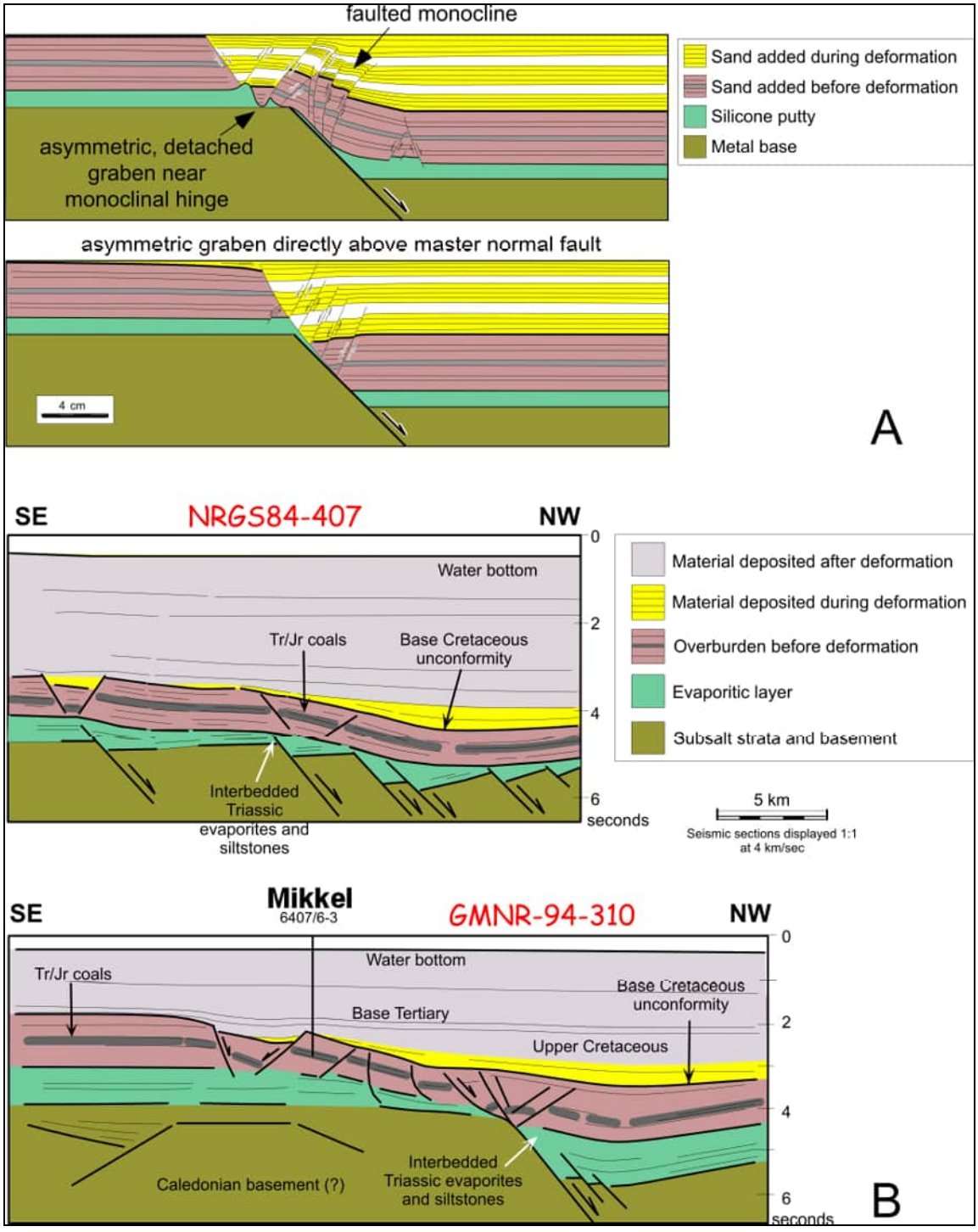


**Figure 12: A. Cross sections through analog models with dry sand and putty (after Withjack and Callaway, 2000). B. Haltenbanken area, offshore Norway. (top) Line drawing of time-migrated seismic section (NRGS84-407) across Smørbukk structure, offshore Norway (after Withjack *et al.* 1986, 1990; Withjack and Callaway 2000) (bottom). Line drawing of time-migrated seismic section (GMNR94-310) across Mikkel structure, offshore Norway (after Withjack and Callaway 2000). In the models and seismic examples, extension produced basement-involved normal faults. In response, fault-propagation folds and detached normal faults formed in the sedimentary cover.**

Based on the above observations, we believe that the west- to northwest-striking detached normal faults mapped on 3D seismic data in the Terra Nova oilfield area of the Jeanne d'Arc Basin reflect northeast-southwest crustal extension. It should be noted that such detached faults occur exclusively to the east and above the border fault of the Jeanne d'Arc basin (*i.e.* the Murre fault, Fig. 1). Thus, the pre-existing Murre fault must have provided an anisotropic crustal feature that would have been re-activated with both normal and strike-slip components of displacement during the mid-Cretaceous extension.

## Conclusions

Uplift at the south end of the Jeanne d'Arc basin occurred during the Hauterivian to Barremian, causing a forced regression of the coastline and northward progradation of stacked shoreface parasequences. Crustal extension in Aptian-Albian times caused development of detached W- to NW-striking normal faults in the sedimentary column. This tectonically-controlled extension resulted in an increase in subsidence and accumulation of thick, stacked and back-stepping coastal plain and shallow marine strata. Differential sediment compaction caused the most prominent syn-rift faults to propagate upward as sediments accumulated during the Late Cretaceous and Tertiary. These tectonic events and their related stress regimes must be integrated into analysis of the opening history of the North Atlantic Ocean.

## References


Ainsworth, N.R. and L.A. Riley, 2003, Mobil Well Ben Nevis I-45, Offshore Eastern Canada Biostratigraphy of the interval 1,600m – 3,110m, report prepared for Husky Oil, 28p.

Ainsworth, N.R., L.A. Riley, W. Braham, and H.W. Bailey,2004 Canterra *et al* Well Beothuk M-05, Offshore Eastern Canada Biostratigraphy of the interval 900m– 3,780m, report prepared for Husky Energy, 4 p.

Balkwill, H.R. and F.D. Legall, 1989, Whale Basin, offshore Newfoundland: extension and salt diapirism, *in* A.J. Tankard, A.J. and H.R. Balkwill, eds, Extensional Tectonics and Stratigraphy of the North Atlantic Margins, AAPG Memoir 46, p.233-245.

Core Laboratories, 1985, Core Analysis Petro-Canada Exploration Inc. PCI *et al.* North Trinity H-71 Wildcat, Eastcoast Offshore, report 70175-85-560C, available from the Canada-Newfoundland and Labrador Offshore Petroleum Board.

Deptuck, M. E., R. A. MacRae, J. W. Shimeld, G. L. Williams, R. A. Fensome, 2003, Revised Upper Cretaceous and lower Paleogene lithostratigraphy and depositional history of the Jeanne d'Arc Basin, offshore Newfoundland, Canada, AAPG Bull., v 87, p 1459-1483.

Driscoll, N.W., J.R. Hogg, N. Christie-Blick, and G.D. Karner, 1995, Extensional tectonics in the Jeanne d'Arc Basin, offshore Newfoundland: implications for the timing of break-up between Grand Banks and Iberia, *in* R.A. Scrutton, M.S. Stoker, G.B. Shimmield, and A.W. Tudhope, eds., The Tectonics, Sedimentation and Palaeoceanography of the North Atlantic Region, Geol. Soc. Lond. Special Publication 90, p.1-28.

Enachescu, M.E., 1987, Tectonic and structural framework of the northeast Newfoundland continental margin, in C. Beaumont and A.J. Tankard, eds., Sedimentary Basins and Basin-forming Mechanisms. Can. Soc. Petrol. Geol., Memoir 12, p.117-146.

Grant, A.C., K.D. McAlpine, and J.A. Wade, 1986, The continental margin of eastern Canada: geological framework and petroleum potential, *in* M.T. Halbouty, ed., Future Petroleum Province of the World, AAPG., Memoir 40, p.177-205.

Grant, A.C., L.F. Jansa, K.D. McAlpine, and A. Edwards, 1988, Mesozoic-Cenozoic geology of the eastern margin of the Grand Banks and its relation to Galicia Bank, *in* G. Boillot, E.L. Winterer, et al., eds., Proceedings of the Ocean Drilling Program, Scientific Results: College Station, Texas, v.103, p.787-807.

Harding, S., 1988, Facies interpretation of the Ben Nevis Formation in the North Ben Nevis M-61 well, Jeanne d'Arc Basin, Grand Banks, Newfoundland, *in* D.P. James and D.A. Leckie, eds, Sequences, Sedimentology: Surface and Subsurface, Can. Soc. Petrol. Geol., Memoir 15, p.291-306.

Haugen, E., J. Costello, L. Wilcox, E. Albrechtsons, and I. Kelly, 2007, Reservoir management challenges of the Terra Nova offshore field: lessons learned after five years of production, OTC paper 109587, presentation at the 2007 SPE Annual Technical Conference and Exhibition held in Anaheim, California, 11-14 November 2007, 15p.

Hiscott, R.N., R.C.L. Wilson, S.C. Harding, V. Pujalte, D. Kitson, 1990, Contrasts in Early Cretaceous depositional environments of marine sandbodies, Grand Banks — Iberia: Bulletin of Canadian Petroleum Geology, v.38, p.203-214.

Hosler, W.T., G.P. Clement, L.F. Jansa, and J.A. Wade, 1988, Evaporite deposits of the North Atlantic rift, *in* W. Manspeizer, ed. Triassic-Jurassic Rifting Continental Breakup and the origin of the Atlantic Ocean and Passive Margins, Part B, Chapter 22, p 525-556.

Hubbard, R. J., J. Pape, and D. G. Roberts, 1985, Depositional sequence mapping to illustrate the evolution of a passive continental margin, *in* O. R. Berg and D. Woolverton, eds., Seismic stratigraphy II: an integrated approach to hydrocarbon exploration: AAPG Memoir 39, p.93-115.

Hudec, M. R., and Jackson, M. P. A., 2006, Advance of allochthonous salt sheets in passive margins and orogens: AAPG Bulletin, v.90, p.1535-1564.

Hudec, M.R. and Jackson, M.P.A., 2007. Terra infirma: Understanding salt tectonics. Earth-612 Science Reviews, v. 82, p. 1-28.

Jansa, L.F., J.P. Bujak, and G.L. Williams., 1980, Upper Triassic salt deposits of the western North Atlantic: Canadian Journal of Earth Sciences, v. 17, p. 547-559.

Jansa, L.F., F.M. Gradstein, G.L Williams, and W.A.M. Jenkins, 1977, Geology of the Amoco Imp Skelly A-1 Osprey H-84 well, Grand Banks, Newfoundland. Geol. Surv. Can., Paper 77-21, 17 p.

Kaderali, A., M. Jones, and J. Howlett, 2007, White Rose seismic with well data constraints: A case history, The Leading Edge, June 2007, p. 742-754.

Locke, W., 2006, Economics of Newfoundland and Labrador's Offshore Oil Industry: Separating Fact from Myth, Presentation at NOIA Annual Conference 2006. http://www.em.gov.bc.ca/DL/offshore/Reports/noia_presentation_2006_final.pdf

McAlpine, K.D., 1990, Mesozoic stratigraphy, sedimentary evolution and petroleum potential of the Jeanne d'Arc Basin, Grand Banks of Newfoundland. Geol. Surv. Can., Paper 89-17, 50 p.

McIntyre, J., N. DeSilva, T. Thompson, 2004, Updated Regional Mapping of Jeanne d'Arc Basin Based on Released 3-D Seismic Data, Canada-Newfoundland and Labrador Report GP-CNOPB-04-01, 14p., 9 map enclosures.

Meneley, R.A., 1986, Oil and gas fields in the east coast and Arctic basins of Canada, *in* M.T. Halbouty, ed., Future Petroleum Provinces of The World. AAPG. Memoir. 40, p.143-176.

Pemberton, S.G., M. Spila, A.J. Pulham, T. Saunders, J.A. MacEachern, D. Robbins and I.K. Sinclair, 2001, Ichnology and Sedimentology of Shallow to Marginal Marine Systems: Ben Nevis & Avalon Reservoirs, Jeanne d'Arc Basin, Geological Association of Canada, Short Course Notes 15, 353 p.

Petroleum Research Atlantic Canada (PRAC), 2005, Socio-Economic Benefits From Petroleum Industry Actvity in Newfoundland and Labrador 2003 and 2004, Jacques Whitford Report, PROJECT No. FS10870, 29 p.

Sclater, J.G. and P.A.F. Christie, 1980, Continental stratching: an explanation of the post-mid-Cretaceous subsidence of the central North Sea, Journal of Geophysical Research, v.85, p.3711-3739.

Sinclair, I.K., 1988, Evolution of Mesozoic-Cenozoic sedimentary basins in the Grand Banks area of Newfoundland and comparison with Falvey's (1974) rift model. Bull. Can. Petrol. Geol., v.36, p.255-273.

Sinclair, I.K., 1993, Tectonism: the dominant factor in mid-Cretaceous deposition in the Jeanne d'Arc Basin, Grand Banks. Marine and Petroleum Geology, v.10, p.530-549.

Sinclair, I.K., 1994, Tectonism and Sedimentation in the Jeanne d'Arc Basin, Grand Banks of Newfoundland. Ph.D. thesis, University of Aberdeen, 248 p. plus appendices and enclosures.

Skaug M., K. Kerwin, and J. Katay, 2001, Reservoir Development Plan for the Terra Nova Field, OTC paper 13024, presentation at the 2001 Offshore Technology Conference held in Houston, Texas, 30 April–3 May 2001, 9p.

Tankard, A. J., and H. J. Welsink, 1987, Extensional tectonics and stratigraphy of Hibernia oil field, Grand Banks, Newfoundland: AAPG Bull., v.71, p.1210–1232.

Tankard, A.J., H.J. Welsink, and W.A.M. Jenkins, 1989, Structural styles and stratigraphy of the Jeanne d'Arc Basin, Grand Banks of Newfoundland, *in* A.J. Tankard and H.R. Balkwill, eds., Extensional tectonics and stratigraphy of the North Atlantic margins: AAPG Memoir 46, p.266-282.

Wilcox, L.B., D.E. Couturier, and M.D. Hewitt. 1991, The integration of geophysical, geological and well test studies into a reservoir description for the Terra Nova oilfield offshore eastern Canada. Thirteenth World Petroleum Congress, Topic 11, John Wiley & Sons, Chichester, p.1-9.

Withjack, M., J. Olson, and E. Peterson, 1990, Experimental models of extensional forced folds: AAPG. Bull., v.74, p.1038-1054.

Withjack, M., K. Meisling,, and L. Russell, 1989, Forced folding and basement-detached normal faulting in the Haltenbanken area, offshore Norway: *in* A. J. Tankard and H. R. Balkwill, eds., Extensional Tectonics and Stratigraphy of the North Atlantic Margins: AAPG Memoir 46, p.567-575.

Withjack, M.O. and S. Callaway, 2000, Active Normal Faulting Beneath a Salt Layer: An Experimental Study of Deformation Patterns in the Cover Sequence, AAPG Bull., v.84, p.627–651.

Withjack, M.O., and R.W. Schlische, 2005, A review of tectonic events on the passive margin of eastern North America, *in* P. Post, ed., Petroleum Systems of Divergent Continental Margin Basins: 25th Bob S. Perkins Research Conference, Gulf Coast Section of SEPM, p.203-235.

**BACK**

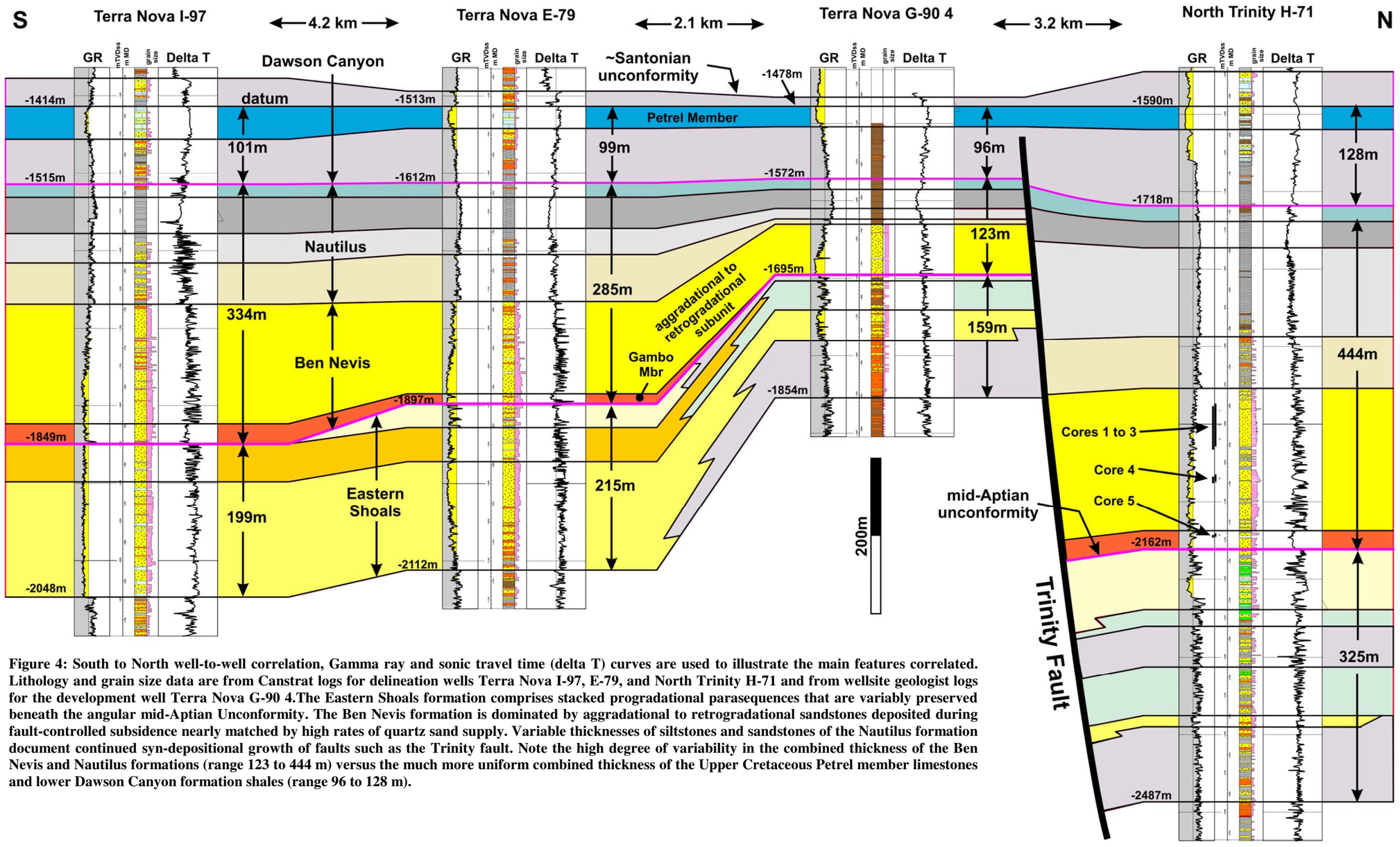


**Figure 4: South to North well-to-well correlation, Gamma ray and sonic travel time (delta T) curves are used to illustrate the main features correlated. Lithology and grain size data are from Canstrat logs for delineation wells Terra Nova I-97, E-79, and North Trinity H-71 and from wellsite geologist logs for the development well Terra Nova G-90 4.The Eastern Shoals formation comprises stacked progradational parasequences that are variably preserved beneath the angular mid-Aptian Unconformity. The Ben Nevis formation is dominated by aggradational to retrogradational sandstones deposited during fault-controlled subsidence nearly matched by high rates of quartz sand supply. Variable thicknesses of siltstones and sandstones of the Nautilus formation document continued syn-depositional growth of faults such as the Trinity fault. Note the high degree of variability in the combined thickness of the Ben Nevis and Nautilus formations (range 123 to 444 m) versus the much more uniform combined thickness of the Upper Cretaceous Petrel member limestones and lower Dawson Canyon formation shales (range 96 to 128 m).**

BACK

# Reservoir Connectivity Analysis, Hydrocarbon Distribution, Resource Potential and production Performance in the Clastic Plays of the Sable Subbasin, Scotian Shelf

**Bill Richards**
ExxonMobil Canada
1701 Hollis Street
P.O. Box 517
Halifax, Nova Scotia B3J 3MB
Canada
e-mail: bill.richards@esso.ca

**Lee H. Fairchild**
Gorge Geotechnical
Mt.Hood/Parkdale, Oregon 97041
USA

**Peter J. Vrolijk**
ExxonMobil Upstream Research Company,
P.O. Box 2189
Houston, Texas 77098
USA

**Susan J. Hippler**
ExxonMobil Exploration Company
233 Benmar
Houston, Texas 77060
USA

## ABSTRACT

Reservoir Connectivity Analysis (RCA) is a systematic approach to understanding reservoir "plumbing" based on well-known physical principles). It is central to understanding fluids, pressures and field/pool size distribution in the clastic reservoirs of the Sable Subbasin. We will illustrate this approach with examples from the five producing Sable gas fields, other significant discoveries, and, the recent, third tranche of exploration and delineation drilling.

Hydrocarbon traps in the clastic system at Sable vary progressively from linear, low relief, extensional fault bend folds (which have small scale internal faulting), to high relief, heavily faulted domes where salt movement is involved in addition to listric faulting. It was recognized pre-production that despite complex overpressure distribution (attributed to recent charge) hydrocarbon accumulations are dominantly controlled geometrically, by "fill & spill" mechanisms: spill and break-overs at structural saddles, and critically, juxtapositional connections at internal and bounding faults. Because the Sable Subbasin is predominantly a high net-to-gross, marginal marine system with limited thick top seals there is - with a few very important exceptions - a propensity for "leaky traps", short hydrocarbon columns, and numerous small hydrocarbon pools.

In the absence of direct seismic indications of hydrocarbons, RCA has been the most effective technique for fluid prediction ahead of the drill. Previous speculation that fault processes and ensuing

"fault rocks" would provide lateral seals, with longer gas columns and a larger resource is inconsistent with drilling results and production history.

## Introduction

This talk is about insights gained over the last decade through Reservoir Connectivity Analysis (RCA) (Vrolijk *et al*. 2005) in the clastic plays of the Sable Subbasin. This period of activity included development of the five producing Sable gas fields (the "Sable Project" operated by ExxonMobil Canada Properties), and an associated exploration and appraisal program. The focus of this talk is specifically on the clastic plays in the Subbasin, without comment on recent industry activity in the Abenaki Carbonate Bank or the Scotian Slope.

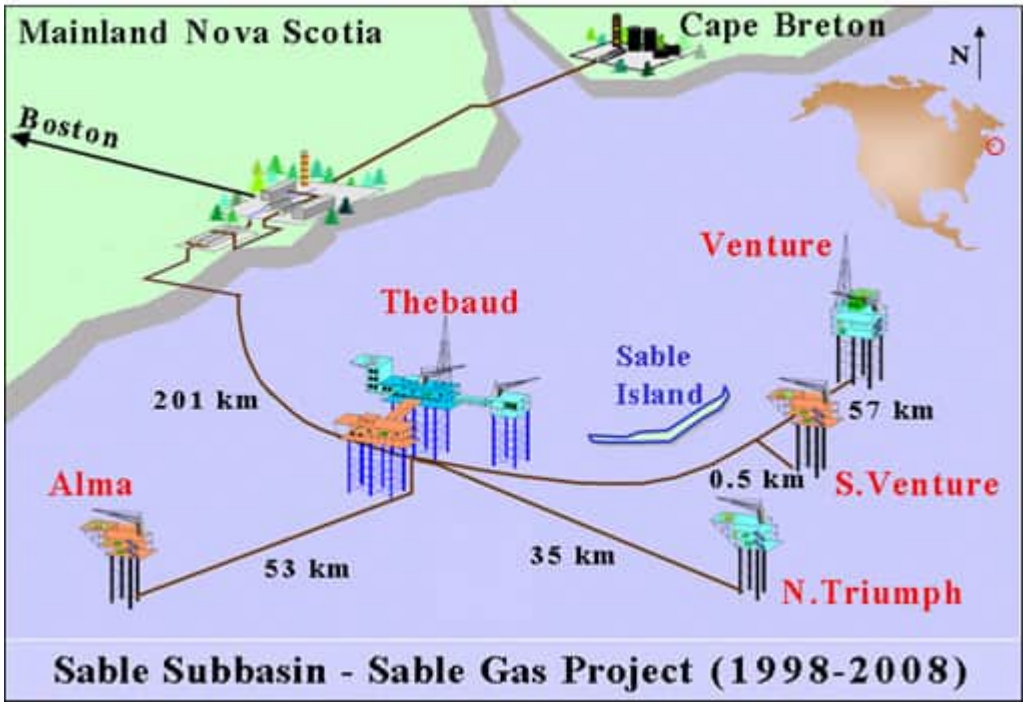


**Figure 1. Location map. Sable Subbasin and Sable Gas Project.**

The Sable Project involved installation of seven platforms, a pipeline system and associated onshore facilities (Fig. 1). Twenty production wells have typically achieved 400-500 MMcf/d of gas and condensate production from multiple reservoirs at varying pressures and temperatures in multiple fields - a successful, but complex and expensive engineering project in a harsh operating environment. As a subset of the Sable Project, owner companies concurrently undertook further extensive 3D seismic acquisition and regional studies, and re-evaluated a further 15 much smaller significant discoveries that were made in two previous tranches of drilling - about 80 wells drilled between 1969 & 1985 based on 2D seismic (Fig. 2).

Between 2000 and 2004, three exploration wells (Emma N-03, Adamant N-97 and Cree I-34) encountered limited gas. A sixth Sable Project field, Glenelg, was not developed subsequent to an appraisal well in 2003 (H-59). A development well at South Venture field (P-60) had a significant appraisal component, adding some volumes in the main reservoir interval, but a speculative upside that was ruled out. Potential deep reservoirs in the same well were of poor quality.

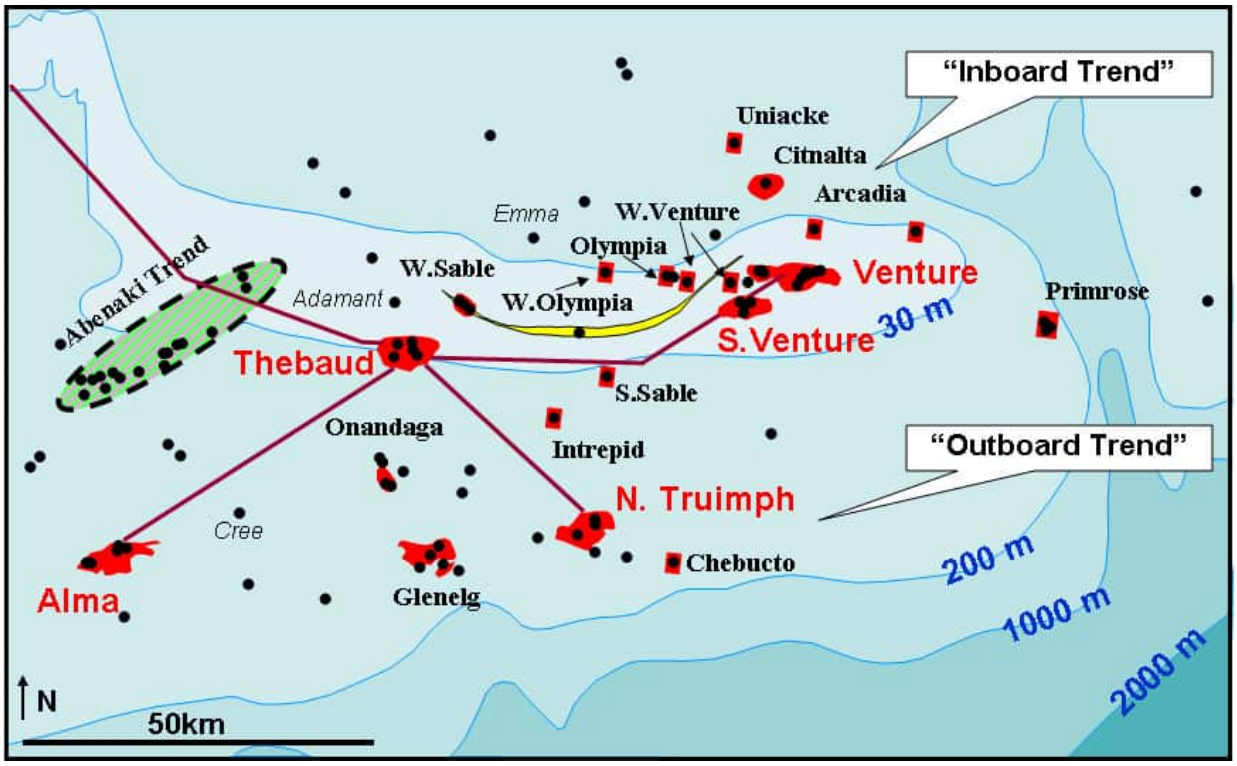


**Figure 2. Sable Producing Gas Fields and Significant Discoveries.**

The fundamental play elements of the Sable Subbasin hydrocarbon system (Fig. 3) were well understood by the early 1980s, and it was recognised that hydrocarbon accumulations are likely to be dominantly gas and generally small and widely dispersed, both vertically and laterally (Grant *et al.*,1984). The underlying cause of this wide dispersal is the high degree of reservoir connectivity resulting from the spatial arrangement of play elements. Where reservoir is abundant and high quality there is generally a lack of well-developed top seals. At depth, reservoir degradation due to diagenesis is often an issue. The few large gas accumulations occur where the balance of reservoir presence and quality, seal thickness and structural configuration are optimum. Reservoir Connectivity Analysis (RCA) has proved important in understanding the distribution of in-place hydrocarbon volumes, in risking exploration and appraisal opportunities, in evaluating resource potential, and in rationalising and predicting production performance.

## Reservoir Connectivity Analysis

Reservoir Connectivity Analysis is a systematic, rigorous process defining reservoir plumbing, which integrates and reconciles fluid types, fluid pressures, contacts, and geologic interpretations. It was developed at ExxonMobil and subsequently published (Vrolijk *et al*. 2005). RCA is based on well-known physical principles and types of seals and connections:

- buoyancy,
- reservoir geometry controlled by folding, faulting, stratigraphy and diagenesis,
- mechanical and capillary seal capacity (Sales 1997).

In the 2005 ExxonMobil publication (Vrolijk *et al.* 2005) three basic components of Reservoir Connectivity Analysis are defined.

6. **Describe reservoir compartments.**
7. **Define connections between compartments.**
8. **Build an RCA model.**

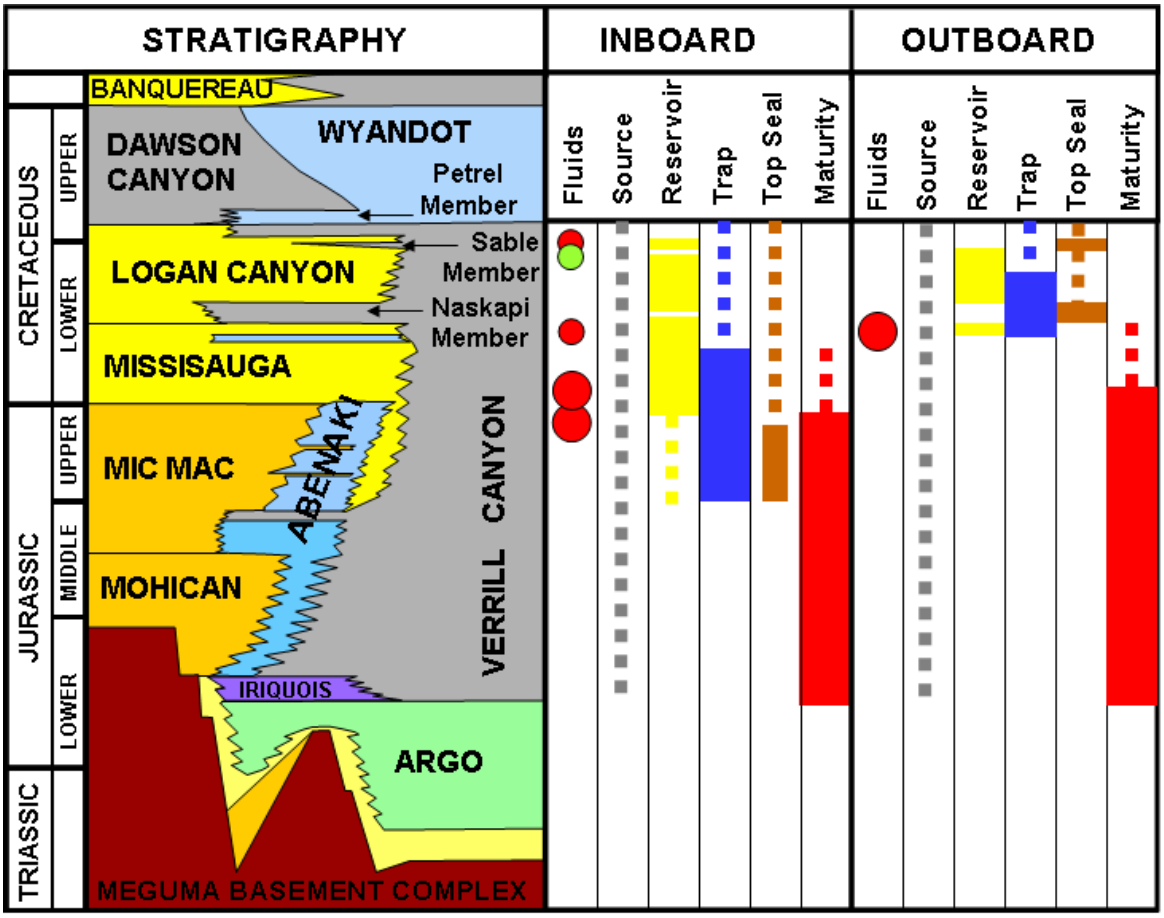


**Figure 3. Stratigraphic Chart and Play Elements.**

In practice, RCA often instigates considerable iteration of basic interpretations, often reveals unexpected insights and complexities, and often yields multiple possible scenarios, some not previously recognised. RCA models are built at various scales, various levels of detail, and are presented in different ways. During Sable development, a map-montage style was employed, comprising structure maps at all productive levels in each field, with compartments and potential connections rigorously described and defined based on structure, fluids, pressures and reservoir presence and quality. In subsequent projects at ExxonMobil, reservoir connectivity models are defined in "connectivity diagrams", essentially box diagrams, or flow-charts. In this talk, annotated perspective views from geologic models are presented, with some supporting seismic data and simplified connectivity diagrams.

The basic concepts of structural geometric connectivity are illustrated schematically in Figures 4 and 5, beginning with "spill", "break-over", "perched water" and "stair-stepping" and continuing to a range of seal/leak mechanisms that occur where there is reservoir-to-reservoir juxtaposition at faults (and an active influx of fluids and pressure to a spatially confined compartment). These ideas are then extended to a schematic illustration of an optimum trap configuration at Sable (see Fig. 8) and a key complexity is introduced - that in a number of fields reservoir pressures increase incrementally with depth from hydrostatic to almost lithostatic.

The range of trap types and trap effectiveness observed at Sable is revealed at Alma, South Venture, Thebaud, and West Sable (Figs. 6-7, 9-10). The Venture Field is illustrated in Figures 11-14, with focus on how overpressure distribution might be controlled by very limited cross-fault juxtapositions between reservoir systems. Reservoir juxtapositions at faults were identified deterministically at Sable via 3D seismic mapping and construction of fault plane profiles ("Allan diagrams"). It is outside the scope of

this presentation, but uncertainties in stratigraphy and fault offset were addressed by extensive use of a stochastic multi-fault approach to fault seal analysis (James *et al*. 2004).

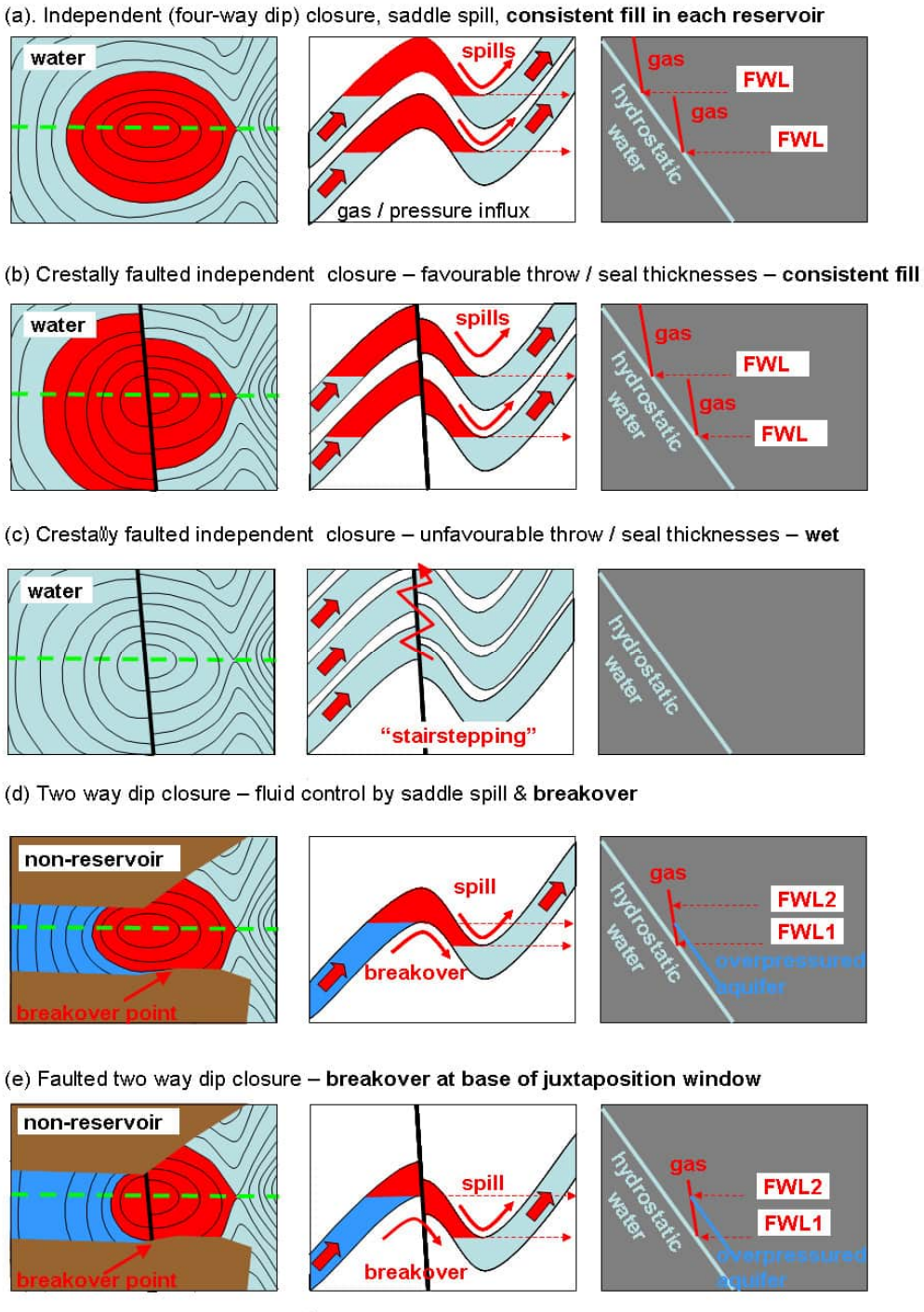


**Figure 4. Structural Geometrical Controls on Fluid Distribution & Pressures. (Map View, Schematic Cross Section, Schematic Pressure-depth)**

The connectivity concepts illustrated in Figure 4 are initially rudimentary, beginning with saddle spill from a simple anticline, with and without crestal faulting (Fig. 4a and Fig. 4b). Upward migration of hydrocarbons by repeated cross-fault leak, termed "stair-stepping", results from a sub-optimum

combination of crestal faulting and bed geometry. This is illustrated in Figure 4(c) and occurs as shown in two dimensions, but is also common in three dimensions where there is substantial change in throw along a fault (*i.e.* a "high delta throw" fault). Each of these situations is observed in fields and drilled prospects in the Sable Subbasin. The concept of an isolated structural low, containing "perched" or "ponded" water at elevated pressure, is illustrated in Figures 4(d) and 4(e). The free water level (FWL) associated with a perched water accumulation is controlled by a "break-over point", that can be viewed as the lowest point of the "dam" between the isolated and open aquifers (Vrolijk *et al*. 2005).

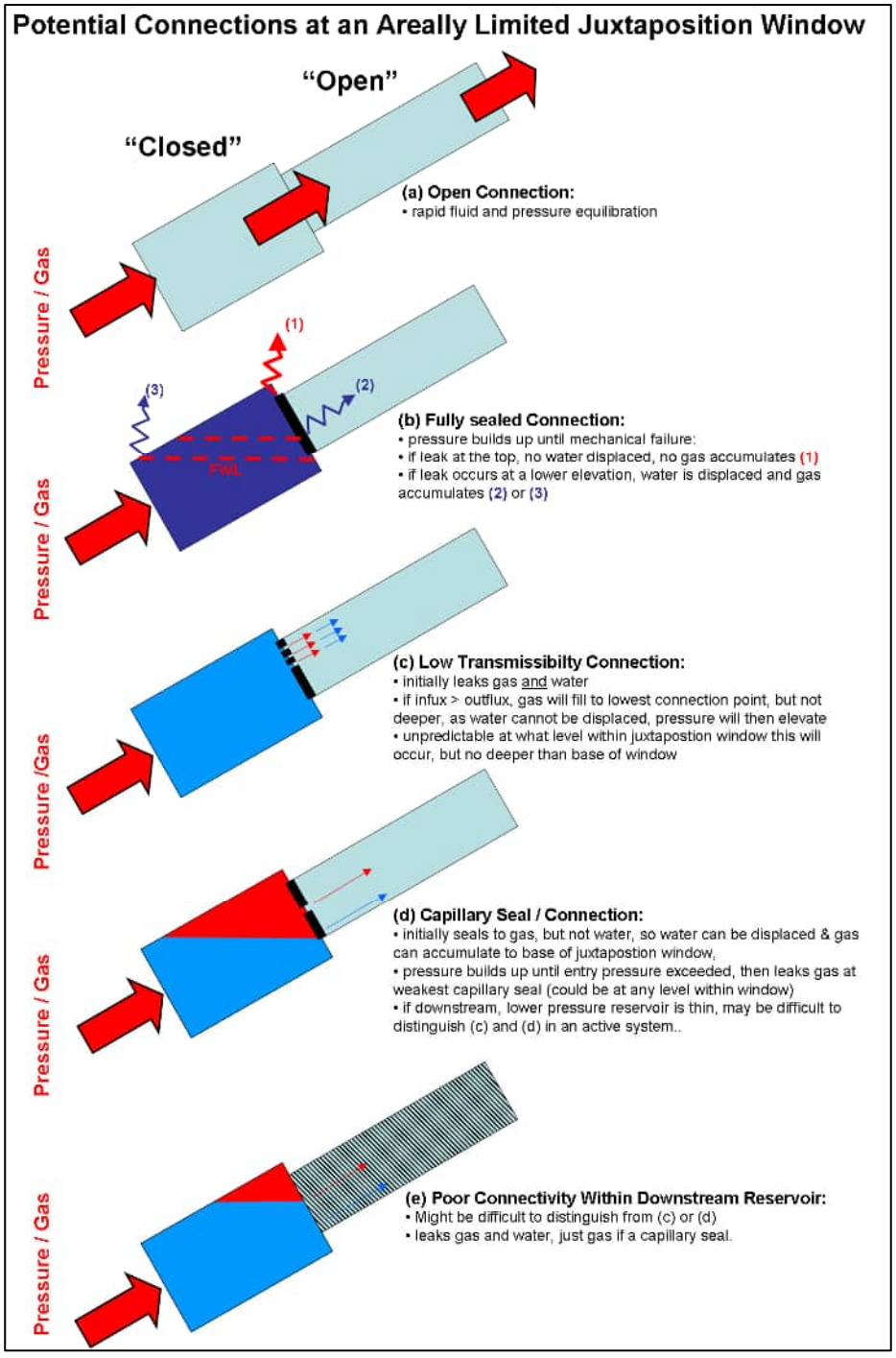


**Figure 5. Connectivity at Cross-Fault Reservoir Juxtapositions.**

Reservoir juxtapositions at faults (Fig. 5) exhibit a range of connectivity. An open connection, is illustrated in Figure 5(a). In RCA it is a key working principle that a high proportion of reservoir-to-reservoir juxtapositions at faults are open to fluid flow at geologic time scales and this is supported by observed fluid distribution in the Sable Subbasin and by recent drilling results (and predictions) including wells at South Venture and Glenelg. Conversely, reservoir to non-reservoir juxtapositions typically seal.

More complex juxtaposition controls occur when "fault rocks" are present due to shale smear, cataclasis or cementation. In principle fault rocks can inhibit fluid flow across a reservoir-to-reservoir juxtaposition window until mechanical failure pressures are attained (Fig. 5(b)), but it is more common that transmissibility is reduced (Fig. 5(c)), or that a capillary seal is formed (Fig. 5(d)). A further complication is that inhibition to fluid flow caused by these mechanisms can be difficult to discriminate from inhibition caused by stratigraphic degradation or discontinuity (Fig. 5(e)). There is wide consensus that "fault rocks" impede fluid and pressure equilibration at production time scales, and even during periods of rapid hydrocarbon charge, but there is controversy as to how prevalent or predictable seal by these mechanisms is over geologic time. In outcrop, fault rocks such as shale gouge are often discontinuous and heterogeneous, including permeable and impermeable lithologies. Identifying clear instances of seal by fault rocks is often compromised by limitations in structural and stratigraphic imaging and depth control close to faults.

Figure 5(b) illustrates a juxtaposition seal by fault rocks that ultimately fail mechanically when increased pressure from fluid influx becomes sufficient to open new or existing fractures. Hydrocarbon fill in a high-pressure compartment of this type is controlled by the point at which mechanical failure occurs. If mechanical leak occurs at the top of the compartment, pressure and hydrocarbons are released, but little or no water is displaced creating the voidage necessary to form a hydrocarbon accumulation. If mechanical leak occurs at some lower elevation, then water exits the compartment and hydrocarbons fill from the top down to the elevation at which mechanical leak occurs.

Between these end members, connectivity at fault juxtapositions is inhibited in two ways. Reduced transmissibility often results from discontinuous low permeability fault rock, but Darcy flow of hydrocarbons and water is not terminated (Fig. 5(c)). When water in fine capillaries in fault rocks prevents flow to hydrocarbons, essentially due to surface tension, capillary seals are formed, but these become ineffective when capillary entry pressure is exceeded (either due to additional pressure influx or the buoyancy associated with a hydrocarbon column). A common aspect of these mechanisms is that it is difficult to predict how much hydrocarbon column can be trapped and at what elevation a free-water level (FWL) might occur. In each case, unless there is an open connection elsewhere, the FWL cannot occur below the base of the juxtaposition window (assuming that water is incompressible).

## Play Elements: Reservoir, Seal, Source, Maturation

The Sable Project initially comprised six gas fields that may be viewed as part of two trends based on shared play elements. An "outboard trend" near the shelf edge includes Alma, Glenelg and North Triumph fields, and an "inboard trend" near Sable Island includes Thebaud, Venture and South Venture fields (Fig. 2). Stratigraphy and play elements in each trend are illustrated in Figure 3.

In the outboard trend marginal marine sandstones of the Barremian Upper Missisauga Formation are structurally trapped below a thick topseal, the Aptian age Naskapi Shale. These reservoirs are relatively shallow (2700-3800 m) and are essentially normally-pressured. All of the commercial gas at North Triumph is in a single contiguous accumulation (pool) and at Alma about 80%.

In the inboard trend, seals comprise thin intra-formational shales, limestones and tight sandstones. Gas pools are structurally trapped at multiple levels, from about 3800-6000 m, in marginal marine sandstones of the Late Jurassic MicMac Formation and the Early Cretaceous Lower Missisauga Formation. In Thebaud and Venture fields all except the shallowest gas-bearing reservoirs are confined to an expansion trend - a thick accumulation of sediment confined to a linear accommodation zone controlled by syn-depositional, down-to-basin, listric faulting. The Venture expansion trend extends west through significant discoveries at West Venture C-62 and West Venture N-91 to Olympia and West

Olympia. Diagenesis is an important control on reservoir quality in both the inboard and outboard trends, in particular where the presence of chlorite in several key intervals, has inhibited reservoir degradation due to quartz cementation.

Each of the inboard fields has gas at (or near) hydrostatic pressures in the shallowest commercial reservoirs and aquifer pressures increase relative to hydrostatic pressure with depth (increasing overpressure, or excess pressure), ultimately approaching lithostatic pressures. Similarly, the outboard fields are underlain by an overpressured section, but currently without commercial hydrocarbon reservoirs.

The relative distribution of reservoirs and seals is an important control on reservoir connectivity at Sable. At each field, below the major producing reservoirs, net-to-gross ratios are low with thick non-reservoir intervals reflecting a distal depositional setting and limited influx of coarse clastics. Net-to-gross ratios increase upwards, reflecting the change to a more proximal marginal marine setting in which non-reservoir intervals are thin (less than about 50 m). The two key exceptions are the Naskapi Shale in the outboard trend that exceeds 200m thickness, and the locally developed Lower Missisauga, Thebaud Shale (about 120m). Shales that occur at relatively shallow depths in the Upper Logan Canyon Formation, Dawson Canyon Formation and Tertiary are locally significant as top seals, where Albian / Cenomanian age Logan Canyon sandstones are draped over salt diapirs.

Gas at Sable is interpreted to be sourced from shales that are interbedded with, and are the distal equivalents of, the MicMac and Missisauga reservoir intervals - the Verrill Canyon Shale. These shales contain terrestrially sourced type III organic matter. In the Sable Island area, a variety of indicators suggest full maturity currently occurs in the Lower Missisauga Formation with the transition to over-maturity within the MicMac Formation. (Grant *et al.* 1984). Williamson and Smyth (1992) conclude from burial history, thermal and maturation models that Jurassic source rocks at Glenelg, in the outboard trend, began significant gas generation at 115 Ma, and at Venture, in the inboard trend, at 85 Ma.

## Play Elements: Structure - Reservoir Connectivity and Trap Effectiveness

The Scotian Shelf is a passive continental margin, and structures in clastic reservoirs (excluding drape over the Abenaki carbonate bank) have formed by two main mechanisms: (1) sediment loading, resulting in down-to-basin, listric faulting with and without associated fault bend folds (which may or may not be internally or crestally faulted), (2) movement of underlying Lower Jurassic, Argo salt. Structures in the Sable Subbasin can be categorised by the intensity of each of these mechanisms and the degree of interaction between them. In many cases, two or more trap styles are exhibited within the same field. The following discussion begins with fault dependent traps that have little or no independent closure, moves to low relief four way dip closures formed as fault bend folds above listric faults (with and without crestal faulting), and then to moderate-to-high relief faulted four way dip closures where structural relief has been enhanced by salt movement at intermediate depths visible seismically.

### Fault dependent traps (with no independent, four way dip, closure)

These can be very effective traps in the outboard trend where Upper Missisauga reservoirs are overlain by thick Naskapi Shale and underlain by thick Verrill Canyon Shale. At Alma field (Fig. 6) the west structural culmination contains gas trapped by juxtaposition seal to Verrill Canyon Shale to the north and juxtaposition seal to Naskapi Shale to the southwest.

In the inboard trend where there are thin intraformational seals, fault-dependent traps of this type are inconsistent, trapping gas sporadically in short columns in a small proportion of available reservoirs. Examples in the Venture complex include West Venture C-62, West Venture N-91 and Venture B-52. (Figs. 12-14).

Figure 6, at Alma, also provides an illustration of a simple connectivity diagram, with three compartments in the Missisauga A reservoir. Gas in the west and east culminations is connected as the intervening saddle occurs above the FWL inferred from pressure-depth data. Fluid exit occurs to the

northeast where the north-bounding fault bifurcates, reducing fault offset and allowing self-juxtaposition of the Missisauga A reservoir to the fault block to the north. An alternative scenario is that the east culmination spills to a small northeast culmination, which similarly leaks by self-juxtaposition to the footwall block (or possibly spills to the northeast). One of the key utilities of RCA is in systematically identifying alternate scenarios, which are risked, assessed, and aggregated to facilitate business decisions.

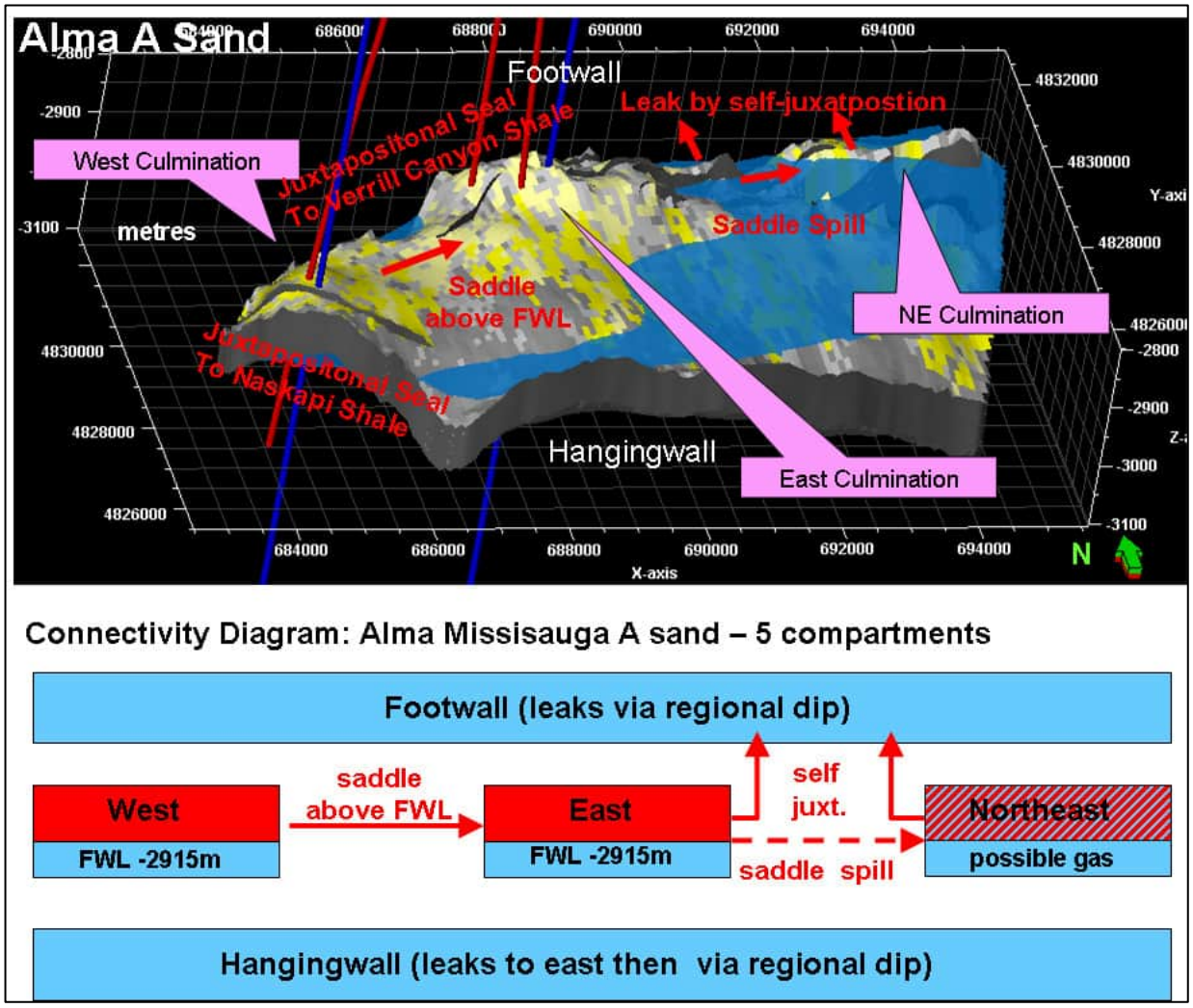


**Figure 6. Perspective View of Alma Field A Reservoir and connectivity diagram. The west culmination is sealed by juxtaposition to Verrill Canyon Shale to the north and by juxtaposition to Naskapi Shale to the southwest. Leak occurs via self -juxtaposition to reservoir in the footwall where fault throw diminishes to the northeast. No connection to the hanging wall to the south. (Vertical Exagerration 10:1).**

## Four way dip closures (no apparent crestal faulting)

This type of structure forms effective traps, typically with each reservoir level filled to a similar controlling spill or cross-fault leak point. South Venture (Fig. 7) contains multiple, normally pressured reservoirs with gas column heights between 40 and 80m dependent on juxtaposition leak at the north bounding fault. Pre-development, a low probability scenario was considered that the bounding fault might seal and the structure fill to a down-dip saddle. (The single pre-development exploration well has "gas-on-rock" in each reservoir). Consistent with RCA predictions, this scenario was not confirmed by development drilling results. Similarly the northwest fault block at Glenelg, appraised in 2003, is

interpreted to leak by cross-fault juxtaposition at its respective north bounding fault, again consistent with pre-drill RCA predictions.

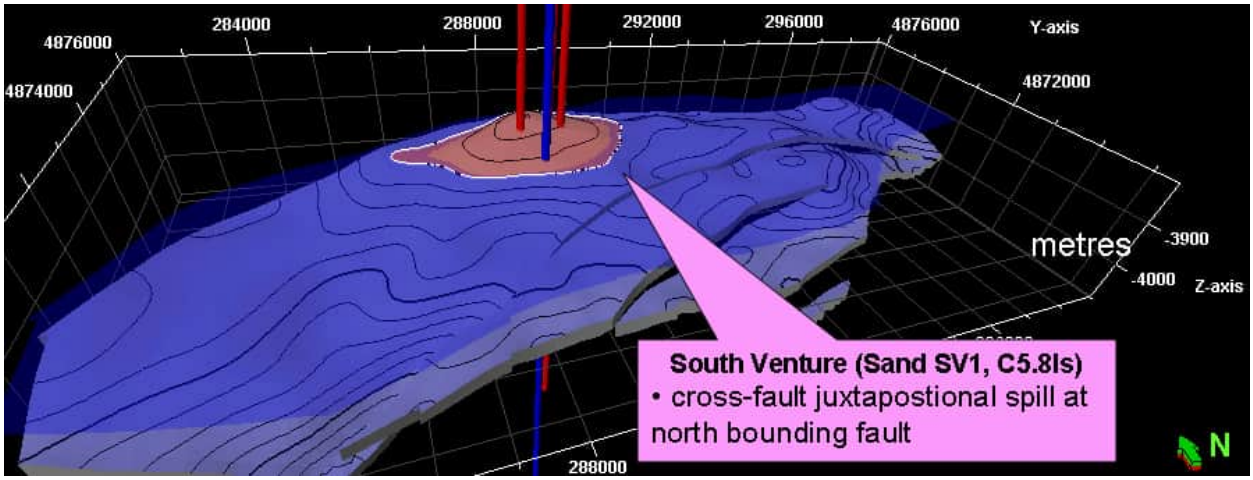


**Figure 7. Perspective View of South Venture Field SV1 reservoir. Gas fill at mutiple reservoir levels is limited by cross-fault juxtaposition to the north. (Vertical Exagerration 10:1).**

At South Venture, structural closure diminishes upward limiting trap extent vertically. Below the main reservoirs there is increased propensity for both juxtaposition seal at the north-bounding fault, and reservoir degradation. Deep, marginal quality, overpressured, gas reservoirs seen in the South Venture O-59 exploration well, were further degraded and unproducible in the subsequent development well (P-60).

Citnalta field has a similar configuration to South Venture, as does the western culmination at Venture (Figs. 12, 13 and 14). At Venture west culmination, FWLs are not controlled by cross-fault leak to the north, but by saddle spills to the east and west.

## Four way dip closures (with crestal faulting)

This configuration, shown schematically in Figure 8, forms effective traps if internal fault offsets are less than intraformational seal thicknesses. The Missisauga reservoirs in the east culmination at Alma (Fig. 6), and the Missisauga and Micmac reservoirs in the east culmination at Venture are examples (Figs. 12-14). The effectiveness of this configuration is easily compromised by small changes in the relative thickness of internal seals to internal fault throws or by stratigraphic incision and breach of thin intra-formational seals. These factors, plus reservoir quality, limited the success of the exploration wells drilled at Adamant, Emma and Cree.

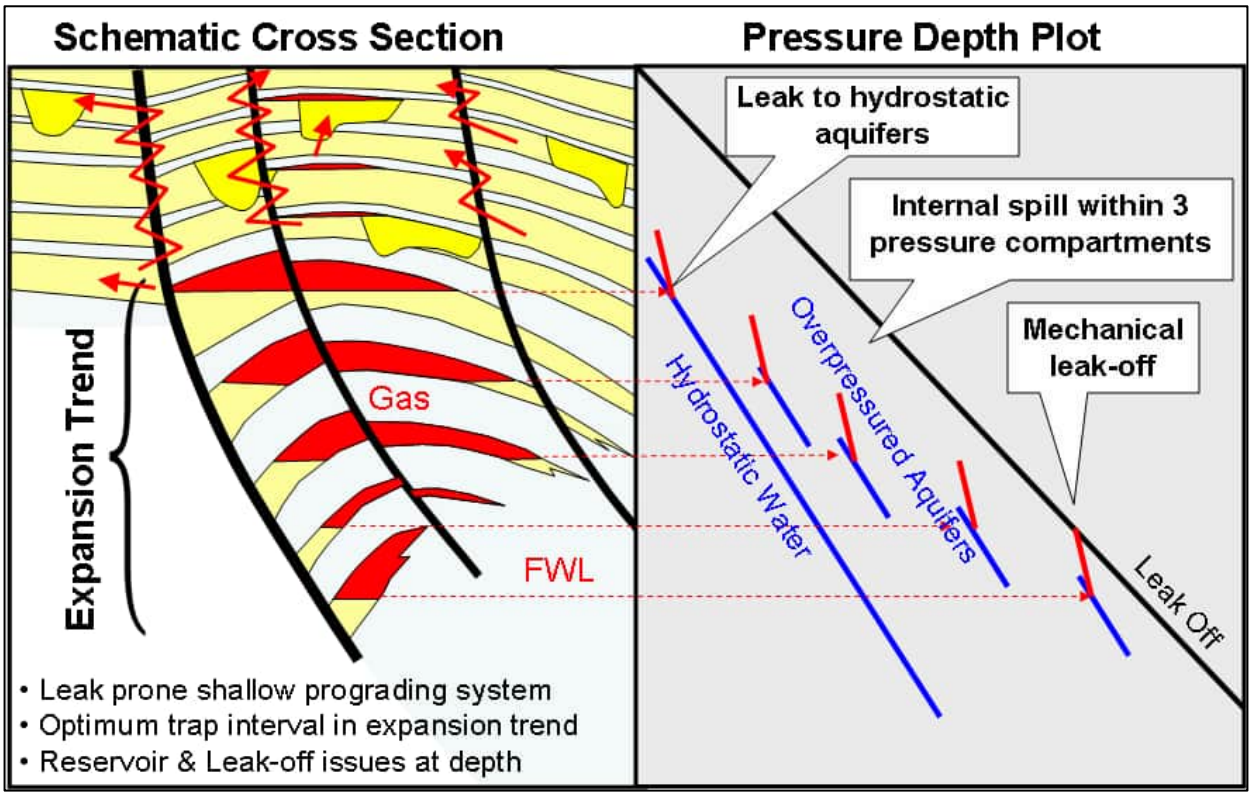


**Figure 8. Schematic Cross Section and Pressure-Depth plot illustrating optimum trap configuration in the Sable Gas Fields.**

## Four way dip closures (with crestal faulting). Relief enhanced by salt movement

These structures are essentially fault bend folds, which have enhanced relief due to salt movement up the footwall of major listric faults. They are characteristically circular in map view with radial crestal faulting. A group of these structures, including West Sable, Thebaud, Onondaga and Glenelg, forms a NNW-SSE trend, possibly related to basement structure. Trap effectiveness is controlled by the same interplay of seal thickness and fault throws as seen in crestally faulted fault bend folds. At moderate relief, with a well-developed topseal, these can be very effective traps, for example, the Missisauga A/B reservoirs below the Thebaud Shale at Thebaud field (Fig. 9). Above the Thebaud Shale at Thebaud a faulted high net to gross reservoir section predominantly leaks due to "stair-stepping", with a few small, sporadic gas accumulations formed where reservoirs juxtapose shale at faults.

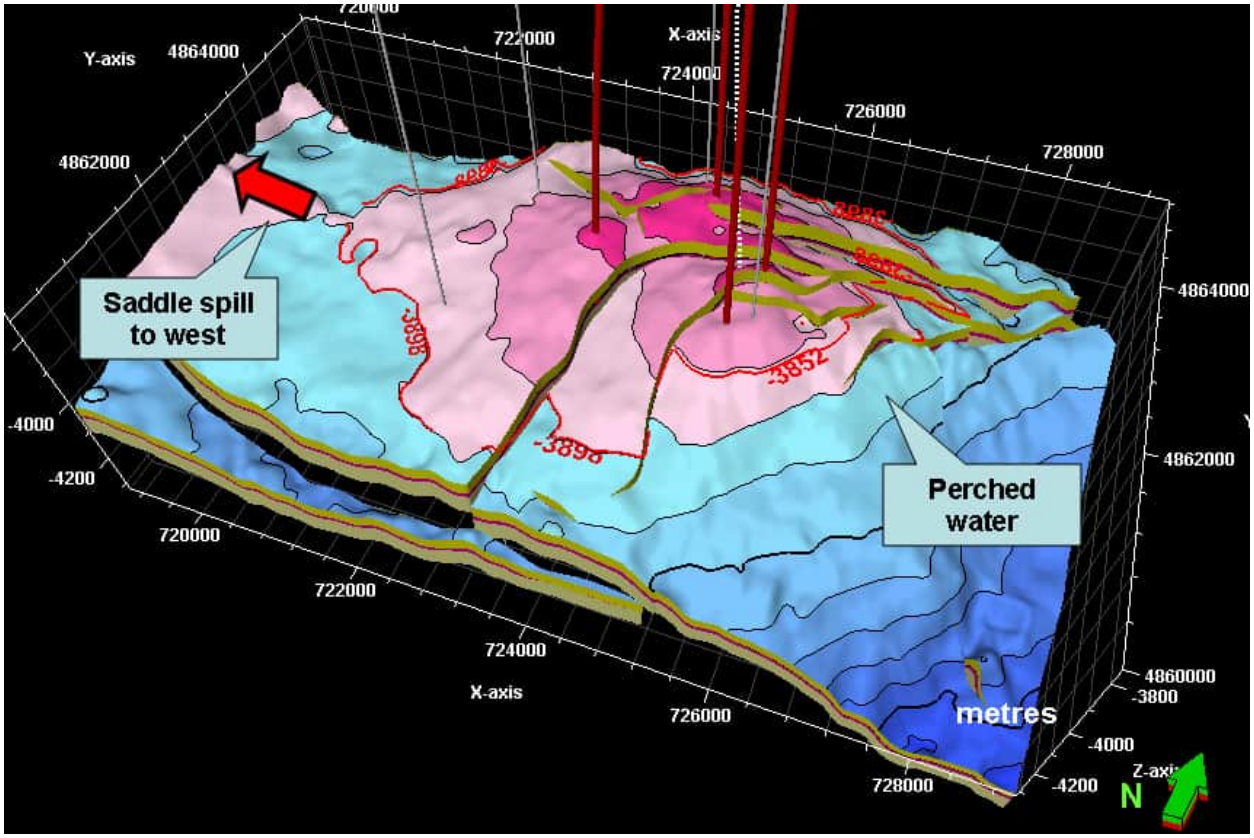


**Figure 9. Perspective View of Thebaud Field A/B reservoir. Gas spills at a saddle to the west. (Vertical Exagerration 10:1).**

Where salt movement is more pronounced than at Thebaud, for example at West Sable (Fig. 10), there is a very high propensity for upward leak of hydrocarbons by "stair-stepping" and the West Sable field has multiple small accumulations extending up to the Late Cretaceous Lower Dawson Canyon Formation. West Sable is one of a few fields in the Sable Subbasin that has significant DHI (direct hydrocarbon indicator), and this is consistent with juxtaposition leak predicted by RCA.

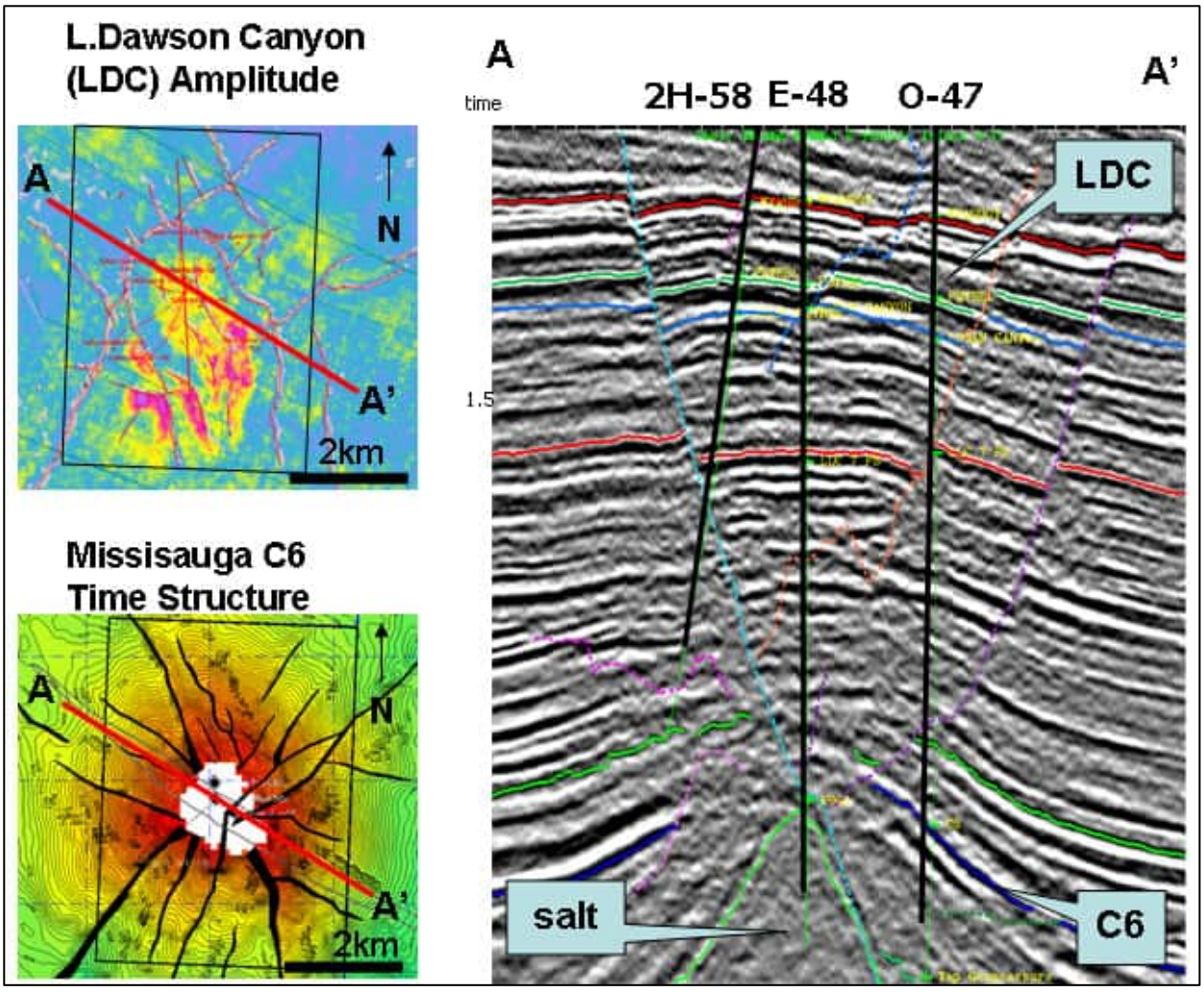


**Figure 10. West Sable Seismic Traverse, Amplitude Map on Lower Dawson Canyon hydrocarbon reservoir and structure map on Missisauga C6 resevoir. Structure results from diapiric salt.**

## Overpressures and Reservoir Connectivity

Figure 8 illustrates an optimal trap configuration at Sable, with a pressure regime typical of the inboard fields. At extreme depth, hydrocarbons and water are encountered at very high pressures resulting from a combination of stratigraphic isolation, (usually within expansion trends) and an active source of pressure - probably a combination of ongoing hydrocarbon migration from encasing over-mature shales and disequilibrium compaction due to Tertiary sediment loading. The relative importance of these mechanisms has been the subject of some discussion (Williamson and Smyth, 1992, Yassir and Bell, 1994). In deep compartments, pressure is retained and builds up until the mechanical seal capacity of encasing rocks is reached. At this point, there is sufficient pressure to open existing fractures or create new ones in either the topseal or at faults. Fluids escape until pressures decline to the point where fractures once again close. The underlying evidence to support this interpretation is that pressures in the deepest reservoirs are commonly close to leak-off pressures measured in wells, and quite close to lithostatic pressure. In these compartments, gas accumulations are limited by seal capacity, and the high level of overpressure infers that reservoir extent and pool size is limited.

After exiting the deepest reservoirs via seal failure, gas then progressively migrates upwards, filling local structural highs in each pressure compartment and displacing water, apparently via peripheral cross-fault juxtaposition connections. These cross-fault connections are excluded from Figure 8 for simplicity, but are identified and illustrated at Venture field in some detail below. Gas eventually reaches shallow, hydrostatic reservoirs that are leak-prone due to a high degree of stratigraphic and cross-fault connectivity. The mechanism by which large pressure differences are maintained across these peripheral juxtaposition windows is open to discussion. A series of possibilities is introduced and illustrated in Figure 5. The favored mechanisms are slow Darcy flow across low transmissibility connections in an actively charged or pressured system, or ongoing, or episodic, capillary leak of gas across capillary seals at juxtaposition windows. In either case, a connected system where lower pressure "downstream" reservoirs are progressively either thinner, poorer quality or more discontinuous than those upstream inhibits the release of pressure from the system.

Venture field is one of the best examples of this type of trap / overpressure situation. A pressure-depth plot (Fig. 11) shows large pressure steps between the major aquifers, from Sand 2 / hydrostatic, to Sand C, to Sand 3, to Sands 4/5 to Sands 6/7/8 to Sand 11 and Sand 13. Minimum leak-off pressures are typically 10,000 kPa to 20,000 kPa or more above maximum reservoir pressures except at Venture B-43 where a group of leak-off pressures at (or below) reservoir pressures appears anomalous. Based on juxtaposition analysis, there is mappable geometric connectivity between Sands 6/7/8 and all sands above, but no geometric connectivity between these sands and Sands 11 and deeper (which are also closer to leak-off pressures than those above). Thus, it is inferred that mechanical seal failure, or fracture closure pressure controls connectivity in the deep sands and geometric connectivity above.

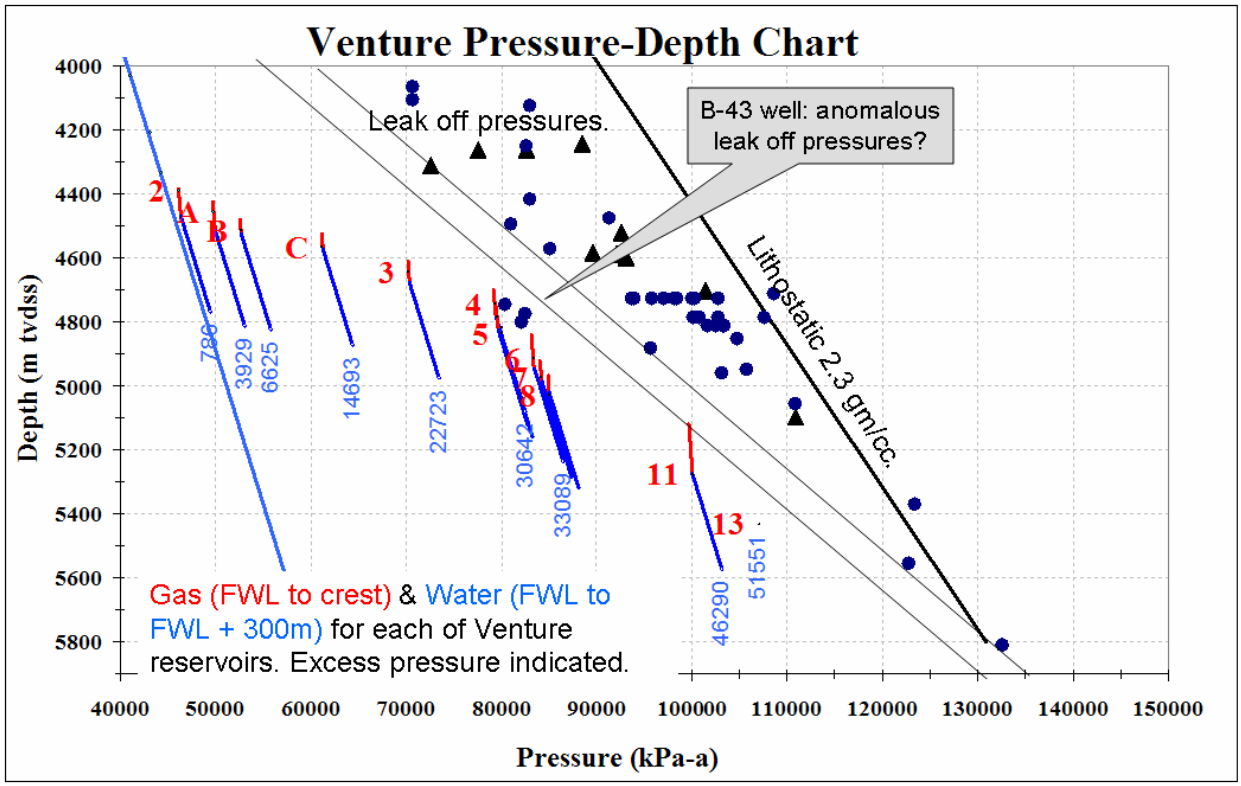


**Figure 11. Venture Field Pressure-depth Plot**

A 3D perspective view of Venture Sand 6 and a simplified connectivity diagram are provided in Figure 12. Six compartments and the connections between them are annotated. Influx of gas via mechanical leak from reservoirs below is interpreted. The WB52 and B52 compartments are interpreted

to leak to the east via cross-fault connections to Sands 4/5 at high delta throw faults. The West culmination spills to the East culmination at the intervening saddle, and the East culmination spills via a shallower cross-fault leak point to Sand 4ab in the southeast compartment across a high delta throw fault. Sand 4ab in the SE compartment then also juxtaposes thin, poor quality, Sands 4d and 5 back in the East compartment, completing the connection between the 6/7/8 aquifers and the 4ab/4c/4d/5a aquifers. At Sand 6 level the eastern high delta throw faults limits hydrocarbon fill, but in Sand 4ab, Sand 3 and Sands A, B and C it is the high delta throw fault on the east of the WB52 compartment that becomes important.

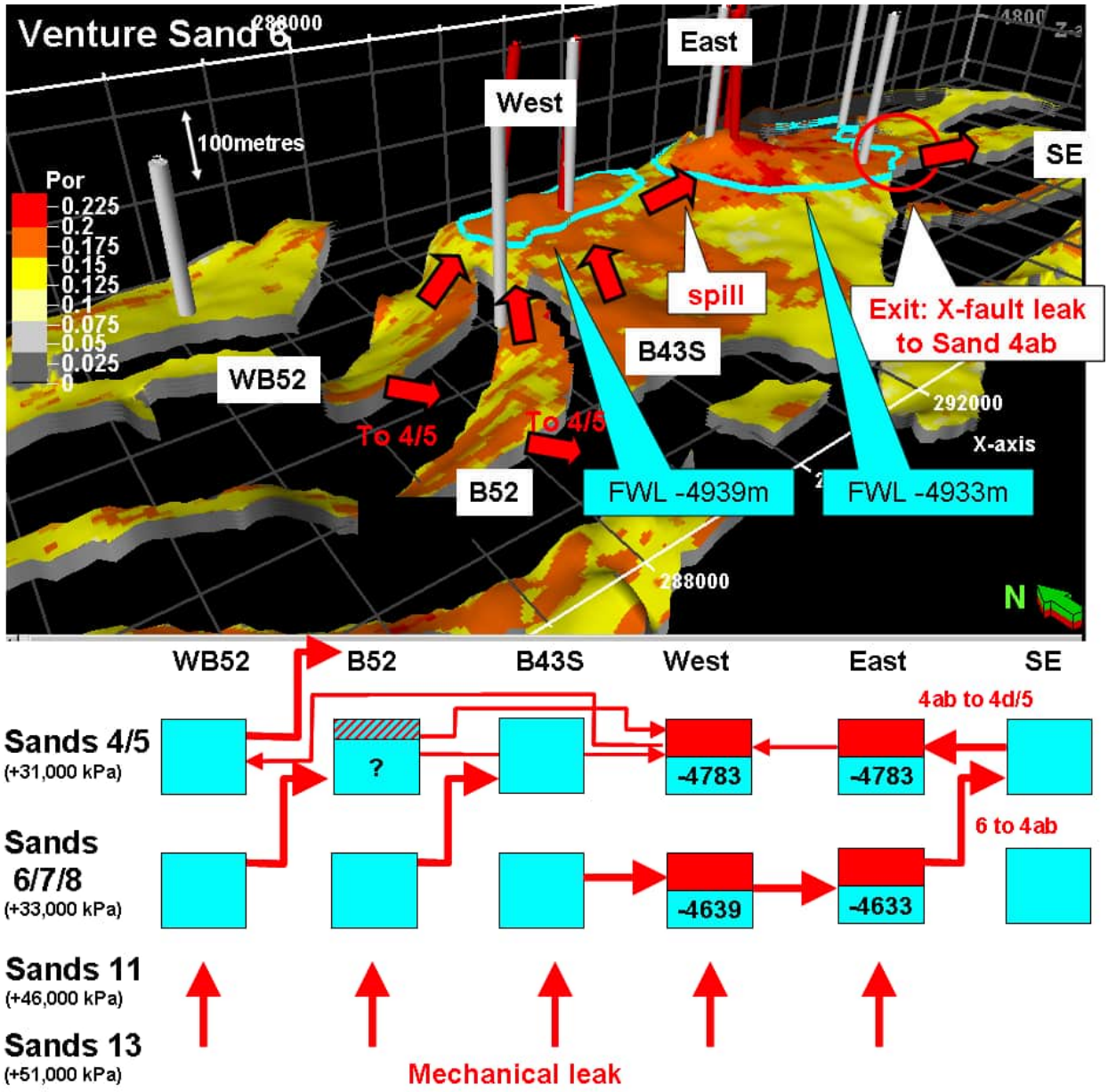


**Figure 12. (a) 3D perspective view of Venture Sand 6. (Vertical Exagerration 5:1). Average porosity is indicated, derived from seismic amplitudes calibrated at wells. (b) Simplified connectivity diagram of Venture Sand 6, and Sands 4/5 above.**

At Sand 3a level (Fig. 13), gas enters the B52 block from Sand 4ab in the WB52 block and enters the WB52 block similarly from the next block to the west - drilled by West Venture C-62. The East

culmination spills to the West culmination, which spills to the WB52 compartment. The WB52 compartment has a high delta throw fault to its east linking Sand 3 to Sand C and so any gas that spills from the West culmination to WB52 exits Sand 3. The B52 compartment has a small accumulation sealed by simple juxtaposition to non-reservoir that spills to the West culmination.

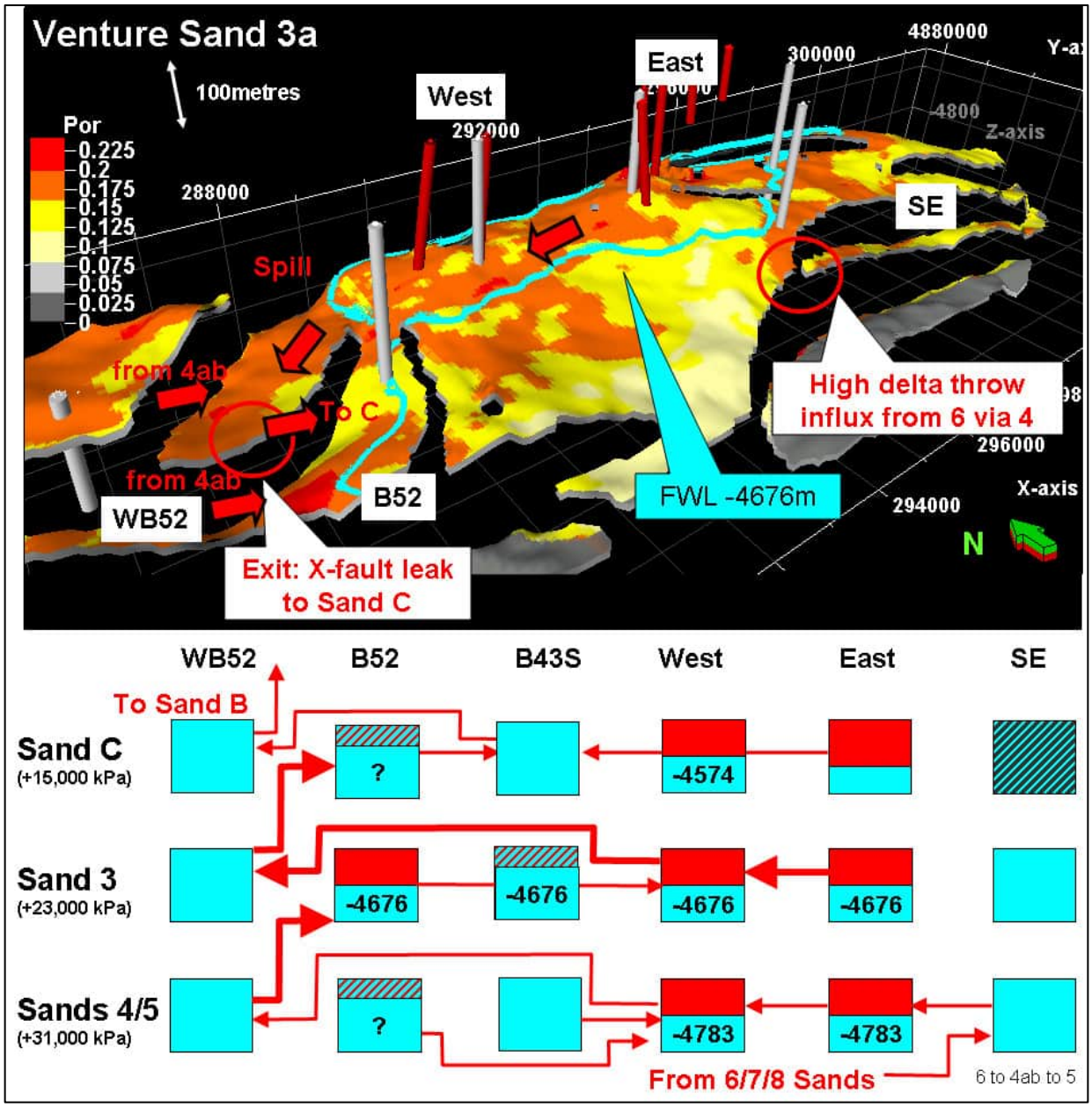


**Figure 13 (a). 3D perspective view of Venture Sand 3. (Vertical Exagerration 5:1). Average porosity is indicated, derived from seismic amplitudes calibrated at wells. (b) Simplified connectivity diagram of Venture Sand 3, Sand C above and Sands 4/5 (common aquifer, but multiple gas columns) below.**

At the high delta throw fault on the east side of WB52 this relationship is repeated a number of times between pressure compartments and gas accumulations at different levels, with an overall progressive "downstream" deterioration in the quality of reservoirs. This configuration continues from Sand C through the poor quality Sand B and Sand A and up to Sand 2, where because of a stratigraphic trap on the west side of Venture this high delta throw fault is "switched off" (Fig. 14). Sand 2 fills to a

larger column height than would otherwise occur and spills by cross-fault leak at the high delta throw fault to the east, to the SE compartment, the same fault that limits gas in Sand 6. The stratigraphic trap on the west and south sides of Venture Sand 2 results from the combination of a shale-filled slope canyon and a tight sand channel. Both are penetrated by wells and mapped seismically. Within the B43S compartment this stratigraphic and structural configuration potentially traps perched water, and early water production at one well which subsequently diminished was explained this way.

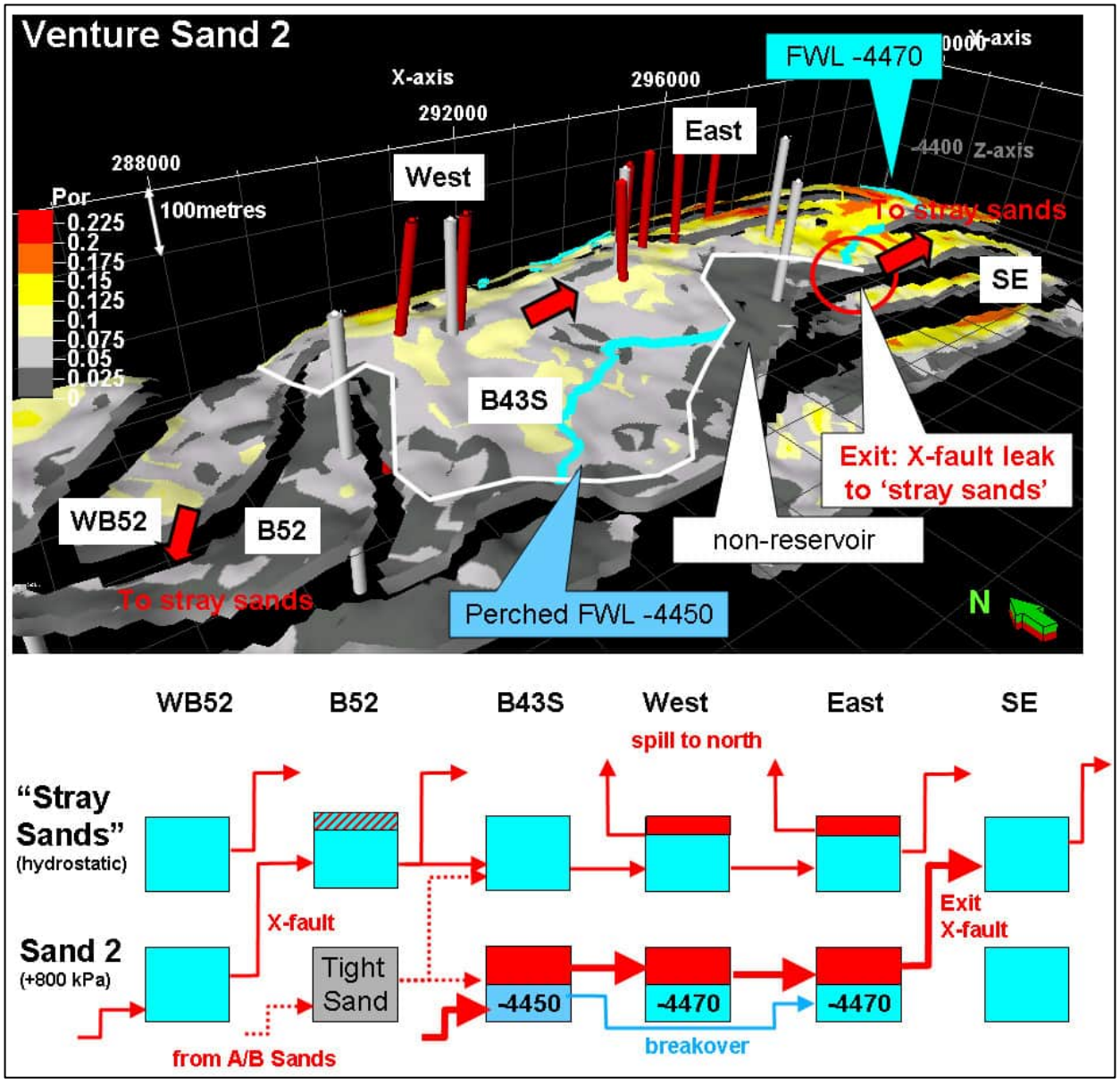


**Figure 14 (a) 3D perspective view of Venture Sand 2 (Vertical Exagerration 5:1). Average porosity is indicated, derived from seismic amplitudes calibrated at wells. (b) Simplified connectivity diagram of Venture Sand 2 and Venture "Stray Sands". Stray sands are minor reservoirs above Sand 2 with minor independent closure and thin gas legs in the west and east culminations. Sand 2 is eroded by a shale-filled slope canyon in the east (H-22 well) and is a tight sand channel fill in the west (B-52 well). Both cause dimming of seismic amplitude.**

These simplified connectivity diagrams illustrate and explain much of the geometrically connected system at Venture, certainly the major aquifer compartments. A full understanding requires all reservoir and fault block compartments to be described, and the connections between them defined.

## Impacts of Reservoir Connectivity Analysis at Sable

### Exploration: Hydrocarbon Distribution and Resource Potential

Analysing and understanding the way reservoirs are connected or "plumbed" is critical at Sable to finding, assessing, developing and producing commercial reservoirs - as in any basin. The insights gained from this sort of analysis are used to predict and assess undrilled opportunities and resource potential as a whole. RCA has been the most effective tool in predicting fluids ahead of the drill, in a basin where DHIs are few and far between.

The key observation at Sable is that there is a high degree of reservoir connectivity. At a high level, the combination of an abundant supply of coarse clastic sediments with passive, shelf-scale tectonics, results in an abundance of reservoir but a paucity of thick seals. Faulting associated with gravity-driven and salt related structures breaches most seals allowing extensive cross-fault connectivity and upward migration of hydrocarbons. This history results in a widely distributed resource trapped in numerous small accumulations and a few large fields, which themselves often comprise multiple stacked pools.

In Figure 15 hydrocarbon column heights in the major Sable reservoirs are compiled, and for comparison column heights in the largest accumulations in the Jeanne d'Arc and Beaufort-Mackenzie basins are included. These Canadian frontier basins share parallel exploration histories with the Scotian shelf and are both Atlantic margin basins - if the Beaufort-Mackenzie is regarded as the termination of the tectonic system related to opening of the Atlantic. These basins differ in two key respects from the Scotian Shelf, which results in considerably larger hydrocarbon column heights than in the Sable Subbasin. Firstly, thick seals are present in each basin, the Fortune Bay, Whiterose and Nautilus Shales in the Jeanne d'Arc and the Richards, Bituminous Zone and Mackenzie Bay in the Beaufort-Mackenzie Basins. Each acts as an effective topseal trapping major fields. Secondly, these basins were exposed to multiple episodes of major tectonic deformation, which have resulted in large structural closures. In the Beaufort-Mackenzie Basin late rotation of Alaska has generated major south-north anticlines and in the Jeanne d'Arc Basin interplay between late Triassic, late Jurassic and Aptian-Albian phases of extension, as well as some salt movement, has generated large south-north anticlinal structures.

(Continued on next page.)

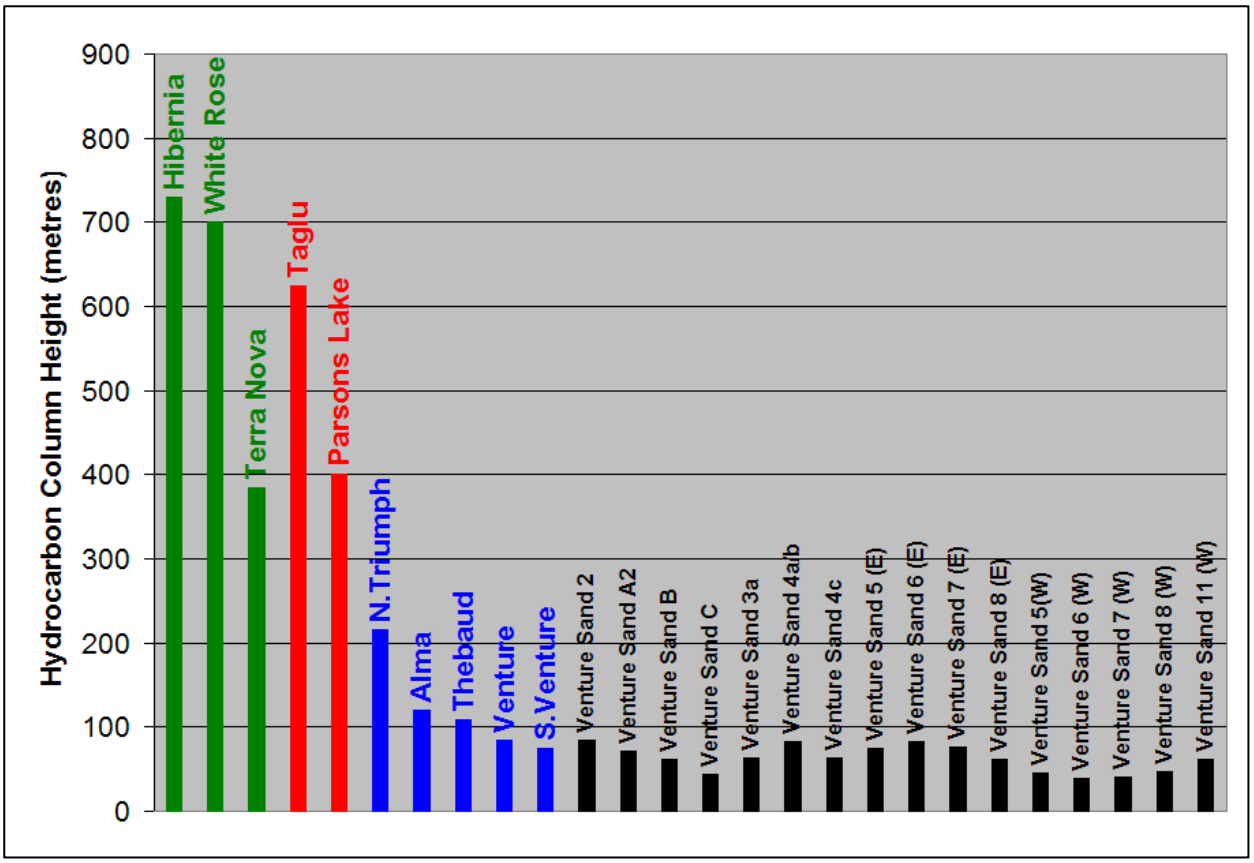


**Figure 15. Maximum hydrocarbon column heights in individual pools in: the producing Sable gas fields (blue), the three largest fields in the Jeanne d'Arc Basin, offshore Newfoundland (green), and the two largest onshore fields in the Beaufort-Mackenzie Basin, northwestern Canada (red). Column heights for individual producing reservoirs are shown for Venture field (black) and are designated where different between the west and east structural culminations.**

## Development and Production

Hydrocarbon column height is a useful comparative measure, particularly in connectivity analysis, but fails as a proxy for gas-in-place. Even if there is the same pore volume in two traps, the one with the larger column height (assuming this means it has greater overall relief) will have greater gas in place - because it will contain a larger proportion of fully saturated reservoir above the transition zone (which results from water retained by capillary forces above the FWL). In addition, the lower relief structure will have a greater propensity for early water breakthrough, particularly where high permeability intervals, sometimes laterally confined, link perforations to a nearby aquifer, and this can have ramifications for sand control in well bores. These types of considerations, related to and understood by connectivity analysis, have been important in managing and understanding the Sable reservoirs. The multiple hydrocarbon columns at Venture field are also illustrated in Figure 15, all less than 100 m and some as low as 40 m between crest and FWL (and perforation to FWL height may be less, depending on porosity or permeability distribution). From a development and production perspective, this situation is very different from a field like North Triumph where all the gas occurs in a single normally pressured reservoir. The complexity of developing multiple accumulations at Venture is compounded by the differences in pressures between reservoirs. A strategy of "bottom up", progressive pressure depletion and commingling has been effective but well recompletions and interventions are costly.

A further consideration is the presence of perched waters. These have been encountered in the Thebaud A/B sandstones and in one well in Sand 2 at Venture, as described. They were not predicted

ahead of the drill, but once encountered RCA enables the mechanism and areal limits of these aquifers to be understood.

In several reservoirs, notably at Alma and Citnalta, it is observed that when transition zone saturation profiles derived from resistivity logs are extrapolated downwards below "low known gas" the implied FWL is significantly deeper (15-25m) than the FWL interpreted from pressure-depth plots. An explanation for this phenomenon, which at Alma has been invoked to history match production performance, is that paleo-FWLs are present in some reservoirs. In essence, gas once filled down to a deeper FWL than at present. Possible mechanisms include structural readjustment of controlling saddle points or fault movement, or "pressuring up" of compartments thereby reducing gas volume. In the interval between the paleo and current FWLs, low saturation gas, sometimes called "trapped gas" is retained, typically at about 25% gas saturation. Recognising paleo-FWLs is important in volumetric assessments as imbibition instead of drainage saturation height functions should be used and trapped gas inhibits aquifer influx as well as contributing some small volumes to production.

## Conclusions

Reservoir Connectivity Analysis is an effective procedure for understanding and predicting the detailed distribution of hydrocarbons within fields, groups of fields, or more extensively, within a hydrocarbon system. RCA provides detailed insights, well over and above those achieved by simply identifying and describing play elements, and it is a very important consideration in evaluating resource potential.

The recognition of an unusual degree of reservoir connectivity at Sable, and how that affects hydrocarbon distribution, has had important ramifications for development and production, particularly the effects of relatively short hydrocarbon columns on transition zones, water breakthrough and recoverable volumes. This recognition has also been important for exploration and resource assessment, especially in conjunction with an understanding of the optimum circumstances in which the larger fields are formed.

In the recent decade of activity, deterministic RCA, and the associated stochastic multi-fault analysis, have been the most effective tools for predicting fluids ahead of the drill in the Sable Subbasin. DHIs are infrequently observed in the Sable Subbasin.

Drilling results and tightly constrained fluid mapping support the notion that fluid communication across-fault juxtaposition windows is a dominant control on fluid distribution - even where large pressure differentials exist between pressure compartments. Speculation that large pressure differences between compartments infer volumetrically extended trap capability (and larger gas accumulations) is unsupported by drilling results.

The last decade of activity in the Sable Subbasin has shown that Reservoir Connectivity Analysis is a key technology at all business stages and the knowledge gained from this project could have significant impact in future exploration and development projects.

## Acknowledgements

The authors wish to acknowledge: the Sable Project Owner Companies for permission to publish (ExxonMobil, Shell, Imperial Oil, Pengrowth and Mosbacher), and the Geological Survey of Canada and the Canada Nova Scotia Offshore Petroleum Board for access to data bases and literature. Many Geoscience and Reservoir Engineering colleagues from each of the owner companies contributed to multiple teams in Halifax, Calgary and Houston. In particular, we should acknowledge Bill James, formerly of ExxonMobil Upstream Research, prime-mover of RCA, Ron Hamm and Andrei Moore of Shell, and Fred Haynes of ExxonMobil who developed ideas around paleo-FWLs at Sable. Doug Thompson of Imperial Oil and Steve Matthews of ExxonMobil reviewed this manuscript and provided helpful guidance.

## References


Grant, A.C. *et al.,* 1984, The Geological Margin of Eastern Canada: Geological Framework and Petroleum Potential, *in* Halbouty, M.T. (ed.), Future Petroleum Provinces of the World: A.A.P.G, Tulsa, Oklahoma, p.177-205.

James, *et al.,* 2004, Fault-seal analysis using a stochastic multifault approach: AAPG Bulletin, v.88, no.7, p.885-904.

Sales, J.K., 1997, Seal strength vs trap closure - a fundamental control on the distribution of oil and gas, *in* Surdam, R.C. (ed.), Seals, traps and the petroleum system: AAPG Memoir 67, p.57-83.

Vrolijk, *et al.,* 2005, Reservoir Connectivity Analysis - Defining Reservoir Connections and Plumbing: Society of Petroleum Engineers Middle East Oil Show and Conference, SPE Paper 93577.

Williamson, M.A., and C. Smyth, 1992, Timing of gas and overpressure generation in the Sable Basin offshore Nova Scotia: implications for gas migration dynamics: Bulletin of Canadian Petroleum Geology, v.40, no.2, p.151–169.

Yassir, N.A. and Bell, J.S, 1994, Relationships Between Pore Pressure, Stresses, and Present-Day Geodynamics in the Scotian Shelf, Offshore Eastern Canada: AAPG Bulletin, v.78, no.12, p.1863-1880.


**BACK**

# Regional Setting of the Late Jurassic Deep Panuke Field, Offshore Nova Scotia, Canada – Cuttings-based Sequence Stratigraphy and Depositional Facies Associations Abenaki Formation Carbonate Margin

**Leslie Eliuk**
Dalhousie University
Department of Earth Sciences
Halifax, Nova Scotia B3H 4J1
Canada
e-mail: geotours@eastlink.ca

## ABSTRACT

Deep Panuke, discovered in 1998, is the only carbonate gas field in the eastern North America continental shelf. Several recently published studies (Weissenberger *et al.*, 2006; Wierzbicki *et al.,* 2005, 2006; EnCana 2006) give details on the hydrothermally-dolomitized reef margin gas field itself. Expanding on those studies using mainly cuttings and core data, Panuke is placed in a larger context between the northeast contemporaneous major Sable Island paleodelta prograding ramp shelf and the southwest thicker cleaner carbonate platform. Wells can be grouped based on geometry and position relative to the shelf margin as follows: prograding ramp margin (only a few of the numerous wells in the Sable Island paleodelta are included), margin slope, margin with full shoaling sequence, margin with paleohighs and encased pinnacles (typical of Deep Panuke area), margin inboard flexure with shoals, interior platform oolitic shoals, interior platform shaly lagoon and 'moat' and near-shore ridge/siliciclastic-rich. The large-scale (second order?) vertical full-shoaling stratigraphic sequence is seen in nearly all margin wells. It comprises a basal transgressive oolite usually, then forereef with microbial mud mounds, then shallow coral-coralline sponge reefs, then oolites and two types of capping beds – either oolites (with or without sandstone interbeds) or lithistid sponge-rich beds. Only Deep Panuke does not show this pattern. Laterally there is a curious pattern to the argillaceous sponge-rich cap beds in being flanked by wells with oolite caps both nearer the delta and south-westward of the Panuke area wells. There is also a regional trend in the color from darker to lighter (and finally even red in the slope beds) away from the Sable Island paleodelta. These facies trends relative to the Sable Island delta and the associated early, deep prodeltaic burial are key factors that contributed to Deep Panuke's reservoir, trap, seal and charge properties.

## Introduction and Exploration Background

Deep Panuke is so far unique in the North American Atlantic offshore for being the only hydrocarbon field in carbonates. Located near Sable Island offshore Nova Scotia, it is near the northeast end of a Late Jurassic gigaplatform that formed the continental shelf edge from the Grand Banks to Florida with a few intervening siliciclastic depocentres (Poag 1991). In 1998-1999 EnCana (Pan-Canadian) discovered gas between the two oldest wells on the Late Jurassic-earliest Cretaceous carbonate margin in commercial quantities at Deep Panuke (EnCana 2006 - probabilistic mean recoverable $17.8X10^9$ m3 or 632 BCF, perhaps 1TCF in place). The Abenaki Formation carbonates were first drilled in 1970 in the type well Shell Oneida O-25 (McIver 1972, Given 1977). The margin was drilled in 1973 at Mobil-TETCO Cohasset D-42 and in 1974 at Shell Demascota G-32 which found and cored all three Jurassic reef types – coral reef, sponge reef mound and microbial mud mound (Dromart *et al.* 1994, Eliuk 1978, 1981, 1985, 1998; Eliuk and Levesque 1989; Ellis 1984, Ellis *et al*. 1985, 1990; Jansa 1981, 1993;

Jansa et al. 1982, 1989; Kidston *et al*. 2005; Pratt 1982, 1995; Pratt and Jansa 1989). The discovery well, Panuke PP-3C (J-99), was deepened from a production platform slated for abandonment of a depleted oil field in Lower Cretaceous sandstones draped over the carbonate shelf edge.

The Deep Panuke carbonate reservoir burial diagenesis (Wierzbicki *et al.* 2006) and its lithofacies-sequence stratigraphy (Weissenberger *et al.* 2006) have recently been published. Their depositional facies subdivision (given in more detail in Wierzbicki *et al.* 2002) is followed here since it is based in part on earlier published work (Eliuk 1978, Eliuk and Levesque 1988). Because cuttings and core work was done for EnCana's new wells, their sequence stratigraphy is followed with a listing of the criteria used and an emphasis on interpretation of the cuttings lithologies that had been integrated into their larger data set by the EnCana workers. That data set includes their 3D seismic from which 2D lines illustrate seismic stratigraphic support for some of their sequences (Weissenberger *et al.* 2006, their Fig. 13). Rather than repeat their third order field sequence stratigraphy some of the larger scale (second order) and more regional relationships will be reviewed here. And illustration of sequence use in some example well summary reports will be given in the final sections on the Abenaki carbonate margin facies associations. A regional Abenaki study (Kidston *et al.* 2005 on CD by Canada-Nova Scotia Offshore Petroleum Board = CNSOPB) gives brief well reviews that are illustrated by recent seismic through the wells. That is the source of much of the seismic data used by me (see Table 1). Little diagenesis is discussed here but late burial diagenesis is critical for dolomitzation and reservoir development in contrast to Eliuk's (1978) mixing zone hypothesis. In Eliuk (2004) the failed early-dolomitization mixing model was reviewed and compared with the better interpretation by the EnCana workers (Wierzbicki *et al.* 2006 detailed publication on diagenesis).

This extended abstract summarizes work in progress relevant to the setting of Deep Panuke in a PhD study at Dalhousie University with the goal of understanding the regional effects of a Late Jurassic-Early Cretaceous large delta on a contemporaneous thick extensive carbonate platform adjacent to the southwest. Note that where appropriate figure captions are enlarged rather than using only text body comments and discussion. The paleogeography of the contemporaneous Sable delta and adjacent Abenaki carbonate bank is shown in Figure 1 (see Table 1 to further identify wells). The hypothesis of a point-source clastic influx affecting the carbonate margin at progressive distances is shown by a depositional block diagram (Fig. 2). Figure 2 also shows schematically the prograding carbonate ramp style near the Sable Delta that is made possible by the basin-filling siliciclastics. This contrasts with the much thicker carbonates and relatively stationary aggrading margin typical of the Abenaki carbonate platform to the southwest. See Eliuk and Wach (2008, this conference CD) for more details on mixed carbonates-siliciclastics and the prograding ramps.

Deep Panuke gas accumulation is located in the carbonate platform margin within perhaps 50 km or less of the contemporaneous Late Jurassic Sable Island delta and prodeltaic shales onlapping the toe of the carbonate slope. The Marquis L-35 and whipped L-35A well are even closer within the transition from platform to ramp. All these new Abenaki wells (17 of 32 are post-1997 with a decadal gap so also post-1987) nearly double the control in this area of asymmetrically varying siliciclastic and likely nutrient influx amounts along the margin. Thus the wells may show an asymmetric spectrum of depositional and early diagenetic changes in the margin carbonates particularly when compared to the much more distant wells to the far southwest. These unusual features are not a coincidence but result from a "natural experiment" cataloguing the influence (increased nutrients and turbidity; reduced salinity, oxygen and illumination; potential fouling, hard substrate loss and burial – list modified from Leinfelder 1997 and Mount 1984) of the Sable Island siliciclastic depo-centre in modifying other paleo-oceanographic controls on the Abenaki carbonate platform and its reef margin to the southwest. This is the focus of the PhD research.

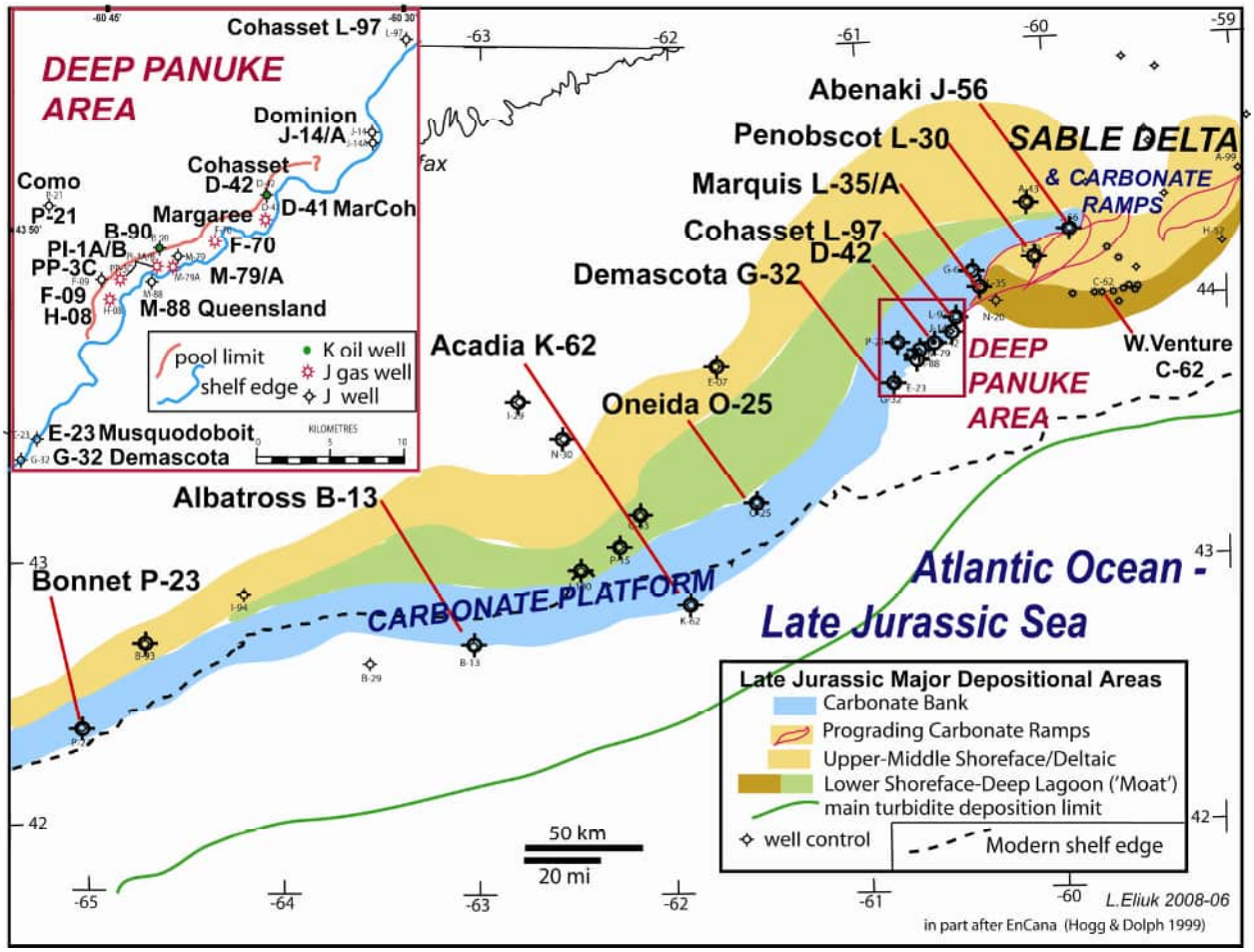


**Figure 1. Paleogeographic map for southwest Nova Scotia offshore Late Jurassic showing well control with inset of wells in Deep Panuke area (based in part after Wierzbicki *et al.* 2006, Wade and MacLean 1990 and Eliuk 1978 with wells labeled by Unique Well Identifier letter-number). Note the two main areas of Sable Island delta and associated carbonate ramps and of Abenaki Formation carbonate platform with nearly-stationary aggrading margin and increasingly siliciclastic-rich shelf interior and near-shore zones of MicMac-Mohawk formations.**

But perhaps of more immediate economic significance, this transitional paleogeographic setting and likely associated early burial by the younger continued deposition of the Sable Island deltaic siliciclastics may be the key ingredients to the Deep Panuke gas accumulation and Abenaki reef hydrocarbon system. Margaree F-70 seismic and well schematic (Fig. 3 modified from EnCana 2006) shows the seismically mapped dolomitic porosity (HPRF = High Permeability Reef Front) and the loss of porosity vertically and laterally even within carbonates. But a closer look at the carbonates shows not only gross dolomite to limestone lithologic changes but also changes within the limestone facies that likely focused the later diagenesis as there was progressive stratigraphically-upward changes into deeper and/or more argillaceous facies. Laterally a stratigraphic trap updip of porous reef margin limestones and dolomites is formed from tight limestones that were depositionally-shallower oolite. These relationships will be examined more closely later.

| Year | Operator | Name | ID | FTD (m) | Status (m of gas) | Comments (of Kidston et al 2005) | Litholog (of Eliuk) | S=Schematic log X=Seismic | I=Sequence ID P=%s W=words | Core #'s |
|---|---|---|---|---|---|---|---|---|---|---|
| 1970 | Shell | Oneida | O-25 | 4110 | D&A | Platform-basement structure | 1978, d | X | | |
| 1971 | Shell | Abenaki | J-56 | 4569 | D&A | Platform-salt diaper flank | 1978, d | X | | |
| 1972 | Shell | Mohican | I-100 | 4393 | D&A | Platform-over salt swell | 1978, d | X | | 5 |
| 1973 | Mobil | Cohasset | **D-42** | 4427 | D&A | Bank edge/back reef-some ϕ, K, oil disc | 1978, d, s | S···X | I(E)·····P W | |
| 1974 | Shell | Demascota | **G-32** | 4672 | D&A | Bank edge--186m, ϕ, test W | 1978, d, s W | S···X | ·····P | 5 |
| 1976 | PetroCanada | Penobscot | **L-30** | 4267 | D&A | (*)Bank edge/back reef- no ϕ | 1981/85, s W | S?···X | | |
| 1977 | PetroCanada | Moheida | P-15 | 4298 | D&A | Platform-basement structure | 1978, p | X | | 2 |
| 1978 | Chevron | Acadia | **K-62** | 5283 | D&A | Bank edge-good ϕ | 1981, s, p W | S?···X | | 5 |
| 1978 | Mobil | Cohasset | **L-97** | 4872 | D&A | (*)Bank edge-minor ϕ | d, s, | S···X | I·····PW | 1 |
| 1984 | Husky | Glooscap | C-63 | 4542 | D&A | Platform,-salt swell | | X | | |
| 1984 | PetroCanada | Bonnet | **P-23** | 4336 | D&A | Back reef- major lost circ' | (to log)···· W | X | | |
| 1984 | PetroCanada | Dover | A-43 | 4525 | D&A | Platform-fault block | d,·····W | X | | |
| 1985 | Mobil | West Venture | **C-62** | 5522 | Gas | Shelf lime beds under delta | Core only | x | See Cummings 2004 | 2+ |
| 1985 | PetroCanada | Albatross | **B-13** | 4046 | D&A | (*)Bank edge-some ϕ | d, s | S···X | | 1 |
| 1985 | Shell | Kegeshook | **G-67** | 3540 | D&A | Platform-basement structure | (to log)···· W | S···X | | |
| 1986 | Shell | Panuke | **B-90** | 3445 | D&A-oil | (*)Bank edge- no ϕ, K oil disc | d,·····W | X | I·(E)·····PW | |
| 1987 | PetroCanada | Como | **P-21** | 3540 | D&A | Platform-basement structure | d,·····W | S···X | I?·····PW | 1 |
| 1998 | PanCanadian | Panuke PP-3C | **J-99** | 4163 | Gas -97 | Bank edge- Ab5 gas disc' | d, s | x | I(E)·····P | |
| 1999 | PanCanadian | Panuke PI-1A | **J-99** | 4030 | Gas -6.9 | Bank edge-thin gas · .·. whip | d, s | S?···X | I(E)·····P | 1 |
| 1999 | PanCanadian | Panuke PI-1B | **J-99** | 4046 | Gas -49 | Bank edge-24.2m pay | d, s | ^X | I(E)·····P | |
| 2000 | PanCanadian | Panuke | **H-08** | 3682 | Gas -112 | Bank edge-108m pay | d, s | X | I(E)·····P | 1 |
| 2000 | PanCanadian | Panuke | **M-79** | 4598 | D&A-14 | Bank edge-no gas · .·. whip | d, s·····W | S···? | I(E)·····P | 1 |
| 2000 | PanCanadian | Panuke | **M-79A** | 3935 | Gas -21 | Bank edge-11.4m pay | d, s | ^X | I(E)·····P | |
| 2000 | PanCanadian | Panuke | **F-09** | 3815 | D&A-27 | (*)Back reef- low ϕ, oolite | d, s | S···X | I(E)·····PW | |
| 2001 | PanCanadian | Musquodoboit | **E-23** | 3818 | D&A | Bank edge- no ϕ | d, s | S···X | | |
| 2002 | PanCanadian | Queensland | **M-88** | 4401 | D&A | Fore reef- no ϕ, by-pass sst | d, s | S···X | ·I?·····PW | |
| 2002 | ElPaso (CdnSup) | Marquis | **L-35/A** | 4501 | D&A | Bank edge - no ϕ, whipped | d, s | S···X | I?·····PW | |
| 2003 | EnCana | Margaree | **F-70** | 3677 | Gas-76 | Bank edge —70m pay | d, s | S···X | I(E)·····PW | 1 |
| 2003 | EnCana | MarCoh | **D-41** | 3625 | Gas-122 | Bank edge —100m pay | d, s | S···X | I(E)·····PW | |
| 2006 | EnCana | Dominion | **J-14/A** | 3700 | D&A | Bank edge — no ϕ, whipped | d, s | S | I·····PW | |

**Deep Panuke Gas Field** = all gas wells plus M-79, F-09. **NOTE**: Dauntless D-35, Sauk A-57, Mohawk B-93 logs in Eliuk 1978; * = lithofacies not in agreement with geometry-based interpretation of Kidston et al. 2005; ϕ = porosity; Litholog: 'year' = published year; d = detailed log; s = schematic log; p = preliminary/partial/text; W = needs more work.

Seismic: Kidston et al. & EnCana 2006

(E)=EnCana info

**Table 1. Abenaki margin wells – litho/depofacies analyses Versus CNSOPB CD (Kidston *et al.* 2005)**

| | |
|---|---|
| PROGRADING RAMP MARGIN | NORTHEAST ..... SOUTHWEST<br>Penobscot L-30 (to NE numerous wells with 'younger' limestone beds -- cf. Wade and McLean 1990)<br>.....(West Venture C-62 #9 Limestone under shelf margin deltas but has core with shale contact)<br>Dauntless D-35 and Sauk A-57 near NE margin yet older limestone suggest different setting or older NE delta |
| MARGIN SLOPE | Queensland M-88 (still has basal oolite even if mostly slope carbonate sediment then shales above) |
| MARGIN — **full shoaling sequences with basal oolite** | (**capping beds sponge rich**, then oolite, shallow reef, forereef & mud mounds)<br>Cohasset L-97*, Dominion J-14 & 14A (anomalous shale over MMd), Musquodoboit E-23(?), Demascota G-32*<br>(**capping beds oolite rich**, then shallow reef, forereef & mud mounds)<br>Marquis L-35 (top=prograding oolite/sst, base=shallow reefal) & 35A (more slope), PANUKE GAP, Acadia K-62*, Albatross B-13* (red microbial Mud Mounds & no basal oolite) |
| **MARGIN — paleohighs and encased pinnacles (sponge-rich cap)** | MarCoh D-41, Margaree F-70, Panuke M-79* &79A, Panuke J-99s (PP-3C, PI-1A, PI-1B), Panuke H-08<br>(lower distal forereef & mud mounds not developed; D-41 & F-70 lack ooids & have landward forereef dips) |
| **MARGIN — inboard flexure and shoal** | Cohasset D-42* (sponge cap), Panuke B-90 (thin sponge cap), Panuke F-09 (thin sponge cap), Bonnet P-23* |
| **INTERIOR PLATFORM — oolitic shoals** | Abenaki J-56*, Kegeshook G-67, Como P-21, Oneida O-25* (top eroded/reddened & 4 sequences) |
| **INTERIOR PLATFORM — shaly lagoon/moat** | Glooscap C-63*, Moheida P-15* (sponge cap), Mohican I-100* (post-Misaine sequences = 4 at least) |
| **NEARSHORE RIDGE &/or SILICICLASTIC RICH** | Dover A-43, Ojibwa E-7, Naskapi N-30, Sambro I-29, Mohawk B-93 (also mid Cretaceous Roseway carbonates)<br>**NOTE**: In the above columns an asterisk (*) by the well = **penetrates Scatarie Member** below Misaine shale |

**Table 2. Abenaki wells – Sequence Styles and Facies Tract Setting - west of Sable Island.**

Major facies tract settings or magna-facies are based on both position relative to the seismically defined shelf edge (and internal geometries) and well lithofacies (see Table 2 for wells and Table 3 for core control). These facies subdivisions – slope and forereef, margin reef types, margin and shelf shoals and final capping sponge-rich beds - define the paper's later subdivisions as well as the poster topics that complete the overview given as a Conjugate Margin talk. Excerpts from a well-by-well summary that is in progress (see Table 1 for status) will be used to illustrate the characteristics of each of these major subdivisions with seismic through the wells from seismic shown in Kidston *et al.* (2005 or EnCana 2006, or MacLean and Wade 1993).

## Methodology and Facies-Sequences Background

This research is mainly based on cuttings studies over 35 years during exploring (for Shell Canada, Eliuk 1978) or consulting (to EnCana and others, Wierzbicki *et al.* 2002, 2005) and additional subsequent logging of the Abenaki Formation. Cuttings in carbonates are critical in the absence of core or, better yet, supplemented by very limited whole core (and in the Deep Panuke field by rotary sidewall cores) to give support and insight for the proper interpretation of the off-setting cuttings (see Table 3). Fortunately some of the main depositional facies subdivisions are quite distinguishable in Abenaki cuttings because of their unique fabric such as oolite and reefal framebuilders. In fact even subdivision of reef types is possible because lithistid sponges, stromatoporoids and chaetetids (both coralline sponges) and even particular types of corals (such as microsolenids with their useful deeper/more turbid tolerance) can be identified in small rock chips. Unfortunately some fossils, such as corals, are under-represented due to some genera with large corallite size and more often to diagenesis affecting their original aragonite mineralogy. Unlike the hexacorals and ooids of many other geological ages, Late Jurassic ooids were not aragonite but originally calcite, a more stable mineralogy, that is less likely to leach and more likely to be

preserved and even cemented with burial resulting in poor reservoir development. Dolomitization makes most cuttings unusable for depositional interpretation although in cores and sidewall cores sometimes identifiable texture is preserved. Other cuttings interpretation required insights from the post-1970s carbonate research literature. For instance now many peloid textures can be attributed to microbial deposition-cementation occurring in reefs and on the distal carbonate slope rather than just in lagoons as fecal pellets.

| MagnaFACIES Association | DELTA--NEAR OR IN | PANUKE-COHASSET | WESTERN SHELF MARGIN and *Baltimore Canyon Trough margins* |
|---|---|---|---|
| **Sponge (deep) Reef Mounds & inter-reef** | West Venture C-62 #13 (thin cap ?) | (MarCoh D-41 & Margaree F-70 & Panuke M-79 SWCs)···Demascota G-32 #1 | Moheida P-15 #1 (interior)<br>*Hyena 0317 #2; Civet 0337 #1; Rhino 0336 #2* |
| **Shelf & Margin Shoal and shallow Ramp (oolites)** | Penobscot L-30 #1 | (Panuke F-09 SWCs) | Acadia K-62 #1-3 (dolomite)<br>Albatross B-13 (ooids)<br>*Hyena #3&4; Civet #2; (Rhino #1-LK)* |
| **Reef Flat-margin** | -- | (Panuke M-79 SWCs)<br>Musquodoboit E-23 | Acadia K-62 #4 (oncolite) |
| **Shallow Reef** | -- | Margaree F-70 #1 (base-reef &/or forereef debris & SWCs)<br>(Panuke M-79, PI-1A & MarCoh D-41 SWCs)<br>Panuke PI-1A #1 (dolm), H-08 #1<br>Demascota G-32 #2, 3, 4 (dolomite) | *Rhino 0336 #3&4 (interior or prograding reef)* |
| **Transitional? ?reef & slope** | -- | Cohasset L-97 #1 (deep coral-microbial)<br>Margaree F-70 #1 (deepens up; sandy proximal slope=dolomite) | -- |
| **Slope-Microbial Mud Mound** | West Venture C-62 #13<br>Penobscot L-30 #2 | (Queensland M-88 SWCs)<br>Demascota G-32 #5 | Acadia K-62 #5<br>(Albatross B-13 SWCs red mud mounds, thin section only, not rotary drilled)<br>*Civet 0337 #3* |
| NOTE: SWC = sidewall core (rotary drilled, ca. 2.5 cm diameter) D-41 = 51, F-70 = 45, M-79 = 99, PI-1A = 44, F-09 = 31, E-23 = 5 | | | |

**Table 3. Abenaki (upper-Baccaro/Artimon) core control listed by magnafacies associations.**

Another more recent less fortunate innovation affecting cuttings analysis is more rapid carbonate drilling using PDC (Polycrystalline Diamond Compact) bits and turbine motors that give very fine, lighter-colored, chalkified and fractured cuttings making "back-to-the-future" emphasis on newer well cuttings interpretation sometimes problematic (see Fig. 8 inset for example). Most of the examination of both cuttings and core is only by low-power binocular microscope. This was supplemented by thin section study from the recent and archived sidewall cores and many from whole cores. Although time consuming, the potential for contribution from cuttings study is great. However the long time-line of this geologist's work makes necessary re-study of some older already-studied wells for newly recognized features in cuttings and other unstudied wells. Because of that and even re-examination of old core that has yet to be done I must apologize for the incomplete nature of this summary. All the newly drilled post-1998 Abenaki wells have been logged by me. An examination of Table 1 shows what wells remain to be done or redone. To illustrate major carbonate facies associations and show how the wells are being summarized against the dip seismic through the wells included in the CNSOPB Abenaki study (Kidston *et al.* 2005), some examples of well write-ups are included later in this contribution (Cohasset L-97, Margaree F-70, Panuke F-09). The lithofacies have been summarized schematically in lithofacies well schematics with greater than 10% reef framebuilders (lithistid sponges shown separately from corals and coralline sponges – stromatoporoids mainly), and ooid or peloid grain-supported limestones highlighted and unique textures like microbialites shown by symbols. Some sequence intervals on maps or well

sections are summarized by pie diagrams based on percentage lithofacies (Fig. 5 has a key or legend applicable to other figures where absent).

The depositional facies of the upper Baccaro and Artimon members of the Abenaki have been presented as Wilson-style (1975, from Shell-style) facies templates (Eliuk 1978) that have been updated with new data (Eliuk and Levesque 1988) particularly from Deep Panuke (Wierzbicki *et al.* 2002, 2005; reshown here as Fig. 11). Because of the needs for field development and the many new wells near the margin, EnCana workers (Weissenberger *et al.* 2006) developed detailed sequence stratigraphy with seven third-order units for the Abenaki including the basal Scatarie (AB I) and Misaine shale members (lower AB II) and culminating in thin sponge-rich argillaceous limestones of the upper Artimon Member (AB VII). Much earlier, a four-fold subdivision of the upper Abenaki (Baccaro-Artimon members) was possible (Eliuk 1978, his Fig. 14 and 18) for the margin and platform interior based on deeper-shallower or transgression-regression trends but the EnCana seven-fold sequence is followed here.

With the addition of the recent wells, criteria useful for depositional sequence (defined with subaerial unconformities) or parasequences (shoaling sequences) contact identification were developed for logs and cuttings. They include the following three diagnostic groups of indicators. First, 'gamma-sonic/density log characters' are shale-argillaceous carbonate above or below a break, gamma 'notch' (shelf interior) and possibly porosity underlying a break. Second, 'lithofacies changes' are shale/argillaceous carbonate above or below, glauconitic shale/argillaceous carbonate above, organic-rich black shale above, sandstone above (reworked or palimpsest in transgression), sandstone below (lowstand by-pass, karst fill), oolitic caps (shoaling trends) and oolitic bases (initial shallow transgression). Third, "biota-lithofacies changes" are lithistid sponge reef caps (in deeper water on microbialites), coralline (stromatoporoid-chaetetid) sponge reef caps, coral-coralline sponge reef caps, reefal bases (initial shallow transgression), bryoderm (bryozoa-echinoderm) argillaceous beds (transgression-shale influx), microbial-peloid grainstone-cement-rich zones (slower sedimentation/hiatus on slope). Use of these criteria can be seen applied on Figure 5 and in some specific well reviews used as examples in the Abenaki carbonate margin facies association sections in the latter part of the write-up.

## A Unique Setting and Different Depositional Styles

From the Sable Island area southwest, the Late Jurassic Nova Scotia offshore shelf has two major paleogeographic subdivisions – the Sable Island deltaic area with its upper-middle-lower shorefaces and associated relatively thin carbonate ramps versus the carbonate platform with its slope and margin reefal facies and outer shelf of mainly oolitic beds and the more interior deep lagoon/'moat' to lower shoreface to middle and upper shoreface of the nearshore ridges (see Figs.1, 2). More details of the prograding ramp and deltaic areas are given in Eliuk and Wach (2008, this conference CD) with examples of Late Jurassic mixed carbonate-siliciclastics wells on the carbonate slope (Queensland M-88) or in the carbonate ramp (Penobscot L-30) or in the Venture area shelf margin delta (West Venture C-62). The large-scale sequence styles and facies tracts or association settings with their wells are given in Table 2. More details on the Abenaki carbonate margin facies associations are given in the last five sections of this extended abstract and correspond to the Conference posters – 1) facies template and percentage pie diagrams, 2) slope/forereef settings and microbialites, 3) various reef types, 4) shelf margin oolites and 5) sponge reef beds relate to deltas.

The Abenaki may be unique or at least very rare in the world in being a thick reef-bearing carbonate platform laterally adjacent to and possibly dissected by a large delta – the Sable Island paleodelta. This juxtaposition is opposed to the not uncommon mixed carbonate-siliciclastic situations of relatively thin carbonate layers or small buildups within thick siliciclastic-volcaniclastic regimes or isolated carbonate banks or platforms across deeps from major siliciclastic influxes or carbonate shelves with nearshore siliciclastics. In the modern, tropical shallow-water reef-forming scleractinian corals are adapted to nutrient poor or oligotrophic conditions and are stressed to extirpation with high nutrients and clayey sedimentation particularly at high sedimentation rates. However this modern analogue may not be strictly applicable to Late Jurassic corals even if they are scleractinian hexacorals because oligotrophy

apparent was not yet fully developed (Leinfelder *et al.* 2002). Based on the occurrence in Panuke-Cohasset margin wells that have seismically defined settings, Abenaki coral-rich or 'reefal' beds occur between an outer margin flexure in relatively shallow but still deeper waters than oolite sedimentation of the inner margin flexure. The corals lived in less energetic slightly deeper waters since they usually have carbonate mud matrices and wacke- packstone interbeds. They may have been more tolerant of greater amounts of nutrients and minor clays. Demascota G-32, the first well drilled right at the margin (in fact a little beyond the outer margin flexure based on better seismic - MacLean and Wade 1993, Kidston *et al.* 2005) shows all three of Leinfelder's (1994) Late Jurassic reef types (Fig. 4) – sponge reef mounds, coral-coralline sponge reefs and microbial mud mounds.

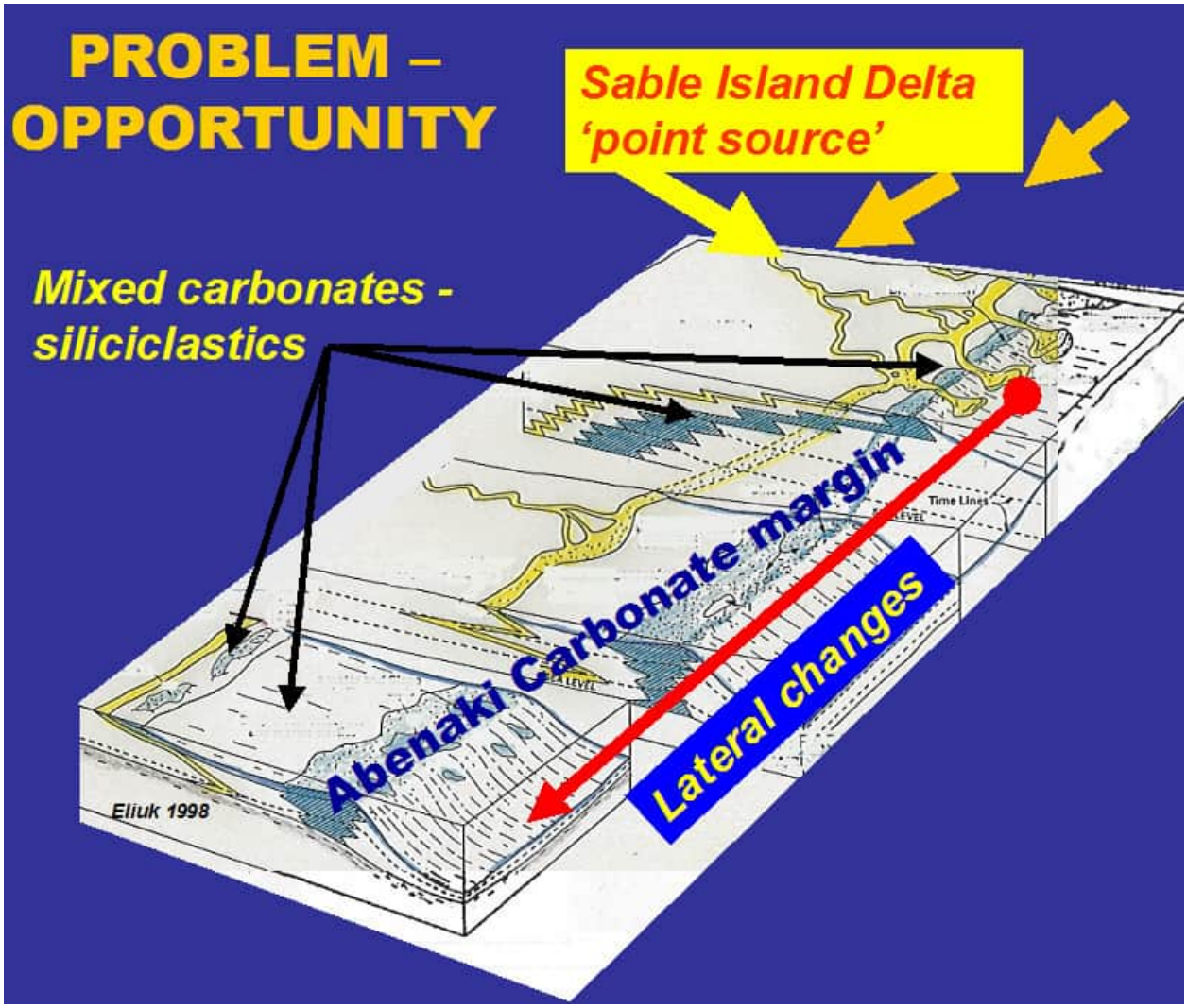


**Figure 2. Schematic depositional block diagram shows relationship of Abenaki carbonate margin with hypothesized main influx of fine siliciclastics and nutrients from the northeast Sable Island siliciclastic depo-centre. Close to the delta, basin-filling sand and shale allow progradation of carbonate ramps but further away the carbonate platform is influenced progressively over time by influx of finer siliciclastics and nutrients particularly along the deeper slope and during periods of higher relative sea-level stands. Alternation of relative sea level also allows variations in proximity and amount of mixed carbonates-siliciclastic in the shelf interior (deep lagoon-'moat') and nearshore ridge areas (diagram modified from Eliuk 1998).**

The vertical distribution of the buildup types is typical of much of the Abenaki wells (see Table 2). It reflects a large-scale shoaling sequence from slope microbial "mud" mounds to shelf-margin coral reefs to marginal oolite shoals then a reversal as the beds deepen and/or 'dirty' upwards with clay influx into sponge-rich reef mounds as shown in Figure 5 - a dip section of deep wells at Deep Panuke with G-32 projected in. Tight or low-porosity wells bracket M-79 that has typical dolomite-associated porosity of the margin amongst shallow reef or reef-derived limestones. Panuke F-09, although highly oolitic reflecting the original shallow and energetic crest of the platform margin, has its original depositional porosity occluded, as it was in the on-strike earlier-drilled Panuke B-90 and Cohasset D-42. F-09 is tight enough to act as a partial stratigraphic trap for Deep Panuke gas and this cementation is attributed to rapid burial and probable original calcite ooids that would not have been as easily leached either in early subaerial exposure or in later corrosive burial fluids.

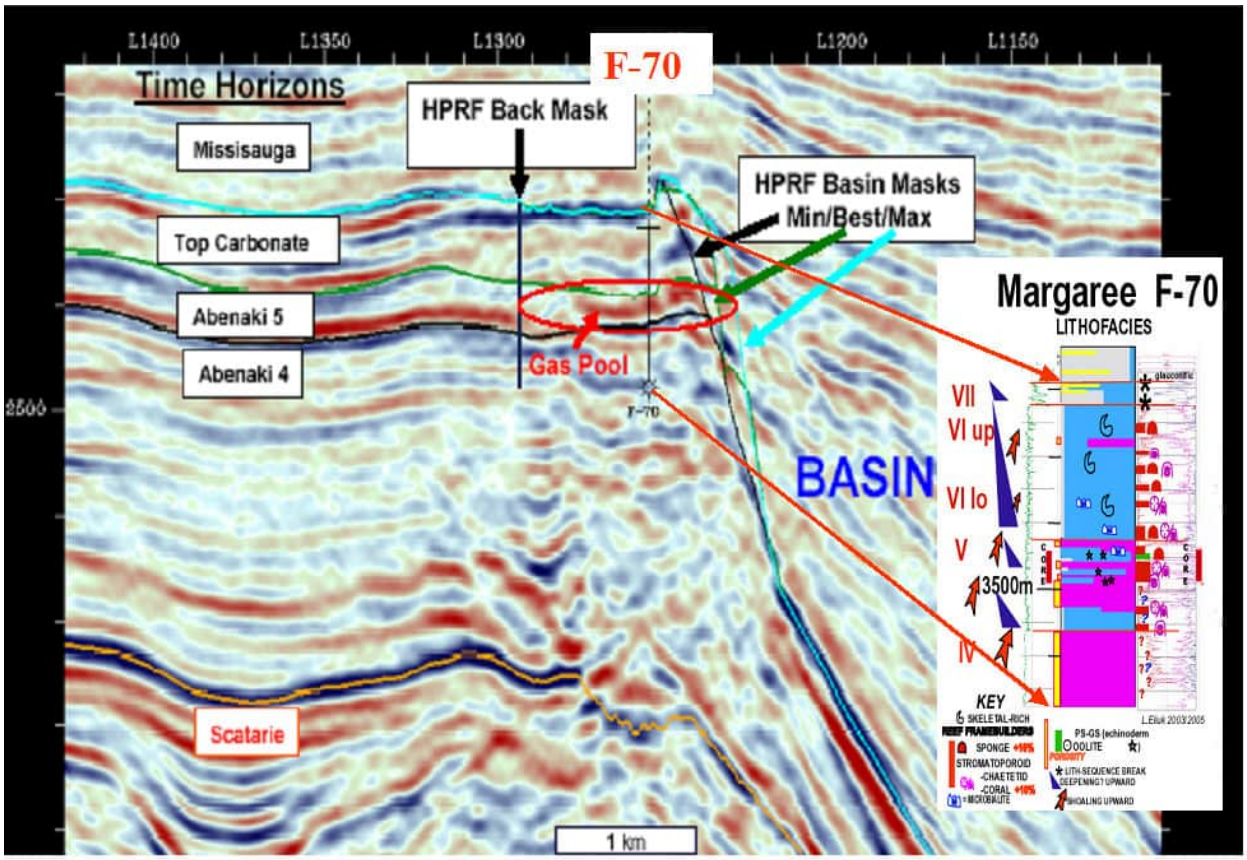


**Margaree F-70 Seismic** Encana - Deep Panuke Report 2006

**Figure 3. EnCana et al. Margaree F-70 dip seismic section and well lithofacies schematic in the north half of the Deep Panuke shelf margin gas accumulation (combined from EnCana 2006 Fig. 2.25 by Eliuk and Fig.2.48). Note the gas pool mainly developed in the Abenaki V sequence and the porosity is visible as a low amplitude event (HPRF = High Permeability Reef Front reservoir region) that allowed reservoir mapping when calibrated to the well control. F-70 drilled the shelfward side of a carbonate-encased pinnacle between an inner and outer shelf flexure. Dip-meter and core indicate that proximal forereef beds dip northwestward toward the Nova Scotia shelf rather than the Atlantic basin. This is similar to the situation in MarCoh D-41. Both wells lack oolite indicating that the these shelf margin upper slope buildups were too small for ooid shoals yet had too much relief for slope deposition of shelf-derived allochthonous ooids.**

Down dip in Queensland M-88 and in the lower section of Demascota G-32 (similar seismically to just off-bank and far off-bank settings in Fig. 3 and Fig. 17 or Fig. 22, see Kidston *et al.* 2005 for more seismic at the wells), limestone is microbial peloid mudstones to grainstones that were formed in deeper

water of the distal forereef slope. Again the limestone is tight and in many cases cemented on the seafloor. This is interpreted from cuttings supported by sidewall core and inferences from similar settings in at least three cores, including some with thick submarine cements and stromatactis (Fig. 4), of off-setting wells (see Table 3). Therefore subsequent corrosive or dolomitizing fluids lacked permeability pathways to enhance porosity during burial and stylolitization resulted in further cementation.

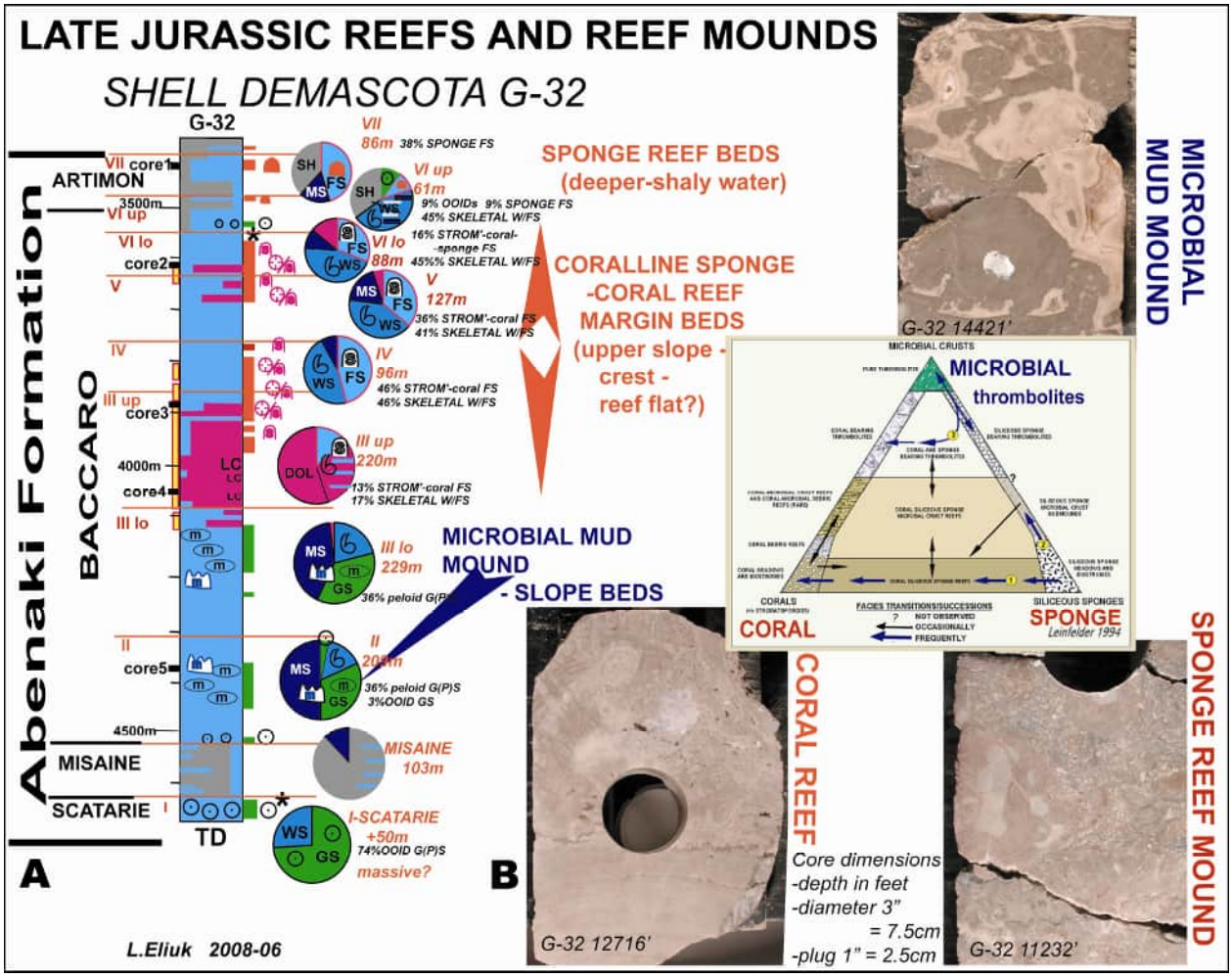


**Figure 4. Late Jurassic reef-reef mound types (triangular diagram from Leinfelder 1994 and in Wierzbicki *et al.* 2002) and Demascota G-32 well schematic column with the Abenaki four member stratigraphic subdivision and EnCana's seven sequence stratigraphic units. A) Demascota G-32 first sampled all three Abenaki reefal types in cuttings and cores and showed that buildups occur in a variety of settings on the distal slope as microbialite 'mud' mounds, most typically just in front of the shallowest part of the margin as coral-coralline sponge debris reefs and finally capping the Abenaki during 'drowning' or deeper more argillaceous periods as lithistid demosponge-siliceous sponge reef mounds; B) Leinfelder's (1994) triangular Late Jurassic reef type classification developed initially from a study of reefs and carbonate ramps in Portugal showing various common transitions and illustrated here from portions of G-32 cores. Note the common bioerosion by bivalves and sponges in the coral reef and sponge reef mound with framebuilders in the latter of much smaller overall size. The microbialites show thrombolitic textures and some stromatolitic to branching habits with occasional well-developed submarine cements and even stromatactis which are both evident in this core photograph.**

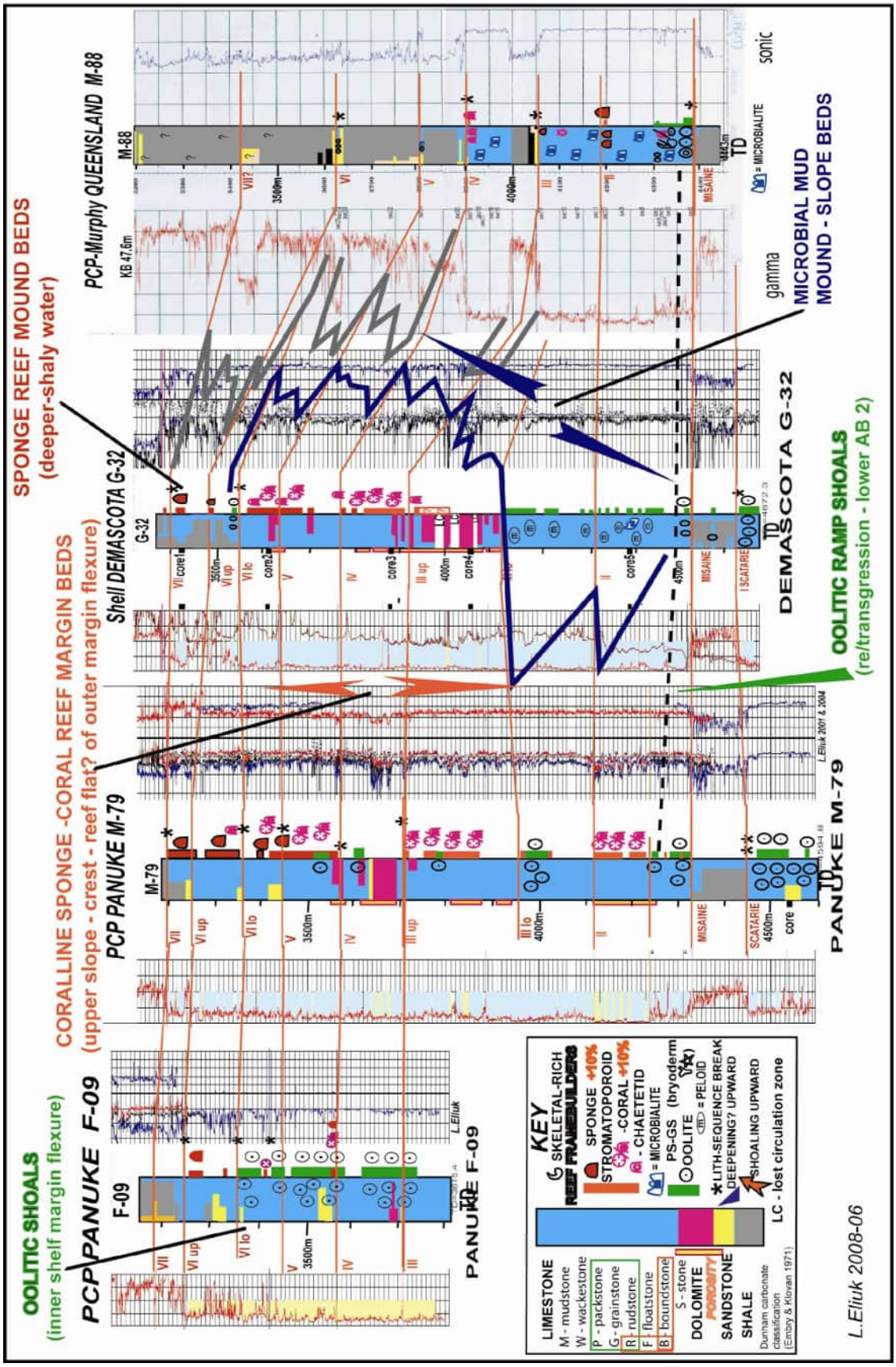


**Figure 5. Detailed caption on next page.**

**Figure 5. Shelf margin dip stratigraphic section in the Deep Panuke area showing the development of major different carbonate margin facies associations and the EnCana (2006, Weissenberger *et al.* 2006) sequence stratigraphy. See Fig. 1 map inset for well locations from northwest (left) F-09 inner shelf margin flexure rich in oolite through mixed oolite and increasing amounts of shallow reefal sections in M-79 and G-32 (projected in from the southwest) to the outer shelf flexure with distal slope beds rich in microbialite 'mud' mounds on the southeast (right) M-88 slope-basin beds (some of the shales may be prodeltaic to the Sable Island delta). Note that the seven EnCana sequences (Weissenberger *et al.* 2006 and EnCana 2006) are defined on the shelf by inferred unconformities identified mainly by sandy-shaly breaks interpreted to be lowstand influx or reworked at base of next sequence during maximum regression capping shoaling sequences indicated by oolite or reefal beds. In deeper reefal margin and especially lower or distal slope settings, unconformities are unlikely and sequence breaks are based on indications of maximum regression such as greater hard-peloid grainstones (G-32), lithistid or coralline sponge or deep-water coral caps on microbialites especially when overlain by shales and particularly dark possibly dysoxic shales (M-88). For the uppermost Abenaki (Artimon Member) of sequences AB VI Upper (the latter is easily seen in wells but not on seismic) and AB VII the tops may not be unconformable exposure surfaces but drowning surfaces resulting not only from relative sea-level rise but also from high nutrient and clay influx inimical to carbonate formation due even to sponge growth. Note that the base of the Baccaro Member has a regionally developed oolite (and sometimes coral reef beds). It is immediately above the Misaine shale considered the second order maximum flooding event or surface (MFS of Weissenberger *et al.'s* 2006 AB II sequence which includes the overlying basal oolite).**

Considering the area of the Abenaki platform there is low well control (about 30). It is concentrated along the margin particularly in the Deep Panuke area with assessment wells. There are vertical changes that allow cycles and sequences to be defined. These are interpreted to be a result of relative sea-level fluctuations but do shown overall vertical trends as discussed above and in the next section. Areally those wells can be grouped as on Table 2 from basin to nearshore shelf interior with characteristic facies associations (see Fig.11 and later sections). These go from slope microbialite-rich lower energy to highest wave energy in shelf margin oolitic shoals shelfward of the greatest reef development and various interior platform shoals before lower energy and more argillaceous beds of the far interior platform open lagoon or 'moat' and finally the siliciclastic-rich, sometimes coaly, nearshore ridge zone. Along the margin the shallower water reef complexes seem to have developed as discontinuous buildups giving local bathymetric/topographic relief in slightly deeper water between the oolitic inner shelf margin flexure and an outer slope flexure. Thus there is great local variability of the resultant facies and morphologies as shown in Figure 9 and the Margaree F-70 well review. That and particularly the fault-and-fracture-associated late diagenesis also give great reservoir variability. The deleterious influence of the enlarging Sable Island delta during higher sea-level stands results in the demise of the shallow-water bank and formation of sponge-rich beds adjacent to prodeltaic shales. In even closer proximity to the Sable Island delta, sandstones overwhelm even shallow-water oolitic and biostromal limestones diachronously without the development of sponge-rich beds.

## Varied Vertical Sequences

Variations along the carbonate margin are shown in section (see Figs. 5, 6 the latter includes some older interior wells and a nearshore ridge well) and map view (Fig. 7) for wells that reached the Misaine shale. Except in the Deep Panuke area they all have a shoaling upward pattern from the maximum flooding (MFS) of the Misaine shale through microbial-rich slope beds to shallow reefs to oolite that could be considered a second order sequence from the MFS to the near the top of the Abenaki. This larger sequence encompassing the whole Baccaro Member and the underlying Misaine and perhaps capping Artimon members has been further subdivided into six second-order sequences (AB II to AB VII) by Weissenberger *et al.* (2006, also EnCana 2006) as they analyzed their new seismic and well data at Deep Panuke and sub-regionally. Their basal sequence AB I applies to the underlying Scatarie Member limestone which in fact may comprise three or more sequences in itself given the regionally developed threefold cyclicity (Eliuk 1978) and its long age-range and varying stratigraphy (Wade and MacLean 1990, their Fig. 5.24).

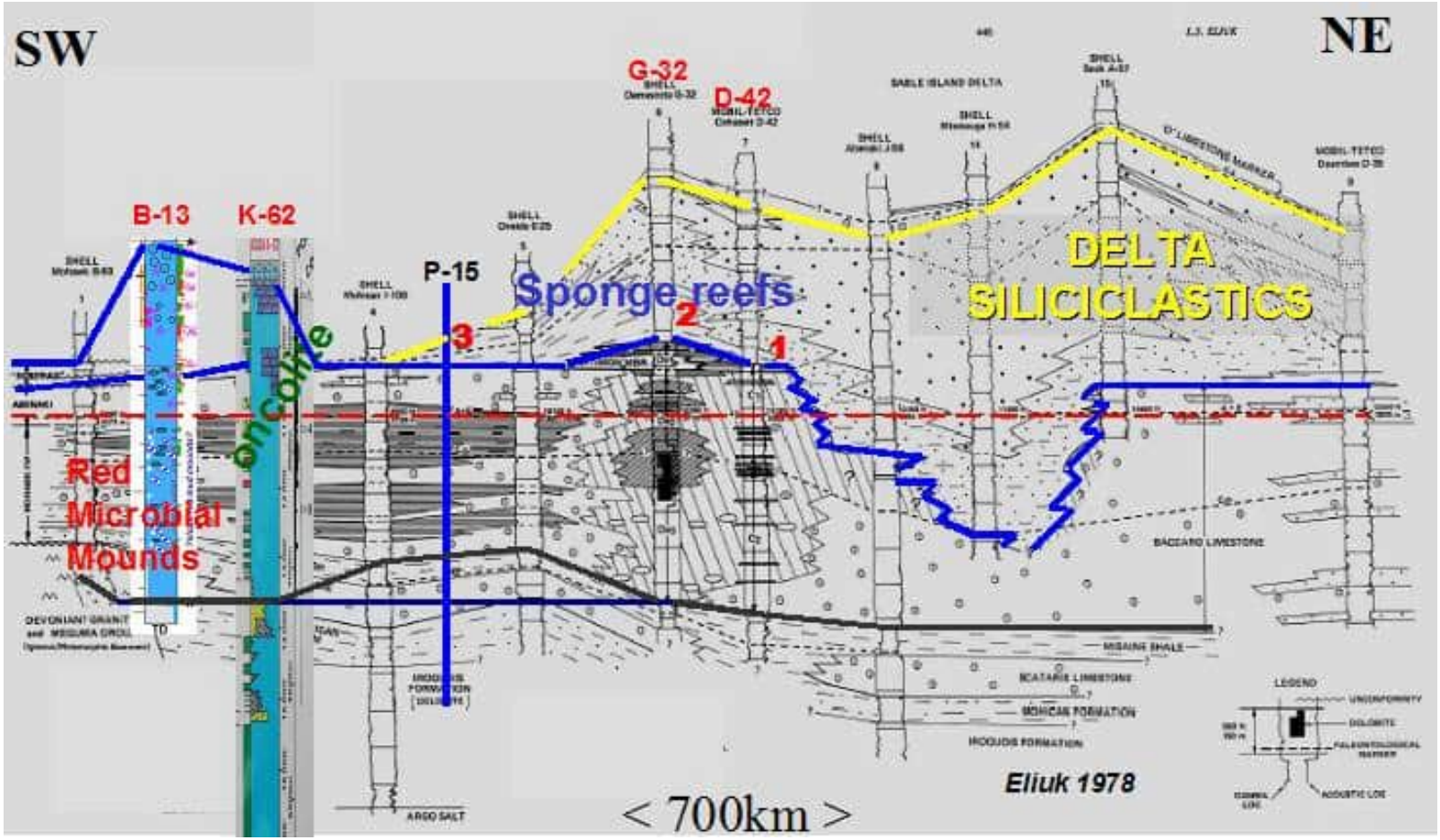


**Figure 6. Regional strike section (from Eliuk 1978 Fig. 13 with datum on a biostratigraphic marker) with overlay of some more recent wells (K-62 and B-13 datumed with G-32 on the top Misaine, P-15 hung on top Abenaki) to show the relationship of the Sable Island siliciclastics to the Abenaki capping sponge-rich beds and the continued carbonate platform growth to the southwest away from the major siliciclastic influence. D-42 is in the north end of the Deep Panuke field. The transgressive-regressive (deeper-shallower oolitic-reefal) sequences are apparent even in the old platform interior and margin wells. The sponge-rich intervals are progressively younger (1= D-42, 2= G-32, 3= P-15) as the prodeltaic beds onlap the "drowned" Abenaki (dating by Graham Williams in Eliuk 1985). The lower third to half of Baccaro in the shelf margin K-62 and B-13 are slope microbialites of much lighter color and even reds as compared to similar facies in the Deep Panuke margin. Note that immediately northeast of the Sable delta at Sauk A-57 the likely progradational pattern of ramp carbonates over siliciclastic fill as proposed by Wade and MacLean (1990 and similar to Fig. 5 of Eliuk 1978) is better interpretation than that shown here from Eliuk (1978, note questions marks below A-57 on Fig. 6). The older Jurassic dating and thickness/amount of limestone in Dauntless D-35 may indicate the existence of a northeast bank or requires another older deltaic source for Wade and MacLean's (1990) progradational ramp hypothesis to apply.**

For the rest of the Abenaki, depending on the location the top may consist of sponge-rich beds (Artimon Member, diachronous condensed sedimentation may include Early Cretaceous ages, Eliuk and Levesque 1988) or of oolite with interbedded sandstones either closer to the Sable Island delta or oolites without interbedded sandstones on the Western Shelf to the far southwest with carbonate deposition continuing beyond the Berriasian into the younger Early Cretaceous (Jansa 1993). The discontinuous sponge-rich capping beds (Figs. 6,7) and their relationship to the prograding prodelta of the Sable Island delta is discussed in the final Abenaki carbonate margin facies association section in figure captions (Figs. 24, 25). The Artimon sponge-rich beds are now believed to reflect the deleterious effects of siliciclastics and associated nutrients in deeper water that limits shallow carbonate sedimentation but allows sponges to exist during low-level clay influx. Some of the upper sequences AB VI and AB VII may not be capped by subaerial unconformities but simply by maximum regression intervals in an overall deepening ('shaling') trend. In fact the AB VI sequence can often be easily split into an upper and lower part based on shallower reefal or even oolitic facies in the lower section versus more argillaceous and sponge-rich limestones in the upper. This break is not resolvable seismically.

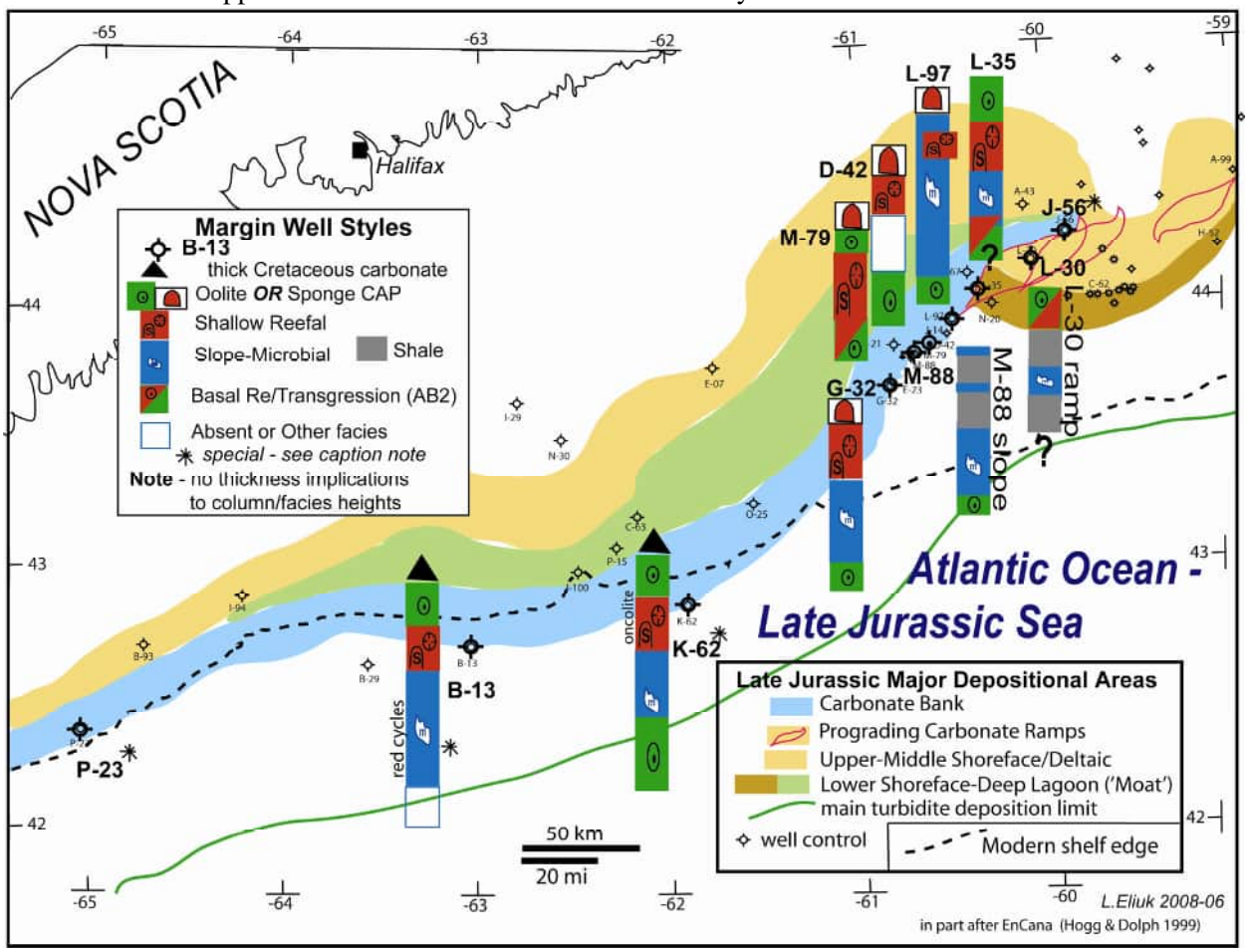


**Figure 7. Margin well styles showing large-scale vertical second-order sequence patterns of the Abenaki platform edge from wells with Misaine shale (L-35 nearly reaches Misaine and the L-30 ramp well bottoms well above Scatarie-Misaine). At the northeast end near the Sable Island delta, a ramp well (L-30) prograding over prodeltaic shales and one basin-slope well (M-88) are the two thick mixed siliciclastic-carbonate wells in this series. Except for two other wells (D-42 and M-79 in Deep Panuke which lack distal slope beds) the wells show a shoaling up succession from slope microbialites through shallow coral reefal beds up into oolite in most wells on both sides of Deep Panuke. However at Deep Panuke the wells are dominantly shallow coral reefal above microbialite then capped by argillaceous sponge beds. Nearly all wells show a surprisingly oolitic (occasionally shallow reefal) limestone immediately above the Misaine Member shale which has the maximum**

**flooding surface of the Abenaki second order sequence; this relationship may represent a drastic forced regression for AB II sequence (AB II basal limestone is shallow oolite or reef in all wells except B-13 and very thin in L-97). *NOTE* P-23 has yet to be logged by the author and is 5 km from the margin; B-13 has no basal oolite in AB II but does show several white-up-to-red and white-up-to-pink cycles in slope microbialites; K-62 has to be re-logged but does have an unusual oncolite-ooid-reef flat facies above slope microbialites; J-56 on the flank of a salt dome but probably is near the north end of the Abenaki carbonate platform.**

An interesting anomaly is the occurrence of an oolitic interval between the Misaine shale, and the usual development of the deeper-water distal slope peloid-microbial beds in the lower Baccaro in most margin wells that is overlain by successively shallower facies. Only Albatross B-13 (see Fig. 7) has no basal oolite just dark argillaceous limestone above the Misaine shale before the change to cyclic red and white slope microbialites. This would be a more elegant, uninterrupted second-order sequence of shallowing from a Misaine MFS. But that basal oolite is nearly ubiquitous and is could be considered a transgressive event of the second-order sequence. Panuke M-79 lacks significant distal slope microbialites and for that reason is interpreted to have always been a paleohigh localizing reefs from the inception of the Baccaro (AB II). This rapid apparent change in depositional depth at the outset of Baccaro sedimentation was elaborated on by Weissenberger *et al.* (2006, their Fig. 13) in their third order AB II sequence that included the second order maximum flooding surface (Misaine shale). Between Demascota G-32 and Deep Panuke, they showed seismic evidence for offlap and the basinward location of the AB II margin as compared to the AB III margin. Yet in Demascota G-32, the upper AB II and lower AB III are distal microbial slope so a significant transgression followed the Middle AB II regression. Because this abrupt regressive relationship is so widespread and dated as Callovian-Oxfordian, a correlation to the Middle-Late Jurassic forced regression and disconformity on the Portuguese carbonate ramp of Azeredo *et al.* (2002) seems like a very reasonable interpretation for these not quite conjugate cross-Atlantic margins. However there may not be any exposure-disconformity in the Abenaki but just a major submarine transgression-regression-transgression. Clearly more conjugate research is needed.

## Proposed Deep Panuke Hydrocarbon System

A hydrocarbon accumulation requires a trap, seal, reservoir, migration path and source rock – the petroleum or hydrocarbon system. Awhile after the Cohasset D-42 and Demascota G-32 tested the carbonate margin and seemed to have found only methane gas dissolved in formation water, Eliuk (1978) outlined Abenaki hydrocarbon potential. The key requirements in order of increasing difficulty included: potential traps, seals (including "even nonporous carbonates within the Abenaki" required since the margin dipped into the basin), reservoirs (problematic due to deep burial and apparent lack of regional exposure but aided by local shelf-edge porous limestone and dolomite interpreted to have formed in freshwater lenses of exposed islands with mixing zone dolomite) and migration/source rocks that were seen as the greatest difficulty. "Unless source rocks occur in the basin-filling Late Jurassic and Cretaceous shales immediately seaward of the Abenaki carbonate platform and shelf-edge fracturing is adequate as a migration path, the hydrocarbon potential of the Abenaki must be considered low" (Eliuk 1978, p.475). This discouraging prophecy, like my mixing-zone dolomite, turned out to be false but the predicted need for fractures was true for both reservoir development and charge (Eliuk 2004, Wierzbicki *et al.* 2006). Instead, perhaps ideas on direct porosity indicators in the Abenaki margin seismic (Harvey and MacDonald 1990), probably the impending abandonment of a production facility and definitely the willingness to again explore the Abenaki led to to the PanCanadian (EnCana) discovery. Amplitude anomalies on 3D seismic shot during development of the overlying oil pool in 1990 but occurring basinward of it in the carbonate margin were successfully tested in Panuke PP-3C (Weissenberger *et al.* 2006). For those exploring the Baltimore Canyon Trough offshore Delaware USA, the same unhappy prediction could be made regarding the need for an as yet inknown source rock for nearly all the play types tested in the mid 1980's. That area with the rest of the United States East Coast offshore along with Georges Bank just on the Canadian side are in drilling moratorium at least until the 2012 and hopefully this second prophecy will eventually also turn out to be false.

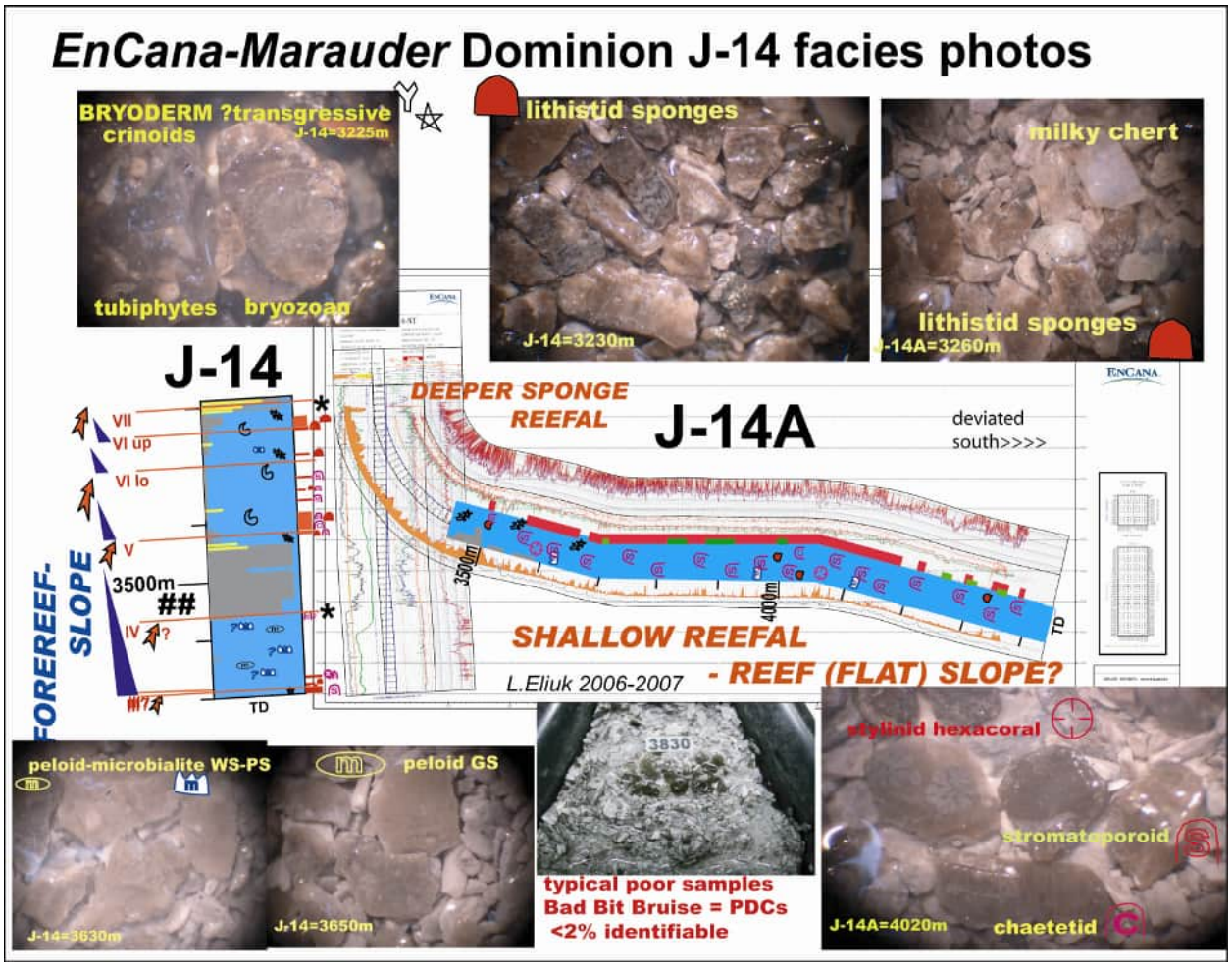


**Figure 8. EnCana-Marauder Dominion J-14 and J-14A sidetrack with examples of carbonate facies recognizable in cuttings (no whole or sidewall cores were taken nor FMI logs but, as shown by the photographs, some of the cuttings allowed depositional facies to be assigned in the 4 sequences penetrated; PDC = polycrystalline diamond compact bits result in very poor cuttings). For the Deep Panuke margin wells, both shale (in AB V the usual reservoir interval) and slope microbialites (in AB IV) are unique whereas AB VII and upper AB VI are typical in being slightly argillaceous sponge-rich beds as is lower AB VI in having a mix of lithistid and coralline sponge (stromatoporoid and chaetetid) reefal beds. Located at the northeast end of a broad promontory extending from the Deep Panuke area (see Fig. 1 inset and Fig. 9) J-14 tested a seismic anomaly generated from shale rather than porosity contrasts and J-14A drilled nearly horizontally 1 km to the south in the AB V sequence successfully found stromatoporoidal-coral reefal beds but unfortunately no porosity nor dolomite. Seismic mapping (EnCana 2006, Fig. 2.55) indicates the shale is a limited pod behind the reef margin carbonates that may or may not open north-northeastward to a basinal embayment. This shale may indicate that by AB V deposition at the north end of the Deep Panuke platform salient the prodeltaic beds were at least temporarily nearly as high as the Abenaki platform top-lapping distal slope microbialites within a local embayment. Compare this to the apparent uncompacted 300 m of relief 18 km or so to the southwest at Queensland M-88 between the top of the AB V slope shales and platform (see Fig. 5). Alternatively instead of by-passing the margin to be deposited basinally, the shales may have been trapped in a upper foreslope mini-basin between carbonate ridges and buildups that unlike the Margaree-MarCoh areas did not get carbonate filled. This change to much reduced carbonate productivity over this relatively short distance may reflect the stress of increased nutrients-clays on shallow-water carbonate organisms following a deepening event that initiated AB V deposition.**

Diagenetic study of the Deep Panuke reservoir (Wierzbicki *et al.* 2006) made a strong argument for porosity creation by burial dolomitization and limestone dissolution, likely late post-stylolitization deeper burial. Pathways for the diagenetic fluids were related to fracturing and faulting near the carbonate margin due to wrench-faulting and instablity of the margin over basement highs. Early diagenesis was not

a subject of that study but the tight nature of most limestones including updip oolites that actually contribute to stratigraphic trapping show that early cementation (in the microbial slope beds) and mainly rapid burial cementation are critical components of the accumulation. Reservoir development is highly variable (Figs. 8, 9) and required side-tracking of three initially tight wells in the reservoir zone with economic success in two cases and a 'technical success' of finding reefal beds instead of shale that unhappily were still not porous. From a regional point of view, dolomite is seen to some extent in all shelf margin wells from Deep Panuke south. This includes Bonnet P-23 which, eventhough it is 5 km behind the margin, has major faulting easily seen on seismic (Jansa 1991, MacLean and Wade 1993, Kidston *et al.* 2005). To the northeast of Deep Panuke, Cohasset L-97 is the only well with some 100% dolomite beds although they are of limited thickness. Marquis L-35 and the whip-stocked L-35A both had oolitic, reefal and microbial distal slope limestone but no significant porosity. So looking for faulting, fracturing and direct porosity indicators for deep burial diagenesis rather than reefal margin paleohighs of the failed mixing-zone dolomite subaerial-leaching model is required.

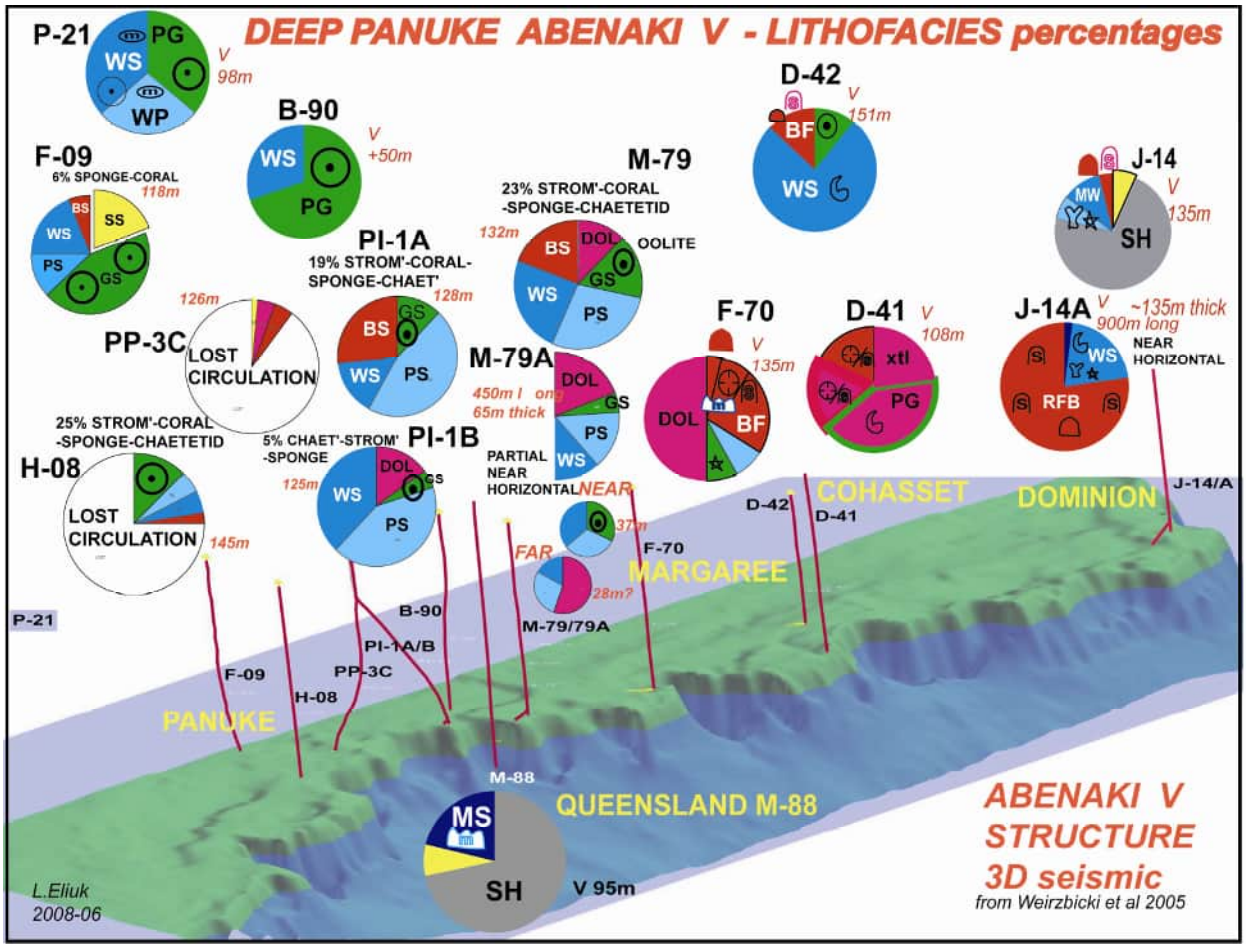


**Figure 9. Deep Panuke area lithofacies map of AB V sequence with percentages shown as pie charts (see Fig. 5 Key for symbol-letter definition and Table 1 for well identification, PI/PP = Platform Injector/Producer). Based on cuttings analysis strongly supplemented by rotary sidewall cores (F-09, PI-1A, M-79, F-70, D-41) and very rarely whole cores (H-08, PI-1A, M-79=Scatarie Member only, F-70 = only long core of 24m). Lost circulation zones ("Vuggy Limestone" zone based on petrophysical logs and FMI images) and thick dolomite ("High Permeability Reef Front" zone) development are proxies for good reservoir porosity (see EnCana 2006 for details on reservoir zones and complete pool analysis). Oolite-rich wells can be non-porous and form lateral seals for stratigraphic trapping (F-09 and B-90 on the inner margin flexure. P-21 shelf interior well is 8 km behind the shelf edge with more lagoonal pellets than ooids). Northeast trapping along strike is partly structural but also due to both shale and tight reefal limestone in J-14 and J-14A (see Fig. 8). Reservoir (and**

**lithofacies) variation over short distances required side-tracking in three wells with favorable porosity or lithofacies results – PI-1A to PI-1B with porous dolomite, M-79 to M-79A with porous dolomite and J-14 to J-14A with shallow reefal beds instead of shale but still not porous. Similarly rapid changes over just 1 km (and a 30 year gap) separate Cohasset D-42, drilled an anticlinal feature just behind the margin and abandoned in 1973 as unproductively tight, from MarCoh D-41 with greater than 120m of gas-filled porosity nearer the margin. D-42 is analogous to the inner-flexure tight highly oolitic wells B-90 and F-09 but has much less oolites and more but thin reefal beds plus more skeletal wackestones. Note the great amount of reefal and skeletal float-wacke-packstones amongst the shallow reefal boundstones (and dolomites) that support the slightly downslope location of these reefs inferred from seismic and limited core. The oolite beds occupy the shallowest platform margin crest.**

Unfortunately, even this better understanding of the play factors leaves some nagging reservoir risks that increase as the risk of charge and perhaps seal decreases. In rare cases the amplitude anomalies might be shale as in Dominion J-14 (Fig. 8) just as some of the build-up relief might be non-reservoir argillaceous sponge reefs. The earlier discussed association of prodeltaic shales and deeper-water argillaceous sponge reef limestones acted as super- and intra-formational seals. Both are more likely closer to the distal prodeltaic shales of the Sable Island delta which is also the most likely area for dispersed, lignitic, gas-prone source rocks (Williamson and DesRoches 1993). They also described a source rock model for the widespread Sable subbasin gas accumulations. Their analysis of source rock maturation gives a likely timing of 110 MA for maturation of a Late Jurassic (152 MA) Verrill Canyon Formation shale. At that time the Abenaki margin at Deep Panuke would have been at 2 km burial depth which with perhaps a higher heat flow would already have occluded most of the porosity that was not enhanced by subsurface diagenetic fluids. With these apparent required ingredients – rapid burial for seals and gas-prone source rock – the Abenaki hydrocarbon system at least at Deep Panuke requires proximity to and early burial by the Sable delta summed up in Figure 10. The presence of oil-filled sandstones in drape structures above the carbonate margin at Panuke and Cohasset might have resulted from a change in carbonate reservoir-seal properties between the time of oil versus gas generation and migration. Or complex multiple source rocks (Mukhopadhyay & Wade 1990 found some potential thin oil-prone as well as gas-prone Verrill Canyon Formation source rocks) and complicated migration paths and histories are involved.

## Summary Review – A unique reef margin gas field without analogues

Deep Panuke is a gas accumulation in a Late Jurassic platform margin reef complex on the northwestern edge of the then small proto-Atlantic Ocean. Its location near a large delta complex makes it unique or at least very uncommon lacking close analogues in the Recent and possibly even in the geologic record. But considering the great number of Jurassic reefs (Leinfelder *et al.* 2002) and huge volume of Jurassic hydrocarbon reserves worldwide and particularly in the Middle East; it is surprising to learn that less than 1% of hydrocarbon reserves in carbonate buildups are of Jurassic age. Greenlee and Lehman (1993) list Miocene then Devonian, Paleocene and Pennsylvanian as the ages with the largest reef reserves. The Jurassic does not merit a place on their chart eventhough the Late Jurassic has the second or third greatest number of reef sites for Phanerozoice supersequences after the Late Devonian and before/same as the Miocene (Kiessling 2002 Fig. 2, but reservoir quality is perhaps only fifth, Fig. 30). Perhaps that low Jurassic statistic might be slightly under-estimated by the possible exclusion of data on shelf-edge reef hydrocarbon fields in the Carpathian-Caucasus regions of the Ukraine (Izotova and Popadyuk 1993, Lukin 1999, and unfortunately a not easily accessed literature). Nevertheless, it does reflect the fact that most large Jurassic fields are low-relief structures with carbonate shelf interior reservoirs and typically wholly or partly evaporitic top seals (including the Ukrainian reefs). The example of such non-reef fields begins with Ghawar in Saudi Arabia - the world's largest oil field having a Late Jurassic reservoir in the Arab D Formation.

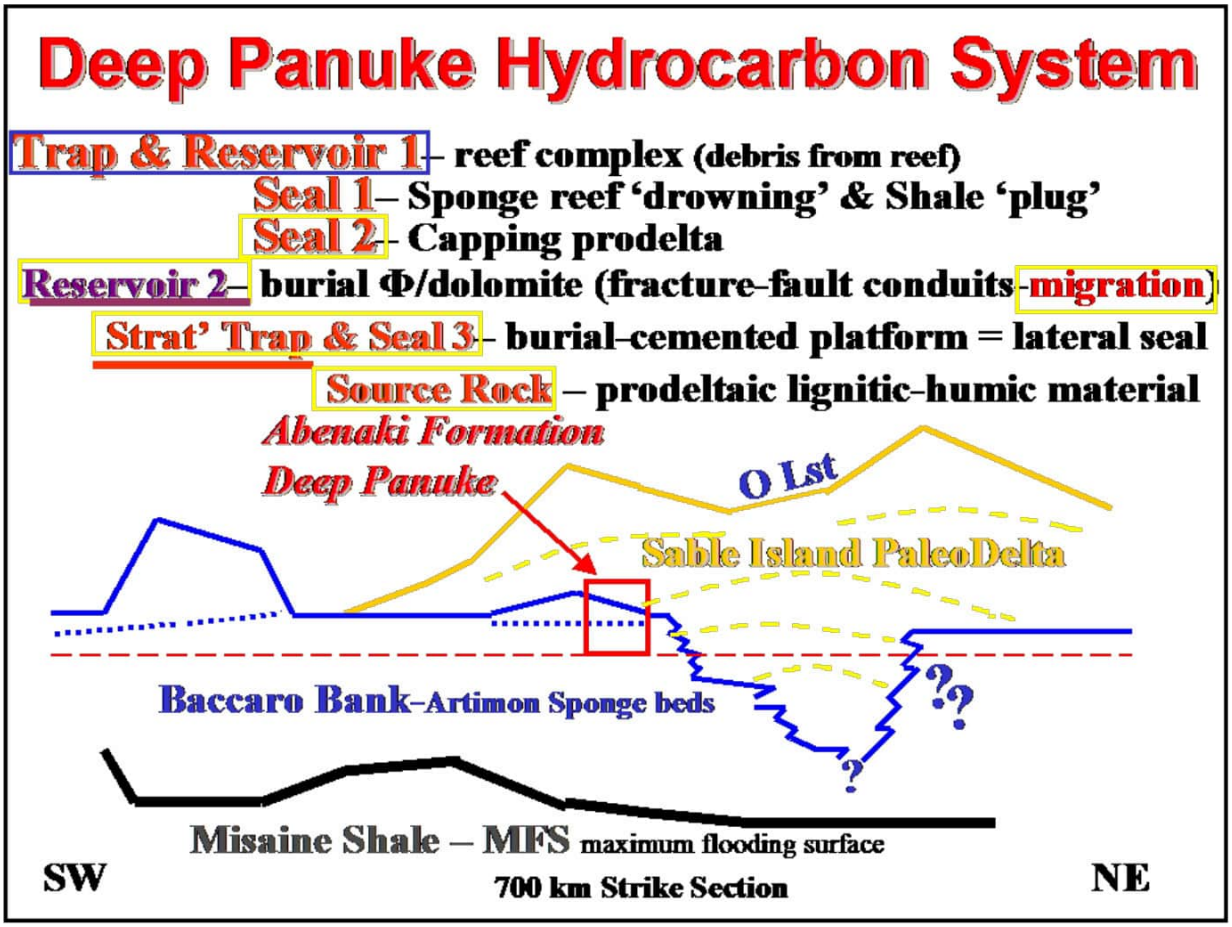


**Figure 10. Deep Panuke Hydrocarbon System. - summary of hydrocarbon system components above a schematic line drawing of regional strike section (see Fig. 6) to show relation of Deep Panuke on carbonate platform margin to Sable Island siliciclastic depocentre. Although carbonates and siliciclastics tend to be incompatible due to high sedimentation rates and highly variable environmental stresses associated with fluvial-deltaic sedimentation in particular, the proximity of the Sable Island delta to the Abenaki carbonate bank in combination with the reefal buildup relief is interpreted to have provided all the ingredients for an effective hydrocarbon/petroleum system. The Abenaki buildup provided the initial structure-trap (and in fact the low relief anticlinal trap for the overlying Lower Cretaceous oil field) and early reefal debris and reef-derived slope/backreef lime sands that were subsequently burial dolomitized or leached. But the delta provided top and lateral sealing facies due to argillaceous content (sponge-rich limestones) and prodeltaic-basinal shales (Verrill Canyon Formation) and tight clean limestones due to early and deep burial cementation (oolitic limestones on the shelf), source rock from prodeltaic lignitic-humic material, and arguably fracture conduits for diagenetic and reservoir fluids due to loading and failure of the reef margin. As a play type these shelf-margin reefs could be considered analogous to the shelf-margin deltas of Cummings and Arnott (2005) without the growth faults and overpressures.**

In contrast, Deep Panuke platform-margin coral-coralline sponge reef complex adds to a limited collection of circum-Atlantic-Gulf of Mexico Jurassic reef fields that include a coral-microbial reef mound on oolite shoals in a southern England intra-cratonic basin (Sun and Wright 1998), early dolomitized shallow-water microbialite mounds on basement ridges and nearshore microbialite-high energy shoal stratigraphic trap in Smackover Formation restricted embayments in Alabama (Mancini *et al.* 2003, 2008), stacked inner ramp margin coral-microbialite reef complex and outer ramp thrombolite-sponge limestone pinnacles of the Cotton Valley Lime in deep East Texas Basin (Montgomery *et al.* 1999a & 1999b). It is intriguing that what reef-reef mound reservoir works in one basin does not

necessarily work in another. Deep Panuke differs from all these ramp-associated reefs and most significantly in its much larger estimated reserves and the importance of late burial diagenesis for reservoir porosity because of loss of original depositional porosity with early deep burial near a delta. Deep Panuke is the only carbonate gas field on the North American Atlantic continental shelf. It is the youngest hydrocarbon-bearing reef reservoir in Canada. It is still being developed and hopefully will not continue to be unique but become an analogue for more Jurassic reef fields.

## Acknowledgements

This work is being carried out at Dalhousie University as a PhD project under the supervision of Prof. Grant Wach and includes data originally worked on while consulting for EnCana (formerly PanCanadian) on Deep Panuke and as a Shell Canada geologist much earlier. I thank both companies and Royal Dutch-Shell and management for permission to use, publish and continue working with the data. I particularly thank EnCana's geologists Rick Wierzbicki and Nancy Harland and more recently Norm Corbett who have generously shared some of their insights. ElPaso Canada (no longer extant, Sandra Bleu technologist) assisted with figure-size well logs used in some of the well studies after I helped them with the Marquis drilling and analysis. Some others I thank for sharing ideas, data, thin sections, and/or various other help include: Eric Bogoslowski (PetroCanada), David E. Brown (CNSOPB), Tony Cortis (Shell Canada), Jeff Dravis (consultant), Alison Essery (ex-Shell Canada), John Harper (Conoco-Phillips), John Hogg (ex-EnCana), Lubomir Jansa (GSC), Darcy Schau (Shell Canada), Mary-Jean Verrall (CNSOPB), Clint Tippett (Shell Canada), John Weissenberger (ex-PanCanadian) , Nancy White (CNSOPB), and Hans Wielens (GSC).

## References

Azeredo, A.C., V.P. Wright and M.M. Ramalho, 2002, The Middle-Late Jurassic forced regression and disconformity in central Portugal: eustatic, tectonic and climatic effects on a carbonate ramp system; Sedimentology v.49, p.1339-1370.

Conway, K.W., J.V. Barrie and M. Krautter, 2004, Modern siliceous sponge reefs in a turbid siliciclastic setting: Fraser River delta, British Columbia, Canada; Neue Jahrbuch Palaeontologie Mh, 2004, p.335-350.

Cummings, D.I., and R.W.C. Arnott, 2005, Growth-faulted shelf-margin deltas: a new (but old) play type, offshore Nova Scotia. Bulletin of Canadian Petroleum Geology: v.53, p.211-236.

Dromart, G., C.L.F. Gaillard and l. Jansa, 1994. Deep-marine microbial structures in the Upper Jurassic of Western Tethys. *in* J. Bertrand-Sarfati and C. Monty, eds., Phanerozoic Stromatolites II, p.295-318.

Erlich, R.N., Longo, Jr., A.P. and Hyare, S. 1993. Response of carbonate platform margins to drowning: evidence of environmental collapse. In, Loucks, R.G. and Sarg, J.F. (ed.), Carbonate Sequence Stratigraphy – Recent Developments and Applications, American Association of Petroleum Geologists, Memoir 57, p.241-286.

Eliuk, L.S., 1978. Abenaki Formation, Nova Scotia shelf, Canada - depositional and diagenetic model for a Mesozoic carbonate platform: Bulletin of Canadian Petroleum Geology, v.26, p.424-514.

Eliuk, L.S., 1981. Abenaki update: variations along a Mesozoic carbonate shelf, Nova Scotia Shelf, Canada: *in* F. Stoakes, ed., Canadian Society of Petroleum Geologists Annual Core and Field Sample Conference, p.15-19 (extended abstract).

Eliuk, L.S. 1985. Artimon Member: *in* G.L Williams, L.R Fyffe, R.J.Wardle, S.P.Colman-Sadd, R.C. Boehner and J.A.Watt, eds., Lexicon of Canadian Stratigraphy - Atlantic Region, v.6, p.11-12, Canadian Society of Petroleum Geologists.

Eliuk, L.S., 1998. Big bivalves, algae and the nutrient poisoning of reefs: a tabulation with examples from the Devonian and Jurassic of Canada: *in* P.A. Johnston and J.W. Haggart, ed., Bivalves: An eon of Evolution; University of Calgary Press, p.157-184.

Eliuk, L.S. 2004. History of the practical application of a failed? dolomite model (mixing zone) to the "Demascota Dolomite Beds" of the Abenaki Formation, Nova Scotia offshore Late Jurassic paleocontinental shelf

carbonate margin – Case Study for Core Conference, CSPG Dolomite Conference January 13-15th (15 pages on CD).

Eliuk, L.S., S.C. Cearley, and R. Levesque, 1986. West Atlantic Mesozoic carbonates: Comparison of Baltimore Canyon and Offshore Nova Scotian Basins: AAPG Bulletin, v.70, p.586-587 (abstract).

Eliuk, L. and R. Levesque, 1988, Earliest Cretaceous sponge reef mound Nova Scotia shelf (Shell DemascotaG-32): *in* H.H.J.Geldsetzer, N.P. James and G.E.Tebbutt, eds., Reefs, Canada and Adjacent Areas. Canadian Society of Petroleum Geologists, Memoir 13, p.713-720.

Eliuk, L.S. and S.G Pemberton, 2002. Bioerosion in the Upper Jurassic Abenaki margin – preliminary survey: Appendix to Weirzbicki et al. (2002), p.95-101.

Eliuk, L.S. and B.E. Prather, 2005. Baltimore Canyon Trough Mesozoic Carbonate Margin Cores, Offshore USA Atlantic: Abstract and core conference article – CSPG-AAPG Convention June core conference in Calgary AB (31 pages on CD).

Eliuk, L. and G. Wach, 2008 (this conference CD), Carbonate and siliciclastic sequence stratigraphy - examples from the Late Jurassic Abenaki limestone and West Venture deltaic beds, offshore Nova Scotia, Canada

Ellis, P.M., 1984. Upper Jurassic carbonates from the Lusitanian Basin, Portugal and their subsurface counterparts in the Nova Scotian Shelf: Unpublished PhD. Thesis, Open University, England.

Ellis, P.M., P.D. Crevello and L.S. Eliuk, 1985. Upper Jurassic and Lower Cretaceous deep-water buildups, Abenaki Formation, Nova Scotian shelf: *in* P.D. Crevello, and P.M. Harris, eds., Deep-water Carbonates, SEPM Core Workshop No. 6, p. 212-248

Ellis, P. M., R. C. L. Wilson, and R. R. Leinfelder, 1990, Controls on Upper Jurassic carbonate buildup development in the Lusitanian Basin, Portugal: *in* M. E. Tucker, J. L. Wilson, , P. D. Crevello, J. R Sarg. and J. F. Read,, eds. Carbonate Platforms - Facies, Sequences and Evolution. International Association of Sedimentology Special Publication 9: p.169-202, Oxford.

Embry, A.F, and J.E. Klovan, 1971, A late Devonian reef tract on northeastern Banks Island, N.W.T.; Bulletin of Canadian Petroleum Geology, v.19, p.730-781.

EnCana Corporation, 2006, Deep Panuke Offshore Gas Development, Volume 2 – Development Plan. (Document No: DMEN-X00-RP-RE-00-0003 Rev. 01U), 313 p. (available on the CNSOPB website).

Given, M.M., 1977, Mesozoic and early Cenozoic geology of offshore Nova Scotia: Bulletin of Canadian Petroleum Geology, v.25, no.1, p.63-91.

Greenlee, S.M. and P.J. Lehmann, 1993, Stratigraphic framework of productive carbonate buildups: *in* R.G. Loucks and J.F. Sarg, eds., Carbonate Sequence Stratigraphy; AAPG Memoir 57, p.43-62.

Harvey, P.J. and D.M. MacDonald, 1990, Seismic modeling of porosity within the Jurassic aged carbonate bank, offshore Nova Scotia: Canadian Journal of Exploration Geophysicists, v.26, p.54-71.

Izotova, R.S., and I.V. Popadyuk, 1993, Oil and gas in Jurassic reefal complexes of the west Ukrainian Carpathian foredeep; AAPG Bulletin, v. 7, p.1663-1664 (abstract).

James, N.P. and P-A. Bourque, 1992, Reefs and mounds: *in*, R.G. Walker and N.P. James, eds. Facies Model: Response to sea level change, p.323-347.

Jansa, L.F., 1981, Mesozoic carbonate platforms and banks off the eastern North American margin: Marine Geology, v.44, p.97-117.

Jansa, L.F., 1991. Lithostratigraphy 9: Carbonate buildup morphology: *in*, East Coast Basin Atlas Series: Scotian Shelf, Geological Survey of Canada, Atlantic Geoscience Centre, p.69.

Jansa, L.F., 1993, Lower Cretaceous carbonate platforms of the northeastern North American margin: *in* J.A.T. Simo, R.W. Scott and J.P. Masse, eds., Cretaceous Carbonate Platforms: AAPG Memoir 56, p.111-126.

Jansa, L.F. and Lake, P.B. 1991a. Lithostratigraphy 8: Isopach maps – Roseway Unit and Abenaki Formation: *in*, East Coast Basin Atlas Series: Scotian Shelf, Geological Survey of Canada, Atlantic Geoscience Centre, p.65.

Jansa, L.F. and P.B. Lake, 1991b, Lithostratigraphy 9: lithofacies and depositional environment – Scatarie and Baccaro members: *in*, East Coast Basin Atlas Series: Scotian Shelf, Geological Survey of Canada, Atlantic Geoscience Centre, p.67.

Jansa, L.F., B.R. Pratt, and G. Dromart, 1988, Deep water thrombolite mounds from the Upper Jurassic of offshore Nova Scotia: *in* H.H.J. Geldsetzer, N.P. James and G.E. Tebbutt, eds., Reefs, Canada and Adjacent Areas. Canadian Society of Petroleum Geologists, Memoir 13, p.725-735.

Jansa, L.F., G. Termier et H. Termier, 1982, Les biohermes a algaes, spongiaires et coraux des series carbonatees de la flexure bordiere du "paleoshelf" au large du Canada oriental: Revue de Micropaleontologie, v.25, p.181-219.

Kiessling, W., 2002, Secular variations in th Phaerozoic reef ecosystem; *in* W. Kiessling, E. Flugel and J. Golonka, eds., Phanerozoic Reef Patterns: SEPM Special Publication No. 72, p.625-690.

Kidston, A.G., D.E. Brown, B.M. Smith, and B. Altheim, 2005, The Upper Jurassic Abenaki Formation offshore Nova Scotia: a seismic and geologic perspective: Canada-Nova Scotia Offshore Petroleum Board CD publication , 168p.

Leinfelder, R.R., 1994. Distribution of Jurassic reef types: a mirror of structural and environmental changes during breakup of Pangea: *in* A.F. Embry, B. Beauchamp, and D.F. Glass, ed., Pangea: Global Environments and Resources: Canadian Society of Petroleum Geologists Memoir 17, p. 677-700.

Leinfelder, R.R., 1997, Coral reefs and carbonate platforms within a siliciclastic setting: General aspects and examples from the Late Jurassic of Portugal: 8th International Coral Reef Symposium, Panama City, Proceedings, v.2, p.1727-1742.

Leinfelder, R.R., D.U. Schmid, M. Nose and W. Werner, 2002, Jurassic reef patterns – the expression of a changing globe: *in* W. Kiessling, E. Flugel and J. Golonka, eds., Phanerozoic Reef Patterns: SEPM Special Publication No.72, p.465-520.

Lukin, A., 1999, Oil and gas potential of the reef-carbonate reservoirs of Ukraine; AAPG Bulletin, v.83, p.1296-1300. (extended abstract, p.333-336 of AAPG Int. Conf and Exhibit.)

MacLean, B.C. and J.A. Wade, 1993, Seismic Markers and Stratigraphic Picks in the Scotian Basin Wells: East Coast Atlas Series, Geological Survey of Canada, 276p.

Mancini, E.A., J.C. Llinas, W.C. Parcell, M. Aurell, G. Badenas, R.R. Leinfelder and D.J. Benson, 2004, Upper Jurassic thrombolite reservoir play, northeastern Gulf of Mexico; AAPG Bulletin, v.88, p.1573-1602.

Mancini, E.A., W.C. Parcell, W.M. Ahr, V.O. Ramirez, J.C.Llinas and M. Cameron, 2008, Upper Jurassic updip stratigraphic trap and associated Smackover microbial and nearshore carbonate facies, eastern Gulf coastal plain: AAPG Bulletin, v.92, p.417-442.

McIver, N.L. 1972. Cenozoic and Mesozoic stratigraphy of the Nova Scotia Shelf: Canadian Journal Earth Sciences, v.9, p.54-70.

Meyer, F., 1989, Siliciclastic influenced development of the Mesozoic Wilmington Platform, Western Atlantic: *in* P.D. Crevello, J.L. Wilson, J.F. Sarg, and J.F. Read, eds., Controls on Carbonate Platforms: SEPM Special Publication No.40, p.213-232.

Montgomery, S.L., T.H. Walker, G.P. Wahlman, R.C. Tobin and D. Ziegler, 1999a. Upper Jurassic "reef" play, East Texas Basin: An updated overview: Part 1 – background and outboard trend; AAPG Bulletin, v.83, p.707-726.

Montgomery, S.L., R. Karlewicz and D. Ziegler, 1999b, Upper Jurassic reef play, East Texas Basin: An updated overview: Part 2 – inboard trend; AAPG Bulletin, v.83, p.869-888.

Mount, J.F., 1984, Mixing of siliciclastic and carbonate sediments in shallow shelf environments: Geology, v.12, p.432-435.

Mukhopadhyay, P.K. and J.A. Wade, 1990, Organic facies and maturation of sediments from three Scotia Shelf wells; Bulletin of Canadian Petroleum Geology, v.38, p.407-425.

Poag, C.W., 1991, Rise and demise of the Bahamas-Grand Banks gigaplatform, northern margin of the Jurassic proto-Atlantic seaway: Marine Geology, v.102, p.63-130.

Prather, B.E. 1991. Petroleum geology of the Upper Jurassic and Lower Cretaceous, Baltimore Canyon Trough, western North Atlantic Ocean: AAPG Bulletin, v.72, p.258-277.

Pratt, B.R., 1982. Stromatolitic framework of carbonate mud mounds: Journal of Sedimentary Petrology. v.52, p.1203– 1227.

Pratt, B.R., 1995. The origin, biota and evolution of deep-water mud-mounds: *in* C.L.V Monty, D.W.J. Bosence, P.H. Bridges and B.R. Pratt, eds., Carbonate Mud-Mounds, Their Origin and Evolution: International Association of Sedimentology Special Publication, v.23, p.49– 123.

Pratt, B.R. and Jansa, L.F. 1988. Late Jurassic shallow water reefs of offshore Nova Scotia: *in* H.H.J. Geldsetzer, N.P. James and G.E. Tebbutt, eds., Reefs, Canada and Adjacent Areas: Canadian Society of Petroleum Geologists, Memoir 13, p.741-747.

Schlager, W., 2005, Carbonate Sedimentology and Sequence Stratigraphy. SEPM Concepts in sedimentology and Paleontology #8, 200p.

Sun, S.Q. and V.P. Wright, 1998, Controls on reservoir quality of an Upper Jurassic reef mound in the Palmers Wood Field area, Weald Basin, southern England; AAPG Bulletin v.82, p.497-515.

Wade, J.A. 1991. Lithostratigraphy 4: MicMac and Abenaki Formations *in*, East Coast Basin Atlas Series: Scotian Shelf, Geological Survey of Canada, Atlantic Geoscience Centre, p.57.

Wade, J.A. and B.C. MacLean, 1990, The Geology of the southeastern margin of Canada: Chapter 5 *in* M.J. Keen and G.L. Williams, ed. Geology of the Continental Margin of Eastern Canada, Geological Survey of Canada, Geology of Canada No.2, p.167-238.

Weissenberger, J.A.W., R.A. Wierzbicki, and N.J. Harland, 2006, Carbonate sequence stratigraphy and petroleum geology of the Jurassic Deep Panuke Field, offshore Nova Scotia, Canada. *in* P.M. Harris and L.J. Weber, eds., Giant Hydrocarbon reservoirs of the World: From rocks to reservoir characterization and modeling: AAPG Memoir 88/SEPM Special Publication, p.395-431.

Wierzbicki, R., J.J. Dravis, I. Al-Aasm, and N. Harland, 2006. Burial dolomitization and dissolution of Upper Jurassic Abenaki platform carbonates, Deep Panuke reservoir, Nova Scotia, Canada. AAPG Bulletin, v.90, p.1843-1861.

Wierzbicki, R., Gillen, K., Ackermann, R., Harland, N., Eliuk, L. with a contribution by J. Dravis. 2005. Interpretation of a Fractured Dolomite Core: Margaree F-70, Deep Panuke, Nova Scotia, Canada. Abstract and core conference article – CSPG-AAPG Convention June core conference in Calgary AB (25 pages on CD).

Wierzbicki, R., Harland, N. and Eliuk, L. 2002. Deep Panuke and Demascota core from the Jurassic Abenaki Formation, Nova Scotia – Facies model, Deep Panuke, Abenaki Formation. Canadian Society of Petroleum Geologists 75th Diamond Jubilee Convention Core Conference Abstracts including extended abstracts, p.71-94. (plus Appendix see above; also on CD as PDF in color; note the same paper used in Halifax core conference as Wierzbicki and Harland 2003).

Williamson, M.A. and K. DesRoches, 1993, A maturation framework for Jurassic sediments in the Sable Subbasin, offshore Nova Scotia; Bulletin of Canadian Petroleum Geology, v.41 p.244-257.

Wilson, J.L. 1975. Carbonate Facies in Geologic History: Springer, New York, 471p.

**BACK**

# Lithology-based, High-Resolution Sequence Stratigraphic Framework of Lower Cretaceous, Mixed Carbonate-Siliciclastic Sediments, Atlantic Coastal Plain, Eastern United States

**Richard A. Sunde**
University of North Carolina
N.C. Geological Survey
205 Perry Creek Drive
Chapel Hill, NC, 27514
United States
e-mail: rsunde1@sfu.ca

**Brian P. Coffey**
Dept. of Earth Sciences
Simon Fraser University
8888 University Drive
Burnaby, BC, V5A 1S6
Canada

## ABSTRACT

A lithology-based sequence stratigraphic framework for the Lower Cretaceous mixed carbonate-siliciclastic sediments of the subsurface Albemarle Basin of eastern North Carolina was developed using thin sectioned well cuttings, wireline logs, and 2D seismic. Thin sections were analyzed to characterize lithology, fossil components, depositional facies, and diagenetic events, because the study interval is confined to the deep subsurface in a basin lacking core control. Integration of lithologic data with 2D seismic data and biostratigraphic control allowed regional correlation of major transgressive-regressive events between wells, resulting in the generation of a sequence stratigraphic framework for the onshore basin. Dominant lithofacies include: (shallow to deep): sandstone, skeletal sandstone, variably sandy mollusk packstone/grainstone, siltstone to shale, skeletal wackestone, variably sandy (quartz and glaucony) lime mudstone, and marl.

Comparison of observed facies with cores and wireline logs from the Baltimore Canyon and Southeast Georgia Embayment confirms that many updip sequences consist of upward-shoaling siliciclastic shoreface successions, with basal open shelf mollusk-rich carbonates often marking transgressive events. Basin-scale depositional trends indicate greater accumulation of the carbonate facies in the southern portion of the basin, with increased fine siliciclastic material to the north. This trend may reflect a major siliciclastic point-source in the vicinity of the ancestral Chesapeake region. The depositional and diagenetic models generated provide insight into the facies and reservoir properties in coeval offshore units comprising frontier exploration targets along the Western Atlantic margin of the U.S. and Canada.

## Introduction

Hydrocarbon exploration wells have been drilled in the Albemarle Embayment of eastern North Carolina almost 100 years, but there have been relatively few published studies that focus on the subsurface Mesozoic strata. This project presents a lithology-based depositional model and sequence stratigraphic framework for the subsurface Early Cretaceous sediments of the Albemarle Embayment. This framework provides an analogue for coeval strata along the North Atlantic margin. It also provides

an updip stratigraphic reference section for offshore exploration targets within the basin (Manteo Prospect; Vigil 1998).

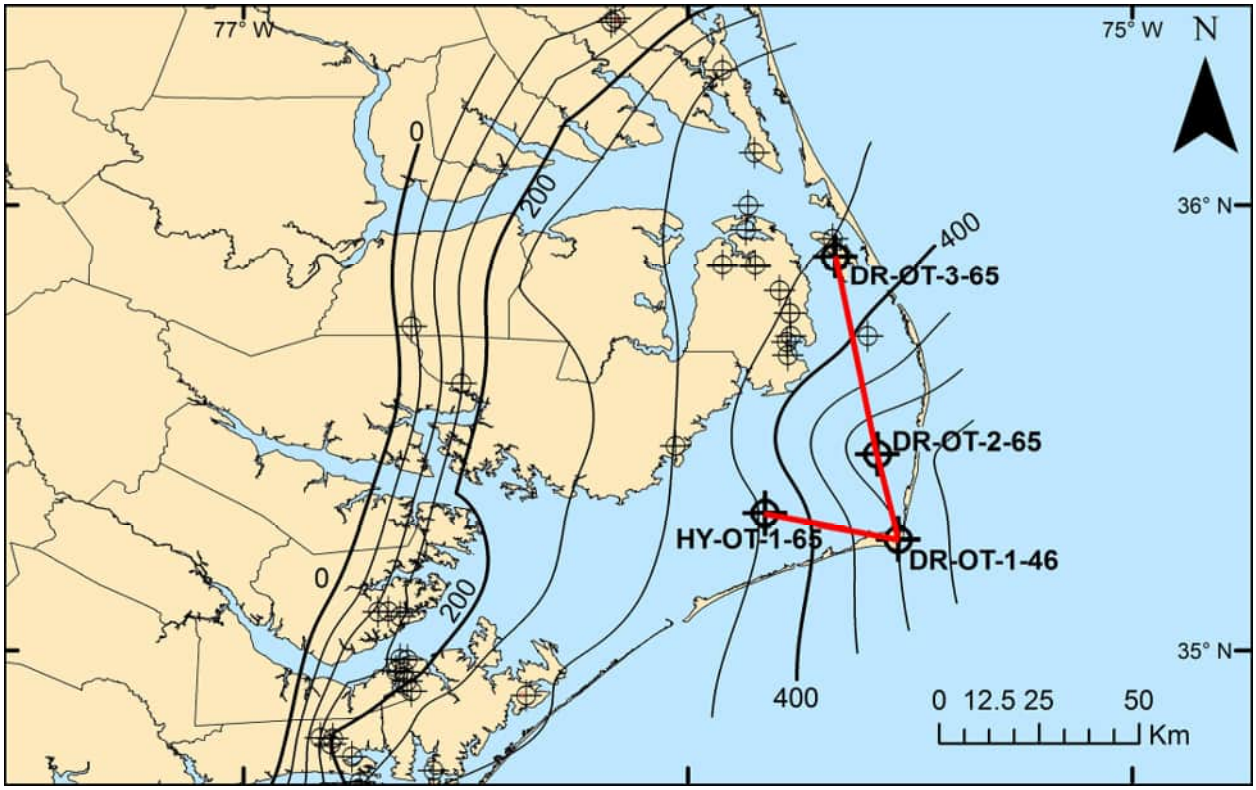


**Figure 1. Study area in the onshore Albemarle Embayment, eastern North Carolina (USA). Lower Cretaceous marine sediments are isolated to the subsurface; contours show thickness of this package in meters. Wells used in the study are labeled. The cross-section shown in Figure 4 indicated in red.**

The datasets employed in this project were vintage well and 2D seismic data (Fig. 1). As discontinuous core was recovered from only one well within the basin, cuttings samples provided invaluable lithologic control. Cuttings are rarely studied in academia, though they commonly are utilized in industry. The observed lithologies were compared to core from more recently drilled offshore wells in adjacent basins (Baltimore Canyon Trough and Southeast Georgia Embayment) to confirm stacking patterns and discern environments of deposition. Figure 2 displays the regions stratigraphic nomenclature.

The successful use of these vintage datasets in generating a regional stratigraphic framework is of great value, as many under-explored basins in the world lack modern, easily workable datasets. By applying the methods and techniques utilized in this study, costly exploration activities may be better planned, or avoided entirely.

## Depositional Model

The observed mixed carbonate-siliciclastic lithologies were grouped into ten facies associations (Table 1) that were deposited in environments ranging from marginal marine to deep, open shelf. Sediments were deposited on a low angle, high-wave energy shelf or ramp (Fig. 3). The tropical paleolatitude of the basin, throughout the Early Cretaceous, favoured carbonate sedimentation during periods of reduced siliciclastic transport to the basin from the proximal Appalachian Mountains (Scotese, 1995).

| Facies Association | FA 1<br>Coal | FA 2<br>Quartz and Skeletal Quartz Sandstone | FA 3<br>Sandy Molluscan Packstone and Grainstone | FA 4<br>Shale and Siltstone | FA 5<br>Deep Marine | FA 6<br>Restricted Tidal Flats | FA 7<br>Ooid Grainstone & Packstone | FA 8<br>Peloidal Packstone | FA 9<br>Skeletal Packstone | FA 10<br>Hardground |
|---|---|---|---|---|---|---|---|---|---|---|
| **Dominant Constituent Facies** | Dominated by carbonaceous cuttings fragments. | **FA 2A**: Medium- to coarse-grained quartz sand and finer-grained quartz sandstone<br>**FA 2B:** Skeletal- and glauconite-bearing quartz sandstone. | Quartz sandy molluscan packstone and grainstone. | Shale and siltstone. | **FA 5A:** Planktonic foraminifera siltstone and diatomaceous shale.<br>**FA 5B:** Marl, fine-grained skeletal wackestone and planktonic foraminifera packstone and wackestone. | **FA 6A:** Bedded evaporites (Anhydrite and Gypsum).<br>**FA 6B:** Most abundant, algal laminites and lime mudstones.<br>**FA 6C:** Miliolid packstone and wackestone as well as lime mudstones. | Dominated by quartzose sand-bearing ooid grainstones and packstones. Rare peloid and skeletal packstones present. | Dominated by mollusc peloid packstone. | Dominated by bryozoan and brachiopod skeletal packstones that show little re-working. | Phosphatic sandstone and hardground, glauconitic sandstone, and chert near the base of studied interval. |
| **Biota** | Plant type not identified. | Local disarticulated, abraded bivalves. Rare echinoderms. | Dominantly bivalves (oysters, rudists, and inoceramis); rare corals and gastropods. | None identified. | Planktonic foraminifera and diatoms. Rare sponge spicules and thin walled bivalves | Miliolids benthic foraminifera, rare bivalves, ostracodes, or gastropods. | Coated mollusks and rare echinoderms are commonly associated. | Rare, micrite rimmed bivalves. | Bryozoans and brachiopods dominate. Rare large benthic foraminifera, bivalves, and echinoderms. | Planktonic and benthic foraminifera, and mollusks are locally present. |
| **Stratigraphic Occurrence & Thickness** | Rarely present in up-dip positions, typically overlies quartz sandy units. Mean thickness is 1.8 m | Abundant throughout the basin. Typically overlies shaley or silty units, as well as units rich in molluscan fragments. Mean thickness is 5.5 m. | Abundant throughout the basin. Though variable, commonly found with shale-rich and quartzose sand-bearing units. Mean thickness is 5 m. | Abundant throughout the basin. Found with quartz sandstone and mollusc packstone. Mean thickness is 4.9 m. | Low abundance association largely confined to basinal regions. Typically associated with shale. Mean thickness is 4.6 m. | Rarely present, found in the southern and down dip portions of the basin. Typically overlying ooid-bearing facies. Mean thickness of 3.8 m. | Rarely present, observed in southern and down dip portions of the basin. found with restricted facies and mollusc-rich facies. Mean thickness: 3 m. | Rarely present; found in the southern and down dip portions of the basin. Found with mollusc and other skeletal packstones. Mean thickness of 4 m. | Rarely present, observed in the southern and down dip portions of the basin. Found with peloid packstone and marly facies. Mean thickness of 5.2 m. | Low abundance, though present throughout the basin. Largely interpreted as surficial coatings, much less than 1 m thickness. |
| **Interpreted Depositional Environment & Setting** | Marginal marine back-barrier, delta plain, or tidal flat setting: Peat swamps or foreshore marshes. | High-energy, inner shelf setting. Mainly shoreface and barrier island settings. | Open marine, shallow shelf; middle ramp depositional setting. Subject to periodic storm wave reworking. | Low-energy setting below fair-weather wave base. Distal delta and offshore settings, rare protected lagoons or estuaries. | Open marine, deep shelf; basinal ramp depositional settings. | Deposited in the inner ramp setting, in an environment subject to restricted circulation. Shallow sub tidal to supra tidal water depths. | Ooids formed and were deposited in the high-energy inner ramp setting, in shallow subtidal water depths. | Deposited in a mid- to outer-ramp setting, likely below storm wave base. | Deposited in outer-ramp settings, below storm wave base. | Deposited during transgression, in areas of low sedimentation rate, during periods of sea bed erosion, or due to winnowing by nutrient-rich semi-permanent bottom-water currents. |

**Table 1: Albemarle Basin Facies Associations**

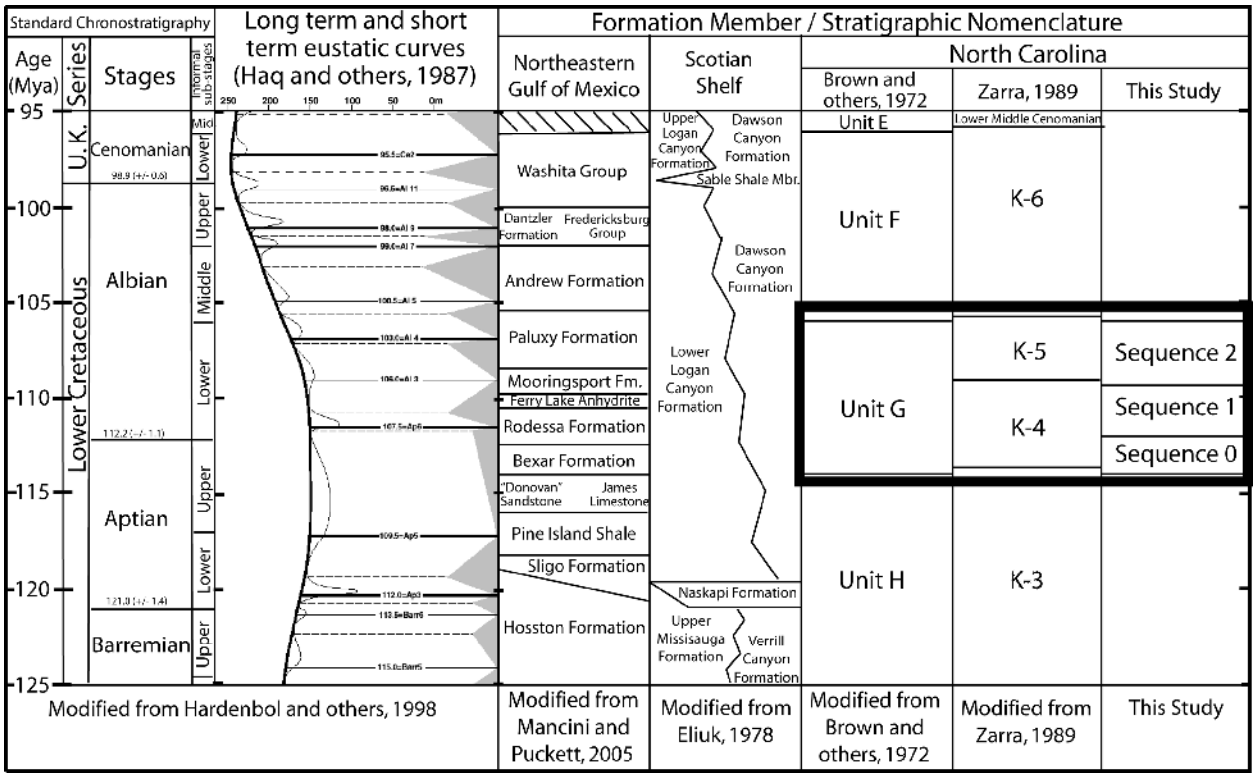


**Figure 2. Regional Stratigraphic framework for the Lower Cretaceous in Eastern North America. The focus interval of this study is shown on the far right.**

The more common, siliciclastic-dominated system (Fig. 3A) consisted of marginal marine environments (lagoons, coastal and delta plains), which graded seaward to open shelf settings. Biostromes consisting dominantly of mollusks (likely rudist bivalves) existed locally on the shallow shelf in areas downdip of the quartzose, sand-dominated shoreface. Proximal to terrigenous point sources, abundant siliciclastic material limited carbonate productivity, resulting in thicker accumulations of siliciclastics. The deep, open shelf setting was dominated by pelagic and hemipelagic sedimentation, typified by shale, diatomaceous shale, planktonic foraminifera-bearing siltstone, and marl in more distal settings.

The carbonate-dominated system (Fig. 3B) was prominent only during the late highstand systems tract of the upper studied sequence (Sequence 1). It consisted of restricted tidal flats and lagoons, which graded seaward to high-energy quartzose sand-bearing, shallow subtidal, ooid shoals and barriers. The system graded basinward to open-marine, mollusc-rich biostrome accumulations of the middle ramp. Mollusc-rich carbonates were periodically reworked by storm and swell waves. As water depth increased, more carbonate mud accumulated, which was reworked with benthic biota to form sediment dominated by mollusks and peloids. In nutrient-rich, deep waters of the outer ramp, bryozoans and brachiopods flourished, resulting in the local deposition of skeletal packstone showing little evidence of reworking. The deep shelf was characterised by marls with abundant planktonic foraminifera. Minor amounts of siliciclastic material were deposited within the carbonate succession; storm mixing processes or longshore drift probably transported this material downdip onto the shelf from sand-rich coastal regions.

During short-term transgressions, much of the siliciclastic material was trapped in updip estuaries (*cf.* Galloway and Hobday 1996), favouring biogenic carbonate production on the open shelf (Milliman *et al.* 1968; Ginsburg and James 1974). Molluscan carbonate production likely was widespread during these periods, with pelagic sedimentation occurring in deep shelf settings. Localised hardground surfaces developed in regions characterised by minor sedimentation and/or bottom scouring by nutrient-rich currents.

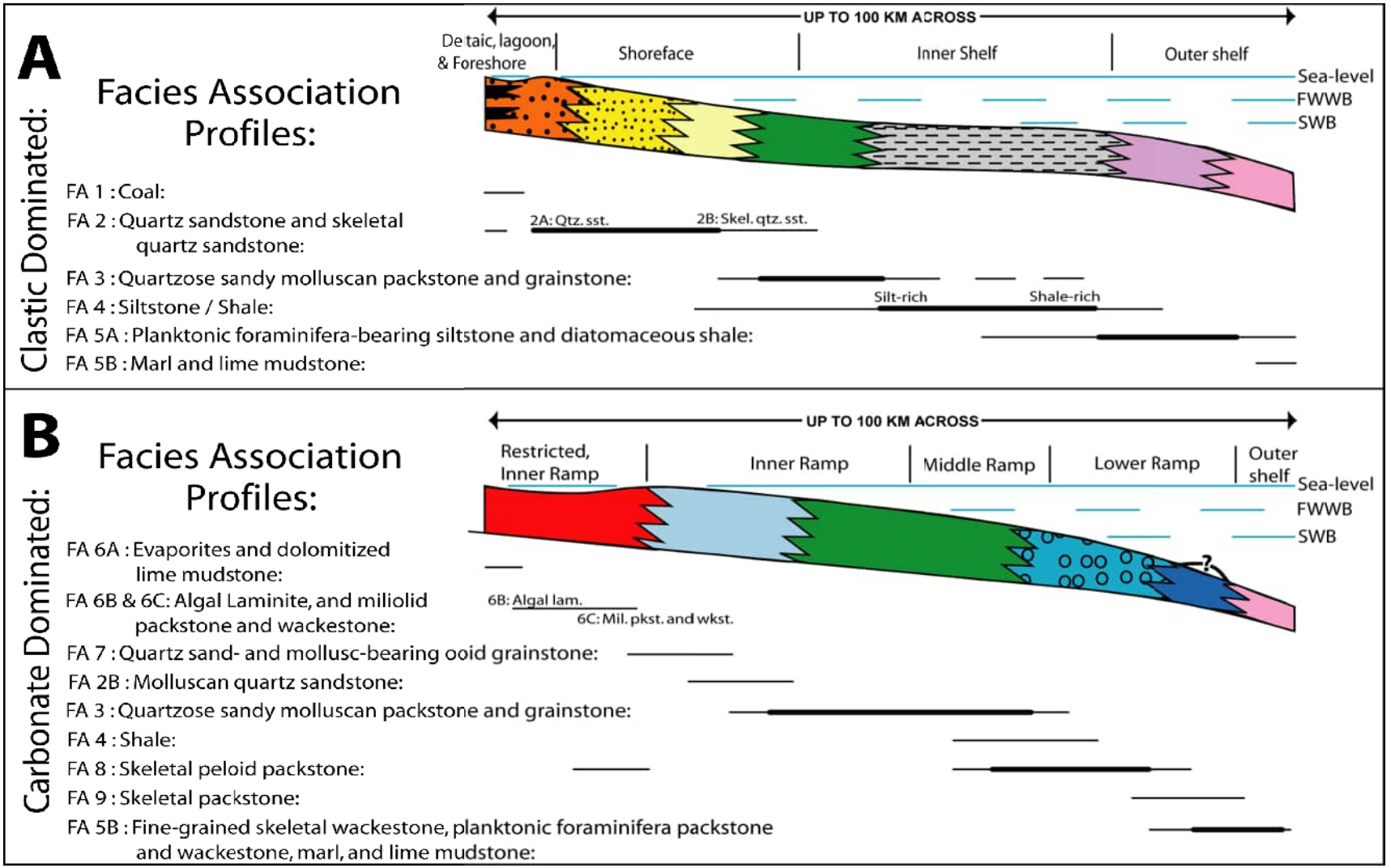


**Figure 3. Generalised facies association profiles of the Early Cretaceous sediments in the Albemarle Embayment of North Carolina. Siliciclastic-dominated sedimentation (profile A) is most common. Carbonates (profile B) accumulated primarily during periods of low siliciclastic input to the shelf, largely during the relative sea-level lowstand transitioning from Sequence 1 to Sequence 2. Shelf setting indicated at top. Heavy lines represent region of maximum accumulation of facies types; light lines represent zone of likely accumulation. Facies association legend can be found on Figure 3**

This study documents a very heavily admixed carbonate-siliciclastic depositional system (Fig. 3). It also corroborates the contention that climate plays a major role in controlling carbonate- versus siliciclastic-dominated sedimentation patterns in times of global greenhouse climate. Arid climate cycles favour carbonate sedimentation, whereas humid climate cycles favour siliciclastic sedimentation (Wilson 1975; Riggs 1984; Read 1995). Sea-level also plays a major role in controlling carbonate versus siliciclastic abundance (Wilson 1975; Martindale and Boreen 1997). However, the late highstand, carbonate-rich sediments of the upper sequence studied demonstrate that relative sea-level falls do not always favour siliciclastic sedimentation.

## Sequence Stratigraphic Summary

Sequence stratigraphic surfaces were identified in a manner similar to that employed by Coffey and Read (2004). Regionally correlatable, upward-shoaling packages 15 to 20 m (50 to 70 ft) thick were identified in all of the studied wells. These packages were interpreted as parasequences; and likely record high frequency changes in relative sea-level. Parasequences were grouped into parasequence sets characterised by either progressive progradational or retrogradational stacking patterns. Sequence boundaries were assigned to the tops of progradational highstand parasequence sets (HST) that sometimes corresponded with downlapping reflectors on seismic data. Maximum flooding surfaces were placed below facies interpreted to record the deepest-water facies association capping transgressive, retrogradational parasequence sets (TST). These surfaces typically coincide with regional seismic reflectors upon which downlaps occur. Lowstand sediments were not identified in the study area (criteria used were shallow-water facies associations occupying a basinal position and wedge-like, onlapping geometries expressed on seismic profiles). If developed, they are believed to be present downdip of the study area. On this basis, transgressive flooding surfaces are considered to closely coincide with the underlying sequence boundaries.

Three third-order sequences were identified, each with a maximum duration of approximately four million years (Fig. 2). The oldest (Sequence 0) is dominated by siliciclastics, with regionally extensive marls and shales marking the maximum flooding surface. The middle sequence (Sequence 1; Fig. 4) is siliciclastic-dominated at the base, but grades into carbonate-dominated facies associations during late highstand conditions. The maximum flooding surface in this interval is seismically traceable in updip regions, but due to either thickness changes or facies transitions, it is not seismically resolvable in basinal areas. The youngest identified sequence (Sequence 2) contains a carbonate-dominated transgressive package that grades abruptly to siliciclastic-dominated associations during the following relative sea-level highstand. The maximum flooding surface is marked by a marl/shale unit in southern regions, and by a thick, diatomaceous marl/shale in the northern regions.

In all sequences, the highstand systems tract is thicker than the transgressive systems tract, and it typically possesses shingled seismic reflectors indicative of strongly progradational sedimentation. A large, carbonate-dominated shelf-margin wedge is suspected to be present downdip, deposited during the time interval spanning the sequence boundary (SB 2.0) separating Sequence 1 and Sequence 2. This is based on the late highstand systems tract of Sequence 1 being carbonate-dominated and capped by evaporites (indicative of restricted conditions downdip of the study area).

The sequence boundaries identified in this project generally correspond to the positions of the sequence boundaries identified by Zarra (1989). However, important differences exist between this and previously-published studies. This study provides a more comprehensive sequence stratigraphic framework that includes major flooding surfaces in addition to the sequence boundaries. This study also identifies a previously unrecognised sequence within the study interval. Most importantly, this study provides valuable depositional and stratigraphic models that incorporate lithologic, biostratigraphic and geophysical datasets from a mixed carbonate-siliciclastic system that developed on an open shelf during a time of global greenhouse climate.

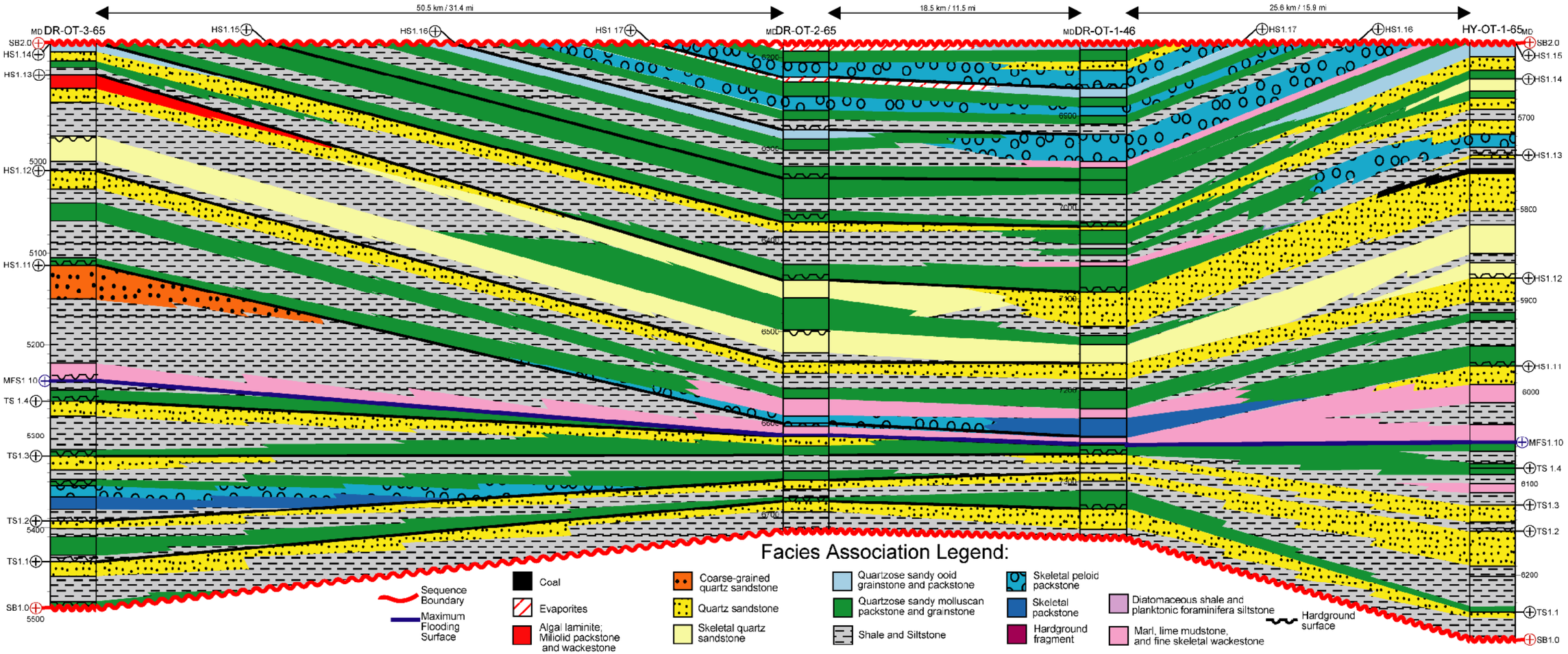


**Figure 4. Interpreted stratigraphic cross section of Sequence 1. Gross correlations were accomplished by incorporating available 2D seismic data; while more detailed correlations were accomplished using Waltherian principles (1894). Surface names are shown at the extreme left and right. Flooding surfaces are black, maximum flooding surfaces are blue, and composite sequence boundaries and transgressive flooding surfaces are red. Orientation of cross section is shown on Figure 1. Facies association legend can be found in Figure 3. Measured depth is displayed (in feet). Section is flattened on the overlying sequence boundary, as this architecture most closely resembled that shown by the seismic reflectors.**

## References


Brown, P.M., Miller, J.A. and Swain, F.M., 1972. Structural and Stratigraphic Framework, and Spatial Distribution of Permeability of the Atlantic Coastal Plain, North Carolina to New York, Washington, Geological Survey Professional Paper, v.796, 79p.

Coffey, B.P., and Read, J.F., 2004. Mixed carbonate-siliciclastic sequence stratigraphy of a Palaeogene transition zone continental shelf, southeastern USA: Sedimentary Geology, v.166, p.21-57.

Eliuk, L.S., 1978. The Abenaki Formation, Nova Scotia Shelf, Canada – A depositional and diagenetic model for a Mesozoic carbonate platform: Bulletin of Canadian Petroleum Geology, v.26, n.4, p.424-514.

Galloway, W.E., and Hobday, D.K., 1996. Terrigenous Clastic Depositional Systems, Applications to Fossil Fuel and Groundwater Resources, New York, N.Y., USA, Springer, second edition, 489p.

Ginsburg, R.N., and James, N.P., 1974. Holocene carbonate sediments of continental shelves. *In:* C.A. Burk, and C.L. Drake, eds., The Geology of Continental Margins, New York, Springer-Verlag, p.137-155.

Hardenbol, J., Thierry, J., M.B. Farley, M.B., Jacquin, Th., De Graciansky, P.C. and P.R. Vail, 1998. Mesozoic and Cenozoic Sequence Chronostratigraphic Framework of European Basins. *In:* P.-C. De Graciansky, J. Hardenbol, Th. Jacquin, and P.R. Vail, eds., Mesozoic and Cenozoic Sequence Stratigraphy of European Basins, SEPM Special Publication 60, CD-ROM.

Haq, B.U., Hardenbol, J., and Vail, P.R., 1988. Mesozoic and Cenozoic chronostratigraphy and eustatic cycles. *In:* Wilgus, C.K., Hastings, B.S., Kendall, C.G.S.C., Posamentier, H.W., Ross, C.A., and Van Wagoner, J.C., (eds.), Sea-Level Changes: An Integrated Approach, SEPM Special Publication No. 42, p.71-108.

Mancini, E.A., and Puckett, T.M., 200., Jurassic and Cretaceous Transgressive-Regressive (T-R) Cycles, Northern Gulf of Mexico, USA: Stratigraphy, v.2, n.1, p.31-48.

Martindale, W., and Boreen, T.D., 1997,. Temperature-stratified Mississippian carbonates as hydrocarbon reservoirs – examples from the foothills of the Canadian Rockies. *In:* N.P. James, and J.A.D. Clarke, eds., Cool-Water Carbonates, Tulsa, Oklahoma, Society for Sedimentary Geology, SEPM special publication no. 56, p.391-409.

Milliman, J.D., Pilkey, O.H., and Blackwelder, 1968. Carbonate sediments on the continental shelf, Cape Hatteras to Cape Romain, Southeastern Geology, v.9, p.245-267.

Poag, C.W., 1982, Stratigraphic reference section for Georges Bank Basin – Depositional model for New England passive margin: The American Association of Petroleum Geologists Bulletin, v.66, n.8, p.1021-1041.

Poag, C.W. and Valentine, P.C., 1988, Mesozoic and Cenozoic stratigraphy of the United States Atlantic continental shelf and slope. *In*: R.E. Sheridan, and J.A. Grow, eds., The Atlantic Continental Margin, U.S., The Geology of North America, Vol. I-2,: Geological Society of America, Boulder, p.67-85.

Read, J.F., 1995. Overview of carbonate platform sequences, cycle stratigraphy and reservoirs in greenhouse and ice-house worlds. *In:* J. F. Read, C. Kerans, L.J. Weber, J.F. Sarg, and F.M. Wright, eds., Milankovitch Sea-Level Changes, Cycles, and Reservoirs on Carbonate Platforms in Greenhouse and Ice-House Worlds, SEPM Short Course No.35., p.1-102.

Riggs, S.R., 1984. Paleoceanographic model of Neogene phosphorite deposition, U.S. Atlantic Continental Margin, Science, v.223, n.4632, p.123-131.

Vigil, D.L., 1998. North Carolina/Minerals Management Service Technical Workshop on Manteo Unit Exploration: February 4-5, 1998, OCS Study MMS 98-0024, U.S. Dept. of the Interior, Minerals Management Service, Gulf of Mexico OCS Region, New Orleans, 168p.

Wilson, J.L., 1975. Carbonate Facies in Geologic History, New York, Springer-Verlag, 471p.

Zarra, L., 1989. Sequence Stratigraphy and Foraminiferal Biostratigraphy for Selected Wells in the Albemarle Embayment, North Carolina: North Carolina Geological Survey, Open-File Report 89-5, 48p.


**BACK**

# Distribution of Diagenetic Minerals in Lower Cretaceous Sandstones within a Depositional Facies and Sequence Stratigraphic Framework: Glenelg, Thebaud, and Chebucto Fields, Offshore Scotian Basin

**Atika Karim**
**Georgia Pe-Piper**
Saint Mary's University
Department of Geology
Halifax, Nova Scotia, B3H 3C3
Canada
e-mail: atika.karim@smu.ca

**David J.W. Piper**
Geological Survey of Canada-Atlantic
P.O. Box 1006
Dartmouth, Nova Scotia, B2Y 4A2
Canada

## ABSTRACT

The spatial and temporal distribution of diagenetic cements has been constrained in relationship to lithofacies and sequence stratigraphy of the Lower Cretaceous sandstones from the Glenelg, Chebucto, and Thebaud fields in the Sable sub-basin. Quartz and lithic grains coated with illite and chlorite occur in transgressive systems tracts (TST) in Glenelg N-49 and Thebaud I-93, and are cemented by Fe-calcite. Early kaolinite occurs as booklets and vermicular stacking textures principally in sandstones immediately beneath the TSTs, particularly in cross-bedded, coarse-grained, channel sandstones. Illite occurs as fibrous crystals, which in the Chebucto K-90 are included by ankerite. Fe-rich chlorite rims, found only in the Thebaud samples, have developed from earlier Fe-rich clay.

Pore-filling chlorite occurs in contact with detrital quartz grains on which diagenetic quartz cement has not developed. This chlorite is commonly associated with illite. Quartz cement, well developed in medium- and coarse-grained sandstones, postdates kaolinite and predates most other cements. Calcite, Fe-calcite, Mg-calcite, ankerite and siderite are the major cementing minerals in the studied wells. In Glenelg H-59, two siderite cements were defined; the earlier one occurs in TSTs as large, corroded crystals and is low in Mg. The late microcrystalline siderite (< 10 μm) is Mg-rich (~ 9 wt.%). It forms the tiny crystals that fringe detrital grains and fill intercrystalline micropores. Early calcite cement is found principally in bioturbated sandstones and mudstones with bioclasts, typical of the highstand systems tract (HST). In samples from the Glenelg field, perthite is replaced by Fe-calcite. Late framboidal pyrite in carbonate cement indicates burial under both reducing and alkaline conditions. Rare traces of francolite (1 to 6 wt.% $P_2O_5$) are found in the Glenelg wells associated with illite and calcite cements.

This study demonstrates that the distribution of diagenetic minerals and their impact on reservoir-quality evolution can be better elucidated when linked to a sequence stratigraphic framework.

BACK

# Hyperpycnal River Floods and the Deposition of Lower Cretaceous Sands, Scotian Basin

**David J.W. Piper**
Geological Survey of Canada-Atlantic
P.O. Box 1006
Dartmouth, Nova Scotia, B2Y 4A2
Canada
e-mail: dpiper@nrcan.gc.ca

**Atila Karim**
**Heidi Pratt**
**Ryan Nftall**
**Kathleen Gould**
**James Foley**
**Georgia Pe-Georgia**
Saint Mary's University
Department of Geology
Halifax, Nova Scotia, B3H 3C3
Canada

## ABSTRACT

The large supply of sand that reached the Scotian basin in the latest Jurassic and early Cretaceous resulted from tectonic reactivation and erosion of the Appalachian hinterland. The rivers that transported this sediment were steep and braided, based on sediment calibre and sedimentary structures preserved in the Chaswood Formation. Such rivers have the propensity to discharge hyperpycnally during floods. The importance of such hyperpycnal flows can be evaluated from sedimentological criteria in conventional core.

Thick-bedded reservoir sandstones from fields such as Thebaud and Venture appear to be inner shelf hyperpycnal deposits (facies 9), forming graded sandstone beds decimetres to metres thick, with Bouma Ta-Tc sequences, abundant phytodetritus, detrital intraclasts of mudstone and siderite, and minor bioturbation at the top of beds. This facies passes stratigraphically upward into tidally influenced river-mouth and river-channel sandstones (facies 4) and downward into thinner, graded sandstone beds with interbedded mudstone (facies 0). Highly bioturbated thin-bedded sandstones (facies 2) in places show hummocky cross-stratification, concentration of shells at the base of beds, and wave-ripples, suggestive of storm reworking. In the Glenelg field, tidally-influenced hypopyncal silts interbed with hyperpycnal sands and both change character distally. Turbidites in the middle Missisauga Formation in the Tantallon M-41 well show petrography and sedimentary structures that indicate deposition from overbank hyperpycnal flows.

Exploration models for the Scotian basin must take account of this reinterpretation of the major sandstone facies. The presence of widespread hyperpycnal flows means that there may have been a major transfer of sand to deep water. The rapid deposition of hyperpycnal flow sands, overlain by slowly sedimenting transgression surfaces, may have strongly influenced the style of early diagenesis and the neoformation of iron-rich clays that transformed on burial to chlorite rims.

BACK

# River Source and Dispersion of Lower Cretaceous Sands Scotian Basin

**Georgia Pe-Piper**
**Stavros Triantafyllidis**
Saint Mary's University
Department of Geology
Halifax, Nova Scotia, B3H 3C3
Canada
e-mail: georgia.pe-piper@smu.ca

**David J.W. Piper**
Geological Survey of Canada-Atlantic
P.O. Box 1006
Dartmouth, Nova Scotia, B2Y 4A2
Canada

## ABSTRACT

Understanding the source and dispersion of Lower Cretaceous deltaic sandstones is important for predicting (1) the distribution of sandstone; (2) the availability of quartz; and (3) regional variation in diagenesis. Many analytical techniques to identify sediment provenance have been applied to samples from conventional cores from the offshore Naskapi N-30 well in the west to the Dauntless D-45 well in the east. The results were compared with similar analyses of onshore Chaswood Formation samples.

Geochronology of detrital monazite shows several modes: ~330 and ~400 Ma at the Naskapi N-30 well; ~400 Ma in wells from the Alma field to the Venture field, with minor ~1.0 and ~1.65 Ga modes; and predominant ~1.0 and ~1.8 Ga modes at the Peskowesk A-99 well, with a minor ~380 Ma mode. Detrital zircons show similar modes. However, the ~1.0 Ga mode predominates from the Alma field to the Venture field, and an additional ~650 Ma mode is present. Morphology and texture show that 45-80% of detrital zircon is of first cycle igneous origin, with the proportion of polycyclic zircon decreasing stratigraphically upward. Sources of monazite and zircon are further constrained by mineral chemistry. Variation in abundance and chemical composition of heavy minerals, notably chromite, tourmaline and garnet, has been determined.

Bulk-rock geochemistry provides information on the total source area, whereas mineralogical studies emphasize source rocks containing heavy minerals. The Ti content of Scotian basin shales is almost double the world average due to detrital ilmenite. Fe is also abundant and Ca very low. Sandstones show geochemical variability within the basin; however, shales are more uniform geographically.

The integration of this data suggests that the Naskapi N-30 well was supplied by a river that also furnished sediment to the Chaswood Formation in central Nova Scotia. The sands in the area from the Alma field to the Venture field were sourced from a major river draining Newfoundland. Sandstones on the eastern Scotian Shelf were sourced by one or more separate rivers, also draining Newfoundland.

BACK

# NOTES

# Session 2C:
# PETROLEUM SYSTEMS

Husky Energy

## KEYNOTE ADDRESS


**PETROLEUM SYSTEMS DEVELOPED ALONG THE NW AFRICA OFFSHORE MARGIN: CHALLENGES FACING EXPLORATION & PRODUCTION COMPANIES**
**Chaney, Alistair John**

**CONTROLS ON FACIES DISTRIBUTION AND RESERVOIR DEVELOPMENT OF UPPER TRIASSIC RIFT CONTINENTAL SYSTEMS IN INTERMONTANE RIFT SETTINGS: A COMPARATIVE STUDY OF EXTENSIVE OUTCROPS IN SW MOROCCO**
Redfern, Jonathan; Mader, Nadine; Fabuel Perez, Ivan; Hodgetts, David and El Ouataoui, Abedelmajid

**FUTURE PROSPECTS OF OIL AND GAS WITHIN SELECTED TARGET AREAS OF SCOTIAN SHELF AND SLOPE, OFFSHORE NOVA SCOTIA, EASTERN CANADA: EVALUATION BASEDON PETROLEUM SYSTEMS RISK ASSESSMENT**
Prasanta K., Mukhopadhyay (Muki) and Harvey, Paul, J.

**CONTINENTAL RIFT BASIN FILLS: EVOLUTION FROM OPENED TO CLOSED STAGE (WOLFVILLE/ BLOMIDON FM, NOVA SCOTIA)**
Leleu, Sophie

**PERMO-TRIASSIC BASINS FROM IRELAND TO NORWAY: BASIN ARCHITECTURE AND CONTROLS**
Stolfova, Katerina and Shannon, Patrick M.

**EARLY INFILL OF THE TRIASSIC FUNDY BASIN: ARCHITECTURE OF THE WOLFVILLE FORMATION AND FLUVIAL EVOLUTION**
Leleu, Sophie; Hartley, Adrian J.; Jolley, David W. and Williams, Brian P.J.

**RESERVOIR QUALITY, DIAGENETIC HISTORY AND PROVENANCE OF THE LATE TRIASSIC SANDSTONES OF THE WOLFVILLE FORMATION, BAY OF FUNDY, NOVA SCOTIA, CANADA**
Kettanah, Yawooz; Kettanah, Muhammad and Wach, Grant D.


**BACK**

# Petroleum Systems Developed Along the Northwest African Offshore Margin: Challenges Facing Exploration & Production Companies

**Alistair Chaney**
Tullow Oil Plc
3rd Floor, Building 11, Chiswick Park
566 Chiswick High Rd.
London, W4 5YS
United Kingdom
e-mail: Alistair.Chaney@Tullowoil.com

## ABSTRACT

The offshore NW African Atlantic margin extends from northern Morocco to the Guinea Fracture Zone in the south and comprises up to 6km of Mesozoic and Cenozoic siliciclastics and carbonates overlying Triassic salt.

The primary source rocks are Albian, Cenomanian and Turonian mudrocks, with lesser contributions from Palaeocene intervals that are thought to have reached marginal maturity in some areas, and restricted Liassic shelfal carbonates. Deep water gravity deposits provide the main reservoirs and include confined canyon systems and unconfined turbidite lobes. Less well explored plays include carbonate reefs and deltaic topsets further up-dip. The most prominent trapping mechanism along the length of the NW African margin is related to halokinesis. Allochthonous salt diapirs and canopies (largely absent from offshore Western Sahara, Senegal, Gambia and Guinea Bissau) have generated proven and unproven traps including sub-salt, salt stock, and supra salt closures. Other trapping mechanisms include tilted fault blocks (some are counter regional faults), stratigraphic pinchout (*e.g.* Banda gas discovery), extensional roll-over folds, and toe trust compressional folding.

The under explored nature of the NW African Atlantic margin provides E&P companies with numerous challenges. The relative lack of well control makes prediction of sandstone problematic, particularly as many of the canyons appear to be by-pass systems. Where geobodies have been mapped, the low quality of seismic data often makes it difficult to differentiate with confidence between prospective sheet turbidite sandstones and reservoir-poor debrites, particularly in the deeper Cretaceous section. Other pitfalls have recently come to light after drilling. These include reef-like morphologies along the carbonate platform break of slope that are possibly contourites of siliceous ooze, and bright seismic amplitude anomalies that are not hydrocarbon filled sands, but low velocity shales.

These challenges are generally prospect specific, but there are further difficulties which relate to the cost of exploration in immature basins. Increasing water depth places restrictions on rig availability, and requires increasingly larger prospects to be considered commercially viable. As the restrictions imposed by the water depth drive companies to explore deeper in the basin it becomes more likely that prospects will be overpressured as they are in other deep passive margins (*e.g.* Nigeria, Borneo). This will only increase well costs, placing still greater pressures on commerciality.

## Introduction

The conjugate margins of the northwest African plate and the corresponding American plate are excellent examples of passive margins. By and large, the structural and sedimentological evolution along the offshore northwest African Atlantic margin from north Morocco to the Guinea Fracture Zone in the south is extremely consistent (Figs. 1, 2). The offshore basins tend to be larger and preserve a thick succession of Mesozoic and Cenozoic sediments recognisable anywhere along the passive margin of northwest Africa, compared to the smaller, more tectonically complex onshore marginal counterparts. The

northwest African basins were created during the continental break-up and development of the Atlantic Ocean, and as a result share a similar basin fill to the conjugate equivalent basins of Nova Scotia (Fig. 2) and the east coast of the United States (Davison 2005).

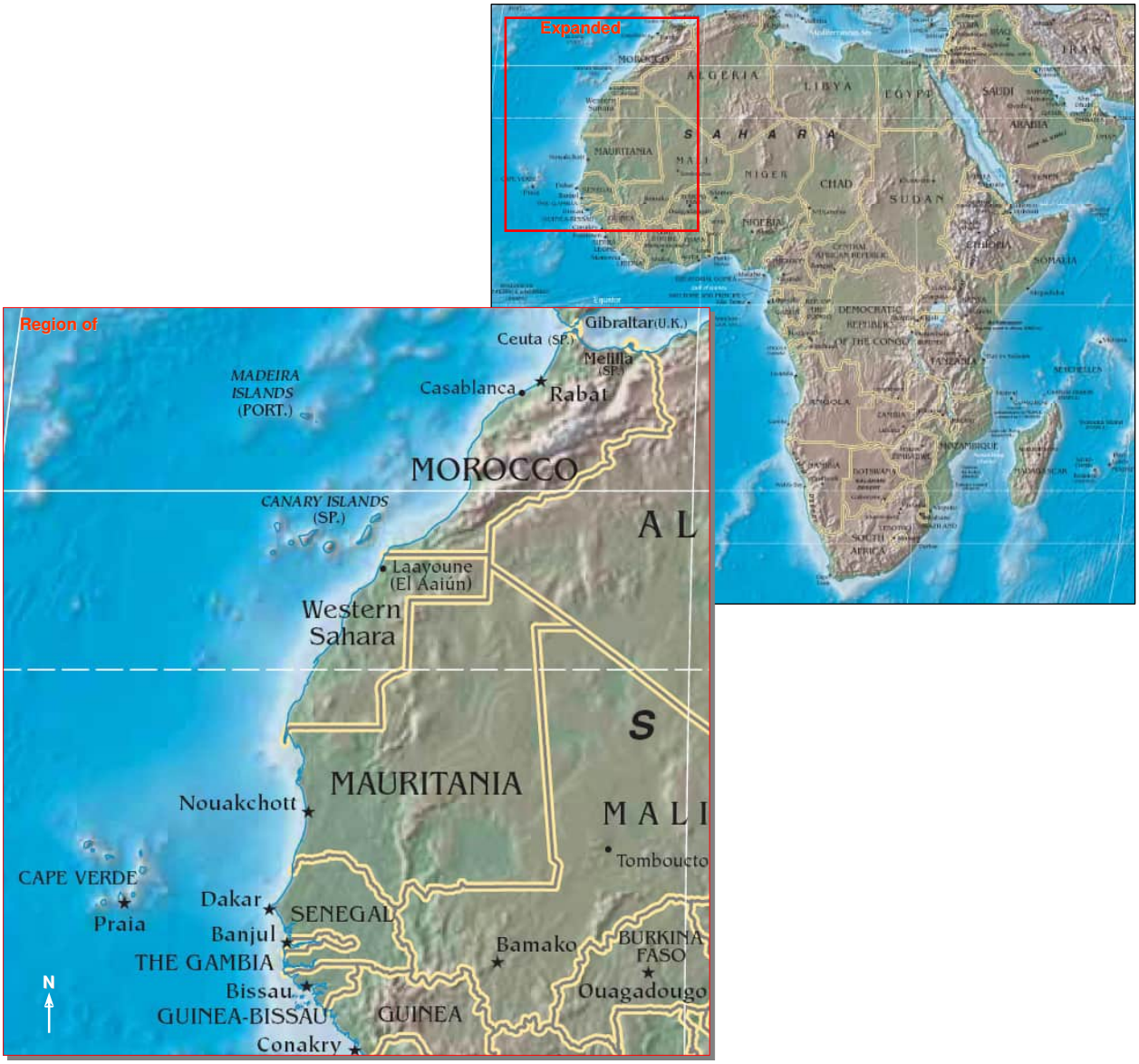


**Figure 1. Location map of northwest African coastline and countries.**

Break-up was initiated with continental rifting in the late Triassic to early Jurassic (Scotese 2008, Davison, 2005 and Tari *et al.* 2003) which, with continued extension, resulted in oceanic spreading and the formation of the proto-Atlantic around 180-170 Ma (Davison 2005). It was during the last stages of the early rift phase that thick sequences of evaporites were deposited in many of the rift basins along the NW African margin during the early Jurassic (Tari *et al.* 2003).

The earliest deposition in the offshore basins is inferred from well data in the onshore Essaouira Basin of Morocco where the syn-rift basinal fill has been defined as Triassic continental red-beds overlain by Liassic evaporates (Davison 2005, Vear 2005 and Hafid 2000). Continued extension led to a marked change in depositional environment as the proto-Atlantic flooded the early rift basin in the Middle

Jurassic This led to the deposition of extensive marine shales and the development of a prominent carbonate platform which can be traced almost continuously along the entire northwest African margin. Ongoing extension during the Cretaceous and Tertiary led to the deposition of up to 6 km of clastic deep water, deltaic and shoreface sediments (Fig. 3). It is this huge accumulation of marine and marginal marine deposits that have generated the petroleum systems currently being explored.

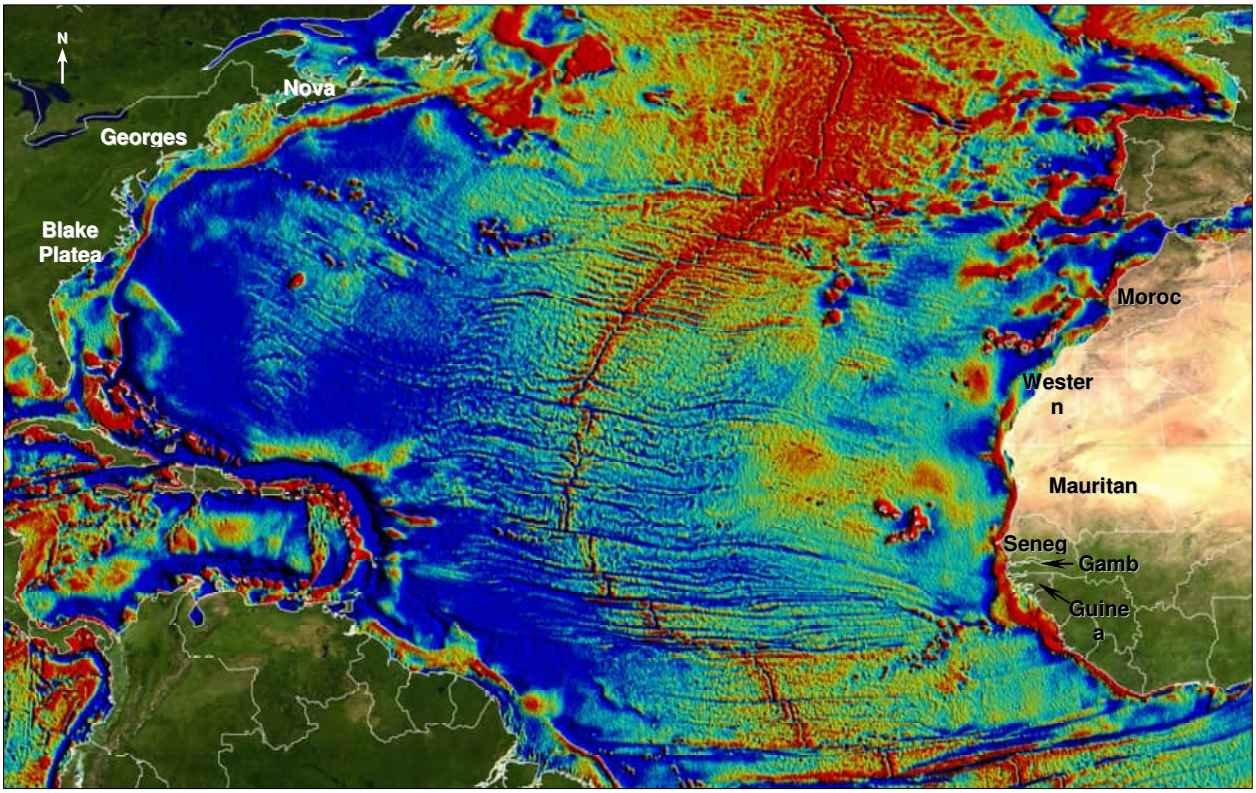


**Figure 2. Free air gravity map of Atlantic Ocean illustrating the conjugate equivalents of northwest Africa are the eastern United States and Nova Scotia.**

## Sedimentological Evolution of the NW African Margin

There is no record or well penetrations of the earliest Triassic-Jurassic syn-rift sediments deposited in the offshore rift basins. The age and style of deposition has been inferred from wells that have drilled the onshore Essaouira Basin in Morocco. Outcrop observations describe the basal syn-rift infill as continental red-bed conglomerates, sandstones and claystones of Late Triassic age (Brown, 1980). The most complete sub-surface stratigraphy was penetrated in the JRP-1 well (Davison 2005) and the in-situ salt encountered was dated as early Jurassic. Although there are other well penetrations that encountered evaporate sequences along the northwest African margin, it is all allochthonous salt.

The Middle Jurassic was dominated by marine shales which are overlain by an extensive carbonate bank, which can be traced, almost unbroken, along the whole of the NW African continental margin (Vear 2005 and Davison 2005). This appears to mark a major transgression of the proto-Atlantic as rifting and continental break-up progressed. The arid conditions that generated the syn-rift red-bed sequences created a sediment starved margin favourable for the deposition of a significant carbonate platform once there was ingression of marine conditions (Vear 2005). The carbonate system lasted from the Late Jurassic to the Valanginian, when exposure and subsequent flooding terminated carbonate development along the entire margin. Exposure of the carbonate bank has in many places generated karst weathering, which has important implications for reservoir development.

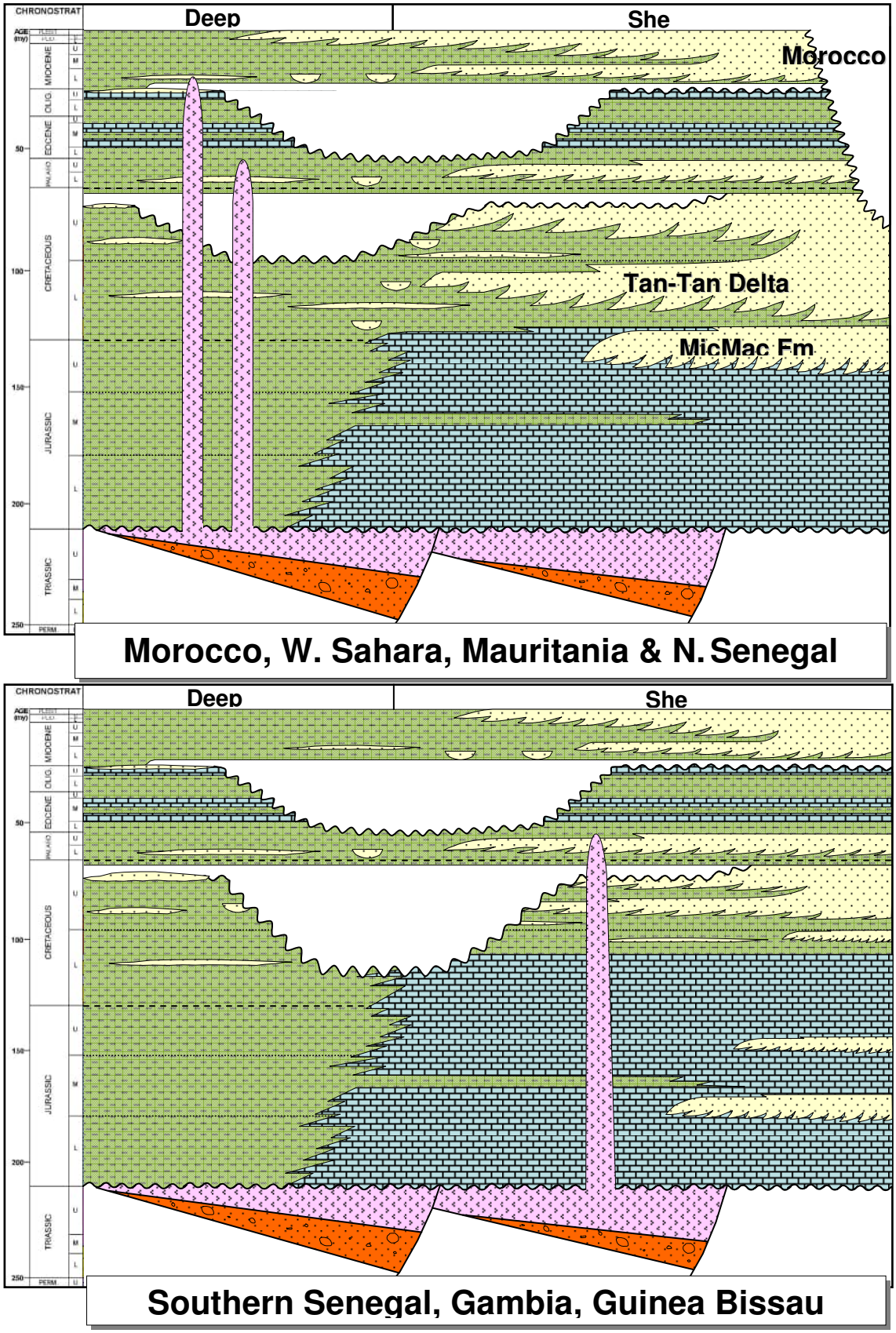


**Figure 3. Stylised stratigraphic columns for the northwest African offshore passive margin.**

The end of carbonate build-up is marked by the onset of almost continuous clastic deposition. Deep marine conditions prevail to the west, with inferred deltaic and shoreface development probably controlled by the buried carbonate bank break of slope. The extent of Early Cretaceous delta and shoreface progradation is inferred from the existence of deep water turbidites further westwards. The westward extent of the shoreline systems is unknown as there are few proximal wells that have drilled deep enough, and the seismic resolution is not sufficient to pick out any clinoformal features.

From onset of clastic deposition in the Early Cretaceous to the end of the Tertiary, sedimentary evolution along the length of the passive margin has been punctuated by significant regional flooding events (such as the Albian-Aptian and Cenomanian-Turonian) and numerous low-stand events, which are marked by laterally extensive unconformities, prominent canyons and turbidite development downdip.

## Context and Comparison

On the face of it, it may appear that the development of passive margin sedimentation and the structural evolution along the northwest African margin can be compared directly to the rest of West Africa and the corresponding passive margin sediments on the American plate. Whilst there are similarities, there are also some fundamental and important differences in evolution, and therefore relevance to direct comparison.

Evaporite development in the basins of northwest Africa is older (Triassic to early Jurassic) than the larger salt deposits that dominate the southern conjugate Atlantic margin in Brazil and Angola. Evaporite sedimentation in northwest Africa was restricted to the relatively small early syn-rift basins. By comparison, evaporite deposition across the southern margin was Aptian in age and during the post-rift thermal subsidence phase of margin evolution (Tari *et al*. 2003). The primary difference, therefore, is that the salt deposits along the northwest African margin are less extensive and not as thick as the younger accumulations further south. The result is that halokinesis on the southwest African margin is far more intense, and wide spread, generated by large scale basinward sliding of the post-rift sediments along a decollement of the mobile evaporite units. Whilst similar passive margin down-slope sliding and halokinesis is present along the northwest African margin, it is less prevalent than the prolific hydrocarbon basins of the southwest African margin (Fig: 4).

A second consideration when comparing the northwest and southwest Atlantic hydrocarbon basins is post-rift sediment supply. The basins along the southwest margin have been infilled by very large, long lived deltaic systems, fuelled by a humid climate. By comparison, the northwest margin has only developed significant deltas periodically throughout the Cretaceous and Tertiary, which has resulted in a petroleum system that is sparser in terms of reservoir and source rock development. It is quite possible that this is a result of a more arid climate as North Africa began to dry, ultimately forming the Sahara Desert. As a consequence, exploration of the larger basin of the southwest Atlantic margin is more advanced when compared to that of the northwest Atlantic conjugate basins.

Differences in the climatic evolution across the northwest Atlantic are important in terms of direct comparison between the two conjugate margins. This is most evident when comparing the reservoir development of the Tarfaya Basin (Morocco) and the Scotian Basin (Canada), which are conjugate equivalents (Fig. 2 and 5). Delta and shoreface progradation in the Scotian Basin has been largely continuous from the late Jurassic with the deposition of the Mohawk and Mic Mac formations to the present day, with occasional, but significant regional transgressions throughout the post-rift period. In contrast, the Tarfaya Basin is characterised by discrete pulses of delta progradation (such as the Tan Tan Delta of the Early Cretaceous) directly attributed to individual tectonic events (Fig. 6). Given that the evolution of the two basins is coeval and structurally very similar, one explanation for this difference is a marked variation in climatic evolution, with the southwest Canadian margin remaining temperate, and the northwest African margin becoming arid, resulting in the creation of the Sahara Desert. The driving force for this difference is the relative plate movement as the Atlantic Ocean formed. The American plate drifted into more northerly latitudes while north Africa remained just north of the equator throughout the Cretaceous and Tertiary (Scotese 2008, and Blakey 2005) (Fig. 7).

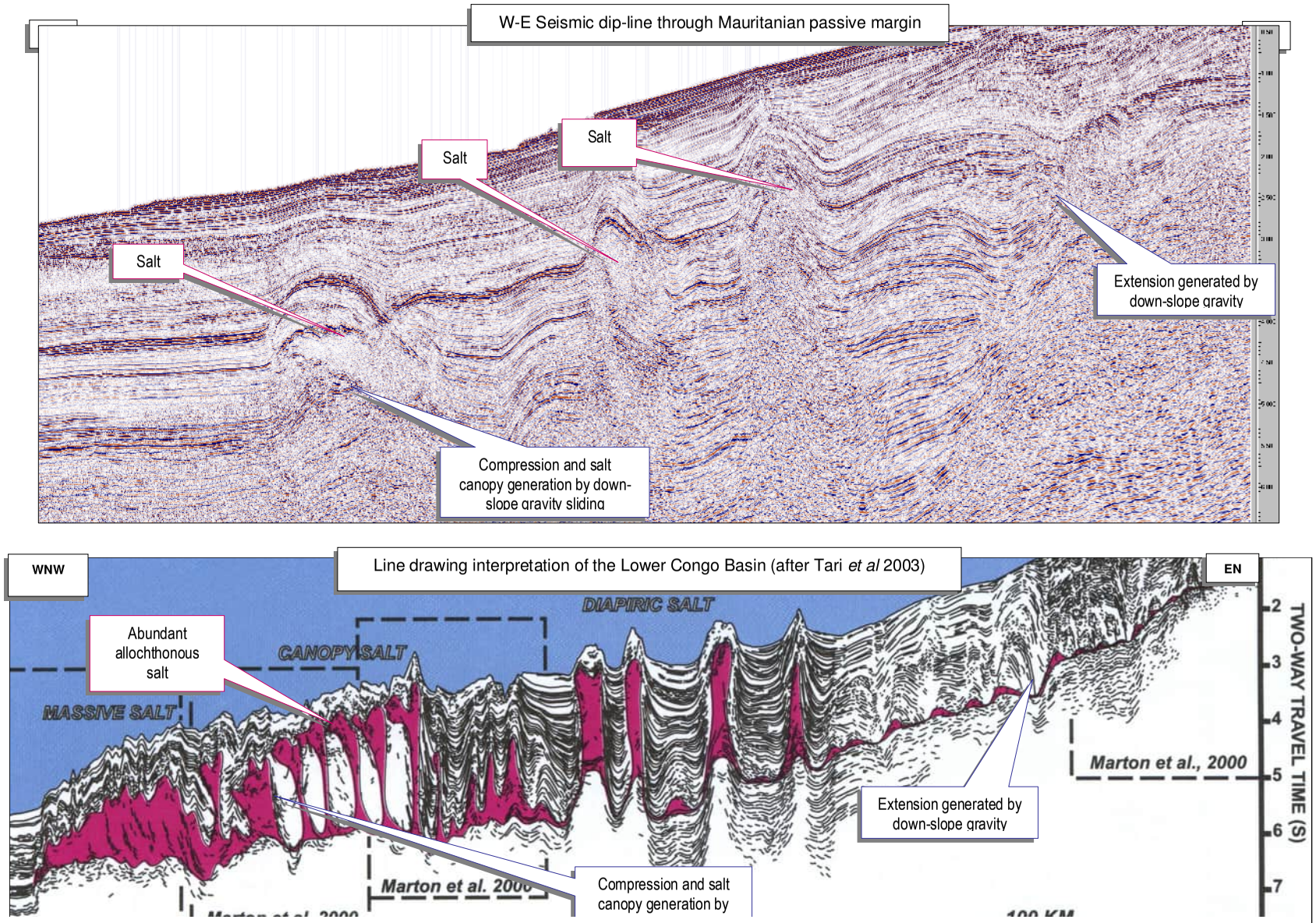


**Figure 4. Comparison of seismic lines between offshore Mauritania and Lower Congo Basin, illustrating the difference and density of halokinesis and downslope gravity sliding between the northwest and southwest African margins (Congo section after Tari *et al.* 2003).**

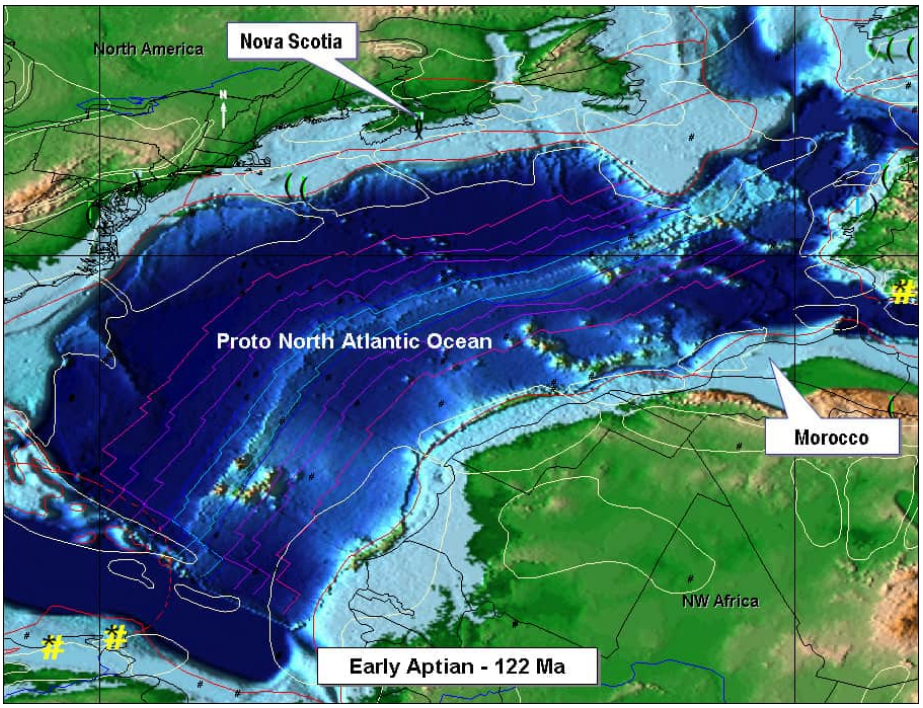


**Figure 5. Detail of Atlantic opening plate reconstruction demonstrating the conjugate nature of the Scotian Basin in Canada and the Tarfaya Basin in Morocco. (Modified after, Scotese ©2008, PALEOMAP Project).**

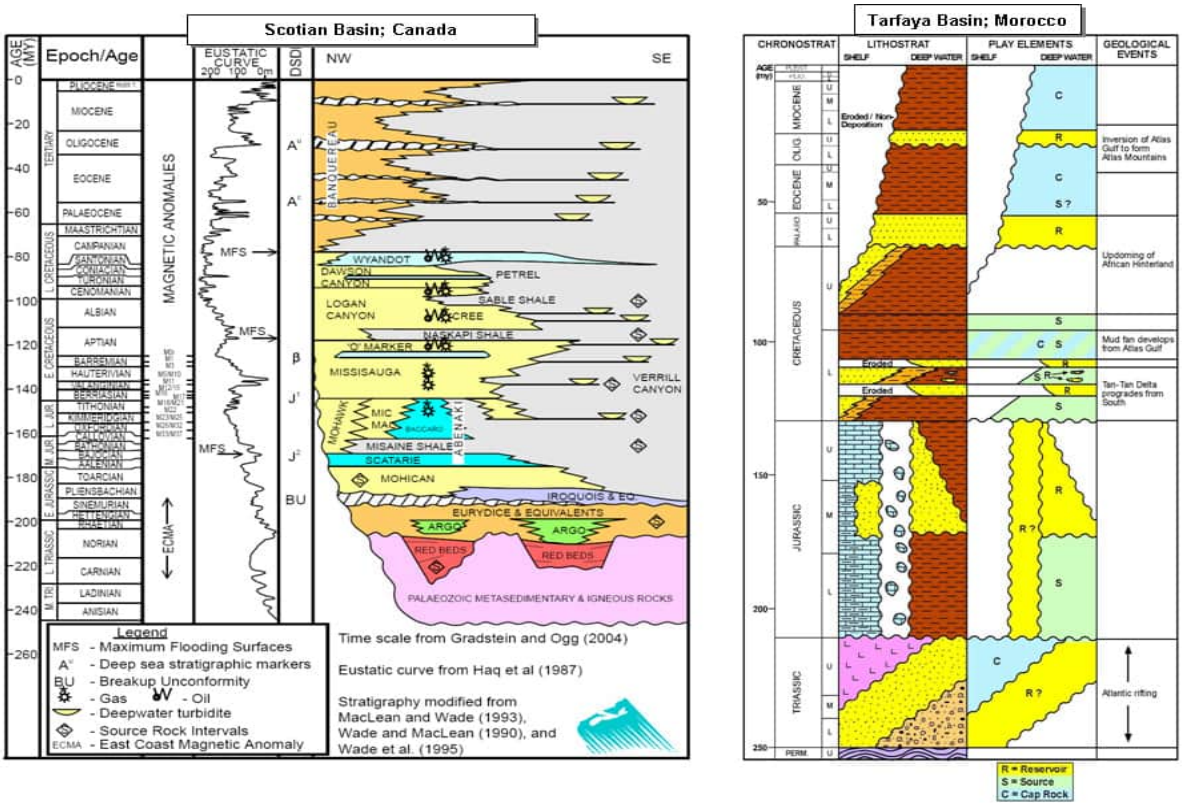


**Figure 6. Comparison of Scotian Basin and Tarafaya Basin stratigraphic columns to illustrate the difference in respective longevity of shelfal deposystems during the Cretaceous and Tertiary. (Scotian Basin after Kidston *et al.* 2005).**

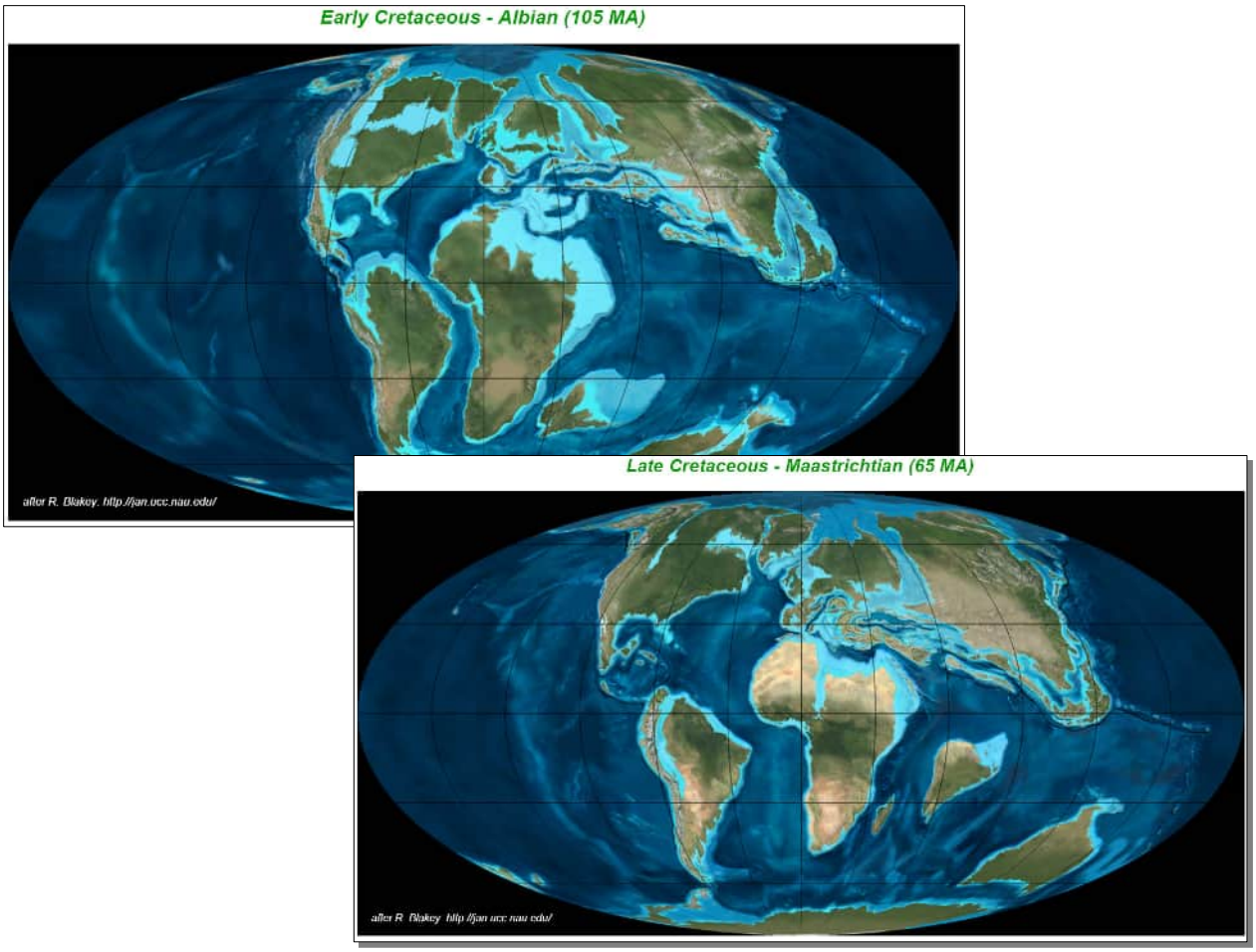


**Figure 7. Plate reconstructions for the Cretaceous. Note the relative latitude of northwest Africa to those Atlantic margin basins that have had long lived deltaic systems during the Cretaceous and Tertiary (*e.g.* Nova Scotia, Angola, Nigeria and Brazil). This reconstruction suggests that desertification of northern Africa is well advanced by the end of the Cretaceous.**

## The Petroleum System

### Source Rocks

The primary source rocks are Cretaceous in age, with the Albian, Cenomanian and Turonian mudrocks being the major contributors. The Cenomanian-Turonian interval is the proven source across much of northern and northwest Africa, with TOC ranging from 2-31% (Luning 2003). There are, however, other shales of various ages that have a high organic content, and given the correct burial depth are also productive. Secondary source rocks include some highly organic rich Palaeocene intervals that are thought to have reached marginal maturity where burial has been sufficient. Restricted Liassic shelfal carbonates inboard of the Jurassic carbonate platform edge are thought to have charged the Cap Juby oil discovery in Morocco (Vear 2005, Davison 2005, and Jarvis 1999) as well as oil shows in the Ras el Baida–A1 well in Block 8 of Mauritania and possibly the Wolof-1 well in Senegal (Vear *ibid.*). Charge is usually not problematical, with hydrocarbons encountered throughout the Cretaceous and Tertiary reservoirs. There are, however, some areas which are believed to be within migration shadows.

## Reservoir Development and Seal

Changing sea-level during the development of the Cretaceous and Tertiary sequences has generated a regular supply of sand into the deepening Atlantic basin. Downdip these are gravity deposits, which can be confined within canyons or unconfined basin-floor fans and slope-channel complexes deposited during progradational episodes. Closer to shore, there is extensive development of high net-to-gross deltaic and shoreface systems, which, given favourable trapping geometries in the older sediments, have been proven to be a valid play in southern Senegal and Guinea Bissau. Compared to other petroleum systems along the Atlantic margin, the basins of northwest Africa are relatively reservoir poor, in that deposition has been restricted to episodic pulses of coarse clastic material (often related to tectonic uplift), rather than continuous sedimentation from long lived deposystems. As a result, the development of deep water gravity driven deposits and the associated updip feeder systems is localised, rather than ubiquitous along the entire continental margin. Furthermore, in some cases (*e.g.* parts of Mauritania) it appears that the palaeo-basin floor, during the Tertiary in particular, is further outboard than other regions and thus the deposition of potential basin floor fans is beneath water depths beyond the reach of conventional exploration limits. The prominent feeder canyons to a more distal basin floor are within easy exploration limits, but represent deposition on the continental slope and in some cases act as by-pass conduits bringing sediment to the basin floor.

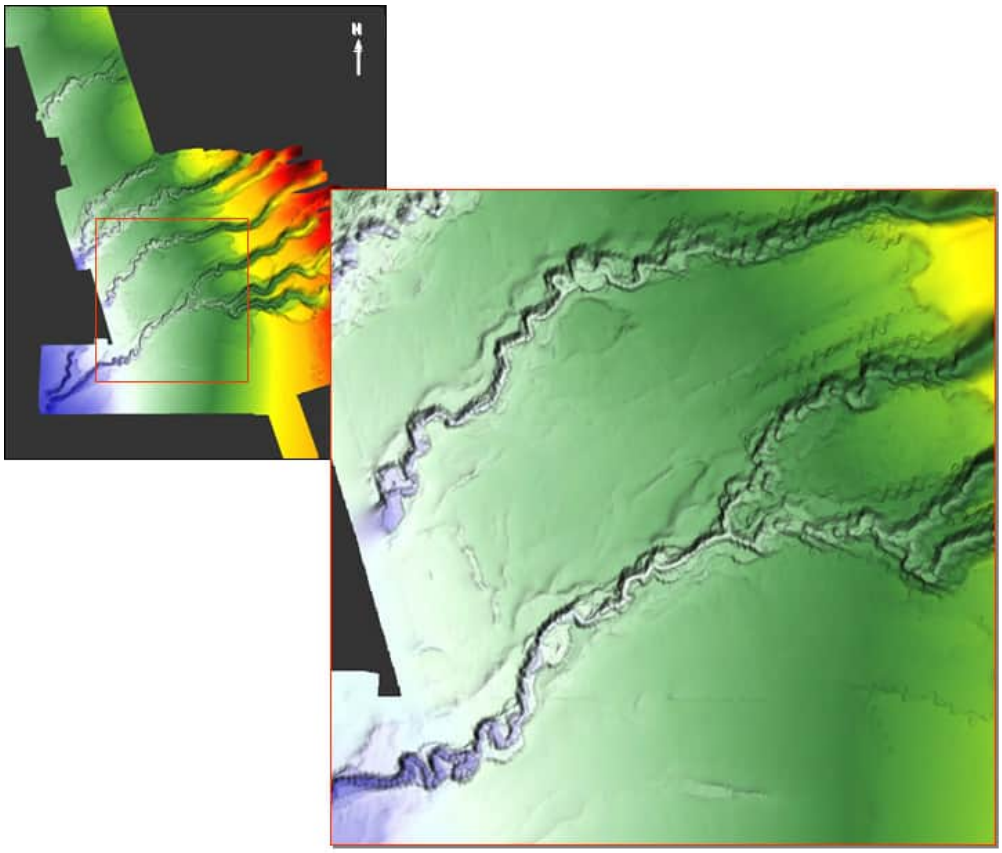


**Figure 8. Map generated from seismic interpretation of the modern day sea-floor, offshore Mauritania. Note the highly sinuous nature of channels within the canyons, suggesting an anastomosing reservoir system of relatively low net-to-gross rather than braided or sheet sand amalgamation.**

The net-to-gross of the canyon fill turbidites is variable. A combination of seismic character and drilling results indicate that these deposystems are a series of anastomosing meandering channel systems, confined within the large canyon cuts. Mapping of the modern sea-floor canyon system reveals that the

basal channels are highly sinuous in nature (Fig. 8) and sub-surface analysis of the Tertiary equivalent channels would suggest that the older deposits are no different in morphology. As a result the distribution of sand within the confines of any given canyon will vary dramatically. In the Chinguetti canyon, for example, (which includes the Tevet and Banda discoveries) net-to-gross ranges from 54% to 22% (Vear 2005). In the case of the Tertiary reservoirs, where the temperatures are low, there has been little in the way of diagenetic cementation and porosities average around 26% with permeabilities in the Darcies (Vear *ibid.*). In places excellent porosities can also be preserved in Cretaceous sandstones though elsewhere it has been found to be tightly cemented. Net-to-gross has so far proven to be significantly lower than those encountered in the Tertiary. The updip Cretaceous equivalent deltaic and shoreface deposits have, unsurprisingly, much improved reservoir quality; Autruche-1 east of Block 1 in Mauritania has recorded porosities up to 20-30% and net-to-gross between 40-70%. This would suggest that there are locations downdip where the net-to-gross of the Cretaceous turbidite play could be expected to increase down-slope of the main input points. The deltaic topset play, however, suffers from lack of top seal where the net:gross is very high.

For the deep water gravity deposits, seal is rarely a problem given that they are deposited on a low energy slope setting dominated by mud and silt sedimentation. The high net:gross of the more proximal deltaic and shoreface deposits on the other hand, suffer from a lack of potential topseal (and often structural trapping mechanisms).

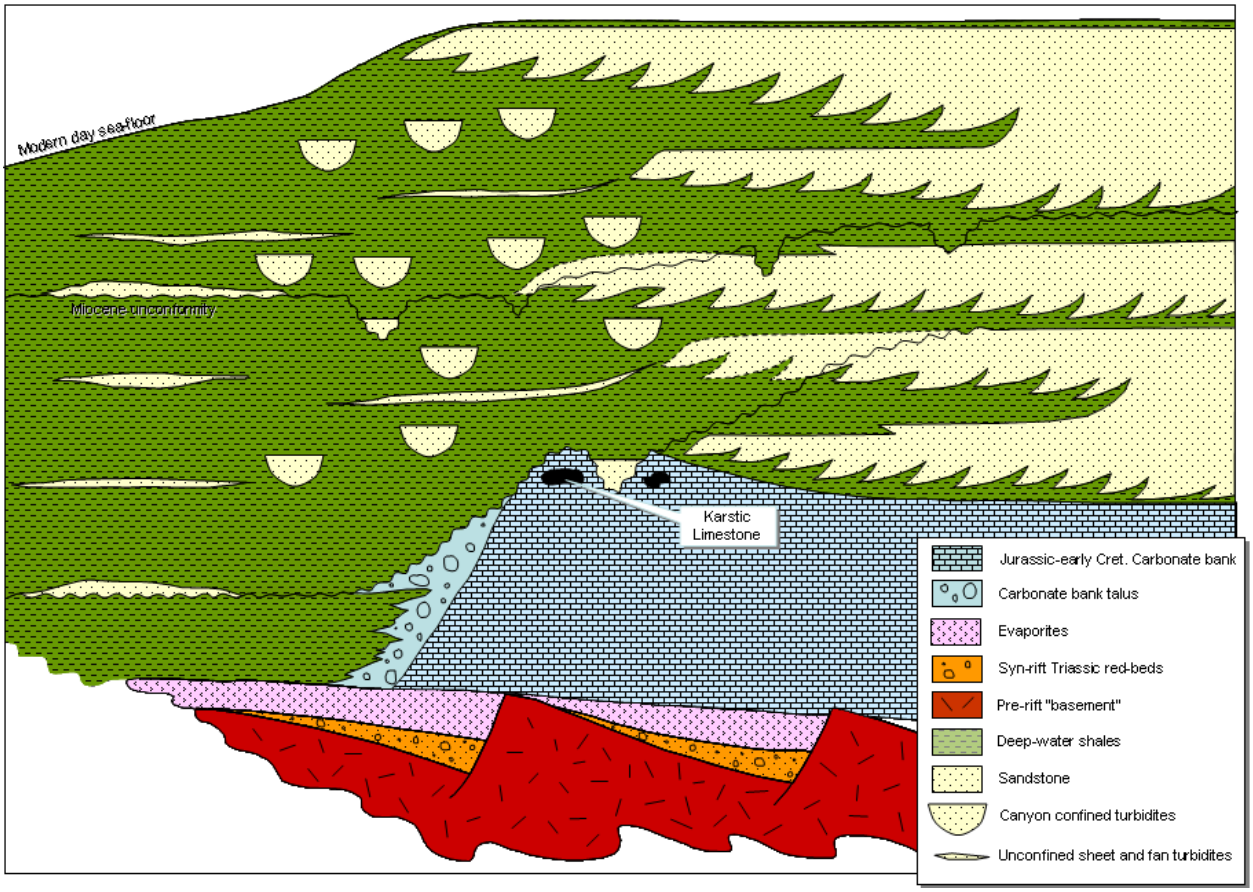


**Figure 9. Stylised illustration depicting the style of reservoir development along the northwest African margin. Note that this is purely a sedimentological depiction, and does not include the major structural elements such as halokinesis, gravity sliding, toe thrusts and extensional faulting and collapse.**

The regional development of an extensive carbonate platform along the northwest African margin during the Jurassic provides the possibility of a reefal carbonate reservoir (Fig. 9). Exposure of the carbonate bank to atmospheric weathering has created the opportunity of a karst play in the limestones. This is virtually untested on the northwest African margin, with the notable exception of the non-commercial heavy oil Cap Juby discovery in Morocco, which proves the validity of the play. There are numerous undrilled closures all along the carbonate bank edge where seismic character would suggest karstic weathering. More successful examples exist on the North American equivalent margin, and suggest that this is a play that has yet to be thoroughly explored on the African side.

### Trapping Mechanisms

Along the length of the northwest African margin the most prominent trapping mechanism is related to halokinesis. Allochthonous salt diapirs and canopies intrude into the Cretaceous and Tertiary succession offshore Mauritania, Guinea Bissau and Morocco, but are largely absent from offshore Western Sahara, Senegal and Gambia. Proven and unproven traps include sub-salt, salt stock, and supra-salt closures, of which only the supra-salt style has been proven at Chinguetti (Mauritania). Other trapping mechanisms are mostly associated with gravitational collapse along the passive margin and include tilted fault blocks (including counter regional faults), stratigraphic pinchout (Banda and Tiof discoveries), extensional roll-over folds, and toe trust compressional folding (Fig. 10).

## Challenges Facing E&P Companies, and Possible Solutions

The under explored nature of the northwest African Atlantic margin provides exploration and production (E&P) companies with numerous challenges, many of which derive from a lack of detailed well control.

### A Sand-Poor System?

The depositional systems in the Cretaceous and the Tertiary display highly variable net-tp-gross, which, coupled with difficulties in correlating age equivalent events, makes prediction of sandstone problematic. In addition, many of the seismic facies and morphologies that can be identified cannot differentiate between debrites and slope channel complexes. Furthermore, sheet turbidites in the Cretaceous are seismically un-resolvable. Canyon systems provide a prominent conduit for remobilised sandstone to be deposited, but in many cases the relationship between the palaeo-basin floor and present day water depth means that the most promising areas for reservoir accumulation are at the limits of "drillable" water depths. Where sandstones have been preserved within major Cretaceous canyon systems updip decapitation of the channels is hard to establish, since there are no AVO effects to aid the interpreter.

The prediction of sand presence is a fundamental issue facing the development of exploration prospects across the northwest African margin. Unlike the rest of the Atlantic margin (*e.g.* Canada, Brazil, Angola and Nigeria) the northwest African margin lacks any form of long lived large deltaic system throughout the Cretaceous and Tertiary. As described previously, a probable explanation for this is the latitude of northwest Africa during this period, and the resulting increase in aridity during the formation of the Sahara Desert has meant that large river systems have tended to be ephemeral in nature. Consequently periods of significant coarse clastic deposition along the northwest African margin have been episodic. In the case of Morocco these are related to local tectonic events, such as the uplift of the Atlas Mountains. Well results from Morocco to Guinea Bissau demonstrate that there have been significant periods of sand input into the offshore basins, but that this is diachronous and variable in quantity. The challenge is predicting these sweet spots of sufficient reservoir.

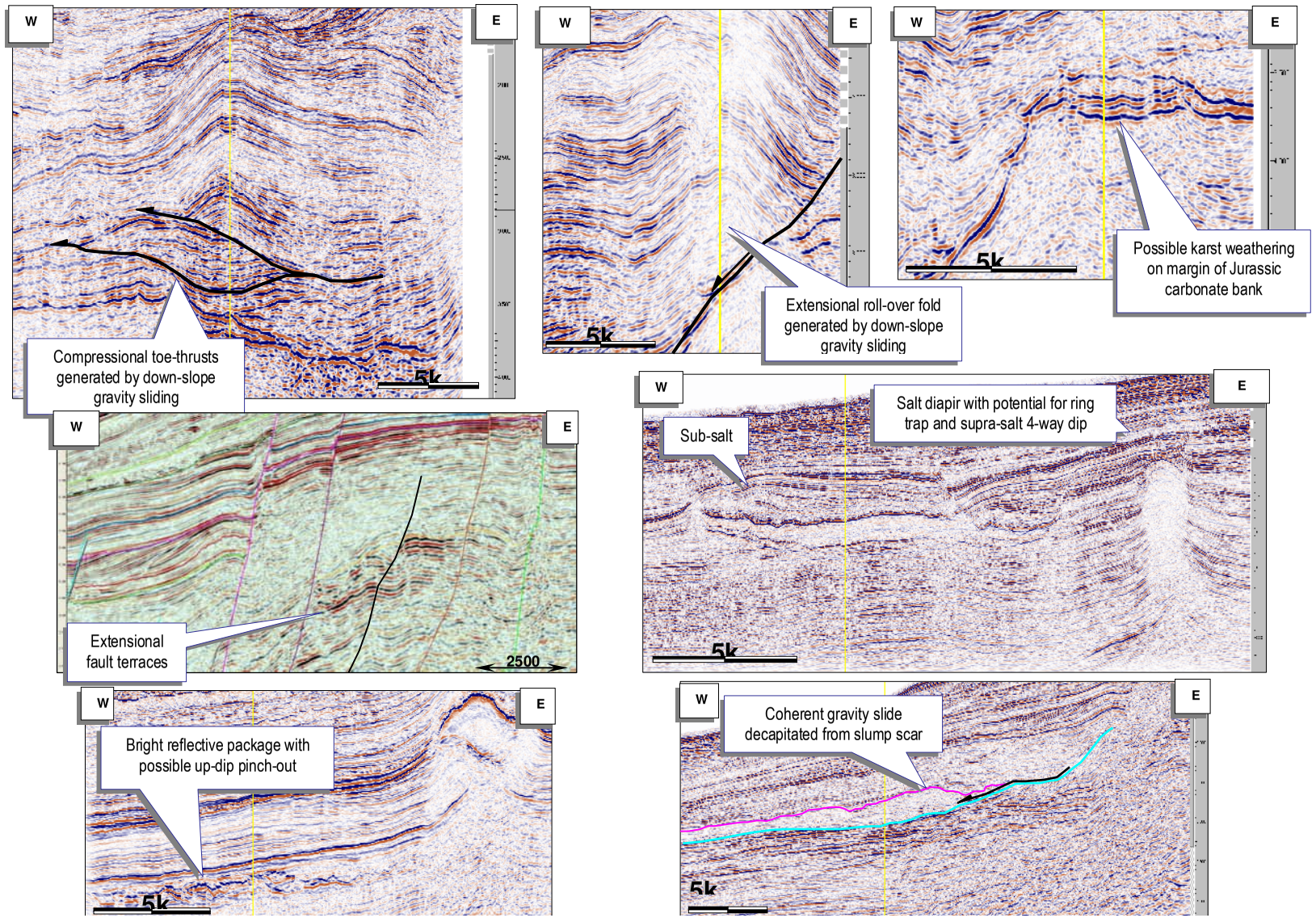


**Figure 10. Seismic lines to demonstrate examples of trapping style along the northwest African margin**

Indentifying reservoir within the Tertiary deep water and associated deltaic and shoreface deposystems is aided considerably by seismic amplitude, where strong amplitudes tend to represent channels of high net-to-gross. There were several significant lowstands during the Tertiary, which resulted in a series of prominent canyon systems, along which remobilised sediment from the more proximal shoreline systems has been deposited as a series of meandering channels. The presence of an effective AVO response has also significantly reduced the risk of up-dip pinchout failure where there is no structural closure. Hence, downdip Tertiary turbidite systems tend to be confined to the deeply incised slope canyons, where prediction of reservoir is possible. The equivalent Cretaceous deep-water play, however, is far more problematic. Canyonisation is either less common, or down-cutting less severe and basin floor sheet turbidites are seismically un-resolvable. Consequently, seismic attributes cannot be used for the prediction of reservoir. Identification of the most favourable regions along the northwest African margin for reservoir development depends on a sound sedimentologically derived depositional model. Given that the overall climatic conditions of northwest Africa since the opening of the Atlantic Ocean have been of increasing aridity, and there is no long lived sediment input system along much of the coastline, the palaeo-fluvial systems providing sediment during the Cretaceous and Tertiary will be abandoned drainage systems. Landsat imagery (Fig. 11) over Mauritania has revealed scars of ancient drainage systems beneath the sand dunes of the Sahara Desert, which is also supported by hydrological analysis of the digital elevation model. As much of the north African craton south of Morocco has been stable with no major collisonal events since the opening of the Atlantic, it can be inferred that ancient drainage systems along the west coast of Africa have acted as conduits for Cretaceous sediments as they have in more humid and temperate environments (*e.g.* the Niger and Congo river systems). Therefore, the subsequent identification of dried out ancient fluvial systems quite probably represent the major sediment input points since the opening of the Atlantic Ocean. Comparison of these input points, with the mapped extent of shelfal sand development, appears to corroborate the hypothesis (Fig. 12)

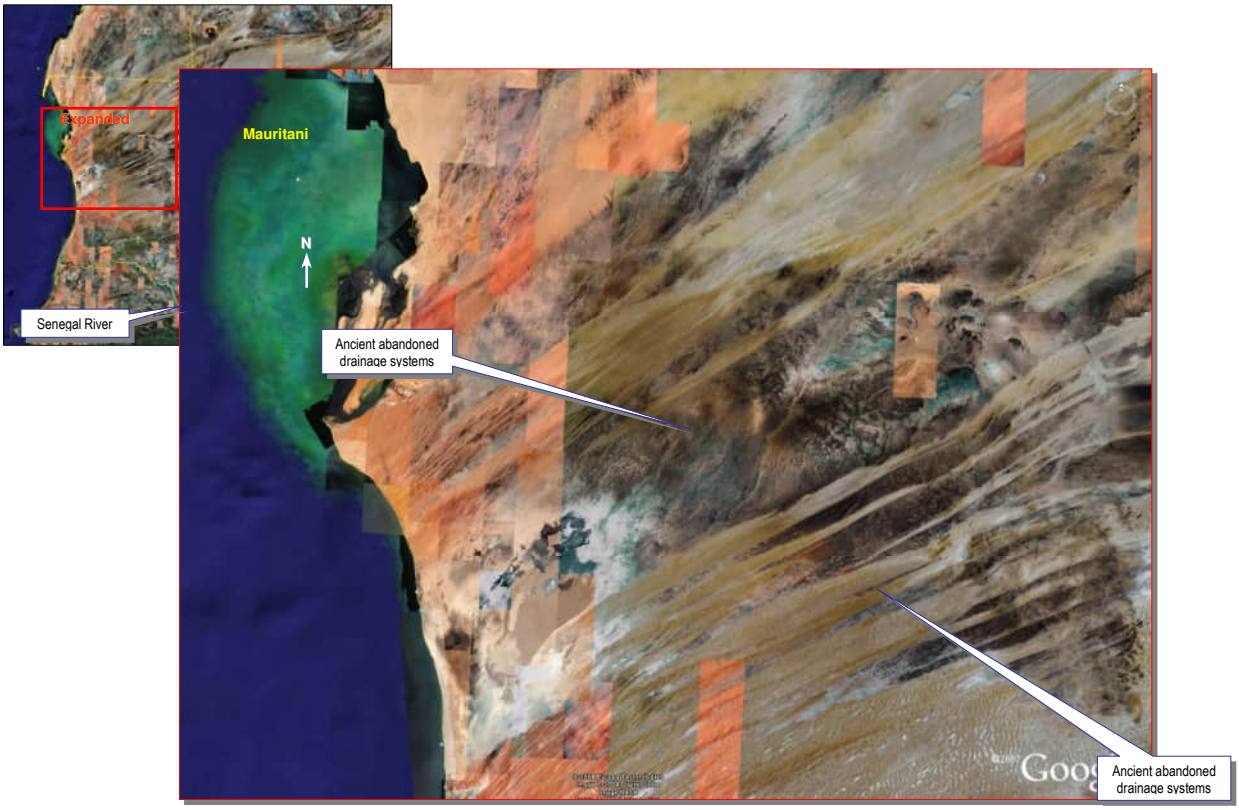


**Figure 11. Image from Google Earth that identifies ancient drainage systems that have been partially buried by the sands of the Sahara Desert. Such drainage basins are likely to have been in existence from the Cretaceous onwards, as they have in the Congo and Niger Basins.**

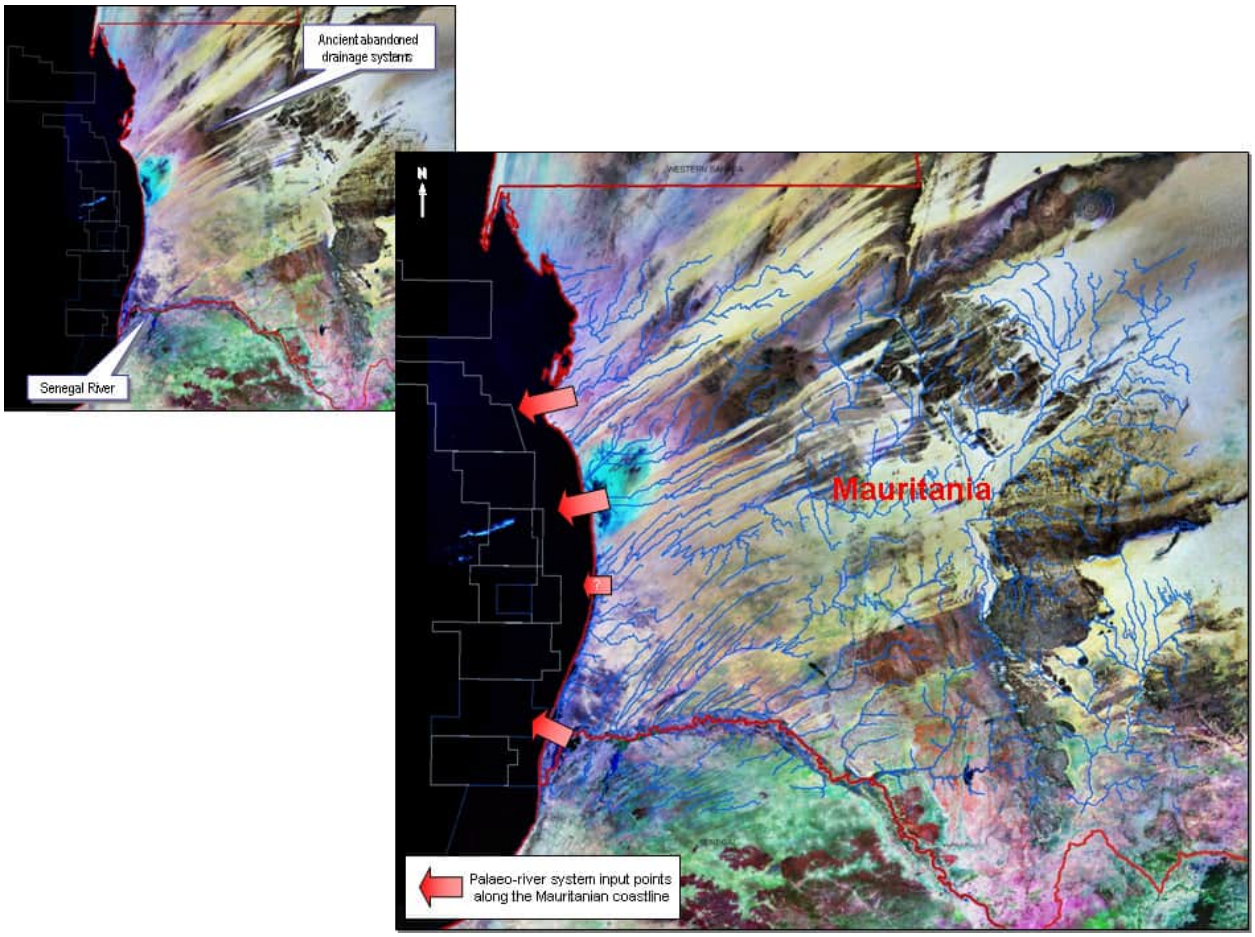


**Figure 12. Hydrological analysis of the digital elevation model illustrates possible input points along the Mauritanian coastline, should the buried drainage basins be Cretaceous/Tertiary in age.**

South of the Cap Vert Peninsula in Senegal the issues concerning reservoir distribution are different. Plate reconstructions (Scotese 2008) show that the North American plate split from Africa earlier than the South American plate, leaving the two continents joined just south of Guinea Bissau (Figs. 13A and B). The deposition of the Jurassic-early Cretaceous fringing carbonate bank along the margins of the proto-Atlantic was prior to the complete separation of the South American craton from the African craton. As a result, the carbonate bank was developed from northwest Africa to northeast South America as a continuous morphological feature. The subsequent extensional tectonics that joined the north and south proto-Atlantic split the carbonate bank in two. From southern Senegal, Gambia and Guinea Bissau, therefore, the carbonate bank margin diverges from the northwest African coastline westwards creating a much larger shallow water platform than further north for Cretaceous and Tertiary sediments to prograde across. Well data in the region demonstrates that Cretaceous shelfal systems were further inboard than the current coast line. This, coupled with the larger carbonate platform meant that there was less opportunity for coarse clastic sediments to reach the deep water environment west of the carbonate platform shelf break (Fig. 14). This does not hinder the possibility of reservoir deposition over the platform top, but sealing mudstones are less prevalent, and structural trapping is reliant on salt tectonics (which is restricted to parts of Guinea Bissau) or very subtle closures created by sediment compaction.

The combination of mapping known shelfal deposits relative to ancient sediment input points could provide a powerful tool in de-risking the presence of reservoir in the Cretaceous deep water, and possibly deltaic topset, plays.

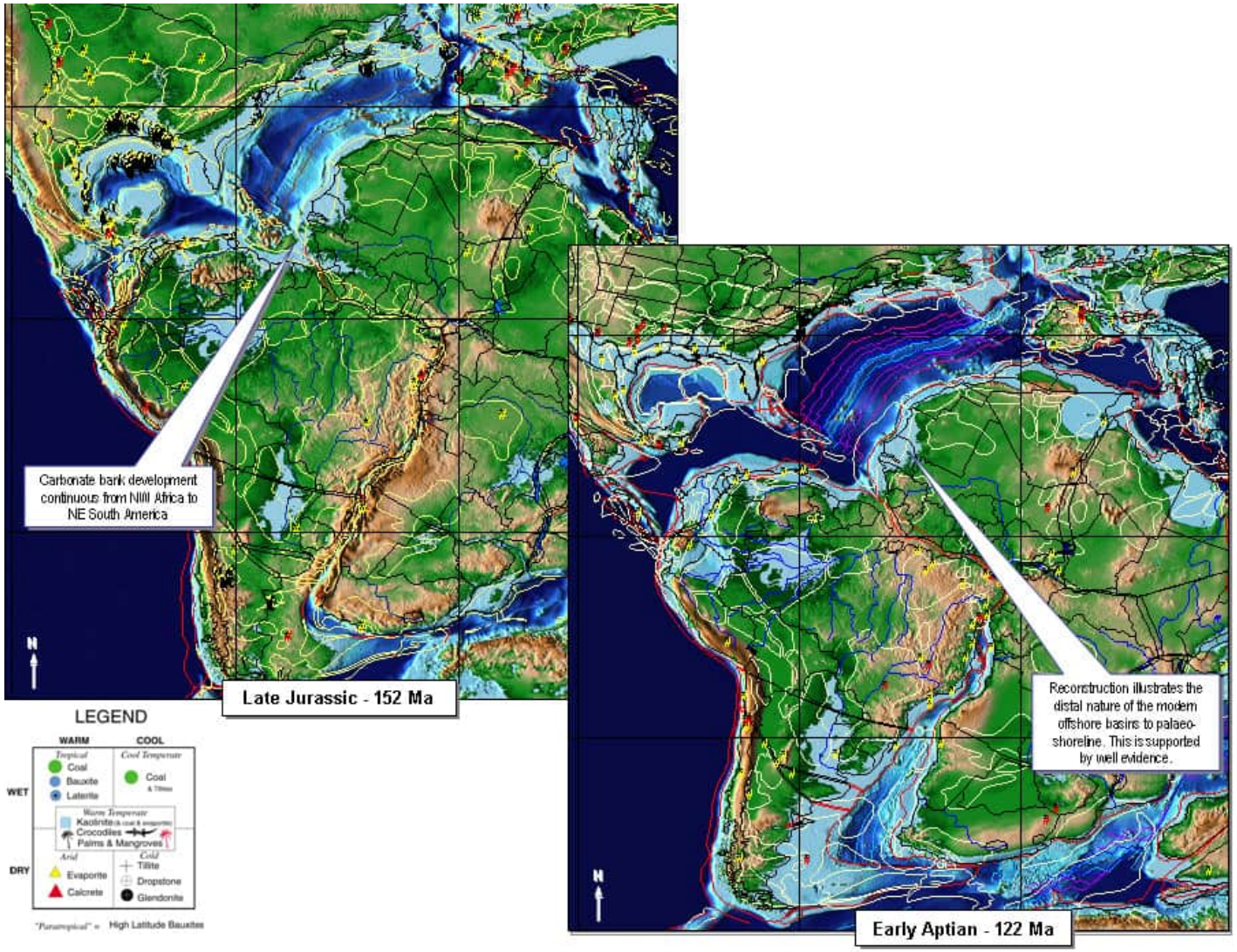


**Figure 13A. Plate reconstruction of Proto Atlantic (After Scotese © 2008, PALEOMAP Project). Note that the Jurassic carbonate platform would have extended continuously from Africa to South America, only breaking up in Albian times when extension is sufficient to join the south and north Atlantic "seas".**

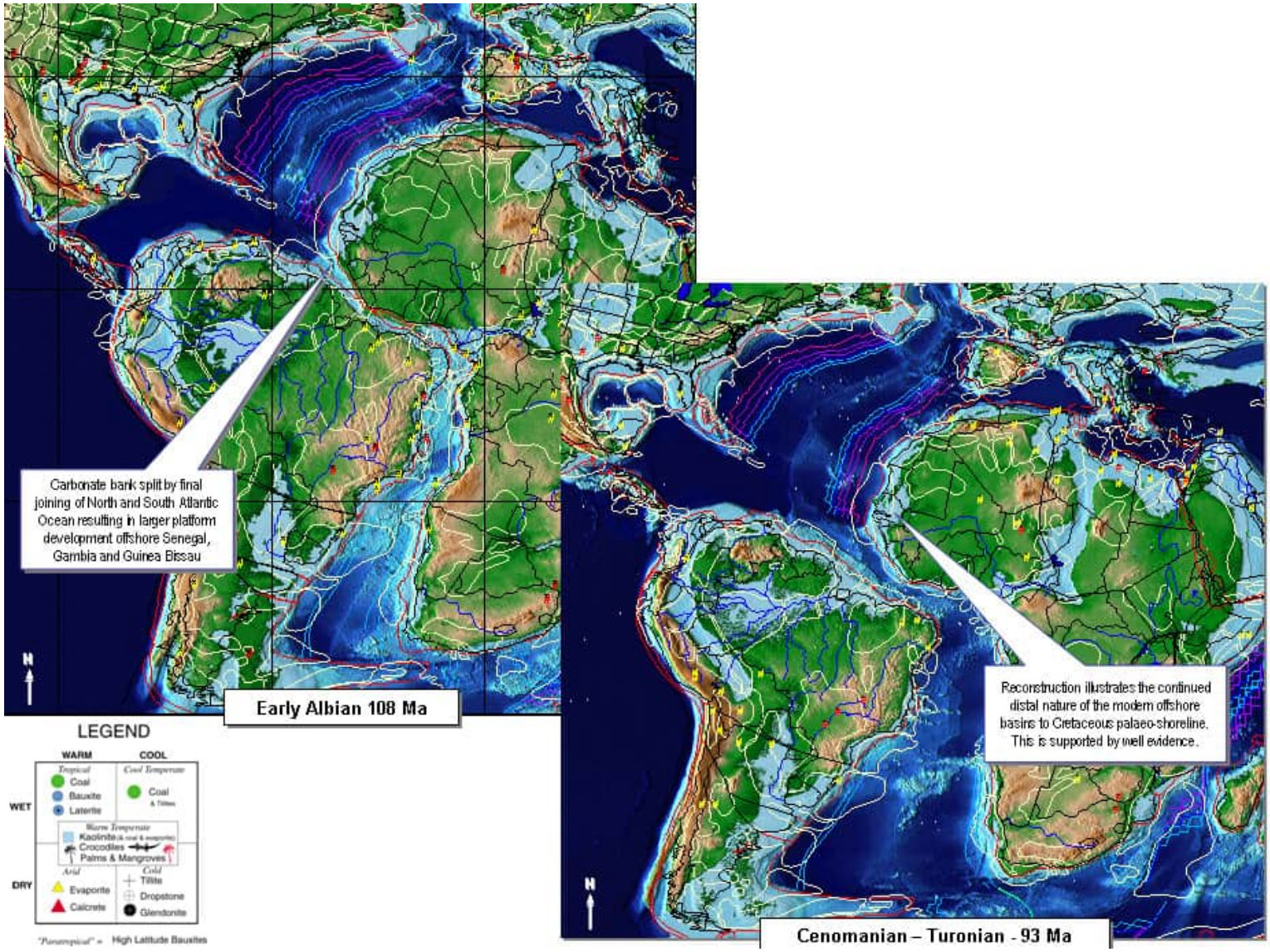


**Figure 13B. Plate reconstruction of Proto Atlantic (After Scotese © 2008, PALEOMAP Project). Note that the Jurassic carbonate platform would have extended continuously from Africa to South America, only breaking up in Albian times when extension is sufficient to join the south and north Atlantic "seas".**

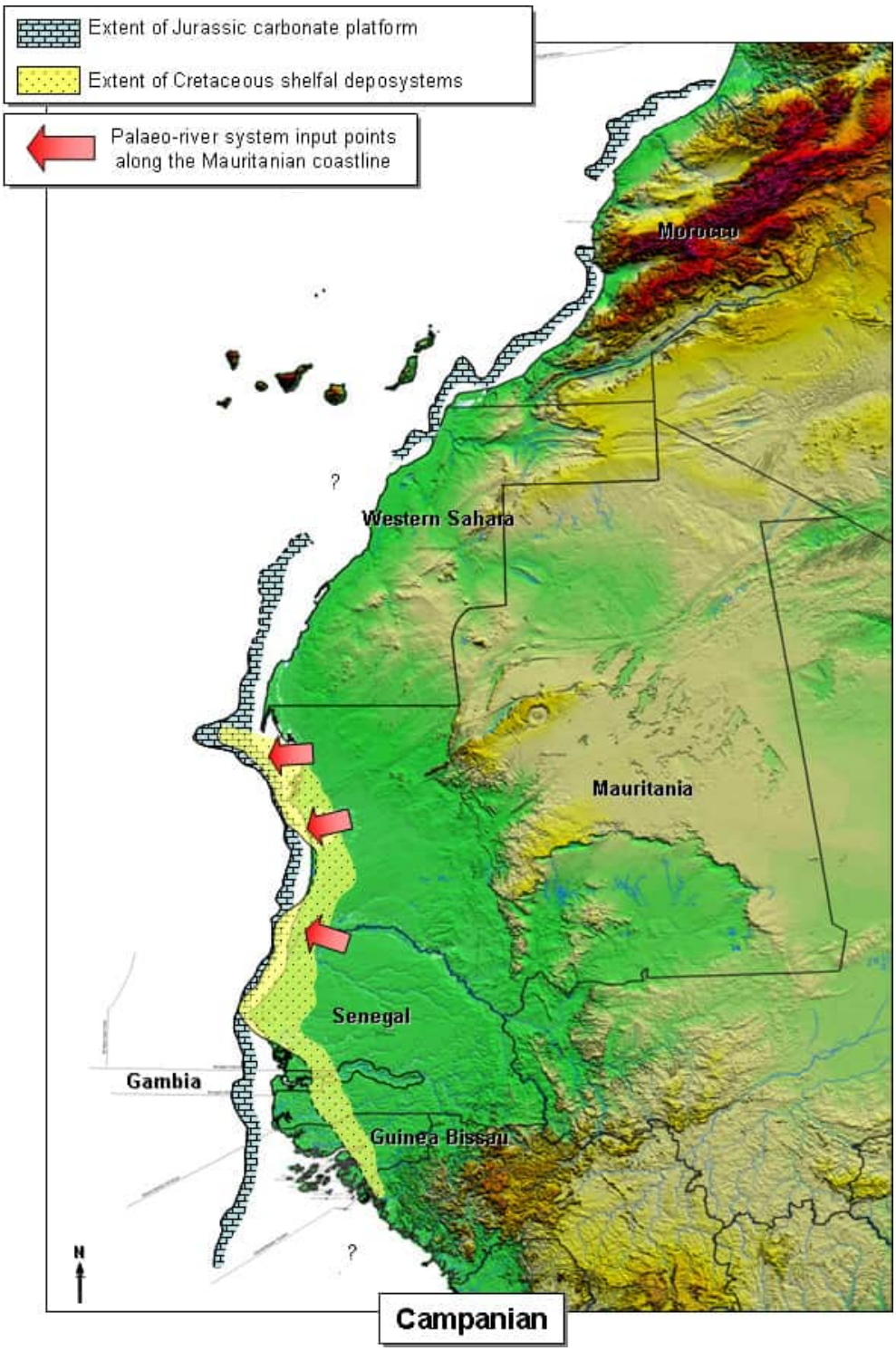


**Figure 14. One of several paleogeographic reconstructions (based on well evidence) illustrating the extent of the shelfal system during the Campanian along the northwest African margin. Note that the major input points identified from modern day aerial imagery in Mauritania correspond to regions of maximum shelfal progradation. This is a feature repeated throughout the Cretaceous.**

## Misleading Seismic Morphologies

Other pitfalls have recently come to light after drilling. The Flamant-1 well (Block 8, Mauritania) targeted one of many mounded morphological features that run along the carbonate platform shelf break. These mounds appear to be shallow water carbonate build-ups in nature forming discrete four-way dip closures, many of which are associated with possible gas clouds (Fig. 15).

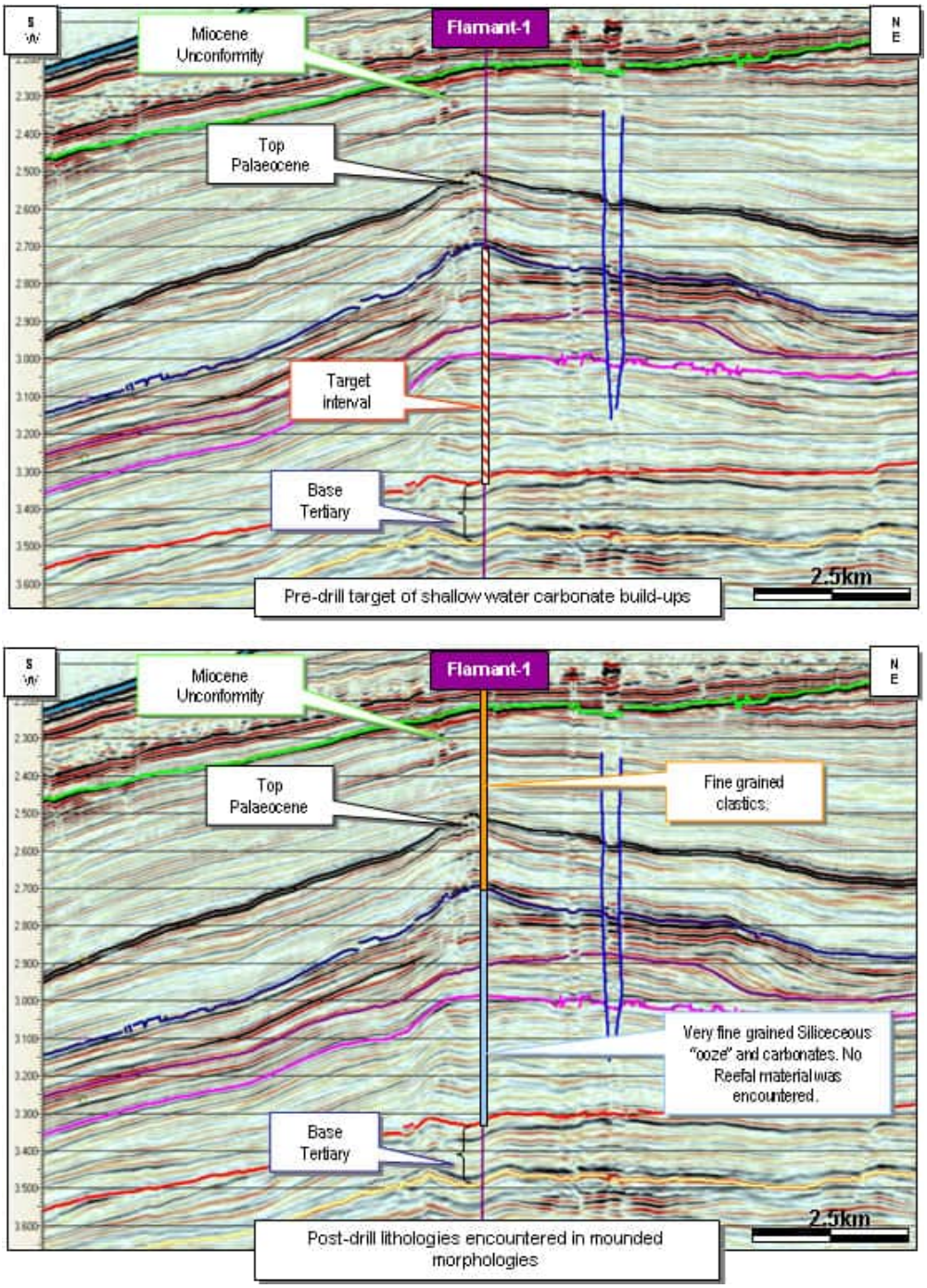


**Figure 15. West-East seismic lines illustrating the pre- and post-drill difference between seismic morphology and actual lithology at Flamnat-1, Mauritania. (Reproduced with kind permission from Dana Petroleum)**

The well in fact encountered a predominance of extremely fine grained siliceous lithologies (only identifiable by a combination of XRD analysis, calcimetry and petrography), suggesting deep water depositional environments. This conclusion was supported by micro-palaeontological evidence. The morphological characteristics of the seismic so reminiscent of a carbonate build ups, given the lithological make-up of the structures, have now been re-interpreted as generated by siliceous contourites.

## Misleading Seismic Attributes

As already described, many of the successes in Tertiary deep-water deposits have been associated with a strong seismic amplitude and AVO response. It is no surprise, therefore, that bright amplitude anomalies in the deeper Cretaceous section have proved to be attractive targets in the past. Faucon-1 (Block 1 Mauritania) targeted what was interpreted to be a three-way dip closed Cretaceous turbidite, downdip of a large salt diapir which provided the updip seal. The prospect was identified entirely on prominent seismic amplitudes which increased updip towards the salt diapir, but did not conform to structure. It was assumed that the lateral extent of the amplitudes, and therefore the prospect, were defined by the lateral limits of the interpreted turbidite.

The well was a non-commercial discovery, intersecting two thin gas bearing sands just below the amplitude anomaly. Post-well analysis clearly demonstrated that the original target amplitude was not a result of the gas bearing sands, but a thin low velocity shale (Fig.16). The discovery of the hydrocarbon bearing reservoir beneath had been entirely serendipitous. Whilst the well has proven a working Cretaceous petroleum system, it demonstrates that seismic attributes in the deeper sections of the stratigraphy can be misleading without a sound sedimentological model and highlights the difficulty in targeting reservoirs that are often seismically unresolvable.

## Karst Play

Exposure of the carbonate platform in the early Cretaceous has generated prospectivity along the entire northwest African margin by karstic weathering of the exposed limestones. Cap Juby in Morocco, is to date the only discovery in this play on the African side of the North Atlantic There has been a more successful discovery on the Canadian margin in Deep Panuke. Porosities in Cap Juby range from 1-20%, the shallower units exhibiting the better reservoir characteristics as the weathering has been greater.

There are two proven oil accumulations, MO-2 which discovered 12$^{o}$ API biodegraded oil, and MO-8 which encountered a deeper accumulation of 38$^{o}$ API oil. Although good quality oil has been discovered, it is in a part of the reef that is not as heavily weathered as the shallower units, and as a result suffers from poor porosity-permeability characteristics that after acidising and fracturing only flowed 16 bbls/day. The biodegradation of the oil accumulation in the parts of the reservoir that has good reservoir has been attributed to the downcutting of the base Tertiary unconformity, which has eroded into the top of the carbonate bank, allowing meteoric waters from the overlying Tertiary sands to degrade the trapped hydrocarbons.

Many similar prospects located along the northwest African margin also suffer from contact with, or close proximity to, the base Tertiary unconformity. This results in an increased risk of discovering low viscosity hydrocarbons in what is already a problematic reservoir. If large karst closures can be identified along the margins of the carbonate bank that are sufficiently deeper than the base Tertiary unconformity, then these will become valid and important targets for the future development of the hydrocarbon province along the entire northwest African margin.

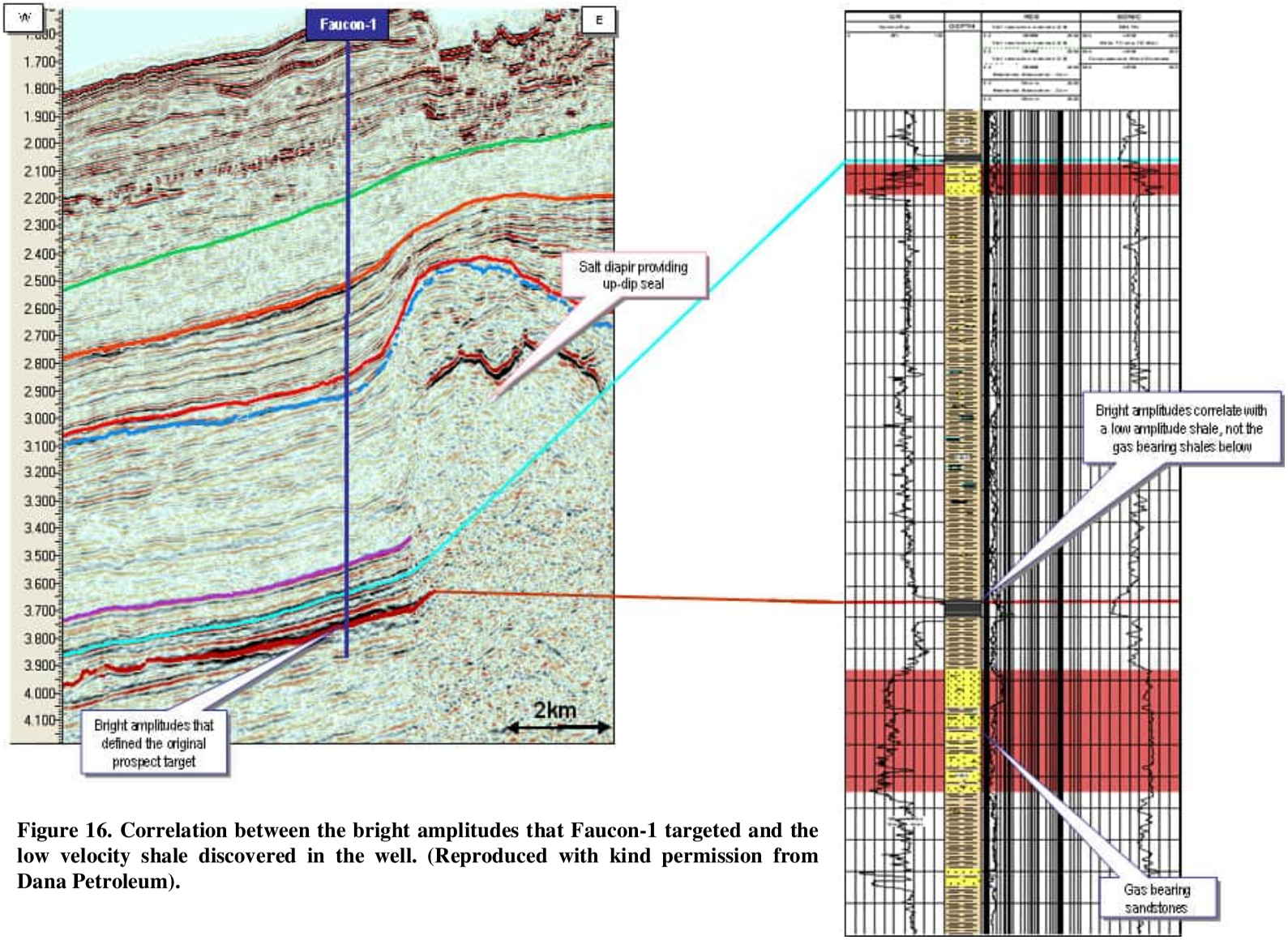


**Figure 16. Correlation between the bright amplitudes that Faucon-1 targeted and the low velocity shale discovered in the well. (Reproduced with kind permission from Dana Petroleum).**

### Hydrocarbon Migration and Charge

The pervasive existence of numerous sealing lithologies through the deep-water stratigraphy not only increases the chance of sealing hydrocarbons, but in many cases it also presents the possibility of migration shadows. This is a particular issue for prospects further downdip, where faulting and deformation as a result of passive margin gravity sliding becomes less of an influence, and seismically identifiable conduits from the Albian-Aptian and Cenomanian-Turonian source rocks are often absent. It is also possible that the numerous salt diapirs could act as effective baffles to hydrocarbon migration.

The lack of a long lived deltaic system on the northwest African margin means there is considerably less sediment being deposited into the offshore basins than there is along the southern Atlantic conjugate margin. The knock-on effect on source rock maturity is that the burial required for the younger source rock intervals is insufficient to generate and expel hydrocarbons, thus reducing the over all extent of possible source kitchen when compared to similar aged rocks and petroleum systems elsewhere with higher sedimentation rates.

### Water Depth and Commerciality

The challenges described above are generally prospect specific issues, but there are further challenges which relate more to the cost of exploration in relatively immature basins. Water depth provides its own specific problems with rig availability and ability to drill certain prospects at all, but the cost of drilling wells, and the lack of infra-structure means that a discovery does not necessarily lead to development. With many of the identified prospects and leads being beneath 2,000m of water the full potential of this margin can only be realised with advances in drilling and development technology. The advent of Liquefied Natural Gas (LNG) provides the welcome possibility of developing what had previously been stranded gas discoveries, but as in all relatively immature basins, more than one large discovery is required to kick-start the development of the offshore petroleum system of northwest Africa as a whole. This should not deter any exploration effort.

### Overpressure

As the restrictions on commerciality and ability imposed by the water depth drive companies to explore ever deeper in the basin it becomes increasingly likely that prospects will be overpressured as they are in other deep passive margins. This will increase well costs, placing greater pressure on discovering larger accumulations to ensure commerciality. Whilst there are serious implications to cost in exploring overpressured reservoirs, there are also un-tapped opportunities. The presence of overpressure demonstrates a sealed system, faults tend to be sealing, providing the prospect of viable targets in hanging wall fault blocks. In passive margins such as northwest Borneo and Nigeria, this has generated a viable play in the deeper, faulted deltaic high net-to-gross topset sandstones.

## Conclusions

The northwest African margin shares a similar stratigraphic and geological evolution to the prolific, Angolan, (Nigerian) Brazilian and Canadian Atlantic margins. It has, therefore, attracted comparisons that a similarly prolific petroleum system may exist. Such a comparison can only lead to misplaced disappointment. The northwest African margin has had less coarse clastic input, which has had a fundamental impact on reservoir abundance and source rock maturity and the salt basins are smaller resulting in fewer structural traps. In terms of prospectivity these are significant differences, and direct comparison of these other provinces with the northwest African margin is probably misleading. The offshore basins from Morocco to Guinea Bissau have been demonstrated to contain functioning petroleum systems, with discoveries along the whole length of the margin. Exploration has been proven to be viable, and the absence of a long lived delta does not mean that this is a hydrocarbon province suffering from

unfulfilled expectations. It does mean, however, that geoscientists need to employ a combination of more imaginative and varied techniques to discover potentially commercial prospects than in other geologically blessed basins in a similar tectonic setting.

## Acknowledgments

Tullow Oil Plc, Petronas Carigali Sdn. Bhd., Dana Petroleum Plc, Roc Oil, Premier Oil, Gaz De France, KUFPEC, SMH and Wintershall Holding AC

## References

Brown, R.H. 1980, Triassic rocks of the Argana Graben, southern Morocco, and their regional structural implications. Bulletin American Association of Petroleum Geologists, v.64, p.988-1003.

Blakey, R. 2005 : http://jan.ucc.nau.edu/

Davison, I. 2005, Central Atlantic margin basis nod North West Africa: Geology and hydrocarbon potential (Morocco to Guinea). Journal of African Earth Sciences, v.43, p.245-274.

Hafid, M. 2000, Triassic-early Liassic extensional systems and their Tertiary inversion, Essaouira Basin (Morocco). Marine and Petroleum Geology, v.17, p.407-429

Jarvis, J. and T. Garwood, J. Glover, 1999, The evolution and hydrocarbon potential of the deep-water Tarfaya Basin. Bulletin American Association of Petroleum Geologists, v.83, p.1319.

Kidston, A.G., D.E. Brown, B.M. Smith, and B. Altheim, 2005. The Upper Jurassic Abenaki Formation offshore Nova Scotia: A seismic and geologic perspective. Canada-Nova Scotia Offshore Petroleum Board, Halifax, Nova Scotia, 165p. (CD-ROM and http://www.cnsopb.ns.ca

Luning, S. and S. Kolonic, E.M. Belhadj, Z. Belhadj, L. Cota, G. Baric, T.Wagner. 2003, Integrated depositional model for the Cenomanian-Turonian organic-rich strata in North Africa. Earth-Science reviews, v.64, p.51-117.

Scotese, C.R., 2008. ArcGIS PaleoAtlas, *In* Cretaceous, PALEOMAP Project, Arlington, Texas http://www.scotese.com, v.2.

Scotese, C.R., 2008. ArcGIS PaleoAtlas, *In* Jurassic & Triassic, PALEOMAP Project, Arlington, Texas http://www.scotese.com, v.3.

Tari, G. J. Molnar, and P. Ashton, 2003, Examples of salt tectonics from West Africa: a comparative approach. *In* T.L. Arthur, D.S. Macgregor & N.R. Cameron (eds), Petroleum geology of Africa: New themes and developing technologies: Geological Society, London, Special Publication. no.207, p.85-104

Vear, A. 2005, Deep-water plays of the Mauritanian continental margin. *In* A.G. Dore & B.A. Vinning (eds) Petroleum Geology: North-West Europe and Global Perspectives – Proceedings of the 6th Petroleum Geology Conference. v.2, p.1217-1232.

**BACK**

# Controls on Facies Distribution and Reservoir Revelopment of Upper Triassic Continental Systems in Intermontane Rift Settings: A Comparative Study of Extensive Outcrops in Southwest Morocco

**Jonathan Redfern**
**Ivan Fabuel Perez**
**David Hodgetts**
University of Manchester
School of Earth Atmospheric and Environmental Sciences
Williamson Building, Oxford Road
Manchester M13 9PL
United Kingdom
e-mail: jonathan.redfern@manchester.ac.uk

**Nadine Mader**
Hess
Level 9
The Adelphi Building
1-11 John Adam Street
London WC2N 6AG
United Kingdom

**Abedelmajid El Ouataoui,**
ONHYM
34, Avenue Al Fadila
BP 8030 NU
10500 Rabat
Morocco

## ABSTRACT

Upper Triassic (Carnian) sediments in SW Morocco comprise a continental red bed sequence deposited in discrete rifted basins following the break up of Pangea and opening of the Atlantic. This comparative study examines extensive outcrops of the Oukaimeden Sandstones Formation (F5) in the High Atlas and Unit T6 in the Argana Basin, SW Morocco, deposited within a series of narrow fault bounded intermontane basins. Both contain a variety of braided fluvial, overbank, shallow ephemeral lacustrine, alluvial fan and aeolian facies.

Traditional sedimentological data (sedimentary facies logs, palaeocurrent information, gamma ray logs etc) has been combined with high resolution 3D laser (LIDAR) and Differential Global Positioning System (DGPS) to map these outcrops and provide a detailed dataset.

On a basin scale, the often complex facies distribution evident in the Argana Basin suggests a highly variable fill within these basin types. Correlation of individual facies elements is often difficult and relies on identification of key stratal surfaces. Local tectonics control accommodation and influences facies patterns, such as development of alluvial fans and entry points of major drainage systems. Significant changes in fluvial style, from ephemeral to perennial, are recognized in both basins within this interval, which suggests rejuvenation of the source areas and a potential interplay of climatic and tectonic control. An overall drying upward pattern is observed, with increasing influence of aeolian processes towards the top of both the Oukaimeden sandstone (F5) and T6 of Argana. This supports previous work

that has demonstrated a change from humid to increasingly arid conditions during the Upper Triassic, recognized both throughout SW Morocco and in the Fundy Basin, Canada, and highlights the climatic control on the depositional system.

These studied sections offer potential analogues for subsurface Triassic hydrocarbon systems in similar settings, and provide valuable information on the tectonic and climatic control on depositional facies and architecture. Analysis of basin-wide facies variation, provenance and sediment pathways provide regional scale analogue data. More detailed field scale reservoir models have also been developed for the high net-to-gross intervals in the Oukaimeden sandstone.

## Introduction

Upper Triassic (Carnian) sediments in southwest Morocco comprise a continental red bed sequence deposited following the break up of Pangea and opening of the Atlantic, strongly influenced by a low palaeolatitude (between 10° to 20° N) climatic regime. This comparative study examines extensive outcrops of the Oukaimeden Sandstones formation (F5) in the High Atlas Oukaimeden Basin, and the Tadrart Ouadou Sandstone member (T6) in the Argana Subbasin in southwest Morocco. Both contain a variety of braided fluvial, overbank, shallow ephemeral lacustrine, alluvial fan and aeolian facies, deposited within fault bounded intermontane basins. The study combines traditional sedimentological data (sedimentary facies logs, palaeocurrent information, gamma ray logs etc) with high resolution 3D laser (LIDAR) and Differential Global Positioning System (DGPS). The comparison between these basins provides valuable regional information on the tectonic and climatic control on depositional facies and architecture, and offers potential analogues for subsurface hydrocarbon systems in similar settings.

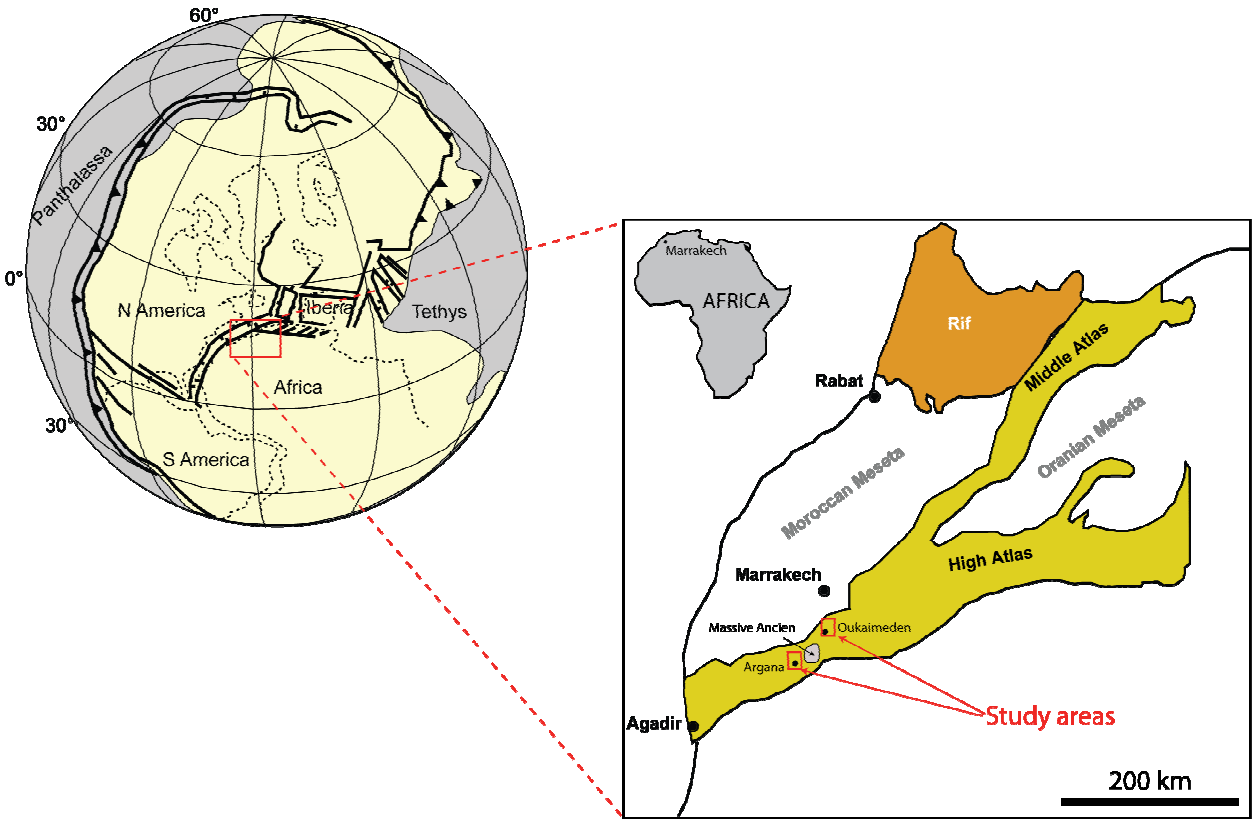


**Figure 1. Location Map of studied basins in SW Morocco, showing the outline of the High Atlas. Global palaeogeography adapted from Ziegler (1990).**

## Location

Upper Triassic continental deposits were examined in two areas located in southwest Morocco (Fig. 1). The Argana outcrops are exposed along the southwest flank of the High Atlas mountain chain (Fig. 2), and the Oukaimeden deposits are located within the High Atlas (Fig. 3). Both basins are fault controlled. They are separated by the Ancien Massif, which was a positive feature formed during the Hercynian, acted as a major sediment source.

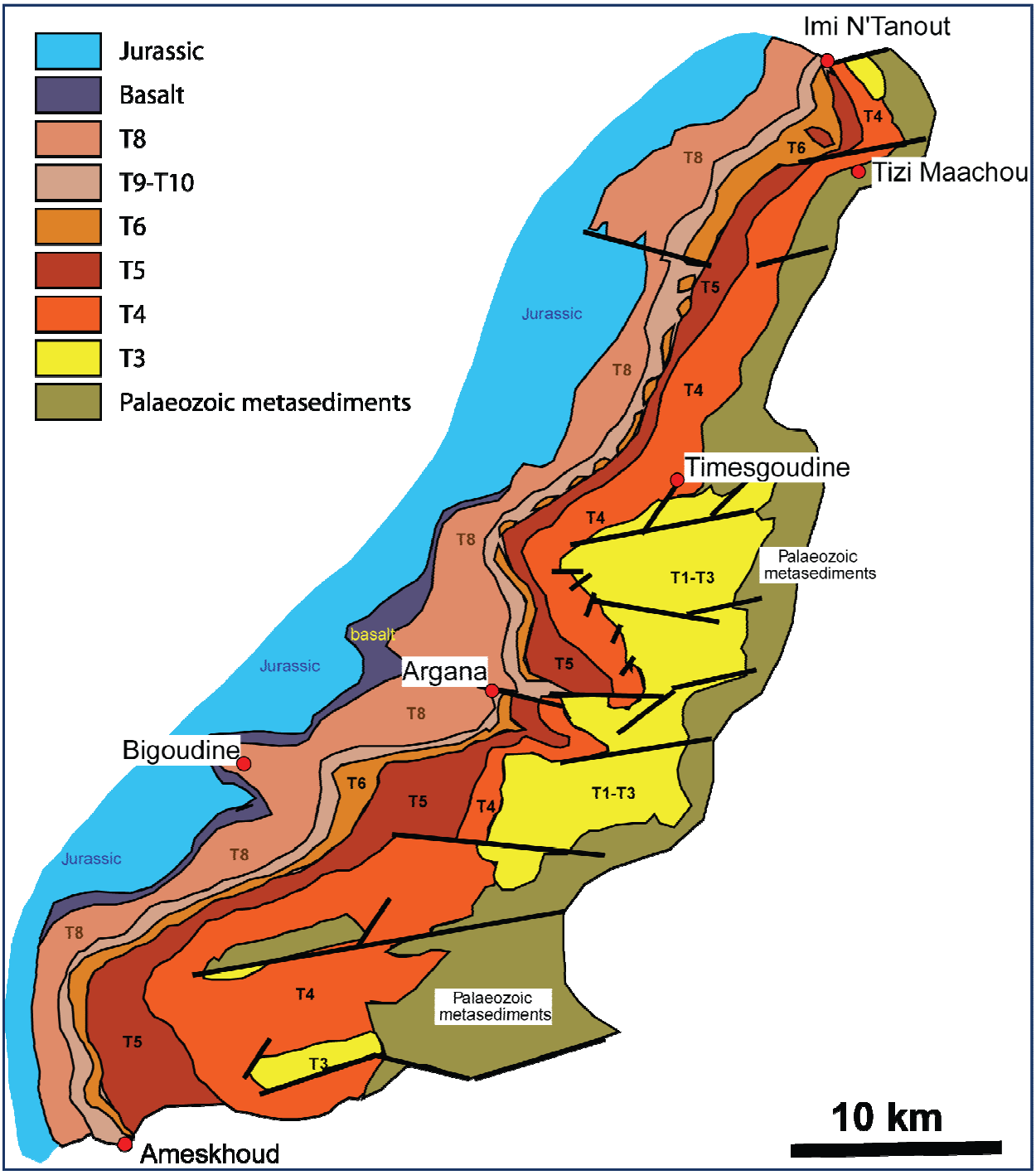


**Figure 2. Simplified geological map of the Argana Basin (based on Tixeroint 1973)**

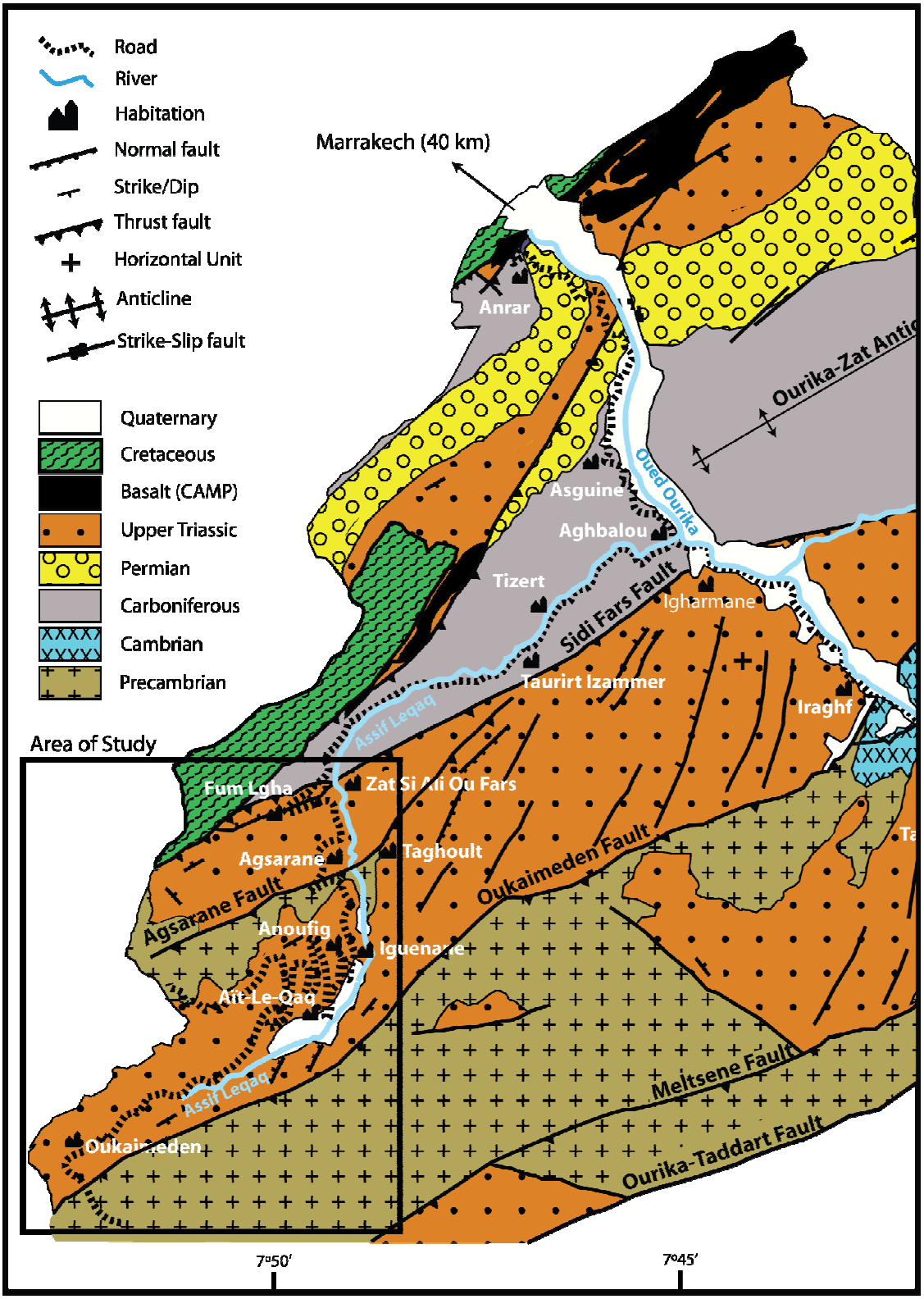


**Figure 3. Simplified geological map of Oukaimeden**

## Stratigraphy

The Permian and Triassic successions overlie a major unconformity developed on rocks deformed by the Hercynian and older orogenies and are conformable with the overlying Jurassic marine deposits (Van Houten 1977). In both basins dating of this interval is generally poor due to the dominantly continental nature of the deposits.

Initial deposition is coarse continental clastics; the T1 and T2 in Argana (Tixeront 1973) and F1 and F2 in Oukaimeden (Mattis 1977; Biron 1982). These have been dated as possibly Permian using paleontological (Dutuit 1976), radiometric (Van Houten 1977) and palynomorphic data (Cousminer & Manspeizer 1975; Olsen *et al.* 2003a & b, 2005). Units T3 to T7 in Argana and F3 to F6 in Oukaimeden are Upper Triassic in age (Cousminer & Manspeizer, 1975). The Tadrart Ouadou Sandstone Member (T6) is Upper Carnian to Lower Norian age (Tourani *et al.* (2000). The Oukaimeden sandstone (F5) is also tentatively dated as Carnian based on palynoflora (Biron and Courtinat 1982). Lower Triassic assemblages have not been recovered to-date in any location (Cousminer & Manspeizer 1975; Olsen *et al.* 2003a; Olsen *et al.* 2003b).

## Depositional Facies

The Upper Triassic section in both basins is dominated by continental, mixed fluvial-aeolian deposits, which record high degree of lateral facies variability (Fig. 4). A number of facies associations have been recognized: Alluvial Fan, Braided River Fluvial Facies, Floodplain (Playa), Aeolian and Tidal (Oukaimeden only)

Detailed correlation of the T6 and F5 intervals shows similar facies and depositional evolution. The basal depositional environments of both the T6 and F5 represent contemporaneous coarse alluvial fan and ephemeral fluvial braidplain deposits. In the Argana Subbasin, a major fluvial bounding surface recognized midway within T6 has been interpreted as a regional re-activation surface, and is believed to have been formed in response to a change in fluvial regime from ephemeral to perennial. This records a probable change in climate in the hinterland source province. In Argana, an axial drainage system flowed from north to south and was fed by several channel systems from the east/northeast/north, sourced in part from the Ancien Massif. A similar pattern can be seen in the Oukaimeden, with a significant erosional surface marking the change to a perennial system within the middle member of the F5. The overlying package comprises a major stacked sandstones deposited in a low sinuosity braided channel belt sourced from the Ancien Massif, in this case flowing to the northwest.

The upper part of the succession in both areas is marked by mixed fluvial–aeolian deposition. The recognition of extensive aeolian facies is interpreted to indicate a regional change to more arid conditions. In Oukaimeden, the top of the succession is characterised by the presence of tidally influenced facies recording the first marine incursion into the basin from Tethys to the northeast. No marine influence was recorded in Argana, suggesting the Massif Ancien remained a positive feature at this time. Both the T6 and F5 are capped by a mudstone dominated units (F6 and T7), and a regionally extensive basalt that provide a regional correlation surface.

## Climatic Versus Tectonic Controls

Sedimentary facies distribution, both spatially and temporally, is strongly influenced by the interplay between tectonics and climate. Basin architecture is controlled by tectonics, which has a significant influence on facies distribution. The main fluvial systems show strong tectonic control on their location, with axial river systems parallel to the main bounding faults and lateral drainage comprising alluvial fans and feeder river systems entering at fault linkage/ transfer zones. The basin bounding faults have controlled accommodation, local sediment input and the orientation of the main channel belts. Local erosion of footwall highs in both basins has acted as a source for coarse alluvial fan breccias. Floodplain and/or aeolian sediments predominate in areas of reduced accommodation, or away from the main drainage systems.

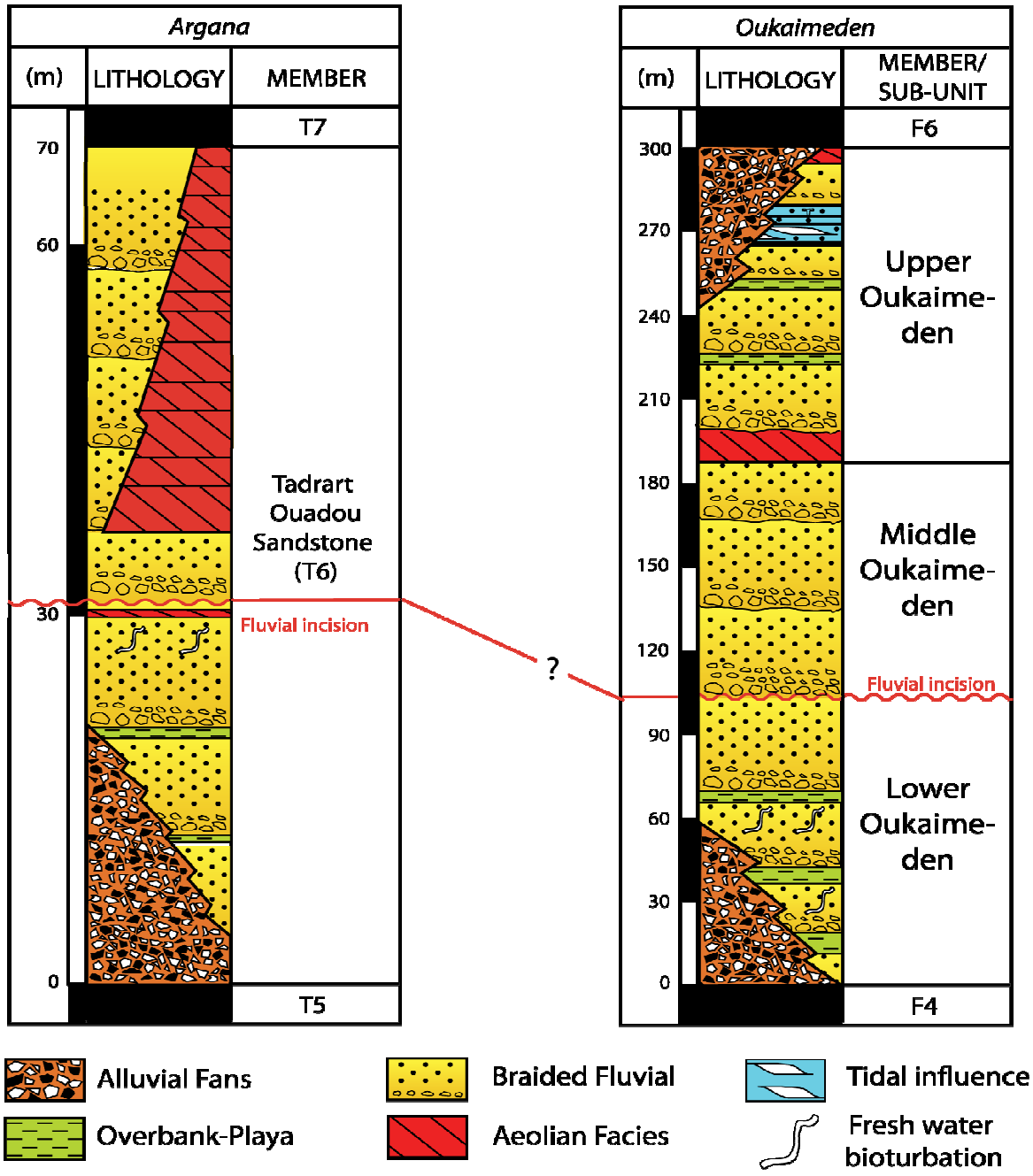


**Figure 4. Correlation of the studied interval, the Oukaimeden Formation (F5) in the Ourika Valley and Tadrart Ouadou Sandstone Member (T6) of the Argana sub-basin, highlighting the main facies recorded and correlated surfaces.**

A major erosion surface within units T6 and F5 is tentatively correlated between basins (Fig. 4), marking a change from ephemeral to perennial fluvial conditions. This is interpreted to record a regional change to a wetter climatic in the hinterland resulting in increased run-off from the catchment area. This was followed by widespread aeolian dune deposition in both studied areas that is interpreted to record a climatic shift back to dry conditions. The evolution towards a more arid climate has also been observed in other Triassic basins along the Central Atlantic conjugate margins (Olsen *et al.* 1996; Smoot 1991; Olsen 1997; Arche and Lopez-Gomez 2005).

## Conclusions

On a basin scale, the complex facies distribution evident in these basins suggests a highly variable basin fill. Correlation relies on identification of key stratal surfaces and architectural styles because of the lack of biostratigraphic control or any other chronostratigraphic surfaces. In both the Argana and Oukaimeden basins, local tectonics control accommodation and influences facies patterns, such as development of alluvial fans and entry points of major drainage systems. Significant changes in fluvial style, from ephemeral to perennial, are recognized within the studied intervals, which suggests rejuvenation of the source areas and a potential interplay of climatic and tectonics. An overall drying upward pattern is observed, with increasing influence of aeolian processes towards the top of both the Oukaimeden sandstone (F5) and Tadrart Ouadou Sandstone member (T6) of the Argana.

These studied sections offer potential analogues for subsurface hydrocarbon systems in similar settings, and provide valuable information on the tectonic and climatic control on depositional facies and architecture. Analysis of basin-wide facies variation, provenance and sediment pathways provide regional scale analogue data.

## References


Arche, A. and Lopez-Gomez, J., 2005. Sudden changes in fluvial style across the Permian-Triassc boundary in the eastern Iberian Ranges, Spain: Analysis of possible causes. Palaeogeography, palaeoclimatology, palaeoecology, 229 (1-2): p.104-126.

Biron, P. and Courtinat, B., 1982. Contribution palynologique à la connaissance du Trias du Haut Atlas de Marrakech. Geobios, 15 (2): p.231-235.

Cousminer, H. and Manspeizer, W., 1976. Triassic pollen data Moroccan High Atlas and the incipient rifting of Pangaea as Middle Carnian. Science, 191: p.943-945.

Dutuit, J.M., (1976). Introduction à l'étude paléontologique du Trias continental marocain. Description des premièrs Stégocéphales recueillis dans le couloir d'Argana. Mém. Mus. Natn. Hist. nat., Paris C 36: p.253.

Dutuit, J.M., (1977). Palaeorhinus magnoculus, phytosaure du Trias supérieur de l'Atlas Marocain. Géologie Méditerranéenne 4: p.225-238.

Dutuit, J.M., (1988). Diplocaulus minimus n. ps. (Amphibia; Nectridea), Lepospondyle de la formation d'Argana, dans l'Atlas occidental marocain. C.R. Acad. Sci. Paris II 307: p.851-854.

Hunt, A.P. and Lucas, S.G., (1991). The Palaeorhinus Biochron and the correlation of the non-marine Upper Triassic of Pangaea. Palaeontology 34: p.487-501.

Jalil, N.E., (1999). Continental Permian and Triassic vertebrate localities from Algeria and Morocco and their stratigraphical correlations. Journal of African Earth Sciences 29(1): p.219-226.

Jalil, N.E. and Dutuit, J.-M., (1996). Permian captorhinid reptiles from the Argana Formation, Morocco. Palaeontology 39(4): p.907-918.

Lucas,S.G., (1998). Global Triassic tetrapod biostratigraphy and biochronology. Palaeogeography, Palaeoclimatology, Palaeoecology 143: p.347-384.

Olsen, P. E. and Kent, D. V., 1996, Milankovitch climate forcing in the tropics of Pangea during the Late Triassic. Palaeogeography, Palaeoclimatology, and Palaeoecology, v.122, p.1-26.

Olsen, P. E. 1997. Stratigraphic record of the early Mesozoic breakup of Pangea in the Laurasia-Gondwana rift system. Annual Reviews of Earth and Planetary Science v.25, p.337-401.

Smoot, J.P. 1991. Sedimentary facies and depositional-environments of early Mesozoic Newark supergroup basins, Eastern North-America. Palaeogeography, Palaeoclimatology, and Palaeoecology, v.84 (1-4), p.369-423.

Olsen, P.E., Kent, D.V., Et-Touhami, M., Puffer, J.H., 2003a. Cyclo-, magneto-, and bio-stratigraphic constraints on the duration of the CAMP event and its relationships to the Triassic-Jurassic boundary. The Central Atlantic Magmatic Province: Insights From Fragments of Pangaea, Geophysical Monograph Series, 136: p.7-32.

Olsen, P.E., Kent, D.V., Sues, H.D., Koeberl, C., Huber, H., Montanari, A., Rainforth, E.C., Fowell, S.J., Szajna, M.J., Hartline, B.W., 2003b. Ascent of dinosaurs linked to an iridium anomaly at the Triassic-Jurassic boundary (Reply to Thulborn). Science, 301: p.169.

Tixeront, M., (1973). Lithostratigraphie et minéralisations cuprifères et uranifères stratiformes syngenetiques et familières des formations detritiques permo-triassiques du couloir d'Argana, Haut Atlas occidental (Maroc). Notes du service geologique du Maroc 33 (249): p.147-177.

Tourani, A., Lund, J. J., Benaouiss, N. and Gaupp, R., (2000). Stratigraphy of Triassic syn-rift deposition in Western Morocco. Zentralblatt für Geologie und Paläontologie, Teil 1, Heft 9-10: 1193-1215.

Van Houten, F. B., (1977). Triassic-Liassic deposits of Morocco and E North America: comparison. AAPG Bulletin 61 (1): p.79-99.

Ziegler, P. A. (1990). Geological Atlas of Western and Central Europe. The Hague, Shell Internationale Petroleum Maatschappij.

**BACK**

# Future Prospects of Oil and Gas within Selected Target Areas of Scotian Shelf and Slope, Offshore Nova Scotia, Eastern Canada: Evaluation based on Petroleum Systems Risk Assessment

**Prasanta K., Mukhopadhyay (Muki)**
Global Geoenergy Research Ltd.
427 – 1657 Barrington Street
Halifax, Nova Scotia, B3J 2A1
Canada
e-mail: muki@global-geoenergy.com

**Paul, J. Harvey**
Nova Scotia Department of Energy
Halifax, NS, B3J 3P7
Canada
e-mail: harveypj@gov.ns.ca

## ABSTRACT

Recent deepwater drilling surrounding the Sable Subbasin within the Scotian Slope, Eastern Canada has indicated that the successes/failures in finding economic hydrocarbon discoveries are closely related to complex petroleum systems and mobilization of Jurassic salts compared to deepwater basins of both the Gulf of Mexico and Angola. New comprehensive research combining seismic stratigraphy, heat flow assessment, geochemical fingerprinting, and petroleum system modeling of the Triassic-Tertiary sediments from the Scotian Slope reveals that the formation, timing, and fluidity of several large allochthonous salt canopies (Sable Subbasin) or autochthonous salt diapers (area between Sable and Shelburne Subbasins) are closely connected to source rock anoxia, bypassing of turbidite sands (in early Tertiary and late and middle Cretaceous), and the survival of hydrocarbons within various play types. Early mobilization of Jurassic salt forming large canopies (especially within the Tertiary sediments of the Sable Slope) possibly originated from enhanced heat flow and three-phase fluid flow in the late Jurassic-early Cretaceous.

Our study indicates that the various play types (especially the salt flank and salt top reservoirs) in the late Jurassic and early Cretaceous may possibly be charged with three petroleum system hydrocarbons (gas-condensate, light oil-gas and heavy oil-gas) within the Sable (beyond 2500 m water depth) and Shubenacadie-Shelburne Slopes (beyond 1500 m). The late Triassic/Early Jurassic lacustrine and Jurassic/Cretaceous Verrill Canyon marine source rocks are the most significant components within various petroleum system hydrocarbons although the timing of hydrocarbon charge could be significantly different in various parts of the Scotian Basin.

BACK

# Continental Rift Basin Fills: Evolution from Opened to Closed Stage (Wolfville / Blomidon Formations, Nova Scotia).

**Sophie Leleu**
University of Aberdeen
Meston Building
Aberdeen, Scotland, AB24 3UE
United Kingdom
e-mail: sophie.leleu@abdn.ac.uk

## ABSTRACT

Rift basins in continental settings tend to display a similar sedimentary evolution with an initial stage (1) characterized by alluvial fan deposition around the basin flanks and fluvial sequences in the basin centre and a later stage (2) dominated by lacustrine sedimentation in the basin centre. The syn-rift Late Triassic sedimentary succession of the Minas sub-basin (Bay of Fundy, Nova Scotia) shows this evolution. The sedimentary succession comprises the lower fluvio-aeolian Wolfville Fm (stage 1 deposits) and the overlying ephemeral fluvial/lacustrine/ playa Blomidon Fm (stage 2 deposits). This contribution presents a facies analysis of the transition between the two stages. The Wolfville Fm displays a complex interplay of coarse and fine-grained fluvial sandstones, aeolian dune deposits and alluvial fan sediments. The upper part of the Wolfville Fm (250 m of vertical section) which occurs beneath and is transitional into the lacustrine/ playa deposits of the Blomidon Fm is described here. Cyclicity within the sedimentary succession is illustrated by well organized and repetitive alternations of fluvial/ ephemeral fluvial/ lacustrine and aeolian sediments, which suggests a gradual evolution from stage 1 and stage 2 and a strong climatic influence on depositional architecture.

BACK

# Permo-Triassic Basins from Ireland to Norway: Basin Architecture and Controls

**Kateřina Štolfová**
**Patrick M. Shannon**
UCD School of Geological Sciences
University College Dublin
Belfield, Dublin 4
Ireland
e-mail: katerina.stolfova@ucd.ie
e-mail: p.shannon@ucd.ie

## ABSTRACT

A series of rift basins along the northwest European Atlantic margin often contain Permo-Triassic strata. The original depositional extent of the Permo-Triassic basins and their large-scale geometries are poorly constrained due to their burial beneath younger strata, combined with tectonic effects of later rifting and continental breakup. Permo-Triassic basin geometries include (a) long-lived, large-scale growth fault-controlled depocentres, (b) ephemeral and subtle broad fault-controlled geometries with switching depocentres and fault polarity and (c) simple uniform thicknesses across large regions. The basin architecture is controlled by a complex interplay of (1) crustal thickness and thermal structure, (2) inherited Variscan, Caledonian and older basement fabrics, (3) pre-rift palaeotopography and (4) spatial and temporal rift history.

## Introduction and Geological Setting

Permo-Triassic strata are preserved as a series of elongate rift basins along the northwest European Atlantic margin. Following Caledonian and Variscan orogenies and plate amalgamation, these rift basins developed due to continental breakup and extension. The original depositional extent and large-scale geometries of the Permo-Triassic basins are poorly constrained, due to their often deep burial beneath Jurassic, Cretaceous and Cenozoic strata, combined with effects of later tectonism and continental break-up.

This study uses seismic and well data, supplemented by outcrop information, to compare Permo-Triassic large-scale basin geometries along 3000 km of the northwest Atlantic Margin in Irish, UK and Norwegian offshore sectors (Fig. 1). Their structural setting range from basins overlying hot, thickened Variscan crust in the Irish offshore to those developed above normal temperature crust, sometimes with inherited Caledonian structural fabrics, west of UK and Norway.

## Irish Sector

Permo-Triassic strata have been recorded in the Celtic Sea, south of Ireland, in the Irish Sea region east of Ireland (not dealt with in this paper) and in the Atlantic Margin basins (Slyne, Erris, Porcupine and Rockall basins). The basin geometries vary from simple half-graben to structurally complex basins and the Permo-Triassic geometries frequently indicate that the depositional limits of the basins extended significantly beyond the currently preserved basin limits.

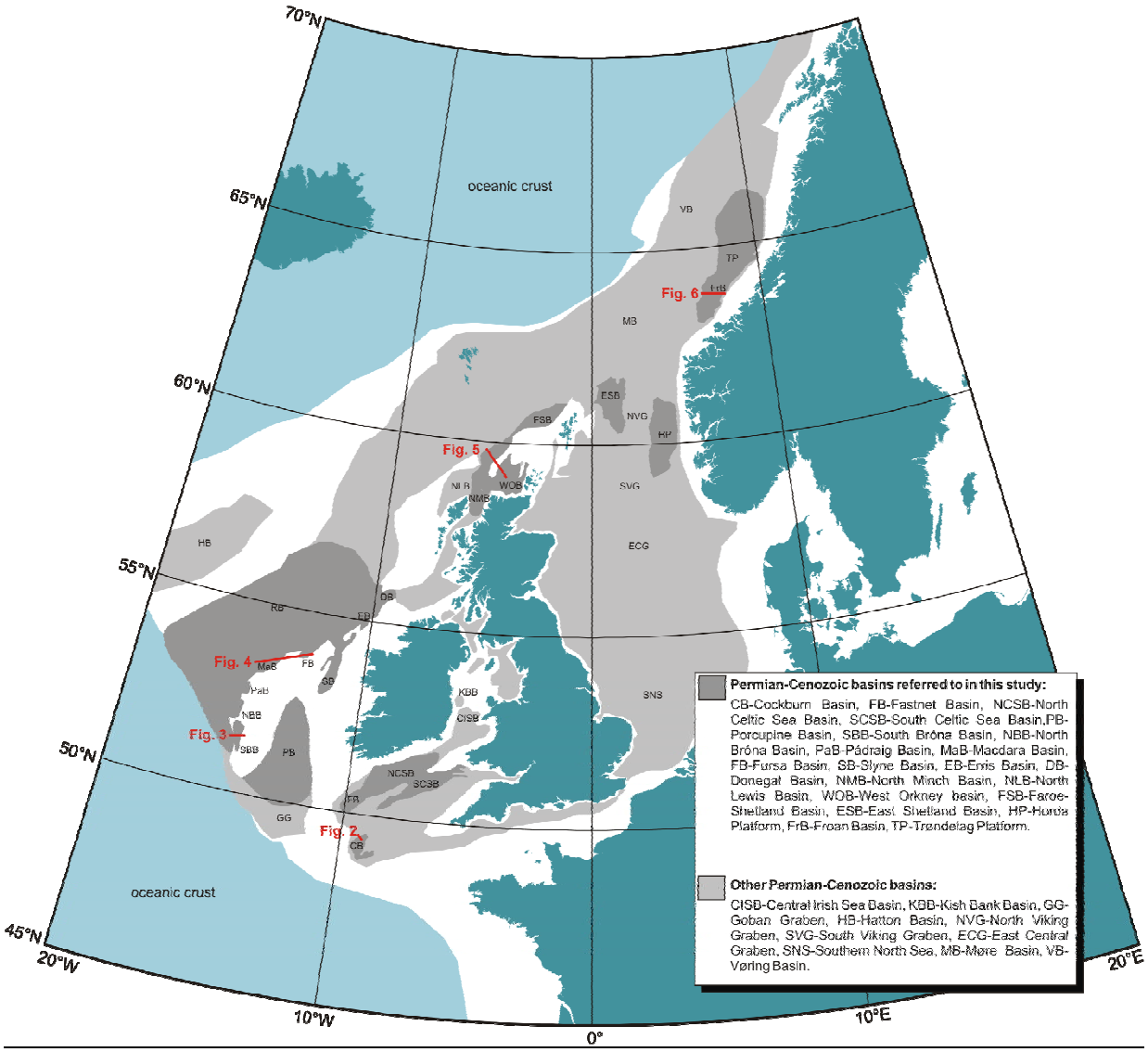


**Figure 1. Map of NW Atlantic margin. Approximate limits of Permian-Cenozoic basins are shown in grey (see legend for basin names). Locations of Figures 2-6 are indicated.**

## Celtic Sea basins

Basins south of Ireland trend east-northeast–west-southwest to northeast-southwest, parallel to inherited Caledonian and Variscan basement structures. While the Triassic in the Celtic Sea basins is proven by wells, Permian successions were not encountered and are only inferred from seismic evidence (Van Hoorn 1987, Smith 1995, Shannon 1995). The South Celtic Sea Basin contains thick salt sequences, which are also locally preserved along the southern margin of the North Celtic Sea Basin. In the Cockburn Basin, inferred Permian strata are restricted to half-grabens preserved beneath an angular unconformity at the base of Triassic (Shannon 1995, Smith 1995). These half-grabens are fault-controlled, probably by reactivated Variscan structures, and show stratal wedging. The interpreted Triassic succession is areally extensive and has an approximately uniform thickness (Fig. 2). The inferred Permian strata could have developed by post-orogenic collapse of thickened hot Variscan crust, while the Triassic could represent a later stage of Pangea break-up, when the crust was cooler and thinner.

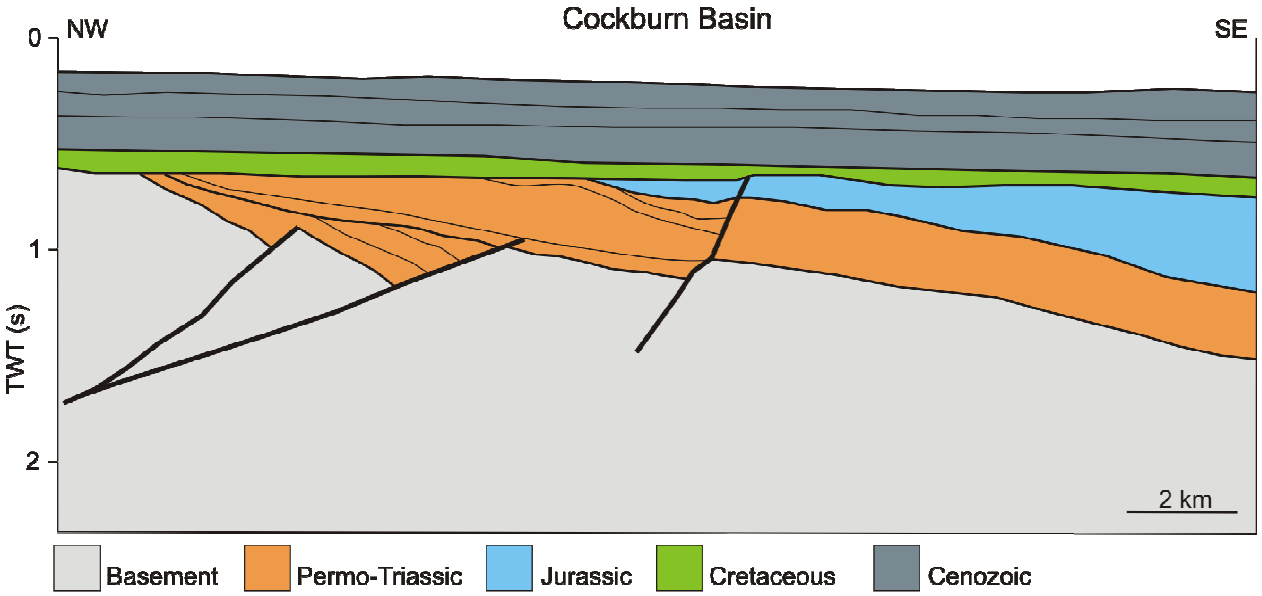


**Figure 2. Geoseismic profile from Cockburn Basin. Inferred early wedging strata are locally preserved in small half-grabens, while unconformably lying younger Triassic strata are deposited over extensive area and exhibit uniform thickness with subtle internal variations.**

### Atlantic Margin Basins

Permo-Triassic strata are preserved as elongate fault-controlled rift basins, typically 'perched' in the footwall of the large Porcupine and Rockall basins. Well data has encountered an extensive succession in the northeast-southwest trending Slyne and Erris basins (Naylor *et al.* 1999, 2002, and Dancer *et al.* 2005). Cores from the Corrib gas field in the Slyne Basin comprise sandstones with minor mudstones and siltstones of presumed Lower Triassic age. The fluvial sandstones are very well sorted, containing some reworked aeolian grains and show a general absence of gravel or pebble material. The sandstones often exhibit planar cross-bedding and lamination. They represent the deposits of distal part of mature fluvial system, with the possibility of coexistence of nearby aeolian dune fields. The mudstone and siltstone beds show rare bioturbation and occasional desiccation cracks and they are interpreted as deposits of floodplain or playa origin.

Several small basins, perched in the eastern and western footwalls of the Rockall Basin, contain interpreted Permo-Triassic strata and show a broadly regionally correlateable internal stratigraphy (Fig. 3). Interestingly, some seismic lines show possible minor halokinetic structures (Fig. 4). In the northern part of the area the presumed Permo-Triassic strata exhibit often stratal wedging, while in the south they are uniformly thick with few internal unconformities. Their geometries suggest that the original deposition extent of the Permo-Triassic was greater than is presently preserved in the 'perched' basins.

## UK Sector

The Permo-Triassic offshore basins described in this section are situated to the north and to the west of Scotland. Their characteristics are illustrated by examples studied from the North Minch Basin, the Solan Bank High and the East Shetlands Basin regions.

### North Minch Basin

The North Minch Basin is located between Lewis and the Northern Scotland mainland. It is a half-graben with Triassic syn-depositional normal faulting (Steel and Wilson 1975). The presence of

Permo-Triassic strata has been proven by drilling, with more than 1 km of mainly red, poorly dated sandstones, siltstones and mudstones (Fyfe *et al.* 1993). The Permo-Triassic depocentre migrated northwestwards by approximately 15 km, with progressive cessation of activity on faults and the development of new growth faults. The southeast-dipping faults are estimated to have accommodated up to 3 km of Permo-Triassic sedimentation (Fyfe *et al.* 1993). The half-graben geometry is interpreted as a response to migrating strain localization in a narrow rift system.

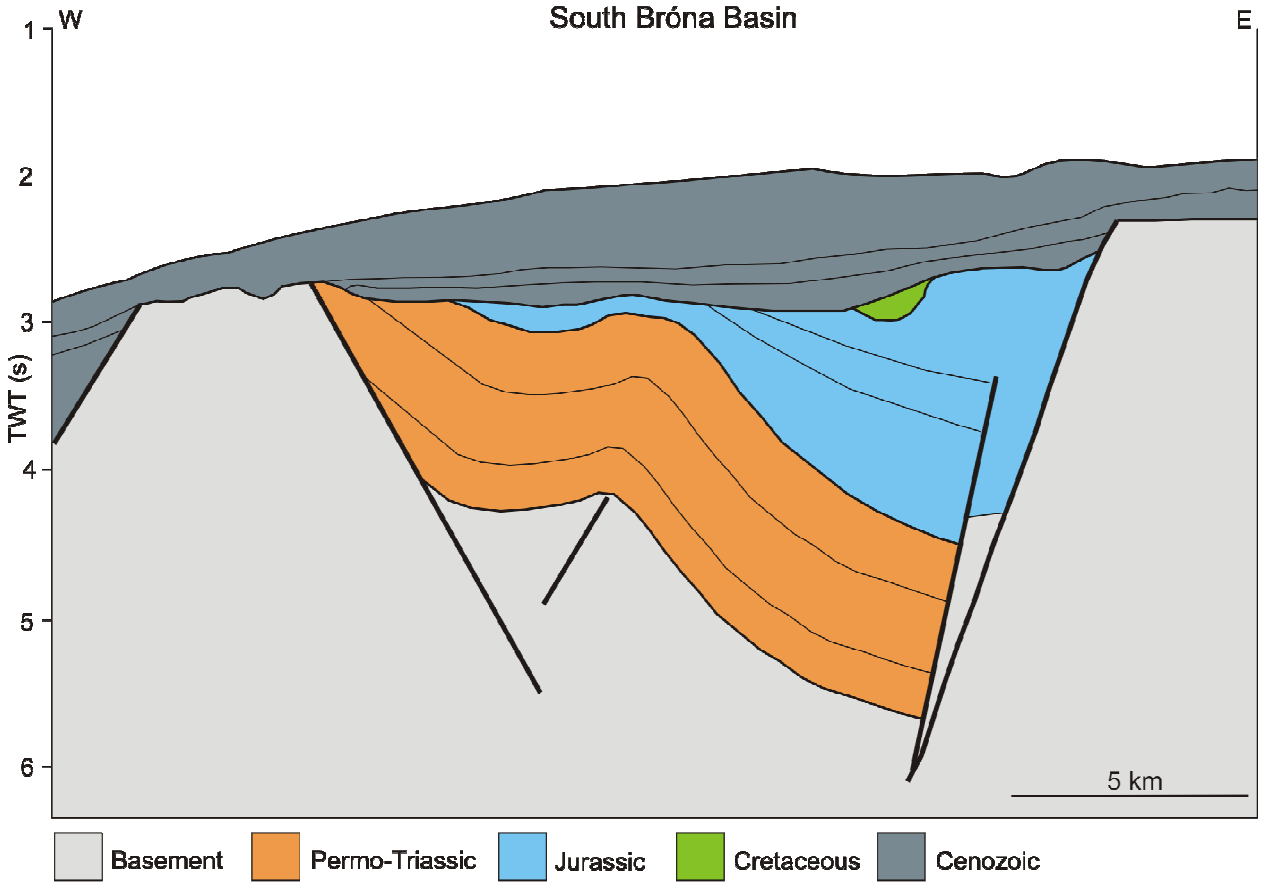


**Figure 3. Geoseismic profile from South Bróna Basin. The interpreted Permo-Triassic strata have uniform thickness. Jurassic strata show wedging towards west-dipping basin-bounding fault. The Permo-Triassic geometry suggests that the depositional limits of basin extended significantly beyond the currently preserved basin.**

## Solan Bank High Area

The area north of the Scottish mainland and west of the Orkneys can be divided into two regions by the Solan Bank High, a northeast-southwest trending horst. The Permo-Triassic is extensively preserved and proven by BGS boreholes and exploration wells. The succession to the southeast of the Solan Bank High consists of small half-grabens with Permo-Triassic sediment wedges showing classical growth fault geometries. The succession to the northwest of the Solan Bank High is thick and parallel-bedded suggesting the interpreted Permo-Triassic strata had an originally greater extent than is preserved in the basin (Fig. 5). The basin was tilted by later movement on the northwest Solan Bank High listric fault and deeply eroded. The basin architecture can be explained by low-magnitude multiple extension (wide rift).

### East Shetland Basin

The interpreted Permo-Triassic is preserved in eroded, southeast-dipping tilted fault blocks, which are onlapped by major basin fill of Cretaceous age. The Permo-Triassic sequence can be divided into two successions: The lower one shows variable thickness and the upper one seems to wedge towards the southeast. The Permo-Triassic geometry appears to be consistent with initial palaeotopographic infill followed by minor narrow rifting.

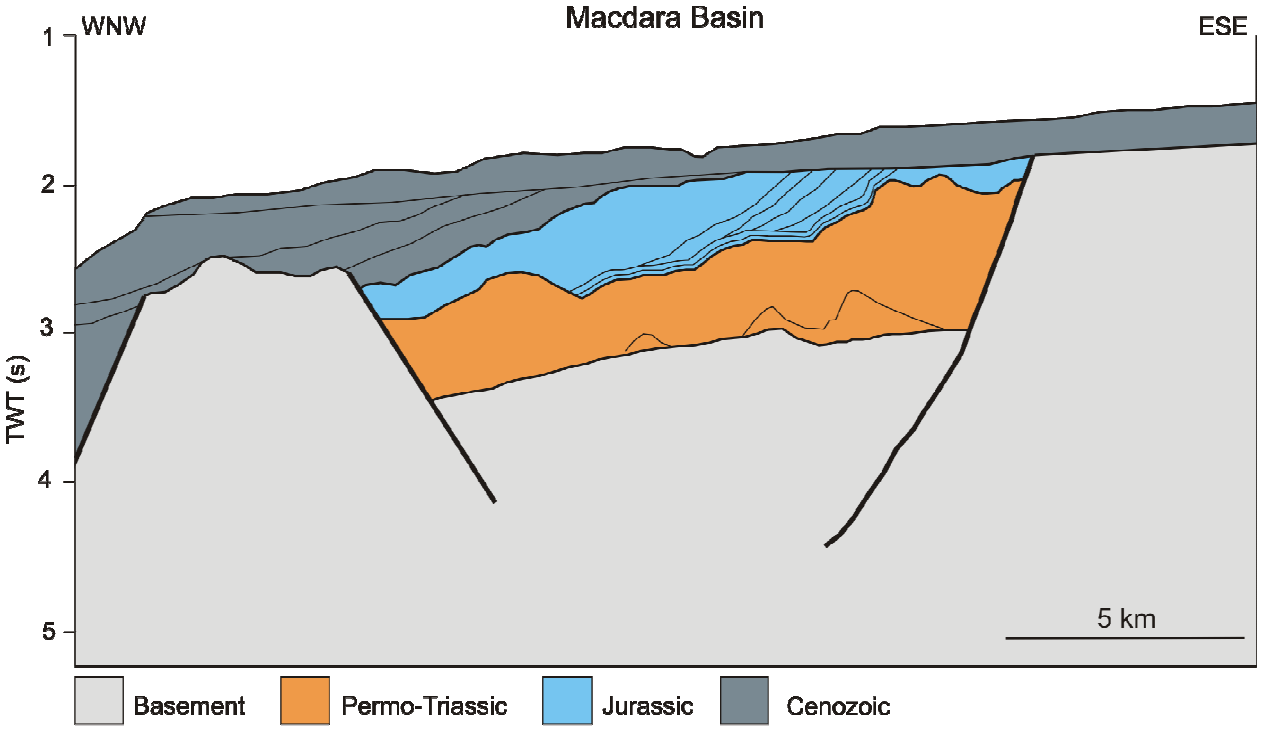


**Figure 4. Geosesmic profile from Macdara Basin. Interpreted halokinetic structures are present in the lower part of interpreted Permo-Triassic succession. Those structures are mirrored by basal part of the overlaying Jurassic sequence. Middle and upper parts of Jurassic succession show dip change of seismic reflectors resulting in downlap onto basal part.**

## Norwegian Sector

Permo-Triassic strata on the continental margin have been proven by numerous wells in the Norwegian North Sea area between 60° and 69° north. In the south, the Horda Platform shows fault-controlled half-graben geometries with thick Triassic strata. A block-faulted terrane generated by probable Late Permian episodic rifting occurs beneath the Trøndelag Platform and the Halten Terrace. During the Triassic some block faulting continued in the area of the Frøya High (Blystad *et al.* 1995). The Trøndelag Platform is a major structural element and includes the Froan Basin, Frøya High, Vega High and the Ylvingen Fault Zone.

### Horda Platform

The Permo-Triassic succession in the Horda Platform region shows growth fault geometry within half-grabens. Faulting shifted progressively to the southeast giving rise to new depocentres. The lowermost syn-rift sequence overlying basement is of Permian-Scythian age and occurs in the northwest and central sub-basins. The syn-rift sequence is overlain by three post-rift sequences (Steel and Ryseth,

1990). The initial syn-rift and the first post-rift sequence are consistent with narrow rifting, with progressive southeast migration of strain localization. The two upper sequences, of Carnian-Rhaetian and Rhaetian-Sinemurian age, exhibit broadly tabular shapes which can be interpreted as low-magnitude multiple extension basin geometry.

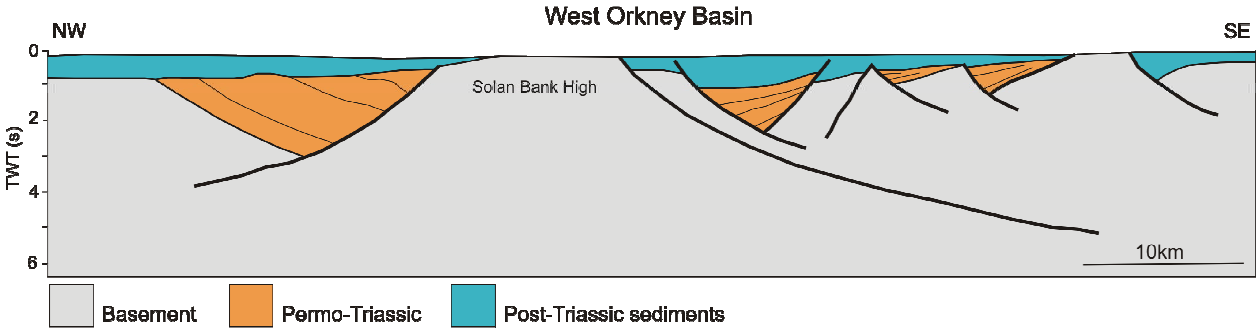


**Figure 5. Geoseismic profile from West Orkney Basin area. The succession to the SE of the Solan Bank High consists of small half-grabens with Permo-Triassic sediment wedges showing classical growth fault geometries. The succession to the NE of the Solan Bank High is thick and parallel-bedded.**

### Froan Basin

The Froan Basin lies in the southwest part of the Trøndelag Platform. The eastern flank of the adjacent north-south trending Frøya High represents the basin-bounding fault. In the southernmost part of the area, the oldest part of the interpreted Permo-Triassic succession shows half-grabens with pronounced wedging towards the southeast, overlain in the central part of the section by a set of half-grabens with smaller scale southeast-dipping growth faults. The upper part of the section, proven to be Triassic in age, has subtle thickness changes and consists of several internal stratal wedges. The basin experienced fault polarity changes as well as migration of depocentre through time. Further north the Permo-Triassic sequence is intensively faulted and can be divided into three seismic packages (Fig. 6). The oldest package shows clear growth faulting, the central package exhibits less dramatic growth faulting and the youngest strata have a broadly tabular geometry with some internal thickness variations. The basin architecture is compatible with initial narrow rift overlain by wide rift geometry. The main western basin-bounding fault was long-lived and controlled the depocentre during Permo-Triassic times.

### Ylvingen Fault Zone area

The last section described in this study is from the Ylvingen Fault Zone and the Vega High area. The oldest interpreted Triassic package thickens slightly towards the SE and may represent a combination of palaeotopographic infill and early rifting. The middle package shows pronounced northwest stratal wedging reflecting growth faulting and a northwest migration of the sediment depocentre. The upper package has a uniform thickness and is generally devoid of syn-depositional faulting. The deposits may represent a distal part of latest low-magnitude rifting. Minor layer-bound faulting and other structural features may be due to salt movement.

## Discussion

Theoretical modes of crustal extension, based on assumptions of initial crustal thickness, initial heat flow and strain rate, predict that extensional basin domains may be either narrow or wide rifts (Buck 1991, 1999 and Hopper *et al.* 1996). Narrow rifts characterize regions of cold crust with normal initial crustal thicknesses while wide rift zones, often composed of multiple low-magnitude rifts, are predicted in areas of warm crust. In addition, inherited crustal features, together with the extensional response to

orogenic thickening following crustal amalgamation (Core complex mode as defined by Buck, 1991), can control the rift basin geometry. Pre-rift palaeotopography can also influence the resulting large-scale sedimentary geometry. The study area, extending northwards from the region of thick crust in the Variscan frontal region of the southern Irish offshore through to areas of normal, unthickened crust west of Norway, also crosses a number of zones containing major Caledonian structures west of Scotland and elsewhere.

Small, localized half-grabens of presumed Permian age south of Ireland overlie hot thickened Variscan crust. These basins may have been initiated as early post-Variscan orogenic collapse structures within a zone of thickened crust. Thick, broadly uniform Triassic strata were deposited over a large region in the Irish and UK offshore and fit a model of crustal extension with delocalized strain developing a wide rift, multiple low-magnitude basin geometry in a region of heated crust. These are characterized by fault polarity changes and subtle internal wedging of individual seismic packages within a broadly uniform succession. A number of examples are seen locally in the UK and Norwegian offshore that conform to the narrow rift model showing syn-rift graben or half-graben deposits overlain by post-rift thermal subsidence sequences. These are interpreted to reflect zones of cooler crust coinciding with episodes of Triassic extension. The location, orientation and rejuvenation of inherited features (Variscan, Caledonian or older) also played a role in localizing Triassic extensional strain and the resulting characteristic basin geometries are illustrated in several parts of the study area, especially in the Irish and UK offshore.

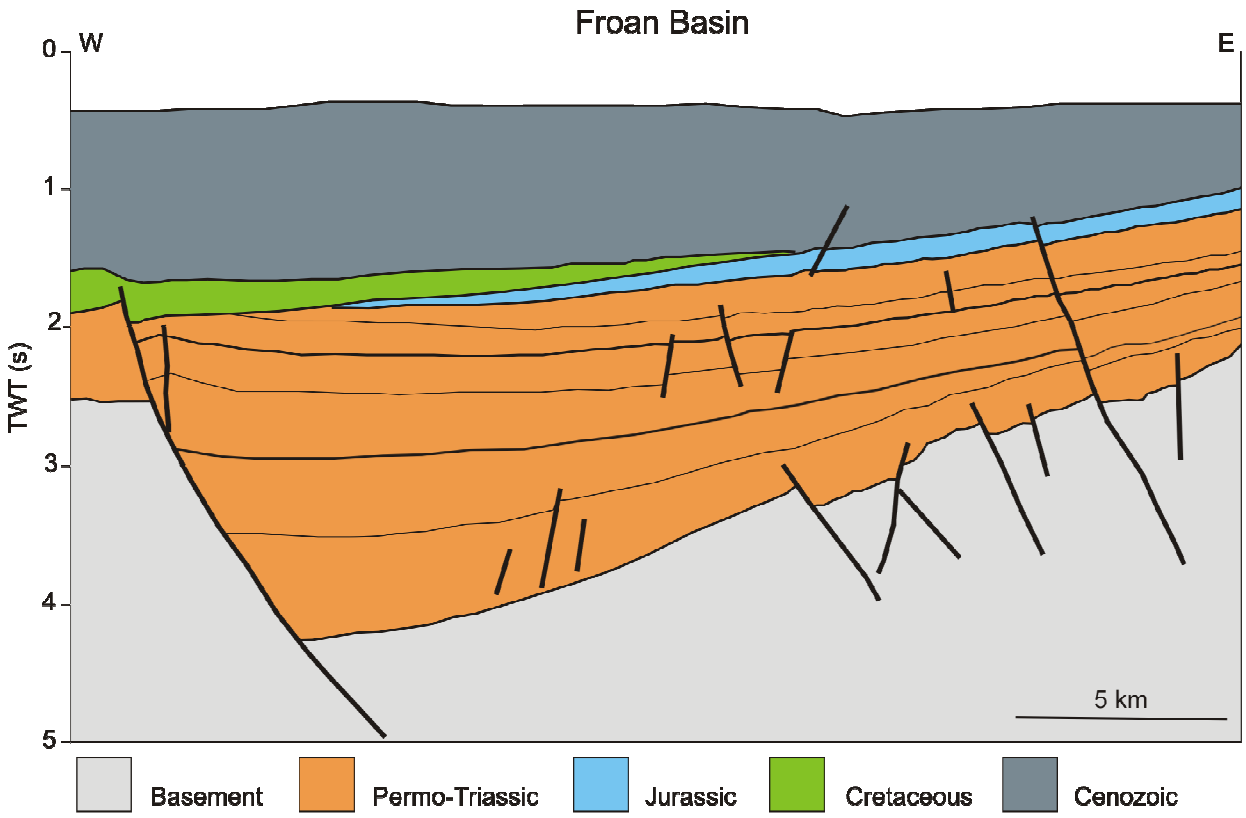


**Figure 6. Geoseismic profile from Froan Basin. Permo-Triassic sequence is intensively faulted and is divided into three seismic packages. The oldest package shows clear growth faulting, the central package exhibits less dramatic growth faulting and the youngest strata have a broadly tabular geometry with some internal thickness variations.**

## Conclusions

There are extensive occurrences of proven (but often poorly dated), largely non-marine, Permo-Triassic strata along the Irish, UK and Norwegian sectors. Although the large-scale regional depositional geometries have been modified by later Jurassic and Cretaceous tectonism, sufficient evidence is seen on seismic data enabling to build a model of basin-scale regional depositional architectures. The regional Permo-Triassic geometries include (a) long-lived, large-scale growth fault-controlled depocentres, (b) ephemeral and subtle broad fault-controlled geometries with switching depocentres and fault polarity and (c) simple uniform thicknesses across large regions. The basin architecture is controlled by a complex interplay of (1) crustal thickness and thermal structure, (2) inherited Variscan, Caledonian and older basement fabrics, (3) pre-rift palaeotopography and (4) spatial and temporal rift history.

## References


Van Hoorn, B., 1987, The South Celtic Sea – Bristol Channel Basin: origin deformation and inversion history: Tectonophysics, v.137, p.309-334.

Smith, C., 1995, Evolution of the Cockburn Basin: implications for the structural development of the Celtic Sea basins, *in* P.F. Croker and P.M. Shannon, eds., The Petroleum Geology of Ireland's Offshore Basins: Geological Society Special Publication, n.93, p.279-295.

Shannon, P.M., 1995, Permo-Triassic development of the Celtic Sea region, offshore Ireland, *in* S.A.R. Boldy, ed., Permian and Triassic rifting in Northwest Europe: Geological Society of London Special Publication 91, p.215-237.

Naylor, D., P.M. Shannon, and N. Murphy, 1999, Irish Rockall Basin region—a standard structural nomenclature system, PAD Special Publication, 42p.

Naylor, D., P.M. Shannon, and N. Murphy, 2002, Porcupine-Goban region—a standard structural nomenclature system, PAD Special Publication, 65p.

Dancer, P.N., S.M. Kenyon-Roberts, J.W. Downey, J.M. Baillie, N.S. Meadows, and K. Maguire, 2005, The Corrib gas field, offshore west of Ireland, i*n* A.G. Doré and B.A. Vining, eds., Petroleum Geology: North-West Europe and Global Perspectives, Proceedings of the 6th Petroleum Geology Conference: Geological Society London, p.1035-1046.

Steel, R.J. and A.C. Wilson, 1975, Sedimentation and tectonism (?Permo-Triassic) on the margin of the North Minch Basin, Lewis: Journal of Geological Society London, v.131, p.183-202.

Fyfe, J.A., D. Long, and D. Evans, 1993, The Geology of the Malin – Hebrides sea area: United Kingdom Offshore Regional Report, British Geological Survey, 91p.

Blystad, P., H. Brekke, R.B. Færseth, B.T. Larsen, J. Skogseid, and B. Tørudbakken, 1995, Structural elements of the Norwegian continental shelf, Part II: The Norwegian Sea Region: NPD-Bulletin Number 8, 45p.

Steel, R. and A. Ryseth, 1990, The Triassic–early Jurassic succession in the Northern North Sea: megasequence stratigraphy and intra-Triassic tectonics, *in* R.F.P. Hardman and J. Brooks, eds., Tectonic Events Responsible for Britain's Oil and Gas Reserve: Geological Society Special Publication, n.55, p.139-168.

Buck, W.R., 1991, Modes of Continental Lithospheric Extension: Journal of Geophysical Research, v.96, n.B12, p.20, 161-20, 178.

Buck, W.R., L.L. Lavier, and A.N.B. Poliakov, 1999, How to make a rift wide: Phil. Trans. R. Soc. London, v.357, p.671-693.

Hopper, J.R. and W.R. Buck, 1996, The effect of lower crustal flow on continental extension and passive margin formation: Journal of Geophysical Research, v.101, n.B9, p.20, 175-20,194.


**BACK**

# Early Infill of the Triassic Fundy Basin: Architecture of the Wolfville Formation and Fluvial Evolution

**Sophie Leleu**
**Adrian Hartley, Adrian**
**David W. Jolley**
**Brian P. Williams**
University of Aberdeen
Meston Building
Aberdeen, Scotland, AB24 3UE
United Kingdom
e-mail: sophie.leleu@abdn.ac.uk

## ABSTRACT

The Fundy Basin forms one of a series of early Mesozoic rift basins developed along the northwestern Atlantic margin. Syn-rift continental sediments were deposited during Late Triassic times within the basin. The sedimentary succession comprises the lower fluvio-aeolian Wolfville formation, the overlying ephemeral fluvial/playa Blomidon formation capped by basaltic lava. Three subbasins are present in the Fundy Basin: the Fundy subbasin, the Minas subbasin to the east and the Chignecto subbasin to the north.

The Wolfville formation displays a complex interplay of coarse and fine-grained fluvial sandstones, aeolian dune deposits and alluvial fan sediments. This study focuses on the Wolfville formation stratigraphy and correlation within the gravely- and younger sandy-dominated fluvial deposits of the Minas subbasin. This contribution will present a detailed analysis of the large scale architecture (27 km) of a gravely braided river system deposited within this endorheic basin, and will discuss the major changes in fluvial style within the basin. The palaeogeography of the Wolfville formation is analyzed by determining the size of the braided river system and by taking an allostratigraphic approach to the recognition and correlation of extensive bounding surfaces.

The bounding surfaces and cycles within both coarse and fine-grained fluvial units allow correlation across the basin. Together with a palynological analysis, the stratigraphy of the Wolfville formation is assessed in the Minas subbasin. This new scheme of the Wolfville Fm architecture in a better-constrained timescale has the potential to help predict sand-fairways and reservoir architecture within similar coarse-grained alluvial deposits.

BACK

# Reservoir Quality, Diagenetic History and Provenance of the Late Triassic Sandstones of the Wolfville Formation, Bay of Fundy, Nova Scotia, Canada

**Yawooz Kettanah**
**Muhamma Kettanah**
**Grant D. Wach**
Department of Earth Sciences
Dalhousie University
Halifax, NS, B3H 4J1
Canada
e-mail: kettanah@dal.ca

## ABSTRACT

The reservoir characterization and provenance of the Wolfville formation sandstones are investigated using petrography, heavy minerals and microprobe analysis of tourmaline and garnet. These fluvial sandstones are calcite cemented feldspathic litharenites to lithic feldsarenites and consist of quartz, lithics, feldspars, minor amounts of mica and heavy minerals. They are derived from metasedimentary and granitic rocks of Meguma terrane during early stages of rifting along the Minas sub-basin as part of the Fundy Basin rift zone postdating the earlier Paleozoic collision orogenies which were culminated by the Appalachian orogeny. Their heavy minerals are mostly iron oxides (magnetite, hematite, ilmenite and their alteration products) and garnet with minor amounts of apatite, chlorite, zircon, tourmaline, biotite and lesser amounts of rutile, staurolite, hornblende, and rarely epidote. They have a recycled orogenic provenance and the main source of these sediments are the Paleozoic rocks underlying the Wolfville Formation dominated by the Meguma supergroup, the South Mountain batholith, Horton and Windsor groups with a possible minor contribution from other Paleozoic formations. The lowermost part of the Wolfville Formation has relatively low porosity (~6%). The Wolfville formation has a considerable thickness beneath the Bay of Fundy where it overlies the Horton Bluff formation, Meguma and/or Avalon terranes which should be investigated further to determine the reservoir potentiality especially where it overlies the organic rich shales of the Horton Bluff formation, as a source rock.

## Geology

The Bay of Fundy is an important part of the geological history of eastern Canada formed during early rifting of Pangaea in the early Mesozoic time along a wide valley in the direction of the Avalon/Meguma suture line which is the extension of Cobequid-Chedabucto fault system. Mesozoic sediments were deposited during various stages of rifting and the early development of the Bay of Fundy. They are exposed along the margins of the Minas sub-basin, part of the northeastern Bay of Fundy (Fig.1). The exposed Mesozoic strata are relatively limited in comparison to their wide extent beneath the Bay of Fundy. Petroleum companies became interested in synrift sediments and explored in the Bay of Fundy during 1968-1983. Seismic surveys were conducted and two exploration wells were drilled in the southwestern part of the Bay of Fundy (Fig.2) (Wade *et al*. 1996).

The Bay of Fundy is part of the northern Appalachian Mountains which was divided by Williams (1979) on the basis of tectonism, metamorphism, plutonism, metallogenesis and stratigraphy into five "lithotectonic zones or terranes". These terranes are from south to north: Meguma, Avalon, Miramichi (Gander), Dunnage and Humber. The Meguma terrane forms the southern part of Nova Scotia and the adjacent continental shelf; it comprises thick turbiditic sediments of the Cambrian-Ordovician Meguma

supergroup, Silurian metasediments and volcanics of White Rock, Kentville and New Canaan formations, and the Early Devonian Torbrook formation. The Meguma Supergroup consists of sand-dominated, metamorphosed turbidites of the Goldenville formation and overlying silt/shale-dominated metamorphosed turbidites of the Halifax Formation. The South Mountain batholith (Late Devonian) has intruded the older formations (Fig.1). The Avalon terrane occupies southern New Brunswick and northern Nova Scotia and comprises late Precambrian and early Paleozoic mafic volcanics and continental metasediments intruded by granites (Rast *et al.* 1976; Keppie, 1979). The Bay of Fundy forms a half graben at the boundary of Meguma and Avalon zones (Wade *et al.* 1996). Both zones were affected by many tectonic events including the Acadian orogeny during mid-Paleozoic which deformed and metamorphosed these rocks. The Mesozoic formations are underlain by Carboniferous formations in the northeastern parts of the Bay of Fundy and by Meguma and/or Avalon terrane rocks towards the southwestern part as indicated from the seismic profiles and sections studied by Wade *et al.* (1996) (Fig.2).

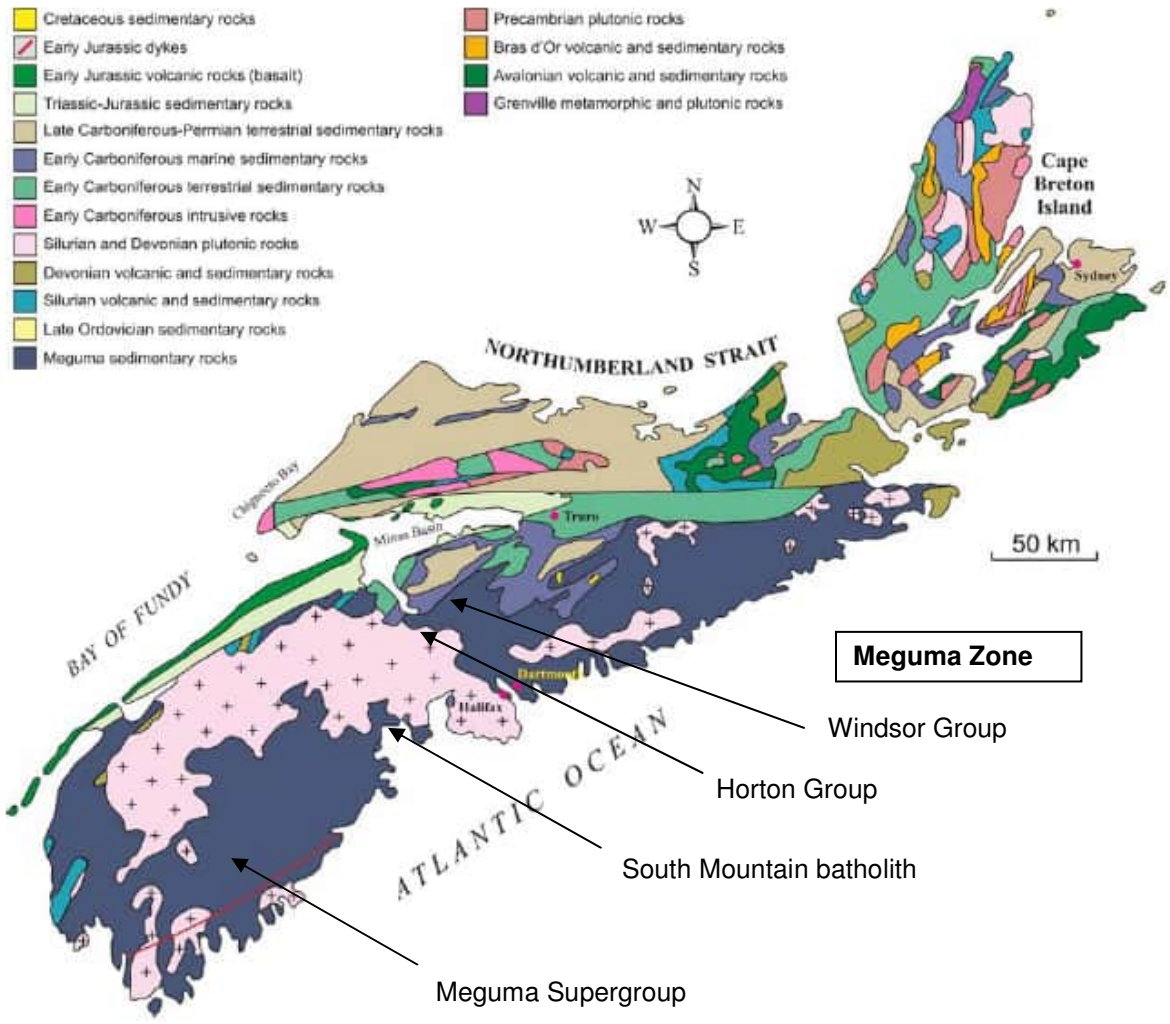


**Fig. 1: Geology of Nova Scotia (Fensome and Williams 2001) showing the location of Cambridge Cove.**

The Horton group in the Minas Basin covers a large area and rests unconformably on lower Paleozoic rocks of the Meguma Supergroup and is conformably to unconformably overlain by Windsor group of Early Carboniferous age (Fig.1). The Mesozoic formations underlying the Fundy sub-basin (Fundy Group) in these sections are from older to younger: Wolfville, Blomidon, North Mountain Basalt, and Scots Bay/McCoy Brook (Fig.2). The Wolfville formation (Fig.1) is exposed on both coasts of the Minas subbasin and Cobequid Bay and also in the Annapolis Valley (Keppie 1979). It unconformably overlies Carboniferous and older Paleozoic sedimentary/metasedimentary rocks (sandstones, conglomerate and minor siltstones and shale) or granitoids of the South Mountain batholith. They were deposited in continental environments by fluvial (braided rivers) and aeolian processes under semi-arid conditions (Klein 1962; Hubert and Forlenza 1988; Wade *et al.* 1996). The red brown color of these sediments indicates that they were deposited in an oxidizing subareal environment.

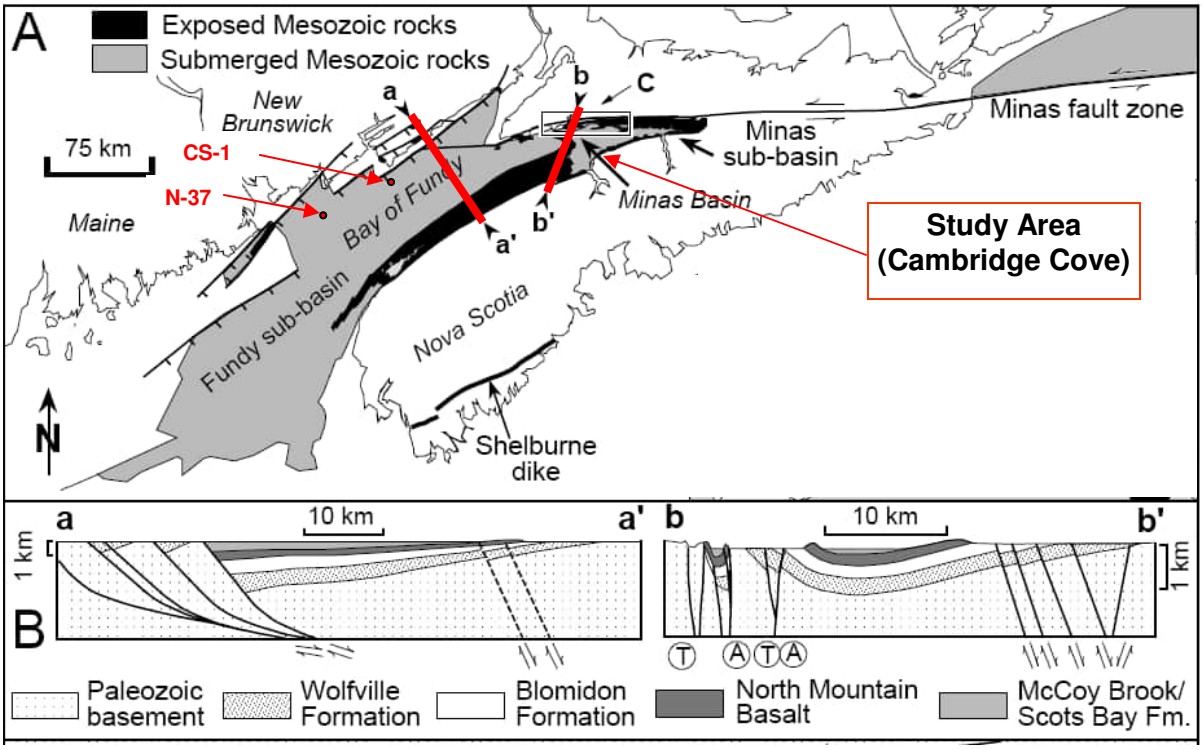


**Fig. 2: Map of Fundy basin and a cross section through the Minas Basin showing the stratigraphy of Mesozoic formations beneath the basin and onshore (from Olsen and Schlische 1990). N-37 = Chinampas N-37 well; CS-1 = Cape Spencer No.1 well.**

The Wolfville formation has been studied by many authors since 1828 as part of the Newark Group by Powers (1916), and as part of the Fundy Group by Klein (1962), and more recently by Wade *et al.* (1996). The thickness of the Lower Triassic Wolfville formation, the oldest formation in the Fundy Group, varies in outcrop from 60m to 833m (Williams *et al.* 1985). It is exposed on both sides of Minas subbasin. The thickness of the Wolfville Formation beneath the Bay of Fundy increases toward the southwest from 1308m in the Irving Cape Spencer-No.1 well to >1718m in the Chinampas N-37 well, and is believed to increase to >3000 m east of Grand Manan Island (Wade *et al.* 1996). The Wolfville formation is well exposed in the southern coast of Minas Basin where it unconformably overlies the Horton Bluff formation. The angular unconformity between the two formations is sharp and very distinct in Cambridge Cove (Fig.3), and the nearby Rainy and Clemment coves.

**Figure 3. Field view of the unconformity between the Triassic Wolfville formation and the Late Devonian-Early Mississippian Horton Bluff formation at Cambridge Cove, Minas Basin, Bay of Fundy.**

The Early Carboniferous Horton Bluff formation has a thickness of 325m and is disconformably overlain by the Cheverie formation and together they form the Horton group. It is separated from the older Meguma Group or the South Mountain batholith by an angular unconformity or fault contact (Williams 1985). The Horton Group has been deposited in fluvial-lacustrine environments as alternating grey to black very fine to very coarse grained clastic sediments ranging from shale to conglomerate, and it is commonly of sublitharentic to orthoquartzitic types. In the Cambridge Cove area the Horton Bluff Formation consists of highly deformed alternating very hard brownish gray siltstones and grayish thinly laminated hard shales (Fig.3). The siltstones are homogeneous in grain size and the quartz grains are cemented by calcite. Two wells (Kennetcook #1 and #2) were drilled in 2007 in the Windsor Basin of Nova Scotia investigating hydrocarbon potential of the Horton Bluff formation shales (The Oil & Gas Magazine Online, June 24, 2008). Related news release in January 30, 2008 announced the discovery of substantial amounts of gas with an estimated resource of 89 to 109 Bcf of OGIP per square mile (http://www.wallstreet-online.de/diskussion/1137920-neustebeitraege/news-news-triangle-pet).
According to this news release, the total gas content of the shales range from 7.9 to 190 $ft^3$/ton with an average TOC of 10% for all shales containing organic matter of type II/III to III which have a maturity of 1.53% to 2.07% placing them within the peak window for natural gas generation.

## Petrography and Diagenesis

Eleven sandstone samples from the thickest part of the Wolfville formation at Cambridge Cove were studied. The samples were chosen to represent the dominant thick sandstone/conglomerates beds which have average thicknesses of 2 to 4 m. These beds are channel fills and some times become thinner as shown in Fig.3; they are separated by thin silty claystones. Sieving results showed they are mostly medium grained, poorly sorted, fine skewed and platykurtic.

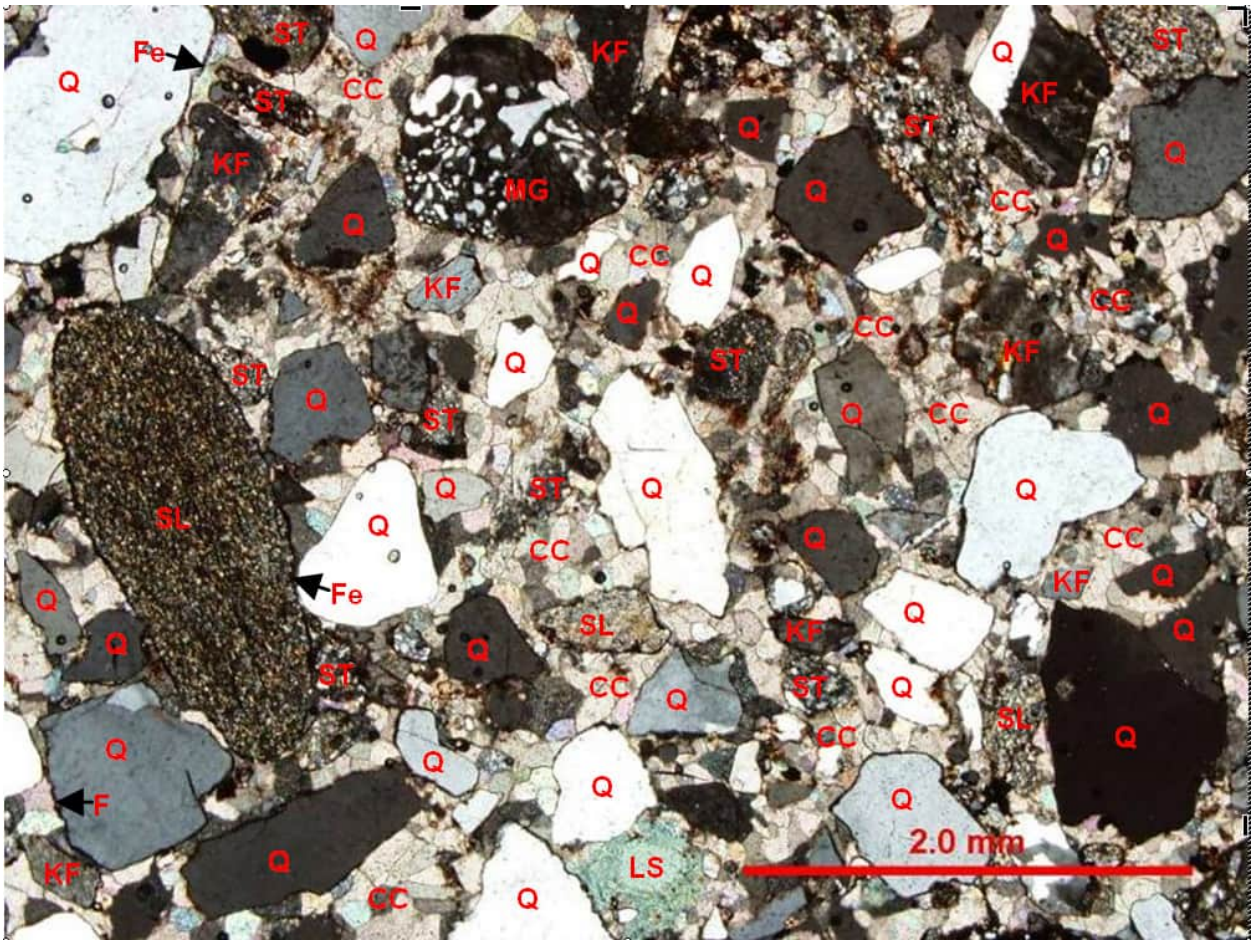


**Fig.4: Calcite cemented sandstones of Wolfville Formation showing the main constituents. [Q=quartz; KF=K-feldspar; SL=slate; ST=siltstone; LS=limestone; MG=micrographic granite; CC=calcite cement; Fe=iron rim (cement)]**

The Wolfville sandstones are mostly feldspathic litharenites and lithic feldsarenites (Fig.4 and 5E). They consist of cement (dominated by sparry calcite and minor iron oxide and clays) (36.4%), quartz (31.8%), lithics (16.1%), feldspars (9.9%), heavy minerals (0.8%), and mica and chlorite (0.5%) with the remainder representing pore spaces (Fig.4). The average percentage of alkali feldspars/plagioclase is 10.4%. The lithics are in their order of abundance: slate, siltstone, granite, limestone, sandstone, quartzite, chert, and schist. These percentages were obtained by separately counting 1200 points in each thin section of the rock and their heavy mineral fraction. Counting of framework grains was done according to the Gazzi-Dickinson method (Gazzi 1966; Dickinson 1970) which has the advantage of using the data for provenance interpretation (Dickinson 1985; Dickinson *et al.* 1983; Dickinson and Suczek 1979; Ingersoll and Suczek 1979). The Gazzi-Dickinson method reduces the effect of composition dependence on grain

size used in traditional methods by restricting lithic fragments to microcrystalline aphanetic material which contains no crystals larger than the silt size (62.5 μm). Traditional methods, following the procedure of Pettijohn (1972) were also performed for counting the relative abundance of lithics in these sandstones (Fig.5F). XRD analysis of clay fraction separates from the studied sandstones showed that they consist of illite, montmorillonite, kaolinite and chlorite.

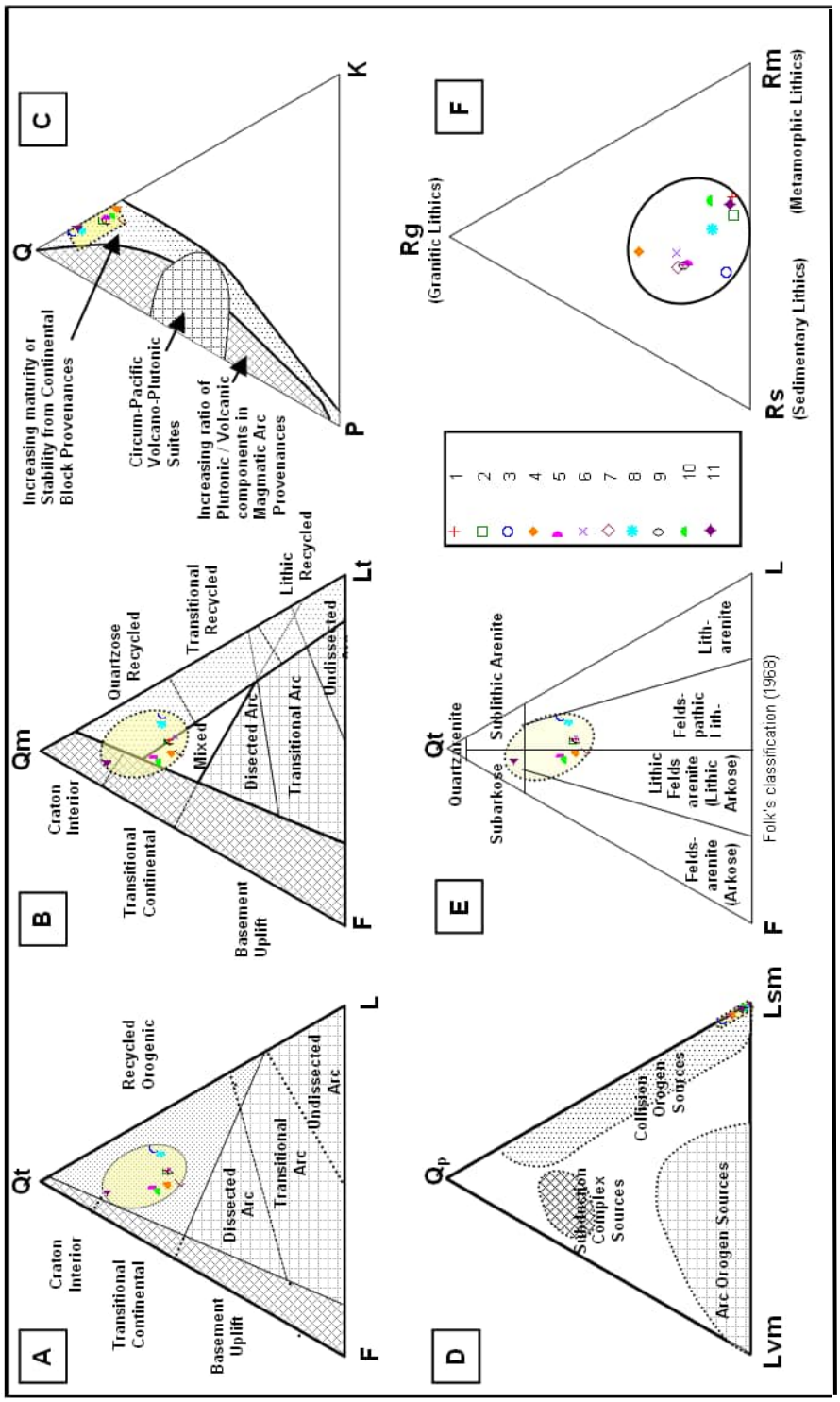


**Fig. 5: Detrital constituents of the Wolfville Formation sandstones plotted on the provenance indicator triangular diagrams of Dickinson (1985), and Dickinson and Suczek (1979) (A, B, C, D) and on Folk's (1968) sandstone classification triagle (E). (F) Lithic fragment's triangular diagram; Qm=monocrystalline quartz; Qp=Polycrystalline quartz (chert & quartzite); Qt=Qm+Qp; F=feldspars; L=Lithics; Lt =L+Qp; Lsm=MetasedimentaryLithics; Lvm=Metavolcanic lithics; Rg=Granitic lithics; Rs=Sedimentary lithics; Rm=Metamorphic lithics.**

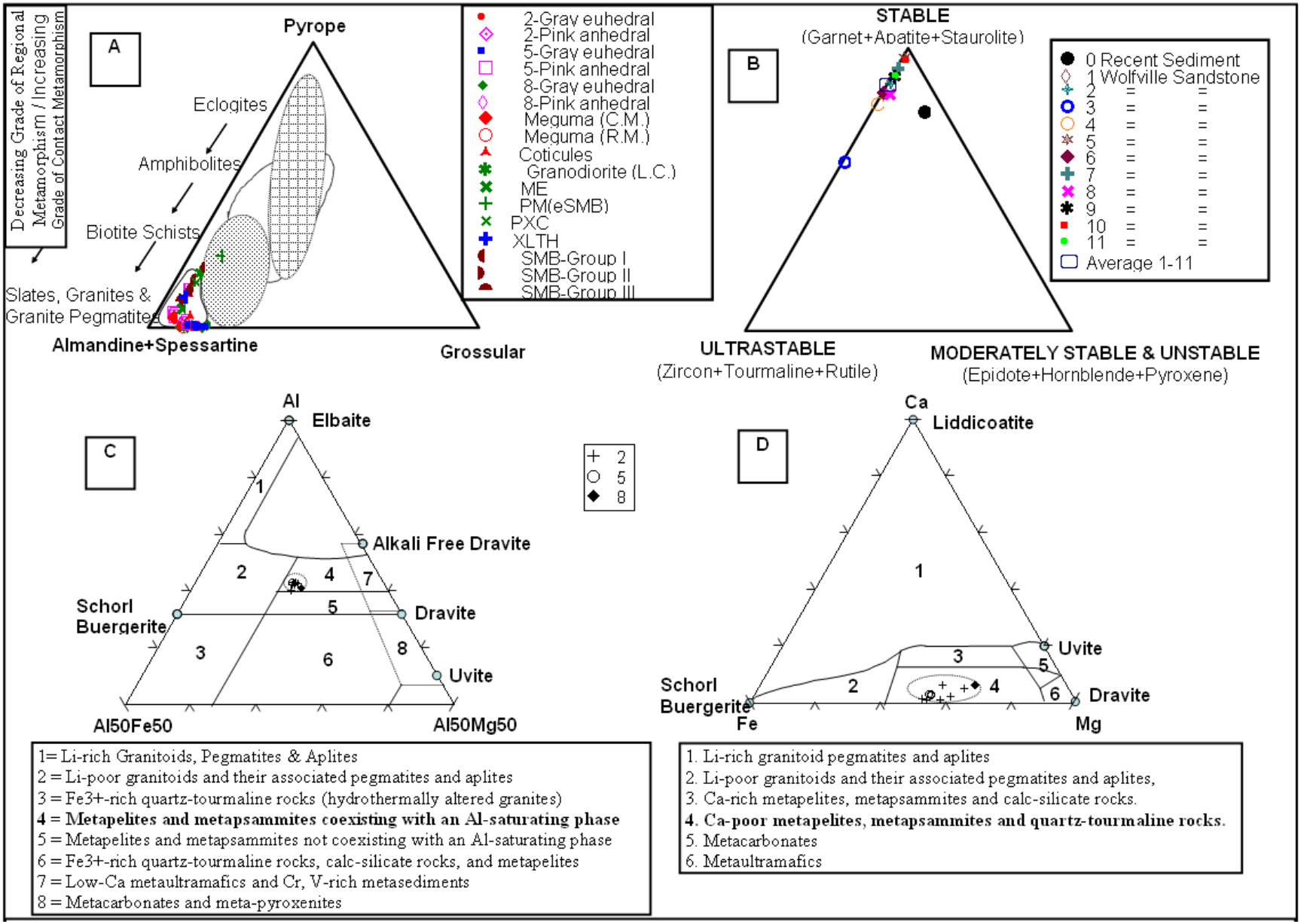
A
Decreasing Grade of Regional Metamorphism / Increasing Grade of Contact Metamorphism
Pyrope
Eclogites
Amphibolites
Biotite Schists
Slates, Granites & Granite Pegmatites
Almandine+Spessartine
Grossular
2-Gray euhedral
2-Pink anhedral
5-Gray euhedral
5-Pink anhedral
8-Gray euhedral
8-Pink anhedral
Meguma (C.M.)
Meguma (R.M.)
Coticules
Granodiorite (L.C.)
ME
PM(eSMB)
PXC
XLTH
SMB-Group I
SMB-Group II
SMB-Group III
B
STABLE
(Garnet+Apatite+Staurolite)
ULTRASTABLE
(Zircon+Tourmaline+Rutile)
MODERATELY STABLE & UNSTABLE
(Epidote+Hornblende+Pyroxene)
0 Recent Sediment
1 Wolfville Sandstone
2 = =
3 = =
4 = =
5 = =
6 = =
7 = =
8 = =
9 = =
10 = =
11 = =
Average 1-11
C
Al
Elbaite
Alkali Free Dravite
Schorl
Buergerite
Dravite
Uvite
Al50Fe50
Al50Mg50
2
5
8
D
Ca
Liddicoatite
Uvite
Schorl
Buergerite
Dravite
Fe
Mg
1= Li-rich Granitoids, Pegmatites & Aplites
2 = Li-poor granitoids and their associated pegmatites and aplites
3 = Fe3+-rich quartz-tourmaline rocks (hydrothermally altered granites)
4 = Metapelites and metapsammites coexisting with an Al-saturating phase
5 = Metapelites and metapsammites not coexisting with an Al-saturating phase
6 = Fe3+-rich quartz-tourmaline rocks, calc-silicate rocks, and metapelites
7 = Low-Ca metaultramafics and Cr, V-rich metasediments
8 = Metacarbonates and meta-pyroxenites
1. Li-rich granitoid pegmatites and aplites
2. Li-poor granitoids and their associated pegmatites and aplites,
3. Ca-rich metapelites, metapsammites and calc-silicate rocks.
4. Ca-poor metapelites, metapsammites and quartz-tourmaline rocks.
5. Metacarbonates
6. Metaultramafics

**Fig. 6: (A) Composition diagram of Wolfville Formation sandstones plotted on slightly modified (Almandine+Spessartine) – (Pyrope) – (Grossular) triangular diagram of garnets of Wright (1938) (in Preston et al., 2002). The plotted data are from the study area (numbers 2, 5, and 8) as well as Meguma Group and South Mountain Batholith (SMB), Nova Scotia taken from other references. R.M. are averages of representative garnet analysis from low grade regionally metamorphosed Meguma Group slates and sandstones (Halifax Formation - Mosher's Island Member); C.M. are representative garnet analysis from the contact metamorphic zone of Meguma Group sandstones (Halifax Formation - Mosher's Island Member) with South Mountain batholith, southern Nova Scotia around Mahon Bay (from Hicks, R.J., 1996). SMB are averages of three groups of garnets from South Mountain batholith around Halifax and in the central part of the Batholith (from Allen and Clarke, 1981). L.C. is a garnet analysis from granodiorite body in Liscomb Complex, South Mountain Batholith (Cameron and Zentilli, 1997). ME, PM (eSMB), PXC and XLTH are averages of many garnets from xenoliths within South Mountain Batholith and its contact zones with the Meguma Group (Halifax Formation), Nova Scotia (from Erdmann, 2006). (B) Triangular diagram of the transparent heavy minerals of Wolfville Formation sandstones. (C and D) Composition diagram of Wolfville Formation sandstones plotted on the triangular plots of Henry and Guidotti (1985).**

Soon after the deposition of Wolfville formation sandstones, paragenesis commenced by early compaction which appears to have limited effect indicated from the nature of sandstones, as most of the detrital grains do not have common contacts, but are separated by calcite cement. Iron cement was the earliest to develop around the detrital grains as thin rims. The source of iron was the detrital Fe and Fe-Ti oxide grains which are the most abundant heavy minerals. Oxidation of these grains to hydrous oxides resulted in staining the water in pore spaces and their subsequent deposition as thin films around the detrital grains. This was followed by the enrichment of the pore space water by calcium carbonates derived from the source terranes which were drained by rivers; and also from the detrital carbonate grains within the sandstones which have spherical and ovoidal shapes, possibly developed by systematic dissolution of their boundaries and/or by transportation effect. The carbonate enriched pore water was then precipitated as sparry calcite filling most of the pore spaces and resulted in a calcite cement-supported sandstone. Minor amounts of fibrous radiating clays were also deposited at the same time as calcite filling minor portions of pore spaces.

Further burial caused another stage of compaction indicated by selective microfracturing and breaking of most quartz grains which are more brittle than the accompanying feldspars and lithics. These quartz grains either possessed microfractures prior to deposition and under burial compaction were broken along these planes of weaknesses; or due to their brittle nature were fractured and broken during effective compaction pressure. Dissolution has partly affected the calcite cement and also the feldspars some of which were already partially altered in the source rocks and/or during transportation and deposition. Fracturing and breaking of quartz grains and partial dissolution of feldspar grains and calcite cement produced secondary porosity. Dissolution of altered feldspars resulted in the production of kaolinite which was deposited in vermicular form with noticeable intercrystalline porosity filling few pore spaces. The final stage of compaction produced sandstones of limited complex porosity. The average porosity of these sandstones is 6% (1.7 to 15.6%) in the form of primary and secondary porosity. Most of the primary intergranular pores were filled by sparry calcite cement; however many types of secondary porosity were developed during diagenesis. The secondary porosity types are dissolution, microfracturing (particularly of quartz), grain-boundary, intracement and intragranular.

## Tectonic Provenance

The counting results based on Gazzi-Dickinson methodology were plotted on the provenance indicator triangular diagrams of Dickinson (1985), and Dickinson and Suczek (1979) (Fig.5). The sandstone falls in the field of "recycled orogenic provenance" (FQtL diagram) (Fig.5A), "mixed" and "quartzose recycled" (FQmLt diagram) (Fig.5B), "increasing maturity or stability from continental block provenance" (PQmK diagram) (Fig.5C) and "collision orogen source" (LvmQmLsm diagram) (Fig.5D). The triangular diagrams of the grain counts indicated that these sandstones are of "recycled orogenic

provenance". This means that they are derived from the Pre-Triassic Paleozoic rock units which were part of the Appalachian Mountains formed under collision tectonic settings.

The main source of the studied synrift sediments is the Meguma terrane which has a collision contact relation with the older Avalon terrane to the north of the Cobequid fault system. Both terranes are part of the Appalachian Mountains and were also affected by the mid-Paleozoic Acadian Orogeny (Wade *et al.* 1996). The geologic map of the Bay of Fundy area, where the Wolfville formation is located in both in outcrops and subsurface, shows that the most probable source rocks of the studied sandstones are the Meguma supergroup and the South Mountain batholith. The absence of any volcanic rock fragments among the studied sandstones grains; and also the absence of heavy minerals which could be of volcanic origin such as pyroxenes indicates either the absence of pre-Triassic volcanic body exposures in the area, or that the contribution of rock units to the north of the Bay of Fundy in New Brunswick which contain Devonian and Silurian volcanic rocks was very limited. The Recent beach sediments at Cambridge Cove contain the same heavy mineral suites with nearly the same proportions as the nearby Wolfville formation, but they also contain basalt rock fragments and heavy minerals which have a basaltic origin such as pyroxene. This means that volcanic outcrops of North Mountain Basalt (earliest Jurassic) are the source of these basaltic rock fragments and the pyroxene.

The Wolfville sandstones and conglomerates contain quartz, various feldspars (alkali feldspars/plagioclase ≈11) and rock fragments (slate-schist, siltstone-sandstone, granitoids, quartzite, limestone, and chert). The Wolfville formation is underlain by formations ranging in age between Cambrian to Carboniferous which contains all lithologies that exist in Wolfville formation suggesting that they are the dominant source of the studied sandstones and conglomerates of Wolfville formation. The Meguma group is probably the dominant source of the major part of rock fragments (slate, schist, siltstone, sandstone, and quartzite). The South Mountain batholith is the source of granitoid lithics, and the Windsor group is a possible source of limestone lithics. The other formations are also the possible source of some of these deposits because there is more than one type of each rock grain.

The absence of volcanic lithics and/or heavy minerals of volcanic origin such as pyroxene preclude sources other than the Meguma supergroup and the South Mountain batholith as the major source of the studied sandstones. This is because of the similarity of the rock fragments (slates some of which are garnetiferous, siltstones, quarztites, and micrographic granites) and the heavy minerals (iron oxide, garnet, apatite and ultrastable minerals – zircon, tourmaline-rutile, as well as few staurolites, hornblende, and micas) to the main lithology of these two major rock units which are widely exposed in Nova Scotia. The major part of quartz, K-feldspars, plagioclase, granitoid lithics, mica, and some heavy mineral (ultrastable group) are derived from the South Mountain batholith which occupies important part of central Nova Scotia as well as tens of scattered smaller similar outcrops to the east and west. The source of most lithics (excluding granitoids), part of quartz, feldspars, chlorite and many heavy minerals is Meguma Supergroup which occupies large areas of Nova Scotia (Fig.1).

## Heavy Mineral Provenance

The heavy minerals consist of Fe and Fe-Ti oxides (magnetite, hematite, ilmenite, and their alteration products: goethite, limonite and leucoxene) (76%), garnet (13.6%), apatite (3.3%), chlorite (3.3%), zircon (1.4%), tourmaline (1.3%), biotite (1%) and minor amounts of rutile, staurolite, hornblende, and rarely epidote. Triangular diagram of the transparent heavy minerals (Fig.6B) showed that the stable heavy minerals are the dominant group followed by the ultrastable group with negligible amount of the unstable and moderately stable group.

For comparison, a sample of recent beach sediments indicated the presence of moderately stable minerals (pyroxene, epidote and hornblende) in addition to the groups which are present in the Wolfville sandstones; these moderately stable heavy minerals are obviously derived from the volcanic outcrops in the area including North Mountain Basalts which were not formed during the deposition of Wolfville formation sediments. Garnets and tourmalines are very useful provenance indicator minerals because of

their diversity and stability (Morton 1991; Wright 1938; Preston *et al.* 2002; Henry and Guidotti 1985).These two minerals, which are abundant in the Wolfville formation sandstones were analyzed by electron microprobe and their compositions plotted on the provenance triangles of Wright (1938) and Preston *et al.* (2002) for garnet (Fig.6A), and Henry and Guidotti (1985) for tourmaline (Fig.6C, D). All garnets were plotted in the field of "pelites and granites and granite pegmatites" in the (Almandine+Spessartine)-(Pyrope)-(Grossular) triangle (Fig.6A). The tourmalines were plotted in the field of "metapelites and metapsammites that coexist with an Al-saturating phase" and "Ca-poor metapelites, metapsammites and quartz-tourmaline rocks" in the $Al_{50}Fe_{50}$-Al-$Al_{50}Mg_{50}$ and Fe-Al-Mg triangles respectively (Fig. 6C, D).

The abundant garnet as the major transparent heavy mineral in the studied sandstones is particularly important as a provenance indicator. Two types of garnet exist: a dominant euhedral, gray under the microscope, rich in inclusions and spessartine in type; and minor amounts of anhedral, clear, pink under the microscope and almandine in type but still Mn-rich. Both types fall in the field of pelites, granites and granite pegmatites in the (pyrope)–(almandine+spessartine)–(grossular) triangle (Fig.6A) suggesting Meguma supergroup and SMB as their provenance. The spessartines are closely clustered near the almandine+spessartine corner along the grossular line direction while the almandine is sparser and fall closer to the almandine+spessartine corner but mostly along the pyrope line direction (Fig.6A). One of the characteristics features of the Meguma supergroup (particularly the Halifax formation) is that they contain spessartine garnets. Comparisons were made with those garnets which exist as xenoliths in the SMB and its contact zone with Meguma supergroup in central Nova Scotia studied by Erdmann (2005). The studied almandines also have similarities with those studied by Allen and Clarke (1981) from various parts of the SMB and also with those studied by Cameron and Zentilli (1997) from SMB (Liscomb complex).

Garnet was also reported by Cullen (1984) as accessory grains in the metaquartzites and schists of Folly River in Bass River Complex, Cobequid Highland within the Avalon zone of Maritimes; however they were not analyzed to allow chemical comparison with the garnets of Wolfville formation. Triangular provenance diagrams of Henry and Guidotti (1985) (Figs. 6C, D) showed that the studied tourmalines fall in the field of "metapelites and metapsammites coexisting with an Al-saturating phase" and "Ca-poor metapelites, metapsammites and quartz-tourmaline rocks" again suggesting Meguma supergroup sediments and possibly SMB as their source. The vast majority of the rock-forming minerals as well as most of the heavy minerals found in the sandstones of Wolfville formation were also found and mostly analyzed by Hick (1996) which included quartz, albite, biotite, muscovite, chlorite, carbonates, apatite, epidote, garnet, rutile, titanite, tourmaline, zircon, and hematite.

## Conclusions

The result of the grain size analysis, petrography and heavy mineral studies of Cambridge Cove sandstones concludes that:

**(1)** The Wolfville formation sandstones transported by braided rivers and deposited as channel fills and on flood plains are mostly feldspathic litharenite, poorly sorted, fine to strongly fine skewed, platykurtic to very platykurtic and medium in grain size.

**(2)** They predominantly consist of quartz as well as considerable amounts of rock fragments and feldspars as detrital grains which were cemented by calcite and minor iron oxides and clays.

**(3)** Iron oxides and garnets are the predominant heavy minerals in these sandstones with minor amounts of apatite, zircon and tourmaline and negligible amounts of others. These minerals are of low grade metamorphic and silicic (granitic) igneous rock provenances. Unstable minerals are very rare.

**(4)** The provenance indicator triangles for results of detrital grains and heavy minerals in general, and those of tourmaline and garnet in particular, indicated that the Wolfville Formation sediments have recycled orogenic provenance (collision setting) and derived mostly from the Meguma terrane located to the south of Cobequid (Minas) fault zone. The main source rocks are the Meguma supergroup and South Mountain batholith with minor contributions from the carbonate-bearing formations such as the Windsor Group. The lack of rock fragments and heavy minerals attributable to volcanics and high grade

metamorphic rocks exclude the Avalon terrane and other rock units of the Appalachian Mountains in New Brunswick as a contributing source.

**(5)** The average porosity of the studied sandstones is 6% which is relatively low to fair. They have both primary and secondary porosity. The Wolfville formation is overlaying the Carboniferous Horton Bluff formation which is made up of siltstones, sandstones and organic-rich shales. They both extend below the Bay of Fundy area at depth for considerable extent. Two exploration wells drilled in the southwestern Bay of Fundy also showed low porosity of sandstones (~4%). However the Wolfville formation has considerable thickness and the upper parts are of aeolian origin (Klein 1962; Wade *et al*. 1996) and may have better porosity. If there is a regional seal to the Wolfville Formation sandstones, the system could be an attractive hydrocarbon target since the organic-rich shales of Horton Bluff formation may act as a source and the Wolfville formation as a reservoir. Drilling in 2007 through the shales of Horton Bluff formation onshore proved that these argillaceous rocks have high potential as a source of natural gas.

**(6)** The paragenesis of diagenetic and related events deduced from the study is summarized in Figure 7.

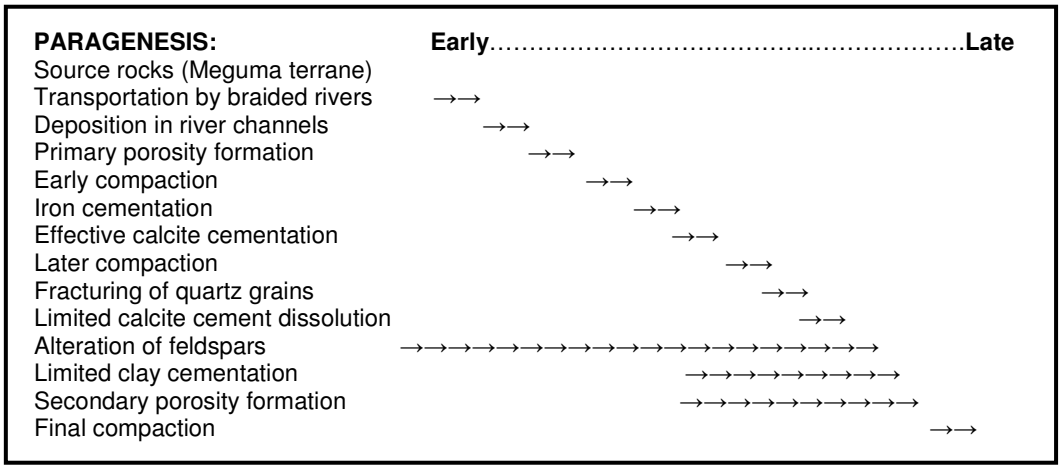


**Fig.7: Paragenesis of the diagentic and related events of the Wolfville Formation sediments.**

## References


Allen, B.D. and Clarke, D.B., 1981. Occurrence and origin of garnets in the South Mountain Batholith, Nova Scotia. Canadian Mineralogist, v.19, p.19-24.

Cameron, B.I. and Zentilli, M., 1997. Geochemical characterization of the mineralized transition between the Goldenville and Halifax formations and the interaction with adjacent granitoid intrusions of the Liscomb Complex, Nova Scotia. Atlantic Geology, v.33, p.143-155.

Cullen, M.P., 1984. Geology of the Bass River Complex, Cobequid Highlands, Nova Scotia. Unpublished M.Sc. thesis, Dalhousie University, 183p.

Dickinson, W.R., 1970. Interpreting detrital modes of greywacke and arkose. Journal of Sedimentary Petrology, v.40, p.695-707.

Dickinson, W.R., 1985. Interpreting provenance relations from detrital modes of sandstones. In: Zuffa, G.G. (ed.) Provenance of arenites. Reidel Publishing Co., Dordrecht, p.331-361.

Dickinson, W.R., Beard, L.S., Brakenridge, G.R., Erjavec, J.L., Ferguson, R.C., Inman, K.F., Knepp, R.A., Lindberg, F.A., and Ryberg, P.T., 1983. Provenance of North American Phanerozoic sandstones in relation to tectonic setting. Geol. Soc. America, Bull., v.94, p.222-235.

Erdmann, S., 2006. Country-rock contamination and assimilation in the South Mountain batholith, Unpublished Ph>d. thesis. Dalhousie University, 209p.

Fensome, R.A. and Williams, G.L., 2001. The Last Billion Years: A Geological History of the Maritime Provinces of Canada. Atlantic Geoscience Society, Nimbus Publishing, 212p.

Folk, R.L., 1968. Petrology of sedimentary rocks. Hemphill Publishing Company, Austin, Texas, 182p.

Gazzi, P., 1966. Le arenarie del flysch sopracretaceo dell'Appennino modenese; correlazioni con il flysch di Monghidoro:Mineralog. Et Petrog.Acta, v.12, p.69-97.

Henry, D.J. and Guidotti, C.V., 1985. Tourmaline as petrogenic indicator mineral: an example from the staurolite-grade metapelites of Northern Maine. American Mineralogist, v.70, p.1-15.

Hicks, R.J., 1996. Low-grade metamorphism in the Meguma Group, Southern Nova Scotia. Unpublished M.Sc. thesis, Dalhousie University, 352p.

Hubert, J.F. and Forlenza, M.F., 1988. Sedimentology of braided-river deposits in Upper Triassic Wolfville redbeds, southern shore of Cobequid Bay, Nova Scotia, and Canada. In Triassic-Jurassic Rifting: Continental Breakup and the origin of the Atlantic Ocean and Passive Margins. Edited by Manspeizer. Elsevier, Amsterdam. The Netherlands, p.231-247.

http://www.wallstreet-online.de/diskussion/1137920-neustebeitraege/news-news-triangle-pet.,2008. Triangle Petroleum announces analytical results for its two exploratory wells in the Windsor Basin of Nova Scotia, Canada. January 30, 2008.

Ingersoll, R.V. and Dickinson, W.R., 1979. Petrology and provenance of Neogene sands from Nicobar and Bengal fans, DSDP sites 211 and 218. Journal of Sedimentary Petrology, v.49, p.1217-1228.

Ingersoll, R.V. and Suczek, C.A., 1979. Petrology and provenance of Neogene sand from Nicobar and Bengal fans, DSDP sites 211 and 218. Journal of Sedimentary Petrology, v.49, p.1217-1228.

Keppie, J.D., 1979. Geological Map of the Province of Nova Scotia, Nova Scotia Department of Mines, and Scale 1:500,000.

Klein, G. de V., 1962. Triassic sedimentation, Maritime Provinces, Canada. Geological Society of America Bulletin, 73, p.1127-1146.

Morton, A.C., 1991. Geochemical studies of detrital heavy minerals and their application to provenance studies, in Morton, A.C., Todd, S.P. and Haughton, P.D.W., eds. Developments in Sedimentary Provenance Studies: geological Society of London. Special Publication 57, p.31-45.

Olsen, P.E. and Schlische, R.W., 1990. Transtensional arm of the early Mesozoic Fundy rift basin: Penecontemporaneous faulting and sedimentation. Geology, v. 18, p. 695-698.

Pettijohn, F.J., Potter, P.E., and Siever, R., 1972. Sand and Sandstone: Berlin, Springer-Verlag, 618 p.

Powers, S., 1916. The Acadian Triassic. Journal of Geology, pp.1-26, 155-122, 254-268.

Preston, J., Hartley, A., Mange-Rajetzky, M., Hole, M, May, G., Buck, St. and Vaughan, L., 2002. The provenance of Triassic continental sandstones from the Beryl Field, Northern North Sea: Mineralogical, geochemical and sedimentological constraints. J. Sed. Petrology, v.72, no.1, p.18-29.

Rast, N, Kennedy, M.J. and Blackwood, R.F., 1976. Comparison of some tectonostratigraphic zones in the Appalachians of Newfoundland and New Brunswick. Canadian Journal of Earth Sciences, v.13, p.868-875.

Schiller, E.A. and Taylor, F.C., 1965. Spessartine-quartz rocks (coticules) from Nova Scotia. The American Mineralogist, v.50, p.1477-1481.

Schlische, R.W. and Olsen, P.E., 1990. Quantitative filling model for continental extensional basins with applications to early Mesozoic rifts of eastern North America. Journal of Geology, 98, pp.135-155.

The Oil & Gas Magazine Online: oilworks.com, 2008. Kennetcook #1 & #2 Drilling and Evaluation Programs, 24 June 2008. info@oilandgasmagazine.ca

Wade, J.A., Brown, D.E., Traverse, A., and Fensome, R.A., 1996. The Triassic-Jurassic Fundy Basin, eastern Canada: regional setting, stratigraphy, and hydrocarbon potential. Atlantic Geology, v.32, 189-231.

Williams, G.L., Fyffe, L.R., Wardle, R.J., Colman-Sadd, S.P., and Boehner, R.C. 1985. Lexicon of Canadian Stratigraphy, volume vi, Atlantic Region. Canadian Society of Petroleum. Geologists, 572p.

Wright, W.I., 1938. The composition and occurrence of garnets. American Mineralogist, 23, 436-449.

**BACK**

# MARGIN EVOLUTION & DEVELOPMENT

## Poster Session 1

---

**1. 4D RIFT ANALYSES FOR THE JEANNE D'ARC BASIN**
Baur, Friedemann; Jauer, Chris; Littke, Ralf and Wielens, Hans

**2. BASIN, PETROLEUM SYSTEM AND PLAY ANALYSIS IN THE WEST AFRICAN ATLANTIC BASINS**
Beglinger, Suzanne; Cloetingh, Sierd and Doust, Harry

**3. PREDICTIVE TRENDS IN SALT MORPHOLOGY DERIVED FROM SYSTEMATIC ASSESSMENT OF MERGED 3D SEISMIC COVERAGE OVER ENTIRE BASINS**
Bird, Tim; Johnstone, David and Martin, Mark

**4. VARIATION IN CRUSTAL EXTENSION AND ITS IMPLICATION FOR HYDROCARBON HABITAT IN THE DAKAR - RUFISQUE AREA, OFFSHORE SENEGAL**
Bottomley, Steven and Jeans, Pete

**5. TECTONO-STRATIGRAPHIC EVOLUTION OF SALT STRUCTURES AND DEPO-CENTER MIGRATION IN THE ABENAKI SUB-BASIN AND ITS DEEPWATER EXTENSION, OFFSHORE NOVA SCOTIA**
Campbell, Clarke; Tyler; MacDonald, Cody; Cribb, Jonathan; Adam, Jürgen; Nedimovic, Mladen; Louden, Keithand; Krezsek, Csaba

**6. ANALOGUE MODELLING OF SALT TECTONIC PROCESSES AND DEPOCENTER MIGRATION ON THE SHELF AND DEEPWATER SLOPE, WESTERN LAURENTIAN SUB-BASIN**
Cribb, Jonathan; Campbell, Clarke; MacDonald, Cody; Adam, Jürgen; Nedimovic, Mladen; Louden, Keith; Krezek, Csaba and Grujic, Djordje

**7. MAPPING POST RIFT SILLS ALONG THE NEWFOUNDLAND PASSIVE MARGIN**
Deemer, Sharon; Hurich, Charles and Hall, Jeremy

**8. A REGIONAL TRANSECT ACROSS THE SOUTH NEWFOUNDLAND BASIN, A NONVOLCANIC MARGIN**
Deemer, Sharon; Hall, Jeremy; Solvason, Krista; Lau, Helen; Louden, Keith; Srivastava, Shiri and Sibuet, Jean-Claude

**9. U.S. EAST COAST: CONTINENTAL MARGIN EVALUATION WITH NEW TOOLS, DATA AND TECHNIQUES**
Dickson, William; Odegard, Mark and Post, Paul J.

**10. THE NOVASPAN PROJECT: DEEP IMAGING OF AN ENIGMATIC CONTINENTAL MARGIN**
Dinkelman, Menno G. and Shimeld, John W.

**11. THE LAST 100 MILLION YEARS ON THE SCOTIAN MARGIN, OFFSHORE EASTERN CANADA: AN EVENT STRATIGRAPHIC SCHEME EMPHASIZING BIOSTRATIGRAPHY**
Fensome, Rob; Gard, Gunilla; MacRae, Andrew; Williams, Graham; Thomas, Frank; Fiorini, Flavia; and Wach, Grant

**12. LOW-T THERMOCHRONOLOGY PROVIDES NEW INSIGHTS IN THE MESOZOIC TO PRESENT**
Ghorbal, Badr; Bertotti, Giovanni; Foeken , Jurgen; Stuart, Fin and Andriessen, Paul

**13. SEQUENCE STRATIGRAPHIC EVOLUTION OF THE DEMERARA RISE, SURINAME, SOUTH AMERICA- TRANSITION FROM A RIFTED TO PASSIVE MARGIN; POSSIBLE ANALOGUE TO THE SCOTIAN SLOPE**
Goss, Shawn; Mosher, David; and Wach, Grant D.

**14. QUANTITATIVE KINEMATIC AND THERMOMECHANICAL ANALYSIS OF THE EVOLUTION OF THE MOROCCAN RIFTED CONTINENTAL MARGIN**
Gouiza, Mohammed; Bertotti, Giovanni; Hafid, Mohamed; and Ghorbal, Badr

**15. THE EVOLUTION OF THE PERDIDO FOLD BELT IN THE CONTEXT OF SALT TECTONICS OF THE NORTHWESTERN MARGIN OF THE GULF OF MEXICO – INSIGHTS FROM NUMERICAL MODELING**
Gradmann, Sofie; and Beaumont, Christopher

**16. SEISMIC STRATIGRAPHY, SALT STRUCTURES AND THERMAL AND PETROLEUM SYSTEMS MODELS ACROSS THE CENTRAL NOVA SCOTIA SLOPE BASIN**
Louden, Keith; Mukhopadhyay, P.K; Wu, Yue; Negulic, Eric; and Nedimovic, Mladen

**17. SEQUENCE STRATIGRAPHIC ANALYSIS OF ATLANTIC MARGIN ON NEW JERSEY COASTAL PLAIN: IMPLICATIONS TO GLOBAL SEA-LEVEL STUDIES**
Mizintseva, Svetlana F

**18. NEW PROFILE MODELS OVER THE U.S. EAST COAST CONTINENTAL MARGIN**
Odegard, Mark; Post, Paul J. and Dickson, William

**19. THE LUSITANIAN BASIN (PORTUGAL) STRATIGRAPHIC AND GEODYNAMIC CORRELATION WITH OTHER PORTUGUESE AND MOROCCAN BASINS**
Pena Reis, Rui; Pimentel, Nuno; and Garcia, Antonio

**20. CONTROLS ON FACIES DISTRIBUTION AND RESERVOIR DEVELOPMENT OF UPPER TRIASSIC RIFT CONTINENTAL SYSTEMS IN INTERMONTANE RIFT SETTINGS: A COMPARATIVE STUDY OF EXTENSIVE OUTCROPS IN SW MOROCCO**
Redfern, Jonathan; Mader, Nadine; Fabuel Perez, Ivan; Hodgetts, David and El Ouataoui, Abedelmajid

**21. LITHOSPHERIC DENSITY VARIATIONS AND MOHO STRUCTURE OF THE IRISH RIFTED CONTINENTAL MARGIN FROM CONSTRAINED 3-D GRAVITY INVERSION**
Welford, J. Kim; Hall, Jeremy and O'Reilly, Brian

**22. STRUCTURE AND RIFTING EVOLUTION OF THE NORTHERN NEWFOUNDLAND BASIN FROM ERABLE MULTICHANNEL SEISMIC REFLECTION PROFILES ACROSS THE SOUTHERN MARGIN OF FLEMISH CAP**
Welford, J. Kim; Smith, Julie; Hall, Jeremy; Deemer, Sharon; Srivastava, Shiri ; Sibuet, Jean-Claude

**23. THERMOCHRONOLOGY EVIDENCE FOR MESOZOIC AND CENOZOIC INVERSIONS OF THE CONTINENTAL MARGIN OF NOVA SCOTIA, CANADA**
Zentilli, Marcos; Grist, A.M.; Ryan, R.J.; Ravenhurst, C.E. and Li, G.

**BACK**

# NOTES

# 4D Rift Analysis for the Jeanne d'Arc Basin Using Inverse Basin-Modelling

**Friedemann Baur**
RWTH Aachen University
Institute of Geology and Geochemistry of Petroleum and Coal
Lochnerstr. 4-20, Haus B
52056 Aachen
Germany
e-mail: baur@lek.rwth-aachen.de

**Chris Jauer**
**Hans Wielens**
Geological Survey of Canada (Atlantic)
Bedford Institute of Oceanography
PO Box 1006
Dartmouth, Nova Scotia B2Y 4A2
Canada
e-mail: cjauer@nrcan.gc.ca
e-mail: hwielens@nrcan.gc.ca

**Ralf Littke**
RWTH Aachen University
Institute of Geology and Geochemistry of Petroleum and Coal
Lochnerstr. 4-20, Haus B
52056 Aachen
Germany

**Thomas Fuchs**
Integrated Exploration Systems (IES)
Ritterstr. 23
52072 Aachen
Germany

## ABSTRACT

The study provides for the first time a full 4D (space and time) analysis of heat flow-, subsidence-, maturation- and compaction history for the Jeanne d' Arc basin, located offshore Newfoundland. The Jeanne d'Arc basin is a typical failed rift basin, whose development and burial history is based on crustal thinning processes Therefore, the basin is an ideal place to quantify and verify rift-related processes such as heat flow history depending on the magnitude of the stretching of the crust and other factors. The study compares the results of simulated geological and geophysical processes and their mutual effects for variations of the McKenzie approach, mostly related to the stretching behavior of the upper mantle. These assumptions have been applied to a 4D numerical basin model extending from the Port au Port area in the south to the Adolphus area in the north in the Jeanne d'Arc basin. The model was simulated with a software package PetroMod®, developed by Integrated Exploration Systems. Additionally, a special workaround has been applied to simulate not only single rift events but also multiple-sequence rift events. The simulation technique uses an inverse approach with respect to the traditional McKenzie approach and is called advanced McKenzie approach. Based on the known burial history, the tectonic subsidence is

calculated by back-stripping and decompaction. In a second step, the stretching factors can be determined by adjusting them to fit the tectonic subsidence. Lastly, the heat flow history can be calculated based on the calculated stretching factors. The 4D regional Jeanne d'Arc basin model uses the results of over 45 individual 1D models (well locations) and calibration data from 61 wells. Thus, the study of the Jeanne d'Arc basin quantifies the impacts of diverse rift- and heat flow scenarios on the basin based on a non-steady-state finite-element simulation.

.

## Introduction

The study will provide for the first time a full 4D (space and time) analysis of the heat flow-, tectonic subsidence-, stretching factor-, maturation-, temperature- and compaction-history for the Jeanne d'Arc basin, offshore Newfoundland. The study area extends almost 125 km in the south north direction from the Port au Port J-97 well region to the Adolphus D-40 area (Fig. 1).

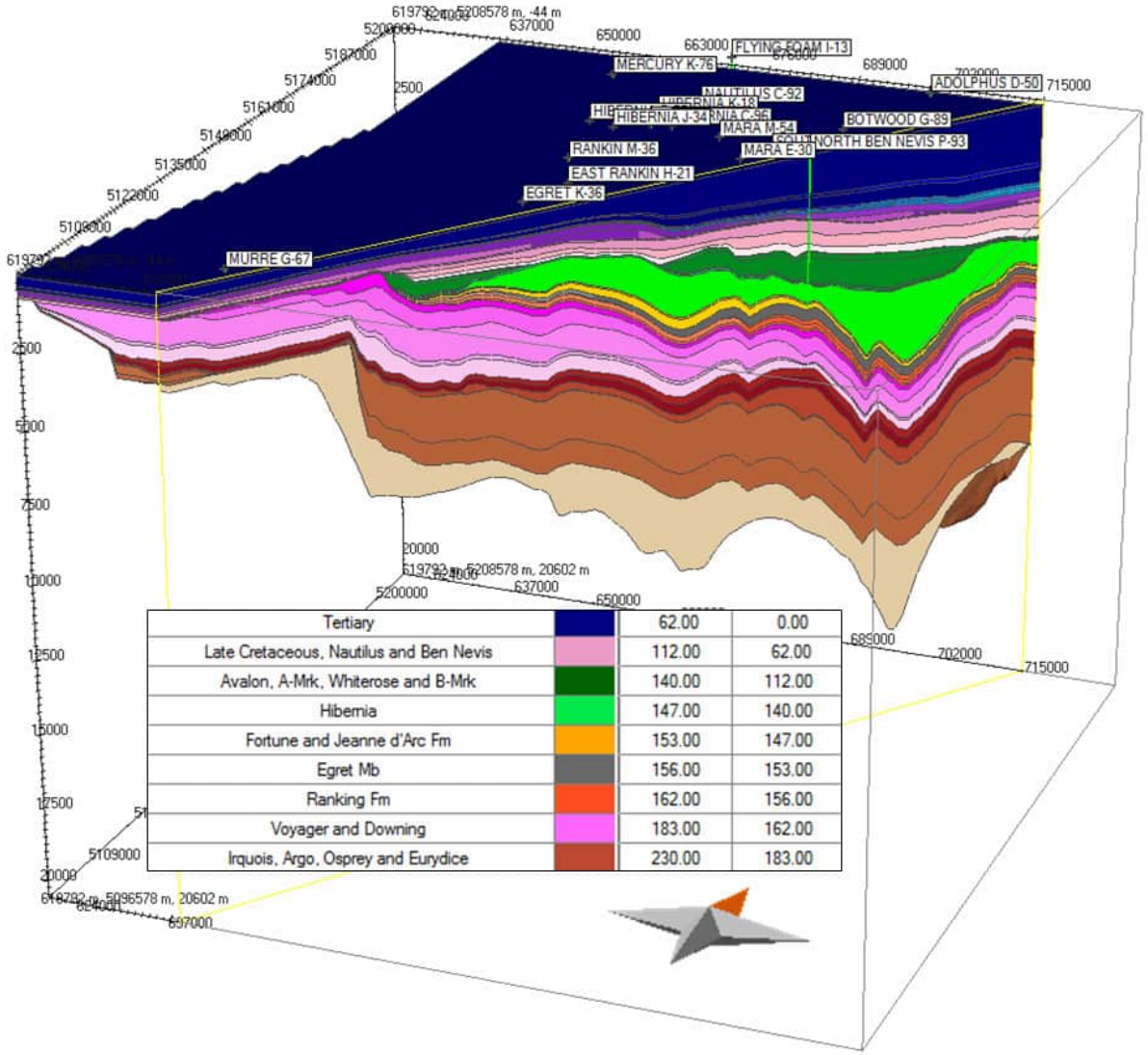


**Figure 1: 3D model of the Jeanne d'Arc Basin with a slice cut away (outlined by the yellow border) to show a 2D section. The orange arrow points north. The major formations are indicated; they have been further subdivided in the model. The slower subsidence in the blue, pink and dark green formations contrasts with the faster subsidence induced by the first rift.**

The Jeanne d'Arc basin is a typical confined and failed rift basin, whose development and burial history is controlled by crustal stretching and thinning processes such as described by Coward 1986, Lister *et al.* 1986, McKenzie 1978 and Wernicke 1985. Therefore, the purpose of this study is to quantify and verify rift-related geo-processes and other major processes as well as parameters of the petroleum system.

## Method

During this first year the study has emphasized geodynamic aspects such as heat flow development through time. Normally, the heat flow history is calculated based on vitrinite reflectance data but this causes various uncertainties. Therefore, it is prudent to use a second method to verify or falsify the heat flow evolution, which is the most important and sensitive factor for the generation of oil and gas. A discontinuous, pure shear stretching model, reflecting the timing and the magnitude of stretching factors of crust and mantle and other related geo-factors, has been applied to the numerical model. The so called "advanced" McKenzie approach is mostly related to the different rheological stretching behaviour of the brittle crust and the ductile upper mantel and is theoretically suitable only for non-volcanic symmetrical pure-shear passive margins (Jarvis and McKenzie 1980). This geodynamic approach has been applied using a sophisticated software package for basin analysis called PetroMod®, developed by Integrated Exploration Systems (IES). The simulation technique uses an inverse approach compared to the traditional McKenzie approach. Based on the known burial history, the tectonic subsidence is calculated by backstripping and decompacting the sediments. In the second step, the stretching factors derived from the advanced McKenzie approach are calculated and adjusted to the tectonic subsidence of the basin model. This adjustment is optimized by a least-squares fit method. Finally, the heat flow history can be deduced using the stretching factors. Because of multiple rift events, which are proposed by the literature, a new workaround simulates not only single-rift events but also multiple-sequence rift events. Thus, the study quantifies the impacts of possible different rift- and heat flow scenarios based on a non-steady-state finite-element simulation and the result is heat flow maps for each defined time step. Those maps can be adjusted in detail to perform a calibration on, for example, vitrinite reflectance and temperature. Results from deep refraction seismic have been used to determine pre-Triassic crustal thickness to 35 or 40 km. The thermal history has been improved additionally by integrating available Apatite Fission Track data.

Besides the geodynamic aspect, the study gives new insights into a 4D numerical basin model of the Jeanne d'Arc basin and some new detailed and depth-converted maps. Apart from this, over 45 individual 1D models have been built for each well location and calibration data from 61 wells have been used to improve the results of the 4D regional model.

## Results

First results show that for a complete understanding of the post-Jurassic thermal evolution of the Jeanne d'Arc basin it is important to take into account the earlier Triassic rifting history. This earlier rift event generates the structural framework of the Jeanne d'Arc basin in which most of the sediments are deposited, whereas the second rift (Iberian rift) might have resulted only in the deposition of coarser clastics, limestone and finer clastics. But analyzing all 1D burial histories (Fig. 2) from well positions it is clear that most burial histories have higher sedimentation rates during the Early and Middle Jurassic and appear smooth without any stronger subsidence during the Late Jurassic and entire Cretaceous. But if a real heat pulse in combination with a rift event would have affected the Jeanne d'Arc basin by the end of Jurassic or beginning of Cretaceous, a more rapid burial would be expected at that time. So, the strong subsidence during the Jurassic is definitely related to the Triassic heat event and can be fully explained and simulated this way.

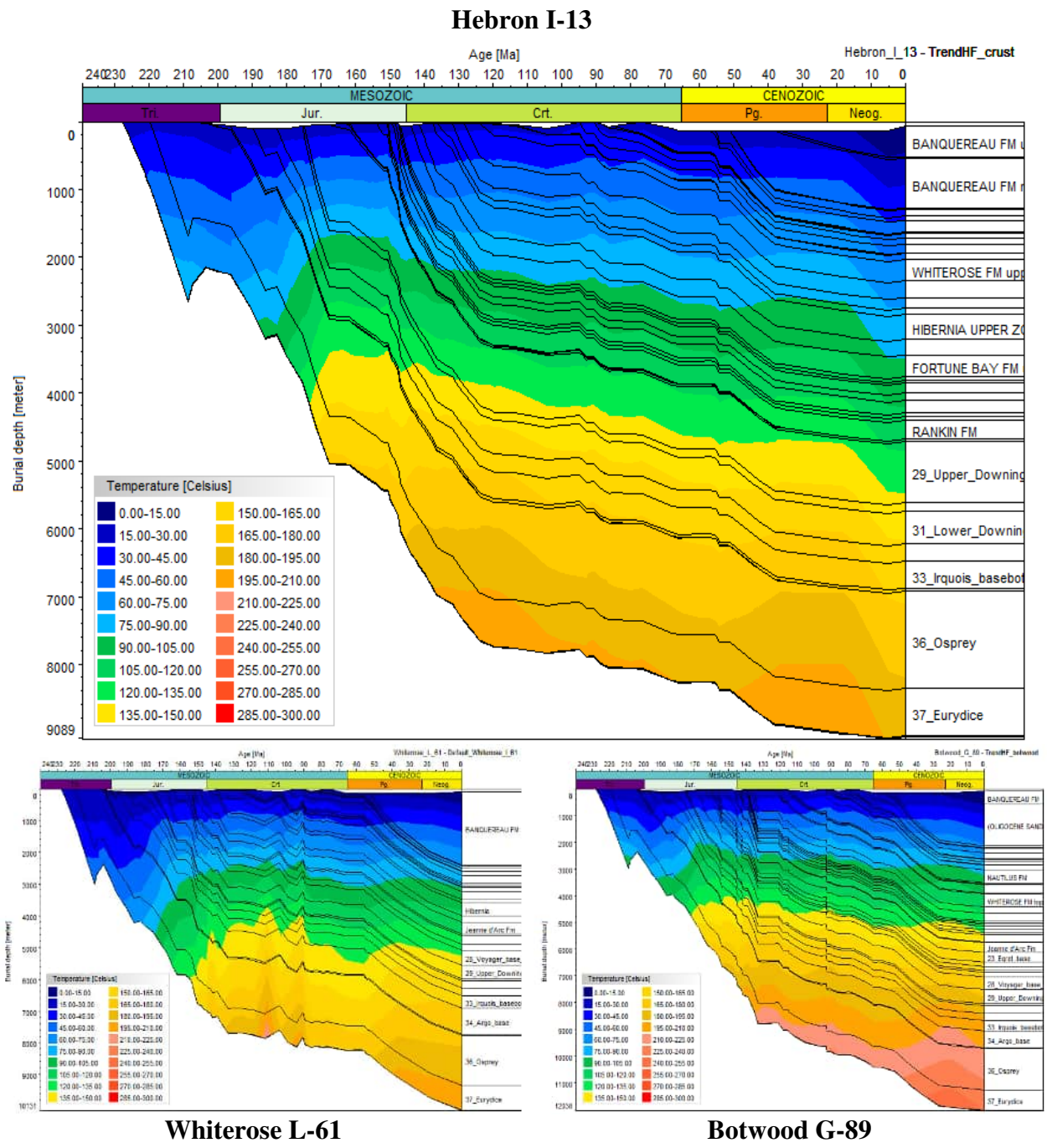


**Figure 2: Burial Histories for different wells in the Jeanne d'Arc basin with temperature overlay**

In general, the impact of a rift scenario on a burial history is marked by an initial subsidence caused by the stretching during the rift and a thermal subsidence caused by thermal relaxation of the passive margin. At least one of those two processes should leave its mark and it can be identified normally quite easily from the burial history of other locations worldwide e.g. the North Sea. Most of the wells in the Jeanne d'Arc basin have strong subsidence during the Early and Middle Jurassic (before ~ 155 Ma) which is too early to associate with the Iberian rift. The Iberian rift is assumed to be somewhere between 155 and 125 Ma, depending on the author and absolute age dates.

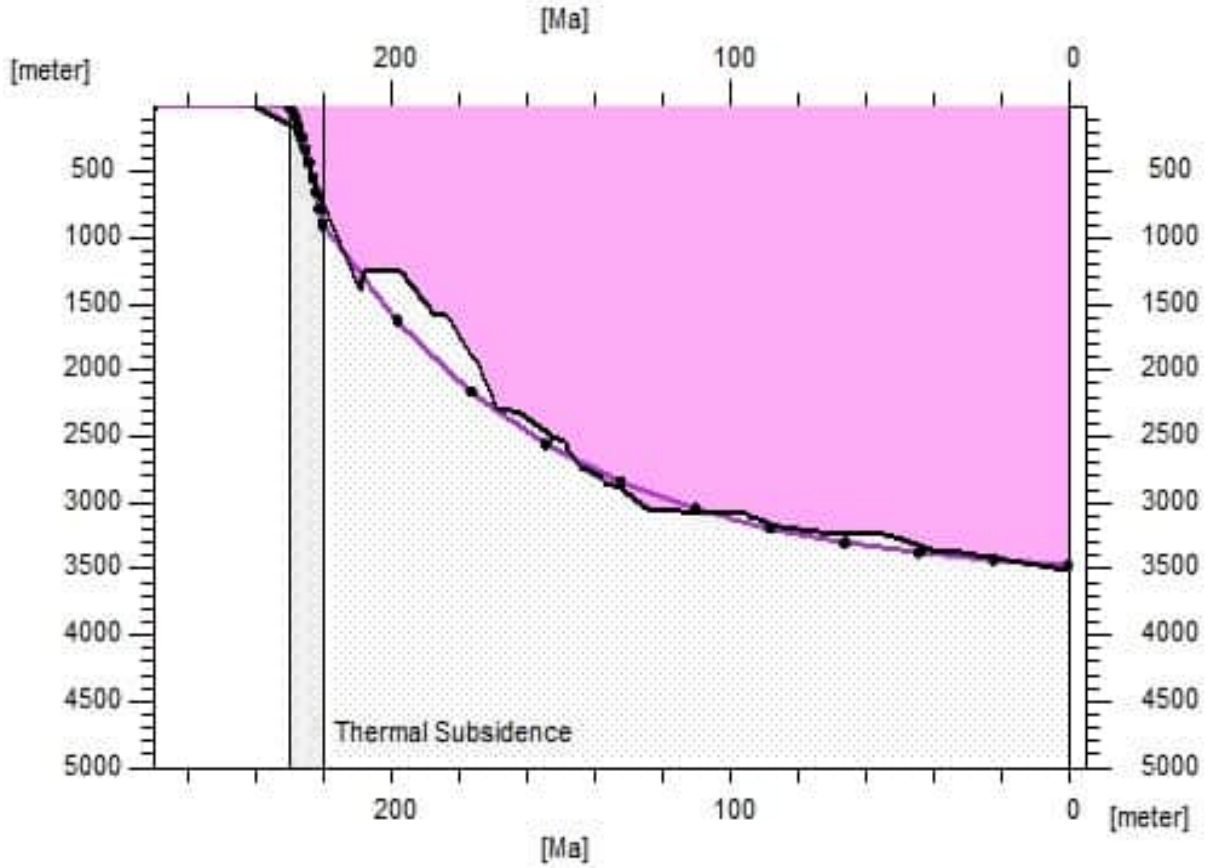


**Hebron I-13** Rift from: 230 Ma
Beta: 1.8 Rift to: 220 Ma
Gamma: 3 Subsidence to: 0 Ma

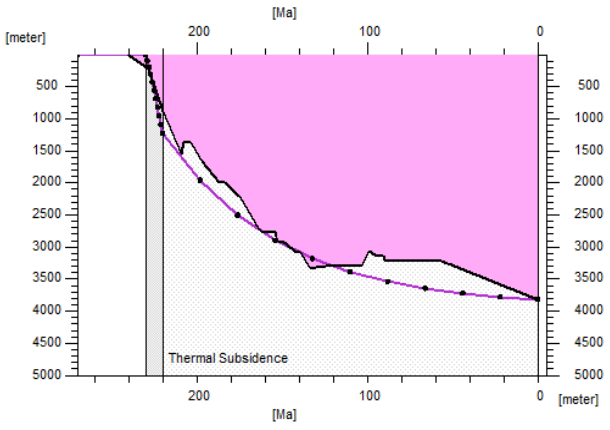


**Whiterose L-61** Rift from: 230 Ma
Beta: 1.95 Rift to: 220 Ma
Gamma: 3 Subsidence to: 0 Ma

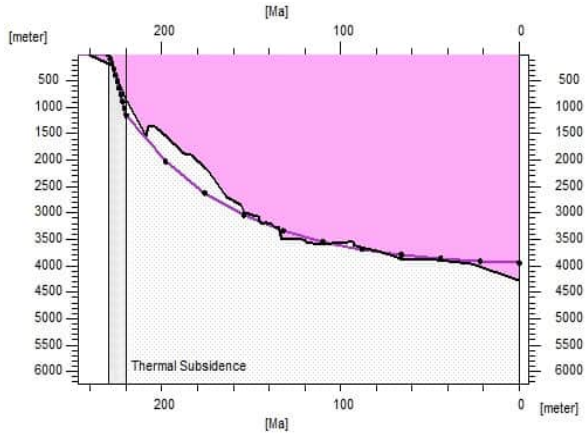


**Botwood G-89** Rift from: 230 Ma
Beta: 2.4 Rift to: 220 Ma
Gamma: 3.8 Subsidence to: 0 Ma

**Figure 3: Tectonic subsidence curves: pink area marks subsidence derived from the burial history of the well and line with dots marks calculated tectonic subsidence derived from the McKenzie approach. Tectonic subsidence is calculated for a water-loaded basin.**

Besides the analysis of the pure burial history it is remarkable that the total tectonic subsidence (combination of initial subsidence and thermal relaxation) of the basin model can be simulated and

matched fairly well by using only one single rift event during the Late Triassic (Fig. 3). Different scenarios have been checked (sensitivity runs; compare also the schematic sketches in Figure 4) but it is impossible to insert a McKenzie type second rift event without ending up with a far too deep tectonic subsidence curve. Ideally there would have to be two phases of strong subsidence, which could be calibrated to two individual rift events (see schematic Figure 4a). But in reality it looks more like that the entire tectonic subsidence, up to the present day, can be matched with just one Triassic rift event (Figure 4b). It is conceivable to have other, less important processes, which do not follow the rules of the McKenzie approach to optimize the fit between calculated and real tectonic subsidence (Figure 4c). Those processes can lead to the basin subsiding several tens of meters during Cretaceous and Cenozoic without any big thermal influence. The driving mechanism could be an ultra-slow rift, for example. Hence, one is able to infer that at least one of those rifts was not a McKenzie type and that was most probably the Iberia rift.

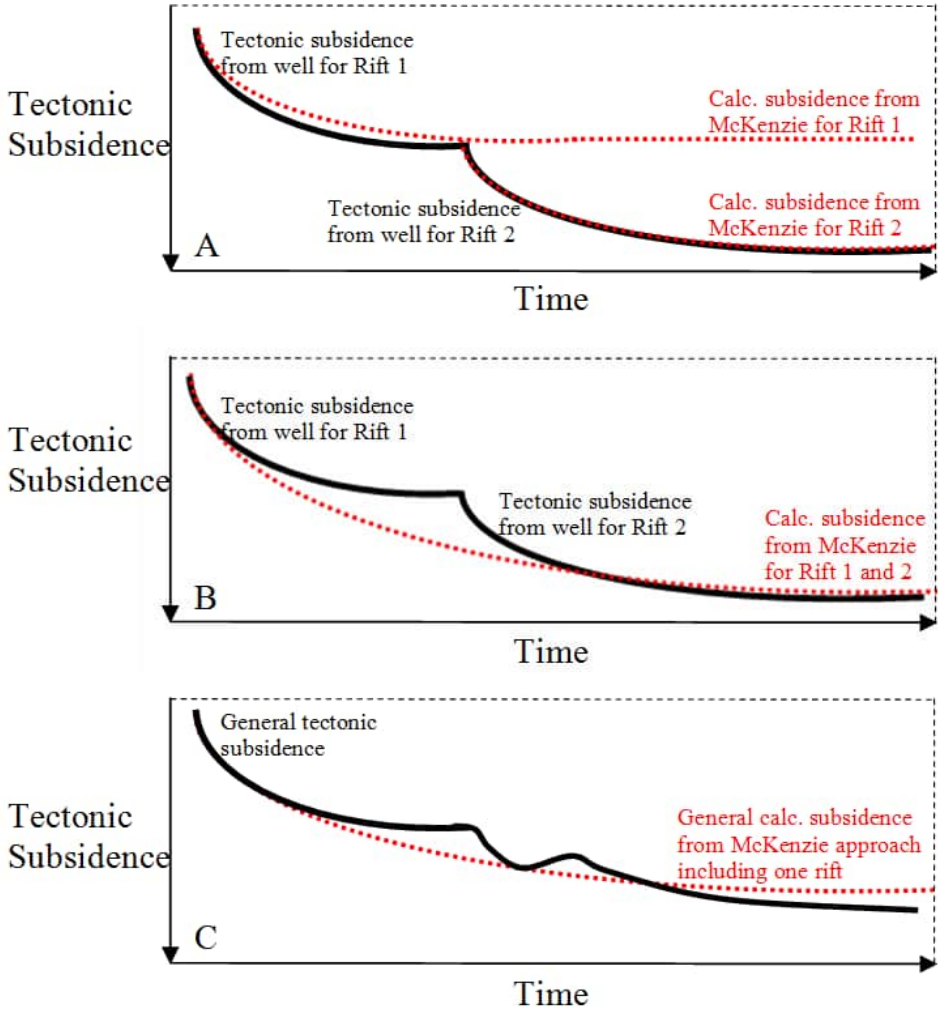


**Figure - 4a: Black line is the idealised shape of the burial history (bh) including two phases of rifting and associated subsidence; dotted line is calculated tectonic subsidence for this double rift - 4b: Black line shows ideal shape of bh; dotted line shows calculated actual tectonic subsidence - 4c: Black line shows general tectonic subsidence deduced from the well; dotted line shows the general tectonic subsidence. A second McKenzie subsidence event does not fit this profile.**

## Interpretation

Finally, we conclude that the Triassic rift event was associated with a real heat pulse, but not strong enough to split the continent. Later, during the end of Jurassic and Early Cretaceous, Iberia splits off from the Grand Banks but caused an ultra-slow and long rift effect on the continental crust in the west. The rift, which developed to the east, possibly pushed against the passive margin and stabilized the continental crust. The heat, generated by the slow rift on the continental crust, was likely dissipated as soon as it came up. If the Iberia rift would have been a real McKenzie rift, the Jeanne d'Arc basin would most probably have broken apart, due to its general unstable condition at that time. Therefore, the Jeanne d'Arc basin is a failed rift, due to a stronger rift event during a tectonically stable time (Triassic) and of an ultra slow rift during an instable plate tectonic phase. That means that the Mackenzie decay can be used for the Triassic rift only and not for the Iberia one. Calibration with vitrinite reflectance and apatite fission track data agree with those results.

The heat flow history deduced from this part of the study will be implemented later on, together with geochemical analysis, into a 4D model in which petroleum-related geochemical processes will be quantified in detail.

## References


Coward, M.P., 1986, Heterogeneous stretching, simple shear and basin development, Earth and Planetary Science Letters 80, p.325-336.

Jarvis, G.T. and McKenzie, D.P., 1980, Sedimentary basin formation with finite extension rates, Earth and Planetary Science Letters 48, p.42-52.

Lister, G.S., Etheridge, M.A. and Symonds, P.A., 1986, Detachment faulting and the evolution of passive continental margins, Geology 14, p.246-250.

McKenzie, D.P., 1978, Some remarks on the development of sedimentary basins, Earth and Planetary Science Letters 40, p.25-32.

Wernicke, B., 1985, Uniform-sense normal simple shear of the continental lithosphere, Canadian Journal of Earth Sciences 22, p.108-125.


**BACK**

# Basin, Petroleum System and Play Analysis in the West African Atlantic Basins

**Suzanne E. Beglinger**
**Harry Doust**
**Sierd Cloetingh**
VU University Amsterdam
de Boelelaan 1085
1081 HV Amsterdam
The Netherlands
Email: suzanne.beglinger@falw.vu.nl

## ABSTRACT

We report on a study of the relationship between tectono-stratigraphic basin evolution and petroleum system development in West African marginal basins between Angola and Cameroon. For this analysis, a novel framework model has been created. The basins have evolved since the Early Cretaceous from a lacustrine synrift, through a transitional hypersaline stage into a postrift, characterized initially by a shallow marine carbonate, secondly by a deep marine and finally a deltaic depositional environment. This history reflects intra-cratonic rifting followed by the creation of the South Atlantic passive margin: all basins considered have experienced a similar tectonic and sedimentary basin evolution. The petroleum systems identified in these basins can be related to common source facies and may be grouped into families or Petroleum System Types (PSTs). Two proven regionally extensive PSTs and two probably local PSTs have been identified. The regionally extensive PSTs are the Lacustrine Synrift PST and the Marine Postrift PST. The probably local PSTs are the Restricted Marine Hypersaline Transitional PST and the Deltaic/Deep Marine Postrift PST. Families of petroleum accumulations (or plays) that characterize these petroleum systems, and which are defined by their reservoir lithofacies and trap type, are also similar in each of these basins. This group of similar basins therefore demonstrates the close link between tectonic- and sedimentary basin evolution on the one hand, and petroleum system and play development on the other. We call such a group of basins a basin family; one which can be used for analogue purposes in basin studies.

## Introduction

Most of the world's basins originate in some way in a rifting episode and subsequently pass through a syn-rift to post-rift evolution. Despite the often complex sedimentary and tectonic development of the various stages, they can most frequently be correlated with phases in tectonostratigraphic development, or to mega-sequences separated by unconformities. Similarly, although the depositional environment and tectonic situation may change considerably over short distances, basic sedimentary patterns and structural styles can usually be recognized. If the development of characteristic hydrocarbon habitats can be related to these basic patterns, we can make broad scale comparisons of petroleum systems between different basins with a similar geological history. This can aid us in recognizing common petroleum system types with related parameters, as well as the plays likely to be associated with them, and thus assist in the evaluation of opportunities in un- or under-explored rift basins (Doust and Sumner 2007). The study area is the West African South Atlantic Margin, extending from Cameroon to Namibia and comprising the Douala Basin, Rio Muni Basin, Gabon Coastal Basin, Lower Congo Basin, Congo Fan Basin, Kwanza Basin and Namibe Basin (Fig 1). The area is a very prolific producer of oil and gas. However, some areas of the West African margin remain under-explored.

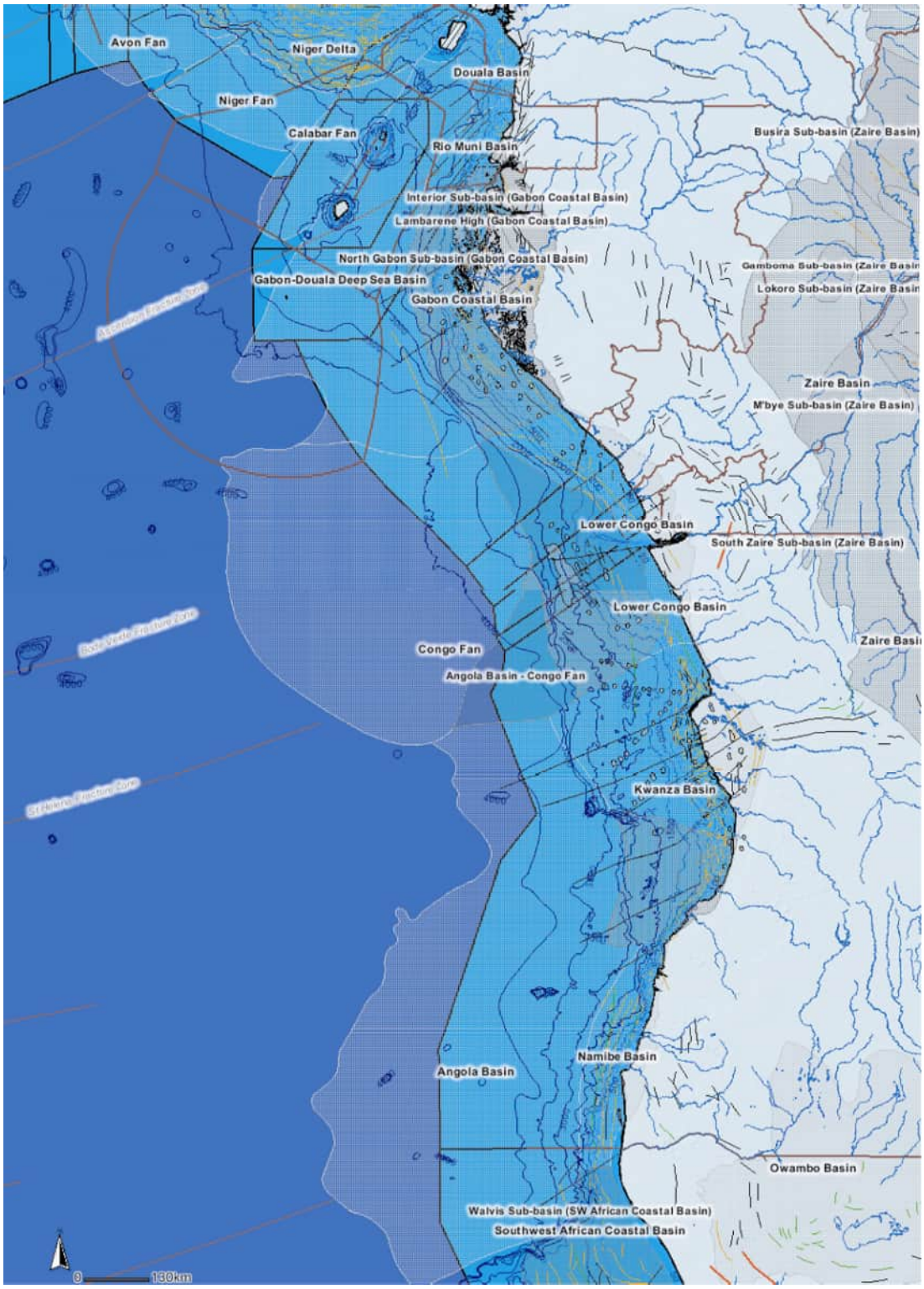


**Figure 1: Location map of the West African South Atlantic Basins, also showing the main tectonic features, bathymetric contours and main drainage systems. The West African South Atlantic Basins comprise (from north to south) the Douala -, Rio Muni -, Gabon Coastal - (Interior-, North- and South- Gabon Basins), Lower Congo -, the Congo Fan -, Kwanza -, and Namibe Basins (IHS 2008).**

## Methodology

A specific framework model has been developed (Fig. 2), the first step of which is to recognize and identify the tectonic stages the basin passes through. Each basin stage is often characterized by a certain sedimentary sequence and type of petroleum system tract (PST). The PST is defined by the source rock depositional environment and its stage in the basin evolution. The associated reservoir levels may be located within the same basin stage, in another basin stage or may even occur throughout the basin sequence. Within the PST, plays are defined by the reservoir lithofacies and the associated trap types.

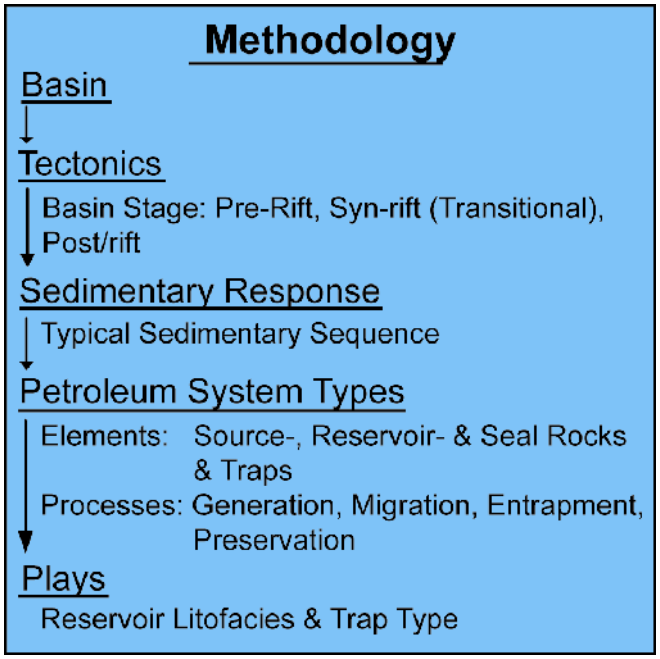


**Figure 2. Framework of the hierarchic model used for basin-, petroleum system- and play analysis in West African South Atlantic Basins.**

## Basin Analysis

Four tectonostratigraphic stages have been recognized in the West African South Atlantic basins: pre-rift, syn-rift (interior fracture), transitional and post-rift (thermal marginal sag) (Fig. 3). The western coast of Africa and the eastern coast of South America were once joined together in the super-continent Gondwana, but reactivation of zonal weaknesses in the Precambrian basement during the Permian, Triassic and Jurassic, resulted in the formation of localized sag basins. The two continents separated at the end of the Jurassic and the very beginning of the Cretaceous by a process of rifting and oceanic suturing.

The continental extensional breakup was initiated by a thermal doming event, followed by at least two active rifting episodes. As the split between the continental landmasses developed continental alluvial, fluvial and lacustrine pre- and syn-rift sediments were deposited. Oceanic emplacement began in the south and advanced northwards: the oldest oceanic crust south of the Walvis Ridge is Jurassic, while north of this ridge it is Cretaceous. Accordingly, the syn-rift and transitional stages of the West African South Atlantic Margin start and terminate later in the northern basins than in the southern basins, in agreement with the zipping open of the South Atlantic from south to north (Fig. 3).The end of rifting was associated with salt deposition during the transitional period (the period defined by the transition from rifting conditions to full drift conditions).

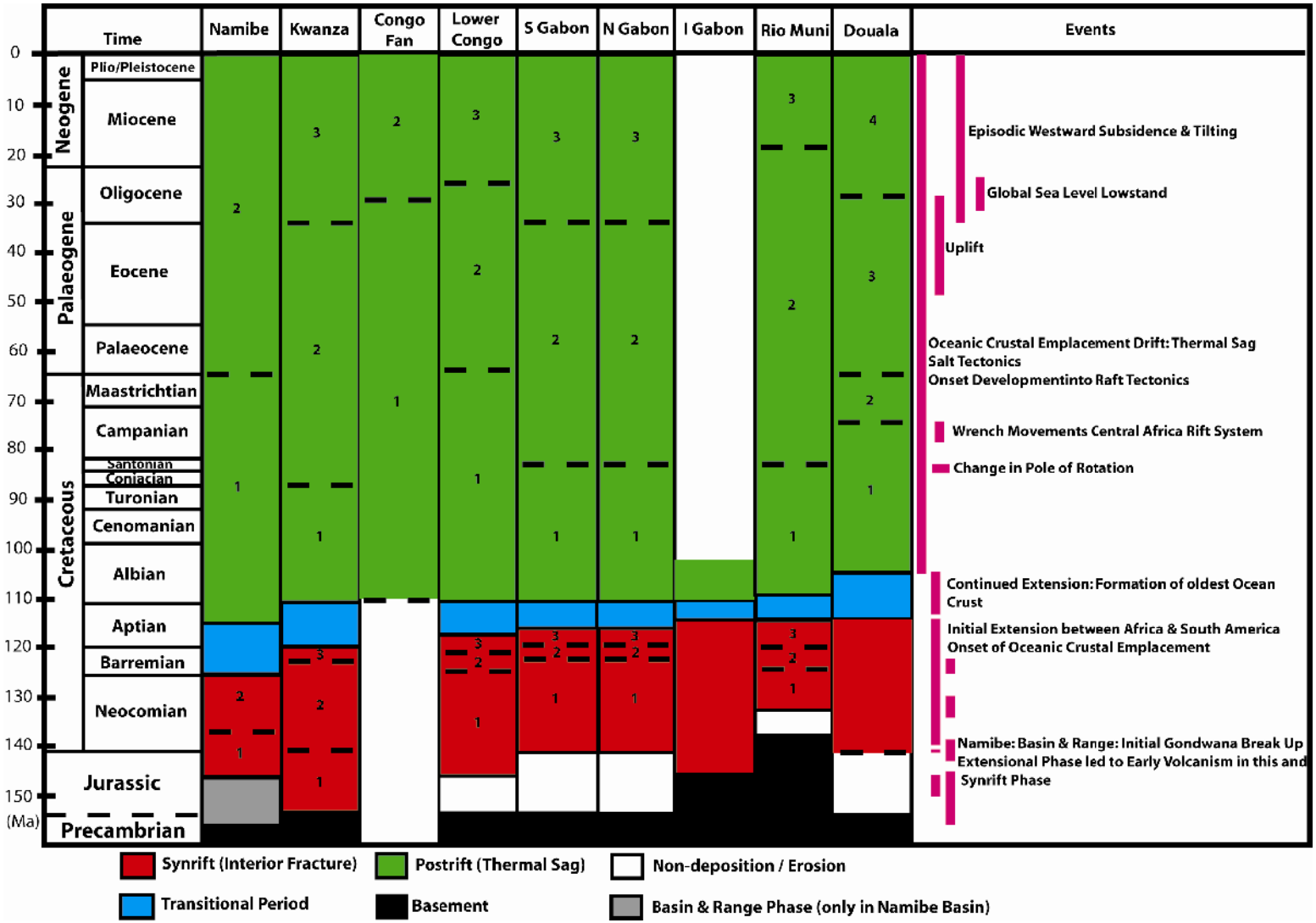


**Figure 3. Basin tectonic evolution chart, summarizing the timing of each basin stage in basin evolution in each West African South Atlantic Basin. Every individual basin has experienced a similar tectonic evolution and has been subject to the same tectonic events (right column). Note that the syn-rift and transitional period tend to start and terminate later when moving northwards, related to the zipping open of the South Atlantic from south to north (after data IHS Energy 2008).**

The divide between the rift and drift sections of the West African South Atlantic basins is defined by the Aptian peneplain unconformity and the overlying Albian Salt layer. The salt deposits were laid down in a region of poorly circulating waters north of the volcanic Walvis Ridge and Rio Grande Rise. Following the period of evaporite deposition, further extension led to the opening of the South Atlantic and the deposition of a series of post-Aptian shallow to deep marine clastic and carbonate post-rift sediments as the margin shelves subdued.

The evaporite deposits are particularly important in determining patterns of fan- and turbidite systems. Post-depositional salt movement also created various trap types within the overlying sediments: extensional structures developed in the upper margin of the basins and compressional structures in the deeper basinal parts (Dupré *et al*. 2007; Cramez and Jackson 2000). The passive margin conditions, which started in the Albian with subsidence associated with oceanic crustal cooling, have persisted to the present day.

A way to illustrate the evolution of a basin is to use trajectory plots. On the X-axis of a trajectory plot, the main tectonic basin stages are plotted, and on the Y-axis, the depositional environments. Each basin is characterized by a specific trajectory path in this diagram, but each of the West African South Atlantic basins has experienced a similar sedimentary evolution: a fluvial/lacustrine syn-rift, followed by a restricted hypersaline transitional stage and a shallow to deep marine postrift. The latest phase of the postrift is characterized by the local development of deltaic systems on the shelf and associated turbidite systems in the deeper parts of the basin (Fig. 4).

## Petroleum System Analysis

### Source, Reservoir- and Seal Rocks

With the use of IHS field data, every proven, potential and hypothetical source rock interval in the West African South Atlantic Margin has been identified (Fig. 5). The source rocks were deposited during certain periods in the tectonic- and sedimentary evolution, and each interval produces hydrocarbons with a particular signature (although there may be some mixing, (Katz and Mello 2000).

The syn-rift source rocks are lacustrine in origin. Generally, two generative shale intervals have been recognized, the most important of which comprises organic-rich, thick type I and II lacustrine shales with TOC contents averaging 2 to 6.1 wt.%. The oils generated by syn-rift lacustrine shales are paraffinic. The restricted marine hypersaline environment of the transitional stage led to the deposition of organic-rich shale intervals within the evaporite unit in the Douala Basin: sea water entering the Proto-South Atlantic from the south had trouble reaching the most northerly basins. Evaporite deposition was less pronounced there.

The dominantly marine post-rift is characterized by several intervals of marine shale and marl type II/III source rocks. These shales average 3 to 5 wt.% TOC and many are known to be mature and to have generated hydrocarbons. The latest phase of the postrift is in some areas characterized by the development of extensive deltas, which allowed deltaic source rocks to mature and generate hydrocarbons. The kerogens are type II and II/III. In other basins, where no such delta development has taken place, equivalent shales can only generate hydrocarbons, when deposited in deep troughs or in areas with an abnormal high thermal heat flow.

The hydrocarbon accumulations are located in both non-marine and marine stratal packages, and in both carbonates and siliciclastics. Figures 5 and 6 summarize the proven reservoir lithofacies within each basin stage of each basin. The pre-rift is mainly associated with volcanic reservoir lithofacies, although alluvial, fluvial and aeolian lithofacies are expected in this stage also. The syn-rift is characterized by lacustrine and fluvial lithofacies, while the transitional stage includes also some shallow marine facies. Within the post-rift, there is the greatest variety in reservoir lithofacies with fluvial, deltaic shoreline, tidal, shallow marine and deep marine facies. This means that during basin evolution, the

number of potential reservoir lithofacies increases. Further, the reservoir lithofacies show a general deepening through time.

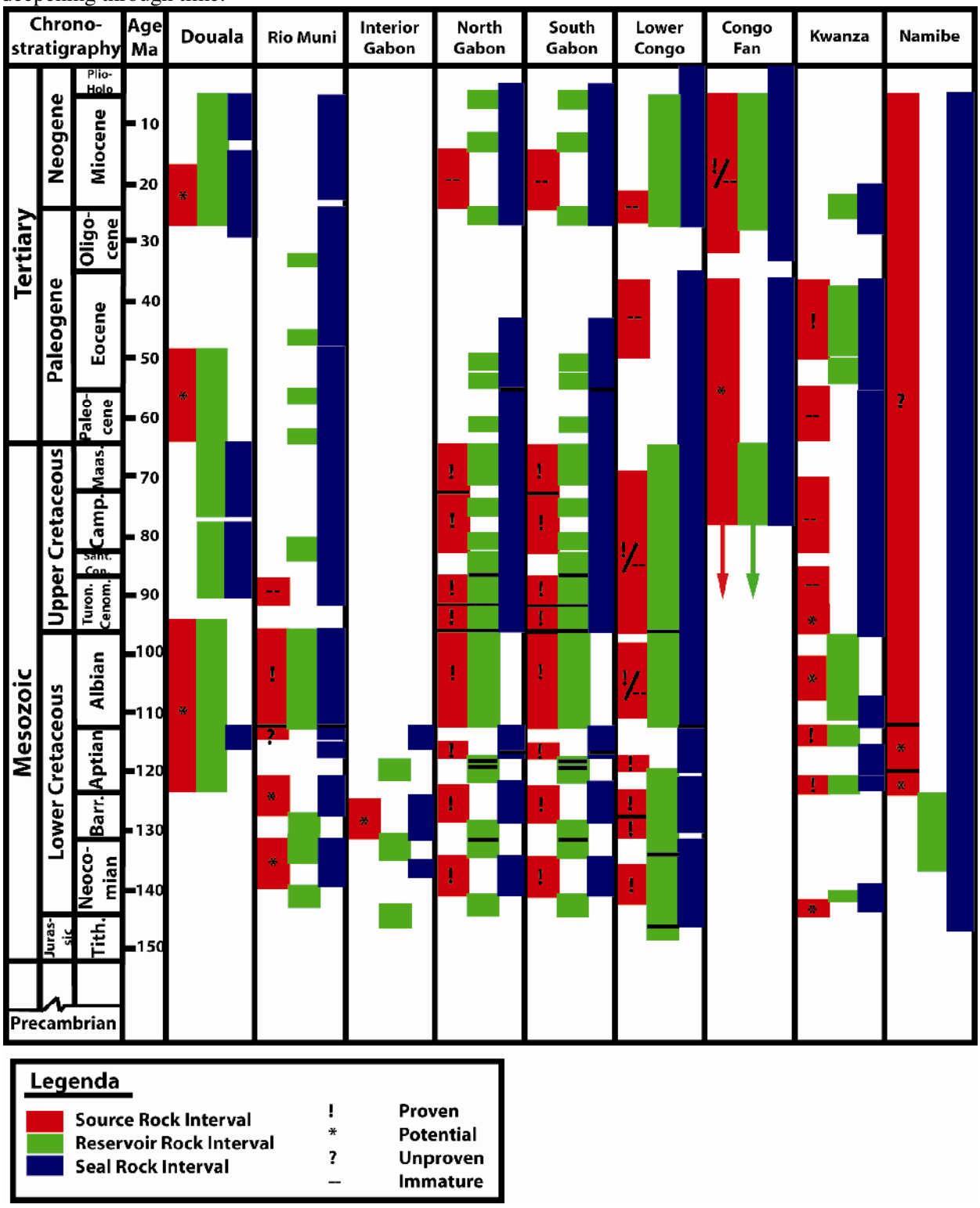


**Figure 5.Diagram summarizing all source-, reservoir-, and seal rock intervals identified in each West African South Atlantic Basin (after data IHS Energy 2008).**

The most important seal is provided by the Aptian evaporite layer, separating syn-rift systems from post-rift systems. In areas, where salt windows are present, either due to non-deposition or salt tectonic movement, hydrocarbons generated in the syn-rift are able to migrate into the post-rift reservoirs. Many shale and clay layers are present throughout the stratigraphy of all West African South Atlantic basins, and these lacustrine, deltaic and marine shales act as intra-formational seals, as well as providing source potential (Fig. 5).

| Basin Stage | Reservoir Lithofacies | Trap Class | | | | | | |
|---|---|---|---|---|---|---|---|---|
| | | Structural | Stratigraphic | Statigraphic-Structural | Stratigraphic-Unconformity | Structural-Unconformity | Stratigraphic-Structural-Unconformity | Unknown |
| Pre-rift | Volcanics | | | X | | | | |
| | ... | | | | | | | |
| | ... | | | | | | | |
| Synrift | Volcanics | | | | | | | |
| | Alluvial | | | X | | | | |
| | Lacustrine | X | | X | | | X | X |
| | Fluvial | X | | X | | | X | X |
| | Deltaics | | | | | X | | |
| | Shoreline | X | | X | | | | |
| | Tidal | | | | | | | |
| | Coastal | | | X | | X | | |
| | Shallow Marine | | | | | | | |
| | Deep Marine | | | | | | | |
| | Unknown | X | | X | | X | X | |
| Transitional | Volcanics | | | | | | | |
| | Alluvial | | | | | | | |
| | Lacustrine | X | | X | X | | | |
| | Fluvial | X | | X | | X | | X |
| | Deltaics | | | | | X | | |
| | Shoreline | X | | X | | X | | X |
| | Tidal | | | | | | | |
| | Coastal | | | | | | | |
| | Shallow Marine | | | | | X | | |
| | Deep Marine | | | | | | | |
| | Unknown | X | | X | | X | | X |
| Postrift | Volcanics | | | | | | | |
| | Alluvial | | | | | | | |
| | Lacustrine | | | | | | | |
| | Fluvial | X | | X | | | | X |
| | Deltaics | X | X | X | | | | |
| | Shoreline | X | | X | | | | |
| | Tidal | X | | X | | | | X |
| | Coastal | X | | X | | | | |
| | Shallow Marine | X | X | | | X | X | X |
| | Deep Marine | X | X | X | X | X | X | X |
| | Unknown | X | X | X | | | | X |

**Figure 6. Diagram summarizing the different play types identified in each basin. Note the increase of the number of play types with basin evolution (after data IHS Energy 2008).**

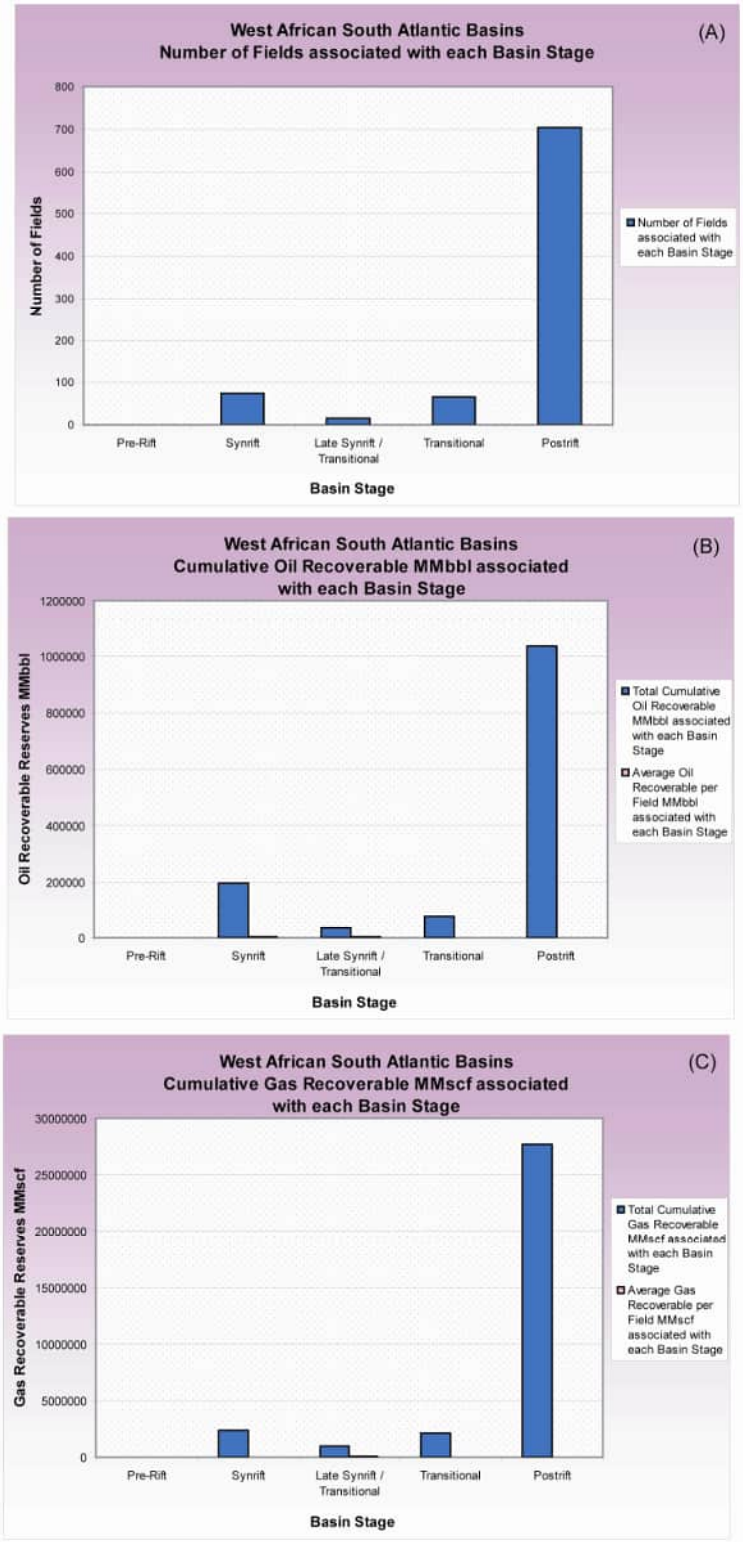


**Figure 7. Basin stage analysis. A) Number of fields associated with each basin stage. B) Cumulative oil recoverable reserves associated with each basin stage. C) Cumulative gas recoverable reserves associated with each basin stage (after data IHS Energy 2008).**

### Petroleum Systems

A petroleum system is defined as a natural system encompassing a pod of active source rock and all related oil and gas accumulations – including all the necessary processes of maturation and generation. Within the West African South Atlantic basins, four types of Petroleum System may be recognized: Lacustrine Syn-rift PST, Restricted Hypersaline PST, Marine Post-rift PST and Deltaic Post-rift PST.

### Plays

A play is defined by its reservoir lithofacies and trap type. Unfortunately, only minimum information is publicly available about the actual trapping architecture of the fields. We have distinguished structural, stratigraphic, and combination traps with or without a sealing unconformity. Figure 6 summarizes all occurring reservoir lithofacies in the pre-rift, syn-rift, transitional stage and post-rift, and their associated trapping character.

## Discussion

This study demonstrates that each of the West African South Atlantic basins has experienced a similar tectonic and sedimentary evolution. Four basin stages, characterized by specific depositional environments and separated by major unconformities, have been identified: a continental pre-rift, a lacustrine syn-rift, a restricted hypersaline transitional stage and a marine (and later deltaic) post-rift. Most fields are located within the post-rift section. The largest volumes of oil and gas have also been found in the post-rift section, but significant accumulations are also present within the syn-rift and transitional stages (Fig. 7).

As a consequence of the similar basin evolution, similar types of petroleum systems (PSTs), associated with each basin stage, were able to develop. Four PSTs have been recognized: Lacustrine Syn-rift PST (PST I), Restricted Hypersaline Transitional PST (PST II), Marine Post-rift PST (PST III) and Deltaic Post-rift PST (PST IV). Many fields are charged by solely one PST, but even more fields are charged by a mixture from several PSTs (Fig. 8). Most fields are associated with PST I and PST III, with a mixture of PST I and III, or with a mixture of PST I, III and IV. PST I and III are the main oil and gas producers, but PST IV also contributes an important part to the total gas production. Condensates are mainly produced by PST I.

Because of the development from an interior fracture basin to a passive margin, many different reservoir lithofacies occur, representing the wide variety of depositional environments. Most fields are associated with shallow or deep marine clastics and carbonates. This is because most fields are located in the post-rift section, which is dominated by a marine depositional environment. However, a significant volume of oil is also associated with fluvial and shoreline reservoir lithofacies (Fig. 9).

In this study, all proven play types have been identified for each basin stage. It can be concluded that with basin evolution, the number of play types increases: the post-rift is characterized by the greatest variety of depositional environments, providing the most possible reservoir lithofacies, and the greatest variety of trapping structures, due to strong salt-tectonics.

Exploration density is not uniform across the West African South Atlantic Margin. Some areas are mature, but many others appear to be under-explored. Most fields have been drilled in the Lower Congo Basin, followed by the North Gabon and Congo Fan Basin (Fig. 10). The Lower Congo and North Gabon Basin are the main oil producers. The Lower Congo Basin also holds significant volumes of gas, together with the Congo Fan Basin. The Douala Basin, with relatively few wells, also contains a relatively large volume of recoverable gas.

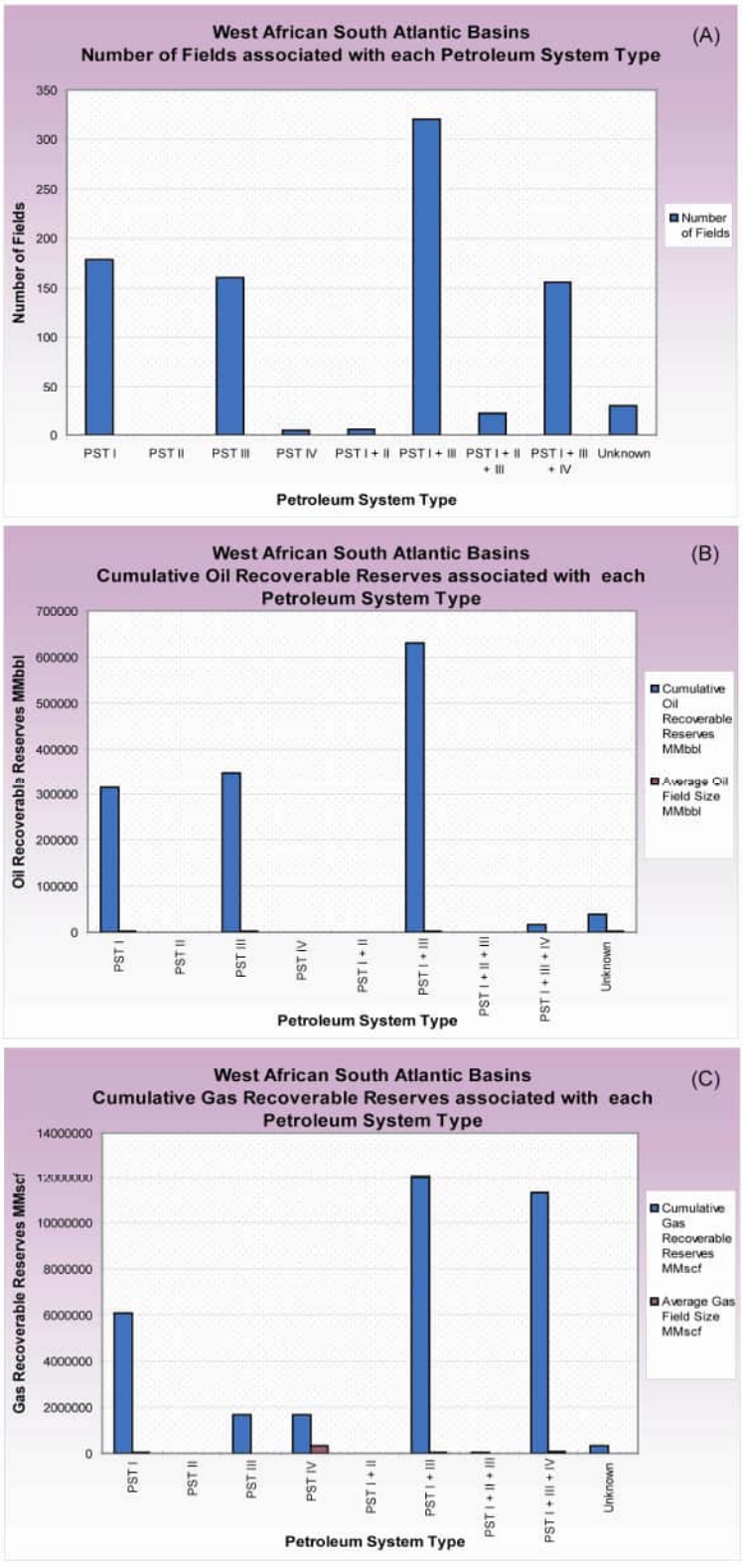


**Figure 8. PST analysis. A) Number of fields associated with each PST. B) Cumulative oil recoverable reserves associated with each PST. C) Cumulative gas recoverable reserves associated with each PST (after data IHS Energy 2008).**

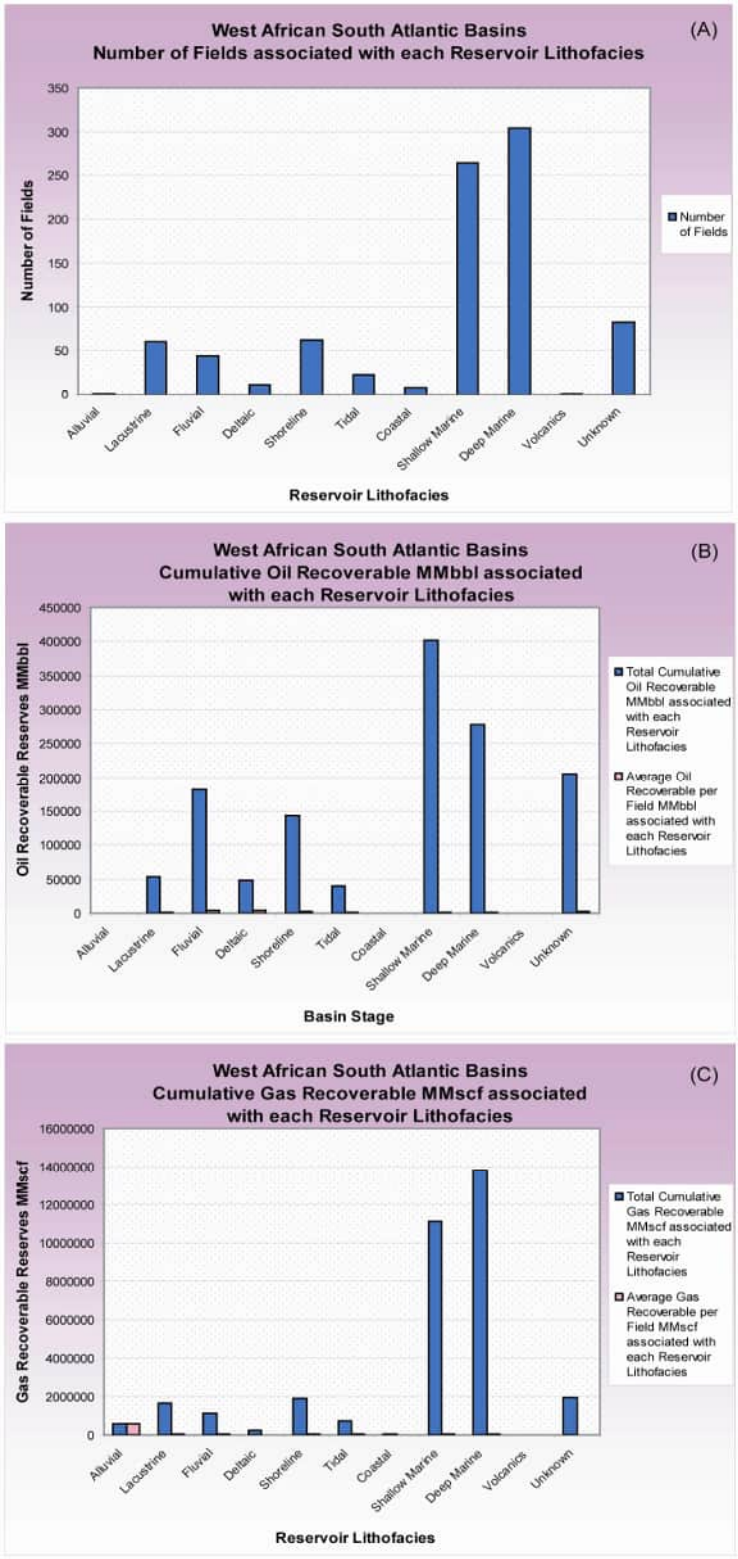


**Figure 9. Reservoir lithofacies analysis. A) Number of fields associated with each reservoir lithofacies. B) Cumulative oil recoverable reserves associated with each reservoir lithofacies. C) Cumulative gas recoverable reserves associated with each reservoir lithofacies (after data IHS Energy 2008).**

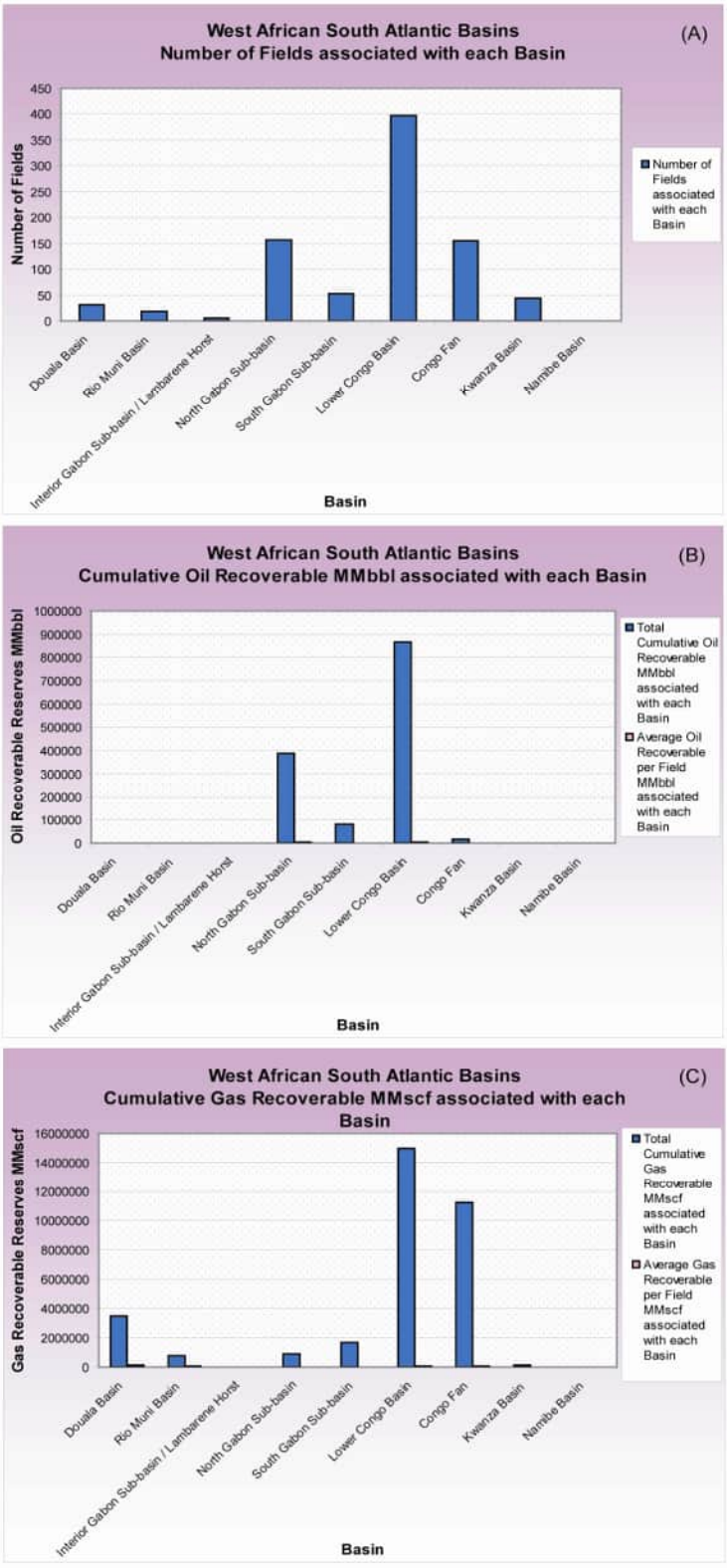


**Figure 10. Basin analysis. A) Number of fields associated with each basin. B) Cumulative oil recoverable reserves associated with each basin. C) Cumulative gas recoverable reserves associated with each basin (after data IHS Energy 2008).**

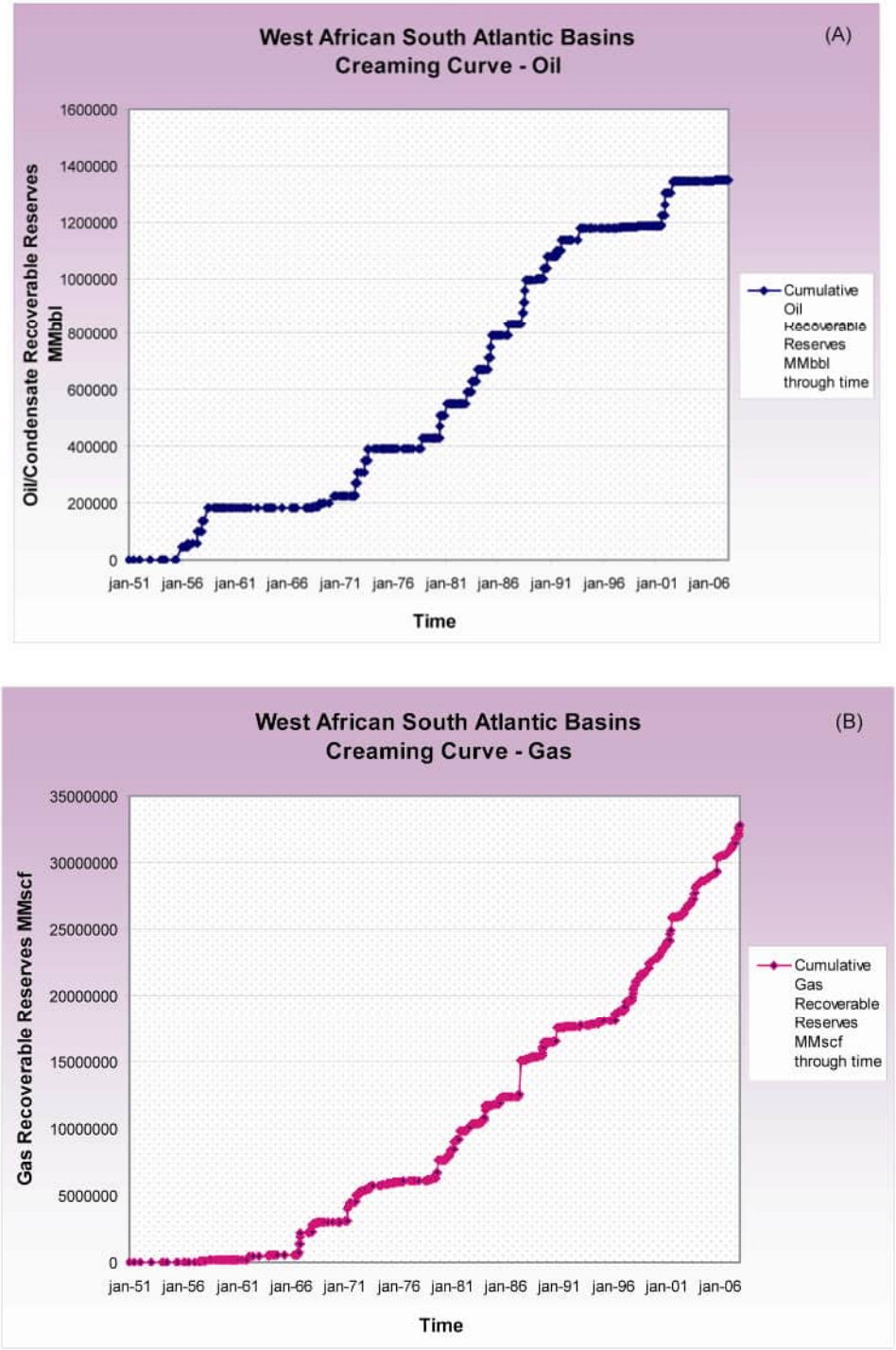


**Figure 11. Creaming curves, describing hydrocarbon production through time. A) Oil creaming curve. B) Gas creaming curve (after data IHS Energy 2008).**

The creaming curve is a way to display the discovery history of a basin or group of basins through time. Hydrocarbon production started in 1951. The oil creaming curve (Fig. 11) shows four major jumps in recoverable oil reserves. The first jump in the late 1950s was associated with major oil finds in the post-rift section of the North Gabon Basin and syn-rift section of the Lower Congo Basin. The second

jump in the early 1970s was due to increased exploration and production in the post-rift section of mainly the Lower Congo and Kwanza basins. The enormous jump extending from the late 1970s till the early 1990s, corresponded to extensive exploration in the syn-rift and transitional sections in the Lower Congo, Gabon Coastal and Douala basins. The last jump during the years 2001 and 2002 was associated with mainly post-rift exploration in the Gabon Coastal, Congo Fan and Rio Muni basins. The curve shows signs of creaming in the last few years, suggesting that the West African South Atlantic basins are becoming mature oil provinces. Gas exploration flourished from 1966 onwards.

The creaming curve shows an almost straight line, suggesting that the area as a whole is not yet a mature gas province. The Douala Basin is under-explored with relatively small discoveries and two not fully understood petroleum systems (IHS, 2008). In the Rio Muni Basin, potential remains in the poorly defined pre-salt section (IHS 2008). The Gabon Coastal Basin (North-, South- and Interior Gabon basins) is mature in terms of drilling and seismic density and moderately prospective in terms of reserves discovered. Exploration is immature, however, in the North Gabon syn-rift section, in the deeper water parts of the Ogooue River Delta and in the post-rift section of the South Gabon Basin (IHS 2008). The Lower Congo Basin is mainly a gas province, but some significant oil accumulations have also been identified.

Future prospects are expected mainly in the deep waters and at greater depths, where turbidite systems may be identified on 3D seismics (IHS 2008). Exploration in the Congo Fan Basin is immature for both oil and gas. Due to the multi-country and mainly ultra-deep water, much of the basin has been poorly explored. Even on the shelf, for many years little geological attention was paid to the Tertiary section. In recent years, the massive hydrocarbon potential of the Tertiary has been demonstrated, and exploration has been moving into the deep and ultra-deep waters of the Congo Fan Basin (IHS 2008). The deep water province of the Kwanza Basin remains substantially undrilled. The whole area is now covered with a large 2D seismic grid and major areas of 3D seismic coverage. The recognition of potential deep water mature source sequences coupled with the Upper Cretaceous and Tertiary deltaic and turbidite potential provides this area with interesting exploration potential (IHS 2008). The Namibe basin is a frontier basin and considerable work is needed to establish it as a viable exploration region. In view of the rapid increase of water depth away from the Angolan and Namibian coastline, it is likely that most exploration effort will be in the hinge line and central graben regions, in which structural-stratigraphic traps are likely to be best developed (IHS 2008).

## Conclusions

Because exploration density is not uniform across the West African South Atlantic Margin, some areas are already mature, while others remain under-explored. The Douala Basin, the pre-salt section of the Rio Muni and North Gabon Basin and the deep to ultra-deep waters of the Ogooue Delta, and Lower Congo, Congo Fan and Kwanza Basin are such under-explored areas with high exploration potential. The Namibe Basin is a frontier area. Four PST's are responsible for the discovered hydrocarbon accumulations. The Lacustrine Syn-rift PST, the Marine Post-rift PST and the Deltaic Post-rift PST are the main hydrocarbon producers. Often, hydrocarbons generated by these systems, mix prior to accumulating in structures. The greatest volume of hydrocarbons accumulates in traps located in the post-rift sections, but significant accumulations are also present within the syn-rift and transitional stages. The post-rift section is also characterized by the greatest variety of plays: the depositional environments associated with the passive margin architecture are most diverse, and many different structures are able to develop due to salt tectonics. The similar tectonic and sedimentary evolution of the individual West African South Atlantic basins, has led to the development of similar PSTs and plays in these basins. Therefore, these basins can be used as analogues for evaluating exploration opportunities in basins with similar evolution.

## References


Doust, H & Sumner, H.S., 2007, Petroleum Systems in Rift Basins – a Collective Approach in Southeast Asian Basins: Petroleum Geoscience, v.13, n.2, p.127-144.

IHS Energy, 2008: Databases.

Brownfield, M.E. & Charpentier, R.R., 2006, Geology and Total Petroleum Systems of the West-Central Coastal Province (7203), West Africa: U.S. Geological Survey Bulleting 2207-B, 52p.

Dupré, S., Bertotti, G. & Cloetingh, S., 2007, Tectonic history along the South Gabon Basin: Anomalous early post-rift subsidence: Marine and Petroleum Geology, v.24, p.151-172.

Cramez, C., Jackson, M.P.A., 2000, Superposed deformation straddling the continental-oceanic transition in deep-water Angola: Marine and Petroleum Geology, v.17, n.10, p.1095-1109.

Katz, B.J. and Mello, M.R., 2000, Petroleum Systems of South Atlantic Marginal Basins – An Overview, *in* M.R. Mello and B.J. Katz, (eds.)., Petroleum Systems of South Atlantic Margins: AAPG Memoir 73, p.1-13.


**BACK**

# Predictive Trends in Salt Morphology Derived from Systematic Assessment of Merged 3D Seismic Coverage over Entire Basins

**Tim Bird**
**David Johnstone**
PGS Reservoir
17 Marlow Road
Maidenhead, Berkshire, SL6 7AA
United Kingdom
e-mail: tim.bird@pgs.com

**Mark Martin**
PGS Exploration
Walton-on-Thames
Surrey, KT12 1RS
United Kingdom

## ABSTRACT

3D seismic 'MegaSurveys' over three major salt basins in the North and South Atlantic Margin Provinces have been analysed to compare and contrast the geometries of salt structures in three distinctly different structural and depositional settings. Superficially the halokinetic features in these basins appear to have strikingly similar characteristics. Systematic measurement of the geo-spatial statistics of these features allows quantification of the degree of similarity in styles and highlights the local differences associated with each basin. Some of the more complex geometries can be explained as the interaction of multiple phases of deformation with different orientations, timing and stress fields.

## Introduction

Salt geometries have been interpreted on over 75,000 $km^2$ of 3D seismic data covering three major salt basins – the Southern Permian Zechstein Basin in the Netherlands and UK Southern North Sea, the deepwater Campos Basin offshore Brazil and the southern portion of the Lower Congo Basin, deepwater Angola. All three areas are characterised by large salt wall features extending for tens of kilometres. These features are typical narrow, generally 2 km in width, ranging to a maximum of approximately 5 km locally, often with relief in excess of 2000 m. They can generally be seen to follow an underlying, pre-existing structural grain, with a regular spacing of 10-15 km. Several, often near-orthogonal trends are recognised in all three areas, leading to complex geometries where the trends intersect. Geometries are further complicated by the multiple phases or pulses of salt re-activation in response to changing stress regimes, both extensional and compressional. Compressional geometries are identified in all three case study areas.

## Data

The data used for the evaluation of each basin were PGS 'MegaSurveys'. MegaSurveys are patchworks of tens to hundreds of individual interlacing and overlapping 3D surveys which are merged, re-binned, phase and amplitude matched, and normalised into a single contiguous 3D seismic dataset covering entire basin systems.

These merged MegaSurvey datasets are calibrated by all available well control, re-interpreted into a consistent regional framework and used to interpret 5 to 8 seismic mega-sequence boundaries or regional marker horizons for each basin. Such consistent 3D coverage over a whole region enables new insights into the detailed geometries of basins.

No 3D MegaSurvey projects yet exist in the Central Atlantic Margin Province. However, three such 'MegaSurveys' covering major salt basins from either side the South Atlantic Margin Province and the North Sea have been studied with the aim of better understanding and differentiating generic, 'global' trends in salt morphology from local basin-specific styles. These three major salt basin areas were selected for study as having distinctly different basin histories, exhibiting varying tectonic development and depositional settings enabling assessment of the similarities and differences between salt body geometries in different tectono-stratigraphic settings.

## Statistical Analysis

By systematically measuring and cross-plotting the spatial distribution and dimensions of all the halokinetic features within the entirety of each basin, it is possible to examine patterns in, for example, wavelength and amplitude, and the ranges and statistical distribution of these parameters. The general trends in these attributes appear to be consistent and independent of the tectono-stratigraphic history of the various salt basins, as a result of which each basin exhibits differences in the age and thickness of the salt, along with variations in the age and character of the overlying sediments. For instance, the spatial distribution and aspect ratios of salt walls are found to be limited to a relatively narrow range for all three basin areas studied. Salt walls rarely exceed 2-5km in width, irrespective of wall length or height. Different clusters are observed for the three main generic classes of salt structural styles – walls, stocks and pillows – and consistent ranges can be extracted for height to width, and length to width (elliptical eccentricity of major axis length to minor axis width) for each class.

Three major salt basin areas with distinctly different basin histories, exhibiting varying tectonic development and depositional settings were studied to assess the similarities and differences between salt body geometries. These are briefly summarised in the following sections.

## South Permian / Zechstein Basin, Southern North Sea (SNS), Netherlands & UKCS

### Geology

The structural grain of the Anglo-Dutch offshore portion of the Zechstein Basin has been strongly influenced by fault systems in the basement that came into existence during the Variscan orogeny (Late Carboniferous - Permian phases). Late Jurassic to Early Cretaceous extensional tectonics dominates the structural configuration of the Dutch subsurface, involving Cimmerian reactivation of pre-existing Permo-Carboniferous faults. Late Jurassic and Early Cretaceous subsidence of basins and uplift of flanking platforms, combined with effects of salt movement, reflect the development of a complex structural setting. The geological setting during the Late Jurassic was characterized by erosion of elevated platforms together with the accumulation of sediment in the local basins along the edges of the uplifted blocks. Late Jurassic depositional areas are relatively small as compared to the Permian, Triassic and Cretaceous basins. Strong halokinetic movements took place in the northern offshore and the north-eastern onshore area. The thickness of Zechstein shows strong local variation. Salt pillows, walls and diapirs have been active since the Late Triassic. Both intensity and (re-)activation of salt movement varies strongly across the basin.

### Data

The SNS MegaSurvey covers the majority of the Southern North Sea Basins located in shallow water between the southeast coast of England and the Netherlands. The survey is a merge of over 50 input 3D seismic surveys creating a patchwork approximately 270km x 250km with a contiguous live trace area of over 45,000 $km^2$ (Fig. 1). Over 900 wells were used to calibrate this dataset.

### Interpreted salt structures

The style of salt structures in the Southern North Sea Zechstein Basin is dominated by elongate salt walls along three distinct axes (Fig. 1). A northwest striking Variscan trend predominates in the west, with an average spacing of 15km aligned with the structural grain of the underlying Carboniferous rotated fault blocks and fold axes. A second northeast-striking trend predominates in the east, especially in the Dutch Central Graben and Terschelling Basin. This trend is seen in the cross-faults that compartmentalize many of the Permian Rotliegendes and Carboniferous sandstone reservoirs which form the traps beneath the Zechstein salt that create the majority of the gas fields discovered in the Netherlands and UK Southern North Sea Basin. A third, north-south trend is associated with several of the most continuous, tall narrow salt wall structures on the UK side. Approaching 50 discrete salt structures have been identified and detailed dimensions recorded. This basin has a greater representation of pillow structures than the other two basins analysed.

## Deepwater Campos Basin, Brazil

### Geology

During the Early Cretaceous, a northeast-southwest rift-valley system split South America and West Africa. A series of horst and graben basins resulted from this extension developed on both the South American and West African margins of the expanding South Atlantic. During the subsequent drift phase of ocean floor spreading and subsidence up to 9,000 m of Early Cretaceous to Holocene sediments were deposited into the individual basins along the conjugate margins. One of these, the Campos Basin, offshore Brazil, covers an area of about 100,000 $km^2$. The Campos Basin is the most prolific petroleum bearing basin in Brazil, with over 70 accumulations containing 80% of Brazil's reserves, most concentrated in a handful of giant fields in the deeper water regions of the basin.

The initial rift phase of margin development occurred in the Late Hauterivian to Early Aptian, with a complex rift lake graben system evolving in a tectonic setting similar to the present day East African rift system. Up to 3,500m of organic rich lacustrine mudstones were deposited, which now form one of the major hydrocarbon source rocks in the region, the Lagoa Feia formation, with a TOC of over 6 percent. Carbonate reservoirs comprising peleycepod coquinas and reefs with porosities of 15%-20% and permeabilities of 200-500mD, were deposited at the lake margins or on uplifted crests of rotated fault blocks, while alluvial fan and fan-delta sands deposition occurred on the margins of these graben systems.

A transition phase occurred during the Aptian with thick evaporite sequences deposited across the entire basin. Salt thicknesses, after halokinesis, reach over 5,250 milliseconds TWT, equating to almost 4,000m of mobilised salt in local diapiric structures. Movement of the salt was initially triggered by reactivation of earlier Cretaceous rift-related fault systems and the salt layer acts as a regional decollement surface for the listric faults that accommodate extension in the overlying later Cretaceous and Tertiary sedimentary cover.

Onset of the drift phase occurred in the Albian, with the Macae formation carbonates comprising algal calcarenites and interbedded micrites, developed in a restricted shallow water marine environment. Oil accumulations occur locally in the lower Macae formation where porosity is high.

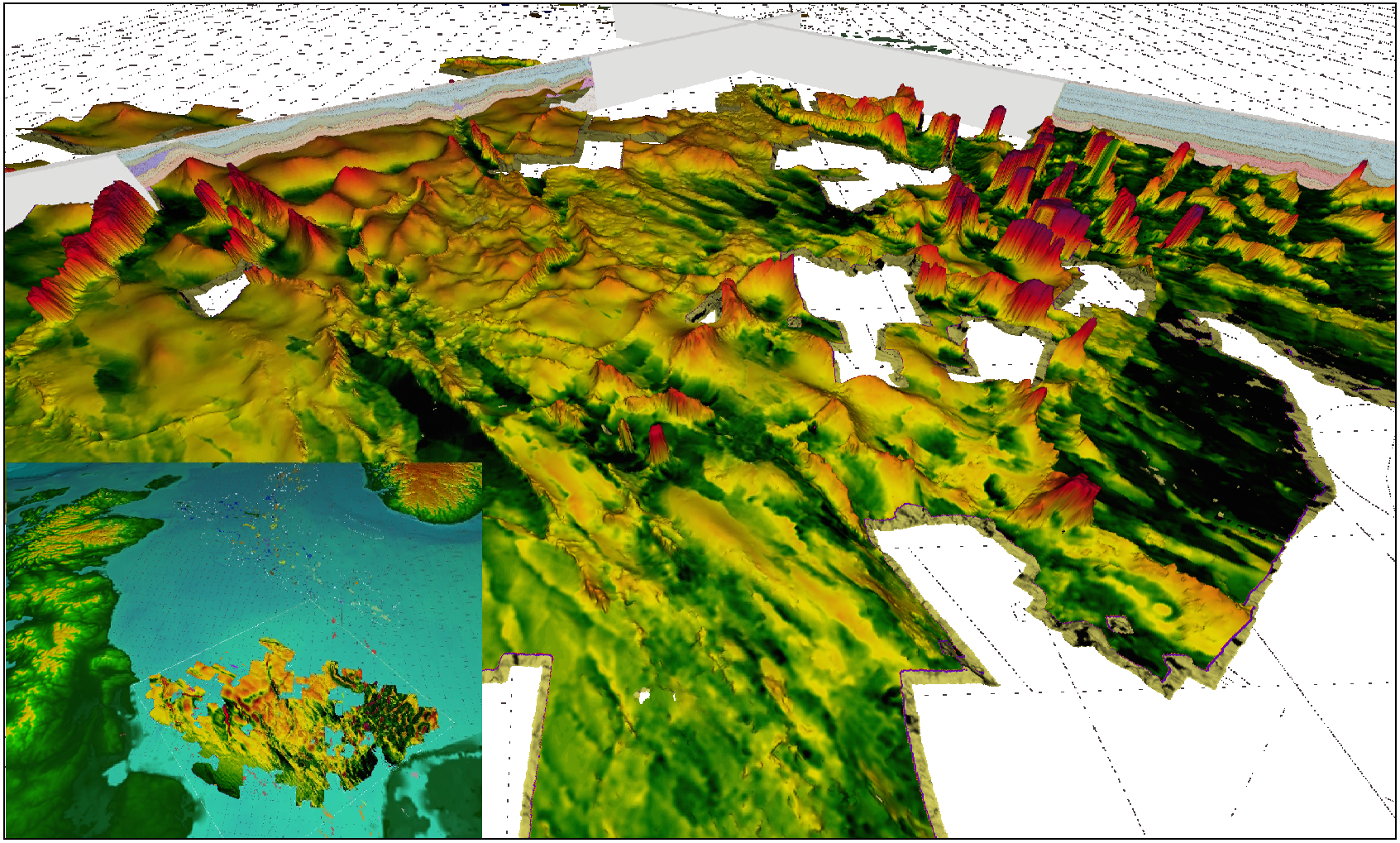

**Figure 1: 3D view from south of the Southern North Sea (SNS) 3D seismic MegaSurvey showing top salt two-way time (twt) structure of the northern portion of the Southern Permian Basin present in the Netherlands and UK Continental Shelf (UKCS). The twt structure horizon is draped with the isochron of salt thickness. Dark green colours indicate thin to absent, grading through 'hotter' yellow-red-purple colours to maximum preserved thickness approaching 2 seconds twt, approximately 1500m. Image shows dominance of salt walls many of which are continuous features over > 40 km, yet are rarely wider than 2-5 km. Scale is indicated by block outlines which are 22 km x 15 km in the UKCS ; Location of 3D seismic MegaSurvey in Southern North Sea is shown in inset map; SNS MegaSurvey is approximately 270km x 250km with a**

The drift phase continued throughout the Late Cretaceous to Tertiary with a series of turbidites deposited in a deep water environment. Sand-rich turbidites with thicknesses of 30m to 100m occur over a large area, 6,000km$^2$. These massive, slightly friable sands, with net-to-gross ratios up to 95 percent, typical porosities greater than 30% and permeabilities reaching 5.4 Darcy are the most important reservoir facies offshore Brazil.

### Data

The PGS Campos 3D seismic MegaSurvey dataset is located approximately 200 km offshore Brazil, due east of Rio in waters ranging from 500m to over 3000m depth (Fig. 2) . The dataset is composed of 7 modern-vintage 3D surveys re-binned on a north-south grid approximately 250 km long by 160 km east-west, forming a contiguous live trace area of approximately 18,000 km$^2$. The MegaSurvey is calibrated by log data and tops for over 160 wells available from the Brazilian Agência Nacional do Petróleo (ANP) Banco de Dados E&P (BDEP) Exploration and Production Databank, re-interpreted into a consistent regional tectono-stratigraphic framework. The 3D MegaSurvey is integrated more regionally to a grid of super-regional 2D lines, up to 400 km long, providing seismic ties onto key wells on the shelf area to the west and the adjacent areas north and south of the contiguous 3D coverage.

## Interpreted Salt Structures

This deepwater sector of the Campos Basin is in the 'diapir province' which here is dominated by large salt walls, many extending for in excess of 40 km (Fig. 2). Three main trends of diapiric structure can be distinguished in this project area: a trend of persistent south south-east striking high-relief walls with approximately 20km spacing; a subsidiary trend of shorter north-south trending salt walls with 15-20km spacing and a series of laterally-extensive east-west salt walls with a wider 30-40km spacing that cut and offset the other two trends, indicating that this is the latest orientation to be active. Within this 3D MegaSurvey dataset the salt structures divide into two distinctive provinces separated by a prominent south south-east striking wall feature transecting the middle of this portion of the basin. To the north, the northwest-southeast trend of elongate walls dominates. Typically, these walls have high relief up to almost 4,000 m in places, with most restricted to an average width of 2km, but a group of broader high relief walls occurs in the east that have widths of 8-10km. This orientation of salt structures is offset by the east-west trend and linked by the north-south trend. To the south, the later east-west trending salt walls dominate, with a prominent northeast-striking wall extending for over 50 km in the southeast of the dataset. These and the north-south trending structures are offset by the later east-west orientated structures.

In the north of the dataset, abundant, small-scale NNE-striking faults and folds are observed in the top surface of the salt layer as a result of downward creep caused by regional oceanward tilting. In the southeast of the area, in an region of broad, low relief pillow-style salt geometry, persistent crenulations are observed in the top surface of the salt with regular, repeated short wavelength folding that arcs around from an eastward movement direction to a southward spreading direction. These crenulations are offset by a trend of west-east lineaments, which evidently post-date the crenulation features.

Salt welds and penetrating faults, seen as possible conduits for hydrocarbon migration from kitchen areas of mature source rocks are more prevalent in the north and east where diapirism occurs on a larger scale. Distinctive salt withdrawal synclines with concentric fault systems are observed in sediments overlying areas of lateral salt migration and radial systems of faults are identified in Tertiary sequences recording the extension above active diapiric structures.

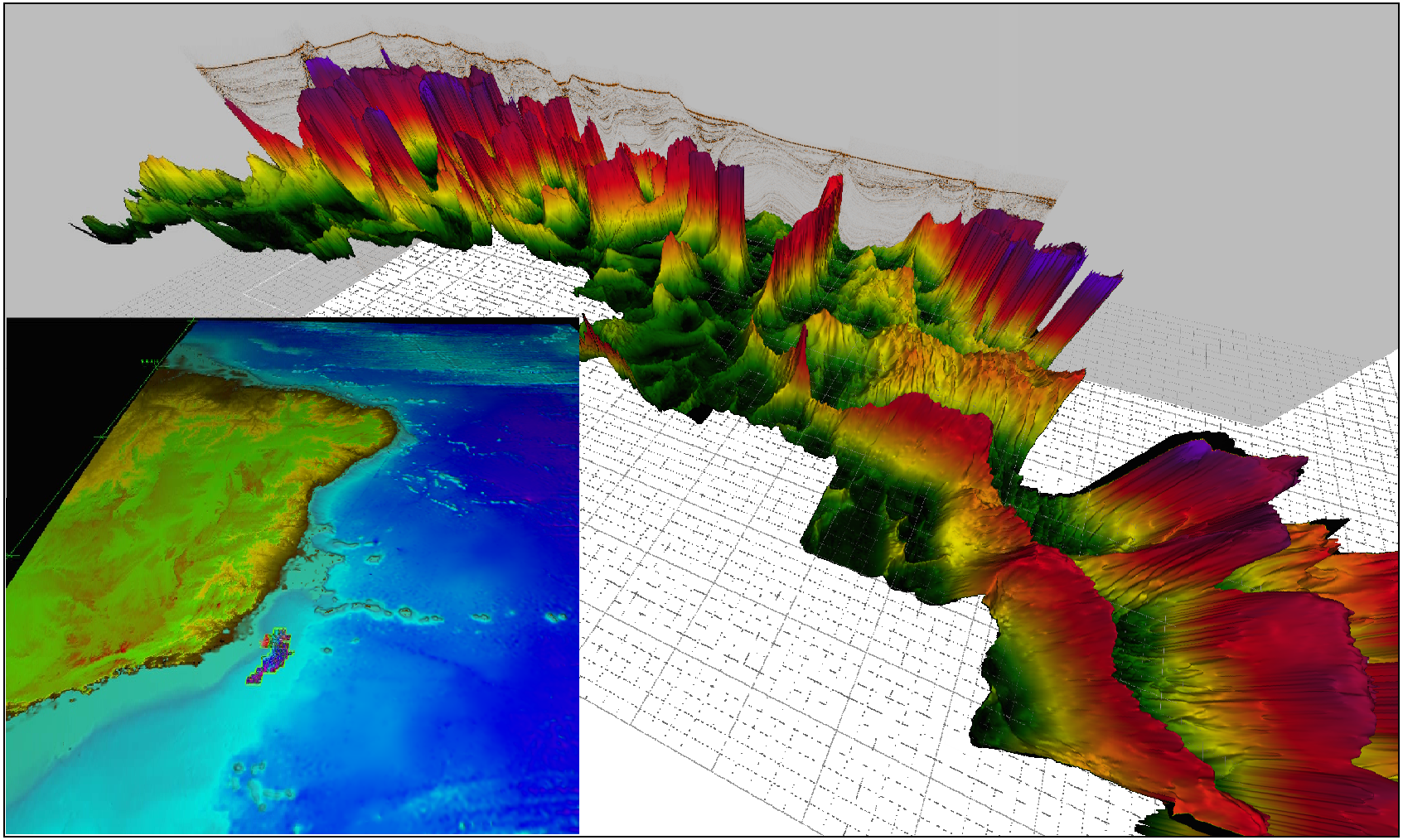

**Figure 2: 3D view from southwest of deepwater Campos Basin 3D seismic MegaSurvey showing top salt two-way time (twt) structure draped with isochron of salt thickness. Dark green colours indicate areas where salt is thin to absent, grading through 'hotter' yellow-red-purple colours to a maximum thickness of over 3 seconds twt, equating to approximately 2250m. The image shows the dominance of salt walls, many of which are continuous features over 40 km yet are rarely wider than 2-5 km. Scale is indicated by background grids: small grid cells are 2km x 2km; large grid cells are 10km x 10km; The location of the 3D seismic MegaSurvey in deepwater Campos Basin is shown in inset map; The Campos Basin MegaSurvey is approximately 250km x 160km, forming a contiguous live trace area of approximately 18,000 km$^2$**

## Lower Congo Basin, Deepwater Angola

### Geology

An initial rifting phase is recognised along the West Africa margin with extensional faulting of the basement, subsidence and associated volcanics pre-dating Atlantic separation. During the Neocomian to Barremian, locally-derived continental conglomerates and alluvial fan/fan-delta sands of the Lucula formation were developed at the faulted margins of a complex lake system that evolved in rift graben, with up to 1400m of organic rich lacustrine mudstones deposited in deep, anoxic rift lakes with water depths up to 650m (Bucomazi formation). Coquina carbonates and sandy carbonate sediments were deposited at the lake margins or on basement highs (Toca formation), reaching thicknesses of up to 300m.

A transition to regional thermal subsidence during the Early Aptian created a relatively undeformed sag basin. Following a relative lake level fall, the exposed Toca/Upper Bucomazi formations were truncated by erosion, creating the Chela unconformity regionally, above which a large prograding, transgressive deltaic sequence, the Chela formation, was deposited., this interval, which reaches a thickness of 300m in total, consists of fluvial sandstones and conglomerates (a lag deposit) at the base grading upwards, with increasing marine affinity into lagoonal facies (siltstones and shales) as lake water salinity increased due to an increasingly dry and humid climate. By the mid-Aptian extension of the lower crust and mantle upwelling caused regional uplift of the basin margin, creating a regionally extensive, shallow-water, restricted marine salt basin environment. Climate was very dry with low humidity (<35%) and limited clastic delivery to the basin, with intermittent inundation and evaporation of marine water led to the deposition of Loeme salt formation evaporites up to 2000 m thick. This salt acts as a decollement zone for post-salt growth-fault structures.

The start of ocean spreading in the Late Aptian marks the start of the drift phase of margin development, with thermal subsidence causing the continental margin to tilt basinward, resulting in and a major marine transgression. Extensive, shallow marine, platform carbonates (dolomite), developed, interbedded with clastic fan deltas which deposited along the basin margin (Binga formation).

In the Early Albian, fine-grained, neritic carbonate shoals with high energy algal calcarenites and oolitic limestones were deposited on bathymetric highs produced by salt diapirs and swells in the basin margin (Pinda-Catumbela formation). Albian deposition was terminated by continued thermal subsidence and sea level rise. This carbonate sequence started to slide basinwards on top of the salt shortly after deposition and created highly extended geometries with isolated, rotated fault-blocks, known as ‘rafts’ separated by large fault plane gaps. This gravity-driven sliding on a regional decollement surface at the base of the salt created the primary influence on later basin fill and hence salt movement.

Epi-orogenic uplift of southwest Africa in the Late Cretaceous resulted in strong basinward tilting of the Angolan margin. This combined with continued thermal collapse resulted in a widespread marine transgression with gradually deepening marine conditions into which sand rich deepwater turbidites were locally deposited (Iabe formation).

The drift phase continued throughout the Tertiary. Rapid subsidence in response to increased siliciclastic input from the Congo Fan delta led to the deposition of extensive turbidite channel systems within a thick clastic wedge building out from shelf to deepwater. Updip erosional truncations occurred as a result of margin uplift and basinward tilting, whilst down dip rafting and salt tectonics continued in response to sediment loading and gravitational sliding.

### Data

The PGS Angola Phase 1 3D MegaSurvey dataset is located approximately 150 km west of Luanda (Fig. 3) in waters ranging from 500 to 3000 m. The dataset is composed of 9 modern-vintage 3D surveys re-binned on a north-south grid approximately 190 km long by 160 km east-west, and is calibrated by all the released wells available in the area.

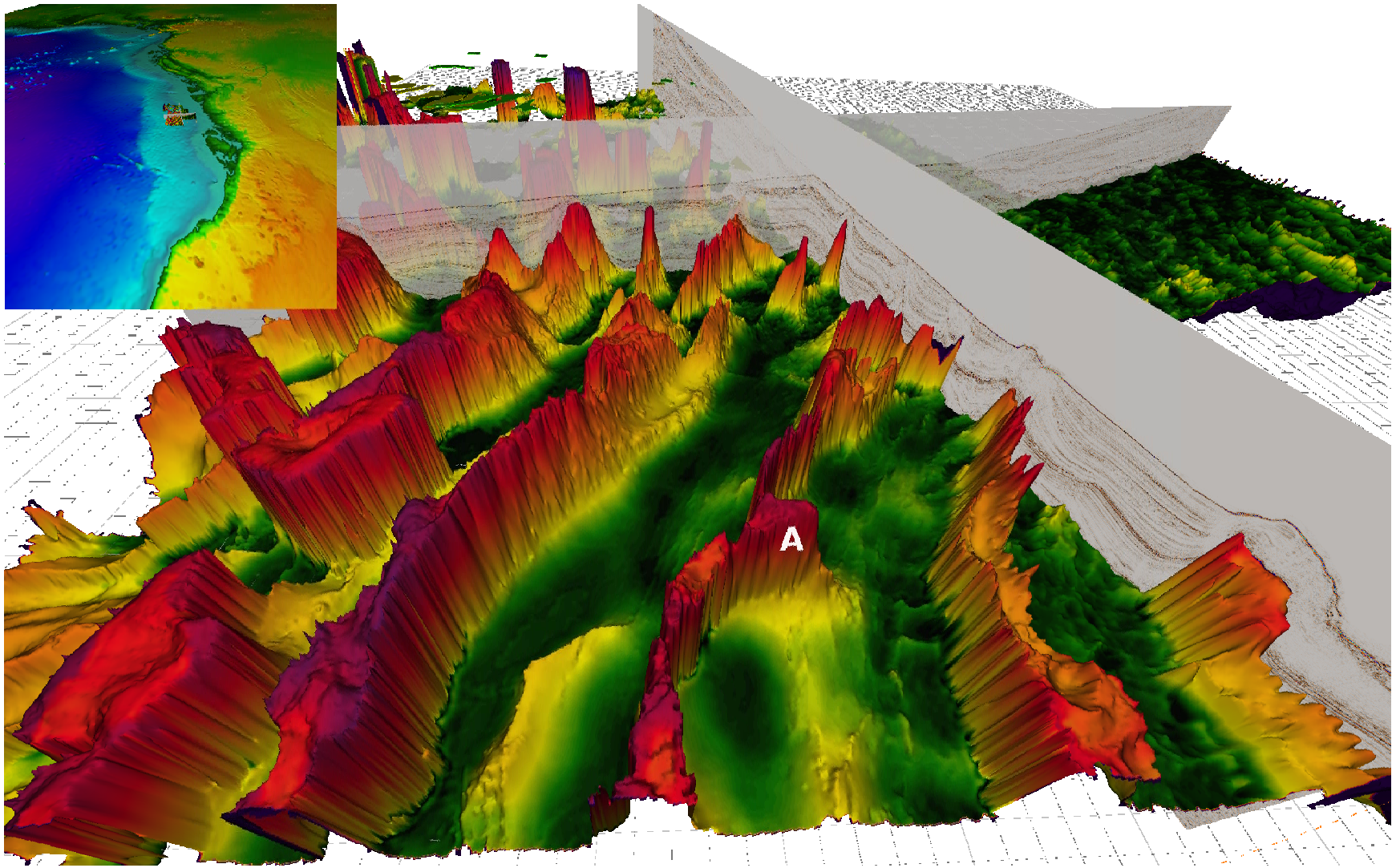


**Figure 3: Salt Structures of the Lower Congo Basin, deepwater Angola**

### Interpreted salt structures

Salt walls predominate the salt geometries in the Lower Congo Basin, Angola. Almost 40 discrete salt bodies have been indentified, the majority of which are continuous salt walls with maximum length of 64 km. They typically range from 2 to 5 km in width. These salt walls range from 1000 metres to 2000 metres in height and on average their height increases basinwards toward the west, with the maximum diapir height being almost 2.5km.

Three main orientations of salt structures are observed in the 3D MegaSurvey data area. A prominent southwest-striking trend of tall, narrow, elongate salt walls is dominant in the south of the area.

In the northern portion of the area a trend of walls striking southeast dominate. A number of wall structures are seen to be offset by a later east-west trend. Complex geometries are formed where these trends intersect.

In cross-section and from isochron maps, salt withdrawal can be seen to have commenced early creating development of locally thick sedimentary depocentres in sequences from the Late Cretaceous onwards. The location of these depocentres can be seen switching basinward and then landward through time.

## Complex Multi-Phase Geometries

In addition to the three main classes of salt geometries of walls, stocks and pillows many more complex geometries result from the interaction of several phases of salt activation with different orientations and axes of compression. By examining in detail the geometric relationships in terms of thickening, thinning and termination of stratigraphic units around and above salt structures the timing of episodes of active salt movement can be interpreted. The distribution of interpreted turbidite facies within deepwater units also provides important clues as to which salt bodies were positive bathymetric features at the time of deposition. This enables the systematic mapping of the salt trends which were active at any particular period. Combined with the cross-sectional geometries of these features, the regional stress orientations at the time can be inferred.

An example of this approach is illustrated (Fig. 4). An unusual T-shaped diapiric geometry is seen part of the way along one of several northeast-striking salt walls in the southeast of the MegaSurvey dataset. By examining the facies distribution of a turbidite system in the Lower Miocene, one can deduce which orientations of salt structure were active during the Early Miocene. Using an RMS attribute map of the Lower Miocene draped on the base Miocene (top Oligocene) surface, a turbidite system can be seen entering from the hinterland area to the southeast and transecting two southwest-northeast trending salt walls in the top left quadrant of the image. These walls would therefore appear not to have been actively up-building in the Early Miocene. The channel is then seen to deflect southwards through approximately ninety degrees, suggesting that this portion of the southwest-striking wall in the centre of the view was a positive bathymetric feature at this time. The channel then trends, un-deflected, across the T-piece of the central salt feature, suggesting that this orthogonal limb protruding from the wall is a later feature developed when the regional stress fields were oriented northwest-southeast. The channel continues for a further 20km in what is interpreted to be the basin floor synclinal axis of the salt wall withdrawal basin. Finally, the channel is again deflected sharply westwards across the salt wall to form a terminal lobe on the western side of the salt wall. Apparently this portion of the salt wall was not such a positive barrier at this time.

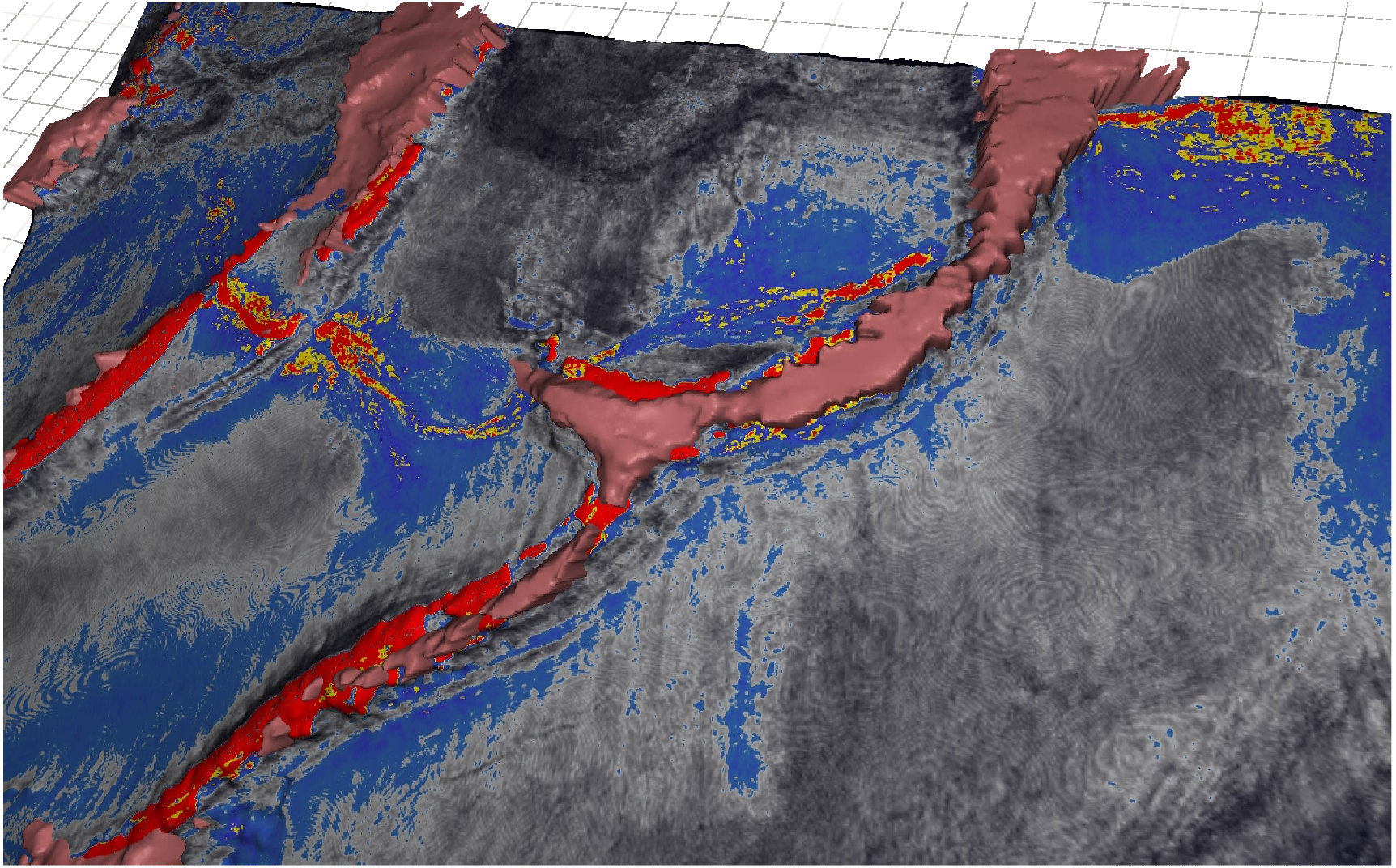

**Figure 4: Timing of salt re-activation in Lower Congo Basin, Angola**

## Conclusions

3D seismic data is acknowledged to have significantly increased both drilling success rate and our understanding of the subsurface geology within localised areas of a basin by revealing detailed 3D relationships between structural geometries and stratigraphy which could not be discerned from a grid of 2D cross-sections. In recent years, the computational power and expertise have developed to merge discrete interlacing and overlapping 3D surveys into a single contiguous 3D seismic dataset covering entire basin systems. we have examined such 'MegaSurveys' over basins on both margins of the South Atlantic and from the North Sea with particular reference to the geometries of salt structures developed and their influence over sag-phase sediment deposition.

The importance of salt movement for hydrocarbon trap formation and as a control on reservoir distribution is well documented, yet drilling results frequently indicate that the dimensions; i.e., the thickness, height and lateral extent of the salt, is often over- or under-estimated. These parameters from several independent and widely distributed basins, give a valuable calibration for examining salt features in other basins.

## References

None cited.

BACK

# Variation in Crustal Extension and its Implication for Hydrocarbon Habitat in the Dakar – Rufisque Area, Offshore Senegal.

**Steven Bottomley**
Premier Oil plc,
23, Lower Belgrave Street
London SW1W 0NR
United Kingdom
e-mail: SBottomley@premier-oil.com

**Pete Jeans**
PJ Exploration Ltd.
3, The Paddocks
Whiteshoots Hill
Bourton on the Water GL54 2LS
United Kingdom
e-mail: pete@pj-exploration.com

## ABSTRACT

This poster postulates that the variation in post-rift hydrocarbon habitat in the Dakar–Rufisque area of offshore Senegal is primarily controlled by the variation in syn-rift crustal extension between adjacent sectors of the continental margin.

It is postulated that, during rifting of the Central Atlantic in the Triassic – Early Jurassic, the sector of the Senegal margin between the Rufisque and Cayar Fracture Zones (the "Dakar Compartment") suffered a higher degree of crustal extension than the sectors to the north and south. It is expected that the opposite situation will occur on the conjugate margin, with a "low extension" segment aligning with the Dakar Compartment.

As a result, when post-rift sediments loaded the more highly extended crust in Albian–Late Cretaceous times, the Dakar Compartment subsided more rapidly, and, accumulated a greater thickness of sediment. In addition, this compartment was also intruded by basic igneous rocks, reflecting the relative ease of magmatic invasion of the extended crust and the "leaky" nature of the bounding transforms.

In Santonian times, north-south directed compression caused uplift of the rigid, less extended Rufisque High to the south of the Rufisque transform. Subsequently, the Rufisque High subsided little during Senonian–Palaeogene times, in contrast to the Dakar Compartment to the north.

In the Oligo–Miocene, the Dakar-Cayar-Rufisque area suffered a regional hypabyssal–volcanic igneous event, with pronounced intrusion into the shallow section in the Dakar-Cayar area. This resulted in the thermally-driven inversion of the pre-existing Late Cretaceous and Palaeogene basin, which has resulted in the present topographic expression of the Dakar Peninsula. Well data from the Rufisque High indicates anomalously high temperatures (77°C at 1005 m below derrick floor in Rufisque-1), but the wells did not encounter any igneous intrusives, implying a more deep-seated magmatic emplacement.

Several basin-scale observations are postulated to be directly related to the syn-rift compartmentalisation of the margin and the more highly extended nature of the crust in the Dakar Compartment:-

- Post-rift passive continental margin depositional systems and facies reflect the additional accommodation space. This is most clearly demonstrated by the lateral offset, across the Rufisque transform, of the Late Jurassic-Early Cretaceous carbonate bank sequence, coeval to that of the Scotian Shelf

- Late Cretaceous source rock bearing sequences are thicker within the Dakar Compartment as a result of the greater accommodation space created over the thinned crust at the time of deposition. The authors do not have sufficient data to conclude if this thickening is at the expense of quality (dilution)
- Outboard of the carbonate margin, in the Dakar compartment, source rocks are thermally over-mature (within the gas generation window) due to their greater depth of burial and higher heat flow from the extended crust. The same source rocks in the compartments to the north and south of the Dakar Compartment are prognosed to be thinner, and geochemical modeling suggests significantly lower maturity levels.
- The present Dakar Peninsula is the topographic expression of an east-west, thermally driven, Neogene inversion of the Dakar Compartment. The inversion is clearly expressed on offshore seismic data and is accomplished through the contrast in rigidity between the thinner crust under the Dakar Compartment in contrast to the adjacent, more rigid (thicker), crust under the Rufisque area.
- The Cayar Dome, an igneous edifice of presumed Tertiary age, is located on the northern accommodation zone of the Dakar Compartment, as are the Cape Verde Islands further offshore, illustrating its importance as a crustal scale feature.
- Neogene inversion of the Dakar Peninsula may have resulted in avulsion of drainage of the Senegal River from the Dakar area (where thick Late Cretaceous–Early Tertiary deltaic sands are exposed) northward to its present position.

Syn-rift compartmentalisation of the shelf to deep water sectors of the Senegal margin is postulated to have had a profound effect on the petroleum geology, by influencing:

- reservoir fairways and facies distribution within the post-rift section
- diagenetic alteration of reservoirs (primarily by differential burial and igneous intrusion)
- thickness of source rocks (variation in accommodation space)
- heat flow, and hence, maturity of source sequences

Recognition of these factors can enable the prediction of optimal areas for hydrocarbon exploration through an integrated model of source rock distribution, timing of maturation, expulsion pathways and accumulation in favourable reservoir facies, and improve the prediction of hydrocarbon phase. The distribution of oil and gas shows within the post-rift section in Senegal reflects these controls.

**BACK**

# Tectono-Stratigraphic Evolution of Salt Structures and Depocentre Migration in the Abenaki Subbasin and its Deepwater Extension, Offshore Nova Scotia

**Clarke Campbell**
**Cody MacDonald**
**Jonathan Cribb**
**Mladen Nedimovic**
Salt Dynamics Group
Department of Earth Sciences
Dalhousie University
Halifax, Nova Scotia, B3J 3J5
Canada
e-mail: ctcampbe@dal.ca

**Jürgen Adam**
Department of Geology
Royal Holloway University of London
Egham, Surrey
United Kingdom

**Louden, Keith**
Department of Oceanography
Dalhousie University
Halifax, Nova Scotia, B3J 3J5
Canada

**Kreszek, Csaba**
Chevron Norge AS
Karenslyst Alle 2, P.O. Box 97
Sköyen, 0212 Oslo
Norway

## ABSTRACT

Despite extensive exploration activity on the Scotian Margin, the latest round of drilling has yielded disappointing results. An in-depth analysis of the interplay between salt tectonic processes and sediment input is required to better understand the regional tectono-stratigraphic framework of the Scotian Basin and its individual sub-basins.

We are using scaled analogue experiments to simulate coupled salt tectonic processes and depocentre migration in the Abenaki sub-basin and its deepwater extension. Experiments simulate the salt tectonics history from the early post-rift stage to the allochthonous salt nappe formation on the modern margin. The experiments are constrained by sedimentation patterns and rates, original salt basin thickness, and basement morphology deduced from the GXT NovaSPAN survey and public-domain 2D seismic reflection data.

Seismic interpretation results of the Abenaki subbasin show a complex salt basement morphology, which includes a mid-basin high implying variable salt thickness in the early post-rift salt basin. Experiment results suggest that the complex basement morphology and variable salt thickness had a strong effect on the initial salt mobilization and early post-rift depocentres, and that it controlled the pattern of sediment transport from the Jurassic to the Cretaceous. During the Cretaceous, seaward salt extrusion in the deepwater slope of the Abenaki sub-basin created an allochthonous salt nappe system with new mini-basins developing on this secondary source level. Mechanically constrained salt tectonic concepts and seismic interpretation templates deduced from the experiments will aid further seismic interpretation of the Abenaki sub-basin.

These concepts will also give insight into how basement morphology influenced salt structure development, and how sedimentation rates and patterns affect depositional styles. This integrated approach will contribute to our understanding on the evolution of the Abenaki sub-basin and how its evolution relates to the timing of adjacent sub-basins on the Scotian Margin.

BACK

# Analogue Modelling of Salt Tectonic Processes and Depocentre Migration on the Shelf and Deepwater Slope, Western Laurentian Subbasin

**Jonathan Cribb**
**Clarke Campbell**
**Cody MacDonald**
**Mladen Nedimovic**
**Djordje Grujic**
Salt Dynamics Group
Department of Earth Sciences
Dalhousie University
Halifax, Nova Scotia, B3J 3J5
Canada
e-mail: jonathan.cribb@dal.ca

**Jürgen Adam**
Department of Geology
Royal Holloway University of London
Egham, Surrey
United Kingdom

**Keith Louden**
Department of Oceanography
Dalhousie University
Halifax, Nova Scotia, B3J 3J5
Canada

**Csaba Kreszek**
Chevron Norge AS
Karenslyst Alle 2, P.O. Box 97
Sköyen, 0212 Oslo
Norway

## ABSTRACT

The Scotian Basin is situated on the Atlantic continental margin offshore Nova Scotia and is composed of a series of interconnected Mesozoic-Cenozoic sub-basins resulting from the rifting of North America from Africa. Thick deposits of late syn-rift Argo Salt coupled with complex basement morphologies and varied sedimentation patterns along the margin have resulted in a complex and laterally variable basin evolution. Unsatisfactory results from the recent round of hydrocarbon exploration in the deepwater slope demonstrate that a better understanding is required about the link between early post-rift salt mobilization and late post-rift formation of canopies and allochthonous salt nappes, and their relation to depocentre migration. We are using scaled analogue experiments comprised of sand and silicone putty to gain such an understanding by simulating basin evolution and salt tectonic processes constrained by seismic data. First-order model parameters of the western Laurentian subbasin analogue experiment including sedimentation rates and patterns, basement morphologies, and initial salt thickness were constrained by GXT NovaSPAN and public-domain seismic data.

Experiment results confirmed appropriate timing and speculation of the evolution of this region with diverse structural processes including; (1) numerous passive downbuilding events throughout basin evolution, (2) extension focused in the Cretaceous forming a ramp flat geometry, and (3) minimal contraction in the upper Cretaceous. The next phase of this project includes modeling the interaction of sediment progradation and salt tectonics between the inter-connected Laurentian, Abenaki and Sable subbasins. This experiment will evaluate the role of margin parallel sediment transport from the northeast via the Laurentian Channel during the early post rift stage of basin evolution and salt tectonics in the northeast Scotian Margin. Insight from both models, when compared to regional seismic data, will contribute to our understanding of the structural evolution of the western Laurentian subbasin and determine the influence of margin parallel sedimentation.

BACK

# Mapping Post Rift Sills along the Newfoundland Passive Margin

**Sharon Deemer**
**Charles Hurich**
**Jeremy Hall**
Memorial University of Newfoundland
Dept. of Earth Sciences
St. John's NL, A1B 3X5
Canada
e-mail: sdeemer@esd.mun.ca

## ABSTRACT

A high amplitude reflector package at the base of the sedimentary sequence in the Newfoundland Basin sampled during ODP Leg 210 results from thin diabase sills. Chemical analyses and dating suggest that the sills were emplaced in two separate post-rift thermal events, probably related to hot spot activity. Seismic data tied to the borehole reveal that the sills are widespread and continuous over hundreds of square kilometers. Spectral decomposition is used here on high quality seismic profiles (migrated near trace gathers) in order to map the peak energy frequency variation of the U reflections throughout the basin, which is then related to thickness of sills.

The analysis is complicated due to limited signal bandwidth and the complexity of the sill geometries but trends are apparent throughout the basin. The lowest frequencies (thickest sills) are associated with the central basin, particularly towards the south. Higher frequencies (thinner sill) are associated with the upper sill in the north but the upper sill in the south central basin is low frequency. Based on sill thickness variations, the source of magma is proposed to be in the south central basin close to the present day Newfoundland Seamounts.

BACK

# A Regional Transect Across the South Newfoundland Basin, a Nonvolcanic Margin

**Sharon Deemer**
**Jeremy Hall**
Memorial University of Newfoundland
Dept. of Earth Sciences
St. John's NL, A1B 3X5
Canada
e-mail: sdeemer@esd.mun.ca

**Krista Solvason**
Nexen, Inc.
801-7th Avenue S.W.
Calgary, AB, T2P 3P7
Canada

**Helen Lau**
Cambridge University
Bullard Laboratories
Madingley Road
Cambridge, CB3 0EZ
United Kingdom

**Keith Louden**
Department of Oceanography
Dalhousie University
Halifax, NS, B3H 4J1
Canada

**Shiri Srivastava**
Geological Survey of Canada-Atlantic
P.O. Box 1006
Dartmouth, NS, B2Y 4A2
Canada

**Jean-Claude Sibuet**
Ifremer Centre de Brest
Département des Géosciences Marines
B.P. 70
29280 Plouzané
France

## ABSTRACT

New seismic reflection data from the Grand Banks of Newfoundland and the Newfoundland Basin add to the knowledge of composition, structure and history of this nonvolcanic margin. Two parallel profiles over the shelf platform image deep crustal fabric representing Precambrian or possibly Appalachian deformation as well as Mesozoic extension. Progressively more intense extension of continental crust is imaged oceanward below the continental slope without the highly reflective detachments frequently seen on profiles off Galicia.

A landward-dipping event 'L' is imaged sporadically and appears to be analogous to a similar event on the approximately conjugate Iberian IAM9 profile. The transition zone is probably unroofed serpentinized mantle as interpreted off the Iberian margin although there appears to be a difference in the character of ridge development and reflectivity. The distinctive 'U' reflection in the Newfoundland Basin is highly regular and continuous except where interrupted by basement highs. 'U' is also seen to have a major impact on the ability to image underlying basement. A full transect from completely unextended continental crust to oceanic crust has provided two estimates of extension and the pre-rifting location of the present continental edge; 85 km based on faulting and 120 km based on crustal thickness.

BACK

# U.S. East Coast: Continental Margin Evaluation with New Tools, Data and Techniques

**William Dickson**
Dickson International Geosciences (DIGs)
10260 Westheimer Rd, Suite 320
Houston, TX 77042-3160
United States
e-mail: billd@hal-pc.org

**Mark Odegard**
Grizzly Geosciences, Inc.
14019 SW Freeway, Suite 301-735
Sugar Land, TX 77478
United States

**Paul J. Post**
Minerals Management Service
1201 Elmwood Park Blvd.
New Orleans, LA 70123
United States

## ABSTRACT

Exploration discussions of the Central Atlantic margins typically omit the U.S. East Coast Continental Margin (ECUS) which has been dormant, without drilling since 1984, despite on-going E&P activities to the north (offshore Nova Scotia), south (offshore northern Cuba), and on the conjugate African margin (Morocco to Mauritania). Shell has documented its exploration success with new ideas and new technology. After a more than twenty year hiatus, we too have new data, technology and ideas along the ECUS, suggesting that timing is favourable for a thorough review.

Our data compilation began with advanced coverage of public domain bathymetry, gravity and magnetic data, all re-leveled, cross-correlated and merged. Our Central Atlantic data set includes five million-odd line-kms each of gravity and magnetic profiles plus a half-million data points. Each data set was carefully merged to regional backgrounds derived from multiple satellites. Stunning imagery of bathymetry, gravity, magnetic and auxiliary data were generated from the final 4 km (super-regional) and 1 km (basin-level) grids. Including multiple data attributes that are somewhat area-dependent, we generated about 40 images, each with specific and general interpretation value.

Evolution of passive margins and adjacent oceanic crust has been studied extensively since the mid-1980's, with continued academic work along the ECUS. The Minerals Management Service is conducting a re-analysis of pre-1985 drilling and seismic data augmenting the older ECUS literature. We make initial comparisons between published interpretations and our new imagery, presenting adjustments, revisions, extrapolations and some speculation. While the dominant structural features are largely unchanged, they are better delineated. This includes evidence of more subtle correlations with published depictions of play-defining features such as areas of salt tectonics and carbonate bank edges. The interaction of these features with plate tectonic elements is also better defined. Each of these observations is illustrated with specific imagery on which feature changes and extensions are highlighted.

BACK

# The NovaSPAN Project: Deep Imaging of an Enigmatic Continental Margin

**Menno G. Dinkelman**
ION Geophysical
2105 CityWest Boulevard, Suite 900
Houston, Texas, 77042-3847
United States
e-mail: menno.dinkelman@iongeo.com

**John W. Shimeld**
Geological Survey of Canada-Atlantic)
P.O. Box 1006
Dartmouth, Nova Scotia, B2Y4A2
Canada

## ABSTRACT

The 2003 NovaSPAN data set comprises over 3400 km of 2-D regional reconnaissance seismic data designed to image down to the base of the crust using large guns (>4200 in³) with a 9 km long cable and 18-second record lengths. The data has undergone Prestack Time Migration (PSTM) as well as Prestack Depth Migration (PSDM - to 40 km).

The primary objective of the NovaSPAN survey was to deliver critical insight into the geologic evolution and basin architecture of the Scotian Margin, and the resultant temporal and spatial history of regional petroleum systems.

The NovaSPAN survey provides a useful regional structural and stratigraphic framework. An initial fast-track seismic stratigraphic interpretation, largely on the PSTM data, has yielded the following preliminary results:

The discovery of rotated crustal blocks in front of the margin provides evidence of significant changes across this zone along the margin, suggestive of transtension along a transform fault zone. If true, there may be important relationships within a zone of comparatively high basement underlying the slope to shifts of major basin elements such as the basement hinge zone and the position of allochthonous salt basins.

The geometry and nature of syn-rift basins along portions of the LaHave Platform may prove important for understanding how the rifting occurred, while the presence of salt within some of the basins might affect evaluation of overlying prospects in the Abenaki carbonate bank.

The long transects across the upper rise and lower slope allow for detailed subdivision of the seismic stratigraphy which in turn aids correlation of units through areas of complex deformation.

A remarkably high rate of sedimentation during the Late Jurassic is manifested by an extensive synkinematic wedge occurring above a salt detachment system in the eastern part of the survey area toward the Laurentian Channel. The implication of this feature is that the southern limit of allochthonous salt deposition lies roughly 100 km further north than previous workers have assumed. More recent work underscores the enigmatic nature of the deeply buried basement structure and crustal nature.

The GXT SPAN™ surveys provide sufficient aperture and illumination, when combined with the right imaging tools, to reveal how complex basin structuring is controlled by Tertiary, Mesozoic and older deformational events and early basin tectonics. We suggest that these data sets, in conjunction with other detailed “prospect-level” surveys, will aid industry in defining petroleum systems and new plays, especially at great depth and in deeper waters and can considerably reduce basin exploration risk.

The NovaSPAN data set is now at the core of a regional re-interpretation effort of the Scotian Margin by the Nova Scotia Department of Energy in conjunction with the GSC and the Departments of Geology of Dalhousie and St Mary’s universities to build a new tectono-stratigraphic framework and a post-mortem of recent deep water drilling failures.

BACK

# The Last 100 Million Years on the Scotian Margin, Offshore Eastern Canada: an Event Stratigraphic Scheme Emphasizing Biostratigraphy

**Rob Fensome**
**Graham Williams**
**Frank Thomas**
Geological Survey of Canada-Atlantic
P.O. Box 1006
Dartmouth, Nova Scotia, B2Y 4A2
Canada
e-mail: rfensome@nrcan.gc.ca

**Gunilla Gard**
5915 Mesa Brook Lane
Houston, TX, 77041
United States

**Andrew MacRae**
Dept. of Geology
Saint Mary's University
Halifax, Nova Scotia, B3H 3C3
Canada

**Flavia Fiorini**
Smithsonian Tropical Research Institute
Ancon, Panama

**Grant D. Wach**
Dept. of Earth Sciences\
Dalhousie University
Halifax, Nova Scotia, B3H 3J5
Canada

## ABSTRACT

In the 1970s and 1980s, the principle biostratigraphic groups used for dating the Late Cretaceous-Cenozoic interval were foraminifera, nannofossils and dinoflagellate cysts (dinocysts), although in recent years the last-named group has been the most intensively used. No concerted efforts were made in the early days to marry results from the different microfossil groups, and this was sometimes reflected in diverse age schemes for individual exploration wells. The present study is based mainly on studies of material from seven exploration wells, selected to provide a composite section: Demascota G-32, Hesper I-52, Onondaga E-84, Sauk A-57 and Shelburne G-29 (all on the shallow water shelf), and Shubenacadie H-100 and Wenonah J-75 on the deep water slope. The Late Cretaceous-Cenozoic interval from each of these wells was analyzed for dinocysts and pollen and spores and, in some of the wells, for calcareous nannofossils and planktonic and benthic foraminifera. The integration of data from different sub-disciplines, especially the calibration of dinocyst events with nannofossil events and thus indirectly with the largely deep-sea-based magnetostratigraphic timescale, has made possible for the first time a detailed sequence of biostratigraphic events.

BACK

# Low-T Thermochronology Provides New Insights in the Mesozoic to Present

**Badr Ghorbal**
**Giovanni Bertotti**
**Paul Andriessen**
VU University-Isotope Geochemistry
De Boelelaan 1085
Amsterdam, 1081 HV
Netherlands
e-mail: badr.ghorbal@falw.vu.nl

**Jurgen Foeken**
**Fin Stuart**
Scottish Universities Environmental Research Centre
East Kilbride, Scotland, G75 0QF
United Kingdom

## ABSTRACT

To constrain upward and downward vertical movements in NW Africa we have sampled for low-T thermochronology a 500km long transect from the Mediterranean coast to the Anti Atlas of Morocco. The analysis of this large data set has provided major surprises requiring a reconsideration of generally accepted ideas.

The data we have produced document an Early to Middle Jurassic stage of subsidence and of Late Jurassic to Early Cretaceous exhumation affecting a large elongated region stretching from the Moroccan Meseta to the Anti Atlas. These domains are typically considered as stable during the same time span. Late Jurassic to Early Cretaceous exhumation caused the erosion of a large amount of terrigenous sediments transported offshore and deposited in the otherwise monotonous and fine-grained succession of the Moroccan Atlantic passive continental margin.

Alpine deformations began in the Late Cretaceous and continue until present. They were initially associated with the development of large scale, WNW-ESE trending folds and then with localization of shortening and exhumation in the Atlas system.

BACK

# Continental Margin Development of the Equatorial Atlantic Gateway: Suriname, South America

**Shawn Goss**
Department of Earth Sciences
Dalhousie University
Halifax, Nova Scotia, B3H 4J1
Canada
e-mail: sgoss@dal.ca

**David Mosher**
Geological Survey of Canada (Atlantic)
1 Challenger Drive. P.O. Box 1006
Dartmouth, Nova Scotia, B2Y 4A2
Canada
e-mail: dmosher@nrcan.gc.ca

**Grant Wach**
Dalhousie University
Halifax, Nova Scotia, B3H 4J1
Canada
e-mail: gwach@dal.ca

## ABSTRACT

The Suriname margin of South America is an ideal location for studying late stage continental rifting and margin development in the equatorial Atlantic. This location was the last junction of South America and West Africa, separating the North and South Atlantic Oceans. Mid to Late Cretaceous break-up resulted in final separation of the two continents and formation of a water passageway between the North and South Atlantic. Recently acquired 2D and 3D industry seismic reflection data bridge the shelf to slope transition along the Suriname margin. These data in combination with offshore industry wells and ODP Leg 207 results allow for detailed investigation of the development of the Suriname margin.

Seismic reflection profiles off the Suriname margin indicate a passive rifted margin reflecting sedimentary sequences of subsidence infill and overall progradation. Post-break up erosion was extensive, resulting in a prominent mid-Cretaceous (Aptian/Albian) unconformity. Early post-rift oceanic conditions were highly anoxic, leading to deposition of a thick (~90 m) interval of Cretaceous organic black shales on the Demerara Rise. Several other significant regional unconformities within the Cenozoic indicate episodes of extensive erosion. In deep water, the Cenozoic sequence is thin, but under the continental shelf and slope, the section is expanded with shelf-to-slope progradational stratigraphic architecture. Stratigraphic and seismic-geomorphologic features suggest a combination of progradation, off-shelf sediment transport and sediment mass-failure on the slope as the dominant Cenozoic processes responsible for construction of the margin. This wedge-shaped architecture indicates sediment slope by-pass is minimal.

## Introduction

The Suriname margin represents the location of the last vestige of the proto-Atlantic, before West Africa's final rifting from South America (Gouyet *et al.*1994). Along the margin is the Demerara Rise

(DR); a deep water plateau that is a fragment of continental crust that sheared from its conjugate, the Guinea Plateau of West Africa. This Cretaceous rifting resulted in formation of a passageway between the North and South Atlantic Oceans. The Suriname margin lies in water depths ranging from 100 m to >3000 m on its seaward flanks (east and west). The area, therefore, is ideal to study the youngest record of rifting and passive margin development anywhere in the Atlantic. From a paleoceanographic perspective, it recorded opening of the Atlantic Gateway in the Middle to Late Cretaceous. Its equatorial setting is ideal to investigate Cenozoic oceanic scale deep and shallow water current development far from the poles. Uninfluenced by glacial processes, it is also an ideal location to study more recent margin progradation; analogous to older periods elsewhere along the Atlantic (*e.g.* Nova Scotia). It is the intent of this paper to investigate the Suriname margin seismic stratigraphy and sedimentology to understand warm climate passive margin development and to use this insight to infer processes that occurred in earlier time periods elsewhere in the Atlantic. 2D and 3D seismic reflection data contributed from industry, in combination with drill results from Ocean Drilling Program (ODP) Leg 207 and industry well data, provide information on the distribution, structure, and thickness of the sedimentary formations; helping to understand it's geologic evolution.

## Background

The Suriname continental margin is underlain by Precambrian to early Mesozoic-aged continental crust. It is conjugate to West Africa at about the position of Guinea (Fig. 1). It formed the southern border of the central Atlantic margin during the Jurassic prior to rifting and opening of the Atlantic gateway (Benkhelil *et al.* 1995; Erbacher *et al.* 2004). Geographically at that time, the Suriname margin would have been located somewhat south of the present day location of Dakar, Senegal (Erbacher *et al.* 2004). In this area of the central Atlantic, north-south rifting initiated about 180 Ma resulting from east-west extension with a large component of dextral shearing (Fig .2) (Mascle *et al.* 1986; Gouyet *et al.* 1994). Complexities caused by plate rotation resulted in a late compressional phase before final rifting. This compression resulted in en echelon folding and flower structures within the Demerara Rise (Gouyet *et al.* 1994). Subsidence of the margin followed rapidly, initially due to thermal cooling of the crust (Benkhelil *et al.* 1995; Pindell and Kennan 2005).

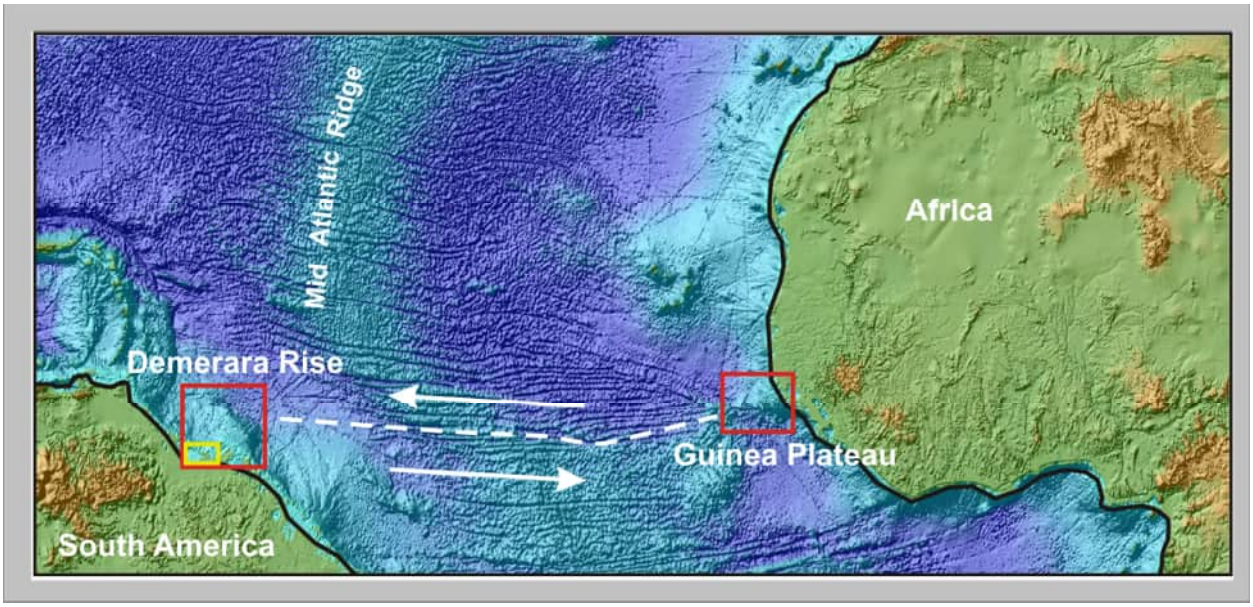


**Figure 1. Equatorial Atlantic showing location of the Suriname Margin and its conjugate Guinea Plateau.**

Beneath the Demerara Plateau, Late Aptian and Late Albian unconformities are reported within the sedimentary section (Gouyet *et al.* 1994). The earlier unconformity may be correlated with the formation of the en echelon folds, while the late Albian event resulted from the main compressional phase (Benkhelil *et al.* 1995; Erbacher *et al.* 2004; Mosher *et al.* 2005).

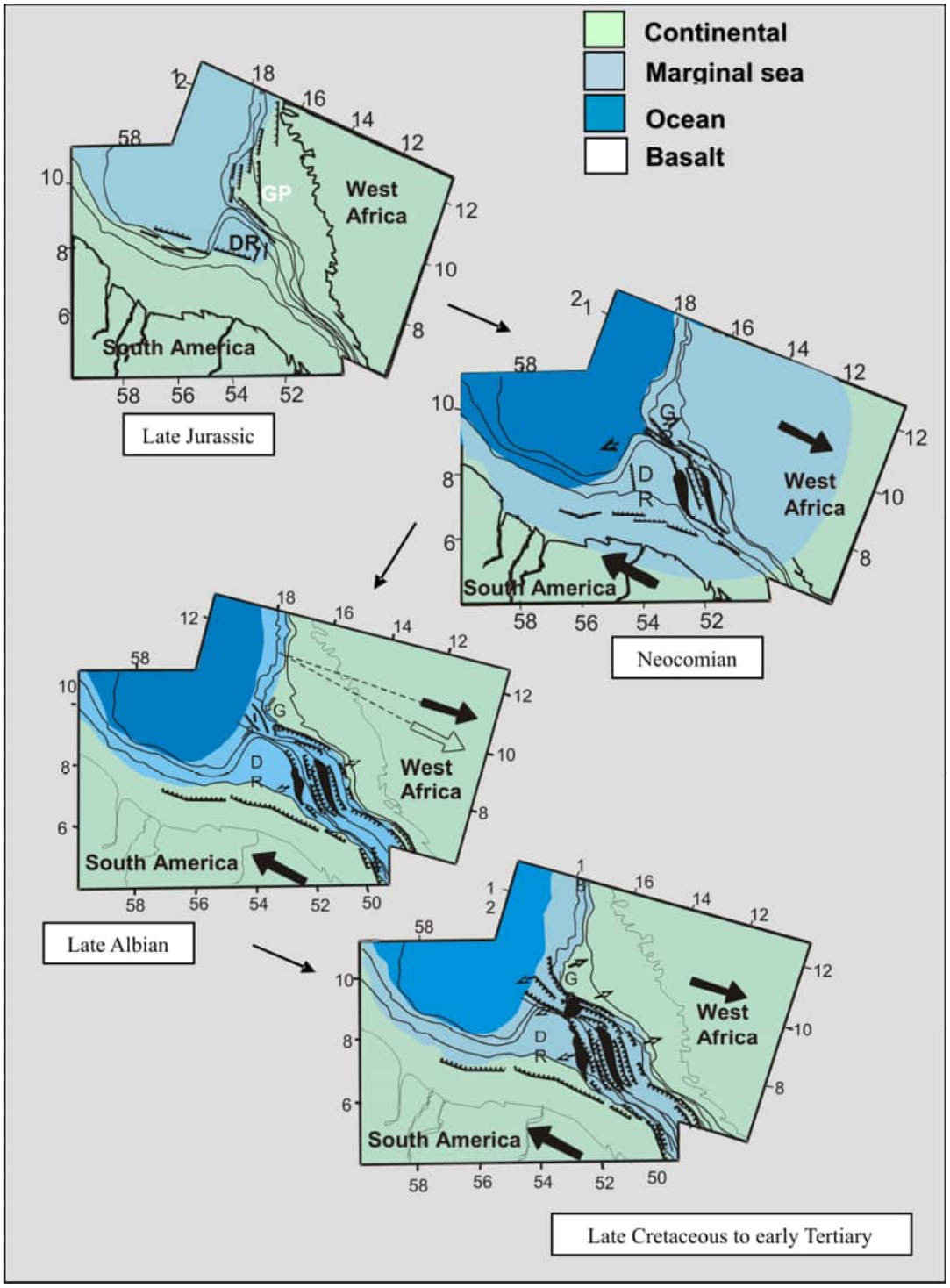


**Figure 2. Schematic stages of Mesozoic evolution of the Equatorial Atlantic (Modified afterGouyet *et al.* 1994, Benkhelil *et al.* 1995).**

Following the minor recurrence of compressive tectonics, an extensional regime ensued during the Late Cretaceous. Extension is characterized by a general collapse of the margin resulting in the final parting of the African and South American continental plates and the creation of oceanic crust (Fig. 2) (Benkhelil *et al.* 1995). Subsidence was presumably rapid, along with continental synrift sedimentation filling accommodation space provided by this subsidence (Flicotaux *et al.* 1988; Erbacher *et al.* 2004). Global sea-level continued to rise throughout this period, and reached its highest levels in the Turonian (Haq *et al.* 1988). Tectonic deformation ceased in the Late Cretaceous followed by normal cooling subsidence as a largely clastic cover was deposited over the previous rift graben on the Demerara Rise (Fig. 2) (Gouyet *et al.* 1994). Largely east-west separation of the West African and central South American margins continued. A feature of this extension is the Guinea fracture zone; a transform fault that forms the eastern outer margin of the Demerara Rise off Suriname (Fig. 1).

## Methods

2D and 3D seismic reflection data were used for this study. The RepsolYPF Block 30 3D seismic volume covers 3074 $km^2$ of the outer shelf and uppermost slope of the Suriname margin. Regional 2D seismic reflection profiles (w99-108, w99-108) provided by Statsolie and RepsolYPF allow for correlation of the inner and outer portions of the margin and tie to industry and (ODP) Leg 207 data on the outer DR (see Erbacher, Mosher, Malone *et al.* 2004 for details). Industry and ODP Leg 207 well data on the Suriname margin allowed for age correlation of seismic horizons. *North Coronie 1* (NC-1) (1976) is the principle industry well used for the correlations for the Suriname margin. NC-1 lies directly within RepsolYPF Block 30 3D seismic volume, inboard of the shelf-to-slope transition in the eastern portion of the study area. Age correlations were also tied to nearby industry wells *Sinna Mary 1* (1975), *Esso A2-1*(1978) and drilling results from (ODP) Leg 207 spanning the central and north-eastern DR. Age picks are based on published micro-fossil assemblages, biostratigraphic observations, and synthetic seismograms to confirm correlation of the seismic data to (ODP) drilling and well results (see Erbacher *et al.* 2005).

## Results

For organizational purposes, the seismic reflection results for the Suriname margin have been divided into two main units of Mesozoic and Cenozoic ages respectively. The Cenozoic unit can then be further subdivided into the Paleogene and Neogene units based on significant regional erosional unconformities.

### Mesozoic

Cretaceous and Early Tertiary sequences are best observed on the outer DR, where they are shallowly buried and well preserved, as demonstrated in the ODP Leg 207 investigations (Erbacher *et al.* 2005; 2006). Two prominent regional unconformities of Aptian/Albian age span much of the Suriname margin and are recognizable to modern abyssal water depths. These unconformities exhibit high amplitude returns, and show strong coherency. The Albian unconformity defined as the "C" unconformity identified from Leg 207 seismic results, erodes the underlying Aptian unconformity (Fig. 3). Below this unconformity, the section is heavily faulted and folded, presumably a result of synrift tectonics and sedimentation (Mosher *et al.* 2005). On the outer DR and immediately overlying the Albian unconformity, seismic reflections are largely parallel continuous and of moderate to high amplitude to the overlying Paleocene horizon. This sequence is of relatively constant thickness of 120 to 150 ms on the outer DR. At this position, a significant portion of this interval correspond with Cenomanian to Santonian claystone rich in organic matter (black shales) (Erbacher *et al.* 2004; Mosher *et al.* 2007). It is about 1.5 s thick under the modern continental slope and maintains that thickness in the intervening basin between the slope and the outer DR. On the DR, the top of this interval is termed the "B" horizon by Mosher *et al.* (2005, 2006) and it corresponds to a significant Paleocene unconformity recognized in the 3D seismic

volume of the upper slope of the Suriname margin (Fig. 3). At the ODP sites of the outer DR, this horizon appears to correspond with the Cretaceous-Tertiary boundary found in drill results.

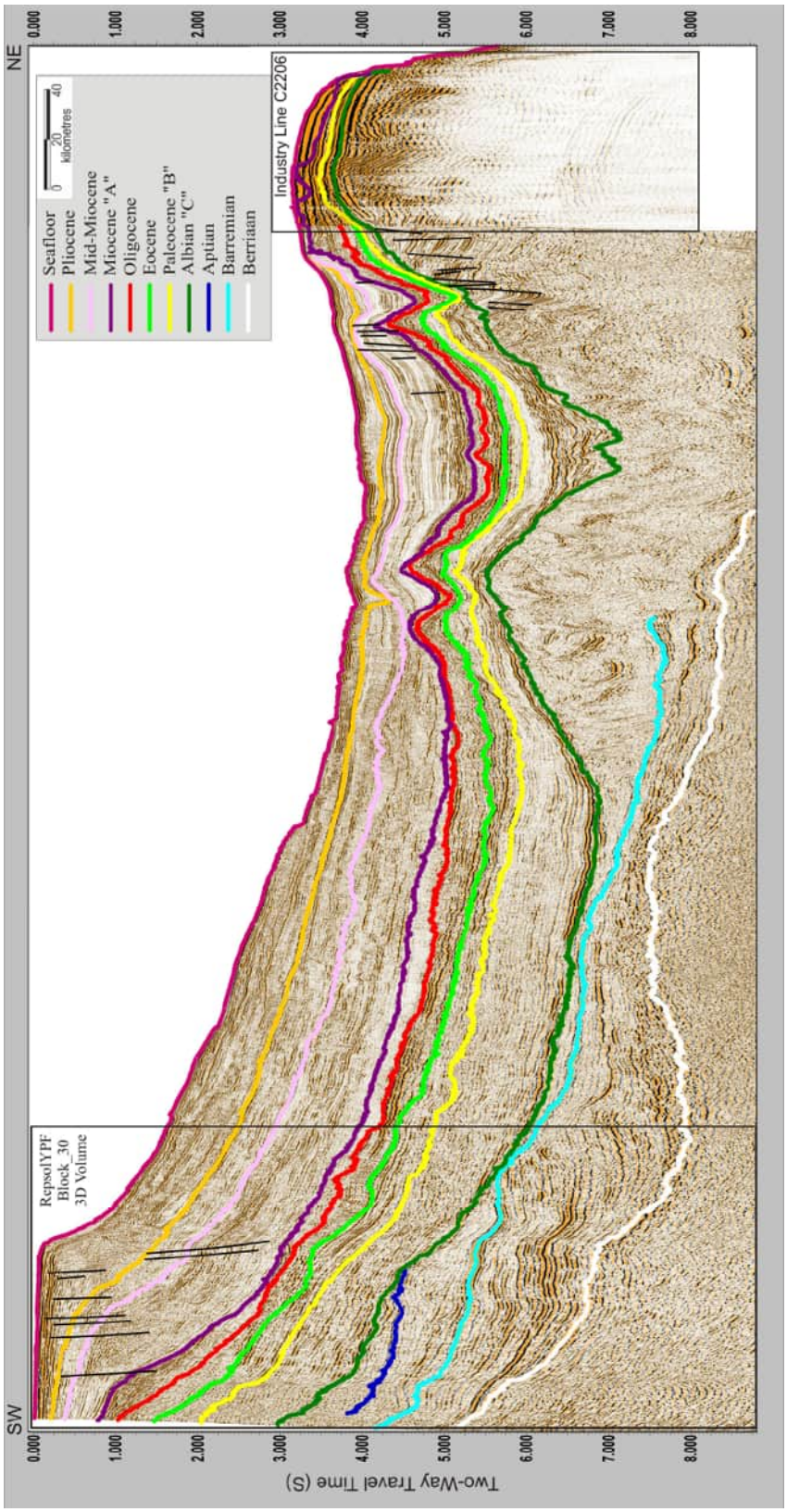


**Figure 3. Seismic profile of line W99-109 integrated with industry seismic profile C2206. Horizon age picks based on microfossil assemblages from ODP drill site 1257, and industry wells North Coronie-1, A2-1 and Sinna Mary 1. Note the correlation of "A" "B" & "C" uncomformities from the northeastern Demerara Rise to the RepsolYPF Block 30 Seismic Volume on the on the Suriname.**

### Cenozoic

The Cenozoic section is thin to absent on the outer DR but thickens substantially inboard, to nearly 2.5 s thick beneath the continental shelf (Fig. 3). On the outer DR, it is largely composed of foraminiferal and nannofossil ooze with varying amounts of terrigenous material. In general description of the seismic data, the entire sequence forms a progradational wedge from the shelf to the intervening basin. Paleo-shelf edges are obvious throughout the section, observed as inflexion points in seismic horizons (Fig. 4). The Cenozoic unit indicates several major erosional unconformities. These reflection events are marked by high amplitude and strong coherency within the Oligocene, Miocene, Mid-Miocene, and Pliocene.

### Paleogene

The Paleogene unit is marked by various erosional unconformities. In general, sequences thin and pinch out northward approaching the outer flanks of the DR plateau. A major erosional event is marked by a regional Oligocene unconformity that spans the entire Suriname margin, becoming virtually non-existent on the DR to the northwest (Fig. 3). This unconformity is clearly defined in the NC-1 well data due to the abundance of planktonic microfauna within the chalky Oligocene-age limestones. Below the modern shelf break, reflection configurations exhibit high amplitude discontinuous to sub-parallel character to the overlying Oligocene unconformity. This Paleogene to Oligocene sequence is approximately 1 s thick under the shelf and maintains a relatively constant thickness throughout the slope and intervening basin but thins rapidly as it approaches the outer flanks of the DR.

### Neogene

A regional Miocene unconformity is easily recognized throughout much of the Suriname margin and has been identified as the “A” horizon for Leg 207 drilling results (Fig. 3). O’Regan and Moran (2007), estimate in excess of 220 m of clastic sediment removal during this event over the DR, but approximations over the Suriname margin and intervening basin are still hard to define. Reflection configurations above this erosive horizon consist of distinctive sequences of continuous parallel to sub-parallel, coherent reflections under the present day continental shelf. Evidence of listric faulting is prevalent in the sequence up to the present day seafloor (Fig. 4); as well incoherent reflection configurations on the slope indicate evidence of sediment mass-failure, such as slump deposits (Ingram et al., in press). Sediment thickness of this interval remain consistent at approximately 1 s under the shelf and intervening basin, but thin drastically approaching the outer flanks of the outer DR. Directly overlying this sequence, a mid- to late Miocene erosive event is well defined within seismic profiles (Fig. 3). Strong reflection coherency of this horizon makes it easily distinguishable throughout the Suriname margin and the underlying stratigraphy. Reflection coherency is poor to moderate above this horizon up to a defined Pliocene unconformity. Abundant listric faults in this sequence under the shelf are responsible for tens of meters offset of mainly flat-lying, moderate to high amplitude continuous reflections. Reflection configurations clearly define the inflection points of a preserved paleo shelf-break throughout this sequence and provide evidence of rates of margin progradation. The shelf to slope transition is defined as reflections become low amplitude and chaotic to discontinuous in character, evidence suggesting sediment mass failure and off-shelf transport. Thickness of this sequence is relatively consistent under the present day continental shelf, slope and intervening basin at approximately 500 ms but tapers out on the outer flanks of the DR (Fig. 3).

The present day seafloor within the 3D seismic volume is generally expressionless without any significant regional or large-scale morphological features. In seismic profiles, high amplitude returns are indicative of hard substrate, perhaps the result of a transgressive cycle and little modern sediment input. At the shelf break outcropping reflections are identified as well as small gullies possibly created by the influence of present day off-shelf currents. Fault offsets are expressed on the seafloor on the outer

continental shelf, creating anomalous rises in the sea bed, one in particular parallels much of the shelf break within the 3D volume.

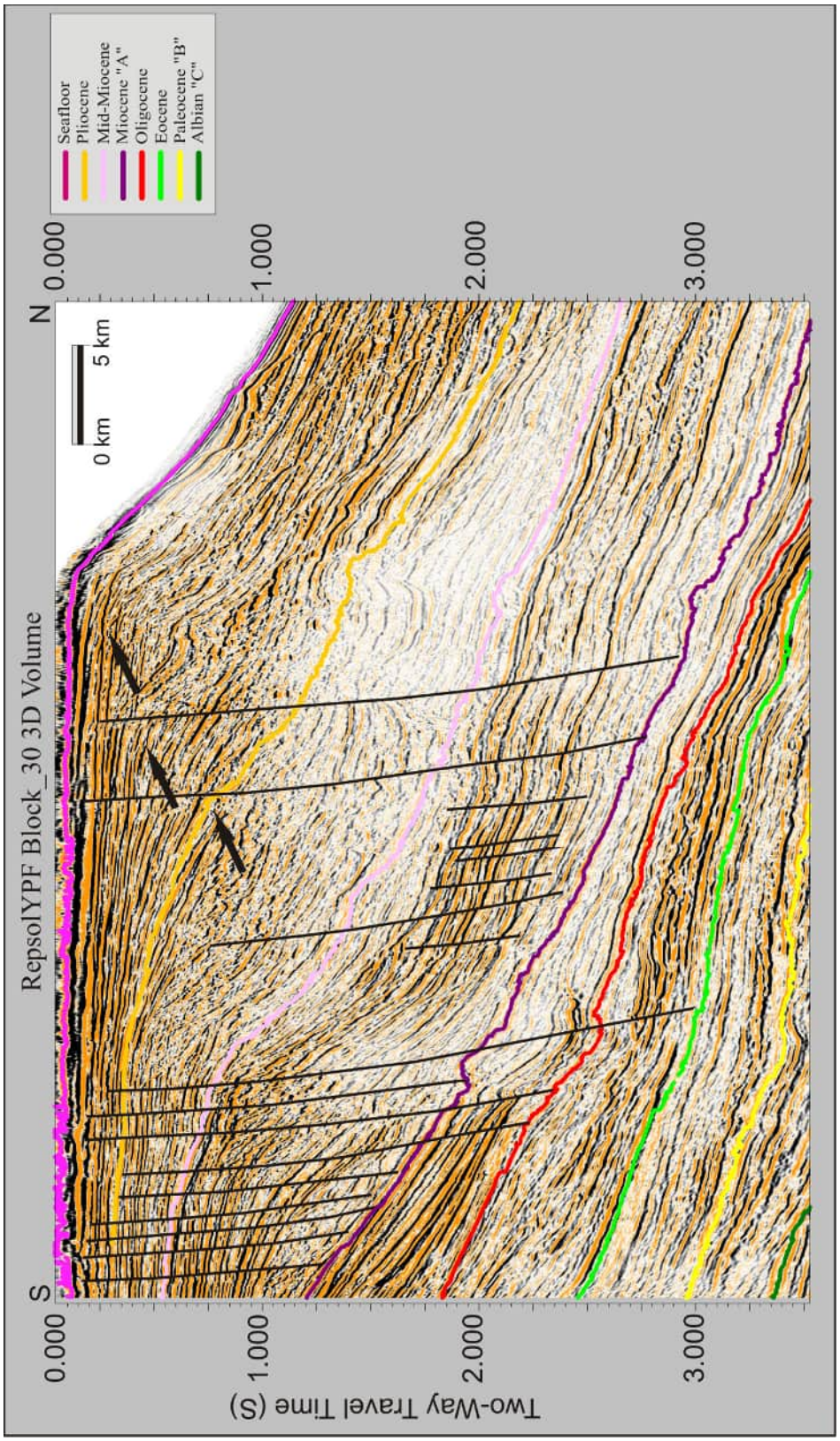


**Figure 4. Seismic profile of Repsol Block 30 indicating the distribution of faulting in the shelf region. Note the sediment thickness above the "A" horizon relative to the underlying units, and the classic shelf-to-slope progradational bedding structures.**

## Discussion

Final rifting between Africa and South America in the Mid-Cretaceous occurred between present-day Suriname and Guinea and resulted in providing a passageway between the North and South Atlantic oceans. Ocean currents flowing through this young shallow water passageway are likely responsible for developing the strikingly prominent Albain unconformity (Fig. 3) observed on seismic records and in drill cores (Erbacher *et al.* 2004). Pre-Albian rocks below this unconformity are heavily faulted and folded, likely due to break-up tectonics and subsidence.

The late Cretaceous sequence, including the Aptian to Turonian, corresponds to a marine platform, in relatively shallow waters and calm environment, with marine influence becoming strong at the top of this interval. Dip-meter analysis from NC-1 well indicates a south east sediment deposition of Albian to early Turonian beds, consistent with a deep North Coronie anticline. Although the early Turonian sequence is located above this Albian unconformity, sediment distribution was heavily influenced by the shape of this surface. A mean dip of 2° is reported up to the Oligocene where a ~60° change in sediment distribution direction occurs and trends become approximately north passing to the southwest. Subsequent thermal subsidence, allowed for deposition of a consistently thick (~90 m) unit of black shale, between Cenomanian and Santonian times (Erbacher *et al.* 2004). These black shales contain up to 30% TOC (Meyers and Bernasconi 2007), making them a first class hydrocarbon source rock. Rocks of similar age and lithology are known to account for 29% of the world's hydrocarbon reserves (Workman 2000).

The remaining Cenozoic section follows the northward trend of the Oligocene and is in accordance with the north plunging regional structural features. The Paleocene unconformity correlated along the Suriname margin identified as the "B" horizon by Erbacher *et al.* (2004) defines the apparent Cretaceous-Tertiary boundary (Fig. 3). In the position of the NC-1 well on the Suriname margin, the Campanian to Paleocene sequence forms a detrital megasequence with a sandy base fining upward to silty clays, and intermixed calcareous chalks deposited in a marine environment. Structural and sedimentologic evidence in the NC-1 well indicates a slope environment at the time of deposition with a sandy series representative of a probable deep sea fan. Above this horizon lower to middle Tertiary sediments were deposited under similar conditions up to the mid-Miocene unconformity, except for occasional sediment mass failure, minor channels and hiatuses.

The mid-Miocene unconformity recognized by Erbacher *et al.* (2004) and Ingram *et al*. (In press), correlates to an extensive erosional event across the entire Suriname margin and DR (Fig. 3). Above this unconformity sediment input was largely terrigenous and on the inner slope a much shallower depositional environment then previous units. Northward trending beds indicate sediment transport from north to south over the Suriname margin. Sediments were presumably transported onto the slope by ocean/tidal currents, minor sediment mass failures and off-shelf hyperpycnal flow forming channel corridors.

The regional Pliocene unconformity is marked by a sharp change at NC-1 in lithology and sediment physical properties. This unconformity is easily correlated throughout the 3D seismic volume (Figs. 3, 4). Continuous sedimentation is defined by laterally continuous reflections within the sequence. A number of subsurface horizon show evidence of gully cutting at the shelf break. This evidence in combination with minor thicknesses of interpreted mass failure deposits suggests that Cenozoic shelf progradation and continental slope construction has been governed by off-shelf transport of sediment, probably by hyperpycnal flows, and occasional sediment mass failure. Shelf-edge shallow faults further indicate that mass failure at this position is on ongoing process leading to slope construction.

## Conclusions

The Suriname margin of South America is an ideal location for studying late stage continental rifting and margin development in the equatorial Atlantic. The location is the youngest rifted margin in the Atlantic, separating from West Africa in the Early to Mid-Cretaceous. Early post-rift oceanic

conditions were highly anoxic, leading to deposition of a thick (~90 m) interval of Cretaceous black shales. Subsequent Cenozoic deposition was largely progradational with several significant regional unconformities. These unconformities likely represent major episodes of global oceanographic change, related to sea level and development of polar glaciations, rather than local influences such as mass-failure. In deep water, the Cenozoic sequence is thin. It was heavily eroded in the Oligocene and again in the Miocene. Plio-Pleistocene sedimentation rates appear to be very low in deep water. Under the continental shelf and slope, the Cenozoic section is expanded with shelf-to-slope progradational stratigraphic architecture. Stratigraphic and seismic-geomorphologic features suggest a combination of progradation, off-shelf sediment transport and sediment mass-failure on the slope as the dominant Cenozoic processes responsible for margin construction, implying minimal slope by-pass.

## References


Benkhelil J, Mascle J and Tricart P (1995): The Guinea continental margin; an example of a structurally complex transform margin. Tectonophysics 248: p.117-137.

Erbacher, J., Mosher, D.C., Malone, M. and shipboard scientific party. (2004). Initial Results, ODP Leg 207, Demerara Rise. Initial Results V. 207, Ocean Drilling Program, Texas A&M University, 89 pp. + CDRom.

Erbacher, J., Mosher, D.C., Malone, M. and shipboard scientific party. (2004): Drilling probes past carbon cycle perturbations on the Demerara Rise. EOS, v.85, p.57.

Flicoteaux R, Latil-Brun MV, and Michaud L (1988): Histoire de la subsidence post-rift du bassin cotier mauritano-senegalo-guineen, relation avec l'amincissement crustal pendant la periode jurassique a Cretace inferieur; comparaison avec l'evolution des marges peri-atlantiques au niveau de l'Atlantique central et equatorial (cote est des U.S.A., Sud-Sahara, Cote d'Ivoire et Plateau du Demerara) *In:* The West African connection; evolution of the central Atlantic Ocean and its continental margins. Sougy J, Rodgers, J. (eds) Journal of African Earth Sciences 7: p.345-359.

Gouyet S, Unternehr P and Mascle A, (1994) The French Guyana margin and the Demerara Plateau; geological history and petroleum plays. In: Mascle A (ed) Hydrocarbon and petroleum geology of France. Special Publication of the European Association of Petroleum Geoscientists 4: 411-422.

Haq, B.U., Hardenbol, J., and Vail, P.R. (1998): Response: Sea Level History. *In:* Sea-level Change: an Integrated Approach. Wilgus, C.K., Hastings, B.J., Posamentier, H., van Wagoner, J.C., Ross, C.A. and Kendall, C.G. St. C. (Eds.) SEPM Spec. Pub, 42: p.71-108

Ingram, W., Mosher, D.C., and Wise, W., (In press): Anatomy of a Deep-Water Mass-Transport Deposits on Demerara Rise: Implications for passive continental margins. *In:* Shipp, C., Weimer, P, and Posamentier, H. (eds.), The Importance of Mass-transport Deposits in Deepwater Settings. SEPM Special Publication.

Mascle J, Marinho M and Wannesson J (1986): The structure of the Guinean continental margin: implications for the connection between the central and South Atlantic Oceans. Geol. Rundsch. 75: p.57-70.

Mascle J, Blarez E and Marinho M (1988): The shallow structures of the Guinea and Ivory Coast Ghana transform margins: Their bearing on the Equatorial Atlantic Mesozoic evolution. Tectonophysics 155: p.193-209.

Mosher, D.C.. Erbacher, J. and Malone, M.J. (Eds.), (2007): Proc. ODP, Sci. Results, 207: College Station, TX (OceanDrillingProgram). Doi: 10.2973/odp.proc.sr.207.2007.

Mosher, D.C.. Erbacher, J. and Malone, M.J., (2007): Synthesis: Extreme warmth, organic-rich sediments and an active deep biosphere: Cretaceous to Paleogene paleoceanographic depth transect at Demerara Rise, western tropical Atlantic. *In:* Mosher, D.C., Erbacher, J. and Malone, M. (Eds.). Proc. ODP, Sci. Results, 207: College Station, TX (Ocean Drilling Program), 1-15. Doi:10.2973/odp.proc.sr.207.101.2007.

Mosher, D C; Erbacher, J; Zuelsdorff, L; Meyer, H; ODP Leg 207 Shipboard Scientific Party; (2005): Stratigraphy of the Demerara Rise, Suriname, South America: a rifted margin, shallow stratigraphic source rock analogue. *In:* Exploring energy systems: 2005 Canadian Association of Petroleum Geologists-American Association of Petroleum Geologists Joint Annual Convention: abstracts; 2005; 8 pages (ESS Cont.# 2004341)

Sancho, J. (1976): Well Completion Report North Coronie-1. Staatsolie C-103.

O'Regan M., and Moran, K., (200): Compressibility, permeability, and stress history of sediments from Demerara Rise. In Mosher, D.C.. Erbacher, J. and Malone, M.J. (Eds.), (2007). Proc. ODP, Sci. Results, 207: College Station, TX (Ocean Drilling Program). Doi: 10.2973/odp.proc.sr.207.2007.

Workman, W. (2000): Guyana basin: A new exploration focus. World Oil Magazine, p.55-60.

**BACK**

# Quantitative Kinematic and Thermomechanical Analysis of the Evolution of the Moroccan Rifted Continental Margin

**Mohammed Gouiza**
**Giovanni Bertotti**
**Badr Ghorbal**
VU University Amsterdam
De Boelelaan 1085
Amsterdam
Netherlands
e-mail: mohammed.gouiza@falw.vu.nl

**Mohamed Hafid**
Université Ibn Tofail
Kenitra 14000
Morocco

## ABSTRACT

The Atlantic passive margin of Morocco developed during Mesozoic times in association with the opening of the Central Atlantic. Extension caused the development of extensional basins along the future continental margin and, further to the E, the Atlas rift system. Therefore, this must be considered as part of the rift system, which led to the formation of the passive continental margin of Morocco. It was inverted in Alpine times to form the present-day High and Middle Atlas Mountains.

To provide a first quantitative analysis of the evolution of the rifted margin, we have constructed a crustal section from the Anti-Atlas (the plate interior) to the Atlantic Ocean crossing the Atlas system, the Meseta and the Atlantic continental margin in the Doukkala Basin segment. We applied numerical models to test quantitative relations between amounts and distribution of extension and isostasy-related vertical movements. A region of particular interest is the Moroccan Meseta, which is generally considered as a stable region separating the subsiding Atlas and Atlantic margin system. This picture is incompatible with the recent findings, which, on the basis of low-thermochronology, have demonstrated the existence of a Late Triassic to Middle Jurassic stage of subsidence followed by a Late Jurassic to Early Cretaceous exhumation.

We use the results of the quantitative analysis presented above to address the importance and regional tectonics of these syn-rift and post rift vertical movements.

BACK

# The Evolution of the Perdido Fold Belt in the Context of Salt Tectonics of the Northwestern Gulf of Mexico: Insights from Numerical Modelling

**Sofie Gradmann**
**Christopher Beaumont**
Department of Earth Sciences
Dalhousie University
1355 Oxford Street
Halifax, NS, B3H 4J1
Canada
e-mail: s.gradmann@dal.ca

## ABSTRACT

The Perdido Fold Belt is a prominent salt-cored deep-water structure in the northwestern Gulf of Mexico. In the last decade it has become a major target for hydrocarbon exploration. It is characterised by a unique geometry (thick, pre-kinematic, kink-folded sedimentary section, lack of significant syn-kinematic sedimentation, seaward tilt of the fold envelope) and its location above the pinch-out of the autochthonous salt and adjacent to and below the extensive Sigsbee Salt Canopy.

We use 2D finite-element models to study the evolution of the PFB by gravitational spreading during sediment progradation, in which a viscous salt layer is overlain by a frictional-plastic passive margin sedimentary sequence. Model experiments include sediment compaction, flexural isostasy, loading by the overlying water column, and parametric calculations of the effects of pore-fluid pressures in the frictional-plastic sediments.

Limit analysis calculations of the stability of this system reveal that the PFB can have formed by gravity spreading alone if moderately high pore-fluid pressure ratios of approximately 0.8 developed. Under these circumstances, the numerical finite-element model fold belt shows good correlation with the kink-type folds, geometry and dimensions of the PFB. Timing, rate, and extent of folding in the model fold belt are shown to be controlled by the system parameters of overburden strength, continental slope width, salt thickness, and salt viscosity. Variability in the latter two generates two end-member fold belt types: toe-of-slope folding that propagates progressively seaward, and synchronous toe-of-salt folding above the distal section of the salt layer. The numerical model results are interpreted to imply that landward Cretaceous toe-of-slope folding started long before the Oligocene-Miocene folding of the PFB. This allowed proximal allochthonous salt structures to develop through breached anticlines in the propagating fold belt while distal sedimentation continued. Only later did folding propagate and fold the PFB, which represents only the nose of a much older and larger fold belt.

## Introduction

The Perdido Fold Belt (PFB) in the northwestern Gulf of Mexico (GoM) is a prominent deep-water salt-tectonic structure that has recently become a focus of intensive hydrocarbon-related studies, but still remains imperfectly understood. Deep-water fold and thrust belts develop on continental margins as a result of gravity spreading and gliding above a weak substratum (such as salt) which produces paired proximal extensional and distal compressional domains.

The PFB is the best studied salt-cored deep-water fold belt worldwide and several unique features distinguish it from many other deep-water fold belts. These include the large, 4.5 km, thickness of the pre-kinematic section and the absence of earlier folding, the highly symmetric kink folds extending for

60-100 km, the seaward tilt of the entire fold belt, the almost synchronous evolution of its folds within less than 10 Ma during Oligo-Miocene times and its vicinity to the large allochthonous salt structure of the Sigsbee Canopy.

The goal of this work is to explain the first-order structures of the PFB in a dynamical context by comparing its evolution with those of a series of finite element model experiments. The modelling is designed to place quantitative constraints on the conditions under which the PFB may have evolved (overburden strength and geometry, sedimentation rates, salt thickness, salt geometry and salt viscosity), to test whether the system was driven by gravity alone, and to enhance the general understanding of the evolution of gravity-driven deep-water fold belts.

## Limit Analysis for Stability of Continental Margin

Gemmer *et al.* (2005) developed an analytic description for the forces acting on a simplified salt bearing continental margin. By balancing the seaward and landward acting forces, a description of the condition of failure can be obtained. We expand the existing calculations to include the isostatic response to sediment loading and a description of pore-fluid pressure that is related to the mean stress instead of the lithostatic stress and apply it to the Oligocene northwestern Gulf of Mexico. Using estimated values for the geometry of the salt basin and sedimentary overburden as well as respective densities, we obtain values for the maximum sediment strengths that allows gravity spreading to set in of $\varphi_{eff}$=5-6.5°. The effective angle of friction $\varphi_{eff}$ is a combination of internal angle of friction of the dry sediment $\varphi_0$ and pore-fluid pressure ratio $\lambda$ ($\sin \varphi_{eff} = (1- \lambda) \sin \varphi_0$). For fine grained clastic material ($\varphi_0$=25°), the implied pore-fluid pressures correspond to $\lambda$=0.8, representing moderately overpressured sediments, commonly found in large, deep sedimentary basins subject to rapid sedimentation. The outcome of the limit analysis shows that gravity spreading alone can be responsible for the formation of the PFB, provided overpressures of this level developed.

## Numerical Modelling

We use 2D finite-element models in which frictional-plastic sediments overlie a viscous salt layer. The models comprise a passive margin sedimentary sequence from shelf to deep water to account for the dynamical interaction of gravity spreading caused by shelf progradation. Model experiments include sediment compaction, flexural isostasy, loading by the overlying water column as well as parametric calculations of the effects of pore fluid pressures in the frictional-plastic sediments.

A reference model that represents a simplified configuration of the Oligocene northwestern Gulf of Mexico continental margin shows the development of a deep-water fold belt driven by gravity spreading (Fig. 1A, B). The salt basin is 260 km wide and 3 km thick, salt has a viscosity of $10^{18}$ Pas and a density of 2200 kg/m$^3$, sediment strength ($\varphi_{eff}$ = 4.8) is chosen according to the calculations of the limit analysis, and sediment density follows a depth-dependent compaction curve from the Gulf of Mexico. Maximum water depth is 3 km, and sediments prograde with a constant rate of 0.5 cm/a. Several parameters of the reference model are changed in subsequent numerical experiments to investigate their influence on the temporal and spatial development of the deep-water fold belt.

The reference model shows good correlation with the natural example from the Gulf of Mexico (Figs. 1B-1D). Both fold belts show approximately 10 km long kink-type folds of the 4.5 km thick pre-kinematic section. The fold belts extend for 60-80 km and are uplifted and tilted seawards. Variations of the model parameters show that lower sediment strength and smaller continental slope width decrease the stability of the system leading to a faster evolution as well as a longer extent of the fold belt. In particular, a stronger sedimentary overburden inhibits gravity spreading and the system remains largely undeformed (apart from vertical subsidence of the shelf overburden where salt is expelled laterally and corresponding moderate seaward inflation of the salt layer). Although the geometry of the salt layer has some effect on the deformation of the fold belt, it is only when the salt is thin (<1 km) that its effect is profound. Here, folding develops at the toe of the slope before propagating to the distal end of the salt basin. The high

basal traction force at the base of the overburden that leads to toe-of-slope folding can also be achieved with higher salt viscosities. Basement steps or different tapers in the distal section can localise and slow down folding, but do not significantly change the nature of the salt-cored fold belt.

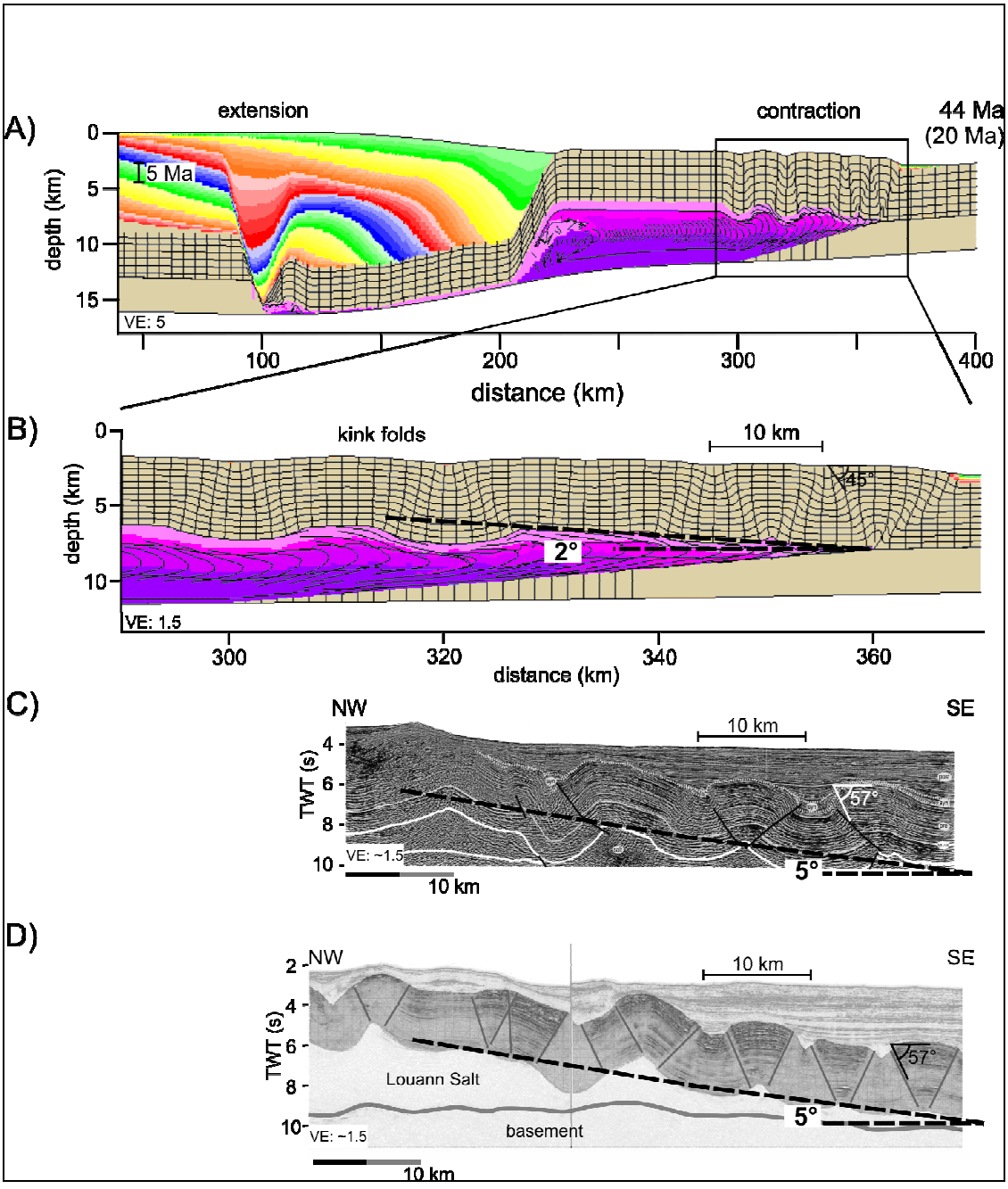


**Figure 1. Comparison of numerical model results with seismic sections from Perdido Fold Belt, northwestern Gulf of Mexico. A) Reference model after 44 Ma model run time (age in brackets denotes time since onset of gravity spreading). The colour scale shows the chronostratigraphy in 5 Ma major bands, each divided into 1 Ma sub-bands. Salt is coloured in magenta. Same coding is used in later figures. B) Close-up of numerical model showing the fold belt with highly symmetric kink folds of ~10 km wavelength. C), D) Seismic sections of PFB (From Rowan *et al.* 2000; Camerlo and Benson, 2006, AAPG©2006, reprinted by permission of the AAPG whose permission is required for further use).**

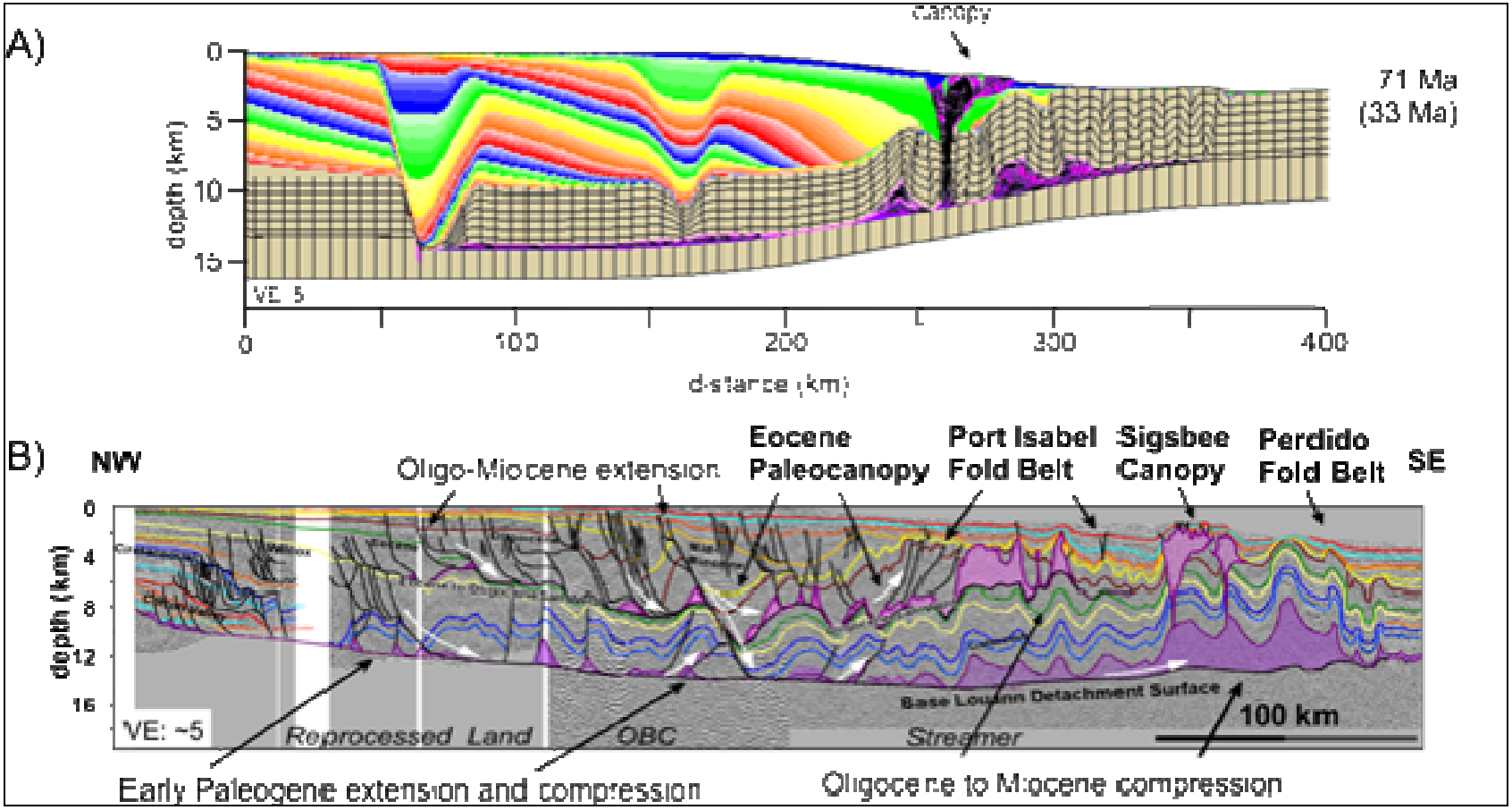


**Figure 2. Comparison of regional numerical model (Fig. 2A, for colour coding and ages see Figure 1) with seismic section from northwestern Gulf of Mexico margin (Fig. 2B) (From Radovich *et al.* 2007). Both sections show landward extension, a distal fold belt and an allochthonous salt canopy located directly adjacent and above the fold belt. Figure 2A shows a simplified model result whereas Figure 2B shows remnants of pre-**

A second set of models was run to investigate the relationship between allochthonous salt structures and deep-water fold belts. Two allochthonous salt structures can be identified from seismic data from the northwestern Gulf of Mexico (Fig. 2B). An early canopy formed during Eocene (Peel *et al.* 1995; Radovich *et al.* 2007), which acted as a shallow detachment surface for the Miocene Port Isabel Fold Belt and is now in most parts deflated. The second structure is the Sigsbee Canopy which formed further seaward in Oligocene times and now partly overlies the PFB. It has recently been inferred from modern seismic data that contraction occurred throughout large parts of the entire Gulf of Mexico deep water (Philippe *et al.* 2005; Guerin *et al.* 2006; Radovich *et al.* 2007). The evolution of allochthonous salt structures in deep water has been associated with compressional deformation, where shortening of salt-cored folds leads to breaching of the anticlines and expulsion of salt onto the seafloor (Vendeville and Gaullier, 2005).

For the numerical experiments we chose values for the model parameters that lead to toe-of-slope folding (thinner salt layer and higher salt viscosity) in order to achieve folding over a wider region and salt expulsion landward of a fold belt located over the distal end of the basin. A comparison of numerical model results and a seismic section is shown in Figure 2. The model presented in Figure 2A develops an allochthonous salt canopy directly adjacent to or above the distal fold belt (similar to the modern Sigsbee Canopy in Figure 2B). By also changing the width of the salt basin we obtain models (not shown here) that develop allochthonous salt canopies >100 km landward of the distal fold belt (similar to the Eocene paleo-canopy).

## Conclusions

Using numerical models and analytic calculations we are able to reconstruct the evolution of a Perdido-like deep-water salt-cored fold belt. Gravity spreading in the Oligocene Gulf of Mexico has been a sufficiently strong mechanism to fold the sediment carapace above the salt provided the overburden developed moderate pore-fluid pressures. Timing and extent of the folding of the model fold belt are shown to be controlled by system parameters such as overburden strength, continental slope width, salt thickness and salt viscosity. The numerical model results are interpreted to imply that landward Cretaceous toe-of-slope folding started long before the Oligocene-Miocene folding of the PFB. This allowed proximal allochthonous salt structures to develop through breached anticlines in the propagating fold belt while distal sedimentation continued. Only later did folding propagate and fold the PFB. By implication, the modern PFB is only the nose of a much older and larger fold belt.

## Acknowledgements

We would like to thank Markus Albertz for many discussions and contributions to the development of this research and Steven Ings for the GoM sediment compaction parameters. Funding for this project was provided by an Atlantic Innovation Fund contract to Dalhousie University, an IBM Shared University Research grant, a Killam Scholarship and a Government of Canada Award to S.G., and the Canada Research Chair in Geodynamics to C.B. We would also like to thank Shell International Exploration and Production, Inc. and Frank Peel for their kind support and advice, and Chris Connors for providing Figure 2B.

## References

Camerlo, R.H. and E.F. Benson, 2006, Geometric and seismic interpretation of the Perdido fold belt; northwestern deep-water Gulf of Mexico: AAPG Bull., v.90, p.363-386.

Gemmer, L. *et al.*, 2005, Dynamic modelling of passive margin salt tectonics: effects of water loading, sediment properties, and sedimentation patterns: Basin Research, v.17, p.383-402.

Guerin, G. *et al.*, 2006, Impact of amount of gravity-driven compression and intermediate decollement levels on the Sigsbee Salt Canopy formation, Gulf of Mexico: AAPG Annual Convention Abstracts.

Peel, F.J. *et al.*, 1995, Genetic structural provinces and salt tectonics of the Cenozoic offshore U.S. Gulf of Mexico: a preliminary analysis, *in* M.P.A. Jackson, D.G. Roberts, and S. Snelson, eds., Salt tectonics, a global perspective: AAPG Memoir, v.65, p.153-175.

Philippe, Y. *et al.*, 2005, Importance of gravity-driven compressional tectonics in northern offshore and deep-offshore Gulf of Mexico: New observations and implications for subsalt interpretation: AAPG Annual Convention Abstracts.

Radovich, B. *et al.*, 2007, Deep imaging of the Paleogene, Miocene structure and stratigraphy of the western Gulf of Mexico using 2D pre-stack depth migration of mega-regional onshore to deep water, long-offset seismic data: GCSSEPM Conference Proceedings, p.307-322.

Rowan, M.G., *et al.,* 2000, Deep-water, salt-cored foldbelts: Lessons from the Mississippi Fan and Perdido Foldbelts, northern Gulf of Mexico, *in* W. Mohriak and M. Talwani, eds., Atlantic rifts and continental margins, Geophys. Monograph, v.115, p.173-191.

Trudgill, B.D. *et al.*, 1999, The Perdido fold belt, northwestern deep Gulf of Mexico; Part 1, Structural geometry, evolution and regional implications: AAPG Bull., v.83, p.88-113.

Vendeville, B. and V. Gaullier, 2005, Salt diapirism generated by shortening and buckle folding: AAPG Annual Convention Abstracts.

**BACK**

# Seismic Stratigraphy, Salt Structures and Thermal and Petroleum Systems Models across the Central Nova Scotia Slope Basin

**Keith Louden**
Department of Oceanography
Dalhousie University
Halifax, Nova Scotia B3H 4J1
Canada
e-mail: Keith.Louden@Dal.Ca

**P. K. Mukhopadhyay**
Global Geoenergy Research Ltd.
Halifax, Nova Scotia B3J 2A1
Canada
e-mail: muki@global-geoenergy.com

**Yue Wu**
**Eric Negulic**
**Mladen Nedimovic**
Department of Earth Sciences
Dalhousie University
Halifax, Nova Scotia B3H 4J1
Canada

## ABSTRACT

Two regional deep seismic profiles, GXT NovaSPAN 1400 and Lithoprobe 88-1A, are used to better characterize the sediment, salt and basement structures across the Central Nova Scotian Slope Province. Imaging of deeper structures is especially improved, using either pre-stack depth migration with the long offset streamer (NovaSPAN 1400) or a combination of pre-stack time migration and wide-angle velocity models (Lithoprobe 88-1A). Seaward of the salt, basement morphology and crustal velocities suggest that highly-stretched and rotated continental crustal blocks extend further into the ultra-deep basin. Beneath the salt, basement is also well-defined except locally beneath major salt diapirs.

Petroleum systems models are derived along the two profiles for various potential source rocks and reservoirs. Along both profiles, salt flank and salt crest Late Jurassic and Early Cretaceous reservoirs form the primary exploration targets. However, significant differences also exist for the two profiles, primarily associated with variations in salt structures. Along NovaSPAN 1400, the Jurassic Verrill Canyon formation is the main source rock for both the Jurassic and Cretaceous reservoirs. For the Early Cretaceous reservoir, hydrocarbons may contain a major volume of liquids (>75%) with an API of 45-55$^{o}$ and only mild overpressures. Along Lithoprobe 88-1A, Early Jurassic lacustrine and Late Jurassic salt-associated marine reservoirs are potential exploration targets, although these would lie within an over-pressured, dry-to-wet gas regime. Mass balance calculations for both seismic lines indicate that more preserved hydrocarbons are expected within the various reservoirs on NovaSPAN 1400.

Model calculations of present-day sea-floor heat flow predict a gradual landward reduction from 55 mW/m$^2$ in the ultra deep-water basin to 45 mW/m$^2$ on the upper slope. However, large variations are caused by high conductivity associated with salt diapirs, yielding values as high as 85 mW/m$^2$. In July 2008, we plan to take detailed measurements along both profiles in order to verify these predictions.

## Introduction

Rifting on the Scotian margin occurred in the Late Triassic to Early Jurassic (~230-190 Ma), when red beds, evaporites and dolomites formed in fault-controlled half-grabens (*e.g.* Jansa and Wade, 1975). Basement subsidence continued in three main post-rift periods during the Jurassic, Cretaceous and Tertiary. The result of this subsidence was to create a number of major sedimentary subbasins (Fig. 1). Most studies have previously been undertaken in the Sable Subbasin leading to the discovery of significant gas reserves. The sandstone reservoirs are located within shallow marine to deltaic sediments and are probably sourced from the Late Jurassic to Early Cretaceous prodelta to pelagic shales of the Verrill Canyon formation (Welsink *et al.* 1989; Wade and McLean 1990). Maturation of the source rock was accomplished by increased post-rift subsidence during the Late Jurassic to Early Cretaceous. Other, more minor occurrences of both gas and oil are associated with Early Cretaceous clastic sequences (Missisauga and Logan Canyon formations) and are related to the edge of the Late Jurassic Abenaki formation carbonate bank following the present shelf edge (Fig. 1).

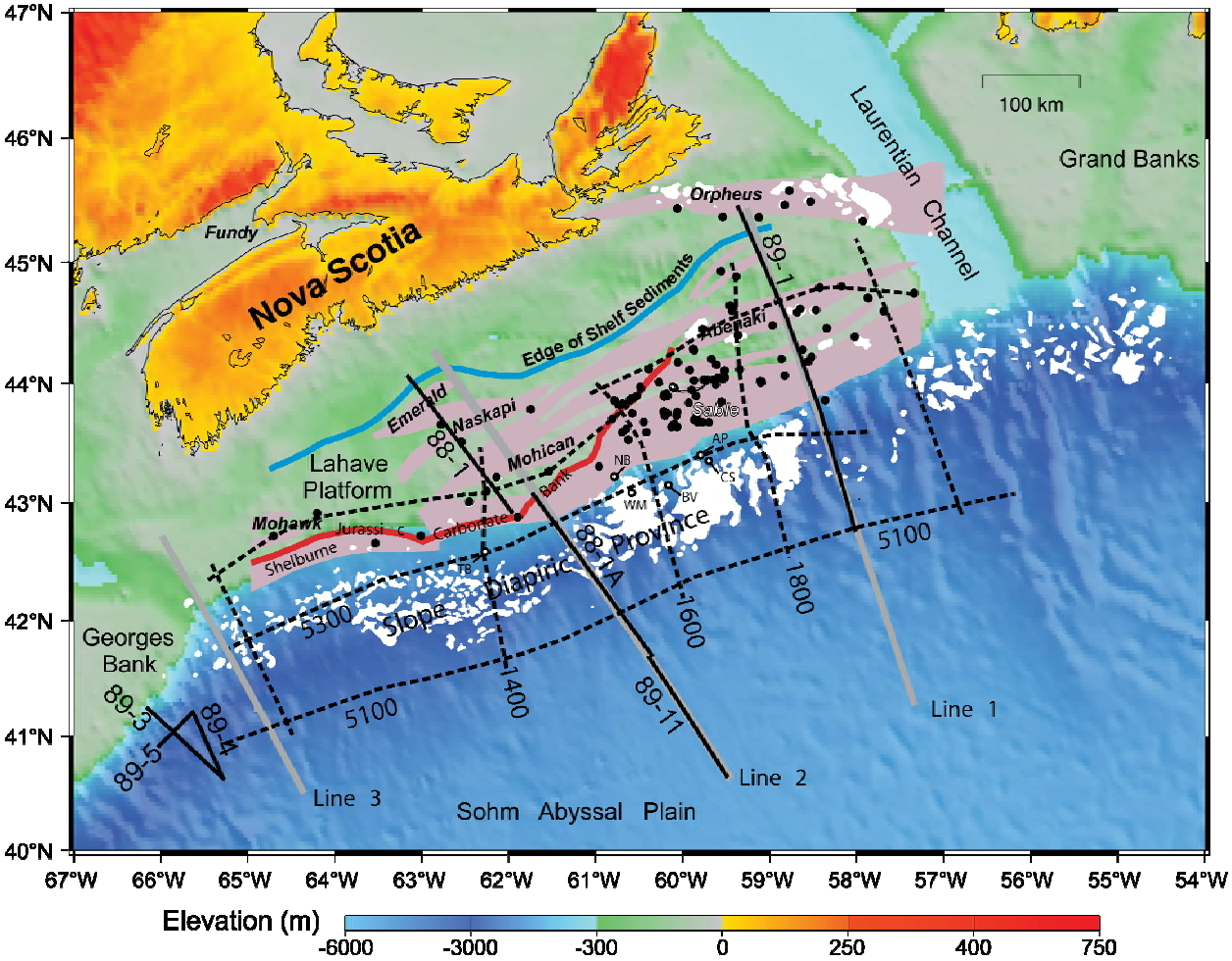


**Figure 1 Location map of seismic profiles and sediment structures across the Nova Scotian margin. Seismic profiles include GXT NovaSPAN MCS profiles (broken lines), Lithoprobe and BGR MCS profiles (solid black) and SMART wide angle profiles (solid gray). Sediment structures include shallow-water basins (solid pink fill) and boundaries of shelf sediment and Jurassic carbonate bank (blue and red lines) from Enachescu and Hogg (2005), and major salt bodies (white fill) from Shimeld (2004). Also shown are exploration wells (filled circles, with selected deep water wells identified as TB=Torbrook, NB=Newburn, WM=Weymouth, BV=Balvenie, AP=Annapolis, CS=Crimson) and shaded seafloor topography (colour scale).**

Further offshore, large thicknesses of sediment also occur beneath the lower continental slope and rise of the Sable and Shelburne subbasins (Fig. 1). It was expected that reservoirs for these deepwater prospects might be associated with Cretaceous and Early Tertiary channels, turbidites and fan deposits, trapped by the steep walls of salt diapirs (Hogg 2000) that extend along the margin within the Salt Diapiric Province southwest of seismic profile 89-1 (Fig. 1). The location of the salt previously had been used to mark the offshore boundary between the rifted continental crust and post-rift formation of oceanic crust. However, recent seismic models now suggest that highly thinned continental crust may in places extend well seaward of the salt (Wu *et al.* 2006) into the ultra-deep water basin (>4000 m). The apparent lack of reservoir indicated by more recent wells on the upper slope, and especially those closest to the Sable gas fields (Fig. 1), suggests the need for wider investigations of the petroleum system in other areas of the margin (Enachescu and Wach 2005). The purpose of this work is to produce petroleum systems models based on new interpretations of these seismic data across the entire region of potential hydrocarbon generation, beginning first with the central slope region.

## Seismic Profiles GXT1400 and Lithoprobe 88-1A

In this paper, we use two profiles, GXT NovaSPAN 1400 and Lithoprobe 88-1A, to better characterize the sediment, salt and basement structures across the Central Slope Province. Imaging of deeper structures in depth section is especially improved, using either pre-stack depth migration with the 9-km-long offset streamer (NovaSPAN 1400) or a combination of pre-stack time migration and wide-angle velocity models (Lithoprobe 88-1A; Wu 2007). Stratigraphic and lithologic interpretation of the profiles is shown in Figure 2, based on neighboring wells and previous interpretations (*e.g.* Kidston *et al.* 2002; Young 2005). Note, however, that there are no hard ties to these interpretations over most of the deep water and it is difficult to tie reflectors which much certainty across the salt. Seaward of the salt, basement morphology and crustal velocities on Lithoprobe 88-1A suggest that highly-stretched and rotated continental crustal blocks extend further into the ultra-deep basin. Beneath the salt, basement is also well-defined except locally beneath major salt diapirs.

## Petroleum System Models

Petroleum systems models, following on previous work by Mukhopadhyay (2006), are derived along the two profiles for various potential source rocks and reservoirs (*e.g.* Figs. 2 and 3). Along both profiles, salt flank and salt crest Late Jurassic and Early Cretaceous reservoirs form the primary exploration targets. However, significant differences also exist for the two profiles, primarily associated with variations in salt structures and stratigraphic thicknesses.

As revealed on line 88-1A, since 35 Ma the Jurassic Verrill Canyon and Cretaceous Verrill Canyon source rocks are situated within the wet gas and dry gas zone. They have expelled 90% of the generated hydrocarbons. The Early Jurassic lacustrine source rocks, which remain within the dry gas zone since 90 Ma, have been fully depleted in generated hydrocarbons (maturity >4% Ro). Distinct prospects of dry gas saturation exist within the syn-rift Early Jurassic reservoirs of the ultra-deep water (beyond 3500 m water depth). These hydrocarbons were solely saturated by the syn-rift Early Jurassic source rocks between 145 and 65 Ma. Although the reservoir contains more than 10% porosity, the reservoirs lie within a temperature $\geq 200^{\circ}$C and pore pressure >125 MPa. The Late Jurassic reservoirs contain a ratio of 90:10 dry to condensate that has not been fully charged with gas and oil until 65 Ma in two distinct expulsion phases. These reservoirs were mainly charged from the Jurassic Verrill Canyon source rock. The Early Cretaceous reservoirs contain a ratio of 60:10 dry gas and condensate. Although both the Late Jurassic and Early Cretaceous reservoirs may have a porosity >10-15%, both reservoirs will be within the overpressure regime.

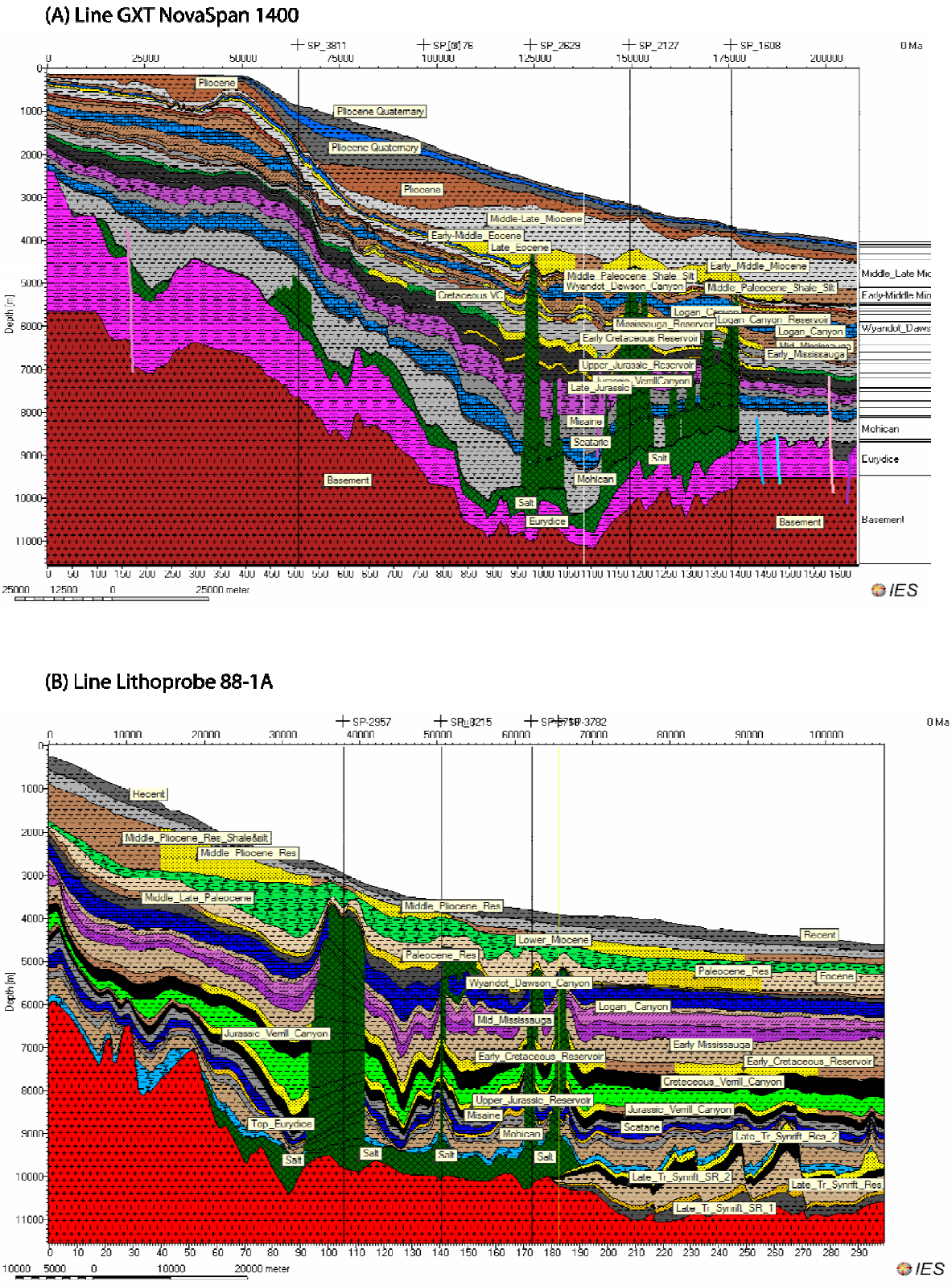


**Figure 2 Lithologic and stratigraphic units interpreted along seismic profiles (A) GXT NovaSPAN 1400 and (B) Lithoprobe 88-1A. Yellow dotted areas are conceptual target sandstone reservoirs and dark and medium gray units are potential source rocks, as identified.**

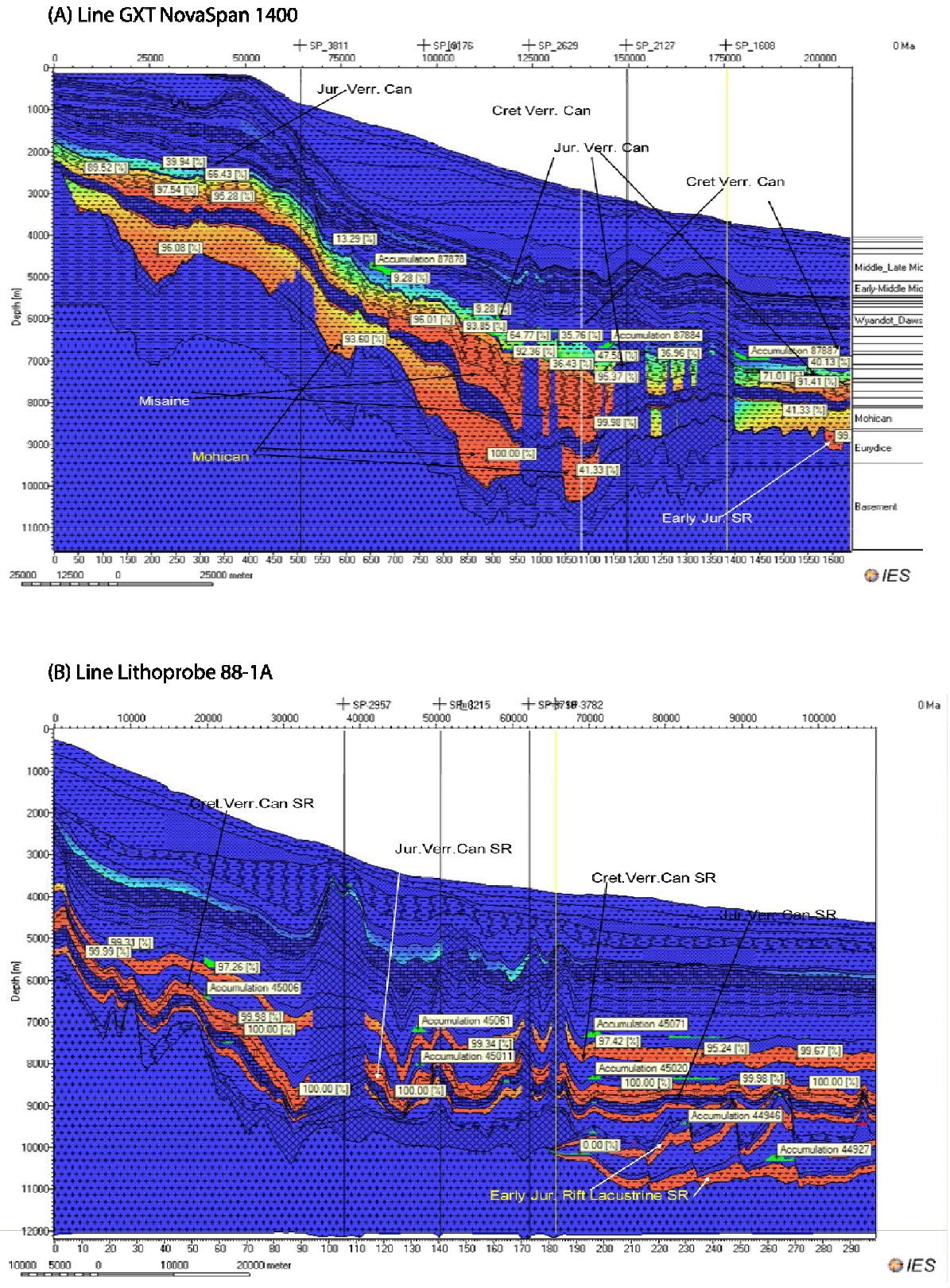


**Figure 3 Simulation output file showing the variations in hydrocarbon transformation ratios in various source rocks and target reservoirs for (A) GXT NovaSPAN 1400 and (B) Lithoprobe 88-1A.**

On line GXT NovaSPAN 1400, the Early Jurassic source rocks occur within the dry gas zone while both the Jurassic and Cretaceous Verrill Canyon source rocks still remain within the oil window (0.5% to 1.35% Ro). Only the source rocks older than the Jurassic Verrill Canyon have expelled more than 50% hydrocarbons. Jurassic Verrill Canyon source rocks have contributed major volumes of hydrocarbons within various reservoirs. The Late Jurassic and Early Cretaceous reservoir hydrocarbons will contain a major component of liquids (>75% for Early Cretaceous with 50% C15+; 40% [low C15+]). The Early Cretaceous reservoirs may lie within moderate pore pressure regime with a temperature <100ºC, while the Late Jurassic reservoirs would remain within the overpressure regime with a temperature >100ºC. These reservoir hydrocarbons were mainly derived from the Jurassic Verrill canyon source rocks. The Late Jurassic reservoir hydrocarbons may contain a liquid to gas mixture of 60:40 with an API of 55º.

**Table 1**

| Seismic Line | Total Mass Generated ($10^9$ kg/m$^3$) | Total Mass Expelled ($10^9$ kg/m$^3$) | Total Mass Accumulated ($10^9$ kg/m$^3$) | Total Hydrocarbons Lost ($10^9$ kg/m$^3$) | Main Hydrocarbon Reservoirs (%) |
|---|---|---|---|---|---|
| Lithoprobe 88-1A | 5253 | 4853 | 247 | 4601 | U. Jurassic (60%)<br>Syn-rift (34%) |
| NovaSPAN 1400 | 6906 | 3165 | 1326 | 1839 | E. Cretaceous (75%)<br>L. Jurassic (25%) |

## Summary

The mass balance reservoir hydrocarbons of both seismic lines (Table 1) indicate that more preserved hydrocarbons could be expected within various reservoirs for line GXT NovaSPAN 1400. For both lines, the salt flank and salt crest Late Jurassic and Early Cretaceous reservoirs could be best for future exploration targets. On line 1400, reservoir hydrocarbons may contain a major volume of liquids (>75% for Early Cretaceous with 50% C15+; 40% [low C15+]) with an API of 45-55º. Jurassic Verrill Canyon is the main source rock for both the Jurassic and Cretaceous reservoirs. On line 88-1A, Early Jurassic lacustrine and Late Jurassic salt-associated marine reservoirs could also become potential exploration targets for future exploration. Both data indicates that stratigraphically older reservoirs (Early Jurassic and Late Jurassic) could be future exploration targets. However, deep drilling is necessary in order to verify these predictions.

Model calculations of present-day sea-floor heat flow predict a gradual landward reduction of 55 mW/m$^2$ in the ultra deep water basin, to 45 mW/m$^2$ on the upper slope. Within this trend, large variations are caused by high conductivity associated with salt diapirs, yielding values as high as 85 mW/m$^2$. There are presently only a few poorly resolved measurements across the slope (Lewis and Hyndman 1976). In July 2008, detailed measurements along both profiles are planned in order to verify these predictions.

## References

Enachescu, M.E. and Hogg, J.R.., 2005. Exploring for Atlantic Canada's next giant petroleum discovery. CSEG Recorder, 30 (5), p.19-30.

Enachescu, M. and Wach, G., 2005. Exploration offshore Nova Scotia: Quo vadis? Ocean-Resources, 23(3), 5p.

Hogg, J.R., 2000, The Scotian basin, new exploration trends for the nest decade, offshore Nova Scotia, Canada: GeoCanada 2000, Conference CD, Abstract No. 1096, 4p.

Jansa, L.F. and Wade, J.A., 1975, Geology of the continental margin off Nova Scotia and Newfoundland: in Offshore Geology of Eastern Canada, Vol. 2, Regional Geology, Van der Linden, W.J.M. and Wade, J.A. (Eds.), Geol. Sur. Can., Paper 74-30, p51-106.

Kidston, A.G., Brown, D.E., Altheim, B., and Smith, B.M., 2002. Hydrocarbon potential of the deep-water Scotian slope, Canada-Nova Scotia Offshore Petroleum Board, 111p.

Lewis, J.F., and Hyndman, R.D., 1976. Oceanic heat flow measurements over the continental margins of eastern Canada, Can. J. Earth Sci., 13, p.1031.

Mukhopadhyay, P.K., 2006. Evaluation of the petroleum systems by 1D and 2D numerical modeling and geochemical analysis in the area of most recent exploration wells on the deepwater Scotian slope, offshore Nova Scotia, Nova Scotia Department of Energy, unpublished report.

Shimeld, J., 2004. A comparison of salt tectonic subprovinces beneath the Scotian Slope and Laurentian Fan, in: Post, P.J. et al. (Eds.), Salt-sediment interactions and hydrocarbon prospectivity: Concepts, applications and case studies for the 21st century, Proc. 24th Bob Perkins Conf., Gulf Coast Section SEPM, p.291-306, CD-ROM, ISSN 1544-2462.

Wade, J.A. and McLean, B.C., 1990. The geology of the southeastern margin of Canada: in Keen, M.J. and Williams, G.L. (Eds.), Geology of the Continental Margin of Eastern Canada, The Geology of North America, Vol. I-1, Geol. Sur. Can., p.169-238.

Welsink, H.J., Dwyer, J.D., Knight, R.J., 1989. Tectono-stratigraphy of the passive margin off Nova Scotia: Extensional Tectonics and Stratigraphy of the North Atlantic Margin, Tankard, A.J. and Balkwill, H.R. (Eds.), Am. Assoc. Pet. Geol., Mem. 46, p.215-231.

Wu, Y., 2007. Crustal structure of the central Nova Scotia margin and the transition from volcanic to non-volcanic rifting off eastern Canada, Ph.D. thesis, Dalhousie University, 341p.

Wu, Y., Louden, K.E., Funck, T., Jackson, H.R., and Dehler, S.A., 2006. Crustal structure of the central Nova Scotia margin off Eastern Canada, Geophy. Jour. Int., 166, p.878-906.

Young, J.L., 2005. The stratigraphy and structural history of the Mesozoic and Cenozoic of the central Nova Scotian Slope, eastern Canada, M.Sc. thesis, Memorial University of Newfoundland, 229p.

**BACK**

# Integrated Late Santonian-Early Campanian Sequence Stratigraphy, New Jersey Coastal Plain: Implications to Global Sea-Level Studies

**Svetlana F. Mizintseva**
**James V. Browning**
**Kenneth G. Miller**
Department of Geological Sciences
Rutgers University
Piscataway, NJ 08854
United States
e-mail: svetik@rci.rutgers.edu

## ABSTRACT

Our studies on New Jersey Coastal Plain indicate existence of the Santonian-early Campanian (Merchantville Formation) unconformity-bounded sequences that originated from sea-level changes. The ages of the Merchantville sequence boundaries are similar to those of Russian platform and northwestern Europe implicating a global cause of their origin. The ages of the Santonian-early Campanian sequences boundaries appear to match the ages of deep-sea benthic foraminiferal $\delta^{18}$ increases from ODP 511 site (Franklin plateau), implying that the Santonian-Campanian $\delta^{18}$ signature was, at least in part, due to development of ice sheets. Miller et al. (2003) explained the presence of ice sheets in the greenhouse world of the Late Cretaceous by proposing that the ice sheets were restricted to Antarctica and paced by Milankovitch forcing. Modeling of Milankovitch forces suggests that about 1/3 of the $\delta^{18}$ increase is attributed to ice and the 2/3 to deep-water cooling. The eustatic falls calculated from Milankovitch orbital solutions are similar to those obtained from the New Jersey margin backstripping analysis. The match of calculated results with our experimental sea-level estimates suggests that the Merchantville sequences on the New Jersey Coastal Plain are connected to the upper Santonian-lower Campanian global climatic variations and provides evidence for existence of small, ephemeral size ice sheets in Antarctica in the greenhouse world.

BACK

# New Profile Models over the U.S. East Coast Continental Margin

**Mark Odegard**
Grizzly Geosciences, Inc.
14019 SW Freeway, Suite 301-735
Sugar Land, TX, 77478
United States
e-mail: meo@grizgeo.com

**Paul J. Post**
U.S. Department of the Interior
1201 Elmwood Park Blvd.
New Orleans, LA, 70123
United States

**William Dickson**
Dickson International Geosciences (DIGs)
10260 Westheimer Rd, Suite 320
Houston, TX, 77042-3160
United States

## ABSTRACT

Profile-based models are excellent for incorporating multiple data sets to illustrate basin architecture. New models across the U.S. East Coast Continental Margin incorporate reprocessed seismic lines, depth-stretched with projected well data, stacking functions and published refraction velocities. Four dip profiles (ranging from 220-480 km each) were tied to a composite (~2,300 km) strike profile; then extended landward and seaward to model long-wavelength crustal variations (from unthinned continental to fully oceanic regimes) defined by our latest gravity and magnetic data.

The seismic interpretation constrains shallower horizons while deep crustal structure derives largely from potential field and published refraction data. Intermediate levels, especially acoustic basement, are revealed as other layers are defined. Models frequently constrain the nature and volume of intrusives such as the lamprophyre dike swarm cored Great Stone Dome (Schlee Dome), and allochthonous salt diapirs, as targeted in the profile model. The feature extents were then interpreted areally, away from seismic coverage, based on gravity and magnetic imagery.

Comparing our profiles with published interpreted and modeled seismic lines; *i.e.*, DNAG volumes, the authors note significant differences. Previously interpreted "salt structures" in the Georges Bank Basin (GBB) do not exist. Salt structures in the Baltimore Canyon Trough (BCT) appear limited to a small, seismically defined diapir and the salt penetrated in the Hudson Canyon 676-1 well on the flank of Schlee Dome. We validated salt structures in the Carolina Trough (CT), although the CT appears to be more complex and separate from the Blake Plateau Basin and BCT. Sediment thickness maxima in the GBB were confirmed on one model and matched to gravity data that improves the definition of previously indicated sub-basins with some exploration potential. Ongoing work is extending the interpretation of the models across the entire margin and will no doubt reveal further interpretation changes.

BACK

# The Lusitanian Basin (Portugal) – Lithostratigraphic and Geodynamic Correlation with other Portuguese and Moroccan basins

**Rui Pena dos Reis**
Dep.Ciências Terra FCTUC, C.Geociências UC
Lg. Mq.de Pombal
3049 Coimbra
Portugal
e-mail: PenaReis@dct.uc.pt

**Nuno Pimentel**
Dep. Geologia e Centro Geologia, FCUL.
Campo Grande C-6, 4º.
1749-016 Lisbon
Portugal
e-mail: Pimentel@fc.ul.pt

**Antônio Garcia**
Núcl.Est.Rec.Nat./D.E.A.
Univ. Federal de Sergipe
Aracaju-SE
Brasil
e-mail: AJVGarcia@yahoo.com.br

## ABSTRACT

The Lusitanian Basin is located at the western Atlantic edge of Iberia, representing the response to the Cretaceous opening of the North Atlantic. It is a conjugate to other basins in northeast North America. However, its Late Triassic to Early Cretaceous evolution reveals important relations with both the Central Atlantic and the Alpine Tethys oceans. This fact can be better understood by looking at other nearby basins, such as the Cacém and Algarve basins (100 and 200 km to the south), and the Moroccan basins of the Atlas (700 km to the southeast). The comparison of the sedimentary infilling of these basins is reviewed, focusing on their paleoenvironmental significance and geodynamic correlation. Opening of the Central Atlantic, Alpine Tethys spreading, linkage with the Central Atlantic and spreading of the North Atlantic, are discussed as the main controls of the Lusitanian Basin's evolution.

## Introduction

The Iberian and northern Morocco regions are located in the eastern edge of the Central-North Atlantic (Fig. 1), therefore sharing evidence of the main regional geodynamic controls. These regions were affected by a strong tectonism at the end of Paleozoic times, associated to the Pangea accretion, and by the break-up of that supercontinent at the early Mesozoic. This created several marginal basins that are exposed today along the Atlantic margins of Iberia and in the Atlas mountain chain (Morocco). The stratigraphic successions preserved in those basins record major basinal events and present strong signatures influenced by the Tethys Ocean to the east, and later by the opening of the Atlantic Ocean to the west.

The purpose of the study is to compare the major basins in the western and southern borders of the Iberian plate (Lusitanian Basin, with its north, centre and south sectors, Santiago do Cacém Basin, Algarve Basin - data from Azerêdo *et al.* 2003; Rey *et al.*. 2006; and Pena dos Reis *et al*. 2008) and the

High Atlas Moroccan Basin.(data from Pique *et al*. 2007; and Souhel *et al*. 2007) (Fig. 1). This approach has been taken in order to assess the signals of the major geodynamic events and to improve regional paleogeographic reconstructions.

**Fig. 1. Location of the Lusitanian Basin and other basins referred in this work at the eastern edge of the North and Central Atlantic. 1, 2 & 3 – Lusitanian Basin: North, Central and Southern Sectors; 4 – Santiago do Cacém Basin; 5 – Algarve Basin; 6 – Northern Morocco Atlas Basin.**

## Correlation and Geodynamic Steps

A comparative approach to these basins supports important geodynamic correlations related to the opening of the Central and North Atlantic, as well as the spreading of the Alpine Tethys and detachment of the Iberian plate.

The areas considered in this study are thought to have been bounded at early Mesozoic times by different continental blocks (Iberia, Northwest Africa, Grand Banks and North America, as proposed in Fig. 3), being influenced by three major oceanic domains: the Central Atlantic to the south, the Western Tethys to the east, and North Atlantic to the west (Manspeizer 1988; Ziegler 1988; Cavazza *et al*. 2004).

This broad framework encompasses comparison of the different basins through the description of their infill successions with a set of eight major geodynamic steps are defined that span from the Late Triassic until the latest Cretaceous (Fig. 2). The paleogeographic and geodynamic framework for some of these steps are presented in Figure 3 as an attempt to integrate the different basins into a regional framework.

### Step 1

The initial rifting episode has a Central Atlantic rifting signature, related with the Sinemurian break-up in the western Moroccan margin (Fig. 3). Step 1 began during Late Triassic times and led to the definition of a system of sub-meridian grabens and half-grabens filled with siliciclastic red beds and capped by a broad evaporitic event in every basin that marks the Hettangian transition to the post-rift interval. The volcanics associated to the top of the evaporitic deposits may be correlated to the CAMP event. They gradually decrease to the North as they get further away from the rifting sector, thus underlining a Central Atlantic signature, which faded out prior to the transgression of Step 2.

### Step 2

The southern intra-continental rifting changed to oceanic spreading in the western Morocco sector. There is a general marine invasion, starting with the installation of lagoonal sabkha systems and grading later into shallow carbonate platform geometries in most places. Dolomitic deposition seems to be dominant in most of the basins, related with shallow seas with meteoric influences.

### Step 3

A major regional unconformity underlines the beginning of the Step 3. This is characterized by a general and rapid deepening in every basin, except in two small sectors (Arrábida and Santiago do Cacém Basins), possibly due to some structural control inhibiting stronger subsidence between the Algarve and the Lusitanian basins. Large carbonate-marl ramps developed by then, and most of the domains contain high TOC in bituminous shaly marls, these being considered as very promising source rocks. These changes are interpreted as the result of a major syn-rift event in the Tethyan realm.

### Step 4

The rift event described in Step 3 changed to post-rift in the Atlas Basin (Early Toarcian), several million years earlier than in the other Portuguese basins (Early Aalenian) suggesting a northward propagation of the rifting influence. These changes are recorded in basin-wide unconformities, whose expression is a long hiatus observed in the Atlas Basin (Fig. 2) that gradually disappears northwards. In the northern Lusitanian Basin, it corresponds just to a short depositional hiatus (*ca.* 1 Ma), and is only detectable due to detailed biostratigraphic control. The change in sedimentation shows an overall tendency to prograding carbonate platforms as the accommodation space decreased.

### Step 5

Step 4 ends with a broad uplift event, leading to a shallowing-upward sedimentation pattern and later karstification of the carbonate platforms. These changes are recorded by a major unconformity with a variable hiatus duration of late Callovian to early Oxfordian age. The ocean spreading in the Central Atlantic sector must have produced an eastwards migration of the African plate promoting the lining-up of the Lusitanian rifting with the Central Atlantic spreading. As a result, an intense period of rifting occurred, followed by a progradation of a thick clastic sequence that records both terrestrial and deep marine systems. This Atlantic influence is also suggested by the southwestward orientation of the drainage patterns and the deeper systems to the southwest in the Lusitanian Basin's sedimentary record.

At this time, terrestrial sedimentation was occurring in the Atlas Basin that was still connected to the Tethyian domain.

According to different palaeogeographic reconstructions, during most of the time between earliest Jurassic until latest Jurassic, the West Iberian basins were separated from the Central Atlantic by the Grand Banks continental block. This explains why during the first rifting episode and subsequent sag interval that the marine influence was dominated by the Tethys Ocean, with marine incursions coming in from both a northern Iberian boreal corridor and southern Mesogean Tethys domain.

### Step 6

Following this major intra-continental rifting event, the drifting phase related with the North Atlantic rifting and spreading offshore the Lusitanian Basin began to set up at the end of Berriasian (earlier Cretaceous). Different authors suggest a three-step northward propagation of the North Atlantic Ocean spreading initiation. This is recorded in different sectors by three major surfaces, each overlain by clastics, and are interpreted as break-up unconformities. The data points to the rifting beginning via a south branch of 300 km in length, followed by a central branch about 200 km long and a finally a northern branch of 300 km long, all separated by transform faults. The complete process is thought to have duration of c.30 Ma. As a result of this process, the Tethys influence was definitely interrupted, leading to an Atlantic-directed drainage system in every sector, including in the High Atlas Basin.

### Step 7

Step 7 is marked by a global eustatic sea level rise (Cenomanian-Turonian transgression) defining a transgressive pattern with shallow open platform carbonates recorded in all the basins of the considered area. There is already a clear Atlantic context which is spreading everywhere in the region.

### Step 8

In the northern border of Iberia, changes related with local geodynamic accommodation between moving plates lead to a north–south compression from the late Cretaceous on, initiating the Tertiary inversion of different basins and sectors, with erosional areas, uplift and installation of mostly terrestrial depositional systems.

## Conclusions

The analysis of the respective basin's sedimentary successions together with comparison of their interpreted tectonic controls, reveal five significant insights:

1. There is a set of major unconformities that separate depositional packages and can be followed across several basins in the region.
2. These surfaces display some minor variations in timing and duration, suggesting differences in accommodation space related to the controlling factors.
3. It is possible to model, as shown, the combination of both Atlantic and Tethys influences as far as geodynamic changes are concerned.
4. The Tethys influence is dominant during the early Mesozoic times, whereas the Atlantic signature is prominent in late Jurassic and beyond.
5. The paleogeographic influence of the Grand Banks continental block is likely to have been very relevant in separating the Iberian basins from the Central Atlantic influences during the early Jurassic times.

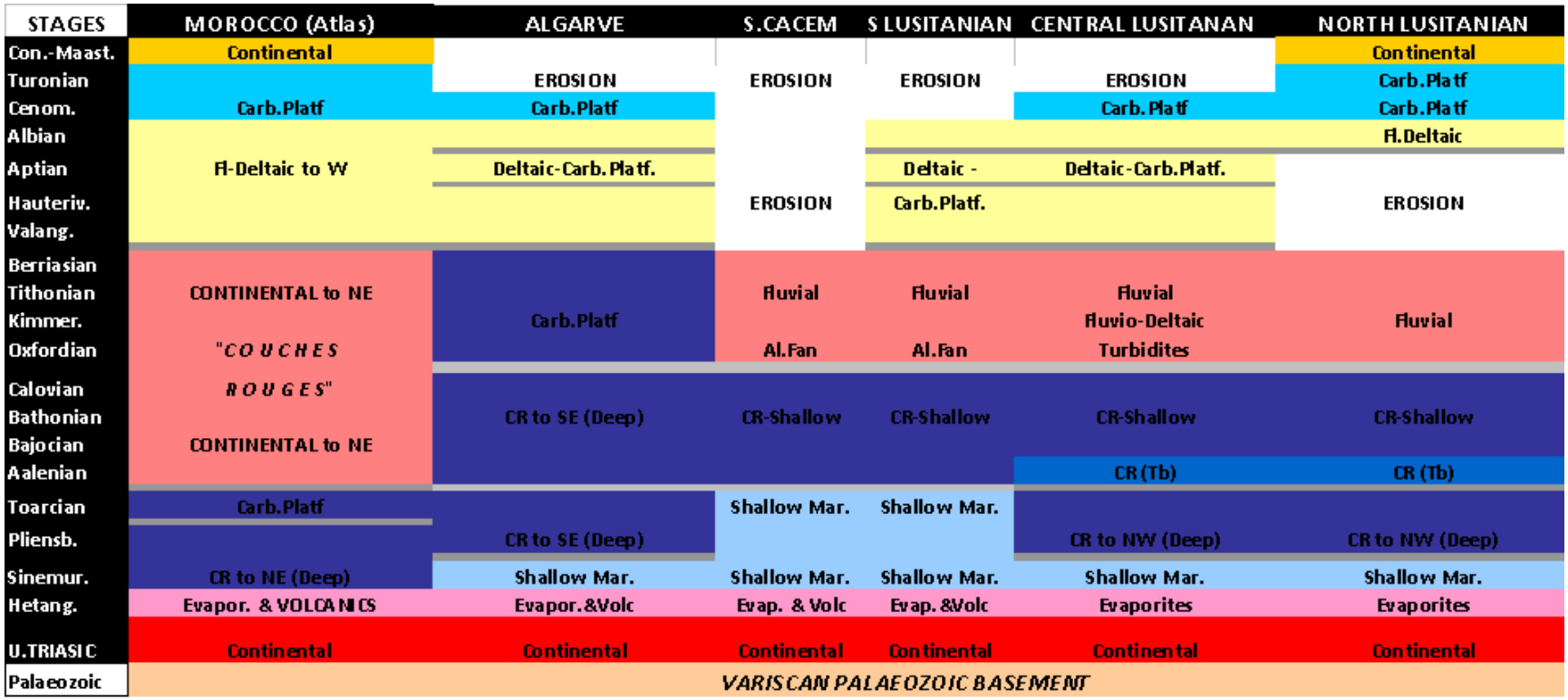


**Fig. 2 – Correlation between the synthetic columns of the sedimentary filling of the studied basins (emphasis on their paleoenvironmental significance) with geodynamic steps numbered from 1 to 8 (see text for explanations). Unconformities are represented as gray horizontal lines and by white horizontal bars whenever they include a significant depositional hiatus. Data from Azeredo *et al.* 2003; Rey *et al.* 2006; Pique *et al.* 2007; Souhel *et al.* 2007; Pena dos Reis *et al.* 2008.**

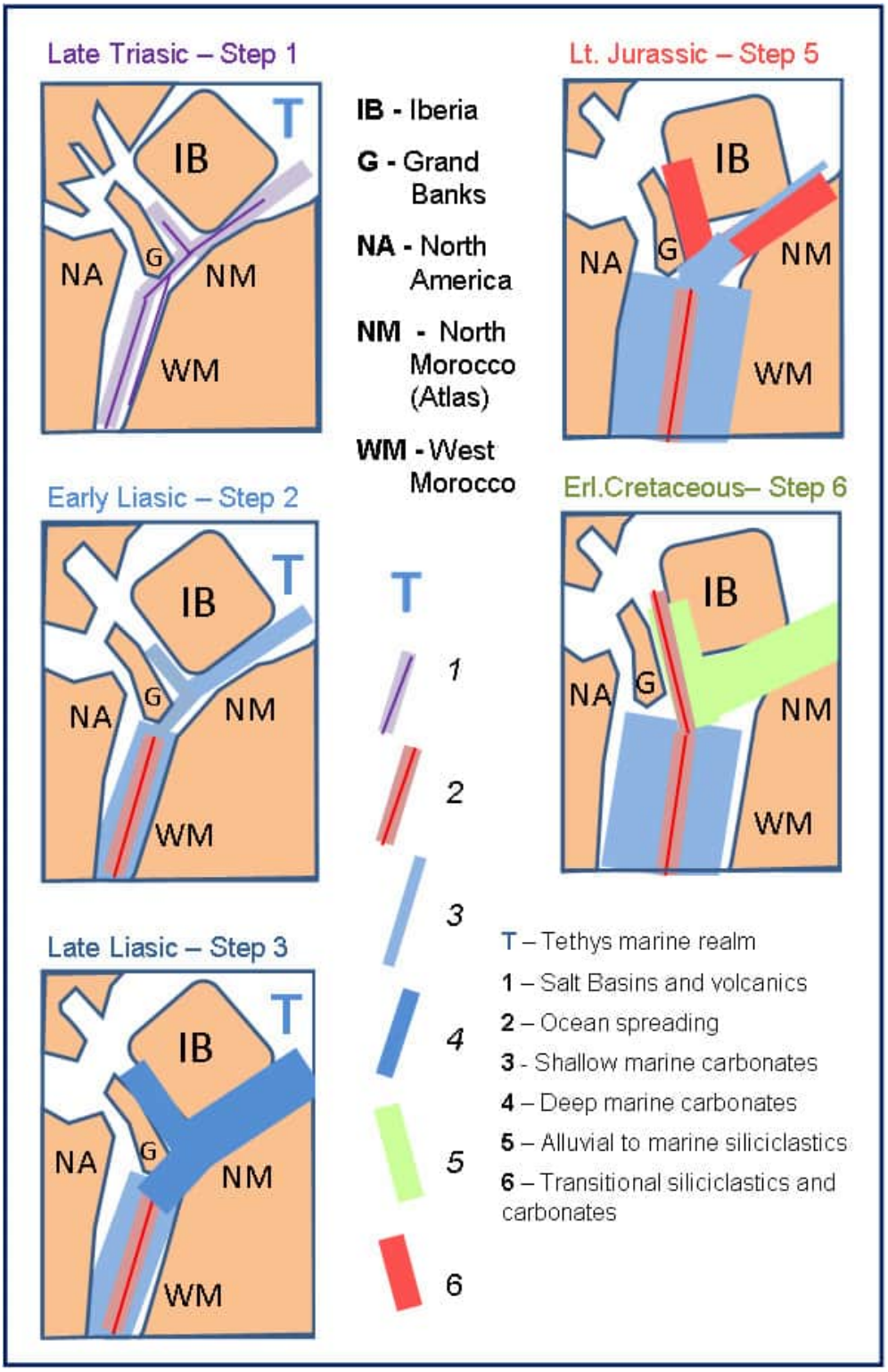


**Fig. 3 – Schematic paleogeographic reconstructions for the main steps defined in this work (*see* Figure 2), as a proposal for the integration of the Lusitanian Basin in its regional geodynamic framework.**

## References


Azerêdo, A.C.; Duarte, L.V.; Henriques, M.H.; Manuppella, G. (2003) - Da Dinâmica Continental no Triásico aos Mares do Jurássico Inferior e Médio. *Cad. Geol.Portugal*, INETI, Lisboa, 43p.

Cavazza, W.; Roure, F.; Spakman, W.; Stampfli, G.M.; Ziegler, P.A. (Eds.) (2004) - *The TRANSMED Atlas. The Mediterranean Region from Crust to Mantle*. Geological and Geophysical Framework Mediterranean Consortium for the 32nd International Geological Congress. 141p.

Manspeizer, W. (Ed.), 1988 - Triassic-Jurassic Rifting, continental breakup and the origin of the Atlantic Ocean and Passive Margins. Developments in Geotectonics 22, Part A & Part B, 998p. Elsevier, Amsterdam.

Pena dos Reis, R.P.; Pimentel, N.L. & Bueno, G.V. (Eds.) (2008) – *III Curso de Campo na Bacia Lusitânica – Roteiro*. Coimbra, 140p.

Pique, A.; Soulaimani, A.; Hoepffner, C.; Bouabdelli, M. ; Laville, E. ; Amrhar, M. ; Chalouan, A. (2007) - *Geologie du Maroc*. Ed. Geode, 287p.

Rey, J. ; Dinis, J.L., Callapez, P; Cunha, P.P. (2006) - Da Rotura Continental à Margem Passiva, Composição e Evolução do Cretácico de Portugal. *Cad. Geol.Portugal*, INETI, Lisboa, 75p.

Souhel, A.; Ettachfini, El.M.; Hariri, K. El; Canérot, J. Chafiki, D.; Bchari, F.El; Lowner, R. (2007) – *From rifting to collision in Central High Atlas: sedimentary and tectonic evolution of na intracontinental peri-tethyan basin*. MAPG International. Conference.& Exhibition., Field Trip Guidebook Exc.5, 70p., Marrakech.

Ziegler, P.A. (1988) – Post-Hercynian plate reorganization in the Tethys and Arctic – North Atlantic domains. *In* Manspeizer, W. (Ed.): *Triassic-Jurassic Rifting, continental breakup and the origin of the Atlantic Ocean and Passive Margins,* p.711-755.


**BACK**

# Controls on Facies Distribution and Reservoir Development of Upper Triassic Continental Systems in Intermontane Rift Settings: A Comparative Study of Extensive Outcrops in Southwest Morocco

**Jonathan Redfern**
**Ivan Fabuel Perez**
**David Hodgetts**
University of Manchester
School of Earth Atmospheric and Environmental Sciences
Williamson Building, Oxford Road
Manchester M13 9PL
United Kingdom
e-mail: jonathan.redfern@manchester.ac.uk

**Nadine Mader**
Hess
Level 9
The Adelphi Building
1-11 John Adam Street
London WC2N 6AG
United Kingdom

**Abedelmajid El Ouataoui,**
ONHYM
34, Avenue Al Fadila
BP 8030 NU
10500 Rabat
Morocco

## ABSTRACT

Upper Triassic (Carnian) sediments in southwest Morocco comprise a continental red bed sequence deposited in discrete rifted basins following the break up of Pangea and opening of the Atlantic. This comparative study examines extensive outcrops of the Oukaimeden Sandstones Formation (F5) in the High Atlas and Unit T6 in the Argana Basin, SW Morocco, deposited within a series of narrow fault bounded intermontane basins. Both contain a variety of braided fluvial, overbank, shallow ephemeral lacustrine, alluvial fan and aeolian facies.

Traditional sedimentological data (sedimentary facies logs, palaeocurrent information, gamma ray logs etc) has been combined with high resolution 3D laser (LIDAR) and Differential Global Positioning System (DGPS) to map these outcrops and provide a detailed dataset.

On a basin scale, the often complex facies distribution evident in the Argana Basin suggests a highly variable fill within these basin types. Correlation of individual facies elements is often difficult and relies on identification of key stratal surfaces. Local tectonics control accommodation and influences facies patterns, such as development of alluvial fans and entry points of major drainage systems. Significant changes in fluvial style, from ephemeral to perennial, are recognized in both basins within this interval, which suggests rejuvenation of the source areas and a potential interplay of climatic and tectonic control. An overall drying upward pattern is observed, with increasing influence of aeolian processes towards the top of both the Oukaimeden sandstone (F5) and T6 of Argana. This supports previous work

that has demonstrated a change from humid to increasingly arid conditions during the Upper Triassic, recognized both throughout southwest Morocco and in the Fundy Basin, Canada, and highlights the climatic control on the depositional system.

These studied sections offer potential analogues for subsurface Triassic hydrocarbon systems in similar settings, and provide valuable information on the tectonic and climatic control on depositional facies and architecture. Analysis of basin-wide facies variation, provenance and sediment pathways provide regional scale analogue data. More detailed field scale reservoir models have also been developed for the high net-to-gross intervals in the Oukaimeden sandstone.

## Introduction

Upper Triassic (Carnian) sediments in southwest Morocco comprise a continental red bed sequence deposited following the break up of Pangea and opening of the Atlantic, strongly influenced by a low palaeolatitude (between 10° to 20° N) climatic regime. This comparative study examines extensive outcrops of the Oukaimeden Sandstones formation (F5) in the High Atlas Oukaimeden Basin, and the Tadrart Ouadou Sandstone member (T6) in the Argana Subbasin in southwest Morocco. Both contain a variety of braided fluvial, overbank, shallow ephemeral lacustrine, alluvial fan and aeolian facies, deposited within fault bounded intermontane basins. The study combines traditional sedimentological data (sedimentary facies logs, palaeocurrent information, gamma ray logs etc) with high resolution 3D laser (LIDAR) and Differential Global Positioning System (DGPS). The comparison between these basins provides valuable regional information on the tectonic and climatic control on depositional facies and architecture, and offers potential analogues for subsurface hydrocarbon systems in similar settings.

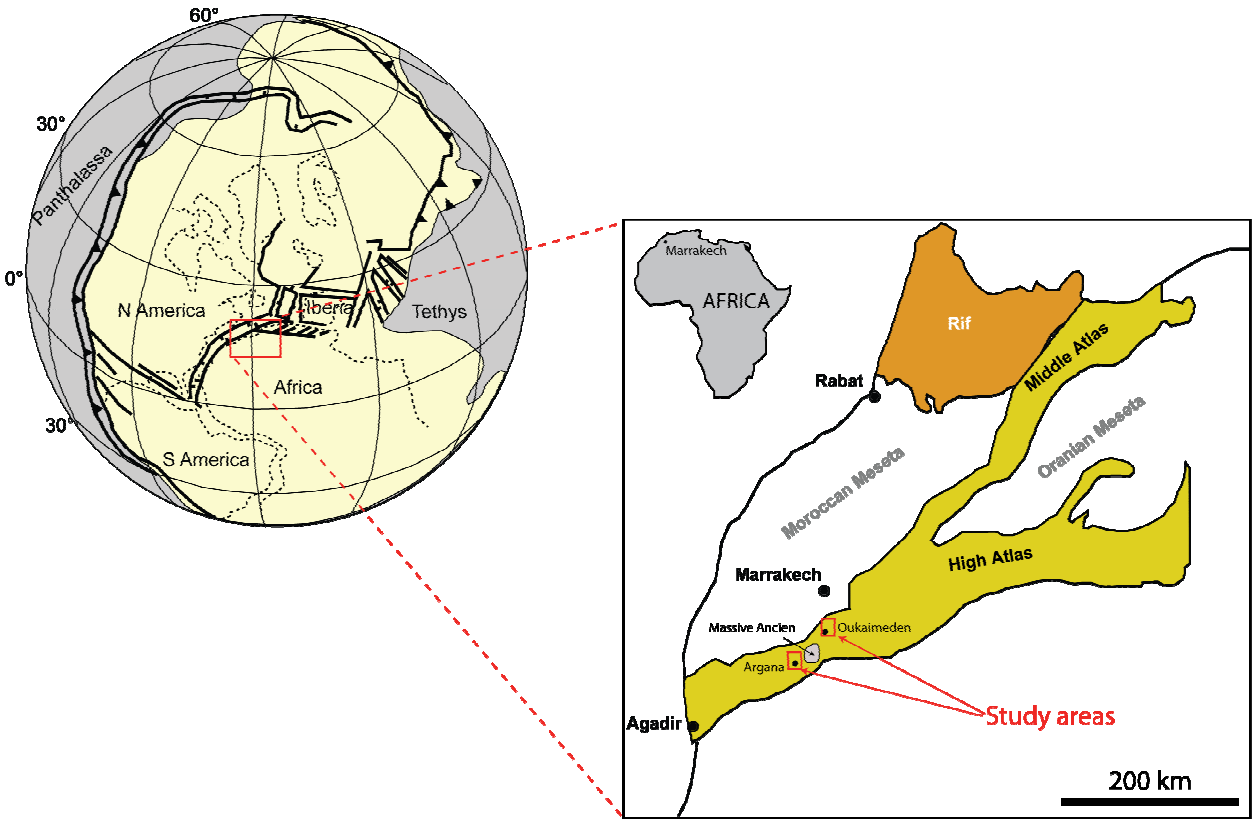


**Figure 1. Location Map of studied basins in southwest Morocco, showing the outline of the High Atlas. Global palaeogeography adapted from Ziegler (1990).**

## Location

Upper Triassic continental deposits were examined in two areas located in southwest Morocco (Fig. 1). The Argana outcrops are exposed along the southwest flank of the High Atlas mountain chain (Fig. 2), and the Oukaimeden deposits are located within the High Atlas (Fig. 3). Both basins are fault controlled. They are separated by the Ancien Massif, which was a positive feature formed during the Hercynian, acted as a major sediment source.

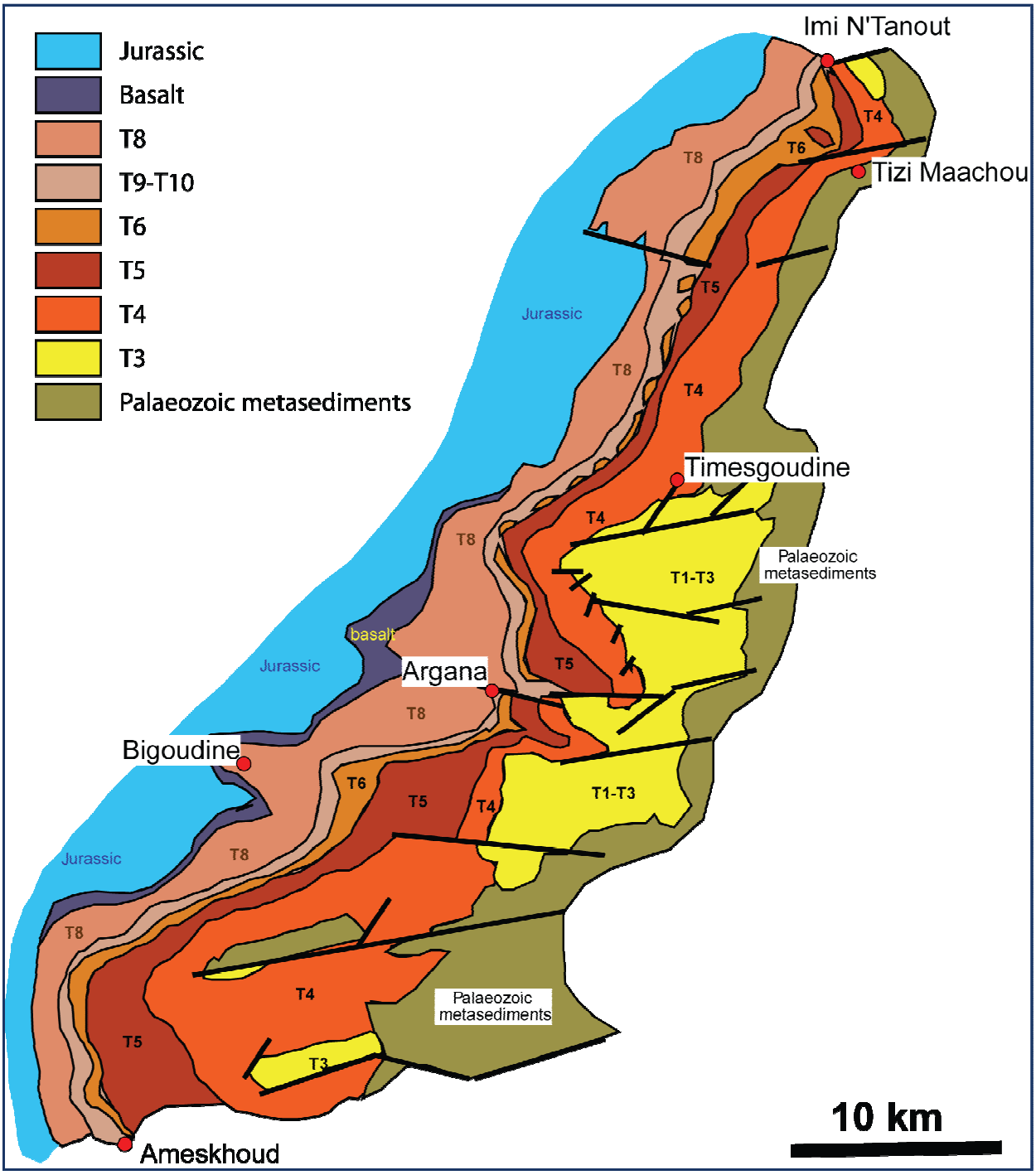


**Figure 2. Simplified geological map of the Argana Basin (based on Tixeroint 1973)**

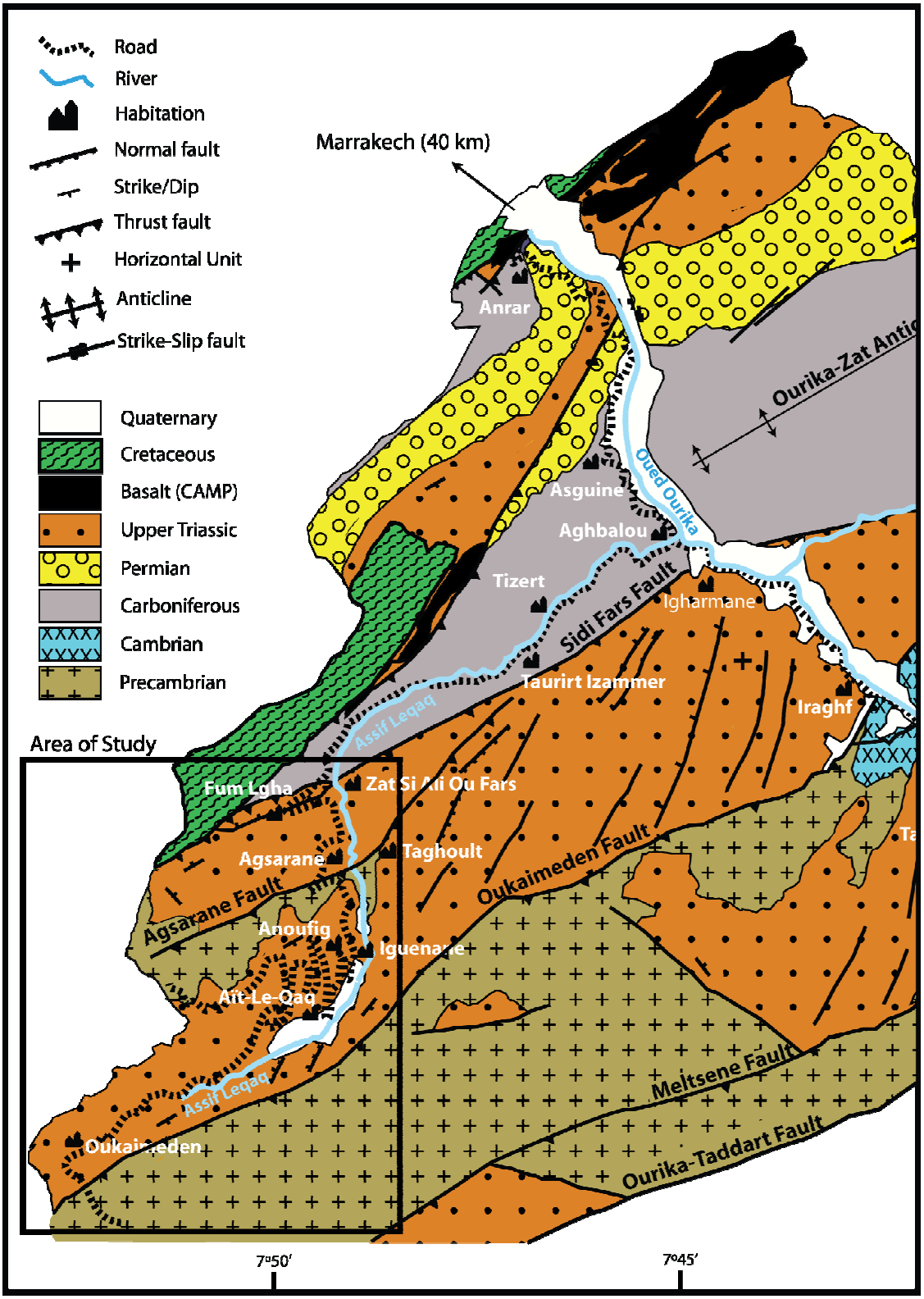


**Figure 3. Simplified geological map of Oukaimeden**

## Stratigraphy

The Permian and Triassic successions overlie a major unconformity developed on rocks deformed by the Hercynian and older orogenies and are conformable with the overlying Jurassic marine deposits (Van Houten 1977). In both basins dating of this interval is generally poor due to the dominantly continental nature of the deposits.

Initial deposition is coarse continental clastics; the T1 and T2 in Argana (Tixeront 1973) and F1 and F2 in Oukaimeden (Mattis 1977; Biron 1982). These have been dated as possibly Permian using paleontological (Dutuit 1976), radiometric (Van Houten 1977) and palynomorphic data (Cousminer & Manspeizer 1975; Olsen *et al.* 2003a & b, 2005). Units T3 to T7 in Argana and F3 to F6 in Oukaimeden are Upper Triassic in age (Cousminer & Manspeizer, 1975). The Tadrart Ouadou Sandstone Member (T6) is Upper Carnian to Lower Norian age (Tourani *et al.* (2000). The Oukaimeden sandstone (F5) is also tentatively dated as Carnian based on palynoflora (Biron and Courtinat 1982). Lower Triassic assemblages have not been recovered to-date in any location (Cousminer & Manspeizer 1975; Olsen *et al.* 2003a; Olsen *et al.* 2003b).

## Depositional Facies

The Upper Triassic section in both basins is dominated by continental, mixed fluvial-aeolian deposits, which record high degree of lateral facies variability (Fig. 4). A number of facies associations have been recognized: Alluvial Fan, Braided River Fluvial Facies, Floodplain (Playa), Aeolian and Tidal (Oukaimeden only)

Detailed correlation of the T6 and F5 intervals shows similar facies and depositional evolution. The basal depositional environments of both the T6 and F5 represent contemporaneous coarse alluvial fan and ephemeral fluvial braidplain deposits. In the Argana Subbasin, a major fluvial bounding surface recognized midway within T6 has been interpreted as a regional re-activation surface, and is believed to have been formed in response to a change in fluvial regime from ephemeral to perennial. This records a probable change in climate in the hinterland source province. In Argana, an axial drainage system flowed from north to south and was fed by several channel systems from the east/northeast/north, sourced in part from the Ancien Massif. A similar pattern can be seen in the Oukaimeden, with a significant erosional surface marking the change to a perennial system within the middle member of the F5. The overlying package comprises a major package of stacked sandstones deposited in a low sinuosity braided channel belt sourced from the Ancien Massif, in this case flowing to the northwest.

The upper part of the succession in both areas is marked by mixed fluvial–aeolian deposition. The recognition of extensive aeolian facies is interpreted to indicate a regional change to more arid conditions. In Oukaimeden, the top of the succession is characterised by the presence of tidally influenced facies recording the first marine incursion into the basin from Tethys to the northeast. No marine influence was recorded in Argana, suggesting the Massif Ancien remained a positive feature at this time. Both the T6 and F5 are capped by a mudstone dominated units (F6 and T7), and a regionally extensive basalt that provide a regional correlation surface.

## Climatic Versus Tectonic Controls

Sedimentary facies distribution, both spatially and temporally, is strongly influenced by the interplay between tectonics and climate. Basin architecture is controlled by tectonics, which has a significant influence on facies distribution. The main fluvial systems show strong tectonic control on their location, with axial river systems parallel to the main bounding faults and lateral drainage comprising alluvial fans and feeder river systems entering at fault linkage/ transfer zones. The basin bounding faults have controlled accommodation, local sediment input and the orientation of the main channel belts. Local erosion of footwall highs in both basins has acted as a source for coarse alluvial fan breccias. Floodplain and/or aeolian sediments predominate in areas of reduced accommodation, or away from the main drainage systems.

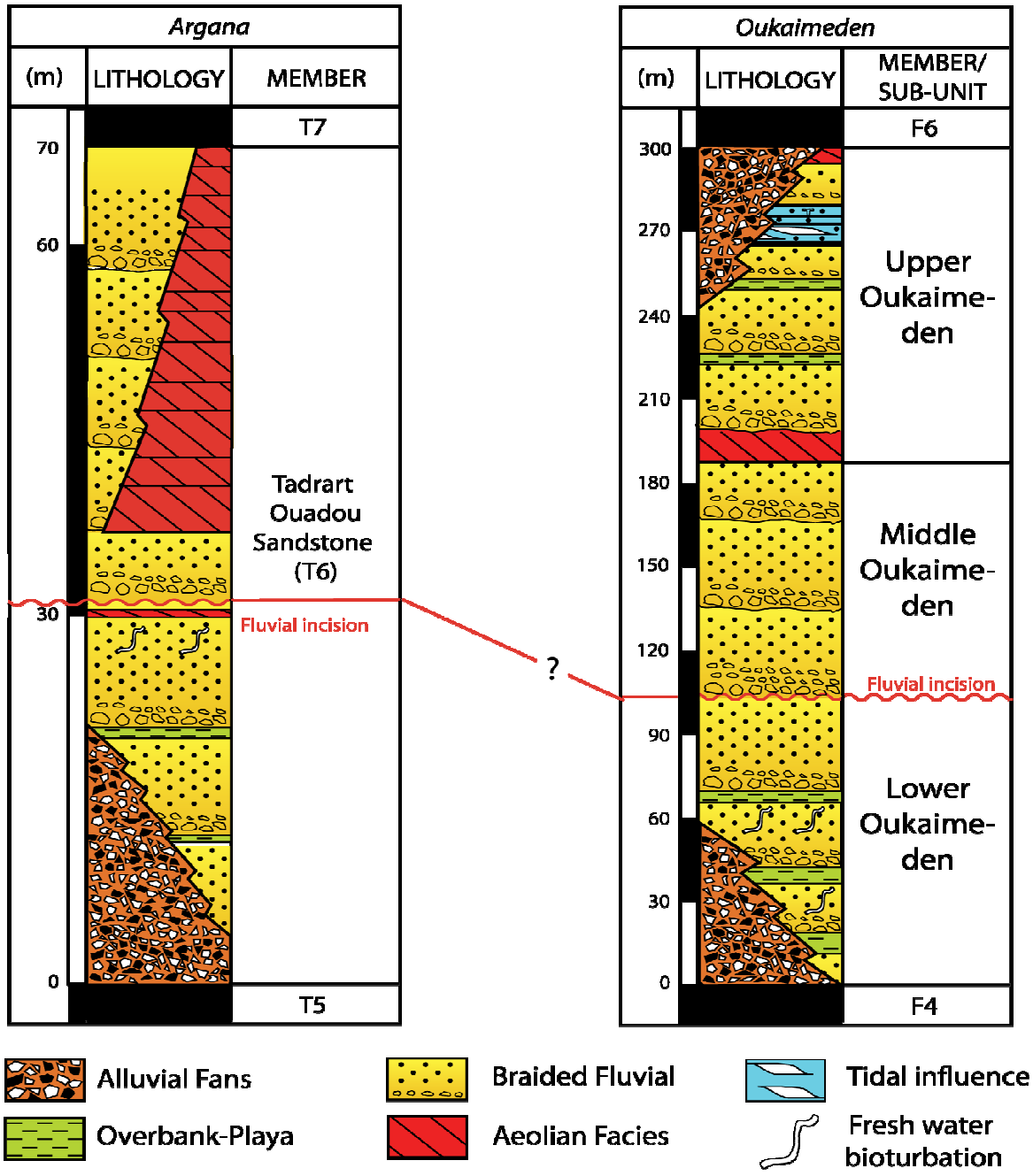


**Figure 4. Correlation of the studied interval, the Oukaimeden Formation (F5) in the Ourika Valley and Tadrart Ouadou Sandstone Member (T6) of the Argana sub-basin, highlighting the main facies recorded and correlated surfaces.**

A major erosion surface within units T6 and F5 is tentatively correlated between basins (Fig. 4), marking a change from ephemeral to perennial fluvial conditions. This is interpreted to record a regional change to a wetter climatic in the hinterland resulting in increased run-off from the catchment area. This was followed by widespread aeolian dune deposition in both studied areas that is interpreted to record a climatic shift back to dry conditions. The evolution towards a more arid climate has also been observed in other Triassic basins along the Central Atlantic conjugate margins (Olsen *et al.* 1996; Smoot 1991; Olsen 1997; Arche and Lopez-Gomez 2005).

## Conclusions

On a basin scale, the complex facies distribution evident in these basins suggests a highly variable basin fill. Correlation relies on identification of key stratal surfaces and architectural styles because of the lack of biostratigraphic control or any other chronostratigraphic surfaces. In both the Argana and Oukaimeden basins, local tectonics control accommodation and influences facies patterns, such as development of alluvial fans and entry points of major drainage systems. Significant changes in fluvial style, from ephemeral to perennial, are recognized within the studied intervals, which suggests rejuvenation of the source areas and a potential interplay of climatic and tectonics. An overall drying upward pattern is observed, with increasing influence of aeolian processes towards the top of both the Oukaimeden sandstone (F5) and Tadrart Ouadou Sandstone member (T6) of the Argana.

These studied sections offer potential analogues for subsurface hydrocarbon systems in similar settings, and provide valuable information on the tectonic and climatic control on depositional facies and architecture. Analysis of basin-wide facies variation, provenance and sediment pathways provide regional scale analogue data.

## References


Arche, A. and Lopez-Gomez, J., 2005. Sudden changes in fluvial style across the Permian-Triassc boundary in the eastern Iberian Ranges, Spain: Analysis of possible causes. Palaeogeography, palaeoclimatology, palaeoecology, 229 (1-2): p.104-126.

Biron, P. and Courtinat, B., 1982. Contribution palynologique à la connaissance du Trias du Haut Atlas de Marrakech. Geobios, 15 (2): p.231-235.

Cousminer, H. and Manspeizer, W., 1976. Triassic pollen data Moroccan High Atlas and the incipient rifting of Pangaea as Middle Carnian. Science, 191: p.943-945.

Dutuit, J.M., (1976). Introduction à l'étude paléontologique du Trias continental marocain. Description des premièrs Stégocéphales recueillis dans le couloir d'Argana. Mém. Mus. Natn. Hist. nat., Paris C 36: p.253.

Dutuit, J.M., (1977). Palaeorhinus magnoculus, phytosaure du Trias supérieur de l'Atlas Marocain. Géologie Méditerranéenne 4: p.225-238.

Dutuit, J.M., (1988). Diplocaulus minimus n. ps. (Amphibia; Nectridea), Lepospondyle de la formation d'Argana, dans l'Atlas occidental marocain. C.R. Acad. Sci. Paris II 307: p.851-854.

Hunt, A.P. and Lucas, S.G., (1991). The Palaeorhinus Biochron and the correlation of the non-marine Upper Triassic of Pangaea. Palaeontology 34: p.487-501.

Jalil, N.E., (1999). Continental Permian and Triassic vertebrate localities from Algeria and Morocco and their stratigraphical correlations. Journal of African Earth Sciences 29(1): p.219-226.

Jalil, N.E. and Dutuit, J.-M., (1996). Permian captorhinid reptiles from the Argana Formation, Morocco. Palaeontology 39(4): p.907-918.

Lucas,S.G., (1998). Global Triassic tetrapod biostratigraphy and biochronology. Palaeogeography, Palaeoclimatology, Palaeoecology 143: p.347-384.

Olsen, P. E. and Kent, D. V., 1996, Milankovitch climate forcing in the tropics of Pangea during the Late Triassic. Palaeogeography, Palaeoclimatology, and Palaeoecology, v.122, p.1-26.

Olsen, P. E. 1997. Stratigraphic record of the early Mesozoic breakup of Pangea in the Laurasia-Gondwana rift system. Annual Reviews of Earth and Planetary Science v.25, p.337-401.

Smoot, J.P. 1991. Sedimentary facies and depositional-environments of early Mesozoic Newark supergroup basins, Eastern North-America. Palaeogeography, Palaeoclimatology, and Palaeoecology, v.84 (1-4), p.369-423.

Olsen, P.E., Kent, D.V., Et-Touhami, M., Puffer, J.H., 2003a. Cyclo-, magneto-, and bio-stratigraphic constraints on the duration of the CAMP event and its relationships to the Triassic-Jurassic boundary. The Central Atlantic Magmatic Province: Insights From Fragments of Pangaea, Geophysical Monograph Series, 136: p.7-32.

Olsen, P.E., Kent, D.V., Sues, H.D., Koeberl, C., Huber, H., Montanari, A., Rainforth, E.C., Fowell, S.J., Szajna, M.J., Hartline, B.W., 2003b. Ascent of dinosaurs linked to an iridium anomaly at the Triassic-Jurassic boundary (Reply to Thulborn). Science, 301: p.169.

Tixeront, M., (1973). Lithostratigraphie et minéralisations cuprifères et uranifères stratiformes syngenetiques et familières des formations detritiques permo-triassiques du couloir d'Argana, Haut Atlas occidental (Maroc). Notes du service geologique du Maroc 33 (249): p.147-177.

Tourani, A., Lund, J. J., Benaouiss, N. and Gaupp, R., (2000). Stratigraphy of Triassic syn-rift deposition in Western Morocco. Zentralblatt für Geologie und Paläontologie, Teil 1, Heft 9-10: 1193-1215.

Van Houten, F. B., (1977). Triassic-Liassic deposits of Morocco and E North America: comparison. AAPG Bulletin 61 (1): p.79-99.

Ziegler, P. A. (1990). Geological Atlas of Western and Central Europe. The Hague, Shell Internationale Petroleum Maatschappij.

**BACK**

# Lithospheric Density Variations and Moho Structure of the Irish Rifted Continental Margin from Constrained 3D Gravity Inversion

**J. Kim Welford**
**Jeremy Hall**
Memorial University of Newfoundland
Department of Earth Sciences
300 Prince Philip Drive
St. John's, Newfoundland A1B 3X5
Canada
e-mail: kwelford@mun.ca
e-mail: jeremyh@mun.ca

**Brian O'Reilly**
Dublin Institute for Advanced Studies
5 Merrion Square
Dublin 2
Ireland
e-mail: bor@cp.dias.ie

## ABSTRACT

The structurally complex Irish margin was separated from its conjugate pair, the northern Flemish Cap/Orphan Basin region, during Late Cretaceous rifting of the North Atlantic. Whilst crustal-scale 2D seismic surveys have been collected across many parts of the margin, the results generated from these surveys cannot easily be interpreted in a regional sense due to their sparse sampling. We have undertaken a 3D gravity inversion of the free air data over the Irish margin in order to generate a 3D density anomaly model that can be compared with the seismic results and used to gain insight into regions lacking seismic coverage. We use the GRAV3D inversion algorithm and constrain our inverted model with bathymetric and sediment thickness information. We are able to closely reproduce the observed gravity anomalies over the margin and use the resultant density anomaly model to interpret the regional Moho structure by identifying a density isosurface appropriate for the crust-mantle transition. Our interpreted Moho shows good correspondence with Moho depths from seismic results whilst providing a more detailed Moho depth map over the region. This map allows the lateral extent of crustal thinning beneath the Rockall Trough, the Porcupine Seabight Basin and south of Goban Spur to be investigated. We present regional cross-sections through the 3D model to highlight lateral variations in Moho structure and lithospheric densities. We also compare sediment and crustal thickness across the margin to show deviations from local isostatic compensation. These deviations correlate with faults and rifting trends along the boundaries of most of the main structural features. Ultimately, the insights provided by our results must act as constraints for future paleoreconstructions of North Atlantic rifting.

## Introduction and Tectonic Setting

Potential field methods provide a tool for bridging gaps in seismic coverage and tracking deep structures regionally. With the development of algorithms for 3D inversion of gravity data which can incorporate geological and geophysical constraints (*e.g.,* Li and Oldenburg 1998), regional density anomaly models for rifted continental margins can be constructed which satisfy geometrical constraints from existing seismic profiles and which provide information about unsampled regions. We undertake a 3D gravity inversion study over the Irish rifted continental margin in order to enhance existing knowledge

about regional crustal structures and to provide insights for future palaeoreconstructions of the North Atlantic region prior to rifting.

Separation of the Irish continental margin from its conjugate pair, the northern Flemish Cap/Orphan Basin region of Newfoundland, Canada, occurred during the Late Cretaceous (Tucholke *et al.,* 1989; Hopper *et al*., 2006). As a consequence of the rifting that led to this separation, a number of offshore basins developed on the Irish continental margin, with the geometry of these basins controlled largely by pre-existing Caledonian and Variscan basement structures and fabrics (Shannon, 1991). The Caledonian basement structures and fabrics trend southwest/northeast and resulted from the closing of the Iapetus Ocean by late Ordovician and Silurian times (Landes *et al.* 2005). Following the Caledonian orogeny, by Late Carboniferous times, an east/west trending fabric was superimposed on the basement of the Irish continental margin by northward migration of deformation from the Variscan orogeny to the south (Landes *et al.* 2005).

Several of the rift basins on the Irish margin have been studied extensively such as the Celtic Sea basins, the Rockall Trough and the Porcupine Basin. While the Celtic Sea basins and the Rockall Trough have a southwest/northeast Caledonian orientation, the Porcupine Basin has a north/south orientation and appears to have been more strongly influenced by east/west extension due to the opening of the North Atlantic Ocean rather than by pre-existing basement fabrics (Shannon 1991). Extreme thinning of the crust has been imaged across the Porcupine Basin where simple shear extension resulted in the exhumation of serpentinized mantle (Reston *et al,* 2004, O'Reilly *et al.* 2006). Similar structures have been imaged across the Rockall Trough where crustal thinning was not as severe (O'Reilly *et al.* 1996). The range of structural trends and crustal thicknesses resolved for different regions of the Irish continental margin highlight the complexity of this margin and act as the motivation for seeking an improved regional view of the margin structures in 3D.

## Gravity Data and Inversion

The gravity data used in the inversion are the free air gravity point measurements obtained from satellite altimetry data (Sandwell and Smith, 1997). We use the GRAV3D inversion algorithm developed by Li and Oldenburg (1996; 1998) to invert gravity observations at the Earth's surface and obtain a subsurface 3D density anomaly distribution (relative to a background density of 2670 kg/m$^3$) below the observation locations. Our model mesh onto which the 3D density anomaly distribution is modelled consists of flattened cubes with lateral dimensions of 15 km by 15 km and which are 500 m deep. The horizontal extent of the mesh corresponds to the study area shown in Figure 1 and contains 50 cells in the easting direction, 57 cells in the northing direction and 50 cells in depth.

For our inversion, we opted for GRAV3D to generate a 3D density anomaly model that was smooth over length scales of 150 km in the easting and northing directions and smooth over a length scale of 6 km in depth. In terms of fitting the data, given the coarseness of the mesh and the dense data coverage, we opted for a misfit value of twice the number of data points.

## Constraints

Bathymetric data for the Irish margin were obtained from satellite altimeter data (Smith and Sandwell 1997) and were incorporated into the reference density anomaly model by forcing all model prisms above the bathymetric depths to contain density anomalies corresponding to ocean water. These anomalies were kept fixed during the inversion.

Estimates of sediment thickness (Fig. 1C) which were obtained from the National Oceanic and Atmospheric Administration (NOAA) and which were compiled from isopach maps, ocean drilling results and seismic reflection profiles, were used with the bathymetric data to determine the depth to acoustic basement across the study region. This information was incorporated into the reference density anomaly model by assigning density anomalies consistent with sediments to the prisms lying between the seabed and the basement. These anomalies were allowed to vary within a prescribed range during the

inversion and this range was chosen to force the prisms to contain reasonable densities for sedimentary rocks whilst allowing the inversion to stratify (as needed) the densities within the sedimentary column and within individual basins.

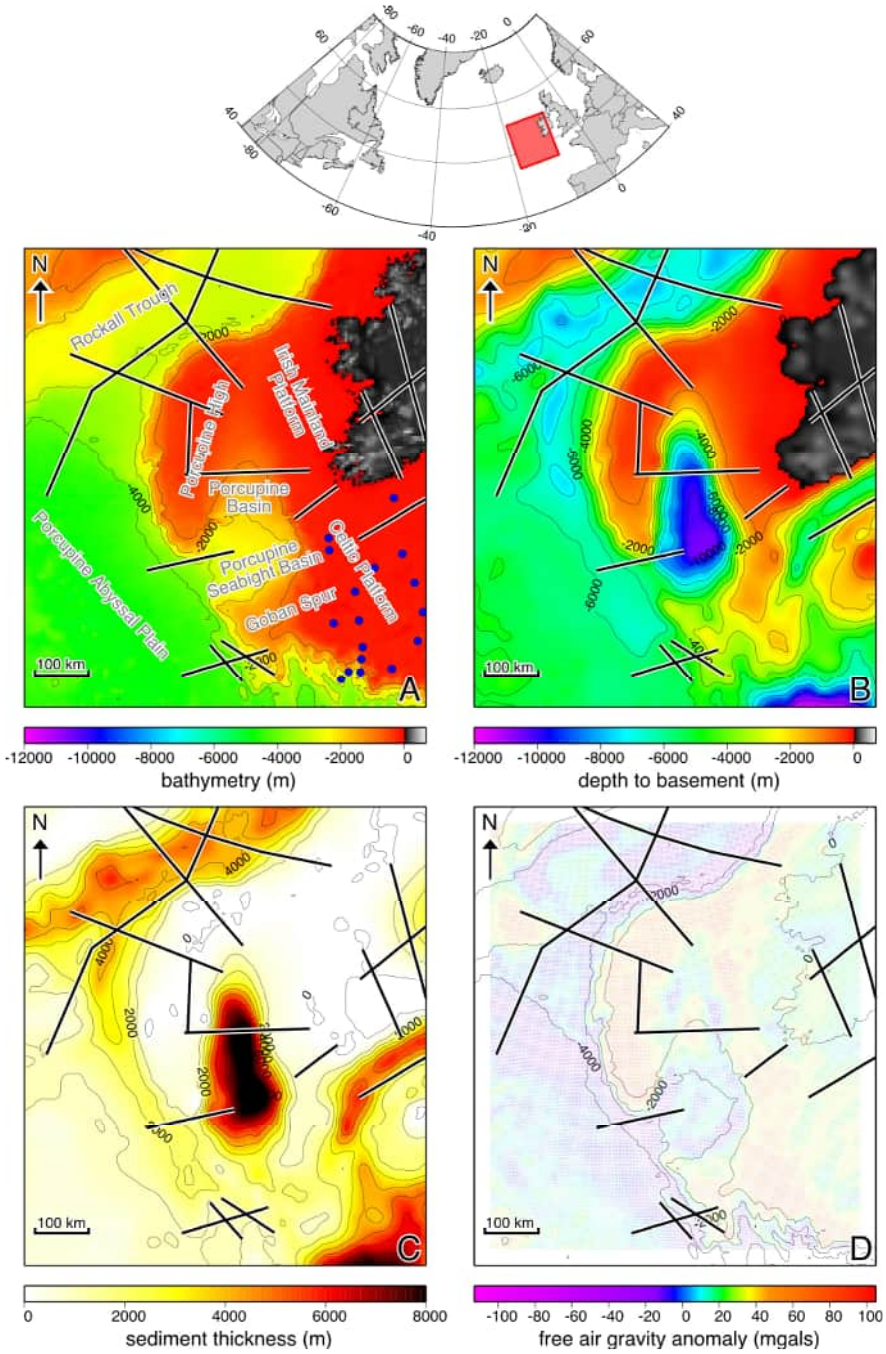


**Figure 1. Maps of (A) bathymetry, (B) depth to basement, (C) sediment thickness and (D) free air gravity anomalies for the study region. A location map is plotted at the top of the figure with the study area shown as the red box. On all of the study area maps, the locations of deep seismic profiles acquired over the margin are indicated with black lines outlined in white. Blue circles in (A) show the location of the Moho constraints provided by the gravity study of Lefort *et al.* (1999). Key bathymetric structures of the margin are labeled in grey on plot (A).**

Once the ocean water and sedimentary portions of the reference density anomaly model were assigned, all remaining mesh prisms were assigned a density anomaly corresponding to the background density. During the inversion, the density anomaly in each of these prisms was allowed to vary within a broader range. Thus, below the base of sediments, the inversion was given great flexibility in assigning density anomalies to reproduce the observed gravity response and no constraints were placed on which prisms should correspond to crustal rocks and which prisms should correspond to upper mantle rocks.

Several wide-angle seismic reflection/refraction surveys have been conducted over the portion of the Irish rifted continental margin considered in our study. The results from these surveys are summarized by Whitmarsh *et al.* (1974), Horsefield *et al.* (1994), Landes *et al.* (2005) and Kelly *et al.* (2007). Whilst these 2D crustal-scale seismic refraction/wide-angle reflection profiles could not be used as constraints for the inversion due to their sparse sampling of the margin, they were used locally to test the reliability of the inversion results.

## Inversion Results

We generate a 3D density anomaly model that is able to successfully reproduce the gravity observations along the Irish margin. All of the main observed gravity features are reproduced and the magnitudes of the gravity field values match well with differences generally less than 20 mgals throughout the study region.

## Moho Variations

The Moho depths resolved from the various 2D seismic refraction profiles and from a gravity study of Lefort *et al.* (1999) were used to generate an interpolated Moho depth map for the Irish margin (Fig. 2A). These sparse Moho depth constraints (white circles in Fig. 2A) produce a coarse and smeared out representation of Moho depths across the margin.

By selecting a density contrast of 350 kg/m$^3$ as a proxy for the Moho in our inverted density model, we obtain an inverted-gravity-constrained Moho model for the Irish margin (Fig. 2B). Since our inverted model does not extend below 25 km depth (for reasons explained in Welford and Hall, 2007), the resulting Moho model is also restricted to 25 km depth. However, if we supplement the inverted Moho with the available seismic and other constraints below 25 km depth and interpolate in between, we obtain the hybrid Moho model illustrated in Fig. 2C. The resulting hybrid Moho map is much more interpretable and bears a closer resemblance to the depth to basement map of the margin (Fig. 1B) which points to a great degree of isostatic compensation.

We generate a number of cross-sections in the west-southwest/east-northeast (Fig. 3) and north/south (Fig. 4) orientations in order to provide a broad view of margin structures. In Figure 3, slice A extends from the Porcupine Abyssal Plain and along the axis of the Rockall Trough. Whilst the interpolated seismic results show a steady deepening of the Moho from 10 km to 15 km towards the northeast, the gravity inversion results predict a Moho with more variable topography. Since the upper mantle beneath the Rockall Trough has been interpreted as consisting of serpentinized mantle (O'Reilly *et al.,* 1996), the Moho topography from the gravity inversion may be reflecting lateral variations in the degree of serpentization (and thus density) along the axis of the trough with the actual Moho topography corresponding to the seismically-modelled Moho. Further south, profile B crosses from the Abyssal Plain through the Porcupine High, the northernmost extent of the Porcupine Basin and onto the Irish Mainland Platform. In general, the two Mohos are in good agreement at the western limit of this slice. A poorer fit is obtained between the two Mohos along profile C to the south where the hybrid Moho beneath the Porcupine Seabight Basin arguably is more reliable given the sparser seismic coverage in this area. Our hybrid Moho shallows immediately beneath the basin where extreme crustal thinning and the exhumation of serpentinized mantle is interpreted to have taken place (Reston *et al.,* 2004 O'Reilly *et al.* 2006). Lastly, profile D starts in the Abyssal Plain and crosses the Goban Spur onto the Celtic Platform. As with B, the two Mohos are generally in good agreement along this profile.

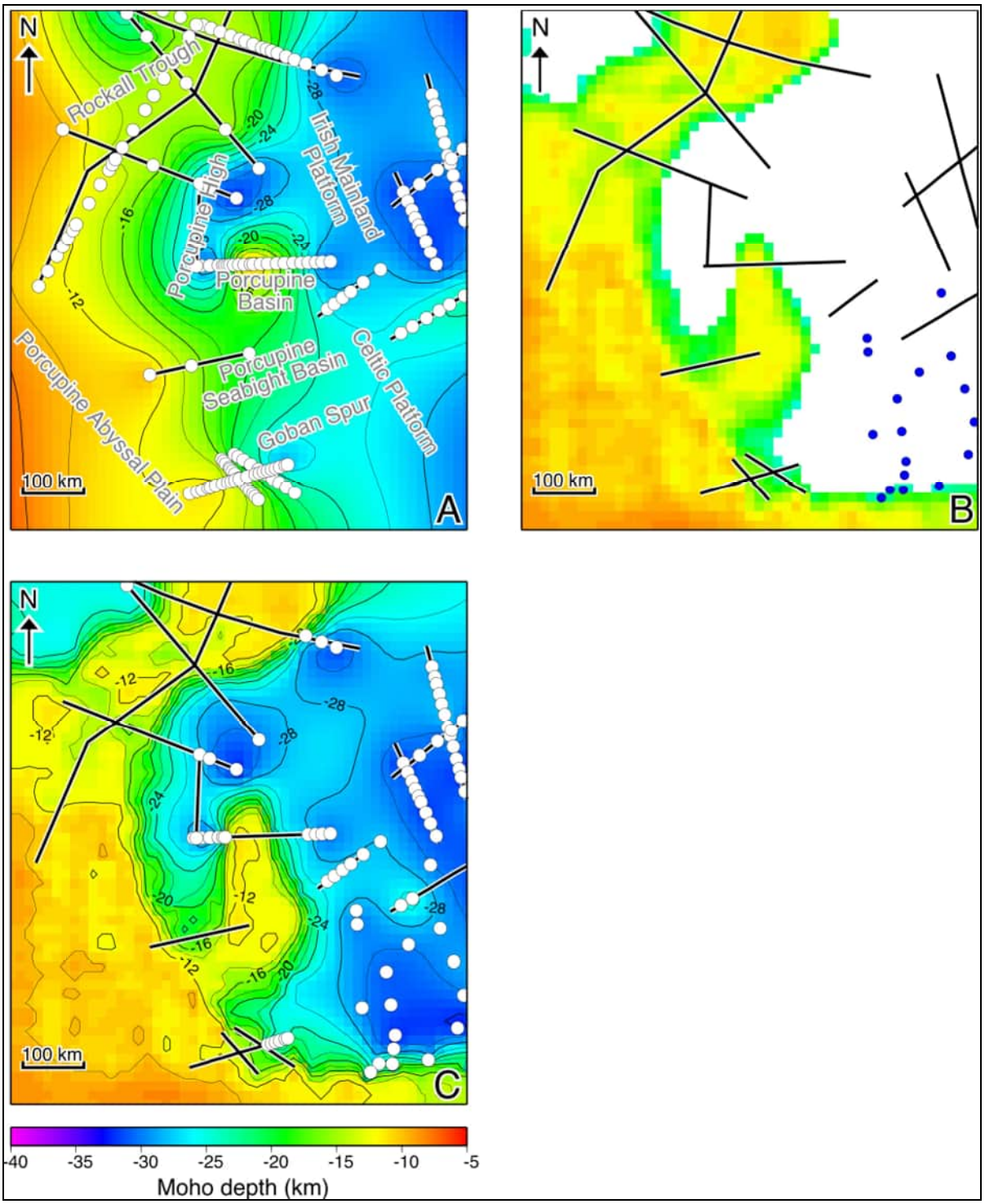


**Figure 2. Maps of Moho depths: (A) interpolated from digitized Moho picks along seismic profiles and from Lefort et al. (1999); (B) from the 350 kg/m$^3$ anomaly isosurface of the inverted density anomaly model (regions without Moho constraints have been masked in white); and (C) from the combination of the isosurface in (B) with seismic and Lefort *et al.* constraints below 25 km depth in (A). On plots (A) and (C), the seismically-constrained Moho pick locations used in the interpolation are shown as white circles. On all maps, the locations of deep seismic profiles acquired over the margin are indicated with black lines outlined in white. In (B), the locations of Moho constraints from Lefort *et al.* (1999) are shown as blue circles. Key bathymetric structures of the margin are labeled in grey on plot (A).**

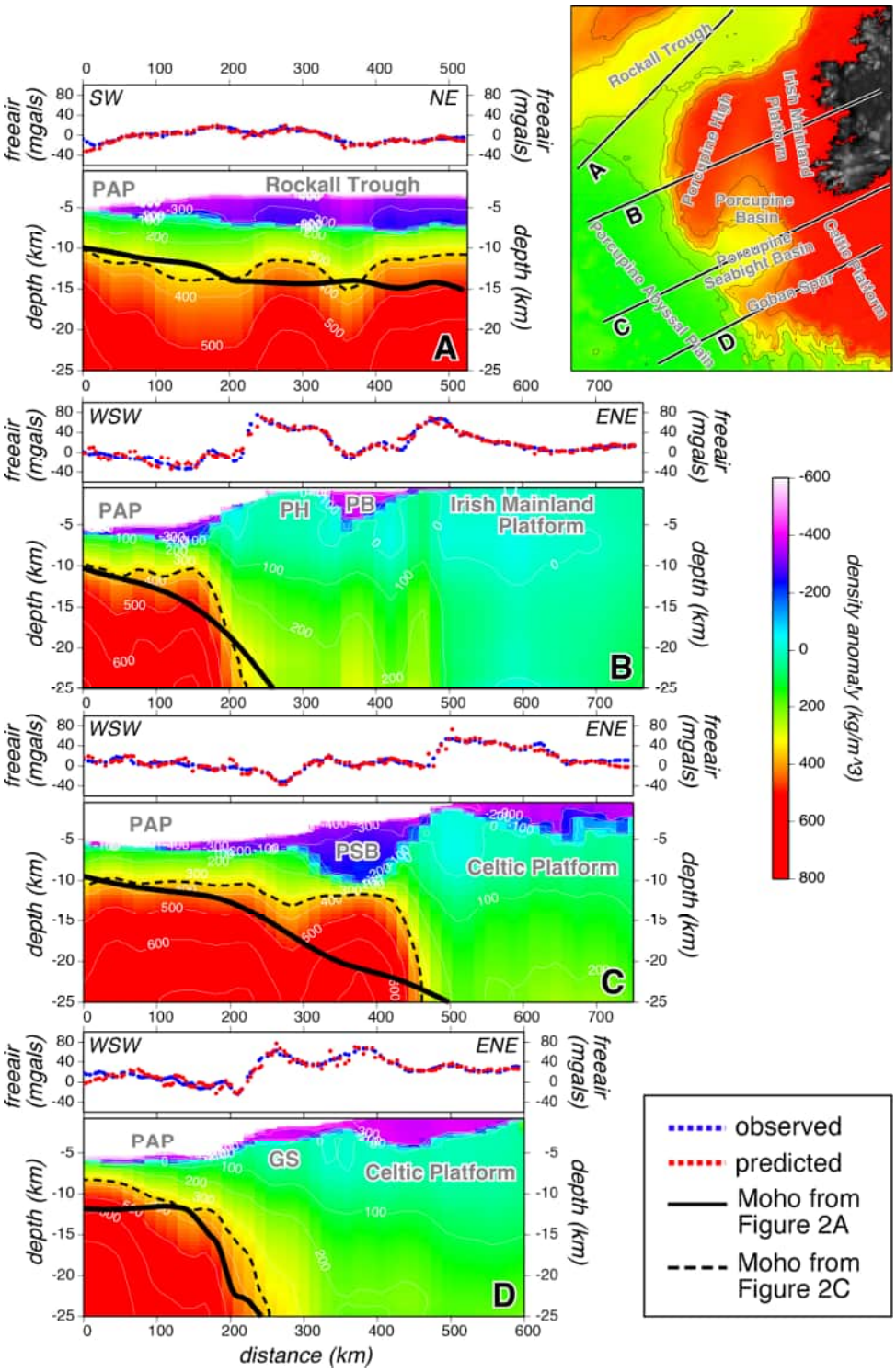


**Figure 3. Arbitrary west-southwest/east-northeast slices through the inverted density anomaly model with the slice locations plotted on the bathymetry map in the top right. The overlain thick dashed black lines correspond to the hybrid Moho depths obtained from Figure 2C and the thick solid black lines correspond to the interpolated seismically-constrained Moho depths obtained from Figure 2A. Above each slice, the comparison between the observed free air gravity anomalies (blue lines) and the anomalies predicted for the inverted density anomaly model (red lines) are plotted. Key bathymetric features of the margin are labeled in grey on the slices and on the map. Abbreviations: GS, Goban Spur; PAP, Porcupine Abyssal Plain; PB.**

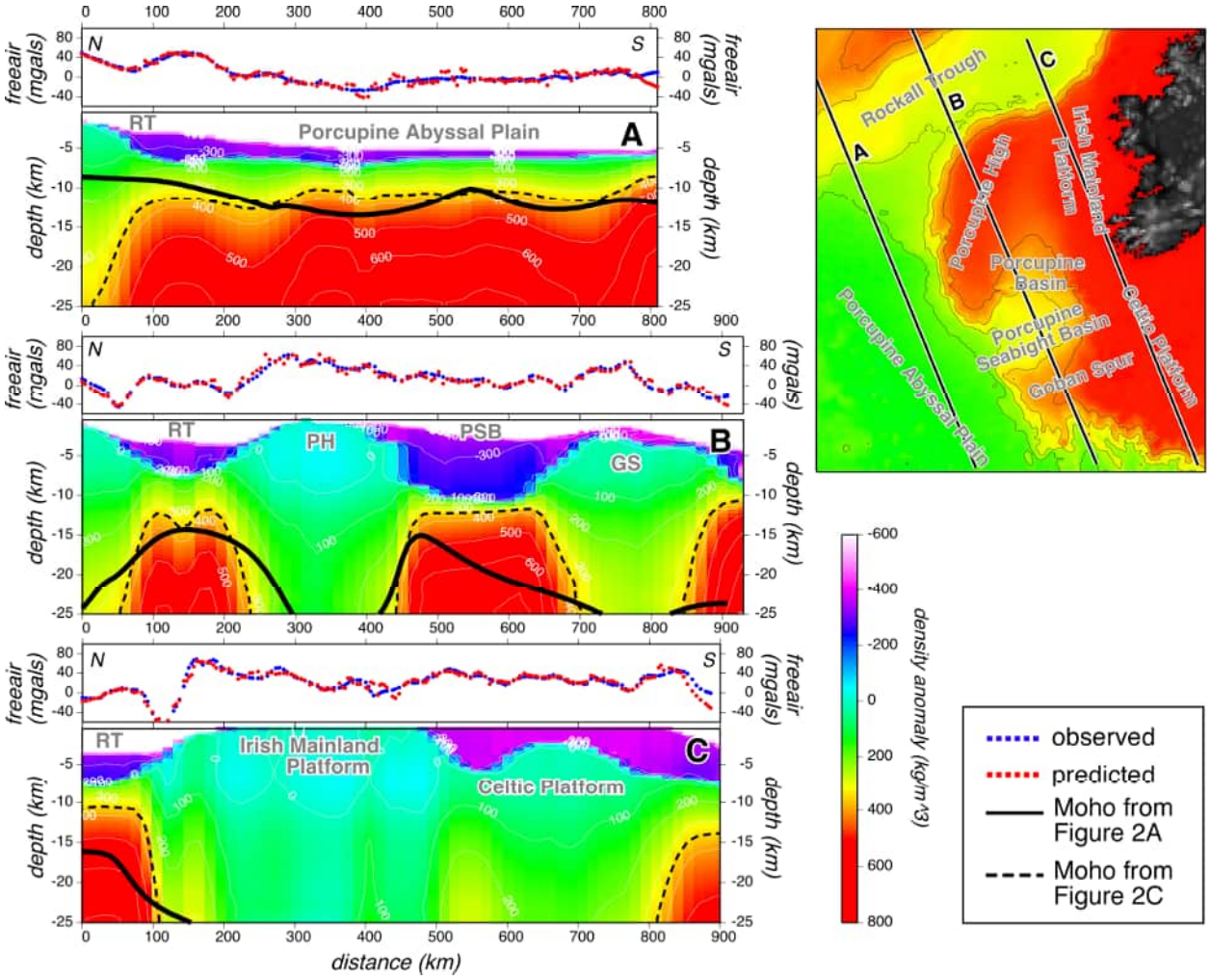


**Figure 4. Arbitrary north/south slices through the inverted density anomaly model with the slice locations plotted on the bathymetry map in the top right. The overlain thick dashed black lines correspond to the hybrid Moho depths obtained from Figure 2C and the thick solid black lines correspond to the interpolated seismically-constrained Moho depths obtained from Figure 2A. Above each slice, the comparison between the observed free air gravity anomalies (blue lines) and the anomalies predicted for the inverted density anomaly model (red lines) are plotted. Key bathymetric features of the margin are labeled in grey on the slices and on the map. Abbreviations: GS, Goban Spur; PH, Porcupine High; PSB, Porcupine Seabight Basin; RT, Rockall Trough.**

The north/south slices displayed in Figure 4 show the major variation in density structure across the Irish margin. The Moho along profile A beneath the Porcupine Abyssal Plain remains consistently between 10 and 12.5 km depth for both the seismic and our gravity inversion results although the Moho topographies differ. The large discrepancy between the Mohos at the northern end of the profile is due to a lack of seismic constraints at this location. Profile B has the most laterally complex density anomaly structure with Moho shallowing beneath the Rockall Trough, the Porcupine Seabight Basin and finally south of Goban Spur. Whilst these shallowings are evidenced both by the interpolated seismic results and the gravity inversion results, their geometries differ greatly. Again, the inversion results are arguably more reliable since the seismic constraints are sparser and heavily influenced by the interpolation routine. Finally, our hybrid Moho shallows at both ends of profile C beneath the Rockall Trough and south of the Celtic Platform whilst the seismic results only show a more moderate shallowing beneath the Rockall

Trough. Again, this discrepancy can be explained by the sparseness of the seismic constraints used at the edges of our study area.

## Density Variations in the Crust

As in Welford and Hall (2007), we will loosely define upper crust as corresponding to density anomaly values of less than 100 kg/m$^3$, middle crust as corresponding to density anomaly values between 100 and 200 kg/m$^3$ and lower crust as corresponding to density anomaly values between 200 and 350 kg/m$^3$. These approximate divisions are intended to simplify description of the crustal density variations and aid in their interpretation.

The broad coverage provided by the cross-sections in Figures 3 and 4 allow for regional conclusions to be drawn regarding the density anomaly distribution within the crust of the Irish margin. On profile A (Fig. 3) through the Rockall Trough, the upper crustal layer thins towards the north and is almost completely pinched out in the middle of the profile, consistent with seismic refraction modelling results (O'Reilly *et al.* 1996). Meanwhile, lower crustal densities become more dominant to the northeast. Further south along profiles B, C, and D (Fig. 3), the crust beneath the Porcupine High, the Goban Spur and the Celtic Platform all appear to have similar density distributions whilst the Irish Mainland Platform looks distinctly different and contains upper crustal densities to greater depth. This character is also evident on the three north/south profiles in Figure 4 although the middle crust of the Goban Spur along profile B (Fig. 4) is thinner. Meanwhile, the density structure of the Porcupine Abyssal Plain remains similar along the length of the margin, arguably becoming dominated by lower crustal densities to the south as seen on profiles D (Fig. 3) and A (Fig. 4).

## Discussion

The 3D density anomaly model derived from the gravity inversion provides an alternate view of the Irish margin that complements existing seismic datasets and provides further insight into the structure of the margin. Combining the depth to basement constraints (Fig. 1B) with the hybrid Moho depth model obtained by combining the density results with deep seismic and other constraints (Fig. 2C), we are able to generate a map of crustal basement thickness across the margin (Fig. 5A).

Comparing the inferred crustal basement thickness (Fig. 5A) with the observed sediment thickness (Fig. 5B), we can map sediment excess and deficiency across the Irish margin. If we assume local Airy compensation and constant densities for sediments ($\rho_s$), crust ($\rho_c$) and mantle ($\rho_m$), then sediment thickness (s) is inversely proportional to the amount of crustal thinning (dt) below the sediments such that

$$s = dt(\rho_m - \rho_c)/(\rho_m - \rho_s) \quad (1)$$

Assuming that the crust was 30 km thick before thinning (Lowe and Jacob, 1989) and that $\rho_s$ , $\rho_c$ and $\rho_m$ are 2200, 2850 and 3300 kg/m$^3$ respectively, we obtain a relationship between sediment and crustal thickness.

In Figure 5C, we map the deviations from our model of isostatically compensated sediment thickness for a given crustal thickness, highlighting areas of sediment deficiency (in blue) and those of excess (in red). Sedimentary deficiency is large over deep water, because the Airy model assumes that sediments occupy all of the available accommodation space. To give a better indication of departures from local Airy compensation, we have compensated for the change in gravitational load due to water by adding a term to the sediment thickness equation such that

$$s = dt(\rho_m - \rho_c)/(\rho_m - \rho_s) - W(\rho_m - \rho_w)/(\rho_m - \rho_s) \quad (2)$$

where the water depth (W) is obtained from the bathymetry and the density of water ($\rho_w$ ) is set to 1030 kg/m$^3$. This redistribution is illustrated in Figure 5D which takes into account the variations in water depth across the margin.

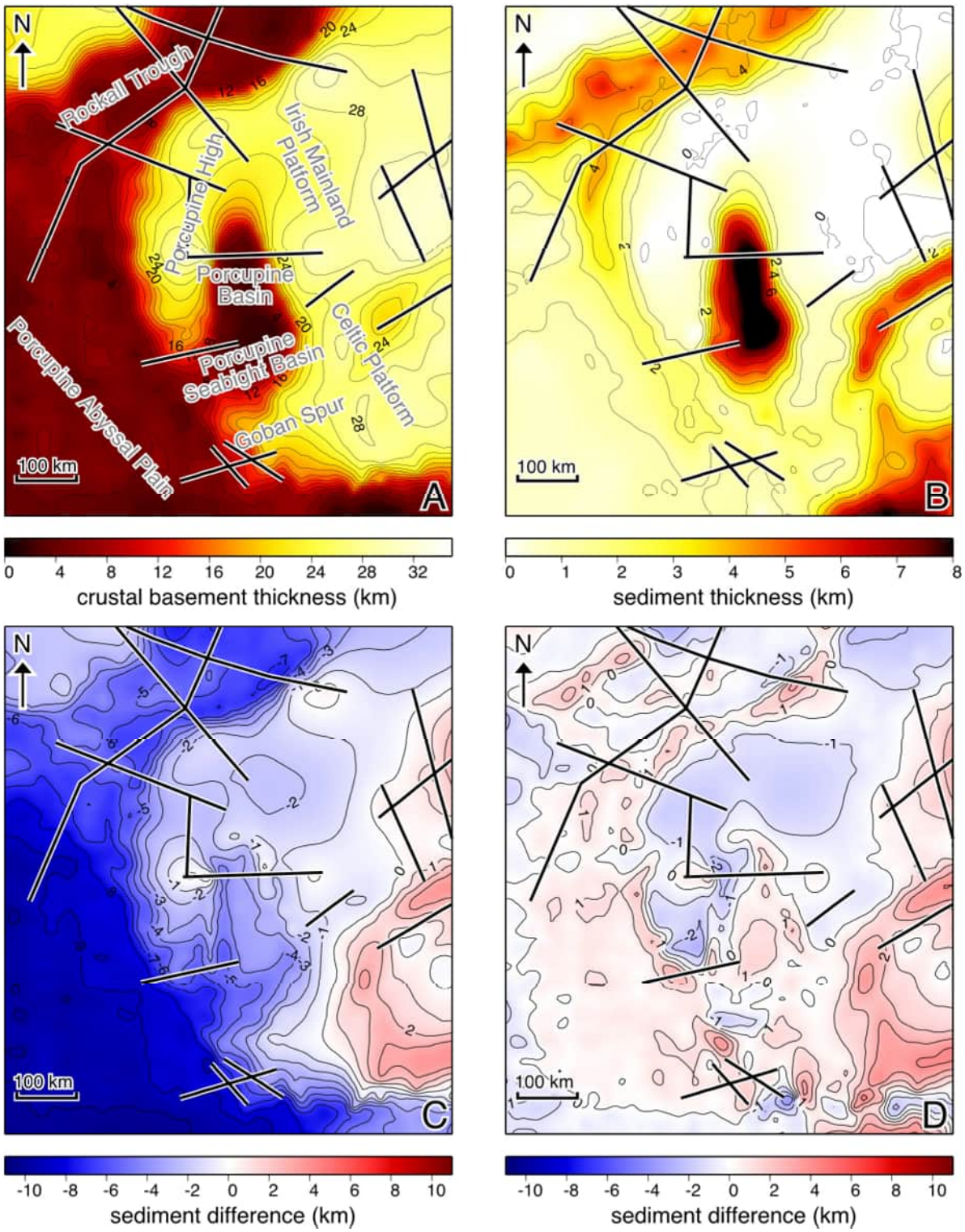


**Figure 5. Maps of (A) crustal basement thickness computed from depth to basement (Fig. 1B) and our interpreted Moho depth surface (Fig. 2C), (B) sediment thickness, (C) the difference between the observed sediment thickness for a given crustal thickness and the expected sediment thickness for an isostatically compensated crust, and (D) the sediment thickness difference in (C) after water depth compensation. The locations of deep seismic profiles acquired over the margin are indicated with black lines outlined in white. In (A), key bathymetric structures of the margin are labeled in grey.**

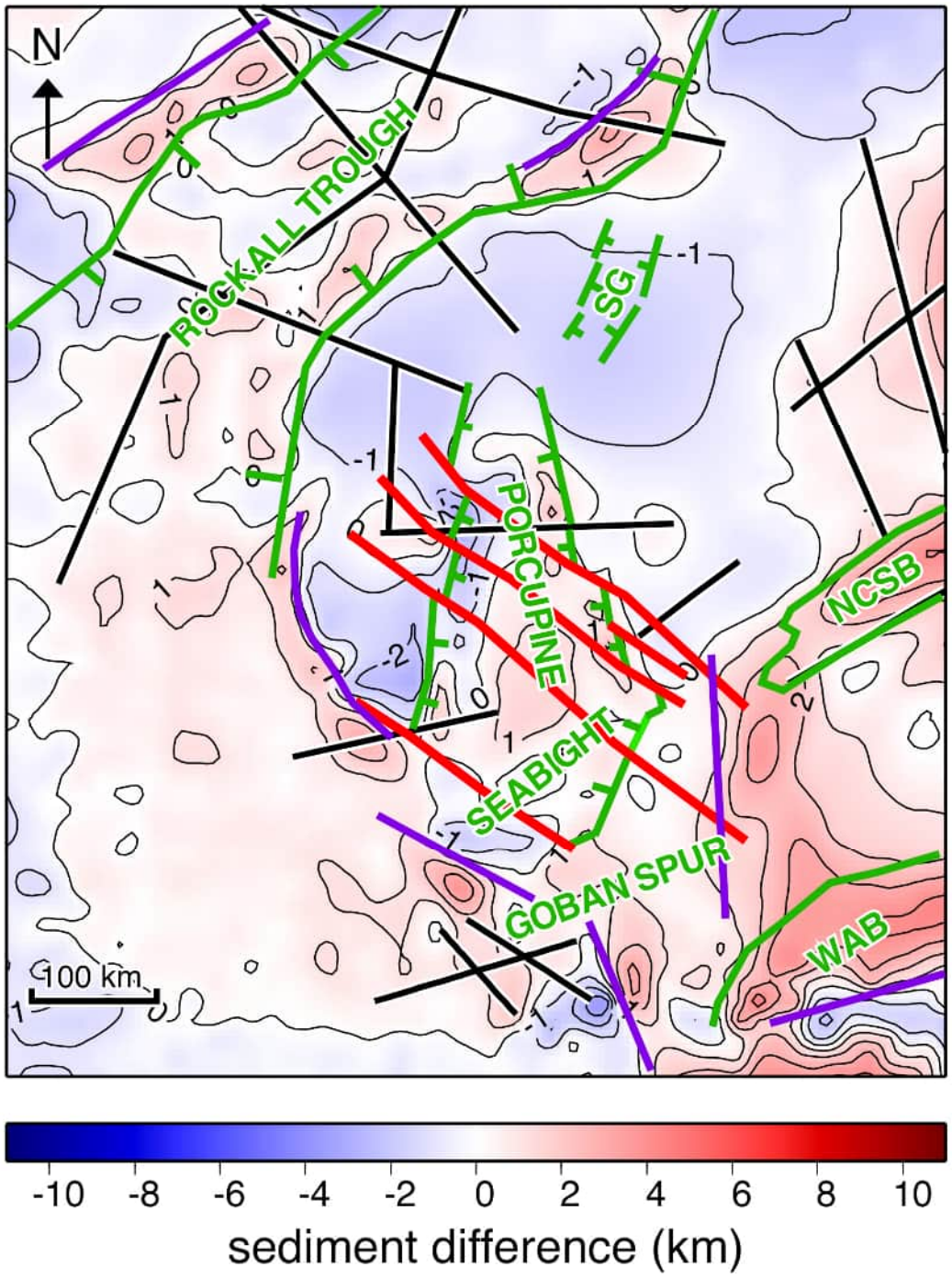


**Figure 6. Interpreted sediment thickness difference after water depth compensation from Figure 5D. The main basin bounding faults are shown as green lines and basin names are labeled in green. Purple lines highlight regions where there is a strong gradient in sediment thickness difference that is not associated with specific basin bounding faults. Dominant northwest/southeast faults within the Porcupine-Seabight basin are shown in red. The locations of deep seismic profiles acquired over the margin are indicated with black lines outlined in white. Abbreviations: S.G., Slyne Graben (as shown in Lefort *et al.* (1999)); N.C.S.B., North Celtic Sea Basin (as shown in Shannon (1991)); WAB, Western Approaches Basin (as shown in Tate (1993)).**

Figure 6 displays the map from Figure 5D with the main bounds of the sedimentary basins of the margin indicated in green. Regions with strong gradients that have not been associated with specific basins are indicated with purple lines.

Since the development of the Irish offshore basins is thought to have been controlled largely by pre-existing Caledonian and Variscan basement structures and fabrics (Shannon 1991), it is not surprising that many of the trends in the sediment difference map (Fig. 6) follow the trends associated with those orogenies. For instance, most of the strong gradients in the sediment difference map arguably have northwest/southeast trends which are perpendicular to and which highlight faults with a southwest/northeast Caledonian orientation. Examples of this are the faults along the edges of the Rockall Trough, the North Celtic Sea Basin and the Western Approaches Basin. Curiously, no corresponding trend in sediment difference is observed for the Slyne Graben (Fig. 6).

Strong gradients oriented east/west and southwest/northeast mark the edges of the Porcupine Basin and both the northern and southern edges of the Goban Spur which itself contains several basins. These gradients which are perpendicular to and which delineate faults that are aligned with the continent-ocean boundary, are likely associated with east/west extension and opening of the North Atlantic Ocean. The same extension possibly caused the north/south trending region of sediment excess that bridges between the North Celtic Sea Basin and the Western Approaches Basin. Shannon (1991) argues that these zones do not follow the Caledonian or Variscan trends because the basement structures were not well developed in these areas.

Overall, our sediment difference map (Fig. 6) appears to highlight ancient Caledonian basement structures and fabrics for most areas of the margin. Meanwhile, areas where pre-existing Caledonian and Variscan trends are not apparent may represent zones where the deformation from those orogenies was less pronounced or zones of anomalous crust. Ultimately, the unique view of the Irish continental margin provided by our study may prove useful for future more detailed paleoreconstructions of the North Atlantic region prior to rifting.

## References


Hopper, J., R. Funck, B. Tucholke, K. Louden, W. Holbrook, and H.C. Larsen, 2006, A deep seismic investigation of the Flemish Cap margin: implications for the origin of deep reflectivity and evidence for asymmetric break-up between Newfoundland and Iberia: Geophysical Jour. International, v.164, no.3, p.501–515.

Horsefield, S.J., R.B Whitmarsh, R.S. White, and J.-C. Sibuet, 1994, Crustal structure of the Goban Spur rifted continental margin, northeast Atlantic: Geophysical Jour. International, v.119, p.1–19.

Kelly, A., R.W. England, and P.K. Maguire, 2007, A crustal seismic velocity model for the UK, Ireland and surrounding seas: Geophysical Jour. International, v.71, p.1172–1184.

Landes, M., J. Ritter, P. Readman, and B. O'Reilly, 2005, A review of the Irish crustal structure and signatures from the Caledonian and Variscan Orogenies: Terra Nova, v.17, no.2, p.111–120.

Lefort, J., B. Agarwal, and M. Jaffal, 1999, A tentative chronology of the Moho undulations in the Celtic sea region: Jour. of Geodynamics, v.27, p.161–174.

Li, Y. and D.W. Oldenburg, 1996, 3D inversion of magnetic data: Geophysics, v.61, no.2, p.394–408.

Li, Y. and D.W. Oldenburg, 1998, 3D inversion of gravity data: Geophysics, v.63, p.109–119.

Lowe, C. and A.B. Jacob, 1989, A north-south seismic profile across the Caledonian Suture zone in Ireland: Tectonophysics, v.168, p.297–318.

O'Reilly, B.M., F. Hauser, C. Ravaut, P.M. Shannon, and P.W. Readman, 2006, Crustal thinning, mantle exhumation and serpentinization in the Porcupine Basin, offshore Ireland: evidence from wide-angle seismic data: Jour. of the Geological Society, London, v.163, p.775-787.

O'Reilly, B.M., F. Hauser, A.W.B. Jacob, and P.M. Shannon, 1996, The lithosphere below the Rockall Trough: wide-angle seismic evidence for extensive serpentinisation: Tectonophysics, v.255, p.1-23.

Reston, T.J., V. Gaw, J. Pennell, D. Klaeschen, A. Stubenrauch, and I. Walker, 2004, Extreme crustal thinning in the south Porcupine Basin and the nature of the Porcupine Median High: implications for the formation of non-volcanic rifted margins: Jour. of the Geological Society, London, v.161, p.1-16.

Sandwell, D.T. and W.H. Smith, 1997, Marine gravity anomaly from Geosat and ERS 1 satellite altimetry: Jour. of Geophysical Research, v.102, no.B5, p.10039–10054.

Shannon, P., 1991, The development of Irish offshore sedimentary basins: Jour. of the Geological Society of London, v.148, p.181–189.

Smith, W. and D. Sandwell, 1997, Global seafloor topography from satellite altimetry and ship depth soundings: Science, v.277, p.1957–1962.

Tate, M.P., 1993, Structural framework and tectono-stratigraphic evolution of the Porcupine Seabight Basin, offshore western Ireland: Marine and Petroleum Geology, v.10, p.95–123.

Tucholke, B., J. Austin, and E. Uchupi, 1989, Crustal structure and rift-drift evolution of the Newfoundland basin, *in* A. Tankard and H. Balkwill, Extensional tectonics and stratigraphy of the North Atlantic margins: AAPG Memoir, v.46, chap.16, p.247–263.

Welford, J. K. and J. Hall, 2007, Crustal structure across the Newfoundland rifted continental margin from constrained 3D gravity inversion: Geophysical Jour. International, v.171, p.890–908.

Whitmarsh, R., J. Langford, J. Buckley, R. Bailey, and D. Blundell, 1974, The crustal structure beneath the Porcupine Ridge as determined by explosion seismology: Earth and Planetary Science Letters, v.22, p.197–204.

**BACK**

# Structure and Rifting Evolution of the Northern Newfoundland Basin from ERABLE Multichannel Seismic Reflection Profiles Across the Southern Margin of the Flemish Cap

**J. Kim Welford**
e-mail: kwelford@mun.ca
**Julie Smith**
**Jeremy Hall**
**Sharon Deemer**
Memorial University of Newfoundland
Department of Earth Sciences
300 Prince Philip Drive
St. John's, Newfoundland A1B 3X5
Canada

**Shiri Srivastava**
Geological Survey of Canada
Bedford Institute of Oceanography
P.O. Box 1006
Dartmouth, Nova Scotia B2Y 4A2
Canada
e-mail: shsrivas@nrcan-rncan.gc,ca

**Jean-Claude Sibuet**
Ifremer, Centre de Brest
Département des Géosciences Marines
B.P. 70
29280 Plouzané
France
e-mail: jcsibuet@ifremer.fr

## ABSTRACT

We present four multichannel seismic reflection profiles from the 1992 ERABLE experiment collected over the southern margin of Flemish Cap and extending into the Newfoundland Basin. These profiles are between and sub-parallel to lines 1 and 2 from the 2000 SCREECH seismic experiment and provide more comprehensive data coverage over the region. Combining these data with the SCREECH seismic profiles, two ODP drill sites, and other geophysical data has allowed the mapping of distinct zones of continental, transitional, and oceanic crust in this region. Comparisons with mapped crustal boundaries on the Iberian margin from detailed seismic surveys and drilling show asymmetry in the conjugate pair, with the zone of extended continental crust and transitional crust being much wider on the Iberian margin compared to the Newfoundland margin. Furthermore, whilst detachment faulting is evidenced on both margins, it appears to be less widespread on the Newfoundland margin. For the southern portion of our study area, we propose either a simple shear, or, simple shear/pure shear combination model involving a westward dipping detachment fault, with the Newfoundland margin acting as the upper plate. However, along strike variations in the present day structure of the Flemish Cap margin deviate significantly from the simple 2D rifting model and are explained within the context of Late Jurassic to Early Cretaceous rifting and breakup.

## Introduction and Tectonic Setting

The Newfoundland continental margin is a key location for investigating the process of rifting and the opening of ocean basins. We present multichannel seismic reflection profiles collected in 1992 as part of the ERABLE project along four seismic lines across the southern margin of Flemish Cap extending into the deeper waters of the Newfoundland Basin. These profiles bridge between two of the lines from the more recent Study of Continental Rifting and Extension on the Eastern Canadian Shelf (SCREECH) project collected in 2000. The SCREECH profiles revealed very different structures, despite their close proximity, and the newly presented ERABLE profiles allow for a more detailed understanding of how the margin varies over short spatial scales.

Flemish Cap is a prominent sub-circular submarine knoll on the offshore Newfoundland margin. At 30 km in thickness, this flat-topped block of continental crust is located northeast of the Grand Banks and lies under less than 200 m of water. From paleoreconstructions of the margin at M0 time based on regional aeromagnetic data, the southern margin of Flemish Cap is conjugate with the Galicia Bank off the western Iberian margin. These margins were separated from Late Jurassic to Early Cretaceous during the second of three major phases of rifting to affect the Newfoundland margin starting during the Late Triassic (Tucholke *et al.* 1989; Grant and McAlpine 1990). The northeast margin of Flemish Cap separated from the Goban Spur, offshore Ireland, during the third phase in the Late Cretaceous (Tucholke *et al.* 1989; Hopper *et al.* 2006). From recent work, it is thought that the Flemish Cap originated in the region now occupied by the Orphan Basin out of which it was rotated as a whole in a clockwise direction 43 degrees during the Late Triassic-Early Tertiary and was further translated 200-300 km southeastward relative to North America (Srivastava and Verhoef 1992; Enachescu 2006; Sibuet *et al.* 2007).

The transition zone between continental and oceanic crust is well constrained on the Iberia margin from both seismic and drilling data. The transition zone within the Newfoundland basin has been explored in less detail, but is the focus of recent studies. It is the aim of our study to use the ERABLE profiles to gain a better understanding of the evolution and formation of the northern Newfoundland Basin, with emphasis on the southern margin of Flemish Cap (Fig. 1). By placing boundaries on continental, transitional, and oceanic crust, we obtain valuable geometrical constraints on rifting and propose a plan-view rifting and breakup model for this section of the margin.

## Data Acquisition and Processing

In 1992, the ERABLE project was undertaken jointly by the Geological Survey of Canada's Atlantic Geoscience Centre (AGC) and the Institut Français de Recherche pour l'Exploitation de la Mer (IFREMER). The project involved the acquisition of multiple 2D multichannel seismic reflection profiles in the Newfoundland Basin and along the margins of Flemish Cap. The seismic source was generated by an air gun array with a shot spacing of 100 m. Data were recorded by a 96 channel, 2.4 km long streamer using a sampling rate of 4 ms. Trace lengths varied between 12288 ms (E33) and 17408 ms (E36, E53, E54 and E56). The resulting common-midpoint (CMP) spacing was 12.5 km and the nominal CMP fold was 12.

The four ERABLE profiles that we present were processed using similar processing flows consisting of frequency filtering, amplitude gaining, normal-moveout (NMO) correction, spiking deconvolution, F-K linear noise filtering, multiple suppression (F-K filtering for the shelf, Radon transform filtering for the slope and deep water), near trace muting, stack, post-stack predictive deconvolution, trace mixing and post-stack Kirchhoff time migration. Finally, each section was balanced using time variant scalars.

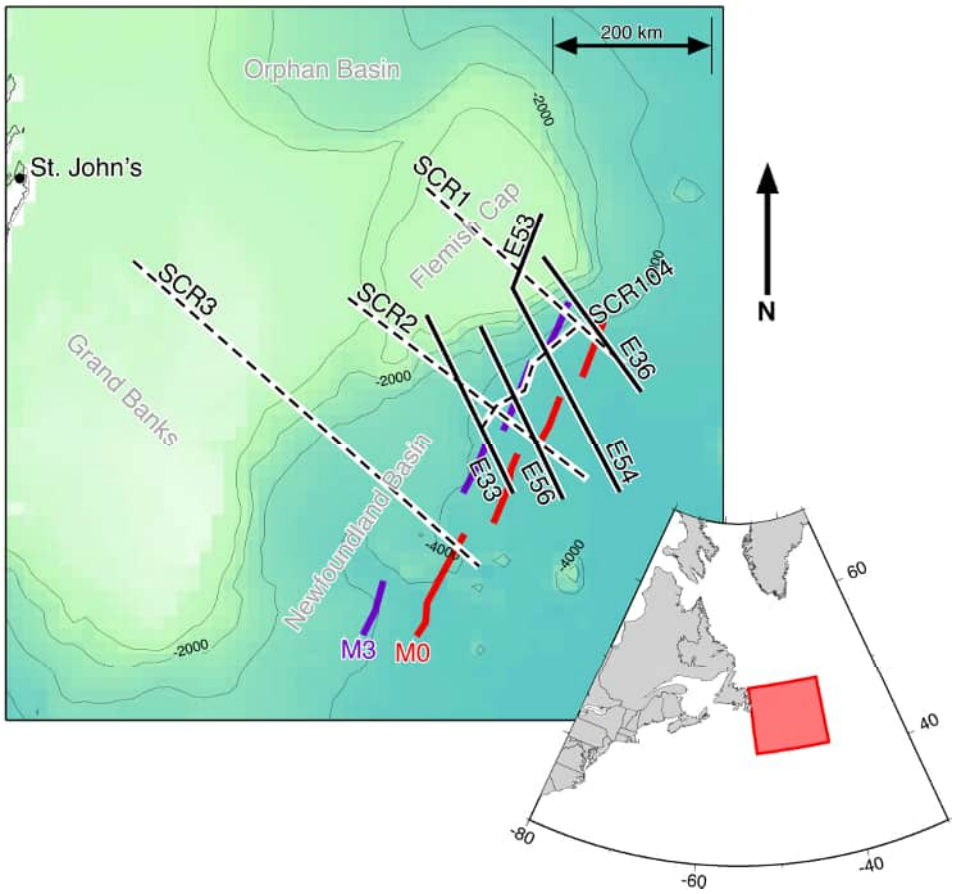


**Figure 1. Bathymetric map of study region. Multichannel seismic reflection profiles plotted as black lines with solid lines corresponding to the ERABLE experiment (lines E33, E36, E53, E54 and E56) and dashed lines corresponding to the SCREECH experiment (lines SCR1, SCR2, SCR3 and SCR104). Locations of magnetic anomalies M0 and M3 identified by Srivastava *et al.* (2000) are plotted as red and blue line segments respectively. Key bathymetric features are labelled in grey. A broader location map is plotted in the bottom right with the study area highlighted as the red box.**

## Results

### ERABLE Profile 33

E33 (Fig. 2: NB: Large 11x17 in. figure – see end of paper) is the southernmost seismic profile investigated in our study. This profile is sub-parallel and intersects with SCREECH profile 2 (SCR2; Shillington *et al.,* 2006) with which it shares many seismic characteristics. At its landward end, unambiguous continental crust thins seaward as evidenced by the presence of multiple rotated fault blocks. The easternmost rotated block (CDPs 11500-13000) coincides with the intersection point with the SCR2 profile where this same block is interpreted as the seaward limit of thinned continental crust. The only intra-crustal reflections imaged within the continental crust occur within this block and are interpreted as corresponding to the base of pre-rift sediments (Shillington *et al.* 2006). Reflections from the top of the mantle are interpreted between 9 and 10 s at the western end of the profile and at 8 s beneath the easternmost rotated continental block. Whilst Moho depth constraints are not available from seismic refraction surveying along this profile, the Moho obtained from a regional gravity inversion (Welford and Hall 2007) is time-converted (using regional bathymetric and sediment thickness estimates and velocities of 1500, 3000 and 6000 m/s for the water, the sediments and the crust respectively) and is overlain as the dark grey line on Figure 2. This Moho correlates well with the interpreted Moho reflection

beneath the rotated continental block but overestimates the depth of the Moho beneath the continental shelf (possibly due to our choice of crustal velocity). A second time-converted Moho using the bathymetric and sediment thickness constraints digitized from the seismic profile itself is overlain as the light grey line and shows a similar fit.

Seaward of the easternmost continental block, transitional zone T1 (CDPs 11500-6000) spans 75 km and is characterized by minimal relief and a poorly imaged basement surface due to the overlying strong U-reflection. The U-reflection has been drilled by the ODP project and found to be composed of two diabase sills separated by sediments (Shipboard Scientific Party 2004). We interpret this T1 zone as corresponding to serpentinized exhumed mantle rocks, similar to those observed on the conjugate Iberia margin (*e.g.,* Pickup *et al.* 1996; Dean *et al.* 2000; Whitmarsh and Wallace 2001). A similar zone along SCR2 was interpreted as corresponding to thinned continental crust (van Avendonk *et al.* 2006) or a combination of continental crust with magmatic intrusions/exhumed mantle/thin ocean crust (Shillington *et al.,* 2006) which are also plausible interpretations but which are at odds with the interpretation for SCR3 to the southwest (Lau *et al.* 2006a; 2006b).

Moving further seaward between CDPs 5800-1800, basement relief increases moderately and the basement surface itself is imaged. We interpret this transitional zone T2 as corresponding to a peridotite ridge with a lateral extent of 50 km. The western limit of this section corresponds to the M3 magnetic anomaly that was once considered as a seafloor-spreading anomaly in this region (e.g., Srivastava et al., 2000; Shipboard Scientific Party, 2004), but now is hypothesized to be produced by serpentinized peridotites (Sibuet *et al.* 2007). A similar T2 domain is identified on the SCR2 profile and is also hypothesized to have formed through exhumation and serpentinization of mantle rocks. Interpreted Moho reflections within this section agree well with the gravity-inverted Moho.

From CDP 1800 seaward, the basement surface remains shallow and basement relief is relatively smooth. This section of the profile contains the M0 magnetic anomaly (CDP 1000) which is in close proximity to a basement low. This low is likely correlated with a similar basement low on the SCR2 profile near the M0 anomaly where a change in the velocity gradient has been modelled and interpreted as typical Atlantic Ocean crust (van Avendonk *et al.* 2006). Thus, the landward limit of oceanic crust is similarly placed just landward of the M0 anomaly on the E33 profile. The disagreement between the interpreted Moho reflection and the gravity-inverted Moho beneath this section may simply reflect that the Moho picked from the inverted density model should have corresponded to a higher density contrast beneath the oceanic crust.

## ERABLE profile 56

The E56 profile (Fig. 3: NB: Large 11x17 in. figure – see end of paper) is parallel to and immediately to the east of E33. Both profiles intersect with SCR2, and have very similar seismic reflection characters. As on profile E33 (Fig. 2), rotated fault blocks make up the continental slope along E56. An angular crustal block (CDPs 14000-13500) containing stratigraphic layering that parallels its surface correlates with similar blocks along E33 and SCR2 and marks the seaward limit of thinned continental crust.

Seaward, a transitional zone T1 (CDPs 13500-10000) closely resembles the T1 zone identified on E33 although its lateral extent is limited to roughly 40 km. Again, we interpret this T1 zone as corresponding to serpentinized exhumed mantle rocks. Interpreted Moho reflections beneath this zone match well with those from the gravity-inverted Moho.

Between CDPs 10000-7000, a transitional zone T2 spanning roughly 40 km is interpreted where basement relief increases and the basement surface itself is imaged. As on profile E33, this section contains the M3 magnetic anomaly which is thought to be produced by exhumed serpentinized peridotites (Sibuet *et al.* 2007).

The landward limit of normal oceanic crust is placed near the M0 anomaly on profile E56 (CDP 6000). From this point seaward, basement relief is much more pronounced than on profile E33 whilst interpreted Moho reflections occur at similar times. Again, the disagreement between the interpreted

Moho reflections and the gravity-inverted Moho beneath this section may simply reflect that the Moho picked from the inverted density model should have corresponded to a higher density contrast beneath normal oceanic crust.

## ERABLE Profiles 53 and 54

E53 and E54 (Fig. 4: NB: Large 11x17 in. figure – see end of paper) are located further northeast along the southern Flemish Cap margin. E53 images the continental shelf of Flemish Cap where shallow water depth, combined with a hard water bottom reflection, makes noise from multiple reflections a severe problem. Although various multiple removal techniques were used in the processing flow, the signal to noise ratio remains very low. Below the thin sediment layer, basement is detected from refracted arrivals but no intra-crustal reflections have been successfully imaged along the shelf. A package of horizontal reflections between 9-11 seconds (~32 km depth using an average crustal velocity of 6.35 km/s) corresponds with the expected depth of the Moho, and continues south across the shelf shallowing to 8-10 seconds near the slope break (~29 km depth). These Moho reflections are consistent with the gravity-inverted Moho.

Along the continental slope there is little evidence of rotated fault blocks as observed on Galicia Bank (Reston *et al.* 1996) and the Iberian Abyssal Plain (Whitmarsh *et al.* 2000; Pickup *et al.* 1996). However, velocity models from an early refraction experiment (Todd and Reid 1989) confirm the presence of continental crust. The crustal block at CDPs 10000-11000 may represent a smaller westward dipping fault block adjacent to a horst that is bounded by a high angle landward dipping normal fault to the west, and a seaward dipping normal fault to the east.

Farther seaward, a crustal block of unknown origin is present between CDPs 11500-12000. Adjacent to this crustal block there is a change in the top of basement reflectivity character, and deeper reflections are more evident. A seaward dipping reflection, that likely represents a fault, coincides with this change in basement character. The basement surface of this block is very angular, demonstrating a similar shape to the top of a rotated fault block. Two similar crustal blocks near the foot of the slope on the SCR1 profile that lies north of E54, have been interpreted as continental crust by some authors (Funck *et al.,* 2003; Hopper et al., 2004) and the blocks on E54 may correlate with those identified on SCR1.

Immediately seaward of this block, Todd and Reid (1989) model a high velocity gradient within the crust and interpret the crust as oceanic. Similarly on SCR1, thin ocean crust is interpreted to lie just seaward of the two crustal blocks interpreted as continental crust extending for about 60 km until normal ocean crust thickness is reached (Funck *et al.* 2003; Hopper *et al.* 2004; Hopper *et al.* 2006). Thus, we adopt the same interpretation of thin ocean crust for this region on the E54 profile. Interpreted Moho reflections beneath this thinned oceanic crust show a good match with the gravity-inverted Moho.

A subtle change in the basement reflectivity occurs near the M0 magnetic anomaly located at ~CDP 17500. As with the other profiles, we interpret that this anomaly marks the landward limit of normal oceanic crust.

## ERABLE Profile 36

Furthest to the northeast, E36 (Fig. 5: NB: Large 11x17 in. figure – see end of paper) is sub-parallel to and intersects with SCR1. As with profile E54, no intra-crustal reflections have been successfully imaged along the shelf, but a package of horizontal reflections located between 8-10 seconds (~29 km depth using an average crustal velocity of 6.35 km/s) corresponds with the expected depth of the Moho, and are consistent with the gravity-inverted Moho.

Along the continental slope, several small rotated fault blocks are observed although these are not as clear as those imaged on the lines to the south. The crustal block at CDPs 6400-6800 may correlate with a similar block along SCR1 which marks the seaward limit of continental crust. Below this block, seismic refraction modelling results (Funck *et al.* 2003) reveal a pronounced shallowing of the Moho. We identify a prominent landward dipping reflector that is consistent with the Moho from the refraction

modelling and so provide the same interpretation. This interpreted Moho surface differs significantly from the gravity-inverted Moho which likely means that the upper mantle in this region is of anomalously low density and that the Moho picked from the gravity-inverted density model should have been at a lower density in this region.

As on profile E54, adjacent to the most seaward crustal block, there is a change in the top of basement reflectivity character along profile E36. A seaward dipping reflection, that likely represents a fault, coincides with this change in basement character and we interpret thin oceanic crust seaward of this fault.

Farther seaward, the location of the change from transitional thin oceanic crust to normal oceanic crust is difficult to pinpoint. A subtle change in the basement reflectivity occurs near the M0 magnetic anomaly located at ~CDP 9300 however the pronounced shallowing of the gravity-inverted Moho beneath this anomaly and seaward makes an interpretation of normal oceanic crust suspect at this location. Thus, we interpret the landward limit of normal oceanic crust to lie near CDP 11000 where the basement surface begins to shallow, basement relief increases and the gravity-inverted Moho deepens. Again, the disagreement between the interpreted Moho reflections and the gravity-inverted Moho beneath this section may simply reflect that the Moho picked from the inverted density model should have corresponded to a higher density contrast beneath oceanic crust.

## Discussion

The crustal domains interpreted on the ERABLE profiles considered in this study and those interpreted for the nearby SCREECH lines are mapped with simple linear interpolation to extend the interpretations off the lines (Fig. 6). This map view illustrates the complexity of the Newfoundland margin and highlights the need for a comprehensive rifting and breakup model that allows for rifting in the south and anomalous sea-floor spreading in the north.

The lateral extent of transitional crust generally decreases as we move northeastward along the margin such that serpentinized mantle ceases to exist somewhere between profiles E56 and E54 on the southeastern edge of Flemish Cap. Meanwhile, the conjugate Iberian margin is characterized by a much wider zone of serpentinized exhumed mantle that narrows to the north moving into the Galicia Bank region but does not disappear entirely. This wider zone of serpentinized exhumed mantle on the Iberian margin is also accompanied by a much wider zone of extended continental crust than on the Flemish Cap margin. This marked asymmetry is possibly the result of simple shear extension with a westward-dipping primary detachment or a simple shear/pure shear combination model (Fig. 7).

Whilst a simple 2D rifting model may be adequate for explaining the structures observed in the south of our study area, a more complex rifting model is clearly required to explain the significant along-strike variations. In particular, the complexities involved in the proposed rotation of Flemish Cap (Sibuet *et al.,* 2007), and possibly subsequent oblique shearing along the southern Flemish Cap margin (Todd and Reid, 1989) require a plan-view rifting and breakup model from the Late Jurassic to Early Cretaceous. We offer such a model for the evolution of the southern margin of Flemish Cap (Fig. 8).

Our model leaves North America (NA) fixed. A rifting triple junction active during the Late Jurassic is proposed with three branches that extend into: 1) East Orphan Basin, 2) along the southern margin of Flemish Cap, and 3) into the (future) Flemish Pass Basin (Fig. 8A). In addition to extension, dextral strike slip motion occurs along all three branches, and accommodates rotation and southeast displacement of Flemish Cap and southeast translation of the Iberian (IB) plate with respect to NA (Fig. 8B). Thus, the Flemish Pass Basin formed in a transtensional regime that accommodated movement and rotation of Flemish Cap (Sibuet *et al.* 2007).

A new major triple junction forms between NA, IB, and Eurasia (EU), as rotation of Iberia and northeast translation of EU creates additional rifted crust with breakup occurring along the Central Grand Banks during M3, progressing along the southern margin of Flemish Cap possibly through oblique shear mechanisms, and into the Bay of Biscay by M0 time (Figs. 8C and 8D). Finally, breakup occurs along the northeast edge of Flemish Cap during Albian time (C34; Fig. 8E).

Our proposed model contains rift and spreading segments that have been offset by oblique shearing (Fig. 8C). The margin geometry inherited from this model is consistent with the present-day structure of the Flemish Cap margin delineated using the seismic profiles interpreted in our study (Fig. 8F). Future work will involve extending this plan-view rifting model into depth so that the evolution of our 2D rifting model in the south can be adapted northward to satisfy our subsurface geometry constraints. This evolution may require a more complicated 2D rifting model than can be envisioned within the pure shear to simple shear spectrum.

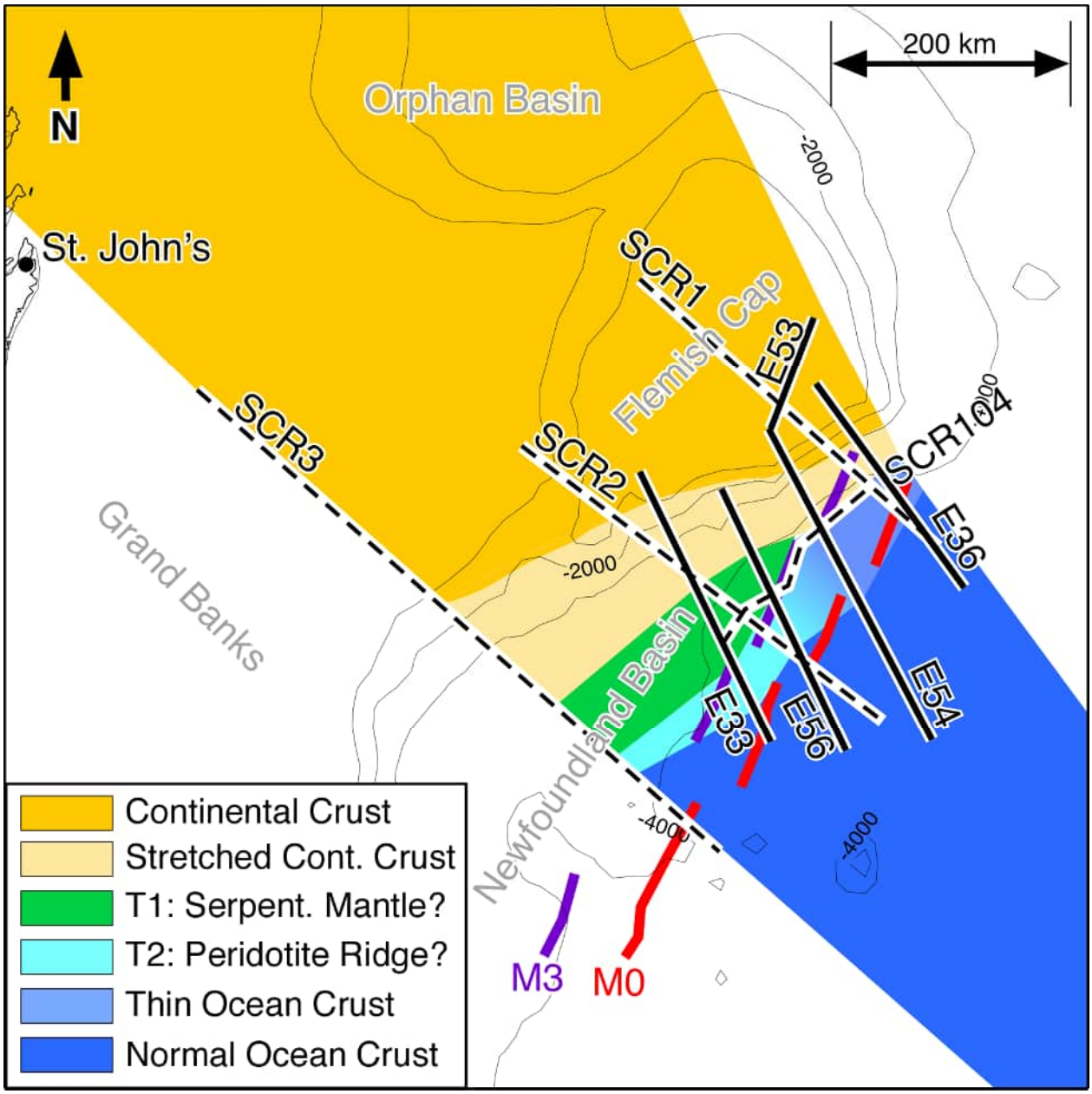


**Figure 6. Map of project area showing bathymetry (contours) and the interpreted crustal boundaries and domains from the SCREECH and ERABLE profiles considered in this study. The location of magnetic anomalies M0 and M3 are taken from Srivastava *et al.* (2000).**

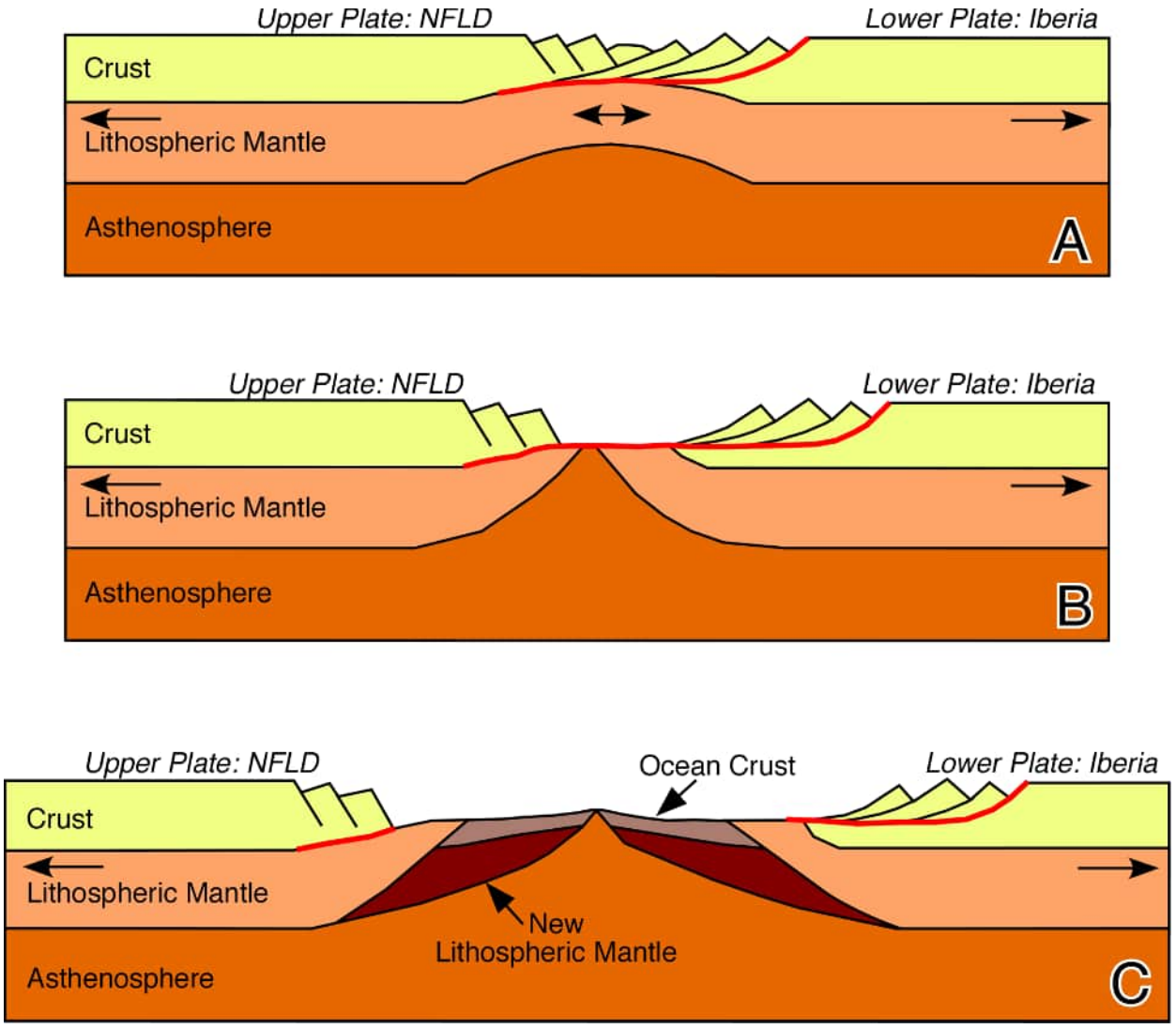


**Figure 7. Simple shear and pure shear combination model of A) crustal thinning, B) mantle exhumation and C) sea-floor spreading, where a detachment fault (outlined in red) penetrates the crust and soles at the crust/mantle boundary (modified from Keen *et al.* (1989) and Lister *et al.* (1991)). Pure shear stretching accommodates sub-crustal extension. Note that layer thicknesses are not drawn to scale.**

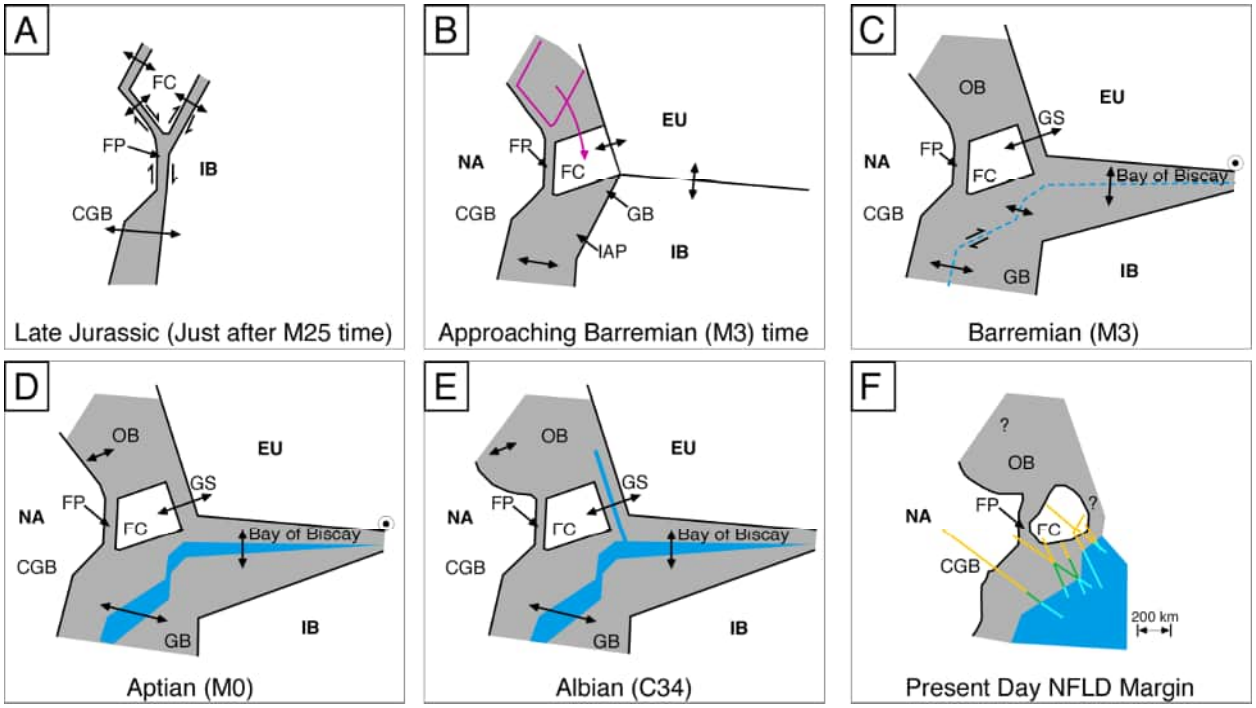


**Figure 8. Plan-view model illustrating how rifting and breakup between Newfoundland and Iberia may have evolved with time. CGB=Central Grand Banks, EU=Eurasia, FC=Flemish Cap, FP=Flemish Pass Basin, GB=Galicia Bank, GS=Goban Spur, IAP=Iberia Abyssal Plain, IB=Iberia, NFLD=Newfoundland, OB=Orphan Basin. Solid blue areas indicate formation of ocean crust, the blue dashed line outlines the location of imminent break-up. The bull's eye in C and D corresponds to the pole of rotation for IB. The seismic lines considered in this study are overlain on plot F with the continental, transitional and ocean crust segments highlighted in yellow, green and light blue respectively.**

## References


Dean, S.M., T.A. Minshull, R.B. Whitmarsh, and K.E. Louden, 2000, Deep structure of the ocean-continent transition in the southern Iberia Abyssal Plain from seismic refraction profiles: The IAM-9 transect at 40 20'N: Jour. of Geophysical Research, v.105, p.5859-5886.

Enachescu, M.E., 2006, Structural setting and petroleum potential of the Orphan Basin, offshore Newfoundland and Labrador: Recorder, v.31, no.2, p.5–13.

Funck, T., J.R. Hopper, H.C. Larsen, K.E. Louden, B.E. Tucholke, and W.S. Holbrook, 2003, Crustal structure of the ocean-continent transition at Flemish Cap: seismic refraction results: Jour. of Geophysical Research, v.108, no.B11, doi:10.1029/2003JB002,434.

Grant, A., and K. McAlpine, 1990, The continental margin around Newfoundland, *in* M. Keen and G. Williams, eds., Geology of the continental margin of Eastern Canada: Geological Survey of Canada, Geology of Canada, no.2, chap.6, p.239–292.

Hopper, J., R. Funck, B. Tucholke, K. Louden, W. Holbrook, and H.C. Larsen, 2006, A deep seismic investigation of the Flemish Cap margin: implications for the origin of deep reflectivity and evidence for asymmetric break-up between Newfoundland and Iberia: Geophysical Jour. International, v.164, no.3, p.501–515.

Hopper, J.R., T. Funck, B.E. Tucholke, H.C. Larsen, W.S. Holbrook, K.E. Louden, D.J. Shillington, and H. Lau, 2004, Continental breakup and the onset of ultraslow seafloor spreading off Flemish Cap on the Newfoundland rifted margin: Geology, v.32, no.1, p.93–96.

Keen, C., C. Peddy, B. de Voogd, and D. Matthews, 1989, Conjugate margins of Canada and Europe: results from deep reflection profiling: Geology, v.17, p.173-176.

Lau, K.H., K.E. Louden, T. Funck, B.E. Tucholke, W.S. Holbrook, J.R. Hopper, and H.C. Larsen, 2006a, Crustal structure across the Grand Banks-Newfoundland Basin continental margin - I. Results from a seismic refraction profile: Geophysical Jour. International, v.167, p.127–156.

Lau, K.H., K.E. Louden, S. Deemer, J. Hall, J.R. Hopper, B.E. Tucholke, W.S. Holbrook, and H.C. Larsen, 2006b, Crustal structure across the Grand Banks- Newfoundland Basin continental margin - II. Results from a seismic reflection profile: Geophysical Jour. International, v.167, p.157–170.

Lister, G.S., M.A. Etheridge, and P.A. Symonds, 1991, Detachment models for the formation of passive continental margins: Tectonics, v.10, p.1038-1064.

Pickup, S.L.B., R.B. Whitmarsh, C.M.R. Fowler, and T.J. Reston, 1996, Insight into the nature of the ocean-continent transition off West Iberia from a deep multichannel seismic reflection profile: Geology, v.24, p.1079-1082.

Reston, T.J., C.M. Krawczyk, and D. Klaeschen, 1996, The S reflector west of Galicia (Spain): Evidence from prestack depth migration for detachment faulting during continental breakup: Jour. of Geophysical Research, v.101, p.8075-8092.

Shillington, D.J., W.S. Holbrook, H.J. van Avendonk, B.E. Tucholke, J.R. Hopper, K.E. Louden, H.C. Larsen, G.T. Nunes, and O.L.S. Party, 2006, Evidence for asymmetric nonvolcanic rifting and slow incipient oceanic accretion from seismic refraction data on the Newfoundland margin: Jour. of Geophysical Research, v.111, no.B09402, doi:10.1029/2005JB003,981.

Shipboard Scientific Party, 2004, Leg 210 summary, *in* B.E. Tucholke, J.-C. Sibuet, A. Klaus, et al., eds., Proceedings of the Ocean Drilling Program, Initial Reports: Ocean Drilling Program, v.210, p.1-78.

Sibuet, J.-C., S. Srivastava, M.E. Enachescu, and G. Karner, 2007, Early Cretaceous motion of Flemish Cap with respect to North America: implications on the formation of Orphan Basin and SE Flemish Cap-Galicia Bank conjugate margins, *in* G. Karner, G. Manatschal, and L. Pinheiro, eds., Imaging, mapping and modelling continental lithosphere extension and breakup: Geological Society of London, Special Publications, v.282, p.63–76.

Srivastava, S., and J. Verhoef, 1992, Evolution of Mesozoic sedimentary basins around the North Central Atlantic: a preliminary plate kinematic solution, *in* J. Parnell, Basins on the Atlantic Seaboard: petroleum geology, sedimentology and basin evolution: Geological Society Special Publication, v.62, p.397–420.

Srivastava, S.P., J.-C. Sibuet, S. Cande, W.R. Roest, and I.D. Reid, 2000, Magnetic evidence for slow seafloor spreading during the formation of the Newfoundland and Iberian margins: Earth and Planetary Science Letters, v.182, p.61-76.

Todd, B.J., and I. Reid, 1989, The continent-ocean boundary south of Flemish Cap: constraints from seismic refraction and gravity: Canadian Jour. of Earth Sciences, v.26, no.7, p.1392-1407.

Tucholke, B., J. Austin, and E. Uchupi, 1989, Crustal structure and rift-drift evolution of the Newfoundland basin, *in* A. Tankard and H. Balkwill, Extensional tectonics and stratigraphy of the North Atlantic margins: AAPG Memoir, v.46, chap.16, p.247–263.

van Avendonk, H. J., W.S. Holbrook, G.T. Nunes, D.J. Shillington, B.E. Tucholke, K.E. Louden, H.C. Larsen, and J.R. Hopper, 2006, Seismic velocity structure of the rifted margin of eastern Grand Banks of Newfoundland, Canada: Jour. of Geophysical Research, v.111, no.B11404, doi:10.1029/2005JB004,156.

Welford, J.K., and J. Hall, 2007, Crustal structure across the Newfoundland rifted continental margin from constrained 3-D gravity inversion: Geophysical Jour. International, v.171, p.890–908.

Whitmarsh, R.B., and P.J. Wallace, 2001, The rift-to-drift development of the west Iberia nonvolcanic continental margin: A summary and review of the contribution of ocean drilling program leg 173, *in* M.O. Beslier, R.B. Whitmarsh, P.J. Wallace, and J. Girardeau, eds., Proceedings of the Ocean Drilling Program, Scientific Results: Ocean Drilling Program, v.173, p.1-36.

Whitmarsh, R.B., S.M. Dean, T.A. Minshull, and M. Tompkins, 2000, Tectonic implications of exposure of lower continental crust beneath the Iberia Abyssal Plain, Northeast Atlantic Ocean: Geophysical evidence: Tectonics, v.19, p.919-942.

**BACK**

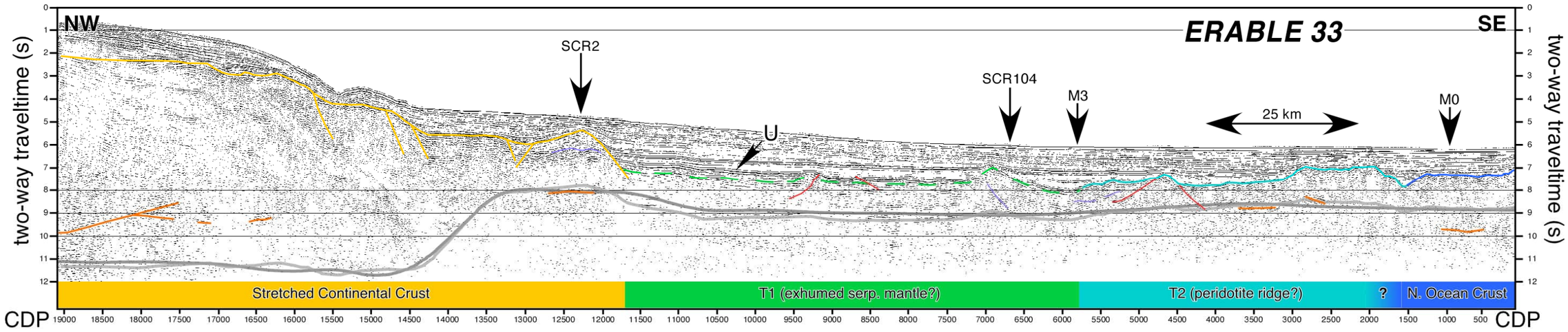


**LEGEND**

- Faults
- Intra-crustal Reflections/Faults?
- Continental Crust
- T1: Unreflective Transitional Crust (exhumed serpentinized mantle?)
- T2: Reflective Transitional Crust (peridotite ridge?)
- Normal Ocean Crust
- Unaltered or Serpentinized Mantle
- Gravity Inverted Moho
- Modified Gravity Inverted Moho

**Figure 2. Time migration of the ERABLE 33 (E33) seismic reflection profile. Magnetic anomalies M0 and M3 identified by Srivastava *et al.* (2000) and crossovers with other seismic lines are outlined as black arrows. Interpretation of crustal boundaries is discussed in text. U refers to the U-reflection.**

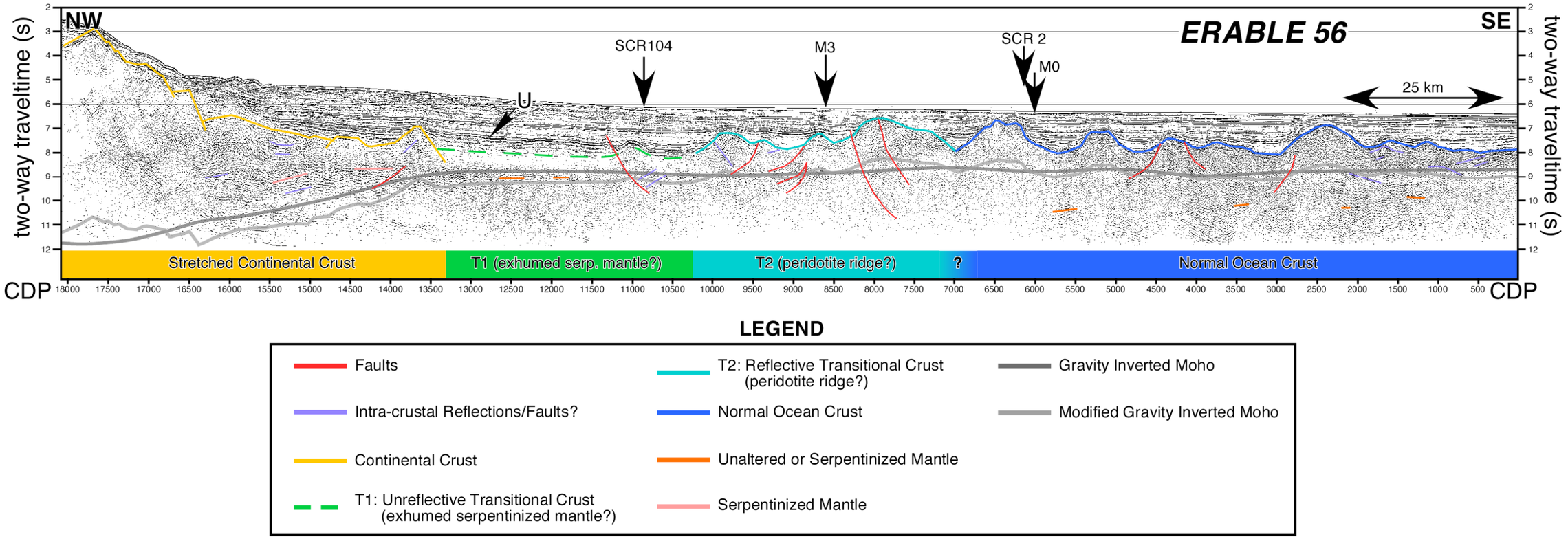


**Figure 3. Time migration of the ERABLE 56 (E56) seismic reflection profile. Magnetic anomalies M0 and M3 identified by Srivastava *et al.* (2000) and crossovers with other seismic lines are outlined as black arrows. Interpretation of crustal boundaries is discussed in text. U refers to the U-reflection.**

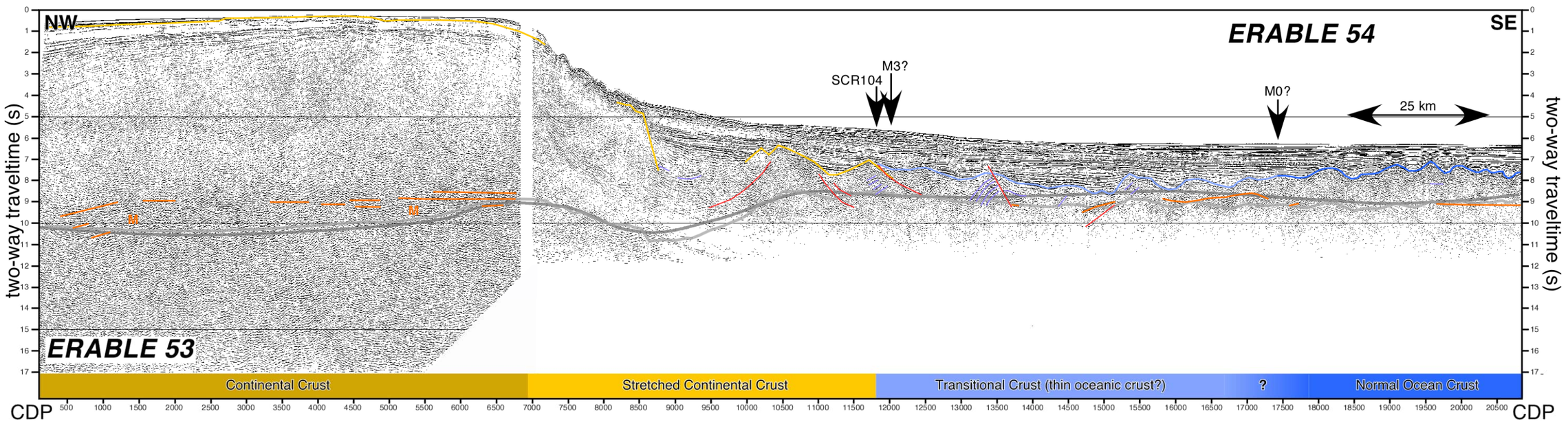


**Figure 4. Time migration of the combined ERABLE 53 and 54 (E53 and E54) seismic reflection profiles. Magnetic anomalies M0 and M3 identified by Srivastava *et al.* (2000) and crossovers with other seismic lines are outlined as black arrows. Interpretation of crustal boundaries is discussed in text.**

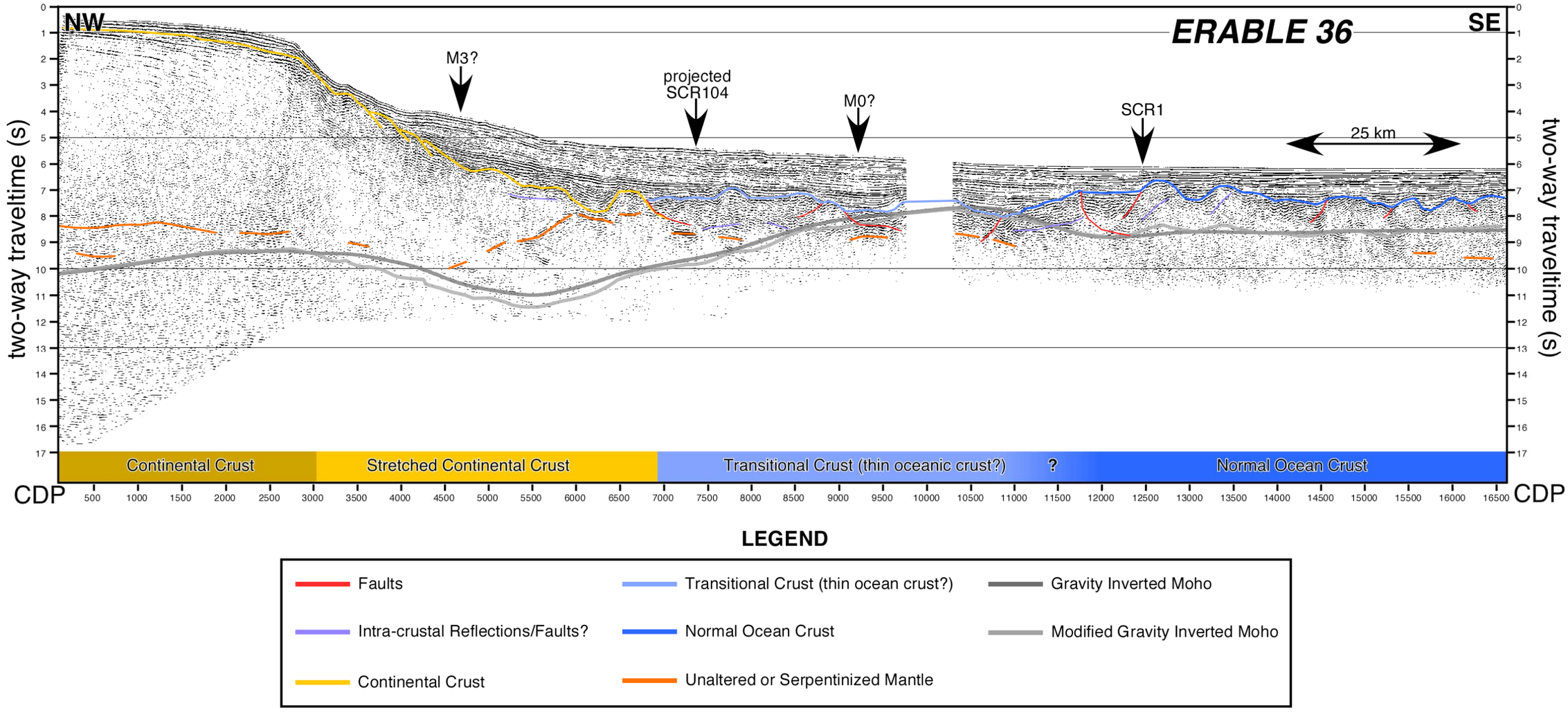


**Figure 5. Time migration of the ERABLE 36 (E36) seismic reflection profile. Magnetic anomalies M0 and M3 identified by Srivastava *et al.* (2000) and crossovers with other seismic lines are outlined as black arrows. Interpretation of crustal boundaries is discussed in text.**

# Thermochronology Evidence for Mesozoic and Cenozoic Inversions of the Continental Margin of Nova Scotia, Canada

**Marcos Zentilli**
**Casey E. Ravenhurst**
**G.Li**
Dept. of Earth Sciences
Dalhousie University
Halifax, Nova Scotia, B3H 4J1
Canada
e-mail: marcos.zentilli@dal.ca

**A.M. Sandy Grist**
Department of Earth Sciences
University of Queensland
Brisbane, Queensland 4072
Australia

**Robert J. Ryan**
Nova Scotia Department of Natural Resources
P.O. Box 698
Halifax, NS, B3J 2T9
Canada

## ABSTRACT

Considerable erosion followed the folding, metamorphism and grainotoid intrusion (ca. 380 Ma) of the Devonian Acadian Orogeny. By the Early Carboniferous (ca. 350 Ma) coarse clastics - followed by extensive marine carbonates and evaporites - were deposited non-conformably on exhumed granitoids and metamorphic rocks. The Carboniferous-to-Permian Maritimes Basin developed, accumulating clastic sediments in excess of 12 km in its depocentre further north. Maximum burial of the basin was attained in the Late Carboniferous (ca. 300 Ma), and the youngest sediments preserved in this basin are Lower Permian in age.

Apatite fission track thermochronology studies have shown that basin inversion led to erosion of ca. 5 km of strata in the Late Triassic, coinciding with the Atlantic break-up unconformity, and preceding extensive but short-lived basaltic magmatism (ca. 200 Ma). The traditional view of gradual exhumation and peneplanation of the Nova Scotia margin since the Triassic-Jurassic is untenable. During the Aptian-Albian, continental sediments were deposited throughout Atlantic Canada over a weathered surface that included karst and has wide expression along the margin. The exhumation of the land went hand in hand with deposition in the adjacent Scotian Basin, part of the present Atlantic passive margin, an active depositional basin from the Late Triassic-Early Jurassic to the present. In such a passive margin it was expected that rocks deep in offshore wells would be at their maximum temperature today. However, our apatite fission track thermochronology data indicates that rocks in offshore wells were once tens of degrees hotter (e.g. within the oil window) than at present, and that substantial post-Paleocene cooling has occurred.

Although higher paleo-mean annual surface temperatures in the Late Cretaceous may account for some of the thermal anomaly detected, the most probable cause for this cooling is inversion of the margin and erosion of ca. 1 km of post-Albian cover from onshore and offshore, probably in the Eocene - Oligocene. This Tertiary inversion may have important implications for hydrocarbon maturation, the distribution of deep-water sand bodies, overpressures, and post-Paleocene canyons and unconformities.

BACK

# NOTES

# PETROLEUM SYSTEMS

## Poster Session 2

**24. VARIATION IN PORE CONNECTIVITY WITHIN ABENAKI FORMATION CARBONATE LITHOFACIES, OFFSHORE NOVA SCOTIA**
Blissett, Donovan; Butler, Karl; and Keighley, David

**25. OLIGOCENE CANYON AND FAN DEVELOPMENT: THE RESPECTIVE ROLES OF SEA LEVEL AND SEDIMENT DELIVERY IN EVOLUTION OF THE EASTERN SCOTIAN MARGIN**
Brake, Virginia; Mosher, David and Wach, Grant D.

**26. MIDDLE CENOZOIC DEPOSITIONAL PROCESSES ALONG THE WESTERN SCOTIAN MARGIN**
Campbell, Calvin; Mosher, David and Wach, Grant D.

**27. COMPARING CONTROLS ON DEPOSITION OF MESOZOIC AND CENOZOIC MIXED CARBONATE-SILICICLASTIC SYSTEMS FROM THE CENTRAL ATLANTIC MARGIN, NORTH CAROLINA, USA**
Coffey, Brian P. and Read, Fred

**28. INTEGRATED RESERVOIR CHARACTERISATION, DEEP PANUKE GAS POOL, OFFSHORE NOVA SCOTIA**
Corbett, Norman; Uswak, Gordon and Skrypnek, Terrance

**29. THE MOHICAN CHANNEL GAS HYDRATE ZONE, SCOTIAN SLOPE: GEOPHYSICAL STRUCTURE**
Cullen, Janette; Mosher, David C.; Schlesinger, Angela; Haacke, Ross and Louden, Keith

**30. ABENAKI CARBONATE MARGIN FACIES ASSOCIATIONS: POSTER 1 - UPDATED DEPOSITIONAL FACIES TEMPLATE AND VERTICAL-LATERAL MARGIN VARIATIONS AS PIE DIAGRAM SECTIONS-MAPS**
Eliuk, Leslie

**31. ABENAKI CARBONATE MARGIN FACIES ASSOCIATIONS: POSTER 2 - SLOPE-FOREREEF SETTINGS AND SPECTRUM OF MICROBIAL MUD/REEF MOUNDS**
Eliuk, Leslie

**32. ABENAKI CARBONATE MARGIN FACIES ASSOCIATIONS: POSTER 3 - VARIETIES OF REEFS AND REEF MOUNDS OF THE OUTER MARGIN**
Eliuk, Leslie

**33. ABENAKI CARBONATE MARGIN FACIES ASSOCIATIONS: POSTER 4 - SHELF EDGE OOLITIC SHOALS OF THE INNER MARGIN AND ONCOLITE, BYPASS SAND, UNCONFORMITY THOUGHTS**
Eliuk, Leslie

**34. ABENAKI CARBONATE MARGIN FACIES ASSOCIATIONS: POSTER 5 - SPONGE REEFS AND ARGILLACEOUS SPONGE-RICH CARBONATES RELATED TO DELTAS: THE JURASSIC-CRETACEOUS BALTIMORE CANYON-NOVA SCOTIA ABENAKI EXAMPLES COMPARED TO THE MODERN FRASER PRODELTA EXAMPLE**
Eliuk, Leslie

**35. CARBONATE AND SILICICLASTIC SEQUENCE STRATIGRAPHY- EXAMPLES FROM THE LATE JURASSIC ABENAKI LIMESTONE AND WEST VENTURE DELTAIC BEDS, OFFSHORE NOVA SCOTIA, CANADA**
Eliuk, Leslie, and Wach, Grant D.

**36. CHARACTERIZATION OF PARALIC PALEOENVIRONMENTS USING BENTHIC FORAMINIFERA AND THECAMOEBIANS FROM EARLY CRETACEOUS SEDIMENTS (SCOTIAN SHELF)**
Fiorini, Flavia; Wach, Grant D and Scott, David B.

**37. CONTINENTAL SLOPE SEDIMENTATION MODELS: LAURENTIAN CHANNEL AND HALIBUT CHANNEL REGIONS, EASTERN CANADA**
Giles, Michael; Mosher, David C.; Piper, David J.W; Nedimovic, Mladen and Wach, Grant D.

**38. SEAFLOOR DIAGENESIS OF THE SCOTIAN BASIN: THE ROLE OF FE, TI, AND P**
Okwese, Ann Chioma; Pe-Piper, Georgia and Piper, David J.W

**39. BIOSTRATIGRAPHIC STUDY OF CENOZOIC STRATA OF THE GRAND BANKS, NEWFOUNDLAND**
Skilliter, Deborah; Williams, Graham L; Fensome, Robert A; Guerstein, G.R; MacRae, R. Andrew and Wach, Grant D.

**40. LOWER TERTIARY MASS TRANSPORT SYSTEMS EXHIBITED IN UPPER CRETACEOUS WYANDOT CHALK**
Smith, Brenton M.

**41. A QUANTITATIVE 3D OUTCROP MODEL OF A GRAVEL DOMINATED FLUVIAL SYSTEM (LATE TRIASSIC, MINAS BASIN, NOVA SCOTIA, CANADA)**
van Lanen, Xavier; Hodgetts, David; Redfern, Jonathan; Williams, Brian and Leleu, Sophie

**BACK**

# Variations in Pore Connectivity within Abenaki Formation Carbonate Lithofacies, Offshore Nova Scotia

**Donovan John Blissett**
**Karl Butler**
**Dave Keighley**
University of New Brunswick
P.O. Box 4400
Fredericton, NB
Canada E3B 5A3
e-mail: blissett@unb.ca

## ABSTRACT

The Scotian Basin, offshore Nova Scotia, hosts the Cohasset-Panuke oil field, which produced until 1999, various gas fields of the Sable project, and the Deep Panuke gas field, which will begin production in 2010. The reservoir for the latter field is part of an Upper Jurassic carbonate platform. Previous investigations of this carbonate platform have concentrated on lithostratigraphy, facies and diagenetic modeling, fracture analyses, burial dolomitization and seismic interpretation. This study examines pore distribution, geometry and pore connectivity within various carbonate lithofacies forming the carbonate platform with the aim of better understanding the overall early diagenetic processes that have influenced reservoir quality.

## Geological Background

The Scotian Basin underlies much of the Scotian Shelf and is typically subdivided into various structural highs, and lows or sub-basins (Fig. 1). The stratigraphy of the Basin (Fig. 2), as described by Kidston *et al*. (2005) and references therein, is most completely developed in the depocentres of the sub-basins. Here, the succession can be summarized as comprising Paleozoic metasedimentary and igneous rocks overlain by Triassic-Middle Jurassic red beds, salt, dolostone, and sandstone; a Middle-Upper Jurassic succession of interfingering sandstone, siltstone, shale and carbonate; Cretaceous-Neogene strata characterized by sandstone, siltstone, shale, mudstone and chalk; and Quaternary sediment. It is the Jurassic carbonate, assigned to the Abenaki Formation, and the reservoir rock for the Deep Panuke gas field, that is the subject of this investigation. This carbonate was deposited in a platformal setting (low topographic relief, shallow-marine sedimentary expanse (Tucker and Wright 1990)) and on the passive Scotian continental margin of the widening Atlantic Ocean. The carbonate platform was best developed in the west of the Basin, away from clastic-delta depocentres to the northeast, and is most prominent at the hinge zone between the La Have Platform and the Shelburne and Sable subbasins (Fig. 1).

The Abenaki Formation is subdivided into four members. The basal Scatarie Member is primarily a grainstone unit consisting of ooliths, fossil fragments and quartz grains formed during progradation of the platform into deeper waters. The Misaine Member comprises gray calcareous shale interbedded with micritic pelletoidal limestone, and represents a marine transgressive phase. Renewed expansion of the platform is represented by the overlying Baccaro Member, dominated by oolitic grainstone alternating with pelletal mudstone which is locally interbedded with shale and sandstone, and the Artimon Member which locally caps the succession and consists of grey calcareous shale and argillaceous fossiliferous limestone.

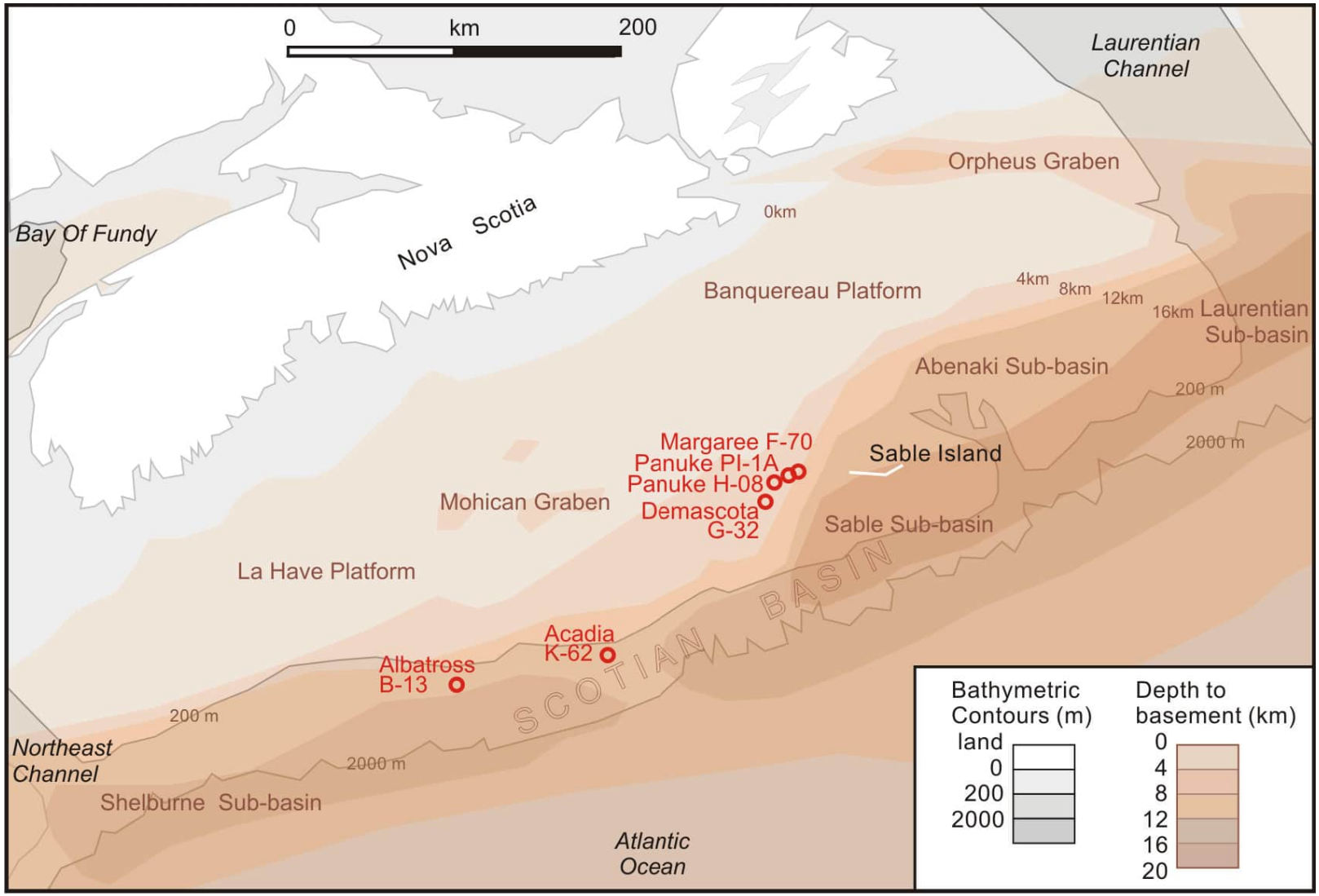


**Figure 1. Map of offshore Nova Scotia showing depth to pre-Mesozoic basement and main depositional basins, bathymetric contours, and approximate location of wells (red circles) from which samples were taken. Adapted from Wade (2000) and N.S. Dept. of Energy map DOE 2007-1.**

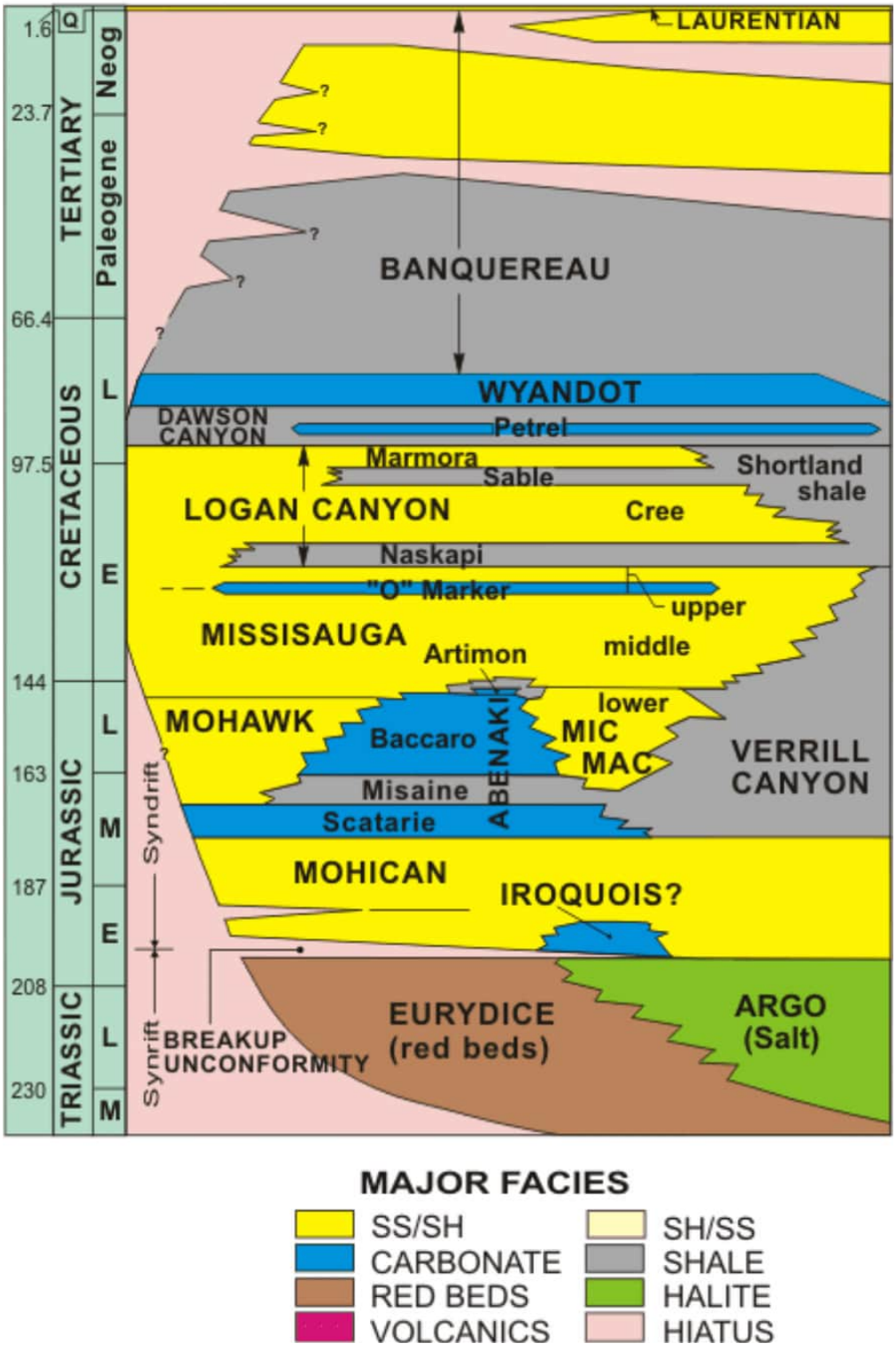


**Figure 2. Generalized stratigraphy of the Scotian shelf. Reproduced with the permission of Natural Resources Canada 2008, courtesy of the Geological Survey of Canada.**

Based on a set of sequence stratigraphic criteria, the formation is alternatively divided into Abenaki 1-7 (Wierzbicki *et al*. 2002) as shown in Table 1. Facies and subfacies associations (Fig. 3) are the other type of divisions reported from the Abenaki Formation (Wierzbicki *et al*. 2002). Further detailed stratigraphic analyses, inclusive of facies distribution and types, diagenetic history and regional geology, are described in McIver (1972), Given (1977), Eliuk (1978), Wierzbicki and Harland (2004), Wierzbicki et al. (2002, 2005) and Kidston *et al*. (2005).

| Division | Member | Dominant Lithology |
|---|---|---|
| Abenaki 1 | Scatarie | grainstones |
| Abenaki 2 | Misaine | calcareous shales |
| Abenaki 2-6 | Baccaro | oolitic grainstones |
| Abenaki 7 | Artimon | calcareous shales |

**Table 1. Table depicting the distribution of sequence stratigraphic divisions within the Abenaki Formation along with the general lithology of each Member. Note that Abenaki 2 is a basal segment of the Baccaro Member and is transitional from the underlying Misaine. Abenaki 3-5 together constitute the bulk of the Member and represents lagoonal, oolitic, reef, reef margin and talus facies. Abenaki 6 represent a deeper water facies (Wierzbicki *et al.* 2002).**

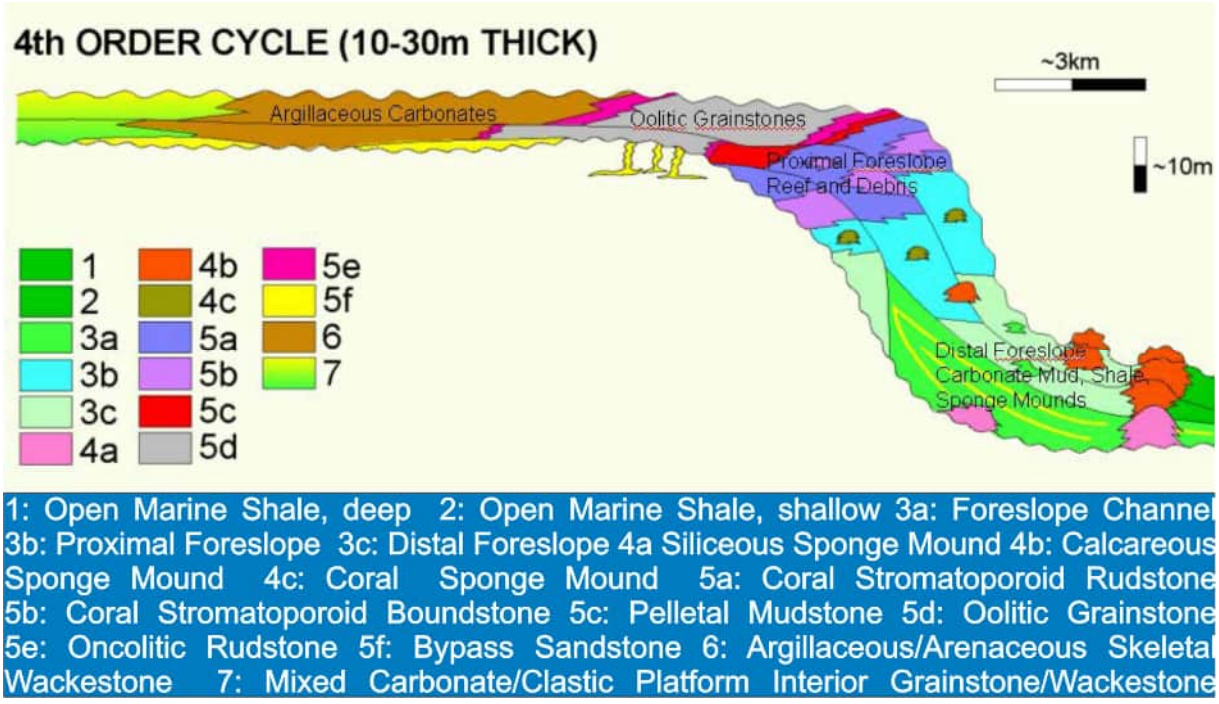


**Figure 3. Schematic diagram of the Abenaki facies model. Reproduced with the permission of R. Wierzbicki and L. Eliuk.**

## Materials and Methods

This investigation examines Abenaki carbonate reservoir characteristics with respect to pores and their connectivity. The significance of fabric selective porosity types within differing carbonate facies and the importance of various diagenetic fabrics within these facies are also examined. Accordingly, twenty-two sample core chips from six wells, detailed in Table 2, were obtained. Different lithologies and porosity types were targeted with a bias towards sections of the cores having carbonate lithofacies with obvious vugs, stylolites and, or, fossil remnants. Samples from Panuke H-08 (labelled Pan3A, 3C, 5 and 12) were of biosparite-biopelmicrite with vugs and micro-fractures. Those from Demascota G-32 (Dem1-7) were of sparse–packed biomicrite with micro-stylolites and fractures. Acadia K-62 material (Acad1-3) included a dolomitic limestone, packed biomicrite and biopelmicritic with micro-stylolites and pyrite inclusions. Samples from Margaree F-70 (Marg1-6) were of drusy dolostone-bioclastic dolostone, and calcitic dolomite. One sample of dolomite-cemented oolitic grainstone with calcite-filled fractures was taken from Albatross B-13 (Alba1) and a drusy dolostone with zoned dolomite crystals and micro-fractures was sampled from Panuke 1A/1 (1A/1).

Material from the chips were prepared and mounted for analyses as either unpolished thin sections for standard and enhanced light microscopy, unpolished slabs for Scanning Electron Microscopy (SEM) analyses, or cylindrical mini-cores for Micro Computed Tomography (MicroCT) scanning. The enhanced light microscopy utilized an epiflourescence microscope (see Dravis and Yurewicz 1985, and Dravis, 1991 for techniques). For SEM analyses, a JEOL JSM 6400 instrument was employed with an attached Genesis 4000 Energy Dispersive X-ray Analyzer (EDAX). Elemental analyses produced by this instrument were used to investigate mineralogical variation. The fragile/friable nature of the samples prevented us from applying the polishing process required for rigorous quantitative EDAX elemental analyses. We therefore used elemental ratios (rather than individual elemental abundances) to compare the mineralogies of different fabrics within the samples.

MicroCT imaging was undertaken using a Skyscan-1072 table-top instrument that measure spatial variation in X-ray attenuation within samples up to 11 mm in diameter and up to 30 mm in height. At energies less than 100KeV the photoelectric effect is primarily responsible for attenuation, and the attenuation coefficient is a function of the effective atomic number (Zeff) of the material examined, with attenuation increasing with Zeff. Consequently, carbonate mineral grains and crystals that are sufficiently large to be resolved by the instrument (>18μm), and display contrasting Zeff (*e.g.* calcite = 15.88; dolomite = 13.94) can be distinguished, as can pore space. Such heterogeneity can be visualized by plotting grey-scale images of attenuation variations within 2D slices through the sample. Alternatively, data from many slices may be combined to render 3D illuminated grey-scale images to better illustrate pore geometry and connectivity.

Image-analysis techniques are used to quantify porosity or specific mineral phases. Preparation of samples to obtain effective porosity entailed an initial MicroCT scan of the 'dry' sample, in which pores were filled with air having low Zeff followed by a second 'wet' scan after the sample had been saturated with high Zeff potassium iodide (KI) solution. Precise alignment and subtraction of these two images removed the common (solid and isolated pore) component and left an image of the connected pore space (Agbogun *et al*. 2007).

(Continued on next page.)

| Sample # | Depth (m) | Descriptions | Facies |
|---|---|---|---|
| Marg1 | 3441.0 | Fossiliferous biomicrite with microfractures and stylolite development. Dolomitization and pyritization occurs along stylolite | Sponge microbial micro reeflet; stromatoporoid-chaetetid micro reef; microsolenid cap reeflet on shallow coral debris reef= sub facies 3b, proximal foreslope. Facies association 3=foreslope |
| Marg2 | 3447.4 | Packed biomicrite-calcitic dolomite with micritized rims, intercrystalline pores and multiple fractures with pyrite inclusions. Sutured crystalline boundaries | |
| Marg3 | 3451.2 | Drusy dolomite having intercrystalline porosity and second generation fracture porosity | |
| Marg4 | 3455.1 | Calcitic dolomite showing late stage dolomitization, sparse to packed biomicrite. Drusy dolostone with intercrystalline porosity. fluid inclusions | |
| Marg5 | 3461.0 | Drusy bioclastic dolostone with intercrystalline porosity and fused crystal interface | |
| Marg6 | 3464.6 | Limestone-drusy, coraliferous, peloidal dolomitic limestone with zoned crystals and mouldic porosity | |
| 1A/1 | 4030.5 | Intercrystalline limestone to dolomitic limestone with zoned dolomite crystal having various vug sizes, dedolomite crystal, sutured crystal boundaries and irregular crystal contact, stylolitic and intercrystalline pore space | Coral-stromatoporoid-chaetetid-algal reef (eg. Backreef patch reef, rubble of reef flat, back- and forereef)=sub facies 5b. Facies association 5=Open marine platform margin |
| Dem1 | 3424.0 | Sparse to packed biomicrite with micro stylolites, oolites and fractures. Bioclast includes bryozoans, sponge spicules and foraminifers. Porosity is low and, fabric selective, occurs in dolomitized mouldic areas and in fractures | Siliceous sponge reef= sub facies 4a and Lithistid sponge-chaetetid-stromatoporoid= sub facies 4b respectively. Facies association 4= Foreslope (deeper-water). |
| Dem2 | 3428.0 | Fossiliferous micrite with bryozoans, fenestrae foraminifers and oolites as clasts | |
| Dem3 | 3608.0 | Fossiliferous-sparse biomicrite with fabric selective porosity | Coral-stromatoporoid-chaetetid-algal reef (eg. Backreef patch reef, rubble of reef flat, back- and forereef)=sub facies 5b. Facies association 5=Open marine platform margin |

**Table 2. List of designated sample numbers, relating depths, lithologic descriptions and corresponding facies/subfacies association. Lithofacies subfacies association is in accordance with Wierzbicki et al., 2002, Abenaki facies model Fig. 3 herein. Note that not all represented facies were sample based on our concentration on carbonates. Specific well associated with sample numbers are Panuke H-08 (Pan3A, 3C, 5 and 12), Demascota G-32 (Dem 1-7), Acadia K-62 (Acad1-3), Margaree F-70 (Marg1-6), Albatross B-13 (Alba 1), Panuke IA/1 (IA/1).**

## Transmitted Light Microscopy and SEM Observations

Pore space of secondary origin is evident in the samples examined with the transmitted light microscope. Such pores are interpreted to be the result of one or more of four main diagenetic processes: micritization, neomorphism, dissolution and dolomitization. Diagenesis commenced with micritization of most bioclasts and locally of matrix (Fig. 4A-D), producing microporosity. In numerous samples, pores that are irregular in shape (average diameter of 0.5 mm) formed by concomitant or subsequent, partial or complete, dissolution of shell fragments (Figs. 4,5). Other pores, rounded in shape, are of more enigmatic. Neomorphism likely followed, and dolomitization appears to be the final process, resulting in dolomite crystals growing from the inner rim of micritized fossil fragments to potentially fill a void (Fig. 5B).

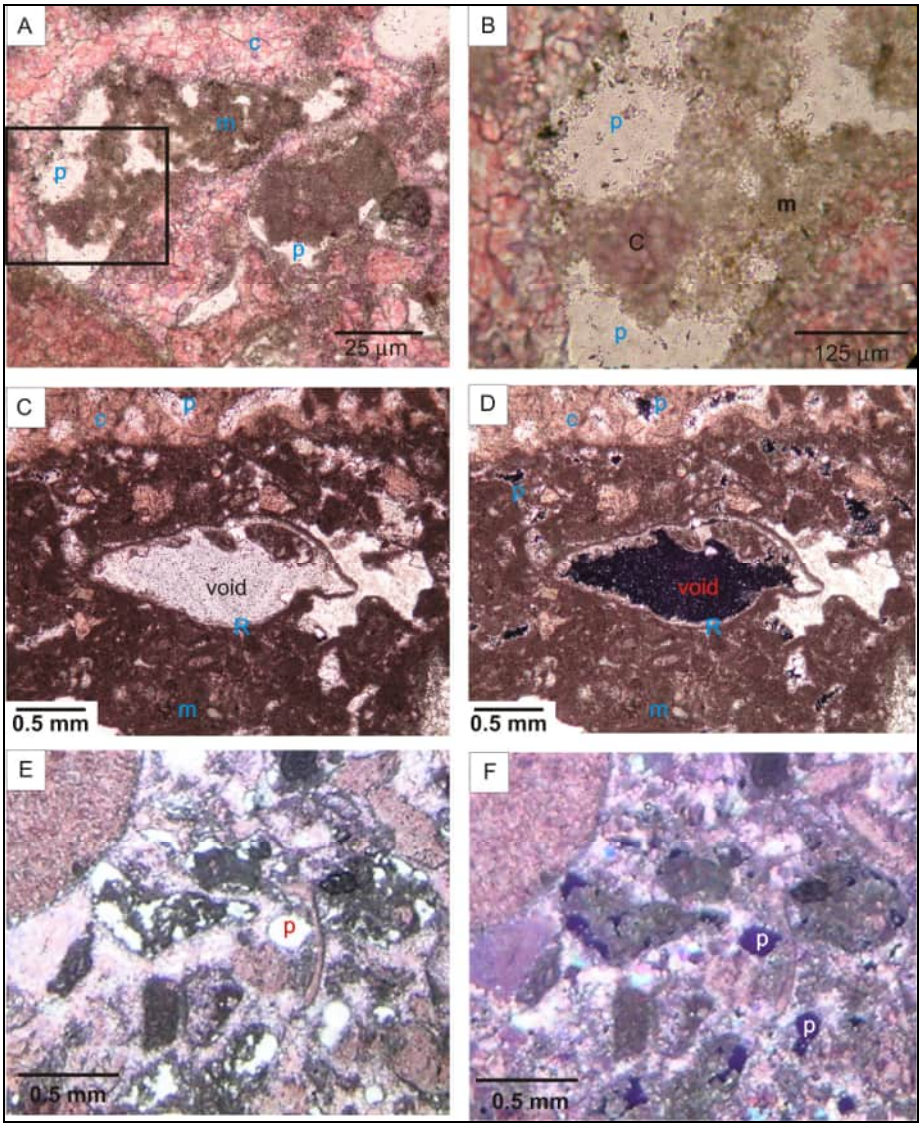


**Figure 4. A. Photograph of an area of a thin section (Pan 3A) taken using a transmitted light microscope. Showing pore space (p), micrite (m), calcite crystals (c) and fossil rim (R). B. Enlarged picture of the area outlined in A. Note neomorphic crystallization (C) occurring within pore space adjacent to micrite. C. and E. Examples of various styles of pore space observed within samples from Dem 5 and Pan 3A respectively. D. and F. Cross-polarized equivalent of C. and E. All slides were stained.**

Other samples exhibit either extensive fabric-preserving or fabric-destroying dolomitization (Fig. 5C-D). The latter is more common within the sample suite. Preservation of intercrystalline pore spaces is also common. In order to preserve primary fabrics high-magnesium calcite has to be present and a balance between dissolution of fossil fragments and dolomite precipitation has to be reached (Sibley, 1982; Tucker and Wright 1990). Fabric destruction occurs when dolomitization rates are high (greater influx of magnesium into the system) normally in the presence of the stable low magnesium calcite (Sibley 1982; Scoffin 1987).

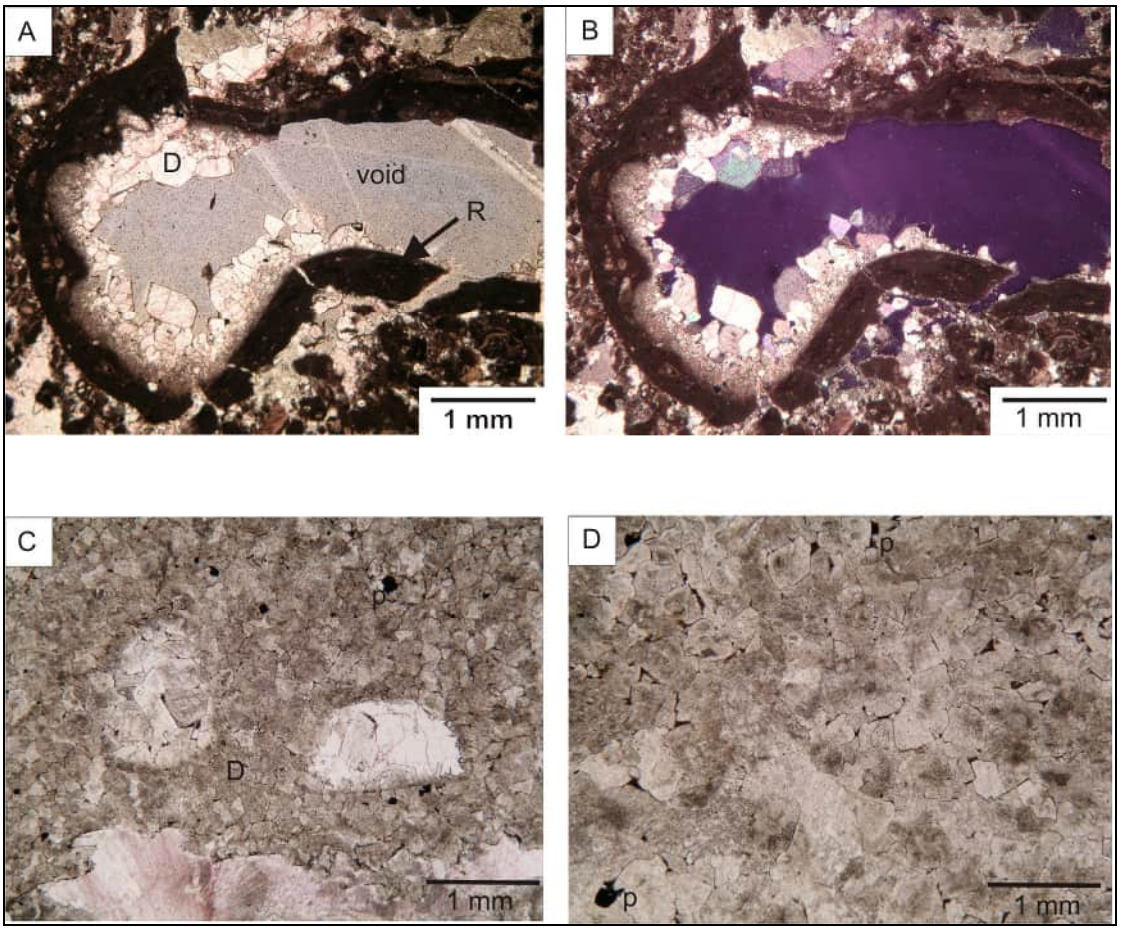


**Figure 5. Photographs of stained thin sections. A. Micritized rimmed fossil fragment with void within a crystalline matrix from sample # Dem 3. B. Cross-polarized equivalent of A. C. Dolomitized example showing the preservation of original fabrics within sample Marg 2. D. Dolomitized example showing the non-preservation of original fabric within sample Marg 2. Key: R=micritized rim, D=dolomite crystal and p=pore space.**

SEM-EDAX analysis of sample Pan 3A (Panuke H-08) has shown variation in Mg/Ca ratios in both fossils and matrix. The Mg/Ca ratio is lower close to the fossil/matrix boundary than it is in the core of the fossil and the distal matrix (Fig. 6). This may indicate that at some stage in the early diagenetic history of the sample, Mg was diffusing from the fossil into pore waters. Later matrix cements with a higher Mg component would indicate equilibrium was eventually reached. Ongoing analyses are aimed at determining whether similar variation occurs adjacent to secondary pore boundaries as an aid to understanding the origin of these pores.

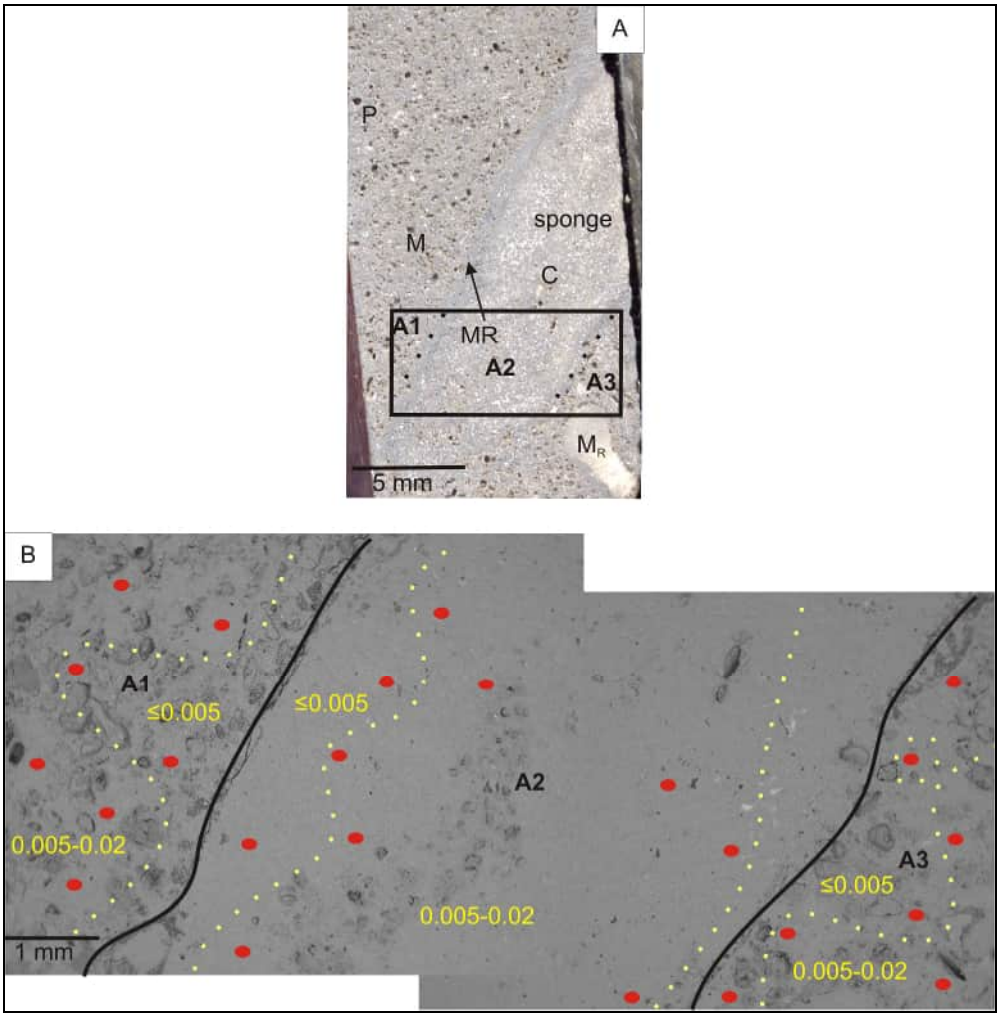


**Figure 6. A. Carbon coated, unpolished slab, sample Pan3A (Panuke H-08), used in obtaining EDAX data, rectangle represents area of the SEM images in B. B. Mosaic SEM images with red spots representing points where EDAX data were taken. Dotted lines represent contours of Mg/ca ratios. Solid lines represent fossil fragment boundary. Symbol designation: A1-3= areas grouped for analyses, C=core of micritized rimmed, fossil remnants, $M_R$=fossil fragment, P=pore space, M=matrix and numerical notations represents range of Mg/Ca ratios for contouring.**

## MicroCT Imaging

A sample (Pan 5) from Panuke H-08 has been analyzed for effective porosity. Comparison of a total porosity image obtained for a dry sample versus its KI-saturated wet equivalent and their difference is illustrated in Figure 7. Total porosity (from the dry image) and the effective porosity (from the difference image) have been calculated in a region of interest measuring 3.5 mm in diameter and extending 12 mm into the sample (ROI in Fig. 7A1-A3).

The total porosity of 16% contrasts with an effective porosity of just 8%. In comparison, the He-porosity of 13% from a CoreLab sample at a similar depth suggests much better reservoir quality. The

differences are due to natural variation in lithology from the location of the CoreLabs sample and that of our analyses. There is also localized lithological variation within and between each imaged slice.

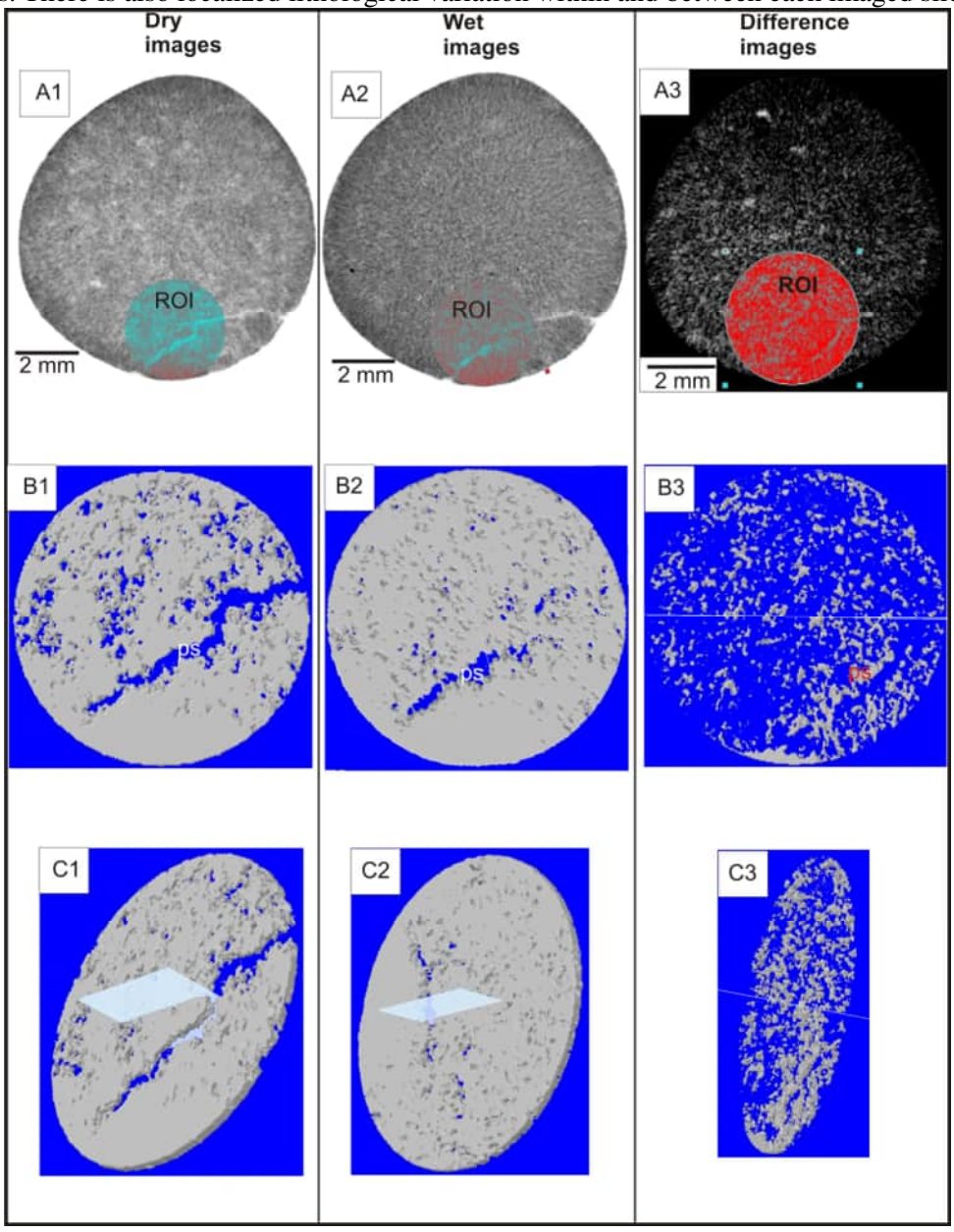


**Figure 7. Images of slices from Pan 5 (Panuke H-08) showing fractures and pore spaces. A1-A3. Dry, wet and difference images of corresponding slices. B1-B3. 3D plan view of region of interest (ROI) depicted in A1-A3. C1-C3. Corresponding rotated view of six slices from the ROI. In the dry and wet images pores spaces are open and denoted ps whereas in the difference images they are solid (ps). Note the prominence of fractures, pore spaces and in A3 the effect pore space. Specs. X-ray voltage=61Kv, thickness of slice=18 µm.**

The MicroCT unit can also be used to examine pore geometry, and whether or not suspected pore blockages exist. A sample from Demascota 32, Dem 4, was imaged and 45 slices located in the highlighted region of the radiograph image in Figure 8 were examined. The size and shape of the pores were determined by the enlargement of generated images of individual slices (Fig. 9). If necessary,

smaller sample diameters, 5 mm or less, could have been used, enabling the magnification setting on the MicroCT to be greatly increased to produce larger, undistorted, images.

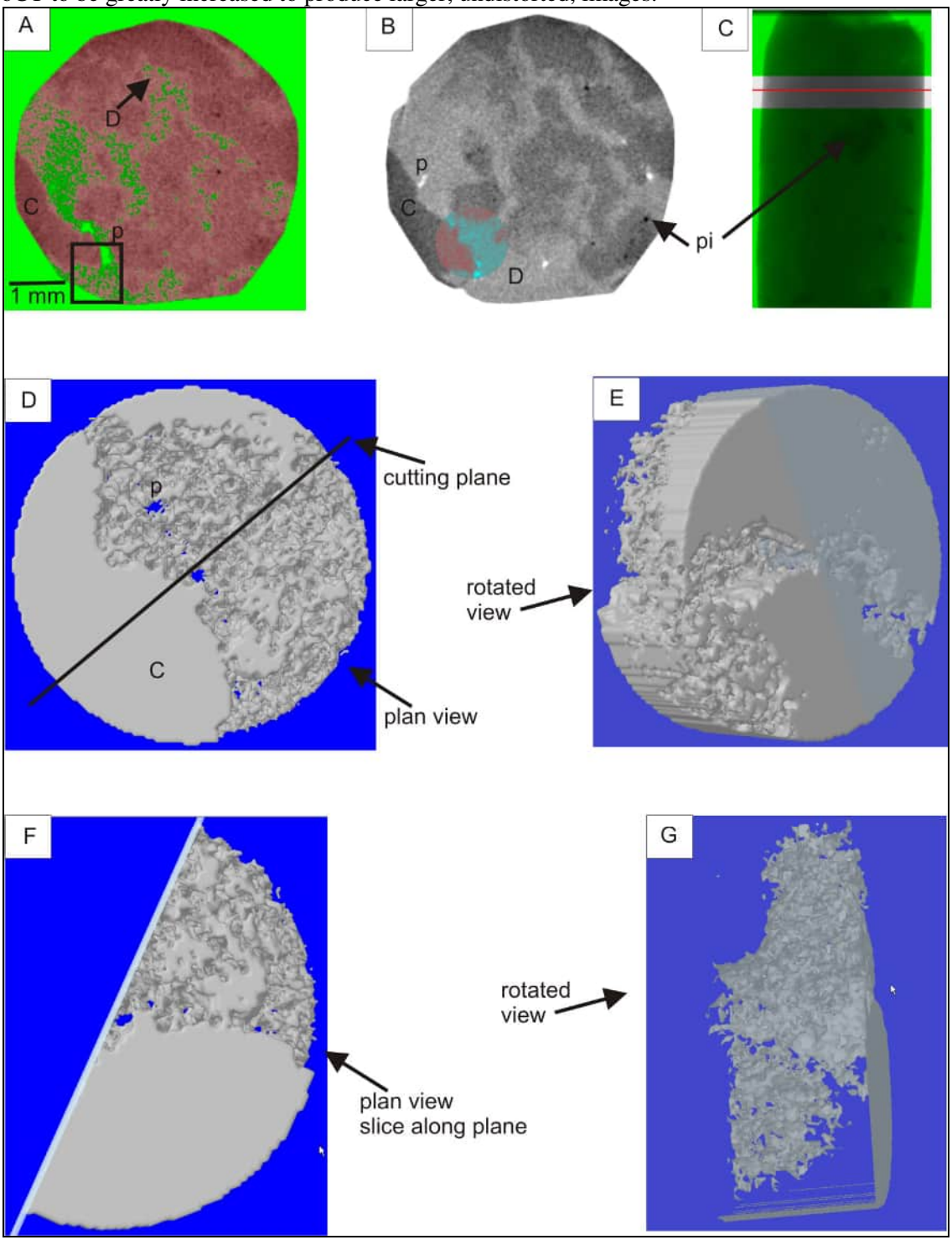


**Figure 8. Generated MicroCT images of sample Dem 4, Demascota G-32. A. Slice showing threshold pore spaces, green (porosity=4.8%). Rectangular area is related to Figure 9. B. Shows the location of ROI (diameter 14 mm). C. Radiograph image of mini-core, showing region, upper faded area where 45 slices for projection (D-G). D-G. Various projections of the 3D images of the 45**

**slices. Symbols definitions: p=pore space, C=calcite, D=dolomite, pi=pyrite inclusion. Spec. X-ray voltage=90Kv, thickness of slice=11 µm, pixel size=11 µm.**

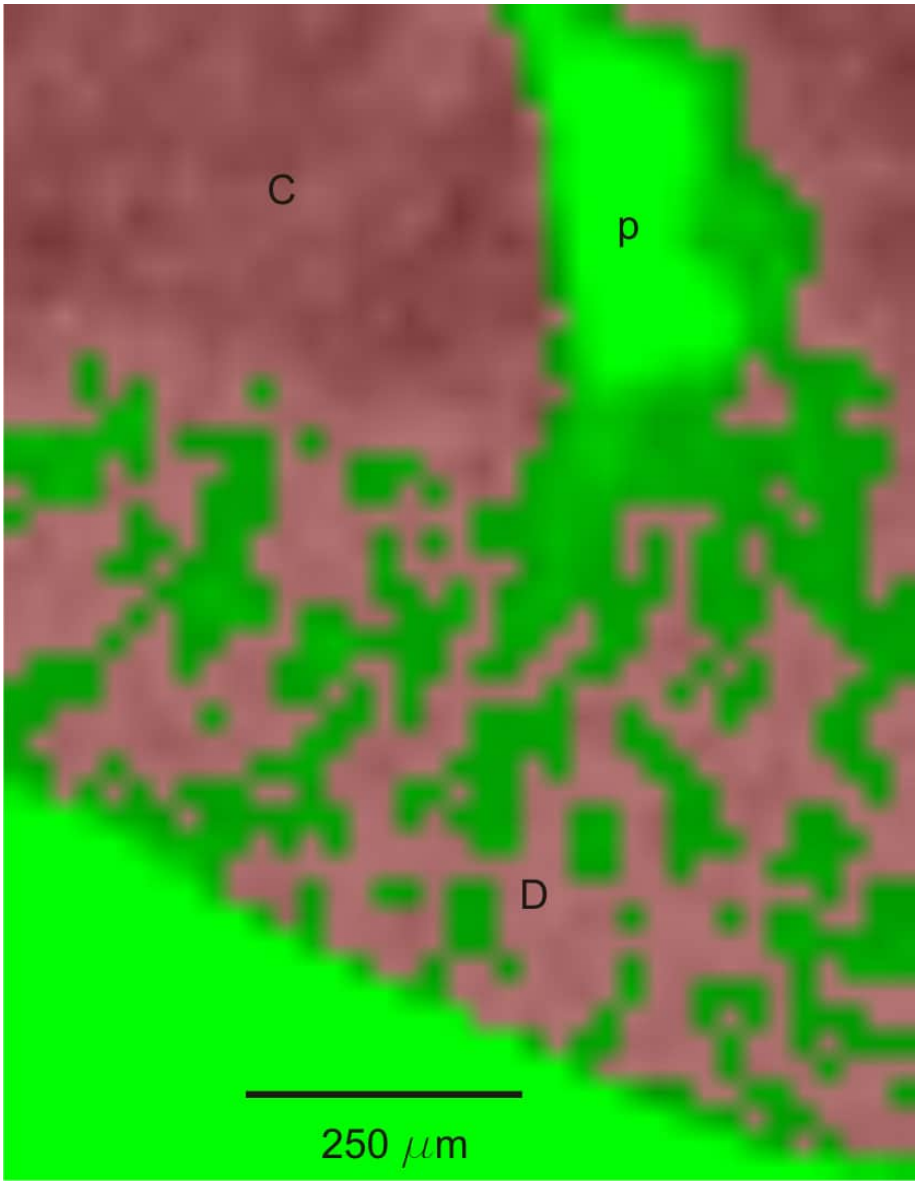


**Figure 9. Pixellated image of the rectangular area depicted in Figure 8. Green areas represent micro-pore space. Symbols definitions: p=pore space, C=calcite, D=dolomite.**

## Conclusions

An investigation of pore characteristics in the Abenaki carbonate reservoir of the Scotia Basin is ongoing. To date, it has been recognized that the abundance of secondary porosity is a result of the combination of total and partial micritization, dissolution and neomorphism. Also, Mg/Ca ratios are found to vary between the micritized rim and core of fossil fragments, and within the matrix. Magnesium diffusion from fossils into pore waters is implied.

MicroCT techniques allow quantification and visual comparisons of total and effective porosity which differ by a factor of two for the sample presented here. The method can also be used to examine pore connectivity, pore geometry, and types of pore obstructions.

## Acknowledgements

Funding for this project is provided by the Atlantic Innovation Fund through the Pan-Atlantic Petroleum System Consortium (PPSC). H. Agbogun is thanked for his assistance with software techniques and A. Park for several spirited discussions on physical chemistry. We thank the technical staff of the Institute of Material Visualization and Analysis (IMAV), MicroCT lab, the Microscopy Microanalysis Unit, and the Geology Preparation Lab, University of New Brunswick. We also wish to thank L. Eliuk, R. Wierzbicki, the Nova Scotia Department of Energy and Natural Resources Canada, and the Geological Survey of Canada for granting us permission to reproduce their published figures.

## References

Agbogun, H.M., L.C. Cavé, and T.A. Al, 2007, High resolution measurement of porosity and solute concentration in a diffusion experiment using computed tomography: 60th Canadian Geotechnical Conference & 8th Joint CGS/IAH-CNC Groundwater Conference Ottawa, October, 2007, CD-Rom, p.612-619.

Dravis, J.J., 1991, Carbonate petrography-update on new techniques and applications: Jour. Sedimentary Petrology, v.61, p.626-628.

Dravis, J.J. and D.A. Yurewicz, 1985, Enhanced carbonate petrography using fluorescence microscopy: Jour. Sedimentary Petrology, v.55, p.795-804.

Eliuk, L.S., 1978, The Abenaki Formation, Nova Scotia Shelf, Canada-A depositional and diagenetic model for a Mesozoic carbonate platform: CPG Bull., v.26, p.424-514.

Given, M.M., 1977, Mesozoic and early Cenozoic geology of offshore Nova Scotia: CPG Bull., v.25, p.63-91.

Kidston, A.G., D.E. Brown, B, Smith, and B. Altheim, 2005, The Upper Jurassic Abenaki Formation, Offshore Nova Scotia: A Seismic and Geologic Prespective; CNSOPB, Halifax, Nova Scotia, 168p.

McIver, N.L., 1972, Cenozoic and Mesozoic stratigraphy of the Nova Scotia Shelf: Canadian Jour. Earth Science, v.9, p.54-70.

Moore, H.C., 1989, Carbonate diagenesis and porosity: Elsevier, Amsterdam, 338p.

Putnis, A. and J.D.C. McConnell, 1980, Principles of mineral behaviour: Elsevier, New York, 257p.

Scoffin, T.P., 1987, An introduction to carbonate sediments and rocks: Chapman and Hall, New York, 274p.

Sibley, D.F., 1982, The origin of common dolomite fabrics: clues from the Pliocene: Jour. of Sedimentary Petrology, v. 2, p.1087-1100.

Tucker, M.E. and V.P. Wright, 1990, Carbonate Sedimentology: Blackwell Scientific Publications, Oxford, 482 p.

Wierzbicki, R. and N. Harland, 2004, Diagenetic model: Deep Panuke reservoir, offshore Nova Scotia, Canada; Search and Discovery Article #40135.

Wierzbicki, R., N. Harland, and L.S. Eliuk, 2002, Deep Panuke and Demascota core from the Jurassic Abenaki Formation, Nova Scotia- Facies model, Deep Panuke, Abenaki Formation: CSPG Diamond Jubilee Convention, Cd-rom of Abstracts, Paper # 12345678, p.31.

Wierzbicki, R., J.J. Dravis, I. Al-Asam, and N. Harland, 2006, Burial dolomitization and dissolution of Upper Jurassic Abenaki platform carbonates, Deep Panuke reservoir, Nova Scotia, Canada; AAPG Bull., v.90, p.1843-1861.

Wierzbicki, R., K. Gillen, R. Ackerman, N. Harland, and L. Eliuk, (with contribution from Jeff Dravis). 2005. Interpretation of a fractured dolomite core: Margaree F-70, Deep Panuke, Nova Scotia, Canada: CSPG, Annual Meeting, Core Convention Extended Abstracts, p.339-363.

BACK

# Oligocene Canyon and Fan Development: The Respective Roles of Sea Level and Sediment Delivery in Evolution of the Eastern Scotian Margin

**Virginia Brake**
**Grant Wach**
Dalhousie University
Department of Earth Sciences
Halifax, Nova Scotia B3H 4J1
Canada
e-mail: vbrake@dal.ca

**David Mosher**
Geological Survey of Canada (Atlantic)
1 Challenger Drive
P.O. Box 1006
Dartmouth, Nova Scotia B2Y 4A2
Canada

## ABSTRACT

The Cenozoic sedimentary section of the eastern Scotian margin is characterized as a progradational sequence incised by canyons, valleys and gullies. These features provide conduits for offshelf sediment transport, slope by-pass and deposition on the continental rise and abyssal plain during periods of low relative sea level. The Stonehouse 3D seismic volume, spanning outer shelf and upper slope terrain of a portion of the modern eastern Scotian Slope, provides an opportunity to study the detailed Cenozoic stratigraphy and modern and buried seafloor morphologies in this critical shelf to slope transition zone. Sequence stratigraphic concepts were applied to the Neogene section of this depth-migrated 3D data set to map the distribution of seismic facies and their bounding unconformities. Several widespread unconformity surfaces were identified and compared to the present-day seafloor. Canyon incision appears to be episodic throughout the Cenozoic section. As with the modern seafloor, ancient canyon systems are fundamental to slope sedimentary processes and sediment delivery mechanisms. Canyon formation requires significant removal of slope material to the deep ocean floor, following which these canyons act as sediment pathways. A particularly widespread Oligocene (?) erosive surface has a complex morphology that is potentially analogous to the modern Sable Gully canyon system that "drains" much of the central and eastern Scotian Shelf through a system of feeder channels and valleys. The implications of repeated canyon formation on the Scotian Slope imply that the residence period of sediments on the slope is geologically short and that preservation potential is confined to periods of canyon fill or local reductions in gradient. Canyon formation on the slope presumably requires significant sea level lowering, so repeated canyon formation raises the question of eustatic versus tectonic controls on sedimentary processes. Given the extent of the Oligocene (?) erosional unconformity, it is suggested that eustatic change alone cannot explain this consequence, thus tectonic inversion on this passive margin may have contributed to sea level lowering.

**Adapted from extended abstract prepared for CSPG CSEG CWLS Convention, "Back to Exploration" May 12-15, 2008 – Calgary, Alberta, Canada*

## Introduction

Passive continental margin sedimentation responds to sediment influx and first order forcing mechanisms such as tectonic and sea level fluctuations. As a result, margin sedimentary sequences demonstrate periods of progradation, aggradation and erosion, leading to development of stratigraphic sequences. The modern seafloor of the outer Scotian Shelf and upper slope appears highly eroded with deeply incised canyons that were generated in response to lower sea level stands and high sediment input rates during Quaternary glacial and particularly de-glacial periods (Mosher *et al*. 2004). The following study investigates a section of base Cenozoic to recent strata on the eastern Scotian continental margin using seismic reflection and well data (Fig. 1). Within this interval there is an unconformity of presumed Oligocene-age exhibiting a canyon system comparable to the modern eastern Scotian Slope. It is the purpose of this study to apply seismic geomorphologic and sequence stratigraphic techniques to help interpret mechanisms of formation of this and other ancient seafloor surfaces to understand Neogene development of the region.

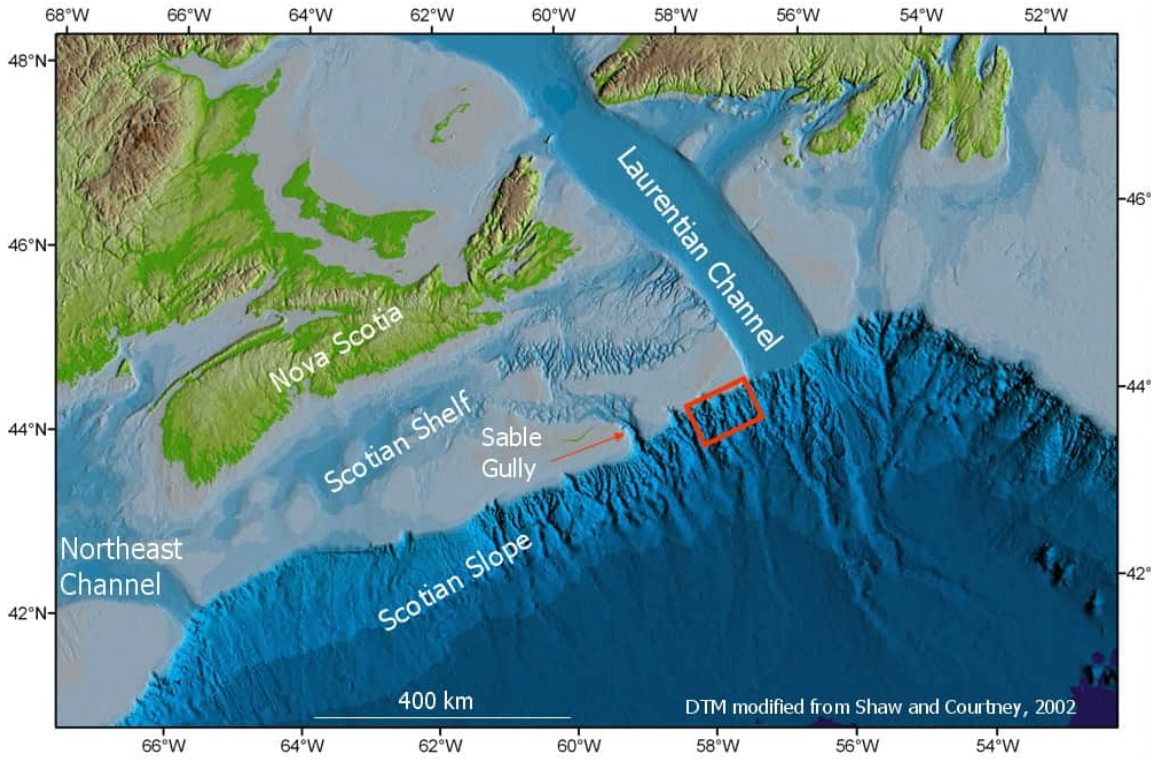


**Figure 1. Location map of study area: The Stonehouse 3D seismic cube spans modern outer shelf and upper slope terrain of the heavily incised eastern Scotian Slope between the Sable "Gully" and the Laurentian Channel. The study area is located beneath modern water depths of ~ 65 m – 2500 m, with a regional slope of 2.5˚ to 4˚.**

The Oligocene is documented worldwide as an unconformity in the geologic record. Noted on the sea level curves of Vail and Mitchum (1977), Haq *et al.* (1987), and Miller *et al*. (2005), the Oligocene is generally accepted as the onset of generalized cooling that continued into the Pleistocene. On the eastern Scotian margin the Oligocene is documented as a sub-regional unconformity consisting of multiple unconformable surfaces that locally merge. The canyon morphology of the Oligocene surface within the Stonehouse area is similar to present canyon systems. It is possible that buried canyons once linked shoreward (shelf) channels and gullies, however the similarities to today's morphology are under investigation.

## Seismic Interpretation

Seismic facies, seismic sequence stratigraphic and seismic geomorphologic techniques were applied to a pre-stack depth-migrated 3D seismic volume to investigate the geology of a region of the easternmost upper Scotian Slope. Several widespread erosive unconformity surfaces were investigated and compared to erosional morphologies on the present-day seafloor.

Canyon incision appears to have been episodic through the Cenozoic history of the Scotian margin. During periods of low relative sea level, canyons provided conduits for off-shelf sediment transport resulting in slope by-pass and deep water deposition. Canyon systems appear to have evolved through multiple phases of cut-and-fill; new systems often re-occupying old. Within the Neogene interval the Oligocene unconformity exhibits a large canyon system comparable in extent to the Sable Gully of the modern Scotian Slope. Because of its age, canyon formation cannot be the result of glaciation as is the modern surface (Fig. 2).

## Results

On the eastern Scotian margin the Oligocene unconformity represents the last phase of canyon incision of a system consisting of two major incisional phases and several small scale erosive events. Within the study area the Oligocene unconformity is represented by two or more unconformities that locally merge. The widespread Oligocene erosive surface indicates incision of up to 900 m of strata in a canyon that is ~9 km wide. Multiple phases of deposition ultimately led to complete infill of this canyon resulting in a relatively smooth seafloor. A modern canyon system subsequently cut into these infill deposits (Fig. 3).

Canyon fill of the Oligocene canyon system is complex, consisting of multiple erosive phases separated by periods of fill. Although the processes that cut and fill the canyon system are uncertain, seismic facies act as indicators for sedimentary processes. The lower canyon fill facies is distinguished by high amplitude chaotic reflectors that suggest active sediment gravity flows erode and partially fill the channel. In contrast, the upper fill facies is continuous with low to moderate amplitude reflectors, suggesting a passive fill that, given the lack of channels, could have formed from non-erosive muddier flows or contourites.

The extent of the Oligocene canyon system is beyond the limits of the 3D seismic volume although extension of this surface through an extensive grid of 2D seismic reflection data indicates it is part of a much larger system. 2D seismic reflection data on the shelf indicate the Oligocene canyon system cuts back tens of kilometres onto the shelf deeply incising shelf strata. Given the magnitude of shelf incision and the continuation of the canyon system onto the abyssal plain, the canyon may have once been linked to a fluvial network, indicating subaerial exposure during a major sea level lowstand or tectonic uplift of the shelf.

## Conclusions

Canyon formation requires significant removal of slope material to the deep ocean floor. Canyons also act as conduits for sediment transported from other sources to the canyon head after incision. Therefore, as with the modern surface Neogene canyons are likely fundamental to slope sedimentary processes and sediment delivery mechanisms.

The implications of repeated canyon formation on the Scotian Slope indicate a limited residence period of slope sediments with erosion and slope by-pass delivering sediment to the continental rise and abyssal plain. Insight on the depth and extent of the Oligocene surface has implications for reservoir distribution on the remainder of the Scotian Slope and its future as a prospective hydrocarbon system. This study provides a stratigraphic framework for the eastern Scotian slope that can be used as a model for further research, hydrocarbon exploration and regional comparison.

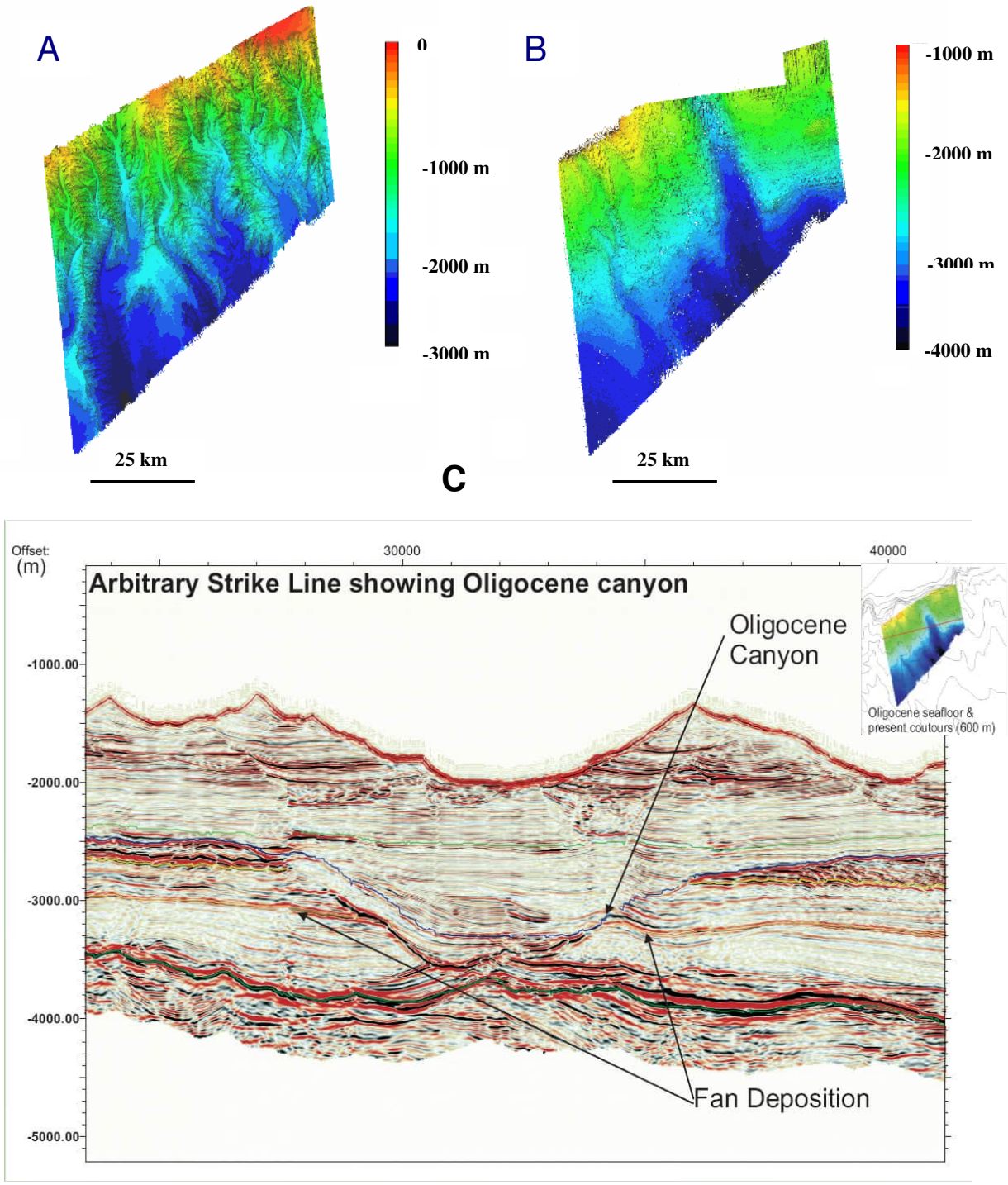


**Figure 2: A) Seismic geomorphologic image of the modern seafloor, heavily incised by canyons, valleys and gullies. B) The Oligocene geomorphologic surface indicates a major canyon system with implications for slope by-pass. C) Arbitrary strike line showing the relationship of the Oligocene canyon to the modern seafloor. Colorbars indicate depth below sea level.**

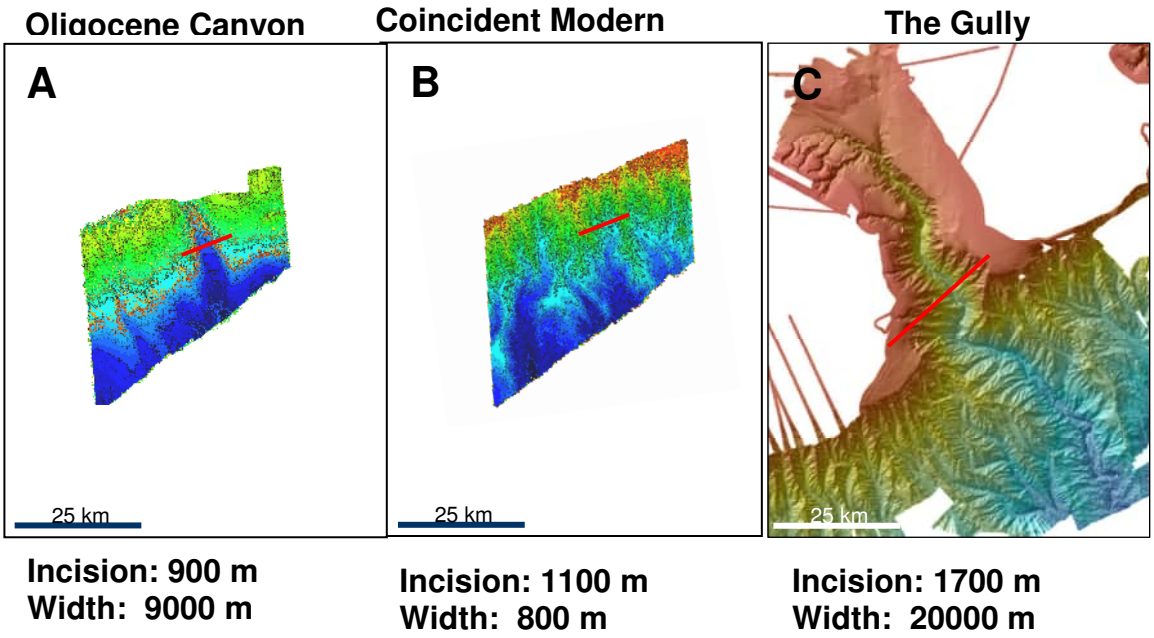


**Figure 3: History of canyon incision on the eastern Scotian margin: A) Seismic geomorphologic image of the Oligocene seafloor illustrating the final phase of canyon incision before a switch to deposition. B) Seismic geomorphologic image of the modern seafloor with a canyon system coincident to the Oligocene canyon system. C) Comparison to the modern "Gully"; could the Oligocene canyon system be comparable in magnitude? Variation in incision and width measurements are due in part to variation in shelf break location.**

## References

Haq, B.U., Hardenbol, J., and Vail, P.R., 1987, Chronology of Fluctuating Sea Levels since the Triassic: Science, 235, p.1156-1167.

Miller, K.G., Kominz, M.A., Browning, J.V., Wright, J.D., Mountain, G.S., Katz, M.E., Sugarman, P.J., Cramer, B.S., Christie-Blick, N., and Pekar, S.F., 2005, The Phanerozoic record of global sea-level change: Science, 310, p.1293-1298.

Mosher, D.C., Piper, D.J.W., Campbell, D.C., and Jenner, K.A., 2004, Near-surface geology and sediment-failure geohazards of the central Scotian Slope: AAPG Bulletin, 88, p.703-723.

P.R. Vail, R.M. Mitchum, in Seismic Stratigraphy-applications to hydrocarbon exploration. C.E. Payton, Ed. AAPG Memoir 26, p.83-97.

BACK

# Middle Cenozoic Depositional Processes along the Western Scotian Margin

**Calvin Campbell**
**Grant D. Wach**
Dept. of Earth Sciences
Dalhousie University
Halifax, Nova Scotia, B3H 4J1
Canada
e-mail: cacampbe@nrcan.gc.ca

**David Mosher**
Geological Survey of Canada-Atlantic
P.O. Box 1006
Dartmouth, Nova Scotia, B2Y 4A2
Canada

## ABSTRACT

Extensive 2D and 3D seismic exploration data on the deep water margin off Nova Scotia reveals prospective hydrocarbon bearing structures, yet seven recent exploration wells met with only moderate success. The difficulties encountered in finding quality reservoirs reveal that geologic models successfully applied in other parts of the world need to be refined for the Scotian margin. It is the purpose of this study to develop an understanding of margin-scale geologic process relevant to the middle Cenozoic section of the Scotian margin in order to develop appropriate exploration models.

Published studies of the Oligocene to Pliocene geological history of the outer Scotian margin show that canyon incision on the slope and local depositional lobe progradation dominates sedimentation during periods of relative sea-level lowstands. During this same period, development of Antarctic glaciation and opening of Arctic Ocean circulation established North Atlantic oceanic currents that influenced sedimentation on the lower slope and rise. There is also evidence for occasional tectonic activity, presumably due to changes in intra-crustal stress, salt migration, and movement along ancient faults. Throughout the Cenozoic, large scale sediment mass-wasting events wield considerable influence over the evolution of depositional systems along parts of the margin.

Preliminary analysis of 2D and 3D seismic reflection data from the western Scotian margin reveals evidence of widespread erosion and associated depositional elements, which, through correlation with biostratigraphic data at the Shubenacadie H-100 and Shelburne G-29 wells, are of Oligocene to Miocene age. Here, the geological history of the outer margin records a complex interplay of down-slope and along-slope processes. The relationship of these various processes; sea level change, canyon cutting, contour current intensification, tectonics, sediment slope by-pass and sediment instability, for example, is unknown at this time but is critical, both for understanding the geology of the Scotian margin and how continental margins evolve in general.

BACK

# Comparing Controls on Deposition of Mesozoic and Cenozoic Mixed Carbonate-Siliciclastic Systems from the Central Atlantic Margin, North Carolina, USA

**Brian P. Coffey**
Simon Fraser University/University of North Carolina-Chapel Hill
205 Perry Creek Drive
Chapel Hill, North Carolina 27514
USA
e-mail: bcoffey@email.unc.edu

**J. Fred Read**
Dept. of Geosciences,
Virginia Tech
4044 Derring Hall
Blacksburg, Virginia 24061-0420
USA
e-mail: jread@vt.edu

## ABSTRACT

Regional lithology-based sequence stratigraphic frameworks constructed across the subsurface of the Albemarle basin of eastern North Carolina (USA) from Jurassic, Cretaceous, and Paleogene time intervals reveal striking similarities within each of these passive margin shelf successions. Studied units were deposited over a broad temporal range at different paleolatitudinal positions and global climatic regimes.

Previous interpretation of the Paleogene depositional facies successions concluded that deposition was heavily influenced by paleolatitudinal position (subtropical to warm-temperate), oceanographic controls (boundary currents and nutrients), and with the major global transition from greenhouse to icehouse conditions. However, examination of more deeply buried Lower Cretaceous mixed carbonate-siliciclastic strata from the same basin reveals carbonate lithofacies that resemble late Paleogene updip shelf facies and stacking patterns consisting of admixed quartz sands/silts and mollusk-foraminifera dominated skeletal carbonate sands. Deep shelf marls also are comparable. Preliminary analyses suggest that facies similarities also exist into the underlying Upper Jurassic interval.

These observations suggest that while eustasy and climate strongly influence thickness and stacking patterns, the paleogeographic position of the shelf as a promontory exposed to open ocean wave energy and currents plays a major role in facies development through time. This region of the Atlantic margin was subjected to repeated pulses of ocean-derived elevated nutrient levels, similar to the modern palimpsest Carolina shelf. These observations further suggest that boundary currents (cool, proto-Labrador and warm, ancestral Gulf Stream) may have existed and mixed in this study area during Mesozoic times, albeit with lower intensities than observed in late Paleogene-Neogene icehouse conditions.

## Introduction

This paper presents data compiled from an integrated sequence stratigraphic study of outcrop, core, well, and seismic data from the Paleogene and Lower Cretaceous section of the North Carolina coastal plain (Fig. 1). Lithologic information collected from well-cuttings, when constrained by

biostratigraphic and seismic reflection data, provide valuable insight into the complicated stratigraphy exposed in quarries and updip portions of the basin by revealing regional facies relationships from much thicker portions of the basin. This approach has broad application in basins with sparse outcrop coverage, but relatively thick, laterally extensive subsurface sections. Discussions of detailed stratigraphy and sequence stratigraphic relationships have been minimized in order to focus on long-term trends observed in outcrop and subsurface lithologic data from the Albemarle Basin. Detailed descriptions of facies and supersequence are discussed in greater detail by Coffey and Read (2004, 2007) and Sunde (2008). The goal of this study is to demonstrate the complex interaction of climatic, oceanographic, and eustatic controls on deposition on a high energy passive margin in both greenhouse and icehouse times. Results from this work show that these processes were active in both global climatic regimes, their expression in the rock record varies considerably.

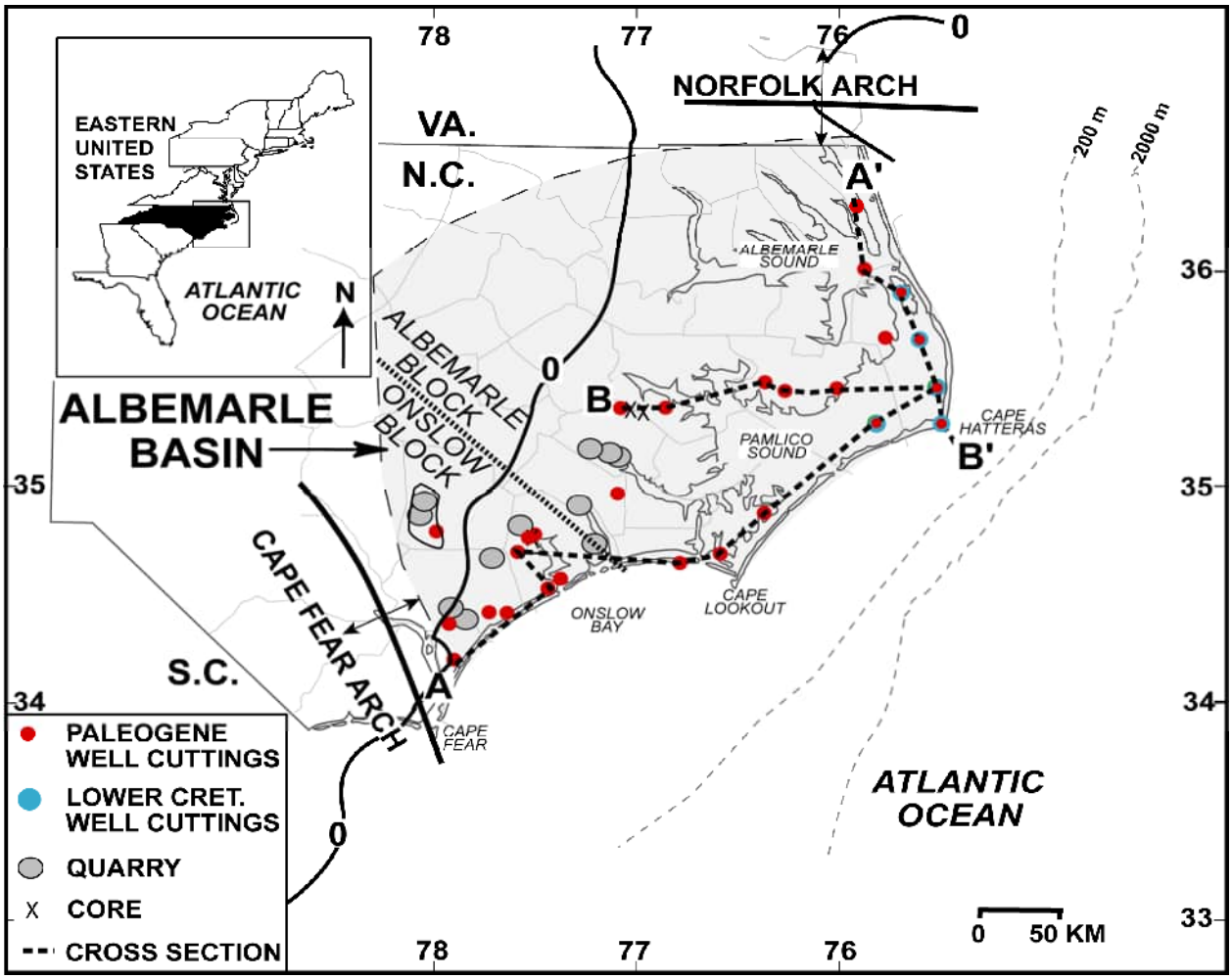


**Figure 1. Map of the study area in eastern North Carolina (inset shows location on eastern US Atlantic margin). Wells, outcrops, and cores included in this study are shown. Cross section A-A' corresponds with Figure 4 (NB: Figure 4 is located at the end of this paper as it is a large-scale cross-section).**

## Regional Setting

The Albemarle Basin of eastern North Carolina is bounded on the south by the Cape Fear Arch and on the north by the Norfolk Arch (Fig. 1; Bonini and Woollard 1960; Harris 1975). Low subsidence rates on this passive margin (1.4 to 4 cm/ky; Steckler and Watts 1978) postdate the bulk of thermo-

tectonic subsidence related to Mesozoic rifting. Cretaceous through Paleogene strata form a seaward-thickening wedge, with erosional remnants near the present fall line. The continental shelf shows a distinctive evolving profile on seismic profiles, consisting of an inner-shelf and inner-shelf break, as well as a deeper outer shelf, which breaks seaward onto the continental slope.

During mid-late Paleogene sea-level highs, the ancestral Gulf Stream became active, cutting across Florida via the Suwannee Straits during sea-level highstands, and then flowing northeastward along the southeastern U.S. margin (Pinet and Popenoe 1985; Huddleston 1993). This provided relatively constant warm waters to the shelf during sea-level highstands. Similarities in lithofacies from the Lower Cretaceous interval suggest similar currents may have been active at this earlier time. Northward drift of the North American plate during the Paleogene positioned the North Carolina shelf between 30 and 36 degrees north latitude, while it lied near 25 degree north latitude (Scotese 1995).

## Stratigraphic Setting

The three time intervals presented in the paper, Upper Eocene through Oligocene, Paleocene through Middle Eocene, and Lower Cretaceous (Aptian-Albian) have loosely defined stratigraphic frameworks that have been based heavily on biostratigraphic age control (Fig. 2). Limited detailed lithologic study has been conducted away from thin, heavily discontinuous outcrop belts. The study area appears to straddle the broad transition zone between siliciclastic-dominated shelf successions to the north, and the carbonate-dominated successions to the south in both Paleogene and Lower Cretaceous times. Consequently, facies commonly are mixed carbonate-siliciclastic types. In addition, the shelf succession records the effects of the ancestral Gulf Stream (Popenoe 1985; Riggs 1984; Lynch-Stieglitz *et al.* 1999), which influenced water temperatures, nutrient supply, and eroded deep shelf sediment bodies for hundreds of kilometers along strike.

## Depositional Setting

The Paleogene and Lower Cretaceous depositional systems were comprised of heavily admixed carbonate and siliciclastic sediment in nearly all interpreted depositional settings. Figure 3 presents a summary of depositional profiles in Paleogene end-members, and a Lower Cretaceous depositional profile is presented by Sunde and Coffey (this volume). Deposition was generally characterised by wide, strike-parallel facies belts that developed in response to extensive storm and swell wave sweeping on this open ocean continental margin. This energy, coupled with limited sedimentation rates, resulted in a distinctive, dual-break shelf profile (Fig. 3). Limited sedimentation rates resulted from a combination of tectonic and oceanographic controls that included the passive margin setting (siliciclastic supply) and nutrient enriched waters (carbonate factory). The combined effects of a high energy depositional system and limited sedimentation resulted in extensive erosional reworking of sediments and incomplete expression of depositional sequences, especially in updip areas of the basin.

Nearshore deposition was dominated by coarse, well-washed siliciclastic sands that contained variable amounts of admixed skeletal carbonate, predominantly mollusk. Mid-shelf settings are prone to condensed sedimentation, with common development of heavily abraded skeletal sands and gravels rich in phosphate and glaucony. Middle to deep shelf deposition was dominated by variably muddy carbonate skeletal sands that included echinoderms, bryozoa, benthic foraminifera, and brachiopods. These skeletal carbonate fabrics were best developed in the early Paleogene, but fragments of comparable lithofacies also were observed in the other two time intervals (Fig. 4: NB. Large 11x17 inch figure. See end of article). Deep shelf deposition was dominated by argillaceous lime mudstones (marls) that contained abundant planktonic foraminifera and glaucony in all time intervals.

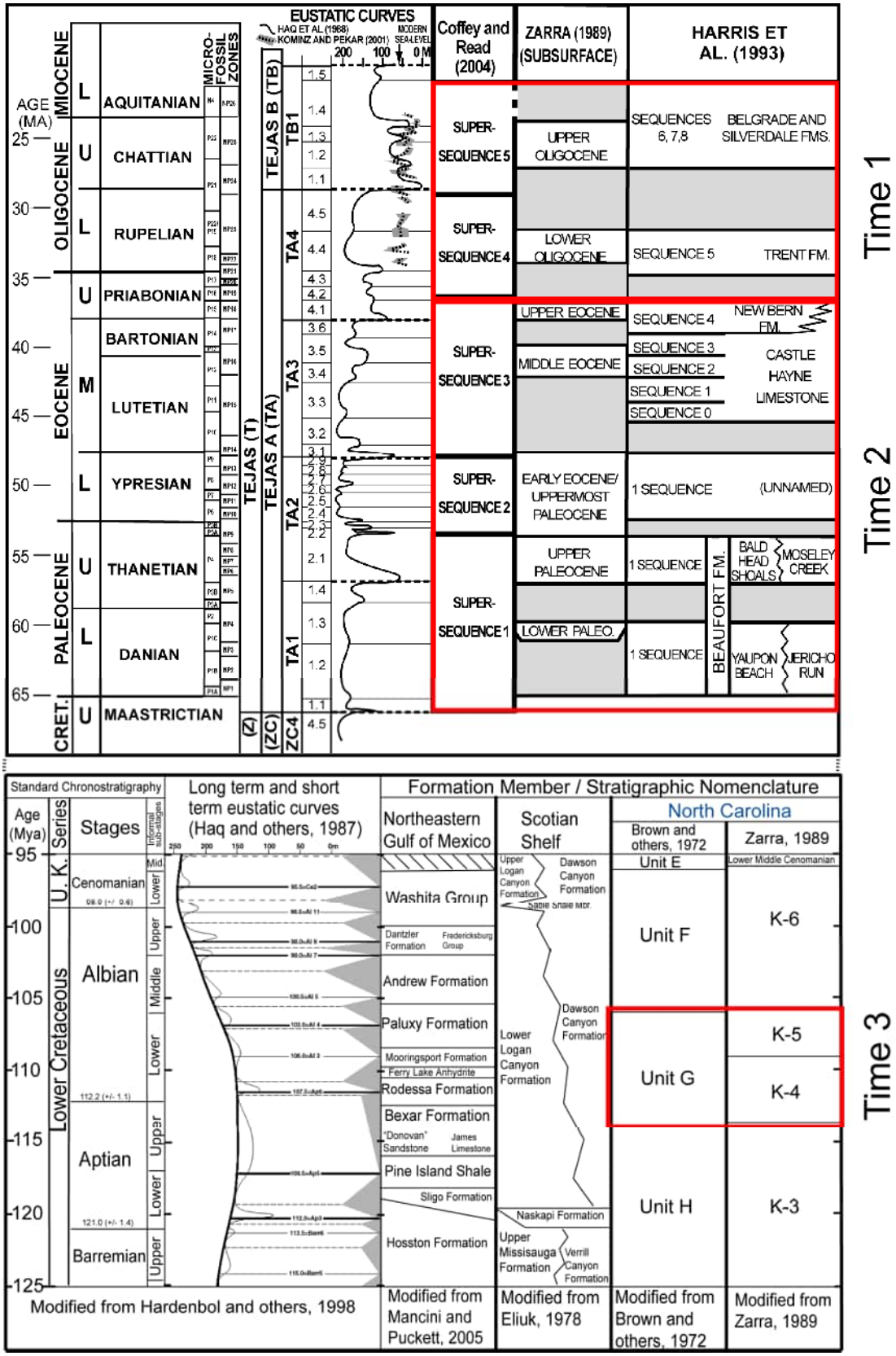


**Figure 2. Stratigraphic framework for the three time intervals studied (red boxes).**

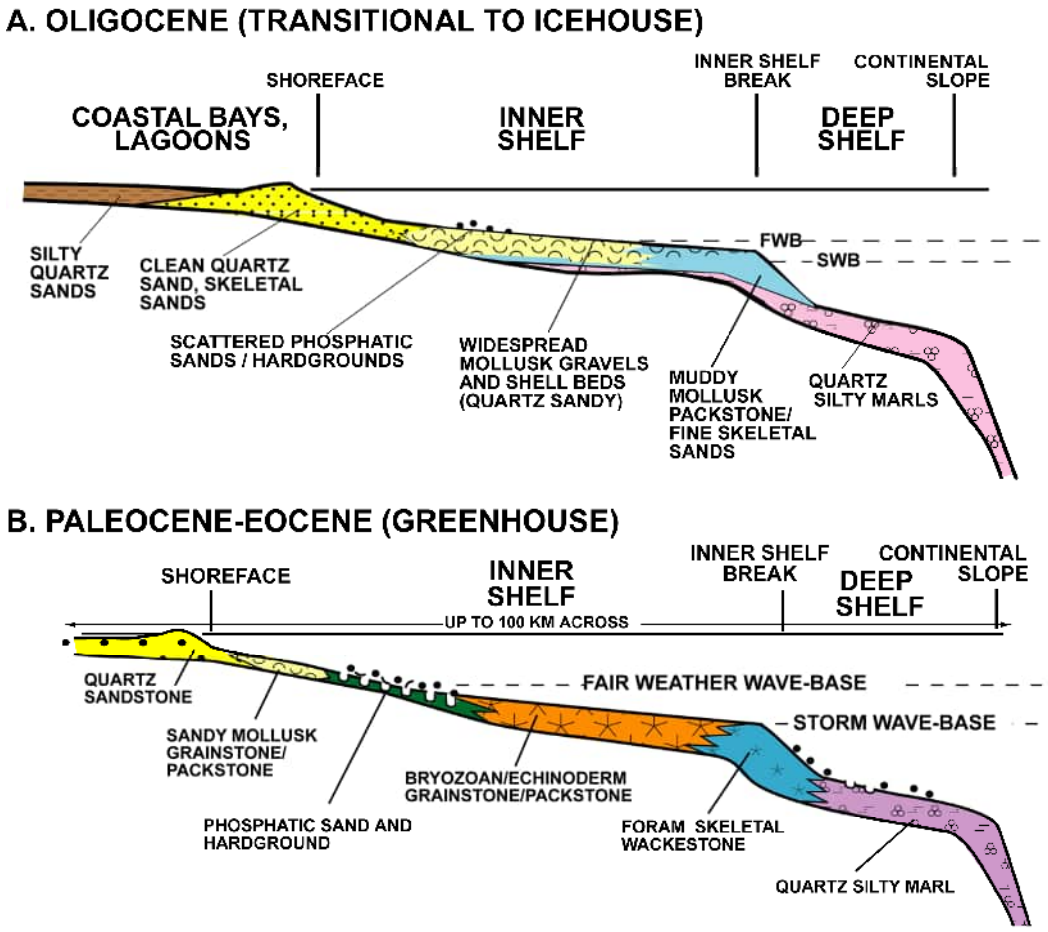


**Figure 3. Interpreted depositional profiles for Oligocene (A) and Paleocene-Eocene (B) time intervals. Depositional profiles for the Lower Cretaceous interval are presented by Sunde and Coffey (This volume). This basin is characterised by a distinctive dual-break shelf profile, with predominant siliciclastic materials in nearshore to shallow inner shelf settings, heavily wave-swept mid-shelf, and carbonate dominated deep shelf deposition.**

## Sequence Stratigraphic Model

Sequence stratigraphic correlation of lithologic data between wells incorporated regional seismic and biostratigraphic data, which indicated overall progradational stacking patterns. Progradational geometries prevailed on seismic in all intervals, with increased development in the Oligocene and Lower Cretaceous packages that were dominated by siliciclastic depositional styles. Progradational geometries in the Eocene were concentrated in central areas of the shelf basin (Figs. 4, 5). Transgressive packages are highly thinned in all three studied time intervals, often below the resolution of seismic data. They tended to consist of heavily reworked sands and gravels (both carbonate and siliciclastic grains) with abundant associated phosphate and glaucony. Lowstand packages were not observed in onshore well data, but onlapping wedge geometries in offshore seismic data suggest their development in the Paleogene; they likely also are present further offshore in the Cretaceous, but these data have not been investigated.

The magnitude and rate of relative sea-level change differed greatly in the studied time intervals, with more subtle facies transitions in much of the Paleocene-Eocene and rapid shifts in lithofacies in the Oligocene. The Lower Cretaceous appears to more closely resemble the Oligocene lithofacies stacking patterns, but with higher rates of sediment accumulation and progradation.

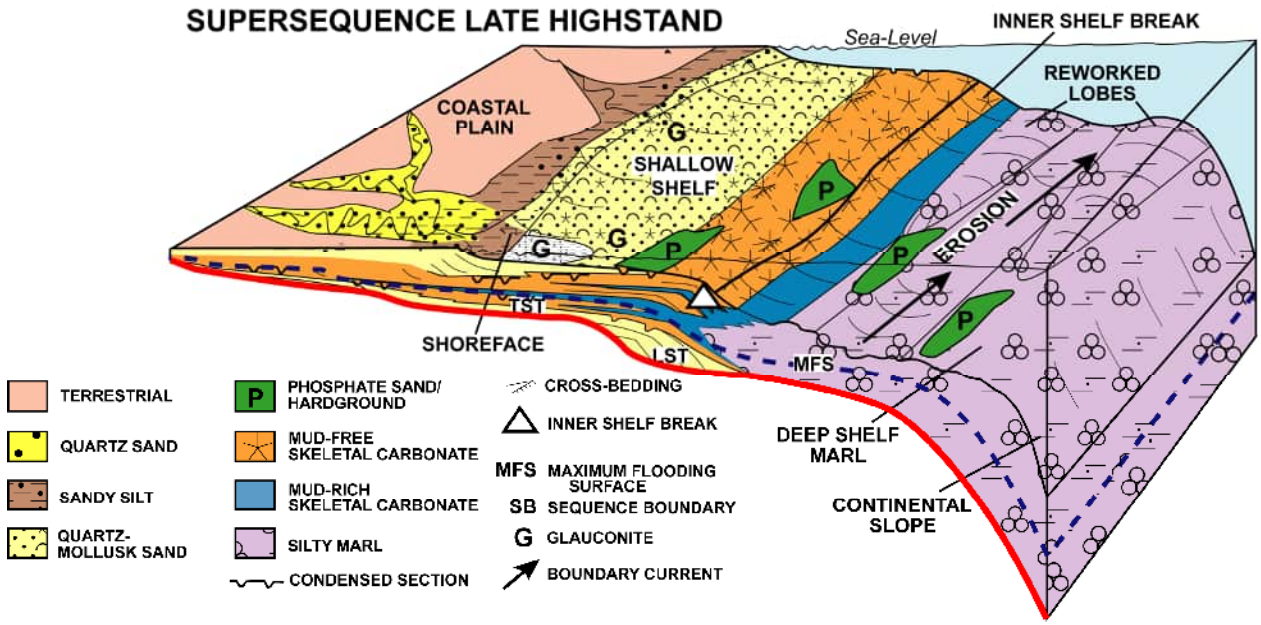


**Figure 5. Conceptual depositional model for supersequence highstand deposition, whereby moderate inner shelf progradation occurred updip and extensive scouring by boundary currents occurred on the deep shelf. Note sporadic distribution of phosphatic materials, rather than regionally correlatable surfaces.**

## Controls on Deposition

The open shelf position of this passive margin subjected the shelf to extensive storm and swell wave abrasion, which combined with limited rates of terrigenous sediment supply, resulted in extensive reworking of sands on the shelf and winnowing of fines into the deep ocean basin. As such, much of the inner shelf deposition was dominated by admixed siliciclastic sands and reworked skeletal material.

An additional explanation for the predominance of siliciclastic materials in shallow shelf setting is elevated levels of nutrients across the shelf. This phenomenon would limit the ability of highly-productive phototrophs to develop in shallow marine settings. Instead, the rock record shows extensive development of phosphatic hardgrounds/gravels with admixed encrusting benthic organisms. These fabrics occur at many times within sequences, not exclusively at maximum floods or transgressive surfaces; some are laterally continuous, but many are not (Fig. 5). Elevated nutrient levels are thought to have developed in response to contour current-generated upwellings on the shelf. These features may have been driven by gyres spalled off of the main boundary current when it intersected positive bathymetric elements on the shelf (*cf.* Riggs, 1984). Localised to regional upwelling events likely provided nutrient-enriched waters to the shelf, which favoured development of the oligotrophic to eutrophic skeletal carbonate assemblages observed. However, these non-reef building biota were unable to tolerate the extensive wave energy in updip portions of the shelf, leading to their isolation on deeper portions of the ramp that generally were below the influence of wave abrasion.

Boundary currents also were responsible for extensive shore parallel incision of the deep shelf during highstands in times of global icehouse, when they appear to have had much greater intensity. This resulted in extensive removal and along-strike transport of deep shelf marls, with complete removal of the deep shelf and slope sediment record during major lowstands (Fig. 5; Popenoe 1985).

One of the major complicating factors in reconstructing sequence stratigraphic frameworks in this basin is that the sand-prone depositional system was prone to extensive reworking, due largely to the absence of early lithification. Coastal environments consisted of silt and sand-dominated deposition that was very prone to erosion and cannibalisation during subsequent eustatic changes. Non-reef building, delicate carbonate biotas also were very susceptible to reworking by swell waves on the deeper portions of the inner shelf, making it difficult to identify clear sequence stratigraphic surfaces downdip.

Development of phosphatised hardgrounds on the shelf appears to be one of the primary means of sediment preservation, as materials beneath these hardened surfaces were protected from reworking during subsequent sea-level changes. In updip outcrops, these surfaces tend to mark sequence boundaries that are overlain by transgressive gravel lags rich in phosphate and marine skeletal debris, yet some surfaces have yielded stable isotopic data that clearly indicates subaerial exposure (Baum and Vail 1988). This complication shows that the most likely surfaces to be used as correlative time markers by geologists constructing sequence stratigraphic analyses within the basin actually may be developed as localised features that develop in a time-transgressive manner across the shelf, often actually signifying major diastems in updip settings.

## Conclusions

This study provides a rare opportunity to compare open marine shelf strata that were developed on a passive margin in very different global climatic regimes. The findings verify that climate does play a major role in sedimentation in mixed carbonate-siliciclastic depositional styles, but that related oceanographic changes on the deep shelf also have a major impact on deposition (and perhaps preservation). It is important to incorporate these influences when developing stratigraphic frameworks, particularly on open shelf, wave-swept settings like the Western Atlantic Margin.

## References


Baum, G.R., and Vail, P.R., 1988, Sequence stratigraphic concepts applied to Paleogene outcrops, Gulf and Atlantic basins: *in* C.K. Wilgus, B.K. Hastings, H. Posamentier, J. Van Wagoner, C.A. Ross and C.G.St.C. Kendall, (editors), Sea-Level Change: An Integrated Approach: SEPM, Special Publication 42, p.309-327.

Bonini, W.E., and Woollard, G.P., 1960, Subsurface geology of North Carolina-South Carolina coastal plain from seismic data: AAPG Bulletin, v.44, p.298-315.

Brown, P.M., Miller, J.A., and F. M. Swain, 1972, Structural and Stratigraphic Framework, and Spatial Distribution of Permeability of the Atlantic Coastal Plain, North Carolina to New York, Washington, Geological Survey Professional Paper, v.796, 79p.

Coffey, B. P., and Read, J.F., 2004, Mixed carbonate-siliciclastic sequence stratigraphy of a Palaeogene transition zone continental shelf, southeastern USA: Sedimentary Geology, v.166, p.21-57.

Coffey, B. P. and Read, J.F., 2007, Subtropical to warm-temperate facies from a transition zone, mixed carbonate-siliciclastic system, Paleogene, North Carolina, U.S.A.: Sedimentology, v.54 (2), p.339-365.

Eliuk, L. S., 1978, The Abenaki Formation, Nova Scotia Shelf, Canada – A depositional and diagenetic model for a Mesozoic carbonate platform: Bulletin of Canadian Petroleum Geology, v. 26, no. 4, p. 424-514.

Haq, B. U., Hardenbol, J., and Vail, P.R., 1988, Mesozoic and Cenozoic chronostratigraphy and eustatic cycles: in Wilgus, C.K., Hastings, B.S., Kendall, C.G.S.C., Posamentier, H. W., Ross, C.A., and Van Wagoner, J.C., (editors), Sea-Level Changes: An Integrated Approach, SEPM Special Publication No. 42, p. 71-108.

Hardenbol, J., Thierry, J., Farley, M.B., Jacquin, T., De Graciansky, P.-C., and Vail, P.R., 1998, Mesozoic and Cenozoic Sequence Chronostratigraphic Framework of European Basins. *In:* P.-C. De Graciansky, J. Hardenbol, Th. Jacquin, and P. R. Vail, eds., Mesozoic and Cenozoic Sequence Stratigraphy of European Basins, SEPM Special Publication 60, CD-ROM.

Harris, W.B., 1975, Stratigraphy, petrology, and radiometric age (upper Cretaceous) of the Rocky Point Member, Peedee Formation, North Carolina [unpublished PhD thesis]: University of North Carolina-Chapel Hill, 190p.

Harris, W., Zullo, V., and Laws, R., 1993, Sequence stratigraphy of the onshore Paleogene, southeast Atlantic coastal plain, USA: Special Publications of the International Association of Sedimentologists, v.18, p.537-561.

Huddleston, P., 1993, A Revision of the Lithostratigraphic Units of the Coastal Plain of Georgia: The Oligocene: Georgia Geological Survey Bulletin 105,152 p.

Lynch-Stieglitz, J., Curry, W.B., and Slowey, N., 1999, Weaker Gulf Stream in the Florida Straits during the Last Glacial Maximum: Nature, v.402, p 644-647.

Mancini, E. A., and Puckett, T.M., 2005, Jurassic and Cretaceous Transgressive-Regressive (T-R) Cycles, Northern Gulf of Mexico, USA: Stratigraphy, v.2, no.1, p.31-48.

Huddleston, P., 1993, A Revision of the Lithostratigraphic Units of the Coastal Plain of Georgia: The Oligocene: Georgia Geological Survey Bulletin 105, 152p.

Popenoe, P., 1985, Cenozoic depositional and structural history of the North Carolina margin from seismic stratigraphic analyses, in Poag, W.C. (editor), Stratigraphy and Depositional History of the U. S. Atlantic Margin: Stroudsburg, PA, Van Nostran Reinhold, p.125-187.

Riggs, S.R., 1984, Paleoceanographic model of Neogene phosphorite deposition, U.S. Atlantic Continental Margin, Science, v.223, n.4632, p.123-131.

Scotese, C.R., 1995, Phanerozoic Plate Tectonic Reconstructions, PALEOMAP Progress Report # 36, Department of Geology, University of Texas at Arlington, 82 pp. (copyrighted in 1997).

Steckler, M.S., and Watts, A.B., 1978, Subsidence of the Atlantic-type continental margin off New York: Earth and Planetary Science Letters, v.41, p.1-13.

Sunde, R.F., 2008, Well-Cuttings Based, Sequence Stratigraphic Framework of the Mixed Siliciclastic-Carbonate Lower Cretaceous Sediments of the North Carolina Coastal Plain, [unpublished M.Sc. Thesis], Simon Fraser University, 23 p.

Vigil, D.L., 1998, North Carolina/Minerals Management Service Technical Workshop on Manteo Unit Exploration: February 4-5, 1998, OCS Study MMS 98-0024, U.S. Dept. of the Interior, Minerals Management Service, Gulf of Mexico OCS Region, New Orleans, 168p.

Zarra, L., 1989, Sequence Stratigraphy and Foraminiferal Biostratigraphy for Selected Wells in the Albemarle Embayment, North Carolina: North Carolina Geological Survey, Open-File Report 89-5, 4 p.

**BACK**

# PALEOCENE-EOCENE STRIKE SECTION

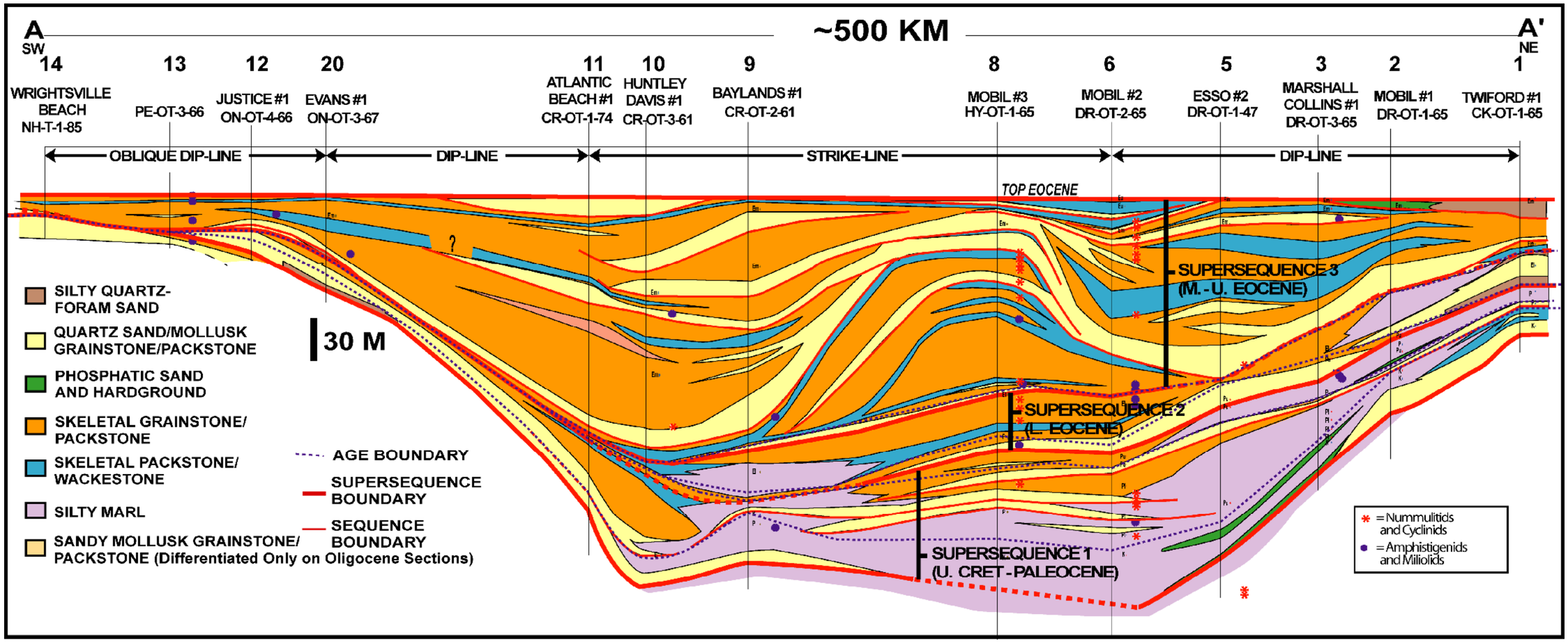


**Figure 4. Strike cross section A-A' showing distribution and correlation of Paleocene and Eocene strata from the Albemarle basin, North Carolina. The section extends across the basin (roughly parallel to modern coastline). Correlation geometries between wells were constrained with biostratigraphic and seismic data in this heavily admixed carbonate-siliciclastic system.**

BACK

# Integrated Reservoir Characterisation, Deep Panuke Gas Pool, Offshore Nova Scotia

**Norman Corbett**
**Gordon Uswak**
**Terrance Skrypnek**
EnCana Corporation
EnCana on 9th
150 -9th Avenue
Calgary, Alberta, T2P 2S5
Canada
e-mail: norm.corbett@encana.com

## ABSTRACT

The Deep Panuke gas pool is the first, significant carbonate reservoir gas discovery on the Scotian Shelf. Development of the pool is currently proceeding. The Jurassic Abenaki Formation-hosted, lean, slightly-sour gas accumulation was delineated in two rounds of drilling involving seven wells resulting in five successes. Well test rates exceed 50 million cubic feet per day per well.

Diagenesis controls secondary porosity development in the Deep Panuke fractured dolostone and associated leached vuggy limestone reservoir. Three litho-types were defined in the reservoir characterisation process: non-reservoir unleached limestone, porous vuggy limestone and dolostone. Petrophysical analysis of the wells defines relationships between lithology, porosity, Sw and fracturing for each litho-type. In particular, it has been important to recognize the presence of a bimodal porosity distribution in the High Permeability Reef Front (HPRF) region of the pool, which contains 80% of the gas resource. The bimodality is a consequence of the presence of both dolostone and unleached limestone litho-types. Similar reservoir characteristics have been documented at Simonette, Alberta (Duggan, 2004). Neural Net methods were used to integrate the petrophysical results with 3D seismic-derived rock properties, resulting in bimodal low/mid/high case porosity predictions for the HPRF. This multi litho-type approach and aquifer modeling has led to significant improvements in the integrated reservoir characterisation, well test matches and in the static and dynamic reservoir simulation models.

The approved development plan involves subsea tie-back of wells to a new jack-up production field centre and new export pipeline to shore.

BACK

# The Mohican Channel Gas Hydrate Zone, Scotian Slope: Geophysical Structure

**Janette Cullen**
Department of Earth Sciences
Dalhousie University
Halifax, Nova Scotia, B3H 4J1
Canada
e-mail: jcullen@dal.ca

**Angela Schlesinger**
School of Earth and Ocean Sciences
University of Victoria
P.O. Box 3055
Victoria, BC, V8W 3P6
Canada

**Ross Haacke**
Geological Survey of Canada –Atlantic
P.O. Box 1006
Dartmouth, Nova Scotia, B2Y 4A2
Canada

**Keith Louden**
Department of Oceanography
Dalhousie University
Halifax, Nova Scotia, B3H 4J1
Canada

## ABSTRACT

The Cenozoic section of the Scotian margin largely consists of turbidity current, mass transport and glacial sediments, with related canyon and valley formation. A significant portion of the continental slope of this margin falls within the methane gas hydrate stability zone (GHSZ), yet a prominent bottom simulating reflector (BSR) was identified at only one location. 3D seismic reflection, ocean bottom seismometer (OBS) and long offset (9 km) pre-stack 2D multichannel seismic data were used to study the velocity structure, geophysical characteristics and volume of this Mohican Channel gas hydrate zone. The Mohican Channel area shows a double BSR 0.35 to 0.45 s below the seafloor within channel levee deposits in water depths of 1,200 to 1,500 m. Primary and secondary BSRs are ~280 km2 and 50 km2 in area. A system of polygonal faults extends from an apparent gas-charged zone at ~1.2 s subbottom (Miocene-Eocene Unconformity) to ~0.3 s subbottom. Some faults form vertical chimneys and appear as conduits for gas leakage into the GHSZ. Some chimneys reach the seafloor producing positive-relief gas-charged mounds. A total of 39 OBSs were deployed along 3 profiles; one strike line and 2 dip lines. A few of the P and S-wave velocity profiles derived from these data over the BSR show anomalies consistent with the presence of hydrate and free gas, but others are ambiguous. Dissimilarities within the low velocity zone (LVZ) and amplitude variations suggest hydrate is laterally inhomogeneous. Shear-wave anisotropy appears related to changes in density of polygonal faults. As in any petroleum system, source, pathway, reservoir and trapping mechanisms are necessary for hydrate occurrence. Rare appearance of BSRs on the Scotian margin with low gas and hydrate concentrations imply that gas hydrates are in far less abundance than theoretical calculations suggest.

BACK

# Abenaki Carbonate Margin Facies Associations 1: Updated Depositional Facies Template and Vertical-lateral Margin Variations as Pie Diagram Sections-Maps

**Leslie Eliuk**
Dalhousie University
Department of Earth Sciences
Halifax, Nova Scotia B3H 4J1
Canada
e-mail: geotours@eastlink.ca

Although artificially static, a carbonate facies template and schematic carbonate facies model are useful for high-lighting the general relationship of facies in a dip transect of a carbonate platform from shore to basin. The biological-sedimentological criteria in cuttings and core for facies association identification are thus tabulated. However contemporaneous local variability such as channels versus reef buildups versus skeletal shoals at the margin are more difficult to show sometimes even on 3D models. And in some cases facies many not be contemporaneous locally such as argillaceous sponge reef beds versus clear-water deeper coral or microbialite reefs or mounds.

While perhaps in the same depositional depth and relative position, they occur widely separated in space and/or time but are shown on a single facies template or model for practical presentation and simplification. Modified from Wilson-style (1975) template of Eliuk (1978), Eliuk and Levesque (1988) then Wierzbicki, Harland and Eliuk (2002), the Abenaki facies associations (Fig. 11) are as follows: 1) Open marine shale – bathyal/deep, 2) open marine shale – neritic/shallow, 3A) foreslope channel, 3B) proximal foreslope (forereef), 3C) distal foreslope including microbial mounds (see 5C), 4A) 'deep' siliceous sponge reef mound & intermound, 4B) 'shallow' siliceous/lithistid sponge mound, 4C) 'shallow' lithistid-stromatoporoid/coral sponge reef, 5A) skeletal rich, 5B) shallow coralgal reef (coral-coralline sponge), 5C) pelleted 'mud' (see 3C), 5D) oolitic, 5E) oncolitic, 5F) thin bypass sandstones, 6) 'moat' open inner shelf (deep lagoon), 7) mixed carbonate-siliciclastic platform interior (nearshore ridge), 8) coastal deltaic-interdeltaic-restricted lagoon (loferite)-continental (coals).

As discussed in the preceding sections, geometry and position relative to the shelf margin (see seismic in Kidston *et al.* 2005) is another way of subdividing the well 'magnafacies' especially when they have a particular vertical depofacies pattern (see Table 2 and Fig. 7). Yet another method of viewing relative changes is showing percentage lithofacies-essential biotic-sedimentological components on pie diagrams placed vertically on sections or areally on maps by stratigraphic sequences (see Figs. 9, 12).

(Continued on next page.)

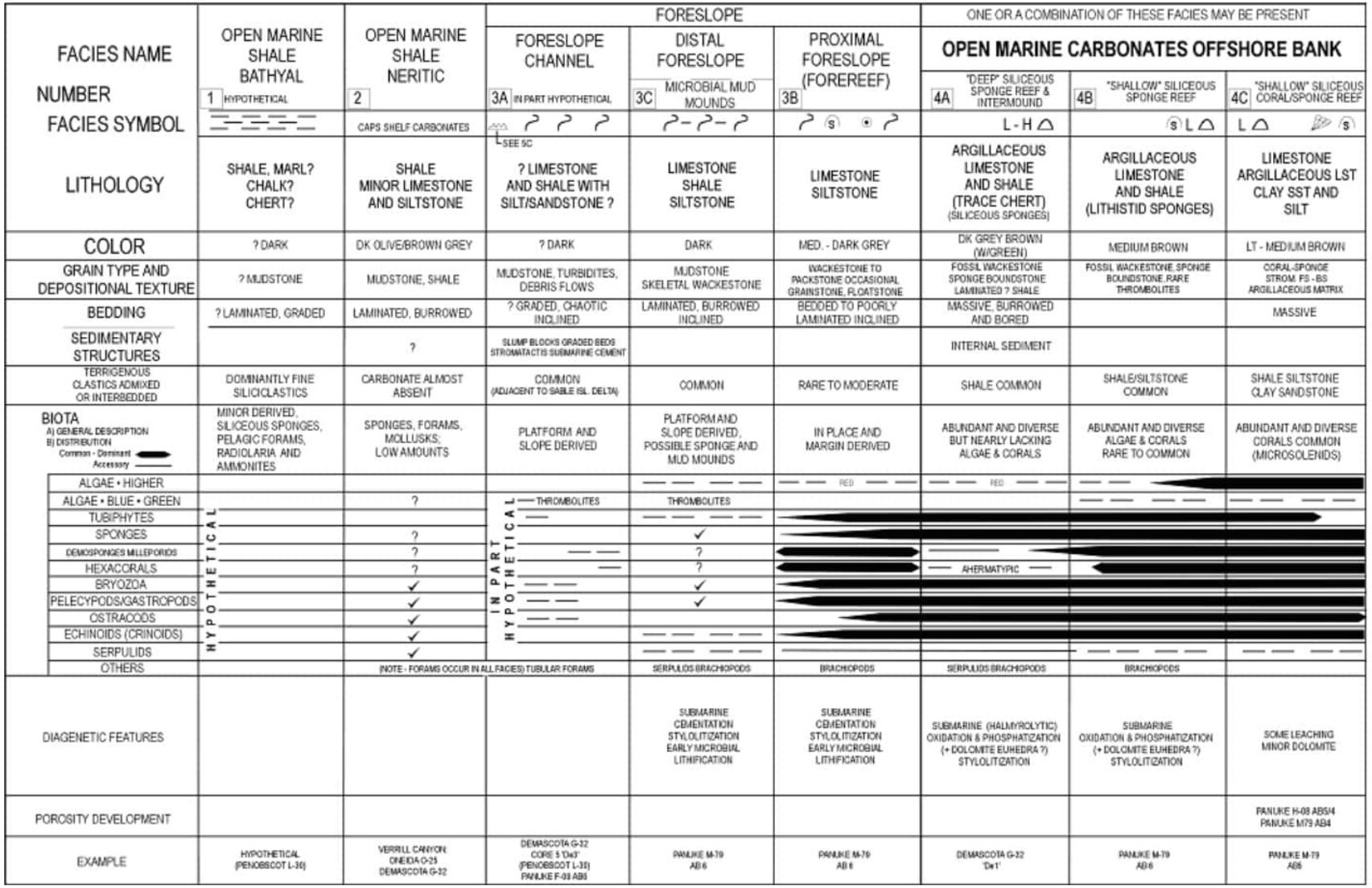


**Figure 11 (left and right). - Abenaki Carbonate Facies Template (from Wierzbicki *et al.* 2002 shown as left half then right half, modified after Eliuk 1978 and Eliuk and Levesque 1988 in style of Wilson 1975).**

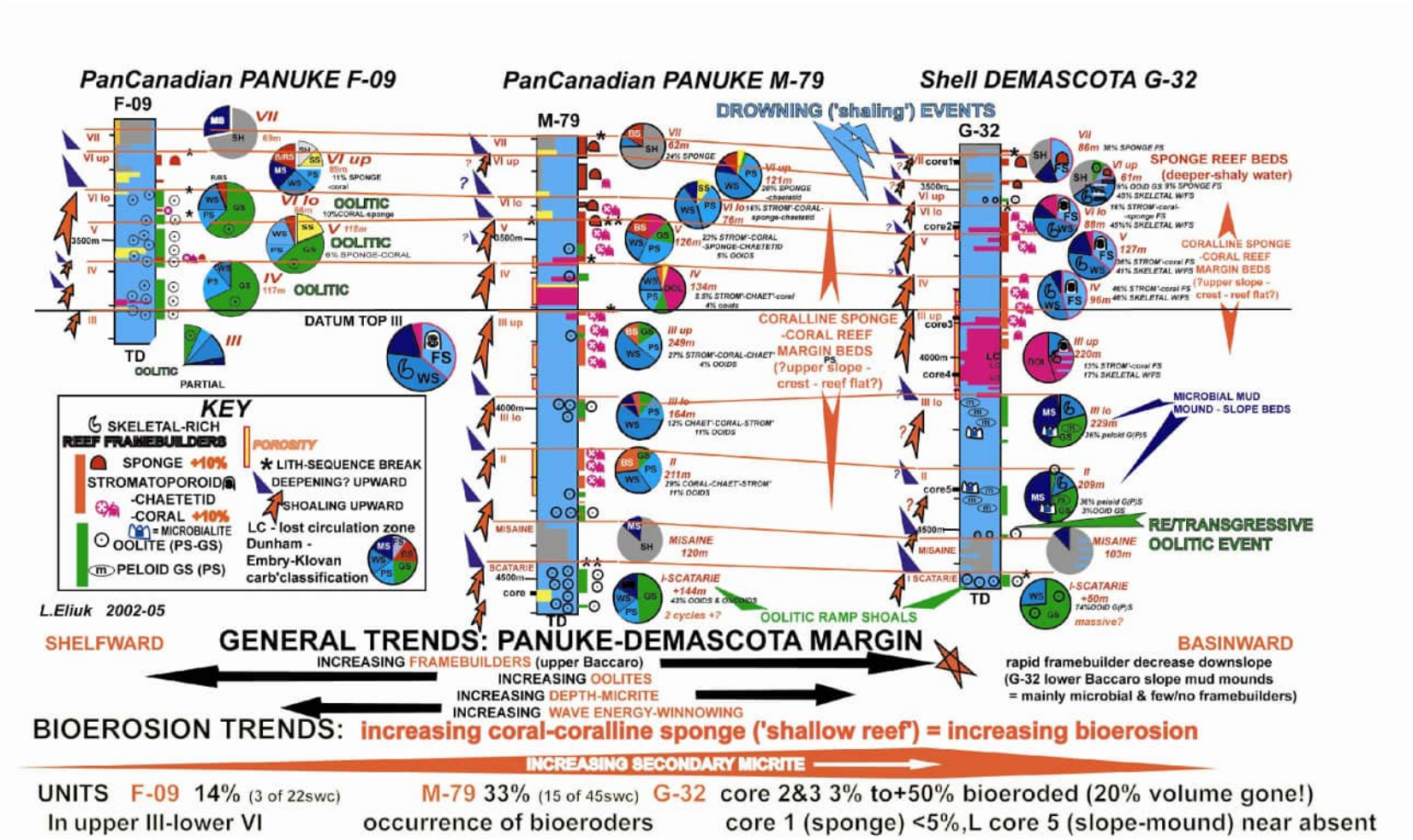


**Figure 12. Panuke F-09 to M-79 to Demascota G-32 dip section with percentage lithfofacies by sequences (modified from Eliuk and Pemberton 2002). This can be compared to Fig. 5 that has electric log traces and major facies. This figure shows some of the inferences available from inter- and intra-sequence comparisons of averaged lithofacies derived from cuttings and cores as well as some preliminary observations on degree of bioerosion seen in whole and sidewall cores. Note the large-scale or second order sequence pattern of shallowing upward and shelfward until a reversal with the capping argillaceous limestones characteristically rich in lithistid sponges in upper AB VI and AB VII. The coral-stromatoporoid reefal beds in G-32 are quite micritic indicating the lower-energy and slightly deeper setting of the reefs between the oolite-rich inner margin flexure and the outer margin flexure of the steeper slope. Of reservoir development significance in the Deep Panuke area is the lack of porosity in the deeper-water distal forereef-peloid grainstones to mudstone and somewhat surprisingly generally very low porosity in the shallow-water oolitic shoals. Porosity development is burial diagenetic in leached "vuggy limestone" and dolomite but is located within reefal beds in proximal forereef and reef flat carbonate sands and debris.**

# Abenaki Carbonate Margin Facies Associations 2: Slope-Forereef Settings and Spectrum of Microbial Mud/Reef mounds

**Leslie Eliuk**
Dalhousie University
Department of Earth Sciences
Halifax, Nova Scotia B3H 4J1
Canada
e-mail: geotours@eastlink.ca

With the exception of M-79 in Deep Panuke and Cohasset D-42 that is a bit back of the margin flexure, all thick shelf margin wells (Marquis L-35 & L-35A, Cohasset L-97, Dominion J-14, Demascota G-32, Acadia K-62, Albatross B-13) have a significant portion of their lower and middle sections (lower Baccaro Member or EnCana's Sequences AB II and AB III) in a microbial-hard peloid-carbonate mudstone lithofacies rich in calcite cements. These lithofacies are interpreted as distal carbonate slope with microbial mud/reef mounds. This is strongly supported by core (G-32, K-62, sidewall cores in B-13 and core at the base of the Baltimore Canyon Trough 'Civet' OCS-0337 well; see Fig. 13) which show isopachous submarine cements, marine geopetals, microbial thrombolitic-stromatolitic and even stromatactis textures.

The amount and variety of associated biota, degree and openness of submarine cavity systems and presence of debris flows varies, possibly systematically with distance from the Sable Island delta. Color changes (Fig. 13) show this with B-13 most distal and white and red. In contrast, two wells with core (Penobscot L-30, West Venture C-62) in the Sable Island paleodelta with prograding ramp geometries have microbial mud mound facies that are considerably darker and less biotically varied compared to those of cores in wells to their southwest.

Queensland M-88 is the only well drilled completely on the Abenaki carbonate slope to test possible bypass sandstone reservoirs immediately basinward of the Deep Panuke field. Cuttings, strongly supported by drilled sidewall cores, indicate a distal slope setting with abundant microbial mud/reef mound facies. In addition thin sponge or stromatoporoid-rich limestone beds define the sequence boundaries with overlying often-black shales. Proximal slope or forereef facies are fairly common in most margin wells especially in Deep Panuke. There, these generally sandier carbonates are often 'leached' limestones or dolomites forming much of the porous reservoir. Even in core, distinguishing forereef from reef flat sands can be a difficult interpretive problem. However in the Margaree F-70 core, the inclined dips and interbedding of thin *in situ* relatively low-energy hence deeper-water microbial-sponge-microsolenid coral reeflets support a proximal forereef interpretation for the dolomites and graded echinodermal grainstone interbeds.

## Cohasset L-97 - Example of interpreted mainly slope and deeper reef well

Mobil Cohasset L-97 drilled a faulted structural feature in a near margin test that penetrated the complete Abenaki Formation but left untested amplitude anomalies (Fig. 14). The upper Abenaki had minor oil and gas shows and traces of porosity with some dolomite lenses (Kidston *et al.* 2005). Showing that L-97 is problematic; these authors sometimes called it a "bank edge" test (their Table 1, p.18) and sometimes a "back reef" test (their Table 8, p.101) that was drilled "slightly away from the margin". This problem becomes even more interesting after cuttings analysis indicated that the well may be dominantly in a low energy slope and deeper reef setting rather than back bank or all reefal at the margin (Fig. 15). The *in situ* and phaceloid nature of some of the largest corals in the single L-97 core plus the high amount of microbial content supports a deeper quieter reef setting. But core interpretation is difficult due to

complicated diagenesis (pers. observation; Pratt and Jansa, 1989 their Fig. 6). It has the large scale shoaling up pattern typical of many bank margin wells but the lower 'deeper' beds are dominated by microbial-peloidal mudstones to wackestones with shoaling indicated by lesser amounts of variably thick stromatoporoidal floatstones to packstones (boundstone in core). These reefal and skeletal rich intervals helped to define tops of sequence and subsequence (parasequences?) boundaries.

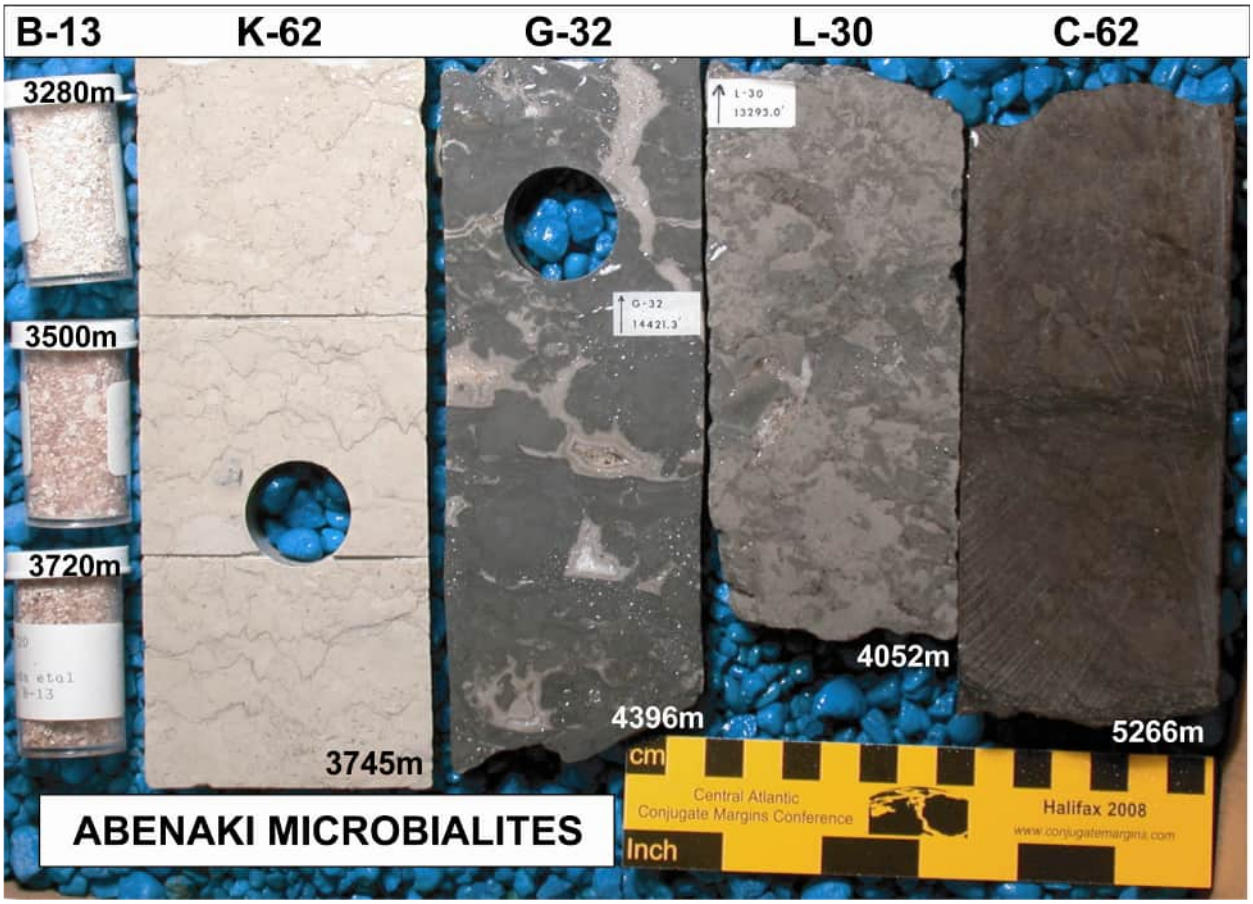


**Figure 13. Microbialite lithofacies of the Abenaki carbonate margin-slope showing color changes from the southwest (left) to northeast (right). See Fig. 1 and Table 1 for well locations: B-13 on far Western Shelf with red and pink capped cycles, L-30 on deep ramp foreslope, C-62 in thin #9 Limestone beneath the Venture shelf-margin delta gas field. The thrombolitic textures are interpreted as due to seafloor microbial cementation and trapping of lime peloids and mud that also is shown by ubiquitous geopetal infill of cavity systems of various sizes. Some cavities (G-32) are large enough to allow multiple isopachous submarine cements with some showing stromatactis characteristics (similar patterns can be seen even at a microscopic 'fractal' level as in B-13 that only has cuttings and limited old "shotgun-type' percussion sidewall cores). The color changes are tentatively attributed to proximity to nutrients (and sometimes minor clays) closer to the Sable Island area siliciclastic source with lighter colors due to greater oxidation (K-62) that in the extreme becomes white-to-red then pink-to-red cycles (B-13). However some changes could be interpreted as burial (or even slope depositional) depth related (C-62, G-32, L-30) under the influence of the prodeltaic clays-nutrients with fluctuating redox conditions. The alternative interpretations are not mutually exclusive.**

**AB7** although argillaceous is rich (4-20%) in stromatoporoids with much less amounts of lithistid sponges and associated microbial textures. Byrozoans and crinoids are also common. So a somewhat shallower reef or reef-derived setting can be inferred than for solely lithistid sponge reef or microbial mounds. Fossiliferous sandstones overlie the Abenaki with some thin interbeds of skeletal-sponge limestones. **AB6 U** has only one thin stromatoporoid-sponge bed and is mainly peloidal-skeletal-

microbial wackestone indicating a distal slope setting capped by 15 m of calcareous dolomite. **AB6 L** shows a long shoaling trend from all microbial-peloid-skeletal mudstones to packstones up to 40 m continuous section of microbially-encrusted corals and stromatoporoids that core shows includes *in situ* boundstone reef that has not suffered wave or storm destruction (but has been attacked by early and late diagenesis).

Just below the reefal interval is a 15 m bed of porous dolomite. **AB5** is again more stromatoporoid-rich, especially at the top but also lower down sporadically interbedded with microbial-peloidal beds indicating a mix of distal and proximal slope to reefal environments (or 'true' reefs and microbial mud mounds). **AB4, AB3 U, AB3 L** and **AB2** are all similar in being almost solely microbial-peloidal mudstones to wackestones relieved only by slightly more skeletal-stromatoporoidal content in the uppermost beds of each unit. Considering that these are carbonate mud-rich rocks there is a surprising amount of clear and white calcite spar particularly in the lowermost sequences that is interpreted to be mostly from submarine cements (stromatactis?) of distal slope mud mounds rather than fracture fill. Trace amounts of calcispheres, a Mesozoic deep-water pelagic indicator, occur sporadically in these sequences. The **base of AB2** clean limestone has just 10 metres of skeletal-fragmental wackestone to packstone with one 5m interval containing only 5% ooids instead of the more usual thick basal transgressive oolite seen above the **Misaine** in many other wells. Below the AB2 clean limestone are increasingly argillaceous limestones down into the calcareous Misaine shale with one 5m interval of 'reefal' limestone with chaetetids, byrozoans, lithistid, stromatoporoids. Much of the limestone could be attributed to caving but this bed has nothing obvious to cave from except nearly a kilometre up-hole and was clean on logs. A transitional Baccaro to Misaine member contact is similar to more oolitic Cohasset D-42 in contrast to more abrupt in Panuke M-79 and Demascota G-32.

In summary, Cohasset L-97 is dominated by high carbonate mud content that shows peloid and particularly microbial textures even amongst coral and stromatoporoid-rich reefal intervals. The variably-thick reefal intervals that can be quite thin help define the upper limits of the sequences. The Abenaki is interpreted to be mainly a distal slope of microbial mud mound sediments with increasing amounts of low energy reef or reef-derived beds upward even into the AB7 (= Artimon Member level which does not have good lithistid sponge development). Anomalously the seismically defined "back bank" setting does not accord with the litho-depofacies. Speculatively the whole area may have been a re-entrant in the platform margin that was subsequently structurally uplifted. The apparent lack of a basal transgressive shallow event above the Misaine shale and the greater thickness of L-97 relative to other Panuke trend full Abenaki penetrations, even with a normal fault that should reduce total thickness, is yet another anomaly. It could be explained by a mainly slope setting in the thickest part of a depositional sigmoid for L-97. Therefore an explorationist looking for more favourable facies and reservoir should be directed to "go west young man/woman" towards the main platform a short distance.

## Cohasset L-97 PERCENTAGE LITHOLOGIES by Abenaki "AB" sequences:

(Dunham & lithology initials = M/W/P/G/B/F-mud/wacke/pack/grain/bound/floatstone; SH=shale)

- **AB7** (130m) – 10% SH, 4% sponge WP, 27% stromatoporoid (chaetetid/microbial) WP, 15% fragment W, 13% argillaceous fragment-skeletal W, 31% argillaceous W
- **AB6 U** (80m) – 6% stromatoporoid-microb WP, 13% skeletal W, 56% peloid (microb) W, 25% dolomitic lime skeletal W
- **AB6 L** (200m) – 13% stromatoporoid-coral-microb FBR, 25% peloid-microb P, 55% microb-peloid W, 7% dolomite
- **AB5** (185m) – 5% lost circulation at top, 46% stromatoporoid-microb WF, 8% peloid-microb WP , 43% microb MW
- **AB4** (135m) – 19% peloid-microb PW, 81% microb-peloid WM; **AB 3U** (205m) – 12% stromatoporoid PF, 39% microb-peloid WM. 49% microb M
- **AB3 L** (100m) – 5% stromatoporoid WF, 50% peloid-microb WM, 45% microb (peloid) M
- **AB2** (175m) –11% skeletal-microb ('nearly' stromatoporoidal) P; 40% microb-peloid MW, 43% (microb) M, basal 6% skeletal-fragmental PW with 5m of 5% ooids only

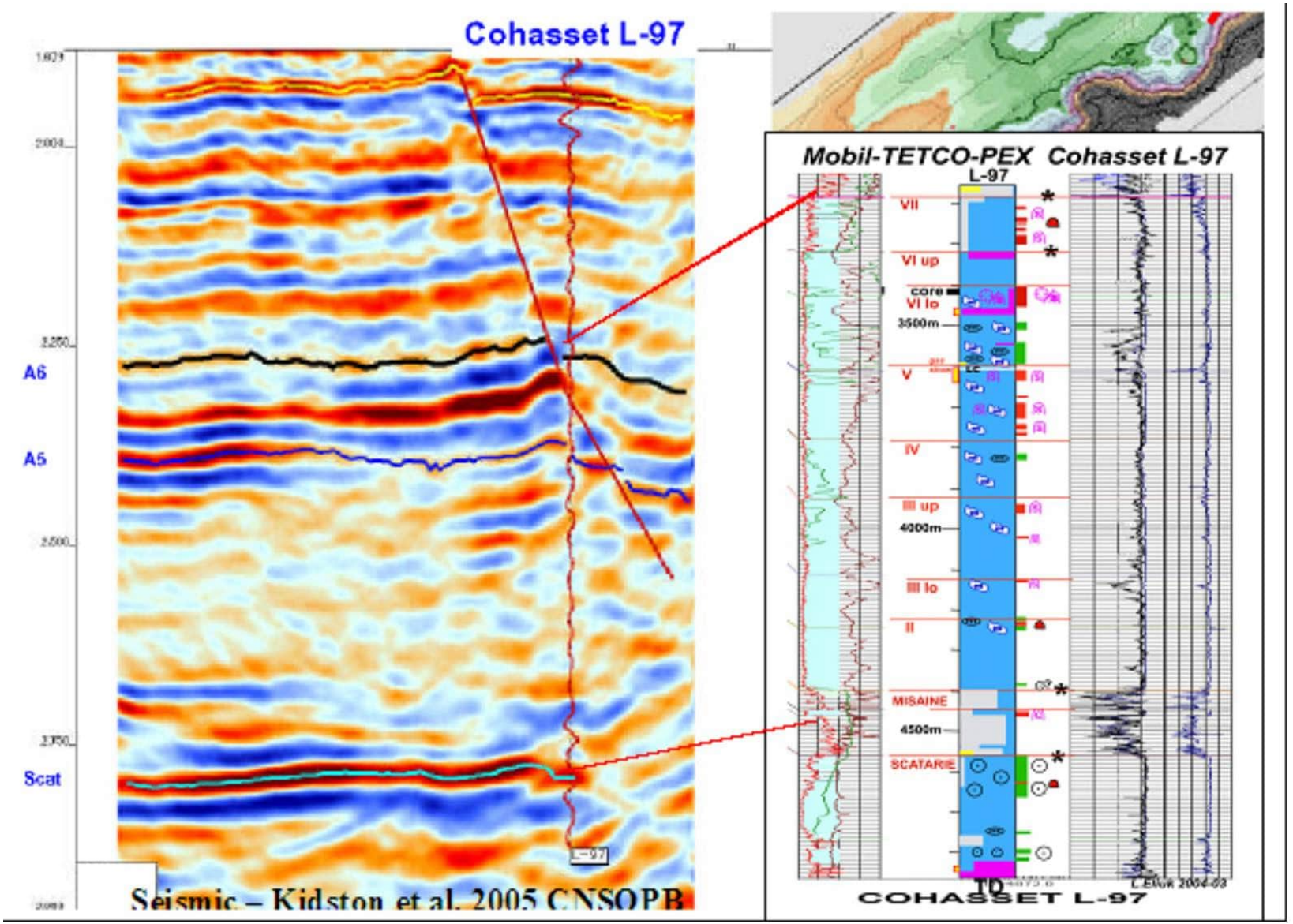


**Figure 14. L-97 example – Abenaki litholog and dip seismic (latter from Kidston *et al.* 2005).**

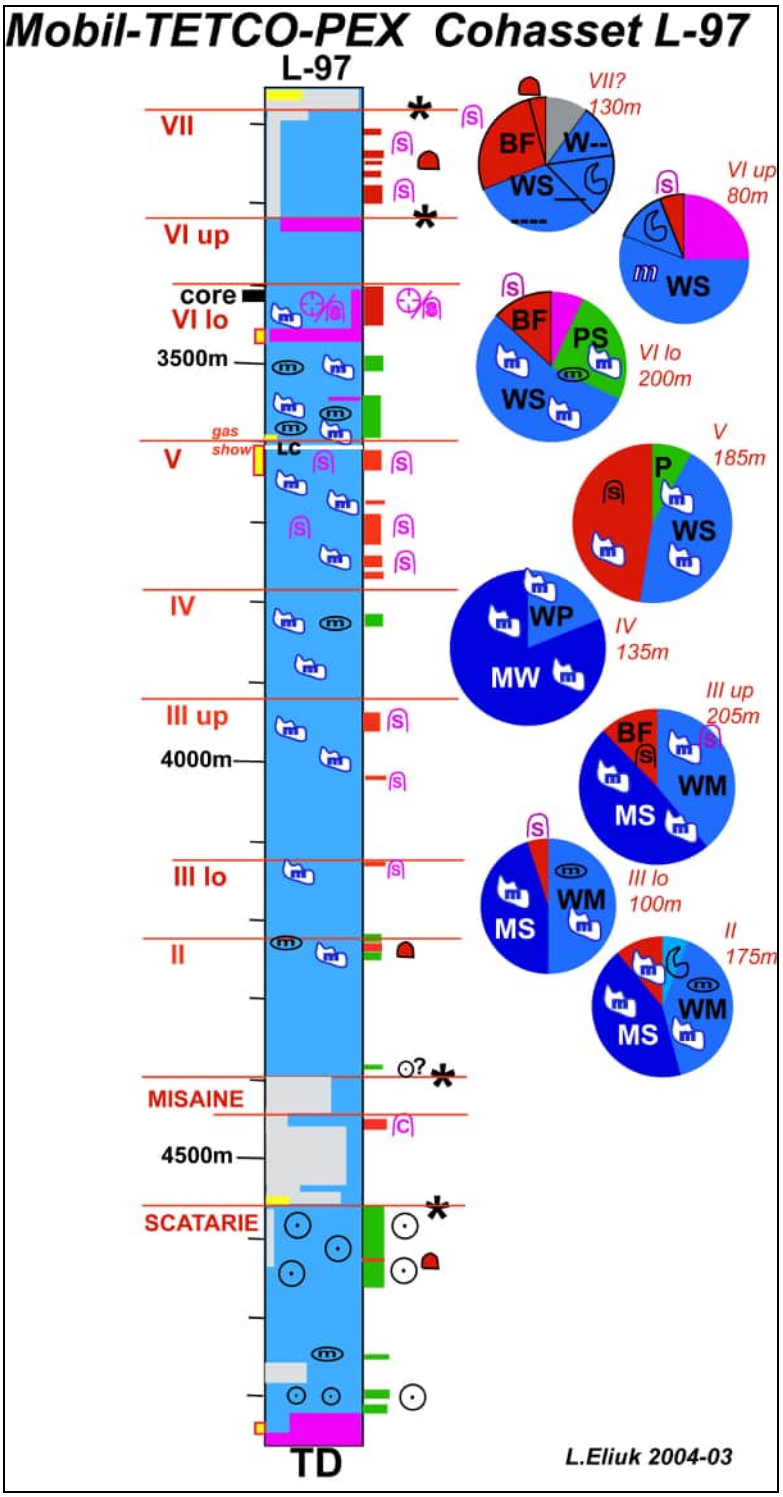


**Figure 15. L-97 example – Abenaki schematic log column with pie percentage lithologies. See Figure 5 or 18 for key to modified Dunham classification (Embry and Klovan 1971) abbreviations and symbols.**

BACK

# Abenaki Carbonate Margin Facies Associations 3: Varieties of Reefs and Reef Mounds of the Outer Margin

**Leslie Eliuk**
Dalhousie University
Department of Earth Sciences
Halifax, Nova Scotia B3H 4J1
Canada
e-mail: geotours@eastlink.ca

Worldwide, the Late Jurassic is noted for great quantities of varied reefs and of hydrocarbons in carbonates (Greenlee and Lehmann 1993, Leinfelder *et al.* 2002). Surprisingly, with just a handful of exceptions, it is not the Jurassic reefs that contain the hydrocarbons but rather platform interior carbonates in structural traps. Deep Panuke is one of those exceptions. The gas is in the reef complex and the trap is partially stratigraphic with even the structural component mainly due to reefal growth. And in the Abenaki margin, all three Jurassic reef-reef mound end-members (Leinfelder 1994, also see Fig. 4 and Fig. 16) are present: coral reefs, siliceous sponge and microbial (mud) reef mounds.

These end-members have intermediate transitional forms but only the shallow-water coral-coralline sponge (stromatoporoids and chaetetids) reef complexes are significant reservoirs. Microbial mud/reef mounds (see Poster 2) are well-cemented limestones and occur in slope facies below the reservoir levels. (As a caution against generalizations, some Jurassic Gulf of Mexico microbialite reefs occur in restricted shallow settings and are hydrocarbon reservoirs – Mancini *et al.* 2004.) Siliceous (lithistid) sponge reefs (see Poster 5) generally occur above the porosity-reservoir levels and actually contribute to the trap seal by their argillaceous content.

These three reef type end-members can be distinguished even in cuttings. But only in core can one appreciate and possibly subdivide the shallow-water reef complex into reef flat, core (typically rubbly from bioerosion then storm and wave action) and proximal forereef (cores in Cohasset L-97, Margaree F-70, Panuke H-08, Demascota G-32, Acadia K-62). And in most cases the common presence of carbonate mud in the matrix, crinoidal debris and encrusting microbialites indicate that, unlike many modern *Acropora*-dominated reefs, these Late Jurassic hexacoral-rich reefs probably grew in slightly deeper margin water not at the crest. Probably particularly true when large phaceloid corals are seen still standing (L-97 core and on FMI in Panuke M-79).

Seismic and dip-meter data clearly show that the reef-prone outer margin slope, between the updip oolitic inner flexure and the distally steepened downdip flexure, has considerable local topography. Some forereef beds on local pinnacle-like buildups even dip landward (MarCoh D-41, Margaree F-70 see well example and Figs. 17-20). Usually that topography is encased by carbonates but Dominion J-14 shows that rarely shale can be trapped between individual buildups (Fig. 8). In Baltimore Canyon Trough, the southward extension of the Jurassic gigaplatform, margin pinnacle reefs keep growing as the shelf interior is drowned and buried in shale (Fig. 24).

## Margaree F-70 – Example of interpreted varied reefs and near-reef slope (+flat?)

EnCana-Murphy Margaree F-70, drilled in 2003, is in the north end of the Deep Panuke field and, unlike all the other field wells with no or very poor core recovery, has the longest single continuous core even for the whole of the Abenaki Formation. The principal reference on this well including the nature of its reservoir and fracturing is Wierzbicki *et al.* (2005) and the following is mainly excerpts from Eliuk's contribution on the lithology and deposition of the Abenaki in the well and core. The well penetrates sequences AB 7 through into the upper part of AB4. While similar to MarCoh D-41 in its deepening up depositional trend, it is much less argillaceous (Figs. 17, 18).

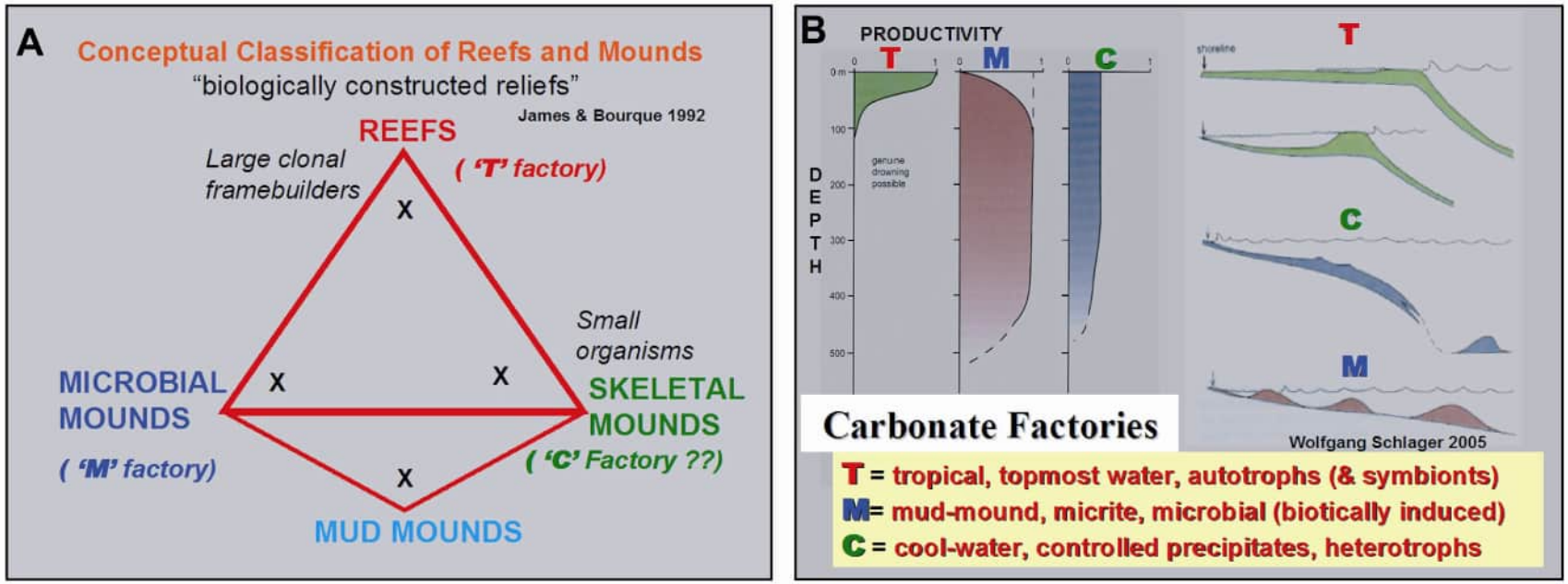


**Figure 16. Reef-reef mound and carbonate factory classifications. A) Quaternary classification of reefs-mounds of James and Bourque (1992) that are interpreted to all be present as end members and transitional forms in the Abenaki and the Late Jurassic (see Leinfelder 1994 and Fig. 4 this paper) with mud mounds mainly represented by microbial buildups on the slope that are cemented very early on the seafloor or even precipitated in part as cements. Note that the reefs and mounds can be (but not always uniquely) related to Schlager's carbonate factories with the best fit to the older original tropical shallow-water coral-reef-rimmed carbonate platform as "T" and mud/microbial mounds as "M" almost by definition. B) Carbonate factory classification of Schlager (2005) is a useful simplification that helps place certain buildups in reasonable depositional settings linking depth and average rate of carbonate productivity. The high productivity 'T' factory may average the same in vertical productivity to the 'M' factory because the generally deeper mud/microbial mound factory does not get as easily redistributed by shallow energetic waters so that it can accumulate *in situ* more continuously. It is arguable whether the Abenaki argillaceous sponge reefs and inter-reef beds, while well placed as 'small organism skeletal mounds', represent 'C' factory sediment since they are likely not cool water. But they probably are subject to reduced productivity because of turbid then deeper conditions that are interpreted to have 'killed-off' or suppressed "T" factory coral reef production. They also likely mimic the underlying substrate morphology and thus may simulate the siliciclastic-style profile of the 'C' factory. It is interesting that the ramp profiles are most usual in proximity to the Sable Island delta after the initial early 'transgressive' carbonate sedimentation of the Scatarie and basal Baccaro members. However the plentiful oolites even on ramp profiles near the Sable Island are not appropriate 'C' factory sediment and show that seawater chemistry and temperature changes with geological age are an important variable.**

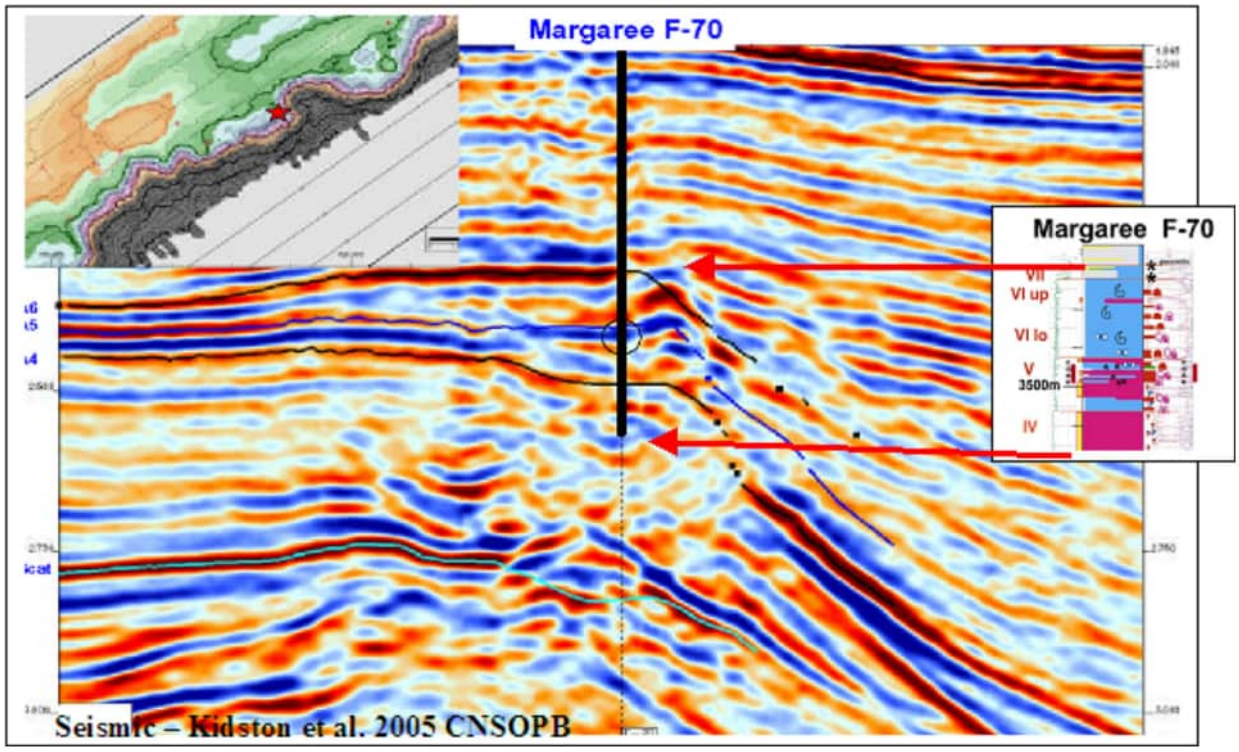


**Figure 17. F-70 example – Abenaki litholog and dip seismic (latter from Kidston et al. 2005).**

Set within an Abenaki section lithofacies transition from dominantly cleaner dolomite-rich carbonates up into slightly argillaceous limestone-rich carbonates, Margaree F-70 core #1 (3434-3458.7 m) also captures a depositional facies transition in reef types and water depths (and/or nutrient-argillaceous content) that increase upward. Jurassic-earliest Cretaceous carbonates show three reef-reef mound type end members – coral (& coralline sponge), siliceous (lithistid) sponge and microbial crust (Leinfelder 1994, Leinfelder *et al.* 2002, Wierzbicki *et al.* 2002).

The relationship of the whole F-70 Abenaki well section to the core is shown in Figure 19 and more detail of core # 1 with its thin reef types named in Figure 20. They tell a story of what happens around an Abenaki reefal build-up from shallower to deeper water or from further to closer proximity to the major Sable Island paleodelta or both. The core has 4 reef examples transitional between the 3 end-member reef types of the mid-Mesozoic Based on F-70 cuttings analysis, the mainly argillaceous-carbonate mud-supported limestone of the upper Abenaki (sequences **AB7** and **AB6**) are interpreted to be dominantly forereef slope with periods of thin deeper-water reef colonization.

Initially these reefs are a mix of corals, coralline sponges (stromatoporoids-chaetetids) and lithistid sponges with a microbial component. But upward there is a progressive decrease in corals (along with microbialite content?) then stromatoporoids leaving only the lithistid sponges. This change indicates increasing water depth and/or nutrient-argillaceous content upward. Tentatively the **AB6 U versus AB6 L** transition can be placed about 3640 m where there is mainly sponge-rich beds above and but microbial and stromatoporoids mixed with lithistid sponges below. A possible reworked surface was seen in a sidewall core at 3374 m.

The lack of even derived oolites as parts of slope debris in the whole section supports the seismic geometries showing that not only was F-70 drilled on the back or bankward-side of a partially collapsed margin-edge build-up but that it penetrated material shed and growing in deeper water on the southwest side of a local pinnacle or raised rim. Downward (sequence **AB5**) there is a decrease in sponge and microbial content and an increase in dolomite to 100% in the bottom 100metres (sequence **AB4**). The presence of abundant crinoids at the top of sequence **AB5** indicates slope deposition continued but interbedded with increasing amounts of coral and stromatoporoid reef or reef-derived sediment downward. Thus the dolomitized sections in **lower AB5** and all of **AB4**, whose depositional facies is problematic even with the help of sidewall cores, are inferred to be reefal or at least shallow-water carbonate bank.

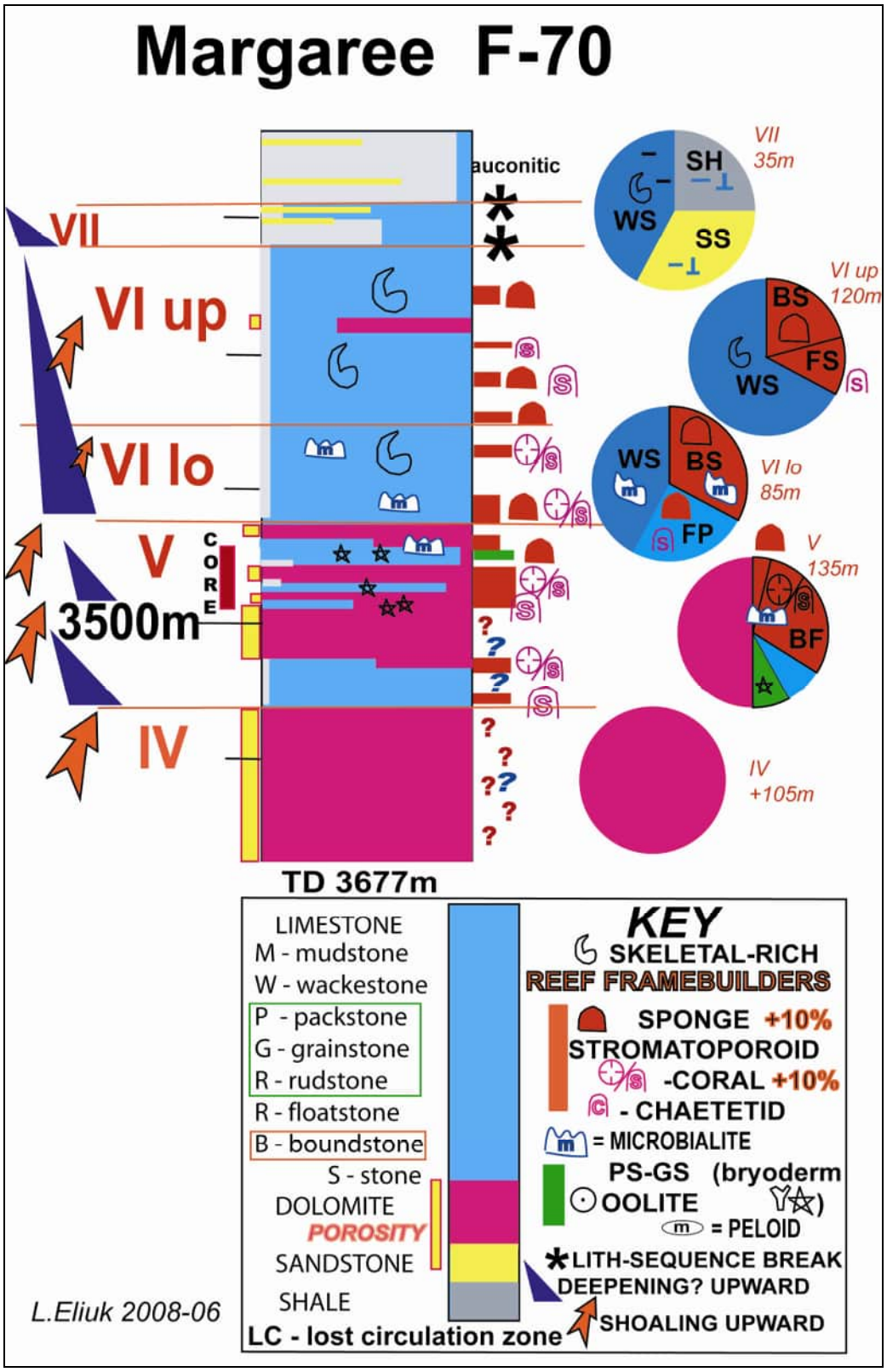


**Figure 18. F-70 example – Abenaki schematic log column with pie percentage lithologies. Carbonate classification is Dunham modified by Embry and Klovan (1971).**

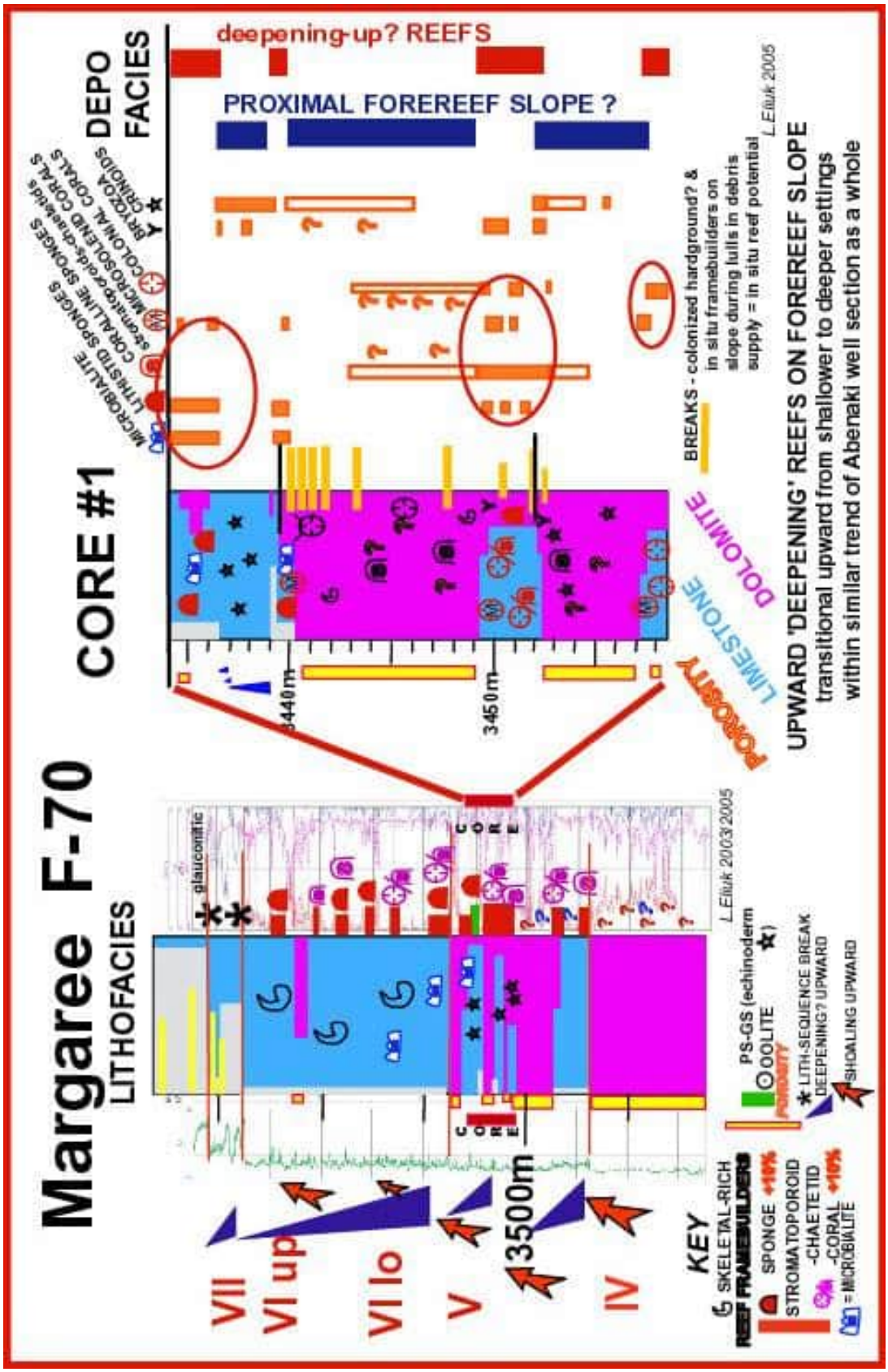


**Figure 19. F-70 example – Abenaki interpretive schematic log column with core log showing distribution of framebuilders and important accessories (also used in EnCana 2006, and Wierzbicki *et al.* 2005 and 2008 core workshop this conference CD that also has rock photographs). Note the upward shift of framebuilder organisms plotted by typical relative depositional depths in life that is used to infer deepening on the slope.**

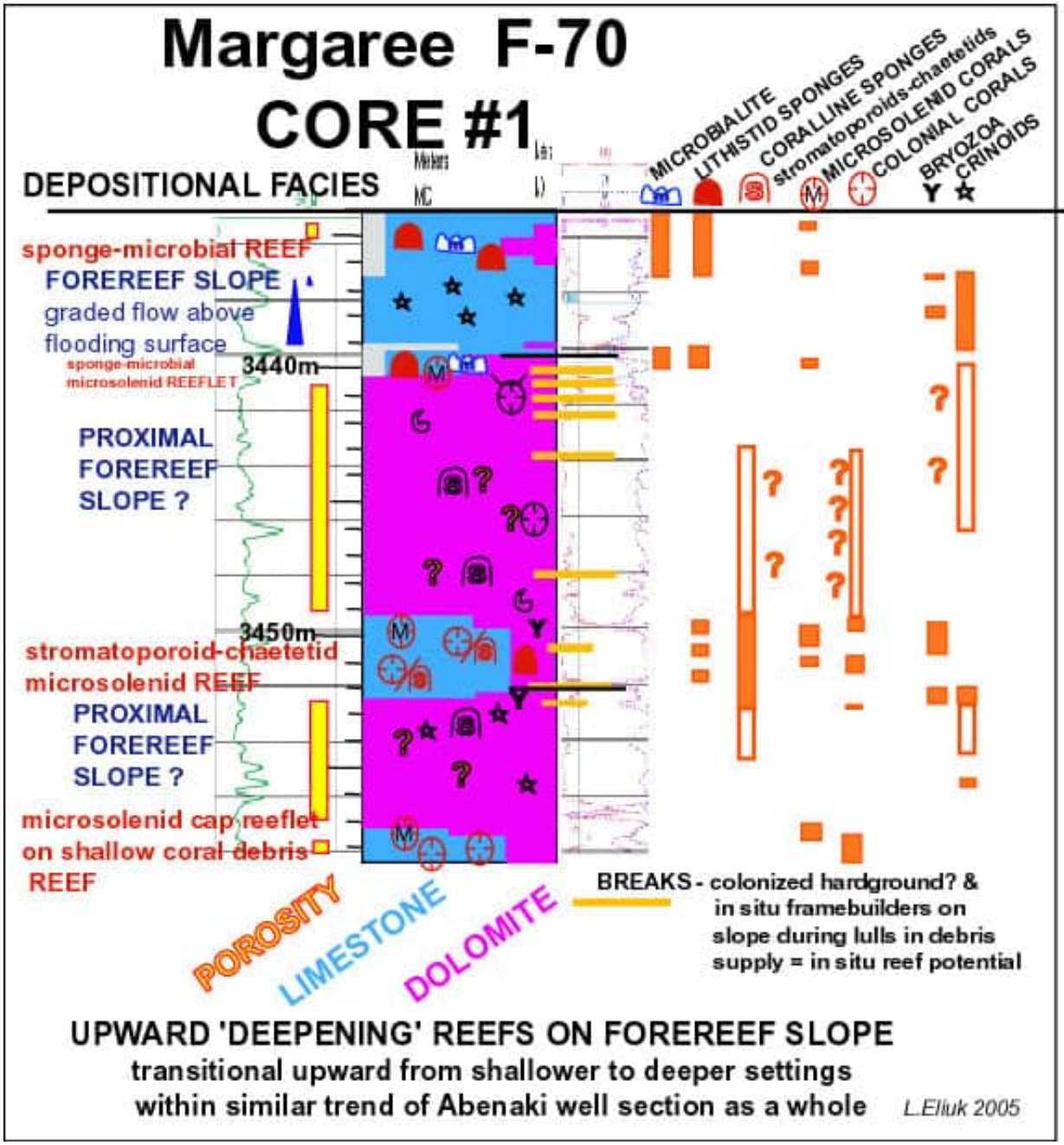


**Figure 20. F-70 example – Abenaki interpretive schematic core log showing distribution of framebuilders and important accessories. Note that the reefal intervals are limestone often slightly argillaceous and interpreted as early cemented and compacted so resistant to burial dolomitization common in grainier reef-derived beds.**

**Core #1**, wholly **in AB5**, is well placed to show the litho- and depo-facies transition of the Abenaki section as a whole (Figs. 19, 20). The limestone intervals are reefal except for 3 metres of well-cemented normal-graded crinoid-rich slope debris beds (slope channel with possible submarine cement) near the core top. The thick dolomite intervals are interpreted to be proximal forereef slopes with debris from a shallower-water coral-stromatoporoid reef intermixed with minor slope material such as crinoids and bryozoa. An originally porous finer lime sand matrix may have localized the dolomitization. During breaks in slope sediment supply, hardgrounds (?) and framebuilder colonization occurred. If the breaks

were long enough a deeper-water reef built up. Analysis of percentage framebuilder contribution shows a progressive change that is interpreted to result from progressively deeper (or/and more nutrient-rich and argillaceous content which due to increased turbidity has the effect of increased depth if the organisms can handle the greater clays-nutrients). The basal few metres of the core have 16% microsolenid hexacorals and 28% other colonial hexacorals in a rudstone indicating shallow-water reef-derived or even storm-affected in-situ reef. These rubbly beds are capped by a 0.5 m in-situ pure microsolenid coral reeflet.

The next limestone reef interval, above a thin crinoid–rich possibly transgressive lag limestone, has less hexacorals (15%) and microsolenids (8%) but more stromatoporoids-chaetetids (21% collectively coralline sponges) and lithistid sponges (14%). Capping the thick foreslope dolomite bed with its increasing number of sedimentation breaks is a microbial-sponge–microsolenid coral reeflet (0.5m thick and 12%, 15% and 11% respectively). Of the colonial hexacorals, microsolenids range into deeper and more turbid waters. At the top of the core a microbialite-lithistid sponge reef with some scattered microsolenids (16%, 21% and 9% respectively) form complex consortia with early-cemented high depositional angles (and possibly structural dip due to later rotation of whole section). Some solitary and/or open branching corals are present. Locally there are crusts of lithistid sponges overgrown by sponge-microbialites capped by bioeroded tabular microsolenid corals. Taken as a whole these changes indicated progressively deeper (more nutrient-rich?) water upward over the cored interval. The presence of periods of reefing on the slope indicate that the forereef slope is not just a sediment sink but supplies significant amounts of its own sediment.

## Margaree F-70 PERCENTAGE LITHOLOGIES by Abenaki "AB" sequences:

(Dunham & lithology initials = M/W/P/G/B/F-mud/wacke/pack/grain/bound/floatstone; SH=shale)

- **AB7** (35m) - 42% argillaceous skeletal-fragmental W, 33% argillaceous-calcareous SST, 25% calcareous SH
- **AB6 U** (120m) - 21% sponge F-B, 12% stromatoporoid-sponge F, 67% fragmental-skeletal W
- **AB6 L** (85m) - 25% sponge-microb WPF, 33% sponge-stromatoporoid-coral F-B, 42% fragmental-microbial W
- **AB5** (135m) - 4% sponge-microb BS, 30% stromatoporoid-coral (microb) F-B, 8% fragmental W, 8% lime and dolo- crinoid G, 50% xtl DOL
- **AB4** (+105m, partial) - 100% xtl DOL

BACK

# Abenaki Carbonate Margin Facies Associations 4: Shelf-Edge Oolitic shoals of the Inner Margin, and Thoughts on Oncolites, Bypass Sands and Unconformities

**Leslie Eliuk**
Dalhousie University
Department of Earth Sciences
Halifax, Nova Scotia B3H 4J1
Canada
e-mail: geotours@eastlink.ca

Worldwide, Jurassic carbonates are also noted for oolites. The Abenaki too has oolite nearly everywhere and in many cases it allows cyclic and sequence subdivision to be made. But rarely are these grainy rocks an important contributor to reservoir porosity at least in the deeply buried Panuke trend, in the carbonate ramp shelf associated with the Sable Island paleodelta, in the basal transgressive beds of the platform, or in the very oolitic Scatarie Member at the base of the Abenaki Formation. Seismically at the inboard margin flexure and sedimentologically, oolites occur in the shallowest carbonate settings and should be subject to effective winnowing and subaerial exposure. Both should create porosity but likely Late Jurassic calcitic seas may have made for less soluble ooids. And most oolites are completely occluded by burial cement except on the Western Shelf where they occur less deeply buried beneath the present-day deep-water slope. At Deep Panuke the oolitic grainstones are impermeable enough to form part of the seal for stratigraphic trapping as opposed to their usual role as platform reservoir rock. There is an interesting range in oolite color that parallels that of the microbialites (Fig. 21). Panuke F-09 illustrates a highly oolitic margin shoal well (see example write-up and Figs. 22, 23).

A very thick oncolitic facies was defined using core in Acadia K-62 (location on Fig. 6 section and Fig. 7 map) where the common presence of ooids, megalodont clams and coral fragments with the large oncoids suggested a reef flat interpretation. Since the oncolite facies is not obvious in other wells, speculatively it may reflect a more local or special event - possibly nutrient enrichment corresponding to the influx of deltaic clays and siliceous sponge reefing closer to the Sable Island delta. Another facies definitely related to siliciclastic influx is thin bypass sands (see Panuke F-09 write-up). These are widespread at particular levels and have been interpreted to represent unconformity related low-stand periods with sand influx. As well the sand may overlie unconformities when reworked during the next transgression. In bracketing the inferred unconformities they represent maximum regression surfaces. Thus they are a key to establishing a sequence stratigraphic framework on the platform whether that is based on transgression-regression or more elaborately on relative sea-level stands of transgressive, high, forced regression and low.

(Continued of the next page.)

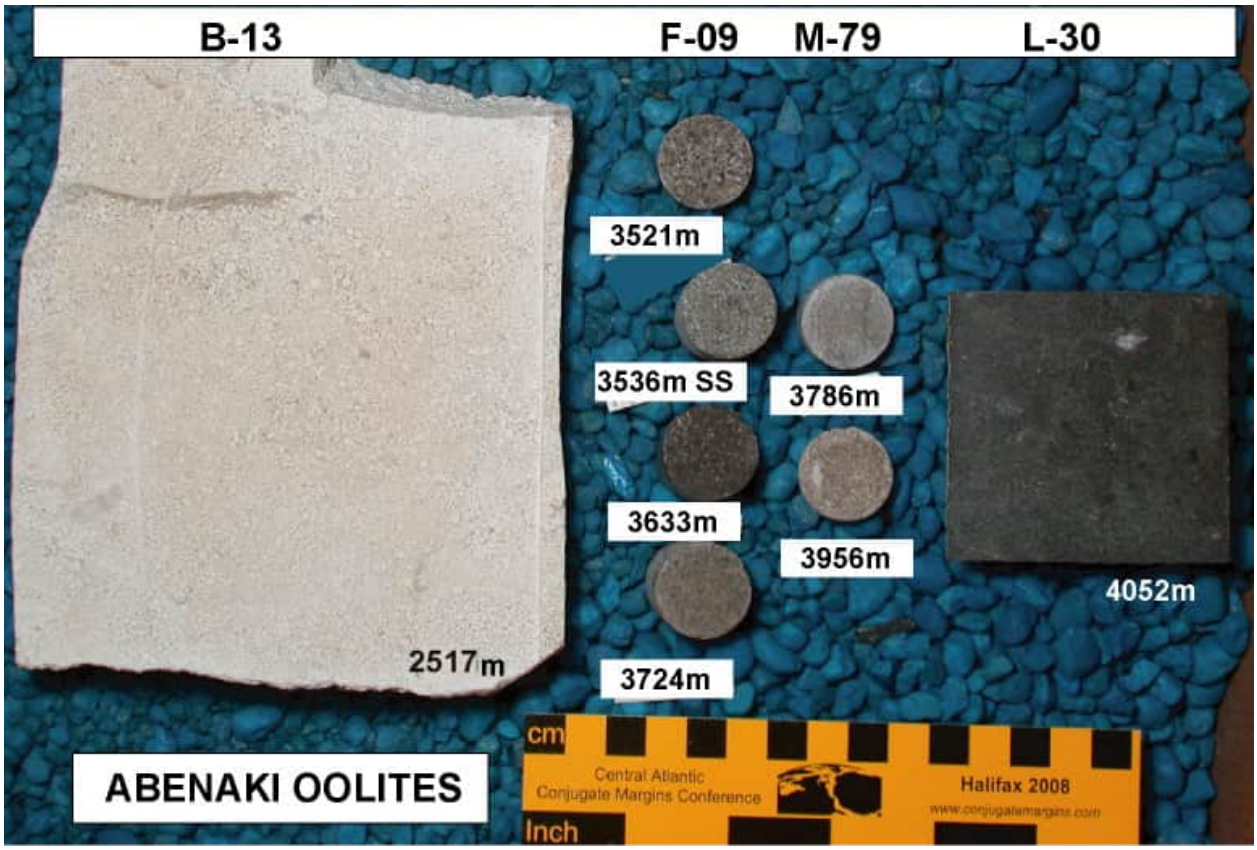


**Figure 21. Oolitic lithofacies of the Abenaki carbonate margin and ramp showing color changes from the southwest (left) to northeast (right). See Fig. 1 and Table 1 for well locations: B-13 on far Western Shelf, F-09 and M-79 rotary drilled sidewall cores, L-30 shallow inner-mid carbonate ramp. The color changes are also tentatively attributed to proximity to nutrients closer to the Sable Island area siliciclastic source but again a burial depth interpretation that is also seen in the greater compaction-closer fit of ooids in L-30 as compared to B-13. SS = sandstone in F-09 3536 m.**

(Continued on the next page.)

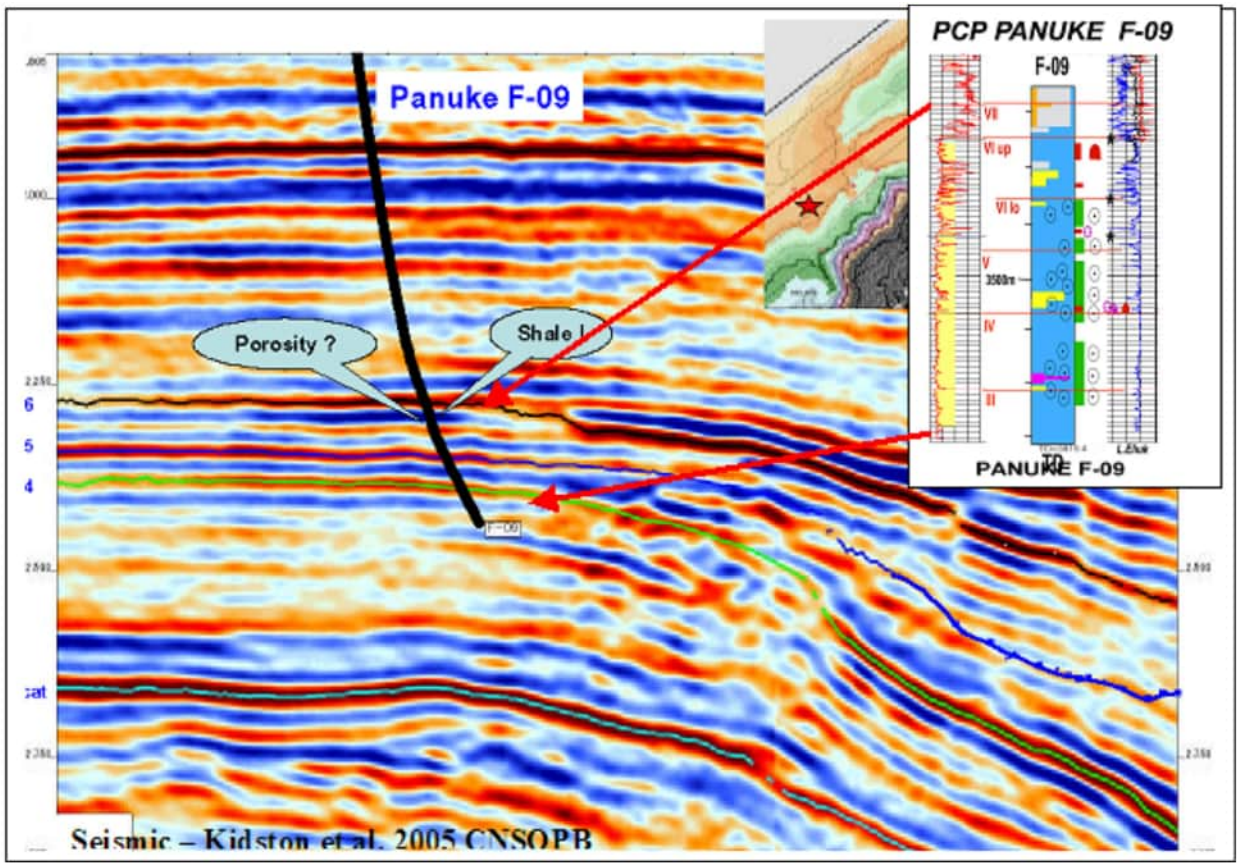


**Figure 22. F-09 example – Abenaki litholog and dip seismic (latter from Kidston *et al.* 2005).**

## Panuke F-09 - Example of oolitic shoals and sandstone sequence breaks

PanCanadian F-09 penetrated nearly 600m of Abenaki going through sequence AB7 into 100 m of AB3. F-09 followed up on early Deep Panuke wells with an attempt to test the backreef of sequence AB5 (Kidston et al. 2005) at the inner-shelf margin up-dip flexure (Figs. 22, 23). It is on trend with the decade older Panuke B-90 well that was 6 km to the northeast but also 1-2 km behind the major margin-slope flexure (see locations Fig. 1 and Fig. 9). Both wells failed to find significant Abenaki reservoir despite high amounts of oolites in sequences below AB6 U that reflect a depositionally shallower position compared to the rest of the Deep Panuke Abenaki margin wells closer to the slope.

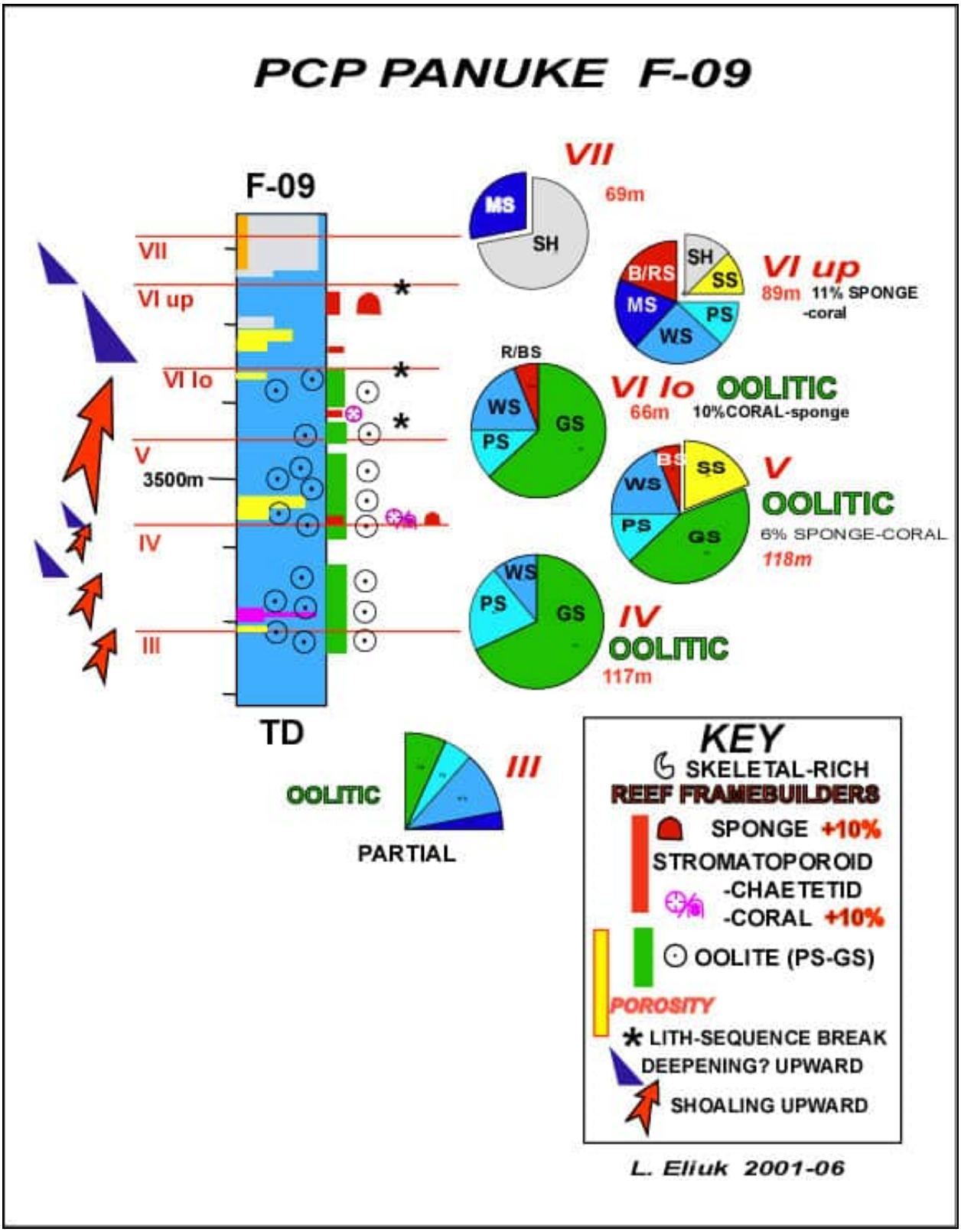


**Figure 23. F-09 example – Abenaki schematic litholog column with pie percentage lithologies. See Figure 5 or 18 for key to modified Dunham classification (Embry and Klovan 1971) abbreviations and symbols.**

Both B-90 and F-09 wells are also similar above AB6 L. **AB7** is dominated by argillaceous limestones and siliciclastics but apparently shalier in F-09 compared to sandier in B-90. In both wells **AB6 U** has more sponge framebuilders zones along with siliciclastics in the limestones. They differ in that the sponges are lithistid (siliceous but now calcified) in F-09 whereas in B-90 sponges are stromatoporoids (coralline sponges) with more intervals high in bryozoans-echinoderms ("bryoderm"). An argument could be made that B-90 is shallower and more proximal to a siliciclastic source than F-09 suggesting transport along the margin from the northeast rather than just across the shelf. The underlying **AB6 L to uppermost AB3** are highly oolitic with skeletal content slightly more concentrated in the lower portions of each sequence. Occasional sandy oolites to sandstone beds occur such as in the lower AB5. Downward there is an increase in peloids from essentially none in AB6 L to a partial replacement of ooid grainstone-packstone beds by lower energy peloid-fragmental wackestones-mudstones below the top 45m oolite of AB3. Within that probably lagoonal interval there was a possible 5m stromatoporoid-oyster patch reef.

## Panuke F-09 PERCENTAGE LITHOLOGIES by Abenaki "AB" sequences:

(Thickness as drilled not true vertical; Dunham & lithology initials = M/W/P/G/B/F-mud/wacke/pack/grain/bound/floatstone; SH=shale, SST=sandstone)

- **AB7** (45m) - 44% silty SH, 56% argillaceous lime M
- **AB6 U** (110m) - 5% SH, 20% SST. 31% sponge W(P), 14% ooid-fragment P, 20% argillaceous MW
- **AB6 L** (70m) - 7% coral, PW, 71% ooid PG, 22 % fragment W
- **AB5** (145m) - 10% SST; 73% ooid PG, 17% fragment W
- **AB4** (140m) - 82% ooid PG, 14% ooid-fragment W 4% dolomite
- **AB3** (+105 partial) – 10% tromatoporoid WF, 38% ooid PG, 14% fragment PW, 33% fragment WM, 5% dolomite.

***Note*** *the original tops unchanged from 2001 and the old pie diagrams are good approximations but are based on every second sample using more detailed Excel calculations aided by sidewall cores. The above have been calculated more generally and similarly to Panuke B-90 and Como P-21 using every sample from an infill of the older 200l logging.*

**BACK**

# Abenaki Carbonate Margin Facies Associations 5: Sponge Reefs and Argillaceous Sponge-rich Carbonates Related to Deltas: the Jurassic-Cretaceous Baltimore Canyon-Nova Scotia Abenaki Examples Compared to the Modern Fraser Prodelta Example

**Leslie Eliuk**
Dalhousie University
Department of Earth Sciences
Halifax, Nova Scotia B3H 4J1
Canada
e-mail: geotours@eastlink.ca

Of the three Jurassic reef-reef mound end-members (see Poster 3), the siliceous sponge reef mounds occur uniquely at the top of the Abenaki and at the top of equivalent carbonates in the Baltimore Canyon Trough (BCT). Thin shales overlie both. A major oceanographic or relative sea-level carbonate drowning event or series of events affecting both areas seemed like an obvious explanation. However a limestone core just below the Venture Field shelf margin delta, diachronous age dating of sponge-rich beds and their limited distribution on the Nova Scotia Shelf (NSS), and the discovery of siliceous sponge reefs adjacent to prodeltaic shales of the Fraser River delta, British Columbia (Conway, Barrie and Krautter 2004, also see Fig. 15), may give an alternative explanation with a modern analogue.

Seismic and Ringer's Valanginian model (in Eliuk and Prather 2005, repeated at this conference, also see Fig. 24) in BCT show that after and perhaps even contemporaneously with the shelf margin pinnacle reefs, sponge mounds formed in nearby deeper water (several 100 feet or ~50-100 m) below the pinnacle reef and in front of small deltas prograding over drowned inner platform carbonate. In the NSS, argillaceous sponge-rich beds at the top of the Abenaki are younger in wells further southwest of the large Sable Island delta (see Fig. 6).

Even further away from the delta on the Western Shelf the Abenaki (Roseway unit) carbonates no longer have a sponge facies but continue in typical shallow platform facies and are younger yet. In the bottom of West Venture C-62 the older thin Late Jurassic #9 Limestone has a few metre thick sponge-microsolenid coral-microbial reef mound capping a pure microbialite reef mound of similar thinness (Eliuk and Wach 2008, this conference CD). Laminated black prodeltaic shales at the base of a 50 m thick shelf-margin deltaic sequence (Cummings and Arnott 2005) abruptly overlie the limestone. This is like a miniature version of the Abenaki carbonate platform terminations to the southwest and ignoring subsidence indicates an initial water depth around 50 m.

The change from microbialite up to sponge-microsolenid coral reef with possible red algae in a total of less than 5m indicates a relative sea-level fall and supports an interpreted forced regression (also see Eliuk and Wach 2008, this conference CD). Like the modern Fraser delta sponge reefs (Fig. 25), these more calcareous Late Jurassic-earliest Cretaceous sponge reefs were in deep quiet nutrient-rich waters but not yet engulfed and buried by clay sediment of an encroaching delta. Such a setting was environmentally untenable for shallow-water carbonate sedimentation that had therefore already "drowned".

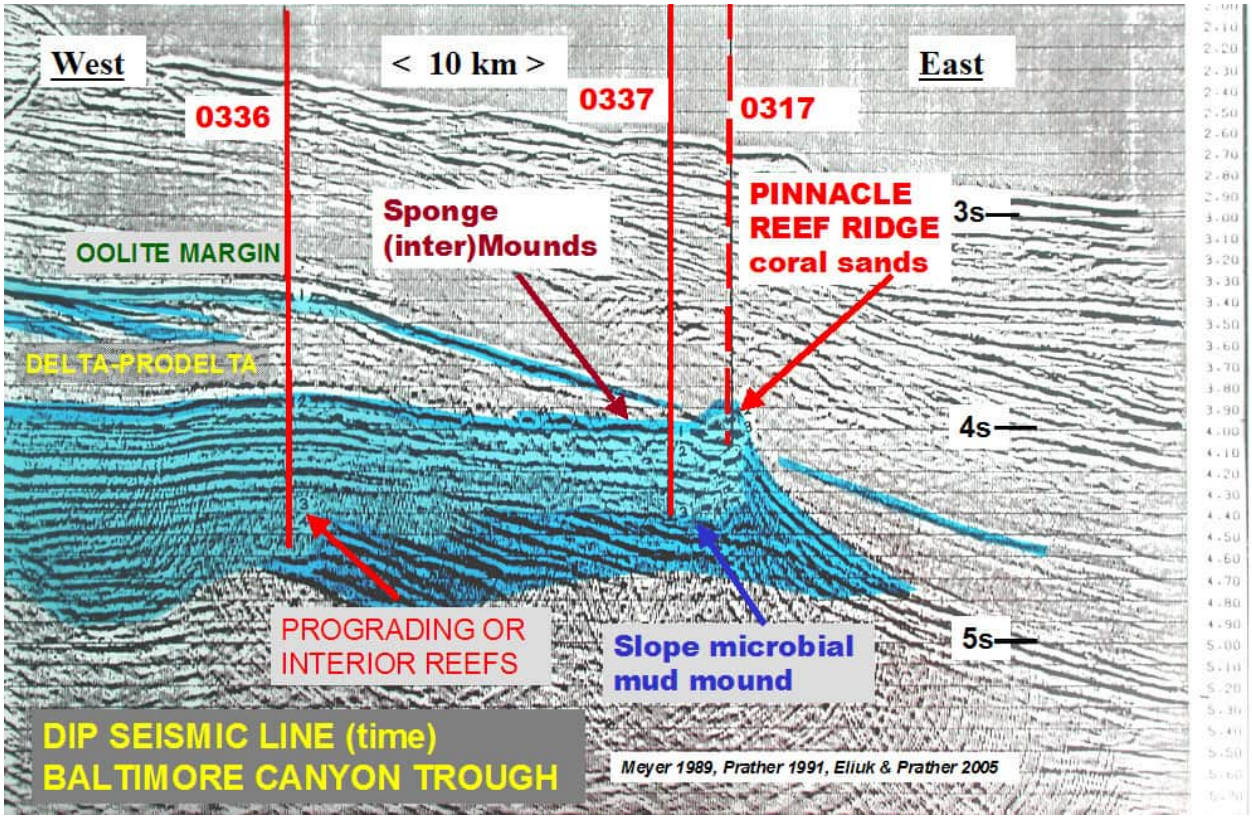


**Figure 24. Baltimore Canyon Trough, USA dip seismic section across Late Jurassic carbonate margin and Lower Cretaceous delta capped by Aptian oolitic limestones. For details on Baltimore Canyon (BCT) see Eliuk and Prather (2005 and 2008 Core Workshop article in this Conference CD). The BCT area off Delaware is very analogous to the Abenaki and Barremian O Limestone of the Nova Scotia Shelf (NSS). Even a morphologic similarity to the NSS along-strike-section (see Fig. 6) with continued younger carbonate deposition away from the influence of the siliciclastics with a margin pinnacle reef (BCT) or continued carbonate sedimentation in the Lower Cretaceous Western Shelf (NSS). Inter-sponge reef mound facies were cored in several BCT wells (well-core #: 336 #2, 337 #1, 317 #2) and from seismic their deeper water setting can be seen relative to the mostly older 'drowned' pinnacle reef and the prograding siliciclastics that show contemporaneous shallower bathymetric depths. The sponge-rich beds occur just in front of the prograding prodeltaic shales and on the drowned reef platform - so the classic solution of combining competing geological hypotheses becomes true (regional relative sea-level rise in stressed conditions for carbonate drowning of Eliuk 1978 and diachronous environmental deterioration of Wade and MacLean 1990, Ehrlich *et al.* 1993, Jansa 1993 and perhaps Graham Williams in Eliuk 1985; Eliuk 1978, p. 470 also offered this alternative but opted for a deep-water drowned platform scenario and supplied a possible modern analogue of a Recent seamount comparison – not the first time I selected maybe the wrong alternative with sound logic but limited analogues – see Fig. 25 for a new analogue that combines deep and prodeltaic but is short on carbonate).**

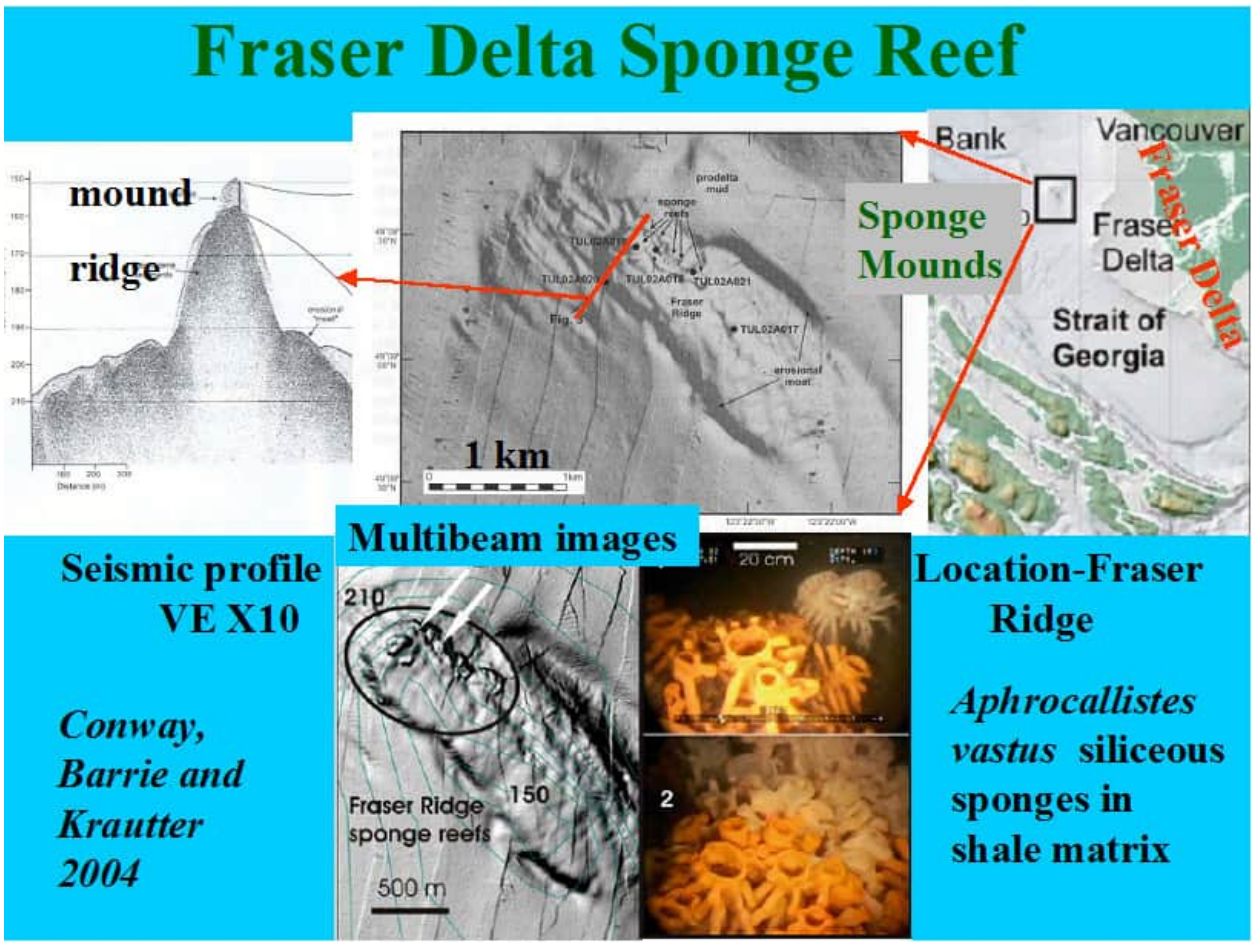


**Figure 25. Modern siliceous sponge reef mounds at the toe of the Fraser River delta, British Columbia Canada showing location, side-scan sonar plan views, seismic cross section and reef mound framebuilding biota. Modern analogues of comparatively common ancient sponge reef mounds are very rare but Canada seems to be the main contributor of examples. Very new additions have been found on a glacial ridge not yet buried in prodeltaic mudstones (Conway *et al.* 2004). Although an appealing analogue for the similarly positioned mid-Mesozoic sponge reef mound occurrences on the western Atlantic carbonate margin, the old ones are argillaceous limestones as opposed to the silica and clay mudstone for the modern. But perhaps this underlines the importance of varying sea-water chemistry with geological time. The Late Jurassic was a time of calcite seas and high carbonate saturations that perhaps expanded the possible types of sponges and perhaps as importantly the associated carbonate-precipitating microbial communities that could be part of such reef mound buildups. An interesting exploration consideration is that such buildups could form geophysically- interesting relief and even have low amplitude 'soft or bright spots' but these would not likely be the hoped for reservoir porosity.**

## Acknowledgements

This work is being carried out at Dalhousie University as a PhD project under the supervision of Prof. Grant Wach and includes data originally worked on while consulting for EnCana (formerly PanCanadian) on Deep Panuke and as a Shell Canada geologist much earlier. I thank both companies and Royal Dutch-Shell and management for permission to use, publish and continue working with the data. I particularly thank EnCana's geologists Rick Wierzbicki and Nancy Harland and more recently Norm Corbett who have generously shared some of their insights. ElPaso Canada (no longer extant, Sandra Bleu technologist) assisted with figure-size well logs used in some of the well studies after I helped them with the Marquis drilling and analysis. Some others I thank for sharing ideas, data, thin sections, and/or

various other help include: Eric Bogoslowski (PetroCanada), David E. Brown (CNSOPB), Tony Cortis (Shell Canada), Jeff Dravis (consultant), Alison Essery (ex-Shell Canada), John Harper (Conoco-Phillips), John Hogg (ex-EnCana), Lubomir Jansa (GSC), Darcy Schau (Shell Canada), Mary-Jean Verrall (CNSOPB), Clint Tippett (Shell Canada), John Weissenberger (ex-PanCanadian) , Nancy White (CNSOPB), and Hans Wielens (GSC).

## References

Azeredo, A.C., V.P. Wright and M.M. Ramalho, 2002, The Middle-Late Jurassic forced regression and disconformity in central Portugal: eustatic, tectonic and climatic effects on a carbonate ramp system; Sedimentology v.49, p.1339-1370.

Conway, K.W., J.V. Barrie and M. Krautter, 2004, Modern siliceous sponge reefs in a turbid siliciclastic setting: Fraser River delta, British Columbia, Canada; Neue Jahrbuch Palaeontologie Mh, 2004, p.335-350.

Cummings, D.I., and R.W.C. Arnott, 2005, Growth-faulted shelf-margin deltas: a new (but old) play type, offshore Nova Scotia. Bulletin of Canadian Petroleum Geology: v.53, p.211-236.

Dromart, G., C.L.F. Gaillard and l. Jansa, 1994. Deep-marine microbial structures in the Upper Jurassic of Western Tethys. *in* J. Bertrand-Sarfati and C. Monty, eds., Phanerozoic Stromatolites II, p.295-318.

Erlich, R.N., Longo, Jr., A.P. and Hyare, S. 1993. Response of carbonate platform margins to drowning: evidence of environmental collapse. In, Loucks, R.G. and Sarg, J.F. (ed.), Carbonate Sequence Stratigraphy – Recent Developments and Applications, American Association of Petroleum Geologists, Memoir 57, p.241-286.

Eliuk, L.S., 1978. Abenaki Formation, Nova Scotia shelf, Canada - depositional and diagenetic model for a Mesozoic carbonate platform: Bulletin of Canadian Petroleum Geology, v.26, p.424-514.

Eliuk, L.S., 1981. Abenaki update: variations along a Mesozoic carbonate shelf, Nova Scotia Shelf, Canada: *in* F. Stoakes, ed., Canadian Society of Petroleum Geologists Annual Core and Field Sample Conference, p.15-19 (extended abstract).

Eliuk, L.S. 1985. Artimon Member: *in* G.L Williams, L.R Fyffe, R.J.Wardle, S.P.Colman-Sadd, R.C. Boehner and J.A.Watt, eds., Lexicon of Canadian Stratigraphy - Atlantic Region, v.6, p.11-12, Canadian Society of Petroleum Geologists.

Eliuk, L.S., 1998. Big bivalves, algae and the nutrient poisoning of reefs: a tabulation with examples from the Devonian and Jurassic of Canada: *in* P.A. Johnston and J.W. Haggart, ed., Bivalves: An eon of Evolution; University of Calgary Press, p.157-184.

Eliuk, L.S. 2004. History of the practical application of a failed? dolomite model (mixing zone) to the "Demascota Dolomite Beds" of the Abenaki Formation, Nova Scotia offshore Late Jurassic paleocontinental shelf carbonate margin – Case Study for Core Conference, CSPG Dolomite Conference January 13-15th (15 pages on CD).

Eliuk, L.S., S.C. Cearley, and R. Levesque, 1986. West Atlantic Mesozoic carbonates: Comparison of Baltimore Canyon and Offshore Nova Scotian Basins: AAPG Bulletin, v.70, p.586-587 (abstract).

Eliuk, L. and R. Levesque, 1988, Earliest Cretaceous sponge reef mound Nova Scotia shelf (Shell DemascotaG-32): *in* H.H.J.Geldsetzer, N.P. James and G.E.Tebbutt, eds., Reefs, Canada and Adjacent Areas. Canadian Society of Petroleum Geologists, Memoir 13, p.713-720.

Eliuk, L.S. and S.G Pemberton, 2002. Bioerosion in the Upper Jurassic Abenaki margin – preliminary survey: Appendix to Weirzbicki et al. (2002), p.95-101.

Eliuk, L.S. and B.E. Prather, 2005. Baltimore Canyon Trough Mesozoic Carbonate Margin Cores, Offshore USA Atlantic: Abstract and core conference article – CSPG-AAPG Convention June core conference in Calgary AB (31 pages on CD).

Eliuk, L. and G. Wach, 2008 (this conference CD), Carbonate and siliciclastic sequence stratigraphy - examples from the Late Jurassic Abenaki limestone and West Venture deltaic beds, offshore Nova Scotia, Canada

Ellis, P.M., 1984. Upper Jurassic carbonates from the Lusitanian Basin, Portugal and their subsurface counterparts in the Nova Scotian Shelf: Unpublished PhD. Thesis, Open University, England.

Ellis, P.M., P.D. Crevello and L.S. Eliuk, 1985. Upper Jurassic and Lower Cretaceous deep-water buildups, Abenaki Formation, Nova Scotian shelf: *in* P.D. Crevello, and P.M. Harris, eds., Deep-water Carbonates, SEPM Core Workshop No. 6, p. 212-248

Ellis, P. M., R. C. L. Wilson, and R. R. Leinfelder, 1990, Controls on Upper Jurassic carbonate buildup development in the Lusitanian Basin, Portugal: *in* M. E. Tucker, J. L. Wilson, , P. D. Crevello, J. R Sarg. and J. F. Read,, eds. Carbonate Platforms - Facies, Sequences and Evolution. International Association of Sedimentology Special Publication 9: p.169-202, Oxford.

Embry, A.F, and J.E. Klovan, 1971, A late Devonian reef tract on northeastern Banks Island, N.W.T.; Bulletin of Canadian Petroleum Geology, v.19, p.730-781.

EnCana Corporation, 2006, Deep Panuke Offshore Gas Development, Volume 2 – Development Plan. (Document No: DMEN-X00-RP-RE-00-0003 Rev. 01U), 313 p. (available on the CNSOPB website).

Given, M.M., 1977, Mesozoic and early Cenozoic geology of offshore Nova Scotia: Bulletin of Canadian Petroleum Geology, v.25, no.1, p.63-91.

Greenlee, S.M. and P.J. Lehmann, 1993, Stratigraphic framework of productive carbonate buildups: *in* R.G. Loucks and J.F. Sarg, eds., Carbonate Sequence Stratigraphy; AAPG Memoir 57, p.43-62.

Harvey, P.J. and D.M. MacDonald, 1990, Seismic modeling of porosity within the Jurassic aged carbonate bank, offshore Nova Scotia: Canadian Journal of Exploration Geophysicists, v.26, p.54-71.

Izotova, R.S., and I.V. Popadyuk, 1993, Oil and gas in Jurassic reefal complexes of the west Ukrainian Carpathian foredeep; AAPG Bulletin, v. 7, p.1663-1664 (abstract).

James, N.P. and P-A. Bourque, 1992, Reefs and mounds: *in*, R.G. Walker and N.P. James, eds. Facies Model: Response to sea level change, p.323-347.

Jansa, L.F., 1981, Mesozoic carbonate platforms and banks off the eastern North American margin: Marine Geology, v.44, p.97-117.

Jansa, L.F., 1991. Lithostratigraphy 9: Carbonate buildup morphology: *in*, East Coast Basin Atlas Series: Scotian Shelf, Geological Survey of Canada, Atlantic Geoscience Centre, p.69.

Jansa, L.F., 1993, Lower Cretaceous carbonate platforms of the northeastern North American margin: *in* J.A.T. Simo, R.W. Scott and J.P. Masse, eds., Cretaceous Carbonate Platforms: AAPG Memoir 56, p.111-126.

Jansa, L.F. and Lake, P.B. 1991a. Lithostratigraphy 8: Isopach maps – Roseway Unit and Abenaki Formation: *in*, East Coast Basin Atlas Series: Scotian Shelf, Geological Survey of Canada, Atlantic Geoscience Centre, p.65.

Jansa, L.F. and P.B. Lake, 1991b, Lithostratigraphy 9: lithofacies and depositional environment – Scatarie and Baccaro members: *in*, East Coast Basin Atlas Series: Scotian Shelf, Geological Survey of Canada, Atlantic Geoscience Centre, p.67.

Jansa, L.F., B.R. Pratt, and G. Dromart, 1988, Deep water thrombolite mounds from the Upper Jurassic of offshore Nova Scotia: *in* H.H.J. Geldsetzer, N.P. James and G.E. Tebbutt, eds., Reefs, Canada and Adjacent Areas. Canadian Society of Petroleum Geologists, Memoir 13, p.725-735.

Jansa, L.F., G. Termier et H. Termier, 1982, Les biohermes a algaes, spongiaires et coraux des series carbonatees de la flexure bordiere du "paleoshelf" au large du Canada oriental: Revue de Micropaleontologie, v.25, p.181-219.

Kiessling, W., 2002, Secular variations in th Phaerozoic reef ecosystem; *in* W. Kiessling, E. Flugel and J. Golonka, eds., Phanerozoic Reef Patterns: SEPM Special Publication No. 72, p.625-690.

Kidston, A.G., D.E. Brown, B.M. Smith, and B. Altheim, 2005, The Upper Jurassic Abenaki Formation offshore Nova Scotia: a seismic and geologic perspective: Canada-Nova Scotia Offshore Petroleum Board CD publication , 168p.

Leinfelder, R.R., 1994. Distribution of Jurassic reef types: a mirror of structural and environmental changes during breakup of Pangea: *in* A.F. Embry, B. Beauchamp, and D.F. Glass, ed., Pangea: Global Environments and Resources: Canadian Society of Petroleum Geologists Memoir 17, p. 677-700.

Leinfelder, R.R., 1997, Coral reefs and carbonate platforms within a siliciclastic setting: General aspects and examples from the Late Jurassic of Portugal: 8th International Coral Reef Symposium, Panama City, Proceedings, v.2, p.1727-1742.

Leinfelder, R.R., D.U. Schmid, M. Nose and W. Werner, 2002, Jurassic reef patterns – the expression of a changing globe: *in* W. Kiessling, E. Flugel and J. Golonka, eds., Phanerozoic Reef Patterns: SEPM Special Publication No.72, p.465-520.

Lukin, A., 1999, Oil and gas potential of the reef-carbonate reservoirs of Ukraine; AAPG Bulletin, v.83, p.1296-1300. (extended abstract, p.333-336 of AAPG Int. Conf and Exhibit.)

MacLean, B.C. and J.A. Wade, 1993, Seismic Markers and Stratigraphic Picks in the Scotian Basin Wells: East Coast Atlas Series, Geological Survey of Canada, 276p.

Mancini, E.A., J.C. Llinas, W.C. Parcell, M. Aurell, G. Badenas, R.R. Leinfelder and D.J. Benson, 2004, Upper Jurassic thrombolite reservoir play, northeastern Gulf of Mexico; AAPG Bulletin, v.88, p.1573-1602.

Mancini, E.A., W.C. Parcell, W.M. Ahr, V.O. Ramirez, J.C.Llinas and M. Cameron, 2008, Upper Jurassic updip stratigraphic trap and associated Smackover microbial and nearshore carbonate facies, eastern Gulf coastal plain: AAPG Bulletin, v.92, p.417-442.

McIver, N.L. 1972. Cenozoic and Mesozoic stratigraphy of the Nova Scotia Shelf: Canadian Journal Earth Sciences, v.9, p.54-70.

Meyer, F., 1989, Siliciclastic influenced development of the Mesozoic Wilmington Platform, Western Atlantic: *in* P.D. Crevello, J.L. Wilson, J.F. Sarg, and J.F. Read, eds., Controls on Carbonate Platforms: SEPM Special Publication No.40, p.213-232.

Montgomery, S.L., T.H. Walker, G.P. Wahlman, R.C. Tobin and D. Ziegler, 1999a. Upper Jurassic "reef" play, East Texas Basin: An updated overview: Part 1 – background and outboard trend; AAPG Bulletin, v.83, p.707-726.

Montgomery, S.L., R. Karlewicz and D. Ziegler, 1999b, Upper Jurassic reef play, East Texas Basin: An updated overview: Part 2 – inboard trend; AAPG Bulletin, v.83, p.869-888.

Mount, J.F., 1984, Mixing of siliciclastic and carbonate sediments in shallow shelf environments: Geology, v.12, p.432-435.

Mukhopadhyay, P.K. and J.A. Wade, 1990, Organic facies and maturation of sediments from three Scotia Shelf wells; Bulletin of Canadian Petroleum Geology, v.38, p.407-425.

Poag, C.W., 1991, Rise and demise of the Bahamas-Grand Banks gigaplatform, northern margin of the Jurassic proto-Atlantic seaway: Marine Geology, v.102, p.63-130.

Prather, B.E. 1991. Petroleum geology of the Upper Jurassic and Lower Cretaceous, Baltimore Canyon Trough, western North Atlantic Ocean: AAPG Bulletin, v.72, p.258-277.

Pratt, B.R., 1982. Stromatolitic framework of carbonate mud mounds: Journal of Sedimentary Petrology. v.52, p.1203– 1227.

Pratt, B.R., 1995. The origin, biota and evolution of deep-water mud-mounds: *in* C.L.V Monty, D.W.J. Bosence, P.H. Bridges and B.R. Pratt, eds., Carbonate Mud-Mounds, Their Origin and Evolution: International Association of Sedimentology Special Publication, v.23, p.49– 123.

Pratt, B.R. and Jansa, L.F. 1988. Late Jurassic shallow water reefs of offshore Nova Scotia: *in* H.H.J. Geldsetzer, N.P. James and G.E. Tebbutt, eds., Reefs, Canada and Adjacent Areas: Canadian Society of Petroleum Geologists, Memoir 13, p.741-747.

Schlager, W., 2005, Carbonate Sedimentology and Sequence Stratigraphy. SEPM Concepts in sedimentology and Paleontology #8, 200p.

Sun, S.Q. and V.P. Wright, 1998, Controls on reservoir quality of an Upper Jurassic reef mound in the Palmers Wood Field area, Weald Basin, southern England; AAPG Bulletin v.82, p.497-515.

Wade, J.A. 1991. Lithostratigraphy 4: MicMac and Abenaki Formations *in*, East Coast Basin Atlas Series: Scotian Shelf, Geological Survey of Canada, Atlantic Geoscience Centre, p.57.

Wade, J.A. and B.C. MacLean, 1990, The Geology of the southeastern margin of Canada: Chapter 5 *in* M.J. Keen and G.L. Williams, ed. Geology of the Continental Margin of Eastern Canada, Geological Survey of Canada, Geology of Canada No.2, p.167-238.

Weissenberger, J.A.W., R.A. Wierzbicki, and N.J. Harland, 2006, Carbonate sequence stratigraphy and petroleum geology of the Jurassic Deep Panuke Field, offshore Nova Scotia, Canada. *in* P.M. Harris and L.J. Weber, eds., Giant Hydrocarbon reservoirs of the World: From rocks to reservoir characterization and modeling: AAPG Memoir 88/SEPM Special Publication, p.395-431.

Wierzbicki, R., J.J. Dravis, I. Al-Aasm, and N. Harland, 2006. Burial dolomitization and dissolution of Upper Jurassic Abenaki platform carbonates, Deep Panuke reservoir, Nova Scotia, Canada. AAPG Bulletin, v.90, p.1843-1861.

Wierzbicki, R., Gillen, K., Ackermann, R., Harland, N., Eliuk, L. with a contribution by J. Dravis. 2005. Interpretation of a Fractured Dolomite Core: Margaree F-70, Deep Panuke, Nova Scotia, Canada. Abstract and core conference article – CSPG-AAPG Convention June core conference in Calgary AB (25 pages on CD).

Wierzbicki, R., Harland, N. and Eliuk, L. 2002. Deep Panuke and Demascota core from the Jurassic Abenaki Formation, Nova Scotia – Facies model, Deep Panuke, Abenaki Formation. Canadian Society of Petroleum Geologists 75th Diamond Jubilee Convention Core Conference Abstracts including extended abstracts, p.71-94. (plus Appendix see above; also on CD as PDF in color; note the same paper used in Halifax core conference as Wierzbicki and Harland 2003).

Williamson, M.A. and K. DesRoches, 1993, A maturation framework for Jurassic sediments in the Sable Subbasin, offshore Nova Scotia; Bulletin of Canadian Petroleum Geology, v.41 p.244-257.

Wilson, J.L. 1975. Carbonate Facies in Geologic History: Springer, New York, 471p.

**BACK**

# Carbonate and Siliciclastic Sequence Stratigraphy- Examples from the Late Jurassic Abenaki Limestone and West Venture Deltaic Beds, Offshore Nova Scotia, Canada

**Leslie Eliuk**
**Grant D. Wach**
Dept. of Earth Sciences
Dalhousie University
Halifax, Nova Scotia B3H 4J1
Canada
e-mail: geotours@eastlink.ca

## ABSTRACT

Relative to their occurrence in thick siliciclastic sections, thin carbonates show utility as sensitive indicators of the surrounding sand and shale sedimentation. When composed of *in situ* framebuilders (microbial and skeletal) as demonstrated by inter-growth position, bioerosion, associated submarine cements and marine geopetals, the carbonates are particularly helpful for environmental inferences. Within the Sable Island paleodelta, cores in Penobscot L-30 and West Venture C-62 show both dark colors and limited biotic diversity with microbial textures. The C-62 cores are particularly interesting because they provide an independent check on the shelf-margin delta model and sequence stratigraphic scenario presented by Cummings and Arnott for the Venture gas field. In less than 7 metres, facies and fauna in limestone change upward from a biotically depauperate marl to a microbial mud mound which is succeeded by an argillaceous sponge-microsolenid coral reef mound with some stromatoporoids and possible red algae. The sequence is interpreted to reflect a forced regression and falling sea level. This closely supports the published deltaic sequence stratigraphy as long as it is appreciated that the "condensed limestone facies" is actually a distal composite, recording changes in sea level, nutrient supply, and ultimately sediment type that replaces the carbonate as the delta progrades. The maximum flooding surface (MFS) occurs during the microbial mound stage, below an abrupt lithologic change across a pyritized hardground which is overlain by laminated black shale. This placement of the MFS reflects problematic differences in sequence stratigraphic concepts of carbonates versus siliciclastics. Relative to understanding the Abenaki platform, the C-62 core provides insights into relationships seen only in cuttings and sidewall cores in Queensland M-88 which drilled the slope and basin facies immediately in front of the Deep Panuke (Abenaki reservoir) gas field. M-88 and C-62 may be potential links for correlating and dating the massive (Abenaki) carbonates and the deltaic siliciclastics.

## Introduction

The Upper Jurassic continental shelf off Nova Scotia has contemporaneous siliciclastic-dominated and carbonate-dominated sedimentation (Fig. 1). The former shows a progradational ramp style that continues on into the middle Cretaceous in the Sable Island area whereas the latter is mainly aggradational southwest of the Sable Island with various types of platform margin reefs developed (Eliuk 1978). Shelf margin deltas have been interpreted for several of the Sable Sub-basin gas fields (Cummings and Arnott 2005). Thus the paleo-shelf edge is of economic interest for both sandstone and carbonate reservoirs with the discovery and development of Deep Panuke (Weissenberger *et al.* 2006, EnCana 2006). Limestone in the mixed-carbonate-siliciclastic settings has not been porous but may give insights into the associated sandstone reservoirs or potential reservoirs and their depositional setting and sequence history. Only two wells have cored limestone in these mixed lithologies; but provide a spectrum from

very thin limestone completely within the delta (West Venture C-62 #9 Limestone) to deep and shallow carbonate ramp settings just in front of the carbonate platform (both cored in Penobscot L-30) to interbedded prodeltaic-slope shales in front of and infilling topography on the thick carbonate platform slope with the mixed slope carbonates and shales drilled but only side-wall cored in Queensland M-88 immediately in front of the Deep Panuke platform margin discovery. This spectrum will be briefly sketched then used as analogues for a closer look at the #9 Limestone beneath the Venture shelf-margin deltaic gas fields.

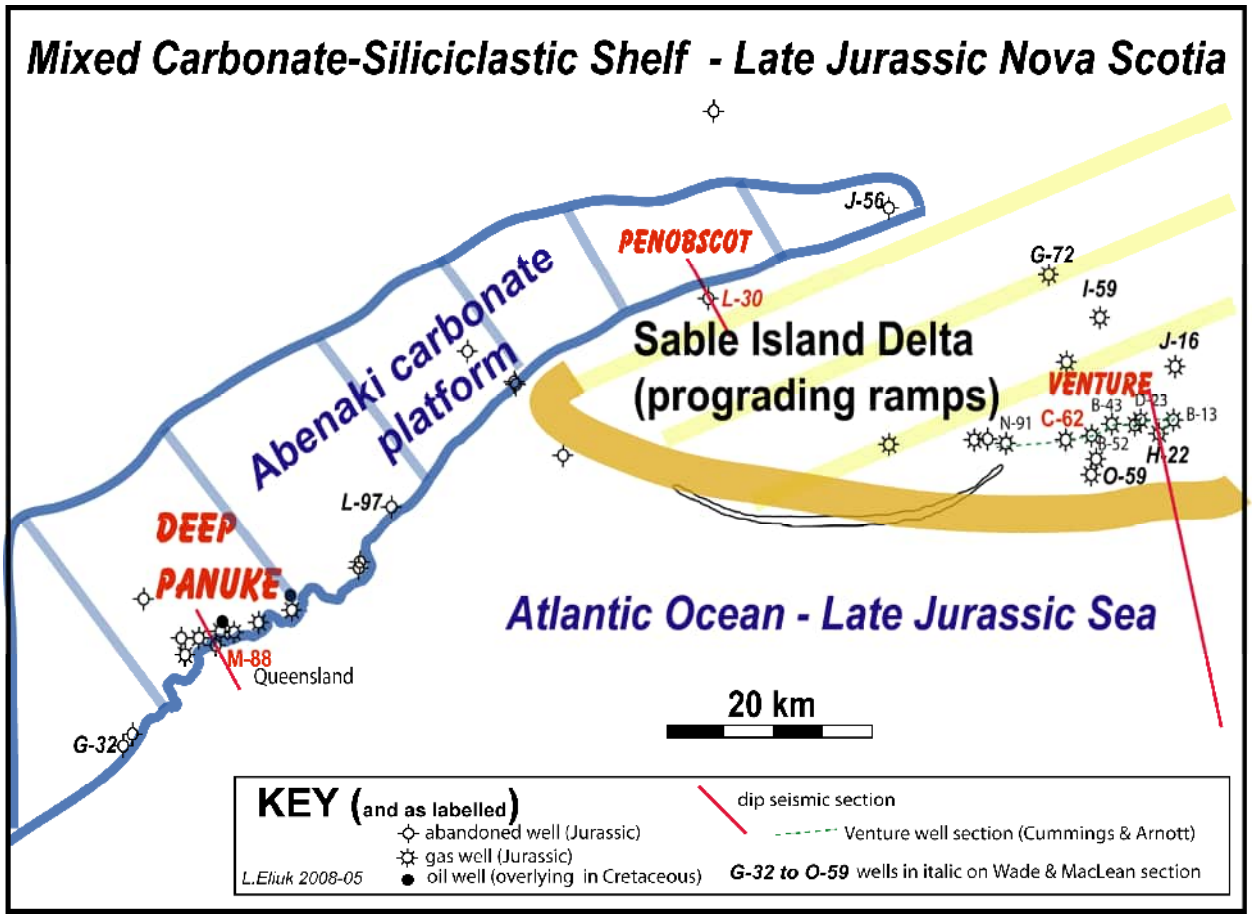


**Figure 1. Regional setting of Late Jurassic carbonate platform and Sable Island delta with intervening prograding ramp showing three key locations, wells and seismic lines approximately – Venture area with West Venture C-62, Penobscot L-30 and Deep Panuke with Queensland M-88 on adjacent reef slope.**

The West Venture C-62 core of the #9 Limestone of the lowermost Missisauga or topmost MicMac formations and cuttings in offsetting wells are used to re-evaluate the basal Facies 1 of Cummings and Arnott's (2005) depositional sequence stratigraphic and shelf-margin delta model for the Venture gas fields. In particular, the C-62 core (see Appendix for schematic core logs with photo details of contained depositional facies) with thin *in situ* microbial mound overlain by skeletal reef mound and the limestone facies of adjacent wells shows a much different story from Cummings and Arnott's Facies 1 "condensed lime mudstone". While that part of their model must change; those changes give paleoecological support for a key piece of evidence for their model that they listed as absent in Venture from their ideal list of criteria. Paleoecological changes from deeper to shallower reef support the relative sea-level fall (forced regression) they had proposed for Venture siliciclastic deposition. In addition the facies distribution of the #9 Limestone shows that the location of the overlying stacked incised channels

in C-62 were likely following a pre-existing bathymetric low on the shelf. Another consequence of this study will be to allow later comparison of the differences of contemporaneous limestones of the Sable Island prograding delta-constructed shelf, considered variously as Abenaki (Eliuk 1978, Jansa and Lake 1991) or MicMac (Wade and MacLean 1990) and the Abenaki Formation aggradation carbonate platform to the southwest.

Correlation between these two areas and even within the siliciclastic-dominated area is complicated by major growth faulting and significant facies differences (Wade and MacLean 1990). Correlation from shelf to basin and subdivision into stratigraphic sequences can be problematic since subaerial unconformities that aid subdivision on the shallow shelf are lacking in the basin and maximum flooding surfaces seen in deeper water may be difficult to discern on the shallow shelf. Poor core control and very thick sequences are a further difficulty; and the long-standing problems of provinciality and regional biostratigraphic zonations and stage terminologies at the Jurassic-Cretaceous boundary is yet another difficulty (Ogg 2004). In fact a depositional sequence stratigraphy compatible between both areas may still be impossible but useful insights are possible from a comparison of the #9 Limestone unit at the base of the Venture area wells and the slope-basinal Queensland M-88 well in front of the Deep Panuke gas field. Separate sequence stratigraphic frameworks have been proposed for Venture (Cummings and Arnott 2005) and for Deep Panuke (Weissenberger *et al.* 2006). Neither attempted a correlation between the areas but Weissenberger *et al.* (*ibid,* Fig. 17) illustrated mixed siliciclastic-carbonate cores from over 50km northeast of Sable Island in Citadel H-52 and Peskowesk A-99. They were used to show the nature of the alternation between the two major lithologies on a core scale where major hiati are inferred and used as an analog for similar relationships seen on the FMI log in Panuke M-79.

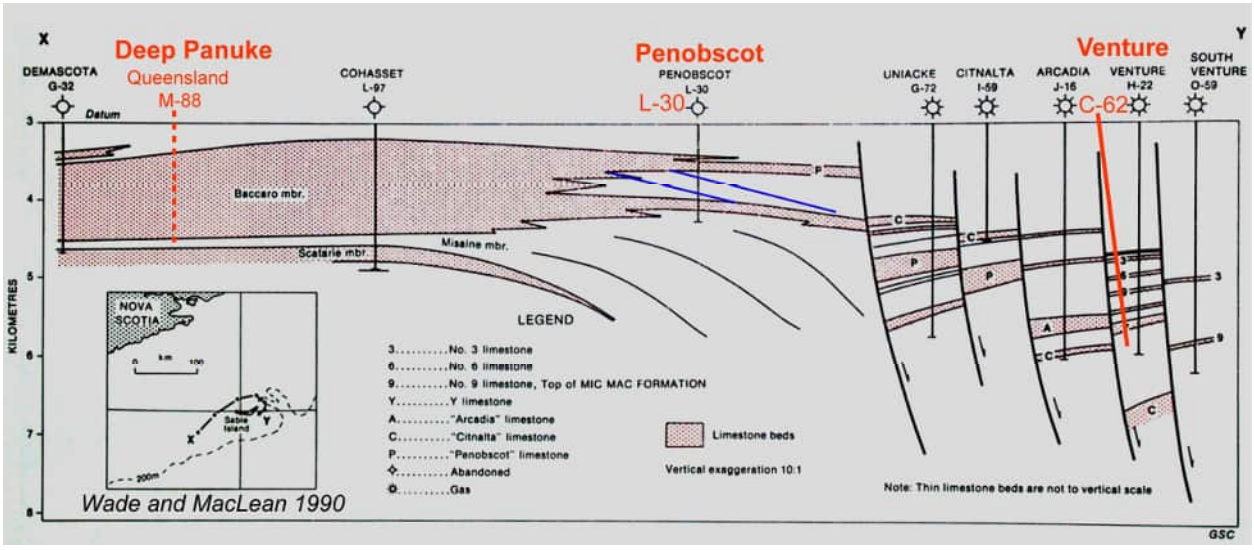


**Figure 2. Regional schematic Late Jurassic well section from the Deep Panuke area through Penobscot L-30 to the Venture area (Wade and MacLean 1990 slightly modified, used by permission). Note the southwest to northeast transition from a thick carbonate platform to a mixed carbonate-siliciclastic progradational ramp to the highly growth-faulted Sable Island paleo-delta area. There is faulting at Penobscot L-30 possibly due to underlying salt movement. Various limestone beds or members are designated by name and placed in the MicMac Formation (Wade and MacLean, 1990).**

## Venture, Penobscot and Deep Panuke (Queensland) Settings

To relate the carbonates to the siliciclastics and to assess the thin #9 limestone cored in West Venture C-62, it is compared against the section in Queensland M-88 near Deep Panuke and the section and cores in Penobscot L-30. The relationship of Upper Jurassic stratigraphy between the Abenaki

carbonate platform, Penobscot L-30 and the various growth fault blocks of the Sable Island area where Venture is located was nicely depicted by Wade and MacLean (1990 and shown here with slight modification as Figure 2). The M-88 Late Jurassic section on the slope in front of Deep Panuke margin becomes increasing siliciclastic-rich upward until only thin limestones separate the shales giving superficial similarity to the Venture area but on the continental slope not a shelf. The L-30 cores from thicker limestones in two seismically and depositional different settings act as facies end-members of limestones interbedded in thick siliciclastics. The comparison is for facies differences only with no exact age or correlation implied except all are Late Jurassic. Between L-30 and the Venture area, the upper "Penobscot" limestone is younger than the #9 limestone and due to growth faulting has about 1.6 km structural separation and perhaps over 2 km stratigraphic separation (Wade and MacLean 1990, see their figure reproduced slightly modified as Fig. 2).

Sedimentation in the over-pressured growth-faulted Sable Island area was indeed rapid. Penobscot L-30 appears to have been drilled just basinward of the Abenaki carbonate platform margin and is closer to the Venture area deltaic sediments than Deep Panuke. It may also show transitional features of the prograding ramp style-Venture deltaic shelf and Deep Panuke platform carbonate slope-basin setting drilled but not cored in Queensland M-88. The microbialite-rich core #2 in Penobscot L-30 and its setting have been previous documented (Dromart et al 1994, Eliuk 1978, 1981, Ellis 1984, Ellis *et al.* 1985, Ellis *et al.* 1990, Jansa, Pratt and Dromart 1988) and many of the microbial boundstone features placed in a broader comparative context (Pratt 1982, 1995). That microbialite represents an end-member in a range of microbialites that occur on the Abenaki slope in wells as far as 300 km southwest.

## DEEP PANUKE – Queensland M-88 Platform Carbonate Slope and Shale

Queensland M-88 drilled seismic geometries of major foresets to test a by-pass sandstone play basinward of Deep Panuke but very little sandstone was found (see Appendix and Fig. 3 schematic log and seismic). These geometries are well supported by the lithologies as being mostly distal carbonate slope deposits and mainly microbial in origin. M-88 has no core but rotary sidewall cores strongly support cuttings that the foreset limestones are mainly microbial-peloidal "mudstones" (mud- to packstone) to microbialite boundstones with early cements. Thin lithistid or coralline (chaetetid and stromatoporoid, very rare delicate branching corals) boundstone layers cap the microbialites before minor sandstone influx and more shale, sometimes initially dark, deposition. Skeletal framebuilders and bivalves are often highly bioeroded. Sequence boundaries (as defined by EnCana for Deep Panuke) are placed at these lithologic breaks above skeletal-rich beds (or based on the biota alone in massive carbonate). Higher in the section shale is dominant with sequences (and seismic reflectors) defined by very thin sponge-microbial limestones. The shallowest thin limestone has ooids (likely allochthonous) with sponges amongst sandy limestone.

This is evidence of shoaling and partial infilling of the reef-front basin by progradation of the prodelta shales. Since oolite only occurs below the lower half of Sequence VI in Deep Panuke wells on the platform, it also is evidence that correlation likely is mid Sequence VI where there are still ooids to be shed. The other occurrence of ooids is as oolite in the regionally developed "basal transgression" of Baccaro Member sedimentation. None of these surfaces are likely to be unconformities but they can be used for practical sequence subdivision as maximum regressive intervals and are quickly overlain by interpreted maximum flooding surfaces. Arguably if located on a shallow shelf they might have been considered condensed intervals during relative sea-level highstand flooding when siliciclastic supply was starved. Comparison with thin limestone cored in West Venture C-62 (which is likely up on the outer shelf in mid-deep neritic depths) gives interesting insights about the nature of these limestones and contacts that are only seen in cuttings.

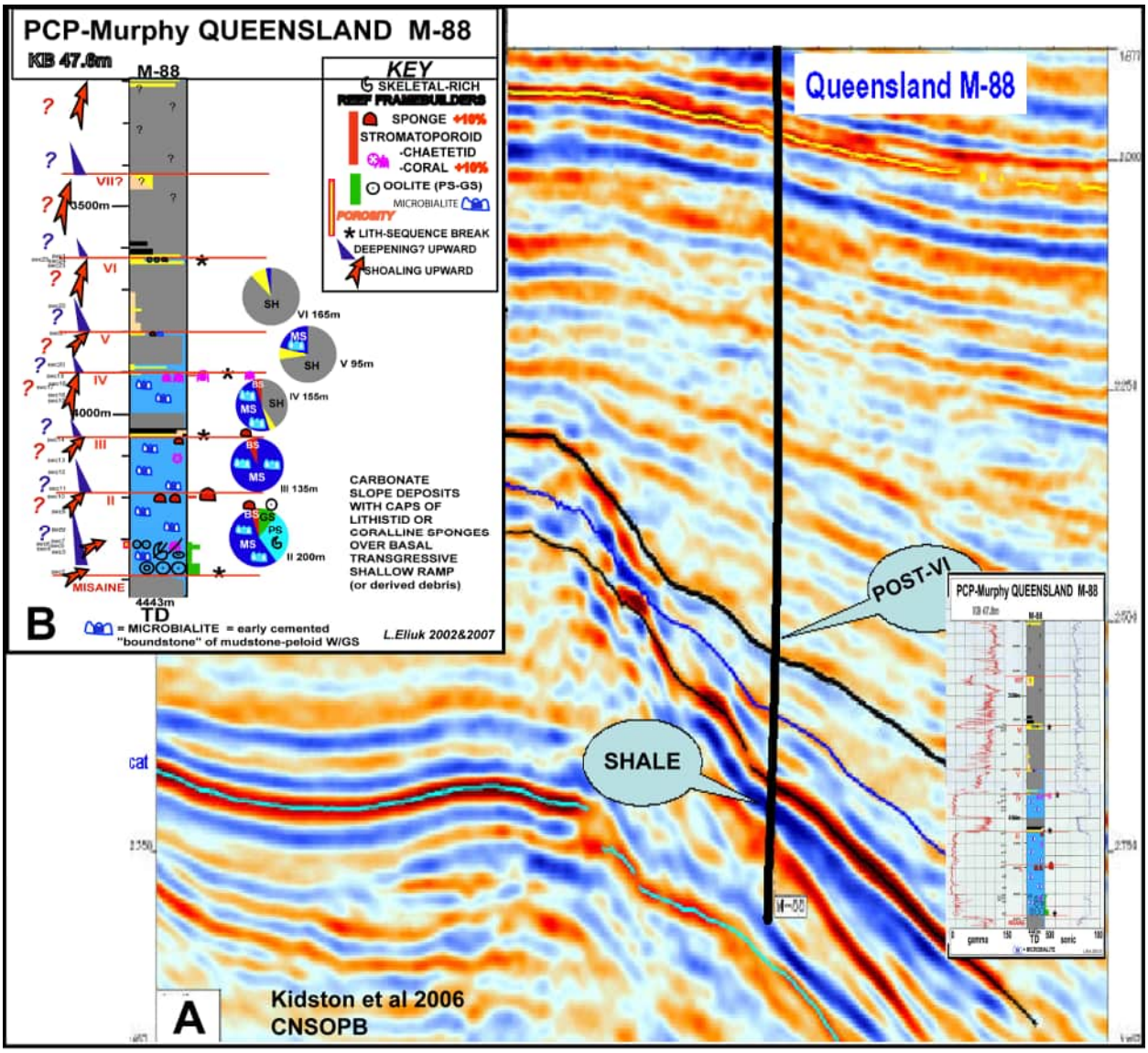


**Figure 3. Queensland M-88 of Deep Panuke area - A) dip seismic section (Kidston *et al.* 2005) with lithology-gamma-sonic log insert, and B) schematic lithologic column with pie charts of lithofacies. Depositional sequences approximate those of Weissenberger *et al.* (2006) and EnCana (2006), but differ slightly. M-88 is located immediately in front of the Deep Panuke gas field on the forereef slope and has a mixed carbonate siliciclastic composition with siliciclastic content increasing upward. As indicated by the question marks the transgressive-regressive (deepening-shoaling) cycles are highly interpretive.**

## PENOBSCOT – Prograded Carbonate Ramp and Slope

Penobscot L-30 tested a probable salt-cored structure. Figure 4 is a collage of seismic, a simplified interpretation and a schematic well log for L-30 (Eliuk 1981, Eliuk *et al.* 1986). Deeper Penobscot L-30 penetrated Upper Jurassic interbedded limestones and sandstones that are relatively flat-lying 'topset' in attitude that overlie inclined major 'foreset' reflectors consisting of limestone and thick shale. The topset limestones connect northwest to the nearby Abenaki platform and prograde over the basin-filling shales and limestones. Penobscot L-30 has both seismic and core control that independently provide criteria for slope sedimentation with foreset geometry having microbial (= thrombolitic) limestones and for shelf-shallow ramp with topset geometry having oolites, thin coral-chaetetid

boundstone biostromes and skeletal-rich muddy limestones that are in part oncolitic (see Appendix for schematic logs and photos of these facies). These lithologies can also be seen more widely in cuttings.

This high variability of shallow carbonate ramp depositional facies reflects the control that highly photic settings subject to great water energy variations has on the biota producing the sediments and where minor transgression-regression can move environments significantly. Even the lithologies of mixed-siliciclastics and carbonates can alternate rapidly in such a setting (see Weissenberger *et al.* 2006 figure of two cores well northeast of Venture and reproduced in Appendix). This characteristic variability is in marked contrast to the uniformity of sediment on the distal slope which is either dark calcareous shale to marl or mainly *in situ* microbial-peloid lime "mudstone" to boundstone similar to what was seen in M-88 slope but in L-30 even less variable with microbialites associated with encrusters like *Tubiphytes*, tubular foraminifer and worm tubes but only very few skeletal framebuilders. Compared to those of L-30, microbialites seen elsewhere in the Abenaki have more associated framebuilders and often show better developed submarine cement-lined cavity systems and lighter colors.

## VENTURE – Shelf Margin Delta and Basal Thin Limestone

In the Sable Sub-basin Cummings and Arnott (2005) included the Venture area with Glenelg and Alma as examples of growth-faulted shelf-margin delta gas fields. For Venture correlations, sedimentary facies units and sequence depositional model are summarized using their elegant diagrams as Figure 5 and Figure 6. Large-scale basinward-dipping seismic clinoforms also occur in front of the Venture area, and were part of Cummings and Arnott's (2005, see their Fig. 3a) major argument for a shelf margin delta setting for the lowermost Lower Missisauga Formation Venture gas field. Their section (Fig. 5) also shows subdivision and interpretation of the upward-coarsening units as prodelta mudstones up into storm-dominated delta front sandstones during relative sea-level rises. They pointed out that the sands thicken toward a growth fault between wells C-62 and B-52. In several wells the coarsening-up units are variously overlain by sharp-based channel units. They interpret a relative sea-level fall for the channel-form units as a strongly tide-influenced estuarine incised valley fill. These relationships and interpretation for a shelf-margin falling sea-level (forced regression) model are summarized in Figure 6 (reproduced from Cummings and Arnott's Fig. 6) and further discussed in the next section. Based on extensive core studies they tabulated 12 facies and one –"Facies 1 – light blue grey carbonate mudstone " interpreted as "offshore carbonate deposits (condensed sections)" occurs only in the Venture and West Venture fields will be discussed as the #9 Limestone in the next section.

## Limestones and the Growth-Faulted Shelf-Margin-Delta Model at Venture

### Cummings and Arnott's model criteria and #9 Limestone problems-potential

The Venture (V) and nearby fields were the geologically oldest of the three field areas that included Alma (A) and Glenelg (G) in Cummings and Arnott's (2005) suite of examples of Missisauga Formation growth-faulted shelf-margin deltas. They assembled seven (reduced to 5 in their abstract) criteria to identify ancient growth-faulted shelf-margin deltas (V, A, G indicates presence): 1) thick upward-coarsening successions (V, A); 2) large-scale clinoform reflections (V, A); 3) stratigraphic position over relatively mudstone-rich deposits (V, A, G); 4) soft sediment deformed intervals and gravity-flow deposits (A, G); 5) growth faults (V, A, G); 6) evidence of storm-wave deposition (V, A, G); 7) paleoecological evidence of rapid shallowing (A). Progradation across a continental shelf to the margin requires very high sediment supply relative to accommodation space. Thus it is aided considerably by relative sea-level fall that reduces accommodation space. In fact such a falling sea-level or forced regression may be the key ingredient and perhaps can only be proved with assurance by paleoecological evidence of rapid shallowing not caused by thick sediment infill. Such evidence was unavailable for the Venture delta. Cummings and Arnott's (2005) shelf-margin depositional model for Venture is best summarized by their diagram (reproduced as Fig. 6). Note the importance of falling sea-level for both progradation and later incision. Also note that for at least three (a, b and c) and possibly four (including

late e) phases of relative sea-level stand there is carbonate sedimentation on the outer shelf. The changes in water depth have a good probability of being reflected in changes in carbonate sedimentation even if perhaps slow or condensed due to environmental stress (turbidity and nutrient excess for instance) of being on a siliciclastic rich shelf.

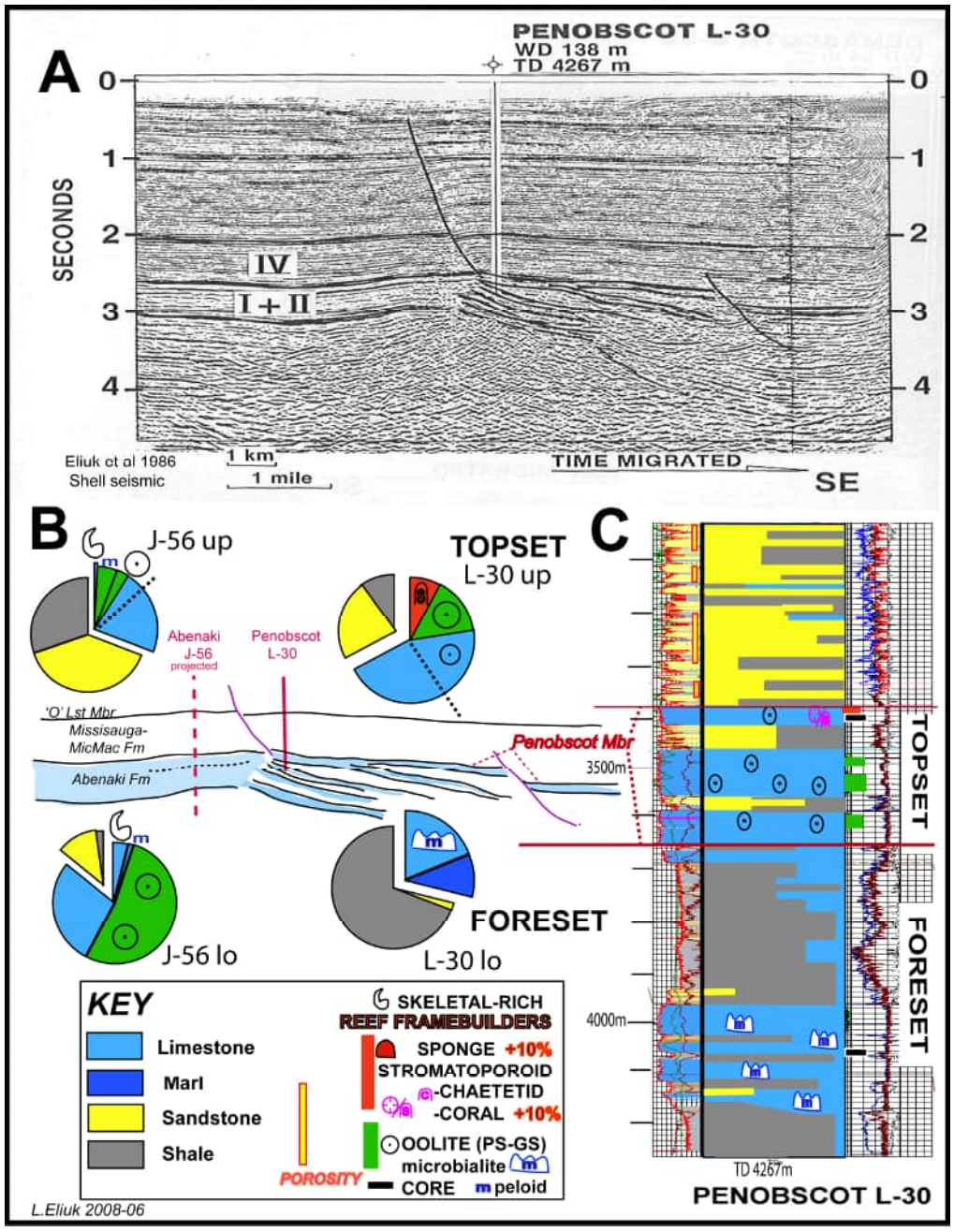


**Figure 4. Penobscot L-30 area - A) dip seismic line (from Eliuk et al (1986) similar but clearer than published seismic line in Ellis et al (1985); IV is - lower Mississauga-MicMac formations below O Limestone and I & II Late Jurassic Abenaki Formation); B) trace of seismic line above with Penobscot L-30 contrasting major lithofacies in topset ramp beds and foreset slope beds basinward of upper and lower Abenaki platform carbonates and siliciclastics in Abenaki J-56 projected south, and C) L-30 schematic lithology-gamma-porosity log showing major lithofacies. Penobscot Member (Wade and MacLean, 1990) dominantly limestone on a prograding ramp basinward of the northeast end of the Abenaki Formation carbonate platform that grades upward into siliciclastics. The deeper ramp and distal platform slope is dominantly shales derived from the Sable Island delta with deep-water limestone interbeds.**

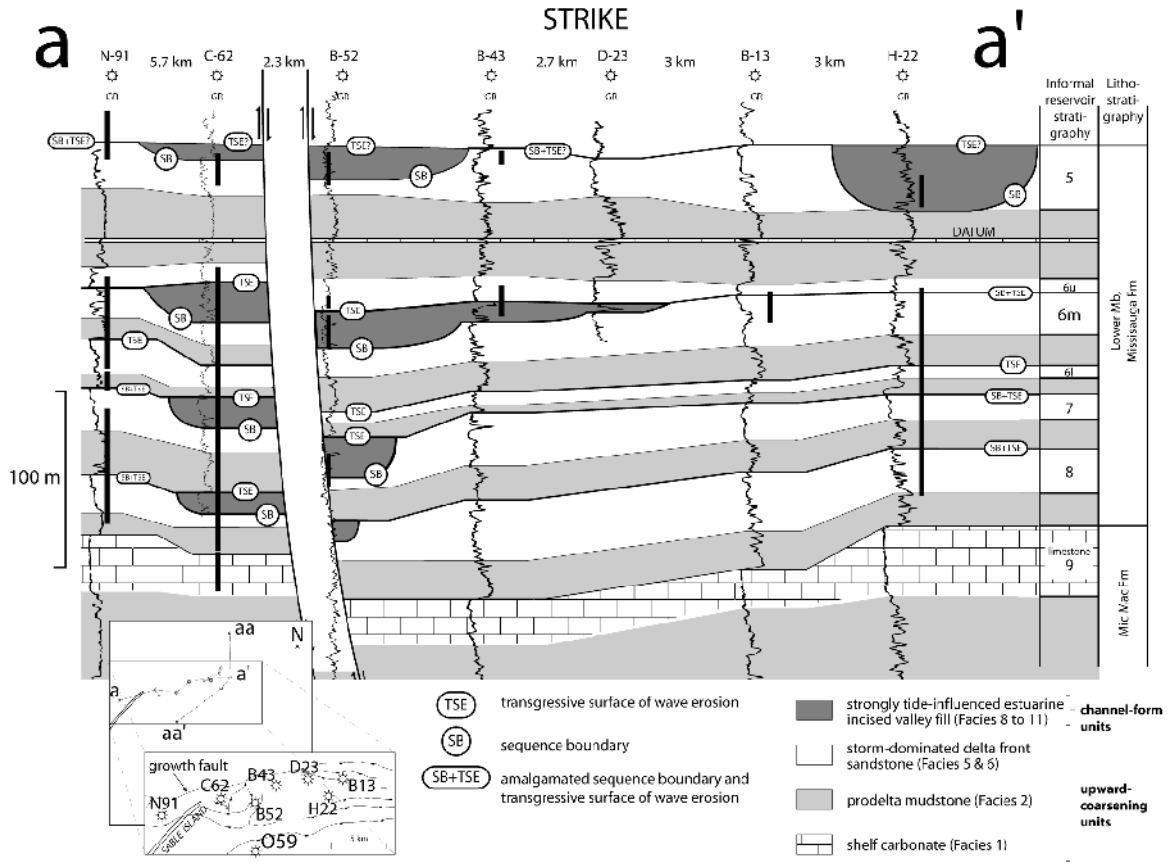


**Figure 5. Venture area – interpreted stratigraphic strike section through the Venture field #5 to #8 sandstones as indicated on included map showing the major facies association groupings and note the stacking of incised channels in the C-62 and B-52 wells (reprinted with permission from Cummings and Arnott 2005, Fig. 5). Insert map from CNSOPB and black bars indicate cored intervals.**

Carbonates can be sensitive indicators of depositional paleo-environment and likely paleo-depths. The #9 limestone may give that missing paleoecological evidence in Venture for at least the initial sequence. We cannot agree with Cummings and Arnott's (2005, p.217) Facies #1 description, as only "carbonate mudstone deposits lacking frame-building organisms, which pass gradationally upward to into prodeltaic mudstone" that were "marine condensed sections formed during maximum transgression". But we may be able to use the limestone to support their interpreted falling sea-level or forced regression and perhaps understand some of the other relationships they observe. A closer look at core in West Venture C-62 and cuttings in five other wells shows that there in fact are a variety of different carbonate facies in the relatively thin #9 limestone. These include microbial 'mud'-boundstone, sponge-microsolenid coral boundstone, sponge float-boundstone, oolite, and others. The 7 m of limestone in C-62 core show paleoecological changes supporting a fall in relative sea-level.

## #9 Limestone Lithologic Observations – cuttings and core

Lithology of the Venture Field area #9 Limestone was logged in five wells based on cuttings (N-91, B-43, B-13 and H-22) and core (C-62). Figure 7 briefly summarizes those lithologies as written vertical sections below their respective wells on Cummings and Arnott's (2005) cross-section. Clean limestone varied from about 5 to 35m thick and the biota and Dunham (Embry and Klovan 1971) texture differed in each well with no single limestone lithology prevalent but all were dark to medium grey.

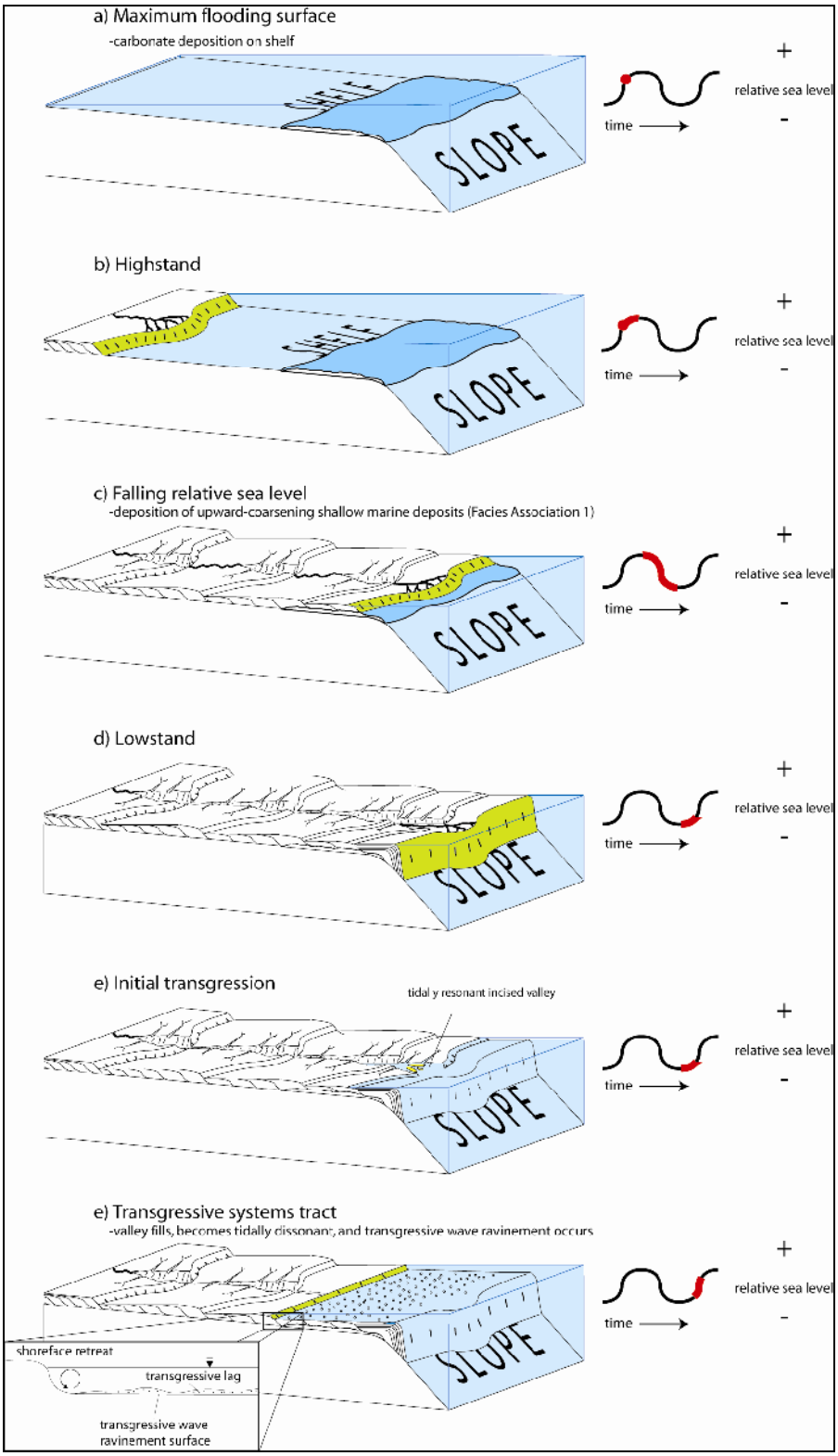


**Figure 6. Sequence stratigraphic depositional shelf-margin delta model Lower Member of Missisauga Formation for Venture, West Venture and South Venture fields near east end of Sable Island (reprinted with permission from Cummings and Arnott 2005, Fig. 6). Note that shelf carbonate (Facies 1) potentially developed during 4 of 6 relative sea-level stand periods.**

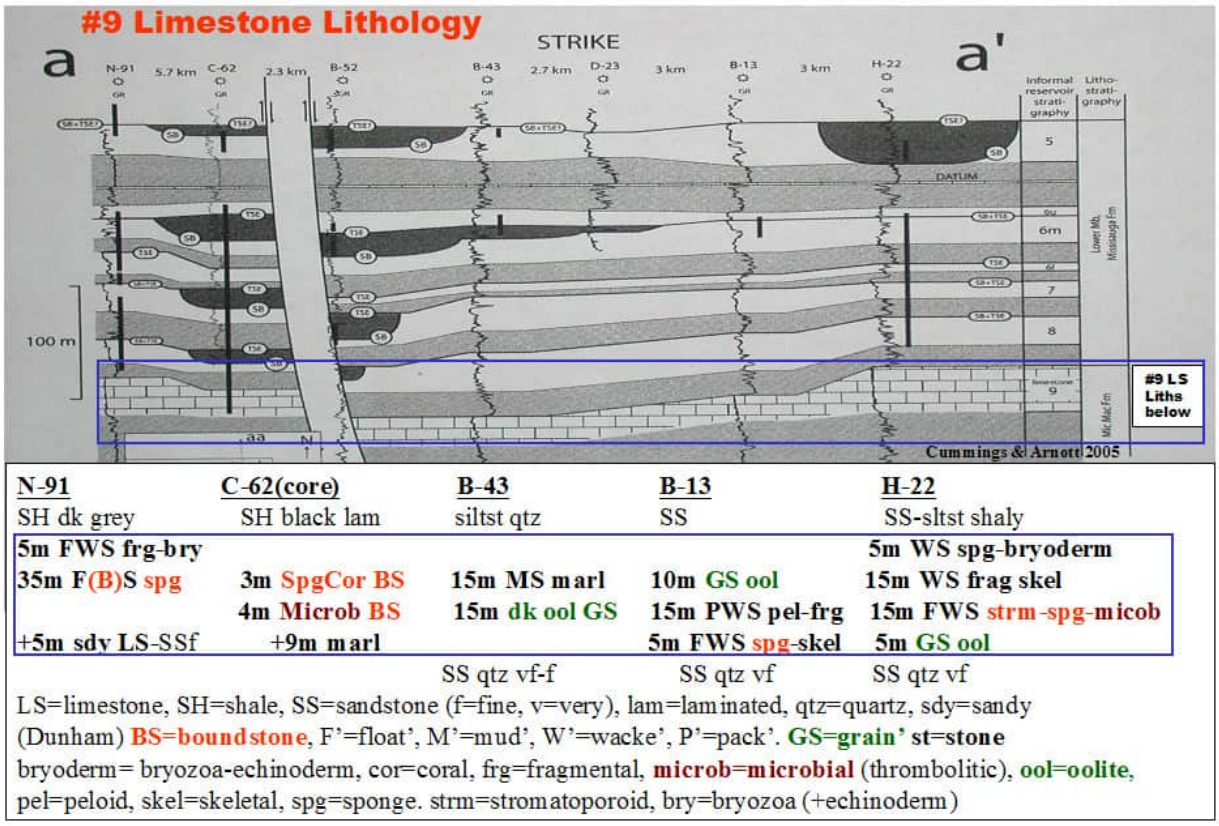


**Figure 7. Venture area #9 Limestone lithologies – based on 5m cuttings samples for all but C-62 well. Colors indicate either red for reefal (10% or greater framebuilders - lithistid/siliceous sponges, stromatoporoids, corals mainly microsolenid) or green for oolite grain/packstones. In Venture B-52 most of the #9 Limestone is faulted out except for 10 m of marl- argillaceous mudstone with minor black ooids.**

The limestones varied from a microbial bindstone (core only) and sponge-coral-stromatoporoid float-boundstone to lithistid sponge only to peloid wacke/packstone to argillaceous lime mudstone (marl) to oolitic grainstone with skeletal-fragmental mud/wackestone perhaps most common. In facies other than oolitic, *Tubiphytes* was always present and for cuttings only the lower sponge-stromatoporoid-rich interval in H-22 had significant (10-15%) microbial textures. In Venture B-52 as shown in Cummings and Arnott (2005, Fig 5) about 100 m of lower Missisauga is faulted out above and possibly including some of the #9 Limestone. The limestone seen in about 10m of cuttings was mainly a slightly argillaceous lime mudstone or "micro-packstone" with a near absence of fossils (trace of *Tubiphytes* and ?bryozoa with pyritized thin shells and round peloids in a large chert chip) similar to the marl interval below the microbialite in core 13 of West Venture C-62 but minor amounts of small black ooids did occur but were most probably allochthonous. Figure 8 shows the C-62 schematic core log opposite portions of Cummings and Arnott's (2005) Venture depositional model. Figure 9 shows sketch facies maps for the lower and upper #9 Limestone for the logged wells.

The deepest core in West Venture C-62 (Fig. 8 and Appendix figures and photos of facies) has a succession of highly calcareous to limestone facies that include from the base upward – 1) an extremely bioturbated calcareous shale to marl lacking body fossils with ichnofauna possibly indicative of deep neritic–upper bathyal depths (*e.g. Zoophycos*), 2) a massive marl (lime mudstone to very fine micro-packstone) with minor amounts of delicate articulated bivalves, sponge spicules and crinoid columnals, 3) a couple decimeter skeletal packstone-floatstone of varied broken fossil fragments including small colonial corals, sponges, *Tubiphytes*, crinoids, bryozoans that in places become microbially encrusted, possibly a storm-derived debris bed from adjacent carbonates that acted as a hard substrate for attachment

of the next facies, 4) 4-5 m microbialite with stromatolitic and thrombolitic textures with encrusting and attaché *Tubiphyte*s, nubeculurid forams and serpulid-terebellid worm tubes as accessories (only a few small lithistid sponges seen; this depauperate biota and microbial fabric are very similar to the slope microbialite in Penobscot L-30 core 2) upward some of the geopetally-filled cavities are quite large and have pendant coelobites, 5) transitional change to 3-4 m of *in situ* mixed microbial-skeletal framebuilders including branching and tabular microsolenid corals, lithistid sponges and lesser amounts of recyrstallized, very fine textured, evenly laminated columnar fossils interpreted as a solenoporids (red algae) with bioerosion by bivalves and sponges very prevalent.

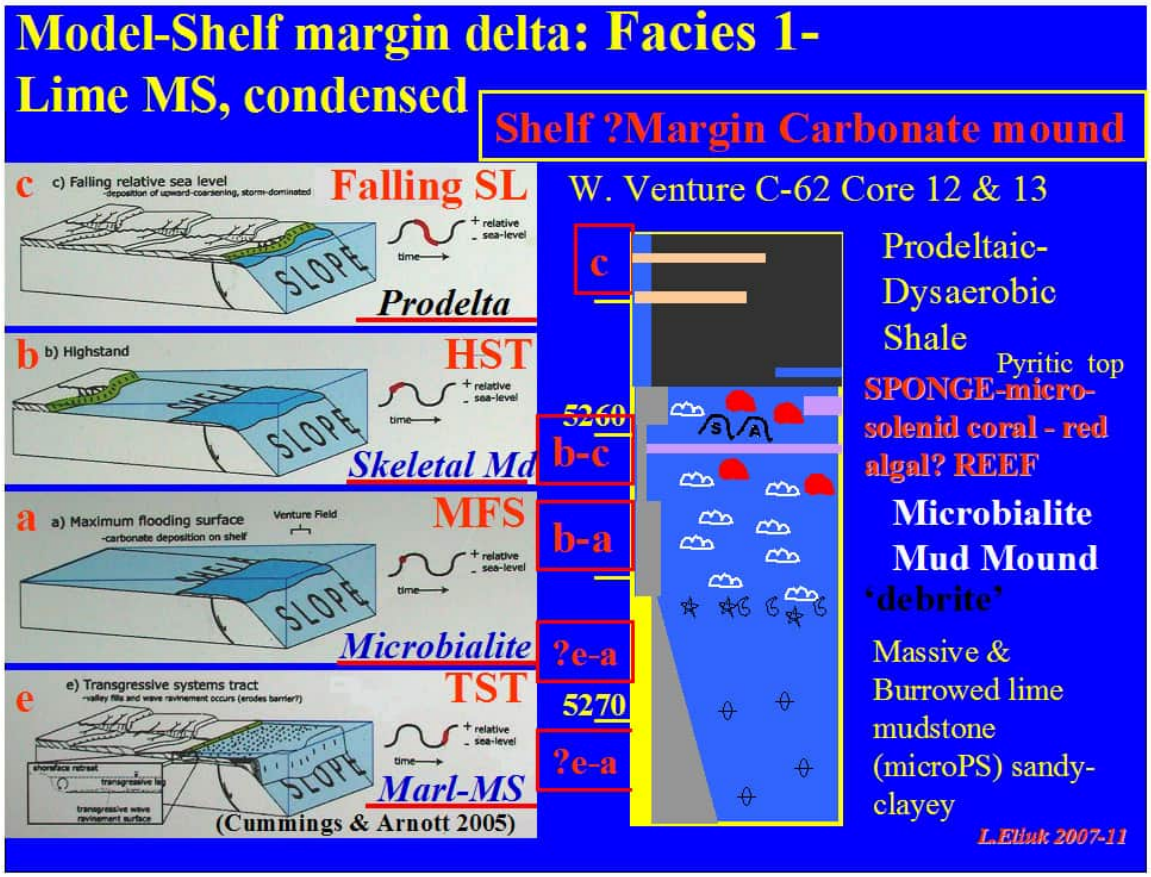


**Figure 8. West Venture C-62 #9 Limestone core depo-lithofacies compared to depositional model of Cummings and Arnott (2005) – note the interpreted transgressive or deepening trend in the relatively thin limestone facies from highly bioturbated deeper-shelf calcareous shale/marl up to massive marl (micro-packstones) then microbial boundstone ("mud mound") compatible with the model's transgressive (TST), maximum flooding (MFS) and highstand systems tracts then the reversal to a regressive or shoaling trend of microbial-microsolenid coral-lithistid sponge-red algal? (solenoporid?) reef mound abruptly overlain by laminated prodeltaic or lower shoreface shales/mudstones with a pyritized hardground contact that is the most abrupt lithologic change, but not the deepest deposition. Given the thinness of the limestone making depositional elevation into photic and less nutrient-rich depths unlikely, this reversal is best explained by falling relative sea-level that allowed skeletal framebuilder replacement of the pure microbialites in spite of the increasing clay content (see Appendix for core gamma log and additional facies illustrations).**

Complex intergrowth of the relatively small framebuilders and initiation on microbial hard surfaces is common. The *in situ* growth and rare still-articulated partial crinoid calycies indicate quiet

water conditions. Accessory fauna includes bryozoa, bivalves including some oyster-like, possible brachiopods, crinoids and similar microbialite micro-encrusters/accessories as in pure microbialite. This skeletal reef mound is abruptly overlain by laminated shale with an intervening pyritized capping interval that has some infiltration by shale and was likely a dysaerobic hiatal surface. That shale is the beginning of a shoaling shoreface section that is depicted on Figure 5 (Cummings and Arnott 2005) as a prodelta mudstone then delta front sandstones. Although not the emphasis here, the core does show diagenetic features of note - pyrite is common in most facies, recyrstallized zones that have been partly dolomitized and others that appear to be argillaceous pressure-solution concentrates with remnant 'refractory' calcite fossils not easily dissolved like *Tubiphytes*, crinoids, and bryozoa. In the bottom of the C-62 well no petrophysical logs are available but a core gamma was measured (shown with the schematic log in the Appendix Fig. A1) and the 'cleanest' or least radioactive interval equates to the pure microbialite with clay amount again increasing upward in the transition to the overlying microbial-skeletal boundstone.

### #9 Limestone Lithologic interpretations – Precursor Limestone Facies to Incised Channels

Core C-62 provides the most comprehensive detail of the facies relationships. If only this core was available, without the data from the cuttings from the other wells, the interpretation of the succession would simply be a vertical sequence of facies, reflecting changing carbonate paleoecology, responding to decreasing then increasing clay influx affecting turbidity, nutrient and oxidation levels in a relatively deep shelf setting (see Appendix Fig. A1, and also supporting Figs. A2-A7). As well, a probable change to increasing photic, conditions first follows the reduced clay sedimentation, but then surprisingly is interpreted to continue increasingly photic in spite of the reversal to an increasing clay influx that ultimately buries the carbonate reef mound in prodeltaic shale. Except for this last inference, either delta lobe switching or relative sea-level fall could apply. But if the argument that in spite of increasing clay influx there was increasing light then the hypothesis of relative sea-level fall (or tectonic uplift; but not thickening sedimentation 'lifting' the seabed into the photic zone given a thin section of less than 8 m) must apply. Just as there are more limestone facies than Cummings and Arnott's (2005) original "facies 1 - condensed lime mudstone" the scenario is more complex but fits and supports their depositional model of relative sea-level changes (Fig. 5 and Fig. 8 where the C-62 core is shown with their model and letters a-e). Implicit in their model is the potential existence of limestone on the outer shelf during 3 to 4 of their six sea-level stages.

With organisms' sensitivity to their environment, changes should be expected and do occur. The base of the cored interval starts during later transgression (TST- Fig. 8 (e)) on an open marine relatively deep siliciclastic shelf indicated by the high bioturbation with *Zoophycos* ichnofauna (Fig. A1). The near lack of macrofossils may indicate some limiting stress perhaps depth. Approaching maximum flooding (TST-Fig. 8 (e) to MFS- Fig. 8 (a), see also Fig. A2) clay supply is nearly absent but over-supply of nutrients continues with perhaps establishment of an upper slope-deep shelf oxygen minimum zone and dysoxic conditions resulting in loss of burrowers with carbonate sediment supplied from the overlying water column and fines winnowed off adjacent shoals and probably silt-sized bioerosion chips from the skeletal boring by clionid sponges. Then slow growth of only microbialite (MFS-Fig. 8 (a) to HST- Fig. 8 (b), also see Figs. A3-A5) is initiated on a microbialite stabilized debris bed derived from a shallower setting with a great variety of invertebrates including some small colonial coral clasts and lithistid sponges but lacking really shallow water indicators like ooids. In spite of increasing influx of clays, the pure microbialite is gradually joined by deep-water sponges-microsolenid corals indicating more oxic conditions.

The presence of a few other types of corals and especially the suspect solenoporid red algae indicate photic conditions prevail and are most easily understood in terms of significant relative sea-level fall (falling rsl- Fig.8 (c), or FSST- Falling Stage Systems Tract; see also Figs.A6, A7). This fall brings with it the forced regression and influx of prodeltaic sediments that kill off the microbial-skeletal reef mound in a dysoxic or even anoxic setting shown by the high amount of pyrite and the abrupt top surface

interpreted as a hardground with infiltered clays. Then the dead limestone is buried in laminated very dark prodeltaic shale showing continued dysoxia. And that clay mudstone shoals and coarsens up into storm-dominated delta-front sandstones that are incised by estuarine valley fill of the maximum lowstand tract and backfill in the next sequence. The C-62 single well core story becomes somewhat more complex when limestones in off-setting wells are included but can still be encompassed within the forced regression model.

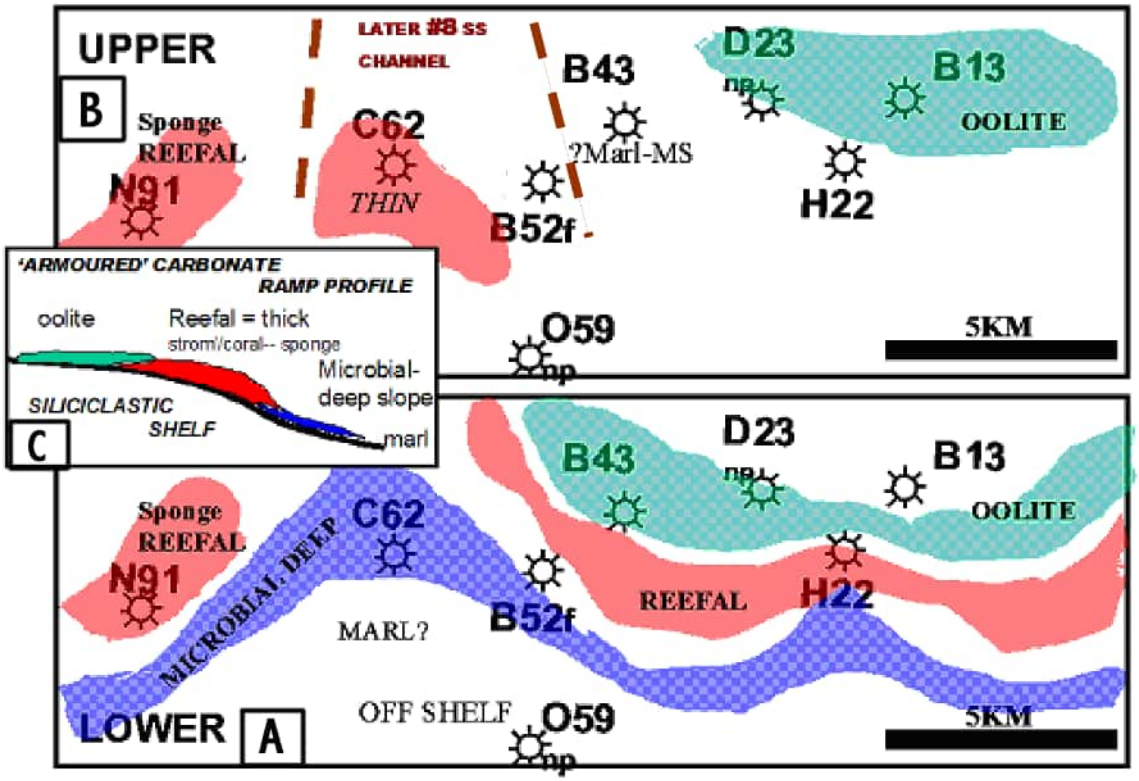


**Figure 9. Venture area #9 Limestone facies sketch maps based on sample lithologies (summarized on Fig. 7; f = faulted, np = not penetrated)) and subdivided into A) lower and B) upper with C) a simplified depositional facies depth-profile of shallow oolite to reefal (coral-stromatoporoid or deeper lithistid sponge) to microbialite to deep marl (excluding the oolite this could also be seen as a trend to greater clays-nutrients-dysoxia). These limestone changes are interpreted to mirror or thinly "armour" pre-existing siliciclastic bathymetry on the shelf or/and over the shelf-slope break. Note that the C-62 relatively thinner limestones with the microbialite 'mud mound' and overlying skeletal-microbial reef mound may all belong in the lower #9 Limestone. Lower #9 Limestone (map A) shows a deep or low on the shelf at the C-62 well where stacked incised channels occur for the #8 to #5 sandstones but to the northeast in a shelfward direction an oolitic shoal-sheltered peloid area (B-43 to B-13) with stromatoporoid-sponge-microbial reefal beds just basinward (H-22) indicating shallower depths or/and less clays-nutrients than the thicker lithistid sponge reefal beds in N-91. Upper #9 Limestone (map B) shows a northeastward shift in oolite deposition and at B-43 dark oolites replaced by marl-argillaceous lime mudstone that is interpreted to be due to the shoaling trend forcing clay input in the deeper areas (future incised channel areas of C-62 and B-52) carried by underflows (hyperpycnal transport of siliciclastics) that allow continued carbonate sedimentation on lateral bathymetric highs until further regression and widespread burial by regressive prodeltaic mudstones that overlie the #9 Limestone.**

Cuttings indicate the #9 limestone is neither solely condensed nor always in a deep-water shelf setting in the Venture area. Although generally thin, the thicker limestones near or beneath overlying incised channels in C-62 and possibly H-22 were deeper-water reefal with possible microbial admixtures while the wells shown between (B-13 and B-43) and located more shelfward (north) had more ooids,

cleaned upwards with B-13 having the shallowest oolitic-pelletal facies in a possible shoaling upward pattern. The B-43 limestone, however, had blackened small ooids that may be allochthonous and were capped by mudstone, indicating decreasing energy upward. Similarly the bit of #9 Limestone not faulted out in B-52 (not included on Fig. 8 and representative of the lower #9) is argillaceous lime mudstone (micro-packstone) with a minor amount of small black ooids, similar to the marl below the microbialite in C-62 core. There are at least a couple of alternatives for the pelletal pack/wackestones in B-13 – either slope microbial peloids or shallow shelf sediments (?lagoonal correlative to the B-43 oolite). Due to the lack of cements, *Tubiphytes* and bryozoa, and, the abrupt change to ooids without reefal beds, the latter (shelf) interpretation is preferred. The only other oolite was a basal 5m, possibly transgressive interval or allochthonous debris, in H-22. H-22 also had the thickest clean blocky outline on gamma logs with N-91 nearly as thick. Both have reefal intervals that were dominantly lithistid sponges in N-91 versus a mixture of lithistid and stromatoporoid (=coralline) sponges in H-22 that upward became fragmental-rich. A 5 m limestone cap in both these wells was *Tubiphytes*-bryoderm (bryozoa-echinodermal) rich possibly indicating a flooding and/or nutrient-siliciclastic influx. The lack of many stromatoporoids in West Venture N-91 may indicate a deeper or more nutrient/clay-rich setting as compared to Venture H-22.

A possible interpretation (refer to Figs. 7, 9) that links the later stacked incised channel locations in C-62 and B-52 and the underlying carbonate fabrics and original depositional settings and depths would place shallower more oolitic facies (B-13 and B-43) on relative paleohighs and more shelfward. These would not become the locus of channeling later. Whereas deeper settings (C-62 and B-52), that also may have been a relative sink for clay and nutrient-rich currents perhaps in part as hyperpycnal flows (and deeps for periodic oxygen minimum zone influx), would favour filter feeders like sponges and stromatoporoids and sessile predators like microsolenid corals, as long as the currents were also strong enough to inhibit sediment burial. It is also likely that the limestones in these two wells were buried by clay mudstone on either the interpreted paleohighs or their unchannelized upper slopes before the end of #9 Limestone deposition, When the lower versus upper #9 Limestone maps (Fig. 9) are compared there is an expansion of deeper water marly facies away from the channel area at C-62 and B-52 up onto the interpreted paleohigh reducing the oolite area. Overall the #9 Limestone is not a condensed limestone but rather a thin shelf carbonate starved of siliciclastics that mimics or "armours" the pre-existing siliciclastic shelf bathymetry. Thicker limestone, particularly since it tends to be reefal, may only indicate a position further down the local ramp slopes (see schematic profile on maps of Fig. 9). A corollary of this second interpretation would be that only relative sea-level fall and not local tectonic uplift would be the overall control; since a local tectonic/structural uplift to explain the inferred shoaling would not leave a low to be occupied by later channels. The mechanism or reason for the topographic lows on the shelf are not wholly understood and could range from underlying salt movement, to previous submarine erosion of the shelf, to carbonate buildup on the shelf forming areas of subtle positive relief.

## Analogues from Jurassic Reef Literature and Nova Scotia Offshore (but not the modern)

Because the Late Jurassic ocean chemistry differed significantly from the modern in having much higher carbonate saturation, finding modern analogues is difficult. As well microbialites (stromatolites and thrombolites and so on) except as supratidal mats are rare in the modern and at one time were also considered rare for most of the marine subtidal Phanerozoic in contrast to their abundance throughout the Precambrian. However more recently, that 'absence of microbialites' is becoming more apparent than real. In an overview article on microbial carbonates Riding (2000) summarized the two competing explanations for their Phanerozoic poor showing and now highly variable occurrence depending on the geologic age. The older hypothesis was "competitive exclusion" due to the rise of skeletal biota (eukaryotes as invertebrates and algae) in grazing or for habitat space so that stromatolites only survive in stressed refugia (e.g. desiccated tidal flats, dysaerobic settings, etc.). The newer "microbial calcification model", that does take into account their now recognized greater but variable Phanerozoic occurrence, proposes geological periods when ocean waters are highly carbonate saturated and allow microbial

biofilms and sheath mucilage to undergo calcification in the extracellular polymeric substances (EPS). With the second hypothesis comes the linkage of plentiful microbialites with greater amounts of ooids and early marine cements during certain geological periods (the Jurassic certainly was one of those). The conclusion is that likely both hypotheses are true, combined with evolutionary changes in the microbes themselves over time. So actualistic applications are limited by this geologic-time dependence on varying seawater. Modern analogues should not be expected for Jurassic occurrences except perhaps the rare example in unusual settings. Fortunately same age comparisons should be possible.

Greater emphasis is placed on "within-basin analogues" than on those from the very large world-wide Jurassic reef literature. But summary reviews of world-wide Jurassic reefs (Leinfelder *et al* 2002), European Late Jurassic reef paleoecology (Leinfelder et al 1996) and microsolenid biostromes (Insalaco 1996) do show the widespread nature of certain reef types and their inferred controls. Just for balance, a cautionary admission is that microbialite–rich reefal intervals are not always deep nor always non-reservoir (Mancini *et al.* 2004), is included. Two Nova Scotia shelf analogue areas, previously outlined above, of mixed carbonates-siliciclastics with cores, or with good side-wall cores and definitive seismic to contrast deeper water slope versus shallow-water platform or ramp settings, are at Deep Panuke as illustrated in Queensland M-88 and at Penobscot L-30. Only the cores in Penobscot L-30 will be briefly reviewed here since the schematic log and discussion of Queensland M-88 was outlined in the "Settings" section, and demonstrates with the seismic data that the microbial textures found on a deeper water distal slope. Penobscot core 1 in the topset ramp position illustrates similar facies to those seen in Venture area cuttings as oolitic and stromatoporoid-coral-and-sponge reefal. Core 2 on the foreset slope is an end-member in regards to microbialite development with almost no admixed skeletal fossils except tiny encrusters. It is very similar to the pure microbialite interval seen in West Venture C-62 core.

## Penobscot L-30 and other mixed-lithology ramp cores

Two mainly limestone cores were recovered from very different settings in Penobscot L-30 described and located previously (also see Fig. 4 and Appendix for schematic core log and photos). In the topset beds, core #1 shows at least three depositional facies in just 8 metres whereas foreset beds of core #2 have two lithologies, calcareous shale and limestone, but both are unvarying in the extreme (Fig. 5). Mixed siliciclastic-carbonate cores were described for Citadel H-52 and Peskowesk A-99 (Weissenberger *et al.* 2006) to support their use of erosional sequence breaks in Deep Panuke where such contacts were not cored. These give yet more core analogues to supplement the comparison base for the shallow to mid ramp environments in core. Again like the L-30 core #1 there is even a greater variation in lithologies and depositional environments over a relatively short vertical interval.

The L-30 core #1 (11231-11259 ft.; 3423.2-3421.7 m) is shown schematically in the Appendix (from Eliuk 1981) and was also described by Ellis (1984). Although stylolitic to horsetail solution seams obscure many intervals and can generate pseudo-packstones from former grainstones, at least three subfacies show the considerable local variation is sedimentation. The upper core is fossil-rich floatstone with matrix of slightly argillaceous peloid-skeletal-superficial ooid wacke-packstone. Large angular uncoated clasts of dark chaetetids (a coralline sponge) are common along with other framebuilders such as various genera of hexacorals, stromatoporoids, lithistid sponges (one particular type characteristically white), bryozoa and some banded milliporellids or solenoporids. Many are bioeroded, mainly by bivalves, particularly the chaetetids. Bivalves (some still articulated and some perhaps brachiopods), echinoid spines, crinoid columnals and small gastropods are common. At around 3423.2 and 3426 m (11231 and 11241 ft.) large belemnite rostra occur. Within this facies some thin decimetre layers of framebuilders are concentrated as rudstones and *in situ* boundstones. Below about 3426.9 m (11243 ft.) the lower core is mainly oolitic with grainstone in the upper intervals interpreted as a cleaning and coarsening upward ooid bar of 2 m or so and possibly composite since there is one abrupt lower contact surface at 3428 m (11247 ft.). Below the more concentrated ooids are burrowed peloid-ooid-oncolitic packstones to wackestones (and rare stylolitically-compacted ooid grainstone layers). Larger clasts tend to be microbially coated. Some of the burrows have finer gray recrystallization in the walls that may be in part dolomite. Some

superficially similar ovoid structures appear to be early dissolved mollusk shells that have been infilled by fine micrite. Elsewhere similar shell casts have been calcite cement lined and filled.

The L-30 core #2 has a lower uniform silty calcareous shale/marl with traces of sponge spicules and an upper limestone. The limestone is almost exclusively dominated by microbialite sediments with associated encrusting *Tubiphytes*, tubular foraminifera (*Nubeculinella* sp (chambered-ish) and *Nubicularia* sp. (more smooth walled branching) of family Nubeculariidae) and worm tubes (agglutinated thartharellids or terebellids and smooth walled serpulids). The microbialite limestone has thrombolitic and stromatolitic textures and was lithified very early on the sea floor and shows geopetal internal sediment and encrusters that even lived as coelobites on the cavity roofs. There are traces of small lithistid sponges as the sparse representation of skeletal framebuilders. More detailed analysis and line tracings of the microbial, micro-encruster, geopetal infill and early cement fabrics in this core are provided by Jansa *et al.* (1988). Pratt (1982, 1995) illustrated some portions of this core when reviewing Phanerozoic microbialites (stromatolites and thrombolites) summarized by age.

The contrast between these two cores reflects their different settings on a ramp margin. Core 1 in a shallow to mid ramp position is always in the photic zone, subject to little restriction or variation in open marine waters but to highly variable wave energy conditions. With small relative changes in sea level or shifts in sedimentation, environments can change radically. Core 2 in a deeper water slope position was either marine shale or, during lulls in that sedimentation, dark limestone formed by slow microbial precipitation or trapping of carbonate under likely aphotic, dysoxic and eutrophic conditions associated with near proximity to prodeltaic river-sourced sedimentation that excluded normal marine skeletal biota. The siliciclastic influx may have been dominantly hyperpycnal following the deeper topography and tending not to foul the carbonate shoals. Both the widespread presence of microbialites and high amount of ooids so close to a major delta indicate that here the Late Jurassic is unlike modern carbonate environments and reflects highly-carbonate-saturated sea waters (see Riding 2000 and Schlager 2005 and references therein or "Calcite Sea" by Mark Wilson on the Wikipedia website, for an introduction to changing ocean chemistry).

## Summary of Late Jurassic Microbialite and Reef Controls

Leinfelder *et al.* (1996) summarized the paleoecology and controls of Western European Late Jurassic reefs giving several models/charts comparing depth, sedimentation rate, oxygen level (=nutrient fluctuation) for reef types and reef organism paleoecology. Microbialites can have a wide range, but pure microbialites associated with limited and particular encruster communities (*Terebella-'Tubiphytes'*) are confined to deeper, dysaerobic and low sedimentation settings under terrigenous influence. Microsolenid corals also have a range of depths but tolerate deeper and more turbid water than most Mesozoic colonial corals (The microsolenids' characteristic septal pattern makes them identifiable even in cuttings thereby increasing their utility). Dromart (1992) reviewed Jurassic deep-water outer shelf-slope deposits of Tethys continental margins composed of microbialites and marls. He argued microbial biostromes represented condensed sections formed under low sedimentation rates and defined maximum flooding surfaces and thus would be useful in carbonate sequence stratigraphy.

In a more comprehensive review of Jurassic reef patterns, Leinfelder *et al.* (2002) concluded that pure microbialite development is a good indicator of eutrophication/oxygen depletion in low sedimentation regimes at least for depths (deeper?) where other limiting factors such as salinity can be ruled out. And they added that the type and nature of associated micro-encrusters refined paleobathymetric interpretations. The warning of other limiting factors or controls that might confuse what seems like a fairly consistent interpretation of the setting for pure microbialites was insightful. The northeastern Gulf of Mexico Upper Jurassic has thrombolite buildups that even act as reservoir located in a number of nearshore embayments on paleohighs. They differ in being shallow ramp occurrences and subject to shallow evaporite-associated dolomitization that result in important reservoirs. The early phases of restricted conditions that resulted in the dolomitization in the eastern areas (Alabama-Florida) may have excluded corals and other skeletal organisms present in buildups further west (or intense diagenesis

may be obscuring their former presence). Clearly these are not very appropriate as analogues with many dissimilarities but they do show microbialite buildups are not always non-reservoir facies as they have been to date in the Abenaki Formation.

## Conclusions

A thin limestone succession is used to give paleoecological support to falling sea level causing forced regression in a shelf-margin delta depositional sequence model of Cummings and Arnott (2005). Initially this support was based on the study of a single cored limestone that was then supplemented by limestone cuttings in nearby wells of the Venture area near Sable Island offshore Nova Scotia, Canada. If only the West Venture C-62 core is considered (Fig. 8) an uncomplicated argument can be made for a fall in relative sea level to explain change from deep-water marl and pure microbial boundstone to microbial-microsolenid coral-sponge boundstone in only a few metres of buildup. The limestone is indeed condensed but has many facies changes as relative sea level and clays-nutrient supply changes caused water clarity and photic changes; still deep but clear and light enough for skeletal framebuilders and possible deep-water red algae (solenoporids). This microbial-skeletal reef mound is shallower than the maximum flooding zone represented by microbialite boundstone and massive marl that has sponge spicules and delicate articulated bivalves (possibly nektonic).

The increase in clays and dysoxia-anoxia with the approach of the prograding delta eventually kills off the carbonate sediment producers and a dysaerobic pyritized submarine hardground is covered by laminated prodelta shale. Thus the changes on the outer shelf in the thin (about 15m) limestone-marl, that shows no evidence for subaerial exposure or even very shallow deposition, mirror and record the relative sea level changes that control the siliciclastic sedimentation and progradation over about 70m (lower Lower Missisauga Formation basal sequence of #8 Sandstone and #9 Limestone) occurring on the inner shelf nearer to shore and to the river mouth as depicted in Cummings and Arnott's (2005) shelf-margin delta depositional sequence model. When more of the #9 Limestone wells (Figs. 7, 9) are included in section and map view, C-62 and B-52 (perhaps H-22) are in relatively deeper facies. And these wells (at least C-62 and B-52) have many overlying channels and thus continued to be a bathymetrically deep or low. The oolite-bearing, more shelfward limestone in wells (B-13 and B-43), suggests an original paleohigh and not surprisingly overlying channels are absent. This could be evidence for early seafloor topography perhaps related to local tectonics that controlled the later positions of channels.

These conclusions follow from a general acceptance of Cummings and Arnott's (2005) depositional model and the assumption that the section from the highly burrowed marls below and up through the limestone and the clay mudstone prodeltaic beds, to the overlying coarsening up sandstones are all a single depositional sequence of a prograding delta during a forced regression. If an alternative channel and delta-lobe switching and/or an independent sub-sequence of carbonate-prone sedimentation is recorded here, then there would be no continuous sequence connection between the overlying siliciclastic sedimentation and the different events recorded in the C-62 core or mapped for the #9 Limestone. The top of the limestone might be the sequence break at a submarine hardground surface during a local switch from maximum regression (the microbial-skeletal reef mound) to transgression (the basal prodeltaic shales) complicated by changes in oxidation levels. The thin limestone would not be just a condensed maximum flooding zone. It might be a complete condensed sequence with the maximum transgression (MFS) in the marl-microbialite and the maximum regression in the top of the skeletal reef mound only 5-8 m higher.

## References


Cummings, D.I., and R.W.C. Arnott, 2005, Growth-faulted shelf-margin deltas: a new (but old) play type, offshore Nova Scotia. Bulletin of Canadian Petroleum Geology, v.53, p.211-236.

Dromart, G., 1992, Jurassic deep-water microbial biostromes as flooding markers in carbonate sequence stratigraphy. Palaeogeography Palaeoclimatology Palaeoecology, v.91, p.219-228.

Dromart, G., C. Gaillard and L.F. Jansa, 1994, Deep-marine microbial structures in the Upper Jurassic of Western Tethys. In: J. Bertrand-Sarfati and C. Monty (eds.), Phanerozoic Stromatolites II, p.295-318.

Eliuk, L.S. 1978. Abenaki Formation, Nova Scotia shelf, Canada - depositional and diagenetic model for a Mesozoic carbonate platform. Bulletin of Canadian Petroleum Geology, v. 26, p.424-514.

Eliuk, L.S. 1981, Abenaki update: variations along a Mesozoic carbonate shelf, Nova Scotia Shelf, Canada. In, Stoakes, F. (ed.) Canadian Society of Petroleum Geologists Annual Core and Field Sample Conference, p.15-19

Eliuk, L.S., S.C. Cearley and R. Levesque 1986, West Atlantic Mesozoic carbonates: comparison of Baltimore Canyon and Offshore Nova Scotian Basins. AAPG Bulletin, v.70, p.586-587 (abstract).

Ellis, P.M. 1984. Upper Jurassic carbonates from the Lusitanian Basin, Portugal and their subsurface counterparts in the Nova Scotian Shelf. Unpublished PhD. Thesis, Open University, England

Ellis, P.M., P.D. Crevello and L.S. Eliuk**,** 1985, Upper Jurassic and Lower Cretaceous deep-water buildups, Abenaki Formation, Nova Scotian shelf. In, P.D. Crevello and P.M. Harris (eds.), Deep-water Carbonates, Society of Economic Paleontologists and Mineralogists, Core Workshop No. 6, p.212-248.

Ellis, P. M., R. C. L Wilson and R. R. Leinfelder, 1990, Controls on Upper Jurassic carbonate buildup development in the Lusitanian Basin, Portugal. In, M. E. Tucker, J. L. Wilson, P. D. Crevello, J. R. Sarg and J. F. Read (eds.): Carbonate Platforms - Facies, Sequences and Evolution. International Association of Sedimentology Spec. Publ. 9, p.169-202; Oxford.

Embry, A.F, and J.E. Klovan, 1971, A late Devonian reef tract on northeastern Banks Island, N.W.T.; Bulletin of Canadian Petroleum Geology, v.19, p.730-781.

EnCana Corporation. 2006, Deep Panuke Offshore Gas Development, Volume 2 – Development Plan. (Document No. DMEN-X00-RP-RE-00-0003 Rev.01U), 313 p. (available on the CNSOPB website).

Flugel, E., 2004, Microfacies of Carbonate Rocks – Analysis, Interpretation and Application. Springer, 976p.

Gradstein, F.M., L.F. Jansa, S.P. Srivastava, M.A. Williamson, G. Bonham-Carter, and B. Stam, 1990, Chapter 8 – Aspects of North American paleo-oceanography. In, M.J. Keen and M.A. Williamson (eds.) Geology of the continental margin of eastern Canada, Geology of Canada No. 2, p.353-388.

Insalaco, E., 1996, Upper Jurassic microsolenid biostromes of northern and central Europe: facies and depositional environment. Palaeogeography, Palaeoclimatology, Palaeoecology, v.121, p.169-194.

Jansa, L.F. and P.B. Lake, 1991, Lithostratigraphy 9: lithofacies and depositional environment – Scatarie and Baccaro members In, East Coast Basin Atlas Series: Scotian Shelf, Geological Survey of Canada, Atlantic Geoscience Centre, p.67.

Jansa, L.F., B.R. Pratt and G. Dromart, 1988, Deep water thrombolite mounds from the Upper Jurassic of offshore Nova Scotia In, Geldsetzer, H.H.J., James, N.P. and Tebbutt, G.E. (eds.), Reefs - Canada and Adjacent Areas. Canadian Society of Petroleum Geologists, Memoir 13, p.725-735.

Kidston, A.G., D.E. Brown, B.M. Smith, and B. Altheim, 2005, The Upper Jurassic Abenaki Formation offshore Nova Scotia: a seismic and geologic perspective. Canada-Nova Scotia Offshore Petroleum Board CD publication , 168p.

Leinfelder, R.R., W. Werner, M. Nose, D.U. Schmid, M. Krautter, R. Laternser, M. Takacs and D. Hartmann, 1996, Paleoecology, growth, parameters and dynamics of coral, sponge and microbolite reefs from the Late Jurassic. In. J. Reitner, F. Neuweiler and F. Gunkel (eds.), Global and Regional controls on biogenic sedimentation I. Reef evolutions, Research Reports, Gottinger Arbeiten zur Geologie and Palaontologie., Sb. 2, p.227-248.

Leinfelder, R.R., D.U. Schmid, M. Nose and W. Werner, 2002, Jurassic reef patterns – the expression of a changing globe. In S. Keisling, E. Flugel and J. Golanka, Phanerozoic Reef Patterns, SEPM Spec. Publ. 72, p.465-520.

Mancini, E.A., J.C. Llinás, W.C. Parcell, M. Aurell, B. Bádenas, R.R. Leinfelder, and D.J. Benson, 2004, Upper Jurassic thrombolite reservoir play, northeastern Gulf of Mexico. AAPG Bulletin, v.88: p.1573-1602.

Ogg, J.G. 2004. The Jurassic Period. In: F.M. Gradstein, J.G. Ogg, and A. G. Smith (eds.) A Geologic Time Scale 2004. Cambridge, p.3007-343.

Pratt, B.R., 1982, Stromatolitic framework of carbonate mud mounds. Journal of Sedimentary Petrology. v.52, p.1203–1227.

Pratt, B.R., 1995, The origin, biota and evolution of deep-water mud-mounds. In: C.L.V. Monty, D.W.J. Bosence, P.H. Bridges, B.R. Pratt (Eds.), Carbonate Mud-Mounds, Their Origin and Evolution. International Association Sedimentology, Tulsa., Spec. Publ. v.23, p.49–123.

Riding, R., 2000, Microbial carbonates: the geological record of calcified bacterial-algal mats and biofilms. Sedimentology, v. 47, p.179-214.

Schlager, W., 2005, Carbonate Sedimentology and Sequence Stratigraphy. SEPM Concepts in Sedimentology and Paleontology #8, 200p.

Swanson, R.G. 1981, Sample Examination Manual, AAPG Methods in Exploration No. 1.

Wade, J.A. and B.C. McLean, 1990, The Geology of the southeastern margin of Canada - Chapter 5. In M.J. Keen and G.L. Williams (eds.); Geology of the Continental Margin of Eastern Canada, Geological Survey of Canada, Geology of Canada No.2, p.167-238.

Weissenberger, J.A.W., R.A. Wierzbicki, and N.J. Harland, 2006, Carbonate Sequence Stratigraphy and Petroleum Geology Of The Jurassic Deep Panuke Field, Offshore Nova Scotia, Canada. In, P.M. Harris and L.J. Weber (eds.), Giant Hydrocarbon reservoirs of the World: From rocks to reservoir characterization and modeling: AAPG Memoir 88 / SEPM Special Publication, p.395-431.

**BACK**

# APPENDIX

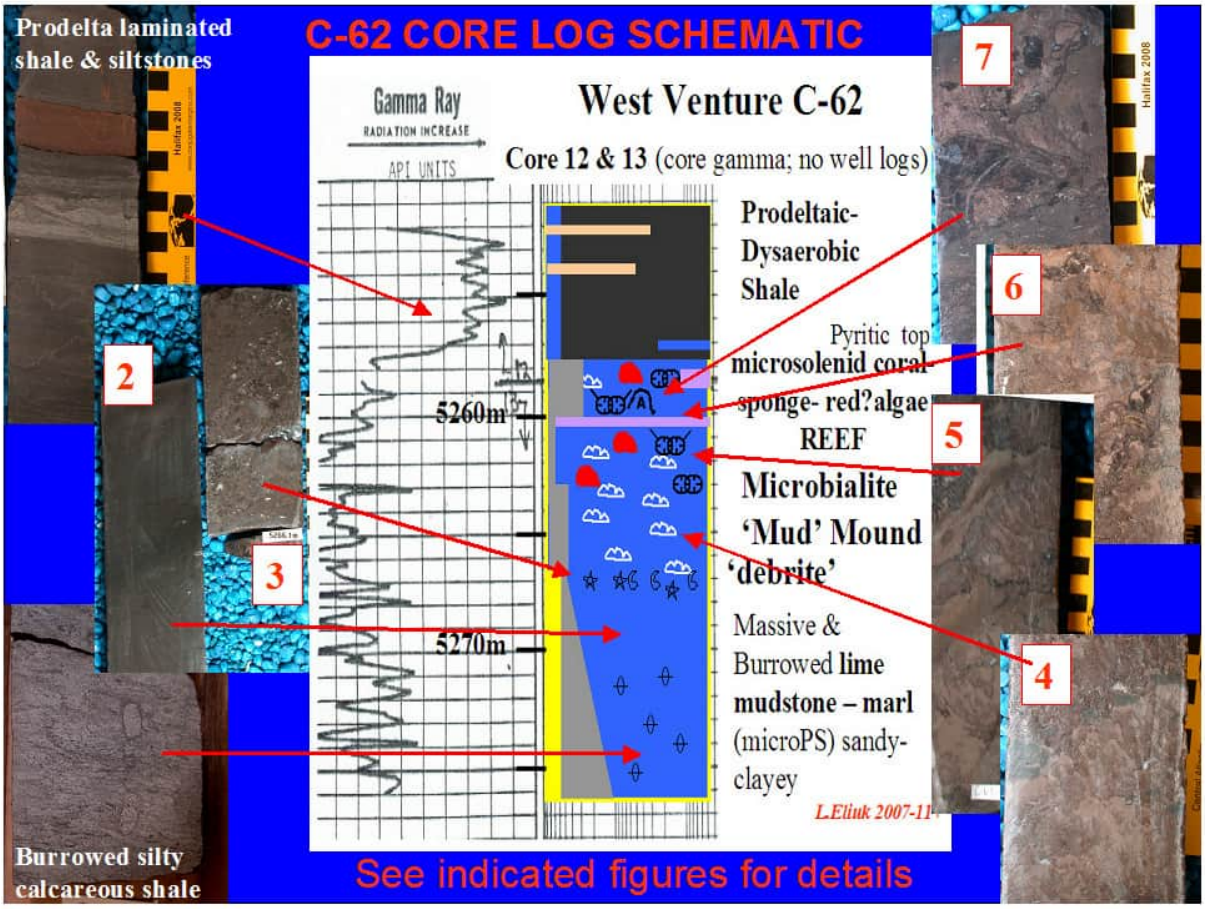


**Figure A1. West Venture C-62 #9 Limestone schematic core log summary – a number of facies features are illustrated in more detail in the following figures as indicated by the numbers (see key in Fig 4 for most symbols, purple lithology is fine crystalline dolomite, star is crinoid). No logs were run in the lower well but a core gamma indicates the relative radioactivity (indicative of argillaceous content or 'clean-dirty'). The main facies are very argillaceous limestone to calcareous shale or marl that can be subdivided into: 1) a highly bioturbated lower interval lacking in body fossils with a great number and variety of ichnofossils including *Zoophycos* indicating a deep shelf-upper slope environment that is overlain by 2) a massive marl to argillaceous micro-packstone then 3) a microbially stabilized debris bed that forms a substrate for colonization by a pure microbialite "mud mound" with a limited variety of micro-encrusters which grades upward with increasing *in situ* skeletal content to a 4) microbial-microsolenid coral-lithistid sponge-red ?algal (= ?solenoporid) reef mound that is abruptly overlain across a pyritized hard ground by 5) dark laminated prodeltaic shales or clay mudstones with some ironstone cemented layers and thin beds of siltstone to fine sandstone that upward become burrowed and more common. Except for the first and last facies these subdivisions are shown in more detail in the following six figures.**

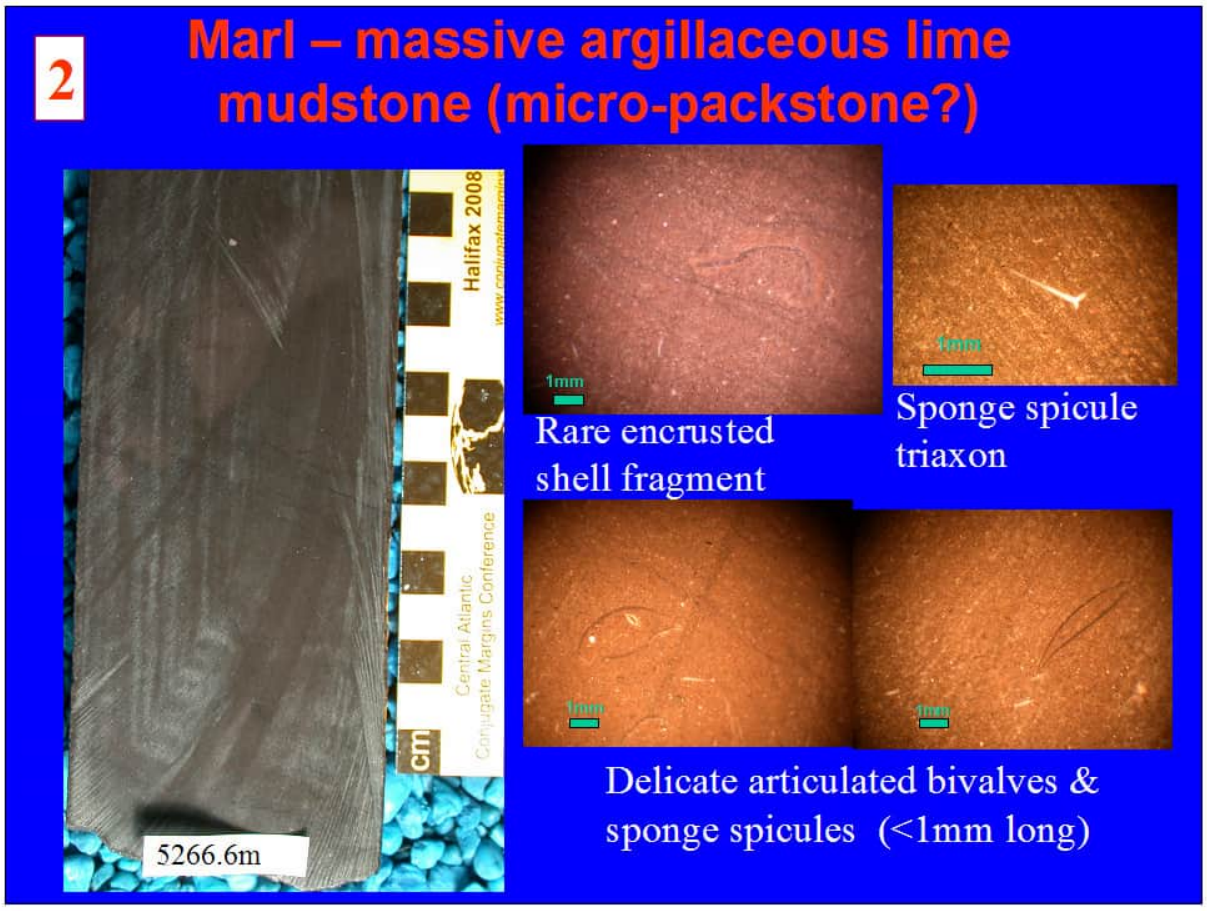


**Figure A2. West Venture C-62 #9 Limestone: marl –massive argillaceous lime mudstone to micro-packstone – this massive-appearing argillaceous limestone is composed of sublithographic to fine particles with only a few larger fossils hence the lime mudstone to micro-packstone designation. Some of the fine fragments appear angular and might be scallops from sponge bioerosion of shallower reefal beds and skeletons Those few fossils are small and include crinoid ossicles, sponge spicules and small bivalve shells. One disarticulated bivalve was microbially coated but the few others were not encrusted and still articulated showing a lack of energy or even bioturbation and possibly originated from a nektonic mode of life. Therefore the lack of lamination is not thought to be due to burrowing but represents the original texture perhaps due to a 'soupy' nature or rapid sedimentation. The carbonate sediment is interpreted to be winnowed from carbonate shoals diluting the low amount of clays coming during near maximum flooding.**

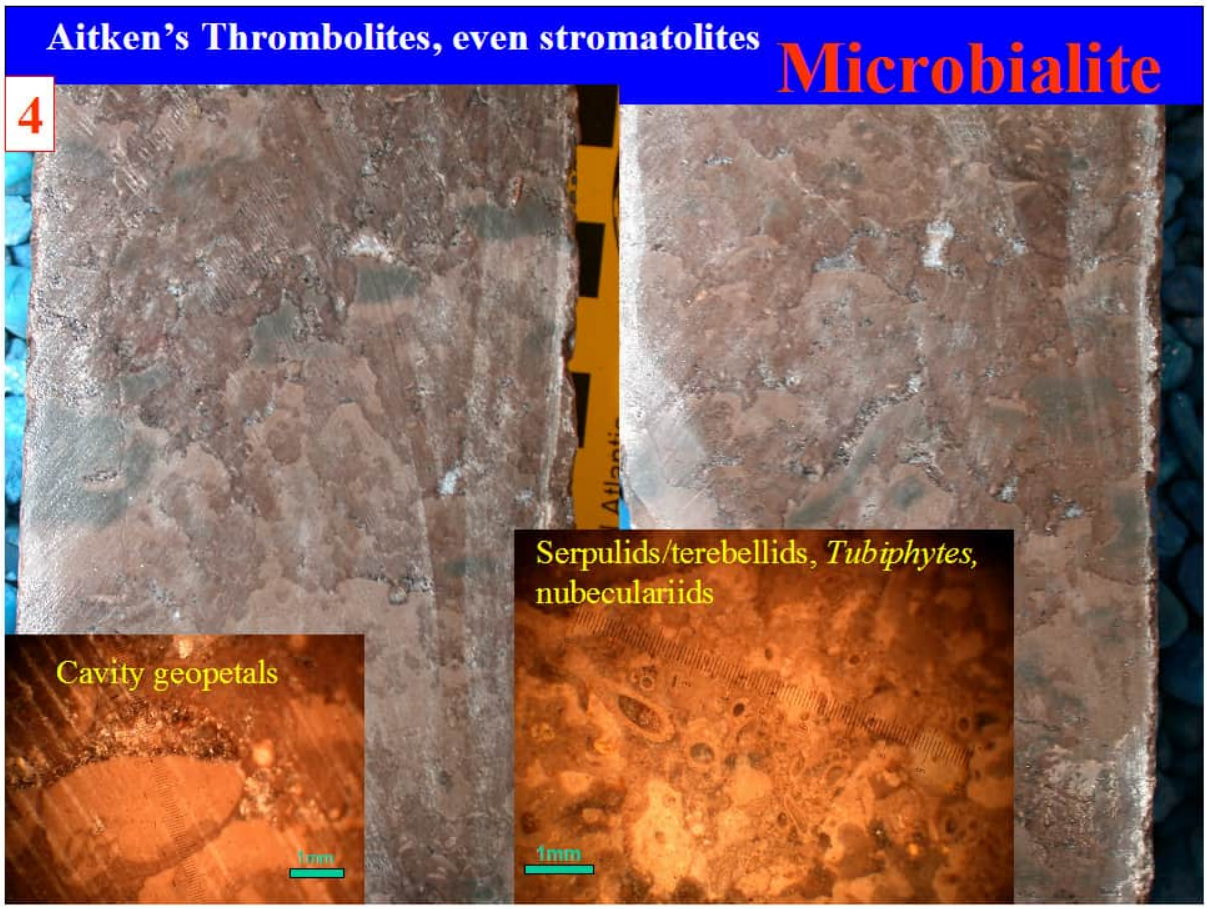


**Figure A3. West Venture C-62 #9 Limestone: skeletal packstone to floatstone debris bed (about 3 decimetres) with microbial stabilization – a great variety of small fossil fragments mostly deeper? heterozoans such as crinoids, bryozoa, *Tubiphytes*, bivalves, gastropods, brachiopods?, sponges, forams but also microsolenid corals and a possible colonial stylinid or oculinid coral. Locally there is microbial encrustation and therefore stabilization of the fossil fragments which are interpreted as storm or avalanche derived debris from shallower carbonates. The whole bed serves as a hard substrate that allows colonization by the overlying microbialite 'mud mound'.**

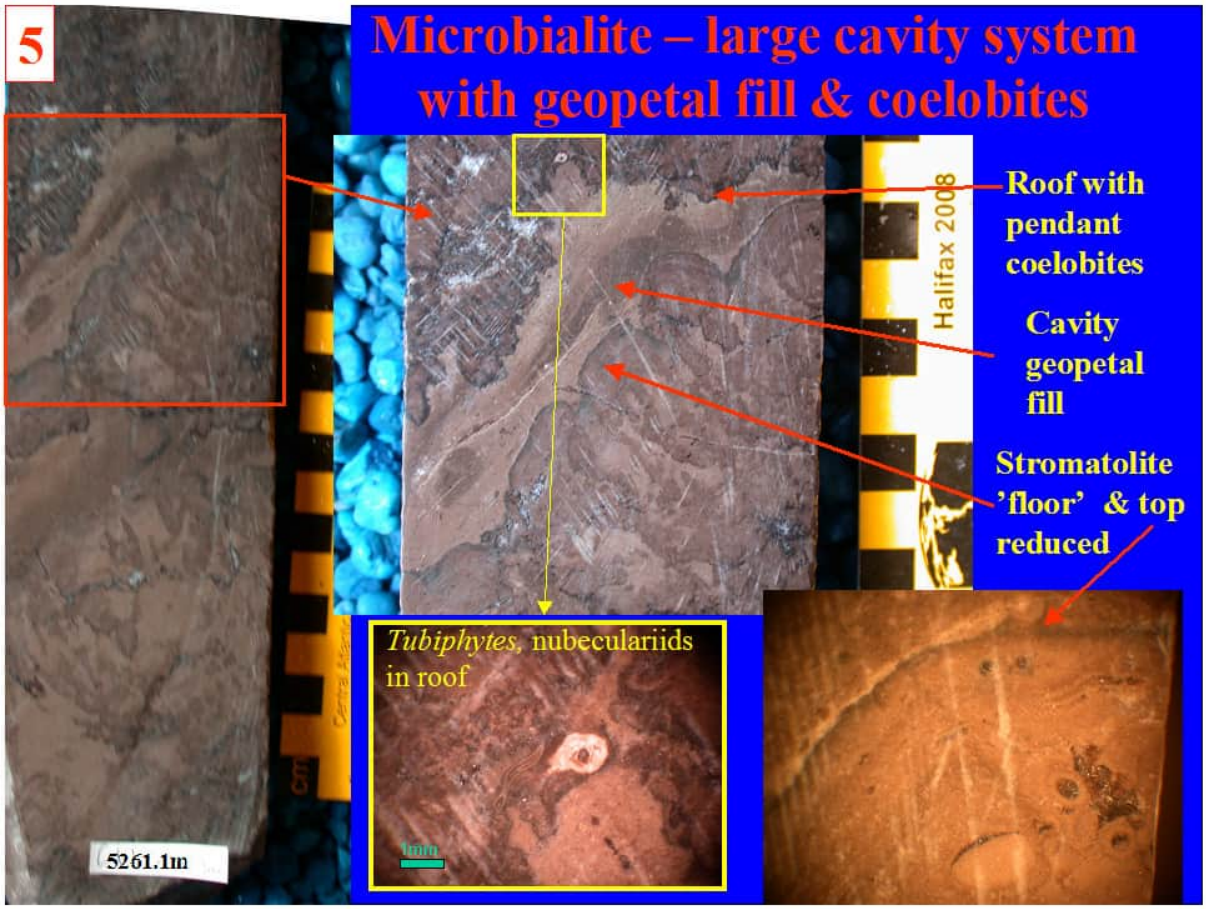


**Figure A4. West Venture C-62 #9 Limestone: pure microbial boundstone with thrombolitic to stromatolitic textures and limited but plentiful micro-encrusters – about 5 m thick of peloidal to massive mudstone with numerous shelter cavities that are geopetally-filled by peloid grainstone with varied development of later calcite cements that often include a thin initial isopachous rim. The micro-encrusters occur in the mudstone but also can encrust both upper and lower microbial surfaces. They include *Tubiphytes* (also known as *Shamovella* and possibly Jurassic foraminiferal-microbial consortium that is characteristically in reef slope debris beds and outer ramps to deeper slopes, Flugel 2004), serpulids-terebellids-thartharelids (various encrusting worm tubes with some smooth-walled calcite, some agglutinated) and nubecularids (tubular foraminifera chambered and branching). Note: Jim Aitken coined the term thrombolite for clotted fabrics interpreted as subtidal stromatolites in Lower Paleozoic rocks in the Southern Canadian Rockies.**

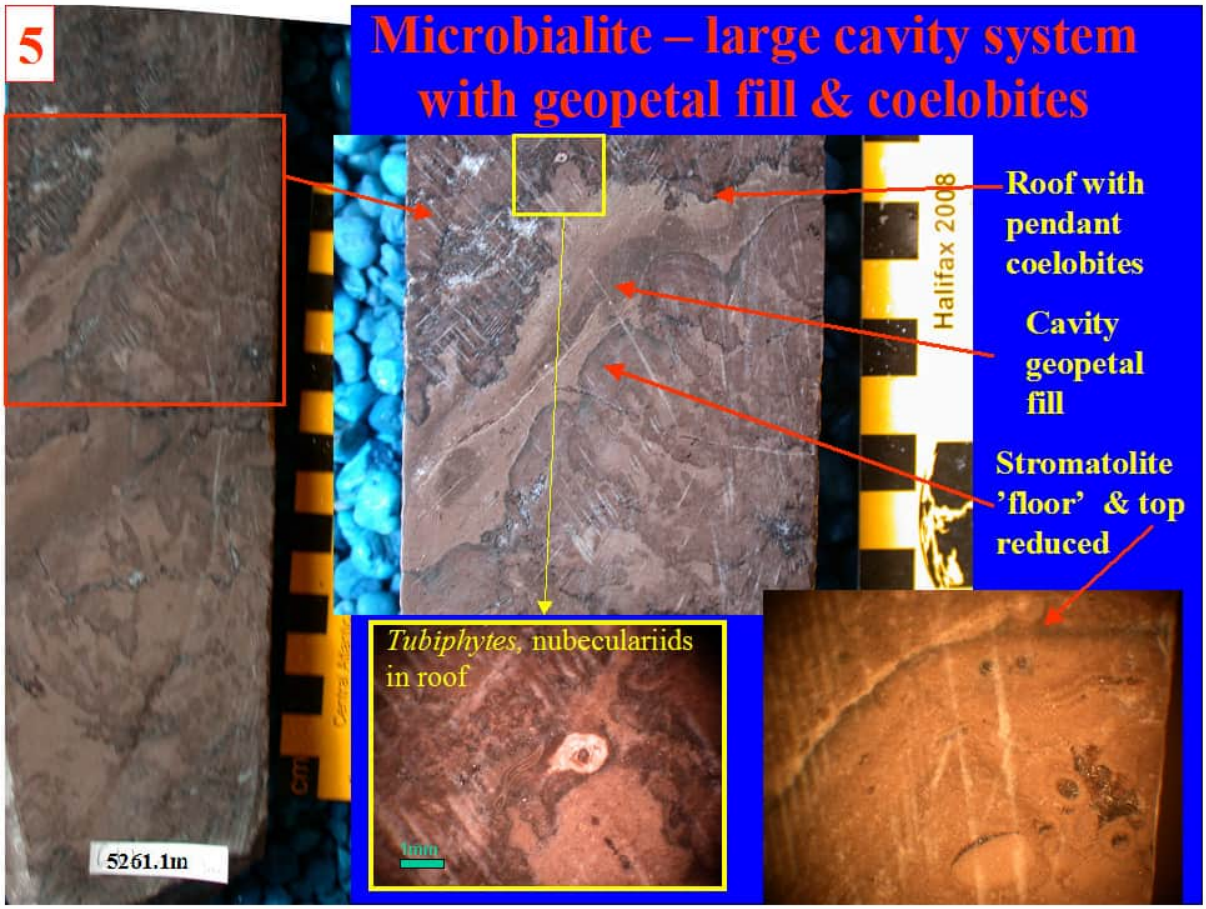


**Figure A5. West Venture C-62 #9 Limestone: pure microbial boundstone large cavity system – larger cavities of several centimeters height occur in the upper part of the microbialite interval and are filled by geopetal muds. Top and bottom surfaces appear slightly darkened grey possibly reduced (such color alteration occurs throughout the microbialite – see previous figure) and may be colonized by micro-encrusters or show pendant microbialites. Often there are bewildering gradational transitions from 'hardened' microbial bindstone fabrics to geopetal infill fabrics.**

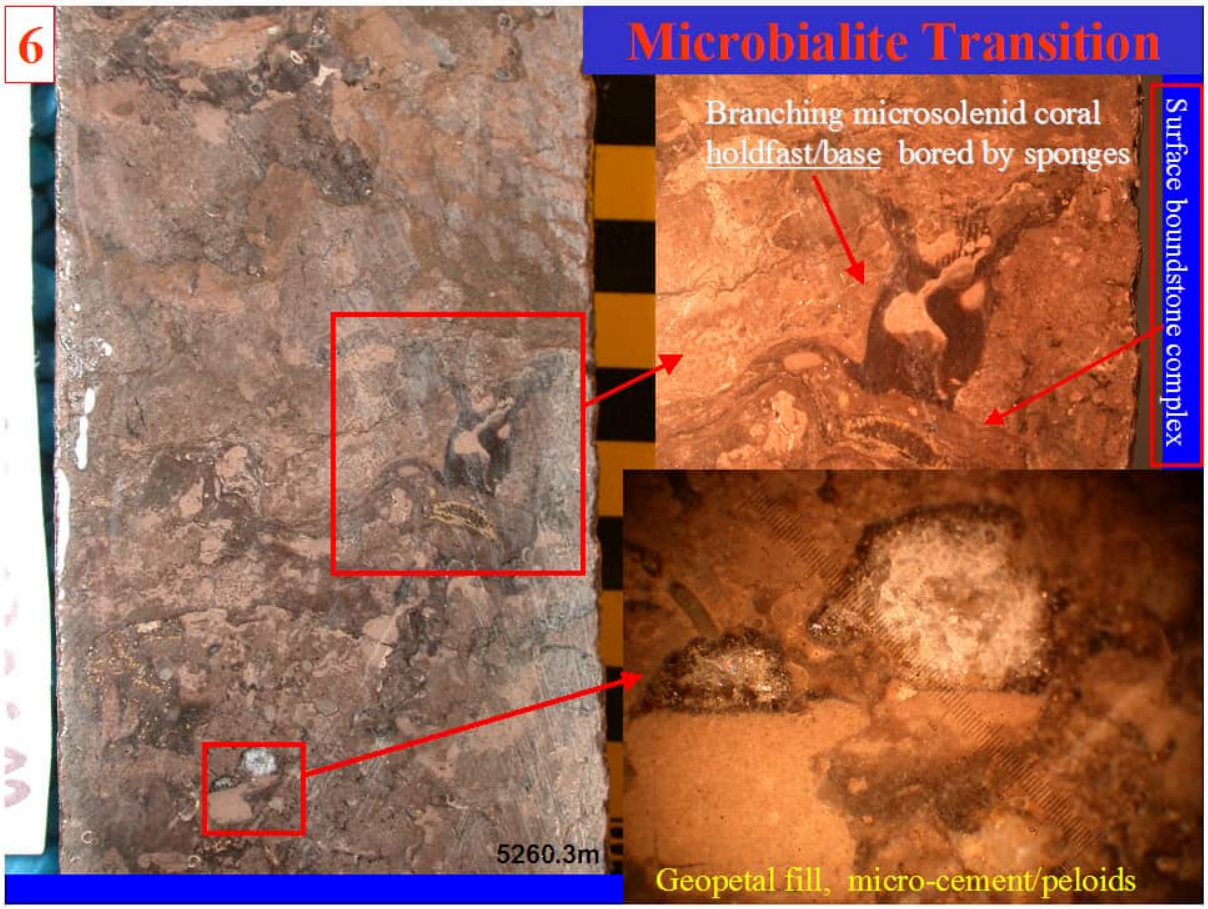


**Figure A6. West Venture C-62 #9 Limestone: pure microbialite to microbial-skeletal boundstone transition – over a metre or so hard microbial bindstone surfaces are increasingly encrusted by tabular skeletal framebuilders (for varieties see Fig. A7) or colonized by holdfasts or bases of branching-columnar framebuilders like this microsolenid corals with a highly bored interior (the sponge-boring *Entobia* makes the coral superficially look like the central cavity of a framework sponge!). An *in situ* lithistid sponge is left of the *in situ* dark coral column.**

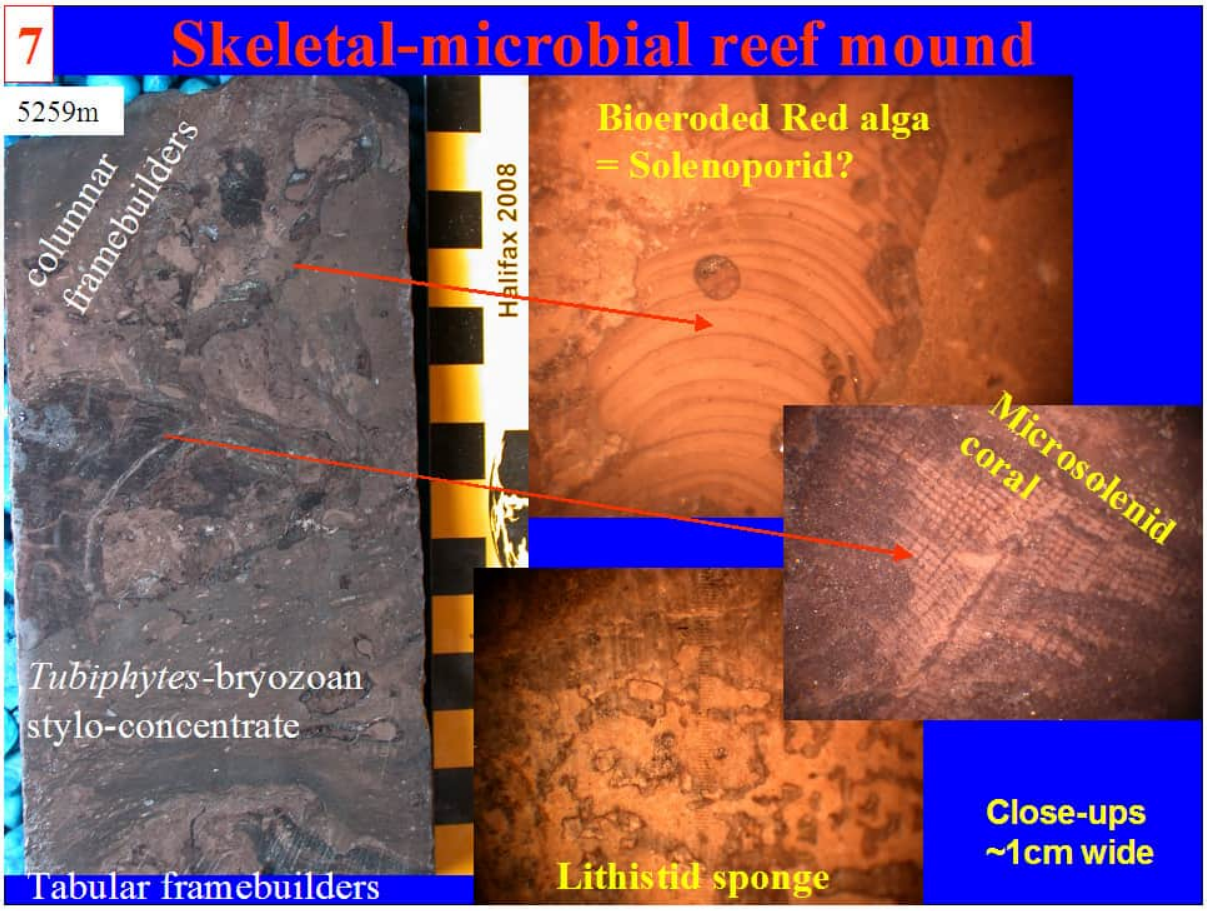


**Figure A7. West Venture C-62 #9 Limestone: skeletal microbial reef mound framebuilders – include lithistid and 'white' sponges, minor chaetetids and microsolenid corals that show complex intergrowth with each other and the microbialites. The preservation of corals due to early dissolution often makes identification problematic but it appears that only microsolenid corals with their characteristic zigzag 'tire-track' pattern (see Fig. A3) are present. All framebuilders are relatively small with the microsolenids perhaps as common as the lithistid demosponges. Their small size and dominantly *in situ* position indicates a low energy, deeper-water probably stressed setting. The high amount of bioerosion of skeletal framebuilders (microbialites are seldom infested) by bivalves (*Gastrochaenolites*) and sponges (*Entobia*) suggest very high nutrient levels. Several occurrences of an extremely finely layered with thin dark and thick light bands is interpreted as a solenoporid (usually considered a red algae). Unfortunately, the finest texture is uniformly recyrstallized and the identification is not positive with less preferred alternatives of milleporid (hydrozoan cnidarian with usually a coarser cell structure than solenoporid and therefore less likely to be completely and uniformly recyrstallized) or of some kind of skeletal stromatolite. In any case the argument for ameliorating and likely increasingly photic conditions for the skeletal reef mound as opposed to that of the pure microbialite is reasonable. Considering the increasing amount of argillaceous content indicated by the gamma log this is surprising unless there is significant relative sea-level fall. Although diagenesis is not the focus this bit of core does show a relatively common fabric due to high amounts of stylolitization aided by the high argillaceous content – solution seams and stylo-concentrates of refractory less soluble calcitic fossils like Tubiphytes-bryozoa-crinoids.**

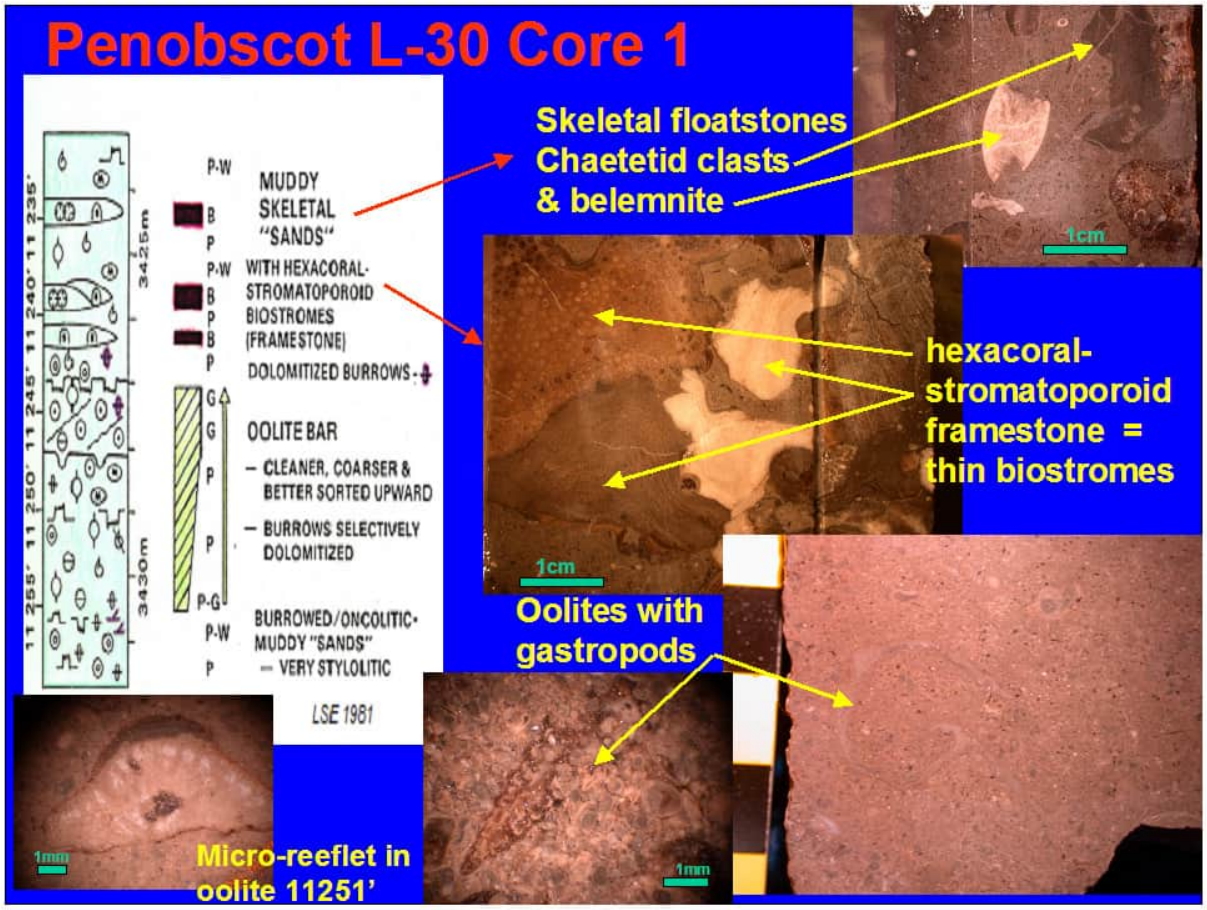


**Figure A8. Penobscot L-30 core 1 schematic log and analogue for shallow inner to mid ramp carbonate facies – coral-stromatoporoid biostromes in broken-fossil-rich packstones-floatstones, oolite and oncolitic-oolitic-peloidal packstone-floatstones (variably and slightly argillaceous) are illustrated (refer to Fig. 4 and Swanson 1981 for symbols). There may be a deepening upward or protected to less protected ramp trend in the core with shelter shallow facies in the lower core that has burrowed 'muddy' ooids, peloids, oncoids and coated fossil clasts including mollusks grading up through an oolite bar complex with gastropods into a more open setting with angular skeletal clasts including dispersed framebuilders like chaetetids and thin reefal rudstones and in situ coral-stromatoporoid boundstones as biostromes plus nektonic forms like belemnites. In a relatively short distance there is a great variety of depositional facies. All of the gastropods are replaced some more typically by spar calcite but some by mud infill indicating early aragonite replacement possibly showing instability in calcitic seawater chemistry. The micro-reeflet in the oolite is a possible small coral shaped for stability in agitated waters and over grown by a chaetetid but soon buried in carbonate ooid sand. Curiously considering the general proximity of siliciclastics, the ooid nuclei are apparently not quartz grains. Stylolites are fairly common and in part reflect the low level argillaceous content and original high carbonate mud amount.**

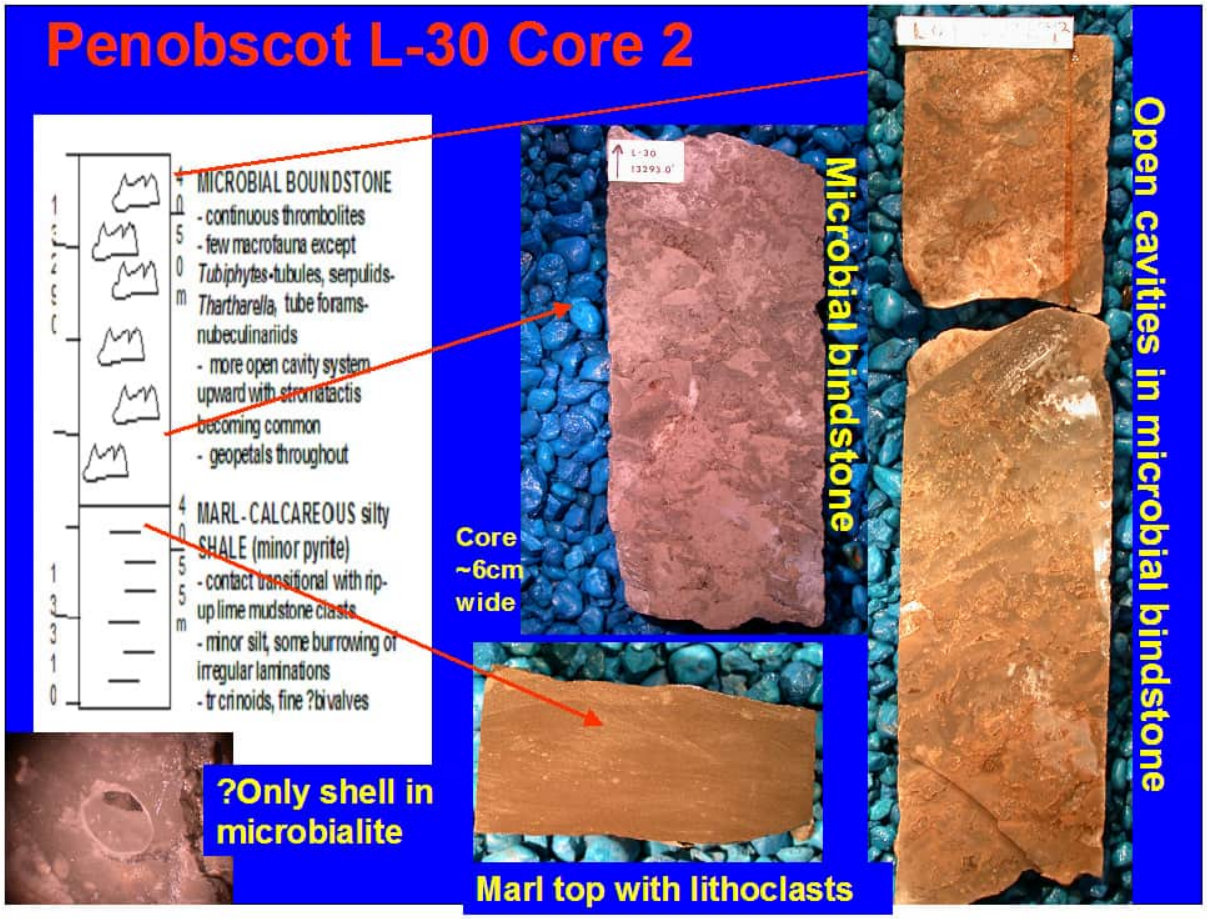


**Figure A9. Penobscot L-30 core 1 schematic log and analogue for deep-water distal ramp and slope under siliciclastic influence – the depauperate 'pure' microbialite boundstone (perhaps 'bindstone' but not by trapping sediment as much as by very early penecontemporaneous cementation by the microbes that also likely produced peloids) with plentiful geopetal shelter fabric and minor but well distributed calcite cement in cavities that range from millimeter to centimeter and larger size in the upper part of the core. Except for a small possible lithistid sponge and small shell (?brachiopod shown) the only accessory biota is a limited variety but plentiful number of micro-encrusters – *Tubiphytes*, serpulids-terebellids-thartharellids (worm tubes) and nubecularid forams. Among the microbialites seen in the Abenaki Formation distal slope this represents an end member in terms of dark color, limited accessory micro-encrusters, uniformity of fabric and lack of different interbeds. The underlying calcareous shale to marl is also fairly uniform throughout with minor silt and some burrowing of irregular laminations and traces of crinoids and fine ?bivalves. The transition to microbialite is abrupt with small (less than a centimetre) limestone lithoclasts just below the contact.**

BACK

# Characterization of Paralic Paleoenvironments using Benthic Foraminifera and Thecamoebians from Early Cretaceous Sediments (Scotian Shelf)

**Flavia Fiorini**
**Grant D. Wach**
Smithsonian Tropical Research Institute
Ancon, Panama

**David B. Scott**
5 Edsel Drive
Halifax, Nova Scotia, B3H 3J5
Canada
e-mail: dscott@dal.ca

## ABSTRACT

The benthic foraminifera and thecamoebians from an early Cretaceous cored interval of Cohasset A-52 well (located on the Scotian Shelf- North Atlantic), were used to interpret the depositional environments of these sediments. Paleoenvironmental interpretation was based on the analysis of samples from four cored intervals of A-52 corresponding to 25 m of interbedded, gray-black shale, mudstone and sandstone belonging to the Cree member of the Logan Canyon formation (Aptian –Albian). The foraminiferal association recovered from the samples is comprised mainly of agglutinated species of Trochammina, Haplophragmoides, Ammobaculites and Verneulinoides which are comparable at the generic level with the microfauna that live in modern marshes. A scattered occurrence of calcareous benthic foraminifera (typical of marginal marine environment) and thecamoebians (freshwater to brackish environment) is also recorded. The comparison of these microfauna with modern and fossil foraminiferal associations from paralic environment suggests that the sediments in the Cretaceous of A-52 were deposited in a marsh-estuarine environment. Additionally the species from A-52 were identical to those found in the Cretaceous of Alberta's Bearpaw formatiom.

BACK

# Continental Slope Sedimentation Models: Laurentian Channel and Halibut Channel Regions, Eastern Canada

**Michael Giles**
**Mladen Nedimovic**
**Grant D. Wach**
Dalhousie University
Dept. of Earth Sciences
Halifax, NS, B3H 4J1
Canada
e-mail: mkgiles@dal.ca

**David Mosher**
**David J.W. Piper**
Geological Survey of Canada-Atlantic
P.O.Box 1006
Dartmouth, Nova Scotia, B2Y 4A2
Canada

## ABSTRACT

Recently acquired seafloor multibeam, and 2D and 3D seismic reflection data of the St. Pierre and Halibut Slope regions provide evidence for successive mass failures at a variety of scales. The occurrence of stacked and regionally extensive mass failures suggests that this is a fundamental process for slope sedimentation in this area; the most recent mass-transport event was in 1929.

There are a variety of factors that explain the significance of mass failures in this area: 1) Drainage of the Great Lakes, which are the largest inland bodies of water in North America, cause the St. Lawrence River and Laurentian Channel to act as major fluvial and sediment transport conduits for most of eastern North America. It was also a major ice-outlet corridor during numerous Quaternary glaciations. As a result, sedimentation rates at the mouth of Laurentian Channel and on Laurentian Fan have been periodically high, leading to potential generation of high pore pressures and a thick column of underconsolidated sediment. 2) Sediment sampling in the region has shown the presence of intra-formational methane gas within the shallow portion of the sediment column. Generation of gas within sediment reduces its strength properties. 3) Gas hydrates, which may be indicated by bottom-simulating reflectors, are interpreted to occur in the region. Their dissociation may provide another potential source for shallow gas. 4) Recognition of buried sedimentary bedforms suggests sandy intervals underlying St. Pierre and Halibut Slope areas. Listric faults extending from surface escarpments into this interval suggests that possible detachment surfaces, perhaps in response to generation of overpressures occur within them. 5) The area overlies the Cobequid-Chedabucto fault, a paleo-transform margin, which appears to have a higher level of seismicity than most of the Canadian east coast margin. Ground accelerations due to earthquakes plays a critical role in initiating sediment failure, as in the 1929 Grand Banks submarine landslide during a M7.2 earthquake.

Mass transport processes are clearly a significant mechanism of sediment delivery in the shelf to slope setting of the greater Laurentian Channel region. These processes are dependent upon a variety of pre-conditioning factors, both lithologic and structural, yet likely initiated by seismicity. The ubiquitous nature of such processes in the Quaternary section is a critical component to understanding reservoir potential of underlying rocks that reside in the same geologic setting.

BACK

# Seafloor Diagenesis of the Scotian Basin: The Role of Fe, Ti And P

**Ann Chioma Okwese,**
**Georgia Pe-Piper**
Dept. of Geology
Saint Mary's University
Halifax, Nova Scotia, B3H3C3
Canada
e-mail: ari4el@yahoo.com

**David J.W. Piper**
Geological Survey of Canada-Atlantic
P.O. Box 1006
Dartmouth, Nova Scotia, B2Y 4A2
Canada

## ABSTRACT

Diagenesis in Lower Cretaceous sandstones of the Scotian basin is an important reservoir quality. Diagenetic processes include the effects of seafloor redox-controlled changes in pore water and the re-mineralization of organic matter; as well as later cementation and secondary porosity resulting from increases in the temperature and pressure with burial and the flux of formation waters and hydrocarbon expelled from compacting shales. Lower Cretaceous rocks of the Scotian basin are deltaic, with cycles of delta progradation characterized by high sedimentation rates capped by transgressive systems tracts typified by low sedimentation rates.

Transgressive systems tracts (TST) in one well (Peskowesk A-99 with 7 conventional cores) from the Scotian basin were identified in conventional cores with the support of available wireline logs, and core photographs (CNSOPB Geoscience Research Laboratory). The TST sediment facies include bioturbated medium- to coarse-grained sandstones with patchy siderite cementation and some bioclasts, grading upward into bioturbated mudstones. Geochemically, the Lower Cretaceous sedimentary rocks of the Scotian basin are unusual in having high titanium (Ti) and iron (Fe) and very low calcium (Ca). As a result, the early diagenetic system is dominated by Fe minerals and locally by phosphorus (P) minerals.

Samples have been collected from conventional cores through representative TSTs and underlying high-sedimentation rate deltaic sandstones in the Peskowesk A-99 well for whole-rock geochemical analysis. The vertical variation in particular Fe, Ti and P can be used to understand the seafloor diagenetic system and its relationship to abrupt changes in sedimentation rates in the TST.

BACK

# Biostratigraphic Study of Cenozoic Strata of the Grand Banks, Newfoundland

**Deborah Skilliter**
Nova Scotia Museum
1747 Summer Street
Halifax, N.S., B3H 3A6
Canada
e-mail: skillidm@gov.ns.ca

**Graham L. Williams**
**Robert A. Fensome**
Geological Survey of Canada-Atlantic
P.O. Box 1006
Dartmouth, Nova Scotia, B2Y 4A2
Canada

**G.R. Guerstein**
Lab de Palinologia, Depart. de Geologia
Universidad Nacional del Sur
San Juan 670
8000 Bahia Blanca
Argentina

**Andrew MacRae**
Dept. of Geology
Saint Mary's University
Halifax, Nova Scotia, B3H 3C3
Canada

**Grant D. Wach**
Dept. of Earth Sciences
Dalhousie University
Halifax, Nova Scotia, B3H 4R2
Canada

z

## ABSTRACT

The only extensively cored Cenozoic sections from offshore eastern Canada were recovered from a series of core holes drilled in 1965 by Pan American Petroleum Corporation (now part of BP P.L.C.) and Imperial Oil Canada. The core holes are from several basins, including the Scotian, Horseshoe, South Whale and Jeanne d'Arc. Previously, only preliminary palynological studies have been made on materials from the core holes. The current study focuses on Core Hole 16 from the southern Jeanne d'Arc Basin and Core hole 2 from Bear Ridge. Core hole 16 penetrates a broadly fining-upwards section through the Banquereau Formation, with excellent dinocyst recovery, spanning the middle Eocene through the middle Miocene. Preliminary results indicate that Core Hole 2 represents a similar sequence through broadly fining-upwards strata in the Banquereau Formation, spanning the Late Eocene to Pleistocene. By incorporating pollen and spores with dinocysts, we plan to consolidate the taxonomy, develop detailed event biostratigraphy, interpret local paleoenvironments, and determine the prevalence and age of offshore currents, particularly the Proto-Gulf Stream. The results will provide new insights into the Cenozoic history of offshore eastern Canada, including an awareness of climate change during this time.

BACK

# Lower Tertiary Mass Transport Systems Exhibited in Upper Cretaceous Wyandot Chalk

**Brenton M. Smith**
Canada Nova Scotia Offshore Petroleum Board
1791 Barrington Street
Halifax, Nova Scotia, B3J 3K9
Canada
e-mail: bmsmith@cnsopb.ns.ca

## ABSTRACT

The Upper Cretaceous Wyandot formation is a thick, continuous package of limestones, marls and chalks representing deposition on a stable, shallow, open-marine continental shelf.

Extremely detailed mapping of this surface is made possible by the strong seismic signature at the top of the Wyandot limestone. Interpretation of 16 3-D surveys covering 12,000 $km^2$ has described a complicated surface with varying degrees of erosion and has detailed several erosional features. The mapping results are displayed as a 3-D surface from which the following can be observed.

A polygonal pattern covering much of the original chalk surface, possibly caused by brittle deformation of the Wyandot, has widths of up to 150 m.

Early tertiary deltas prograding onto the Wyandot surface formed a series of troughs and ridges along the toe of these deltas. This pattern may have been caused by ocean current scour or sediment loading. Most of these patterns were eroded by subsequent mass transport systems.

Slope failure of the prograding Paleocene and Eocene deltas resulted in erosion of the upper Wyandot formation. A failure plane in the upper Wyandot detached creating a clearly defined head scarp of ~80m in height. This scarp is over 100 km in length. A 5 km wide mass transport corridor leading out to the shelf break is also clearly imaged. The fill within this corridor suggests multiple mass transport events.

Large slide blocks over 1 km long within the mass transport systems can be observed. Numerous failure events have overprinted, resulting in a complicated pattern of mass transport systems and varying degrees of Wyandot erosion.

These observations indicate that large quantities of transported Wyandot chalks should have been re-deposited out to at least on the upper slope, although these chalks would be mixed with Tertiary deltaic sediments. Re-deposited chalks are a major reservoir in the North Sea. Demonstrating that Tertiary deltas transported sediments to the slope provides additional evidence that similarly situated, Early and Middle Cretaceous deltas may have also transported sediments to the slope. This process is essential for the development of deep water turbidite reservoirs.

BACK

# A Quantitative 3D Outcrop Model of a Gravel Dominated Fluvial System (Late Triassic, Minas Basin, Nova Scotia, Canada)

**Xavier van Lanen**
**David Hodgetts**
**Jonathan Redfern**
University of Manchester
School of Earth Atmospheric and Environmental Sciences
Williamson Building, Oxford Road
Manchester, Lancashire, M13 9PL
United Kingdom
e-mail: xavier.van-lanen@postgrad.manchester.ac.uk

**Brian Williams**
**Sophie Leleu**
Department of Geology & Petroleum Geology
King's College
Aberdeen, Aberdeenshire, AB24 3UE
United Kingdom

## ABSTRACT

The Wolfville Formation was deposited in a rift basin setting during Anisian to Norian age. It is superbly exposed in both cliff sections and on extensive wave-cut platforms along the Minas Basin shore, Nova Scotia (Canada). This nature of the exposure provides unique three-dimensional sections, offering a valuable insight in the sedimentology and the facies geometries and distribution of a red bed braided fluvial-aeolian facies suite.

The selected study area is located on the southern Minas Basin shore and represents the lower unit of the Wolfville Formation. The area measures 400 m by 350 m and comprises Carnian to Norian age sediments that show a cyclicity of conglomerate / pebbly rich sandstone to a coarse lithic sandstone with sparse pebble sized clasts. The limited amount of preserved finer grained material throughout this gravel dominated system contains the faunal remains and palaeosol horizons. The base is characterised by the discordant contact with the Carboniferous and a thin alluvial breccia unit.

To obtain quantitative outcrop data, both LiDAR and DGPS data were collected and integrated with traditional geological field and laboratory data into a digital outcrop model (DOM). In the DOM the observed geological object are mapped and their geometries and distribution evaluated. The results offer a better understanding of the depositional system, and provide a geological framework for reservoir models. Such information aids improved reservoir characterisation and geostatistical modelling, as well as help explain seismic reflection data and improve flow model simulations for subsurface reservoirs.

BACK

# NOTES

# CORE WORKSHOP

## Presentations by Stratigraphy

**1. THE MONTAGNAIS METEORITE IMPACT STRUCTURE, WESTERN NOVA SCOTIAN SHELF**
Lubomir Jansa and Georgia Pe-Piper

**2. DEEP SHELFAL CHALK RESERVOIRS OF THE UPPER CRETACEOUS WYANDOT FORMATION, PRIMROSE SALT STRUCTURE AREA, OFFSHORE NOVA SCOTIA**
Andrew MacRae

**3. PRODELTAIC DEFORMATION FACIES FROM THE ALMA AND TANTALLON FIELDS**
David Piper and Georgia Pe-Piper

**4. HYPERPYCNAL FLOW DEPOSITS FROM THE THEBAUD FIELD**
David Piper and Atika Karim

**5. TIDALLY-INFLUENCED DELTAIC RESERVOIRS IN THE UPPER JURASSIC-LOWER CRETACEOUS MICMAC AND MISSISAUGA FORMATIONS (GLENELG AND ARCADIA FIELDS), OFFSHORE NOVA SCOTIA**
Andrew MacRae

**6. VARIED CARBONATE FACIES FROM THE JURASSIC-CRETACEOUS GIGAPLATFORM MARGIN OF BALTIMORE CANYON TROUGH OFF DELAWARE, USA.**
Les Eliuk & Brad Prather

**7. REEF MARGIN CARBONATE RESERVOIRS OF THE UPPER JURASSIC-LOWER CRETACEOUS ABENAKI FORMATION (DEEP PANUKE)**
Les Eliuk *for* Rick Wierzbicki, Kevin Gillen, Rolf Ackermann, Nancy Harland, Leslie Eliuk, with a contribution by Jeff Dravis

**BACK**

# NOTES

# The Montagnais Meteorite Impact Structure, Western Nova Scotian Shelf

**Lubomir F. Jansa**
Geological Survey of Canada-Atlantic
P.O. Box 1006
Dartmouth, N.S., B2Y 4A2
Canada
e-mail: lujansa@nrcan.gc.ca

**Georgia Pe-Piper**
Dept. of Geology
Saint Mary's University
Halifax, N.S. B3H 3C3
Canada.
e-mail: gpiper@smu.ca

## ABSTRACT

The first of only three known offshore impact structures, Montagnais has a short core from fractured Meguma Group (Cambro-Ordovician) recovered in Union et al. Montagnais I-94. In 1987 a report in Nature (v.327, p. 612-614) was followed up by a 1989 larger article by Jansa, L.F., Pe-Piper, G. Robertson, P.B., and Friedenreich, O. in Geological Society of America, v. 101, p.450-463. Although the effects of meteorite impacts on land has been relatively well studied (including as significant hydrocarbon-bearing structures) those on the 70% of the water-covered earth are much less understood. An underwater extraterrestrial impact crater occurs on the North Atlantic continental shelf, 200 km southeast of Nova Scotia, Canada. The impact, in late early Eocene (51 Ma) produced a complex structure with a submarine crater, a central structural high and an inner topographic ring. The crater is filled with breccia, which exhibits shock deformation features. Lack of enrichment of the melt rocks in siderophile elements compared with basement rocks and a slight enrichment in iridium suggest that the impactor was either a stony meteorite or a cometary nucleus. The diameter of the impactor is estimated to be about 2-3 km.

The cored section is about 400 m below the top of basement in the central uplift of the crater. Megascopically, it resembles Meguma Group metagreywackes and phyllites exposed on land in southern Nova Scotia. The metagreywackes from the core have hairline microfractures and rare undecorated shock lamellae in quartz grains, visible in thin sections. Other evidence for the impact structure was based on petrographic examination of cuttings and included the recognition of thick breccias, melt zones of rhyolitic composition containing calcic plagioclase, and shock-induced features of minerals including isotropization and shock-induced lamellae.

BACK

# Deep Shelfal Chalk Reservoirs of the Upper Cretaceous Wyandot Formation, Primrose Salt Structure Area, Offshore Nova Scotia

**Andrew MacRae**
Dept. of Geology
Saint Mary's University
Halifax, N.S. B3H 3C3
Canada
e-mail: andrew.macrae@smu,ca

## ABSTRACT

Chalks of the Upper Cretaceous (Turonian-Maastrichtian) Wyandot Formation form an extensive stratigraphic marker on the Scotian Margin and parts of the Grand Banks. Although not commercial, significant discoveries of natural gas occur at two sites on the Scotian Margin, Eagle and Primrose, where the Wyandot Formation serves as the main reservoir. This core display will show selected examples of the reservoir intervals at the Primrose field.

At Primrose the Wyandot Formation is characterised by well-bioturbated chalk and minor marlstone with a diverse ichnofauna dominated by subhorizontal feeding and dwelling traces (e.g., *Thalassinoides*, *Zoophycos*, *Chondrites*), and body fossils of inoceramid clams. There are some subtle indications that firmground surfaces may occur within some intervals of the chalk. The nature of the ichnofauna and of published rock-eval data (Wielens et al. 2002) implies well-oxygenated bottom conditions at the time of deposition. These are clearly "autochthonous" chalks that have formed in-situ rather than being redeposited "allochthonous" chalks (Ings et al. 2005).

Stratigraphic relationships with the overlying Campanian-Neogene Banquereau Formation indicate these chalks were probably deposited in water depths in excess of 200-300m, and were located outboard of most of the clastic sedimentary input. Despite the significant water depths, they were still inboard of the main continental slope of the Upper Cretaceous, and are therefore described as forming in a "deep shelf" setting.

Porosity within the Wyandot Formation is as high as 20-30%, but, as for most chalks, it is extraordinarily fine-grained. Porosity declines significantly even within the approximately 200m thickness of the unit at Primrose, likely due to compaction-related cementation. It is probably the relatively shallow depths (<1600m) that have allowed the reservoirs to remain significant here (Ings et al. 2005). This issue probably precludes major reservoirs in this interval on the deeper parts of the Scotian Margin, however, were redeposited chalks and early hydrocarbon charge to occur as in the central North Sea, promoting porosity preservation, deeper reservoirs may still be possible.

BACK

# Prodeltaic Deformation Facies from the Alma and Tantallon Fields

**David J.W. Piper**
Geological Survey of Canada-Atlantic
P.O. Box 1006
Dartmouth, N.S., B2Y 4A2
Canada
e-mail: dipper@nrcan.gc.ca

**Georgia Pe-Piper**
Dept. of Geology
Saint Mary's University
Halifax, N.S. B3H 3C3
Canada
e-mail: gpiper@smu.ca

## ABSTRACT

Conventional core through foresets of Lower Cretaceous deltas at the Alma field and in Tantallon M-41 show a wide range of sediment deformation facies. In particular, facies that have shallow-water sedimentological features (tidal-flat structures, wave ripples) occur in blocks of sizes ranging from centimeters to metres overlying a zone of sedimentary mylonite, with highly deformed sediments interpreted as the deforming base of a submarine landslide. Failure to recognise the allochthonous nature of these sediments has led to misinterpretation of the depositional environment and also has consequences for the connectivity of sandstone bodies. The range of observed allochthonous facies will be illustrated with core from Alma and Tantallon.

BACK

# Hyperpycnal Flow Deposits from the Thebaud Field

**David J.W. Piper**
Geological Survey of Canada-Atlantic
P.O. Box 1006
Dartmouth, N.S., B2Y 4A2
Canada
e-mail: dipper@nrcan.gc.ca

**Atika Karim**
Dept. of Geology
Saint Mary's University
Halifax, N.S. B3H 3C3
Canada
e-mail: akarim@smu.ca

## ABSTRACT

Hyperpycnal flow deposits, or "delta-front turbidites", are becoming increasingly recognised as important components of some deltaic systems. The presence of Bouma $T_{abce}$ or $T_{bce}$ sequences in sandstones, with unidirectional climbing current ripples and basal flute marks are the most diagnostic sedimentological evidence of prodeltaic hyperpycnal flows (Bhattacharya and Tye, 2004; Hampson and Howell, 2005; Myrow et al. 2006). Such beds may be capped by wave-generated oscillatory ripples and the tops are commonly strongly bioturbated. Laminae of phytodetritus are common in the sandstones and the $T_e$ division commonly has a high organic content (Rice et al. 1986). Delta-front turbidites show distinctive ichnological suites (MacEachern et al. 2005) as a result of rapid event deposition and changes in oxygenation and salinity. Some coarse-grained cross-bedded sandstones have been interpreted as deposits of predominantly by-passing prodeltaic hyperpycnal flows (Edwards et al. 2005) and turbidite channels and lobes are interpreted as significant components of shelf facies models (Pattison, 2007). Hyperpycnal mud turbidites are also recognised in prodelta settings (Leithold and Dean, 1998), with sedimentological characteristics summarized by Piper and Stow (1991). Delta-front turbidites show many similarities to sandstone beds termed tempestites, which are interpreted to result from storm resuspension of littoral sand. Myrow et al. (2002) have demonstrated that well sorted sandstone beds showing Bouma sequences and basal unidirectional flute marks have climbing ripples with convex-up and sigmoidal foresets that are characteristic of mixed wave and current motion.

These concepts will be illustrated by selected core, principally from the Thebaud field. Thick bedded reservoir sandstones from fields such as Thebaud appear to be inner shelf hyperpycnal deposits (facies 9), forming graded sandstone beds decimeters to metres thick, with Bouma Ta-Tc sequences, abundant phytodetritus, detrital intraclasts of mudstone and siderite, and minor bioturbation at the top of beds. This facies passes stratigraphically upward into tidally influenced river-mouth and river-channel sandstones (facies 4) and downward into thinner graded sandstone beds with interbedded mudstone (facies 0). More highly bioturbated thin bedded sandstones (facies 2) in places show hummocky cross-stratification, concentration of shells at the base of beds, and wave-ripples, suggestive of storm reworking. In the Glenelg field, tidally-influenced hypopyncal silts interbed with hyperpycnal sands and both change character distally. The recognition of hyperpycnal flow deposits has important implications for reservoir geometry and diagenesis.

BACK

# Tidally-influenced Deltaic Reservoirs in the Upper Jurassic-Lower Cretaceous Micmac and Missisauga Formations (Glenelg and Arcadia Fields), Offshore Nova Scotia

**Andrew MacRae**
Dept. of Geology
Saint Mary's University
Halifax, Nova Scotia, B3H 3C3
Canada
e-mail: andrew.macrae@smu.ca

## ABSTRACT

The sedimentary and ichnological signatures of tidal environments are well known from modern and ancient settings, but they are often tricky to recognize within core. This core display will demonstrate some of the diagnostic traits of tidal rhythmite deposits and associated trace fossils in a deltaic setting at the Arcadia (MicMac Formation) and Glenelg (Upper Missisauga Formation) fields. These two sites represent the approximate location of the front of the delta system in the Sable Subbasin in the Late Jurassic and Early Cretaceous, respectively.

At Arcadia J-16, core 2 consists of a succession of "massive" and crossbedded medium sandstones interbedded at metre-decimetre scale with distinctly rhythmically-bedded (mm-cm scale) fine sandstone and mudstone. The rhythmites show varying degrees of overprinting by bioturbation, from none to moderate, showing how rapid deposition and/or exclusion of much of the biota is often a prerequisite for rhythmite preservation. The fauna is low diversity and dominated by simple vertical or horizontal burrows (mostly Skolithos, Planolites, and occasionally Teichichnus). The rhythmites show clear indications of diurnal inequality and spring-neap cycles, including "crossover", that unambiguously identify them as being produced by tidal processes. At the acme of some cycles the current became strong enough to generate current ripples.

At Glenelg N-49 the cored interval consists of medium-coarse dune-crossbedded or unstructured sands with coarse rip-ups and rare preserved mud drapes. These are interbedded at metre-decimetre scale with fine, occasionally rippled sand-mud rhythmites. Unlike the rhythmites at Arcadia, diurnal inequality is not evident, and although there are thickness variations consistent with spring-neap cycles, the cycles are incomplete, suggesting that this site experienced a different current regime. The succession generally fines upwards, and is capped by bioturbated sands (Diplocraterion & Skolithos), rooted mudstones (tidal flat?) and coal, together interpreted as a channel fill. Below the channel is an interval of finer sand-mud rhythmites with rare bioturbation, reactivation surfaces, and current ripples that is interpreted as a more distal setting, perhaps in front of a distributary mouth, but still relatively sheltered from wave processes and influenced by tides.

Both of these sites demonstrate that throughout the long history of the succession of delta lobes referred to as the "Sable Delta", there were intermittent periods when tidal processes were locally significant, and these can be used to infer the proximity of the delta front at the time.

BACK

# Varied Carbonate Facies from the Jurassic-Cretaceous Gigiplatform Margin of Baltimore Canyon Trough off Delware, USA

**Leslie S. Eliuk**
Dept. of Earth Sciences
Dalhousie University
Halifax, Nova Scotia, B3H 4R2
Canada
GeoTours Consulting Inc.
e-mail: geotours@shaw.ca

**Bradford E. Prather**
Shell International E&P
Houston, TX
United States
e-mail: bradford.prather@shell.com

## ABSTRACT

In 1984 three wells operated by Shell tested various types of Jurassic-Cretaceous carbonate shelf and margin plays in deep water offshore New Jersey. Eleven cores were recovered: OCS-A 0336 cores R1-4, OCS-A 0337 cores C1-3 and OCS-A 0317 cores H1-4. Representative core intervals on display are keyed to seismic morphology and show litho-biofacies from three geometrically and stratigraphically separate shelf edges:

Oxfordian-Kimmeridgian prograded margin (R1+2) and slope (C3), Late Kimmeridgian-Berriasian aggraded margin capped by pinnacle reefs (C2, H3+4), then an extensive deeper-water mounded sponge-rich interval of Berriasian and Valanginian age (R2, C1, H2) and finally a back-stepped Barremian-Aptian reef margin (R1) on prodeltaic shales. Alternatively cores can be facies grouped into deeper-water upper slope microbial(?) mound (C3) and reef complex (R3–foreslope? + R4-reef framework & sands) of the prograded margin, shelf-edge shallow-water skeletal sands (H3+4, C2) in the aggraded margin, and deep-water carbonates capping a drowned shallow-water shelf (R2, C1, H2) then mid-Cretaceous shallow-water shelf-edge oolite (R1).

Previously unpublished paleoenvironmental models by Edwin Ringer and Harvey Patten illustrate the depositional facies relationships. No analogue is perfect, but older (and with the 1999 Panuke gas discovery many more recent) Nova Scotia (NS) shelf-edge wells also sample the Jurassic-Cretaceous gigaplatform margin. Though similar enough to apply the same formational terminology, and a very similar vertical depositional progression including 'drowning', the Baltimore Canyon wells in general sample much more carbonate-sand-rich beds. Whereas the NS margin wells sample muddier but much more reef framebuilder-rich beds. The basins have some major difference but these biofacies differences may indicate a "sampling" bias; possibly shallow-water J-K reefs simply grew in slightly deeper water. The best depositional model will integrate both data sets. Degree of dolomitization remains a significant difference.

This presentation is repeated (with slight modification) by permission from the Canadian Society of Petroleum Geologists 2005 Core Conference and with permission of Royal Dutch-Shell.

BACK

# Reef Margin Carbonate Reservoirs of the Upper Jurassic – Lower Cretaceous Abenaki Formation (Deep Panuke)

**Leslie Eliuk**
**(For Rick Wierzbicki, Kevin Gillen, Rolf Ackermann, Nancy Harland and Leslie Eliuk, with a contribution by Jeff Dravis)**
Dept. of Earth Sciences
Dalhousie University
Halifax, Nova Scotia, B3H 4R2
Canada
GeoTours Consulting Inc.
e-mail: geotours@shaw.ca

## ABSTRACT

The purpose of this presentation is to show the facies, diagenesis, and fracture interpretation of the fractured and dolomitized margin of the Abenaki carbonate platform at Deep Panuke. Core from F-70, H-08, and PI-1B will be displayed.

The Deep Panuke gas reservoir was discovered in 1999, 250 km offshore of Halifax Nova Scotia. Gas is trapped in dolomite and limestone at the margin edge of the Jurassic aged Abenaki carbonate complex. Analysis of well test data had indicated that platform margin edge wells were connected to a highly permeable reservoir, assumed to be fractured or vuggy dolomite/limestone.

In 2004, data was obtained on the high permeability reservoir, when 24 meters of core was recovered from the F-70 well bore. The F-70 core encountered foreslope and reefal limestone and fractured vuggy dolomite in the upper portion of the reservoir. The core was examined and facies described in detail by Les Eliuk. Thin sections were examined and a diagenetic interpretation provided by Jeff Dravis.

The core and associated FMI image from F-70 was interpreted by Kevin Gillen. Data from his interpretation and interpretation of all of the FMI data by HEF Petrophysical were used by Rolf Ackerman (Beicip Inc.) to build a discrete fracture network model of the reservoir. The parameters and insights gained have been used to constrain the flow simulation model of the reservoir.

NOTE: Repeated with only minor modification by permission from Canadian Society of Petroleum Geologists 2005 Core Conference in Calgary Alberta. Additions have been made to Eliuk's section on depositional setting and that will be the emphasis of the 2008 display. Also a brief appendix has been added with information on cores from Panuke PI-1A and H-08. Panuke M-79 has a 5m core in the basal Scatarie Member rich in quartz grains and ooids that will not be shown.

BACK

# NOTES

# NOTES

We sincerely thank all our sponsors, partners and supporters who contributed to the success of the

# Conjugate Margins Conference | Halifax 2008

## Diamond $15,000+

OETR

CNSOPB — CANADA-NOVA SCOTIA OFFSHORE PETROLEUM BOARD

NOVA SCOTIA Department of Energy

## Platinum $10,000 – $14,999

PETROBRAS

bhpbilliton resourcing the future

## Gold $6,000 – $9,999

ExxonMobil

Husky Energy

Atlantic Canada Opportunities Agency | Agence de promotion économique du Canada atlantique — Canada

EnCana energy for people

## Bronze $2,000 – $3,999

CANADIAN SUPERIOR ENERGY INC.

RPS Energy

ion

## Patron $1,000 – $1,999

Schlumberger

Petroleum Research Atlantic Canada

## Partners $500 – $999

Natural Resources Canada | Ressources naturelles Canada

Canada

Minerals Management Service

## Supporters

Canadian Society of Petroleum Geologists

American Association of Petroleum Geologists 1917

AGS

Boston Geological Society 1929

Geological Journal

PESGB

Dalhousie University Inspiring Minds